OPEN ACCESS
Online ISSN: 2831-2597
Volume 3, 2024

Water Emerging Contaminants & Nanoplastics

Published Articles 2024

WECN
https://oaepublish.com/wecn

EDITORIAL BOARD

Editor-in-Chief

Daoji Li (China)
Joana C Prata (Portugal)

Founding Editor-in-Chief

Antoni Ginebreda (Spain)

Associate Editors

Laurent Dufossé (France)
Xuetao Guo (China)
Roberto Rosal (Spain)
Jie Wang (China)
Quan Wang (China)
Defeng Xing (China)

Regional Editors

Julian Aherne (Canada)
Elvis Dartey Okoffo (Australia)
Giuseppe Suaria (Italy)

Editorial Board Members

Denis Abessa (Brazil)
Richard Bade (Australia)
Xue Bai (China)
Amit Bhatnagar (Finland)
Julian Blasco (Spain)
Lucila Candela (Spain)
Hongzhe Chen (China)
Jiawei Chen (China)
Wei Chen (China)
Zhijie Chen (Australia)
Gabriel Enrique De-la-Torre (Peru)
Mohammad Hadi Dehghani (Iran)
Marc Elskens (Belgium)
Cheng Fang (Australia)
Francisca Fernandez-Piñas (Canada)
Francois Gagné (Netherlands)
Karina Yew Hoong Gin (Singapore)
Leobardo Manuel Gómez-Oliván (Mexico)
Laodong Guo (USA)
Changseok Han (South Korea)
Hafiz M.N. Iqbal (Mexico)
Nicole JAFFREZIC-RENAULT (France)
Hongru JIANG (China)
Ioannis K Konstantinou (Greece)
Shan Liu (China)
Xianhua Liu (China)
Mallavarapu Megharaj (Australia)
Vincenzo Naddeo (Italy)
Ravi Naidu (Australia)
Miguel Oliveira (Portugal)
Marta Otero (Spain)
Lokesh Padhye (New Zealand)
Marco Parolini (Italy)
Paolo Pastorino (Italy)
Marco Race (Italy)
Alexandra Ribeiro (Portugal)
Didier Robert (France)
Jorge Jesús Rodríguez Chueca (Spain)
Ajit Sarmah (New Zealand)
Joaquim Rovira Solano (Spain)
Qian Sui (China)
Jing Sun (China)
Yuanyuan Tang (China)
Berrin Tansel (USA)
Sara Valsecchi (Italy)
Paola Verlicchi (Italy)
Lin Wang (China)
Yan Wang (China)
Youji Wang (China)
Yongkui Yang (China)
Wenke Yuan (China)
Yingxin Zhao (China)
Lijun Zhou (China)
Lixin Zhu (China)

GENERAL INFORMATION

About the Journal

Water Emerging Contaminants & Nanoplastics is an international peer-reviewed, open access journal.

Information for Authors

Manuscripts should be prepared in accordance with Author Instructions.
Please check https://www.oaepublish.com/wecn/author_instructions for details.
All manuscripts should be submitted online at https://ucenter.oaepublish.com

Copyright and License to Publish

Copyright is retained by authors. Authors are required to sign a License to Publish (which can be downloaded from the journal's Author Instructions), granting *Water Emerging Contaminants & Nanoplastic*s, which identifies itself as the original publisher, exclusive rights to publish their articles, and granting any third party the right to use the articles freely as long as the integrity is maintained and the original authors, citation details and publisher are identified.

Disclaimer

The information and opinions presented in the journal reflect the views of the authors and not of the journal or its Editorial Board or the Publisher. Publication does not constitute endorsement by the journal. Neither the *WECN* nor its publishers nor anyone else involved in creating, producing or delivering the *WECN* or the materials contained therein, assumes any liability or responsibility for the accuracy, completeness, or usefulness of any information provided in the *WECN*, nor shall they be liable for any direct, indirect, incidental, special, consequential or punitive damages arising out of the use of the *WECN*. The *WECN*, nor its publishers, nor any other party involved in the preparation of material contained in the *WECN*represents or warrants that the information contained herein is in every respect accurate or complete, and they are not responsible for any errors or omissions or for the results obtained from the use of such material. Readers are encouraged to confirm the information contained herein with other sources.

Publisher

OAE Publishing Inc.
245 E Main Street Ste 107, Alhambra, CA 91801, USA
Website: www.oaepublish.com

Contacts

E-mail: watercontaminants@oaemesas.com
Website: https://www.oaepublish.com/wecn

Water Emerging Contaminants & Nanoplastics

CONTENTS

Volume 3

Published Articles 2024

Volume 3, Issue 1

Volume 3, Issue 2

Volume 3, Issue 3

Volume 3, Issue 4

OPEN ACCESS
Online ISSN: 2831-2597
Volume 3, Issue 1, March 2024

Water Emerging Contaminants & Nanoplastics

WECN
https://oaepublish.com/wecn

Yaranal *et al. Water Emerg Contam Nanoplastics* 2024;3:1
DOI: 10.20517/wecn.2023.46

Water Emerging Contaminants & Nanoplastics

Research Article

Open Access

Identification, removal of microplastics and surfactants from laundry wastewater using electrocoagulation method

Naveenkumar Ashok Yaranal, Saket Apparao Kuchibhotla, Senthilmurugan Subbiah, Kaustubha Mohanty

Department of Chemical Engineering, Indian Institute of Technology Guwahati, Guwahati 781039, India.

Correspondence to: Kaustubha Mohanty, Department of Chemical Engineering, Indian Institute of Technology Guwahati, Surjyamukhi Rd, Guwahati 781039, India. E-mail: kmohanty@iitg.ac.in

How to cite this article: Yaranal NA, Kuchibhotla SA, Subbiah S, Mohanty K. Identification, removal of microplastics and surfactants from laundry wastewater using electrocoagulation method. *Water Emerg Contam Nanoplastics* 2024;3:1. https://dx.doi.org/10.20517/wecn.2023.46

Received: 19 Aug 2023 **First Decision:** 19 Sep 2023 **Revised:** 4 Oct 2023 **Accepted:** 16 Oct 2023 **Published:** 8 Nov 2023

Academic Editors: Christine C. Gaylarde, Antoni Ginebreda **Copy Editor:** Dong-Li Li **Production Editor:** Dong-Li Li

Abstract

Microplastics (MPs) and surfactants are generally recognized as emerging contaminants with complicated ecotoxicological impacts. The majority of study data refers to laundry wastewater as a substantial source of MPs and surfactants in the aquatic system, which reaches aquatic environments through sewer discharges even when wastewater treatment facilities retain them. This study focused on releasing and removing contaminants from laundry wastewater, particularly MPs and surfactants. The electrocoagulation method was used to remove the pollutants from laundry wastewater. According to the results, a reference load of 2 kg of synthetic materials releases 92,700 to 1,14,300 synthetic microfibers (MFs). MFs, surfactants, and chemical oxygen demand (COD) removal efficiency are higher at neutral pH. The percentage removal efficiency of MFs, surfactants, and COD was 97.9%, 91.2%, and 86.3%, respectively, at an operating time of 25 min, a current density of 300 A/m^2 with optimum power consumption. The total operation cost of laundry wastewater treatment by electrocoagulation was US\$0.53 /m^3. The readers will gain a complete understanding of the removal of MFs and surfactants from laundry wastewater using the electrocoagulation technique.

Keywords: Microplastics, microfibers, surfactant, laundry wastewater, electrocoagulation

INTRODUCTION

Domestic laundry wastewater is a kind of greywater. The report estimates that there are 590 million washing machines in 38 countries, and the average yearly water use of each washing machine is approximately 10 m^3[1,2]. If such a huge volume of laundry effluent is released straight into the environment without treatment, it will enormously impact the ecosystem. Direct discharge of laundry wastewater may not only cause eutrophication but may also impair the functioning of wastewater treatment plants. The majority of laundry effluent enters the wastewater treatment facility directly via municipal wastewater piping, which, if reused after treatment, can conserve water resources. Laundry activities generate a large amount of wastewater high in lint, dye, oils, fats, suspended particles, surfactants, and microplastics (MPs)[3-5]. Surfactants and MPs are two common contaminants in laundry effluent that can affect the ecosystem. Surfactants have been shown in studies to not only harm the morphology and physiology of plants but also to significantly reduce sludge dewaterability[1,6,7]. The substantial majority of research data suggests that a significant source of microfibers (MFs) (Microplastics in the form of fibers: size is less than 5 mm) in the freshwater system is from laundry outlets[8-12]. For instance, De Falco *et al.* (2018), Belzagui *et al.* (2019), and Galvão *et al.* (2020) determined that laundry outlets released MFs at rates of 1.75×10^5 - 5.6×10^5, 12×10^5 and 30×10^5 MFs/kg of cloth loads, respectively[8,9,11]. A significant accumulation of MPs and surfactants, along with their degraded products in aquatic environments, resulted in frequent exposure to living species, causing an ecological imbalance[13-15]. To date, the majority of research has focused on surfactant concentration, microplastic sources, distributions, estimates, and hazardous consequences[1,8,10,11,16-18]. Globally, the removal of MFs and surfactants from laundry outlets is a significant problem as well as a challenging task. There is an immediate need to take steps to eliminate these contaminants from laundry effluent.

Several literatures on the treatment of laundry wastewater based on various methodologies have been reported. The most often used methods include adsorption, chemical coagulation, biological, membrane filtration, electrocoagulation, floatation, and sand filtration or a combination of these techniques[4,17,19-22]. In spite of satisfactory results, each process has its own drawbacks. For example, adsorption is a pH-dependent process that requires longer treatment time, decreases adsorption capacity as the number of cycles increases, and requires high energy for regeneration. Similarly, the chemical coagulation approach necessitates the use of several chemicals. It cannot form flocs across a larger pH range. The pH must be regulated during the process, with the addition of acids and various coagulants. During the coagulation-precipitation process, a significant number of secondary pollutants, such as chloride and sulfates, are produced, and a large amount of sludge is also produced, which causes serious environmental issues[23]. In biological treatment, a large amount of space and prolonged time is required for effluent treatment. When it comes to membrane filtration, it causes fouling, which has a negative influence and reduces permeate flow. In this method, equipment and cleaning costs are expensive[19,24]. Floatation can easily separate microplastics from water or sediment. The drawback of this technique is that the removal efficiency is affected by the surface hydrophilicity of microplastics. The sand filtration technique is an easy and alluring option for wastewater treatment. However, it is reported that MPs can easily escape from sand filtration media in the presence of surfactants[25]. As a result, there is an urgent need for more reliable and cost-effective technologies that use fewer chemicals, consume less energy, and have a high capacity for pollutant removal. Electrocoagulation has gained widespread acceptance for pollutant removal from industrial and municipal wastewater. The reason could include the simple equipment design, ease of operation, rapid reaction rate, integration with various treatment techniques, and low operating costs[26,27].

Various researchers have also studied this process's effectiveness in removing MPs and surfactants from multiple sources. Shen *et al.* (2022) reported the removal of MPs from synthetic wastewater[22]. The findings indicate that aluminum anodes performed better than iron anodes in terms of removal rate, which was over 90%. Perren *et al.* (2018) reported the removal of microbeads from synthetic wastewater using electrocoagulation with removal efficiency ranging from 90% to 99%[28]. Similarly to this, Elkhatib *et al.* (2021) collected final effluent from municipal wastewater and incorporated the synthesized MPs[21]. The finding indicated that 96.5% of MPs were removed using the aluminum electrode from electrocoagulation. Oktiawan *et al.* (2021), the study focused on the removal of surfactants using electrocoagulation[5]. Study results revealed that the efficiency of removal of surfactants was higher in aluminum electrodes compared to iron electrodes. From the literature, it is envisaged that electrocoagulation with the aluminum electrode is best suited for eliminating MPs and surfactants from wastewater. Therefore, electrocoagulation with an aluminum electrode is selected for the present study for the treatment of laundry wastewater; to the best of our knowledge, the electrocoagulation technique has not been investigated much for the treatment of laundry wastewater, especially focusing on MFs and surfactants.

This study provides insight into the discharge of MFs and anionic surfactants from regular household washings. Optical microscopy and Attenuated total reflectance - Fourier transform infrared spectroscopy (ATR-FTIR) spectroscopy were used for checking microfiber counts and chemical compositions. In addition, the methylene blue active substance (MBAS) method was used to determine surfactant concentration. A cost-effective and straightforward method was adopted to reduce the MFs, chemical oxygen demand (COD), and surfactant concentration from laundry wastewater. Further, a preliminary economic evaluation of the electrocoagulation process, which includes the overall power consumption and mass of electrode material utilized for treating laundry wastewater, was carried out. Consequently, based on this quantification, an estimate of the number of MFs released into the environment is performed and compared to previously published studies. The current study will assist readers in developing a thorough grasp of the features and treatment of laundry wastewater comprising key contaminants such as MFs and surfactants.

MATERIALS AND METHODOLOGY

Materials

All the chemicals used in the experimental study were Analytical and laboratory reagent-grade chemicals. Chloroform ($CHCl_3$) and phenolphthalein indicator ($C_{20}H_{14}O_4$) were purchased from Finar Chemicals. Methylene blue dye ($C_{16}H_{18}ClN_3S$), and sodium dodecylbenzene sulfonate/linear alkylbenzene sulfonate ($C_{18}H_{29}NaO_3S$) were purchased from Merck Life Science Pvt. Ltd, Mumbai, India. Hydrogen peroxide 30% (H_2O_2), hydrochloric acid 37% (HCL), ethanol 99% (C_2H_6O), sodium hydroxide (NaOH) and sodium chloride (NaCl) were purchased from Sigma-Aldrich Chemical Pvt. Ltd. Sulfuric acid 98% (H_2SO_4) was procured from Thermo Fisher Scientific Pvt. Ltd. Nile red dye ($C_{20}H_{18}N_2O_2$), sodium Lauryl Sulfate ($C_{12}H_{25}NaO_4S$), sodium bicarbonate ($NaHCO_3$) and sodium carbonate anhydrous (Na_2CO_3) were purchased from HI-Media Laboratories Pvt. Ltd, Mumbai, India. Polycarbonate track etching (pore size 0.2 m, dia 25 mm) and nylon (pore size 0.2 m, dia 47 mm) filter papers were purchased from Sterlitech Corporation, USA and Axiva Sichem Pvt. Ltd, respectively. The electrocoagulation technique was carried out using aluminum electrodes. In order to maintain the effectiveness of the electrodes, diluted HCl (0.01 M) was used to clean the electrodes.

Washing machine discharge collection

Polyester lining fabrics were brought from different stores in India and washed (2 kg fabric materials). A top-load convection washing machine and liquid detergent were used. The quick program option in the washing machine was used to conserve energy and water (15 min, 45 L of ambient temperature water). Regularly, the discharge from washing machines was collected from residential areas, and it was determined that the sample's average residual turbidity was 145 NTU (Lutron, TU-2016). The washing machine effluent was turbid and muddy in color. Before beginning the experiment, the washing machine went through several blank washes to clean it.

Sample preparation

The fabrics were measured in terms of length and weight and classified based on materials before starting the experiments. After washing fabrics, machine outlet samples were collected and stored in glass containers at 4 °C. Further stored samples were characterized and utilized for electrocoagulation tests. To calculate the number of MFs present in washing machine outlet samples, 1 L washing machine outlet samples were taken and digested with hydrogen peroxide to remove organic and dirt materials[29,30]. After digestion, samples were filtered with polycarbonate track etching or nylon filter paper. To prevent contamination, the filters were always stored in glass Petri dishes. Subsequently, the filtered membrane was dried at 50 °C for 24 h and then characterized. Complete sample filtration was conducted in laminar flow to avoid any airborne MPs. Throughout the experiments, no plasticware was used, and special precautions were taken to avoid contamination.

Electrocoagulation experiment

The electrocoagulation operation was carried out using an electrochemical setup (semi-batch process) built of acrylic material with a 1.2 L volumetric capacity. Both of the electrodes were made with aluminum sheets with a surface area of 6.42×10^{-3} m^2 and dimensions of 0.088 m × 0.073 m. In order to deliver consistent current, anode and cathode electrodes were connected to a direct current (DC) power source (0-30 V/10 A, DC Crown regulated power supply). Induced polarization takes place when a voltage is applied to the electrode ends, leading to the monopolization of the whole assembly. The distance between electrodes was maintained at 5 mm. A detailed schematic diagram of the electrocoagulation system is shown in Figure 1. Several current densities, ranging from 100 to 400 A/m^2, were applied. It is observed that the removal effectiveness of the process approaches saturation when trials are carried out at current densities of more than 300 A/m^2. These investigations demonstrated a comparable decrease in percentages in terms of pollutant concentration. However, current densities of less than 200 A/m^2 were unable to completely eliminate all the contaminants that were over the acceptable limit. As a result, the experiments' ideal current density of 300 A/m^2 was chosen. Similarly, an electrocoagulation duration of 25 min was determined as the best working time since continuing the trials beyond this point results in negligible pollutant removal. As a result, the optimum conditions for all following experiments were 300 A/m^2 (current density) and 25 min (treatment duration). To properly spread the coagulant matter generated by anodic oxidation, a magnetic stirrer with a continuous stirring speed of 180 rpm was used. The experiments were carried out using aluminum electrodes. The entire experimental and analysis process took place at room temperature. The after-electrocoagulation process samples were allowed to settle overnight, and then the supernatant solution was decanted for further MFs and surfactant analysis. The reactions that take place during electrocoagulation (at the anode, cathode, and bulk medium) are detailed below[31].

At anode:

$$Al(s) \rightarrow Al^{3+} (aq) + 3e^- \qquad (1)$$

$$2H_2O \rightarrow O_2 (g) + 4H^+ (aq) + 3e^- \qquad (2)$$

At cathode:

$$2H_2O + 2e^- \rightarrow H_2\,(g) + 2OH^-\,(aq) \tag{3}$$

In solution:

$$Al^{3+}\,(aq) + 3OH^- \rightarrow Al(OH)_3\,(s) \tag{4}$$

After settling the sludge, the supernatant solution was taken gently to further analyze MFs, anionic surfactants, and COD concentrations. The sludge was separated and then dried for 24 h at 45 °C in a vacuum drying oven. Each experiment was repeated three times. To study the influence of initial pH, the pH values were adjusted by using diluted H_2SO_4 and NaOH solutions.

Visual inspection, quantification, chemical composition, and morphological characterization

After the sample preparation, filtered membranes were subjected to visual sorting under an optical microscope, which is the most generally used approach for identifying MFs. Microfiber particles were categorized based on their forms and sizes. To determine the functional groups contained in the obtained samples, FTIR analysis of the MFs sample was performed using PerkinElmer Spectrum II. This type of spectroscopic investigation enables the accurate identification of the smallest synthetic plastic particles. After each electrocoagulation experiment, the sludge was recovered and dried at 45 °C for 48 h and further examined with a field emission scanning electron microscope (FESEM) (Manufacturer: Carl Zeiss; Model: Gemini 300) to study the morphological characterization of the sludge and MFs.

Anionic surfactant

Anionic surfactants were assessed via spectrophotometric techniques using methylene blue as the active substance, and this standard method was utilized to determine surfactant concentration in tap water (IS 3025: Part 78: 2021, which is identical to ISO 16265: 2009). The technique works by forming an ionic pair between anionic surfactants and methylene blue. Anionic surface-active agents form salts in reaction with methylene blue in an alkaline medium. These salts are extracted with chloroform and acid treatment of the chloroform solution. Later, the absorbance of the isolated organic phase at the maximum absorption wavelength of 650 nm was measured by a double-beam UV spectrophotometer (Shimadzu, UV-2600)[3,32,33]. Identification of surfactant concentration using the UV spectrophotometer method was a tedious process, which has been simplified in the schematic diagram and shown in Figure 2. A detailed analytical procedure for determining anionic surfactant has been mentioned in the Supplementary material.

RESULTS AND DISCUSSION

The characteristics of laundry wastewater effluent parameters are shown in Table 1. Effluent waste from laundry was collected from domestic in October 2022 at IIT Guwahati, Assam, India. In this study, the results shown in Table 1 are the mean values of three test samples. The experiment was conducted at room temperature. Sample pH, turbidity, COD anionic surfactant, and concentration of MFs were analyzed.

Effect of pH

The pH of laundry wastewater is a very significant factor in the performance of the electrocoagulation process. To investigate the influence of pH, the laundry effluent pH was adjusted with dilute aqueous NaOH and H_2SO_4. Figure 3 depicts the removal efficiency of MFs, surfactant concentration, and COD at different pH after 25 min of electrocoagulation operation. From the figure, it can be seen that the removal efficiency of MFs in all the samples was above 90%, with pH levels ranging from 4 to 10. However, the removal efficiency of MFs at pH = 4 and 10 is slightly lower compared with pH = 6-8. Further, the removal efficiency

Table 1. Characteristics of laundry wastewater before and after electrocoagulation treatment

Sl. No.	Parameters	Initial effluent characteristics	Electrocoagulation operating parameters and cost estimation	After electrocoagulation treatment
1	pH	9.1 ± 0.5	T= 25 min, pH= 7, CD 300 A·m^{-2}, Stirring speed 180; 0.53 US\$·m^{-3} (44 Rs·m^{-3})	8.9 ± 1
2	Turbidity	145 ± 10 NTU		1.2 ± 0.7 NTU
3	COD	830 ± 25 (mg/L)		112 ± 5 (mg/L) (> 85%)
4	Anionic surfactant	48 ± 3 (mg/L)		4.3 ± 1 (mg/L) (> 90%)
5	MFs	2,300 ± 240 MFs/L		50 ± 18/L (> 95%)

COD: Chemical oxygen demand; MFs: microfibers; NTU: nephelometric turbidity units.

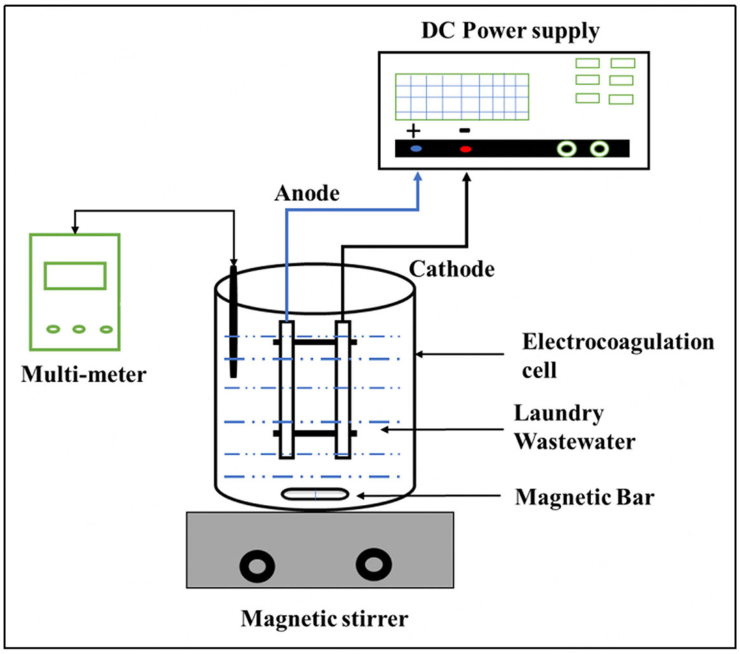

Figure 1. Schematic diagram of the electrocoagulation set up. DC: Direct current.

of surfactant and COD was 91% and 85%, respectively, at pH 7. At pH = 7, the maximum removal efficiency of all contaminants was determined to be optimal. The results show that a more neutral pH is likely to provide greater removal due to the favorable formation of coagulants at neutral pH, which is in line with the results of Perren *et al.* (2018) and Dimoglo *et al.* (2019)[26,28]. The difference in removal efficiency with pH is due to the hydrolysis and polymerization of Al^{3+} in the pH range of 6-8, which leads to the formation of particles Al(OH)$^{2+}$, [Al$_2$(OH)$_2$]$^{4+}$, Al(OH)$_3$, and highly charged polymeric hydroxy complexes [Al$_{13}$(OH)$_{32}$]$^{7+}$, which are effective for coagulation. As the pH rises over 10, the main hydrolysis product is Al(OH)$_4$, which inhibits the synthesis of anodized aluminum species as well as the adsorption of dispersed particles. The adsorption effect is negligible at low pH = 4 because only aluminum ions are present[14,26,28].

Effect of current density

Current density is an essential parameter in electrocoagulation operations since it is an operating factor that may be directly regulated using the DC power source. Figure 4 depicts the average removal rates for the various current densities from 100 to 400 A/m^2. It can be observed from the figure that the change in current density has a considerable impact on the removal efficiency of MFs, surfactants, and COD

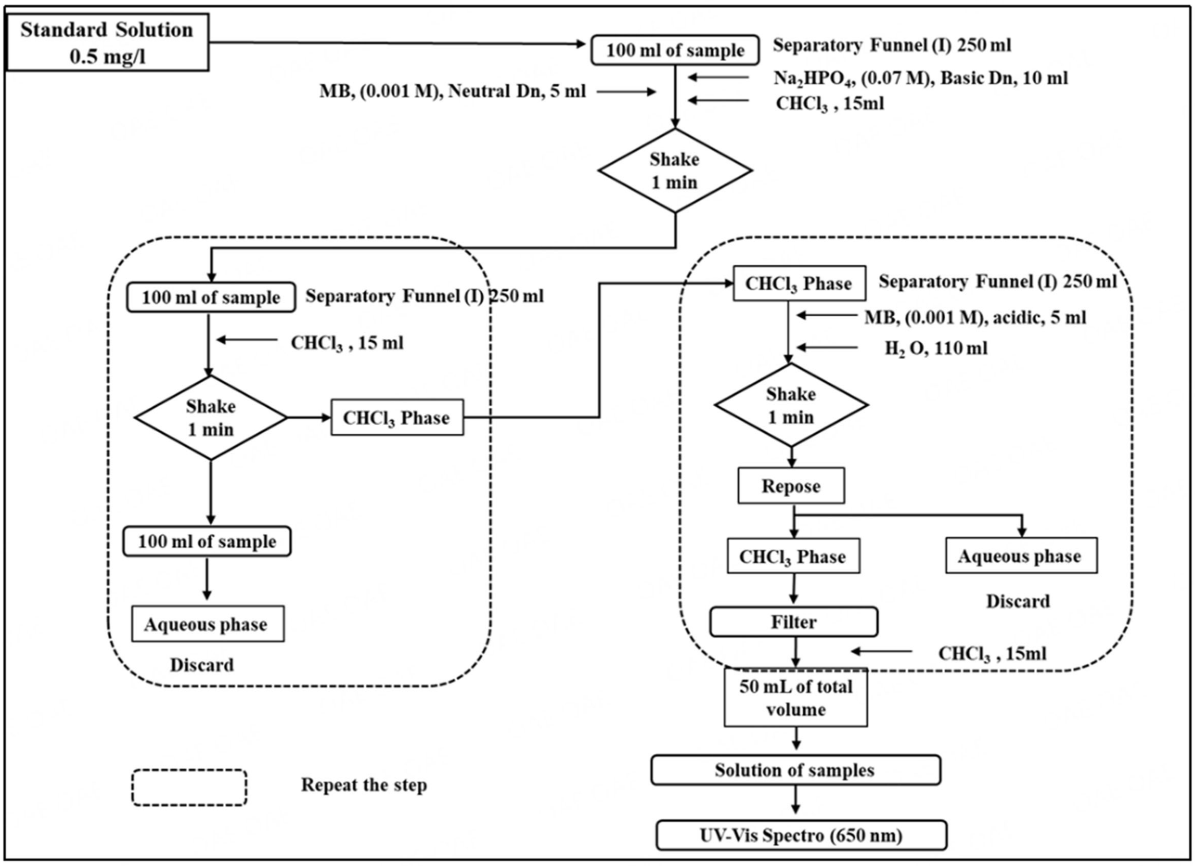

Figure 2. Schematic representation of the normalized analytical method for identifying anionic surfactants.

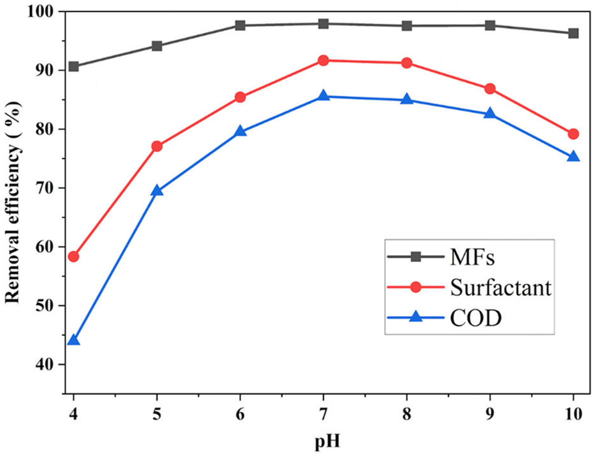

Figure 3. Efficiency of removing MFs, surfactants, and COD after 25 min of electrocoagulation at various starting pH levels. Electrode spacing is 0.5 cm, stirring speed is 180 rpm, and current density is 300 A/m^2. COD: Chemical oxygen demand; MFs: microfibers.

concentrations. The removal efficiency increased with an increase in current densities. This is in line with Faraday's law of electrolysis. When the current density of the cell is increased, metal ions released from the electrodes are also increased, and flocculants are likely to be present at high current density. Yet, there was

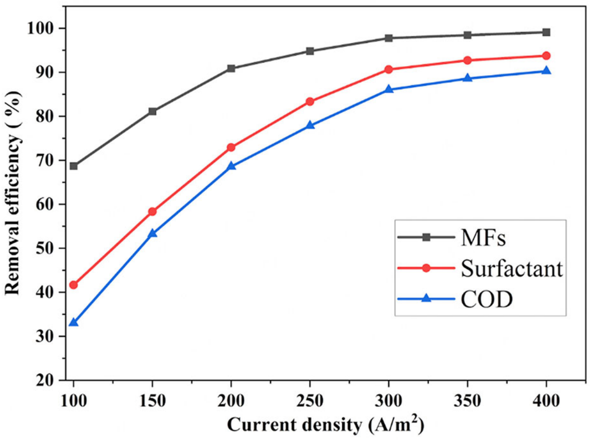

Figure 4. The effect of current density on MFs, surfactant, and COD removal efficiency reaction time 25 min time, pH 7, electrode spacing 0.5 cm, and stirring speed of 180 rpm. COD: Chemical oxygen demand; MFs: microfibers.

no apparent change in removal efficiency between 300 and 350 A/m^2; taking operational cost into consideration, a current density of 300 A/m^2 was found to be optimum, with a removal efficiency of 97%, 90.6%, and 86% for MFs, surfactants, and COD, respectively. Hence, 300 A/m^2 has been considered for further experiments.

Effect of processing time

The results of MFs, surfactant, and COD removal from laundry wastewater by electrocoagulation as a function of processing time are depicted in Figure 5. Contaminant removal efficiency starts increasing when the electrolysis duration is raised from 5 to 35 min, as seen in the figure. The results show that reaction time has a favorable influence on electrochemical treatment efficiency. Anodic electro-dissolution causes the release of coagulating species during electrocoagulation. Pollutant removal efficiency is directly related to metal ion dissolution concentration. The concentration of metal ions and associated hydroxide flocs in the water solution increases as the electrolysis duration increases. An increase in the treatment time results in a significantly greater removal. The time when coagulants are in excess and flocculation takes control appears to be between 20 and 25 min since current density seems to have a greater impact on contaminate elimination during this time period. Running the reactor for more than 25 min would result in excess coagulant with minimum effect on removal efficiency.

Additionally, prolonged operation results in increased electrode and energy consumption. Therefore, the operating time of 25 min was found to be optimum with a removal efficiency of 97.9%, 91.2%, and 86.3% for MFs, surfactant, and COD, respectively, at pH 7 and 300 A/m^2. The initial turbidity decreased from 145 ± 10 to 1.2 ± 0.7 NTU.

Characteristics of microfibers and flocs

Optical microscopic analysis

Laundry wastewater was observed under an optical microscope. The results confirmed the existence of MFs in all of the laundry wastewater samples [Figure 6A]. It was observed that laundry wastewater contained around 2,300 ± 240 MFs/L or 46,350 -57,150 MFs/kg fabrics. The length of the collected MFs varied between 20 to 5,000 μm with a diameter between 10 to 20 μm. After electrocoagulation, the supernatant solution and sludge were observed under the optical microscope.

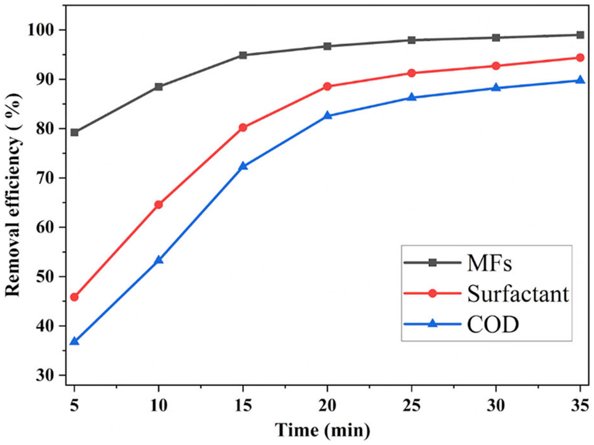

Figure 5. Effect of electrolysis time on the removal efficiency of MFs, surfactants and COD. Reactor CD 300 is A/m^2,pH 7, electrode spacing 0.5 cm, and stirring speed 180 rpm. COD: Chemical oxygen demand; MFs: microfibers.

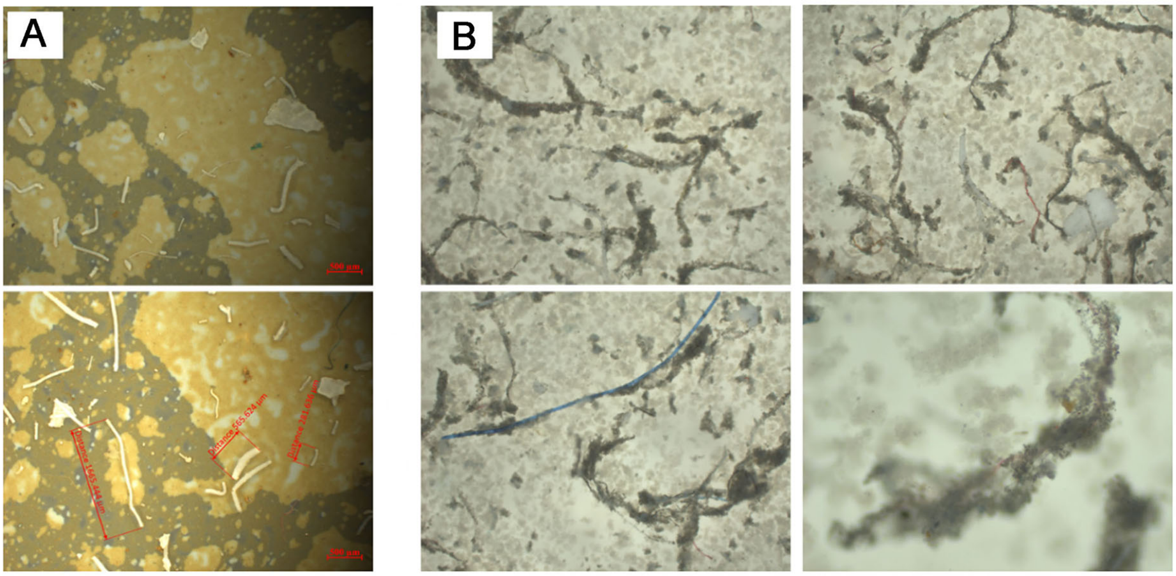

Figure 6. (A) Microscopic images of MFs in laundry effluent; (B) sludge obtained after electrocoagulation. MFs: Microfibers.

Around 50 ± 18 MFs/L was observed in the supernatant solution. It was found that there was a huge deposition of organic and inorganic particles (soil/dust, surfactants, dye, heavy metals) on the surface of MFs, which makes the MFs precipitate easily [Figure 6B].

FTIR analysis

A total of ten samples of laundry effluent were collected, including replicates. After the procedure, the validation of microfiber polymer types was performed using ATR-FTIR. Spectra were scanned in the range of 4,000-400 cm^{-1}. The raw spectra were processed using Bio-Rad KnowItAll software and identified the composition of MFs polymers. The graph obtained from the ATR-FTIR of microfiber particles was examined and depicted in Supplementary Figure 1. It can be seen from the figure that laundry wastewater contained a polyester type of polymer. The results were compared with reference samples using Bio-Rad KnowItAll software.

FESEM analysis

After electrocoagulation, the flocs were analyzed using scanning electron microscopy. The presence of MFs in the sludge can be clearly seen in FESEM images, as shown in Figure 7. The FESEM study is reliable, consistent, and accurate, making it possible to measure the size of fibers present in laundry wastewater and sludge. The MFs are long and thick and often occur in aggregates within flocs. The size of the flocs was > 50 µm, which was confirmed using a scanning electron microscopic technique.

A proposed possible mechanism

Electrocoagulation is a complicated process that uses a combination of procedures that work together to remove contaminants from wastewater. It allows for anodic oxidation and the formation of *in situ* active adsorbent (for example, aluminum hydroxides). Simultaneously, cathodic reactions take place, and H_2 gas is generated, allowing the absorbents to float[28,34]. The produced Al^{3+} ions instantaneously hydrolyze to form equivalent hydroxides and poly hydroxides at a suitable pH. Generated aluminum hydroxides and aluminum poly hydroxides have a stronger attraction to collect the contaminants in the wastewater, producing more coagulation compared to the typical aluminum coagulants[35,36]. Furthermore, the gas bubbles produced by water electrolysis might promote the floating of contaminants and coagulated materials. A possible mechanism is proposed based on the results obtained [Figure 8].

Natural clay particles, heavy metals, and dyes are usually negatively charged[28,37,38]. Monomeric species such as $Al(OH)^{2+}$, $Al(OH)_2^{+}$, $Al_2(OH)_2^{+}$, $Al(OH)_4$, and polymeric species such as $Al_6(OH)_{15}^{3+}$, $Al_7(OH)_{17}^{4+}$, $Al_8(OH)_{20}^{4+}$, $Al_{13}O_4(OH)_{24}^{7+}$, $Al_{13}(OH)_{34}^{5+}$, can neutralize the surface charges of heavy metals[23,31] dye, and clay particles[35,39], which ultimately leads to their surface deposition onto MFs during electrocoagulation.

(ii) Amorphous flocs of aluminum hydroxides have a wide surface area, which is advantageous for faster MFs adsorption[22,37].

(iii) Anionic surfactants are adsorbed on MFs, and the negative surface charges can be neutralized with an opposite charge or floc of aluminum hydroxides generated during the process. Further, it leads to the formation of larger flocs, and these flocs can be removed from the aqueous medium by precipitation or hydrogen flotation.

Operating cost analysis of electrocoagulation

The operating cost (US$·$m^{-3}$ of effluent) of the electrocoagulation process mainly includes electricity and electrode costs. The operational cost was calculated using Equation 5[23].

$$Operating\ cost_{(electrocoagulation)} = a \times Q_{electrode} + b \times Q_{energy} \tag{5}$$

where $Q_{electrode}$ and Q_{energy} denote electrode material and electrical energy usage, respectively. "*a*" indicates the cost of the electrode (2.82 US$·kg of aluminum), and "*b*" means the cost of electricity use (0.0924 US$·kW·$h^{-1}$). Faraday's law was used to determine the consumption of electrode material[31]:

$$Q_{energy} = \frac{I \times V \times t}{V_L} \tag{6}$$

$$Q_{electrode} = \frac{I \times t \times M.W}{F \times z \times V_L} \tag{7}$$

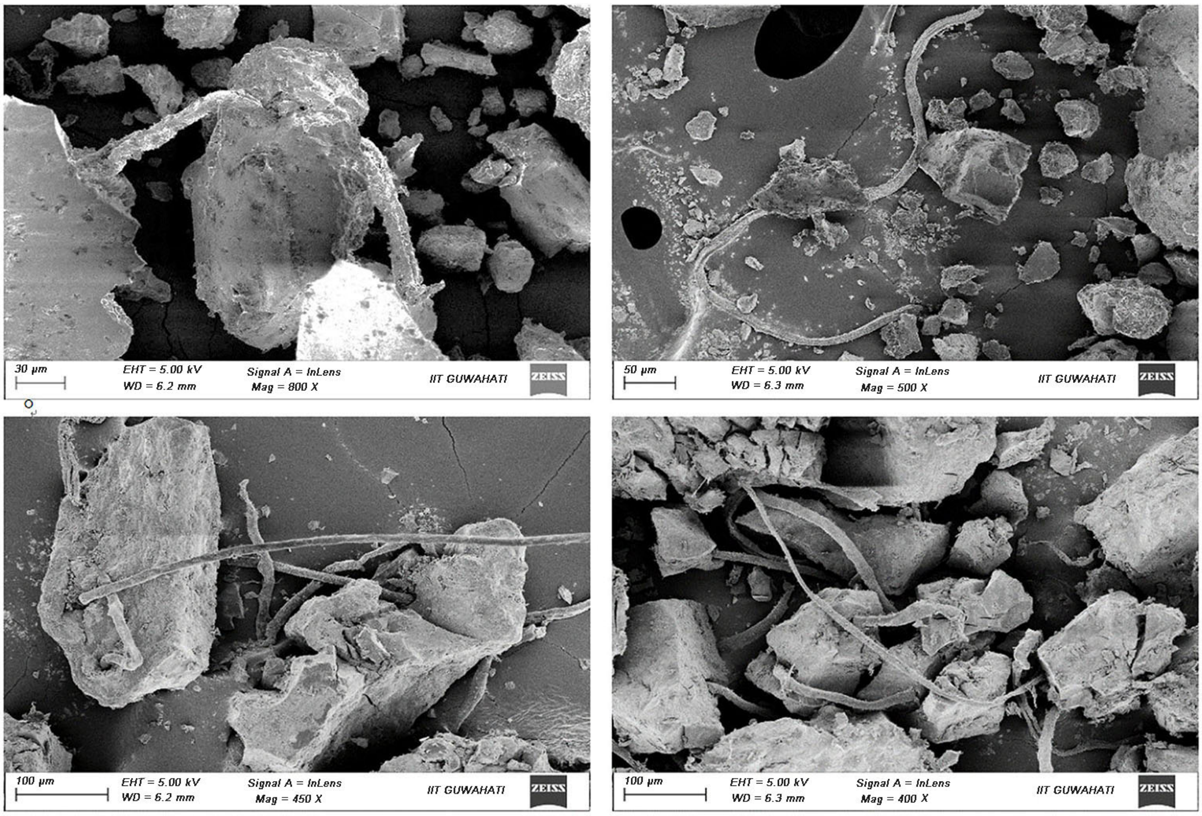

Figure 7. Scanning electron microscopic images of MFs flocs after electrocoagulation. MFs: Microfibers.

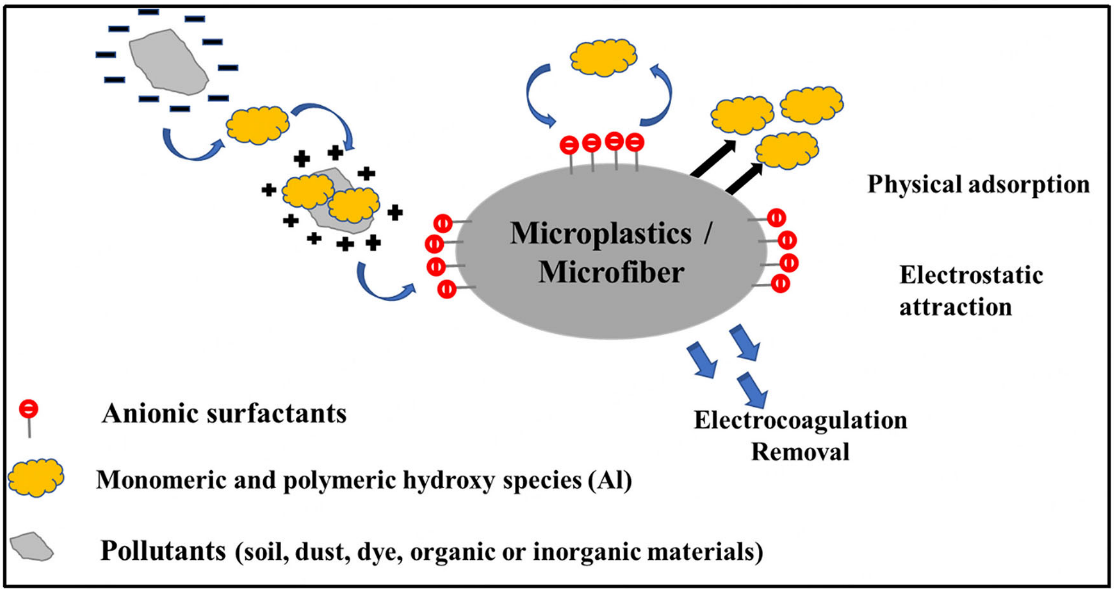

Figure 8. Schematic illustration of surfactant stealth effect of MPs/MFs during coagulation. MFs: Microfibers; MPs: microplastics.

where I designates the current (A), t indicates the time of electrocoagulation process (s), $M.W$ is the molar mass of aluminum (26.98 g·mol^{-1}), V is the voltage (V), V_L is the effluent volume (m^3), F is the Faraday's constant (96,487 $C\cdot mol^{-1}$), and z is the number of electrons transported ($z = 3$). The energy and electrode costs for the electrocoagulation process increase with increasing current density. This is due to increased energy consumption and greater anodic oxidation. At 25 min of study, the total operation cost was 0.53 $US\$\cdot m^{-3}$ with a rising current density of 300 $A\cdot m^{-2}$.

A comparative study with various literature

The release of MFs from the laundry is influenced by various parameters, including textile properties (for example, fabric type and age), washing temperature, detergent properties and dosage, and abrasion during laundry[40,41]. New clothes shed more MFs during washing because of residues from the fabric production process[9]. Various literature estimates MFs detachment from fabrics. However, their results are difficult to compare since they employed utilized materials, different washing durations, and other detergents are presented in different units. A summary of these previously published works is shown in Table 2. According to what can be observed in the table, our data show fewer MFs than those of earlier studies. This may be due to less washing time, lower water temperature (25-30 °C), and use of liquid detergent, which resulted in less release of MFs in laundry outlets. Similar interference was also reported by[40,41].

The studies on the removal of MFs and surfactants in various wastewater using the electrocoagulation process are shown in Table 3. Significantly, the available research on the removal of MFs and surfactants from laundry wastewater by the electrocoagulation process is very limited. The comparison of targeted parameters and data based on pollutant removal obtained in this work suggests that aluminum electrodes are best suited compared to other electrodes. This is also comparable with the studies that have used aluminum electrodes for pollutant removal from various wastewater, as shown in the table. Further, the research conducted in this work could serve as benchmark data in the field of treatment of MFs and surfactants from the laundry industry.

CONCLUSION

Synthetic MFs accumulation and deposition in the aquatic ecosystem are presently undeniable. This work aimed to evaluate the presence of MFs in laundry wastewater and the effective removal of pollutants by the electrocoagulation process. From the study, it was envisaged that initial pH, operating time, and current density have a substantial impact on the removal of contaminants from laundry wastewater. The removal efficiency of MFs, surfactants, and COD is higher at neutral pH. The percentage removal efficiency of MFs, surfactants, and COD was 97.9%, 91.2%, and 86.3%, respectively, at an operating time of 25 min, a current density of 300 A/m^2 with optimum consumption of electrodes. The Electrocoagulation system was effective in reducing more than 86% of the amount of pollutant concentration in laundry wastewater. Further research should look at the impact of NaCl percentage and current density on the efficiency and cost operations. A two-stage, continuous electrocoagulation reactor with membrane or adsorption or sand-based separation appears to be the most practical solution for a large-scale industrial electrocoagulation process. Additional studies may be conducted to investigate different reactor designs and combinations to improve the process.

Table 2. Comparison of various works of literature with the present work

Type of fabric	New clothes	MFs numbers	MFs length	Surfactant concentration	Ref.
Commercial garments (polyester, polypropylene)	Yes	12×10^5 - 35.40×10^5 MFs/kg	20 to 2,000 m	n.d	De Falco *et al.* (2018)[9]
Commercial garments (polyester)	Yes	6.40×10^5 - 15×10^5 MFs/kg	Avg. 360-660 m	n.d	De Falco *et al.* (2019)[10]
Textile garments (Polyester, polyester-elastane and polyamide-elastane)	Yes	30,000-465,000 MFs/m^2	20 to 5,000 m (avg. 0.2-0.4 mm)	n.d	Belzagui *et al.* (2019)[8]
Household clothes and linens (cotton, polyester, polyamide, viscose, elastane, acrylic)	No	30×10^5 MFs/kg	0.17 mm (50 to > 500 m)	n.d	Galvão *et al.* (2020)[11]
Polyester, polyamide, and polyacetate fabrics	Yes	74,816 ± 10,656 MFs/m^2	5-4,000 m (avg. polyester: 499.49 ± 505.65 μm, polyamide: 1,056.53 ± 761.42 μm, acetate: 1,128.00 ± 750.72 μm)	n.d	Yang *et al.*, (2019)[41]
Household clothes	No	4,400-10,800 MFs/L	6-4,000 μm	8 ± 2 to 800 ± 50 (mg/L)	Luo *et al.* (2022)[1]
Household lining fabric	No	2,300 ± 240 MFs/L or 46,350-57,150 MFs/kg	> 50 to 5,000 μm	48 ± 3 (mg/L)	Present work

Avg.: Average length; MFs: microfibers; n.d: not determined.

Table 3. Removal of MFs and surfactants in various wastewater using the electrocoagulation process

Type of wastewater	Pollutants	Treatment method	Electrode	Removal efficiency	Ref.
Domestic wastewater (PE, PVC)	MPs	Electrocoagulation-electroflotation and membrane filtration	Al and Fe	MPs 100% (Electrocoagulation and membrane)	Akarsu *et al.* (2021)[20]
Effluent from the local wastewater treatment plant	Polyester MPs (25 mg/L) were added	Electrocoagulation	Al	MPs 96.5%	Elkhatib *et al.* (2021)[21]
Synthetic wastewater	MPs (PE, PMMA, CA, PP)	Electrocoagulation	Al and Fe	For Al: PE 93.2%, PMMA 91.7%, CA 98.2%, PP 98.4%. For Fe: PE 71.6%, PMMA 58.6%, CA 85.4%, PP 82.7%.	Shen *et al.* (2022)[22]
Secondary effluent of the sewage treatment plant	PE MPs (25 mg/L) were added	Electrocoagulation	Al	Surfactants 97.5%	Xu *et al.* (2022)[12]
Laundry wastewater	Surfactants	Electrocoagulation	Al	Surfactants 80%	Ramcharan and Bissessur (2017)[18]
Laundry wastewater	Surfactants	Electrocoagulation/ electroflotation	Al	Surfactants 90%	Dimoglo *et al.* (2019)[26]
Laundry wastewater	Surfactants	Electrocoagulation	Al-Al, Fe-Fe, Al-Fe, and Fe-Al	72.89% in Al-Al, 54.33% in Fe-Fe, 62.70% in Al-Fe, and 49.01% in Fe-Al	Oktiawan *et al.* (2021)[5]
Laundry wastewater	MFs and surfactants	Electrocoagulation	Al	MFs 97.9%, Surfactants 91.2%,	Present work

Al: aluminum; CA: Cellulose acetate; Fe: iron; MFs: microfibers; MPs: microplastics; PE: polyethylene; PMMA: polymethyl methacrylate; PP: polypropylene; PVC: polyvinyl chloride.

DECLARATIONS

Acknowledgment

The authors are thankful to the Central Instrument Facility and Center for Nanotechnology at the Indian Institute of Technology, Guwahati (IITG), India, for providing all analytical facilities. We are grateful to

Prof. Purkait MK (Department of Chemical Engineering, IIT Guwahati) for allowing us to utilize the instruments and Mr. Anweshan and Pranjal Das (Research Scholar, Department of Chemical Engineering, IIT Guwahati) for helping out during the experiments.

Authors' contributions

Conceptualization, methodology, validation, formal analysis, investigation, writing - original draft: Yaranal NA
Experimentation, analysis: Kuchibhotla SA
Conceptualization, supervision, resources, writing - review and editing: Subbiah S, Mohanty K

Availability of data and materials

Not applicable.

Financial support and sponsorship

None.

Conflicts of interest

All authors declared that there are no conflicts of interest.

Ethical approval and consent to participate

Not applicable.

Consent for publication

Not applicable.

Copyright

REFERENCES

1. Luo J, Jin X, Wang Y, Jin P. Advanced treatment of laundry wastewater by electro-hybrid ozonation-coagulation process: surfactant and microplastic removal and mechanism. *Water* 2022;14:4138. DOI
2. Pakula C, Stamminger R. Electricity and water consumption for laundry washing by washing machine worldwide. *Energy Effic* 2010;3:365-82. DOI
3. Kruszelnicka I, Ginter-Kramarczyk D, Wyrwas B, Idkowiak J. Evaluation of surfactant removal efficiency in selected domestic wastewater treatment plants in Poland. *J Environ Health Sci Eng* 2019;17:1257-64. DOI PubMed PMC
4. Santiago DE, Hernández Rodríguez MJ, Pulido-melián E. Laundry wastewater treatment: review and life cycle assessment. *J Environ Eng* 2021;147:03121001. DOI
5. Oktiawan W, Samadikun BP, Junaidi, et al. Effect of electrode configuration and voltage variations on electrocoagulation process in surfactant removal from laundry wastewater. *IOP Conf Ser Earth Environ Sci* 2021;896:012049. DOI
6. Badmus SO, Amusa HK, Oyehan TA, Saleh TA. Environmental risks and toxicity of surfactants: overview of analysis, assessment, and remediation techniques. *Environ Sci Pollut Res Int* 2021;28:62085-104. DOI PubMed PMC
7. Kaleta J, Elektorowicz M. The removal of anionic surfactants from water in coagulation process. *Environ Technol* 2013;34:999-1005. DOI PubMed
8. Belzagui F, Crespi M, Álvarez A, Gutiérrez-Bouzán C, Vilaseca M. Microplastics' emissions: microfibers' detachment from textile garments. *Environ Pollut* 2019;248:1028-35. DOI PubMed
9. De Falco F, Gullo MP, Gentile G, et al. Evaluation of microplastic release caused by textile washing processes of synthetic fabrics. *Environ Pollut* 2018;236:916-25. DOI
10. De Falco F, Di Pace E, Cocca M, Avella M. The contribution of washing processes of synthetic clothes to microplastic pollution. *Sci Rep* 2019;9:6633. DOI PubMed PMC
11. Galvão A, Aleixo M, De Pablo H, Lopes C, Raimundo J. Microplastics in wastewater: microfiber emissions from common household laundry. *Environ Sci Pollut Res Int* 2020;27:26643-9. DOI PubMed
12. Xu R, Yang Z, Niu Y, et al. Removal of microplastics and attached heavy metals from secondary effluent of wastewater treatment plant using interpenetrating bipolar plate electrocoagulation. *Sep Purif Technol* 2022;290:120905. DOI

13. Elizalde-Velázquez GA, Gómez-Oliván LM. Microplastics in aquatic environments: a review on occurrence, distribution, toxic effects, and implications for human health. *Sci Total Environ* 2021;780:146551. DOI PubMed
14. Tripathi SK, Tyagi R, Nandi BK. Removal of residual surfactants from laundry wastewater: a review. *J Dispers Sci Technol* 2013;34:1526-34. DOI
15. Yaranal NA, Subbiah S, Mohanty K. Microplastics in the environment: sources, pathways, and abundance. IGI Global; 2022, p. 49-70. Available from: https://www.igi-global.com/chapter/microplastics-in-the-environment/305542. [Last accessed on 26 Oct 2023].
16. Li J, Dagnew M, Ray MB. Effect of coagulation on microfibers in laundry wastewater. *Environ Res* 2022;212:113401. DOI PubMed
17. Patil VV, Gogate PR, Bhat AP, Ghosh PK. Treatment of laundry wastewater containing residual surfactants using combined approaches based on ozone, catalyst and cavitation. *Sep Purif Technol* 2020;239:116594. DOI
18. Ramcharan T, Bissessur A. Treatment of laundry wastewater by biological and electrocoagulation methods. *Water Sci Technol* 2017;75:84-93. DOI PubMed
19. Šostar-turk S, Petrinić I, Simonič M. Laundry wastewater treatment using coagulation and membrane filtration. *Resour Conserv Recycl* 2005;44:185-96. DOI
20. Akarsu C, Kumbur H, Kideys AE. Removal of microplastics from wastewater through electrocoagulation-electroflotation and membrane filtration processes. *Water Sci Technol* 2021;84:1648-62. DOI PubMed
21. Elkhatib D, Oyanedel-craver V, Carissimi E. Electrocoagulation applied for the removal of microplastics from wastewater treatment facilities. *Sep Purif Technol* 2021;276:118877. DOI
22. Shen M, Zhang Y, Almatrafi E, et al. Efficient removal of microplastics from wastewater by an electrocoagulation process. *Chem Eng J* 2022;428:131161. DOI
23. Das PP, Anweshan, Mondal P, et al. Integrated ozonation assisted electrocoagulation process for the removal of cyanide from steel industry wastewater. *Chemosphere* 2021;263:128370. DOI
24. Deepti, Bora U, Purkait MK. Promising integrated technique for the treatment of highly saline nanofiltration rejected stream of steel industry. *J Environ Manage* 2021;300:113781. DOI PubMed
25. Jiang Y, Yin X, Xi X, Guan D, Sun H, Wang N. Effect of surfactants on the transport of polyethylene and polypropylene microplastics in porous media. *Water Res* 2021;196:117016. DOI PubMed
26. Dimoglo A, Sevim-Elibol P, Dinç Ö, Gökmen K, Erdoğan H. Electrocoagulation/electroflotation as a combined process for the laundry wastewater purification and reuse. *J Water Process Eng* 2019;31:100877. DOI
27. Priya M, Jeyanthi J. Removal of COD, oil and grease from automobile wash water effluent using electrocoagulation technique. *Microchem J* 2019;150:104070. DOI
28. Perren W, Wojtasik A, Cai Q. Removal of microbeads from wastewater using electrocoagulation. *ACS Omega* 2018;3:3357-64. DOI PubMed PMC
29. Yaranal NA, Subbiah S, Mohanty K. Distribution and characterization of microplastics in beach sediments from Karnataka (India) coastal environments. *Mar Pollut Bull* 2021;169:112550. DOI PubMed
30. Yaranal NA, Subbiah S, Mohanty K. Identification, extraction of microplastics from edible salts and its removal from contaminated seawater. *Environ Technol Innov* 2021;21:101253. DOI
31. Das PP, Mondal P, Anweshan, et al. Treatment of steel plant generated biological oxidation treated (BOT) wastewater by hybrid process. *Sep Purif Technol* 2021;258:118013. DOI
32. Barz G, Gordalla B, Vega I, Lewis J. Water quality - Determination of surfactants - Part 1: Determination of anionic surfactants by measurement of the methylene blue index (MBAS). 1996. Available from: https://cdn.standards.iteh.ai/samples/24784/e633ec389b134ad1a402a1dc8a976bfd/ISO-7875-1-1996.pdf. [Last accessed on 26 Oct 2023].
33. Jurado E, Fernández-Serrano M, Núñez-Olea J, Luzón G, Lechuga M. Simplified spectrophotometric method using methylene blue for determining anionic surfactants: applications to the study of primary biodegradation in aerobic screening tests. *Chemosphere* 2006;65:278-85. DOI
34. Jang YC, Lee J, Hong S, Lee JS, Shim WJ, Song YK. Sources of plastic marine debris on beaches of Korea: more from the ocean than the land. *Ocean Sci J* 2014;49:151-62. DOI
35. Bayramoglu M, Kobya M, Can OT, Sozbir M. Operating cost analysis of electrocoagulation of textile dye wastewater. *Sep Purif Technol* 2004;37:117-25. DOI
36. Wang CT, Chou WL, Kuo YM. Removal of COD from laundry wastewater by electrocoagulation/electroflotation. *J Hazard Mater* 2009;164:81-6. DOI PubMed
37. Shen M, Song B, Zeng G, Zhang Y, Teng F, Zhou C. Surfactant changes lead adsorption behaviors and mechanisms on microplastics. *Chem Eng J* 2021;405:126989. DOI
38. Xia Y, Xiang XM, Dong KY, Gong YY, Li ZJ. Surfactant stealth effect of microplastics in traditional coagulation process observed via 3-D fluorescence imaging. *Sci Total Environ* 2020;729:138783. DOI PubMed
39. Shim HY, Lee KS, Lee DS, et al. Application of electrocoagulation and electrolysis on the precipitation of heavy metals and particulate solids in washwater from the soil washing. *J Agric Chem Environ* 2014;3:130. DOI
40. Le LT, Nguyen KQN, Nguyen PT, et al. Microfibers in laundry wastewater: problem and solution. *Sci Total Environ* 2022;852:158412. DOI
41. Yang L, Qiao F, Lei K, et al. Microfiber release from different fabrics during washing. *Environ Pollut* 2019;249:136-43. DOI

Brown *et al. Water Emerg Contam Nanoplastics* 2024;3:2
DOI: 10.20517/wecn.2023.54

Water Emerging Contaminants & Nanoplastics

Research Article

Open Access

A baseline for microplastic occurrence in three New England estuaries

Bonnie Brown[1], Gregg Moore[1], Hanna Mogensen[1], Taja Sims-Harper[1], Jennifer Gibson[1], Bo-Young Lee[1], Catherine Wardinski[1,2], Gabrielle Jarrett[1]

[1]Department of Biological Sciences, University of New Hampshire, Durham, NH 03824, USA.
[2]College of Natural and Computational Sciences, Hawai'i Pacific University, Honolulu, HI 96813, USA.

Correspondence to: Bonnie Brown, Department of Biological Sciences, University of New Hampshire, 38 Academic Way, Durham, NH 03824, USA. E-mail: Bonnie.Brown@unh.edu

How to cite this article: Brown B, Moore G, Mogensen H, Sims-Harper T, Gibson J, Lee BY, Wardinski C, Jarrett G. A baseline for microplastic occurrence in three New England estuaries. *Water Emerg Contam Nanoplastics* 2024;3:2. https://dx.doi.org/10.20517/wecn.2023.54

Received: 2 Sep 2023 **First Decision:** 31 Oct 2023 **Revised:** 16 Nov 2023 **Accepted:** 27 Nov 2023 **Published:** 30 Nov 2023

Academic Editor: Quan Wang **Copy Editor:** Dong-Li Li **Production Editor:** Dong-Li Li

Abstract

Although microplastics (MP) have been documented in estuarine habitats, limited published data exist for New Hampshire and northern Massachusetts hampering meaningful, regional comparison with other geographies. Here we synthesize previously unpublished data from several independent baseline studies spanning three estuarine systems including Great Bay Estuary (GBE), Hampton-Seabrook Estuary (HSE), and Great Marsh Estuary (GME) to compare geographic data for MP to other published regional studies. Data include water column in GBE (n = 179 from 7 sites), surface waters and salt marsh sediment cores from HSE (n = 72 water samples from 12 sites and n = 77 sediment cores from 8 sites), and surface waters from GME (n = 42 water samples at 17 sites). Samples were analyzed for MP characteristics initially via either automated confocal microscopy or light microscopy, allowing initial estimation of the number and size distribution of putative MP. Particles from representative samples were analyzed using laser direct infrared spectrometry (LDIR) to determine elemental analysis. MP were found in > 98% of samples collected including surface waters, water column, and marine sediments. Counts ranged from 1 to 144,000 MP particles m^{-3} and mean MP differed significantly among regions, sites within regions, and across years. In the GBE water column, MP tended to peak during June-August in 4 of the 5 years studied. Most MP were roughly circular and ~50 μm in diameter. LDIR confirmed that many types of plastics are in these estuarine waters and also revealed that despite the digestion processes, biogenic materials often remained, predominantly chitin, rubber, wood, and coal. These data allow us to address the realistic levels of risk that estuarine MP pose in NH and northern MA estuaries and can be used to populate existing hydrodynamic models that will predict the tributary sources, movements, and fate of MP within these aquatic habitats.

Keywords: Microplastic, estuary, rural runoff, New England

INTRODUCTION

As early as the 1970s, marine scientists noted the occurrence of microplastic particles (MP, particles < 5mm) in nearly every aquatic system studied[1-7] and because of their persistence, MP is an emerging water pollutant of concern[8]. Recent studies have confirmed the roles that coastal systems play in attenuating microplastics[9], including deposition in marine sediments[10] and salt marsh peat[11-13]. Subsequently plastics have been found to serve as the substrate for the growth of microbes, both prokaryote and eukaryote[6,14-17], and as such, scientists have posited that MP are responsible for movement and redistribution of organisms both benign and harmful, within and across ecosystems[15,16,18-23]. Having codified that this new "Plastisphere"[17] realm constitutes a new and diverse microbial niche with biogeochemical consequences[21,24-26], there now exists a series of questions regarding the environmental fate and consequences of plastics and their epiplastic communities[27]. Numerous studies show that zooplankton, mollusks, fishes, crustaceans, birds, and cetaceans consume MP, and those particles are found in soft tissues, muscle, liver, and gut (10-1,000 s of particles per individual)[8,28-37]. Recent reports quantify actual levels of MP in seafood[38-42] with specific reference to MP location (gut, gills, tissues) within organisms. Numerous studies indicate that MP may damage aquatic organisms (including higher trophic levels) by blocking digestive tracts, and by altering feeding and reproductive patterns. To understand how MP are acquired and concentrated in living resources, data are needed for the ambient occurrence of MP in aquatic systems. A recent study of MP in Great Bay Estuary sediments[10] found levels as high as 100 ± 50 MP·g^{-1}. Results of inputting MP sediment data into a hydrodynamic and particle transport model suggested the highest MP deposition occurs in regions with weaker hydrodynamic flows and lower bed shear stress such as eelgrass meadows and along the fringes of the Bay. Other models of MP settlement in estuaries recently have been published[43], and together such tools will enable prediction of the tributary sources, movements, and fate of MP within these aquatic habitats. To better inform such hydrodynamic models, data are needed for the ambient quantities, types, densities, sizes, *etc*. of MP currently present within these estuaries. Because MP have not been well studied in estuarine habitats of New England, additional studies were performed in three estuarine systems in this geography, including Great Bay Estuary (GBE) in New Hampshire, Hampton-Seabrook Estuary (HSE) in New Hampshire and Great Marsh Estuary (GME) in Massachusetts to gather baseline knowledge of ambient levels of MP in the water column and intertidal sediments. Provided here is a summary of MP data from samples derived from contemporaneous independent studies conducted by our group. While it is important to note there are differences in approach, analysis, and study goals reported herein, the data constitute an important regional summary and a baseline in support of future work in this region.

METHODS

Sampled regions

The coastal GBE is surrounded by rural, agricultural, and forested areas and is fed by 7 tributaries that are typically low-discharge systems, providing limited freshwater[44]. In contrast, HSE and GME are barrier marsh systems that were formed behind the multi-state barrier beach system, serving as the primary coastal landform that protects homes, businesses, infrastructure, and estuarine resources of the marsh complex. Although these two systems each have their individual tidesheds, both ecologically and hydrologically, HSE is a component of GME, collectively spanning 10 municipalities from Cape Ann, Massachusetts to Hampton, New Hampshire. These three estuarine systems [Figure 1] contain some of the most outstanding

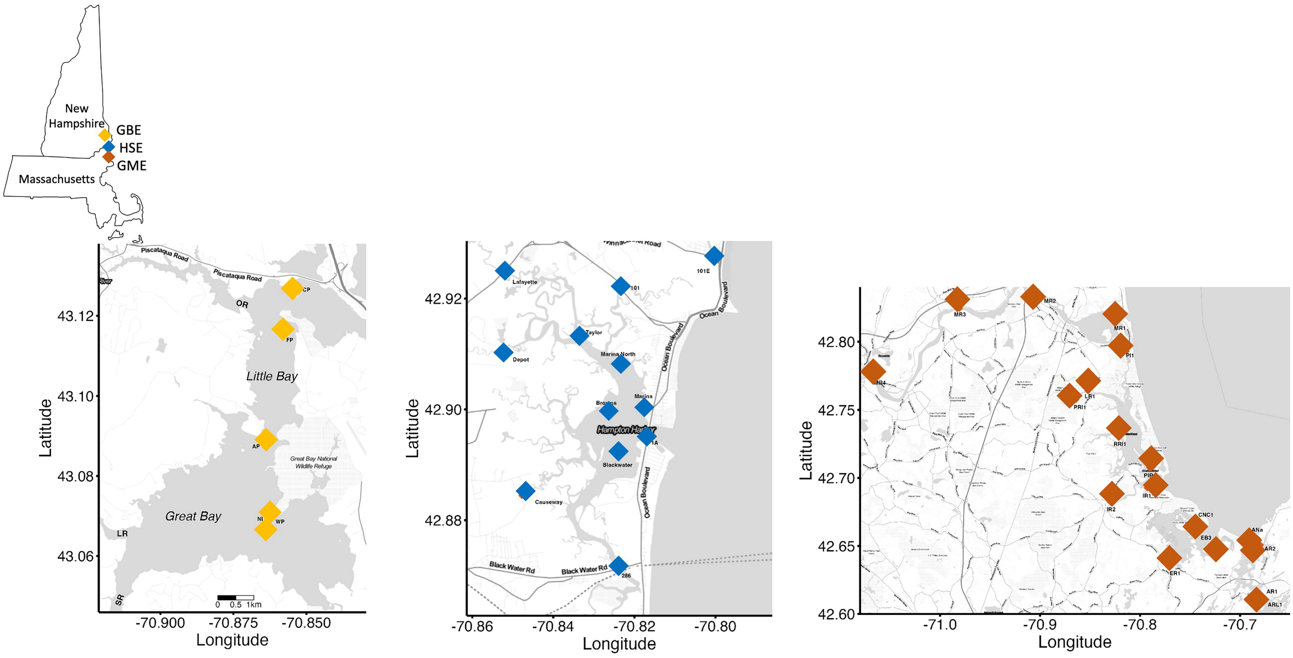

Figure 1. Map of New England (top left) and individual maps of estuarine sites where samples were analyzed for microplastics between 2018-2023. (A) GBE, New Hampshire; (B) HSE, New Hampshire; (C) GME, Massachusetts. GBE: Great Bay Estuary; GME: Great Marsh Estuary; HSE: Hampton-Seabrook Estuary.

ecological and economic resources on the Eastern Seaboard thanks to unparalleled conservation actions and coordination of multiple regional organizations and agencies.

Multiple sites and sampling approaches within three New England regions were accessed to assemble a regional summary of MP in the geography provided herein [Table 1]. Although each of these studies is reported here, it should be noted that these efforts were not necessarily coordinated efforts; thus there are differences in methodology and approach. Nevertheless, all resulting data were analyzed using a uniform approach to create this summary regional report. In GBE and HSE, both in New Hampshire, water samples of different types (bulk and manta trawl) were collected. The GBE water column samples had been collected previously (2018-2022) for a multiyear survey of oyster larva abundance. Analysis of archived samples from a previous study of sediment size characteristics provided data for MP in GBE sediments[10]. Thus, sediment cores were collected only in HSE (at high and low marsh areas in 2021). There were no prior samples from GME, which is situated on the north shore of Massachusetts. At that site, only water samples were collected between 2021-2023 [Figure 1].

Field collections

Water sampling (GBE, HSE, and GME)

Water column samples from GBE were derived from samples archived from a prior study designed to document presence of oyster larvae. Previously preserved samples were derived from replicate horizontal tows using a 64 μm mesh net held at ~0.3 m below the surface, resulting in an average of 38 m^3 of water sampled per tow[45]. In a separate study area, surface water in HSE was sampled using both manta trawl with 330 μm mesh[46,47] and bulk sampling[47] whereas surface water sampling in GME employed only the 330 μm mesh manta trawl. At both HSE and GME, horizontal surface-water tows were performed resulting in an average of 166 m^3 of water sampled per tow. Tows in GBE were made at slack tide and sample collections were timed to be as unaffected as possible by rainfall. Tows in HSE and GME were collected on an outgoing tide and rainfall within 48 hours was noted. The collected material was preserved and stored in the dark

Table 1. Details of samples from three New England estuaries that were investigated for microplastic content

Sampling location	Sampling sites	Number of samples	Sampling period	Collection method	Flow rate ($m \cdot s^{-1}$)	Filter size cutoff
GBE water (Column)	7	179	Feb-Nov 2018-2022	Subsurface trawl	0.5-1.0	5 µm - 5 mm
HSE water (Surface)	12	72	Jul-Sep 2021	Bulk	N/A	5 µm - 5 mm
HSE water (Surface)	12	72	Jul-Sep 2021	Manta trawl	0.2 ± 0.01 (0.003-0.6)	5 µm - 5 mm
HSE intertidal sediment	9	18	Jul 2021	4 cm × 10 cm cores	N/A	1 µm - 5 mm
GME water (Surface)	17	42	May-Nov 2021-2023	Manta trawl	0.5 ± -0.04 (0.2-1.3)	5 µm - 5 mm

GBE: Great Bay Estuary; GME: Great Marsh Estuary; HSE: Hampton-Seabrook Estuary.

until processed for MP. Field blanks were integrated with sampling; one blank was collected for every six environmental samples[47-49]. Manta trawl blanks were taken by rinsing the outside of the clean net with 1 gallon of DI water and transferring liquid within the cod end into a glass jar[47].

Bulk water sampling (HSE)

Bulk samples were collected in tandem with all manta trawl samples at HSE. At each site, 1 L glass jars triple-rinsed with filtered H_2O were used to collect water samples by submerging the jar just below the surface, allowing it to fill, and capping it underwater. Field blanks were integrated into the sampling plan, with one blank taken for every six samples collected by pouring ~1 L of DI water into a glass jar in the field[47]. All blanks were taken at established sampling locations to best replicate actual sampling conditions[47-49]. To assess variability among samples, replicates also were collected in the field[50,51] immediately following the initial sample collection.

Sediment core sampling

A prior published study[10] provides MP data for GBE. To investigate the potential for differential deposition by habitat location, HSE sediments were sampled in both high and low marsh habitats. A piston coring device (4 cm diameter and 10 cm long) was used to collect sediments proximal to surface water sampling sites in HSE [Figure 1]. The top 10 cm of the core was used for MP determinations, representing approximately 35-40 years of sediment accretion based on regional accretion rate data[52]. Cores were held on ice for transportation to the laboratory[46] and stored at 40 °F until processed.

Laboratory analyses

Efforts completed across the three estuaries were disparate, and various approaches were used to minimize cross contamination in the field and lab. All studies included filtering all reagents (0.2 µm), triple-rinsing glassware with filtered diH_2O, performing manipulations under a fume hood, wearing cotton garb, and covering all containers with aluminum, glass, or paper lids whenever possible. Given that this report synthesizes data from a number of discrete studies that were not uniform in design or goals, the individual methods applied in each case follow.

Water column MP (GBE)

Preserved material from water column tows was thoroughly mixed and 3-5 µm filtered (47 mm PTFE; Sigma-Aldrich, USA) in a glass funnel system. Biofilms and organic matter were removed by stoppering the funnel and adding a 1:1 mixture of KOH (30%) with NaClO (14%, Alfa Aesar) to the filter and holding at 60 °C for 24 h to digest biogenic matter[53]. The digest was vacuum filtered followed by one rinse with filtered diH_2O and one subsequent rinse with filtered 50% methanol. After plugging the filter again, 2 mL of Nile Red Working Solution (10 μg·mL^{-1} in n-hexane[54-56]) was added and allowed to incubate in the dark at 25 °C for 30 min. Following incubation, the filter was washed with 50% methanol then dried at 60 °C and kept sandwiched between two large glass slides (Home Science Tools, USA) and allowed to dry in darkness until subsequent analysis[57].

Microplastic particle counts were estimated initially using a fluorescent staining and automated imaging approach. Confocal microscopy was performed by scanning filters (or portions thereof) using excitation: 487 nm and emission: 525 nm for Nile Red and (only for the HSE samples - see below) excitation: 409 and emission: 450 nm for DAPI using a Nikon A1R HD according to standard methods described by[10,49,54,56,58]. Depending on the number of particles, either whole, half, or one-quarter of each filter was scanned and the images stitched together to create a composite. Automated image analysis of the full scan was accomplished using the NIS-Elements program (Nikon Instruments Inc., USA).

Following confocal analysis, filters from representative samples (samples across years, sites, and with both high and low MP counts) were handled according to the manufacturer's recommendation to remove MP and analyze them by LDIR. The prior filters were placed in a glass beaker with 2 mL of 70% ethanol and stirred for 15 min to release MP particles into solution. The solution containing MP was introduced into Fastwells™ reagent barrier (Grace Bio-labs, Bend, Oregon, USA) attached to a Kevley MirrIR™ slide (Kevley Technology, Chesterfield, Ohio, USA), covered with a petri dish, and allowed to dry completely. Prepared slides were marked with a black marker along the horizontal edge to improve sample flatness detection prior to automated infrared analysis of count, size, shape, and elemental composition using the Agilent 8700 LDIR[59,60] and the supplied Microplastics Starter spectral library[61] using Clarify™ software. The library contained a default set of > 50 polymer IR spectra plus spectra of biogenic particles such as coal, chitin, and rubber, and spectra of other particle types that might typically be present in an environmental sample, e.g., silica. Counts of MP in these paired samples were analyzed to determine concurrence of the two methods.

Surface water and bulk sample MP (HSE and GME)

Manta trawl samples were wet sieved through stacked 5 and 0.3 (GME) or 0.1 mm (HSE) stainless-steel mesh sieves using diH_2O. Particles remaining on the 5 mm sieve were discarded. Solids collected on the smallest sieve were transferred to a pre-weighed clean glass beaker, covered with aluminum foil, and placed in a drying oven set to 60 °C until completely dry. Due to high amounts of organic matter, samples with more than 15% settled visual organic matter were sub-sampled prior to sieving. Once dry, organic material was eliminated using 30% hydrogen peroxide (30% H_2O_2, LabChem, USA) at 60 °C[46]. Following digestion, samples with sand or sediment were density separated using a $ZnCl_2$ solution (1.5 g·cm^{-1}; Fisher Scientific, USA)[62]. Following digestion and density separation, the remaining sample was vacuum filtered onto 5 μm PTFE filters. GME samples were visually assessed using light microscopy while HSE samples were stained for confocal microscopy. Bulk surface-water samples were immediately filtered onto 5 μm PTFE filters and peroxide digested (*op. cit.*). Subsampling and density separation was not performed for bulk grabs as sand and sediment levels did not require this step.

Samples from HSE were subjected to confocal imaging following the same Nile Red staining process described for GBE, after which MP in surface water and bulk samples were immediately incubated with DAPI (1 mg·mL^{-1}, Sigma-Aldrich, USA)[63] for another 30 min in the dark to counter-stain. This procedure identified putative MP as those reflecting strongly for Nile Red (mean reflectance < 850 nm) but not reflecting strongly for DAPI (max reflectance < 170 nm). Identified particles were counted, measured, and reflectance noted. Samples representing sites and MP count ranges were selected and processed for LDIR analysis as described for the GBE water samples. The LDIR spectra were compared to a library containing 8 different polymer spectra. Samples from GME were analyzed using light microscopy only to identify MP by type and color, and were not subject to confocal or LDIR analysis.

Sediment core processing

Sediment cores were separated into 2 cm segments, dried, homogenized[10], and 1 μm sieved using filtered diH_2O. Filtrates were again dried, digested over two days using wet peroxide at 60 °C[46], and vacuum filtered onto a 5 μm PTFE filter, after which particles were manually identified using light microscopy. Samples containing a large amount of material following digestion were density separated using 25 mL of $ZnCl_2$ solution ($1.5\ g{\cdot}cm^{-1}$; Fisher Scientific, USA)[62]. Floating solids were collected by vacuum filtration onto a 5 μm PTFE filter. MP in this fraction also were identified by type and color using light microscopy, and were not subject to confocal or LDIR analysis.

Statistical treatments

Normal distribution of data was tested by Shapiro-Wilk normality test. Kruskal-Wallis test was performed to investigate ambient MP concentration in all sample types and the P-values were adjusted by Bonferroni correction. Data derived from confocal and LDIR analyses were compared using paired two-sample *t*-test for means. All tests were performed in R.

RESULTS

Across the 179 GBE water column samples analyzed, the range of numbers of MP detected was 0.08-4,528 MP particles m^{-3}, with a mean of 467 ± 811 (median 115) MP particles m^{-3}. Significant variation was observed across GBE sites ($\chi^2 = 15.2$, 6 df, $P = 0.002$), despite the fact that the estuary is uncharacteristically well-mixed[44,64] [Figure 2]. In GBE, where the same sampling procedure was used every year, there was significant variation in MP counts across the 5 years ($P < 0.0001$) [Figure 2]. Within years, because of high levels of variation, there were few significant differences in temporal (monthly) or spatial MP counts in GBE [Figure 3]. The majority of particles observed in GBE were very small, < 100 μm and fairly tightly focused around 50 μm. Elemental morphology of MP in the water column was highly variable where some samples contained only a few polymer types and others had complex mixtures of low and high density (ranging the gamut from PP to PVC), copolymers, and biogenic particles (especially cellulose, chitin, coal, and rubber) [Figure 4]. The size distributions (roughly 50 μm) and polymer variation (variable but often with more high density MP) of GBE water column MP were similar to the distributions observed in GBE sediments[10], an observation that was expected as MP and sediments co-transport[43]. Of recent particular interest is the occurrence of rubber particles (a.k.a. Tire Wear Particles, TWP) that have been identified in areas near urban runoff[65]. Rubber was detected in all GBE samples (ranging from 1%-28% of particles). This proportion is similar to that observed (15%-38% of all "MP" particles) in Guanabara Bay Brazil bottom sediments[65].

Across the 14 manta water samples from HSE, the range of MP counts was 0.45-30 MP particles m^{-3}, with a mean of 11 ± 9 (median 8) MP particles m^{-3}. For the 72 bulk water samples from HSE, the range of numbers of MP detected was 0-143,763 MP particles m^{-3}, with a mean of 27,690 ± 29,860 (median 10,927) MP particles m^{-3}. As observed in GBE, the majority of particles observed in HSE waters were very small, around 50 μm [Figure 5]. Elemental morphology of MP in these water samples also was highly variable generally showing representatives of at least eight polymer types. Bulk grabs in HSE contained significantly more MP per volume than those collected with a manta trawl net. Similar findings have been noted across a range of MP studies comparing discrete grabs with manta trawls[47,66-69]. This outcome can be explained by differences in methodology; 300 mm trawl mesh captures only a subset of MP present, whereas bulk grabs of water

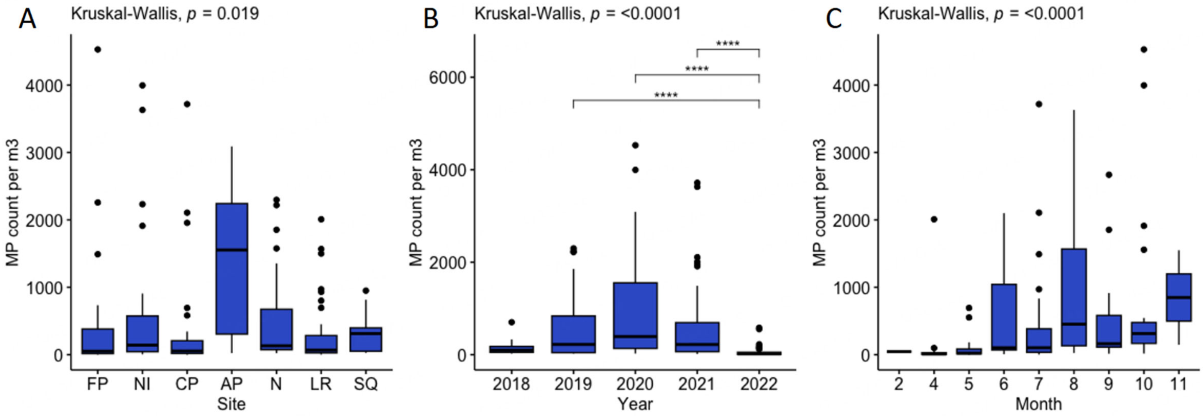

Figure 2. Overall variability in MP counts in water column samples from Great Bay Estuary shown by (A) location sampled; (B) year sampled; and (C) month. Significance level indicated by "*". MP: Microplastics.

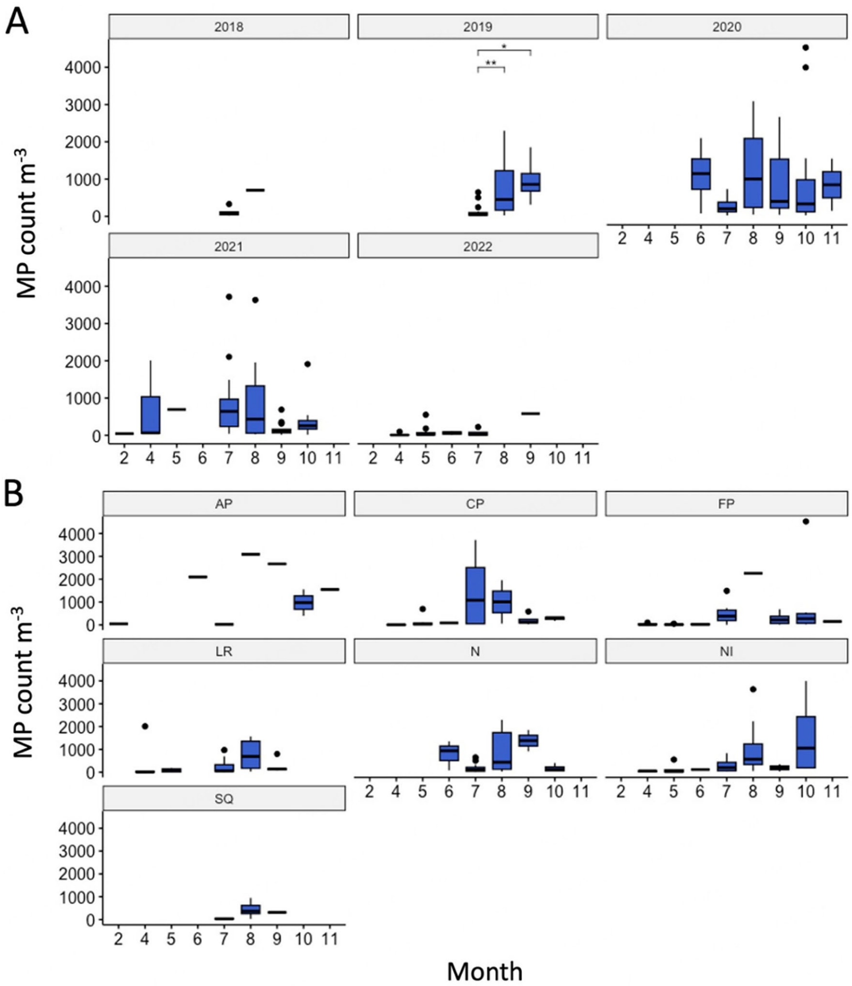

Figure 3. (A) Temporal and (B) spatial variation in MP counts from water column samples collected in GBE. Significance level indicated by "*". GBE: Great Bay Estuary; MP: microplastics.

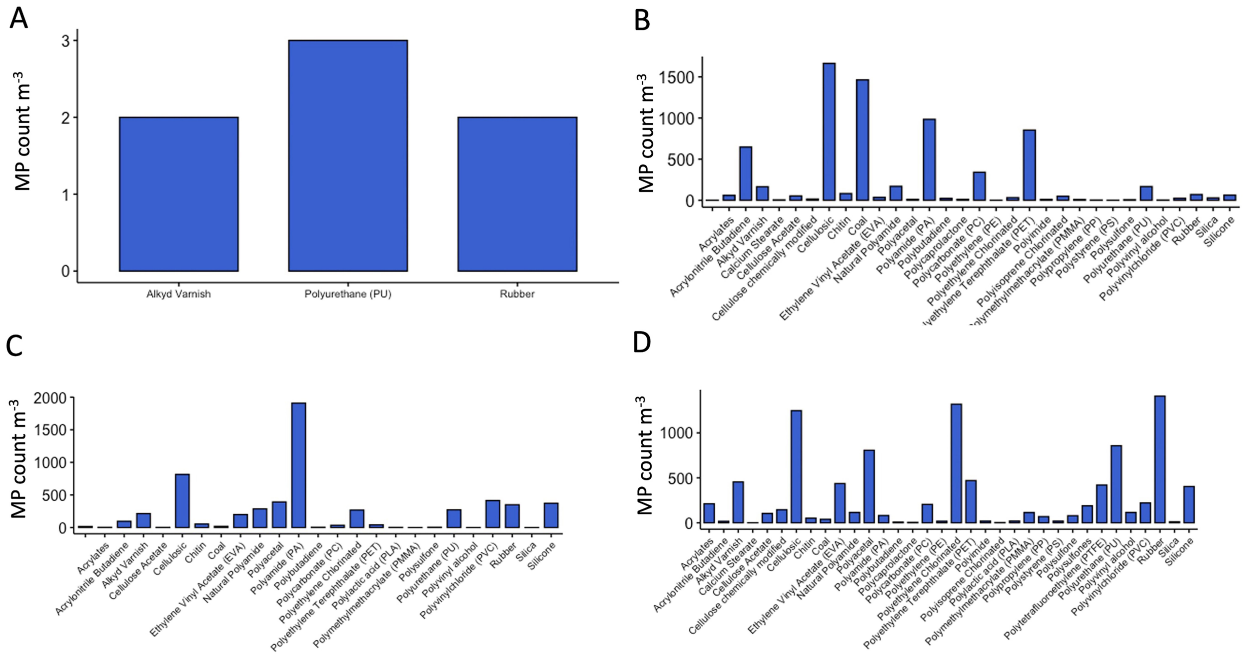

Figure 4. Spectrally determined (LDIR) elemental composition of MP detected in representative water samples from Great Bay Estuary. Panels show data for (A) Nannie Island August 2020; (B) Nannie Island April 2021; (C) Oyster River July 2020; and (D) Adams Point October 2020. LDIR: Laser direct infrared spectrometry; MP: microplastics.

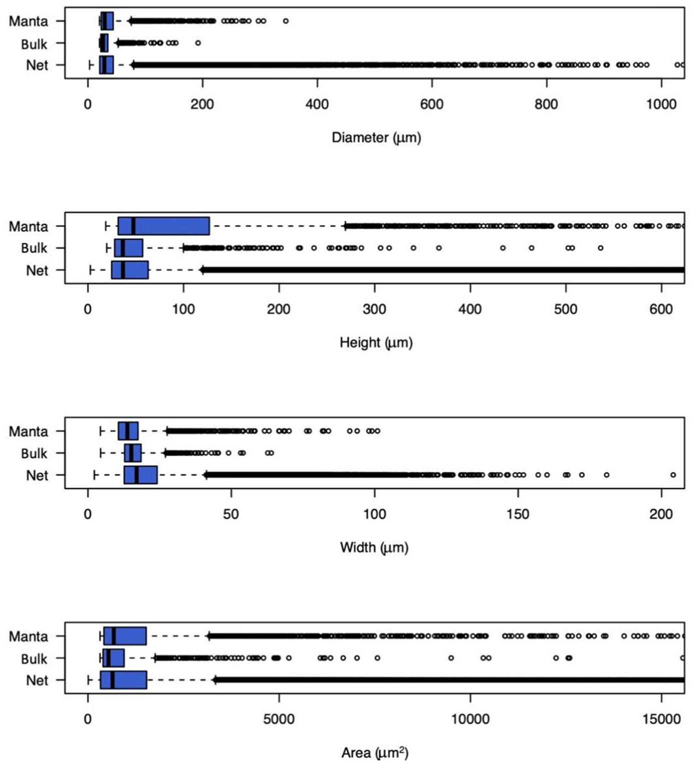

Figure 5. Physical parameters of MP collected in different estuarine water systems of New England using three types of water samplers, all estimated using a confocal microscopic analysis. Manta and bulk sample types were from Hampton-Seabrook Estuary only. Net samples were from Great Bay Estuary. MP: Microplastics.

capture the full size-range of MP[47,70]. When comparing particle abundance derived from nets only (manta trawl in HSE versus plankton net in GBE), far fewer MP were observed in HSE than in GBE waters, very nearly 1,000× fewer particles. Those differences were most likely due to the hydrology of HSE, which has greater ocean influence and flow in/out. It also is possible that differences in particle density could account for lower MP abundance in the HSE surface sampling approach (top 0-0.2 m of the water column), *vs.* the slightly deeper water column GBE sampling (~0.3 m below the surface). Minor differences could be due to differences in spectral libraries used for LDIR, with the library used for the HSE samples having a smaller number of polymer types (8 *vs.* > 50 used for the GBE samples). The GME water samples, being analyzed only via light microscopy, yielded many fewer MP than the samples from other studies that were subjected to confocal fluorescent analysis. Across the 42 GME surface water trawl samples, the range of MP detected was 0.05-5 MP particles m^{-3}, with a mean of 1 ± 0.2 (median 0.6) MP particles m^{-3}. Significant variation was observed across GME sites ($P = 0.002$).

The numbers of MP vary considerably among each of these New England habitats. This is not surprising given the differences in methodologies, hydrology, and particular geographies[71]. The MP counts also are well-within the ranges reported for many other estuaries around the globe [Table 2].

As the study of MP progresses and expands, so do the methods utilized. The fortunate application of both confocal and LDIR analysis for many of the samples accessed in this survey provided for comparison of MP counts derived from both methodologies at two sites and using three sampling methods. In every case, LDIR microscopy yielded more particles than was obtained by confocal microscopy. For samples collected with plankton nets, MP were underestimated by a factor 5× when analyzed by confocal. For bulk samples, MP were undercounted by confocal microscopy by a factor of 6×. Samples collected by manta trawl were undercounted by a factor of 10×.

Across the eight salt marsh locations tested for MP sequestration, there were significant differences in the counts of MP·kg^{-1} ($\chi^2 = 6.8$, df = 7, $P = 3 \times 10^{-6}$). The majority of MP (60%-70%) found in HSE sediments were in the top 4 cm [low marsh (19,800 ± 6,900 kg^{-1}), high marsh (13,900 ± 2,800 kg^{-1})]. More MP particles were found in HSE low marsh sediment samples (16,400 ± 3,900 kg^{-1} dry weight) than were found in high marsh samples (10,600 ± 1,500 kg^{-1}), which floods less frequently than the low marsh on a lunar tidal cycle. The difference translated to 60%-70% more MP particles, but due to high variation among samples this difference was not significant ($P = 0.45$) [Figure 6]. The absolute numbers of MP detected in HSE marsh sediments were within the typical ranges of many other estuarine MP burdens [Table 3] and were an order of magnitude less than the numbers of MP found in GBE sediments[10].

DISCUSSION

Use of fluorescent staining is popular for MP studies because it is inexpensive and can be accomplished with less sophisticated microscopes. This study illustrates the ease with which hundreds of samples can be analyzed by that method but by no means is an endorsement of one approach over another. A caveat is that the numbers of particles can be greatly underestimated by staining for reasons that are well-documented, namely variations in handling (time and temperature of incubation with the stain[84]) and also the lower staining intensity of many polymers. Infrared spectral analysis of representative samples that previously were analyzed with Nile Red confocal fluorescence analysis provided a precise and accurate means to confirm size and shape analyses from the less stringent procedure and provided estimates of the proportional elemental composition of MP from waters and sediments.

Table 2. Microplastic counts in selected estuaries

Sediment location	MP count (max particles m^{-3})	Ref.
Hampton-Seabrook Estuary (USA)	143,763	This study
Great Bay Estuary (USA)	4,528	This study
Great Marsh Estuary (USA)	5	This study
Chesapeake Bay (USA)	0.2	Bikker *et al*. 2020[72]
Delaware Bay (USA)	1	Cohen *et al*. 2019[73]
Estuary (India)	752	Suresh *et al*. 2020[74]
Estuary (China)	4,137	Zhao *et al*. 2014[75]
Estuary (Australia)	172	Hitchcock *et al*. 2019[76]
Estuary (Mauritius)	412,000	Ragoobur *et al*. 2023[77]

MP: Microplastics.

Table 3. Selected studies of microplastic counts in some coastal sediments

Sediment location	MP count (max particles kg^{-1})	Ref.
Hampton-Seabrook Estuary (USA)	20,000	This study
Great Bay Estuary (USA)	675,000	Cheng *et al*. 2021[10]
Narragansett Bay (USA)	13,000	Fulfer and Walsh 2023[78]
Tampa Bay (USA)	290	McEachern *et al*. 2019[66]
Coastal (Belgium)	213	Claessens *et al*. 2011[79]
Estuary (China)	340	Peng *et al*. 2017[1]
Salt marsh (Portugal)	23	Cozzolino *et al*. 2020[80]
Mangrove (Singapore)	63	Nor *et al*. 2014[81]
Lagoon (Italy)	2,175	Vianello *et al*. 2013[82]
Estuary (Mauritius)	135	Ragoobur *et al*. 2023[77]
Beach (Germany)	62,100	Liebezeit *et al* 2012[83]

MP: Microplastics.

Many of the data recounted here were made possible because samples for other (non-MP) studies were archived long ago and still were available. Because the studies took place over multiple years and by investigators in different laboratories, there was variation in the methodologies used to assess MP. Many water samples were collected using a plankton net whereas some other samples were collected using a manta trawl, also constructed of gradient mesh material. It is important to note that net sampling in estuarine waters is nearly always affected to some degree by the ambient levels of organic material, which can vary rapidly and greatly. Mesh can clog with phytoplankton chains, resuspended sediments, and gelatinous creatures such as ctenophonres, cnidaria, and organic debris (i.e., plant material and wrack, especially in estuarine waters). When nets become clogged, particles smaller than the actual mesh size are entrained and maintained in samples. For this reason, grab samples also were utilized in the recent HSE sampling. Furthermore, the increasing accessibility of high-throughput infrared analysis allowed improvement over time in the analysis of plastic type. This allowed the finding that although confocal analysis of Nile Red stained particles is a reasonable method to begin a survey, the LDIR is consistently a more valuable method because it identifies particles that are not effectively stained and the LDIR provides a definitive morphology. In the future, as sampling continues to evolve with apparatus such as the MuMi[85], more precise data can be obtained. Despite the limitations of net mesh sampling, this set of studies provides a remarkably consistent baseline for the presence and types of MP in these New England estuaries.

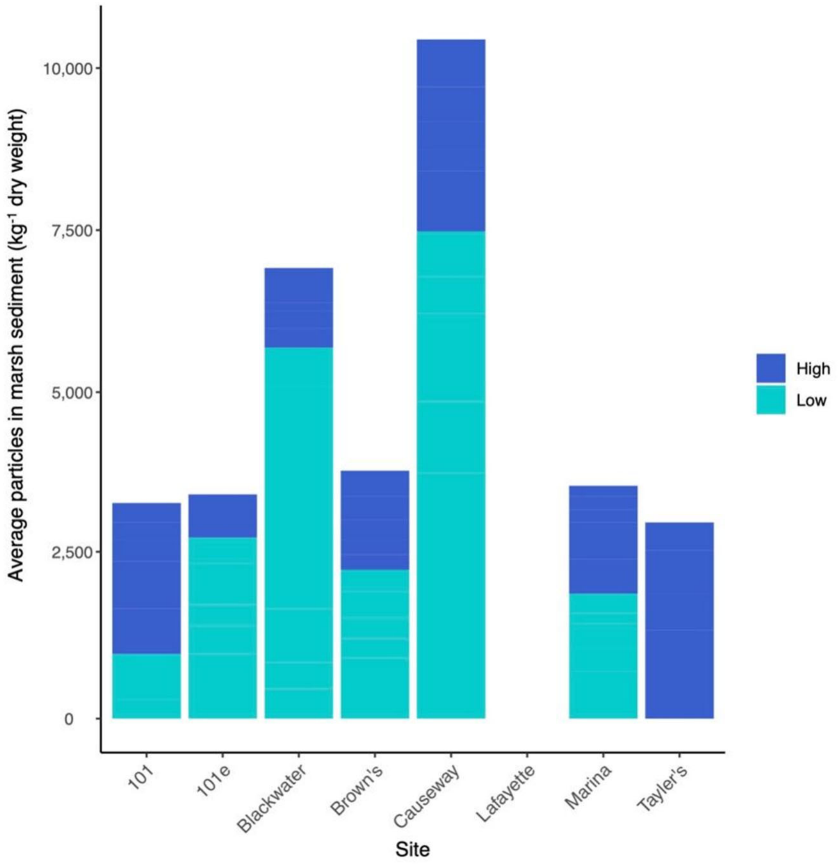

Figure 6. MP found at eight locations in coastal marsh sediments of Hampton-Seabrook Estuary, each subsampled at high and low marsh elevations. MP: Microplastics.

There are a variety of environmental and anthropogenic factors that may influence how MP enter, circulate, and alternatively are sequestered or exit an estuarine system. Variation in watershed size, number of tributaries, water depth, geomorphology, hydrology and tidal energy, and presence intertidal and subtidal coastal habitats can influence MP presence, as can human population densities, amounts and proximity of impervious surface, and the abundance of associated infrastructure. Precipitation events have been tied to increased surface-water MP abundance[86-88], with higher numbers in nearshore waters compared to offshore waters likely due to land-based runoff[87]. Tides have also been found to impact the distribution of MP, with greater amounts of plastic litter found on the outgoing tidal phase[89] and larger MP particles correlated to the spring and flood tidal cycle[90]. Coastal flooding may have a similar impact as precipitation on transporting land-based MP into estuarine environments[86-88]. With increasing storm events and associated surge, flooding events may resuspend and force stranded near-shore marine MP deeper into the estuary[91].

GBE is surrounded by rural, agricultural, and forested areas and is fed by seven tributaries that typically are low-discharge providing limited freshwater[44]. GBE is unique from other estuaries in that it is well-mixed due to strong currents that introduce oceanic water into the Bay, but flushing rates and residence times are slower/longer than HSE and GME. Although the extent to which the tributaries are the primary source of MPs in GBE is unclear, water resource recovery facilities from more than 50 rural communities in New Hampshire and Maine discharge into GBE. Thus, the MP and other point and non-point source pollutants may be higher in GBE. Despite being well-mixed overall, most of the stations in GBE that were sampled are a considerable distance from the estuary's outlet at the mouth of the Piscataqua River. Various authors suggest the flushing time for Great Bay is between 2 and 30 days[64,92,93], depending on the tide and river discharge states involved. The most recent estimate of residence time for Great Bay is between 5 and 20 days[92] which is a more appropriate metric for particles moving through a system. Note that residence time does not account for whether such particles re-enter the system[94].

To our knowledge, quantitative estimates of flushing time have not been published for the HSE, nor were any calculated estimates found in grey literature. However, recognizing that 88% of the water in the estuary is exchanged on each tide and 6% of the ebb tide plume returns to the estuary on the next tidal cycle based on estimates from Public Systems of New Hampshire[95], the flushing time is estimated to be less than one day[96], which is considerably faster than GBE. Although there are no published residence time estimates for HSE and GME, both estuaries have a more direct connection to coastal waters and have higher flushing rates despite the considerable watershed areas and associated population densities. GBE is the smallest of the three estuarine systems studied here at an estimated area of 200 ha with relatively low population density, yet it had orders of magnitude greater MP per unit volume than the significantly larger HSE (5,300 ha) or GME (~10,000 ha) systems.

The uniquely different geomorphology of GBE as a post-glacial drowned river valley landform may play an important role. GBE lacks the extent of broad fringing salt marsh that buffer the waterways in HSE and GME. Unlike the shallow barrier-beach systems of HSE and GME that are flanked by hundreds of hectares of salt marsh[97,98], terrestrial runoff may be washing directly into the waters of GBE with little to no natural filtration through high and low marsh habitats along much of its extent. The salt marshes in GBE are limited to relatively small, narrow and disparate patches that do not extend far seaward from upland shores and many are struggling to keep pace with sea level rise[99]. As a result, GBE is expected to have far less capacity to eliminate MP through sequestration in vegetated wetlands given significantly less acreage of fringing saltmarsh and riparian buffer zones than the barrier beach marsh complexes of HSE and GME. In fact, the high levels of MP in GBE waters have little destiny other than to settle. This corroborates the higher sediment levels of MP in GBE[10] than in GME (current data).

The HSE sediment MP were dramatically lower than found for GBE sediments[10]. Although higher MP concentrations have been correlated with population density[86,100], their presence also can be influenced by point sources such as water resource recovery facilities[101,102]. These facilities are located on two of the seven tributaries to GBE, just upstream of several sampling areas. It is possible that these potential MP point sources, coupled with slower (and lower) tidal flushing rates and diminished ability to sequester MP in fringing salt marsh sediments, could be collectively contributing to the greater abundance of MP in GBE waters as compared to HSE and GME. Similarly, the greater MP in GBE subtidal sediment (100 ± 50 particles g^{-1})[10] as compared to HSE intertidal marsh peat cores (2.3 ± 0.3 particles g^{-1}) may be attributed to lower flush rates and longer residence times allowing denser MP to settle. Together, the detection and comparisons of MP in these New England estuarine waters and sediments illustrate that baseline MP will vary based on anthropogenic impacts (e.g., water treatment methods), hydrology (e.g., estuary type and circulation), and habitat type (e.g., subtidal mudflats *vs*. intertidal salt marshes).

CONCLUSIONS

This work illustrates that the occurrence and fate of MP in the New England estuarine habitats studied vary widely and are generally comparable to the broad ranges of MP identified by other published studies of estuarine waters and sediments. These water and intertidal sediment data complement the only other published study on MP in this geographic area, a study of MP in bottom sediments of GBE[10]. The data are essential to populate new hydrological models that are expected to help trace the sources of MP and other pollutants in GBE. The results provided here are of immediate importance and value to resource users, harvesters, aquaculturists, and managers to inform and evaluate contaminant risks, to choose low MP sites for their activities, and provide information on the time of year with the highest or lowest MP concentrations.

DECLARATIONS

Acknowledgments

Thanks are due to other members of the Brown Lab Team: Kelsey Meyer, Alyssa Stasse, Emily Williams, Kennedy McGrath, and Grant Milne for helping to collect, preserve, and analyze samples. Alyssa Stasse created the maps. Thanks are also due to members of the Moore Lab Team: Kayla Tozier, Grant McKown, Creightanya Brewley, and Emily Dutton who helped collect field samples in HSE. Peter Phippen and Geoff Walker collected GME trawl samples. Kariana Ebel assisted in sample processing. David Shay provided assistance with vessels, nets, and flow meter calibration. Krystin Ward allowed access to one of the sites.

Authors' contributions

Conceptualization: Brown B, Moore G
Methodology: Brown B, Mogensen H, Sims-Harper T, Gibson J, Jarrett G, Wardinski C
Data analysis: Lee BY, Brown B, Mogensen H, Gibson J
Investigation: Sims-Harper T, Brown B, Jarrett G, Wardinski C
Original manuscript preparation: Brown B, Moore G, Gibson J
Authors have read and agreed to the submitted version of the manuscript.

Availability of data and materials

Not applicable.

Financial support and sponsorship

UNH School of Marine Sciences and Ocean Engineering provided fellowship funding to Sims-Harper T and Mogensen H. The College of Life Sciences and Agriculture and NHAES Hatch 1023564 (nh00697) provided funding to Brown B. New Hampshire Sea Grant research project R/RCE-3, pursuant to National Oceanic and Atmospheric Administration Award No. NA18OAR4170090, and The Merrimack Valley Planning Commission provided funding to Moore G.

Conflicts of interest

All authors declared that there are no conflicts of interest.

Ethical approval and consent to participate

Not applicable.

Consent for publication

Not applicable.

Copyright

REFERENCES

1. Peng J, Wang J, Cai L. Current understanding of microplastics in the environment: occurrence, fate, risks, and what we should do. *Integr Environ Assess Manag* 2017;13:476-82. DOI PubMed
2. Carpenter EJ, Smith KL Jr. Plastics on the Sargasso sea surface. *Science* 1972;175:1240-1. DOI PubMed

3. Carpenter EJ, Anderson SJ, Harvey GR, Miklas HP, Peck BB. Polystyrene spherules in coastal waters. *Science* 1972;178:749-50. DOI PubMed
4. Gregory MR. Accumulation and distribution of virgin plastic granules on New Zealand beaches. *N Z J Mar Freshwater Res* 1978;12:399-414. DOI
5. Gregory MR. Virgin plastic granules on some beaches of Eastern Canada and Bermuda. *Mar Environ Res* 1983;10:73-92. DOI
6. Winston JE. Drift plastic - an expanding niche for a marine invertebrate? *Mar Pollut Bull* 1982;13:348-51. DOI
7. Cheng L. Marine insects. 1976. Available from: https://escholarship.org/uc/item/1pm1485b. [Last accessed on 29 Nov 2023].
8. Barboza LGA, Dick Vethaak A, Lavorante BRBO, Lundebye AK, Guilhermino L. Marine microplastic debris: an emerging issue for food security, food safety and human health. *Mar Pollut Bull* 2018;133:336-48. DOI PubMed
9. Dodhia MS, Rogers KL, Fernández-juárez V, et al. Microbe-mineral interactions in the Plastisphere: coastal biogeochemistry and consequences for degradation of plastics. *Front Mar Sci* 2023;10:1134815. DOI
10. Cheng MLH, Lippmann TC, Dijkstra JA, et al. A baseline for microplastic particle occurrence and distribution in Great Bay Estuary. *Mar Pollut Bull* 2021;170:112653. DOI
11. Seeley ME, Song B, Passie R, Hale RC. Microplastics affect sedimentary microbial communities and nitrogen cycling. *Nat Commun* 2020;11:2372. DOI PubMed PMC
12. Li J, Huang W, Xu Y, Jin A, Zhang D, Zhang C. Microplastics in sediment cores as indicators of temporal trends in microplastic pollution in Andong salt marsh, Hangzhou Bay, China. *Reg Stud Mar Scie* 2020;35:101149. DOI
13. Lloret J, Pedrosa-Pamies R, Vandal N, et al. Salt marsh sediment act as sinks for microplastics and reveal effects of current and historical land use changes. *Environ Adv* 2021;4:100060. DOI
14. Carson HS, Nerheim MS, Carroll KA, Eriksen M. The plastic-associated microorganisms of the North Pacific Gyre. *Mar Pollut Bull* 2013;75:126-32. DOI PubMed
15. Jokiel PL. Long-distance dispersal by rafting: reemergence of an old hypothesis. *Endeavour* 1990;14:66-73. DOI
16. Barnes DK. Biodiversity: invasions by marine life on plastic debris. *Nature* 2002;416:808-9. DOI PubMed
17. Zettler ER, Mincer TJ, Amaral-Zettler LA. Life in the “plastisphere”: microbial communities on plastic marine debris. *Environ Sci Technol* 2013;47:7137-46. DOI PubMed
18. Barnes D, Fraser K. Rafting by five phyla on man-made flotsam in the Southern Ocean. *Mar Ecol Prog Ser* 2003;262:289-91. DOI
19. Barnes DK. Natural and plastic flotsam stranding in the Indian Ocean. In: Davenport J, Davenport JL, editors. The effects of human transport on ecosystems: cars and planes, boats and trains. Dublin: Royal Irish Academy; 2004. p. 193-205. Available from: https://nora.nerc.ac.uk/id/eprint/16343/. [Last accessed on 29 Nov 2023].
20. Masó M, Garcés E, Pagès F, Camp J. Drifting plastic debris as a potential vector for dispersing Harmful Algal Bloom (HAB) species. *Sci Mar* 2003;67:107-11. DOI
21. Reisser J, Shaw J, Hallegraeff G, et al. Millimeter-sized marine plastics: a new pelagic habitat for microorganisms and invertebrates. *PLoS One* 2014;9:e100289. DOI PubMed PMC
22. Thompson RC, Olsen Y, Mitchell RP, et al. Lost at sea: where is all the plastic? *Science* 2004;304:838. DOI
23. Plastic rafting: the invasive species hitching, a ride on ocean litter. Available from: https://www.theguardian.com/environment/2021/jun/14/plastic-rafting-the-invasive-species-hitching-a-ride-on-ocean-litter. [Last accessed on 29 Nov 2023].
24. McCormick A, Hoellein TJ, Mason SA, Schluep J, Kelly JJ. Microplastic is an abundant and distinct microbial habitat in an urban river. *Environ Sci Technol* 2014;48:11863-71. DOI
25. Urbanek AK, Rymowicz W, Mirończuk AM. Degradation of plastics and plastic-degrading bacteria in cold marine habitats. *Appl Microbiol Biotechnol* 2018;102:7669-78. DOI PubMed PMC
26. Rogers KL, Carreres-calabuig JA, Gorokhova E, Posth NR. Micro-by-micro interactions: how microorganisms influence the fate of marine microplastics. *Limnol Oceanogr Lett* 2020;5:18-36. DOI
27. Gregory MR. Environmental implications of plastic debris in marine settings--entanglement, ingestion, smothering, hangers-on, hitch-hiking and alien invasions. *Philos Trans R Soc Lond B Biol Sci* 2009;364:2013-25. DOI PubMed PMC
28. Browne MA, Dissanayake A, Galloway TS, Lowe DM, Thompson RC. Ingested microscopic plastic translocates to the circulatory system of the mussel, *mytilus edulis* (L.). *Environ Sci Technol* 2008;42:5026-31. DOI PubMed
29. Cole M, Lindeque P, Fileman E, Halsband C, Galloway TS. The impact of polystyrene microplastics on feeding, function and fecundity in the marine copepod *calanus helgolandicus*. *Environ Sci Technol* 2015;49:1130-7. DOI PubMed
30. Al-Sid-Cheikh M, Rowland SJ, Stevenson K, Rouleau C, Henry TB, Thompson RC. Uptake, whole-body distribution, and depuration of nanoplastics by the scallop pecten maximus at environmentally realistic concentrations. *Environ Sci Technol* 2018;52:14480-6. DOI PubMed
31. Watts AJ, Lewis C, Goodhead RM, et al. Uptake and retention of microplastics by the shore crab *carcinus maenas*. *Environ Sci Technol* 2014;48:8823-30. DOI PubMed
32. Farthing J, Laing I, Dore WJ. Depuration conditions for great scallops (Pecten maximus). *J Shellfish Res* 2003;22:409-14. Available from: https://api.semanticscholar.org/CorpusID:82533626. [Last accessed on 29 Nov 2023]
33. Canniff PM, Hoang TC. Microplastic ingestion by Daphnia magna and its enhancement on algal growth. *Sci Total Environ* 2018;633:500-7. DOI PubMed
34. Sussarellu R, Suquet M, Thomas Y, et al. Oyster reproduction is affected by exposure to polystyrene microplastics. *Proc Natl Acad Sci U S A* 2016;113:2430-5. DOI PubMed PMC

35. Markham E, Brault EK, Khairy M, et al. Time trends of polybrominated diphenyl ethers (PBDEs) in Antarctic biota. *ACS Omega* 2018;3:6595-604. DOI PubMed PMC
36. Dawson AL, Kawaguchi S, King CK, et al. Turning microplastics into nanoplastics through digestive fragmentation by Antarctic krill. *Nat Commun* 2018;9:1001. DOI PubMed PMC
37. Suckling CC. Responses to environmentally relevant microplastics are species-specific with dietary habit as a potential sensitivity indicator. *Sci Total Environ* 2021;751:142341. DOI PubMed
38. Biamis C, Driscoll KO, Hardiman G. Microplastic toxicity: a review of the role of marine sentinel species in assessing the environmental and public health impacts. *Case Stud Chem Environ Eng* 2021;3:100073. DOI
39. Smith M, Love DC, Rochman CM, Neff RA. Microplastics in seafood and the implications for human health. *Curr Environ Health Rep* 2018;5:375-86. DOI PubMed PMC
40. Dehaut A, Cassone AL, Frère L, et al. Microplastics in seafood: benchmark protocol for their extraction and characterization. *Environ Pollut* 2016;215:223-33. DOI
41. Rochman CM, Tahir A, Williams SL, et al. Anthropogenic debris in seafood: Plastic debris and fibers from textiles in fish and bivalves sold for human consumption. *Sci Rep* 2015;5:14340. DOI PubMed PMC
42. Kroon FJ, Motti CE, Jensen LH, Berry KLE. Classification of marine microdebris: a review and case study on fish from the Great Barrier Reef, Australia. *Sci Rep* 2018;8:16422. DOI PubMed PMC
43. Laursen SN, Fruergaard M, Dodhia MS, et al. Settling of buoyant microplastic in estuaries: the importance of flocculation. *Sci Total Environ* 2023;886:163976. DOI
44. Short FT. The ecology of the Great Bay Estuary, New Hampshire and Maine: an estuarine profile and bibliography. PREP Reports & Publications; 1992. p. 222. Available from: https://scholars.unh.edu/prep/376/. [Last accessed on 29 Nov 2023].
45. Stasse A, MLH Cheng, K Meyer, et al. Temporal dynamics of eastern oyster, larval abundance in Great Bay Estuary, New Hampshire. *J Shellfish Res* 2022;40:471-8. DOI
46. Masura J, Baker J, Foster G, Arthur C. Laboratory methods for the analysis of microplastics in the marine environment: recommendations for quantifying synthetic particles in waters and sediments. Available from: https://repository.oceanbestpractices.org/handle/11329/1076. [Last accessed on 29 Nov 2023].
47. Hung C, Klasios N, Zhu X, Sedlak M, Sutton R, Rochman CM. Methods matter: methods for sampling microplastic and other anthropogenic particles and their implications for monitoring and ecological risk assessment. *Integr Environ Assess Manag* 2021;17:282-91. DOI PubMed
48. Brander SM, Renick VC, Foley MM, et al. Sampling and quality assurance and quality control: a guide for scientists investigating the occurrence of microplastics across matrices. *Appl Spectrosc* 2020;74:1099-125. DOI
49. Miller E, Sedlak M, Lin D, et al. Recommended best practices for collecting, analyzing, and reporting microplastics in environmental media: lessons learned from comprehensive monitoring of San Francisco Bay. *J Hazard Mater* 2021;409:124770. DOI
50. Zhu X, Munno K, Grbic J, et al. Holistic assessment of microplastics and other anthropogenic microdebris in an urban bay sheds light on their sources and fate. *ACS EST Water* 2021;1:1401-10. DOI
51. Pasquier G, Doyen P, Kazour M, et al. Manta net: the golden method for sampling surface water microplastics in aquatic environments. *Front Environ Sci* 2022;10:811112. DOI
52. Payne AR, Burdick DM, Moore GE, Wigand C. Short-term effects of thin-layer sand placement on salt marsh grasses: a marsh organ field experiment. *J Coast Res* 2021;37:771-8. DOI PubMed PMC
53. Enders K, Lenz R, Beer S, Stedmon CA, Browman H. Extraction of microplastic from biota: recommended acidic digestion destroys common plastic polymers. *ICES J Mar Sci* 2017;74:326-31. DOI
54. Maes T, Jessop R, Wellner N, Haupt K, Mayes AG. A rapid-screening approach to detect and quantify microplastics based on fluorescent tagging with Nile Red. *Sci Rep* 2017;7:44501. DOI PubMed PMC
55. Shim WJ, Song YK, Hong SH, Jang M. Identification and quantification of microplastics using Nile Red staining. *Mar Pollut Bull* 2016;113:469-76. DOI PubMed
56. Erni-Cassola G, Gibson MI, Thompson RC, Christie-Oleza JA. Lost, but found with nile red: a novel method for detecting and quantifying small microplastics (1 mm to 20 μm) in environmental samples. *Environ Sci Technol* 2017;51:13641-8. DOI PubMed
57. Prata JC, da Costa JP, Duarte AC, Rocha-santos T. Methods for sampling and detection of microplastics in water and sediment: a critical review. *TrAC Trends Analyt Chem* 2019;110:150-9. DOI
58. Scircle A, Cizdziel JV, Tisinger L, Anumol T, Robey D. Occurrence of microplastic pollution at oyster reefs and other coastal sites in the Mississippi sound, USA: impacts of freshwater inflows from flooding. *Toxics* 2020;8:35. DOI PubMed PMC
59. Bäuerlein PS, Pieke EN, Oesterholt FIHM, Ter Laak T, Kools SAE. Microplastic discharge from a wastewater treatment plant: long term monitoring to compare two analytical techniques, LDIR and optical microscopy while also assessing the removal efficiency of a bubble curtain. *Water Sci Technol* 2023;87:39-56. DOI PubMed
60. Nizamali J, Mintenig SM, Koelmans AA. Assessing microplastic characteristics in bottled drinking water and air deposition samples using laser direct infrared imaging. *J Hazard Mater* 2023;441:129942. DOI
61. Whiting QT, O'Connor KF, Potter PM, Al-Abed SR. A high-throughput, automated technique for microplastics detection, quantification, and characterization in surface waters using laser direct infrared spectroscopy. *Anal Bioanal Chem* 2022;414:8353-64. DOI PubMed PMC
62. Coppock RL, Cole M, Lindeque PK, Queirós AM, Galloway TS. A small-scale, portable method for extracting microplastics from

marine sediments. *Environ Pollut* 2017;230:829-37. DOI PubMed

63. Stanton T, Johnson M, Nathanail P, Gomes RL, Needham T, Burson A. Exploring the efficacy of nile red in microplastic quantification: a costaining approach. *Environ Sci Technol Lett* 2019;6:606-11. DOI
64. Brown WS, Arellano E. The application of a segmented tidal mixing model to the Great Bay Estuary, N. H. *Estuaries* 1980;3:248-57. DOI
65. Neto JA, Gaylarde C, Beech I, Bastos AC, da Silva Quaresma V, de Carvalho DG. Microplastics and attached microorganisms in sediments of the Vitória bay estuarine system in SE Brazil. *Ocean Coast Manag* 2019;169:247-53. DOI
66. McEachern K, Alegria H, Kalagher AL, Hansen C, Morrison S, Hastings D. Microplastics in Tampa Bay, Florida: abundance and variability in estuarine waters and sediments. *Mar Pollut Bull* 2019;148:97-106. DOI PubMed
67. Song YK, Hong SH, Jang M, et al. A comparison of microscopic and spectroscopic identification methods for analysis of microplastics in environmental samples. *Mar Pollut Bull* 2015;93:202-9. DOI
68. Barrows APW, Cathey SE, Petersen CW. Marine environment microfiber contamination: global patterns and the diversity of microparticle origins. *Environ Pollut* 2018;237:275-84. DOI PubMed
69. Covernton GA, Pearce CM, Gurney-Smith HJ, et al. Size and shape matter: a preliminary analysis of microplastic sampling technique in seawater studies with implications for ecological risk assessment. *Sci Total Environ* 2019;667:124-32. DOI
70. Cutroneo L, Reboa A, Besio G, et al. Microplastics in seawater: sampling strategies, laboratory methodologies, and identification techniques applied to port environment. *Environ Sci Pollut Res Int* 2020;27:8938-52. DOI PubMed PMC
71. Biltcliff-ward A, Stead JL, Hudson MD. The estuarine plastics budget: a conceptual model and meta-analysis of microplastic abundance in estuarine systems. *Estuar Coast Shelf Sci* 2022;275:107963. DOI
72. Bikker J, Lawson J, Wilson S, Rochman CM. Microplastics and other anthropogenic particles in the surface waters of the Chesapeake Bay. *Mar Pollut Bull* 2020;156:111257. DOI PubMed
73. Cohen JH, Internicola AM, Mason RA, Kukulka T. Observations and simulations of microplastic debris in a tide, wind, and freshwater-driven estuarine environment: the Delaware Bay. *Environ Sci Technol* 2019;53:14204-11. DOI PubMed
74. Suresh A, Vijayaraghavan G, Saranya KS, Neethu KV, Aneesh B, Bijoy Nandan S. Microplastics distribution and contamination from the Cochin coastal zone, India. *Reg Stud Mar Sci* 2020;40:101533. DOI
75. Zhao S, Zhu L, Wang T, Li D. Suspended microplastics in the surface water of the Yangtze Estuary System, China: first observations on occurrence, distribution. *Mar Pollut Bull* 2014;86:562-8. DOI
76. Hitchcock JN, Mitrovic SM. Microplastic pollution in estuaries across a gradient of human impact. *Environ Pollut* 2019;247:457-66. DOI PubMed
77. Ragoobur D, Amode NS, Somaroo GD, Nazurally N. Microplastics in estuarine water and sediment in Mauritius. *Reg Stud Mar Sci* 2023;57:102766. DOI
78. Fulfer VM, Walsh JP. Extensive estuarine sedimentary storage of plastics from city to sea: Narragansett Bay, Rhode Island, USA. *Sci Rep* 2023;13:10195. DOI PubMed PMC
79. Claessens M, De Meester S, Van Landuyt L, De Clerck K, Janssen CR. Occurrence and distribution of microplastics in marine sediments along the Belgian coast. *Mar Pollut Bull* 2011;62:2199-204. DOI PubMed
80. Cozzolino L, Nicastro KR, Zardi GI, de Los Santos CB. Species-specific plastic accumulation in the sediment and canopy of coastal vegetated habitats. *Sci Total Environ* 2020;723:138018. DOI PubMed
81. Nor NH, Obbard JP. Microplastics in Singapore's coastal mangrove ecosystems. *Mar Pollut Bull* 2014;79:278-83. DOI PubMed
82. Vianello A, Boldrin A, Guerriero P, et al. Microplastic particles in sediments of Lagoon of Venice, Italy: first observations on occurrence, spatial patterns and identification. *Estuar Coast Shelf Sci* 2013;130:54-61. DOI
83. Liebezeit G, Dubaish F. Microplastics in beaches of the East Frisian islands Spiekeroog and Kachelotplate. *Bull Environ Contam Toxicol* 2012;89:213-7. DOI PubMed
84. Lv L, Qu J, Yu Z, et al. A simple method for detecting and quantifying microplastics utilizing fluorescent dyes - Safranine T, fluorescein isophosphate, Nile red based on thermal expansion and contraction property. *Environ Pollut* 2019;255:113283. DOI PubMed
85. Montoto-Martínez T, Meléndez-Díez C, Melián-Ramírez A, Hernández-Brito JJ, Gelado-Caballero MD. Comparison between the traditional Manta net and an innovative device for microplastic sampling in surface marine waters. *Mar Pollut Bull* 2022;185:114237. DOI
86. Yonkos LT, Friedel EA, Perez-Reyes AC, Ghosal S, Arthur CD. Microplastics in four estuarine rivers in the Chesapeake Bay, U.S.A. *Environ Sci Technol* 2014;48:14195-202. DOI PubMed
87. Lattin GL, Moore CJ, Zellers AF, Moore SL, Weisberg SB. A comparison of neustonic plastic and zooplankton at different depths near the southern California shore. *Mar Pollut Bull* 2004;49:291-4. DOI PubMed
88. Moore CJ, Moore SL, Weisberg SB, Lattin GL, Zellers AF. A comparison of neustonic plastic and zooplankton abundance in southern California's coastal waters. *Mar Pollut Bull* 2002;44:1035-8. DOI PubMed
89. Manickavasagam S, Kumar S, Kumar K, Rathi Bhuvaneswari G, Paul T, Shukla S. Quantitative assessment of influx and efflux of marine debris in a water channel of South Juhu creek, Mumbai, India. *Reg Stud Mar Sci* 2020;34:101095. DOI
90. Sadri SS, Thompson RC. On the quantity and composition of floating plastic debris entering and leaving the Tamar Estuary, Southwest England. *Mar Pollut Bull* 2014;81:55-60. DOI PubMed
91. Fok L, Cheung PK, Tang G, Li WC. Size distribution of stranded small plastic debris on the coast of Guangdong, South China.

Environ Pollut 2017;220:407-12. DOI PubMed

92. Bilgili A, Proehl JA, Lynch DR, Smith KW, Swift MR. Estuary/ocean exchange and tidal mixing in a Gulf of Maine Estuary: a Lagrangian modeling study. *Estuar Coast Shelf Sci* 2005;65:607-24. DOI
93. Gallagher TW, Mancilla C. MEMORANDUM: calibration of Great Bay Estuary hydrodynamic model and incremental nitrogen estimation. Available from: https://scholars.unh.edu/prep/411/. [Last accessed on 29 Nov 2023].
94. Matso K. Flushing time versus residence time for the Great Bay Estuary. Available from: https://scholars.unh.edu/prep/413/. [Last accessed on 29 Nov 2023].
95. Seabrook station environmental report, vol.1 - construction permit. Available from: https://www.nrc.gov/docs/ML1028/ML102880614.html. [Last accessed on 29 Nov 2023].
96. Trowbridge P. Hydrological parameters for New Hampshire's Estuaries. Available from: https://scholars.unh.edu/prep/130/. [Last accessed on 29 Nov 2023].
97. Eberhardt AL, Burdick DM. Hampton-seabrook estuary restoration compendium. Available from: https://scholars.unh.edu/prep/76/. [Last accessed on 29 Nov 2023].
98. Piscataqua Region Estuaries Partnership. Piscataqua region environmental planning assessment 2015. Available from: https://scholars.unh.edu/prep/358/. [Last accessed on 29 Nov 2023].
99. Payne AR, Burdick DM, Moore GE. Potential effects of sea-level rise on salt marsh elevation dynamics in a New Hampshire Estuary. *Estuaries Coast* 2019;42:1405-18. DOI
100. Barnes DKA. Remote islands reveal rapid rise of southern hemisphere, sea debris. *Sci World J* 2005;5:915-21. DOI PubMed PMC
101. Browne MA, Crump P, Niven SJ, et al. Accumulation of microplastic on shorelines woldwide: sources and sinks. *Environ Sci Technol* 2011;45:9175-9. DOI
102. Estahbanati S, Fahrenfeld NL. Influence of wastewater treatment plant discharges on microplastic concentrations in surface water. *Chemosphere* 2016;162:277-84. DOI PubMed

Fonseca *et al. Water Emerg Contam Nanoplastics* 2024;3:3
DOI: 10.20517/wecn.2023.57

Water Emerging Contaminants & Nanoplastics

Research Article

Open Access

Impact of face masks weathering on the mussels *Mytilus galloprovincialis*

Tainá Fonseca[1], **Carlos Edo**[1,2], **Juliano M. Vilke**[1], **Marina Astudillo-Pascual**[3], **Joanna M. Gonçalves**[1], **Maria J. Bebianno**[1]

[1]CIMA, Centre of Marine and Environmental Research/ARNET - Infrastructure Network in Aquatic Research, University of Algarve, Campus de Gambelas, Faro 8000-139, Portugal.
[2]Department of Analytical Chemistry, Physical Chemistry and Chemical Engineering, University of Alcalá, Alcalá de Henares E-28871, Spain.
[3]Department of Biology and Geology, International Campus of Excellence in Marine Science (CEIMAR), University of Almeria, Almeria E-04120, Spain.

Correspondence to: Prof. Maria J. Bebianno, CIMA, Centre of Marine and Environmental Research/ARNET - Infrastructure Network in Aquatic Research, University of Algarve, Campus de Gambelas, Faro 8000-139, Portugal. E-mail: mbebian@ualg.pt

How to cite this article: Fonseca T, Edo C, Vilke JM, Astudillo-Pascual M, Gonçalves JM, Bebianno MJ. Impact of face masks weathering on the mussels *Mytilus galloprovincialis*. *Water Emerg Contam Nanoplastics* 2024;3:3. https://dx.doi.org/10.20517/wecn.2023.57

Received: 19 Sep 2023 **First Decision:** 14 Nov 2023 **Revised:** 28 Nov 2023 **Accepted:** 12 Dec 2023 **Published:** 15 Dec 2023

Academic Editor: Antoni Ginebreda **Copy Editor:** Pei-Yun Wang **Production Editor:** Pei-Yun Wang

Abstract

The COVID-19 pandemic has triggered an unprecedented need for single-use face masks, leading to an alarming increase in plastic waste globally. Consequently, the improper disposal of face masks has added to the existing burden of plastic pollution in the oceans. However, the complete environmental and marine ecotoxicological impact remains unclear. This study aims to investigate the ecotoxicological impact caused by the weathering of disposable face masks (DFMs) in the marine environment on mussels *Mytilus galloprovincialis* (*M. galloprovincialis*) by assessing biochemical, cytotoxic, and genotoxic effects. The mask leachate was analysed for the presence of nano and microplastics. Furthermore, the leachate was used in *in vivo* and *in vitro* toxicity bioassays to assess its impacts on *M. galloprovincialis*. The *in vivo* exposure of *M. galloprovincialis* to face mask leachate for 14 days induced a significant increase in catalase (CAT) activity in mussel gills, although not enough to prevent oxidative damage to cell membranes. DNA damage was also registered in mussel haemocytes after *in vivo* exposure to mask leachate. The *in vitro* Neutral Red (NR) cytotoxicity assay indicated that leachate concentrations ≤ 0.5 g/L^{-1} pose a significant risk to the health of mussel haemocytes, which seems a reliable tool for the cytotoxicity impact assessment of face masks in the marine environment. Therefore, the leachate obtained from face masks in seawater causes oxidative stress, oxidative damage, cytotoxicity, and genotoxicity in *M. galloprovincialis*, indicating that the plastic burden generated by DFMs in the ocean and its subsequent weathering represents a ubiquitous and invisible threat to the marine biota.

Keywords: Face masks, leachate, microplastics, toxicity, marine mussels

INTRODUCTION

The severe acute respiratory syndrome of coronavirus (SARS-Cov-2), first detected in 2019, gave rise to the COVID-19 pandemic[1]. Social distance, travel restrictions, lockdowns, and sanitary measures were globally adopted to avoid airborne virus transmission and reduce its spreading. One of the most widely accepted actions was the usage of single-use plastics (SUPs)[2], and personal protective equipment (PPEs), including protection suits, surgical face masks, examination gloves, and face shields, employed by frontline health professionals and the general population[3]. As a result of the remarkable shift in the demand for disposable items, a new plastic waste boom emerged, scaling up the already existing plastic pollution crisis[3,4].

In this context, with the mandatory use of disposable face masks (DFMs) worldwide, an explosive demand for its supply at exceptional levels occurred. On the rise of the coronavirus outbreak, projections estimate that 129 billion face masks were used monthly worldwide, amounting to over 1.24 trillion discarded globally since the start of the pandemic[5,6], and in the case of Portugal, PPE usage represents an additional contribution of 4.97% to the municipal solid waste[7].

Global improper disposal of these face masks led to their ubiquitous presence in urbanised areas, lakes, beaches, and mountains worldwide[8-11]. In addition, face masks that end up in landfills or open dumps may easily leak into the surrounding environment and be flushed into rivers and coastlines by rainfall or wind[12,13], ultimately reaching the ocean. Considering the global production, it is estimated that about 1.56 billion face masks entered the marine environment in 2020[14].

Once in the marine realm, DFMs pose a physical threat to marine life through entanglement or ingestion[15]. Moreover, face masks undergo weathering (also known as ageing) by sunlight, mechanical abrasion, oxidation, and biodegradation, breaking down the textile material into microplastics (MPs) and nanoplastics (NPs) (plastic fragments less than 5 mm and 1 μm, respectively), whereby fibres are dominant (70%)[16,17]. Research revealed that a single face mask might release between 3,600 to 1.6×10^7 microfibres into the water, depending on the duration and intensity of physical and chemical disturbances[17-19]. A myriad of synthetic microfibres are dispersed in the marine environment[20,21] and DFMs have been pointed out as a critical secondary source of plastic burden in the ocean[7,16].

Polypropylene is the most used plastic polymer assembled in DFMs, but other polymers like polyurethane, polyester or polyacrylonitrile can also be incorporated into its structure[1]. The release of plastic polymers may act as vectors of hazardous substances, such as persistent organic pollutants (POPs), polycyclic aromatic hydrocarbons (PAHs), polychlorinated biphenyls (PCBs), pesticides, or emerging contaminants. Moreover, chemical additives from face masks' matrices may also be released into the marine environment, including plasticisers, pigments, dyes, metals, antioxidants, stabilisers, and lubricants[13]. The plastic burden from MPs and NPs released from DFMs may enter marine biological systems through ingestion, dermal contact, or filtration[16], particularly in the case of filter-feeding bivalves.

Microfibres are known to be ingested by crustaceans, molluscs, fishes, birds, and seals[22-24]. An extensive body of evidence demonstrated that marine organisms undergo MPs and NPs ingestion, leading to inflammatory responses, oxidative stress, membrane damage, cytotoxicity, genotoxicity, cell death, and reproductive impairments, detected either through *in vivo* or *ex vivo* exposures[25-28]. Likewise, ecotoxicological assessments also indicate the extent of the biological effects following the exposure to microplastic fibres (nylon, polyester, polypropylene polymers) on marine zooplankton representatives[29,30] and mussels[31-33].

However, to the best of the authors' knowledge, the present study is the first marine ecotoxicological assessment conducted on the weathering of DFMs. Considering the high representation of DFMs in the current marine litter composition and the biological disturbances associated with MPs and NPs across several biological levels in the marine biota, there is a pressing need to investigate whether the weathering and fragmentation of DFMs in the ocean pose an additional ecotoxicological threat to the marine environment. The present study hypothesizes that DFMs ageing release plastic particles and further cause biochemical, cytotoxic, and genotoxic injuries to the marine mussel *Mytilus galloprovincialis* (*M. galloprovincialis*). The main objective is to unravel the biological responses posed by DFMs on the mussels through *in vivo* and *in vitro* assays. The use of a cell-based *in vitro* approach conducted with *M. galloprovincialis* haemocytes under DFM leachate exposure revealed a notorious advantage in reducing the considerable number of mussels needed to carry out experiments, allowing the screening of a broader spectrum of exposure conditions and rapid generation of consistent data[34], which is line with demanding regulatory needs of the European Union. The findings herein will shed light on the biological effects that result from the presence of this ubiquitous and unprecedented type of plastic litter on marine mussels.

MATERIAL AND METHODS

Weathering procedure

Due to its broad use during the COVID-19 pandemic and its wide disposal in urban and natural spots, DFM was selected to assess the release of plastic particles to seawater, simulating natural weathering conditions. Instead of applying virgin DFM, timeworn face masks were collected to mimic realistic conditions of the masks ending up in the marine environment. After their collection, the elastic ear loops were removed from the surgical masks.

Twelve DFM (10 g of masks) were immersed in three litres of natural seawater (salinity 35) from the Ria Formosa lagoon, previously UV-sterilized and filtered (FSW) through 0.8 μm glass microfibre filters (Whatman), and the leachate prepared according to the method proposed by Almeda *et al.*[35]. For this purpose, the container was vigorously agitated over 72 h to simulate wave abrasion. After that period, masks were removed and dried in an oven at 60 ºC for three days to identify the polymer composition. The mask leachate was then frozen at -20 ºC until further use. To limit the overestimation of MPs present in the leachate, glassware and cotton clothing were adopted and applied during the whole assay to avoid plastic contamination, and a blank was run in parallel to assess possible MP and NP contamination.

Plastic polymer composition of face masks

Wave-weathered DFMs were analysed using Fourier Transform Infrared Spectroscopy (ATR-FTIR, Thermo Fisher Nicolet iS10) to identify the polymers present in the masks' structure. The spectra were acquired using a resolution of 4 cm^{-1}, 16 scans, 4,000-650 cm^{-1} spectral region, and transmittance mode. The obtained spectra were compared with existing databases using the OMNIC software. This software uses Pearson correlation to give a coincidence value. After the analysis, only the results above 70% of coincidence were considered positive. The different layers from all the masks used to generate the leachate were separated and tested individually, namely the outer lyophobic non-woven layer (O layer), the middle melt-blown layer (M layer), and the inner hydrophilic non-woven layer (I layer).

Analysis of plastic particles in mask leachate

Another leachate from used masks was prepared, following the same procedures described in section "Weathering procedure" to analyse the presence of MPs in the extract. The liquid was filtered through 0.8 μm glass microfibre filters (Whatman) and the filters were dried in an oven at 60 ºC to ensure that the chemical composition of the MPs and NPs was not altered. Filters were evaluated under an Edublue stereomicroscope (Euromex) at ×4 magnification. The present particles were counted, and their colour was assessed. In addition, the particles were measured in length and width, and their equivalent diameter was calculated.

To avoid interference from other submicron materials in seawater, NPs released in mask leachate were determined using artificial seawater (ASW), salinity 35, prepared according to ASTM D1141-98 standard.

To analyse the NPs, total organic carbon (TOC) measurements were performed in a Shimadzu TOC-VCSH equipped with an autosampler. Samples were filtered through Puradisc 25 TF filters (1 μm pore size) and analysed in Non-Purgeable Organic Carbon (NPOC) mode. Moreover, the size of the NPs in the leachate was confirmed with a Malvern Zetasizer Nano ZS apparatus. This equipment uses Dynamic Light Scattering (DLS) technology to analyse the particles present in the submicron portion of the leachates. With this aim, samples were filtered through 1 μm with Puradisc 25 TF filters. Comparison between fragments and fibres was allowed by calculating an equivalent diameter , converting the two flat dimensions into comparable diameters as done elsewhere[36,37].

M. galloprovincialis in vivo bioassay

Mussels *M. galloprovincialis* (*n* = 90; 6.0 ± 0.34 cm shell length) were handpicked during low tide in the Ria Formosa lagoon (Faro, Southern Coast, Portugal) and transported alive to the laboratory, scrap-cleaned and distributed over six glass aquaria containing 7 L of natural seawater. Mussels were acclimated over 5 days, at 16 ± 1 °C, salinity 35 ± 1.0 and pH 8.0 ± 0.2, with continuous aeration during a 12 h light : 12 h dark photoperiod. Seawater was renewed every 48 h during the acclimation period, and organisms were fed with marine microalgae *Tetraselmis chuii.*

After the acclimation period, ninety mussels were randomly selected and exposed for 14 days to each treatment (CT and 100 $mg \cdot L^{-1}$ of DFM leachate) in a triplicate design in 10-L glass aquaria filled with 7 L of seawater (15 animals per aquaria, density = 2 mussels L^{-1}. The seawater was changed every 48 h, and the leachate concentration was re-established. Animals were fed with the only food present in the seawater. Throughout the 14 days of the bioassay, the system was kept under constant aeration, controlled photoperiod, salinity (36), pH (8.0 ± 0.2), temperature (16 ºC), and oxygen saturation (96% ± 4%). On the 14th day of the bioassay, mussels (*n* = 6 per treatment) were collected for the determination of the individual biometric parameters (length, height, and width) and for the calculation of the condition index (CI). For that purpose, the soft and drained body tissues were weighted, and the CI for each organism was calculated according to the equation:

$$CI\ (\%) = \frac{whole\ soft\ tissue\ (wet\ weight) \times 100}{whole\ drained\ body\ tissue}$$

On the last day of the experiment, mussels from each treatment (n = 6) were collected and dissected into gills and digestive glands, which were subsequently flash-frozen in liquid nitrogen and stored at -80 ºC until further biochemical analysis to assess antioxidant and oxidative damage effects by measuring the activity of antioxidant enzymes [superoxide dismutase (SOD), catalase (CAT) and glucose-6 phosphate dehydrogenase (G6PDH)], gllutathiona-S-transferases (GST), lipid peroxidation (LPO) and respective total protein content.

In vitro cytotoxic assessment

Adult specimens of *M. galloprovincialis* (n = 15) from the Ria Formosa coastal lagoon (5.0 ± 0.3 cm shell length) were kept in a 25 L tank filled with clean natural seawater (salinity 35 ± 1), pH 7.8, temperature 18.5 ºC and constant aeration, until haemolymph extraction. Mussels were fed every two days by incorporating ~10 mL microalgae mix of *T. chuii* into the aquaria. After the three days of mussel acclimation, individuals (n = 10) were randomly chosen, and their haemolymph was retrieved under aseptic conditions[38,39]. Briefly, haemolymph was obtained from the posterior adductor muscle using a 2-mL sterile hypodermic syringe. Haemolymph collected from the ten specimens was pulled into one 15-mL Falcon tube and mixed with anti-aggregation solution (pH 6.7; 171 mM NaCl; 0.2 M Tris; 0.15% v/v HCl 1 N; 24 mM EDTA) in a 1:3 ratio, to prevent cell clumping and agglomeration[39,40]. Aliquots of this cell suspension were then used for cell counting in the Neubauer chamber (Hirschmaan, Eberstadt, Germany) through cell staining with the addition of Trypan blue dye (0.4% in physiological solution; v/v). Cell viability was determined by the percentage of live cells in cell suspension (100 cells counted). The following equation was used to calculate cell density:

$$Viable\ cells\ per\ mL = \frac{Viable\ cells}{n^{\underline{o}}\ of\ squares\ counted} \times dilution \times 10{,}000$$

Subsequently, the cell suspension was seeded into 96-well flat microplates (2×10^5 cells·mL^{-1}; 50 µL per well) and exposed, over 24 h in the dark, to a range of leachate concentrations prepared from a stock solution of mask leachate (10 g·L^{-1}) sequentially diluted in Dulbecco's Modified Eagle Medium (hereafter DMEM, pH 7.4) to obtain the following tested concentrations of the leachate: 1, 2.5, 5 and 7.5 g·L^{-1}. These solutions were prepared on the day of the bioassay and maintained at 4 ºC, in the dark, until incubation of mussel haemocytes to the respective exposure conditions. Blanks containing only DMEM cell culture media and anti-aggregation solution, absent of cells, were prepared as a reference, jointly with a negative control group (CT-; cells jointly with an anti-aggregation solution and DMEM) and a positive control group (CT+) prepared with sodium dodecyl surfactant (5 mM SDS, in DMEM), known to cause cytotoxic effects in the endpoint measurement. Eight replicates were prepared per treatment and control conditions. After the 24-h incubation, centrifugation at 1,200 rpm (10 min, at 4 ºC) was carried out to promote cell adhesion to the bottom. The supernatant (medium) was discarded, and cell viability assessed through the NR assay described in section "*NR cytotoxicity assay*".

NR cytotoxicity assay

The NR assay was applied to reveal the viability of mussel haemocytes through the capacity of live cells to incorporate the dye in lysosomes via non-ionic passive[41], according to the protocols of Katsumiti *et al.*[39]

and Fonseca *et al.*[42], with slight adaptations. Subsequently, 50 µL of filtered (Sartorius, 0.22 µm cellulose acetate filters) NR working solution was added to each microplate well and left in the dark for incubation over 1 h. Afterwards, to remove the excess dye from the medium, microplates were again centrifuged and gently washed with PBS until complete removal of the dye from the blanks. An acetic acid and ethanol solution (1:100 v/v) was seeded into a microplate and left over 20 min in the dark at 18 ºC for dye extraction from viable cells. Then, the cell suspension was transferred into a new V-bottom 96 well microplate and centrifuged. The supernatant was carefully placed into a new flat bottom microplate to measure the absorbance obtained from the neutral red extracts of the viable cells (550 nm, Infinite M200 Pro, TECAN®). Live and viable cells present higher absorbance, given the higher embodiment of dye into the lysosomes.

Cell viability and genotoxicity

Haemolymph was extracted as previously described (Section "*In vitro* cytotoxic assessment") and divided into two aliquots: one for the Trypan blue exclusion assay to measure cell viability, and the other was used for the Comet assay to assess genotoxicity.

Cell staining was performed with Trypan blue dye (0.4% in physiological solution; v/v) in a proportion of 1:1 (cell suspension: Trypan Blue 0.4%), whereby the percentage of live cells was determined. Cell viability was obtained through the relative number of viable and non-viable cells by counting blue-stained cells as dead and the translucid ones as alive. Results were expressed as a percentage of viable cells over total cells.

DNA damage was estimated using the alkaline Comet assay, adapted for marine mussels by Gomes *et al.*[43]. Microscope slides were pre-cleaned with ethanol and cast with normal melting point agarose (NMA) in Tris-acetate EDTA. Individual haemolymph aliquots were centrifuged at 3,000 rpm over 3 min (4 ºC), and the pellets were suspended in 0.65% low melting point agarose (LMA, in Kenny's salt solution) and cast over the microscope slides. Cells in the slides were then submitted to a lysis step over 1 h, and electrophoresis was carried out for 5 min at 25 V and 300 mA, followed by immersion in a neutralising solution (0.4 mM Tris, pH 7.5) over 15 min.

For the evaluation of the DNA in the comet tail (tail DNA %), slides were stained with DAPI, and pictures were taken from 50 random cells from each slide under a magnification of ×400 in an optical fluorescence microscope (Axiovert S100) coupled with a camera (Sony). Scoring analysis was performed using Imaging Software Komet 7.1 (Kinetic Imaging Ltd). Results are expressed as mean tail DNA % ± STD.

Biochemical analysis in *M. galloprovincialis*

Antioxidant and biotransformation enzyme activities

Antioxidant (SOD, CAT, G6PDH) and biotransformation (GST) enzyme activities were determined in gills and digestive glands from unexposed and leachate-exposed mussels. For that purpose, tissues of organisms ($n = 6$ per treatment) were individually homogenised in 5 mL of Tris-sucrose buffer (20 mM Tris, 0.5 M sucrose, 0.075 M KCl, 1 mM DTT, 1 mM EDTA, pH 7.6). The homogenate was centrifuged at 500 g, under 4 ºC, and the supernatant re-centrifuged at 12,000 g (45 min, 4 ºC). Cytosolic fraction was isolated and stored at -80 ºC to determine enzymatic activities and total protein content.

SOD activity was determined through the method described by McCord and Fridovich[44], whereby the decrease in the absorbance of the substrate cytochrome-*c*, by competition with the xanthine oxidase/ hypoxanthine system, is measured spectrophotometrically at 550 nm. Results are expressed as $U \cdot mg^{-1}$ protein. To evaluate CAT activity, the decrease in the absorbance of the hydrogen peroxide (H_2O_2) was measured, revealing its consumption at 240 nm. CAT activity is herein presented in $nmol \cdot min^{-1} \cdot mg^{-1}$

protein.

The activity of the housekeeping enzyme G6PDH was indirectly determined through the method described by Glock and McLean[45], adapted by Almeida *et al.*[46], through which the reduction of nicotinamide adenine dinucleotide phosphate (NADP) to NADPH is measured spectrophotometrically at 340 nm. Results are expressed as U·mg^{-1} protein. The metabolism of biotransformation mediated by GST activity was quantified according to the method of Habig *et al.*, adapted for microplate reader, by the conjugation of 0.2 mM reduced form of glutathione (GSH) with 0.2 mM 1-chloro 2,4 dinitrobenzene (CDNB), in a reaction mixture of 0.2 M KH_2PO_4/K_2HPO_4 buffer (pH 7.9), at 340 nm[47]. The respective enzymatic results are expressed as CDNB nmol·min^{-1}·mg^{-1} protein.

Lipid peroxidation

Gills (n = 6) and digestive glands (n = 6) of *M. galloprovincialis* were individually homogenised in Tris-HCl buffer (20 mM, pH 8.6) with butylated hydroxytoluene (BHT) and centrifuged over 45 min (30,000 g, at 4 ºC). The resulting supernatant was stored under -80 ºC for further measurement of total protein content[48] and the determination of lipid peroxidation by-products, namely malondialdehyde (MDA) and 4-hydroxyalkenals (4-HNE), both products of the peroxidation of polyunsaturated fatty acids. The levels of MDA + 4-HNE were determined according to the method described by Erdelmeier *et al.*[49]. For that purpose, malondialdehyde bis-(dimethyl acetal) (Sigma-Aldrich) was used as standard, and the absorbance of the samples was measured at 586 nm in a microplate reader (Infinite M200Pro, TECAN®). Results are expressed as nmol MDA + 4-HNE mg^{-1} protein.

Determination of total protein content

Total protein concentration was determined in the cytosolic fraction of the aliquots regarding the analysis of antioxidant enzyme activity, GST activity and LPO levels, using Bovine Serum Albumin (BSA) as a standard[48]. Absorbance was read at 595 nm, and total protein concentrations were expressed as mg protein g^{-1} wet-weight tissue.

Statistical analysis

Results regarding biomarker responses were first checked for normality and homogeneity by the Kolmogorov-Smirnov and Bartlett's tests using GraphPrism 9 (GraphPad Software, Inc.). Student's t-test was applied to determine significant statistical differences between the effects addressed in paired samples from mask-leachate and control treatments. The critical value for statistical significance was $P < 0.05$.

RESULTS

FTIR analysis

The FTIR analysis of the surgical masks confirmed that the composition of the three protective layers was polypropylene. All the layers showed the same typical bands of this polymer with the CH_3 and CH_2 stretches (asymmetric and symmetric) in the region 3,000-2,850 cm^{-1}, as well as the methyl group present near 1,380 cm^{-1} and the aromatic ring in 1,450 cm^{-1} [Figure 1].

Particle size distribution in the mask leachate

Face mask leachate revealed the presence of 126 microparticles·m^{-3}. The main morphology was fibres (97%) of different colours, except for some coloured fragments, at a density of 3.4 fragments·m^{-3} [Figure 2]. The average size for fibres was 66.5 ± 24.4 µm and 34.6 ± 15.9 µm for fragments, showing the bigger size of the fibres in these samples.

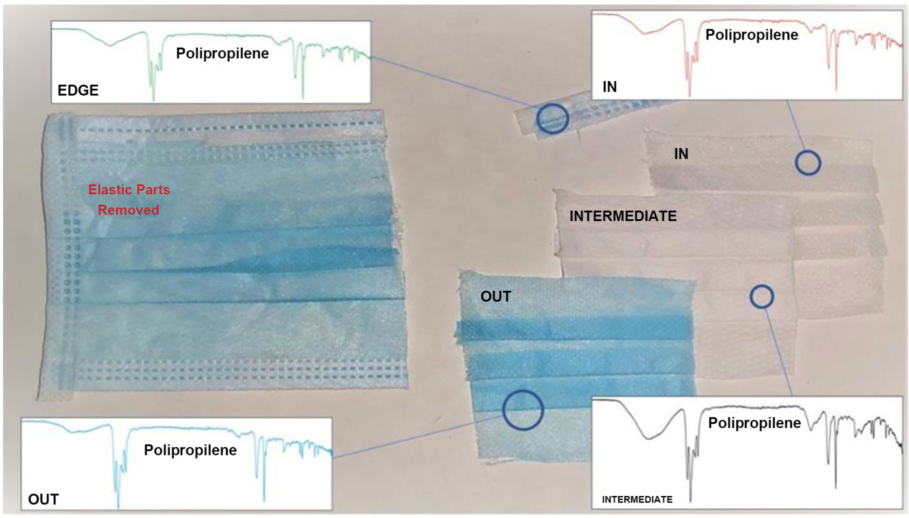

Figure 1. FTIR spectra and visual appearance of the different layers that form the facial masks. Polypropylene was the only polymer present in all layers. FTIR: Fourier Transform Infrared Spectroscopy.

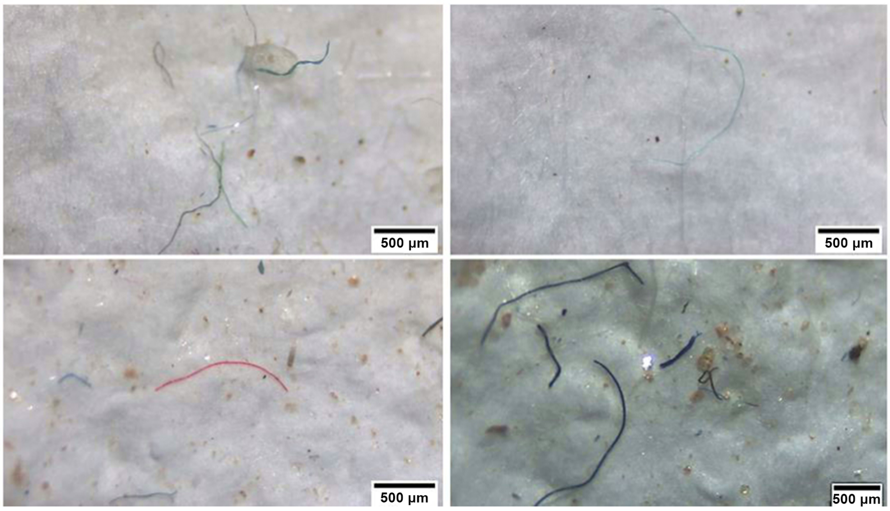

Figure 2. Images from stereomicroscope (×4 magnification) of the microparticles found in the leachate from used masks. Fibres and fragments of different colours were observed.

The TOC calculation determined the presence of NPs (below 1 µm). In all cases, the amount of carbon in leachate was higher than in negative controls. The concentration of carbon after 72 h was 3.21 mg·m^{-3} in leachate, in contrast to the 0.72 mg·m^{-3} found in the ASW control, indicating that NPs have been leached from the facial masks. DLS analysis confirmed the presence of submicron particles in the leachate in the 195.6 ± 96.6 nm range [Figure 3] that were not present in the controls. In addition, few NPs in the 10-100 nm size range were present.

Antioxidant and biotransformation enzyme activities

After 14 days of exposure to the mask leachate, mussels revealed an increasing trend in SOD activity in gills, although not significant compared to controls ($P > 0.05$) [Figure 4A], whereas digestive glands experienced a significant increase in SOD activity compared to unexposed mussels ($P < 0.05$) [Figure 4B]. In contrast, the mechanism that H_2O_2 scavenging exerted by CAT activity increased significantly in leachate-exposed

Size distribution (<1 μm): ASW Control

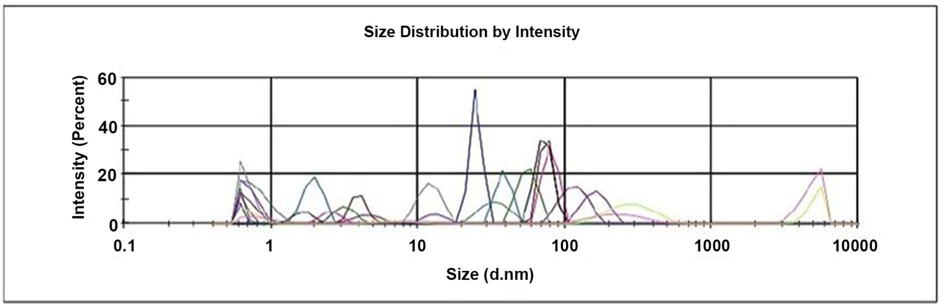

Size Distribution (<1 μm): Mask Leachate in ASW

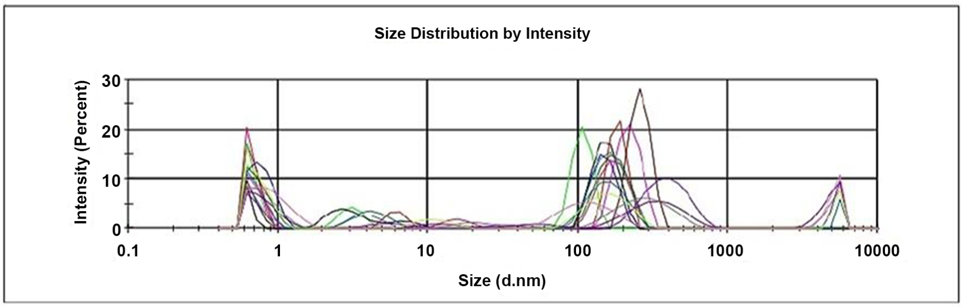

Figure 3. Size distribution of nanosize particles (< 1 μm) in ASW control and in mask leachate measured with DLS in artificial seawater medium (ASTM D1141-98 standard). ASW: Artificial seawater; DLS: Dynamic Light Scattering.

mussels' gills [Figure 4C], while in digestive glands, levels were comparable to the controls ($P > 0.05$) [Figure 4D]. Regarding G6PDH activity, although there was a decreasing trend in the gills exposed to the mask leachate, this decrease was not significant compared to unexposed mussels ($P > 0.05$) [Figure 4E] while in digestive glands, G6PDH activity from leachate exposed mussels significantly decreased in comparison to control levels ($P < 0.05$) [Figure 4F]. The results of the biotransformation metabolism showed that GST activity decreased in the gills of mussels exposed to mask leachate, while there was a slight increase in GST activity in the digestive glands. However, this trend was not significant in either tissue compared to the control group ($P > 0.05$) [Figure 5].

Lipid peroxidation

Levels of LPO by-products detected in gills from mussels exposed to mask leachate were significantly higher (2.7-fold) than those from the controls ($P < 0.05$) [Figure 6A], whereas in digestive glands, no significant differences were detected ($P > 0.05$) [Figure 6B].

Genotoxicity

Haemocytes retrieved from mussels exposed over 14 days to mask leachate experienced a significant increase of 150% of DNA tail compared to the control treatment ($P < 0.05$) [Figure 7].

In vitro cell viability

As observed in Figure 8, haemocytes revealed a significant and monotonic dose-responses relationship with a decrease in cell viability from the concentration of 0.5 $g \cdot L^{-1}$ and onwards ($P < 0.0001$). This significant change in cell viability indicates that concentrations of the leachate > 0.25 $g \cdot L^{-1}$ led to the mussel's haemolymph cell death.

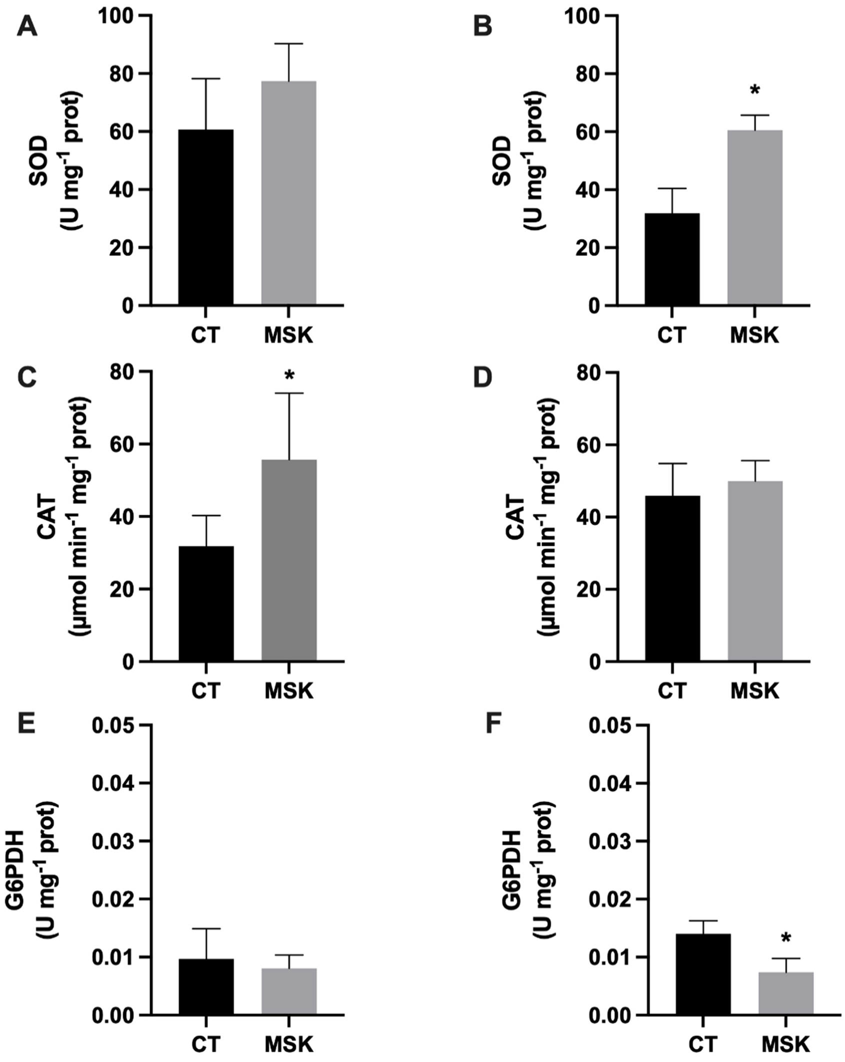

Figure 4. Antioxidant enzymes activity (mean ± STD) of: (A) and (B) SOD; (C) and (D) CAT; and (E) and (F) G6PDH, respectively in gills and digestive glands from unexposed (CT) and mask leachate-exposed mussels, after 14 days of bioassay. Asterisks indicate significant differences between control and mask leachate-exposed mussels (*t*-test; $P < 0.05$). CAT: Catalase; G6PDH: glucose-6 phosphate dehydrogenase; SOD: superoxide dismutase.

DISCUSSION

Findings from the present study are the first data unravelling the biochemical, cytotoxic, and genotoxic disturbances caused by weathering of DFM that releases MPs and NPs into seawater in the relevant marine sentinel species *M. galloprovincialis*.

Simulation of face mask weathering carried out in the present investigation was accountable for generating a total of 126.4 microparticles·m^{-3} in the aquatic system, most of which are fibres (95%). The number of fibres released depicts a high disparity with other weathering assessments with tri-layer masks[17]. Variations in the number of fibres released by non-woven face masks can be noted based on the weathering duration and exposure conditions to which they are submitted[17]. Current challenges were enumerated and emphasised regarding the realistic simulation of fibres pollution due to the lack of harmonisation of techniques applied across studies for analytical detection and quantification of fibres[50,51].

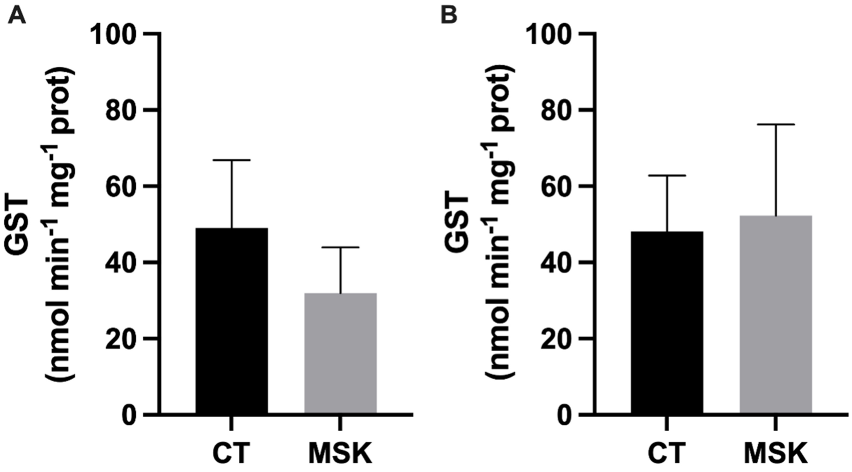

Figure 5. GST activity (mean ± STD) in gills (A) and digestive glands (B) from unexposed (CT) and mask leachate-exposed mussels, after 14 days of bioassay. GST: Gllutathiona-S-transferases.

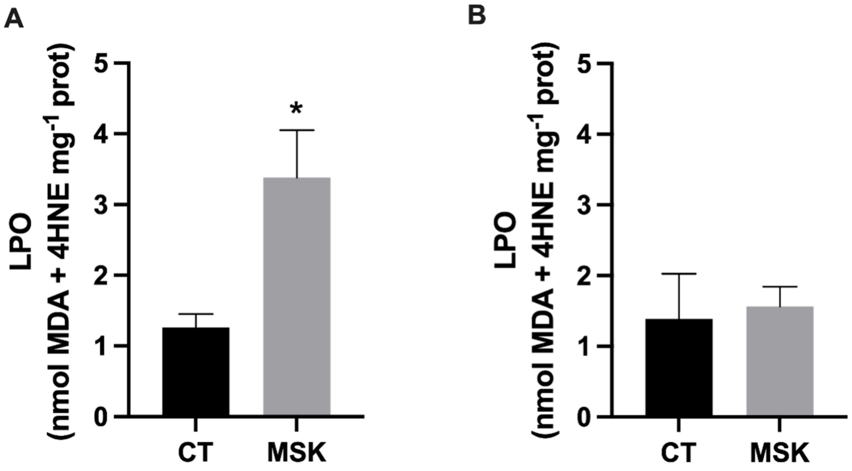

Figure 6. LPO levels by-products (mean ± STD) (nmol MDA+4-HNE mg^{-1} protein) in gills (A) and digestive glands (B) of unexposed (CT) and mask leachate-exposed mussels, after 14 days of bioassay. Asterisks indicate significant differences between control and mask leachate-treated mussels (*t*-test; $P < 0.05$). LPO: Lipid peroxidation; MDA: malondialdehyde; 4-HNE: 4-hydroxyalkenals.

In previous studies, face masks were submitted to mechanical and chemical external forces under laboratory conditions (rotating blender, treatment with alcohol/detergents) that are not similar to those experienced in the open environment[51,52]. Methodologies based on unrealistic simulations of shear stress forces are prone to generate a substantially higher amount of submicron fragments and particles, and the calculation of MPs and NPs generated from mask leachates may be overestimated[6]. The impact of face masks in the marine environment is in its infancy, and therefore, there are currently no standardised methods for analytical procedures and ecotoxicological assessment on this topic. As a consequence, there is a lack of calibrated procedures to ensure the realistic estimation of the impact and weathering of face masks under marine environmental conditions[51,52]. The vibration of functional groups [Figure 2] confirmed the polypropylene composition of the disposable surgical face masks, whose breakdown mainly occurs in the marine environment through photo- and thermo-oxidative degradation[53]. It is hypothesised that the application of used face masks in the present assessment, with different times of utilisation, contributed to contamination of the mask leachate with coloured fibres other than blue and transparent-white[54], potentially from the

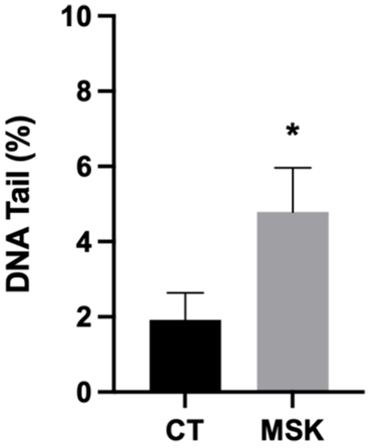

Figure 7. % of DNA tail (mean ± standard deviation) in mussel haemocytes unexposed (CT) and mask leachate-exposed, after 14 days of bioassay. Asterisks indicate significant differences between control and mask leachate-treated mussels (*t*-test; *P* < 0.05).

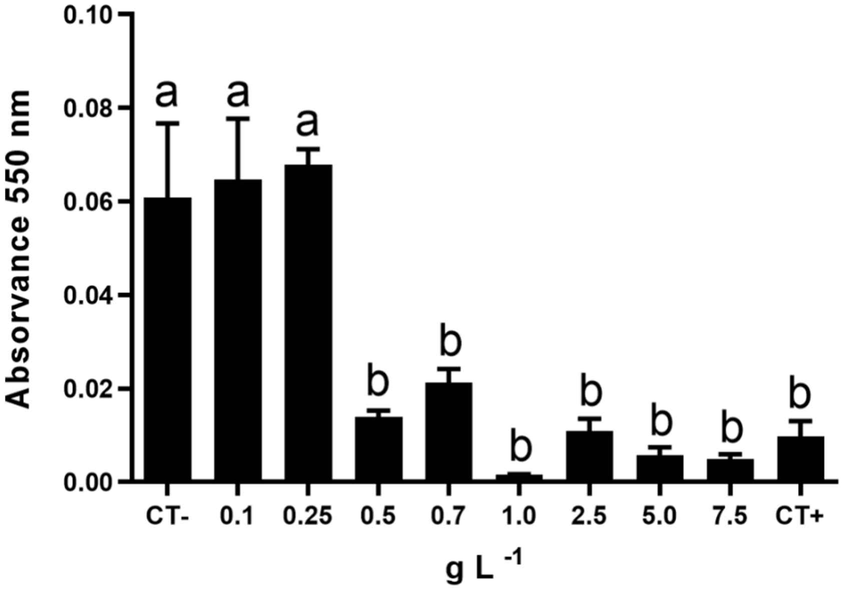

Figure 8. NR assay absorbances levels. Viability of *M. galloprovincialis* cells exposed to leachates, as well as a negative (CT-, unexposed) and positive controls (CT+, exposed to 5 mM SDS). Significant differences among treatments were labelled with different letters (one-way ANOVA test; *P* < 0.0001). NR: Neutral Red.

entrapment of MPs and NPs suspended in the air, or from tissues or clothing which may be accountable for the broader burden of MPs and NPs amount released in the leachate[13,16]. Furthermore, when MPs and NPs are present in seawater, they tend to aggregate[55]. This aggregation might significantly affect the bioavailability of the mixtures of these particles in the marine environment[55,56].

To date, scarce ecotoxicological investigation regarding face mask weathering has been conducted using aquatic species, with few approaches focused on marine biological models[57]. In the present ecotoxicological assessment, the gills of mussels submitted to the mask leachate presented a SOD activity similar to unexposed mussels. However, a significant increase in CAT activity was addressed as a hydrogen peroxide scavenging mechanism [Figure 4C] to counteract the harm generated by the physical stress promoted by

MPs and NPs ingested. Such a trend was also reported in marine mussels *M. galloprovincialis* under exposure to NPs and to emerging chemical contaminants[33,40,55,58], revealing that sources of hydrogen peroxide generation other than upon superoxide anion dismutated by SOD could be operating for CAT activation[59,60]. In contrast, SOD, the first line of defence in protecting tissues against oxidative stress[61], demonstrated to be an efficient response in the digestive glands of *M. galloprovincialis* to overcome the harm caused by the accumulation of the micro and nanoparticles ingested by the mussels[31], potentially jointly with the accumulation of other chemical additives released from the face masks[16,62,63] that were not analysed in the present work. Although CAT activity works in coordination with the activity of SOD, catalysing the reduction of hydrogen peroxide into water, the activity of such enzyme was not significantly altered in digestive glands, possibly due to the H_2O_2 clearance carried by peroxidases present in various subcellular compartments, such as glutathione peroxidases (GPx), which have a critical role in protecting cells against oxidative stress[60,61,64]. The decrease in the activity of G6PDH in gills, although significant only in the digestive gland, hypothesises the interference of the mask leachate on the activity of the glutathione-dependent system. Such an enzyme consists of an additional component of the antioxidant system accountable for catalysing the regeneration of the reduced NADPH. This essential cofactor operates jointly with glutathione reductase (GR) in the regulation of the intracellular supplies of the GSH, a potent *in vivo* antioxidant agent against oxidative damage caused by reactive oxygen species[65]. G6PDH-deficient cells experience a decrease in the GSH recycling mechanism that promptly compromises the ability of the antioxidant systems to detoxify hydrogen peroxide, thus being unable to withstand oxidative stress[66,67].

GST activity is associated with the biotransformation metabolism of organic compounds by catalysing the conjugation of the GSH to non-polar compounds that contain an electrophilic carbon, nitrogen, or sulphur atom[68,69], leading to the generation of less reactive products, with an ultimate protective role against oxidative stress[68,70]. The present findings revealed the absence of a biotransformation mechanism carried out by GST activity after mussels' exposure to mask leachate. This denotes low levels of organic chemicals taken up by mussels, possibly due to the low levels of organic chemicals present in the leachate or on the masks[71,72]. Beyond the physical stress carried out by micro and nano-sized fibres and particles, weathering and deterioration of the face masks are also accountable for contributing to the input of chemical additives in the environment, such as dye compounds, fragrances, and antiviral and antibacterial agents[73]. Sullivan *et al.* addressed the release of leachable inorganic and organic substances from the blue DFMs (like those used herein), namely metals, plastic additives, polyamide-66 monomer and oligomers (nylon-66 synthesis), surfactant molecules, dye-like molecules and polyethylene glycol[54]. These chemicals could have been released and then taken up by mussels in the present case, although further chemical confirmation is required. No significant alterations in GST activity were also registered in the digestive glands of mussels *M. galloprovincialis* exposed to 50 nm NPs (10 $\mu g \cdot L^{-1}$) compared to unexposed individuals, in contrast to a significant suppression in GST activity in the gills of respective animals[28]. Paul-Pont *et al.* also addressed that the biotransformation mechanism was not altered in the digestive glands of *Mytilus* spp. when exposed to polystyrene (PS) MPs (2-6 μm) at 32 $mg \cdot L^{-1}$ over seven days[26]. However, at the end of the depuration period of seven days, following PS-MPs exposure, GST activity significantly increased compared to unexposed individuals. Accordingly, Li *et al.* emphasised that wide variability in GST activity response was also reported in bivalves exposed to MPs and NPs[13].

Likewise, as addressed by Prokić *et al.*, organisms exposed to MPs and NPs exhibited varied responses in their overall antioxidant systems, ranging from no significant changes to a decrease or induction in enzymatic activities[74]. The diversity in ecotoxicological outcomes is influenced by a massive variability between features and parameters, namely the form of the plastic material (e.g., fibres, particle, bead, and powder), polymer composition, size of the particle, time of exposure, and acclimation conditions. These factors are collectively accountable for generating diverse ecotoxicological profiles of responses, which further vary across species and tissues analysed.

Although the reactive oxygen species(ROS)-scavenging antioxidant system was herein activated due to exposure to the mask leachate, the high levels of LPO by-products in the mussels' gills evidenced that the protective mechanisms could not efficiently neutralise ROS to prevent cellular lipids from oxidative damage in this tissue[75,76]; and that micro and nanoparticles induce oxidative damage in the gills. Results from the meta-analysis conducted by Li *et al.*, aiming to elucidate the role of oxidative stress in toxicity elicited by MPs and NPs in marine species, evidenced that end products of LPO are a reliable index of membrane damage when the ability of the cells to maintain redox balance declines, and the antioxidant system is suppressed, leading to cellular damage of the tissues and potentially fitness costs[13].

Accordingly, it is noteworthy that DNA damage was registered in haemocytes under *in vivo* exposure to the mask leachate, indicating genotoxicity, which may be mainly linked to oxidative damage. These findings collectively corroborate with a vast body of research revealing significant disturbances caused by polypropylene microfibres and fragments and NPs on antioxidant systems from *Mytilus* spp.[26,34,77]. Considering the stress depicted by microfibres, Choi *et al.* observed a disruption in SOD and CAT activities, both in the gills and digestive glands of *M. galloprovincialis* exposed to 1 mg·L^{-1} of PET microfibre[33]. In addition, a monotonic dose-response pattern was verified for apoptotic mechanisms and the induction of DNA damage in haemocytes, registered from the concentration of 0.1 mg·L^{-1}[33].

Herein, mussel haemocytes in the *in vitro* NR assay confirmed their sensitivity and reliability in assessing the cytotoxicity posed by weathering and degradation of DFMs in the marine environment. A concentration of 0.5 g·L^{-1} of weathered face masks showed cellular disturbances leading to cytotoxicity and cell death. Sendra *et al.* addressed that after a 3-h exposure of *M. galloprovincialis* haemocytes to PS MPs (1 µm - 10 mg·L^{-1}), a subpopulation of large granular cells exhibited significant cytotoxicity compared to the control group[78]. Additionally, these cells reached values higher than 58% of apoptotic cells when individually exposed to PS NPs of 50 and 100 nm at 10 mg·L^{-1}. Chang and Wang[79] assessed the cytotoxicity of filtered face masks' leachate (300 g·mL^{-1}) on human alveolar basal epithelial cells (A549), revealing significant inhibition in cell proliferation and induction of DNA damage, ultimately leading to cell death with enhanced exposure time, as a result of exposure to multiple phthalate acid esters. However, to date, no studies have been conducted on the cellular disturbances caused by face masks in the innate immune system of marine mussels.

The global problem of plastic pollution caused by MPs and NPs significantly impacts various biological levels in marine species. Given the biological disturbances observed and the subsequent effects on representative marine species it is imperative to incorporate the study of face masks in plastic pollution research, which will facilitate a more accurate projection of the global plastic budget[51]. In addition, the available research evidence suggests that exposure to MPs and NPs can induce more pronounced ecotoxicological effects than microbeads or powdered plastic[80]. Bearing in mind the uncertainties regarding future sanitary crises, there is an urgent need to reduce the environmental impact of the face mask legacy. This necessitates constraints on the amount of these items and the implementation of all measures aimed at preventing their entry into coastal and marine ecosystems. In this sense, the manufacturing use of plasticisers in disposable masks needs strict control and regulation to minimize environmental and public health concerns related to exposure to substances such as phthalates, metals, MPs, and NPs[79,81]. Strong cooperation among scientists, healthcare professionals, industries, and policymakers is essential. Together, they can work towards transitioning to a circular economy that enables the repurposing of products at the end of their life cycle, either for reuse or as raw materials[82].

CONCLUSIONS

Despite the growing scientific evidence on the mechanistic ageing and weathering of single-use face masks and subsequent interactions with aquatic biota, there are still many uncertainties regarding the overall toxicity caused by the multitude of chemical compounds and types of particles that leach from single-use face masks into the marine environment. The present study brings novel findings of the harmful legacy of global face masks in the marine environment by unravelling the oxidative, cytotoxic, and genotoxic disturbances caused by disposable face mask weathering in the mussel *M. galloprovincialis*. Herein, mussel haemocytes arise as a reliable tool for the *in vitro* cytotoxicity assessment regarding the impact of face masks in the marine environment.

DECLARATIONS

Acknowledgements

This work was conducted under the framework of the RESPONSE project (MICROPLAST/0005/2018), funded by Portugal's Science and Technology Foundation (FCT). The authors thank FCT for the funds attributed to CIMA UI/MAR/00350/2020, University of Algarve and to LA/P/0069/2020 granted to the Associate Laboratory ARNET.

Authors' contributions

Study conception and design: Fonseca T, Edo C, Vilke JM, Bebianno MJ
Experimental work and biomarkers analysis: Fonseca T, Edo C, Vilke JM, Astudillo-Pascual M
Analysis and interpretation of results: Fonseca T, Edo C, Vilke JM, Astudillo-Pascual M, Bebianno MJ
Draft manuscript preparation: Fonseca T, Edo C, Vilke JM, Astudillo-Pascual M, Gonçalves JM, Bebianno MJ

Availability of data and materials

Data will be available at the website of RESPONSE the project.

Financial support and sponsorship

This work was funded by the JPI Oceans RESPONSE project (MICROPLAST/0005/2018).

Conflicts of interest

All authors declared that there are no conflicts of interest.

Ethical approval and consent to participate

Not applicable.

Consent for publication

Not applicable.

Copyright

REFERENCES

1. Aragaw TA. Surgical face masks as a potential source for microplastic pollution in the COVID-19 scenario. *Mar Pollut Bull* 2020;159:111517. DOI
2. Filho WL, Salvia AL, Minhas A, Paço A, Dias-Ferreira C. The COVID-19 pandemic and single-use plastic waste in households: a

preliminary study. *Sci Total Environ* 2021;793:148571. DOI

3. Kahlert S, Bening CR. Plastics recycling after the global pandemic: resurgence or regression? *Resour Conserv Recycl* 2020;160:104948. DOI
4. Xanthos D, Walker TR. International policies to reduce plastic marine pollution from single-use plastics (plastic bags and microbeads): a review. *Mar Pollut Bull* 2017;118:17-26. DOI
5. Benson NU, Bassey DE, Palanisami T. COVID pollution: impact of COVID-19 pandemic on global plastic waste footprint. *Heliyon* 2021;7:e06343. DOI
6. Idowu GA, Olalemi AO, Aiyesanmi AF. Environmental impacts of covid-19 pandemic: release of microplastics, organic contaminants and trace metals from face masks under ambient environmental conditions. *Environ Res* 2023;217:114956. DOI
7. Patrício Silva AL, Prata JC, Mouneyrac C, Barcelò D, Duarte AC, Rocha-Santos T. Risks of Covid-19 face masks to wildlife: present and future research needs. *Sci Total Environ* 2021;792:148505. DOI
8. Ammendolia J, Walker TR. Citizen science: a way forward in tackling the plastic pollution crisis during and beyond the COVID-19 pandemic. *Sci Total Environ* 2022;805:149957. DOI
9. Ardusso M, Forero-López AD, Buzzi NS, Spetter CV, Fernández-Severini MD. COVID-19 pandemic repercussions on plastic and antiviral polymeric textile causing pollution on beaches and coasts of South America. *Sci Total Environ* 2021;763:144365. DOI
10. Prata JC, Silva ALP, Walker TR, Duarte AC, Rocha-Santos T. COVID-19 pandemic repercussions on the use and management of plastics. *Environ Sci Technol* 2020;54:7760-5. DOI
11. Okuku E, Kiteresi L, Owato G, et al. The impacts of COVID-19 pandemic on marine litter pollution along the Kenyan Coast: a synthesis after 100 days following the first reported case in Kenya. *Mar Pollut Bull* 2021;162:111840. DOI
12. Hasan NA, Heal RD, Bashar A, Haque MM. Face masks: protecting the wearer but neglecting the aquatic environment? - A perspective from Bangladesh. *Environ Chall* 2021;4:100126. DOI
13. Li B, Huang Y, Guo D, et al. Environmental risks of disposable face masks during the pandemic of COVID-19: challenges and management. *Sci Total Environ* 2022;825:153880. DOI
14. Bondaroff TP, Cooke S. Masks on the beach: the impact of COVID-19 on marine plastic pollution. *OceansAsia* 2020;34:1-79. Available from: https://oceansasia.org/wp-content/uploads/2020/12/Marine-Plastic-Pollution-FINAL.pdf. [Last accessed on 13 Dec 2023]
15. Hiemstra AF, Rambonnet L, Gravendeel B, Schilthuizen M. The effects of COVID-19 litter on animal life. *Anim Biol* 2021;71:215-31. DOI
16. Ma J, Chen F, Xu H, et al. Face masks as a source of nanoplastics and microplastics in the environment: quantification, characterization, and potential for bioaccumulation. *Environ Pollut* 2021;288:117748. DOI
17. Rathinamoorthy R, Raja Balasaraswathi S. Mitigation of microfibers release from disposable masks - An analysis of structural properties. *Environ Res* 2022;214:114106. DOI
18. Huang W, Song B, Liang J, et al. Microplastics and associated contaminants in the aquatic environment: a review on their ecotoxicological effects, trophic transfer, and potential impacts to human health. *J Hazard Mater* 2021;405:124187. DOI
19. Wang Z, An C, Chen X, Lee K, Zhang B, Feng Q. Disposable masks release microplastics to the aqueous environment with exacerbation by natural weathering. *J Hazard Mater* 2021;417:126036. DOI
20. Rebelein A, Int-Veen I, Kammann U, Scharsack JP. Microplastic fibers - Underestimated threat to aquatic organisms? *Sci Total Environ* 2021;777:146045. DOI
21. Saliu F, Veronelli M, Raguso C, Barana D, Galli P, Lasagni M. The release process of microfibers: from surgical face masks into the marine environment. *Environ Adv* 2021;4:100042. DOI
22. Kumar P. Role of plastics on human health. *Indian J Pediatr* 2018;85:384-9. DOI
23. Perez-Venegas DJ, Seguel M, Pavés H, et al. First detection of plastic microfibers in a wild population of South American fur seals (*Arctocephalus australis*) in the Chilean Northern Patagonia. *Mar Pollut Bull* 2018;136:50-4. DOI
24. Le Guen C, Suaria G, Sherley RB, et al. Microplastic study reveals the presence of natural and synthetic fibres in the diet of King Penguins (*Aptenodytes patagonicus*) foraging from South Georgia. *Environ Int* 2020;134:105303. DOI
25. Catalano B, Moltedo G, Martuccio G, et al. Can *Hediste diversicolor* (Nereidae, Polychaete) be considered a good candidate in evaluating PAH contamination? A multimarker approach. *Chemosphere* 2012;86:875-82. DOI
26. Paul-Pont I, Lacroix C, González Fernández C, et al. Exposure of marine mussels *Mytilus* spp. to polystyrene microplastics: toxicity and influence on fluoranthene bioaccumulation. *Environ Pollut* 2016;216:724-37. DOI
27. Sussarellu R, Suquet M, Thomas Y, et al. Oyster reproduction is affected by exposure to polystyrene microplastics. *Proc Natl Acad Sci U S A* 2016;113:2430-5. DOI
28. Gonçalves JM, Bebianno MJ. Nanoplastics impact on marine biota: a review. *Environ Pollut* 2021;273:116426. DOI
29. Au SY, Bruce TF, Bridges WC, Klaine SJ. Responses of *Hyalella azteca* to acute and chronic microplastic exposures. *Environ Toxicol Chem* 2015;34:2564-72. DOI
30. Coppock RL, Galloway TS, Cole M, Fileman ES, Queirós AM, Lindeque PK. Microplastics alter feeding selectivity and faecal density in the copepod, *Calanus helgolandicus*. *Sci Total Environ* 2019;687:780-9. DOI
31. Alnajar N, Jha AN, Turner A. Impacts of microplastic fibres on the marine mussel, *Mytilus galloprovinciallis*. *Chemosphere* 2021;262:128290. DOI
32. Choi JS, Kim K, Hong SH, Park KI, Park JW. Impact of polyethylene terephthalate microfiber length on cellular responses in the

Mediterranean mussel *Mytilus galloprovincialis*. *Mar Environ Res* 2021;168:105320. DOI

33. Choi JS, Kim K, Park K, Park JW. Long-term exposure of the Mediterranean mussels, *Mytilus galloprovincialis* to polyethylene terephthalate microfibers: implication for reproductive and neurotoxic effects. *Chemosphere* 2022;299:134317. DOI
34. Canesi L, Ciacci C, Fabbri R, Marcomini A, Pojana G, Gallo G. Bivalve molluscs as a unique target group for nanoparticle toxicity. *Mar Environ Res* 2012;76:16-21. DOI
35. Almeda R, Gunaalan K, Alonso-López O, et al. A protocol for lixiviation of micronized plastics for aquatic toxicity testing. *Chemosphere* 2023;333:138894. DOI
36. Rosal R. Morphological description of microplastic particles for environmental fate studies. *Mar Pollut Bull* 2021;171:112716. DOI
37. Edo C, Fernández-Piñas F, Rosal R. Microplastics identification and quantification in the composted Organic Fraction of Municipal Solid Waste. *Sci Total Environ* 2022;813:151902. DOI
38. Gómez-Mendikute A, Cajaraville MP. Comparative effects of cadmium, copper, paraquat and benzo[*a*]pyrene on the actin cytoskeleton and production of reactive oxygen species (ROS) in mussel haemocytes. *Toxicol In Vitro* 2003;17:539-46. DOI
39. Katsumiti A, Gilliland D, Arostegui I, Cajaraville MP. Cytotoxicity and cellular mechanisms involved in the toxicity of CdS quantum dots in hemocytes and gill cells of the mussel *Mytilus galloprovincialis*. *Aquat Toxicol* 2014;153:39-52. DOI
40. Fonseca TG, Auguste M, Ribeiro F, et al. Environmental relevant levels of the cytotoxic drug cyclophosphamide produce harmful effects in the polychaete *Nereis diversicolor*. *Sci Total Environ* 2018;636:798-809. DOI
41. Repetto G, del Peso A, Zurita JL. Neutral red uptake assay for the estimation of cell viability/cytotoxicity. *Nat Protoc* 2008;3:1125-31. DOI
42. Fonseca TG, Carriço T, Fernandes E, Abessa DMS, Tavares A, Bebianno MJ. Impacts of *in vivo* and *in vitro* exposures to tamoxifen: comparative effects on human cells and marine organisms. *Environ Int* 2019;129:256-72. DOI
43. Gomes T, Araújo O, Pereira R, Almeida AC, Cravo A, Bebianno MJ. Genotoxicity of copper oxide and silver nanoparticles in the mussel *Mytilus galloprovincialis*. *Mar Environ Res* 2013;84:51-9. DOI
44. McCord JM, Fridovich I. Superoxide dismutase: an enzymic function for erythrocuprein (hemocuprein). *J Biol Chem* 1969;244:6049-55. DOI
45. Glock GE, McLean P. Further studies on the properties and assay of glucose 6-phosphate dehydrogenase and 6-phosphogluconate dehydrogenase of rat liver. *Biochem J* 1953;55:400-8. DOI
46. Almeida EA, Dias Bainy AC, Dafre AL, Gomes OF, Medeiros MHG, Di Mascio P. Oxidative stress in digestive gland and gill of the brown mussel (*Perna perna*) exposed to air and re-submersed. *J Exp Mar Bio Ecol* 2005;318:21-30. DOI
47. Habig WH, Pabst MJ, Jakoby WB. Glutathione S-transferase: the first enzymatic step in mercapturic acid formation. *J Biol Chem* 1974;249:7130-9. DOI
48. Bradford MM. A rapid and sensitive method for the quantitation of microgram quantities of protein utilizing the principle of protein-dye binding. *Anal Biochem* 1976;72:248-54. DOI
49. Erdelmeier I, Gérard-Monnier D, Yadan JC, Chaudière J. Reactions of *N*-methyl-2-phenylindole with malondialdehyde and 4-hydroxyalkenals. Mechanistic aspects of the colorimetric assay of lipid peroxidation. *Chem Res Toxicol* 1998;11:1184-94. DOI
50. Hermsen E, Mintenig SM, Besseling E, Koelmans AA. Quality criteria for the analysis of microplastic in biota samples: a critical review. *Environ Sci Technol* 2018;52:10230-40. DOI
51. Morgana S, Casentini B, Amalfitano S. Uncovering the release of micro/nanoplastics from disposable face masks at times of COVID-19. *J Hazard Mater* 2021;419:126507. DOI
52. Enfrin M, Lee J, Gibert Y, Basheer F, Kong L, Dumée LF. Release of hazardous nanoplastic contaminants due to microplastics fragmentation under shear stress forces. *J Hazard Mater* 2020;384:121393. DOI
53. Tesfaldet YT, Ndeh NT. Assessing face masks in the environment by means of the DPSIR framework. *Sci Total Environ* 2022;814:152859. DOI
54. Sullivan GL, Delgado-Gallardo J, Watson TM, Sarp S. An investigation into the leaching of micro and nano particles and chemical pollutants from disposable face masks - linked to the COVID-19 pandemic. *Water Res* 2021;196:117033. DOI
55. Gonçalves JM, Benedetti M, d'Errico G, Regoli F, Bebianno MJ. Polystyrene nanoplastics in the marine mussel *Mytilus galloprovincialis*. *Environ Pollut* 2023;333:122104. DOI
56. Alimi OS, Farner Budarz J, Hernandez LM, Tufenkji N. Microplastics and nanoplastics in aquatic environments: aggregation, deposition, and enhanced contaminant transport. *Environ Sci Technol* 2018;52:1704-24. DOI
57. De-la-Torre GE, Dioses-Salinas DC, Pizarro-Ortega CI, et al. Face mask structure, degradation, and interaction with marine biota: a review. *J Hazard Mater Adv* 2023;10:100326. DOI
58. Gonzalez-Rey M, Bebianno MJ. Does non-steroidal anti-inflammatory (NSAID) ibuprofen induce antioxidant stress and endocrine disruption in mussel *Mytilus galloprovincialis*? *Environ Toxicol Pharmacol* 2012;33:361-71. DOI
59. Lacy F, Gough DA, Schmid-Schönbein GW. Role of xanthine oxidase in hydrogen peroxide production. *Free Radic Biol Med* 1998;25:720-7. DOI
60. Sies H. Role of metabolic H_2O_2 generation: redox signaling and oxidative stress. *J Biol Chem* 2014;289:8735-41. DOI
61. Regoli F, Giuliani ME. Oxidative pathways of chemical toxicity and oxidative stress biomarkers in marine organisms. *Mar Environ Res* 2014;93:106-17. DOI
62. Adams JK, Dean BY, Athey SN, et al. Anthropogenic particles (including microfibers and microplastics) in marine sediments of the Canadian Arctic. *Sci Total Environ* 2021;784:147155. DOI

63. Islam N, Garcia da Fonseca T, Vilke J, et al. Perfluorooctane sulfonic acid (PFOS) adsorbed to polyethylene microplastics: accumulation and ecotoxicological effects in the clam *Scrobicularia plana*. *Mar Environ Res* 2021;164:105249. DOI
64. Espinoza SE, Guo H, Fedarko N, et al. Glutathione peroxidase enzyme activity in aging. *J Gerontol Series A* 2008;63:505-9. DOI
65. Gong Z, Tian G, Huang Q, Wang Y, Xu H. Reduced glutathione and glutathione disulfide in the blood of glucose-6-phosphate dehydrogenase-deficient newborns. *BMC Pediatr* 2017;17:172. DOI
66. Ho H, Cheng M, Chiu DT. Glucose-6-phosphate dehydrogenase - from oxidative stress to cellular functions and degenerative diseases. *Redox Rep* 2007;12:109-18. DOI
67. Lee HY, Ithnin A, Azma RZ, Othman A, Salvador A, Cheah FC. Glucose-6-phosphate dehydrogenase deficiency and neonatal hyperbilirubinemia: insights on pathophysiology, diagnosis, and gene variants in disease heterogeneity. *Front Pediatr* 2022;10:875877. DOI
68. Hayes JD, Flanagan JU, Jowsey IR. Glutathione transferases. *Annu Rev Pharmacol Toxicol* 2005;45:51-88. DOI
69. Aquilano K, Baldelli S, Ciriolo MR. Glutathione: new roles in redox signaling for an old antioxidant. *Front Pharmacol* 2014;5:196. DOI
70. Hoarau P, Garello G, Gnassia-Barelli M, Romeo M, Girard JP. Purification and partial characterization of seven glutathione *S*-transferase isoforms from the clam *Ruditapes decussatus*. *Eur J Biochem* 2002;269:4359-66. DOI
71. Capolupo M, Gunaalan K, Booth AM, Sørensen L, Valbonesi P, Fabbri E. The sub-lethal impact of plastic and tire rubber leachates on the Mediterranean mussel *Mytilus galloprovincialis*. *Environ Pollut* 2021;283:117081. DOI
72. Provenza F, Rampih D, Pignattelli S, et al. Mussel watch program for microplastics in the Mediterranean sea: identification of biomarkers of exposure using *Mytilus galloprovincialis*. *Ecol Indic* 2022;142:109212. DOI
73. Prata JC, da Costa JP, Lopes I, Duarte AC, Rocha-Santos T. Environmental exposure to microplastics: an overview on possible human health effects. *Sci Total Environ* 2020;702:134455. DOI
74. Prokić MD, Radovanović TB, Gavrić JP, Faggio C. Ecotoxicological effects of microplastics: examination of biomarkers, current state and future perspectives. *TrAC Trends Anal Chem* 2019;111:37-46. DOI
75. Zhang Y, Song J, Yuan H, Xu Y, He Z, Duan L. Biomarker responses in the bivalve (*Chlamys farreri*) to exposure of the environmentally relevant concentrations of lead, mercury, copper. *Environ Toxicol Pharmacol* 2010;30:19-25. DOI
76. Ribeiro F, Garcia AR, Pereira BP, et al. Microplastics effects in *Scrobicularia plana*. *Mar Pollut Bull* 2017;122:379-91. DOI
77. Von Moos N, Burkhardt-Holm P, Köhler A. Uptake and effects of microplastics on cells and tissue of the blue mussel *Mytilus edulis* L. after an experimental exposure. *Environ Sci Technol* 2012;46:11327-35. DOI
78. Sendra M, Sparaventi E, Blasco J, Moreno-Garrido I, Araujo CVM. Ingestion and bioaccumulation of polystyrene nanoplastics and their effects on the microalgal feeding of *Artemia franciscana*. *Ecotoxicol Environ Saf* 2020;188:109853. DOI
79. Chang X, Wang WX. Phthalate acid esters contribute to the cytotoxicity of mask leachate: cell-based assay for toxicity assessment. *J Hazard Mater* 2023;459:132093. DOI
80. Kutralam-Muniasamy G, Pérez-Guevara F, Elizalde-Martínez I, Shruti VC. Review of current trends, advances and analytical challenges for microplastics contamination in Latin America. *Environ Pollut* 2020;267:115463. DOI
81. Khoironi A, Hadiyanto H, Hartini E, Dianratri I, Joelyna FA, Pratiwi WZ. Impact of disposable mask microplastics pollution on the aquatic environment and microalgae growth. *Environ Sci Pollut Res* 2023;30:77453-68. DOI
82. van Straten B, van der Heiden DR, Robertson D, et al. Surgical waste reprocessing: injection molding using recycled blue wrapping paper from the operating room. *J Clean Prod* 2021;322:129121. DOI

Gagné *et al. Water Emerg Contam Nanoplastics* 2024;3:4
DOI: 10.20517/wecn.2023.60

Water Emerging Contaminants & Nanoplastics

Research Article

Open Access

Simple detection of polystyrene nanoparticles and effects in freshwater mussels: method development and *in situ* application to urban pollution

François Gagné, Maxime Gauthier, Chantale André

Aquatic Contaminants Research Division, Environment and Climate Change Canada, Montréal H2Y 1E7, Québec, Canada.

Correspondence to: Prof. François Gagné, Aquatic Contaminants Research Division, Environment and Climate Change Canada, 105 McGill, Montréal H2Y 1E7, Québec, Canada. E-mail: francois.gagne@ec.gc.ca

How to cite this article: Gagné F, Gauthier M, André C. Simple detection of polystyrene nanoparticles and effects in freshwater mussels: method development and *in situ* application to urban pollution. *Water Emerg Contam Nanoplastics* 2024;3:4. https://dx.doi.org/10.20517/wecn.2023.60

Received: 4 Oct 2023 **First Decision:** 29 Nov 2023 **Revised:** 6 Dec 2023 **Accepted:** 15 Dec 2023 **Published:** 21 Dec 2023

Academic Editors: Damià Barceló, Mohammad Hadi Dehghani **Copy Editor:** Pei-Yun Wang **Production Editor:** Pei-Yun Wang

Abstract

The ubiquity of plastics in environments worldwide is raising concerns about their toxicity to organisms. The purpose of this study was to investigate simple means to determine the exposure and effects of nanoplastics (NPs) in the freshwater mussels *Elliptio complanata* (*E. complanata*). NP tissue levels were determined using a plasmonic nanogold sensor probe and effects were determined using the refractive index (RI) and thiol-reaction rates (TRR) in protein-dense tissue extracts. This method was adapted to quantitatively measure the concentration of NPs in tissues using a salting-out extraction in the presence of acetonitrile (ACN). Concentrated solutions of albumin were first spiked with NPs to evaluate changes in RI and TRR to determine crowding effects. The data revealed that NPs readily decreased the RI and TRR in albumin *in vitro*. These three simple assays were then applied on freshwater mussels caged for 3 months at various sites in a largely populated area. Mussels downstream of the city center and found at the street runoff discharge sites were highly contaminated by NPs and the RI and TRR were also reduced. In conclusion, simple and readily accessible assays to assess the NP contamination based on a visual nanogold sensor technology, and the effects of plastics are proposed for freshwater mussels.

Keywords: Polystyrene nanoplastics, nanogold sensor probe, refractive index, thiol-reaction rates, *Elliptio complanata*, municipal effluents

INTRODUCTION

Plastic materials are commonly found in many objects in our daily lives, such as clothing, personal care products, food packages, and drink containers. They provide numerous benefits in the fabrication of domestic and industrial products owing to properties such as their relative inertness, lightweightness, resistance to shock, and low cost of production[1]. Given the global and exponential consumption of plastics and the limited regulation of plastic waste disposal, it is estimated that five trillion fragments exceeding weights of 250,000 tons of plastics already found their way into oceans[2]. In the environment, plastics are gradually degraded into smaller particles termed microplastics (MPs, for sizes between 5 mm to 1 μm) and nanoplastics (NPs, for sizes between 1-1,000 nm[3]). The small size and high surface area of NPs make their analysis tedious in various environmental compartments[4,5]. While MPs are commonly analyzed using microscopic Fourier transform infrared, Raman spectroscopy, and thermo-analytical methods, NPs represent an ongoing challenge. At the moment, methods to detect NPs, which behave differently than MPs and dissolved contaminants, are lacking for organisms. Traditionally, methods used to study plastics involve specialized imaging techniques, separation by chromatographic/field flow techniques, and infrared spectroscopy. An important proportion of plastic materials are retained by municipal effluents and ongoing studies examine ways to remove and degrade plastic on-site[6]. These processes involve separation approaches such as absorption, filtration, and advanced oxidation to separate and degrade these materials at the wastewater treatment plant. The wide range of particle sizes adds to the complexity of global plastic contamination and raises questions as to the ability of the ecosystem to tolerate this pollution on such a large scale. In opposition to MPs, NPs can diffuse across cellular membranes and may perturb cellular physiology. A recent review highlighted that NPs are bioavailable and lead to oxidative stress, inflammation, and potentially cancers[7]. Hence the ability of NPs to diffuse across biological membranes and their ubiquity in the environment may pose risks to the sustainability of aquatic ecosystems and need to be further addressed.

The accumulation of NPs in crowded intracellular compartments can disrupt the complex fractal organization of protein networks[8,9], resulting in the loss of protein function and ultimately impair enzyme activity. These interactions involving hydrophobic surfaces of NPs and local ionic properties of proteins can result in the coating of various proteins [e.g., lysozyme, albumin, and lactate dehydrogenase (LDH)] and can lead to changes in the protein organization. During the aging of NPs, the hydrophobic surface is oxidized by UV or ozone-forming carboxylates at the surface, which can also add to the interaction with the hydrophobic and local positive charges of proteins[10]. The refractive index (RI) of proteins represents a simple and cheap analytical measure to determine the changes in protein concentration, conformation, and composition[11,12]. Changes in the RI per protein mass reveal changes in the conformation and composition of proteins at concentration scales approaching those found in cells (100-400 mg/mL). Within this concentration range, free diffusion of solutes is restricted and could expectedly limit enzyme-catalyzed reaction rates. For example, the LDH activity was decreased by polystyrene (Ps) NPs (PsNPs) of 100 nm diameter[13]. In turn, decreased LDH activity was also reflected by a reduced affinity for pyruvate co-substrate (higher K_M) owing to the reduced fractal dimension of LDH kinetics. Cytoplasmic proteins and lipids could agglomerate during sustained oxidative stress, forming insoluble complexes associated with age-related pigments or lipofuscins[14]. Mediterranean mussels exposed for 7 days to plastic and tire rubber leachates showed elevated levels of oxidative damage and loss of lysosomal stability with increased levels of lipid peroxidation and lipofuscins. When β-amyloid proteins (or other proteins with β-sheet conformation) undergo oxidative degradation, they form insoluble plaques involved with neurodegeneration and amyloidosis in various organs and tissues[15]. Hence, the evaluation of amyloids in organisms exposed to pollution could prove a useful chronic toxicity biomarker associated with the disruption in protein organization in the cytoplasm. These changes could be easily determined by measuring (1) the changes in

RI in concentrated protein suspensions; and (2) the formation of 2-nitro-5-thiobenzoate (TNB), which is produced by the reaction between free thiols and 5,5-dithio-bis-2-nitrobenzoic acid (DTNB). The basis of these simple assays consists of the measurements of the reorganization of dense protein networks by NPs that influence the RI and lower the enzymatic reaction rate in a restricted diffusion microenvironment.

This study aimed to suggest simple and quick markers for the assessment of exposure and effects of PsNPs in aquatic organisms. For this study, we chose a freshwater mussel *Elliptio complanata* (*E. complanata*), endemic to the Saint-Lawrence River, as a sentinel species to reflect the NP contamination in various urban contexts. To assess the exposure of mussels to NPs, a newly developed plasmonic nanogold (nAu) sensor probe allowing the visual detection and quantitation of NPs, requiring only a cell phone camera and free application for color analysis[16], was adapted in biological tissues. Effects of NPs were determined by changes in the RI and thiol-reaction rates (TRR) first with concentrated solutions of albumin *in vitro*. We also tested these markers, along with neutral lipids, aldehydes, and amyloids, in the previously exposed *E. complanata*. These methods were applied to experimentally caged mussels (1) downstream of a large city; (2) in a municipal effluent dispersion plume; (3) at a rainfall/road overflow site, which is an important source of tire wear nanoparticles (TWNPs); and (4) in a pristine lake for comparisons.

MATERIAL AND METHODS

In vitro effects of polystyrene nanoparticles

The influence of PsNPs on the RI and TRR in concentrated albumin was examined *in vitro* to highlight potential biophysical properties of interest in the development of NP biomarkers. A solution of bovine serum albumin (100 mg/mL; MilliporeSigma Canada Ltd., Oakville, Canada), which corresponds to the concentration range of proteins in eucaryotic cell cytoplasm[17] (100-400 mg/mL), was prepared in phosphate-buffered saline (PBS, 140 mM NaCl, 1 mM KH_2PO_4, 1 mM $NaHCO_3$, pH 7.4). The aliquots of 200 µL were exposed to increasing concentrations of PsNPs (0, 0.05, 0.1, and 0.15 µg/mL; Polyscience Inc, Warrington, USA) for 5 min at RT. The PsNPs were uncoated spheres with a diameter of 20 nm, and dilutions were prepared in MilliQ deionized water to limit aggregation. The RI was determined in the albumin-rich solutions using PBS as blank (RI = 1.3326) using an electronic RI device (HDR-P5, Fisher brand, Canada). This preliminary experiment revealed that PsNPs alone did not influence the RI. Then, the TRR was determined by adding 20 µL of 1 mM 5,5'-dithiobis-2-nitrobenzoate (DTNB; MilliporeSigma Canada Ltd., Oakville, Canada) to 200 µL of albumin concentrate[18]. The absorbance was recorded at 412 nm using a microplate reader (model: Synergy-4, Bioteck Instruments, Winooski, USA) for 15 min with 30 s intervals.

Gold nanoparticle - mercaptoundecanoic acid assay

The detection of NPs was achieved using a recently developed nAu plasmonic sensor methodology initially designed for the visualization of NPs in drinking water and from the leaching of heated tea bags or other materials[16]. This methodology was adapted to biological tissues by introducing a preliminary PsNPs salting-out extraction step and recuperation with acetonitrile (ACN) as previously described[19]. The nAu suspension (mean diameter of particles: 14 nm) was commercially obtained from nanoComposix (San Diego, USA) as 50 µg/mL suspension containing 1 mM citrate. The nAu suspension (10 mL) was treated with 0.01% mercaptoundecanoic acid (MUA; prepared in ethanol 100%) for 12 h at RT in the dark to allow binding of the lipophilic acid MUA to nAu to form nAu-MUA complexes [Figure 1]. This solution was filtered through a 0.22 µm cellulose membrane and centrifuged (15,000 × *g*, at 20 °C) for 5 min. The supernatant was discarded, and the pellet was resuspended in half the volume (5 mL) of distilled water (10% ethanol or water) to remove the unbound MUA and citrate. The assay consisted of adding 10 µL of the test sample to 200 µL of the nAu-MUA suspension, followed by the addition of 10 µL of 100 mM HCl (MilliporeSigma Canada Ltd., Oakville, Canada). To investigate the responsiveness of the assay to various

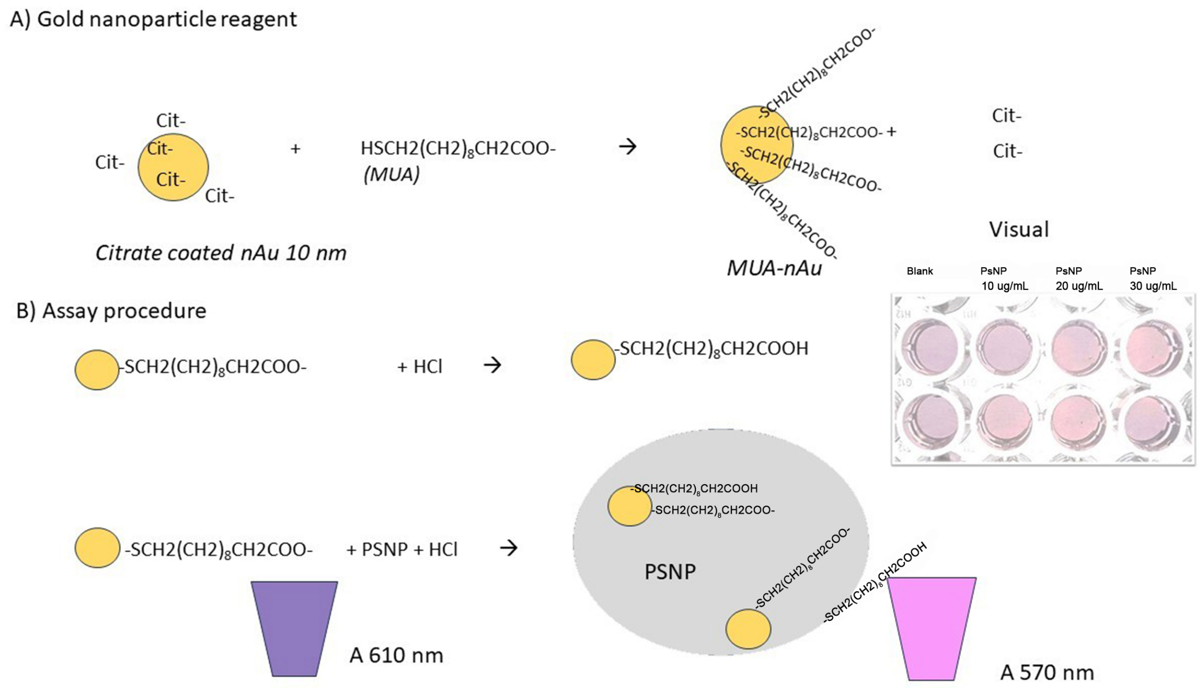

Figure 1. Methodology overview for the nAu sensor for the detection of NPs. Gold nanoparticles (nAu) of 10 nm diameter are first labeled for 24 hr to mercaptoundecanoic acid (MUA) to form nAu-MUA (A). The nAu-MUA complexes are separated from unreacted MUA by centrifugation and resuspension in 10% ethanol. The nAu-MUA is colored violet in the presence of 5 mM HCl in the absence of NPs (B). When it binds to the hydrophobic NPs, the violet color (610 nm) changes to a red wine color (550-580 nm) in a concentration-dependent manner[16]. MUA: Mercaptoundecanoic acid; NPs: nanoplastics; nAu: nanogold.

types of plastics, we examined the following types of plastics: PsNP of different sizes (20, 50, and 100 nm diameter), polyethylene terephthalate (PET) leachates from a 4-year-old water bottle, and tire wear nanoparticles (TWNP) leachates. The different sizes of PsNPs were examined to determine the influence of size on the plasmonic signals at 523 and 610 nm (see below). The TWNP leachates were prepared from drilling dust in new tires with a diamond-coated drilling probe (0.5 cm diameter) and from an ethanol-based commercial formulation of recycled used tire crumbs (particle size: 0.5-1 mm, 40 mg/mL) as previously described[20]. This suspension was exposed to the following cycle three times: frozen at -85 °C, thawed at RT, and sonicated for 1 h on the highest setting. Then, the suspension was filtered through a 0.22 µm cellulose membrane and kept at RT until analysis. For PET water bottles, the bottles (150 mL) were left on a shelf for 4 years under normal light (12-10 h) and dark diurnal (12-14 h) cycles. The bottles were then opened, filtered on a 0.22 µm pore filter and the sample was analyzed directly (no addition of ACN). Without NPs, the addition of HCl causes the bright red color of the nAu-MUA solution (523 nm) to shift to a dark purple color (610 nm). This purple color indicates aggregation of nAu-MUA complexes, whereas monomeric nAu-MUA appears light red. When NPs are present under aggregation conditions (HCl), the nAu-MUA complexes interact with the hydrophobic surface of the NPs, thereby limiting aggregation of the nAu-MUA complex. A blue shift in the absorbance from the aggregated form of the nAu-MUA complex at 610 nm to 560-590 nm indicates increased distance between aggregated nAu-MUA by interaction with NPs[21]. After 5 min, the absorbance (plasmon resonance) was measured (523, 570, and 610 nm) using both a microplate reader (model: Synergy-4, Bioteck Instruments, Winooski, USA) and a Samsung smartphone camera using a free application (RGB color detector) for color analysis (R band). This application analyzes the intensity in the R band of the sample from the picture taken. The limit of detection (blank standard deviation × 2) was estimated at 8 µg/mL for the 50 nm diameter PsNP, which corresponds to tissue concentrations in the order of 50 ng/mg tissues.

Extraction and detection of NPs from mussel homogenates

As stated before, this method was further adapted for biological mussel tissues by conducting a preliminary salting-out extraction of NPs using saturated NaCl (5 M)/ACN[19]. The freshwater mussels were collected at a reference site, a pristine lake 100 km north in the Laurentians area, far from anthropogenic activity. Following an acclimation period of 3 weeks, they were caged (from July to October 2017) at the following sites: (1) a rainfall overflow site (OVF); (2) a site 15 km downstream from the center of Montréal, QC, Canada (Down-city); and (3) a site in the Saint-Lawrence River 8 km downstream of the municipal effluent dispersion plume of the city of Montréal (Down-Effluent). We also selected Down-Effluent, a site where wastewater treatment occurs and where a lower plastic exposure is expected. For each site, three cages containing 20 mussels were placed at 1 m depth. At the end of the 3-month exposure period, mussels were brought back to the laboratory (Montréal, Québec, Canada) and purged in clean water overnight at 15 °C, and their digestive glands were excised and homogenized in Hepes-NaOH buffer (10 mM, pH 7.4) containing 100 mM NaCl, 1 µg/mL aprotinin (protease inhibitors; MilliporeSigma Canada Ltd. Oakville, Canada) and 1 mM ethylenediaminetetraacetic acid (EDTA). The homogenates were centrifuged at 2,500 × *g* (5 min, 20 °C) to remove large tissue debris. The extraction procedure was carried out as follows: the supernatant was mixed with 2 volumes of saturated 5 M NaCl followed by 0.5 volume of ACN. After 15-30 min mixing, the sample was centrifuged (1,500 × *g*, 5 min) to separate the organic phase (upper phase) from the aqueous (lower phase). Preliminary experiments with fluorescently labeled PsNPs (50 to 100 nm) showed that NPs readily partitioned (> 98%) in ACN in high salt conditions. For the detection assay, 200 µL of the nAu-MUA suspension was mixed with 10 µL of samples, and the color changes were measured as described above. Preliminary experiments also revealed that ACN did not influence the reaction process (color changes) and could replace ethanol at 5% concentration [Table 1]. Blanks and additions of PsNPs in the homogenate fractions were prepared in the presence of ACN for method validation [Table 2].

Refractive index, neutral lipids, and amyloid estimations

The changes in RI and TRR were also determined in the digestive gland fractions (10,000 × *g*, 20 min, 2 °C). The levels of proteins were determined in the homogenate and in S10 digestive gland fractions (10,000 × *g*, 30 min, 4 °C) using the Coomassie blue dye binding principle, and bovine serum albumin was used for calibration[22]. The RI was directly measured in homogenate fractions (between 8 and 16 mg/mL protein concentration) as described above. To measure the TRR, the homogenate samples were diluted to 1 mg/mL in PBS and 1 mM of DTNB was added and 412 nm absorbance changes followed for 40 min as described above[18].

The levels of neutral lipids were determined in the homogenates using Nile red dye[23]. Briefly, a 20 µL of the homogenates was mixed with 200 µL of Nile red dye (10 µM, in PBS) and fluorescence was measured (excitation 485 nm, emission 520 nm) with a fluorometer (model: TB-380, Turner Biosystems, San Jose, USA). Calibration was achieved using 0.01% Tween-20 and the data were expressed as mg lipids/mg proteins.

The levels of amyloid proteins were estimated by the centrifugation methodology using Congo red (MilliporeSigma Canada Ltd. Oakville, Canada) as previously described[24]. The principle of the assay resides in the observation that amyloid proteins (insoluble in saline media such as PBS but soluble in distilled water) decrease the absorbance of the dye at 490 nm in a concentration-dependent manner. Briefly, the homogenate 1,500 × *g* fraction was centrifuged at 10,000 × *g* for 10 min and the pellet resuspended in PBS. This process was repeated 4 more times, and the pellet was washed once in distilled water and centrifuged

Table 1. Comparison of the nAu-MUA methodology in the presence of EtOH or ACN

Added PsNP	Absorbance[1] (λ = 570 nm)	Absorbance[2] (λ = 570 nm)	RI[2]
0.0 mg/mL (blank)	0.00	0.00	1.3365
0.6 mg/mL	0.10	0.09	1.3362
1.3 mg/mL	0.15	0.13	1.3363
2 mg/mL	0.23	0.21	1.3363

[1]Final concentration of EtOH = 10%; [2]Final concentration of ACN = 5%. ACN: Acetonitrile; PsNP: polystyrene nanoplastic; RI: refractive index.

Table 2. Calibration of the nAu-MUA assay for PsNPs

Concentration	R signal	Absorbance (λ = 570 nm)	RI	Extrapolated concentration	Concentration standard addition
Direct calibration (external)					
0 (blank)	162	0.00	1.3362		
20 µg/mL	168	0.04	1.3365		
40 µg/mL	174	0.07	1.3363		
60 µg/mL	193	0.10	1.3363		
Standard addition (internal)					
0 (sample)	170			30	27.4 µg/mL
+20 µg/mL	176			53	
+40 µg/mL	181			63	
+60 µg/mL	189			97	

Calibration of the nAu-MUA assay in the presence of 5% ACN using external and standard addition calibration. The detection limit of the assay was determined at 9 µg/mL based on 2 × standard deviations of the blank samples. ACN: Acetonitrile; MUA: mercaptoundecanoic acid; nAu: nanogold; PsNPs: polystyrene nanoplastics; RI: refractive index.

again. The pellet was resuspended once more in distilled water to release amyloids and centrifuged again. The presence of amyloids was determined by the decrease in absorbance at 490 nm (1/490 nm) after adding 10 µM Congo Red in the supernatant and the data were expressed as the inverse of the absorbance/mg proteins in the digestive gland.

The levels of aldehydes were determined in the 10,000 × *g* supernatant of the homogenate using the 4-amino fluorescein fluorescence methodology[25]. Briefly, 20 µL of S10 fraction was mixed with 200 µL of 10 µM 4-aminofluorescein (MilliporeSigma Canada Ltd., Oakville, Canada) in PBS and the fluorescence was taken at 485 nm excitation and 520 nm emission. The data were expressed as relative fluorescence units/mg total proteins. The instrument sensitivity was calibrated with an external standard of 1 µM fluorescein (to 1,000 fluorescence units; supplied with the instrument package).

Data analysis

The experiments were repeated 3 times (n = 3), and the data were presented as mean (± standard error). The data were subjected to the Kruskal-Wallis non-parametric analysis of variance followed by the multiple comparison Conover-Iman test to find differences between groups. Only differences with the reference site were discussed. Correlation analysis was performed using the Pearson-moment procedure. All statistical tests were performed using the StatSoft software package (version 13). The level of significance α of 0.05 was used.

RESULTS AND DISCUSSION

In this study, we adapted and used a simple visualization assay using a nAu sensor probe[16] to assess the exposure of mussels *in situ* to different urban effluents. In addition, we investigated the effects of NPs *in vitro* on the RI and the TRR in an albumin-rich solution and tested these markers, along with neutral lipids and amyloids, in mussels exposed to urban pollution.

Methodological improvement of the nAu-MUA assay

The levels of NPs were determined in biological tissues using the nAu-MUA assay initially developed for the estimation of plastics in simple matrices such as water or plastic tea bag leachates[16]. However, more complex matrices such as digestive gland homogenates inevitably require a primary fractionation step. Therefore, a simple salting-out extraction was designed in the presence of ACN to recuperate NPs in mussel tissues. The nAu-MUA assay was tested in the presence of ACN (5% final concentration). The absorbance at 570 nm and the R color measurements were taken directly in microplates with a smartphone camera or a microplate reader [Table 1]. The absorbance did not change compared to the original method (10% ethanol), suggesting that ACN could also be a suitable solvent for this assay. Additionally, the RI did not change with the addition of PsNPs to nAu-MUA reagent, suggesting negligible aggregation of nAu-MUA. The calibration data revealed that the R color (and the absorbance at 570 nm) increased with the addition of increasing concentrations of PsNPs [Table 2]. Calibration by the standard addition method of a spiked tissue sample revealed the same results as the external calibration method, with regression coefficients ranging from 0.96 to 0.99 [Table 2]. For the standard addition calibration, the test sample was a NaCl/ACN extract of the digestive gland of mussels *E. complanata*. The estimated concentration of PsNPs in the sample was estimated at 30 and 27 μg/mL with the direct and standard addition methodologies, respectively. This suggests that the extraction of PsNPs in ACN from tissues did not introduce important matrix effects. The aggregation of nAu-MUA could be favored by the presence of salts at concentrations over 10 mM, such as HCl or NaCl[16,26]. However, the assay was conducted in ACN fraction devoid of salts. The saturated NaCl/ACN extraction is based on the salting out of large molecules. In this context, less dense plastic particles (usually 0.75-0.95 g/mL) will tend to float at the surface. The ACN step will extract and concentrate these lighter particles. Larger molecules such as peptides/proteins and other large molecules (humic and fulvic acids present in natural organic matter in surface waters) would then precipitate during the centrifugation step[27]. Although the ACN can extract less polar organic compounds (e.g., neutral lipids) along with PsNps (20 to 100 nm in diameter), interference from large amounts of neutral lipids could interfere in the distances between the nAu-MUA-NPs complex. However, significant differences between the direct calibration method and the standard addition method were not found, suggesting the absence of interferences in the conditions used in this study. Moreover, changes in lipids in digestive gland homogenates were not significantly correlated with NPs as determined by the plasmonic nAu-MUA assay. Interference from dissolved organic matter (> 15 mg/L) was observed with the nAu-MUA assay when used directly on surface water samples[27]. In amounts exceeding 15 mg/L, only 15%-20% of the NPs were detected when the assay was used directly on the water samples. An extraction step should be considered when the assay is to be applied directly to the sample with high levels of dissolved organic carbon, as used in the present study.

Responsiveness of the nAu-MUA assay to various plastics

The nAu-MUA assay was tested against various types of plastics such as PsNPs (20, 50, and 100 nm), water from 4-year-old PET water bottles, and tire/recycled tire leachates [Table 3]. As expected, the test responded to PsNPs. Tire wear leachates also elicited a contrasted positive signal compared to the blanks, suggesting that this assay also responds to petroleum-based rubber materials from tire wear and recycled tires. The nAu-MUA assay was tested on water from 4-year-old PET drinking water bottles and the assay also detected the presence of NPs. The nAu-MUA assay responded well to different types and sizes of plastics such as PS, rubber (tire), and PET. The detection of NPs in water bottles corroborates previous findings[16],

Table 3. Response of the nAu-MUA assay to various types of plastics

Materials[1]		**Response factor**[2]
Blank		1.00
Distilled water		1.00
PsNPs	20 nm[3]	1.21
	50 nm[3]	1.17
	100 nm[3]	1.20
Tire wear particle leachates[4]		1.20
Tire crumb[4]		1.14
Water from 4-years-old PET bottle[5]		1.17

[1]10 µL of sample added to 200 µL nAu-MUA; [2]Obtained by dividing the R color sample by the R color blank; [3]15 µg/mL standard solutions; [4]400 µg of ethanol tire wear and aged recycled tire rubber (crumb) powders (1 g/10 mL ethanol); [5]See material and method for details. Note: no extraction or concentration step. MUA: Mercaptoundecanoic acid; nAu: nanogold; PET: polyethylene terephthalate; PsNPs: polystyrene nanoplastics.

i.e., NPs < 100 nm are released from plastic bottles. This assay also proved to work with polypropylene and polyethylene (tea bags) samples and seemed unaffected by the positive or negative charges at the surface of PsNPs, which are likely to be found in aged plastics.

Detection of NPs in mussel digestive glands

The relative levels of NPs were determined in the extract of the digestive gland of the freshwater mussel *E. complanata* following 3 months of caging experiments at various sites in the province of Québec (Canada). We observed a significantly ($P < 0.05$) higher signal for the nAu-MUA assay at the three sites compared to the control [Table 4]. The data revealed that mussels caged 15 km downstream from the city center of Montréal had higher levels of NPs compared to the reference site, in which a very low signal was detected. The levels of NPs were lower in the municipal effluent dispersion plume and were similar to the ones at the overflow site. These results indicate that plastic contamination arises in every site, but more importantly, downstream urban areas, and to a lesser extent, rainfall overflow sites draining nearby roads (tire wear and asphalt erosion) and municipal effluents. In a previous study with caged mussels, similar observations were found in mussels exposed to combined sewer overflows and municipal effluents using size exclusion gel chromatography and fluorescence detection using a molecular rotor probe for NPs in tissues[28]. Increased detection of microplastics and NPs was found in irrigated edible plants downstream municipal wastewater[29]. Interestingly, although plastics are found in most lakes and river samples, their levels were increased at sites close to urban pollution, including street runoffs in combined sewer overflows. The lower NP signals in the digestive gland extracts of mussels exposed to municipal effluent compared to Down city suggest that wastewater treatment retains NPs during the process. Following wastewater treatments, levels of MPs and NPs were shown to be drastically reduced compared to the raw influent wastewater in two different municipal effluents[30]. In this study, the removal of MPs (from 26 to 1.75 µg/L) and NPs (from 12 to 0.71 µg/L) represented diminutions of 93% and 94%, respectively. Although proportions of NPs (particle size: 0.01 to 1 µm) were similar in both effluents, the removal efficiency was least effective with NPs (< 1 µm) compared to MPs (> 1 µm). In another study on larger MPs, the average abundance of MP in the influent was lowered (from 196 to 9 particles/L), which represents efficiency between 90% and 97%[31]. These observations indicate that the removal of MPs by the wastewater treatment plant, yet incomplete, cannot be ignored. This is consistent with the low levels of NPs in the digestive glands of mussels caged downstream of the municipal effluent plume observed in our study compared to the highest downstream of the city site. Another explanation could be that a lowered filtration rate leading to reduced uptake by mussels could also explain the discrepancy observed between both sites. However, this was not evaluated in our study. Decreased filtration rates and acetylcholinesterase activity were found in

Table 4. Case study with caged lake mussels downstream a large city, rainfall overflow, and municipal treated effluent in the Saint-Lawrence River

Caging sites	nAu-MUC method (µg/g)	Lipid (mg/g tissue)	Aldehydes (RFU/mg proteins)	Amyloids 1/ (Abs × mg proteins)
Reference lake	0.02 ± 0.01	16 ± 3 h	110 ± 30	4.9 ± 0.02 h
Down-city	0.11 ± 0.01*	31 ± 5*	200 ± 30*	4.7 ± 0.47 h
Down-Effluent	0.05 ± 0.02*	21 ± 5 h	450 ± 53*	4.3 ± 0.20 h
OVF	0.06 ± 0.01*	21 ± 3*	330 ± 27*	5.5 ± 0.04*

Comparisons were made with the control site. *P < 0.05. nAu: Nanogold; OVF: overflow site.

clams exposed to 80 nm NPs, 6 µm MPs, and ciprofloxacin[32]. Ciprofloxacin, an antibiotic found in municipal wastewater, was shown to worsen the inhibition potential of NPs when co-administered to clams. In another study, marine mussels exposed to elevated PsNP concentrations (0.5 and 5 mg/L) had total antioxidant capacity and acetylcholinesterase activity induced and inhibited, respectively[33]. Acetylcholinesterase activity is usually coupled with filtration rates, indicating that reduced filtration rates could represent an adaptive mechanism to limit exposure and damage caused by NPs. Although not as contrasted as the Down-city site, the overflow site also showed significantly higher NP detection in the mussel digestive glands. This observation suggests that the combined excess of rain and untreated wastewater also contributes to the NPs burden of mussels. The release of NPs from asphalt and tire erosion could also be a contributor to the levels of NPs observed in our study.

Biological and biochemical markers in the mussel digestive glands

In addition to NPs, other biomarkers such as the RI, TRR, aldehydes, neutral lipids, and amyloids in the digestive gland fractions were assessed. Globally, exposure of mussels to urban pollution increased levels of lipids, aldehydes, RI (digestive gland homogenates), and denatured proteins (amyloids). Their levels were highest at the rainfall overflow and downstream the city center sites for lipids and amyloid levels [Table 4]. In our study, we observed a significant increase in neutral lipids at the overflow site and downstream of the city, but not following exposure to the wastewater effluent site [Table 4]. Furthermore, an increased signal for aldehyde formation was observed at all sites [Table 4]. We observed that the RI was significantly lower in mussels downstream of the city as shown below. Interestingly, the highest levels of NPs were also found at this same site. In our study, we also noticed a significant increase in the amyloid contents in mussels exposed to the overflow site [Table 4]. Amyloid formation is involved in several degenerative diseases as a result of a long-term accumulation of oxidatively denatured protein plaques in various tissues and organs[15] (e.g., brain, muscle, and liver) and was referred to as a typical cellular disorder in the physiopathology of aging[34]. To this date, we ignore why amyloids were increased in these mussels, but we observed a significant correlation between amyloids and the RI ($r = 0.66$; $P < 0.01$). This observation strengthens the possible association between these two markers in the digestive gland homogenates.

In vitro investigations of effects of PsNPs in albumin-rich solution and biological matrices

To further investigate the observed changes in the RI and TRRs following exposure to NPs, we conducted an exploratory *in vitro* test to determine the effects of PsNPs on RI and TRRs in an albumin-rich solution and the digestive gland homogenates of *E. complanata* [Figure 2A-D]. Thus, a concentrated albumin solution was prepared at 100 mg/mL near the reported density of intracellular environments[18] and spiked with increasing concentrations of PsNPs. The presence of 50 nm PsNPs decreased the RI of the albumin solution in a concentration-dependent manner (between 0 and 0.15 µg/L, Figure 2A). It is important to state that the addition of PsNPs (without albumin) did not influence the RI of the solution. Furthermore, the TRRs in albumin-rich solutions were determined and revealed a decrease in the reaction rates when over

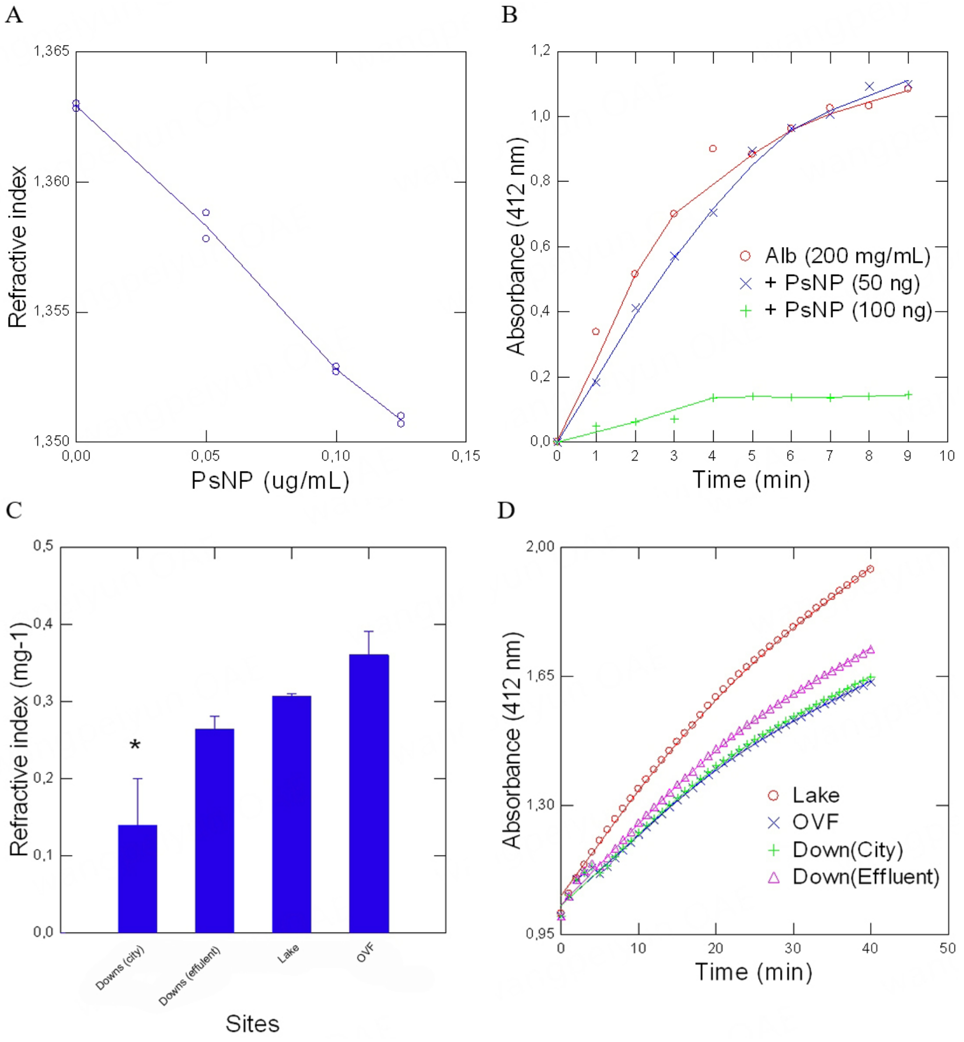

Figure 2. Refractive indexes and TRR following *in vitro* exposure to plastic nanoparticles (A and B) or in *E. complanata* digestive gland extracts following *in situ* exposures (C and D). The RI (A) and the TRR (B) were determined in concentrated albumin solutions. Mussels were encaged for 3 months at various sites and dissected, and digestive glands homogenates were assessed for RI and TRR. OVF: Overflow site; PsNP: polystyrene nanoplastic; RI: refractive index; TRR: thiol-reaction rates.

100 ng of PsNPs were added [Figure 2B]. In turn, this rearrangement could lower the free albumin in the dissolved phase and explain the decreased RI. Overall, these results obtained in albumin-rich solutions contribute to a better understanding of the effects of NPs in protein-rich samples and strengthen the link between the effects of NPs and the biological and biochemical effects observed in the exposed mussel's digestive gland homogenates.

Indeed, albumin could interact with PsNPs, forming local and dense albumin-coated PsNP clusters that restrict the diffusion of substrates[9,35]. Analysis of the reaction rates revealed that the reaction rates over time (a measure of the spectral dimension of the reaction in crowded environments[9]) decreased more strongly in mussels downstream of the urban area compared to the reference lake (results not shown), consistent with the formation of elongated aggregate arrangements of percolation organization. Similarly, TRR could be decreased by the rearrangement of albumin in the presence of PsNPs and perhaps by a non-specific binding of the reagent on the hydrophobic surface of PsNPs. Additionally, the RI and the TRR were also measured in the digestive gland extracts [Figure 2C and D]. The analysis revealed that the RI of the homogenate (normalized to protein content) was significantly decreased at the site with the highest levels of NPs (downstream city center site). Although other contaminants might be at play in these complex environments, it is plausible that NPs contribute to the decreased RI as a result of alteration in protein organization and reaction rates in the digestive gland extracts. Such changes in protein organization were also measured by anisotropic changes in the digestive gland homogenates, consistent with nematic crystal formation in mussels exposed to PsNPs and municipal effluents[36]. The complexation of albumin to PsNPs was previously shown to result from the hydrophobic environment of both albumin and PsNPs[37] and could be positively influenced by the presence of anionic charges on the surface of PsNPs[38]. This complexation is likely to happen given the local cationic patch that albumin displays on its surface and the hydrophobic environment of the NPs, especially when anionic charges are present on aged/weathered NP surfaces. Anionic charges ($R\text{-}COO^-$) were reported to form during the weathering/degradation of plastic materials by UV and ozone[10]. The addition of these anionic charges on the surface of NPs could expectedly weaken the interaction with anionic natural organic matter (e.g., humic acids and alginates) and support interactions with cationic proteinaceous compounds usually found in wastewater. Ultimately, these interactions with NPs could lead to spatial changes in proteins and protein networks and consequently alter enzyme activity. Such influence of PsNPs on the enzymatic activity of LDH was previously reported *in vitro* and mussels exposed to PsNPs[13]. The changes in LDH activity by these NPs were consistent with the altered fractal organization of complex protein networks. Indeed, the calculated fractal dimension of LDH reaction rate was reduced by PsNPs as with F-actin, the natural ligand for LDH, suggesting a loss of affinity for its substrate pyruvate and NADH (increased affinity constant K_M). Indeed, the spectral dimension of the reaction rates reached 1.2, also indicative of a percolation structure (continuous linear dust fragments). Thus, NPs interacting with albumin or protein networks in cells would form percolation-like structures, leading to reduced RI and TRR.

CONCLUSION

In this study, we adapted a simple extraction and detection method for NPs, and we investigated the *in situ* exposure of the freshwater mussel *E. complanata* in polluted urban environments. We also assessed the biochemical effects using several simple markers in exposed mussels and conducted an exploratory *in vitro* test to further understand the effects of NPs in protein-rich samples. Our results suggest that mussels exposed to city effluents are exposed to NPs and show disorders typical of NP exposure. Overall, *E. complanata* proved to be a potential surrogate for NP contamination in biomonitoring studies and responded to various effluents. Given that plastic pollution is ubiquitous and that the traditional NP detection methods (e.g., pyrolysis gas chromatography, thermogravimetric Fourier transformation spectrometry, transmission electron microscopy[39]) are labor- and cost-extensive, the access to quick and cheap assessment methods for the monitoring of plastic contamination and effects are needed. Although this method will need further validation, this study contributes to the development of new accessible tools for institutions and opens new perspectives for preliminary screening strategies to tease out sites with high levels of NPs.

DECLARATIONS

Acknowledgments

The authors are thankful to the Saint-Lawrence Action Plan and Plastics research initiative of Environment and Climate Change Canada for supporting this research. The technical assistance for the mussel caging experiments of Hiba Qchiqach is duly recognized in this project.

Authors' contributions

Conceptualization, methodology, validation, formal analysis, investigation, writing - original draft: Gagné F
Experimentation, analysis, writing -review and editing: Gagné F, Gauthier M, André C
Conceptualization, supervision, resources: Gagné F

Availability of data and materials

Not applicable.

Financial support and sponsorship

None.

Conflicts of interest

All authors declared that there are no conflicts of interest.

Ethical approval and consent to participate

Not applicable.

Consent for publication

Not applicable.

Copyright

REFERENCES

1. Jiang B, Kauffman AE, Li L, et al. Health impacts of environmental contamination of micro- and nanoplastics: a review. *Environ Health Prev Med* 2020;25:29. DOI
2. Eriksen M, Lebreton LCM, Carson HS, et al. Plastic pollution in the world's oceans: more than 5 trillion plastic pieces weighing over 250,000 tons afloat at sea. *PLoS One* 2014;9:e111913. DOI
3. Koelmans AA, Mohamed Nor NH, Hermsen E, Kooi M, Mintenig SM, De France J. Microplastics in freshwaters and drinking water: critical review and assessment of data quality. *Water Res* 2019;155:410-22. DOI
4. Fang C, Luo Y, Naidu R. Microplastics and nanoplastics analysis: options, imaging, advancements and challenges. *TrAC Trend Anal Chem* 2023;166:117158. DOI
5. Lee J, Chae KJ. A systematic protocol of microplastics analysis from their identification to quantification in water environment: a comprehensive review. *J Hazard Mater* 2021;403:124049. DOI
6. Chen Z, Liu X, Wei W, Chen H, Ni BJ. Removal of microplastics and nanoplastics from urban waters: separation and degradation. *Water Res* 2022;221:118820. DOI
7. Kik K, Bukowska B, Sicińska P. Polystyrene nanoparticles: sources, occurrence in the environment, distribution in tissues, accumulation and toxicity to various organisms. *Environ Pollut* 2020;262:114297. DOI
8. Aon MA, Cortassa S, Lloyd D. Chaotic dynamics and fractal space in biochemistry: simplicity underlies complexity. *Cell Biol Int* 2000;24:581-7. DOI
9. Gagné F. Ecotoxicology of altered fractal organization in cells. *Am J Biomed Sci Res* 2020;8:498-502. DOI
10. Li X, Ji S, He E, et al. UV/ozone induced physicochemical transformations of polystyrene nanoparticles and their aggregation tendency and kinetics with natural organic matter in aqueous systems. *J Hazard Mater* 2022;433:128790. DOI
11. Khago D, Bierma JC, Roskamp KW, Kozlyuk N, Martin RW. Protein refractive index increment is determined by conformation as well as composition. *J Phys Condens Matter* 2018;30:435101. DOI
12. Wen J, Arakawa T. Refractive index of proteins in aqueous sodium chloride. *Anal Biochem* 2000;280:327-9. DOI
13. Auclair J, Gagné F. The influence of polystyrene nanoparticles on the fractal kinetics of lactate dehydrogenase. *Biochem Biophys Rep* 2020;23:100793. DOI
14. Capolupo M, Gunaalan K, Booth AM, Sørensen L, Valbonesi P, Fabbri E. The sub-lethal impact of plastic and tire rubber leachates on the Mediterranean mussel *Mytilus galloprovincialis*. *Environ Pollut* 2021;283:117081. DOI
15. Cabaleiro-Lago C, Szczepankiewicz O, Linse S. The effect of nanoparticles on amyloid aggregation depends on the protein stability and intrinsic aggregation rate. *Langmuir* 2012;28:1852-7. DOI
16. Zhou H, Cai W, Li J, Wu D. Visual monitoring of polystyrene nanoplastics < 100 nm in drinking water based on functionalized gold nanoparticles. *Sens Actuators B Chem* 2023;392:134099. DOI

17. Savageau MA. Development of fractal kinetic theory for enzyme-catalysed reactions and implications for the design of biochemical pathways. *Biosystems* 1998;47:9-36. DOI
18. Butterworth PHW, Baum H, Porter JW. A modification of the Ellman procedure for the estimation of protein sulfhydryl groups. *Arch Biochem Biophys* 1967;118:716-23. DOI
19. Gagné F. Isolation and quantification of polystyrene nanoplastics in tissues by low pressure size exclusion chromatography. *J Xenobiot* 2022;12:109-21. DOI
20. Xu EG, Lin N, Cheong RS, et al. Artificial turf infill associated with systematic toxicity in an amniote vertebrate. *Proc Natl Acad Sci U S A* 2019;116:25156-61. DOI
21. Reinhard BM, Siu M, Agarwal H, Alivisatos AP, Liphardt J. Calibration of dynamic molecular rulers based on plasmon coupling between gold nanoparticles. *Nano Lett* 2005;5:2246-52. DOI
22. Bradford MM. A rapid and sensitive method for the quantitation of microgram quantities of protein utilizing the principle of protein-dye binding. *Anal Biochem* 1976;72:248-54. DOI
23. Greenspan P, Mayer EP, Fowler SD. Nile red: a selective fluorescent stain for intracellular lipid droplets. *J Cell Biol* 1985;100:965-73. DOI
24. Pras M, Schubert M, Zucker-Franklin D, Rimon A, Franklin EC. The characterization of soluble amyloid prepared in water. *J Clin Invest* 1968;47:924-33. DOI
25. Xing Y, Wang S, Mao X, Zhao X, Wei D. An easy and efficient fluorescent method for detecting aldehydes and its application in biotransformation. *J Fluoresc* 2011;21:587-94. DOI
26. Choi I, Lee LP. Rapid detection of Aβ aggregation and inhibition by dual functions of gold nanoplasmic particles: catalytic activator and optical reporter. *ACS Nano* 2013;7:6268-77. DOI
27. Pirade F, Lompe KM, Jiménez-lamana J, et al. How suitable is the gold-labelling method for the quantification of nanoplastics in natural water? *AQUA Water Infra Ecosyst Soc* 2023:jws2023278. DOI
28. Gagné F, Roubeau-Dumont E, André C, Auclair J. Micro and nanoplastic contamination and its effects on freshwater mussels caged in an urban area. *J Xenobiot* 2023;13:761-74. DOI
29. Naziri A, Mina T, Manoli K, et al. Looking into the effects of co-contamination by micro(nano)plastics in the presence of other pollutants on irrigated edible plants. *Sci Total Environ* 2023;892:164618. DOI
30. Xu Y, Ou Q, Wang X, et al. Assessing the mass concentration of microplastics and nanoplastics in wastewater treatment plants by pyrolysis gas chromatography-mass spectrometry. *Environ Sci Technol* 2023;57:3114-23. DOI
31. Xu X, Jian Y, Xue Y, Hou Q, Wang LP. Microplastics in the wastewater treatment plants (WWTPs): occurrence and removal. *Chemosphere* 2019;235:1089-96. DOI
32. Guo X, Cai Y, Ma C, Han L, Yang Z. Combined toxicity of micro/nano scale polystyrene plastics and ciprofloxacin to *Corbicula fluminea* in freshwater sediments. *Sci Total Environ* 2021;789:147887. DOI
33. Wang X, Shao S, Zhang T, Zhang Q, Yang D, Zhao J. Effects of exposure to nanoplastics on the gill of mussels *Mytilus galloprovincialis*: an integrated perspective from multiple biomarkers. *Mar Environ Res* 2023;191:106174. DOI
34. Nezelof C. Role of defective intracellular proteolysis in human degenerative diseases. *Bull Acad Natl Med* 2102;196:1587-98. DOI
35. Fang Y, Li H, Ai N, Luo W. Fractal diffusion in a chemical space. *Int J Nonlinear Sci Numer Simul* 2000;1:235-8. DOI
36. Gagné F, Auclair J, André C. Polystyrene nanoparticles induce anisotropic effects in subcellular fraction of the digestive system of freshwater mussels. *Cur Top Toxicol* 2019;15:43-8. Available from: http://www.researchtrends.net/tia/article_pdf.asp?in=0&vn=15&tid=50&aid=6351. [Last accessed on 20 Dec 2023].
37. Kowalczyńska HM, Nowak-Wyrzykowska M, Szczepankiewicz AA, et al. Albumin adsorption on unmodified and sulfonated polystyrene surfaces, in relation to cell-substratum adhesion. *Colloids Surf B Biointerfaces* 2011;84:536-44. DOI
38. Simončič M, Hritz J, Lukšič M. Biomolecular complexation on the “wrong side”: a case study of the influence of salts and sugars on the interactions between bovine serum albumin and sodium polystyrene sulfonate. *Biomacromolecules* 2022;23:4412-26. DOI
39. Jung S, Raghavendra AJ, Patri AK. Comprehensive analysis of common polymers using hyphenated TGA-FTIR-GC/MS and Raman spectroscopy towards a database for micro- and nanoplastics identification, characterization, and quantitation. *NanoImpact* 2023;30:100467. DOI

Iftikhar *et al. Water Emerg Contam Nanoplastics* 2024;3:5
DOI: 10.20517/wecn.2023.58

Water Emerging Contaminants & Nanoplastics

Review

Open Access

Understanding the leaching of plastic additives and subsequent risks to ecosystems

Asmara Iftikhar[1], **Zonaira Qaiser**[1], **Wajiha Sarfraz**[1], **Ujala Ejaz**[2], **Muhammad Aqeel**[3], **Zarrin Fatima Rizvi**[1], **Noreen Khalid**[1]

[1]Department of Botany, Government College Women University, Sialkot 513140, Pakistan.
[2]Department of Plant Sciences, Quaid-i-Azam University, Islamabad 45320, Pakistan.
[3]State Key Laboratory of Grassland Agro-ecosystems, College of Ecology, Lanzhou University, Lanzhou 730000, Gansu, China.

Correspondence to: Dr. Noreen Khalid, Department of Botany, Government College Women University, Kutchehry road, Sialkot 513140, Pakistan. E-mail: Noreen.khalid@gcwus.edu.pk; noreenbasra@gmail.com

How to cite this article: Iftikhar A, Qaiser Z, Sarfraz W, Ejaz U, Aqeel M, Rizvi ZF, Khalid N. Understanding the leaching of plastic additives and subsequent risks to ecosystems. *Water Emerg Contam Nanoplastics* 2024;3:5. https://dx.doi.org/10.20517/wecn.2023.58

Received: 20 Sep 2023 **First Decision:** 17 Nov 2023 **Revised:** 5 Dec 2023 **Accepted:** 26 Dec 2023 **Published:** 4 Jan 2024

Academic Editor: Joana C Prata **Copy Editor:** Pei-Yun Wang **Production Editor:** Pei-Yun Wang

Abstract

Plastic pollutants have emerged as one of the biggest environmental concerns in recent times. The potential hazards arise from the presence of additives within microplastics (MPs), which can leach into the environment. These additives serve a multitude of purposes, resulting in a diverse range of compounds used in plastic formulation. These elements are commonly integrated into plastic molding processes to enhance usability, optimize material performance, and reduce costs. Throughout the lifespan of plastics, there exists a potential for the release of unpolymerized monomers (sometimes more toxic) and additives that are not chemically bound to polymers; these elements pose risks to the environment and, ultimately, human well-being. Assessing the potential impact of MPs on life requires determining the precise chemical composition and the level of exposure to these additives. Phthalates and chemical flame retardants are currently the focus of extensive examination due to their widespread presence in the environment. Following closely behind are stabilizers and antioxidants, which are also undergoing evaluation. Chemical compounds like hexabromocyclododecanes (HBCDs) and polybrominated diphenyl ethers (PBDEs) possess characteristics such as persistence, bioaccumulation, and toxicity. The understanding of the ecotoxicological implications of plastic additives and their discharge from primary plastic materials remains limited at present. The current state of issues concerning the regulations and transparency regarding plastic additive chemicals is marked by a significant lack of openness and clarity. It is paramount to thoroughly comprehend and assess the risks that ecosystems face due to the leaching, degradation, bioaccumulation, and eventual fate of additive compounds when plastics are released into the environment.

Keywords: Plastic leaching, plastic additives, ecotoxicology, microplastics

INTRODUCTION

The use of plastics, a revolutionary invention, has significantly increased in the 20th and 21st centuries. In 2021, global plastic production was estimated at 390.7 million metric tons. This surge in production stems from the manifold economic and social benefits of plastics, which have been instrumental in enhancing the quality of life[1,2]. Synthetic and semi-synthetic materials are part of plastic. Plastics comprise two categories, i.e., thermosets and thermoplastics. Thermoplastics represent a class of plastics that can be easily modified under high-temperature conditions. This category includes polycarbonate (PC), polystyrene (PS), polypropylene (PP), polyarylsulfone (PAS), polyethylene terephthalate (PET), polyvinyl chloride (PVC), polyamides (PA), and thermoplastic elastomers, all of which are commonly found in the environment. Conversely, thermosets denote plastics that retain their form even when subjected to heat, such as vinyl ester, polyurethane, acrylic resin, silicone, melamine resin, phenolic resins, and phenol-formaldehyde[3-7].

Numerous international policies have been established to address the improper disposal of plastic waste; however, mismanagement often leads to the release of such waste, causing detrimental effects on the ecosystem[8,9]. Plastic undergoes degradation via chemical and physical weathering processes, breaking down into smaller fragments known as MPs. These particles come in various sizes, with those measuring < 5 mm categorized as MPs and those smaller than < 1 μm termed nanoplastics[10,11]. Apart from the degradation of large plastics, MPs can also be produced through anthropogenic activities such as in the manufacturing of clothing, cosmetics, nurdles, industrial processes, and wastewater treatment[12].

MPs pose a significant challenge to marine ecosystems globally[13]. Their impact extends beyond the marine environment, as they are increasingly recognized as pollutants across various environmental compartments[14]. Due to their ubiquitous nature and bioavailability, MPs are found extensively in terrestrial environments, marine ecosystems, and plant tissues[4,7,12,15]. This widespread presence potentially amplifies the concentration of contaminants in the environment and burdens biological organisms that inadvertently consume microplastic particles[16]. The interaction between toxic pollutants and MPs presents a considerable environmental concern, impacting the ecosystem and its biota[17,18]. Various toxic chemicals, such as persistent organic pollutants (POPs), also known as hydrophobic organic contaminants (HOCs), include organochlorine pesticides (OCPs), polychlorinated biphenyls (PCBs), and polyaromatic hydrocarbons (PAHs), as well as heavy metals such as lead, copper, zinc, silver, manganese, iron, and aluminum. These contaminants attach to the pitted surfaces of floating MPs in water, facilitated by their wide distribution in water.

Besides contaminants that adsorb onto MPs, additives are another agent that intensifies their ecotoxicity. Approximately 7% of additive compounds are used during the plastic manufacturing process to shape the material and provide specific functions[19,20]. These additives fall into distinct categories such as plasticizers, flame retardants, stabilizers, and antioxidants. Among plasticizers, examples include terephthalates, DEHT, di-2-ethylhexl terephthalate, TOTM, tris-2-ethylhexyl trimellitate, 1,2-cyclohexane dicarboxylic acid, diisononyl ester, and adipates[21]. Beyond their incorporation into MPs, additives find applications in manufacturing biocides, UV protection materials, dye agents, clothing, and formaldehyde-releasing chemicals[22]. Plastic contains a diverse range of additives, monomers, and oligomers. Most of these substances are not chemically bound to the plastic, causing them to leach out and migrate into various matrices (soil, air, water, food, and even human body), leading to harmful consequences[23,24]. For example, the plasticizer di (2 ethyhexyl) phthalate (DEHP) disrupts the endocrine systems of humans and animals. Studies by Tanaka *et al.* demonstrated the accumulation of additives in seabird tissues, revealing the leaching of these substances from plastics, particularly facilitated by the oil components in the digestive tract[25,26]. Moreover, exposure to DEHP for 15-30 days in Carassius auratus (goldfish) resulted in reduced sperm production and diminished motility[27,28].

The existing literature on the leaching of additives from plastic pollution is limited, showcasing a variety of experimental methodologies used in previous studies. Plastic leaching is a widely recognized phenomenon extensively studied in the assessment of potential risks posed by leached additives to various ecosystems. This study aims to investigate the transfer of plastic leachate to organisms in order to address the existing uncertainty and debates surrounding its potential hazards. This paper provides a comprehensive analysis of the distinctive features that differentiate MP additives from other toxic pollutants. Moreover, it investigates the process of additive leaching from MPs and its subsequent dispersion into the environment. Furthermore, it evaluates the environmental impact of MP additives on various ecosystems, including marine, freshwater, and terrestrial environments. Specifically, this study aims to scrutinize the release of these MP additives and their detrimental effects from an environmental perspective.

CO-CONTAMINANTS OF PLASTICS

Microplastics, due to their large surface area, act as transporters of hazardous contaminants in the environment and within organisms. Various pollutants, such as POPs and heavy metals, adhere to the expansive surface area of MPs. According to Maršić-Lučić *et al.*, MPs have the ability to accumulate heavy metals from water, which can then be taken up and consumed by various species[29]. The presence of MPs in the natural environment significantly affects the global transport of detrimental pollutants[30]. In some instances, contaminants may detach from MPs while organisms ingest them.

POPs

POPs, such as PCBs and OCPs, remain in the environment for long periods. Verla *et al.* explained that POPs resist photolytic and biochemical breakdown processes, making them easily transportable and prone to binding with various objects. Due to their poor solubility, organic contaminants tend to adhere to MPs in the environment[31]. Pascall *et al.* demonstrated the presence of 113 chlorinated chemicals among a total of 200 comprising polychlorinated biphenyls, also known as PCBs, in the environment[32]. The first observation of PCB adsorption on polystyrene MPs dates back to 1972[33]. Studies investigating microplastic distribution on New Zealand beaches and in sediments revealed high PCB adsorption on PP microplastic pellets[34]. Subsequent research indicates an increasing adsorption concentration of up to 18,700 ng/g over time[35]. Samples of resin PP pellets were collected from four coastal areas in Japan, revealing polychlorinated chemicals in concentrations ranging from 97 to 117 ng/g. Among 55 polypropylene pellets, a significant quantity of PCBs was detected, indicated by regional differences and discoloration of pellets[36]. Additionally, MPs collected from two beaches in Portugal exhibited concentrations of PCBs ranging from 0.02 to 15.56 ng/g[37]. PAHs, another organic molecule, were found attached to MPs in the North Pacific Gyre, ranging from 39 to 1,200 ng/g in concentration. Researchers noted that when the concentration of connected PAHs increased from 6,100 to 12,000 ng/g, the color of the plastic faded, turning yellow[38].

Heavy metals

Heavy metals refer to metals with a higher density, typically around 5 g/cm^3. Recent studies by several authors have provided evidence supporting the attachment of heavy metals to MPs. In a comprehensive 12-

month investigation conducted by Rochman *et al.*, the attachment of heavy metals to newly manufactured MPs, such as PP, LDPE, PVC, HDPE, and PET collected from three different sites in San Diego Bay, USA, was examined. The final data yielded at the end of 12 months indicated that Zn, Cd, and Pb were found attached to MPs at concentrations of 4.16 µg/g, Cd 3.8 µg/g, and 0.8 µg/g, respectively[39]. Another study focused on eight farms in China, six of which were culture ponds, while two were open area farms for sea cucumber culturing. This study identified the presence of eight heavy metals, including arsenic, cadmium, lead, zinc, manganese, nickel, copper, and chromium, attached to MPs at varying concentrations across these farms[40].

ATTACHMENT AND DETACHMENT MECHANISM OF TOXIC POLLUTANTS ONTO PLASTIC

Attachment mechanism

The attachment of different pollutants to MPs relies significantly on factors like surface structure, affinities towards pollutants, and the types of polymers involved, such as polyethylene (PE), PS, and PP. Toxic chemical pollutants generally become embedded within the pitted surface of MPs[41]. Several key elements of plastics - like surface area, surface chemistry, and size - influence the interaction between MPs and environmental pollutants. For instance, polychlorinated organic pollutants exhibit a higher tendency to be adsorbed by PE pellets than PP pellets, as demonstrated in an *in situ* experiment by[36]. According to Wu *et al.*, alkyl benzenes show higher adsorption onto PVC than onto PE-MPS[42]. This consistent adsorption pattern of MPs towards heavy metals has been observed in numerous studies[43]. For example, when exposed to Zn, PS showed greater adsorption than PVC. Conversely, PVC exhibited higher adsorption when exposed to copper. Moreover, PVC demonstrated increased adsorption after exposure to Cu. Aging also plays a crucial role, potentially affecting the interaction between metal ions and MPs. For instance, in a NaCl solution, the ultraviolet irradiation aging process inhibits the assembly of PS-NPs. Natural organic matter present in natural waters is likely to adhere to plastic surfaces, thereby influencing the properties of plastic particles[44,45]. Ali *et al.* reported that natural organic matter forms a protein layer on the surface of MPs[46]. However, humic acid improves the aggregation of PE-MPs, while sodium alginate enhances the assembly of PS-MPs[47,48].

There are two mechanisms by which MPs attach to various toxic chemical pollutants: (1) attachment of pollutants onto MPs hydrophobically; and (2) incorporation into the biofilm matrix.

Hydrophobic attachment of pollutants

MPs exhibit low surface polarity, rendering them more hydrophobic, facilitating increased adsorption of hydrophobic pollutants. Due to their lower density compared to water, MPs commonly accumulate in the microlayer of seawater. POPs, such as organochlorine (DDT), PAHs, and PCBs, are all lipophilic and typically remain in the upper layer of seawater, where they undergo hydrophobic adsorption with MPs. The combination of the low polarity and a relatively lower pH than most environmental PHs creates favorable conditions for MPs and aqueous metal ions on their surfaces. The pH of the medium, particularly when nearing 0, significantly promotes the electrostatic interaction between polymers and oppositely charged organic compounds. Micelle shaped structures are formed by the attachment of positively charged aqueous ions to the negatively charged surface of MPs. Upon adsorption, the charge is neutralized. In a natural environment, the adsorption or attachment of toxic pollutants onto MPS is a lengthier process compared to artificial laboratory experiments[49]. Research on the degradation of MPs has indicated an increased generation of oxygen groups during the process, altering the surface charge and enhancing polarity, thereby making the plastic surface more reactive. Consequently, it takes longer to reach equilibrium[50,51]. However, laboratory experiments often reach equilibrium more rapidly. For example, Holmes *et al.* performed a lab study exposing virgin PE pellets to six heavy metals: Cr, Cu, Co, Ni, Pb, and Cd, demonstrating a rapid equilibrium[52].

Van der Waal forces: These are the weak intermolecular electric forces between molecules. Polyvinyl chloride and polyethylene microplastic adhere to toxic pollutants through Van der Waal interactions[53,54].

The Pi-Pi (Electron-Donor-Acceptor) interaction: this type of sorption behavior observed in polymers that incorporate benzene rings within their structure. This interaction is non-covalent, involving both electron donation and acceptance. Both the polymer and contaminant types act as electron donors and acceptors. The sorption capacity of polystyrene, polyvinyl chloride, and polyethylene was observed with aromatic organic compounds. Among all phenyl groups, polystyrene plastic shows higher sorption towards organic compounds[55]. PS plastic and tetracycline (TC) demonstrate more sorption via Pi-Pi interaction than polyethylene and polypropylene due to the presence of benzene rings in both PS and TC[56].

Incorporation into biofilm matrix

A phenomenon known as quorum sensing plays a pivotal role in the formation of biofilms. Initially, microbes attach to the surface of MPs, forming micro colonies that eventually mature into biofilms. In addition, biofilms may absorb toxic chemicals due to their unique structure. When virgin MPs come into contact with the bacteria in water, the initiation of biofilm formation within the water can occur in a matter of seconds[57,58]. Temperature and light are essential factors for the formation of biofilm[59,60]. Quorum sensing controls the gene expression of diverse microorganisms that produce extracellular polymeric substances by adhering to each other on non-living or living objects. Studies have shown that biofilms can be present wherever water exists, attaching themselves to hard surfaces or floating freely within the water[61,62]. Extracellular polymeric substances (EPS) govern the distribution and mobility of metals in aquatic environments, either by chelating the metals or by integrating them into their cellular structure[63]. In biofilms, microorganisms create pits on the surface of MPs, thereby increasing the available surface area of MPs available for the sorption of different types of heavy metals. Additionally, this process significantly enhances the hydrophobicity of MPs[63,64].

Detachment mechanism of pollutants

Toxic pollutants may readily attach themselves to MPs via non-covalent bonds, enabling the contaminants attached to plastic surfaces to detach easily [Figure 1]. Goss and Schwarzenbach demonstrated that the forces that hold atoms together include weak van der Waals forces, hydrogen bonds, and the creation of cavities. During the desorption process, pollutants initially travel from their original location to the plastic surface and are then subsequently released into various mediums, such as sediment, water, human or animal bodies, or dirt. The specific desorption mechanisms vary based on the adsorption sites. Moreover, several factors impact desorption, including the type of polymer, the pH of the medium, the salinity of the medium, and the presence of inorganic and organic ligands in the medium[65]. Research by Violante and Pigna revealed that when contaminants discharge into soil or sediment, they tend to adsorb trace elements, humic compounds, inorganic components, and carbonates. Once hazardous pollutants are released from the plastic into an unpolluted environment, the situation is considered resolved[66]. Pollutants, along with organisms in the medium (soil or sediment), also adsorb on the organic and inorganic ligands in the medium[67]. In aqueous environments, the desorption process is largely influenced by medium salinity. According to research by Awet *et al.*, the adsorption of the contaminant DDT onto plastic reduces as the salinity of the solution rises[68].

PLASTIC ADDITIVES

Plastic not only comprises polymers but also contains some other substances known as additives. These

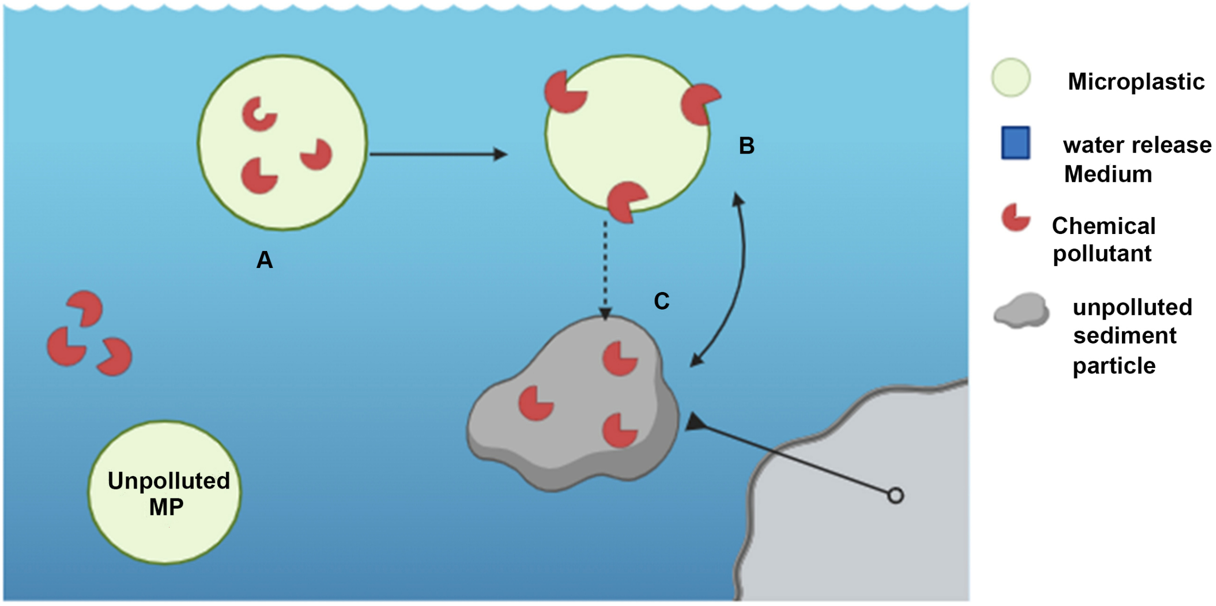

Figure 1. Unpolluted MPs come into contact with chemical pollutants (heavy metals, organic compounds) adsorbed onto MPs (A). When all the organic matter on MPs is used up by pollutants, they slowly move to the outer surface of MPs (B) and migrate to the unpolluted sediment particle that is rich in humic and fulvic acid (C). MPs: Microplastics.

additives serve the purpose of modifying the physical and chemical properties of plastic. The selection of additives significantly influences both the cost and production of plastic materials[69]. The ecotoxicity of MPs is not only affected by their shape and size but also by the concentration, composition, and sheer quantity of additives. The concentration of additive chemicals in MPs surpasses that of toxic anthropogenic pollutants in the environment[20,24]. The specific type of additives plays a crucial role in determining the physicochemical properties of MPs and their behaviors and interactions within the environment[70].

In 2021, the global plastic additives market witnessed substantial growth, reaching 48.41 billion USD with a growth rate of approximately 6%, and is expected to be 51.04 billion dollars by 2026 and 75.29 billion dollars by 2028 (Fortune, plastic additives market size, growth, and forecast report 2022). The manufacturing of plastic involves around 6,000 chemical classes of additives. Along with that, light stabilizers are incorporated to slow down chemical degradation, while added pigments contribute to creating different colors, thereby enhancing the appeal of plastic products.

Identification of MPs-derived pollutants

The current presence of microplastics in the environment can be identified by the chemical additives they contain, such as phthalates, nonylphenol, polybrominated diphenyl ethers, and Bisphenol A (BPA)[47,70]. These pollutants derived from microplastics have been identified through electrochemical oxidation on electrodes. Carbon nanomaterials, including graphene oxides (Gr), carbon nanotube (CNTs), boron-doped diamond (BDD), carbon quantum dots (CQDs), and grapheme oxides (GO), are employed for monitoring and identifying EPS. They are chosen due to their rich surface chemistry, low cost, high conductivity, electrochemical property, chemical stability, and large surface area[71,72]. Jiang *et al.* reported that boron-doped diamond glassy carbon electrode shows a higher detection ability towards bisphenol A than for hydroquinone and 1,2-dihydroxybenzene in urban wastewater[73]. Molecularly imprinted polymers (MIPs) act as synthetic polymeric receptors for dibutyl phthalate and bisphenol A[74,75]. MIPs demonstrate selective identification even in the presence of interfering EPS. For the detection of EPS, carbon materials modify the structure of MIPs, such as QDs, MWCNTs, and CdTe, providing abundant active sites with high stability and surface area, good electrical conductivity, and high sensitivity for bisphenol A analysis[76]. Metal/covalent-organic frameworks (MOFs/COFs) have emerged as excellent electrodes for electrochemical identification of MPs-derived pollutants. When MOFs are modified with CTAB (cetyltrimethylammonium bromide), the response for bisphenol A detection is enhanced threefold compared to MOFs.

The classification of additives is divided into: plasticizers, antioxidants, flame retardants, and monomers, as described in Table 1.

Plasticizers are added to enhance the flexibility and softness of plastics. They encompass substances like phthalates, epoxides, *etc.* On the other hand, antioxidants are incorporated to mitigate the degradation of plastic caused by chemicals, light, or heat.

Antioxidants, including phenols, arylamines, *etc.*, are introduced into plastics to impede oxidation and prevent aging[94]. Similar to other plastic additives, antioxidants sometimes leach out and enter the environment. Particularly in food packaging, antioxidants from containers can migrate into food, posing a threat to food safety.

Flame retardants are used in plastic to meet fire safety standards, rendering the plastic materials resistant to fire or the spread of flames. Various flame retardants are employed, such as halogens and bromine compounds. For instance, BPA is an additive monomer.

MECHANISM OF LEACHING OF PLASTIC ADDITIVES

Since these additives are either loosely attached or not chemically bonded to plastic, they can escape from the plastic during use or after disposal. Once they leach out, they may degrade and form other toxic chemical pollutants, persisting in the environment and accumulating in living organisms[95]. The presence of additives in the environment or MPs largely depends on their origins[96]. However, pinpointing the source can be challenging, as some additives are not exclusively used in plastic but also in various other products. For instance, bisphenol A is used not only in plastic bottle production but also in food can lining and thermal paper manufacturing. Perfluorinated compounds (PFCs), employed in textiles and food packaging, exhibit persistent qualities, remaining in sediment, soil, water, and biota[97].

The leaching of additives from plastic is influenced by various factors, including solubility, volatility, additive size, pH, physical or chemical properties of media, temperature, permeability of the polymer matrix, and gaps between polymer molecules allowing migration [Figure 2]. Additive chemicals possess the ability to migrate from plastic materials to external matrices, such as water, soil, and food, as well as internally within plastic to its surface[20]. In many cases, the unintended and uncontrolled leaching of additives from plastic has significant consequences for the environment and human health. For example, a flame retardant, polybrominated diphenyl ethers (PBDEs), is ubiquitous, environmentally persistent, and accumulates within organisms. It has been banned in the European Union since 2004[98]. However, there are instances where the intentional and controlled migration of additives is beneficial, such as the release of mold agents on the surface to prevent silver oxidation and enhance mechanical, optical, and antistatic properties, thereby improving food preservation[99,100].

The process of leaching/migration of additives from plastics can be categorized into four steps:
1. Diffusion leads to the additive moving towards the surface of polymer.
2. Desorption occurs as the additive separates from polymer surface.

Table 1. Polymers and their additive compounds with different classifications

Polymer type	Additive compound	Classification of additive	Ref.
PS, PP, PA, PE, PVA, HDPE	DEP	Plasticizers	[77,78]
ABS	BHT	Antioxidant	[79]
PC	BPA	Monomers	[80]
PE, PS, PP, PVC	PBDEs	Flame retardants	[81]
PP, PE	Tris (2,4-di-tert-butylphenyl) phosphite	Antioxidant	[82]
PVC, PE	BBP	Plasticizer	[83,84]
Modified PS, PVC, ABS, PS	ATBC	Plasticizer	[85]
PP, PE, PA, PS	2,4-Di-tert-butylphenol	Antioxidant	[77,86]
PVA	Acetic acid	Monomer	[87]
PET, PS, PVC, ABS	TBBPA	Flame retardants	[88,89]
PVC, PET, PS, ABS	TCEP	Flame retardants	[90]
PVA	Diisobutyl phthalate	Plasticizer	[91]
PP, LDPE	Octadecyl 3-(3,5-di-tert-butyl-4-hydroxyphenyl) propionate	Antioxidants	[92]
PVC, PE	DINP	Plasticizer	[83]
PE, PBT	Calcium bis (ethyl 3,5-di-tert-butyl-1-44-hydroxybenzylphosphonate	Antioxidant	[93]

PS: Polystyrene; PP: polypropylene; PA: polyamides; PE: polyethylene; PVA: polyvinyl alcohol; DEP: diethyl phthalate; ABS: acrylonitrile butadiene styrene; BHT: butylated hydroxytoluene; PC: polycarbonate; BPA: bisphenol A; PVC: polyvinyl chloride; PBDEs: polybromodiphenyl ethers; BBP: butyl benzyl phthalate; ATBC: acetyl tributylcitrate; PET: polyethylene terephthalate; TBBPA: tetrabromobisphenol A; TCEP: tris(2-chloroethyl) phosphate; DINP: di-isononyl phthalate; PBT: polybutylene terephthalate.

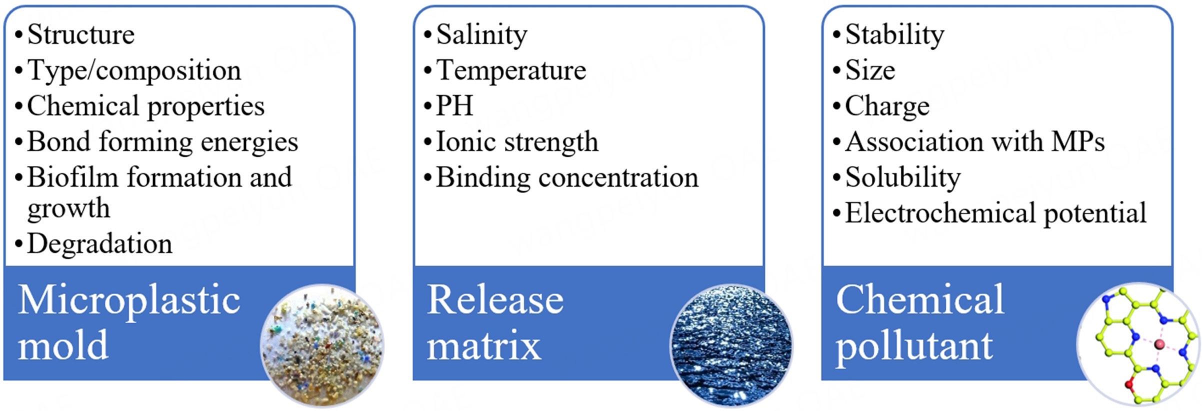

Figure 2. Factors affecting the migration of pollutants from MPs into the medium[18]. MPs: Microplastics.

3. Sorption takes place as the additive becomes absorbed within the plastic matrix in the surrounding medium.
4. Dispersion and absorption occur within the matrix.

Moreover, the leaching or migration of additive chemicals is directly related to the particle size. Smaller particles are more easily and quickly removed. For example, monomers with low boiling points tend to escape even at room temperature. According to Hahladakis *et al.*, these monomers include ethylene, vinyl chloride, butadiene, and formaldehyde. Once released, the additive chemicals become absorbed into a matrix consisting of two phases: a solid phase represented by the polymer, and a liquid phase represented by either water or air[20]. Both adsorption and absorption are part of the sorption concept. During adsorption, the chemical remains at the interface between the solid phase and the fluid phases, while in absorption, additive compounds are embedded and penetrate the layer of the solid phase as polymers[101].

RISK OF LEACHED ADDITIVES ON THE ECOSYSTEM

In recent years, there has been growing evidence indicating the harmful effects of plastics and their constituent substances. This heightened awareness has emerged due to both direct and indirect sources of exposure. According to Wright *et al.*, the intake of plastic particles results in direct poisoning. On the other hand, indirect toxicity occurs when plastic breaks down and releases dangerous chemical components into the environment[102]. This is primarily because most additive components are physically rather than chemically bonded to the plastic.

Effects on marine organisms

The natural compartments of the marine ecosystem serve as reservoirs for all the impurities released by anthropogenic discharges. Across the global marine environment, significant quantities of chemical plastic additives have been identified[103,104]. In a field study, six types of phthalates were detected in sediments, with DEHP accounting for 95% of the total. Additionally, plastic additive compounds have been linked to heavy metals such as Cu, Mn, Ni, Cd, Co, Pb, and Fe. This association has been observed to potentially impact the reproductive and immune systems of *H. diversicolor*[105]. In Osaka Bay, Japan, the plastic additive compounds BPA, NP, and octylphenol (OP) have exhibited bioaccumulation and caused endocrine disruption in *Paraprionospio sp.* (Polychaete)[106]. Furthermore, exposure to leached additives from seven commercially used recyclable plastics has been linked to increased mortality among larvae of *Amphibalanus amphitrite* due to toxicity[47]. Leachates from polypropylene pellets encountered during the embryonic developmental stage of *Perna perna* (mussels) exhibited increased toxicity, inhibiting the growth of the embryos of mussels across all samples[107].

Data were obtained from various marine invertebrate species, including *D. magna*, *Lytechinus variegatus*, *A. amphitrite*, *N. spinipes*, and *P. perna*. The effects of leached additives from three different plastic types on these invertebrate species were observed. It was indicated that additives leached from PVC are more toxic towards species, while PP and PE are less toxic or, in some cases, not toxic towards these diverse species[47,107-109] [Figure 3].

Another study investigated the toxicity and bioaccumulation of PBDEs, a flame retardant, when exposed to *Capitella sp* during the larval settlement stage. Tests were conducted under both hypoxic and normoxic conditions. Under hypoxia, larva settlement was observed[110]. The presence of additives, including flame retardant, had adverse effects on polychaetes, leading to reduced growth and various other biological effects. Moreover, these effects were significantly exacerbated when additional stressors, such as PVC contaminants, were introduced in conjunction with hypoxia conditions and additives, amplifying the impacts on the organisms' immune systems. Table 2 presents an overview of recent studies conducted on the effects of additives found in MPs on various marine species.

Effects on freshwater biota

Wastewater treatment plant effluents often contain various additives of plastics released by industries, dust, sewage sludge, municipal waste, and domestic waste when discharged into freshwater. Another significant contributor to these additives in freshwater is the wear and tear of tire rubber (CTR), which enters freshwater through surface runoff. In their study, Capolupo *et al.* investigated the adverse effects of additives released from tire wear and MPs of PP, PVC, PS, and PET on the freshwater microalga *Raphidocelis subcapitata*. Among the most notable additives detected were cobalt, zinc, and benzothiazole from car tire rubber; antimony and cobalt from PET; acetophenone and lead from PP; and phthalide and zinc from PVC. The quantities of these additives extracted from MPs varied in freshwater, with the highest counts recorded as 19 (PP), 17 (CTR), 9 (PS), 9 (PVC), and 1 (PET). PET, in its purest form, did not exhibit

Table 2. Recent studies on exposure of MP additives to different marine species and the end results

Additives compound	Microplastic type	Species	Exposure time	End results	Ref.
Phthalate; bisphenol A; nonylphenol; brominated flame retardant; boric acid; tris(2-chloroethyl) phosphate	Polystyrene microbeads	*Marenzelleria spp*	1 day	Ingestion by organism	[111]
Phthalate; bisphenol A; nonylphenol; brominated flame retardant; boric acid; tris(2-chloroethyl) phosphate	Polyvinyl chloride, polypropylene, PET	*Nitroca sinipes*	96 h	Leads to mortality	[108]
Polybrominated diphenyl ethers (BDE-47)	Polyethylene	*Laeonereis acuta*	14 days	Bioaccumulation of MPs	[112]
Brominated flame retardant; boric acid	High-density polyethylene, polypropylene, polyvinyl chloride, epoxy resins	*Daphnia magna*	24-48 h	Leads to mortality	[113]
BPA	Polypropylene	*Perinereis aibuhitensis*	4-14 days	Change in the expression of Pa Ga gene	[114]
Polybrominated diphenyl ethers (BDE-47)	Polyethylene	*Pseudochromis fridmani*	2 days	Mortality happens	[115]
Phthalate; bisphenol A; brominated flame retardants; boric acid	Polyvinyl chloride, polyactic acid, high-density polyethylene.	*Arenicola marina*	31 days	Biomass survivorship	[116]
Bisphenol A; nonylphenol; brominated flame retardant; boric acid; tris(2-chloroethyl) phosphate	Polystyrene, polypropylene, polycarbonate, low-density polyethylene	*Amphibalanus amphiteite*	24-96 h	Settlement	[47]
Dibutyl phthalate	Polystyrene	*Galeolaria caespitosa*	15 min - 2.5 h	Toxicity in embryo	[117]
Phthalate; bisphenol A; nonylphenol	Polyvinyl fragments	*Hediste diversicolor*	10-28 days	Organism survived	[118]
Dibutyl phthalate; PA 6,6; PA 11; PA 12; PA 4,6	Polystyrene and polyamide fragments	*Arenicola marina*	106-240 days	Survival of organisms	[119]
Polybrominated diphenyl	Polyethylene	*Capitella sp. I*	1 day	Settlement of larva occurs	[110]
Brominated flame retardant; boric acid; tris(2-chloroethyl) phosphate	Polyurethane, Polymethyl Methacrylate	*Daphina magna*	24 and 48 h	Mortality occurs	[109]
Polybromodiphenyl ethers; PCBs	Polystyrene, polyethylene	*Nereis virens*	28 days	Bioaccumulation of MPs	[120]

MP: Microplastic; PET: polyethylene terephthalate; BPA: bisphenol A; PA: polyamides; PCBs: polychlorinated biphenyls.

any inhibitory effects on the growth of *R. subcapitata* even at 100% leachate concentration. However, the leachates from CTR, PP, PS, and PVC microplastic materials showed full toxicity and resulted in reduced growth of the microalgae[121].

Phthalate compounds, commonly found in polyvinyl chloride plastics, are not chemically bound, allowing them to quickly leach into the environment[122]. These phthalates serve various purposes across multiple products, including medical devices, building materials, electrical cables, food packaging, and toys. Due to their widespread use, these compounds have permeated ecosystems, accumulating in organisms. The presence of MPs, including phthalates, poses a severe threat to freshwater biota, notably keystone species like *D. magna*. This pollution endangers biodiversity and destabilizes entire food systems. *D. magna*, a filter feeder with a diet encompassing particles ranging from 1-70 µm, inadvertently consumes MPs in aquatic ecosystems[123]. Upon ingestion, the chemicals from these microplastics leach into the organisms' gastrointestinal tracts. Particularly, polystyrene carboxylated MPs sized between 20-1,000 nm can permeate the epithelium of *D. magna*, resulting in adverse effects on reproduction, organism growth, and mortality. Recognized as an essential indicator species for environmental pollution, *Daphnia magna* plays a crucial role in detecting contaminants in aquatic ecosystems[124].

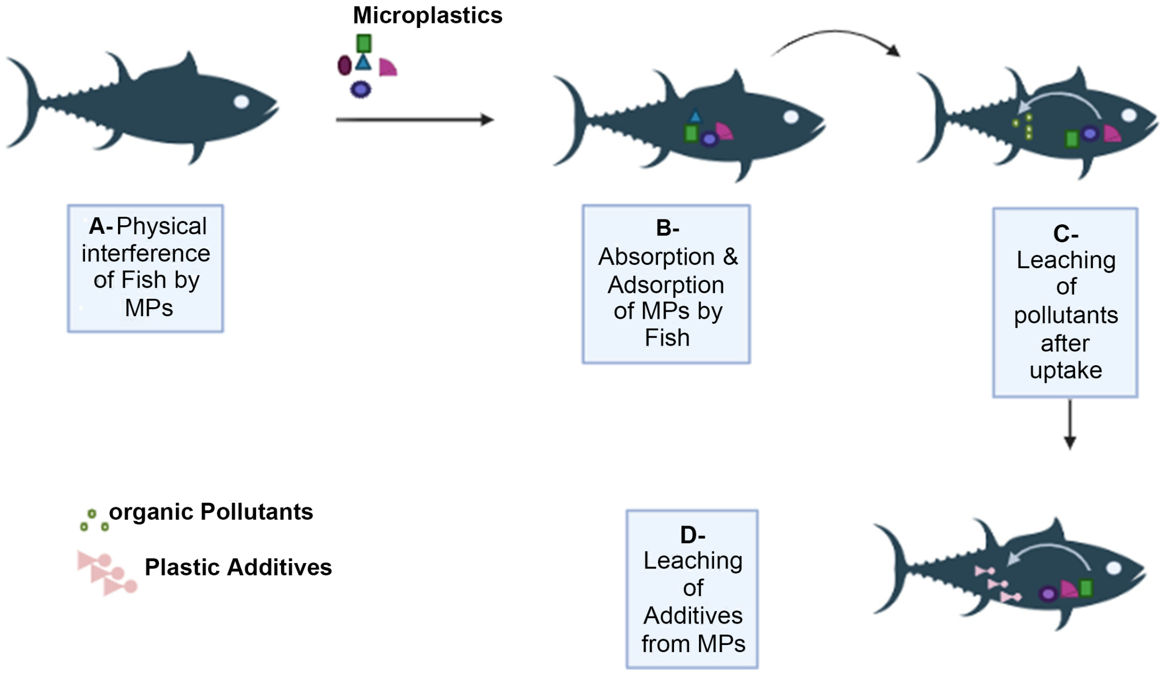

Figure 3. Physical obstruction occurs through different types of MPs encountered by fish in water. A-Sorption occurs after interaction. B-Firstly, pollutants such as chemicals, ions, and C- organic compounds leach from MPs, and then D- additives from plastic released into the fish body. MPs: Microplastics.

Daphnia magna was exposed to three different types of phthalates - DEHP, dibutyl phthalate (DBP), and DEP - ranging from 1-10 μm in concentration. After 14 days of exposure, no significant impact on reproduction or hatching was observed. However, an unexpected outcome emerged: DEHP increased reproduction at a concentration of 1 μm. On the other hand, growth and development were reduced by all the three phthalates, whereas the lipid content of Daphnia increased upon exposure to these substances. Negative effects on the lifespan of *D. magna* were observed with DBP at both 1 and 10 μm concentrations, and with DEP at 10 μm[125]. Blinova *et al.* demonstrated in a laboratory assay the negative impacts of 1-Hydroxycyclohexyl phenyl ketone (1-HCHPK) on two planktonic organisms, *Thamnocephalus platyurus*, *Daphnia magna*, and the benthic organism *Heterocypris incongruens*. 1-HCHPK is a chemical additive used in plastic construction, coating materials, and 3D printing UV-radiation-curable technologies such as 3D printing. This compound enters freshwater systems through consumer waste flows. After 6 days of exposure to 1 HCHPK (25 mg/L), *H. incongruens* exhibited a visible reduction in body size (1.3-1.8-fold) compared to the control[126]. By contrast, Murugan *et al.* found that in *T. platyurus*, hatching was promoted by the introduction of medium calcium into embryonic cells[127]. Zhang *et al.* demonstrate the capacity for biodegradation of dimethyl phthalate (DMP) by three species of freshwater unicellular cyanobacteria, i.e., *Synechocystis sp.*, *Synechococcus sp.*, and a diazotrophic *Cyanothece sp.* Low concentrations of DMP were found to enhance the growth of cyanobacteria, but increased concentrations resulted in reduced growth. At pH 9 and a temperature of 30 °C, degradation of dimethyl phthalate occurred. Cyanothece cyanobacteria exhibited the highest rate of phthalate degradation compared to the other two species. Phthalic acid was identified as an intermediate product of dimethyl phthalate after degradation[128].

Effects on terrestrial ecosystem

Plastic additives have been discovered not only in marine and freshwater ecosystems but also in terrestrial ecosystems, accumulating in the soil and posing risks to human health. A small number of studies have indicated their presence in soil[129]; however, major additives and plasticizers have not been detected yet. One prominent plasticizer found in soil is phthalate, primarily originating from agricultural plastic use[130,131]. Recently, terrestrial ecosystems have been recognized as major receptors of plastic in the environment[132]. MPs in soil degrade into smaller particles through diffusion, the leaching of plasticizers onto their surface, and subsequent release into the soil[129]. The leaching potential of plasticizers depends on the polymer type and physical state of the plastic. Plasticizer content varies in every plastic type; for instance, PE contains minimal plasticizer, while PVC comprises over 80% plasticizers[133].

Billings *et al.* performed a field study in central and southern England (UK), aiming to assess microplastic and leached plasticizer concentrations in UK soil. They collected 19 samples from different sites, including woodlands (7 samples), urban roadsides (3 samples), urban parklands (3 samples), and landfill areas (6 samples). These samples comprised both soil and surface plastic collections. Varying quantities of microplastic items were evident across different land uses. The highest count was found in landfills, registering 42 items per 25 m^2 of soil, followed by urban roadsides with 21 items per 25 m^2, parkland exhibiting 1.3 items per 25 m^2 of, and the lowest amount in woodland, measuring 0.1 items per 25 m^2. Notably, woodlands exhibited the lowest account due to their historical tree cover dating back to 1,600 CE (Natural England, 2021). The high counts in landfills and roadsides are attributed to the widespread disposal of waste by humans[134]. Upon microplastic deposition in soil, additive compounds are released through fragmentation or degradation. Phthalate, for example, is 25 times higher in concentration in urban roadside soil than in landfills (2.3 times), parklands (1.6 times). In deciduous woodlands, the substantial presence of organic matter accelerates plasticizer biodegradation by bacteria[129].

The detrimental impact of phthalates, widely regarded as one of the most hazardous chemicals in plastic, on human health has been well-established. Phthalates enter the human body through dermal contact, eye contact, ingestion, and inhalation. They are present in numerous everyday items, such as personal care and consumer products[135,136]. Additionally, infants are exposed to and ingest phthalates through various sources such as infant formula milk, breast milk, food packaging, or cow milk[137]. Recent studies have revealed the presence of phthalates in cord blood, human breast milk, and other pregnancy specimens[135,138,139]. Colon *et al.* documented the presence of mono-(2ethylhexyl) phthalate (MEHP) and DEHP in 41 Puerto Rican girls, associating it with endocrinal disruption. Moreover, other effects such as damage to the pulmonary system, asthmatic reactions, rhinitis, direct toxicity, and allergies have been observed[140]. In Sweden, a study involving 198 children with asthmatic symptoms and 202 without symptoms, aged between 3 and 8 years, found that asthmatic symptoms were relate to exposure to air with dust containing butyl benzyl phthalate (BBzP)[141].

BPA, an additive compound, finds use in various products such as food can linings, epoxy resins, polycarbonate, polyester-styrene plastics used in containers and other baby bottles, as well as some dental sealants, protective coatings, adhesives, and water storage and supply pipes[142-146]. Many findings have detected the presence of BPA in both animal and human bodies, indicating its effects on thyroid function[147]. Research indicates that women experiencing miscarriages tend to exhibit higher BPA serum levels compared to those who are not parents[148]. A major concern in females is the prevalence of PCOS (polycystic ovary syndrome). It has been evidenced that females facing PCOS issues have a higher level of bisphenol A in their bodies compared to those without PCOS[149,150]. PBDEs are a flame-retardant present in a variety of products, including mattresses, upholstered furniture, televisions, computers, and textiles[151]. A study on humans has shown that exposure to PBDEs causes thyroid hormone level disruption[152].

Urban wastewater serves as a significant source and repository for NPs and MPs. After entering the urban wastewater system, these particles can either travel with the water flow or accumulate within sediment deposits. Notably, NPs have more prominent effects on wastewater treatment processes than MPs. Specifically, PS-NPs (100 nm) impede the removal of nitrogen in activated sludge systems due to their release or induction of reactive oxygen species (ROS) and lactate dehydrogenase (LDH), which cause acute toxicity in activated sludge, consequently suppressing the nitrification and denitrification genes through the reduction of denitrifies and nitrifies[153]. Lee *et al.* also reported the inhibitory effect of nitrification by PS-NPs, which causes disruption of cells membrane potential. Furthermore, NPs show significant effects on the production of hydrogen and methane in anaerobic digestion processes[154].

CONCLUSION AND FUTURE PROSPECTIVE

MPs and plastic additives are both emerging contaminants that have garnered considerable attention from researchers. MPs, together with naturally occurring microorganisms and synthetic chemicals, significantly impact the environment due to the continuous release of chemical pollutants, including heavy metals and organic compounds resulting from human activities. These anthropogenic pollutants have detrimental effects on the environmental matrix. Along with MPs, another major concern is additive compounds constituting the structure of plastic. Additives and plasticizers enhance the stability, shape, and properties of plastic. However, the non-covalent bonding of additives with the polymer often leads to their migration or leaching from plastics. Additives serve as antioxidants to prevent aging and as flame retardants to ensure safety against fire hazards. It is clear that aquatic ecosystems bear a substantial brunt of this pollution. Additionally, terrestrial ecosystems are grappling with issues arising from these additives. Consequently, organisms are exposed to MPs through water, soil, and food ingestion, where these pollutants and additives are retained after physical obstruction. Firstly, pollutants are released from MPs, followed by the detachment of additives due to loss of binding. This results in various dangerous effects on organisms, damaging their endocrine systems and reproductive stages, and ultimately increasing mortality rates.

Currently, there is a significant lack of comprehensive understanding regarding MPs and their leaching into the environment. This knowledge gap spans multiple areas, underscoring the imperative for future research to bridge these limitations. Despite extensive studies on the effects of leached plastic additives on marine and freshwater organisms, there remains a notable scarcity of literature concerning their impact on terrestrial organisms. Terrestrial environments significantly contribute to the accessibility and utilization of MPs from an ecological perspective. Therefore, expanding the experimental investigation of plastic additives to encompass diverse ecosystems, particularly soil, holds significant importance. Further research should prioritize investigating the ecotoxicological impacts of plastic additives on animals, insects, and plants in terrestrial environments. The feasibility of removing MPs from marine water or rivers faces limitations due to their widespread presence and ongoing fragmentation into smaller particles. It is imperative to extensively study methods for removing or converting MPs, assessing their toxicity, and monitoring their presence. Another field that needs to be explored is the potential conversion of these MPs into valuable products as a means of mitigating ecosystem contamination. Efforts targeting the control of MP pollution, particularly focusing on wastewater discharges and leachates, should prioritize transforming MPs into valuable products. Investigating the origins and destinations of MPs and their associated additives in various urban settings is crucial. The development of new technologies and methods is necessary to effectively control MPs in both wastewater treatment plants (WWTPs) and waterways to halt the continued spread of MPs and their subsequent leachates in terrestrial ecosystems.

Moreover, there is a gap in comprehensive research concerning the adsorption of contaminants onto MPs in landfill settings. Understanding the degradation process of MPs and the mechanisms involved in contaminant adsorption in landfills is crucial for the development of an efficient treatment methodology. This significance arises from the fact that leachates within landfills often contain heightened levels of MPs, which may be associated with bound contaminants that can hinder the effectiveness of biological treatment phases. Therefore, acquiring knowledge about MP degradation and contaminant adsorption in landfills is crucial in order to establish an effective treatment strategy. Further investigation is warranted in the area of biological process development. An essential aspect of the study pertains to characterizing microbes, functional enzymes, and their respective genes concerning the degradation of synthetic plastics. Such an understanding not only helps in curbing MP pollution but also aids in mitigating their toxic effects on various organisms.

DECLARATIONS

Acknowledgments

We acknowledge the moral support provided by Jawaria Khalid and Maleeha Ishaq to the first author in writing this manuscript.

Authors' contributions

Writing-original draft: Iftikhar A, Qaiser Z
Data curation, validation, visualization: Iftikhar A, Sarfraz W, Ejaz U
Visualization: Iftikhar A, Aqeel M
Writing-review and editing: Rizvi ZF
Supervision, writing-review and editing: Khalid N

Availability of data and materials

Data and materials will be provided upon request.

Financial support and sponsorship

None.

Conflicts of interest

All authors declare that there are no conflicts of interest.

Ethical approval and consent to participate

Not applicable.

Consent for publication

Not applicable.

Copyright

REFERENCES

1. Thompson RC, Swan SH, Moore CJ, vom Saal FS. Our plastic age. *Philos Trans R Soc Lond B Biol Sci* 2009;364:1973-6. DOI
2. Andrady AL, Neal MA. Applications and societal benefits of plastics. *Philos Trans R Soc Lond B Biol Sci* 2009;364:1977-84. DOI
3. Enyoh CE, Verla AW, Verla EN. Uptake of Microplastics by plant: a reason to worry or to be happy? Available from: https://www.researchgate.net/publication/334083970_Uptake_of_Microplastics_by_Plant_a_Reason_to_Worry_or_to_be_Happy. [Last accessed on 29 Dec 2023].
4. Enyoh CE, Verla AW, Verla EN, Ibe FC, Amaobi CE. Airborne microplastics: a review study on method for analysis, occurrence, movement and risks. *Environ Monit Assess* 2019;191:668. DOI
5. Heskett M, Takada H, Yamashita R, et al. Measurement of persistent organic pollutants (POPs) in plastic resin pellets from remote islands: toward establishment of background concentrations for International Pellet Watch. *Mar Pollut Bull* 2012;64:445-8. DOI
6. Hirai H, Takada H, Ogata Y, et al. Organic micropollutants in marine plastics debris from the open ocean and remote and urban

beaches. *Mar Pollut Bull* 2011;62:1683-92. DOI

7. Zhu F, Zhu C, Wang C, Gu C. Occurrence and ecological impacts of microplastics in soil systems: a review. *Bull Environ Contam Toxicol* 2019;102:741-9. DOI
8. Ritchie H, Samborska Veronika, Roser M. Plastic pollution. 2020. Available from: https://ourworldindata.org/plastic-pollution. [Last accessed on 29 Dec 2023].
9. Oliveira M, Almeida M. The why and how of micro(nano)plastic research. *TrAC Trend Anal Chem* 2019;114:196-201. DOI
10. Baun A, Hartmann NB, Grieger KD, Hansen SF. Setting the limits for engineered nanoparticles in European surface waters - are current approaches appropriate? *J Environ Monit* 2009;11:1774-81. DOI
11. Arthur C, Baker JE, Bamford HA. Proceedings of the International Research Workshop on the Occurrence, Effects, and Fate of Microplastic Marine Debris, September 9-11, 2008, University of Washington Tacoma, Tacoma, WA, USA. Available from: https://repository.library.noaa.gov/view/noaa/2509. [Last accessed on 29 Dec 2023].
12. Ebere EC, Wirnkor VA, Ngozi VE, Chukwuemeka IS. Macrodebris and microplastics pollution in Nigeria: first report on abundance, distribution and composition. *Environ Anal Health Toxicol* 2019;34:e2019012. PubMed PMC
13. Cole M, Coppock R, Lindeque PK, et al. Effects of nylon microplastic on feeding, lipid accumulation, and moulting in a coldwater copepod. *Environ Sci Technol* 2019;53:7075-82. DOI
14. Sridharan S, Kumar M, Singh L, Bolan NS, Saha M. Microplastics as an emerging source of particulate air pollution: a critical review. *J Hazard Mater* 2021;418:126245. DOI
15. Li L, Zhou Q, Yin N, Tu C, Luo Y. Uptake and accumulation of microplastics in an edible plant. *Chin Sci Bull* 2019;64:928-34. DOI
16. Burton GA Jr. Stressor exposures determine risk: so, why do fellow scientists continue to focus on superficial microplastics risk? *Environ Sci Technol* 2017;51:13515-6. DOI
17. Wirnkor AV, Ngozi VE, Medo AC, Chioma LK, Ngozi USM, Christian EE. Biomonitoring of heavy metals in blood and urine of African children from owerrimetropolis, eastern Nigeria. *J Chem Health Risks* 2019;9:11-26. DOI
18. Wirnkor VA, Ngozi VE, Ebere EC, Leizou K, Ndu P. Using physicochemical properties in assessment of river water for consumption and irrigation in Nigeria. *Eurasian J Anal Chem* 2019;5:14-23. Available from: https://www.researchgate.net/publication/334108536_Using_physicochemical_properties_in_assessment_of_river_water_for_consumption_and_irrigation_in_Nigeria. [Last accessed on 29 Dec 2023]
19. Fred-Ahmadu OH, Bhagwat G, Oluyoye I, Benson NU, Ayejuyo OO, Palanisami T. Interaction of chemical contaminants with microplastics: principles and perspectives. *Sci Total Environ* 2020;706:135978. DOI
20. Hahladakis JN, Velis CA, Weber R, Iacovidou E, Purnell P. An overview of chemical additives present in plastics: migration, release, fate and environmental impact during their use, disposal and recycling. *J Hazard Mater* 2018;344:179-99. DOI
21. Schossler P, Schripp T, Salthammer T, Bahadir M. Beyond phthalates: gas phase concentrations and modeled gas/particle distribution of modern plasticizers. *Sci Total Environ* 2011;409:4031-8. DOI
22. Liu H, Yang X, Liu G, et al. Response of soil dissolved organic matter to microplastic addition in Chinese loess soil. *Chemosphere* 2017;185:907-17. DOI
23. OECD. Complementing document to the emission scenario document on plastic additives: plastic additives during the use of end products. 2019. Available from: https://one.oecd.org/document/ENV/JM/MONO(2019)10/en/pdf. [Last accessed on 29 Dec 2023].
24. Hermabessiere L, Dehaut A, Paul-Pont I, et al. Occurrence and effects of plastic additives on marine environments and organisms: a review. *Chemosphere* 2017;182:781-93. DOI
25. Tanaka K, Takada H, Yamashita R, Mizukawa K, Fukuwaka M, Watanuki Y. Facilitated leaching of additive-derived PBDEs from plastic by seabirds’ stomach oil and accumulation in tissues. *Environ Sci Technol* 2015;49:11799-807. DOI
26. Tanaka K, Takada H, Iklenaka Y, Nakayama SMM, Ishizuka M. Occurrence and concentration of chemical additives in plastic fragments on a beach on the island of Kauai, Hawaii. *Mar Pollut Bull* 2020;150:110732. DOI
27. Oehlmann J, Schulte-Oehlmann U, Kloas W, et al. A critical analysis of the biological impacts of plasticizers on wildlife. *Philos Trans R Soc Lond B Biol Sci* 2009;364:2047-62. DOI
28. Golshan M, Hatef A, Socha M, et al. Di-(2-ethylhexyl)-phthalate disrupts pituitary and testicular hormonal functions to reduce sperm quality in mature goldfish. *Aquat Toxicol* 2015;163:16-26. DOI
29. Jasna ML, Jelena L, Pero T, Dubravka BV, Jasna Š, Joško P. Levels of trace metals on microplastic particles in beach sediments of the island of Vis, Adriatic Sea, Croatia. *Mar Pollut Bull* 2018;137:231-6. DOI
30. Lohmann R. Microplastics are not important for the cycling and bioaccumulation of organic pollutants in the oceans - but should microplastics be considered POPs themselves? *Integr Environ Assess Manag* 2017;13:460-5. DOI
31. Verla AW, Enyoh CE, Verla EN, Nwarnorh KO. Microplastic-toxic chemical interaction: a review study on quantified levels, mechanism and implication. *SN Appl Sci* 2019;1:1400. DOI
32. Pascall MA, Zabik ME, Zabik MJ, Hernandez RJ. Uptake of polychlorinated biphenyls (PCBs) from an aqueous medium by polyethylene, polyvinyl chloride, and polystyrene films. *J Agric Food Chem* 2005;53:164-9. DOI
33. Carpenter EJ, Smith KL Jr. Plastics on the Sargasso sea surface. *Science* 1972;175:1240-1. DOI
34. Gregory MR. Accumulation and distribution of virgin plastic granules on New Zealand beaches. *New Zeal J Mar Fresh Res* 1978;12:399-414. DOI
35. Nerland IL, Halsband C, Allan I, Thomas KV. Microplastics in marine environments: occurrence, distribution and effects. 2014. Available from: https://www.miljodirektoratet.no/globalassets/publikasjoner/M319/M319.pdf. [Last accessed on 29 Dec 2023].

36. Mato Y, Isobe T, Takada H, Kanehiro H, Ohtake C, Kaminuma T. Plastic resin pellets as a transport medium for toxic chemicals in the marine environment. *Environ Sci Technol* 2001;35:318-24. DOI
37. Frias JPGL, Sobral P, Ferreira AM. Organic pollutants in microplastics from two beaches of the Portuguese coast. *Mar Pollut Bull* 2010;60:1988-92. DOI
38. Rios LM, Moore C, Jones PR. Persistent organic pollutants carried by synthetic polymers in the ocean environment. *Mar Pollut Bull* 2007;54:1230-7. DOI
39. Rochman CM, Hentschel BT, Teh SJ. Long-term sorption of metals is similar among plastic types: implications for plastic debris in aquatic environments. *PLoS One* 2014;9:e85433. DOI
40. Mohsen M, Wang Q, Zhang L, Sun L, Lin C, Yang H. Heavy metals in sediment, microplastic and sea cucumber *Apostichopus japonicus* from farms in China. *Mar Pollut Bull* 2019;143:42-9. DOI
41. Holmes LA, Turner A, Thompson RC. Interactions between trace metals and plastic production pellets under estuarine conditions. *Mar Chem* 2014;167:25-32. DOI
42. Wu B, Taylor CM, Knappe DRU, Nanny MA, Barlaz MA. Factors controlling alkylbenzene sorption to municipal solid waste. *Environ Sci Technol* 2001;35:4569-76. DOI
43. Brennecke D, Duarte B, Paiva F, Caçador I, Canning-clode J. Microplastics as vector for heavy metal contamination from the marine environment. *Estuar Coast Shelf Sci* 2016;178:189-95. DOI
44. Chen W, Ouyang ZY, Qian C, Yu HQ. Induced structural changes of humic acid by exposure of polystyrene microplastics: a spectroscopic insight. *Environ Pollut* 2018;233:1-7. DOI
45. Wei W, Wang C, Shi X, et al. Multiple microplastics induced stress on anaerobic granular sludge and an effectively overcoming strategy using hydrochar. *Water Res* 2022;222:118895. DOI
46. Ali I, Tan X, Li J, et al. Interaction of microplastics and nanoplastics with natural organic matter (NOM) and the impact of NOM on the sorption behavior of anthropogenic contaminants - a critical review. *J Clean Prod* 2022;376:134314. DOI
47. Li WC, Tse HF, Fok L. Plastic waste in the marine environment: a review of sources, occurrence and effects. *Sci Total Environ* 2016;566-7:333-49. DOI
48. Pradel A, Ferreres S, Veclin C, et al. Stabilization of fragmental polystyrene nanoplastic by natural organic matter: insight into mechanisms. *ACS EST Water* 2021;1:1198-208. DOI
49. Fischer AC, Kroon JJ, Verburg TG, Teunissen T, Wolterbeek H. On the relevance of iron adsorption to container materials in small-volume experiments on iron marine chemistry: ^{55}Fe-aided assessment of capacity, affinity and kinetics. *Mar Chem* 2007;107:533-46. DOI
50. Fotopoulou KN, Karapanagioti HK. Surface properties of beached plastic pellets. *Mar Environ Res* 2012;81:70-7. DOI
51. Artham T, Sudhakar M, Venkatesan R, Madhavan Nair C, Murty KVGK, Doble M. Biofouling and stability of synthetic polymers in sea water. *Int Biodeter Biodegr* 2009;63:884-90. DOI
52. Holmes LA, Turner A, Thompson RC. Adsorption of trace metals to plastic resin pellets in the marine environment. *Environ Pollut* 2012;160:42-8. DOI
53. Wang F, Zhang M, Sha W, et al. Sorption behavior and mechanisms of organic contaminants to nano and microplastics. *Molecules* 2020;25:1827. DOI
54. Fred-Ahmadu OH, Ayejuyo OO, Benson NU. Dataset on microplastics and associated trace metals and phthalate esters in sandy beaches of tropical Atlantic ecosystems, Nigeria. *Data Brief* 2020;31:105755. DOI
55. Hüffer T, Hofmann T. Sorption of non-polar organic compounds by micro-sized plastic particles in aqueous solution. *Environ Pollut* 2016;214:194-201. DOI
56. Xu B, Liu F, Brookes PC, Xu J. Microplastics play a minor role in tetracycline sorption in the presence of dissolved organic matter. *Environ Pollut* 2018;240:87-94. DOI
57. Rummel CD, Jahnke A, Gorokhova E, Kühnel D, Schmitt-Jansen M. Impacts of biofilm formation on the fate and potential effects of microplastic in the aquatic environment. *Environ Sci Technol Lett* 2017;4:258-67. DOI
58. Loeb GI, Neihof RA. Marine conditioning films. In: Baier RE, editor. Applied chemistry at protein interfaces. Washington: American Chemical Society; 1975. pp. 319-35. DOI
59. Johansen MP, Cresswell T, Davis J, Howard DL, Howell NR, Prentice E. Biofilm-enhanced adsorption of strong and weak cations onto different microplastic sample types: use of spectroscopy, microscopy and radiotracer methods. *Water Res* 2019;158:392-400. DOI
60. Rutherford ST, Bassler BL. Bacterial quorum sensing: its role in virulence and possibilities for its control. *Cold Spring Harb Perspect Med* 2012;2:a012427. DOI
61. Solano C, Echeverz M, Lasa I. Biofilm dispersion and quorum sensing. *Curr Opin Microbiol* 2014;18:96-104. DOI
62. Srey S, Jahid IK, Ha SD. Biofilm formation in food industries: a food safety concern. *Food Control* 2013;31:572-85. DOI
63. Richard H. Biofilm facilitates metal accumulation onto new plastic pellets in aquatic environments. 2016. Available from: https://scholarworks.calstate.edu/downloads/z603qz90c. [Last accessed on 29 Dec 2023].
64. Mincer TJ, Zettler ER, Amaral-Zettler LA. Biofilms on plastic debris and their influence on marine nutrient cycling, productivity, and hazardous chemical mobility. In: Takada H, Karapanagioti HK, editors. Hazardous chemicals associated with plastics in the marine environment. Cham: Springer International Publishing; 2019. pp. 221-33. DOI
65. Goss KU, Schwarzenbach RP. Rules of thumb for assessing equilibrium partitioning of organic compounds: successes and pitfalls. *J*

Chem Educ 2003;80:450. DOI

66. Violante A, Pigna M. Sorption-desorption processes of metals and metalloids in soil environments. *J Soil Sci Plant Nutr* 2008;8:95-101. DOI
67. Teuten EL, Rowland SJ, Galloway TS, Thompson RC. Potential for plastics to transport hydrophobic contaminants. *Environ Sci Technol* 2007;41:7759-64. DOI
68. Awet TT, Kohl Y, Meier F, et al. Effects of polystyrene nanoparticles on the microbiota and functional diversity of enzymes in soil. *Environ Sci Eur* 2018;30:11. DOI
69. Mafuta C, Baker E, Rucevska I, et al. Drowning in plastics: marine litter and plastic waste vital graphics. 2021. Available from: https://policycommons.net/artifacts/2390247/drowning-in-plastics/3411476/. [Last accessed on 29 Dec 2023].
70. Oliveira TMBF, Ribeiro FWP, Morais S, de Lima-Neto P, Correia AN. Removal and sensing of emerging pollutants released from (micro)plastic degradation: strategies based on boron-doped diamond electrodes. *Curr Opin Electrochem* 2022;31:100866. DOI
71. Tajik S, Beitollahi H, Nejad FG, et al. Recent advances in electrochemical sensors and biosensors for detecting bisphenol A. *Sensors* 2020;20:3364. DOI
72. Zheng ALT, Andou Y. Detection and remediation of bisphenol A (BPA) using Graphene-based materials: mini-review. *Int J Environ Sci Technol* 2021;19:6869-88. DOI
73. Jiang L, Santiago I, Foord J. A comparative study of fouling-free nanodiamond and nanocarbon electrochemical sensors for sensitive bisphenol A detection. *Carbon* 2021;174:390-5. DOI
74. Ali H, Mukhopadhyay S, Jana NR. Selective electrochemical detection of bisphenol A using a molecularly imprinted polymer nanocomposite. *New J Chem* 2019;43:1536-43. DOI
75. Wang S, Pan M, Liu K, et al. A SiO_2@MIP electrochemical sensor based on MWCNTs and AuNPs for highly sensitive and selective recognition and detection of dibutyl phthalate. *Food Chem* 2022;381:132225. DOI
76. Zhang Y, Zhang W, Zhang L, et al. A molecularly imprinted electrochemical BPA sensor based on multi-walled carbon nanotubes modified by CdTe quantum dots for the detection of bisphenol A. *Microchem J* 2021;170:106737. DOI
77. Fries E, Dekiff JH, Willmeyer J, Nuelle MT, Ebert M, Remy D. Identification of polymer types and additives in marine microplastic particles using pyrolysis-GC/MS and scanning electron microscopy. *Environ Sci Process Impacts* 2013;15:1949-56. DOI
78. Kudo Y, Obayashi K, Yanagisawa H, et al. Development of a screening method for phthalate esters in polymers using a quantitative database in combination with pyrolyzer/thermal desorption gas chromatography mass spectrometry. *J Chromatogr A* 2019;1602:441-9. DOI
79. Herrera M, Matuschek G, Kettrup A. Fast identification of polymer additives by pyrolysis-gas chromatography/mass spectrometry. *J Anal Appl Pyrolysis* 2003;70:35-42. DOI
80. Zhang J, Wang L, Kannan K. Microplastics in house dust from 12 countries and associated human exposure. *Environ Int* 2020;134:105314. DOI
81. Yanagisawa H, Kudo Y, Nakagawa K, Miyagawa H, Maruyama F, Fujimaki S. Simultaneous screening of major flame retardants and plasticizers in polymer materials using pyrolyzer/thermal desorption gas chromatography mass spectrometry (Py/TD-GC-MS). *Molecules* 2018;23:728. DOI
82. Hermabessiere L, Receveur J, Himber C, et al. An Irgafos® 168 story: when the ubiquity of an additive prevents studying its leaching from plastics. *Sci Total Environ* 2020;749:141651. DOI
83. IEC 62321-8:2017. Determination of certain substances in electrotechnical products - Part 8: Phthalates in polymers by gas chromatography-mass spectrometry (GC-MS), gas chromatographymass spectrometry using a pyrolyzer/thermal desorption accessory (Py/TD- GC-MS). Available from: https://webstore.iec.ch/publication/32719. [Last accessed on 29 Dec 2023].
84. Kim JW, Kim YM, Moon HM, et al. Comparative study of thermal desorption and solvent extraction-gas chromatography-mass spectrometric analysis for the quantification of phthalates in polymers. *J Chromatogr A* 2016;1451:33-40. DOI
85. Wang FC. Polymer additive analysis by pyrolysis-gas chromatography. II. Flame retardants. *J Chromatogr A* 2000;886:225-35. DOI
86. Dekiff JH, Remy D, Klasmeier J, Fries E. Occurrence and spatial distribution of microplastics in sediments from Norderney. *Environ Pollut* 2014;186:248-56. DOI
87. Šimon P, Rybár M. Kinetics of polymer degradation involving the splitting off of small molecules: Part 8. Thermal degradation of polyvinyl esters. *Polym Degrad Stab* 1992;38:255-9. DOI
88. Riess M, Thoma H, Vierle O, van Eldik R. Identification of flame retardants in polymers using curie point pyrolysis-gas chromatography/mass spectrometry. *J Anal Appl Pyrolysis* 2000;53:135-48. DOI
89. Rial-Otero R, Galesio M, Capelo JL, Simal-gándara J. A review of synthetic polymer characterization by pyrolysis-GC-MS. *Chroma* 2009;70:339-48. DOI
90. Yanagisawa H, Maruyama F, Fujimaki S. Verification of simultaneous screening for major restricted additives in polymer materials using pyrolyzer/thermal desorption gas-chromatography mass spectrometry (Py/TD-GC-MS). *J Anal Appl Pyrolysis* 2019;137:37-42. DOI
91. La Nasa J, Biale G, Sabatini F, Degano I, Colombini MP, Modugno F. Synthetic materials in art: a new comprehensive approach for the characterization of multi-material artworks by analytical pyrolysis. *Herit Sci* 2019;7:8. DOI
92. Perlstein P, Orme P. Determination of polymeric hindered-amine light stabilisers in plastics by pyrolysis - gas chromatography. *J Chromatogr A* 1985;325:87-93. DOI

93. Wang FCY. Polymer additive analysis by pyrolysis-gas chromatography: I. Plasticizers. *J Chromatogr A* 2000;883:199-210. DOI
94. Lau OW, Wong SK. Contamination in food from packaging material. *J Chromatogr A* 2000;882:255-70. DOI
95. Peng X, Chen G, Fan Y, et al. Lifetime bioaccumulation, gender difference, tissue distribution, and parental transfer of organophosphorus plastic additives in freshwater fish. *Environ Pollut* 2021;280:116948. DOI
96. Sridharan S, Kumar M, Saha M, Kirkham MB, Singh L, Bolan NS. The polymers and their additives in particulate plastics: what makes them hazardous to the fauna? *Sci Total Environ* 2022;824:153828. DOI
97. Schmidt N, Fauvelle V, Ody A, et al. The Amazon river: a major source of organic plastic additives to the tropical North Atlantic? *Environ Sci Technol* 2019;53:7513-21. DOI
98. Gunaalan K, Fabbri E, Capolupo M. The hidden threat of plastic leachates: a critical review on their impacts on aquatic organisms. *Water Res* 2020;184:116170. DOI
99. Chen S, Xu C, Ma M, et al. Application of solubility parameters in the preparation of PMMA with permanent antistatic, high toughness, and excellent optical properties. *Polym Adv Technol* 2021;32:3750-8. DOI
100. Costa JC, Oliveira M, Machado AV, Lanceros-Méndez S, Botelho G. Effect of antistatic additives on mechanical and electrical properties of polyethylene foams. *J Appl Polym Sci* 2009;112:1595-600. DOI
101. Ruthven DM. Principles of adsorption and adsorption processes. 1984. Available from: https://www.wiley.com/en-us/Principles+of+Adsorption+and+Adsorption+Processes-p-9780471866060. [Last accessed on 29 Dec 2023].
102. Wright SL, Thompson RC, Galloway TS. The physical impacts of microplastics on marine organisms: a review. *Environ Pollut* 2013;178:483-92. DOI
103. Bergé A, Cladière M, Gasperi J, Coursimault A, Tassin B, Moilleron R. Meta-analysis of environmental contamination by phthalates. *Environ Sci Pollut Res Int* 2013;20:8057-76. DOI
104. Net S, Sempéré R, Delmont A, Paluselli A, Ouddane B. Occurrence, fate, behavior and ecotoxicological state of phthalates in different environmental matrices. *Environ Sci Technol* 2015;49:4019-35. DOI
105. Cuvillier-Hot V, Gaudron SM, Massol F, et al. Immune failure reveals vulnerability of populations exposed to pollution in the bioindicator species *Hediste diversicolor*. *Sci Total Environ* 2018;613-4:1527-42. DOI
106. Nurulnadia MY, Koyama J, Uno S, et al. Accumulation of endocrine disrupting chemicals (EDCs) in the polychaete *Paraprionospio* sp. from the Yodo River mouth, Osaka Bay, Japan. *Environ Monit Assess* 2014;186:1453-63. DOI
107. Gandara e Silva PP, Nobre CR, Resaffe P, Pereira CDS, Gusmão F. Leachate from microplastics impairs larval development in brown mussels. *Water Res* 2016;106:364-70. DOI
108. Bejgarn S, MacLeod M, Bogdal C, Breitholtz M. Toxicity of leachate from weathering plastics: an exploratory screening study with *Nitocra spinipes*. *Chemosphere* 2015;132:114-9. DOI
109. Lithner D, Damberg J, Dave G, Larsson Å. Leachates from plastic consumer products - screening for toxicity with *Daphnia magna*. *Chemosphere* 2009;74:1195-200. DOI
110. Shin PKS, Gopalakrishnan S, Chan AKY, Qian PY, Wu RSS. Interactive effects of hypoxia and PBDE on larval settlement of a marine benthic polychaete. *Mar Pollut Bull* 2014;85:425-32. DOI
111. Setälä O, Norkko J, Lehtiniemi M. Feeding type affects microplastic ingestion in a coastal invertebrate community. *Mar Pollut Bull* 2016;102:95-101. DOI
112. Díaz-Jaramillo M, Miglioranza KSB, Gonzalez M, et al. Uptake, metabolism and sub-lethal effects of BDE-47 in two estuarine invertebrates with different trophic positions. *Environ Pollut* 2016;213:608-17. DOI
113. Lithner D, Nordensvan I, Dave G. Comparative acute toxicity of leachates from plastic products made of polypropylene, polyethylene, PVC, acrylonitrile-butadiene-styrene, and epoxy to *Daphnia magna*. *Environ Sci Pollut Res Int* 2012;19:1763-72. DOI
114. Zhao H, Zhou Y, Li Y, Li S, Yang D. Molecular cloning and expression of the gene for G protein alpha subunit induced by bisphenol A in marine polychaete *Perinereis aibuhitensis*. *Environ Toxicol Pharmacol* 2014;37:521-8. DOI
115. Hamlin HJ, Marciano K, Downs CA. Migration of nonylphenol from food-grade plastic is toxic to the coral reef fish species *Pseudochromis fridmani*. *Chemosphere* 2015;139:223-8. DOI
116. Green DS, Boots B, Sigwart J, Jiang S, Rocha C. Effects of conventional and biodegradable microplastics on a marine ecosystem engineer (*Arenicola marina*) and sediment nutrient cycling. *Environ Pollut* 2016;208:426-34. DOI
117. Lu Y, Lin M, Aitken RJ. Exposure of spermatozoa to dibutyl phthalate induces abnormal embryonic development in a marine invertebrate *Galeolaria caespitosa* (Polychaeta: Serpulidae). *Aquat Toxicol* 2017;191:189-200. DOI
118. Gomiero A, Strafella P, Pellini G, Salvalaggio V, Fabi G. Comparative effects of ingested PVC micro particles with and without adsorbed benzo(a)pyrene vs. spiked sediments on the cellular and sub cellular processes of the benthic organism *Hediste diversicolor*. *Front Mar Sci* 2018;5:99. DOI
119. Gebhardt C, Forster S. Size-selective feeding of *Arenicola marina* promotes long-term burial of microplastic particles in marine sediments. *Environ Pollut* 2018;242:1777-86. DOI
120. Klosterhaus SL, Dreis E, Baker JE. Bioaccumulation kinetics of polybrominated diphenyl ethers from estuarine sediments to the marine polychaete, *Nereis virens*. *Environ Toxicol Chem* 2011;30:1204-12. DOI
121. Capolupo M, Sørensen L, Jayasena KDR, Booth AM, Fabbri E. Chemical composition and ecotoxicity of plastic and car tire rubber leachates to aquatic organisms. *Water Res* 2020;169:115270. DOI
122. Gao DW, Wen ZD. Phthalate esters in the environment: a critical review of their occurrence, biodegradation, and removal during wastewater treatment processes. *Sci Total Environ* 2016;541:986-1001. DOI

123. Rehse S, Kloas W, Zarfl C. Short-term exposure with high concentrations of pristine microplastic particles leads to immobilisation of *Daphnia magna*. *Chemosphere* 2016;153:91-9. DOI
124. Shaw JR, Pfrender ME, Eads BD, et al. *Daphnia* as an emerging model for toxicological genomics. *Adv Exp Med Biol* 2008;2:327-8. DOI
125. Seyoum A, Pradhan A. Effect of phthalates on development, reproduction, fat metabolism and lifespan in *Daphnia magna*. *Sci Total Environ* 2019;654:969-77. DOI
126. Blinova I, Lukjanova A, Vija H, Mortimer M, Heinlaan M. Toxicity of plastic additive 1-hydroxycyclohexyl phenyl ketone (1-HCHPK) to freshwater microcrustaceans in natural water. *Water* 2023;15:3213. DOI
127. Murugan G, Dumont HJ. Influence of light, DMSO and glycerol on the hatchability of *Thamnocephalus platyurus* Packard cysts. In: Belk D, Dumont HJ, Maier G, editors. Studies on large branchiopod biology and aquaculture II. Dordrecht: Springer Netherlands; 1995. pp. 175-8. DOI
128. Zhang X, Liu L, Zhang S, et al. Biodegradation of dimethyl phthalate by freshwater unicellular cyanobacteria. *BioMed Res Int* 2016;2016:5178697. DOI
129. Billings A, Jones KC, Pereira MG, Spurgeon DJ. Plasticisers in the terrestrial environment: sources, occurrence and fate. *Environ Chem* 2021;18:111-30. DOI
130. Kong S, Ji Y, Liu L, et al. Diversities of phthalate esters in suburban agricultural soils and wasteland soil appeared with urbanization in China. *Environ Pollut* 2012;170:161-8. DOI
131. Zeng LJ, Huang YH, Chen XT, et al. Prevalent phthalates in air-soil-vegetable systems of plastic greenhouses in a subtropical city and health risk assessments. *Sci Total Environ* 2020;743:140755. DOI
132. Horton AA, Walton A, Spurgeon DJ, Lahive E, Svendsen C. Microplastics in freshwater and terrestrial environments: evaluating the current understanding to identify the knowledge gaps and future research priorities. *Sci Total Environ* 2017;586:127-41. DOI
133. CEFIC. Plasticisers fact sheet. Available from: https://www.plasticisers.org/wp-content/uploads/2019/08/Plasticisers_Factsheet_EN_MAY2020.pdf. [Last accessed on 29 Dec 2023].
134. Billings A, Carter H, Cross RK, Jones KC, Pereira MG, Spurgeon DJ. Co-occurrence of macroplastics, microplastics, and legacy and emerging plasticisers in UK soils. *Sci Total Environ* 2023;880:163258. DOI
135. Adibi JJ, Perera FP, Jedrychowski W, et al. Prenatal exposures to phthalates among women in New York City and Krakow, Poland. *Environ Health Perspect* 2003;111:1719-22. DOI
136. Rudel RA, Camann DE, Spengler JD, Korn LR, Brody JG. Phthalates, alkylphenols, pesticides, polybrominated diphenyl ethers, and other endocrine-disrupting compounds in indoor air and dust. *Environ Sci Technol* 2003;37:4543-53. DOI
137. Sathyanarayana S. Phthalates and children's health. *Curr Probl Pediatr Adolesc Health Care* 2008;38:34-49. DOI
138. Latini G, De Felice C, Presta G, et al. In utero exposure to di-(2-ethylhexyl)phthalate and duration of human pregnancy. *Environ Health Perspect* 2003;111:1783-5. DOI
139. Main KM, Mortensen GK, Kaleva MM, et al. Human breast milk contamination with phthalates and alterations of endogenous reproductive hormones in infants three months of age. *Environ Health Perspect* 2006;114:270-6. DOI
140. Colón I, Caro D, Bourdony CJ, Rosario O. Identification of phthalate esters in the serum of young Puerto Rican girls with premature breast development. *Environ Health Perspect* 2000;108:895-900. DOI
141. Bornehag CG, Sundell J, Weschler CJ, et al. The association between asthma and allergic symptoms in children and phthalates in house dust: a nested case-control study. *Environ Health Perspect* 2004;112:1393-7. DOI
142. Factor A. Mechanisms of thermal and photodegradations of bisphenol A polycarbonate. In: Clough RL, Billingham NC, Gillen KT, editors. Polymer durability. Washington: American Chemical Society; 1996. pp. 59-76. DOI
143. Bae B, Jeong JH, Lee SJ. The quantification and characterization of endocrine disruptor bisphenol-A leaching from epoxy resin. *Water Sci Technol* 2002;46:381-7. DOI
144. Brede C, Fjeldal P, Skjevrak I, Herikstad H. Increased migration levels of bisphenol A from polycarbonate baby bottles after dishwashing, boiling and brushing. *Food Addit Contam* 2003;20:684-9. DOI
145. Kang JH, Kito K, Kondo F. Factors influencing the migration of bisphenol A from cans. *J Food Prot* 2003;66:1444-7. DOI
146. Sasaki N, Okuda K, Kato T, et al. Salivary bisphenol-A levels detected by ELISA after restoration with composite resin. *J Mater Sci Mater Med* 2005;16:297-300. DOI
147. Richter CA, Birnbaum LS, Farabollini F, et al. *In vivo* effects of bisphenol A in laboratory rodent studies. *Reprod Toxicol* 2007;24:199-224. DOI
148. Sugiura-Ogasawara M, Ozaki Y, Sonta S, Makino T, Suzumori K. Exposure to bisphenol A is associated with recurrent miscarriage. *Hum Reprod* 2005;20:2325-9. DOI
149. Takeuchi T, Tsutsumi O. Serum bisphenol A concentrations showed gender differences, possibly linked toandrogen levels. *Biochem Biophys Res Commun* 2002;291:76-8. DOI
150. Takeuchi T, Tsutsumi O, Ikezuki Y, Takai Y. Taketani Y. Positive relationship between androgen and the endocrine disruptor, bisphenol A, in normal women and women with ovarian dysfunction. *Endocr J* 2004;51:165-9. DOI
151. Pohl HR, Bosch S, Amata R, Eisenmann CJ. Toxicological profile for polybrominated biphenyls and polybrominated diphenyl ethers. Atlanta,GA: Agency for Toxic Substances and Disease Registry. 2004. Available from: https://stacks.cdc.gov/view/cdc/6740. [Last accessed on 29 Dec 2023].
152. Hagmar L, Bjork J, Sjodin A, Bergman A, Erfurth EM. Plasma levels of persistent organohalogensand hormone levels in adult male

humans. *Arch Environ Health* 2001;56:138-43. Available from: https://www.proquest.com/openview/1e3df4bd68adccfe0d26c318d3acd70c/1?pq-origsite=gscholar&cbl=28654. [Last accessed on 29 Dec 2023].

153. Zhou C, Wu J, Ma W, et al. Responses of nitrogen removal under microplastics versus nanoplastics stress in SBR: toxicity, microbial community and functional genes. *J Hazard Mater* 2022;432:128715. DOI

154. Lee J, Jeong S, Long C, Chandran K. Size dependent impacts of a model Microplastic on nitrification induced by interaction with nitrifying bacteria. *J Hazard Mater* 2022;424:127363. DOI

Kelly *et al. Water Emerg Contam Nanoplastics* 2024;3:6
DOI: 10.20517/wecn.2023.66

Water Emerging Contaminants & Nanoplastics

Research Article

Open Access

Plastic and anthropogenic microfiber pollution on exposed sandy beaches in Nova Scotia, Canada

Noreen E. Kelly[1], Olga Trela[1], Heidi Gavel[1,2], Alyssa Vander Kuylen[1]

[1]Fisheries and Oceans Canada, Bedford Institute of Oceanography, Dartmouth B2Y 4A2, Nova Scotia, Canada.
[2]Department of Environmental Science, St. Mary's University, Halifax B3H 3C3, Nova Scotia, Canada.

Correspondence to: Dr. Noreen E. Kelly, Fisheries and Oceans Canada, Bedford Institute of Oceanography, 1 Challenger Drive, Dartmouth B2Y 4A2, Nova Scotia, Canada. E-mail: noreen.kelly@dfo-mpo.gc.ca

How to cite this article: Kelly NE, Trela O, Gavel H, Vander Kuylen A. Plastic and anthropogenic microfiber pollution on exposed sandy beaches in Nova Scotia, Canada. *Water Emerg Contam Nanoplastics* 2024;3:6. https://dx.doi.org/10.20517/wecn.2023.66

Received: 31 Oct 2023 **First Decision:** 7 Dec 2023 **Revised:** 21 Dec 2023 **Accepted:** 8 Jan 2024 **Published:** 15 Jan 2024

Academic Editors: Quan Wang, Zhijie Chen, Roberto Rosal **Copy Editor:** Pei-Yun Wang **Production Editor:** Pei-Yun Wang

Abstract

This study aimed to assess the initial presence of microplastics on two sandy beaches along a rugged coastline in the Northwest Atlantic, an area with limited prior investigation. Sediment samples were collected from High, Mid, and Low intertidal zones at two beaches on the eastern shore of Nova Scotia, Canada. Microplastics were isolated from 100 g sediment samples using density flotation with a sodium iodide solution. Particle characterization included size, shape, and color analysis, with polymer identification performed using Fourier Transform Infrared (FTIR) spectroscopy. Results indicated that the predominant microplastics were small (< 1.4 mm) transparent microfibers, primarily composed of polyethylene terephthalate (PET), nylon, or alkyd polymers from paints. Mean concentrations were comparable between the two beaches, averaging 5.08 ± 3.20 and 5.58 ± 4.52 microplastics per 100 g of sediment, respectively. Non-plastic microfibers, including natural and semi-synthetic cellulosic materials, were notably more abundant, with mean concentrations ranging from 75.9 ± 60.1 to 97.7 ± 87.9 per 100 g sediment. Statistical analysis revealed no significant differences in microplastic counts across tidal zones due to high variability over small spatial scales (tens of meters). Sources of microfibers were potentially from high recreational use at these sites. This study highlights the lower-than-expected levels of microplastic pollution compared to earlier research at these sites and global beach studies. Future monitoring efforts could focus on longitudinal studies to track microplastic trends on these exposed sandy beaches.

Keywords: Beach sand, density separation, microplastics, microfibers, cellulosic fibers, Northwest Atlantic, local sources, tourism, recreation

INTRODUCTION

Microplastics (MPs), synthetic polymers ≤ 5 mm in size[1], are ubiquitous marine pollutants found in all regions of the world ocean, from the surface[2] to the seafloor[3], and from the poles[4,5] to the tropics[6,7]. Primary MPs originate from the release of small particles into the environment during industrial manufacture, transportation, or use; secondary MPs, on the other hand, form when larger plastics undergo fragmentation due to chemical and/or mechanical abrasion as they disperse throughout the ocean[8]. The persistence of MP pollution on a global scale, combined with their small size, gives rise to concerns about their impacts on the marine environment and biota across all trophic levels[9], from microbes[10] and plankton[11] to marine mammals[12]. MPs have been shown to pose ingestion hazards to marine biota[13], increase exposure to toxic contaminants[14,15], and provide substrate to harmful microorganisms and/or invasive species[16]. Despite the increase in research on plastic pollution over the last decade[17], major gaps in understanding of baseline plastic concentrations remain, particularly in the Northwest (NW) Atlantic[18,19].

Beaches and intertidal environments are at a heightened risk of MP pollution, due to their proximity to plastic pollution sources and their role as (temporary) sinks for plastic pollution[20,21]. Thus, assessing baseline concentrations and patterns of deposition in intertidal areas is necessary for a better understanding of the fate of MPs along shorelines. To date, there have been numerous studies examining the abundance of MPs on beaches and shorelines around the world, reporting a range of particles typically in the 10 to 100s per kg of dry sediment, and a predominance of fibers over other types of particles[20,22-27]. Polyethylene and polyester are the most commonly reported MPs in marine sediments[28]. However, reporting anthropogenic (human-made) non-plastic particles derived from cellulose separately from synthetic, petroleum-based fibers[29-31] is becoming more common.

In contrast, very little research has focused on temperate areas of the NW Atlantic, particularly in Atlantic Canada[19,32]. The first study to investigate MP pollution in intertidal sediments (mud and sand) in Nova Scotia, Canada, documented notably high MP fiber abundances[33]. However, in 2012, Mathalon and Hill were unable to validate the identity of their sampled fibers using spectroscopic or other methods[33]. While these methods were not as prevalent in the literature at the time[34], it is now recognized that visual identification alone is insufficient to accurately determine MP concentrations[35,36]. In addition, Mathalon and Hill suspected laboratory contamination of samples, which is now a well-documented issue[33,37-39]. Given the uncertainty in these MP abundance estimates, yet their widespread use in the scientific literature (cited in 556 publications[40]), repetition of their study is clearly warranted.

The region of Atlantic Canada presents an intriguing opportunity for analysing the distribution of MPs, due to its low human population density but a long history of utilizing its coastal and marine environments, particularly for fishing, shipping, transportation, aquaculture, and tourism and recreation[41,42]. In this study, we investigate concentrations of MPs in beach sediments along an exposed coastline in Atlantic Canada, and compare our results to a previous study conducted in the same region[33] through new investigative tools. Our study contributes additional insight into the fate of a persistent environmental pollutant in an understudied region of the global ocean.

METHODS

Study sites and field sampling

Sediment samples were collected at Rainbow Haven beach (44° 38' 46.69" N, 63° 25' 10.131" W) on April 16, 2019 and at Martinique beach (44° 41' 27.86" N, 63° 08' 18.68" W) on April 17, 2019 in Nova Scotia [Figure 1]. Located along the Eastern Shore of Nova Scotia, Rainbow Haven (https://parks.novascotia.ca/park/rainbow-haven-beach) is a 3.2 km long, primarily sand and cobblestone beach, while Martinique (https://parks.novascotia.ca/park/martinique-beach) is a 5 km long crescent white sand beach that is also a protected area for shorebirds and a wildlife refuge for migratory waterfowl. Both beaches are popular swimming and day-use recreational areas and are located eastward along the coast from Halifax Harbour, a major shipping port and population center in the province. The mean tidal range at both beaches is approximately 1.5 m.

On each beach at low tide, four cross-shore transects, approximately 50 m apart, were created, starting just below the wrack line and extending towards low water. On each transect, one sediment core was collected at High, Mid (at the midpoint between High and Low positions), and Low intertidal positions, following Mathalon and Hill[33]. This resulted in a total of 12 cores per beach. Beach sediment cores were collected using 15 cm tall, 750 mL pre-cleaned glass mason jars with metal lids. Immediately prior to collecting each sample, the jar was inverted (with the lid facing downwards), the lid was removed from the jar, and the jar was then driven into the sand until 2.5 cm of space remained within the jar. This covered an approximate depth of 12.5 cm of sediment. A metal trowel was placed underneath the opening of the jar to prevent the contents from falling out as the jar was removed. The jar was turned upright and the lid was quickly secured and the sample was kept in a cooler with ice packs. After returning from the field, the jars were frozen (at -20 °C) until processed.

Laboratory processing

Prior to processing, jars were thawed at 4 °C for a minimum of 72 h. Once thawed, the sediment representing > 5 cm depth was removed from the jar; the remaining sediment in the jar, representing the 0-5 cm depth, was covered with aluminum foil and placed in an oven at 60 °C until dry (~72 h to 1 week). Once dry, the sediment was transferred to a glass beaker and was homogenized by manually mixing the sediment for 1 min in a laminar flow hood. After mixing, a 100.0 g subsample was removed with a metal spoon, and placed in a 500 mL glass beaker for density flotation.

A maximum density sodium iodide (NaI, Sigma Aldrich) solution (mean density of 1.8 ± 0.04 $g \cdot cm^{-3}$) was prepared, using ultrapure water (Milli-Q®; Millipore Sigma) at 25 °C, to separate plastics from the sediment via floatation[43]. NaI was chosen over other solutions, such as sodium chloride (NaCl), as it can more efficiently extract higher-density MPs, such as polyvinylchloride (PVC, 1.3-1.7 $g \cdot cm^{-3}$) and polyethylene terephthalate (PET, 1.4-1.6 $g \cdot cm^{-3}$)[34]. In a fume hood, the NaI solution (210 mL) was added to the 500 mL glass beaker containing 100.0 g (~70.0 mL volume) of sediment to attain a 3:1 NaI to sediment volume ratio. The solution was manually stirred for 2 min with a glass stirring rod. After stirring, the rod was rinsed with a small amount of ultrapure water into the solution, and the solution was covered with aluminum foil and allowed to stand for 30 min. The supernatant was decanted and vacuum filtered onto a 47 mm, 20 µm polycarbonate membrane filter (PCTE, Sterlitech). The 500 mL beaker (with the remaining sediment) was rinsed three times with ultrapure water to capture any remaining particles on the sides of the beaker, and the remaining small amount of supernatant was pipetted into the vacuum funnel. The sides of the vacuum funnels were also rinsed three times with ultrapure water to ensure all particles were transferred onto the filter. Filters were carefully removed and transferred to Petri slides (Millipore Sigma) and then dried (covered) in a desiccator overnight. Once dried, the Petri slides were stored at room temperature.

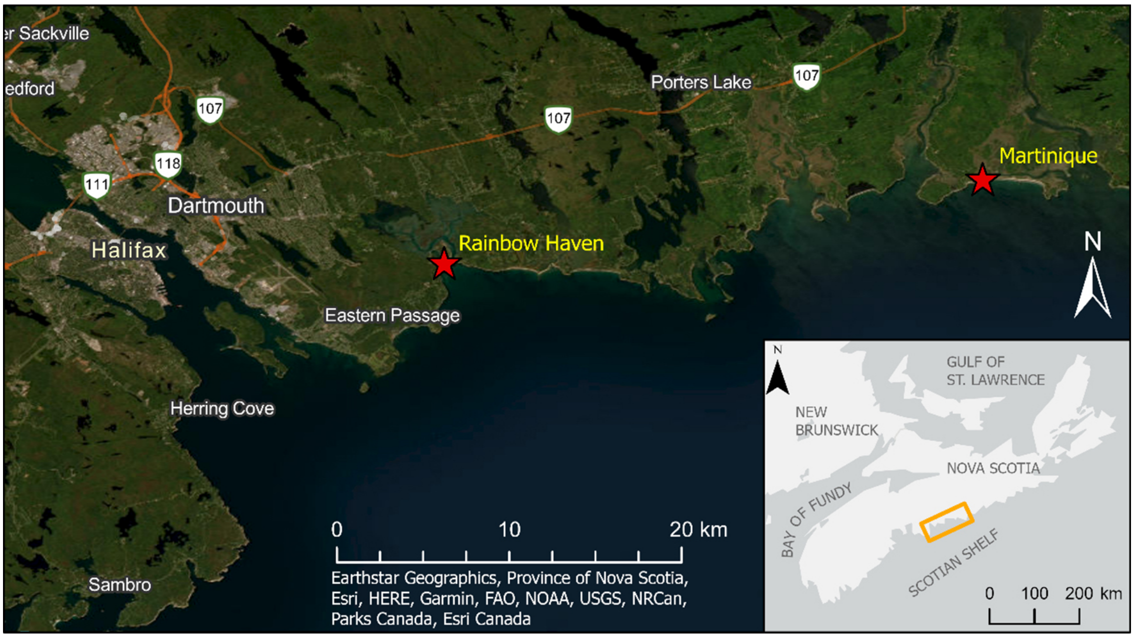

Earthstar Geographics, Province of Nova Scotia, Esri, HERE, Garmin, FAO, NOAA, USGS, NRCan, Parks Canada, Esri Canada

Figure 1. Locations of the two beaches (red stars) sampled in this study. Inset: Sample area (orange box) in relation to the Province of Nova Scotia, Canada.

Particle characterization

Filters were examined under a dissecting microscope at 40-100× magnification. Suspected MPs were removed by hand using ultra fine-tipped jeweler's forceps and placed on double-sided tape in Petri slides. Suspected particles were photographed using a microscope-mounted digital camera (Nikon SMZ-25 fitted with a Di-3 digital camera, Nikon Instruments, Inc.). All suspected particles were classified according to morphology, colour, and transparency, following specific criteria[44-46]. Particle size, measured as the longest dimension, was determined from the microscope photographs using image analysis software (NIS-Elements D, Nikon Instruments, Inc.). We counted all transparent fibers, but only measured the length of a subset of these particles due to their high abundance.

Polymer composition for select particles was identified by Fourier transform infrared (FTIR) spectroscopy at Surface Science Western, University of Western Ontario, London, Ontario, Canada. Selected particles were randomly chosen from each major colour and morphology combination (i.e., transparent fibers, blue fragments, black films, *etc.*), totalling 200 particles or 7% of the dataset. Selected particles were transferred to a diamond compression cell and analyzed by FTIR in transmission mode under the Hyperion 2000 microscope attached to a Bruker Tensor II spectrometer. Particle spectra were matched to a known polymer through manual comparison of individual spectral components using spectral libraries, references, and the knowledge of multiple IR experts; thus, particle matches are considered to be highly certain. For microfibers that had FTIR spectra consistent with a cellulosic material, the method of Cai *et al.* was applied to distinguish between dyed cellulosic textiles (e.g., cottons) and semi-synthetic cellulosic (e.g., regenerated) materials[47]. Each spectrum in question was visually examined for a peak, shoulder, or no peak at ~1,105 cm^{-1}. Particles with spectra that contained a peak at this wavelength were classed as cellulosic fibers; particles with no peak or a shoulder at this wavelength were classed as semi-synthetic fibers. Thus, we report a MP count that includes plastics and alkyds (paints and surface coatings), as well as a separate anthropogenic cellulosic fiber count (following Huntington *et al.*[48]), which includes both cellulosic fibers (i.e., textile fibers made from processed and dyed plant fibers, such as cotton or linen but have been manipulated for human purposes), and semi-synthetic fibers (i.e., particles comprised of rayon or viscose).

Contamination reduction protocols

Following Dimitrijevic *et al.*, many steps were taken to minimize MP contamination during sample collection and processing[49]. In the field, researchers wore clothing made from natural materials (i.e., not fleece) or non-shedding clothing, wore nitrile gloves, and minimized the amount of time samples were exposed to air during the collection process. Mason jars were pre-cleaned in the laboratory and transported to and from the field sites in pre-cleaned totes, and researchers rinsed their gloves with ultrapure water between taking each sample. In the laboratory, researchers wore yellow coveralls (Tyvek 2000, Dupont) or 100% cotton lab coats, a muslin headscarf, and nitrile gloves, which were all cleaned with a lint roller prior to sample processing. Prior to sample processing, all work surfaces, including the laminar flow hood, fume hood, and microscope work area, were cleaned three times using a distinctly-coloured sponge (yellow or pink) dampened with ultrapure water. The microscope work area was covered with plastic sheeting to limit the amount of airborne contamination[37]. Prior to use in density floatation, the NaI solution was vacuum filtered through a 2.7 μm, 90 mm grade D Whatman glass filter and stored in glass jugs. As much field and laboratory equipment as possible was either made of metal or glass and all were rinsed with ultrapure water three times prior to use.

Background and procedural blanks were collected during the laboratory processing of all samples. Individual background blanks for each sample were created by placing a 47 mm, 3 μm PCTE filter, dampened with ultrapure water, in a Petri slide. The background blank was opened whenever its respective sediment sample was exposed to air during sample processing. A procedural blank was conducted each day of sample processing, corresponding to approximately every three samples processed. Each blank was prepared following the same floatation procedure as the sediment samples, but 70 mL of ultrapure water instead of sediment was used. Background and procedural blank filters were examined under 40X magnification and the morphology and colour of any observed particles were recorded.

Statistical analysis

All calculations and statistical analyses were conducted using the R software environment (version 4.2.1, R Core Team[50]) in RStudio (version 2023.06.0, Posit Software).

Particles found in background and procedural blanks were used to correct the final particle counts by establishing a Limit of Detection (LOD) following Dawson *et al.*[51]. The LOD was calculated as the mean + 3* standard deviation (SD) for each particle colour and morphology combination. Corrective action (subtraction of the LOD across all blanks from the number tallied in the sample) was only taken if an item of the same colour and morphology was found in both the blanks and the samples. If the corrected values were less than zero (i.e., subtraction resulted in a negative number), the value was set to zero. Following the blank correction of samples, particle counts per sample were further adjusted to account for the amount of visual identification errors. Using the results of FTIR spectroscopy, the number of particles in each colour-morphology combination was multiplied by a correction factor to account for the amount of visual identification error[46,52]. Final counts were rounded up to the nearest whole integer (to maintain the nature of count data). See Supplementary Materials for original particle counts, LOD values, correction factors, and corrected data.

We tested the difference in particle counts between Beaches (Rainbow Haven, Martinique) and among Intertidal Positions (High, Mid, and Low tide) using generalized linear models (GLMs). We used a negative binomial error distribution to provide a better fit for our over-dispersed count data (number of particles per standard 100 g samples). GLMs for anthropogenic cellulosic fiber counts and MP counts were conducted separately, using the glm.nb function in the MASS package[53]; Tukey post-hoc testing was conducted using the emmeans function in the emmeans package[54]. Model assumptions were assessed from plots of residuals and normal quantiles using the DHARMa package[55].

RESULTS

Background blanks that accounted for airborne laboratory contamination contained a mean of 4.2 ± 5.7 SD particles per sample. Particles found on background blanks were primarily transparent, blue, brown, and black fibers. Procedural blanks that accounted for particle contamination during sample processing contained a mean of 3.6 ± 3.4 SD particles per sample. Particles found on procedural blanks were primarily transparent, red, and blue fibers [Supplementary Materials].

MPs were found in 23 of 24 samples from High to Low intertidal positions, with counts ranging from 0-14 particles per 100 g of sediment. The overall mean concentration was 5.08 ± 3.20 SD and 5.58 ± 4.52 SD MPs per 100 g of sediment at Rainbow Haven and Martinique beaches, respectively. The mean counts of MPs per 100 g of sediment were generally greater at Mid than at High or Low intertidal positions, and High intertidal positions had greater mean counts than Low intertidal positions [Figure 2A]. However, there was no statistically significant difference in mean MP counts per 100 g of sediment detected between Beaches (GLM Likelihood ratio $X^2 = 0.25$, $df = 1$, $P = 0.62$), nor a significant interaction between Beach and Intertidal Position (GLM Likelihood ratio $X^2 = 0.97$, $df = 2$, $P = 0.61$), but there was a significant difference detected in Intertidal Position (GLM Likelihood ratio $X^2 = 6.22$, $df = 2$, $P = 0.045$). Across both beaches, mean MP counts were significantly greater at Mid than Low intertidal position ($P = 0.047$), although there was no significant difference between High and Low ($P = 0.73$) nor High and Mid ($P = 0.23$) intertidal positions [Figure 2A].

At both beaches, anthropogenic cellulosic fibers were up to 19 times more abundant than MP particles, ranging from 1-270 particles per 100 g sediment. The overall mean concentration was 75.9 ± 60.1 SD and 97.7 ± 87.9 SD anthropogenic fibers per 100 g sediment at Rainbow Haven and Martinique beaches, respectively. Mean counts of anthropogenic fibers per 100 g of sediment at Martinique Beach followed the same general pattern across the intertidal zone as for MPs [Figure 2B]. In contrast, at Rainbow Haven, mean anthropogenic cellulosic fiber counts were greatest at the Mid intertidal position, followed by Low and then High intertidal position, respectively [Figure 2B]. Overall, these differences between Beaches (GLM Likelihood ratio $X^2 = 0.94$, $df = 1$, $P = 0.33$), among Intertidal Position (GLM Likelihood ratio $X^2 = 3.89$, $df = 2$, $P = 0.14$), and their interaction (GLM Likelihood ratio $X^2 = 1.38$, $df = 2$, $P = 0.50$), were not statistically significant.

Across all samples combined ($n = 2,220$ particles), 99.2% of all particles extracted from beach sediments were fibers, with the remaining fraction composed of films (0.36%), fragments (0.27%), and foams (0.18%), respectively. Of the subset of particles identified by FTIR spectroscopy ($n = 200$), 93.5% were of anthropogenic cellulosic origin (88% natural, 5.5% semi-synthetic), 5% were plastics [3% were PET, 1% nylon (polyamide), and 1% alkyds], and the remaining 1.5% were either natural particles (i.e., plants) or unable to be identified (i.e., no match in spectral library).

The characteristics of particles (both anthropogenic and plastic) were markedly similar between beaches [Supplementary Figure 1], and thus were compared among intertidal positions for the beaches combined. Particle morphology did not vary among intertidal positions, with fibers dominating at all three tidal heights [Figure 3A]. Transparent particles dominated at all intertidal positions, but yellow, red, blue, and black particle colours were also observed, with the occasional brown, green, and grey coloured-particles

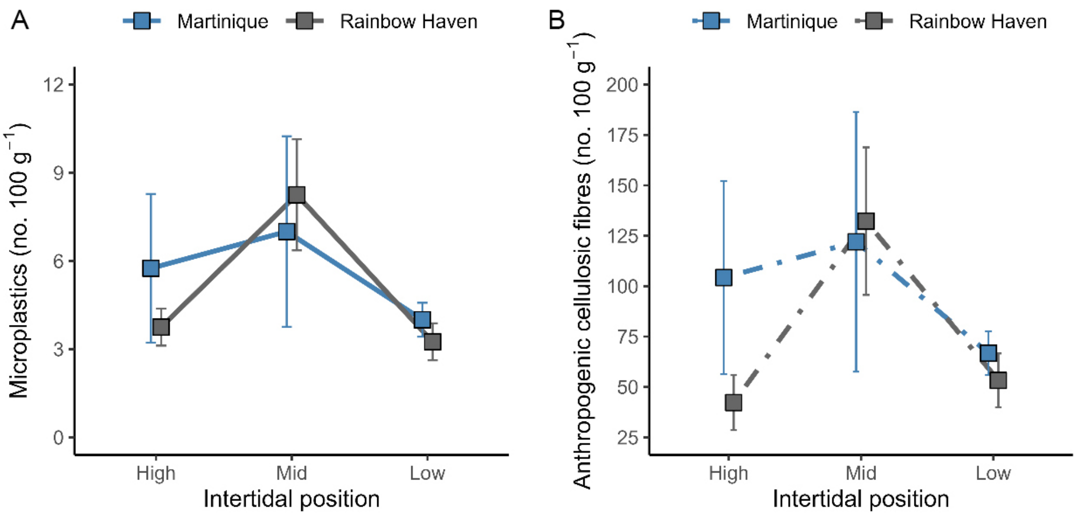

Figure 2. Mean (± SE) (A) MPs and (B) anthropogenic fiber counts (no. particles 100 g^{-1} sediment) by intertidal position sampled at Martinique (blue line) and Rainbow Haven (grey line) beaches. Note the difference in vertical axis scales between panels. MPs: Microplastics.

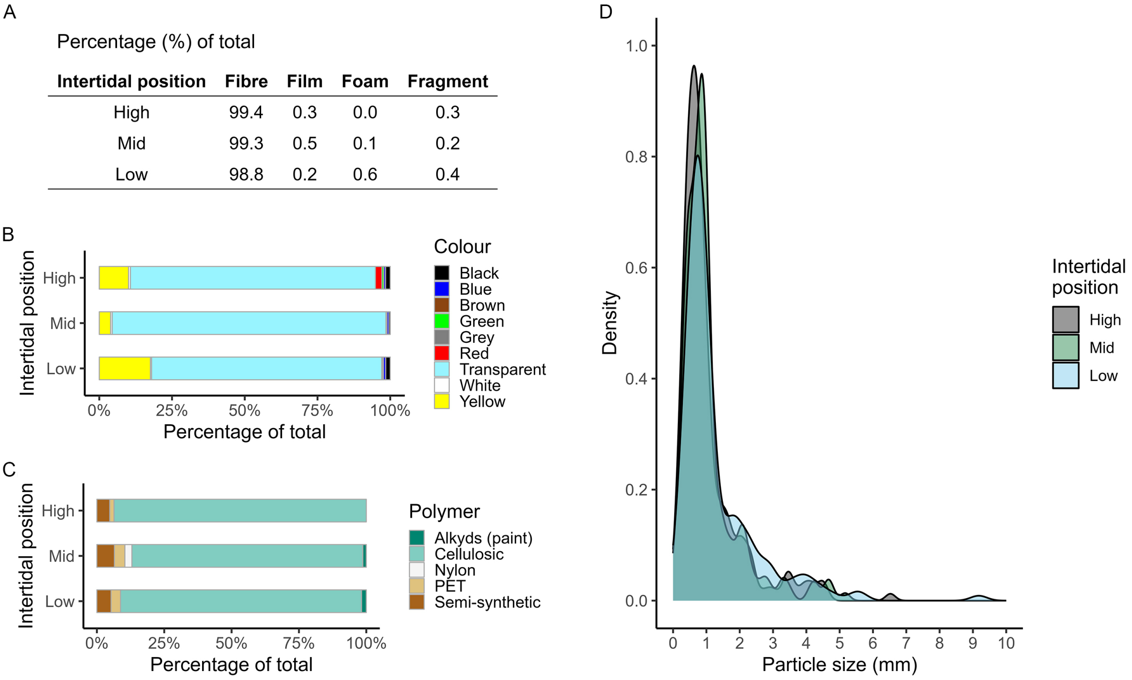

Percentage (%) of total

Intertidal position	Fibre	Film	Foam	Fragment
High	99.4	0.3	0.0	0.3
Mid	99.3	0.5	0.1	0.2
Low	98.8	0.2	0.6	0.4

Figure 3. Characteristics of MPs and anthropogenic particles by intertidal position, collected from Martinique and Rainbow Haven beaches combined. (A) Particle shape and (B) colour, as a percentage of all particles found (*n* = 2,220); (C) polymer composition as a percentage of all particles identified using FTIR spectroscopy (*n* = 200); and (D) size, measured as the longest dimension (in mm). See Materials and Methods for further details. PET: Polyethylene terephthalate; MPs: microplastics; FTIR: Fourier transform infrared.

[Figure 3B]. Yellow particles at Low intertidal positions, and red particles at High intertidal positions, were slightly more abundant than elsewhere. However, we suspect a few of the yellow fibers were actually transparent cellulosic fibers stained from the NaI salts used in the extraction process, suggesting our counts of yellow-coloured fibers may be slightly overestimated.

Of the particles analyzed using FTIR spectroscopy, cellulosic particles were the most common at all tidal heights, followed by semi-synthetic celluloses and PET [Figure 3C]. Alkyds (as paints or surface coatings) were found only at Mid and Low intertidal positions, while nylon (polyamide) fibers were found only at Mid intertidal positions [Figure 3C]. Sodium benzoate was a common secondary contaminant found on 24 (or ~14%) of the anthropogenic cellulosic fibers as identified from FTIR spectroscopy.

While particle sizes ranged from 65-9,176 µm, most anthropogenic and plastic particles were small, being ≤ 1.4 mm (1,400 µm) in longest dimension [Figure 3D]. At Low intertidal positions, there were slightly fewer particles < 1.4 mm and slightly more particles between 1.8-3 mm; otherwise, the distribution of particle lengths was very similar among intertidal positions.

DISCUSSION

In this study, we demonstrate a high abundance of anthropogenic microfiber pollution in the intertidal sediments of two exposed sandy beaches along the Eastern Shore of Nova Scotia. Transparent anthropogenic cellulosic fibers ≤ 1.4 mm in size were the most commonly encountered particle type across the intertidal, being up to 19 times more abundant than MP pollution. Globally, fibers are the dominant MP morphology found on beaches, accounting for 90% of all particles[20,28]. However, in recent years, more attention has been given to documenting human-made, non-plastic microfibers (e.g., anthropogenic celluloses) in addition to synthetic and semi-synthetic textile fibers[29-31]. Similar to our findings, small (≤ 1 mm) non-plastic, cellulosic microfibers have been previously documented to comprise a large portion of sediment samples collected from beaches worldwide, ranging from 19%-93.8% of extracted particle types[20,25,26,56]. Such fibers have also been reported to occur in other marine habitats[31,57], as well as ingested by marine species[58-60], suggesting their distribution is as widespread as other types of plastic pollution. Although the relative rate of degradation is faster for anthropogenic cellulosic fibers than for plastics in marine environments[61] - potentially reducing their persistence in the environment compared to plastics - many anthropogenic celluloses are treated with a range of colourants (dyes, pigments) and finishes (flame retardants, antimicrobial agents, stabilizers, softeners) that may leach into the environment[62,63]. As anthropogenic cellulosic fibers may have similar toxicological impacts as plastics to marine biota once ingested[64], additional research is needed to determine the ecotoxicological risk of anthropogenic microfiber pollution to intertidal fauna in Atlantic Canada and elsewhere.

MP contamination at Rainbow Haven and Martinique beaches was towards the lower end of the range of particles reported by studies in other areas of the globe [Table 1], suggesting low MP pollution at our sites. We identified plastic polymers of nylon, alkyds, PET, and non-plastic semi-synthetic celluloses (e.g., viscose, rayon). Once deposited on the beach, the higher density of these polymers compared to seawater (e.g., nylon = 1.13-1.15 $g \cdot cm^{-3}$; PET = 1.29-1.40 $g \cdot cm^{-3}$; viscose/rayon = 1.53 $g \cdot cm^{-3}$, cellulose = 1.5 $g \cdot cm^{-3}$; alkyds = 1.2-1.7 $g \cdot cm^{-3}$; seawater = 1.027 $g \cdot cm^{-3}$) may make them more likely to be retained within the sediments along this wave-exposed coastline. Further, turbulent mixing of beach sediments during high wave action may bury MPs within the sand, and protect them from washing back into the water column[21]. PET is frequently used in the construction of food packaging, beverage bottles, and clothing, while nylon is widely used in textiles, nets and ropes, and sportswear[49,70]. Fragments of alkyd plastics, frequently used in paints and other surface coatings, suggest an urban or marine source for these particles, possibly from fishing or recreational boats[7,25,46]. However, in combination with the high abundance of anthropogenic celluloses in our samples, some of which were contaminated with sodium benzoate (a widely used antifungal and antimicrobial agent in foods and cosmetics, including sunscreens), it suggests that certain MP sources might be local rather than arriving from distant locations (i.e., from wear and tear of textiles, such as swimsuits, beach towels, blankets, clothing, *etc.*, and fragmentation of plastic containers discarded on the beach).

Table 1. Comparison of MP abundance in sandy sediments reported from other published studies around the globe

Location	MP abundance (no. kg^{-1} d.w. sediment)	Source
Atlantic coast, Canada	50.8 ± 32.0 to 55.8 ± 45.2[a]	Our current study
Atlantic coast, Canada	2,000-8,000[a,b]	Mathalon and Hill[33]
Bay of Fundy, Canada	268 ± 208.7[c]	Forsythe[65]
Atlantic coast, USA	63.8 ± 19.1 to 126.3 ± 43.2	Whitemire and Van Bloem[66]
Pacific coast, USA	38.8 ± 7.2 to 140.0 ± 24.8	Whitemire and Van Bloem[66]
Pacific coast, Mexico	179 ± 50	Piñon-Colin *et al.*[27]
Pacific coast, Gulf of California	76 ± 12	Piñon-Colin *et al.*[27]
Baja California, Mexico	135 ± 92	Piñon-Colin *et al.*[27]
Pacific Islands, USA	98.8 ± 27.7 to 187.5 ± 22.4	Whitemire and Van Bloem[66]
Alaska, USA	21.3 ± 4.3 to 128.8 ± 36.1	Whitemire and Van Bloem[66]
Bohai Sea, China	102.9 ± 39.9 to 163.3 ± 37.7	Yu *et al.*[25]
India	45 ± 12 to 220 ± 50	Tiwari *et al.*[67]
Arabian Gulf	13.5 (range 6-38)	Abayomi *et al.*[56]
Europe, Mediterranean coast	291 ± 62	Lots *et al.*[26]
Slovenia coast	133.3 (median)	Laglbauer *et al.*[68]
Baltic coast	14-532[b]	Stolte *et al.*[24]
Baltic coast	88.10 (median)	Hengstmann *et al.*[69]
Europe, Baltic coast	270 ± 90	Lots *et al.*[26]
Belgian coast	92.8 ± 37.2	Claessens *et al.*[23]
Europe, Atlantic coast	190 ± 35	Lots *et al.*[26]

Values are means ± SD unless otherwise indicated. [a]units converted to no. kg^{-1} sediment to enable inter-study comparison; [b]reported as fibers only; [c]intertidal mud and sand. MP: Microplastic.

Tourism has been implicated as a large contributor of MPs at beaches worldwide[24,25,27,71,72]. Due to their proximity to urban centers, Rainbow Haven and Martinique beaches are popular recreational sites throughout the year[73], lending further support to local tourism as the source of some microfiber pollution in this area.

Combining the results of two previous regional studies[33,65] with our current findings on MP pollution in intertidal zones can shed light on the distribution of this pervasive environmental pollutant on Atlantic Canadian coastlines. Compared to our 0-1.4 MPs per 10 g sediment, Mathalon and Hill documented 20-80 MP fibers per 10 g sediment at Rainbow Haven beach[33]. Given that our sample processing methods differed (Mathalon and Hill used a chemical digestion and short density floatation with NaCl compared to our longer NaI floatation only[33]), it is difficult to directly compare absolute values of MP concentrations between studies. However, at the time, Mathalon and Hill could not validate the identity of their sampled fibers using spectroscopic or other methods, and laboratory contamination of samples was also suspected, suggesting their MP fiber estimates were overestimated by 1-2 orders of magnitude[33]. More recently, Forsythe[65] examined MPs (validated using FTIR) in the intertidal zone at various locations in the Bay of Fundy, an area known for its dynamic tidal range[74], documenting a mean concentration of 268 ± 208.7 MPs per 1 kg sediment, of which 89% were fibers. As in our study, Mathalon and Hill[33] and Forsythe[65] did not find any significant differences in MP quantities across tidal ranges. Collectively, these results suggest MPs and anthropogenic microfibers are evenly distributed along intertidal gradients in the sandy sediments around Nova Scotia. However, the high variability within beaches among samples and transects taken over small spatial scales (10 s of meters) documented in our and these studies also stresses the need for caution when extrapolating to identify broader spatial patterns of pollution in the intertidal zones of Atlantic Canada. More research is clearly needed before the fate of MP pollution is fully understood in these wave-and tidal-dominated systems.

Blue, black, and other brightly coloured MPs are the most frequently detected particles in sediments worldwide[24,28], due to the high global production of plastics with these colours, and/or the ease of visually distinguishing particles of these colours from sediment during sampling[75]. The distribution of colours we report herein may be an indicator of the residence time of these microfibers on Nova Scotia beaches, as the high load of transparent microfibers suggests significant exposure of these particles to UV solar radiation[76]. As we sampled in April before the height of the recreational and tourism season, it is possible that the majority of microfibers were deposited the previous year and lost their colour over the fall and winter through environmental exposure[7]. Future sampling to examine the seasonal deposition of microfibers along the coastline of Nova Scotia would provide additional insight into the sources and residence time of anthropogenic pollution to Atlantic Canadian coastlines. For example, targeted sampling before, during, and after summer could test not only for seasonal changes in plastic loading, but also whether the sources of contamination and MP types change with seasonal recreational use.

Our study documented MP and anthropogenic (non-plastic) microfiber pollution along exposed beaches in Atlantic Canada, and added new investigative tools (e.g., FTIR, contamination control protocols) to refine previous estimates in this understudied region. While our sampling design replicated that of Mathalon and Hill[33] in order to enable a regional comparison, the design shares similarities to those recommended by other monitoring programs for beach litter assessments[77,78]. However, since our results suggest MPs (and anthropogenic microfibers) are patchily distributed over small spatial scales (10 s of m) in this region, many more replicates would be needed to detect differences in the spatial patterns of MP distribution and attribute potential differences to environmental or anthropogenic factors. With additional sampling effort comes increased costs and time, making monitoring potentially less feasible to conduct. Fisner *et al.* suggest that time series assessments may be more realistic than aiming for estimates of absolute particle density[79]. We suggest future work in this region could target Rainbow Haven beach as a focal point for time series analysis of MP change on exposed sandy beaches.

DECLARATIONS

Acknowledgments

The authors wish to acknowledge Harvey C and Zimmerman R for assistance in the field, and Marteinson S and Breeze H for providing financial support for Fourier transform infrared analysis. In addition, we thank our colleagues Gurney-Smith H and Law B, as well as four anonymous reviewers, whose constructive comments helped improve this manuscript.

Authors' contributions

Made substantial contributions to the conception and design of the study and performed data analysis and interpretation: Kelly NE, Gavel H

Performed data acquisition, as well as providing administrative, technical, and material support: Kelly NE, Trela O, Vander Kuylen A

Wrote paper: Kelly NE

Provided comments and review: Gavel H, Trela O, Vander Kuylen A

Availability of data and materials

The dataset for this research is included in the Supplementary Materials attached to this publication.

Financial support and sponsorship
Funding for this work was provided by Fisheries and Oceans Canada to Kelly NE.

Conflicts of interest
All authors declared that there are no conflicts of interest.

Ethical approval and consent to participate
Not applicable.

Consent for publication
Not applicable.

REFERENCES

1. Frias JPGL, Nash R. Microplastics: finding a consensus on the definition. *Mar Pollut Bull* 2019;138:145-7. DOI PubMed
2. Isobe A, Azuma T, Cordova MR, et al. A multilevel dataset of microplastic abundance in the world's upper ocean and the Laurentian Great Lakes. *Micropl Nanopl* 2021;1:16. DOI
3. Harris PT, Maes T, Raubenheimer K, Walsh JP. A marine plastic cloud - Global mass balance assessment of oceanic plastic pollution. *Cont Shelf Res* 2023;255:104947. DOI
4. Isobe A, Uchiyama-Matsumoto K, Uchida K, Tokai T. Microplastics in the Southern Ocean. *Mar Pollut Bull* 2017;114:623-6. DOI
5. Lusher AL, Tirelli V, O'Connor I, Officer R. Microplastics in Arctic polar waters: the first reported values of particles in surface and sub-surface samples. *Sci Rep* 2015;5:14947. DOI
6. Baztan J, Carrasco A, Chouinard O, et al. Protected areas in the Atlantic facing the hazards of micro-plastic pollution: first diagnosis of three islands in the Canary Current. *Mar Pollut Bull* 2014;80:302-11. DOI
7. Ivar do Sul JA, Costa MF, Fillmann G. Microplastics in the pelagic environment around oceanic islands of the Western Tropical Atlantic Ocean. *Water Air Soil Pollut* 2014;225:2004. DOI
8. Andrady AL. The plastic in microplastics: a review. *Mar Pollut Bull* 2017;119:12-22. DOI
9. Ivar do Sul JA, Costa MF. The present and future of microplastic pollution in the marine environment. *Environ Pollut* 2014;185:352-64. DOI
10. Zettler ER, Mincer TJ, Amaral-Zettler LA. Life in the "plastisphere": microbial communities on plastic marine debris. *Environ Sci Technol* 2013;47:7137-46. DOI
11. Prata JC, da Costa JP, Lopes I, Duarte AC, Rocha-Santos T. Effects of microplastics on microalgae populations: a critical review. *Sci Total Environ* 2019;665:400-5. DOI PubMed
12. Kühn S, van Franeker JA. Quantitative overview of marine debris ingested by marine megafauna. *Mar Pollut Bull* 2020;151:110858. DOI
13. Baechler BR, Stienbarger CD, Horn DA, et al. Microplastic occurrence and effects in commercially harvested North American finfish and shellfish: current knowledge and future directions. *Limnol Oceanogr Lett* 2020;5:113-36. DOI
14. Hermabessiere L, Dehaut A, Paul-Pont I, et al. Occurrence and effects of plastic additives on marine environments and organisms: a review. *Chemospher* 2017;182:781-93. DOI PubMed
15. Avio CG, Gorbi S, Milan M, et al. Pollutants bioavailability and toxicological risk from microplastics to marine mussels. *Environ Pollut* 2015;198:211-22. DOI
16. Kirstein IV, Kirmizi S, Wichels A, et al. Dangerous hitchhikers? Evidence for potentially pathogenic *Vibrio* spp. on microplastic particles. *Mar Environ Res* 2016;120:1-8. DOI PubMed
17. Schmid C, Cozzarini L, Zambello E. Microplastic's story. *Mar Pollut Bull* 2021;162:111820. DOI PubMed
18. Haarr ML, Falk-Andersson J, Fabres J. Global marine litter research 2015-2020: geographical and methodological trends. *Sci Total Environ* 2022;820:153162. DOI
19. Melvin J, Bury M, Ammendolia J, Mather C, Liboiron M. Critical gaps in shoreline plastics pollution research. *Front Mar Sci* 2021;8:689108. DOI
20. Harris PT. The fate of microplastic in marine sedimentary environments: a review and synthesis. *Mar Pollut Bull* 2020;158:111398. DOI
21. Zhang H. Transport of microplastics in coastal seas. *Estuar Coast Shelf Sci* 2017;199:74-86. DOI
22. Browne MA, Crump P, Niven SJ, et al. Accumulation of microplastic on shorelines woldwide: sources and sinks. *Environ Sci Technol* 2011;45:9175-9. DOI

23. Claessens M, De Meester S, Van Landuyt L, De Clerck K, Janssen CR. Occurrence and distribution of microplastics in marine sediments along the Belgian coast. *Mar Pollut Bull* 2011;62:2199-204. DOI
24. Stolte A, Forster S, Gerdts G, Schubert H. Microplastic concentrations in beach sediments along the German Baltic coast. *Mar Pollut Bull* 2015;99:216-29. DOI
25. Yu X, Peng J, Wang J, Wang K, Bao S. Occurrence of microplastics in the beach sand of the Chinese inner sea: the Bohai Sea. *Environ Pollut* 2016;214:722-30. DOI
26. Lots FAE, Behrens P, Vijver MG, Horton AA, Bosker T. A large-scale investigation of microplastic contamination: abundance and characteristics of microplastics in European beach sediment. *Mar Pollut Bull* 2017;123:219-26. DOI
27. de Jesus Piñon-Colin TJ, Rodriguez-Jimenez R, Pastrana-Corral MA, Rogel-Hernandez E, Wakida FT. Microplastics on sandy beaches of the Baja California Peninsula, Mexico. *Mar Pollut Bull* 2018;131:63-71. DOI
28. Gago J, Carretero O, Filgueiras AV, Viñas L. Synthetic microfibers in the marine environment: a review on their occurrence in seawater and sediments. *Mar Pollut Bull* 2018;127:365-76. DOI
29. Henry B, Laitala K, Klepp IG. Microfibres from apparel and home textiles: prospects for including microplastics in environmental sustainability assessment. *Sci Total Environ* 2019;652:483-94. DOI
30. Barrows APW, Cathey SE, Petersen CW. Marine environment microfiber contamination: global patterns and the diversity of microparticle origins. *Environ Pollut* 2018;237:275-84. DOI
31. Sanchez-Vidal A, Thompson RC, Canals M, de Haan WP. The imprint of microfibres in southern European deep seas. *PLoS One* 2018;13:e0207033. DOI
32. Anderson JC, Park BJ, Palace VP. Microplastics in aquatic environments: implications for Canadian ecosystems. *Environ Pollut* 2016;218:269-80. DOI
33. Mathalon A, Hill P. Microplastic fibers in the intertidal ecosystem surrounding Halifax Harbor, Nova Scotia. *Mar Pollut Bull* 2014;81:69-79. DOI PubMed
34. Hanvey JS, Lewis PJ, Lavers JL, Crosbie ND, Pozo K, Clarke BO. A review of analytical techniques for quantifying microplastics in sediments. *Anal Methods* 2017;9:1369-83. DOI
35. Lenz R, Enders K, Stedmon CA, Mackenzie DMA, Nielsen TG. A critical assessment of visual identification of marine microplastic using Raman spectroscopy for analysis improvement. *Mar Pollut Bull* 2015;100:82-91. DOI
36. Song YK, Hong SH, Jang M, et al. A comparison of microscopic and spectroscopic identification methods for analysis of microplastics in environmental samples. *Mar Pollut Bull* 2015;93:202-9. DOI
37. Woodall LC, Gwinnett C, Packer M, Thompson RC, Robinson LF, Paterson GLJ. Using a forensic science approach to minimize environmental contamination and to identify microfibres in marine sediments. *Mar Pollut Bull* 2015;95:40-6. DOI
38. Wesch C, Elert AM, Wörner M, Braun U, Klein R, Paulus M. Assuring quality in microplastic monitoring: about the value of clean-air devices as essentials for verified data. *Sci Rep* 2017;7:5424. DOI
39. Prata JC, Reis V, da Costa JP, Mouneyrac C, Duarte AC, Rocha-Santos T. Contamination issues as a challenge in quality control and quality assurance in microplastics analytics. *J Hazard Mater* 2021;403:123660. DOI
40. Web of Science. Citations of Microplastic fibers in the intertidal ecosystem surrounding Halifax Harbour, Nova Scotia 2023. Available from: https://www.webofscience.com/wos/woscc/citation-report/557a62ad-a1dd-4fe6-b153-2235df983f90-aeb88243. [Last accessed on 10 Jan 2024]
41. Lotze HK, Milewski I. Two centuries of multiple human impacts and successive changes in a North Atlantic food web. *Ecol Appl* 2004;14:1428-47. DOI
42. MacLean M, Breeze H, Walmsley J, Corkum J. State of the scotian shelf report. *Can Tech Rep Fish Aquat Sci* 3074. Available from: https://publications.gc.ca/collections/collection_2014/mpo-dfo/Fs97-6-3074-eng.pdf. [Last accessed on 10 Jan 2024]
43. Kedzierski M, Le Tilly V, César G, Sire O, Bruzaud S. Efficient microplastics extraction from sand. A cost effective methodology based on sodium iodide recycling. *Mar Pollut Bull* 2017;115:120-9. DOI
44. Hartmann NB, Hüffer T, Thompson RC, et al. Are we speaking the same language? Recommendations for a definition and categorization framework for plastic debris. *Environ Sci Technol* 2019;53:1039-47. DOI
45. Karlsson TM, Kärrman A, Rotander A, Hassellöv M. Comparison between manta trawl and in situ pump filtration methods, and guidance for visual identification of microplastics in surface waters. *Environ Sci Pollut Res Int* 2020;27:5559-71. DOI PubMed PMC
46. Kelly NE, Feyrer L, Gavel H, et al. Long term trends in floating plastic pollution within a marine protected area identifies threats for endangered northern bottlenose whales. *Environ Res* 2023;227:115686. DOI
47. Cai H, Du F, Li L, Li B, Li J, Shi H. A practical approach based on FT-IR spectroscopy for identification of semi-synthetic and natural celluloses in microplastic investigation. *Sci Total Environ* 2019;669:692-701. DOI
48. Huntington A, Corcoran PL, Jantunen L, et al. A first assessment of microplastics and other anthropogenic particles in Hudson Bay and the surrounding eastern Canadian Arctic waters of Nunavut. *FACETS* 2020;5:432-54. DOI
49. Dimitrijevic J, Kelly NE, Moore AM, Breeze H, Ross PS. Best practices for the extraction and enumeration of microplastics in various marine environmental matrices. *Can Tech Rep Fish Aquat Sci* 3334. Available from https://publications.gc.ca/collections/collection_2019/mpo-dfo/Fs97-6-3334-eng.pdf. [Last accessed on 10 Jan 2024]
50. R Core Team. R: a language and environment for statistical computing. R Foundation for Statistical Computing. Vienna, Austria. 2022. Available from: https://www.R-project.org/. [Last accessed on 10 Jan 2024].
51. Dawson AL, Santana MFM, Nelis JLD, Motti CA. Taking control of microplastics data: a comparison of control and blank data

correction methods. *J Hazard Mater* 2023;443:130218. DOI

52. Covernton GA, Collicutt B, Gurney-smith HJ, et al. Microplastics in bivalves and their habitat in relation to shellfish aquaculture proximity in coastal British Columbia, Canada. *Aquacult Environ Interact* 2019;11:357-74. DOI
53. Venables WN, Ripley BD. Modern applied statistics with S. 4th Edition. New York: Springer; 2002. DOI
54. Lenth RV. emmeans: Estimated marginal means, aka least-squares means. R package version 1.9.0. Available from: https://CRAN.R-project.org/package=emmeans. [Last accessed on 10 Jan 2024].
55. Hartig F. DHARMa: residual diagnostics for hierarchical (multi-level/mixed) regression models. R package version 0.4.6. Available from: https://CRAN.R-project.org/package=DHARMa. [Last accessed on 10 Jan 2024].
56. Abayomi OA, Range P, Al-Ghouti MA, Obbard JP, Almeer SH, Ben-Hamadou R. Microplastics in coastal environments of the Arabian Gulf. *Mar Pollut Bull* 2017;124:181-8. DOI PubMed
57. Suaria G, Achtypi A, Perold V, et al. Microfibers in oceanic surface waters: a global characterization. *Sci Adv* 2020;6:eaay8493. DOI PubMed PMC
58. Remy F, Collard F, Gilbert B, Compère P, Eppe G, Lepoint G. When microplastic is not plastic: the ingestion of artificial cellulose fibers by macrofauna living in seagrass macrophytodetritus. *Environ Sci Technol* 2015;49:11158-66. DOI PubMed
59. Compa M, Ventero A, Iglesias M, Deudero S. Ingestion of microplastics and natural fibres in *Sardina pilchardus* (Walbaum, 1792) and *Engraulis encrasicolus* (Linnaeus, 1758) along the Spanish Mediterranean coast. *Mar Pollut Bull* 2018;128:89-96. DOI PubMed
60. Savoca S, Capillo G, Mancuso M, et al. Detection of artificial cellulose microfibers in *Boops boops* from the northern coasts of Sicily (Central Mediterranean). *Sci Total Environ* 2019;691:455-65. DOI
61. Zambrano MC, Pawlak JJ, Daystar J, Ankeny M, Cheng JJ, Venditti RA. Microfibers generated from the laundering of cotton, rayon and polyester based fabrics and their aquatic biodegradation. *Mar Pollut Bull* 2019;142:394-407. DOI PubMed
62. Sait STL, Sørensen L, Kubowicz S, et al. Microplastic fibres from synthetic textiles: environmental degradation and additive chemical content. *Environ Pollut* 2021;268:115745. DOI
63. Sørensen L, Groven AS, Hovsbakken IA, et al. UV degradation of natural and synthetic microfibers causes fragmentation and release of polymer degradation products and chemical additives. *Sci Total Environ* 2021;755:143170. DOI
64. Athey SN, Erdle LM. Are we underestimating anthropogenic microfiber pollution? A critical review of occurrence, methods, and reporting. *Environ Toxicol Chem* 2022;41:822-37. DOI PubMed
65. Forsythe C. The quantification of microplastics in intertidal sediments in the Bay of Fundy, Canada. 2016. Available from: https://www.viurrspace.ca/server/api/core/bitstreams/46d54dbb-77ae-45d4-bdf8-3e38428545ce/content. [Last accessed on 10 Jan 2024].
66. Whitmire SL, Van Bloem SJ. Quantification of microplastics on National Park Beaches. NOAA Marine Debris Program. Available from: https://marinedebris.noaa.gov/microplastics/quantification-microplastics-national-park-beaches. [Last accessed on 10 Jan 2024].
67. Tiwari M, Rathod TD, Ajmal PY, Bhangare RC, Sahu SK. Distribution and characterization of microplastics in beach sand from three different Indian coastal environments. *Mar Pollut Bull* 2019;140:262-73. DOI PubMed
68. Laglbauer BJL, Franco-Santos RM, Andreu-Cazenave M, et al. Macrodebris and microplastics from beaches in Slovenia. *Mar Pollut Bull* 2014;89:356-66. DOI
69. Hengstmann E, Tamminga M, Vom Bruch C, Fischer EK. Microplastic in beach sediments of the Isle of Rügen (Baltic Sea) - Implementing a novel glass elutriation column. *Mar Pollut Bull* 2018;126:263-74. DOI PubMed
70. United Nations Environment Programme. Chemicals in plastics - a technical report. Available from: https://www.unep.org/resources/report/chemicals-plastics-technical-report. [Last accessed on 10 Jan 2024].
71. Jayasiri HB, Purushothaman CS, Vennila A. Quantitative analysis of plastic debris on recreational beaches in Mumbai, India. *Mar Pollut Bull* 2013;77:107-12. DOI PubMed
72. Gao F, Li J, Hu J, et al. The seasonal distribution characteristics of microplastics on bathing beaches along the coast of Qingdao, China. *Sci Total Environ* 2021;783:146969. DOI
73. Tourism Nova Scotia. 2019 Nova Scotia visitor exit survey overall results. Available from: https://tourismns.ca/sites/default/files/2021-01/2019%20VES%20Full%20Year%20Report.pdf. [Last accessed on 10 Jan 2024].
74. Bundy A, Themelis D, Sperl J, den Heyer N. Inshore Scotian Shelf Ecosystem Overview Report: Status and Trends. 2014. Available from: https://publications.gc.ca/collections/collection_2014/mpo-dfo/Fs70-5-2014-065-eng.pdf. [Last accessed on 10 Jan 2024].
75. Lavers JL, Oppel S, Bond AL. Factors influencing the detection of beach plastic debris. *Mar Environ Res* 2016;119:245-51. DOI PubMed
76. Pinlova B, Nowack B. Characterization of fiber fragments released from polyester textiles during UV weathering. *Environ Pollut* 2023;322:121012. DOI PubMed
77. Cheshire A, Adler E, Barbière J. UNEP/IOC guidelines on survey and monitoring of marine litter. 2009. Available from: https://wedocs.unep.org/20.500.11822/13604. [Last accessed on 10 Jan 2024].
78. Lippiatt S, Opfer S, Arthur C. Marine debris monitoring and assessment: recommendations for monitoring debris trends in the marine environment. Available from: https://repository.library.noaa.gov/view/noaa/2681. [Last accessed on 10 Jan 2024].
79. Fisner M, Majer AP, Balthazar-Silva D, Gorman D, Turra A. Quantifying microplastic pollution on sandy beaches: the conundrum of large sample variability and spatial heterogeneity. *Environ Sci Pollut Res Int* 2017;24:13732-40. DOI

OPEN ACCESS
Online ISSN: 2831-2597
Volume 3, Issue 2, June 2024

Water Emerging Contaminants & Nanoplastics

WECN
https://oaepublish.com/wecn

Olivatto *et al. Water Emerg Contam Nanoplastics* 2024;3:7
DOI: 10.20517/wecn.2023.69

Water Emerging Contaminants & Nanoplastics

Research Article

Open Access

A critical comparison of the main characterization techniques for microplastics identification in an accelerated aging laboratory experiment

Glaucia Peregrina Olivatto[1], **Rômulo Augusto Ando**[2], **Rafaella Ferreira Fernandes**[2], **Nicoli Gomes de Moraes**[1], **Valdemar Luiz Tornisielo**[1]

[1]Center of Nuclear Energy in Agriculture (CENA), University of São Paulo (USP), Piracicaba 13400-970, Brazil.
[2]Fundamental Chemistry Department, Institute of Chemistry, University of São Paulo (USP), São Paulo 05508-000, Brazil.

Correspondence to: Dr. Glaucia Peregrina Olivatto, Center of Nuclear Energy in Agriculture (CENA), University of São Paulo (USP), Av. Centenário, 303, Piracicaba 13400-970, Brazil. E-mail: glauciapolivatto@gmail.com

How to cite this article: Olivatto GP, Ando RA, Fernandes RF, de Moraes NG, Tornisielo VL. A critical comparison of the main characterization techniques for microplastics identification in an accelerated aging laboratory experiment. *Water Emerg Contam Nanoplastics* 2024;3:7. https://dx.doi.org/10.20517/wecn.2023.69

Received: 4 Nov 2023 **First Decision:** 24 Dec 2023 **Revised:** 14 Jan 2024 **Accepted:** 29 Jan 2024 **Published:** 6 Feb 2024

Academic Editors: Antoni Ginebreda, Xuetao Guo, João Pinto Pinto da Costa **Copy Editor:** Dong-Li Li **Production Editor:** Dong-Li Li

Abstract

Many studies have reported the occurrence of microplastics in different environmental compartments, through the description of their morphological characteristics and chemical identification, obtained mainly by spectroscopic techniques. However, the scientific community still lacks the implementation of standardized analytical methods that aim to assess not only the identification of the particle, but also its stage of degradation. It is understood that this information would be extremely useful in helping elucidate the main sources of pollution and contributing to strategies and mitigating measures for the management of solid waste and microplastics in the environment. In this respect, the aim of this study was to evaluate the efficiency of Fourier-transform infrared spectroscopy, Raman spectroscopy, carbon elemental analysis coupled with mass spectrometry, and scanning electron microscopy with energy dispersive X-ray spectrometry for the characterization of virgin and aged polyethylene and polypropylene microplastics samples. The degraded samples were subjected to accelerated aging in a QUV chamber in accordance with American standard for measuring accelerated weather testing (ASTM G-154). This work discusses the efficiency and limitations of each technique for the detailed chemical characterization of microplastic samples collected from the environment.

Keywords: Analytical methods, Fourier-transform Infrared spectroscopy, Raman spectroscopy, carbon elemental analysis coupled with mass spectrometry, scanning electron microscopy with energy dispersive X-ray spectroscopy

INTRODUCTION

Microplastics (MPs) are defined as small polymeric particles (≤ 5 mm) found in the environment[1]. The presence of these particles was first reported in marine environments in 1972[2]. More recently, these particles have been reported in various studies, in different geographical locations, and widely distributed throughout the different environmental compartments, including the hydrosphere, pedosphere, and atmosphere[3-8]. Considering their persistence, small size, and difficult removal from the environment, MPs can be identified as potential persistent pollutants in terms of negative impacts on ecosystems[9,10]. In the aquatic environment, because they are mistaken for food, MPs are easily ingested by various organisms, which can cause harmful effects through physical or physiological mechanisms[11-14]. MPs have also been reported in products intended for human consumption, such as foods and water[8,15,16]. Therefore, humans are also potentially being exposed to MPs through the consumption of these products and also through the contaminated air we breathe, which can cause oxidative stress, inflammation, neurotoxicity, and reproductive toxicity, as well as altering the structure of the intestinal microflora in cells or biota[8,17].

In this way, in order to accurately assess the possible ecological risks of these particles to the environment and potential impacts on human health, the scientific community has dedicated itself to gaining accurate knowledge of the main polluting sources of MPs, and their environmental concentration, composition, and morphology in different environmental matrices, food, drink, and biological samples[8]. It is known that the emission of MPs into the environment occurs throughout the life cycle of the polymeric material, including production, transport, domestic sewage disposal, industrial activities, atmospheric deposition from synthetic fabrics, and the improper disposal of larger plastic objects[18]. The scientific community classifies the entry of these particles into the environment as being from primary or secondary sources[19,20].

Primary MPs are those already produced in small sizes by the plastics industry, called pellets, that are released directly into the environment[18-21]. The industry uses these pellets as raw material for the production of plastic objects in the most varied sectors of society. Accidental loss to the environment occurs during transport and from processing plants[22,23]. In addition, these pellets are used as abrasive “scrubbers” to clean containers, machinery, and ships, and are often found near harbors, in industrial areas, on beach sands, and in the sea[19,24]. Primary source MPs, in micrometer sizes, are also part of the formulation of cosmetics and personal care products for abrasive effects[21,24]. These particles, of different shapes, sizes (from 4 to 2,000 μm), and chemical compositions, are transported to watercourses, for example, through domestic effluents[25,26]. Secondary MPs are small particles of plastic waste derived from the fragmentation of larger objects discarded in the environment. These plastic objects, when exposed to natural stressors, degrade through various processes: photochemical, thermal, mechanical, hydrolysis, and/or ozone-induced[19,27]. These processes are directly related to environmental conditions, the chemical composition of the polymer, and its production process[10,19,27-31].

Studies that report the occurrence of MPs in environmental samples must consider several important factors to provide and accurate analysis and potential exposure risks. These include the abundance of particles in relation to seasonality, and morphological and chemical characterization, as well as the stage of particle degradation, information that helps to elucidate the main pollutant sources. In order to qualitatively analyze the MPs collected, it is essential to use improved analytical techniques, as basic studies that identify MPs only use visual inspection and/or optical microscopy, which is an ineffective analysis and lacks conclusive information, contributing to false positives in the identification of MPs[32].

Currently, the most frequently reported chemical characterization techniques in studies involving MPs are spectroscopic, such as Fourier-transform Infrared spectroscopy (FTIR) and Raman spectroscopy[33]. However, despite the numerous studies involving analytical methods for identifying MPs and the extensive knowledge already clarified about the main characterization techniques used in the analysis of degraded plastics, the scientific community still lacks studies that consider samples of degraded MPs in the implementation of analytical methods[8,27,30]. The qualitative analysis of samples of degraded MPs is extremely important information for assessing the impact of these MPs on the environment and clarifying their classification in terms of the origin and main sources of pollution. This practice could encourage the discussion and comparison of the results of different studies and geographical locations, in order to understand, in greater detail, the extent and distribution of environmental contamination by MPs.

The current study aimed to evaluate the efficiency and limitations of the main techniques used to characterize synthetic organic polymers; FTIR, Raman spectroscopy, carbon elemental analysis coupled with mass spectrometry, and scanning electron microscopy (SEM) with energy dispersive X-ray spectroscopy (EDS), using samples of virgin and aged polyethylene (PE) and polypropylene (PP) MPs. These polymers were selected because they have the highest percentages of production and consumption worldwide[34] and also because they are the most representative of those reported in the environment[35]. In the aquatic environment, for example, due to the low density of these polymers, they float and remain at the top of the photic zone, where they are directly exposed to sunlight, i.e., photochemical degradation. Therefore, the condition of the polymer sample in the aged stage was also considered in this study, in order to be closer to the real condition in the environment and also to include MPs of secondary origin[6,36,37].

METHODS

Materials

High-density polyethylene (HDPE, HE150) and polypropylene polymers (PP, H117) were supplied in the form of pellets by Braskem (Triunfo, Brazil). The density and fluidity index values are 0.948 $g \cdot cm^{-3}$ and 1 g/10 min for HDPE and 0.905 $g \cdot cm^{-3}$ and 45 g/10 min for PP, respectively.

Sample preparation

The PE and PP pellets were used to prepare specimens with dimensions of 105 mm × 75 mm × 2 mm in a heated press (Marconi, model 098) at 185 °C and 38.1 $kgf \cdot cm^{-2}$ for 2 min and cooled to 27 °C. These specimens were subjected to accelerated aging in an accelerated aging chamber (QUV - Accelerated Weathering Tester) in accordance with American standard for measuring accelerated weather testing (ASTM G-154), 2012[38].

After exposure, the specimens of both polymers were ground in a mill (Marconi, Model 580) to obtain MP particles, and the same procedure was also carried out with the virgin pellets. These virgin and aged MPs were then transferred to a stacking system with 1,000 μm (top) and 106 μm (bottom) mesh sieves to ensure their classification by size on the MPs scale (≤ 5 mm).

Accelerated aging

The samples were subjected to thermal and photochemical aging in an accelerated aging chamber (Accelerated Weathering Tester, Q-Lab), which simulates natural weathering, in accordance with the guidelines of ASTM G-154 [Standard Practice for Operating Fluorescent Ultraviolet (UV) Lamp Apparatus] for the exposure of non-metallic materials[38]. The radiation sources were Philips 80W lamps (Cleo Performance WR80 model) with spectral distribution in the UVA region (340 nm). The samples were subjected to the following cycle: 8 h of radiation (irradiance 1.55 $W/m^2/nm$) at 60 °C, controlled by a cooling system, followed by a 2-h condensation cycle. The samples were collected for characterization, in triplicate, after 1,240 h for PP and 2,000 h for PE. It was necessary to reduce the exposure time of the PP polymer due to the accelerated fragmentation and formation of MPs of the specimen inside the aging chamber at 1,240 h.

Analytical methods

FTIR-ATR

In order to identify the polymers, the chemical characterization of the MPs was carried out by FTIR-ATR, in the attenuated total reflectance (ATR) mode, using a Bruker spectrometer (Massachusetts, USA). The spectra were recorded in attenuated total reflectance mode with a 15× Ge crystal objective on a Hyperion microscope coupled to a Vertex 80v. Spectra were acquired with a resolution of 4 cm^{-1} in 64 scans, in the spectral range from 4,000 to 400 cm^{-1}. The spectra were measured in a temperature and humidity-controlled environment and analyzed in absorption mode using Bruker's OPUS 8.0 software. The spectra obtained by FTIR-ATR were also used to characterize the stage of degradation of the surface of the PE and PP polymer MP particles by calculating the carbonyl index (CI) according to Equation 1:

$$CI = \frac{A}{B} \tag{1}$$

where A corresponds to the intensity stretching mode of the carbonyl band between 1,735 and 1,715 cm^{-1} and B to the reference band at 1,471 and 1,460 cm^{-1} due to CH_2 scissor vibrations for PE and PP polymers, respectively[39].

Raman spectroscopy

Raman spectra were recorded using a Witec confocal spectrometer, model Alpha 300R, with a CCD (charge-coupled device) detector, using the exciting radiation at 632.8 nm (He-Ne laser), coupled to a Zeiss microscope. Measurements were acquired in the 500 to 3,000 cm^{-1} range, with a resolution of 4 cm^{-1} in 5 accumulations, with an exposure time of 20 s. Laser power varied from 1 to 5 mW depending on the sample. The spectra were processed using Fityk 1.3.1 software.

Elemental carbon analysis coupled with mass spectrometry

The percentage of carbon by mass of virgin and aged PE and PP MPs samples was determined using an elemental analyzer (EA 1110, Carlo Erba) coupled to a mass spectrometer (Finnigan - Delta Plus). The equipment operated in dynamic flash combustion mode, where around 1.0 mg of each sample was inserted into a quartz tube at 1,000 °C and subjected to combustion, followed by oxidation and reduction reactions. The resulting gases separated by gas chromatography were analyzed by thermal conductivity.

SEM-EDS

For the SEM-EDS characterization, the MP particles were deposited on carbon tape (PELCO Tabs™, Ted Pella, Inc; Redding) mounted on metal stubs. They were then sputter-coated for 180 s with gold to a thickness of 80 nm (Leica ACE 600, Vienna, Austria). Micrographs were taken on an SEM (Jeol JSM-IT300 LV, Tokyo, Japan) operating at 15 kV and the images were digitized. EDS analysis was carried out using the same microscope coupled to an X-ray detector (EDS, Oxford Instruments, Abingdon).

RESULTS AND DISCUSSION

Figure 1 shows the spectra obtained by micro ATR-FTIR for the MPs samples of virgin PE and PP polymers after accelerated aging. The typical spectral profile of PE can be seen in the presence of the bands at 2,915 cm^{-1} (υC–H), 2,845 cm^{-1} (υC–H), 1,472 cm^{-1} (δCH_2), 1,462 cm^{-1} (δCH_2), 730 cm^{-1} (δCH_2), and 720 cm^{-1}

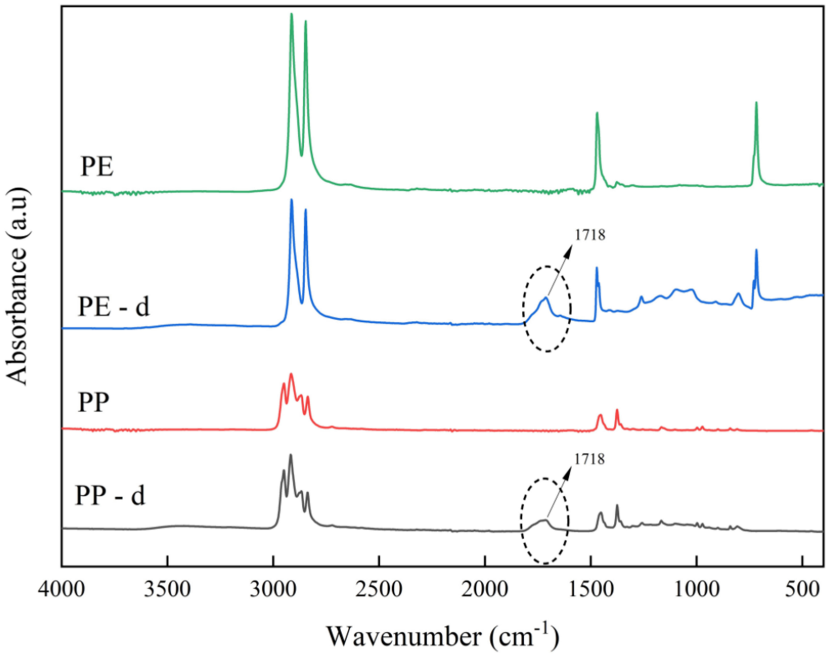

Figure 1. FTIR-ATR spectra of PE and PP polymer samples. PE and PP correspond to virgin samples and PE-d and PP-d correspond to degraded samples after accelerated aging in the QUV. FTIR: Fourier-transform Infrared spectroscopy; ATR: attenuated total reflectance; PE: polyethylene; PP: polypropylene.

(δCH_2). On the other hand, the bands at 2,950 cm^{-1} (υC–H), 2,915 cm^{-1} (υC–H), 2,838 cm^{-1} (υC–H), 1,455 cm^{-1} (δCH_2), 1,377 cm^{-1} (δCH_3), 1,166 cm^{-1} (angular deformation CH and CH_3, stretching C–C), 997 cm^{-1} (δCH_3 and CH), 972 cm^{-1} (δCH_3 and υC–C), 840 cm^{-1} (δCH_2 and $\upsilon C–CH_3$), and 802 cm^{-1} (δCH_2, υC–CH and υC–C) are characteristics of the PP.

Thus, the spectral profiles observed correspond to the chemical signatures of these polymers, which allows for quick, effective, and conclusive identification[40], where υ = stretching and δ = angular deformation.

The stretching bands present in the 1,700 cm^{-1} region (νC=O) in the PE-d and PP-d spectra are evidence of the photodegradation of the material when subjected to thermal and photochemical degradation in the QUV[39]. Knowing that these bands are not characteristic of PE and PP polymers, as polyolefins only have saturated carbon-carbon bonds in their composition, it is clear that the surface of the material has undergone photo-oxidative degradation, i.e., the introduction of oxygen into its polymer chain, due to exposure to UV radiation[41].

The absorption of sunlight by these polymers is due to other chemical groups present in the polymer chain. These could be chemical contaminants produced during the polymerization reaction, chemical compounds added as additives, polymer degradation products, contaminants present in the environment that have been sorbed onto the surface of the material, or even an anomaly in the macromolecular structure[20,42]. A small amount of radiation absorbed by these extrinsic chromophores and/or polymer structures is enough to initiate a free radical chain reaction[42]. This reaction, in the presence of oxygen, produces free radicals, leading to photo-oxidation, which consists of autocatalytic oxidation, with the formation of carbonyl groups such as ketones, aldehydes, and esters[27,42,43].

Due to these degradation reactions, polymers undergo changes in their chemical composition and morphological properties, such as the formation of carbonyl groups, chain scission with a decrease in molar mass, discoloration, and changes in mechanical properties. They become more fragile and break down more easily into small particles[19,20,27,44].

PE and PP polymers are widely used for the production of plastic packaging and utensils and are often reported as the main classes of solid waste disposed of inappropriately in the environment, which can suffer degradation, fragmentation, and the generation of secondary MPs[35]. These same polymers are also used, for example, as microspheres in cosmetics, meaning that they can reach environmental matrices through the discharge of domestic effluents[45].

Therefore, the presence of carbonyl in the FTIR-ATR spectra of the MPs of these polymers may be a relevant and decisive factor in classifying the polluting source. The aged PE and PP samples showed the same chemical alterations as those already mentioned and observed, and high values in the carbonyl index calculation were found at the end of each polymer's aging cycle [Table 1]. The evidence of degradation was more significant for PP than for PE; this is caused by the presence of tertiary carbons in PP with CH bonds with lower energy than those in the primary and secondary carbons. C–H covalent bond scission in the PP chain is thus favored over PE[27]. This explains the results found in the PP samples, with a high CI due to the insertion of the oxygen atom in its structure and faster fragmentation during the aging cycle. Despite the absence of tertiary carbons, the same degradative process of chain scission can also occur with PE, as indicated by the increase in the CI.

In this sense, the possibility of assessing the aging stage of the samples by analyzing the intensity of the band referring to the ν(C=O) mode and calculating the index of the same group highlights the FTIR-ATR technique as a potential tool for non-destructive analysis of MPs.

However, as a disadvantage, qualitative analysis by FTIR-ATR presents a limitation in terms of particle size, as this method generally requires a minimum size of 100 μm in conventional equipment or, using μ-FTIR, MPs with a lower limit of 10 μm and with a spatial resolution of 5 μm[46,47]. In addition, during sample preparation, in conventional FTIR-ATR analysis, MP particles are analyzed individually, and the particle selection step needs to be performed manually, which requires a lot of work and time. Automated analysis of MPs samples on a filter, for example, is only possible with μ-FTIR and often requires the use of a focal plane detector (FPA) or an electron multiplier charge coupled device (EMCCD), which allow multiple points to be measured; these analyses are more complex and require sophisticated instrumentation and a qualified analyst[48]. Another disadvantage is related to the need for sample preparation; FTIR analyses must be purified and dried before detection, otherwise, interferences can occur in the spectra due to the humidity of the samples[49].

Figure 2 shows the spectra obtained by Raman spectroscopy for samples of virgin PE and PP polymers and after accelerated aging. The chemical identification of the polymers is possible and conclusive, due to the presence of two characteristic bands at 2,846 and 2,881 cm^{-1}, referring to the vibrational mode of the PE polymer. Similarly, PP is identified due to the presence of a set of characteristic bands from 2,800 to 3,000 cm^{-1}[50]. However, when comparing the spectra of the same polymers, PE with PE-d and PP with PP-d, in contrast to the spectra obtained by FTIR-ATR, it is not possible to clearly observe evidence of manipulation in the samples subjected to accelerated aging, as the vibrational transitions occurring with this technique do not include the introduction of bands characteristic of the degradation mechanisms occurring in the samples, with the mode referring to carbonyl stretching being much more intense in the infrared,

Table 1. Variation in the carbonyl index as a function of the accelerated aging time of the PE and PP samples

Exposure time QUV (h)	Carbonyl index	
	PE	PP
0	0.0 ± 0.0	0.0 ± 0.0
1,240	-	2.38 ± 0.1
2,000	0.71 ± 0.0	-

PE: Polyethylene; PP: polypropylene.

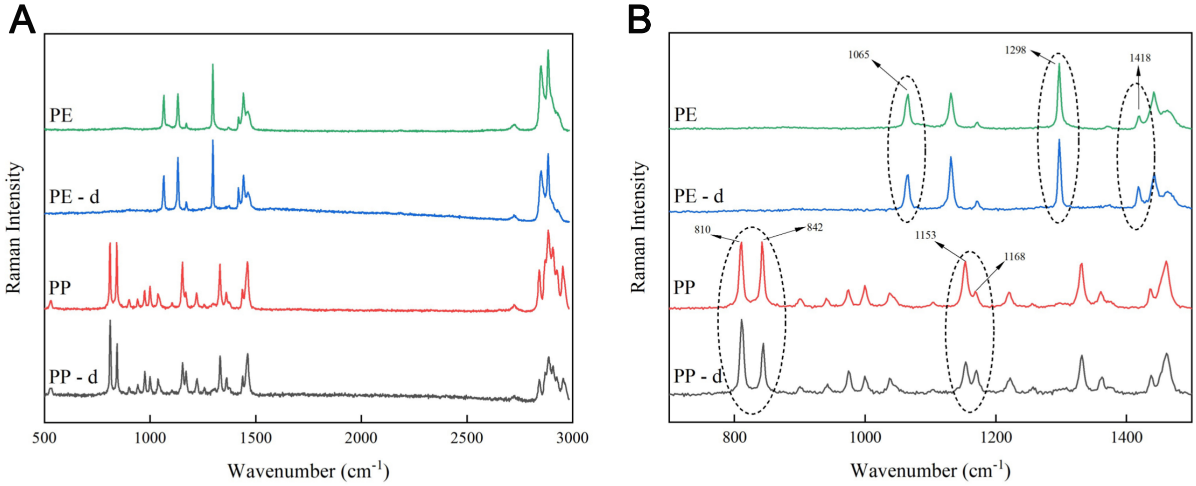

Figure 2. (A) Raman spectra of the PE and PP polymer samples PE and PP correspond to the virgin samples and PE-d and PP-d correspond to the degraded samples after accelerated aging in the QUV; (B) corresponds to the prominence of the altered bands after accelerated aging. PE: Polyethylene; PP: polypropylene.

which requires a more detailed analysis in the Raman analysis of the MPs samples collected in the environment. On the other hand, although the evidence of degradation in the Raman spectra is more subtle and difficult to interpret, it can be identified due to the relationship between the amorphous and crystalline regions, with the increase in crystallinity being related to the aging of the material. For the PE polymer, the intensity of the band at 1,080 cm^{-1}, characteristic of the C–C stretching mode of amorphous chains, decreases as the exposure time increases, representing an increase in crystallinity. Another characteristic indicating degradation is the change and increase in the area of the peaks and the C–C crystalline stretching modes at 1,063 and 1,130 cm^{-1} with the irradiation time. Changes in the 1,400 cm^{-1} region also show a change in the state of degradation, especially in the orthorhombic crystallinity band at 1,418 cm^{-1} and the amorphous band at 1,460 cm^{-1}[51,52]. Considering the PP polymer, the presence of tertiary carbon in its structure makes it more prone to degradation processes compared to PE. The main variations in crystallinity due to aging can be observed through changes in the peaks at around 810, 842, 973, 998, 1,153, and 1,168 cm^{-1}, for example[53].

The analysis of MPs using Raman spectroscopy requires a long measurement time and is more laborious than FTIR analysis, for example, as this technique involves more instrumental variables. It is also more sensitive to interference due to the possibility of chemical additives present in the plastic, such as dyes, or the presence of contaminants, which can cause fluorescence-induced spectral distortion and compromise the analysis, and does not occur in FTIR analysis. On the other hand, as well as FTIR analysis, Raman spectroscopy allows assertive chemical identification of the polymer due to the existence of a spectral library, and also the analysis of MPs on an even smaller size scale than μ-FTIR, with a lower limit of 1 μm. In this respect, it can be considered the most promising technique, depending on the type of sample to be analyzed, for example, for drinking water samples[54]. Another advantage of this technique is the possibility of mapping a certain area with numerous MP particles, like a filter. Finally, like FTIR analysis, Raman analysis represents a non-destructive analysis of the sample[47,49].

Table 2 presents the average results of the mass percentage of carbon in virgin MPs samples and aged PE and PP MPs samples obtained by elemental carbon analysis. As a consequence of the degradation mechanism, it is possible to observe the loss of mass suffered by both polymers subjected to aging, which is more pronounced in PP than in PE. This is due to the presence of tertiary carbon in the PP structure, which facilitates the degradation mechanism by homolytic scission, which further favors the reduction in molar mass[41].

The carbon elemental analysis shows accuracy and good reproducibility of the results, as well as being a relatively low-cost analysis compared to other techniques. The equipment used for elemental analysis only provides %C, and this value, close to 80%, aids in the identification of both virgin and aged MPs, as well as making it possible to observe the loss of carbon mass in aged MPs. However, this analysis alone does not make it possible to discriminate between the chemical identities of the MPs, since they have similar carbon content. There is also the possibility of misinterpreting the result, knowing that other solid materials present in the environment such as biochar, commonly reported in the soil profile, also have a C content similar to that of MPs[55].

Another drawback of elemental carbon analysis is that it is destructive and requires at least 1.0 mg of sample to provide a reliable result. On the other hand, ATR-FTIR requires only one particle to fill the minimum space in the equipment's accessory, which consists of direct contact between the sample and the tip of the germanium crystal lens. In the case of MPs samples collected from the environment, the mass corresponding to 1.0 mg is very significant and often unfeasible.

Figure 3 illustrates the results obtained by SEM-EDS of the virgin and aged PE and PP MPs samples. Both the PE and PP MPs samples showed a loss of mass percentage of carbon and an increase in mass percentage of oxygen after accelerated aging, as well as the presence of some trace elements. The micrographs also make it possible to characterize the morphological alterations resulting from the thermal and photochemical degradation of the samples, with cracks and porosity being observed in the aged samples.

The advantages of SEM-EDS analysis are that it can be used to analyze the surface of small particles and requires only a small amount of the sample. However, this analysis is relatively expensive and does not provide the composition of the entire sample, but only of the elements that are actively selected at a given point, which can result in an inaccurate analysis of the chemical composition of the material. Therefore, it is not possible to identify the MPs with this method, added to which, this is a destructive form of analysis of the sample, and an unfeasible option considering the large number of MPs samples to be analyzed.

CONCLUSIONS

The techniques evaluated here are extremely relevant and are already widely known by the scientific community in the context of characterizing synthetic organic polymers. However, when considering the qualitative analysis of MPs collected in the environment, with the aim of assessing their distribution and identifying the main polluting sources, i.e., the stage of degradation of the particles, it can be concluded that carbon elemental analysis and the SEM-EDS technique are only useful as complementary techniques, which

Table 2. Mass percentage of carbon in PE and PP polymer MPs samples

MPs samples	Average mass (mg)	Average %carbon
PE	1.12 ± 0.01	85.72 ± 0.26
PE-d	1.13 ± 0.00	84.99 ± 0.08
PP	1.13 ± 0.01	86.67 ± 0.49
PP-d	1.13 ± 0.01	78.88 ± 0.39

PE and PP correspond to virgin samples and PE-d and PP-d correspond to QUV-aged samples. PE: Polyethylene; PP: polypropylene; MPs: microplastics.

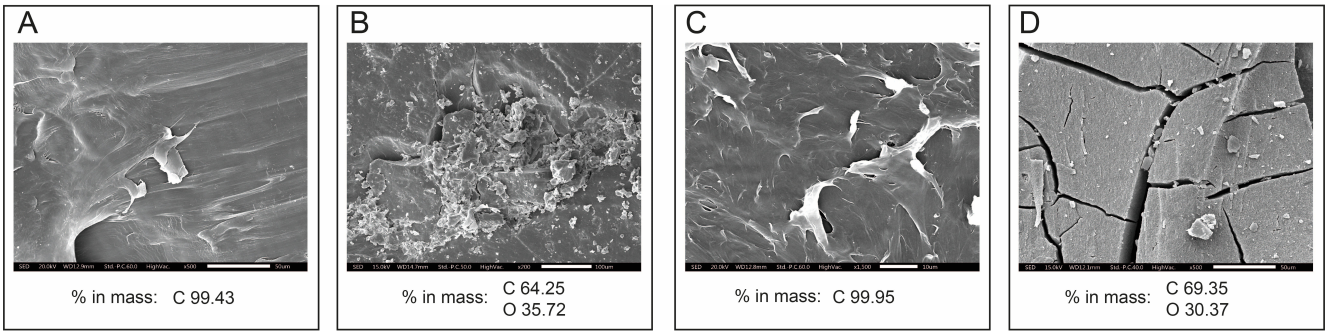

Figure 3. SEM and EDS images of the MPs samples: (A) virgin PE; (B) aged PE; (C) virgin PP; and (D) aged PP. SEM: Scanning electron microscopy; EDS: energy dispersive X-ray spectroscopy; MPs: microplastics; PE: polyethylene; PP: polypropylene.

can help in understanding the degradation of the particles, as shown by the current results from the loss of carbon mass resulting from photodegradation. It should be noted that only the FTIR and Raman techniques can contribute to the conclusive chemical identification of MPs, due to the characteristic spectra of each type of polymer, while μ-FTIR is the most suitable for the analysis of MPs samples in the size range of more than 10 μm, as it easily provides information on the stage of aging, through the quantification of the carbonyl index and, consequently, aids elucidation of the main polluting sources of MPs in the environment.

DECLARATIONS

Acknowledgments

The authors would like to thank the Polymer Processing Laboratory at UNICAMP and the Isotopic Ecology Laboratory at USP for their infrastructure.

Authors’ contributions

Conceptualization, data curation, figures, table, writing - original draft preparation: Olivatto GP
Conceptualization, methodology, writing - reviewing and editing: Ando RA, Fernandes RF, de Moraes NG, Tornisielo VL
Supervision: Tornisielo VL

Availability of data and materials

Not applicable.

Financial support and sponsorship
National Council for Scientific and Technological Development (process number 141021/2019-5).

Conflicts of interest
All authors declared that there are no conflicts of interest.

Ethical approval and consent to participate
Not applicable.

Consent for publication
Not applicable.

REFERENCES

1. Arthur C, Baker JE, Bamford HA. Proceedings of the International Research Workshop on the Occurrence, Effects, and Fate of Microplastic Marine Debris, September 9-11, 2008, University of Washington Tacoma, Tacoma, WA, USA. 2009. Available from: https://repository.library.noaa.gov/view/noaa/2509. [Last accessed on 31 Jan 2024].
2. Carpenter EJ, Smith KL Jr. Plastics on the sargasso sea surface. *Science* 1972;175:1240-1. DOI PubMed
3. Barceló D, Picó Y. Microplastics in the global aquatic environment: Analysis, effects, remediation and policy solutions. *J Environ Chem Eng* 2019;7:103421. DOI
4. Olivatto GP, Carreira R, Tornisielo VL, Montagner CC. Microplastics: contaminants of global concern in the Anthropocene. *Rev Vir Quim* 2018;10:6. (in Portuguese). DOI
5. Alimi OS, Farner Budarz J, Hernandez LM, Tufenkji N. Microplastics and nanoplastics in aquatic environments: aggregation, deposition, and enhanced contaminant transport. *Environ Sci Technol* 2018;52:1704-24. DOI PubMed
6. Hidalgo-Ruz V, Gutow L, Thompson RC, Thiel M. Microplastics in the marine environment: a review of the methods used for identification and quantification. *Environ Sci Technol* 2012;46:3060-75. DOI PubMed
7. Huang Z, Hu B, Wang H. Analytical methods for microplastics in the environment: a review. *Environ Chem Lett* 2023;21:383-401. DOI PubMed PMC
8. Dong H, Wang X, Niu X, et al. Overview of analytical methods for the determination of microplastics: Current status and trends. *Trends Analyt Chem* 2023;167:117261. DOI
9. Worm B, Lotze HK, Jubinville I, Wilcox C, Jambeck J. Plastic as a persistent marine pollutant. *Annu Rev Environ Resour* 2017;42:1-26. DOI
10. Browne MA, Galloway T, Thompson R. Microplastic - an emerging contaminant of potential concern? *Integr Environ Assess Manag* 2007;3:559-61. DOI PubMed
11. Browne MA, Dissanayake A, Galloway TS, Lowe DM, Thompson RC. Ingested microscopic plastic translocates to the circulatory system of the mussel, *Mytilus edulis* (L.). *Environ Sci Technol* 2008;42:5026-31. DOI PubMed
12. Cole M, Lindeque P, Fileman E, et al. Microplastic ingestion by zooplankton. *Environ Sci Technol* 2013;47:6646-55. DOI
13. Wright SL, Thompson RC, Galloway TS. The physical impacts of microplastics on marine organisms: a review. *Environ Pollut* 2013;178:483-92. DOI PubMed
14. Lourenço ALA, Olivatto GP, de Souza AJ, Tornisielo VL. Effects caused by the ingestion of microplastics: first evidence in the lambari rosa (*Astyanax altiparanae*). *Animals* 2023;13:3363. DOI PubMed PMC
15. Kosuth M, Mason SA, Wattenberg EV. Anthropogenic contamination of tap water, beer, and sea salt. *PLoS One* 2018;13:e0194970. DOI PubMed PMC
16. Iñiguez ME, Conesa JA, Fullana A. Author correction: microplastics in Spanish table salt. *Sci Rep* 2018;8:6123. DOI PubMed PMC
17. Bai CL, Liu LY, Hu YB, Zeng EY, Guo Y. Microplastics: A review of analytical methods, occurrence and characteristics in food, and potential toxicities to biota. *Sci Total Environ* 2022;806:150263. DOI PubMed
18. van Wezel A, Caris I, Kools SAE. Release of primary microplastics from consumer products to wastewater in the Netherlands. *Environ Toxicol Chem* 2016;35:1627-31. DOI PubMed
19. Anderson A, Andrady A, Arthur C. Sources, fate and effects of microplastics in the marine environment: a global assessment. London, UK: International Maritime Organization; 2015. Available from: https://research.vu.nl/en/publications/47f9f0e1-f326-4b04-a7e5-

a649218c68b1. [Last accessed on 1 Feb 2024].
20. Cole M, Lindeque P, Halsband C, Galloway TS. Microplastics as contaminants in the marine environment: a review. *Mar Pollut Bull* 2011;62:2588-97. DOI PubMed
21. Boucher J, Friot D. Primary microplastics in the oceans: a global evaluation of sources. Gland, Switzerland: IUCN; 2017. pp 1-43. DOI
22. Turra A, Manzano AB, Dias RJ, et al. Three-dimensional distribution of plastic pellets in sandy beaches: shifting paradigms. *Sci Rep* 2014;4:4435. DOI PubMed PMC
23. Ogata Y, Takada H, Mizukawa K, et al. International Pellet Watch: global monitoring of persistent organic pollutants (POPs) in coastal waters. 1. Initial phase data on PCBs, DDTs, and HCHs. *Mar Pollut Bull* 2009;58:1437-46. DOI
24. Derraik JG. The pollution of the marine environment by plastic debris: a review. *Mar Pollut Bull* 2002;44:842-52. DOI
25. Fendall LS, Sewell MA. Contributing to marine pollution by washing your face: microplastics in facial cleansers. *Mar Pollut Bull* 2009;58:1225-8. DOI PubMed
26. Napper IE, Bakir A, Rowland SJ, Thompson RC. Characterisation, quantity and sorptive properties of microplastics extracted from cosmetics. *Mar Pollut Bull* 2015;99:178-85. DOI PubMed
27. De Paoli MA. Degradation and stabilization of polymers. 2008. (in Portuguese) Available from: http://static.sapucaia.ifsul.edu.br/professores/vmartins/Arquivo/Fundamentos%20de%20Projeto%20de%20Ferramentas/SOPRO/a-introducao.pdf. [Last accessed on 29 Feb 2024].
28. Rocha-santos T, Duarte AC. A critical overview of the analytical approaches to the occurrence, the fate and the behavior of microplastics in the environment. *Trends Analyt Chem* 2015;65:47-53. DOI
29. Andrady AL. Microplastics in the marine environment. *Mar Pollut Bull* 2011;62:1596-605. DOI PubMed
30. Browne MA, Crump P, Niven SJ, et al. Accumulation of microplastic on shorelines woldwide: sources and sinks. *Environ Sci Technol* 2011;45:9175-9. DOI
31. Barnes DK, Galgani F, Thompson RC, Barlaz M. Accumulation and fragmentation of plastic debris in global environments. *Philos Trans R Soc Lond B Biol Sci* 2009;364:1985-98. DOI PubMed PMC
32. Estahbanati S, Fahrenfeld NL. Influence of wastewater treatment plant discharges on microplastic concentrations in surface water. *Chemosphere* 2016;162:277-84. DOI PubMed
33. Xu J, Thomas KV, Luo Z, Gowen AA. FTIR and Raman imaging for microplastics analysis: state of the art, challenges and prospects. *Trends Analytl Chem* 2019;119:115629. DOI
34. Geyer R, Jambeck JR, Law KL. Production, use, and fate of all plastics ever made. *Sci Adv* 2017;3:e1700782. DOI PubMed PMC
35. Koelmans AA, Mohamed Nor NH, Hermsen E, Kooi M, Mintenig SM, De France J. Microplastics in freshwaters and drinking water: critical review and assessment of data quality. *Water Res* 2019;155:410-22. DOI PubMed PMC
36. Andrady AL. The plastic in microplastics: a review. *Mar Pollut Bull* 2017;119:12-22. DOI PubMed
37. Zhang K, Gong W, Lv J, Xiong X, Wu C. Accumulation of floating microplastics behind the Three Gorges Dam. *Environ Pollut* 2015;204:117-23. DOI PubMed
38. American Society for Testing and Materials (ASTM). ASTM G154-12a: Standard practice for operating fluorescent ultraviolet (UV) lamp apparatus for exposure of nonmetallic materials. Available from: https://www.astm.org/g0154-12a.html. [Last accessed on 5 Feb 2023]
39. Rodrigues MO, Abrantes N, Gonçalves FJM, Nogueira H, Marques JC, Gonçalves AMM. Spatial and temporal distribution of microplastics in water and sediments of a freshwater system (Antuã River, Portugal). *Sci Total Environ* 2018;633:1549-59. DOI PubMed
40. Jung MR, Horgen FD, Orski SV, et al. Validation of ATR FT-IR to identify polymers of plastic marine debris, including those ingested by marine organisms. *Mar Pollut Bull* 2018;127:704-16. DOI
41. Hammer J, Kraak MHS, Parsons JR. Plastics in the marine environment: the dark side of a modern gift. In: Whitacre DM, editor. Reviews of environmental contamination and toxicology. New York: Springer; 2012. pp. 1-44. DOI
42. Calvert PD. Polymer degradation and stabilisation. N. Grassie and G. Scott, Cambridge University Press, Cambridge, 1985. pp. 222, price £27.50, $54.50. ISBN 0-521-24961-9. Available from: https://onlinelibrary.wiley.com/doi/10.1002/pi.4980180422. [Last accessed on 1 Feb 2024].
43. Cruz-Pinto JJC, Carvalho MES, Ferreira JFA. The kinetics and mechanism of polyethylene photo-oxidation. *Angew Makromol Chem* 1994;216:113-33. DOI
44. Guo X, Wang J. The chemical behaviors of microplastics in marine environment: a review. *Mar Pollut Bull* 2019;142:1-14. DOI PubMed
45. Napper IE, Thompson RC. Release of synthetic microplastic plastic fibres from domestic washing machines: Effects of fabric type and washing conditions. *Mar Pollut Bull* 2016;112:39-45. DOI PubMed
46. Chen Y, Wen D, Pei J, et al. Identification and quantification of microplastics using Fourier-transform infrared spectroscopy: Current status and future prospects. *Curr Opin Environ Sci Health* 2020;18:14-9. DOI
47. Araujo CF, Nolasco MM, Ribeiro AMP, Ribeiro-Claro PJA. Identification of microplastics using Raman spectroscopy: Latest developments and future prospects. *Water Res* 2018;142:426-40. DOI PubMed
48. Ivleva NP. Chemical analysis of microplastics and nanoplastics: challenges, advanced methods, and perspectives. *Chem Rev* 2021;121:11886-936. DOI PubMed
49. Ye Y, Yu K, Zhao Y. The development and application of advanced analytical methods in microplastics contamination detection: a critical review. *Sci Total Environ* 2022;818:151851. DOI PubMed
50. Dong M, Zhang Q, Xing X, Chen W, She Z, Luo Z. Raman spectra and surface changes of microplastics weathered under natural environments. *Sci Total Environ* 2020;739:139990. DOI

51. Rytelewska S, Dąbrowska A. The Raman spectroscopy approach to different freshwater microplastics and quantitative characterization of polyethylene aged in the environment. *Microplastics* 2022;1:263-82. DOI
52. Fischer J, Wallner GM, Pieber A. Spectroscopical investigation of ski base materials. *Macromol Symp* 2008;265:28-36. DOI
53. Phan S, Padilla-Gamiño JL, Luscombe CK. The effect of weathering environments on microplastic chemical identification with Raman and IR spectroscopy: part I. polyethylene and polypropylene. *Polym Test* 2022;116:107752. DOI
54. Schymanski D, Goldbeck C, Humpf HU, Fürst P. Analysis of microplastics in water by micro-Raman spectroscopy: release of plastic particles from different packaging into mineral water. *Water Res* 2018;129:154-62. DOI PubMed
55. Tsai WT, Liu SC, Chen HR, Chang YM, Tsai YL. Textural and chemical properties of swine-manure-derived biochar pertinent to its potential use as a soil amendment. *Chemosphere* 2012;89:198-203. DOI PubMed

Prata *et al. Water Emerg Contam Nanoplastics* 2024;3:8
DOI: 10.20517/wecn.2023.61

Water Emerging Contaminants & Nanoplastics

Technical Guide

Open Access

Do’s and don’ts of microplastic research: a comprehensive guide

Joana C. Prata[1,2,3], **Jorge Padrão**[4], **Muhammad Tariq Khan**[5], **Tony R. Walker**[6]

[1]Associate Laboratory i4HB, Institute for Health and Bioeconomy, University Institute of Health Sciences, CESPU, Gandra 4585-116, Portugal.
[2]UCIBIO, Applied Molecular Biosciences Unit, Translational Toxicology Research Laboratory, University Institute of Health Sciences (1H-TOXRUN, IUCS-CESPU), Gandra 4585-116, Portugal.
[3]Food Microbiology and Technology Laboratory, Department of Aquatic Production, Instituto de Ciências Biomédicas Abel Salazar (ICBAS), University of Porto, Porto 4050-313, Portugal.
[4]Centre for Textile Science and Technology (2C2T), University of Minho, Guimarães 4800-058, Portugal.
[5]Department of Science and Environmental Studies and State Key Laboratory in Marine Pollution, The Education University of Hong Kong, Tai Po, New Territories 999077, Hong Kong, China.
[6]School for Resource and Environmental Studies, Dalhousie University, Halifax B3H 4R2, Nova Scotia, Canada.

Correspondence to: Prof. Joana C. Prata, Associate Laboratory i4HB, Institute for Health and Bioeconomy, University Institute of Health Sciences, CESPU, Avenida Central de Gandra, 1317, Gandra 4585-116, Portugal. E-mail: joana.prata@iucs.cespu.pt

How to cite this article: Prata JC, Padrão J, Khan MT, Walker TR. Do’s and don’ts of microplastic research: a comprehensive guide. *Water Emerg Contam Nanoplastics* 2024;3:8. https://dx.doi.org/10.20517/wecn.2023.61

Received: 4 Oct 2023 **First Decision:** 31 Jan 2024 **Revised:** 31 Jan 2024 **Accepted:** 20 Feb 2024 **Published:** 4 Mar 2024

Academic Editor: Quan Wang **Copy Editor:** Dong-Li Li **Production Editor:** Dong-Li Li

Abstract

Microplastics are environmental contaminants consisting of small plastics ≤ 5 mm. Concerns over the adverse effects of microplastics have led to a rapid growth in the available literature despite the lack of harmonized methods and materials. Therefore, the field is becoming increasingly daunting to new researchers. A state-of-the-art guide was assembled following a comprehensive literature review of microplastics research with the intent of addressing contemporary challenges, prioritized based on a survey, and introducing best practices. The lack of standardized methods and reference materials, the lack of access to analytical equipment, and the difficulty in working with lower environmental concentrations in laboratory tests (e.g., toxicity assays) remain a great challenge. The present work addresses these issues across three main sections: definitions, sampling, and evaluation of adverse effects. Harmonized methods and greater collaboration were identified as opportunities in this rapidly evolving field. A review of available interlaboratory comparison tests was also conducted to support additional recommendations.

Keywords: Plastic pollution, environmental monitoring, environmental impact, toxicity assays

INTRODUCTION

Microplastics are small plastics ≤ 5 mm that are either fragmented in the environment or resulting from human products and activities[1]. Until recently, most research has been focused on the marine environment, where they were first identified[2]. Concerns have been raised regarding the persistence, ubiquity, and irreversibility of microplastics in the environment[3]. However, the adverse effects of microplastics remain a controversial issue[4]. The lack of standardized methods and reference particles further complicates result interpretation. Still, research continues to proliferate with the term "microplastics" retrieving 16,083 publications in the Web of Science as of January 2024, of which 4,056 were published in 2023 (25,2%). Researchers now entering the field are bewildered and daunted by the large literature base.

A small survey (n = 37) has been conducted during a webinar to summarize difficulties felt by researchers, translating common challenges faced by researchers, worthy of addressing [Supplementary Materials]. The greatest challenges in microplastics sampling and analysis were the lack of standardized methods (78.4%), followed by contamination control (51.4%), lack of specialized equipment in the laboratory (51.4%), and difficulty in identifying microplastics and fibers (35.1%). The greatest challenges in (eco)toxicity studies of microplastics were access to adequate microplastics to be tested (37.8%), quantification of microplastics to prepare solutions or confirm nominal concentrations (37.8%), and use of environmentally relevant concentrations (37.8%). As a result, the present article was idealized with the objective of addressing contemporary challenges and best practices in working with microplastics through a comprehensive literature review.

CHALLENGES IN MICROPLASTICS DEFINITION

What are microplastics?

Plastics are synthetic materials made of long chains of organic polymers, extensively used in a plethora of familiar applications. While thermoset plastics cannot be melted or reshaped by heat once solidified, thermoplastics can be repeatedly melted and molded into different forms. Of the 390.7 Mt of plastics produced globally in 2021, 44% were used in packaging[5]. It has been estimated that 79% of plastics produced as of 2015 persist in landfills or in the natural environment[6]. These plastics can break down into small particles known as microplastics (≤ 5 mm). The term "microplastics" was first used by Dr. Richard Thompson to describe microscopic plastic debris found in seawater samples near Plymouth, UK[7]. Although previous reports of similar particles have been published as early as the 1970s[8], the use of the term microplastics only became popular after Thompson's 2004 publication. Currently, microplastics comprise a class of contaminants characterized by being particles of organic synthetic polymers[9]. Indeed, each microplastic is a unique combination of polymer type, additives, adsorbed contaminants, degradation state, color, size, shape, and biofouling (i.e., accumulation of biogenic matter and organisms on its surface).

How are microplastics defined?

The definition of microplastics is based on size, with the most common upper limit being 5 mm. This limit has been supported by organizations such as the National Oceanic and Atmospheric Administration (NOAA)[10] based on the particle's behavior (e.g., the possibility of being ingested by organisms by accident) and their visibility to the public. The lower limits have been defined as 1 μm based on detection limits of common equipment (e.g., micro-spectroscopy) used in detection and characterization[1]. Therefore, microplastics can be defined as plastic particles of 1 μm to 5 mm in at least one dimension. However, definitions of 1 μm - 1 mm in size have been proposed based on the International System of Units[11]. In these cases, nanoplastics would be defined as plastic particles < 1 μm, although this definition is still debated considering nanoparticles are defined as particles with their size ranging from 10 to 100 nm in at least one of its dimensions[11,12].

Microplastics are also classified based on their origins [Figure 1]. Primary microplastics are those intentionally produced by the industry with ≤ 5 mm, while secondary microplastics originate from the fragmentation of larger plastics[11,13,14]. This classification was challenged when a report classified primary microplastics as those particles reaching the environment with ≤ 5 mm, despite degradative origins (e.g., microplastics from tire wear)[15]. This classification likely originates from particulate matter, which is classified as primary when directly released as particles and secondary when produced in the environment from chemical precursors (e.g., nitrogen oxides)[16]. Since it is not possible to determine if the fragmentation occurred prior to or after arriving at the environment, this classification is not suitable for microplastics. Instead, identifying if microplastics originate from intentional production or fragmentation enables intervention either by banning industrial uses (e.g., microbead ban in cosmetics) or preventing the fragmentation of larger plastics (e.g., avoiding littering)[17].

Another aspect to consider is what physicochemical properties define microplastics. Questions arise about the classification of modified natural polymers (e.g., cellophane), surface coatings (e.g., acrylic paints), and composites as microplastics. As a rule, microplastics should be solid particles, insoluble in water, and made of a synthetic polymeric matrix[1]. Therefore, the following materials should also be considered as microplastics since they contain modified or synthetic polymers in their composition: modified natural polymers (rubber, rayon, cellophane), inorganic or hybrid polymers (e.g., silicone), copolymers [e.g., acrylonitrile-butadiene-styrene (ABS)], composites (e.g., graphite-reinforced epoxy), surface coatings containing synthetic polymers (e.g., acrylic resins), and tire wear particles[11].

How are microplastics formed?

As discussed in the previous point, microplastics may be classified as primary when industrially produced as plastics ≤ 5 mm to be used in products (e.g., exfoliants in cosmetics) or industries (e.g., abrasives to clean ship's hulls). Moreover, microplastics may be produced through the fragmentation of larger plastic objects. Solar ultraviolet radiation initiates an oxidation reaction mainly responsible for plastic degradation[18]. As a result of photooxidation, carbonyl and hydroxyl functional groups are produced[19]. Photooxidation can be delayed by the presence of antioxidant additives in plastics. Plastics may become yellow through the accumulation of degradation products and fragment as a result of mechanical forces (e.g., abrasion with sand) or surface cracking following photooxidation[18]. Other reactions may involve thermal degradation, hydrolysis, and biodegradation[13]. Degradation is an ongoing process, meaning that microplastics are continuously fragmenting into smaller and smaller particles. Nonetheless, complete degradation into simple molecules (e.g., CO_2, H_2O) is expected to take hundreds of years (e.g., 450 years for polyethylene)[20].

Are microfibers also microplastics?

Demand for synthetic fibers has grown, reaching 55.2 million tons in 2014, of which 46.1 million tons is for polyester (a.k.a., polyethylene terephthalate)[21]. Demand for clothing is expected to reach 160 million tons in 2050, of which 63% will be for synthetic fibers (estimated 100 million tons)[22]. The fragmentation of these synthetic fibers (i.e., made of synthetic organic polymers) produces microfibers, which are considered microplastics and are characterized by a minimum 1:3 aspect ratio (i.e., "rod" shape)[23]. Sources of microfibers include textiles, but also fishing equipment and packaging[23]. An estimate of 20%-35% of microplastics are microfibers, although local concentrations vary greatly depending on sources[24]. Due to their shape, fibers may be able to penetrate deeply into the tissue, accumulate, and cause adverse effects to organisms.

Figure 1. Primary microplastic (transparent bead), secondary microplastic (blue fragment), and mesoplastic (white fragment) found on Matosinhos beach, Portugal, in September 2023.

CHALLENGES IN MICROPLASTICS ANALYSIS

Organizations have previously attempted to provide guidance on methodologies (e.g., NOAA, Marine Strategy Framework Directive technical subgroup[10,25]), but mostly focused on larger microplastics in the marine environment. A new attempt of standardization (or harmonization) is under development by the ISO (e.g., ISO/FDIS 24,187 Principles for the analysis of microplastics present in the environment).

Objective, experimental design and statistical analysis

A research question precedes any scientific study, as all planning depends on it. It must be clearly stated as an objective or hypothesis, which is essential to define the scope, provide a foundation for communication, and avoid dispersion to other related topics. Research questions are generally motivated by knowledge gaps arising from previous works, either original articles or literature reviews. It will determine what strategy and methods are necessary to answer this question, also considering the feasibility of its implementation. Defining variables and categories from the start will help in the production of a harmonized database. Ideally, categories should be based on literature to improve comparability between results. For instance, the shape of microplastics could be classified as sphere, spheroid, cylindrical pellet, fragment, film, fiber, and other[11].

Sampling strategies have included different sections, transects, or the use of quadrants[26]. Spatial sampling can include: (i) random sampling, randomly selecting points in an area if a homogeneous distribution is expected (e.g., sampling four random 1 m^2 quadrants in a beach); (ii) systematic sampling, using grids, gradients or transects limited to an area allowing to detect gradients (e.g., sampling a 100 m transect perpendicular to the shoreline); or (iii) stratified random, which subdivides different zones where concentrations are expected to be different and random sampling is conducted inside each zone or stratum (e.g., sampling four random 1 m^2 quadrant in three transects in the beach, each 10 m wide, starting from the shoreline). The objective is to include representative sampling areas. The United States Environmental Protection Agency (EPA) suggests a beach sampling protocol consisting of 12 samples inside 1 m^2 quadrant collected over a 100 m sampling area, collecting samples from four random transects over three lines parallel to the water (high tide line, middle beach, and back beach) [Figure 2][27].

Statistical analysis may be conducted to address the need for a different sampling strategy. For instance, the coefficient of variation, calculated as the standard deviation divided by the geometric mean of replicates from a sampling area, can express data dispersion coming from different samples. A coefficient of variation of ≤ 20% is commonly accepted[28]. If methodological aspects are excluded from causing variation (i.e., variation is not coming from errors in sample collection, processing, and analysis), which can be excluded by running spiked samples, a high coefficient of variation (i.e., high data dispersion) may indicate the need to apply a different sampling strategy. A lower coefficient of variation may be needed for the detection of smaller effect sizes. It is worth considering that microplastic may suffer spatiotemporal variations, for instance, depending on meteorological or seasonal events[29] or on sampling depth[30]. To understand the dynamics of microplastics in the environment, the following aspects should be considered: (i) tridimensional distribution; (ii) measures at regular intervals to account for temporal variation; (iii) source appointment; (iv) particle characteristics related to distribution; and (v) mechanisms influencing distribution[31].

Sampling design, including the number of samples and replicates, depends on the objective of the work. Ideally, statistical approaches should be defined a priori to ensure the data collected serves its function. Data should be recorded in long format, with each row pertaining to a particle (for characterization) or to a replicate (for quantification) and each column to a variable to be assessed (e.g., identification code, color, size, shape, polymer type). Comparisons and conclusions should always be based on a statistical analysis of the data. The chi-square test is commonly used for two categorical variables (e.g., does color vary significatively between areas?). Analysis of quantitative data generally involves t tests or analysis of variance (ANOVA) for parametric datasets, or the corresponding Mann-Whitney U and Kruskal-Wallis tests for non-parametric datasets (e.g., does concentration vary between different areas?). Probability results (i.e., *P*-values) should be reported and compared to the tested significance level (e.g., $\alpha = 0.05$). Categorical variables (e.g., color) should be reported as absolute and/or relative frequencies (i.e., number and/or percentage), and quantitative data should be reported as a mean for parametric datasets, or median for non-parametric datasets, accompanied by a measure of dispersion (e.g., variance, standard deviation, interquartile range).

How to collect samples of microplastics?

The first step is to collect samples containing microplastics, which may include matrices as diverse as water, sediment or soil, air, and biological matter [Figure 3]. The choice of sample collection method depends on the work's objectives. For instance, surface water collection may not be a good estimate of benthic organisms' exposure, especially considering that surface and deep waters may contain different microplastics depending on each particle's sinking behavior (e.g., dependent on density and biofouling)[32]. Moreover, recent publications are mainly focused on collecting the whole size range of microplastics (i.e., 1-5,000 μm). Since smaller microplastics are more abundant (e.g., 92% are < 300 μm in surface water in the South China Sea[33]), smaller sample volumes or weights may be collected. Reporting these smaller microplastics is needed for risk assessment since particles < 150 μm have a higher probability of being internalized by organisms[34]. The choice of sampling methods should also take into consideration principles of green analytical chemistry, which include reducing sample treatment, saving energy and reagents, automation, reducing analytical waste, and avoiding the use of hazardous reagents[35].

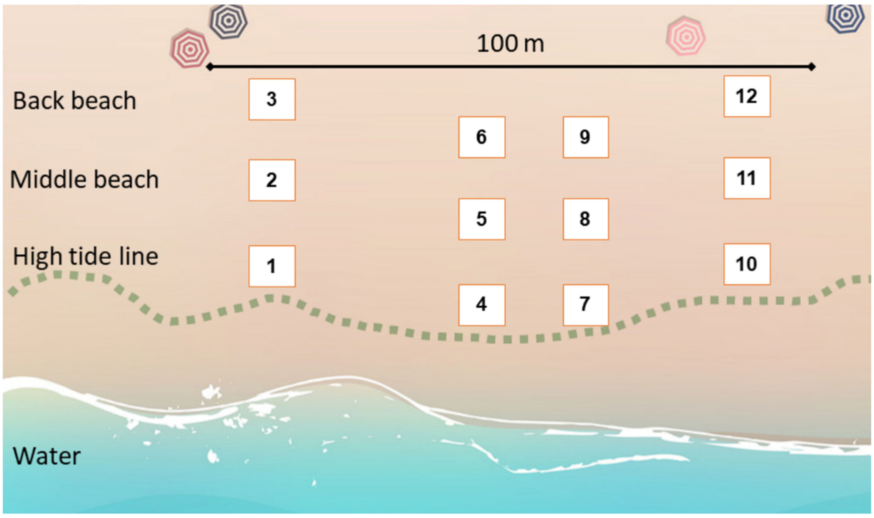

Figure 2. Beach sampling protocol according to the United States Environmental Protection Agency (original artwork).

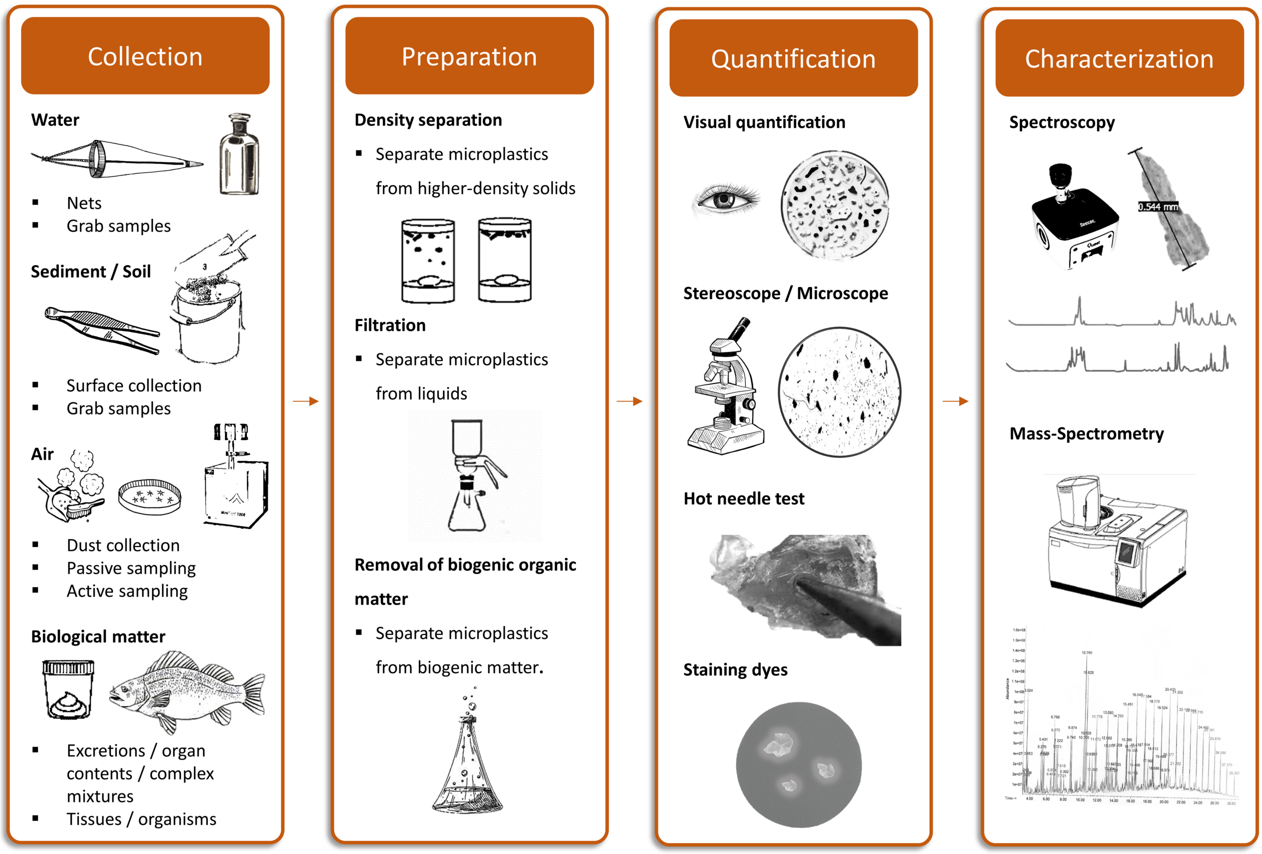

Figure 3. Summary of methods for sampling and analysis of microplastics.

Sampling water

For water, the choice is between using nets (e.g., 330 μm manta trawls) or collecting samples using bottles (i.e., grab samples) to be filtered in the laboratory. Nets may vary in configuration, for instance, sampling either surface water in the case of manta trawls or at a depth of 40-50 cm in the case of neuston nets[26]. Since microplastics may be differentially distributed on the water column (e.g., based on density), the choice of sampling methodology may create a bias on the types of particles found. While nets sample high volumes of water (m^3) with relative ease, they require water flow (e.g., towed by boat), contamination control is difficult, and the precise volume of water filtered is prone to considerable error. Collecting grab samples limits volume (L), either due to transportation or clogging, but allows sampling of smaller particles that are more abundant and more likely to induce adverse effects on organisms. This may include manually using buckets and bottles on surface water or using specialized equipment to collect underwater samples (e.g., Niskin sampler)[36]. Other works have used sieving and/or pumps to collect samples[37]. Grab samples are generally filtered in the laboratory, which may use filter membranes of different compositions and pore sizes. Filtering water through a 1 μm pore filter is expected to retain 40 times more microplastics than using a manta trawl[38]. Moreover, reliable results were produced by collecting 1 L grab samples in four replicates and assessing microplastics > 50 μm[28].

Sampling sediment or soil

For sediments or soil, collection generally requires defining a surface area (e.g., 1 m^2) where the top layer is collected (e.g., top 5 cm) using metal shovels and non-plastic containers (e.g., aluminum, glass). Samples will be taken to the laboratory and separated by density by filtering the supernatant after mixing with saturated solutions. Plastics' densities range between 0.90 and 1.45 $g \cdot cm^{-3}$, whereas sediments possess higher densities, approximately 2.65 $g \cdot cm^{-3}$. Saturated solutions of NaCl, while inexpensive and non-hazardous, produce the lowest recovery rates (75.71%) compared to higher recovery rates (> 85%) of NaBr and $CaCl_2$[39]. This occurs due to the saturated NaCl solution's lower density (1.2 $g \cdot cm^{-3}$), which is insufficient to separate higher-density plastics (e.g., polyvinyl chloride)[39]. Extraction with high-density solutions might need to be repeated to separate all particles from the sediment matrix. Conversely, higher-density solutions may present toxicity and higher costs, which can be alleviated by reusing the solution after filtration, thereby reducing costs and waste production[35]. Other techniques involve the use of complex apparatus for density extraction[40], elutriation[41], or oil-based extraction[42]. Alternatively, microplastics may be collected with tweezers directly from the surface, underwater samples collected by submergible claws (e.g., Van Veen grab), or with sediment core samplers. Results should be reported by the number and weight of microplastics per area and the weight of samples. Moreover, results should be reported in dry weight by drying the sample until no variation in weight occurs (or calculating dry weight based on the weight loss in a subsample). Studies should include details on sediment or soil characterization (e.g., sediment's grain size), since this may help highlight deposition patterns.

Sampling air

For air, samples are collected actively on a filter using an air sampling pump (e.g., flow rate of 5 $L \cdot min^{-1}$ for 24 h[43]), passively by deposition on the surface of a known area (e.g., funnel, Petri dish), or by collecting dust from surfaces using brushes. Samples are generally collected at a human breathing height (1.5 m). Passive sampling has the advantage of not needing specialized equipment but requires longer sampling periods and may not directly translate airborne concentrations (i.e., larger particles are more likely to sediment). Results from passive sampling (e.g., $particles \cdot m^{-2} \cdot h^{-1}$) allows to estimate airborne contamination of other matrices (e.g., water, soil), whereas active sampling ($particles \cdot m^{-3}$) is useful to estimate respiratory exposure, and dust collection allows to estimate the amount of microplastics relative to the total amount of dust collected (e.g., $particles \cdot g^{-1}$). Only particles with aerodynamic diameters < 10 μm (capable of reaching the deep lung) should be considered in the estimation of airborne exposure based on human tidal volume (6 $L \cdot min^{-1}$)[44]. Separation of < 10 μm can be achieved in active sampling by using a selective inlet.

Sampling biological matter

For biological matter, samples may be constituted by excretion products and organ contents (e.g., feces, digestive contents), tissues (e.g., digestive system, food), organisms (e.g., invertebrates), or complex mixtures (e.g., wastewater). Collection will vary according to each case and separation mainly relies on digestion and filtration. It is recommended to limit the amount of sample to reduce filter clogging and physically remove hard tissues (e.g., bones, chitin, or carbonaceous shells). Biological matter is often rich in fat, which must be removed manually, using detergents or ethanol[45]. Moreover, lipids will be subjected to saponification in the presence of alkali solutions (e.g., KOH), which may be removed using hot water. Wastewater samples may be collected as grab samples or through high-volume filtration using sieves[46]. Overall, biological matter is the most challenging matrix to work with. Ideally, new methods will be developed to identify the precise location of microplastics in tissues using histological techniques. Several features of the biological samples should be taken into account: (i) trophic transfer; (ii) correlation with concentrations found in environmental matrices; (iii) microplastics in internal organs (besides the digestive system) as evidence of translocation; (iv) possible accumulation of microplastics in organisms; and (v) presence of related contaminants (e.g., plastic additives). More research on microplastics is needed, especially addressing terrestrial ecosystems.

Sample preparation: removal of biogenic organic matter

Almost all samples require some sort of sample preparation to reduce the number of particles and clean the surface of microplastics [Figure 4]. This is mostly accomplished through digestion (i.e., natural organic matter degradation). The most common solutions used are H_2O_2 (alone or as Fenton's reagent when combined with Fe as a catalyzer), HNO_3, and KOH. H_2O_2 [e.g., 30% (v/v)] is mostly used on environmental samples (e.g., water, sediment) and KOH [e.g., 10% (w/v)] on biological matter (e.g., tissues). Acids are generally not recommended due to the risk of damaging microplastics in the sample[47]. Although enzymes degrade with a high efficiency without damaging microplastics, they are also often prohibitively expensive. Reactions may be accelerated by heating, although temperatures > 60 °C are not recommended as they may destroy microplastics[48]. The use of organic solvents to further clean the surface of microplastics may also cause damage. For instance, acetone may melt polystyrene into a paste[49]. Therefore, it is recommended that sample preparation protocols are tested using positive controls with various representative polymer types (i.e., spiked samples).

Sample preparation: separation of microplastics

Filter membranes are often used in microplastics analysis to separate particles from liquids. The type and pore size of these filter membranes can influence the retained fraction of microplastics, the amount of residual matrix, and the ease of filtration (depending on vacuum pressure). The choice will also depend on treatment and analysis, as it may benefit from materials that are inert (e.g., glass fiber filter), degradable (e.g., cellulose), or present low signal interference in spectroscopic analysis (e.g., silver). Filter structure can also influence the size, shape, and number of particles recovered (e.g., multilayered filters are better at retaining fibers)[50]. While the choice of filter membrane may lead to underestimation, it can also introduce contamination if no decontamination procedure is conducted before use. Similarly, sieve use will depend on pore size and decontamination measures.

Emerging methods for microplastics separation involve chromatographic techniques, such as field flow fraction, which consists of applying a field (e.g., electrical, hydraulic) perpendicular to the flow of particles in a narrow channel leading to the accumulation of particles in one of the walls, and hydrodynamic chromatography, which separates particles by sizes by passing the sample through a column with solid beads, carried by a mobile phase[51]. Dielectrophoretic separation is based on an electric field that separates

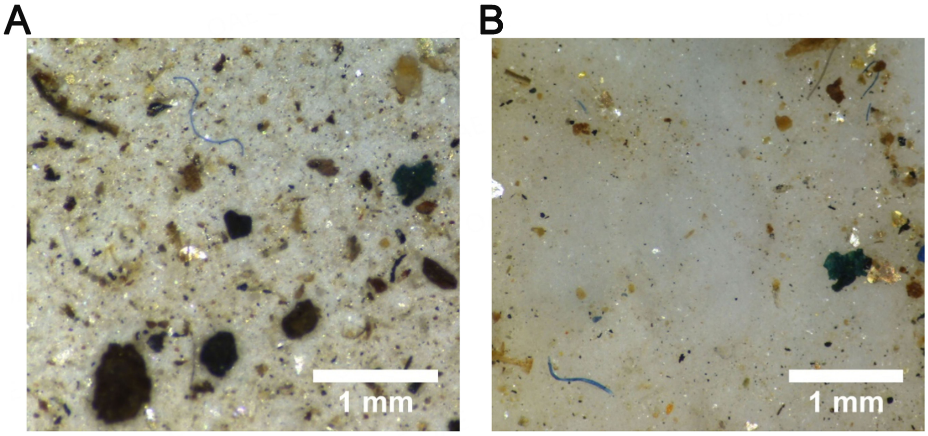

Figure 4. Sediment sample (A) before and (B) after biogenic organic matter removal using 10 mL of 30% hydrogen peroxide and 10 mL of 0.05 M of iron catalyst for 15 min.

particles of different dielectric signatures into microchannels[52]. Alternatively, flow cytometry can be used for sorting and counting and characterizing microplastics based on optical properties, with the advantage of having a high particle throughput[53]. It can be combined with fluorescent dyes and preconcentration steps to improve accuracy. Fractioning could also be used to separate microplastics from liquids, but smaller and less dense particles will require centrifuging at higher speeds for longer periods (e.g., > 3,500 rpm, > 5 min[54]), ideally inside glass tubes to avoid plastic contamination.

How to identify microplastics under the microscope?

Successful microplastics identification depends on proper sample preparation, which is easier in less complex matrices (e.g., in water than in food). Screening microplastics under a stereoscope or microscope is one of the simplest and cheapest methods available. However, it is also subjective and can lead to misclassification of other materials such as microplastics (up to 70%)[55]. Exposing particles to heat (130 °C, 3-5 s)[56] or touching them with a hot needle[57] helps to further separate large melting particles as thermoplastics. The use of a soldering iron instead of a hot needle and a classification criterion (positive if particle melts, bends, or curls) results in ≥ 82% correct classification[58]. While the hot needle test may also be performed, synthetic fibers are visually classified based on their regular and smooth surface, following a classification diagram[59]. Size, shape, and color must be recorded for each particle. Analysis may be aided by image processing software (e.g., ImageJ).

The use of staining dyes provides a more objective criterion if they are selective for plastics or if other stainable particles have been removed (during digestion). Nile Red is the staining dye most frequently used in microplastics screening [Figure 5]. Plastics stained with Nile Red produce a red-to-yellow fluorescence under the blue light (470 nm) when seen through an orange filter or under the UV light (250 nm)[60]. This method seems to reduce the number of false positives, as 90% of fluorescent particles in sediment samples (> 630 µm)[61] and 100% in bottled water samples (> 100 µm)[62] were confirmed as plastics by chemical characterization. Nile Red allows quantification of microplastics > 1 µm when coupled with fluorescence microscopy and can be used as a selection criterion before chemical identification, improving sample throughput[63]. Moreover, staining dyes are inexpensive. Grids or guiding markers are recommended when working with small particles under the microscope to avoid counting them twice.

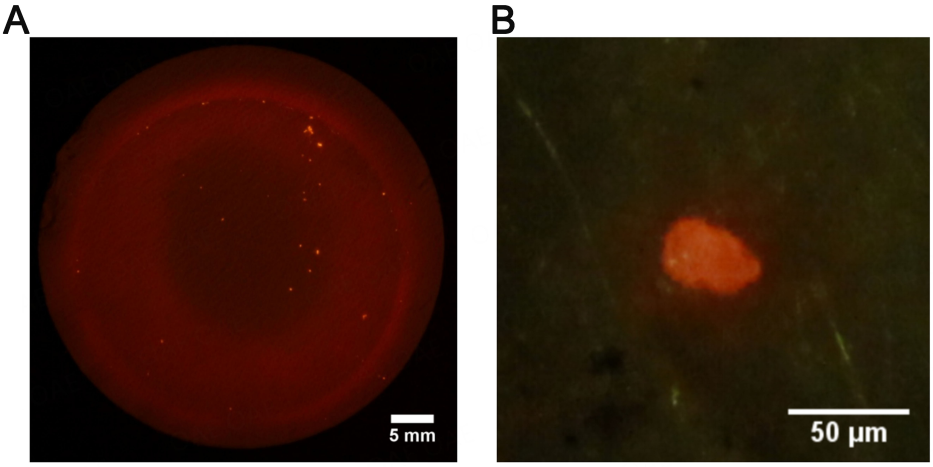

Figure 5. Fluorescent microplastics after Nile Red staining and under 470 nm with an orange lens filter: full glass fiber filter (47 mm) spiked with (A) microplastics and (B) suspected microplastics in river water under the microscope.

How to analyze microplastics by chemical characterization?

Vibrational spectroscopy techniques in microplastic characterization

Visual identification and staining dyes only provide information on suspected microplastics. Chemical characterization is needed for confirmation and polymer identification. The most common techniques are based on vibrational spectroscopy. Fourier transform infrared spectroscopy (FTIR) relies on the detection of the absorption, transmittance, or reflectance of infrared light based on the change in the dipole moment, whereas Raman spectroscopy detects the inelastic scattering of light caused by changes in polarizability within the molecule. It is recommended to characterize at least 10% of suspected microplastics > 100 µm[25]. Micro-spectroscopy techniques (i.e., coupled with microscopy) allow the characterization of particles down to 1-20 µm[64], ideally of a specific area of the filter when scan mode (or mapping) is available or of a group of pre-selected suspected particles (which should be representative of the sample). However, micro-FTIR and micro-Raman spectroscopy are time-consuming (e.g., 6-8 h per sample[65]) and require expensive equipment, which researchers may only have access to through collaborations. Therefore, these techniques are generally not suited for quantification (which still relies on microscopy or staining dyes). Moreover, the presence of contaminants or pigments on microplastics may cause interference, such as titanium dioxide (TiO_2)[66] or black pigments (e.g., carbon black)[67]. Generally, FTIR is more lenient when interference is present, while photo-bleaching (i.e., fluorophore undergoes photo-destruction when the absorption/emission limits are surpassed) may be attempted in micro-Raman spectroscopy[64].

Another challenge in vibrational spectroscopy is the analysis of the fingerprint spectrum. Each peak or band corresponds to vibrations of specific chemical bonds [Figure 6]. Spectra may be subjected to baseline correction, which enables the removal of peaks not in the sample (e.g., CO_2 infrared peak at ~2,360 cm^{-1}). Polymer identification may rely on a personal database of known plastics, on the equipment's database, or on open online databases (e.g., OpenSpecy[68], SiMPle[69]). Besides reporting the relative frequency of different polymer types, the carbonyl and methyl index can be calculated from infrared spectra, which are used as indicators for the weathering state. Carbonyl groups (–C=O) are produced during plastic's degradation through photooxidation, translated as an infrared band between 1,850-1,550 cm^{-1}, centered in 1,715 cm^{-1} (ketone)[70]. Thus, the Carbonyl Index (CI) can be calculated as the ratio between the carbonyl peak (1,715 cm^{-1}) and the reference peak for the polymer (e.g., 1,471 cm^{-1} for polyethylene, 1,458 cm^{-1} for polypropylene, 1,452 cm^{-1} for polystyrene)[19]. In polypropylene, the first stages of degradation lead to the production of volatile oxidation products (e.g., acetone), which are lost by evaporation, resulting in a

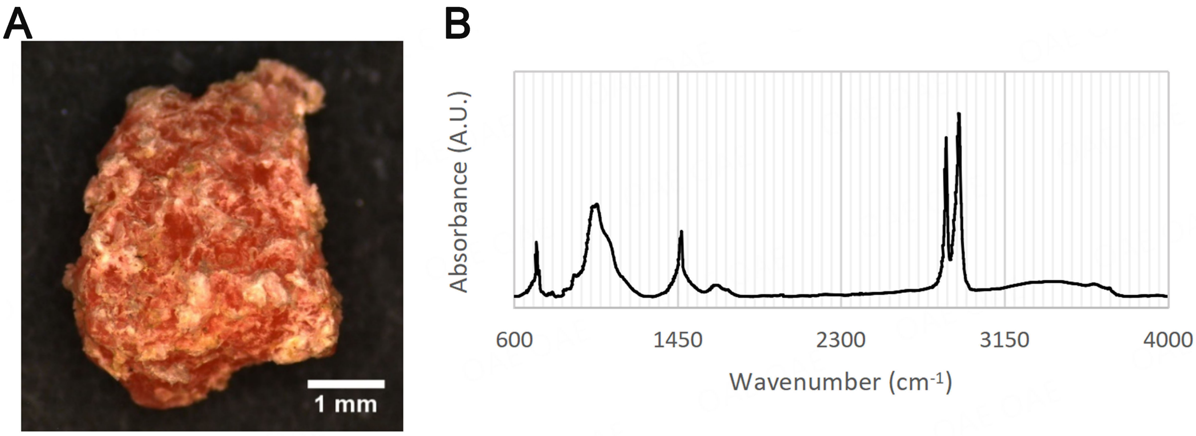

Figure 6. (A) Microplastics collected on a beach in Portugal, and identified as polyethylene based on (B) its infrared spectra.

reduction in methyl groups (-CH$_3$). Thus, the Methyl Index (MI) may be calculated for polypropylene as the ratio between the methyl group (1,377 cm^{-1}) and the reference peak (1,458 cm^{-1})[71]. Comparison between CI should only be conducted for the same polymer type. Particles should be thoroughly cleaned to remove biological debris that may translate into an increased carbonyl band (e.g., using cyclohexane at 80 °C for 48-96 h[72]).

Mass spectrometry techniques in microplastic characterization

Vibrational spectroscopy techniques are non-destructive and allow chemical and physical characterization of particles, which is highly relevant for risk assessment. However, they are time-consuming. Alternatives based on mass spectrometry (MS) [e.g., pyrolysis-gas chromatography-MS (Py-GC-MS), thermoextraction and desorption coupled with gas chromatography-MS, liquid chromatography-MS] allow to gather information from complex matrices without pre-selection, quickly, and even for smaller microplastics sizes[73]. The cons of these methods involve the need for calibration curves for each compound (including considerations on degraded states), sample destruction, and loss of information regarding physical parameters (i.e., only reported as mass, e.g., μg·mg^{-1}).

Py-GC-MS has increased in popularity due to its ability to detect smaller particle sizes (even nanoplastics), with higher sensitivity and lower vulnerability to interference, and being compatible with direct analysis and/or with most sample preparation methods[74]. This technique is based on the thermal decomposition of the sample's molecules into simpler fragments which are separated by a capillary column and detected by mass spectrometry. A specific indicator (fragment) is required for each polymer type to properly detect and quantify them based on calibration curves. An optimized Py-GC-MS method for microplastics has been proposed using a pyrolysis temperature of 700 °C, split ratio of 5, and 300 °C as injector temperature, allowing limits of detection of 1 μg for microplastics[75]. This method performed well when tested on particles previously identified by micro-Raman spectroscopy and correctly identified > 70% of environmental microplastics. Worst results were found for fibers due to their low weight, which could be improved by decreasing the limit of detection using single ion monitoring or pre-concentrating the sample.

Scanning electron microscopy in microplastic characterization

The determination of total organic carbon analysis can be used in the quantification of the total mass of plastics in complex samples after biogenic organic matter removal[76]. Equations are available to make estimate conversions between different types of reporting units[77]. Scanning electron microscopy may be used to characterize the surface of microplastic, while coupling with energy-dispersive X-ray spectroscopy allows for chemical characterization. However, most of the elemental composition of plastics is similar to biological matter (e.g., C, O, H), which may hinder identification.

Other techniques in microplastic characterization

Other techniques of microplastics analysis have been proposed to address challenges in traditional approaches. Hyperspectral imaging is based on spectral fingerprints (e.g., on near-infrared spectrum), which may allow differentiation between polymer types[78]. Matrix-assisted laser desorption/ionization time-of-flight mass spectrometry, which involves ionization and mass-to-charge ratio (m/z) measurement, may be useful in the detection of microplastics, including weathered particles[79]. Dynamic light scattering and nanoparticle tracking analysis are based on light scattering and Brownian motion and can be complementary in the characterization and quantification of particles[80]. Atomic force microscopy scans the sample surface by registering attractive and repulsive forces between the surface and the cantilever[81]. The techniques described in the last two sentences may also be suitable for nanoplastics analysis.

Characterization of nanoplastics

Nanoplastics are more challenging due to the smaller particle sizes (< 1 μm) below most limits of detection and are prone to contamination. Sample preparation also involves the removal of natural organic matter, separation and preconcentration (e.g., filtration, centrifugation), and identification using spectroscopy or mass spectrometry[82]. However, so far, only a few studies have been able to detect nanoplastics in real environmental samples. While scanning electron microscopy has been used to characterize very small plastics (< 10 μm)[83], quantification based on the detection of particles containing carbon has been questioned due to the potential contamination with other similar organic and inorganic materials[84].

How to avoid contamination of microplastics samples?

Microplastics are so ubiquitous that they can easily contaminate samples. Researchers must be aware of the two main sources of contamination, namely, the deposition of airborne microplastics in samples and cross-contamination from solutions and materials used. Reducing airborne contamination requires: (i) regular laboratory cleaning schedules; (ii) proper ventilation and reduced movement; (iii) capping all samples and solutions (e.g., with glass lids or aluminum foil); (iv) conducting work under the fume hood, or ideally, the laminar flow hood; (v) wearing cotton lab coats. Reducing cross contamination requires: (i) filtering all solutions used in cleaning or to be added to the solution; (ii) washing materials between samples, ideally in acid followed by running filtered distilled water; (iii) using only glass and metal materials (i.e., no plastics); (iv) decontaminating inorganic filters (e.g., 3 h at 450 °C). Finally, a relevant number of blanks must be conducted during sample collection (i.e., field blanks) and processing (i.e., procedural blanks and open filters to evaluate airborne deposition). Microplastics found in blanks can be subtracted from results or samples only considered when statistically different from concentrations in blanks.

What can we learn from existing interlaboratory comparison tests?

Interlaboratory tests have been conducted despite not reaching a definitive conclusion regarding recommended methodologies [Table 1]. Since most tests were conducted with pristine microplastics, results may vary when working with environmental samples. For instance, micro-Raman spectroscopy works better with pristine samples since it is susceptible to fluorescence interference and may cause polymer degradation as a result of heating[64]. Studies seem to agree that errors vary greatly between research groups[85,86], which supports conclusions that most are a result of human error[85,87]. Nonetheless, variation is also attributed to microplastics' characteristics, such as particle size (i.e., higher for sizes < 20 μm), shape, and color or matrix properties[85]. While attempts have also been made to harmonize the production of reference materials[88], these are not yet widely available or frequently used. Sample preparation seems to

Table 1. Main conclusions arising from interlaboratory tests conducted on the methods for quantification and characterization of microplastics

Test name	Published date	*n*	Samples	Main conclusions	Ref.
Isobe *et al*., 2019	2019	12	Two bottles with different concentrations of PP, LDPE, HDPE, and NOM in seawater (400-5,700 µm)	High uncertainty (> 50%) likely results from human error (i.e., misidentification or measuring errors) Sample preparation (i.e., chemical treatment, density separation) reduced uncertainty from 40% to 20% Underestimation of 20% for microplastics < 1 mm (spectroscopy recommended)	[87]
Müller *et al*., 2020	2020	17	Sugar water spiked with PE, PVC, PET, PMMA, and PS (8-140 µm)	Better identification of polymer type by micro-Raman spectroscopy and Σ-GC/MS than by micro-FTIR Quantification using microscopy and micro-FTIR worked best	[90]
Becker *et al*., 2020	2020	9	Sediment sample spiked with PP, PS, PE, PET, and suspended particulate matter (2,000-3,000 µm)	Py-GC-MS, TED-GC-MS, TGA-FTIR correctly identified all polymers and produced reasonable results The mean absolute deviation from the median was 14% for PE and PS and > 40% for PP and PET High variability in the analysis of PET likely results in the use of adsorber materials and stationary phase adapted for non-polar compounds Additives in PE could influence the formation of decomposition products and interfere with readings TGA-MS not recommended since it did not confirm the presence of the four polymer types	[93]
Cadiou *et al*., 2020	2020	5	Clean water or sediment spiked with PET, PVC, PC, HDPE, and PP (300-5,000 µm)	Error was < 25% of the absolute value for microplastic counts (60% underestimation and 40% overestimation) Errors in quantification were higher in sediment compared to water samples (18% *vs*. 14% root mean square errors) Laboratories varied greatly in the error of detection of microplastics (2%-3% *vs*. 23%-30%) Regarding shape, films are generally overestimated while others are correctly counted or underestimated Color also influences the correct estimation of microplastics Underestimation might be explained by lack of detection, loss of laboratory material, or loss by being blown out during handling.	[85]
JRC's interlaboratory test	2021	98	One sample of PET in salt water (30-200 µm)	Methods had a high variability depending on research groups Many groups efficiently detected the correct number of plastics in the samples using multiple techniques, including microscopy, micro-FTIR, and micro-Raman spectroscopy Some contamination control measures (i.e., the use of cleaning paper and gloves) seem to be related to the underestimation of microplastics	[86]
WEPAL-QUASIMEME/NORMANs	2021	30	11 samples comprised each of the most common polymer types (PC, PS, PP, PET, LDPE, EPS, PVC) and one blank (2,270-4,310 µm)	Correct chemical identification > 80% (except for low-density polyethylene) Consistent performance of micro-Raman spectroscopy Quantification was often flawed in terms of absolute number and the high dispersion of data (i.e., relative standard deviation of 57%-91%)	[91]
The Plastic Busters MPAs	2021	4	Fish gastrointestinal tract and mussel tissues spiked with PE, PP, and PET (> 200 µm)	The coefficient of variation after digestion and counting under the microscope was < 11% for most samples Recovery rates were 96.7% for 5 mL/g of 10% KOH and 88.8% for 20 mL/g of 15% H_2O_2	[89]

				Changes due to sample preparation were observed as fragmentation (7.1%), discoloration (2.1%), deformation (9.2%), and degradation (17.1%) Microplastics correctly identified by FTIR varied between 47.8% and 69.5%	
De Frond *et al.*, 2022	2022	22	Three samples of PE, PS, PVC, PET, and NOM in drinking water and one blank (1-5,000 µm)	Microscopy allowed for a mean recovery rate of 92% for microplastics > 20 µm and 32% for < 20 µm The mean blank sample count was 91 particles Micro-FTIR accurately identified 95% of microplastics and misidentified 8% of NOM as microplastics Micro-FTIR accuracy was 33% for microplastics < 20 µm Micro-Raman spectroscopy accurately identified 91% of microplastics and misidentified 68% of NOM as microplastics Micro-Raman spectroscopy performed poorly on dyed cellulose fibers due to the interfering fluorescence.	[92]

PP: Polypropylene; LDPE: low-density polyethylene; LDPE: low-density polyethylene; NOM: natural organic matter; PE: polyethylene; PVC: polyvinyl chloride; PET: polyethylene terephthalate; PMMA: polymethyl methacrylate; Σ-GC/MS: thermo-extraction-and-desorption- or pyrolysis- combined with gas chromatography coupled to mass spectrometry; micro-FTIR: micro-Fourier transform infrared spectroscopy; Py-GC-MS: pyrolysis gas chromatography-mass spectrometry; TED-GC-MS: thermal extraction desorption followed by gas chromatography coupled to mass spectrometry; TGA-FTIR: thermogravimetry-infrared spectroscopy; TGA-MS: thermogravimetry coupled to mass spectrometry; PS: polystyrene; EPS: expanded polystyrene.

reduce the errors in the identification of microplastics by removing confounding particles[87,89]. Microscopy, micro-FTIR, and micro-Raman spectroscopy are associated with high recovery rates (> 90%) and spectroscopy methods may also provide information on polymer type[90-92]. Nonetheless, higher errors are expected for smaller microplastic sizes[87]. Alternatively, pyrolysis gas chromatography-mass spectrometry, thermogravimetry-infrared spectroscopy, and thermal extraction desorption followed by gas chromatography coupled to mass spectrometry are also efficient in the quantification and characterization of some polymer types[93]. These techniques also present limitations such as the specificity of adsorber materials and stationary phase compounds for some polymer types or being influenced by additives in plastics[93]. Surprisingly, the most frequently found variation in results was underestimation and not overestimation (expected due to sample contamination)[85-87]. This underestimation likely results from errors in detection or losses to laboratory material or to the air when handling these samples[85]. Therefore, frequent tests are recommended to evaluate the recovery rates of the group's methodologies using a diverse array of microplastics and matrices and improve techniques to reach an acceptable variation.

CHALLENGES IN EVALUATING THE ADVERSE EFFECTS OF MICROPLASTICS

How do microplastics enter the environment?

Microplastics originate from virtually any object made of plastic [Figure 7]. Some relevant sources of microplastics include pellets, microbeads in personal care products, paint, textiles (including garments, household textiles, personal protective equipment, geotextiles used in agriculture), wastewater effluents, synthetic pavement and artificial turf, vehicle tire wear, fishing gear, and littered or mismanaged plastic waste[94-96]. Lack of proper waste management and wastewater treatment greatly contributes to the amount of (micro)plastics entering the environment. Most microplastics are thought to originate from terrestrial areas, especially related to high anthropogenic pressures (e.g., high population density, high industrialization), and then be transported by wind, runoff, or rivers.

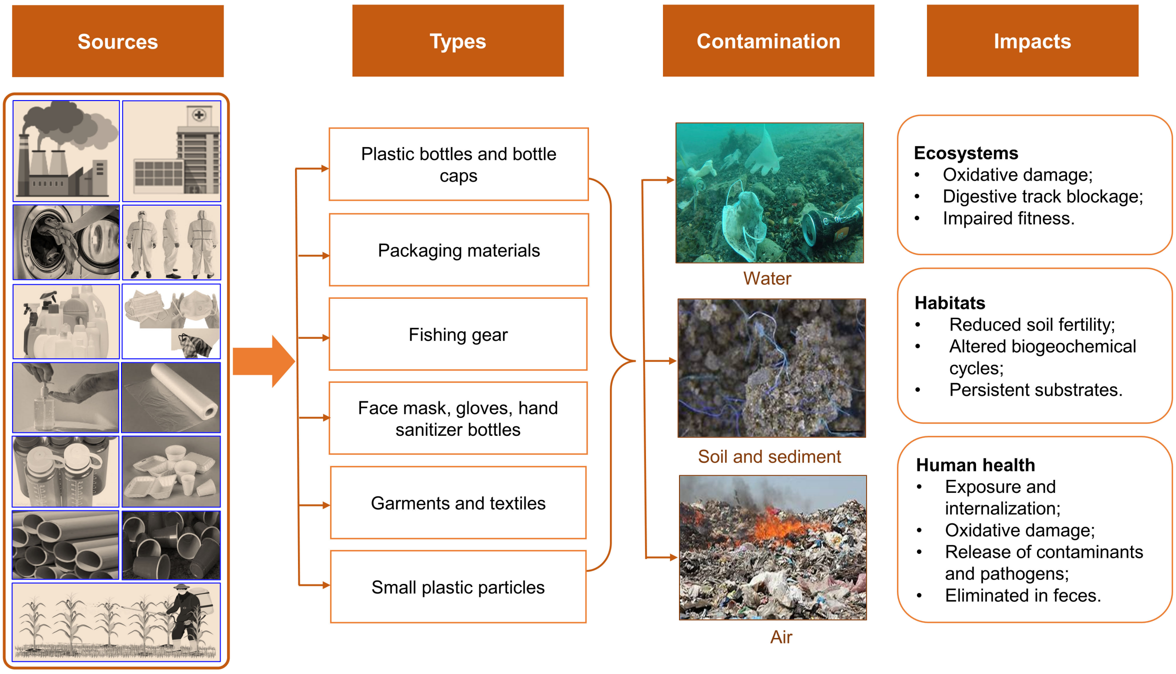

Figure 7. Examples of sources, types, contamination, and impacts of microplastics in the environment.

Estimations indicate that most microplastics reaching the sea originate from river transport[97] whereas atmospheric transport may contaminate remote regions, such as the Tibetan Plateau[98]. The distribution of microplastics may also depend on their surface coverage with organic matter and organisms (i.e., biofouling), for instance, modulating their distribution in the water column[99]. Microplastics may also accumulate in environmental matrices, such as sediments or soils, and can be incorporated into geological formations, being considered markers for the Anthropocene[100]. However, few works have collected data to support the identification of sources and pathways of microplastics in the environment due to the previously addressed methodological challenges.

What are microplastics' effects on the environment?

Biotic effects of microplastics

The presence of microplastics in the environment leads to the exposure of organisms, with these particles being found in the gastrointestinal system of invertebrates (e.g., *Chironomus riparius* larvae)[101] and vertebrates (e.g., *Seriolella violacea* fish)[102]. These studies are often limited to the detection of larger microplastics (e.g., > 500 μm) in the gastrointestinal lumen or tissue. Nonetheless, microplastics in the gut may translocate to internal tissues (e.g., hemolymph of *Mytilus edulis*[103]) and be transferred through the food chain[104]. However, evidence for bioaccumulation and biomagnification in the wild is insufficient[105,106]. Bioindicators are species that can be used to monitor environmental contamination. Bivalves, as filter feeders, have already been suggested as bioindicators for microplastics[107], supported by a significant correlation between concentrations in water and in tissues of *Mytilus edulis* and *Perna viridis*[108]. The use of bioindicator species can provide insights into the spatial distribution of microplastics and their interaction with organisms within the ecosystem.

Laboratory tests on aquatic organisms reveal effects on feeding (e.g., digestive tract blockage), endocrine disruption, metabolism, and gene expression, leading to reduced growth and survival[109]. These likely stem from reactive oxygen species, seemingly the molecular initiating event across different animal species[110]. A species sensitivity distribution determined a threshold effect concentration (HC_5) of 11-521 microplastics·L^{-1}, representing 28% of locations included in the study[38]. Despite the large amount of available literature, most assays have used concentrations 2 to 7 orders of magnitude higher than environmental levels, instead of environmentally relevant concentrations (e.g., ≤ 1 μg·L^{-1} for water)[111]. However, preparing lower concentrations may be challenging due to the lack of methods to quantify microplastics in small volumes, which often involve spectrofluorometry (i.e., when using fluorescent particles) or the use of Neubauer counting chambers[112].

Organisms and microplastics should be selected simultaneously, based on the likelihood of environmental exposure and the availability of international guidelines (e.g., OECD Test Guidelines). Tested microplastics may be acquired (e.g., Sigma-Aldrich; Cospheric; plastic industry) or produced in the laboratory (e.g., using cryomilling or a simple coffee grinder), followed by adequate particle characterization [Figure 8]. Microplastics may also transport adsorbed contaminants or pathogens[113]. Therefore, more complex tests involve aging microplastics under ultraviolet light, producing leachates by incubating them in a pristine solution, or contaminating microplastics with other substances or microorganisms. The contribution of each characteristic to toxicity should be identified (e.g., chemical composition, size, shape).

Abiotic effects of microplastics

Little information is available on those other than marine organisms (e.g., plants) and abiotic effects. Indeed, microplastics may cause abiotic effects on ecosystems, such as favoring species using them as substrates[114], altering the distribution of substances and/or biogeochemical cycles[115], and changing thermal diffusivity and permeability of sediments or soils[116,117]. Thus, marine plastic pollution is already considered a planetary boundary threat due to its accumulation, long-lasting nature, irreversibility, and capacity to disrupt natural processes[3]. Future study designs should encompass the information needed to conduct risk assessment, enabling informed decisions about control and mitigation strategies (i.e., risk management). Work objectives should attempt to fill knowledge gaps following a DPSIR framework (i.e., drivers, pressures, state, impact, and responses)[118].

Plastisphere: life on microplastics

The plastisphere is a unique ecosystem of microorganisms living on the surface of microplastics. It is formed when the surface of particles is covered with biofilms, facilitating further colonization by microorganisms and forming communities with metabolic interactions that might include species with diverse functions (e.g., plastic degradation), which also depends on microplastics' characteristics (e.g., polymer type)[119]. Therefore, microplastics can be considered a novel niche habitat, with longer environmental persistence than natural organic substrates and with hydrophobic surfaces prone to colonization and biofilm formation[120]. A concerning fact is that the microbial communities associated with microplastics differ from those in the surrounding ecosystem, potentially giving rise to microbial invasion, and some contain opportunistic pathogens (e.g., *Vibrio*)[121,122]. Therefore, there is a growing need for research on the plastisphere, not only due to its potential adverse impacts on ecosystems and health but also for the prospects of identifying naturally occurring plastic-degrading species (or communities) that could contribute to mitigating plastic pollution.

Effects of microplastics on human health

Microplastics enter the food chain through water, feed, food, and atmospheric contamination. Moreover, smaller microplastics in suspension in the atmosphere can be inhaled. Human exposure to microplastics through ingestion and inhalation has been estimated as 2.93×10^{10} microplastics·$year^{-1}$[123]. However,

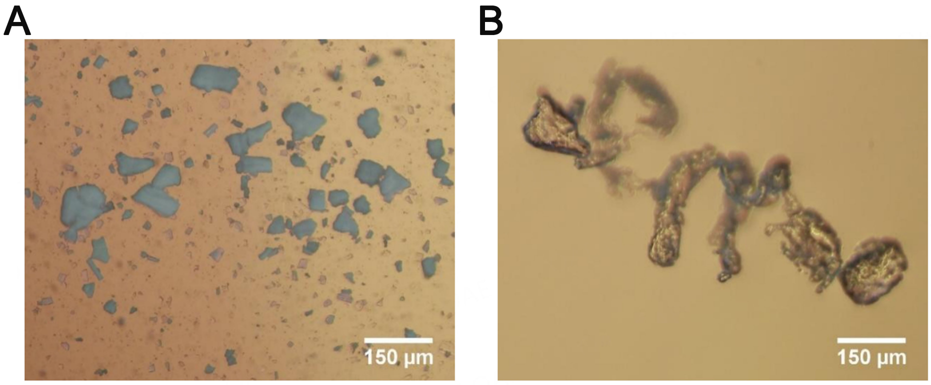

Figure 8. (A) Commercially available polystyrene microplastics; and (B) polypropylene microplastics produced in a coffee grinder in the laboratory.

estimations vary depending on the food types included in the model and the methods used in the original articles (e.g., size limit of detection). An accurate estimation based on uniform methods and estimated daily exposure models is needed. Inhalation is often overestimated due to the use of results from total suspended particulates instead of inhalable or respirable particles (< 100 µm or < 10 µm, respectively). Dermal exposure is not relevant due to the thickness of the stratum corneum. A study of 102 participants found significant correlations between the concentrations of microplastics in feces with exposure to dust and the consumption of bottled water and take-away food[121], supporting inhalation and diet as the main exposure routes.

After exposure of the digestive or respiratory system, only a small amount of smaller microplastics is translocated to internal tissues (< 1%)[122,124]. Some microplastics will find their way into the blood and become systemically distributed until they get caught into narrow capillary beds (e.g., < 5 µm in human lungs)[125] or are removed by the macrophages of the reticuloendothelial system[126]. Microplastics are then eliminated into the bile or the gastrointestinal lumen, where they will be excreted in the feces[127]. Concentrations as high as 139 microplastics·g^{-1} have been found in human feces[128] Additionally, microplastics have been found in human samples including saliva, sputum, bronchoalveolar lavage fluid, pulmonary tissue, blood, liver, kidney, placenta, and breast milk[129].

Despite knowledge gaps, there is no evidence to support the impacts of microplastics on human health[130]. For instance, a single intravenous injection of millions of 3-12 µm microplastics in dogs did not induce significant health effects for up to 4 weeks[131]. However, studies have generally been conducted using pristine microplastics and under acute exposure conditions. The release of monomers, additives, degradation products, adsorbed contaminants, and transport of pathogens may result in different effects of environmental exposure to microplastics, requiring further research. Moreover, microplastics can have adverse effects even when not internalized. Indeed, microplastics may change the human gut microbiome, which is recognized for its importance to human health, leading to dysbiosis[132]. The distribution and toxicity of microplastics may be further clarified by testing radiolabeled particles. Potential pathways of toxicity for microplastics could involve oxidative stress, cytotoxicity, and inflammation.

CONCLUSION

The findings gathered in the “Do’s and Don’ts of Microplastic Research” webinar envisaged the generation of a beginner’s guide for researchers working with microplastics. Another objective was to identify current challenges related to microplastics contaminants in this rapidly emerging field. Overall, the major identified challenges include: (i) the absence of standardized methods; (ii) lack of reference materials; (iii) hindered access to highly expensive equipment; and (iv) resolution problems when working with smaller environmental concentrations (e.g., toxicity assays). To overcome these critical issues, the implementation of a harmonized guideline or standard is warranted and may be achieved through more active and widespread cooperation between researchers of different fields and institutions with paired expertise. During the guideline or standard development, the reference materials should be clearly defined, and thus a comprehensive list of their properties will ensure manufacturing consistency. The highly expensive and specific equipment required for the advanced analysis of microplastics may be circumvented in the short term through a broader collaboration between institutions. Nevertheless, higher funding should be oriented to this pivotal area by governments and funding agencies, for a sustained generation of ubiquitous high-quality microplastic research. With up-to-date equipment, the resolution limitations (i.e., smaller sizes) may be mitigated. Therefore, higher interconnectivity between researchers and institutions is extremely important and should be actively fomented. Moreover, researchers should be involved in dissemination campaigns to increase the public and government's awareness of the importance of microplastic research.

DECLARATIONS

Acknowledgments

Padrão J would like to acknowledge the funding by the Portuguese Foundation for Science and Technology (FCT), European Regional Development Fund (FEDER), Operational Program for Competitiveness Factors (COMPETE), and Portuguese Ministry of Science, Technology and Higher Education (MCTS): [UID/CTM/00264/2021]. The authors would also like to thank the webinar's organizers and participants.

Authors' contributions

Substantial contributions to the conception or design of the work, or the acquisition, analysis, or interpretation of data for the work: Prata JC

Drafting the work or revising it critically for important intellectual content: Prata JC, Padrão J, Khan MT, Walker TR

Final approval of the version to be published: Prata JC, Padrão J, Khan MT, Walker TR

Agreement to be accountable for all aspects of the work in ensuring that questions related to the accuracy or integrity of any part of the work are appropriately investigated and resolved: Prata JC, Padrão J, Khan MT, Walker TR

Availability of data and materials

Not applicable.

Financial support and sponsorship

Padrão J would like to acknowledge the funding by the Portuguese Foundation for Science and Technology (FCT), European Regional Development Fund (FEDER), Operational Program for Competitiveness Factors (COMPETE), and Portuguese Ministry of Science, Technology and Higher Education (MCTS): [UID/CTM/00264/2021].

Conflicts of interest

All authors declared that there are no conflicts of interest. Prata JC is an Editorial Board member of the journal *Water Emerging Contaminants* & *Nanoplastics*.

Ethical approval and consent to participate

Not applicable.

Consent for publication

Not applicable.

Copyright

REFERENCES

1. Frias JPGL, Nash R. Microplastics: finding a consensus on the definition. *Mar Pollut Bull* 2019;138:145-7. DOI PubMed
2. Allen S, Allen D, Karbalaei S, Maselli V, Walker TR. Micro(nano)plastics sources, fate, and effects: what we know after ten years of research. *J Hazard Mater Adv* 2022;6:100057. DOI
3. Villarrubia-gómez P, Cornell SE, Fabres J. Marine plastic pollution as a planetary boundary threat - the drifting piece in the sustainability puzzle. *Mar Policy* 2018;96:213-20. DOI
4. Backhaus T, Wagner M. Microplastics in the environment: much ado about nothing? A debate. *Glob Chall* 2020;4:1900022. DOI PubMed PMC
5. Plastics - the facts 2022. Plastics Europe. Available from: https://plasticseurope.org/knowledge-hub/plastics-the-facts-2022/. [Last accessed on 26 Feb 2024].
6. Geyer R, Jambeck JR, Law KL. Production, use, and fate of all plastics ever made. *Sci Adv* 2017;3:e1700782. DOI PubMed PMC
7. Thompson RC, Olsen Y, Mitchell RP, et al. Lost at sea: where is all the plastic? *Science* 2004;304:838. DOI
8. Carpenter EJ, Anderson SJ, Harvey GR, Miklas HP, Peck BB. Polystyrene spherules in coastal waters. *Science* 1972;178:749-50. DOI PubMed
9. Mehinto AC, Coffin S, Koelmans AA, et al. Risk-based management framework for microplastics in aquatic ecosystems. *Micropl Nanopl* 2022;2:17. DOI
10. Masura J, Baker J, Foster G, Arthur C, Herring C. Laboratory methods for the analysis of microplastics in the marine environment: recommendations for quantifying synthetic particles in waters and sediments. 2015. Available from: https://repository.library.noaa.gov/view/noaa/10296/noaa_10296_DS1.pdf. [Last accessed on 26 Feb 2024].
11. Hartmann NB, Hüffer T, Thompson RC, et al. Are we speaking the same language? Recommendations for a definition and categorization framework for plastic debris. *Environ Sci Technol* 2019;53:1039-47. DOI
12. da Costa JP, Santos PSM, Duarte AC, Rocha-Santos T. (Nano)plastics in the environment - sources, fates and effects. *Sci Total Environ* 2016;566-567:15-26. DOI PubMed
13. Andrady AL. Microplastics in the marine environment. *Mar Pollut Bull* 2011;62:1596-605. DOI PubMed
14. Cole M, Lindeque P, Halsband C, Galloway TS. Microplastics as contaminants in the marine environment: a review. *Mar Pollut Bull* 2011;62:2588-97. DOI PubMed
15. Boucher J, Friot D. Primary microplastics in the oceans: a global evaluation of sources. IUCN International Union for Conservation of Nature. 2017. Available from: https://portals.iucn.org/library/sites/library/files/documents/2017-002-En.pdf. [Last accessed on 26 Feb 2024].
16. Emissions of primary particles and secondary particulate matter precursors. European Environment Agency. 2017. Available from: https://www.eea.europa.eu/data-and-maps/indicators/emissions-of-primary-particles-and-1. [Last accessed on 26 Feb 2024].
17. Walker TR, Fequet L. Current trends of unsustainable plastic production and micro(nano)plastic pollution. *TrAC Trends Anal Chem* 2023;160:116984. DOI
18. Andrady AL. The plastic in microplastics: a review. *Mar Pollut Bull* 2017;119:12-22. DOI PubMed
19. Rodrigues MO, Abrantes N, Gonçalves FJM, Nogueira H, Marques JC, Gonçalves AMM. Spatial and temporal distribution of microplastics in water and sediments of a freshwater system (Antuã River, Portugal). *Sci Total Environ* 2018;633:1549-59. DOI PubMed
20. Jahnke A. A discussion of single-use plastics in medical settings. *Reinf Plast* 2020;64:190-2. DOI
21. Man-made fibers continue to grow. Textile World. 2015. Available from: https://www.textileworld.com/textile-world/fiber-world/2015/02/man-made-fibers-continue-to-grow/. [Last accessed on 26 Feb 2024].
22. A new textiles economy: redesigning fashion's future. Ellen MacArthur Foundation. 2017. Available from: https://www.ellenmacarthurfoundation.org/a-new-textiles-economy. [Last accessed on 26 Feb 2024].
23. Cole M. A novel method for preparing microplastic fibers. *Sci Rep* 2016;6:34519. DOI PubMed PMC
24. Liu J, Yang Y, Ding J, Zhu B, Gao W. Microfibers: a preliminary discussion on their definition and sources. *Environ Sci Pollut Res Int* 2019;26:29497-501. DOI
25. Guidance on monitoring of marine litter in European seas. 2013. Available from: https://op.europa.eu/en/publication-detail/-/publication/76da424f-8144-45c6-9c5b-78c6a5f69c5d/language-en. [Last accessed on 26 Feb 2024].
26. Uddin S, Fowler SW, Habibi N, Behbehani M. Micro-nano plastic in the aquatic environment: methodological problems and challenges. *Animals* 2022;12:297. DOI PubMed PMC
27. EPA's microplastic beach protocol. United States Environmental Protection Agency. 2021. Available from: https://www.epa.gov/system/files/documents/2021-09/microplastic-beach-protocol_sept-2021.pdf. [Last accessed on 26 Feb 2024].

28. Prata JC, Manana MJ, da Costa JP, Duarte AC, Rocha-santos T. What is the minimum volume of sample to find small microplastics: laboratory experiments and sampling of Aveiro Lagoon and Vouga River, Portugal. *Water* 2020;12:1219. DOI
29. Eo S, Hong SH, Song YK, Han GM, Shim WJ. Spatiotemporal distribution and annual load of microplastics in the Nakdong River, South Korea. *Water Res* 2019;160:228-37. DOI PubMed
30. Lenaker PL, Baldwin AK, Corsi SR, Mason SA, Reneau PC, Scott JW. Vertical distribution of microplastics in the water column and surficial sediment from the Milwaukee River Basin to Lake Michigan. *Environ Sci Technol* 2019;53:12227-37. DOI PubMed
31. Zhang S, Wang J, Liu X, et al. Microplastics in the environment: a review of analytical methods, distribution, and biological effects. *TrAC Trends Anal Chem* 2019;111:62-72. DOI
32. Kaiser D, Kowalski N, Waniek JJ. Effects of biofouling on the sinking behavior of microplastics. *Environ Res Lett* 2017;12:124003. DOI
33. Cai M, He H, Liu M, et al. Lost but can't be neglected: Huge quantities of small microplastics hide in the South China Sea. *Sci Total Environ* 2018;633:1206-16. DOI
34. Panel on Contaminants in the Food Chain (CONTAM). Presence of microplastics and nanoplastics in food, with particular focus on seafood. *EFS2* 2016;14:e04501. DOI
35. Picó Y, Barceló D. Analysis of microplastics and nanoplastics: How green are the methodologies used? *Curr Opin Green Sustain Chem* 2021;31:100503. DOI
36. Di Mauro R, Kupchik MJ, Benfield MC. Abundant plankton-sized microplastic particles in shelf waters of the northern Gulf of Mexico. *Environ Pollut* 2017;230:798-809. DOI PubMed
37. Lenz R, Labrenz M. Small microplastic sampling in water: development of an encapsulated filtration device. *Water* 2018;10:1055. DOI
38. Koelmans AA, Redondo-Hasselerharm PE, Mohamed Nor NH, Kooi M. Solving the nonalignment of methods and approaches used in microplastic research to consistently characterize risk. *Environ Sci Technol* 2020;54:12307-15. DOI PubMed PMC
39. He D, Zhang X, Hu J. Methods for separating microplastics from complex solid matrices: comparative analysis. *J Hazard Mater* 2021;409:124640. DOI
40. Coppock RL, Cole M, Lindeque PK, Queirós AM, Galloway TS. A small-scale, portable method for extracting microplastics from marine sediments. *Environ Pollut* 2017;230:829-37. DOI PubMed
41. D'Hont A, Gittenberger A, Leuven RSEW, Hendriks AJ. Dropping the microbead: source and sink related microplastic distribution in the Black Sea and Caspian Sea basins. *Mar Pollut Bull* 2021;173:112982. DOI PubMed
42. Lechthaler S, Hildebrandt L, Stauch G, Schüttrumpf H. Canola oil extraction in conjunction with a plastic free separation unit optimises microplastics monitoring in water and sediment. *Anal Methods* 2020;12:5128-39. DOI PubMed
43. Xumiao L, Prata JC, Alves JR, Duarte AC, Rocha-santos T, Cerqueira M. Airborne microplastics and fibers in indoor residential environments in Aveiro, Portugal. *Environ Adv* 2021;6:100134. DOI
44. Hall JE, Guyton AC. Guyton and hall textbook of medical physiology. 2011. Available from: https://repository.poltekkes-kaltim.ac.id/1147/1/Guyton%20and%20Hall%20Textbook%20of%20Medical%20Physiology%20(%20PDFDrive%20).pdf. [Last accessed on 26 Feb 2024].
45. Silva DM, Almeida CMR, Guardiola F, Rodrigues SM, Ramos S. Optimization of an analytical protocol for the extraction of microplastics from seafood samples with different levels of fat. *Molecules* 2022;27:5172. DOI PubMed PMC
46. Khan MT, Cheng YL, Hafeez S, Tsang YF, Yang J, Nawab A. Microplastics in wastewater. In: Rocha-santos T, Costa M, Mouneyrac C, editors. Handbook of microplastics in the environment. Cham: Springer; 2020. pp. 1-33. DOI
47. Qiu Q, Tan Z, Wang J, Peng J, Li M, Zhan Z. Extraction, enumeration and identification methods for monitoring microplastics in the environment. *Estuar Coast Shelf Sci* 2016;176:102-9. DOI
48. Munno K, Helm PA, Jackson DA, Rochman C, Sims A. Impacts of temperature and selected chemical digestion methods on microplastic particles. *Environ Toxicol Chem* 2018;37:91-8. DOI PubMed
49. Bellon D, Zamudio WH, Tiria LC, Durán SM, Useche IE, Peña J. Effect of expanded polystyrene waste in the creation of waterproofing paint. *J Phys Conf Ser* 2019;1386:012075. DOI
50. Cai H, Chen M, Chen Q, Du F, Liu J, Shi H. Microplastic quantification affected by structure and pore size of filters. *Chemosphere* 2020;257:127198. DOI
51. Rai PK, Kumar V, Sonne C, Lee SS, Brown RJ, Kim K. Progress, prospects, and challenges in standardization of sampling and analysis of micro- and nano-plastics in the environment. *J Clean Prod* 2021;325:129321. DOI
52. Zhao K, Wei Y, Dong J, et al. Separation and characterization of microplastic and nanoplastic particles in marine environment. *Environ Pollut* 2022;297:118773. DOI
53. Tse Y, Lo H, Chan SM, Sze ET. Flow cytometry as a rapid alternative to quantify small microplastics in environmental water samples. *Water* 2022;14:1436. DOI
54. Monteiro SS, Rocha-Santos T, Prata JC, et al. A straightforward method for microplastic extraction from organic-rich freshwater samples. *Sci Total Environ* 2022;815:152941. DOI
55. Hidalgo-Ruz V, Gutow L, Thompson RC, Thiel M. Microplastics in the marine environment: a review of the methods used for identification and quantification. *Environ Sci Technol* 2012;46:3060-75. DOI PubMed
56. Zhang S, Yang X, Gertsen H, Peters P, Salánki T, Geissen V. A simple method for the extraction and identification of light density microplastics from soil. *Sci Total Environ* 2018;616-7:1056-65. DOI

57. Campbell SH, Williamson PR, Hall BD, Schindler D. Microplastics in the gastrointestinal tracts of fish and the water from an urban prairie creek. *FACETS* 2017;2:395-409. DOI
58. Beckingham B, Apintiloaiei A, Moore C, Brandes J. Hot or not: systematic review and laboratory evaluation of the hot needle test for microplastic identification. *Micropl Nanopl* 2023;3:8. DOI
59. Prata JC, Castro JL, da Costa JP, Duarte AC, Cerqueira M, Rocha-Santos T. An easy method for processing and identification of natural and synthetic microfibers and microplastics in indoor and outdoor air. *MethodsX* 2020;7:1-9. DOI PubMed PMC
60. Prata JC, Reis V, Matos JTV, da Costa JP, Duarte AC, Rocha-Santos T. A new approach for routine quantification of microplastics using Nile Red and automated software (MP-VAT). *Sci Total Environ* 2019;690:1277-83. DOI
61. Hengstmann E, Fischer EK. Nile red staining in microplastic analysis-proposal for a reliable and fast identification approach for large microplastics. *Environ Monit Assess* 2019;191:612. DOI PubMed
62. Mason SA, Welch VG, Neratko J. Synthetic polymer contamination in bottled water. *Front Chem* 2018;6:407. DOI PubMed PMC
63. Prata JC, da Costa JP, Fernandes AJS, da Costa FM, Duarte AC, Rocha-Santos T. Selection of microplastics by Nile Red staining increases environmental sample throughput by micro-Raman spectroscopy. *Sci Total Environ* 2021;783:146979. DOI PubMed
64. Araujo CF, Nolasco MM, Ribeiro AMP, Ribeiro-Claro PJA. Identification of microplastics using Raman spectroscopy: latest developments and future prospects. *Water Res* 2018;142:426-40. DOI PubMed
65. Brandt J, Fischer F, Kanaki E, Enders K, Labrenz M, Fischer D. Assessment of subsampling strategies in microspectroscopy of environmental microplastic samples. *Front Environ Sci* 2021;8:579676. DOI
66. Oßmann BE, Sarau G, Holtmannspötter H, Pischetsrieder M, Christiansen SH, Dicke W. Small-sized microplastics and pigmented particles in bottled mineral water. *Water Res* 2018;141:307-16. DOI PubMed
67. Huang Y, Xu EG. Black microplastic in plastic pollution: undetected and underestimated? *Water Emerg Contam Nanoplastics* 2022;1:14. DOI
68. Cowger W, Steinmetz Z, Gray A, et al. Microplastic spectral classification needs an open source community: open specy to the rescue! *Anal Chem* 2021;93:7543-8. DOI
69. Yang J, Monnot M, Sun Y, et al. Microplastics in different water samples (seawater, freshwater, and wastewater): methodology approach for characterization using micro-FTIR spectroscopy. *Water Res* 2023;232:119711. DOI
70. Brandon J, Goldstein M, Ohman MD. Long-term aging and degradation of microplastic particles: comparing in situ oceanic and experimental weathering patterns. *Mar Pollut Bull* 2016;110:299-308. DOI PubMed
71. Arkatkar A, Arutchelvi J, Bhaduri S, Uppara PV, Doble M. Degradation of unpretreated and thermally pretreated polypropylene by soil consortia. *Int Biodeterior Biodegrad* 2009;63:106-11. DOI
72. Knahr K, Pospischill M, Köttig P, Schneider W, Plenk H Jr. Retrieval analyses of highly cross-linked polyethylene acetabular liners four and five years after implantation. *J Bone Joint Surg Br* 2007;89:1036-41. DOI PubMed
73. Dümichen E, Eisentraut P, Bannick CG, Barthel AK, Senz R, Braun U. Fast identification of microplastics in complex environmental samples by a thermal degradation method. *Chemosphere* 2017;174:572-84. DOI PubMed
74. Picó Y, Barceló D. Pyrolysis gas chromatography-mass spectrometry in environmental analysis: Focus on organic matter and microplastics. *TrAC Trends Anal Chem* 2020;130:115964. DOI
75. Hermabessiere L, Himber C, Boricaud B, et al. Optimization, performance, and application of a pyrolysis-GC/MS method for the identification of microplastics. *Anal Bioanal Chem* 2018;410:6663-76. DOI
76. Hong Y, Oh J, Lee I, et al. Total-organic-carbon-based quantitative estimation of microplastics in sewage. *Chem Eng J* 2021;423:130182. DOI
77. Leusch FDL, Ziajahromi S. Converting mg/L to particles/L: reconciling the occurrence and toxicity literature on microplastics. *Environ Sci Technol* 2021;55:11470-2. DOI PubMed
78. Zhu C, Kanaya Y, Nakajima R, et al. Characterization of microplastics on filter substrates based on hyperspectral imaging: laboratory assessments. *Environ Pollut* 2020;263:114296. DOI
79. Wu P, Tang Y, Cao G, et al. Determination of environmental micro(nano)plastics by matrix-assisted laser desorption/ionization-time-of-flight mass spectrometry. *Anal Chem* 2020;92:14346-56. DOI
80. Estahbanati MRK, Rostami S, Ghasemian M, Kiendrebeogo M, Drogui P, Tyagi RD. Chapter 5 - quantitative and qualitative identification, characterization, and analysis of microplastics and nanoplastics in water. In: Current developments in biotechnology and bioengineering. Elsevier; 2023. pp. 99-123. DOI
81. Akhatova F, Ishmukhametov I, Fakhrullina G, Fakhrullin R. Nanomechanical atomic force microscopy to probe cellular microplastics uptake and distribution. *Int J Mol Sci* 2022;23:806. DOI PubMed PMC
82. Cai H, Xu EG, Du F, Li R, Liu J, Shi H. Analysis of environmental nanoplastics: progress and challenges. *Chem Eng J* 2021;410:128208. DOI
83. Zuccarello P, Ferrante M, Cristaldi A, et al. Reply for comment on "Exposure to microplastics (< 10 μm) associated to plastic bottles mineral water consumption: The first quantitative study by Zuccarello et al. [Water Research 157 (2019) 365–371]". *Water Res* 2019; 2019;157:115077. DOI PubMed
84. Oßmann B, Schymanski D, Ivleva NP, et al. Comment on "exposure to microplastics (< 10 μm) associated to plastic bottles mineral water consumption: the first quantitative study by Zuccarello et al. [Water Research 157 (2019) 365-371]". *Water Res* 2019;162:516-7. DOI PubMed
85. Cadiou JF, Gerigny O, Koren Š, et al. Lessons learned from an intercalibration exercise on the quantification and characterisation of microplastic particles in sediment and water samples. *Mar Pollut Bull* 2020;154:111097. DOI

86. Belz S, Bianchi I, Claudia C, et al. Current status of the quantification of microplastics in water - results of a JRC/BAM inter-laboratory comparison study on PET in water. EUR 30799 EN. Publications Office of the European Union. 2021. Available from: https://publications.jrc.ec.europa.eu/repository/handle/JRC125383. [Last accessed on 26 Feb 2024].
87. Isobe A, Buenaventura NT, Chastain S, et al. An interlaboratory comparison exercise for the determination of microplastics in standard sample bottles. *Mar Pollut Bull* 2019;146:831-7. DOI
88. Martínez-Francés E, van Bavel B, Hurley R, et al. Innovative reference materials for method validation in microplastic analysis including interlaboratory comparison exercises. *Anal Bioanal Chem* 2023;415:2907-19. DOI PubMed PMC
89. Tsangaris C, Panti C, Compa M, et al. Interlaboratory comparison of microplastic extraction methods from marine biota tissues: a harmonization exercise of the Plastic Busters MPAs project. *Mar Pollut Bull* 2021;164:111992. DOI
90. Müller YK, Wernicke T, Pittroff M, et al. Microplastic analysis-are we measuring the same? Results on the first global comparative study for microplastic analysis in a water sample*Anal Bioanal Chem* 2020;412:555-60. DOI PubMed
91. van Mourik LM, Crum S, Martinez-Frances E, et al. Results of WEPAL-QUASIMEME/NORMANs first global interlaboratory study on microplastics reveal urgent need for harmonization. *Sci Total Environ* 2021;772:145071. DOI PubMed
92. De Frond H, Thornton Hampton L, Kotar S, et al. Monitoring microplastics in drinking water: an interlaboratory study to inform effective methods for quantifying and characterizing microplastics. *Chemosphere* 2022;298:134282. DOI
93. Becker R, Altmann K, Sommerfeld T, Braun U. Quantification of microplastics in a freshwater suspended organic matter using different thermoanalytical methods - outcome of an interlaboratory comparison. *J Anal Appl Pyrolysis* 2020;148:104829. DOI
94. An L, Liu Q, Deng Y, Wu W, Gao Y, Ling W. Sources of microplastic in the environment. In: He D, Luo Y, editors. Microplastics in terrestrial environments. Cham: Springer; 2020. pp. 143-59. DOI
95. Patrício Silva AL, Prata JC, Walker TR, et al. Increased plastic pollution due to COVID-19 pandemic: challenges and recommendations. *Chem Eng J* 2021;405:126683. DOI PubMed PMC
96. Khan MT, Shah IA, Hossain MF, et al. Personal protective equipment (PPE) disposal during COVID-19: an emerging source of microplastic and microfiber pollution in the environment. *Sci Total Environ* 2023;860:160322. DOI PubMed PMC
97. Schmidt C, Krauth T, Wagner S. Export of plastic debris by rivers into the sea. *Environ Sci Technol* 2017;51:12246-53. DOI PubMed
98. Dong H, Wang L, Wang X, et al. Microplastics in a remote lake basin of the Tibetan Plateau: impacts of atmospheric transport and glacial melting. *Environ Sci Technol* 2021;55:12951-60. DOI
99. Kooi M, Nes EHV, Scheffer M, Koelmans AA. Ups and downs in the ocean: effects of biofouling on vertical transport of microplastics. *Environ Sci Technol* 2017;51:7963-71. DOI PubMed PMC
100. De-la-Torre GE, Dioses-Salinas DC, Pizarro-Ortega CI, Santillán L. New plastic formations in the Anthropocene. *Sci Total Environ* 2021;754:142216. DOI PubMed
101. Silva CJM, Silva ALP, Gravato C, Pestana JLT. Ingestion of small-sized and irregularly shaped polyethylene microplastics affect Chironomus riparius life-history traits. *Sci Total Environ* 2019;672:862-8. DOI PubMed
102. Ory NC, Gallardo C, Lenz M, Thiel M. Capture, swallowing, and egestion of microplastics by a planktivorous juvenile fish. *Environ Pollut* 2018;240:566-73. DOI PubMed
103. Browne MA, Dissanayake A, Galloway TS, Lowe DM, Thompson RC. Ingested microscopic plastic translocates to the circulatory system of the mussel, *Mytilus edulis* (L). *Environ Sci Technol* 2008;42:5026-31. DOI PubMed
104. Welden NA, Abylkhani B, Howarth LM. The effects of trophic transfer and environmental factors on microplastic uptake by plaice, Pleuronectes plastessa, and spider crab, Maja squinado. *Environ Pollut* 2018;239:351-8. DOI PubMed
105. Duis K, Coors A. Microplastics in the aquatic and terrestrial environment: sources (with a specific focus on personal care products), fate and effects. *Environ Sci Eur* 2016;28:2. DOI PubMed PMC
106. Miller ME, Hamann M, Kroon FJ. Bioaccumulation and biomagnification of microplastics in marine organisms: a review and meta-analysis of current data. *PLoS One* 2020;15:e0240792. DOI PubMed PMC
107. Ding J, Sun C, He C, Li J, Ju P, Li F. Microplastics in four bivalve species and basis for using bivalves as bioindicators of microplastic pollution. *Sci Total Environ* 2021;782:146830. DOI
108. Qu X, Su L, Li H, Liang M, Shi H. Assessing the relationship between the abundance and properties of microplastics in water and in mussels. *Sci Total Environ* 2018;621:679-86. DOI
109. Foley CJ, Feiner ZS, Malinich TD, Höök TO. A meta-analysis of the effects of exposure to microplastics on fish and aquatic invertebrates. *Sci Total Environ* 2018;631-2:550-9. DOI PubMed
110. Jeong J, Choi J. Adverse outcome pathways potentially related to hazard identification of microplastics based on toxicity mechanisms. *Chemosphere* 2019;231:249-55. DOI PubMed
111. Lenz R, Enders K, Nielsen TG. Microplastic exposure studies should be environmentally realistic. *Proc Natl Acad Sci U S A* 2016;113:E4121-2. DOI PubMed PMC
112. Prata JC, Venâncio C, da Costa JP, Lopes I, Duarte AC, Rocha-Santos T. Considerations when using microplates and Neubauer counting chamber in ecotoxicity tests on microplastics. *Mar Pollut Bull* 2021;170:112615. DOI PubMed
113. Jasinska EJ, Goss GG, Gillis PL, et al. Assessment of biomarkers for contaminants of emerging concern on aquatic organisms downstream of a municipal wastewater discharge. *Sci Total Environ* 2015;530-1:140-53. DOI
114. Arias-Andres M, Kettner MT, Miki T, Grossart HP. Microplastics: New substrates for heterotrophic activity contribute to altering organic matter cycles in aquatic ecosystems. *Sci Total Environ* 2018;635:1152-9. DOI PubMed

115. Cluzard M, Kazmiruk TN, Kazmiruk VD, Bendell LI. Intertidal concentrations of microplastics and their influence on ammonium cycling as related to the shellfish industry. *Arch Environ Contam Toxicol* 2015;69:310-9. DOI
116. Carson HS, Colbert SL, Kaylor MJ, McDermid KJ. Small plastic debris changes water movement and heat transfer through beach sediments. *Mar Pollut Bull* 2011;62:1708-13. DOI PubMed
117. Wan Y, Wu C, Xue Q, Hui X. Effects of plastic contamination on water evaporation and desiccation cracking in soil. *Sci Total Environ* 2019;654:576-82. DOI
118. Miranda MN, Silva AMT, Pereira MFR. Microplastics in the environment: a DPSIR analysis with focus on the responses. *Sci Total Environ* 2020;718:134968. DOI PubMed
119. Barros J, Seena S. Plastisphere in freshwaters: an emerging concern. *Environ Pollut* 2021;290:118123. DOI PubMed
120. Zettler ER, Mincer TJ, Amaral-Zettler LA. Life in the “plastisphere”: microbial communities on plastic marine debris. *Environ Sci Technol* 2013;47:7137-46. DOI PubMed
121. Yan Z, Liu Y, Zhang T, Zhang F, Ren H, Zhang Y. Analysis of microplastics in human feces reveals a correlation between fecal microplastics and inflammatory bowel disease status. *Environ Sci Technol* 2022;56:414-21. DOI
122. Walczak AP, Hendriksen PJ, Woutersen RA, et al. Bioavailability and biodistribution of differently charged polystyrene nanoparticles upon oral exposure in rats. *J Nanopart Res* 2015;17:231. DOI PubMed PMC
123. Domenech J, Marcos R. Pathways of human exposure to microplastics, and estimation of the total burden. *Curr Opin Food Sci* 2021;39:144-51. DOI
124. Snipes MB, Clem MF. Retention of microspheres in the rat lung after intratracheal instillation. *Environ Res* 1981;24:33-41. DOI PubMed
125. Slack JD, Kanke M, Simmons GH, DeLuca PP. Acute hemodynamic effects and blood pool kinetics of polystyrene microspheres following intravenous administration. *J Pharm Sci* 1981;70:660-4. DOI PubMed
126. Hartenstein V, Martinez P. Phagocytosis in cellular defense and nutrition: a food-centered approach to the evolution of macrophages. *Cell Tissue Res* 2019;377:527-47. DOI PubMed PMC
127. Prata JC. Microplastics and human health: Integrating pharmacokinetics. *Crit Rev Environ Sci Technol* 2023;53:1489-511. DOI
128. Ho YW, Lim JY, Yeoh YK, et al. Preliminary findings of the high quantity of microplastics in faeces of Hong Kong residents. *Toxics* 2022;10:414. DOI PubMed PMC
129. Barceló D, Picó Y, Alfarhan AH. Microplastics: detection in human samples, cell line studies, and health impacts. *Environ Toxicol Pharmacol* 2023;101:104204. DOI PubMed
130. A scientific perspective on microplastics in nature and society. Scientific Advice Mechanism. 2019. Available from: https://scientificadvice.eu/advice/a-scientific-perspective-on-microplastics-in-nature-and-society/. [Last accessed on 26 Feb 2024].
131. Kanke M, Simmons GH, Weiss DL, Bivins BA, DeLuca PP. Clearance of ^{141}C3-labeled microspheres from blood and distribution in specific organs following intravenous and intraarterial administration in beagle dogs. *J Pharm Sci* 1980;69:755-62. DOI PubMed
132. Turroni S, Wright S, Rampelli S, Brigidi P, Zinzani PL, Candela M. Microplastics shape the ecology of the human gastrointestinal intestinal tract. *Curr Opin Toxicol* 2021;28:32-7. DOI

Olivatto *et al. Water Emerg Contam Nanoplastics* 2024;3:9
DOI: 10.20517/wecn.2023.62

Water Emerging Contaminants & Nanoplastics

Research Article

Open Access

Oxy-biodegradable plastics in freshwater environments: degradation and biofouling

Glaucia Peregrina Olivatto[1], **Ana Laura Athayde Lourenço**[1], **Adijailton José de Souza**[2], **Valdemar Luiz Tornisielo**[1]

[1]Center of Nuclear Energy in Agriculture (CENA), University of São Paulo (USP), Piracicaba 13400-970, Brazil.
[2]Luiz de Queiroz College of Agriculture (ESALQ), University of São Paulo (USP), Piracicaba 13418-900, Brazil.

Correspondence to: Dr. Glaucia Peregrina Olivatto, Center of Nuclear Energy in Agriculture (CENA), University of São Paulo (USP), Av. Centenário, 303, Piracicaba 13400-970, Brazil. E-mail: glauciapolivatto@gmail.com

How to cite this article: Olivatto GP, Lourenço ALA, de Souza AJ, Tornisielo VL. Oxy-biodegradable plastics in freshwater environments: degradation and biofouling. *Water Emerg Contam Nanoplastics* 2024;3:9. https://dx.doi.org/10.20517/wecn.2023.62

Received: 17 Oct 2023 **First Decision:** 6 Feb 2024 **Revised:** 22 Feb 2024 **Accepted:** 27 Feb 2024 **Published:** 5 Mar 2024

Academic Editor: Antoni Ginebreda **Copy Editor:** Pei-Yun Wang **Production Editor:** Pei-Yun Wang

Abstract

Growing concern about the impact of plastic pollution on the environment has led to the creation of global public policies and the consumption of "environmentally friendly" products, such as oxy-biodegradable plastics. In this context, "greenwashing" practices can arise, i.e., the product promises more environmental benefits than it actually offers, which can lead to superfluous use, inappropriate disposal, and the generation of microplastics (MPs). However, the scientific literature lacks studies that evaluate the behavior of oxy-biodegradable plastic when exposed to the freshwater environment. In this respect, the aim of the current study was to evaluate the degradation process of oxy-biodegradable plastic bags made from high-density polyethylene (HDPE) in river water. To this end, the current study aimed to assess whether these bags actually meet the label information (which corresponds to the complete degradation of material) or whether they correspond to greenwashing practices. The physical and chemical alterations, and the formation of biological communities that occurred on the surface of the plastic material when exposed to natural aging and submerged in freshwater were monitored using mid-infrared absorption spectroscopy with attenuated total reflectance (FTIR-ATR) and scanning electron microscopy (SEM). The characterization of the samples after 180 days of exposure showed that the oxy-biodegradable bags were not completely degraded, with only fragmentation of the material and generation of MPs. In addition, it was also observed that microorganisms present in the water easily colonized the plastic surface from the start of the experiment. In this way, the oxy-biodegradable bags analyzed correspond to a greenwashing practice, which is extremely harmful, since it can influence the increase in consumption of these products, generating greater improper disposal of these materials, and consequently the generation of MPs and the formation of biofilms, which can carry pathogenic microorganisms to the aquatic biota and to humans.

Keywords: Microplastics, greenwashing, biofilm, polyethylene, plastic pollution, oxy-biodegradable plastics

INTRODUCTION

The unique properties of plastic materials, such as their high durability, malleability, lightness, and low cost, justify their high consumption in various sectors of society; they are considered one of the most widely produced materials today, with recent estimates of global production of 400 million tons[1]. The high consumption of plastic materials combined with inadequate management and disposal has been a cause for great concern among the scientific community and society in general, due to their high persistence in the environment and potential ecological, economic, aesthetic, and public health impacts[2,3].

Plastic bags and disposable packaging made from polypropylene (PP) and polyethylene (PE) polymers are considered to be the most harmful in terms of the quantity of plastic waste in the environment[4], since between 500 billion and 1 trillion of these packages are produced every year[5]. It is estimated that after only 12 min of use, these products are already destined for the natural environment, where they accumulate for many years due to their resistance to degradation[6].

Faced with this problem, as a strategy for mitigating environmental liabilities, various public policies have been introduced, mainly in developed countries[7]. These policies encourage recycling, restrictive use, charging for the use of plastic bags by commercial establishments, and even their prohibition. Examples include California (USA), where the distribution of plastic bags was banned in 2016, and Ireland, where a tax on the use of plastic bags was introduced in 2002[8].

The plastics industry has also proposed alternatives aimed at “low environmental impact”, such as the production of oxy-biodegradable plastic. This type of plastic is made up of conventional polyolefin polymers, such as PE or PP, and also contains additives that accelerate the degradation of the material under certain conditions of temperature, light, and the presence of oxygen, thus causing the chemical bonds in the polymer chain to break, followed by the generation of smaller molecular fragments, until the material is completely degraded.

However, although the degradation of oxy-biodegradable plastic is faster than that of conventional plastic, previous studies have shown that in the marine environment, for example, only the fragmentation and generation of microplastics (MPs), which are pieces of plastic debris less than 5 mm in size, occur more quickly[2]. Despite this, there is still not enough of a reduction in molar mass for these fragments to be biodegraded and bioassimilated by microorganisms[9]. In addition, oxy-biodegradable plastic is a type of waste that makes recycling difficult due to the presence of the degrading additive in its composition. As a result, greenwashing practices emerge, i.e., advertising more ecological and environmental benefits than the product actually has, which influences consumers to buy these products. In addition, this information can encourage the consumption and improper disposal of oxy-biodegradable plastic.

In the aquatic environment, due to their small size, MP particles are easily ingested by biota, from lower trophic levels to higher tropic levels[10]. Depending on the aquatic organism and particle size, this ingestion can have lethal and sublethal consequences, such as obstruction of the digestive tract, malnutrition, suffocation, death, and even possible bioaccumulation and biomagnification processes[11]. MPs are also characterized by having a higher specific surface area - SSA, high porosity, and a hydrophobic character, which translates into greater potential for MPs to retain and transport organic and inorganic contaminants, as well as for the formation of microbial biofilms - which can be formed by both beneficial and harmful microorganisms. In addition, the presence of MPs can potentiate the emergence of antibiotic-resistant microorganisms (ARMs) and the spread of antibiotic resistance genes (ARGs)[12-14].

Knowing that freshwater ecosystems contribute around 80% of the plastic waste that reaches the marine environment and that most of the current research into the dynamics of plastic exposure is concentrated in the marine environment[9,13,15], the need to understand this phenomenon in the freshwater environment is clear. To date, studies that have more specifically evaluated the degradation and microbial formation in polyolefin plastics containing a degrading additive, i.e., oxy-biodegradable plastics, have focused only on the marine environment[9,16-21], with studies carried out in freshwater environments being extremely scarce[22,23].

Therefore, the aim of the current study was to evaluate the degradation process of commercial oxy-biodegradable plastic when exposed to a simulated freshwater environment. To this end, a parallel was drawn between the plastic materials evaluated and their compliance with the information on the product label, which classifies an oxy-biodegradable plastic as any plastic material that degrades completely within various environments and under different conditions[24]. The study also investigated the formation of microbial biofilms on the plastic surface when exposed to this aquatic matrix and whether materials marketed as oxy-biodegradable can be considered greenwashing.

METHODS

Obtaining plastic samples and experimental design

Conventional plastic bags of petrochemical origin, made from high-density polyethylene (HDPE), without a degrading additive (control), and oxy-biodegradable plastic bags made from the same polymer, with a degrading additive (d2w®), were purchased in the city of Piracicaba, São Paulo, Brazil. In the laboratory, experimental samples (n = 90) of each type of plastic bag were prepared by cutting them into strips of similar dimensions (3 cm × 20 cm). Thirty strip samples were added to each stainless steel aquarium filled with freshwater. The experiments were carried out in triplicate for each type of plastic material, totaling 6 different aquariums. Samples were then taken at random from each aquarium, in triplicate for each type of plastic, for chemical characterization at the start of the experiment (T0 = 0 days), after two months of exposure (T1 = 60 days), after four months of exposure (T2 = 120 days), and at the end of the experiment (T3 = 180 days), as well as for morphological characterization after 2 months of the experiment (T1 = 60 days).

Natural freshwater experiment

The simulated freshwater environment was prepared using 20 L of natural freshwater in each stainless steel aquarium. The natural freshwater used was collected from the Piracicaba River Reservoir, Barra Bonita Dam, Anhembi - SP, Brazil (S 22° 37.666’ WO 48° 10.430’). All the aquariums were kept outdoors from June to December 2019, in order to observe the kinetics of degradation and biofilm formation on the plastic surfaces, according to the different weather conditions, considering the light and dark cycles in the natural condition, and thus providing greater environmental relevance. The aquariums were equipped with circulation pumps to keep the water moving. The volume of water in each aquarium was also monitored throughout the experiment, and when necessary, ultrapure water was added. These interventions were necessary to avoid an abrupt increase in salinity in the aquariums[25].

Biological characterization of the river water

In the laboratory, the freshwater samples were diluted using the serial dilution technique and 100 μL were inoculated into petri dishes poured with rich culture medium for bacteria - Plate Count Agar - PCA, and for fungi - Potato Dextrose Agar (PDA). For this, aliquots of 1 mL of the river water sample were transferred to a series of test tubes containing 9 mL of sterile buffer solution - composed of phosphate buffer and magnesium chloride, in order to obtain serial dilutions of up to 10^{-4}. The culture medium used was PCA, for plating and counting bacteria, with the following composition (m/v): 0.5% peptone; 0.25% yeast extract; 0.1% glucose; 1.4% agar; distilled water; pH 7.0 (± 0.2) at 35 °C, and PDA, for plating and counting fungi, with the composition (m/v): 3.9% PDA (potato dextrose agar); distilled water; pH 7.0 (± 0.2) at 28 °C. Plating was carried out on the day the river water sample was collected (T0 = 0 days), in triplicate, using the pour plate technique[26]. Microbial growth counts were expressed in colony forming units (CFU).

Sample characterization

FTIR-ATR

Confirmation of the chemical identity of the polymer and the chemical modifications undergone by the samples during natural aging were assessed using mid-infrared absorption spectroscopy with attenuated total reflectance (FTIR-ATR) (spectrophotometer Cary660, Agilent Technologies). The spectra were collected in absorbance mode and with a resolution of 4,000-400 cm^{-1} at 4 cm^{-1} using Agilent Resolution Pro software in 160 scans. This analysis was also used to identify the increased intensity of carbonyl groups, indicative of photo-oxidative degradation of the HDPE polymer, with a characteristic band around 1,700 cm^{-1}. The carbonyl index (CI) values were calculated in triplicate at the different time intervals to quantify the chemical degradation of the plastic surface, using the absorbance values of the carbonyl band and the reference band, as shown in Equation (1):

$$CI = \frac{a}{b} \tag{1}$$

Where a corresponds to the carbonyl band between 1,735 and 1,715 cm^{-1} and b corresponds to the reference band at 1,471 cm^{-1}[27]. The carbonyl index values were compared using the Student's *t*-test at a 5% significance level.

Scanning electron microscope

For morphological characterization of the plastic surfaces and qualitative analysis of biofilm formation, the samples were prepared on carbon strips, and metalized with gold for 180 s (LEICA ACE 600, Vienna). Scanned micrographs were obtained using a scanning electron microscope (SEM) (Jeol JSM - IT300 LV, Tokyo) operating at 15 kV.

Level of "greenwashing"

The evaluation and identification of greenwashing practices was based on the protocol described by the TerraChoice Environmental Marketing Agency, which points out the seven most common patterns or "sins" of greenwashing [Table 1]. The results obtained from the samples analyzed before and after natural aging were used to evaluate and classify the level of greenwashing in the oxy-biodegradable plastic investigated, according to the claims made on the product label.

RESULTS AND DISCUSSION

Colony counts of bacteria and fungi revealed a high abundance of the culturable microbial community in the freshwater of the Barra Bonita Dam [Table 2]. The CFU·mL^{-1} ranged from 4.5×10^8 to 6.6×10^8 (mean = 5.4×10^8) and 1.0×10^7 to 9.6×10^8 (mean = 3.2×10^8), respectively, for the culturable bacterial and fungal

Table 1. The seven sins of greenwashing according to TerraChoice Environmental Marketing Agency[28]

The seven "sins" of greenwashing	Characteristics
Camouflaging environmental costs	Suggesting that the product is sustainable based on a restricted set of attributes, without attention to other important environmental issues
Lack of proof	An environmental claim that cannot be substantiated by easily accessible supporting information or reliable third-party certification
Uncertainty	A claim so ill-defined or broad that its real meaning is likely to be misunderstood by the consumer
Worship of false labels	A product that, through words or images, gives the impression of third-party endorsement where no such endorsement exists; false labels, in other words
Irrelevance	An environmental claim that may be true, but is not important or does not help consumers looking for environmentally preferable products
"Less worse"	A claim that may be true within the product category, but risks distracting the consumer from the larger environmental impacts of the category as a whole
Lying	Environmental claims that are simply false

Table 2. Quantitative analysis of microorganisms present in river water samples collected from the Piracicaba River Reservoir, Barra Bonita Dam, Anhembi-SP, Brazil

Samples	Bacteria (CFU·mL^{-1})	Fungi (CFU·mL^{-1})
Sample 1	5.1×10^8	9.6×10^8
Sample 2	6.6×10^8	1.0×10^7
Sample 3	4.5×10^8	1.0×10^7
Average	$\mathbf{5.4 \times 10^8}$	$\mathbf{3.2 \times 10^8}$

Values expressed in CFU per milliliter (CFU·mL^{-1}). CFU: Colony forming units.

communities. The sampling site is located in an area that is a long way from polluting sources, because, according to SHELL and colleagues, environmental parameters, such as seasonal characteristics, physical-chemical properties of the water, properties of the biological communities, and, above all, proximity to anthropogenic inputs contribute directly to the behavior of plastic debris dispersed in the environment and the formation of biofilms. However, despite the absence of these inputs at the water sampling site, the presence of these microorganisms was expected, given that aquatic ecosystems host a vast diversity of microorganisms, associated with the quality and maintenance of ecosystem services in this environment[29]. Microbial populations play a crucial role in nutrient cycling, degradation of organic matter, and biodegradation of organic and inorganic pollutants - such as pesticides, antibiotics, oil and petroleum derivatives, and MPs - which are the contaminants frequently reported in bodies of water[30,31].

In addition, microorganisms in aquatic environments are the main precursors of the biodegradation of xenobiotic substances that reach water bodies, such as pesticides, drug residues, easily degraded organic loads, and more recalcitrant materials (e.g., MPs)[32]. Therefore, the microbial community with the highest species richness (cultivable microorganisms > 10^8-10^{10} CFU·mL^{-1}), such as the results reported in this study [Table 2], can promote the rapid colonization of the plastic surface - biofilm formation - which extends both as a microbial mechanism of protection of microbiological life and as a strategy to promote the degradation of complex and recalcitrant substances via extracellular enzymatic activity[33].

The visual inspection of the surface of the oxy-biodegradable plastic by SEM, carried out 2 months after exposure to river water, indicated that, in agreement with the characterization of the water collected, microbial colonization occurred promptly, and it was possible to identify the presence of diatoms, fungi, and possible planktonic bacteria on the surface of the substrate [Figure 1].

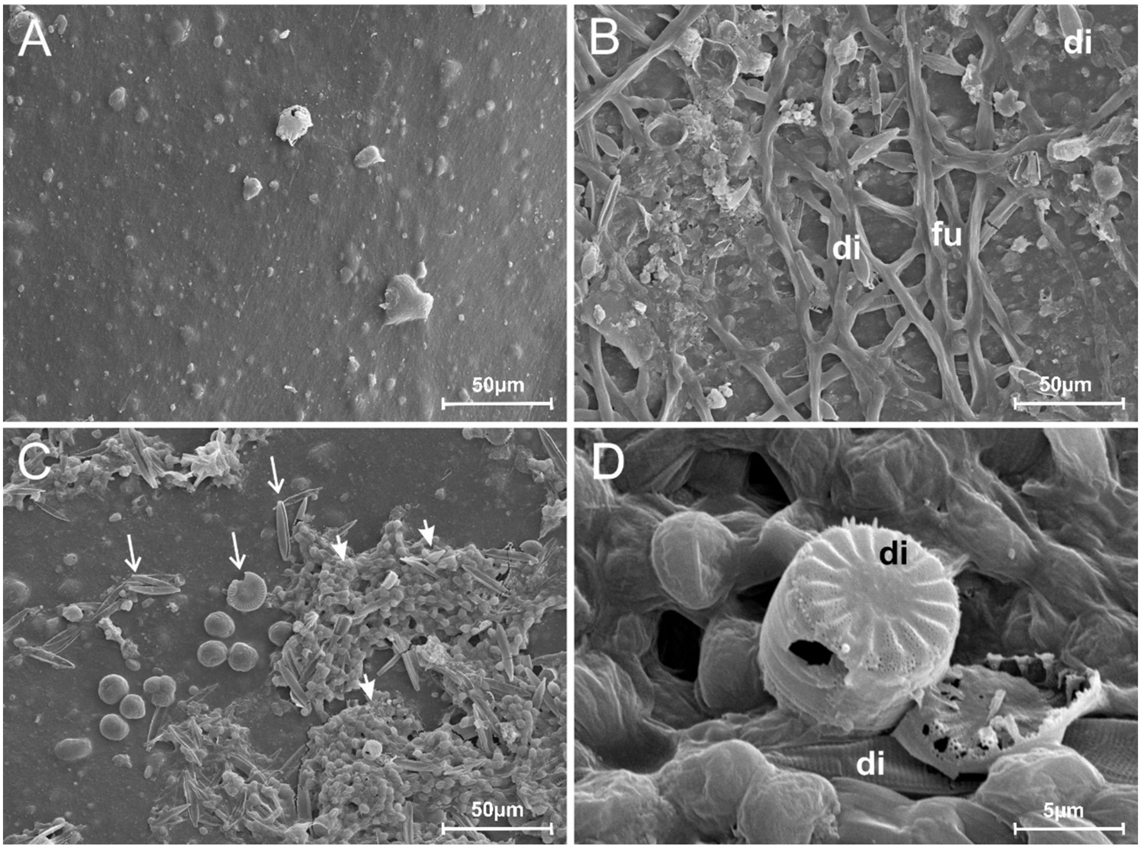

Figure 1. SEM image showing the morphological characterization of the oxy-biodegradable plastic surface. (A) General view at the start of the experiment (T = 0); (B-D) Microbial colonization on the oxy-biodegradable bag substrate after 2 months of exposure (T = 1), where it is possible to see in detail the presence of diatom algae in different shapes (di), intense colonization by fungi (fu), and possible colonization by planktonic bacteria (arrow heads). (A-C) = 50 μm and (D) = 5 μm. SEM: Scanning electron microscopy.

In line with previous findings, where images obtained by SEM showed microbial colonization after a minimum incubation time of 1 month, and indicated through DNA sequencing results the presence of more than 52 bacterial phyla[13], this study also showed rapid microbial colonization on the plastic surface. The major problem with this phenomenon is associated with the possibility of trophic transfer of pathogenic species of bacteria and fungi to the biota, due to the possibility of ingestion of plastic debris in the aquatic environment, which occurs frequently. Therefore, this debris is identified as a potential vector of harmful microorganisms in these environments[10,12,31].

As a specific and complex microbial habitat, plastic debris can also support the selection of unique microorganisms and diverse communities. This fact is associated with the wide distribution and ease of vertical and horizontal transportation of this waste in the aquatic environment, which can lead to the migration of exotic species to other habitats, with profound impacts on the ecological effects of biological communities[12,31]. Furthermore, it is recognized by the scientific community that in addition to microbial attachment to the plastic surface, there is also sorption of contaminants present in the surrounding environment, such as antibiotics, which, in direct contact with certain bacteria, will inevitably lead to the continued increase in ARGs[34]. The production of these resistance genes in the freshwater environment increases the risk of exposure to plastic debris in this environmental matrix, since, in addition to the environmental and ecological importance, this is also a water source for human and animal consumption.

Coincidentally, during the same time period in which microorganisms settled on the plastic surface, changes in the material's physical and chemical properties were observed, such as an increase in the density and sedimentation of the plastic strips at the bottom of the aquariums. The loss of buoyancy of the plastics made up of HDPE polymers, a polymer with a lower density than river water, represents a significant change in the fate of this debris in the water column. By losing buoyancy, this waste can move further from the photic zone in the aquatic environment and suffer less exposure to ultraviolet (UV) radiation, an essential factor in the degradation process of plastic made up of this polymer, which can have an impact on the abiotic degradation kinetics of this plastic waste[12,34].

The study by Lobelle and Cunliffe in 2011 also indicated that the formation of biofilms on the plastic surface led to a loss of buoyancy within 3 weeks. From a hydrodynamic point of view, this may have an impact on the fate of plastics in the aquatic environment, by changing the dynamics of the vertical transport of this low-density waste from the photic zone to the aphotic zone, and also on the bioavailability to benthic organisms.

Figure 2 presents the FTIR-ATR spectra obtained from the surface of the conventional plastic [Figure 2A] and oxy-biodegradable plastic [Figure 2B] samples at the start of the experiment, at increasing exposure intervals, and at the end of the experiment. As expected for the HDPE polymer, the following characteristic bands can be observed: 2,915 cm^{-1} (υC-H), 2,845 cm^{-1} (υC-H), 1,472 cm^{-1} (δCH2), 1,462 cm^{-1} (δCH2), 730 cm^{-1} (δCH2), and 720 cm^{-1} (δCH2), where υ corresponds to stretching modes and δ corresponds to angular deformation[35].

Plastics classified as polyolefins, i.e., made up of the PE polymer, among others, have only carbon and hydrogen in their structure, and their main abiotic degradation mechanism is photo-oxidative degradation, which is induced by the absorption of ultraviolet radiation in the presence of oxygen, allowing oxygen to be introduced into the polymer chain[36]. Thus, the presence of carbonyl groups in the polymer structure after environmental exposure indicates that the surface of the exposed material has undergone photo-oxidative degradation[37], which can be identified and monitored by analyzing the spectrum obtained by FTIR-ATR, or by quantifying the absorbance measurements of the typical carbonyl band, a characteristic band in infrared spectra in the region of 1,700 cm^{-1}[27].

In the conventional plastic, it was possible to observe a slight carbonyl band directly proportional to the exposure time [Figure 2]. When calculating the carbonyl index values for both types of plastic [Figure 3], there was an increase in the carbonyl index during the experiment, indicating that both materials underwent the degradation process over the incubation period (180 days). The carbonyl index values were significantly higher in the 180 d period, where they practically tripled compared to the initial time (T = 0).

As a consequence of photo-oxidative degradation, the plastic surface of both materials showed increased porosity and discoloration after 2 months of exposure to freshwater conditions. In the third month of the experiment, the oxy-biodegradable plastic samples began the fragmentation process, which became more pronounced over the course of the exposure time; the same did not occur with the conventional plastic, which remained intact until the end of the experiment, without suffering fragmentation.

However, despite the more pronounced physical changes in oxy-biodegradable plastic compared to conventional plastic, there was no complete degradation of the material, which corresponds to obtaining degradation products - H_2O, CH_4, or CO_2, according to ASTM D6954 - 18[37], and only the generation of MPs, particles less than 5 mm in size, was observed. These particles had a breakable appearance, most of

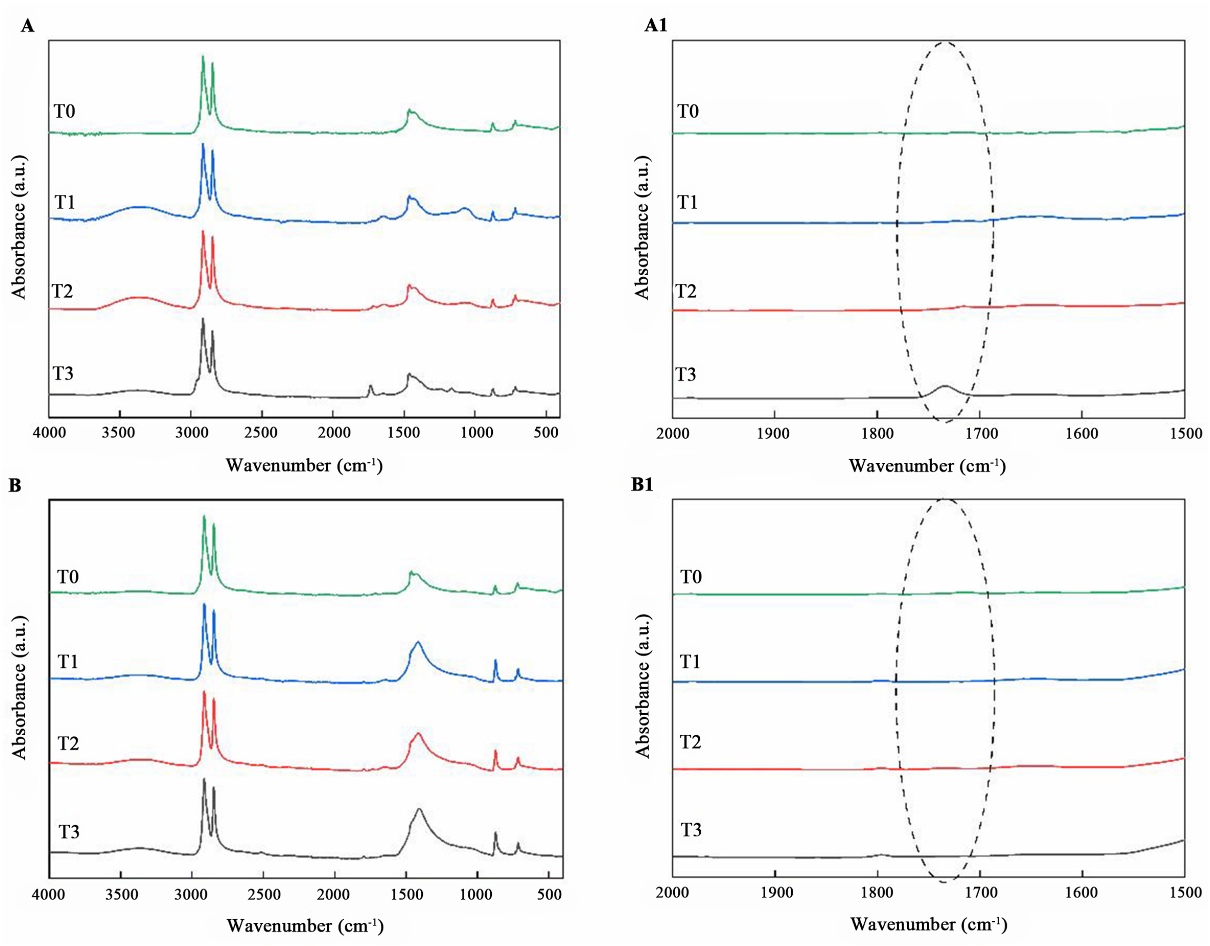

Figure 2. Comparative FTIR-ATR spectra of conventional plastic (A) and oxy-biodegradable plastic (B), at different stages of environmental exposure. Where T0 = initial time, T1 = 60 days of exposure, T2 = 120 days of exposure, and T3 = 180 days of exposure. FTIR: Fourier-transform infrared spectroscopy; ATR: attenuated total reflectance.

which were sedimented at the bottom of the aquarium along with the organic matter, while some were still floating, which made it difficult to carry out a quantitative analysis of the generation of MPs. However, with the absence of plastic strips in their initial dimensions and with just the presence of MP particles, it was only possible to see the fragmentation of the material and not its complete degradation in the aquatic environment.

The presence of MPs in the freshwater environment implies severe consequences for maintaining the quality of this ecosystem, as the removal of these particles is even more challenging than the removal of larger plastics. The ingestion of MPs by freshwater biota is also easier, as well as by organisms from the lower trophic levels, and this fact has already been reported for a wide range of species and, regardless of the type of plastic it comes from, which can cause severe effects depending on the properties and size of the particles and the species involved such as obstruction of the digestive tract, malnutrition, suffocation, death, and even possible bioaccumulation and biomagnification processes[10,11]. In addition, as observed in the current study, plastic waste is considered to be an ideal substrate for the attachment of microbial communities, with MPs being even more favorable due to their specific properties, such as a larger surface area and increased porosity resulting from their longer residence time in the environment, which implies greater potential for biological imbalance through the transfer of microorganisms by these particles and the

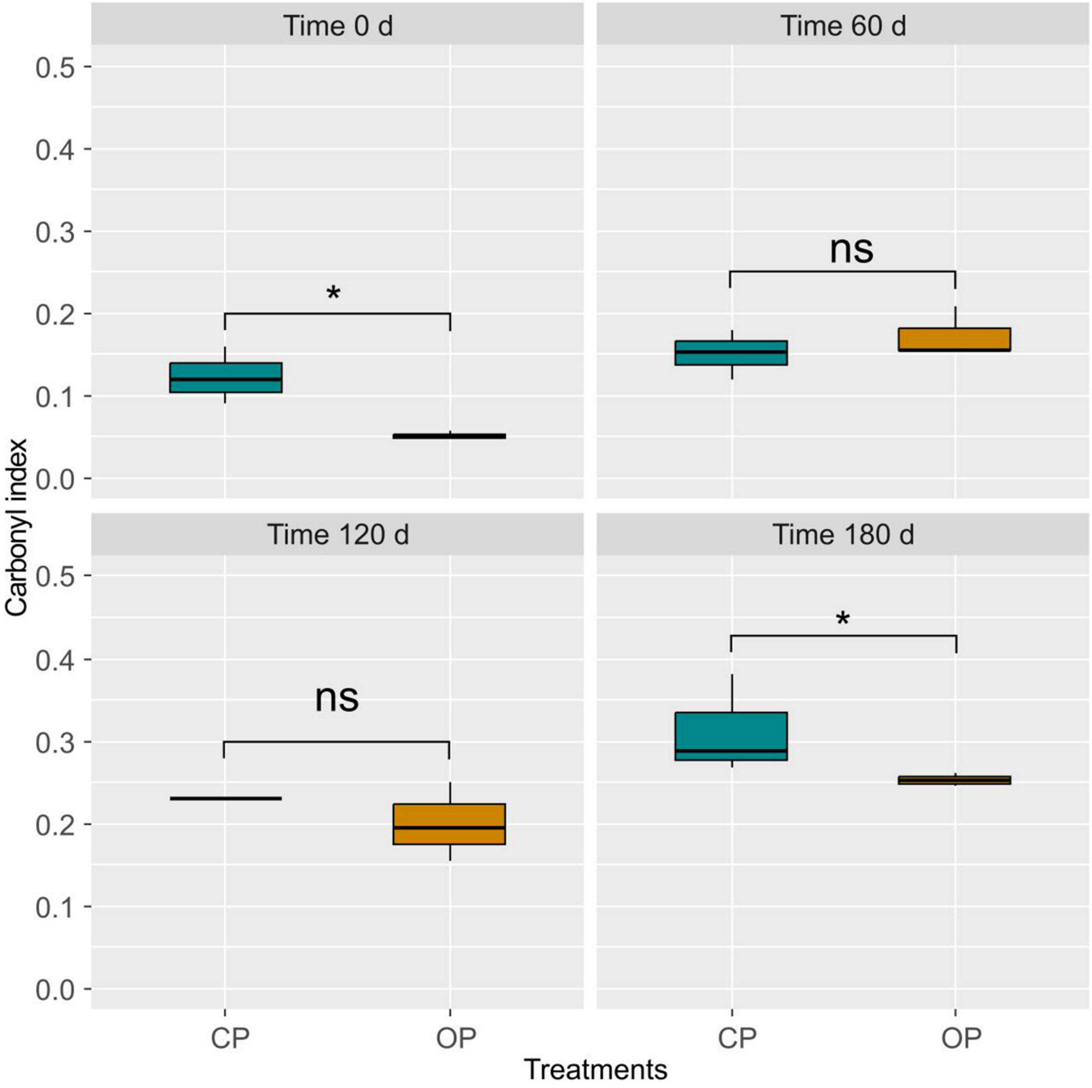

Figure 3. Boxplot of the carbonyl index of CP and OP after 180 days of exposure in the freshwater environment. *There was a difference between the treatments by the Student's *t*-test at a 5% significance level. ns: not significant. CP: Conventional plastic bags; OP: oxy-biodegradable plastic bags.

formation of antibiotic resistance genes[13,34].

Thus, comparing the degradation of conventional plastic with oxy-biodegradable plastic in simulated freshwater environment conditions, we can point out that from an ecological and environmental point of view, oxy-biodegradable plastic did not behave in an advantageous way compared to conventional plastic, i.e., just like conventional plastic there was no complete degradation of the material, only fragmentation over the 180-day period investigated here. In addition, according to the results obtained in this study, we can indicate that oxy-biodegradable plastic is a greenwashing practice, since, according to the parameters listed by the TerraChoice Environmental Marketing Agency, the product has a cult of false labeling and camouflaged environmental costs. Other studies similar to this one, but carried out in simulated conditions of a marine environment and composting, also reached the same conclusion, which indicates the need for the scientific community to act in the assertive investigation of such practices and provide clarification to society, with the aim of raising public awareness[9,24,37]. Therefore, as our study is a pioneer in this field in Brazil, more research is needed to deepen our understanding of the degradation of oxy-biodegradable plastics and the generation of MPs in a freshwater environment, and over a longer period of exposure than that investigated here, considering the importance of this environmental compartment, given that the country holds around 13 percent of all freshwater in the world.

CONCLUSIONS

Oxy-biodegradable plastic bags are composed of the same non-biodegradable polymer of petrochemical origin as conventional plastic bags, with only the addition of a degrading additive. The general results of this study showed that despite indications of degradation, such as an increase in the carbonyl index on the surface of the material, oxy-biodegradable plastic only fragments into MP particles and does not present significantly reduced molecular mass to the point of being bioassimilated by microorganisms, i.e., it does not undergo complete degradation when exposed to fresh water in the presence of microorganisms over a 180-day period. Therefore, the bags analyzed, considering this period of exposure, correspond to a type of greenwashing practice, which is extremely harmful, since it can lead to increased consumption of these products, generating greater improper disposal of these materials and, consequently, the generation of MPs. In addition, microbial colonization on the plastic surface was also identified, which increases the risk of exposure of this waste in the freshwater environment. However, we recommend for future investigations that these same studies be carried out over a longer period of exposure in order to evaluate whether the product may present advantages over conventional plastic in the long term.

DECLARATIONS

Acknowledgments

The authors would like to thank the University of São Paulo (USP) for their infrastructure. This research was carried out with the support of the National Council for Scientific and Technological Development (CNPq) (process number 141021/2019-5 and process number 117292/2019-2) and Coordination for the Improvement of Higher Education Personnel (CAPES, Brazil, Finance Code 001) for granting a scholarship to AJS.

Authors' contributions

Conceptualization, data curation, figures, table, writing - original draft preparation: Olivatto GP
Conceptualization, methodology, figures, writing - reviewing and editing: Lourenço ALA, de Souza AJ
Supervision: Tornisielo VL

Availability of data and materials

Not applicable.

Financial support and sponsorship

Conselho Nacional de Desenvolvimento Científico e Tecnológico (CNPq) process number 141021/2019-5 and Coordination for the Improvement of Higher Education Personnel (CAPES, Brazil, Finance Code 001) for granting a scholarship to de Souza AJ.

Conflicts of interest

All authors declared that there are no conflicts of interest.

Ethical approval and consent to participate

Not applicable.

Consent for publication

Not applicable.

Copyright

REFERENCES

1. Commission delegated regulation (EU) 2020/217 of 4 October 2019 amending, for the purposes of its adaptation to technical and scientific progress, Regulation (EC) No 1272/2008 of the European Parliament and of the Council on classification, labelling and packaging of substances and mixtures and correcting that Regulation. Available from: https://eur-lex.europa.eu/eli/reg_del/2020/217/oj. [Last accessed on 4 Mar 2024]
2. Andrady AL. The plastic in microplastics: a review. *Mar Pollut Bull* 2017;119:12-22. DOI
3. Nielsen TD, Hasselbalch J, Holmberg K, Stripple J. Politics and the plastic crisis: a review throughout the plastic life cycle. *Wiley Interdiscip Rev Energy Environ* 2020;9:e360. DOI
4. Laskar N, Kumar U. Plastics and microplastics: a threat to environment. *Environ Technol Innov* 2019;14:100352. DOI
5. Xanthos D, Walker TR. International policies to reduce plastic marine pollution from single-use plastics (plastic bags and microbeads): a review. *Mar Pollut Bull* 2017;118:17-26. DOI
6. Geyer R, Jambeck JR, Law KL. Production, use, and fate of all plastics ever made. *Sci Adv* 2017;3:e1700782. DOI PubMed PMC
7. Van L, Hamid NA, Ahmad F, Ahmad ANA, Ruslan R, Tamyez PFM. Factors of single use plastic reduction behavioral intention. *Emerg Sci J* 2021;5:269-78. DOI
8. Spranz R, Schlüter A, Vollan B. Morals, money or the master: the adoption of eco-friendly reusable bags. *Mar Policy* 2018;96:270-7. DOI
9. Nazareth M, Marques MRC, Leite MCA, Castro ÍB. Commercial plastics claiming biodegradable status: is this also accurate for marine environments? *J Hazard Mater* 2019;366:714-22. DOI
10. Azevedo-Santos VM, Brito MFG, Manoel PS, et al. Plastic pollution: a focus on freshwater biodiversity. *Ambio* 2021;50:1313-24. DOI
11. Huang W, Song B, Liang J, et al. Microplastics and associated contaminants in the aquatic environment: a review on their ecotoxicological effects, trophic transfer, and potential impacts to human health. *J Hazard Mater* 2021;405:124187. DOI
12. He S, Jia M, Xiang Y, et al. Biofilm on microplastics in aqueous environment: physicochemical properties and environmental implications. *J Hazard Mater* 2022;424:127286. DOI
13. Martínez-Campos S, González-Pleiter M, Rico A, et al. Time-course biofilm formation and presence of antibiotic resistance genes on everyday plastic items deployed in river waters. *J Hazard Mater* 2023;443:130271. DOI
14. Rummel CD, Jahnke A, Gorokhova E, Kühnel D, Schmitt-Jansen M. Impacts of biofilm formation on the fate and potential effects of microplastic in the aquatic environment. *Environ Sci Technol Lett* 2017;4:258-67. DOI
15. Lobelle D, Cunliffe M. Early microbial biofilm formation on marine plastic debris. *Mar Pollut Bull* 2011;62:197-200. DOI
16. Balestri E, Menicagli V, Vallerini F, Lardicci C. Biodegradable plastic bags on the seafloor: a future threat for seagrass meadows? *Sci Total Environ* 2017;605-6:755-63. DOI
17. Emadian SM, Onay TT, Demirel B. Biodegradation of bioplastics in natural environments. *Waste Manage* 2017;59:526-36. DOI
18. O'Brine T, Thompson RC. Degradation of plastic carrier bags in the marine environment. *Mar Pollut Bull* 2010;60:2279-83. DOI
19. Brandon J, Goldstein M, Ohman MD. Long-term aging and degradation of microplastic particles: comparing in situ oceanic and experimental weathering patterns. *Mar Pollut Bull* 2016;110:299-308. DOI
20. Nauendorf A, Krause S, Bigalke NK, et al. Microbial colonization and degradation of polyethylene and biodegradable plastic bags in temperate fine-grained organic-rich marine sediments. *Mar Pollut Bull* 2016;103:168-78. DOI
21. Kedzierski M, D'Almeida M, Magueresse A, et al. Threat of plastic ageing in marine environment. Adsorption/desorption of micropollutants. *Mar Pollut Bull* 2018;127:684-94. DOI
22. Arias-Villamizar CA, Vázquez-Morillas A. Degradation of conventional and oxodegradable high density polyethylene in tropical aqueous and outdoor environments. *Rev Int Contam Ambie* 2018;34:137-47. DOI
23. Chiellini E, Corti A, D'Antone S. Oxo-biodegradable full carbon backbone polymers - biodegradation behaviour of thermally oxidized polyethylene in an aqueous medium. *Polym Degrad Stabil* 2007;92:1378-83. DOI
24. Adamcová D, Radziemska M, Fronczyk J, Zloch J, Vaverkova MD. Research of the biodegradability of degradable/biodegradable plastic material in various types of environments. *Sci Rev Eng Environ Sci* 2017;26:3-14. DOI
25. Kalogerakis N, Karkanorachaki K, Kalogerakis GC, et al. Microplastics generation: onset of fragmentation of polyethylene films in marine environment mesocosms. *Front Mar Sci* 2017;4:84. DOI
26. Tebaldi VMR, Souza AM, de Souza YHS, de Carvalho Alves JN, Piccoli RH. Evaluation of the levels of microbiological contamination of the water of the paraíba do sul river in the urban perimeter of Barra Mansa-RJ. *Braz J Health Rev* 2021;4:17138-53. DOI
27. Rodrigues MO, Abrantes N, Gonçalves FJM, Nogueira H, Marques JC, Gonçalves AMM. Spatial and temporal distribution of microplastics in water and sediments of a freshwater system (Antuã River, Portugal). *Sci Total Environ* 2018;633:1549-59. DOI
28. The sins of greenwashing: home and family edition. 2010. Available from: https://www.twosides.info/wp-content/uploads/2018/05/

Terrachoice_The_Sins_of_Greenwashing_-_Home_and_Family_Edition_2010.pdf. [Last accessed on 4 Mar 2024]

29. de Souza AJ, de Araújo Pereira AP, Pedrinho A, et al. Land use and roles of soil bacterial community in the dissipation of atrazine. *Sci Total Environ* 2022;827:154239. DOI
30. Sun Y, Ren X, Rene ER, et al. The degradation performance of different microplastics and their effect on microbial community during composting process. *Bioresour Technol* 2021;332:125133. DOI
31. Lear G, Kingsbury JM, Franchini S, et al. Plastics and the microbiome: impacts and solutions. *Environ Microbiome* 2021;16:2. DOI
32. Yuan J, Ma J, Sun Y, Zhou T, Zhao Y, Yu F. Microbial degradation and other environmental aspects of microplastics/plastics. *Sci Total Environ* 2020;715:136968. DOI
33. Badea MA, Balas M, Dinischiotu A. Microplastics in freshwaters: implications for aquatic autotrophic organisms and fauna health. *Microplastics* 2023;2:39-59. DOI
34. Wang Y, Zhou B, Chen H, Yuan R, Wang F. Distribution, biological effects and biofilms of microplastics in freshwater systems - a review. *Chemosphere* 2022;299:134370. DOI
35. Jung MR, Horgen FD, Orski SV, et al. Validation of ATR FT-IR to identify polymers of plastic marine debris, including those ingested by marine organisms. *Mar Poll Bull* 2018;127:704-16. DOI
36. Hammer J, Kraak MHS, Parsons JR. Plastics in the marine environment: the dark side of a modern gift. In: Witacre D, editor. Reviews of environmental contamination and toxicology. New York: Springer; 2012. pp. 1-44. DOI
37. ASTM International. Standard guide for exposing and testing plastics that degrade in the environment by a combination of oxidation and biodegradation. Available from: https://www.astm.org/d6954-18.html. [Last accessed on 4 Mar 2024].

Ben-Haddad *et al. Water Emerg Contam Nanoplastics* 2024;3:10
DOI: 10.20517/wecn.2023.70

Water Emerging Contaminants & Nanoplastics

Perspective

Open Access

Per- and polyfluoroalkyl pollution in marine environments: a viewpoint about Africa

Mohamed Ben-Haddad[1], Gabriel E. De-la-Torre[2], Tadele Assefa Aragaw[3], Bilal Mghili[4], Mohamed Rida Abelouah[1], Sara Hajji[1], Aicha Ait Alla[1]

[1]Department of biology, Laboratory of Aquatic Systems: Marine and Continental Environments (AQUAMAR), Faculty of Sciences, Ibn Zohr University, Agadir 80000, Morocco.
[2]Biodiversity, Environment, and Society Research Group, San Ignacio de Loyola University, Lima 15012, Peru.
[3]Faculty of Chemical and Food Engineering, Bahir Dar Institute of Technology, Bahir Dar University, Bahir Dar 6000, Ethiopia.
[4]LESCB, URL-CNRST N° 18, Abdelmalek Essaadi University, Faculty of Sciences, Tetouan 93000, Morocco.

Correspondence to: Dr. Mohamed Ben-Haddad, Department of biology, Laboratory of Aquatic Systems: Marine and Continental Environments (AQUAMAR), Faculty of Sciences, Ibn Zohr University, Dakhla avenue, Agadir 80000, Morocco. E-mail: mohamed.ben-haddad@edu.uiz.ac.ma

How to cite this article: Ben-Haddad M, De-la-Torre GE, Aragaw TA, Mghili B, Abelouah MR, Hajji S, Ait Alla A. Per- and polyfluoroalkyl pollution in marine environments: a viewpoint about Africa. *Water Emerg Contam Nanoplastics* 2024;3:10. https://dx.doi.org/10.20517/wecn.2023.70

Received: 20 Nov 2023 **First Decision:** 22 Feb 2024 **Revised:** 1 Mar 2024 **Accepted:** 14 Mar 2024 **Published:** 1 Apr 2024

Academic Editor: Marta Otero **Copy Editor:** Dong-Li Li **Production Editor:** Dong-Li Li

Abstract

Per- and poly-fluoroalkyl substances (PFAS) represent an extensive and expanding group of chemicals considered contaminants of emerging concern (CECs). These elements have found widespread usage in diverse industrial and commercial sectors since the 1940s. The advancement of modern analytical methods in developed countries has significantly contributed to the increased research on the environmental behavior and risk assessment of PFAS. However, what about developing countries? Over time, the focus on PFAS has expanded beyond legacy PFAS to encompass novel ones. In this perspective, we focus on analyzing the existing knowledge concerning PFAS in the marine environment, aiming to shed light on the limited research pertaining to per- and polyfluoroalkyl pollution in the marine ecosystems of Africa.

Keywords: Per- and polyfluoroalkyl substances, Africa, marine environment, contaminants of emerging concern, pollution, toxicity

INTRODUCTION

Per- and polyfluoroalkyl substances (PFAS) represent a set of anthropogenic organic substances, comprising more than 8,000 distinct acknowledged structures listed in the Toxic Substances Control Act Inventory[1,2]. These compounds are employed in various utilizations in commercial and industrial sectors dating back to the 1940s[2]. Owing to their extensive use in numerous consumer items such as food packaging and water-resistant textiles, coatings, and firefighting foams, these elements are now pervasive throughout the environment[3,4]. Referred to as the “forever chemicals”, PFAS exhibit remarkable persistence in the environment and resist degradation due to the exceptional durability of their carbon-fluorine bonds, making their breakdown particularly challenging. PFAS [e.g., perfluorooctane sulfonate (PFOS) or perfluorooctanoic acid (PFOA)] emissions into the environment originate from multiple sources, including intentional manufacturing, utilization, and disposal processes[5-7]. Furthermore, PFAS can be present as impurities in substances emitted into the environment or can result from the degradation of precursor substances through abiotic or biotic pathways[8].

While the focus on PFAS has primarily revolved around their negative effects on human health, there is an increasing awareness of their bioaccumulation in biota, particularly in marine organisms, owing to the growing number of studies highlighting their presence in these ecosystems[9]. PFAS have demonstrated the capability to disrupt various physiological functions and biochemical routes that are conserved among different phyla, raising concerns regarding their impacts on marine biota[2,9]. To achieve improved risk management objectives concerning PFAS occurrence, bioaccumulation, and biomagnification, it is imperative to further advance our understanding of uptake and elimination kinetics[2]. This necessitates obtaining additional information and data on these crucial processes from several parts of the world, including developing countries.

As of the existing global knowledge concerning PFAS, there is growing concern about their impact on marine environments. PFAS, known for their persistence and bioaccumulative properties, have become a significant environmental issue worldwide[7,10]. Despite extensive research on PFAS pollution, there remains a need to deepen our understanding of their distribution, behavior, and long-term effects on marine ecosystems, particularly in developing countries. In light of the current situation, here we attempted to answer the question: “What is the position of Africa in the current knowledge about PFAS pollution in marine environments?”

CURRENT KNOWLEDGE ABOUT PFAS IN THE MARINE ENVIRONMENT

First, compared with freshwater environments, marine matrices have not attracted significant interest from scientists, especially in Africa[11]. According to a recent review by Khan *et al.*, the majority of worldwide studies concerning PFAS in the marine environment have primarily focused on water and sediment[2]. Limited information is available regarding PFAS bioaccumulation in invertebrates, with most data concentrated on crustaceans and mollusks. In fish, PFAS concentrations are commonly recorded in muscle tissue or fillet, primarily addressing concerns related to seafood safety. However, some studies have also investigated PFAS burdens in whole fish and liver. In the case of seabirds, research on PFAS occurrence and bioaccumulation often involves examining levels in eggs, liver, and blood (or plasma). It is recognized that marine mammals can bioaccumulate these compounds at significant levels, particularly in hepatic and circulatory tissues. Thus, the essential origins of PFAS in the marine environment are land-generated, including pesticides, paints, surfactants, textiles, firefighting foams, and fast food packaging, among several others. These chemicals are transported from land into the marine environment via the water cycle[4]. Then, various ecological phenomena interfere, such as the accumulation in organisms, transfer through food chains, and magnification within ecosystems[12].

Second, the quantification methods of PFAS involved a series of procedures, including preconditioning, extraction, clean-up, and concentration before the analytical instrumentation. Hence, liquid chromatography (LC) coupled with tandem mass spectrometry (MS/MS) is a widely employed technique for PFAS analysis with notable sophistication as well as meticulous calibration and quality control strategies. Indeed, this technique provides high sensitivity, excellent selectivity, and considerable precision even in complex environmental matrices like seawater and sediment. However, this technique may have limitations in detecting all possible PFAS compounds owing to differences in ionization efficiency and fragmentation patterns among various PFAS species[13]. LC-MS/MS methods can be technically complex, expensive, and require expertise for operation and maintenance, which is the main reason for the limited number of studies about PFAS in African and developing countries. Table 1 presents examples of field investigations that unveil the presence of PFAS across diverse marine matrices globally, delineating their geographical distribution, study matrix, identification methodology, and the range of occurrence.

WHAT IS AFRICA’S POSITION IN THE GLOBAL KNOWLEDGE ABOUT PFAS IN THE MARINE ENVIRONMENT?

The studies conducted on PFAS in Africa have predominantly focused on terrestrial aquatic ecosystems, primarily rivers, and lakes. Research efforts have been dedicated to understanding the presence, distribution, and potential ecological impacts of PFAS compounds in sediment and freshwater, mainly in South Africa, Nigeria, and Kenya[31]. Thus, this context forces us to raise relevant questions about the place of marine and coastal environments in the global knowledge of PFAS in Africa. To the best of our knowledge, the two only marine field studies in Africa were carried out in a lagoon area in the north of Tunisia in 2018 and in the Gulf of Guinea in 2022 [Table 1]. The study of Tunisia investigated nine marine species (three fish, two crustaceans, and four mollusks) collected from Bizerte lagoon using (LC-MS/MS) technique, reporting values between 0.20-2.89 ng/g dry weight[29]. The second study utilized the same technique to quantify the amount of PFAS in four fishery products along the Gulf of Guinea, revealing values between 91 and 1,510 pg/g wet weight[30]. In a separate investigation, the assessment of PFAS was conducted on marine shellfish farmed in land-based facilities in South Africa. The PFAS concentrations (expressed in ng/g wet weight) varied between 0.12 and 0.49 in abalone, 4.83-6.43 in mussels, 0.64-0.66 in oysters, and 0.22 ng/g ww in lobsters using UHPLC-MS/MS method[32]. Few other studies included some sampling points in estuaries in global surveys of terrestrial water bodies[11,13,33].

Unfortunately, the lack of studies in Africa is a significant concern. While PFAS pollution has been extensively researched in various parts of the world, there remains a notable gap in our understanding of the presence and impact of these chemicals on this continent. This group of human-made chemicals is widely used in various industrial and consumer products in Africa for their water and grease-resistance properties[34,35]. However, their persistent nature and potential adverse health effects have raised global concerns[36-38] that must not exclude African countries. Despite the growing recognition of PFAS as emerging contaminants, research efforts have predominantly focused on regions such as North America, Europe, and parts of Asia[18].

With its diverse coastal and marine ecosystems and substantial population relying on fisheries, the African continent should not be overlooked in PFAS research. Marine areas in Africa face unique environmental challenges, including industrial activities, burgeoning urbanization, climate change vulnerability, threatened biodiversity hotspots, and increasing plastic waste generation[39-41]. These factors can contribute to the release and accumulation of PFAS in coastal waters, sediments, and organisms, potentially posing risks to both human and ecological health. By expanding studies to include African coasts and marine habitats, researchers can gain valuable insights into the presence, distribution, and potential impacts of PFAS in new

Table 1. Examples of field investigations reporting PFAS are available for various marine matrices worldwide, with only two studies conducted in African marine environments

Country	Location	Matrix	Identification technique	Range (min - max)	Ref.
US	Florida	Seawater Coastal sediment	UHPLC system coupled to mass spectrometer	1.1-113 ng/L (seawater) 0.1-8.4 ng/g (sediment)	[14]
		Coastal waterway	UHPLC-MS/MS	2.47-4.69 ng/L	[15]
Sweden Denmark Germany	Baltic sea	Several marine organisms such as the blue mussel (*Mytilus edulis*), the Atlantic herring (*Clupea harengus*), and the grey seal (*Halichoerus grypus*)	LC-MS/MS	1.1-450 ng/g per wet weight	[16]
Germany	Seaside Büsum village	Coastal atmosphere	GC-MS	8.6-155 pg/m^3	[17]
Antarctica	Ross island	Blood of Weddell seal (*Leptonychotes weddellii*)	UHPLC-MS/MS	0.08-0.23 ng/mL	[18]
	Livingston Island	Seawater Coastal snow Plankton	UFLC-MS/MS coupled to a triple quadrupole mass spectrometer	94-420 pg/L (seawater) 760-3,600 pg/L (snow) 3.1-16 ng/g dry weight (plankton)	[19]
China	Estuaries and Delta of Pearl River region	Coastal water	HPLC-MS/MS	0.003-2.09 items/m^3 of water	[20]
	Bohai sea	Marine mollusks such as *Chlamys farreri*, *Crassostrea talienwhanensis*, *Meretrix meretrix*, and *Mytilus edulis*	Liquid chromatography column equipped with a tandem mass spectrometry system	2.51-1,351 ng/g dry weight	[21]
	South China sea	Seawater Coastal sediment	Ultra-performance liquid chromatograph interfaced with mass spectrometer	38-1,015 pg/L (seawater) 7.5-84.2 pg/g dry weight (sediment)	[22]
Australia	Estuary of Werribee River	Coastal water	HPLC-MS/MS	22-187 ng/L	[23]
France	Bay of Marseille	Coastal water	LC-QTOF-MS	0.11-9 ng/L	[24]
	Several locations in the English channel, the Mediterranean sea, and the Atlantic ocean	Mussel (*Mytilus edulis*, *Mytilus galloprovincialis*) Oyster (*Crassostrea gigas*)	Acquity ultra performance liquid chromatograph coupled to a triple quadrupole mass spectrometer	0.007-0.549 ng/g wet weight	[25]
Chile	Central coast	Coastal litter	HPLC-MS/MS	279-1,211 pg/g	[26]
Saudi Arabia	Red sea	Seawater	QqQ equipped with the AJS-ESI	0-956 ng/L	[27]
Spain	Coastal area of Ebro Delta	Coastal water Coastal sediment	TQ-MS	0-2,775 ng/L (water) 0-22.6 ng/g (sediment)	[28]
Tunisia (Africa)	Bizerte lagoon	Seafood	UPLC system coupled to a LC-MS/MS	0.20-2.89 ng/g dry weight	[29]
Guinea (Africa)	Golf of Guinea	Fishery products	LC-MS/MS	91-1,510 pg/g wet weight	[30]

PFAS: Per- and poly-fluoroalkyl substances; UHPLC: ultra-high performance liquid chromatography; UHPLC-MS/MS: ultra-high-pressure liquid chromatography coupled with tandem mass spectrometry; LC-MS/MS: liquid chromatography and tandem mass spectrometry; GC-MS: gas chromatography coupled with mass spectrometer; UFLC-MS/MS: ultra-fast liquid chromatography-tandem mass spectrometry; HPLC-MS/MS: high-performance liquid chromatography coupled with tandem mass spectrometry; LC-QTOF-MS: liquid chromatography quadrupole time-of-flight mass spectrometry; QqQ: triple quadrupole tandem mass spectrometer; AJS-ESI: jet stream electrospray ionization; TQ-MS: triple quadrupole mass spectrometer; UPLC: ultra-performance liquid chromatography.

environmental conditions. It is essential to evaluate the levels of contamination, identify potential sources, and understand the pathways through which PFAS enter the African marine environment. Moreover, the pervasive presence of PFAS poses a significant risk to marine products intended for export, particularly in the context of food safety. Investigations into the accumulation of PFAS in marine biota are crucial to understanding the potential hazards associated with seafood consumption by human populations. As these substances accumulate in marine life, they can find their way into the food supply chain, posing risks to consumers both domestically and internationally. Therefore, comprehensive studies addressing the bioaccumulation of PFAS in marine species are indispensable for safeguarding the integrity of exported marine products and ensuring global food safety standards.

CONCLUSION

Overall, the existing literature on PFAS in the marine environment, particularly in Africa, reveals a noticeable lack of interest and a limited number of studies conducted in this context. The coasts and marine habitats of Africa remain relatively unexplored and understudied. This knowledge gap calls for urgent attention and increased research efforts to understand the potential presence, distribution, and ecological impacts of PFAS chemicals. Addressing the lack of studies on PFAS in the marine environment of Africa requires collaborative efforts among researchers, environmental agencies, and policymakers. It is imperative to foster more robust international collaborations and partnerships with leading scientists in the field from across the world, such as China, the USA, and Europe. Leveraging the expertise and experience of these prominent researchers can facilitate knowledge transfer, exchange of methodologies, and establishment of standardized protocols for PFAS studies in marine environments. Such initiatives can help generate region-specific data, raise awareness about PFAS pollution, and guide the development of appropriate mitigation and regulatory measures. By shedding light on the presence and potential risks of PFAS in African marine environments, we can work towards safeguarding both the environment and the well-being of the communities relying on these vital ecosystems.

DECLARATIONS

Acknowledgments

The authors would like to thank the editors and reviewers for their efforts in improving the manuscript.

Authors' contributions

Conceptualization, methodology, validation, formal analysis, investigation, and writing - original draft: Ben-Haddad M

Conceptualization, methodology, validation: De-la-Torre GE, Aragaw TA, Mghili B, Abelouah MR, Hajji S, Ait Alla A

Availability of data and materials

Not applicable.

Financial support and sponsorship

None.

Conflicts of interest

All authors declared that there are no conflicts of interest. De-la-Torre GE is an Editorial Board Member of the journal *Water Emerging Contaminants & Nanoplastics*.

Ethical approval and consent to participate

Not applicable.

Consent for publication

Not applicable.

Copyright

REFERENCES

1. Evich MG, Davis MJB, McCord JP, et al. Per- and polyfluoroalkyl substances in the environment. *Science* 2022;375:eabg9065. DOI PubMed PMC
2. Khan B, Burgess RM, Cantwell MG. Occurrence and bioaccumulation patterns of per- and polyfluoroalkyl substances (PFAS) in the marine environment. *ACS ES T Water* 2023;3:1243-59. DOI PubMed PMC
3. Boisvert G, Sonne C, Rigét FF, Dietz R, Letcher RJ. Bioaccumulation and biomagnification of perfluoroalkyl acids and precursors in East Greenland polar bears and their ringed seal prey. *Environ Pollut* 2019;252:1335-43. DOI PubMed
4. Dickman RA, Aga DS. A review of recent studies on toxicity, sequestration, and degradation of per- and polyfluoroalkyl substances (PFAS). *J Hazard Mater* 2022;436:129120. DOI PubMed
5. Buck RC, Franklin J, Berger U, et al. Perfluoroalkyl and polyfluoroalkyl substances in the environment: terminology, classification, and origins. *Integr Environ Assess Manag* 2011;7:513-41. DOI PubMed PMC
6. Kwiatkowski CF, Andrews DQ, Birnbaum LS, et al. Scientific basis for managing PFAS as a chemical class. *Environ Sci Technol Lett* 2020;7:532-43. DOI PubMed PMC
7. Wang Z, Boucher JM, Scheringer M, Cousins IT, Hungerbühler K. Toward a comprehensive global emission inventory of C_4-C_{10} perfluoroalkanesulfonic acids (PFSAs) and related precursors: focus on the life cycle of C_8-based products and ongoing industrial transition. *Environ Sci Technol* 2017;51:4482-93. DOI PubMed
8. Gao K, Chen Y, Xue Q, et al. Trends and perspectives in per-and polyfluorinated alkyl substances (PFASs) determination: faster and broader. *TrAC Trends Anal Chem* 2020;133:116114. DOI
9. Lee JW, Choi K, Park K, Seong C, Yu SD, Kim P. Adverse effects of perfluoroalkyl acids on fish and other aquatic organisms: a review. *Sci Total Environ* 2020;707:135334. DOI
10. Kang P, Zhao Y, Zuo C, et al. The unheeded inherent connections and overlap between microplastics and poly- and perfluoroalkyl substances: a comprehensive review. *Sci Total Environ* 2023;878:163028. DOI
11. Ssebugere P, Sillanpää M, Matovu H, et al. Environmental levels and human body burdens of per- and poly-fluoroalkyl substances in Africa: a critical review. *Sci Total Environ* 2020;739:139913. DOI
12. Du D, Lu Y, Zhou Y, et al. Bioaccumulation, trophic transfer and biomagnification of perfluoroalkyl acids (PFAAs) in the marine food web of the South China Sea. *J Hazard Mater* 2021;405:124681. DOI
13. Mullin L, Katz D, Riddell N, et al. Analysis of hexafluoropropylene oxide-dimer acid (HFPO-DA) by liquid chromatography-mass spectrometry (LC-MS): review of current approaches and environmental levels. *Trends Analyt Chem* 2019;118:828-39. DOI PubMed PMC
14. Griffin EK, Hall LM, Brown MA, et al. PFAS surveillance in abiotic matrices within vital aquatic habitats throughout Florida. *Mar Pollut Bull* 2023;192:115011. DOI
15. Martinez B, Da Silva BF, Aristizabal-Henao JJ, et al. Increased levels of perfluorooctanesulfonic acid (PFOS) during Hurricane Dorian on the east coast of Florida. *Environ Res* 2022;208:112635. DOI
16. de Wit CA, Bossi R, Dietz R, et al. Organohalogen compounds of emerging concern in Baltic Sea biota: levels, biomagnification potential and comparisons with legacy contaminants. *Environ Int* 2020;144:106037. DOI
17. Wang Z, Xie Z, Möller A, Mi W, Wolschke H, Ebinghaus R. Atmospheric concentrations and gas/particle partitioning of neutral poly- and perfluoroalkyl substances in northern German coast. *Atmospheric Environment* 2014;95:207-13. DOI
18. Routti H, Krafft BA, Herzke D, Eisert R, Oftedal O. Perfluoroalkyl substances detected in the world's southernmost marine mammal, the Weddell seal (*Leptonychotes weddellii*). *Environ Pollut* 2015;197:62-7. DOI PubMed
19. Casal P, Zhang Y, Martin JW, Pizarro M, Jiménez B, Dachs J. Role of snow deposition of perfluoroalkylated substances at Coastal Livingston Island (Maritime Antarctica). *Environ Sci Technol* 2017;51:8460-70. DOI PubMed
20. Cheng Y, Mai L, Lu X, et al. Occurrence and abundance of poly- and perfluoroalkyl substances (PFASs) on microplastics (MPs) in Pearl River Estuary (PRE) region: spatial and temporal variations. *Environ Pollut* 2021;281:117025. DOI
21. Meng L, Lu Y, Wang Y, et al. Occurrence, temporal variation (2010-2018), distribution, and source appointment of per- and polyfluoroalkyl substances (PFAS) in mollusks from the Bohai Sea, China. *ACS EST Water* 2022;2:195-205. DOI
22. Wang Q, Tsui MMP, Ruan Y, et al. Occurrence and distribution of per- and polyfluoroalkyl substances (PFASs) in the seawater and sediment of the South China sea coastal region. *Chemosphere* 2019;231:468-77. DOI
23. Allinson M, Yamashita N, Taniyasu S, Yamazaki E, Allinson G. Occurrence of perfluoroalkyl substances in selected Victorian rivers and estuaries: an historical snapshot. *Heliyon* 2019;5:e02472. DOI PubMed PMC
24. Schmidt N, Fauvelle V, Castro-Jiménez J, et al. Occurrence of perfluoroalkyl substances in the Bay of Marseille (NW Mediterranean Sea) and the Rhône River. *Mar Pollut Bull* 2019;149:110491. DOI
25. Catherine M, Nadège B, Charles P, Yann A. Perfluoroalkyl substances (PFASs) in the marine environment: spatial distribution and temporal profile shifts in shellfish from French coasts. *Chemosphere* 2019;228:640-8. DOI PubMed
26. Gómez V, Torres M, Karásková P, Přibylová P, Klánová J, Pozo K. Occurrence of perfluoroalkyl substances (PFASs) in marine plastic litter from coastal areas of Central Chile. *Mar Pollut Bull* 2021;172:112818. DOI PubMed

27. Ali AM, Higgins CP, Alarif WM, Al-Lihaibi SS, Ghandourah M, Kallenborn R. Per- and polyfluoroalkyl substances (PFASs) in contaminated coastal marine waters of the Saudi Arabian Red Sea: a baseline study. *Environ Sci Pollut Res Int* 2021;28:2791-803. DOI PubMed PMC
28. Pignotti E, Casas G, Llorca M, et al. Seasonal variations in the occurrence of perfluoroalkyl substances in water, sediment and fish samples from Ebro Delta (Catalonia, Spain). *Sci Total Environ* 2017;607-8:933-43. DOI
29. Barhoumi B, Sander SG, Driss MR, Tolosa I. Survey of legacy and emerging per- and polyfluorinated alkyl substances in Mediterranean seafood from a North African ecosystem. *Environ Pollut* 2022;292:118398. DOI PubMed
30. Ekperusi AO, Bely N, Pollono C, Mahé K, Munschy C, Aminot Y. Prevalence of per- and polyfluoroalkyl substances (PFASs) in marine seafood from the Gulf of Guinea. *Chemosphere* 2023;335:139110. DOI PubMed
31. Groffen T, Nkuba B, Wepener V, Bervoets L. Risks posed by per- and polyfluoroalkyl substances (PFAS) on the African continent, emphasizing aquatic ecosystems. *Integr Environ Assess Manag* 2021;17:726-32. DOI PubMed
32. Abafe OA, Macheka LR, Abafe OT, Chokwe TB. Concentrations and human exposure assessment of per and polyfluoroalkyl substances in farmed marine shellfish in South Africa. *Chemosphere* 2021;281:130985. DOI PubMed
33. Fauconier G, Groffen T, Wepener V, Bervoets L. Perfluorinated compounds in the aquatic food chains of two subtropical estuaries. *Sci Total Environ* 2020;719:135047. DOI PubMed
34. Nakayama SF, Yoshikane M, Onoda Y, et al. Worldwide trends in tracing poly- and perfluoroalkyl substances (PFAS) in the environment. *TrAC Trends Anal Chem* 2019;121:115410. DOI
35. Xiao F. Emerging poly- and perfluoroalkyl substances in the aquatic environment: a review of current literature. *Water Res* 2017;124:482-95. DOI PubMed
36. Mao W, Li M, Xue X, et al. Bioaccumulation and toxicity of perfluorooctanoic acid and perfluorooctane sulfonate in marine algae Chlorella sp. *Sci Total Environ* 2023;870:161882. DOI
37. Martín J, Hidalgo F, García-Corcoles MT, et al. Bioaccumulation of perfluoroalkyl substances in marine echinoderms: results of laboratory-scale experiments with Holothuria tubulosa Gmelin, 1791. *Chemosphere* 2019;215:261-71. DOI
38. Otero-Sabio C, Giacomello M, Centelleghe C, et al. Cell cycle alterations due to perfluoroalkyl substances PFOS, PFOA, PFBS, PFBA and the new PFAS C6O4 on bottlenose dolphin (*Tursiops truncatus*) skin cell. *Ecotoxicol Environ Saf* 2022;244:113980. DOI PubMed
39. Fayiga AO, Ipinmoroti MO, Chirenje T. Environmental pollution in Africa. *Environ Dev Sustain* 2018;20:41-73. DOI
40. Ouda M, Kadadou D, Swaidan B, et al. Emerging contaminants in the water bodies of the Middle East and North Africa (MENA): a critical review. *Sci Total Environ* 2021;754:142177. DOI
41. Mghili B, Ben-haddad M, Zerrad O, Rangel-buitrago N, Aksissou M. Tackling marine plastic pollution in Morocco: a review of current research, regulatory measures, and future challenges. *Reg Stud Mar Sci* 2024;69:103286. DOI

Zheng *et al. Water Emerg Contam Nanoplastics* 2024;3:11
DOI: 10.20517/wecn.2023.74

Water Emerging Contaminants & Nanoplastics

Review

Open Access

Carbon-based adsorbents for micro/nano-plastics removal: current advances and perspectives

Huifang Zheng[1], **Qian Chen**[2], **Zhijie Chen**[3]

[1]School of Resource and Safety Engineering, Wuhan Institute of Technology, Wuhan 430205, Hubei, China.
[2]School of Civil and Environmental Engineering, University of Technology Sydney (UTS), Sydney, NSW 2007, Australia.
[3]School of Civil and Environmental Engineering, The University of New South Wales, Sydney, NSW 2052, Australia.

Correspondence to: Qian Chen, School of Civil and Environmental Engineering, University of Technology Sydney (UTS), City Campus, Broadway, Sydney, NSW 2007, Australia. E-mail: Qian.Chen-1@student.uts.edu.au; Dr. Zhijie Chen, School of Civil and Environmental Engineering, The University of New South Wales, High St, Kensington, Sydney, NSW 2052, Australia. E-mail: Zhijie.Chen1@unsw.edu.au

How to cite this article: Zheng H, Chen Q, Chen Z. Carbon-based adsorbents for micro/nano-plastics removal: current advances and perspectives. *Water Emerg Contam Nanoplastics* 2024;3:11. https://dx.doi.org/10.20517/wecn.2023.74

Received: 16 Dec 2023 **First Decision:** 5 Feb 2024 **Revised:** 21 Mar 2024 **Accepted:** 22 Mar 2024 **Published:** 1 Apr 2024

Academic Editor: Marta Otero **Copy Editor:** Pei-Yun Wang **Production Editor:** Pei-Yun Wang

Abstract

Carbon-based adsorbents, such as graphene, graphene oxide (GO), activated carbon/biochar (AC/BC), carbon nanotubes (CNTs), metal-modified carbon, and fly ash, are garnering increasing attention due to their exceptional structural properties, enabling their potential effectiveness in removing microplastics and nano-plastics (MPs/NPs) from aqueous solutions. A key attribute contributing to the efficacy of these carbon adsorbents in addressing MPs/NPs is their flexibly tunable surface properties. To advance the applicability of functionalized carbon adsorbents in the context of MPs/NPs removal, it is necessary to highlight their interactions with MPs/NPs in aqueous environments. The review commences by outlining the main adsorption mechanisms. Subsequently, the adsorption behavior of different types of MPs/NPs on carbon-based adsorbents is analyzed and how different factors influence their adsorption performance is examined. Finally, the review concludes by offering insights into prospective avenues for future research concerning functional carbon adsorbents for MPs/NPs removal.

Keywords: Carbonaceous adsorbents, microplastics/nanoplastics, adsorption mechanism, adsorption behavior

INTRODUCTION

Plastics, which exhibit remarkable malleability, versatility, cost-efficiency, durability, exceptional oxygen resistance, and lightweight, have gained extensive usage[1]. In the year 2020, global plastic production reached a staggering 367 million tons[2], and an anticipated increase of 29% is projected for the year 2028[3]. When subjected to environmental conditions, plastics gradually degrade into minute fragments due to factors such as weathering, mechanical wear, solar radiation, and microbial activities[4,5]. These particles are categorized according to their size, shape, density, and the type of polymer from which they are made. Alimi *et al.*[6], Ding *et al.*[7], Jahnke *et al.*[8], Lang *et al.*[9], and Wright and Kelly[10] mentioned that the classification of plastics based on size ranges from macro-plastics (larger than 25 mm), meso-plastics (5-25 mm), microplastics (MPs) (100 nm - 5 mm), to nano-plastics (NPs) (smaller than 100 nm) [Figure 1A-D][11]. MPs are commonly identified as particles between 1 μm and 5 mm, whereas NPs are defined as particles smaller than 0.1 μm[12,13]. These newly recognized entities are now identified as emerging hazardous contaminants for their unique physical and chemical properties, intrinsic stability, and high resistance to biodegradation[14-18]. They are ubiquitously present across diverse landscapes, encompassing sewage systems, wastewater treatment plants (WWTPs), sediment layers, oceans, groundwater reserves, estuaries[19], drinking water sources[6], the atmosphere[20], soil[21], food supplies[22], and even the human body's bloodstream[10,20].

Aquatic organisms, including mammals, birds, fish, zooplankton, and mollusks, are susceptible to mistakenly ingesting MPs/NPs[23]. MPs/NPs can be made from a variety of plastic materials, including polypropylene (PP), polyvinyl chloride (PVC), polyester (PES), polycarbonate (PC), high-density polyethylene (HDPE), low-density polyethylene (LDPE), polystyrene (PS), polyurethane (PU), and polyethylene terephthalate (PET), among others[24-26]. These particles, characterized by their aptitude for adsorbing harmful compounds, serve as carriers for toxic elements such as antibiotics, pharmaceuticals, heavy metals, pesticides, plasticizers, and pathogens[27-29]. Facilitated by their high surface area, reduced dimensions, and pronounced hydrophobic properties[20], these interactions significantly impact the availability, fate, and amplification of these pollutants within ecosystems. Furthermore, the small scale of MPs and NPs renders them prone to being ingested as sustenance by aquatic species, potentially propelling their movement up the food chain and posing a consequential toxicological threat across the entire ecological spectrum[30-32]. Hence, the expeditious removal of MPs and NPs emerges as a pressing priority to safeguard the integrity of aquatic environments.

A diverse array of treatment technologies, encompassing adsorption[33], coagulation[34], advanced oxidation processes[35], photocatalysis[36], bioremediation[37], and filtration[38], has been devised to combat the presence of MPs and NPs in polluted waters. Among these methodologies, adsorption stands out as a cost-effective, straightforward, dependable, and efficacious approach for capturing both MPs and NPs from water sources and sewage systems[15]. Conventional adsorbents encompass a spectrum of materials such as low-cost substances, carbonaceous materials, and modified materials[39]. These versatile adsorbents offer an extensive range of choices and sources, rendering them adaptable to local conditions across diverse countries and regions[40-42]. Significantly, the key attributes of adsorption, notably facile operational procedures, renewable adsorbents, and minimal toxicity, contribute to its broad potential for MPs/NPs removal in water, thereby promising prospects for its wide-scale application[43,44]. Ali *et al.*[2] and Chen *et al.*[45,46] have both conducted reviews on the latest adsorbents for removing MPs/NPs from polluted water. Their reviews encompass a range of emerging adsorbents, including those based on sponge/aerogel, metals, biochar, and other innovative materials. They provide a thorough explanation of the characteristics and adsorption mechanisms of each adsorbent in relation to MPs/NPs. Notably, carbon-based adsorbents are highlighted as particularly promising due to their cost-effectiveness and high adsorption efficiency. However, there is still a

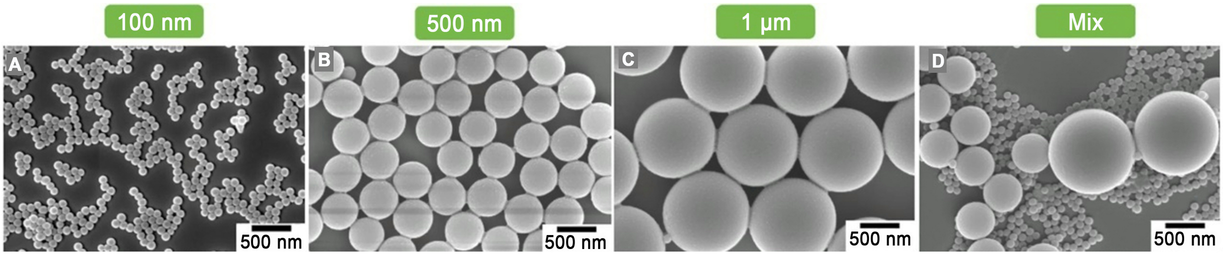

Figure 1. Morphology of PS MPs/NPs with different diameters at (A) 100 nm; (B) 500 nm; (C) 1 μm; and (D) mixed sample[11]. Copyright 2023, Elsevier. PS: Polystyrene; MPs: microplastics; NPs: nano-plastics.

lack of detailed information regarding the removal of MPs/NPs by carbon-based adsorbents. Additionally, a comprehensive and systematic explanation of the adsorption behaviors and mechanisms specific to each type of carbon-based adsorbent is yet to be fully explored.

Carbon-based materials, characterized by carbon as their primary constituent, exist in either powdered or bulk non-metallic solid forms. This category includes activated carbon/biochar (AC/BC)[47,48], CNTs[49], graphene[46], graphene oxide (GO)[50], metal-modified carbon[51,52], and fly ash[53], among others. AC stands as the foremost carbon-based adsorbent employed extensively in wastewater treatment. The versatility of AC allows for the preparation of a broad spectrum of adsorbents tailored to diverse environmental applications, including the removal of MPs and NPs from aqueous solutions[47]. Given the elevated production costs associated with coal-based AC, biochar becomes a cost-effective alternative offering high efficacy in MPs/NPs adsorption[51]. Biochar can be derived from an array of woody biomass sources, encompassing agricultural waste and byproducts such as peanut hulls and dairy manure[54]. Notably, the utility of biochar extends beyond adsorption, encompassing roles such as carbon sequestration, soil fertility enhancement, and environmental remediation, thus establishing its multifunctionality in various domains. Graphene, constituting a single layer of a 2D hexagonal carbon network, is intricately investigated for its application prospects. Meanwhile, GO and reduced GO possess a high specific surface area and abundant surface functional groups, rendering it an ideal adsorbent for MPs/NPs removal[50,55,56]. carbon nanotubes (CNTs), on the other hand, manifest as cylindrical carbon tubes originating from one or multiple layers of graphene. Their well-defined hollow cylindrical structure, extensive surface area, hydrophobic characteristics, and amenability to surface modification contribute to their efficacy. Leveraging their exceptional physicochemical properties, GO and CNTs exhibit considerable advantages within the sphere of adsorption technology, particularly in addressing the removal of MPs/NPs[49].

Although each carbon adsorbent exhibits distinct structural attributes and functionalities, a unifying trait present among all carbon adsorbents is their possession of abundant active surface functional groups. These groups play a pivotal role in shaping the surface chemical properties of carbon-based materials and facilitating the removal of MPs/NPs[57]. The prevailing consensus is that the physical and/or chemical interactions occurring between MPs/NPs and the functional groups on adsorbents substantially contribute to the adsorption process of these minute pollutants. To align with the requirements of water quality criteria, substantial development and refinement efforts have been directed towards diverse carbonaceous materials and their derivatives. Consequently, a multitude of modification techniques have emerged to enhance the removal of MPs/NPs. These approaches include oxidation, magnetization, functional group grafting, and the incorporation of inorganic substances through compositional composites[58].

Chemical and physical alterations to the surface of carbon materials can increase the variety and number of functional groups, enabling the addition of specific heteroatoms. This important area of research focuses on refining carbon materials' surface chemistry, specifically for the targeted capture of MPs/NPs.

These modifications enhance various characteristics of carbon-based adsorbents, such as pore distribution and volume, surface area, as well as increasing the number of functional groups and structural robustness. However, a thorough understanding of how the functional groups on the surface of carbon adsorbents interact with MPs/NPs is still lacking.

This study aims to thoroughly examine recent developments in carbon adsorbents, focusing on their surface functional groups and how these influence the removal and effectiveness against MPs/NPs in water. The papers published from 2015 till the present are summarized and reviewed (All of these papers are related to the MPs/NPs removal via carbon-based adsorbents). The review has two key goals: (1) To explore and clarify the basic processes that control the elimination of MPs/NPs by carbon adsorbents, emphasizing the complex interactions between functional groups and MPs/NPs; (2) To investigate the adsorption patterns of MPs/NPs on carbon adsorbents, highlighting their significant effects. Furthermore, the review will offer forward-looking views on future research into the use of functional groups in carbon adsorbents for the removal of plastic pollutants.

MECHANISM OF MPS/NPS ADSORPTION

The interaction between carbon adsorbents' functional groups and MPs/NPs is intricate, influenced by factors such as the carbon surface's diversity and chemistry, water's ionic composition, and adsorbate characteristics. Adsorbing MPs/NPs onto carbon materials involves various interactions: hydrophobic, hydrogen bonding, van der Waals forces, electrostatic attractions, π–π interactions, pore filling, and intraparticle diffusion [Figure 2][2,56,59]. The impact of these mechanisms on adsorption varies greatly, dependent on the MPs/NPs properties and the adsorbent type.

Chemisorption is important for removing MPs/NPs from water compared to physical adsorption interactions such as electrostatic interactions and pore filling. In specific water conditions, multiple mechanisms such as electrostatic interactions and surface complexation could simultaneously occur, influenced by electrostatic forces, binding site creation, and covalent bonding.

Physical adsorption, a relatively weaker process, involves MPs/NPs migrating into carbon adsorbents' pores and adhering to the carbon surface without forming chemical bonds. This mechanism is significantly affected by the surface area and porosity of carbon adsorbents[47,51,60]. An increase in micropores enhances surface area, favoring physical adsorption, while more mesopores improve contaminant diffusion, thus accelerating adsorption kinetics.

The pore structure of carbon adsorbents plays a crucial role in the physical adsorption process, influenced by factors such as the raw materials used and the carbon synthesis method. This includes carbonization/pyrolysis temperatures for AC/BC[61-63], as well as graphitization for GO and CNTs. The carbon surface's heterogeneity and polarity, along with associated functional groups, also significantly contribute to physical adsorption[56,63]. These elements enable the transfer of MPs/NPs to the carbon surface through forces such as electrostatic attraction and ion-dipole interactions. Although common, physical adsorption is not typically the primary means of adsorbing MPs/NPs. Table 1 lists the recent typical carbon-based adsorbents for MPs/NPs adsorption[47,49-53,64-68].

Table 1. The adsorption mechanism of MPs/NPs on carbon-based adsorbents

MPs/NPs	Carbon adsorbents	Mechanisms	Ref.
PS NPs	Granular activated carbon	Electrostatic attractions; Pore diffusion	[47]
PS MPs	3D RGO	π–π interaction	[50]
PS NPs	Biochar	Electrostatic attractions	[64]
PS NPs	Cu–Ni carbon materials	Electrostatic attractions	[66]
PS MPs	Zn-MBC	π–π interactions, hydrogen bonding, cooperative effect	[52]
PS MPs	Mg/Zn-MBC	Electrostatic interaction and chemical bonding	[51]
Polyethylene microbeads	Activated pine and spruce bark biochar	Physisorption	[67]
PS NPs	Iron-modified fly ash	Electrostatic attraction, complexation, π–π interactions	[53]
PS MPs, COOH-PS MPs, NH2-PS MPs	ChGO	Electrostatic attraction, hydrogen bonding, π–π interactions	[65]
PE, PET, PA	Magnetic CNTs	Hydrophobic interactions, electrostatic attraction, hydrogen bonding, π–π interactions, complexation	[49]
PS NPs	Corncob raw and oxidized biochar	Hydrophobic interaction and hydrogen bonding	[68]

MPs: Microplastics; NPs: nano-plastics; PS: polystyrene; 3D RGO: three-dimensional reduced graphene oxide; Zn-MBC: Zn modified magnetic biochar; Mg/Zn-MBC: Mg/Zn modified magnetic biochar; ChGO: sponge synthesized with chitin and GO; PE: polyethylene; PET: polyethylene terephthalate; PA: polyamide; CNTs: carbon nanotubes.

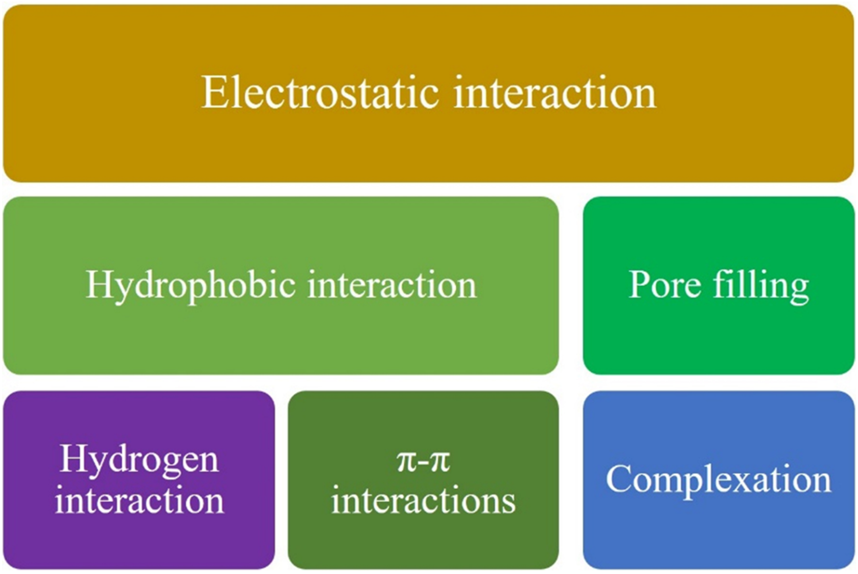

Figure 2. The main adsorption mechanisms of MNs/NPs by carbon-based adsorbents. NPs: Nano-plastics.

MPs/NPs tend to adhere to carbon-based adsorbents in water due to their hydrophobic nature, mainly through hydrophobic interactions. Hydrophobic molecules, which are non-polar, tend to aggregate and exclude water molecules in a polar environment due to hydrophobic interactions. The attachment of adsorbate molecules to the adsorbent's surface is not facilitated by strong ionic, hydrogen, or covalent bonds, but rather through weaker interactions like van der Waals forces[69]. Many types of MPs/NPs exhibit significant hydrophobic characteristics. Similarly, carbon-based adsorbents, which are created at elevated temperatures, possess hydrophobic properties, enabling them to engage in potent hydrophobic interactions with MPs/NPs. For instance, CNTs are capable of bonding with MPs via either hydrophobic or π–π interactions, depending on the hydrophobicity of the MPs. When integrated with magnetic nanoparticles, they form magnetic carbon nanotubes (M-CNTs), which allow for easy separation after absorbing MPs. M-CNTs have demonstrated high efficiency in removing MPs such as polyethylene (PE), PET, and polyamide (PA). They achieved complete adsorption of all MPs at a concentration of 5 g/L within just 5 h, with maximum adsorption capacities for PE, PET, and PA being 1,650, 1,400, and 1,100 mg/g, respectively. Remarkably, the adsorption process by M-CNTs remains effective even in the presence of substances like chemical oxygen demand, phosphate, and ammonia. M-CNTs also show the capability for thermal regeneration, maintaining their magnetic and adsorptive properties close to their original state. They retained about 80% efficiency even after four cycles of reuse[49]. In the adsorption process, hydrophobic interactions were primarily responsible for the adsorption of PE and PET, while π–π interactions were significant in the adsorption of PA and PET. This underscores the versatility and effectiveness of M-CNTs in adsorbing and removing various types of MPs from the environment, highlighting their potential as a sustainable solution for tackling MP pollution[49].

Iron-modified biochar is a notable example, especially when loaded with nanoparticles. It can be easily separated from mixtures using magnetic separation [Figure 3A]. The inclusion of iron species, particularly Fe_3O_4, on the biochar creates active sites for surface complexation with nanoparticles, enhancing its adsorption capacity. This Fe-modified biochar is effective in rapidly removing all NPs from water in as little as 10 min and maintains its efficiency over four reuse cycles[70].

Similarly, biochar modified with magnesium and zinc leverages positively charged $Mg(OH)_2$ and ZnO to enhance the adsorption of PS MPs. This improvement is primarily driven by electrostatic attraction and the formation of PS–O–metal bonds. Beyond its adsorptive qualities, Mg/Zn-MBC features catalytically active sites that exhibit significant hydrogenation activity. This property is particularly beneficial during the thermal treatment of PS MPs, facilitating the degradation of these plastics into smaller molecular compounds, as depicted in Figure 3B. This dual functionality not only aids in effectively removing MPs from the environment but also in breaking down and potentially repurposing these plastic materials[51].

Ganie et al. discovered that BC, synthesized through pyrolysis at 750 °C, exhibited a positive surface charge of 2.85 mV. When this biochar was mixed with PS-based MPs/NPs that carried a negative charge of -39.8 mV, the zeta potential of the resulting combination rapidly shifted to -9 mV. This change signals a significant electrostatic attraction between the components[64].

ChGO sponges demonstrate a remarkable capacity for reuse, maintaining high adsorption efficiencies even after three adsorption-desorption cycles. Specifically, these sponges have shown adsorption capacities of 89.8% for PS, 88.9% for PS-NH_2, and 72.4% for PS-COOH. The adsorption of PS, PS-NH_2, and PS-COOH onto ChGO sponges is facilitated by a blend of electrostatic interactions, π–π interactions, and hydrogen bond interactions. The presence of these varied interaction types is crucial to the sponges' ability to effectively adsorb different derivatives of PS, showcasing their versatility and efficiency as adsorbents in a range of applications[65]. Graphite adsorbents can adsorb MPs/NPs via the π–π interactions. Yuan *et al.* found that the exceptional adsorption capacity (617.28 mg/g) of the three-dimensional reduced graphene oxide (3D RGO) towards polystyrene PS MPs was due to the strong π–π interactions between the graphite layers and the benzene rings in PS[50]. Similarly, Zhou *et al.* reported that the π–π interaction between the sp2-hybridized carbon in CuNi@C and the aromatic rings in PS MPs promoted the removal of PS MPs[71].

ADSORPTION BEHAVIOR OF MPS/NPS

Adsorption kinetic models are pivotal in evaluating the efficiency and identifying rate-determining steps in the removal of MPs/NPs onto carbon-based adsorbents, helping clarify the mechanisms involved in this

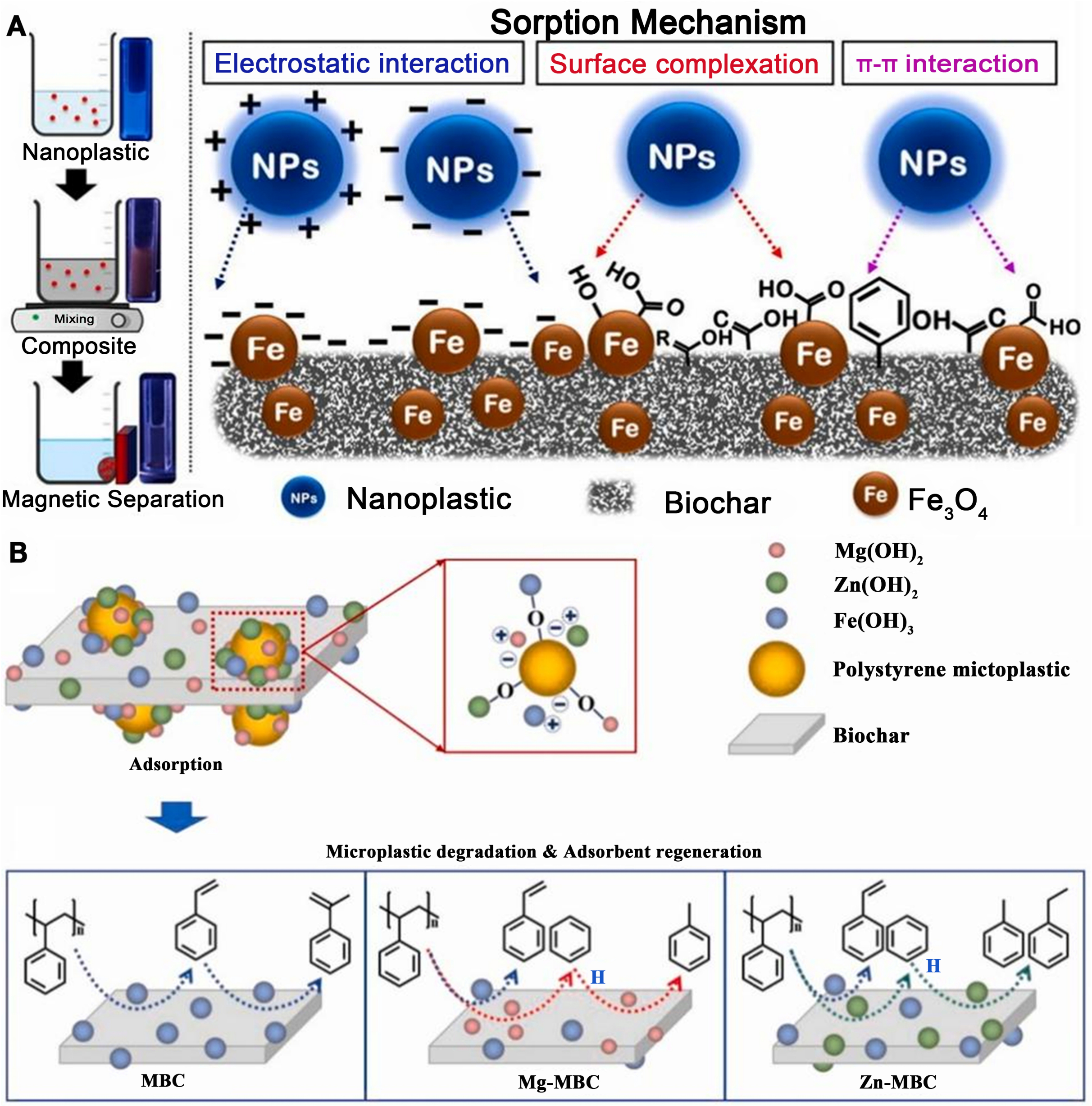

Figure 3. (A) Potential adsorption process and adsorption mechanisms of NPs on Fe-modified biochar[70], Copyright 2021, Elsevier; (B) Potential adsorption mechanisms of MPs on modified Mg/Zn biochar and the degradation of MP via thermal treatment[51], Copyright 2021, Elsevier. NPs: Nano-plastics; MPs: microplastics.

process[72]. The adsorption kinetics generally encompass four steps[73]: (1) bulk transport, which typically happens quickly; (2) film diffusion, a slower process; (3) intraparticle diffusion, also a slower step; and (4) adsorption attachment, which occurs rapidly. The generally used adsorption kinetic models for examining MPs/NPs adsorption on carbon-based adsorbents are the pseudo-first-order[74], pseudo-second-order[75], intraparticle diffusion, and film diffusion models[76]. The pseudo-first-order and pseudo-second-order models are utilized to analyze the entire adsorption process. In contrast, the intraparticle diffusion and liquid film diffusion models are particularly useful for delineating the rate-limiting steps within this process. If the adsorption mechanism's complexity is not adequately captured by the pseudo-first-order and pseudo-second-order models, this can be further elucidated using the intraparticle and liquid film diffusion models, providing a more comprehensive understanding of the adsorption dynamics.

The rate condition inherent in the direct form of both the pseudo-first and pseudo-second request templates can be represented as Qe, as detailed in Equations (1) and (2)[77,78].

$$\log(q_e - q_t) = \log q_e - \frac{k_1}{2.303}t \tag{1}$$

$$\frac{t}{q_t} = \frac{1}{k_2 q_e^2} + \frac{1}{q_e}t \tag{2}$$

The q_t represents the adsorption capacity at time t, q_e denotes the adsorption capacity at equilibrium (mg/g), k_1 is the constant for the pseudo-first-order reaction, and k_2 stands for the pseudo-second-order reaction constant.

Extensive research [Table 2] indicates that both pseudo-first-order and pseudo-second-order kinetic models are effective in characterizing carbon-based adsorbents' adsorption behavior. However, their applicability depends on the specific properties of each adsorbent. The pseudo-first-order model is typically favored for rapid adsorption processes occurring primarily on the adsorbent's surface, and it is suitable for materials where surface interactions are predominant. In contrast, the pseudo-second-order model is better for processes where adsorption kinetics are governed by chemical adsorption mechanisms, involving electron sharing or transfer. This model fits adsorbents with complex surface chemistries or those engaged in deeper adsorption processes. The adsorbent's inherent properties, such as surface area, pore size, functional groups, and chemical structure, are crucial in determining the most suitable model.

Adsorption isotherms are essential for understanding the equilibrium behavior of adsorbents at constant temperature, influenced by the nature of the adsorbate, adsorbent, and adsorption solution properties such as pH, ionic strength, and temperature[79]. Freundlich and Langmuir isotherm models are helpful in discerning the adsorption mechanism, whether linear monolayer coverage or multilayer adsorption[74].

The Freundlich isotherm model, which is used to describe the adsorption characteristics of heterogeneous surfaces, can be expressed in both nonlinear and linear forms. The nonlinear form of the Freundlich isotherm is given by[80]:

$$q_e = K_F C_e^{\frac{1}{N}} \tag{3}$$

$$\log q_e = \log K_F + \frac{1}{N}\log C_e \tag{4}$$

The Freundlich isotherm model is characterized by two coefficients: K_F (L/mg), which indicates the adsorption capacity, and N, which represents the strength of adsorption. These coefficients demonstrate that[78]:

(1) K_F quantifies the maximum amount of adsorbate that can be adsorbed per unit equilibrium concentration, reflecting the adsorbent's capacity to accumulate and retain the adsorbate.

(2) N and its inverse $1/N$ measure the adsorption intensity or the bond strength between adsorbate and

Table 2. The adsorption capacity of MPs/NPs on carbon-based adsorbents and their corresponding adsorption behavior

Carbon adsorbents	Water matrix	Adsorption performance	Adsorption behavior	Ref.
Granular activated carbon	Lake water	Adsorption capacity 6.33 mg·g^{-1}	Pseudo-second-order; Langmuir isotherm	[47]
3D RGO	Tap water	Adsorption capacity 448.60 mg·g^{-1}	Pseudo-second-order; Langmuir isotherm	[50]
Biochar	River water	Adsorption efficiency 75%	Pseudo-first-order; Langmuir isotherm	[64]
Cu–Ni carbon materials	Synthetic wastewater	Adsorption efficiency 99.18%	Pseudo-first-order; Langmuir isotherm	[71]
Zn-MBC	Tap water	Adsorption efficiency >92%	Pseudo-second-order; Langmuir isotherm	[52]
Mg/Zn-MBC	Synthetic solution	Removal efficiency >94%	Pseudo-second-order; Langmuir isotherm	[51]
Iron-modified fly ash	Freshwater	Adsorption capacity 89.9 mg·g^{-1}	Pseudo-first-order; Sips model	[53]
ChGO	Synthetic wastewater	Adsorption efficiency 89.8%	Pseudo-second-order; Langmuir isotherm	[65]
Magnetic CNTs	Synthetic wastewater	Adsorption capacity 1,650, 1,400, and 1,000 mg·g^{-1} for PE, PET, and PA, respectively	Pseudo-second-order; Freundlich isotherm	[49]
Corncob raw and oxidized biochar	Synthetic solution	Removal efficiency >90%	Pseudo-second-order; Langmuir isotherm	[68]

MPs: Microplastics; NPs: nano-plastics; 3D RGO: three-dimensional reduced graphene oxide; Zn-MBC: Zn modified magnetic biochar; Mg/Zn-MBC: Mg/Zn modified magnetic biochar; ChGO: sponge synthesized with chitin and GO; CNTs: carbon nanotubes; PE: polyethylene; PET: polyethylene terephthalate; PA: polyamide.

adsorbent, highlighting the surface's heterogeneity and the interaction's strength.

Unlike models predicting a saturation point, the Freundlich isotherm suggests an unlimited adsorption capacity, implying the potential for multilayer adsorption. The efficiency of the adsorption process under this model can be categorized as follows[81]:
(1) It is deemed efficient or favorable when $0 < 1/N < 1$, indicating a high affinity of the adsorbate for the adsorbent.
(2) It is considered inefficient or unfavorable when $1/N > 1$, indicating a low affinity.
(3) The process is seen as irreversible when $1/N = 1$, meaning the adsorbate, once adsorbed, remains firmly attached to the adsorbent.

The Langmuir model, assuming a uniform adsorbent surface with monolayer adsorption and no interaction between adsorbed molecules, is widely used[72]. The nonlinear and linear forms of the Langmuir model are as follows:

$$q_e = \frac{q_m K_L C_e}{1+K_L C_e} \tag{5}$$

$$\frac{C_e}{q_e} = \frac{C_e}{q_m} + \frac{1}{K_L q_m} \tag{6}$$

where q_m (mg/g) is the maximum adsorption capacity; K_L (L/mg) is the Langmuir isotherm constant.

Based on Table 2, it is clearly seen that the Langmuir isotherm model is predominantly used for describing MPs/NPs adsorption on carbon-based adsorbents, suggesting monolayer adsorption on a homogeneous surface without significant interaction between adsorbed molecules.

EFFECT OF INFLUENCING FACTORS ON THE ADSORPTION PERFORMANCE

The elimination of MPs/NPs from water via adsorption is impacted by the characteristics of the adsorbent as well as the chemical properties of the water. While earlier discussions were centered on how the structure of the adsorbent influences its efficacy, we will now turn our attention to the particular elements that govern the adsorption process of MPs/NPs. These elements include pH level, dissolved organic matter (DOM), metal ions, and anions.

pH value

In aquatic environments, pH value significantly affects both the adsorbents' and MPs/NPs' surface charges, playing a key role in their adsorption process. This factor chiefly determines the electrostatic interactions between the MPs/NPs and carbon adsorbents and influences how the plastic particles cluster together. Research has consistently shown the pH-dependence of the MP/NP adsorption process, noting that a pH range slightly towards the acidic to basic side, usually around 4 to 8, is optimal for enhancing the electrostatic attraction during adsorption. Nonetheless, it is noteworthy that in instances where dominant adsorption mechanisms such as surface complexation are present, the pH's effect on the efficiency of MPs/NPs adsorption may be relatively insignificant.

Metal ions

Metal ions are frequently present in water resources, especially K^+, Na^+, Mg^{2+}, Ca^{2+}, Fe^{3+}, and Al^{3+}. The impact of K^+/Na^+ ions on MPs/NPs adsorption is usually considered to be minimal[53]. The effect of multivalent cations, including those with charges of +2 and +3, on the removal of MPs/NPs has been found to vary across different studies. One observed impact is that these high-valence cations can diminish the adsorption of MPs/NPs. This reduction in adsorption efficiency is attributed to the strong affinity these cations have for the adsorbents, which competes with and potentially hinders the binding of MPs/NPs to the adsorbent surfaces[53,82]. Furthermore, certain metal ions, such as Mg^{2+}, Ca^{2+}, and Fe^{3+}, can improve the aggregation of MPs/NPs through electrostatic attraction. This aggregation process can restrict the diffusion of MPs/NPs into the porous structure of carbon adsorbents, potentially impacting the adsorption effectiveness. However, it is important to acknowledge that ions like Ca^{2+} and Mg^{2+} ions might also enhance the adsorption efficiency. They can create new adsorption sites on the adsorbents through a bridging effect, thereby potentially improving the overall removal efficiency of MPs/NPs [Figure 4][47].

Anions

Anions such as Cl^-, SO_4^{2-}, CO_3^{2-}, and PO_4^{3-} have an impact on the process of adsorbing MPs/NPs. These anions often obstruct the adsorbent-MPs/NPs interactions due to their propensity to bind with the adsorbents. Specifically, when using Cu-Ni/carbon materials for MPs/NPs removal, HCO_3^- largely alters the efficiency. This effect is attributed to the hydrolysis of HCO_3^-, which produces OH^- ions, subsequently raising the pH of the solution. This pH increase leads to stronger electrostatic repulsion between the MPs/NPs and the Cu-Ni carbon, affecting the adsorption dynamics. This relationship between different anions and the adsorption process is also reflected in the studies conducted by Ganie *et al.*[64]. On the other hand, the efficacy of Zn-BMC in adsorbing PS MPs is negatively affected by the presence of anions, with their impact decreasing in the order: $NO_3^- < SO_4^{2-} < Cl^- < HCO_3^- < H_2PO_4^-$. It is suggested that the particularly strong effect of $H_2PO_4^-$ ions stems from their higher charge density, leading to more competitive adsorption on the surface of the adsorbent. This indicates the complexities involved in the adsorption process. Variables such as the concentration of anions, the surface characteristics of MPs/NPs, and the

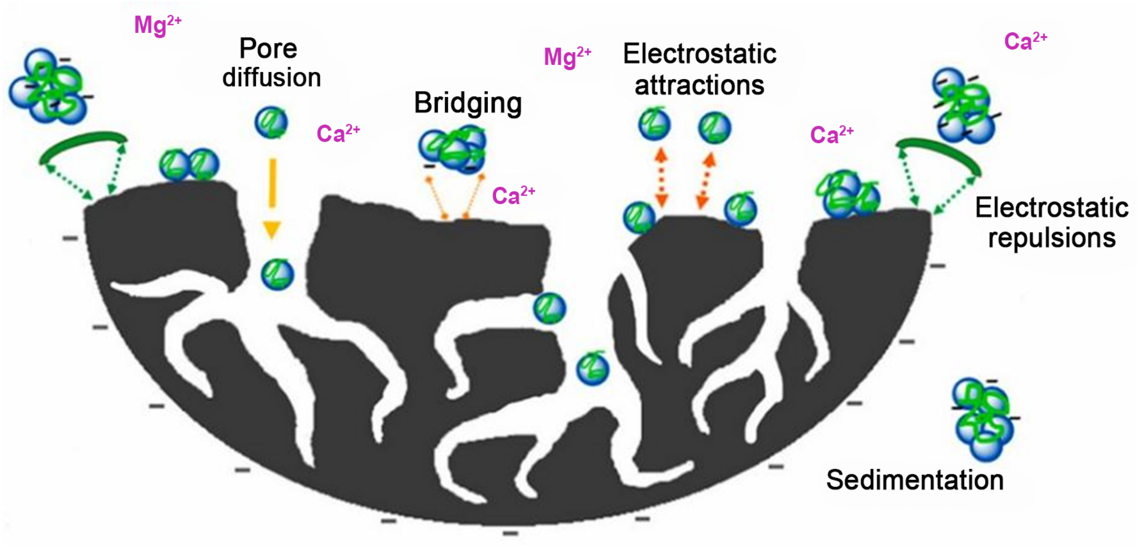

Figure 4. Potential adsorption mechanisms of PS NPs on AC, with the existence of Mg^{2+} and Ca^{2+} ions[47]. PS: Polystyrene; NPs: nanoplastics; AC: activated carbon.

unique features of the adsorbents used contribute to diverse outcomes across different studies. These discrepancies underscore the importance of comprehensively understanding the environmental and material-specific factors that affect adsorption behavior in each distinct situation[52].

DOM

DOM in water systems is a diverse and complex collection of polyelectrolytes. The way DOM interacts with MPs/NPs can affect how MPs adhere to adsorbents, as it changes the surface characteristics of both MPs/NPs and the carbon adsorbents. For example, research[64] has demonstrated that humic acid can notably hinder the adsorption of PS NPs, causing a marked reduction in their removal efficiency (decreasing by 55%-75%). This reduction in adsorption is due to the coating and stabilization of the NPs and the adsorbents, such as BC-750, which creates strong electrostatic repulsion and consequently lowers the effectiveness of the adsorption process. It is important to mention, however, that even in an electrostatically unfavorable environment and in the presence of DOM at concentrations as high as 10 mg/L, sorption of NPs can still occur. This phenomenon can be explained by the more effective complexation of NPs on available adsorption sites, rather than their coverage by DOM[70].

CONCLUSION AND PERSPECTIVES

In this comprehensive review, we delve into the recent advancements in carbon-based adsorbents and their role in eliminating MPs/NPs from water. A key focus is understanding the adsorption mechanism between these adsorbents and MPs/NPs. We then discuss the various methods of synthesizing these adsorbents and analyze their adsorption behaviors. Critical experimental parameters, such as pH value, anions, DOM, and metal ions, can impact the performance of carbon adsorbents to a different degree.

The removal of MPs/NPs from wastewater is crucial for reducing the harmful effects of plastics on various life forms. Despite some advancements, the field of MP/NP adsorption is still emerging, and current research is insufficient for fully resolving this issue. This section outlines challenges and future directions for MP/NP adsorption in water systems:

(1) For adsorbents to be practically viable, their ability to desorb and be reused is vital. Although

regeneration of adsorbents through thermal and chemical processes has been studied, more research is needed to efficiently desorb MPs/NPs, recycle adsorbents, and restore their adsorption capacity.

(2) The longevity and ecological implications of adsorbents are crucial factors. The degradation of adsorbents might result in metal leakage or nanoparticle emission, leading to secondary contamination. Moreover, adsorbents may react with other substances in water to form new pollutants. It is essential to evaluate adsorbents' stability in actual water environments and to develop efficient methods for their post-use removal.

(3) Although adsorption is effective for removing MPs/NPs, it can be influenced by water characteristics and might require significant time for optimal removal efficiency. Merging adsorption with other techniques such as magnetic separation or filtration could improve efficiency and cut costs. Notably, combining adsorption with magnetic separation using magnetic adsorbents has shown potential due to its high effectiveness and easy separation process. Future research should concentrate on creating such hybrid methods for various water environments.

(4) To enhance understanding of adsorbent-MP/NP interactions and facilitate the development of more effective adsorbents, it is necessary to combine the adsorption tests with computational tools. Such methods can assist in designing superior adsorbent materials by providing meaningful insights into adsorption mechanisms.

DECLARATIONS

Authors' contributions

Conceptualization, figures, table, and writing - original draft preparation: Zheng H
Writing - reviewing and editing: Chen Q, Chen Z
Supervision: Chen Z

Availability of data and materials

Not applicable.

Financial support and sponsorship

None.

Conflicts of interest

All authors declared that there are no conflicts of interest. Chen Z is an Editorial Board member of the journal *Water Emerging Contaminants* & *Nanoplastics*.

Ethical approval and consent to participate

Not applicable.

Consent for publication

Not applicable.

Copyright

REFERENCES

1. Zhao K, Wei Y, Dong J, et al. Separation and characterization of microplastic and nanoplastic particles in marine environment. *Environ Pollut* 2022;297:118773. DOI PubMed
2. Ali I, Tan X, Li J, et al. Innovations in the development of promising adsorbents for the remediation of microplastics and nanoplastics - a critical review. *Water Res* 2023;230:119526. DOI PubMed
3. Aslani H, Pashmtab P, Shaghaghi A, Mohammadpoorasl A, Taghipour H, Zarei M. Tendencies towards bottled drinking water

consumption: challenges ahead of polyethylene terephthalate (PET) waste management. *Health Promot Perspect* 2021;11:60-8. DOI PubMed PMC

4. Ali I, Tan X, Li J, et al. Interaction of microplastics and nanoplastics with natural organic matter (NOM) and the impact of NOM on the sorption behavior of anthropogenic contaminants - a critical review. *J Clean Prod* 2022;376:134314. DOI
5. Luo X, Wang Z, Yang L, Gao T, Zhang Y. A review of analytical methods and models used in atmospheric microplastic research. *Sci Total Environ* 2022;828:154487. DOI PubMed
6. Alimi OS, Farner Budarz J, Hernandez LM, Tufenkji N. Microplastics and nanoplastics in aquatic environments: aggregation, deposition, and enhanced contaminant transport. *Environ Sci Technol* 2018;52:1704-24. DOI PubMed
7. Ding J, Li J, Sun C, et al. An examination of the occurrence and potential risks of microplastics across various shellfish. *Sci Total Environ* 2020;739:139887. DOI PubMed
8. Jahnke A, Arp HPH, Escher BI, et al. Reducing uncertainty and confronting ignorance about the possible impacts of weathering plastic in the marine environment. *Environ Sci Technol Lett* 2017;4:85-90. DOI
9. Lang M, Yu X, Liu J, et al. Fenton aging significantly affects the heavy metal adsorption capacity of polystyrene microplastics. *Sci Total Environ* 2020;722:137762. DOI PubMed
10. Wright SL, Kelly FJ. Plastic and human health: a micro issue? *Environ Sci Technol* 2017;51:6634-47. DOI PubMed
11. Chen Y, Kang K, Guo L, Kang J, Qi H. Facile synthesis of functional holocellulose fibers for removal of micro-/nanoparticles of plastics from waste water. *Chem Eng J* 2023;457:141251. DOI
12. Chen Z, Shi X, Zhang J, Wu L, Wei W, Ni BJ. Nanoplastics are significantly different from microplastics in urban waters. *Water Res X* 2023;19:100169. DOI PubMed PMC
13. Wei W, Hao Q, Chen Z, Bao T, Ni BJ. Polystyrene nanoplastics reshape the anaerobic granular sludge for recovering methane from wastewater. *Water Res* 2020;182:116041. DOI PubMed
14. Ali I, Cheng Q, Ding T, et al. Micro- and nanoplastics in the environment: Occurrence, detection, characterization and toxicity - a critical review. *J Clean Prod* 2021;313:127863. DOI
15. Ali I, Ding T, Peng C, et al. Micro- and nanoplastics in wastewater treatment plants: occurrence, removal, fate, impacts and remediation technologies - a critical review. *Chem Eng J* 2021;423:130205. DOI
16. Chen Z, Wei W, Liu X, Ni BJ. Emerging electrochemical techniques for identifying and removing micro/nanoplastics in urban waters. *Water Res* 2022;221:118846. DOI
17. Shi X, Chen Z, Wei W, Chen J, Ni B. Toxicity of micro/nanoplastics in the environment: roles of plastisphere and eco-corona. *Soil Environ Health* 2023;1:100002. DOI
18. Zhuo M, Chen Z, Liu X, Wei W, Shen Y, Ni BJ. A broad horizon for sustainable catalytic oxidation of microplastics. *Environ Pollut* 2024;340:122835. DOI
19. Ya H, Jiang B, Xing Y, Zhang T, Lv M, Wang X. Recent advances on ecological effects of microplastics on soil environment. *Sci Total Environ* 2021;798:149338. DOI
20. Ragusa A, Svelato A, Santacroce C, et al. Plasticenta: first evidence of microplastics in human placenta. *Environ Int* 2021;146:106274. DOI
21. Nizzetto L, Langaas S, Futter M. Pollution: do microplastics spill on to farm soils? *Nature* 2016;537:488. DOI
22. EFSA Panel on Contaminants in the Food Chain (CONTAM). Presence of microplastics and nanoplastics in food, with particular focus on seafood. *EFSA J* 2016;14:e04501. DOI
23. Baudrimont M, Arini A, Guégan C, et al. Ecotoxicity of polyethylene nanoplastics from the North Atlantic oceanic gyre on freshwater and marine organisms (microalgae and filter-feeding bivalves). *Environ Sci Pollut Res Int* 2020;27:3746-55. DOI
24. Sharma S, Basu S, Shetti NP, Nadagouda MN, Aminabhavi TM. Microplastics in the environment: occurrence, perils, and eradication. *Chem Eng J* 2021;408:127317. DOI PubMed PMC
25. Shen M, Song B, Zhu Y, et al. Removal of microplastics via drinking water treatment: current knowledge and future directions. *Chemosphere* 2020;251:126612. DOI
26. Zhang Z, Chen Y. Effects of microplastics on wastewater and sewage sludge treatment and their removal: a review. *Chem Eng J* 2020;382:122955. DOI
27. Chen Z, Wei W, Chen X, Liu Y, Shen Y, Ni B. Upcycling of plastic wastes for hydrogen production: advances and perspectives. *Renew Sustain Energy Rev* 2024;195:114333. DOI
28. Zhang J, Chen Z, Liu Y, Wei W, Ni B. Removal of emerging contaminants (ECs) from aqueous solutions by modified biochar: a review. *Chem Eng J* 2024;479:147615. DOI
29. Shi X, Chen Z, Wu L, Wei W, Ni B. Microplastics in municipal solid waste landfills: detection, formation and potential environmental risks. *Curr Opin Environ Sci Health* 2023;31:100433. DOI
30. Zaki MRM, Aris AZ. An overview of the effects of nanoplastics on marine organisms. *Sci Total Environ* 2022;831:154757. DOI PubMed
31. Wang C, Wei W, Chen Z, Wang Y, Chen X, Ni BJ. Polystyrene microplastics and nanoplastics distinctively affect anaerobic sludge treatment for hydrogen and methane production. *Sci Total Environ* 2022;850:158085. DOI
32. Shi X, Chen Z, Liu X, Wei W, Ni BJ. The photochemical behaviors of microplastics through the lens of reactive oxygen species: photolysis mechanisms and enhancing photo-transformation of pollutants. *Sci Total Environ* 2022;846:157498. DOI
33. Goh PS, Kang HS, Ismail AF, Khor WH, Quen LK, Higgins D. Nanomaterials for microplastic remediation from aquatic environment:

why nano matters? *Chemosphere* 2022;299:134418. DOI PubMed

34. Xu Q, Huang Q, Luo T, Wu R, Wei W, Ni B. Coagulation removal and photocatalytic degradation of microplastics in urban waters. *Chem Eng J* 2021;416:129123. DOI
35. Ricardo IA, Alberto EA, Silva Júnior AH, et al. A critical review on microplastics, interaction with organic and inorganic pollutants, impacts and effectiveness of advanced oxidation processes applied for their removal from aqueous matrices. *Chem Eng J* 2021;424:130282. DOI
36. Ebrahimbabaie P, Yousefi K, Pichtel J. Photocatalytic and biological technologies for elimination of microplastics in water: current status. *Sci Total Environ* 2022;806:150603. DOI PubMed
37. Masiá P, Sol D, Ardura A, et al. Bioremediation as a promising strategy for microplastics removal in wastewater treatment plants. *Mar Pollut Bull* 2020;156:111252. DOI
38. Malankowska M, Echaide-gorriz C, Coronas J. Microplastics in marine environment: a review on sources, classification, and potential remediation by membrane technology. *Environ Sci Water Res Technol* 2021;7:243-58. DOI
39. Fu F, Wang Q. Removal of heavy metal ions from wastewaters: a review. *J Environ Manage* 2011;92:407-18. DOI PubMed
40. Tang X, Zhou Y, Xu Y, Zhao Q, Zhou X, Lu J. Sorption of polycyclic aromatic hydrocarbons from aqueous solution by hexadecyltrimethylammonium bromide modified fibric peat. *J Chem Technol Biotechnol* 2010;85:1084-91. DOI
41. Zhou Y, Chen L, Lu P, Tang X, Lu J. Removal of bisphenol A from aqueous solution using modified fibric peat as a novel biosorbent. *Sep Purif Technol* 2011;81:184-90. DOI
42. Zhou Y, Zhang R, Gu X, Lu J. Adsorption of divalent heavy metal ions from aqueous solution by citric acid modified pine sawdust. *Sep Sci Technol* 2015;50:245-52. DOI
43. Liu Q, Li Y, Chen H, et al. Superior adsorption capacity of functionalised straw adsorbent for dyes and heavy-metal ions. *J Hazard Mater* 2020;382:121040. DOI
44. Asere TG, Stevens CV, Du Laing G. Use of (modified) natural adsorbents for arsenic remediation: a review. *Sci Total Environ* 2019;676:706-20. DOI PubMed
45. Chen Z, Liu X, Wei W, Chen H, Ni BJ. Removal of microplastics and nanoplastics from urban waters: separation and degradation. *Water Res* 2022;221:118820. DOI
46. Chen Z, Fang J, Wei W, Ngo HH, Guo W, Ni B. Emerging adsorbents for micro/nanoplastics removal from contaminated water: advances and perspectives. *J Clean Prod* 2022;371:133676. DOI
47. Arenas L, Ramseier Gentile S, Zimmermann S, Stoll S. Nanoplastics adsorption and removal efficiency by granular activated carbon used in drinking water treatment process. *Sci Total Environ* 2021;791:148175. DOI PubMed
48. Kazemi Shariat Panahi H, Dehhaghi M, Ok YS, et al. A comprehensive review of engineered biochar: Production, characteristics, and environmental applications. *J Clean Prod* 2020;270:122462. DOI
49. Tang Y, Zhang S, Su Y, Wu D, Zhao Y, Xie B. Removal of microplastics from aqueous solutions by magnetic carbon nanotubes. *Chem Eng J* 2021;406:126804. DOI
50. Yuan F, Yue L, Zhao H, Wu H. Study on the adsorption of polystyrene microplastics by three-dimensional reduced graphene oxide. *Water Sci Technol* 2020;81:2163-75. DOI
51. Wang J, Sun C, Huang QX, Chi Y, Yan JH. Adsorption and thermal degradation of microplastics from aqueous solutions by Mg/Zn modified magnetic biochars. *J Hazard Mater* 2021;419:126486. DOI
52. Wang Q, Zhao Y, Shi Z, et al. Magnetic amino-functionalized-MOF(M = Fe, Ti, Zr)@COFs with superior biocompatibility: performance and mechanism on adsorption of azo dyes in soft drinks. *Chem Eng J* 2021;420:129955. DOI
53. Zhao H, Huang X, Wang L, et al. Removal of polystyrene nanoplastics from aqueous solutions using a novel magnetic material: adsorbability, mechanism, and reusability. *Chem Eng J* 2022;430:133122. DOI
54. Kumar R, Verma A, Rakib MRJ, et al. Adsorptive behavior of micro(nano)plastics through biochar: co-existence, consequences, and challenges in contaminated ecosystems. *Sci Total Environ* 2023;856:159097. DOI
55. Li Z, Xie W, Zhang Z, Wei S, Chen J, Li Z. Multifunctional sodium alginate/chitosan-modified graphene oxide reinforced membrane for simultaneous removal of nanoplastics, emulsified oil, and dyes in water. *Int J Biol Macromol* 2023;245:125524. DOI
56. Peng G, Xiang M, Wang W, et al. Engineering 3D graphene-like carbon-assembled layered double oxide for efficient microplastic removal in a wide pH range. *J Hazard Mater* 2022;433:128672. DOI
57. Mehmood T, Mustafa B, Mackenzie K, et al. Recent developments in microplastic contaminated water treatment: progress and prospects of carbon-based two-dimensional materials for membranes separation. *Chemosphere* 2023;316:137704. DOI
58. Yang X, Wan Y, Zheng Y, et al. Surface functional groups of carbon-based adsorbents and their roles in the removal of heavy metals from aqueous solutions: a critical review. *Chem Eng J* 2019;366:608-21. DOI PubMed PMC
59. Zheng B, Li B, Wan H, Lin X, Cai Y. Coral-inspired environmental durability aerogels for micron-size plastic particles removal in the aquatic environment. *J Hazard Mater* 2022;431:128611. DOI
60. Zhu N, Yan Q, He Y, et al. Insights into the removal of polystyrene nanoplastics using the contaminated corncob-derived mesoporous biochar from mining area. *J Hazard Mater* 2022;433:128756. DOI
61. Wang C, Huang R, Sun R, Yang J, Dionysiou DD. Microplastics separation and subsequent carbonization: synthesis, characterization, and catalytic performance of iron/carbon nanocomposite. *J Clean Prod* 2022;330:129901. DOI
62. Li H, Tang M, Wang J, et al. Theoretical and experimental investigation on rapid and efficient adsorption characteristics of microplastics by magnetic sponge carbon. *Sci Total Environ* 2023;897:165404. DOI

63. Liu Y, Li B, Li R, et al. Simultaneous removal of microplastics and doxycycline and preparation of novel hollow carbon nanocakes by pyrolysis. *Chem Eng J* 2023;472:144999. DOI
64. Ganie ZA, Khandelwal N, Tiwari E, Singh N, Darbha GK. Biochar-facilitated remediation of nanoplastic contaminated water: effect of pyrolysis temperature induced surface modifications. *J Hazard Mater* 2021;417:126096. DOI PubMed
65. Sun C, Wang Z, Chen L, Li F. Fabrication of robust and compressive chitin and graphene oxide sponges for removal of microplastics with different functional groups. *Chem Eng J* 2020;393:124796. DOI
66. Cui L, Wang Y, Gao L, et al. EDTA functionalized magnetic graphene oxide for removal of Pb(II), Hg(II) and Cu(II) in water treatment: adsorption mechanism and separation property. *Chem Eng J* 2015;281:1-10. DOI
67. Siipola V, Pflugmacher S, Romar H, Wendling L, Koukkari P. Low-cost biochar adsorbents for water purification including microplastics removal. *Appl Sci* 2020;10:788. DOI
68. Abdoul Magid ASI, Islam MS, Chen Y, et al. Enhanced adsorption of polystyrene nanoplastics (PSNPs) onto oxidized corncob biochar with high pyrolysis temperature. *Sci Total Environ* 2021;784:147115. DOI
69. Atugoda T, Vithanage M, Wijesekara H, et al. Interactions between microplastics, pharmaceuticals and personal care products: implications for vector transport. *Environ Int* 2021;149:106367. DOI
70. Singh N, Khandelwal N, Ganie ZA, Tiwari E, Darbha GK. Eco-friendly magnetic biochar: an effective trap for nanoplastics of varying surface functionality and size in the aqueous environment. *Chem Eng J* 2021;418:129405. DOI
71. Zhou G, Huang X, Xu H, et al. Removal of polystyrene nanoplastics from water by Cu–Ni carbon material: the role of adsorption. *Sci Total Environ* 2022;820:153190. DOI
72. Li H, Wang F, Li J, Deng S, Zhang S. Adsorption of three pesticides on polyethylene microplastics in aqueous solutions: kinetics, isotherms, thermodynamics, and molecular dynamics simulation. *Chemosphere* 2021;264:128556. DOI
73. Ho YS, Ng JCY, Mckay G. Kinetics of pollutant sorption by biosorbents: review. *Sep Purif Methods* 2000;29:189-232. DOI
74. Zhang J, Chen H, He H, et al. Adsorption behavior and mechanism of 9-nitroanthracene on typical microplastics in aqueous solutions. *Chemosphere* 2020;245:125628. DOI
75. Guo X, Liu Y, Wang J. Sorption of sulfamethazine onto different types of microplastics: a combined experimental and molecular dynamics simulation study. *Mar Pollut Bull* 2019;145:547-54. DOI PubMed
76. Zhang H, Wang J, Zhou B, et al. Enhanced adsorption of oxytetracycline to weathered microplastic polystyrene: kinetics, isotherms and influencing factors. *Environ Pollut* 2018;243:1550-7. DOI
77. Wadhawan S, Jain A, Nayyar J, Mehta SK. Role of nanomaterials as adsorbents in heavy metal ion removal from waste water: a review. *J Water Process Eng* 2020;33:101038. DOI
78. Rajendran S, Priya AK, Senthil Kumar P, et al. A critical and recent developments on adsorption technique for removal of heavy metals from wastewater - a review. *Chemosphere* 2022;303:135146. DOI
79. Al-Ghouti MA, Da'ana DA. Guidelines for the use and interpretation of adsorption isotherm models: a review. *J Hazard Mater* 2020;393:122383. DOI PubMed
80. Freundlich H. Over the adsorption in solution. *J Phys Chem* 1906;57:1100-7.
81. Febrianto J, Kosasih AN, Sunarso J, Ju YH, Indraswati N, Ismadji S. Equilibrium and kinetic studies in adsorption of heavy metals using biosorbent: a summary of recent studies. *J Hazard Mater* 2009;162:616-45. DOI PubMed
82. Tiwari E, Singh N, Khandelwal N, Monikh FA, Darbha GK. Application of Zn/Al layered double hydroxides for the removal of nano-scale plastic debris from aqueous systems. *J Hazard Mater* 2020;397:122769. DOI PubMed

Ali *et al. Water Emerg Contam Nanoplastics* 2024;3:12
DOI: 10.20517/wecn.2023.73

Water Emerging Contaminants & Nanoplastics

Review

Open Access

A review on the presence of microplastics in environmental matrices within Southeast Asia: elucidating risk information through an analysis of microplastic characteristics such as size, shape, and type

Ahmad Ammarluddin Mohd Ali[1], Aina Arifah Khalid[1], Nur Izzati Abd Razak[1], Nur Syafiqah Mohd Maulana[1], Nur Sakinah Roslan[1], Raz Shauqeena Batrisyea Razmi[1], Wan Mohamad Akif Wan Ruseli[2], Yusof Shuaib Ibrahim[1,2,3], Maisarah Jaafar[1,3], Rohani Shahrudin[1,3], Khaira Ismail[1], Sabiqah Tuan Anuar[1,3]

[1]Faculty of Science and Marine Environment, Universiti Malaysia Terengganu, Terengganu, 21030 Kuala Nerus, Malaysia.
[2]Institute of Oceanography and Environment (INOS), Universiti Malaysia Terengganu, Terengganu, 21030 Kuala Nerus, Malaysia.
[3]Microplastic Research Interest Group (MRIG), Faculty of Science and Marine Environment, Universiti Malaysia Terengganu, Terengganu, 21030 Kuala Nerus, Malaysia.

Correspondence to: Sabiqah Tuan Anuar, Microplastic Research Interest Group (MRIG), Faculty of Science and Marine Environment, Universiti Malaysia Terengganu, Terengganu, 21030 Kuala Nerus, Malaysia. E-mail: sabiqahanuar@umt.edu.my

How to cite this article: Mohd Ali AA, Khalid AA, Abd Razak NI, Mohd Maulana NS, Roslan NS, Razmi RSB, Wan Ruseli WMA, Ibrahim YS, Jaafar M, Shahrudin R, Ismail K, Anuar ST. A review on the presence of microplastics in environmental matrices within Southeast Asia: elucidating risk information through an analysis of microplastic characteristics such as size, shape, and type. *Water Emerg Contam Nanoplastics* 2024;3:12. https://dx.doi.org/10.20517/wecn.2023.73

Received: 16 Dec 2023 **First Decision:** 6 Mar 2024 **Revised:** 8 Apr 2024 **Accepted:** 11 Apr 2024 **Published:** 19 Apr 2024

Academic Editor: Joana C Prata **Copy Editor:** Pei-Yun Wang **Production Editor:** Pei-Yun Wang

Abstract

Microplastics' ecotoxicological potential in almost all ecosystems makes them a global environmental issue. This review evaluates Southeast Asian microplastic contamination data from 2013 to 2023. This evaluation examined 285 research publications from Scopus, Web of Science, and ScienceDirect, mostly on sediment and water matrices. Based on their size, shape, polymer type, and potential risks from polymer hazards in Southeast Asian countries, this analysis assesses microplastic pollution in biota, sediment, water, and other environmental matrices. The majority of microplastics in this region are small (46%) and large (32%). Within the biota matrix, small microplastics (SMP) and large microplastics (LMP) dominated. Fibers predominated in all matrices, particularly the biota matrix. Polyethylene emerged as the most abundant polymer type (22%), found in all four matrices. Despite being less abundant, polyurethane and polyamide have high hazard scores, raising ecological concerns due to their detrimental effects on environmental matrices. According to the analyzed data, Southeast Asian countries face significant risks due to high levels of microplastic contamination in water, sediments, biota, and other matrices. However, there are noticeable discrepancies in Southeast Asian data, indicating progress in microplastic research, with most data coming from Indonesia, Thailand, Malaysia, Vietnam, and the Philippines and little information in the literature regarding microplastic contamination from East Timor, Laos, Brunei, Myanmar, and Cambodia.

Keywords: Asia and Western Pacific, marine debris, microplastics risk, polymer hazard

INTRODUCTION

The inadequate disposal plans, accidental loss, and fragmentation of larger plastics have contributed to the increasing accumulation of tiny plastic particles and fibers (microplastics with sizes of < 5 mm) in the environment[1]. The path of plastic leakage starts from land to a canal or a river, and then ends up in the water, sediment, biota, and also humans[2-5]. Plastic bags, fishing gear, food containers, and beverages are the most common waste ingredients that contribute to microplastic emissions in rivers[6]. Additionally, microplastics can be categorized as either primary or secondary, depending on their origin. Primary microplastics intentionally produced by humans[7], such as plastic resins and microbeads in cosmetic products, can be carried with wastewaters[8,9]. Conversely, secondary sources result from the breakdown of plastic items into smaller fragments due to processes like oxidation, ultraviolet (UV) radiation, and mechanical forces[10]. During the photodegradation of plastics, sunlight containing UV irradiation triggers oxidation, breaking down the chemical bond of the polymer chains in larger plastics[11,12]; this process also subjects the plastics to mechanical stress and biotic fragmentation[13]. In the water ecosystem, microplastic fragments are easily exposed to sunlight, and their degradation rate increases with higher levels of oxygen[14].

Microplastics exhibit a range of characteristics, encompassing diverse sizes, shapes, and polymeric compositions[15,16]. To illustrate, they are typically classified into two categories based on their dimensions: large microplastics (LMP), ranging from 1 to 5 mm, and small microplastics (SMP), ranging from 0 μm to 1 mm[4]. Various shapes are observed among microplastics, including fragments, fibers, pellets, films, and foam. Certain shapes may predominate in specific water columns[17]. Microplastics in the fragment form, for example, are mostly found on the water surface[18,19], whereas fibers and pellets are found to be dominant in the sediment[20]. Furthermore, as microplastics become smaller in size in the ocean, the potential for microplastics to be ingested by marine organisms increases, with their availability in both pelagic and benthic habitats[21,22]. Microplastics in the aquatic ecosystem take much longer to degrade than those on land due to the presence of salt and the lower temperature[23]. They can also be distributed in specific water columns due to their polymer density[24], and can enter the aquatic food chain from the highest to the lowest trophic levels due to this condition. Consequently, microplastics have been found in a variety of biota[25], including microscopic organisms like zooplankton[26], small marine organisms like barnacles[27], lugworms, mussels[28], and large marine organisms such as pelagic fish[10,22], which inadvertently ingest these particles mistaking them for food.

However, microplastics can leach out chemicals depending on various factors such as the type of plastic, environmental conditions, and the presence of additives[29], raising concerns about potential ecological and human health impacts[30]. When microplastics are ingested by organisms, there is the possibility that the leached chemicals could be transferred through the food web[31]. Therefore, based on the chemical compositions of the plastic polymers, plastic hazard scores have been developed to calculate the risk assessment on the polymer hazard index towards the environmental matrices[32]. Additionally, different polymers have different chemical compositions, and some may contain additives that could be of concern. For example, acrylonitrile butadiene styrene (ABS) and polyvinyl chloride (PVC) may contain additives (i.e., polyisobutylene, polyacrylates, polymetacrylates, oil-soluble polymers and copolymers of allyl and vinyl monomers, derivatives of alkyl naphthalene, and alkylphenols) that are known to be toxic and pose a high risk[32,33]. Hence, polymer risk assessment of microplastics is crucial for several reasons, as it helps understand and reduce the potential environmental and human health impacts associated with the presence of these contaminants in various ecosystems. The lack of such assessments in Southeast Asia poses several challenges and concerns. This region, known for its biodiversity, ecosystems, and high population density, is particularly susceptible to microplastic pollution. Currently, there are limited reports available on polymer risk assessments in Southeast Asia. For instance, the microplastics in surface seawater from the shore of the Rayong province in Thailand were found to contain polypropylene (PP), polyethylene (PE), and polystyrene (PS) polymer, which fell within the medium-risk category[34]. Additionally, research conducted in concentrated and peatland areas of Vietnam detected concentrations of PVC, polycarbonate (PC), and PP, where PVC, extensively utilized in industrial processes, fell into the extremely dangerous risk category[35]. However, there is a gap in reported data on polymer risk assessments in other Southeast Asian countries. Addressing this gap is crucial for developing strategies to protect the ecosystems and biodiversity of these countries from the harmful effects of microplastic polymers. Polymer risk assessments contribute to the development of effective waste management strategies. By understanding the risks posed by specific polymers, authorities can implement targeted measures to reduce their environmental presence.

Plastics found in the world's oceans have been a cause for concern; however, it is only quite recently that attention has turned to plastic waste in various environmental matrices[36,37]. Rivers in Southeast Asia notably contribute to the influx of plastic pollution into the marine environment[38-40]. Over half (58%, n = 29) of the estimated top 50 plastic-emitting rivers in the world are located in Southeast Asian nations[41]. Malaysia, along with the Philippines, Indonesia, and Singapore, is one of the four megadiverse countries in the tropical Associations of Southeast Asian Nations (ASEAN) region, producing an enormous 0.5-1.9 kg/capita/day of municipal solid waste (MSW), with plastic wastes accounting for an estimated 25% of the overall composition[42]. Nonetheless, the field and environmental data on the prevalence of plastic pollution in the marine environment particularly in Southeast Asia is limited, which is one of the continents with the least amount of study on microplastic contamination[38]. This review aims to identify the diverse characteristics of microplastics in different environmental matrices, such as size, shape, and type of microplastic polymers, drawing from various studies reported in Southeast Asia over the last decade. With the compilation of the data, we then evaluate the potential toxicity effects of microplastic polymer in all matrices by conducting polymer risk assessment based on their polymer hazard score. To the best of our knowledge, this is the first scientific paper that estimates how much microplastic research may be under or over-estimating current levels of microplastics based on the impact of microplastics on the environmental matrix, and also provides recommended reporting criteria and a way forward for future improvements on microplastics mitigation frameworks in Southeast Asia.

METHODS

Study area

Southeast Asia consists of 11 countries, namely Brunei Darussalam, Cambodia, Indonesia, Laos (the only land-locked country), Malaysia, Myanmar, the Philippines, Singapore, Timor-Leste, Thailand, and Vietnam. With about 25,000 islands and 150,000 km of coastline, Southeast Asia is a wealthy and biodiverse region that is home to 25%-33% of the world's mangrove forests and 34% of its coral reefs, which are home to a variety of tropical marine animals[43]. Southeast Asian countries share several geographical and environmental characteristics that can contribute to common challenges related to the sources and transport of pollution, including microplastics. Many Southeast Asian countries are connected by the South

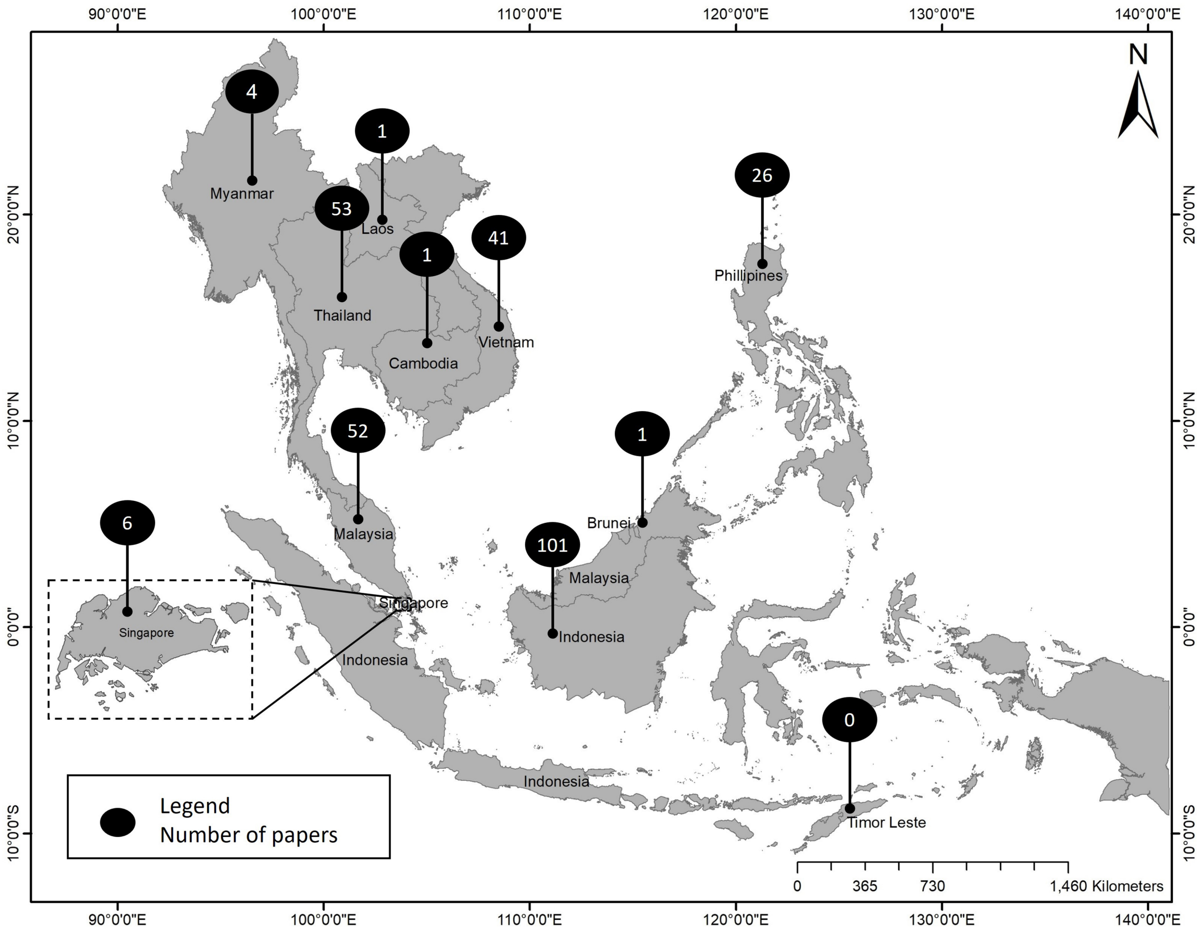

Figure 1. Numbers of reported microplastic pollution papers in Southeast Asian countries (2013-2023).

China Sea, which plays a central role in the region's maritime connectivity[44]. Additionally, the Mekong, Irrawaddy, and Chao Phraya rivers link several countries in Southeast Asia[9,45]. They serve as transportation routes for both plastic debris and microplastics, carrying these pollutants from upstream sources to downstream areas and ultimately to the sea. The countries in Southeast Asia face common environmental challenges, such as deforestation, agricultural runoff, and industrial discharges[46]. These activities can contribute to the introduction of microplastics into aquatic ecosystems. Additionally, Southeast Asia has some of the highest rates of marine plastic pollution in the world; estimates place the combined contributions of Indonesia (10%), the Philippines (6%), Vietnam (6%), Thailand (3%), and Malaysia (3%) to the world's oceans at 30%[47-49]. Four different types of matrices were included in this study, comprising biota, sediment, water, and others [Supplementary Table 1]. Biota samples consist of any living organisms such as fish, bivalves, crustaceans, mussels, and seagrass. Sediments encompass marine, freshwater, beach, and river sediments. Meanwhile, others comprise of atmospheric, face wash, toothpaste, human, and sea salt samples. The numbers of reported studies on microplastic pollution in Southeast Asian countries from 2013 to 2023 are shown in Figure 1. The collected data from a reported study on microplastic pollution in Southeast Asian countries aims to provide information about various characteristics of microplastics. These characteristics typically include size, shape, and types, and the study might investigate these attributes in different environmental matrices.

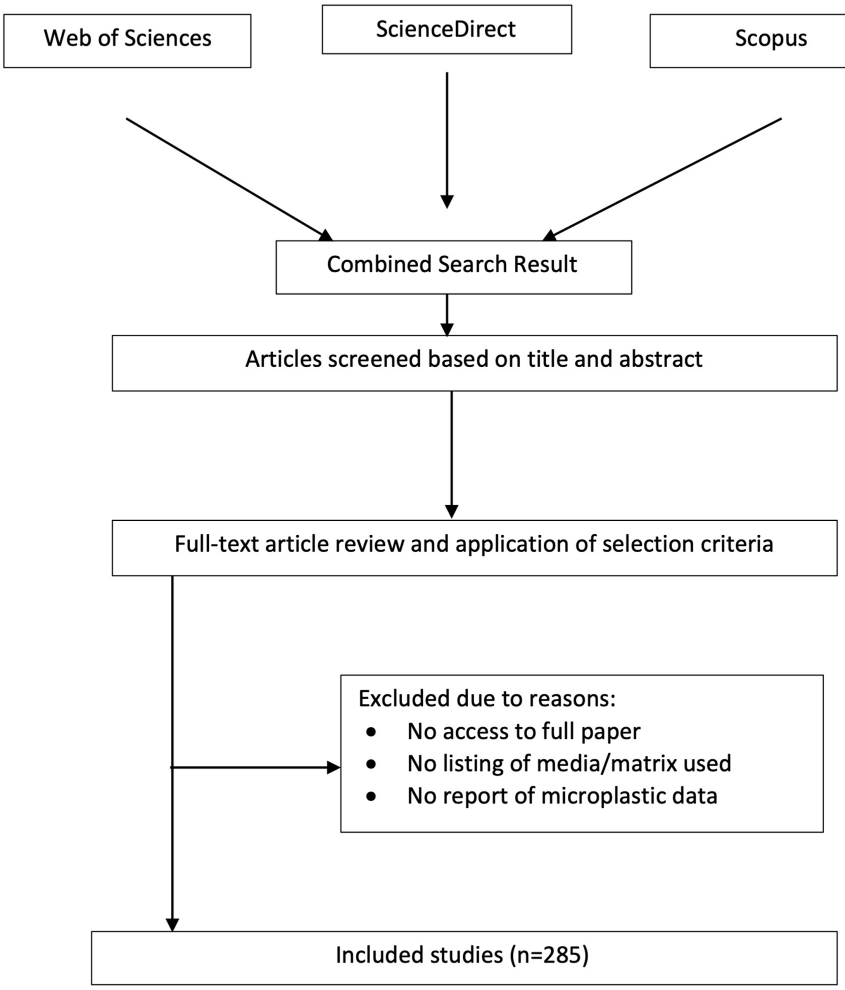

Figure 2. Flow diagram of studies selection including the process of literature identification, screening, and eligibility.

Methodology for literature search - identification of suitable publications

Dataset hunting was attempted using Scopus, ScienceDirect, and Web of Science indexes. The pursuit was directed utilizing the accompanying terms: "Microplastic Southeast Asia" OR "Microplastic" AND "microplastics" OR Malaysia OR Indonesia OR Brunei OR Vietnam OR Thailand OR Cambodia OR Laos OR Philippines OR Singapore OR Myanmar. Following the information base quests, 397 records were found from 2013 until 2023; Microsoft Excel was utilized to arrange the articles. Duplicates were removed, resulting in 285 papers to be evaluated for reasonable titles and abstracts [Figure 2 and Supplementary Table 1]. Several articles from Southeast Asia were examined across multiple matrices, leading to variations in the number of articles and matrices in this review.

The screening interval for the articles on microplastics in Southeast Asia over the last ten years was chosen to provide an up-to-date understanding of the current situation in the region. The abstracts indicate that plastic pollution is a pressing environmental issue in Southeast Asia, with severe impacts on aquatic life, ecosystems, and human health. By focusing on the last ten years, researchers can assess the increasing trends, levels of contamination, sources, and impacts of microplastics in Southeast Asia, providing valuable insights for policy-making, research prioritization, and allocation of resources. This screening interval allows for a comprehensive understanding of the current state of microplastic contamination in the region and helps identify key knowledge gaps that need to be addressed.

Recovery articles and data extracted

The number of recovery articles based on the collection criteria in Southeast Asian countries is shown in Figure 2. Data extracted from the articles included basic information such as author's names, publisher, country, and year of publication. Other materials extracted include the matrices used, abundance, size, shape, and polymer composition of microplastic. Most of the studies were published from 2017 onwards, with the highest number of publications reported in 2023 at 72 articles [Figure 3]. This is also consistent with the timeline of when the term "microplastics" became very significant in the regional context due to the information from[47]. It is important to highlight that, within the context of this analysis, the inclusion of alternative keywords such as "plastic particles" was not taken into account due to their failure to adhere to the specified size parameters for microplastics.

A datasheet was prepared by using Microsoft Excel for the systematic extraction of data. The size of the microplastics was recorded into two categories - SMP (0.1-1,000 μm) and LMP (1,001-5,000 μm). Furthermore, the shape of microplastics was categorized into fragment, fiber, film, foam, and pellet. The most observed polymer composition was PE, PP, PS, polyethylene terephthalate (PET), polyamide/nylon (PA), polyester (PES), and polyurethane (PU). The types of matrices were categorized into sediment, biota, water, and others. However, some studies within the reviewed literature failed to provide information on critical characteristics such as size, shape, and polymer type. Thus, the missing data from the studies was remarked as not available (N/A) in Supplementary Table 1.

Polymer hazard index assessment

To evaluate the polymer hazard index (PHI) of microplastics in sediments, water, biota, and other environmental matrices, data on the chemical composition of microplastic polymers were extracted from each relevant article. The chemical toxicity of different polymer types of microplastics was considered to evaluate their ecological harm[32]. The PHI of microplastics in water[33,50], sediment[51], biota[52,53], and others[54] was calculated using Equation (1):

$$PHI = \sum S_n \times P_n \tag{1}$$

In Equation (1), "*PHI*" represents the computed Polymer Hazard Index resulting from microplastics, where "P_n" corresponds to the percentage of specific polymer types obtained at each sampling location, and "S_n" signifies the hazard scores associated with the polymer types of microplastics as derived[32].

RESULT AND DISCUSSION

Matrices used

The environmental matrices investigated in Southeast Asian countries consisted of water (35%) - being the most studied matrix in the region - followed by sediment (31%), biota (20%), and others (14%) [Figure 4]. Water surfaces serve as a common reservoir for microplastics due to the transport of these particles from land and other sources[55]. Rainfall, wind, and water currents can carry microplastics from urban areas, industrial zones, and river systems into surface water bodies[56,57]. In contrast, sediments act as sinks for microplastics as they can capture and retain these particles over time[58]. Once microplastics enter the water, they may settle and accumulate in sediments due to gravity or interactions with other particles[59]. Microplastics in sediments are of environmental concern because they can persist in the ecosystem for extended periods. Organisms living in or near the water and sediments, including corals, plankton, marine invertebrates, fish, and whales, may come into contact with microplastics, which subsequently enter the

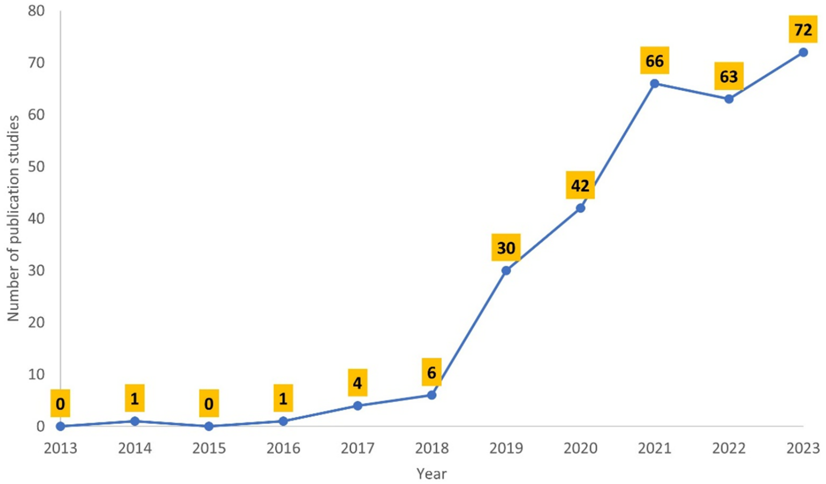

Figure 3. The total number of evaluated articles published in Southeast Asian countries from 2013 until 2023.

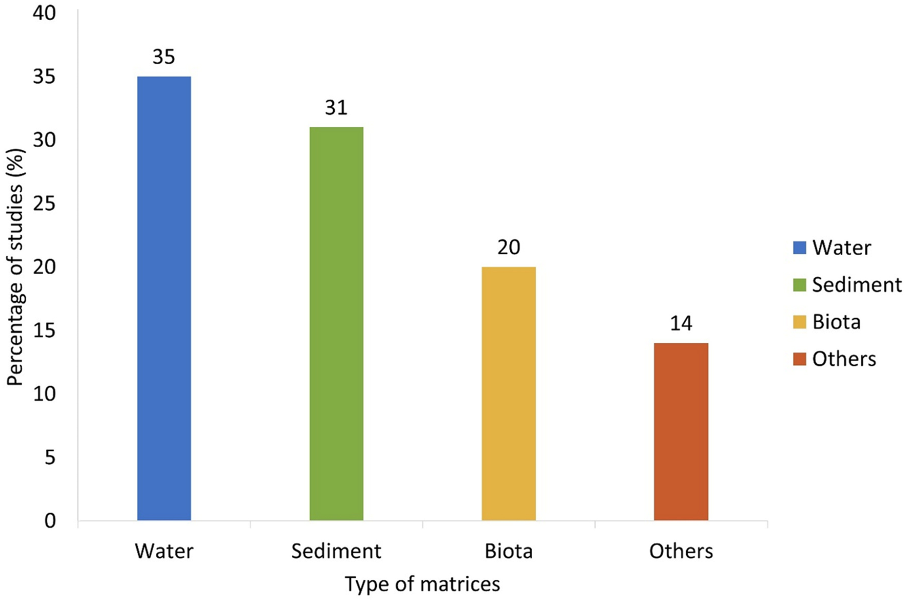

Figure 4. Percentages of different matrices used in the studies.

food chain[60]. When these organisms ingest microplastics, it poses potential ecological and health risks, as the plastics may carry contaminants and affect the feeding behavior of marine life. Moreover, humans are exposed to microplastic pollutants through both ingestion and inhalation pathways[61,62]. Microplastics can enter the human body through the consumption of contaminated food and water[63]. Seafood, for example, may contain microplastics that originate from the ocean. Additionally, microplastics may be present in the air, especially in urban areas with high population density, leading to their potential long-distance atmospheric transport before being deposited onto aquatic surfaces or reaching remote areas[64]. As such, dust and airborne particles that contain microplastics can be inhaled into the respiratory system and cause negative effects on human health[65].

Different sizes of microplastics in Southeast Asia

Based on the dimensions, microplastics can be divided into large and small sizes. Figure 5 demonstrates that

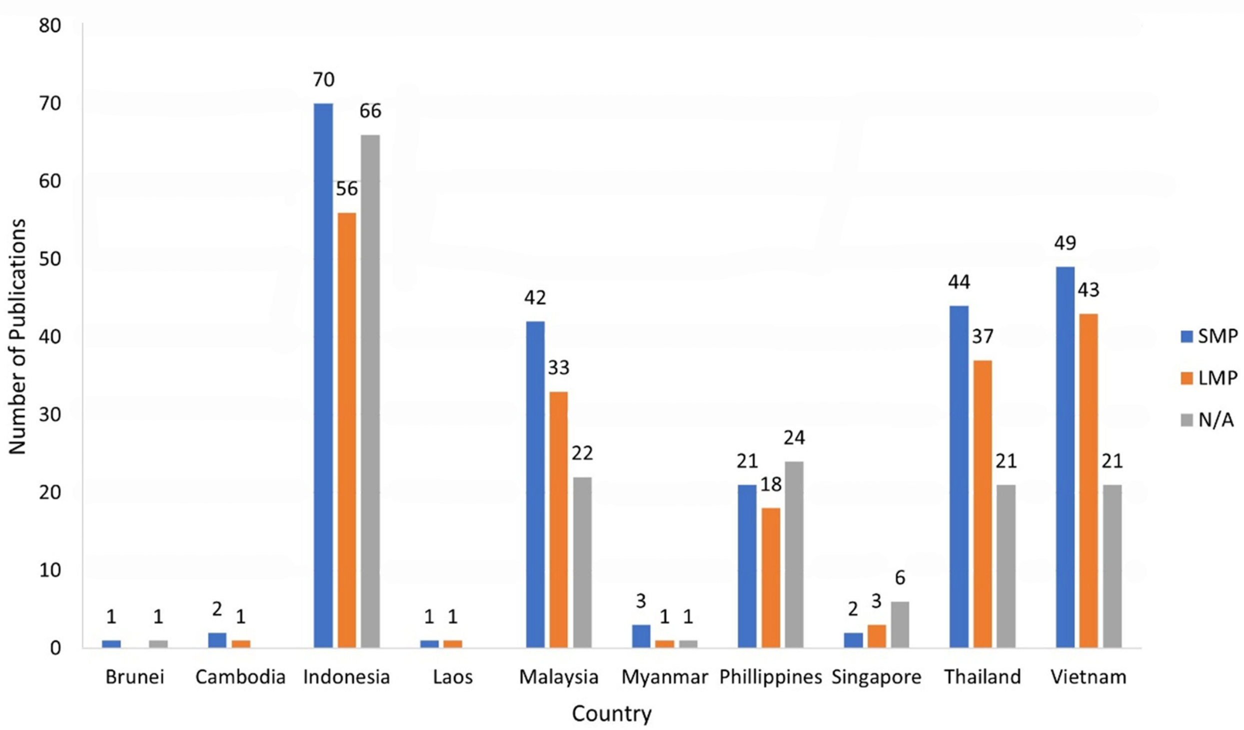

Figure 5. Number of published articles with size measurement. N/A denotes publication without size measurement.

SMP are prominent in practically all Southeast Asia nations. However, some published articles do not indicate the size measurement. Indonesia has the most SMP relative to LMP, followed by Vietnam, Thailand, Malaysia, the Philippines, Singapore, Myanmar, Laos, Cambodia, and Brunei, consistent with the number of published research studies. This study has analyzed the percentage of SMP (0.1-1,000 μm) at 46%, followed by 32% of LMP (1,001-5,000 μm), and 22% of unspecified reports on microplastics [Figure 6A]. According to these published studies, it is evident that the presence of SMP is widespread in the natural environment and corresponding matrices are significantly more abundant than LMPs. Figure 6B shows that SMP occupy the highest percentage at 46%, compared to LMP (37%) in biota samples. This review also demonstrated SMP constituted the majority, accounting for 43% in sediment and 47% in water, followed by LMPs at 29% and 33% in sediment and water, respectively [Figure 6C and D]. While in the other matrices, the percentage of SMP (53%) was also higher than LMP (31%) [Figure 6E]. Nevertheless, comparing the data proved challenging as the various samples found in other matrices were influenced by distinct pathways of microplastic pollutants, resulting in differences across matrices.

It is worth noting that size is one of the important factors that could affect the vertical distribution of the microplastics in water columns[66]. However, in rivers, various degradation processes such as photodegradation, mechanical-physical breakdown, weathering, and biodegradation can lead to a natural decrease in size[67]. As a result, the longer plastic trash is subjected to these degrading processes, the smaller it becomes. The size of the microplastics might have a variety of effects according to their categories. LMP particles may pose a concern to the water treatment plants (WTP) as the majority of water intake is from the river[68]. As such, the high loading of LMP in the water source potentially affects the performance of primary and secondary stages in the WTP. For instance, it was documented that in terms of size fraction, the efficiency of particle removal shows an ascending trend, with filtration playing a crucial role in achieving higher removal rates, particularly for particles sized ≥ 500 μm[69]. Although the abundance of microplastics is decreased by the treatment plant, a significant portion escapes in the treated effluent, especially for the

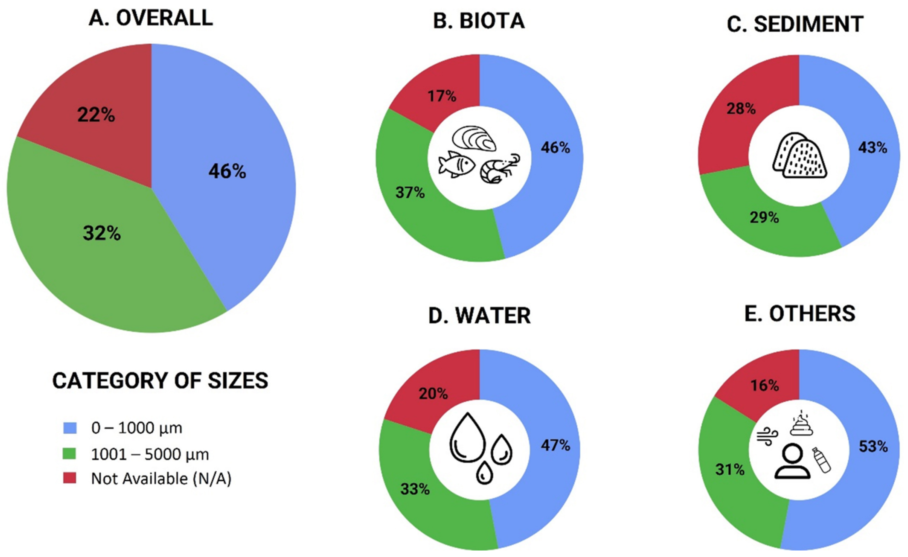

Figure 6. Percentage of microplastic sizes. (A) Overall; (B) Biota; (C) Sediment; (D) Water; (E) Others. N/A indicates the absence of microplastic polymer data in numerous studies.

smaller size fractions. It is reported that microplastics smaller than 2,000 µm tend to be easily mistaken as food and ingested by the marine biota[70,71]. Microplastics of sizes below 1,000 µm were found to be the most abundant in fish intestines, which can translocate across the digestive system to the lymphatic systems of mammals and humans[25].

Previous studies have indicated that SMP tend to dominate due to their strong affinity for natural colloids, leading to increased precipitation rates with sediments over time[72,73]. The concentration of microplastics in sediment samples was determined using sediment properties, sedimentation rates, and the capacity of the microplastics to adsorb or adhere to sediment particles[74]. The predominance of SMP over LMP found in this review may be due to the fact that one LMP can split into numerous SMP (considering the particle abundance that was commonly reported in microplastic studies, not the mass abundance), leading to a steady-state distribution with SMP outnumbering LMP over time. However, the counting of SMP may be underestimated due to variations in the lower size limit and instrument limitations used in different studies, resulting in the exclusion of numerous SMP.

Small-sized plastic particles (< 5,000 µm) tend to be transported over large distances, which ultimately can be transferred along the food chain[75]. The size of microplastics has a significant impact on their mobility in the aqueous environment and whether they may be consumed by animals, which is strongly connected to biosafety[76,77]. Microplastics with particle sizes smaller than 1 mm are found in greater abundance in sediments[78], whereby the likelihood of microplastic abundance in environmental matrices increases as the size of microplastics decreases[79]. Size significantly influences the impact of microplastics on organisms; thus, reporting the size of microplastics is necessary to quantify their potential to interact with the organisms, which intensifies as plastic size decreases[80]. Aquatic organisms such as invertebrates, fish, seabirds, and mammals have all been shown to ingest microplastics, which often comes with negative health consequences[81]. Furthermore, microplastics can absorb concentrated pollutants from the ambient environment, such as polychlorinated biphenyls (PCBs), pharmaceutical and personal care products (PPCPs), and heavy metals onto their surface, and thus can act as a potential carrier for microbial communities, which in turn can accumulate in fish and other organisms, and migrate to the human bodies throughout the food web due to their small size, strong hydrophobicity, and very low density[23,82]. They may then have adverse effects on animals and humans by affecting the body via the skin pores, digestive tract, and respiratory system, causing chemical and physical hazards and inducing neurotoxicity and oxidative damage[83,84].

Different shapes of microplastics in Southeast Asia

The potential negative effects of microplastics differ depending on particle shape. This study focused on the reported shapes of microplastics such as fragment, fiber, pellet, film, and foam. The shapes that were mentioned most commonly in the published articles in Southeast Asia were fiber (28%), fragment (27%), pellet (19%), film (13%), and foam (5%). Another 8% of the articles did not report on the shape data [Figure 7A]. Among them, fragments were the most common shape reported in water (31%) and sediment (34%) samples, while fibers were found to be dominant in biota (35%) and other matrices (28%). The shape of microplastics is significant as it can serve as a basis for traceability and a source of information[85]. Furthermore, the particles can be influenced by the initial structure of the primary microplastics, the surface erosion and degradation mechanisms, and the duration of time the plastic particles remain in the environment[68,86]. Some studies have revealed that the influence of microplastics on adsorption, desorption, and ecological effects can be attributed to the different shapes[87,88]. This current review shows that the data are primarily dominated by secondary microplastics from the breakdown of larger low-density plastics through weathering processes such as fragmentation and fiber formation[89]. In addition, shapes may be used to trace the source of microplastics[90]. Synthetic fibers usually emanate from effluent generated by fishing activities and the textile industry[7]. Fragments and foams are from plastic containers including single-use plastics such as bottles, cups, and food storage containers[91,92], while pellets usually originate from cosmetic products and personal care items[93]. Films, for instance, are made from plastic bags and plastic packaging; however, because they are tiny and translucent, they readily shatter when exposed to sunlight, subsequently producing smaller film particles[94]. Additionally, the proximity of many Southeast Asian countries to rivers and coastal areas facilitates the transport of mismanaged waste to water bodies. For instance, Indonesia, Malaysia, and Thailand have shorelines that are 91,363, 4,809, and 3,150 km long, respectively[95,96]. However, the inconsistent or insufficient regulatory frameworks for waste management in Southeast Asian countries may contribute to ineffective waste disposal practices, which can result in inadequate control over plastic waste[97,98]. Plastic waste carried from the land can undergo fragmentation during transportation, eventually reaching rivers and seas, resulting in microplastics of different shapes[99].

In the biota and other matrices, the shape of microplastics observed followed the order of fiber > fragment > film > pellet > foam [Figure 7B]. Meanwhile, in sediment and water matrices, the order of microplastic shapes can be characterized as fragment > fiber > film > foam > pellet [Figures 7C and D]. However, fibers are also prevalent in both surface water and sediment, as well as other matrices [Figure 7E], making it likely for them to be present in biota as they come into direct contact with these environmental matrix components. The elongated and flexible structure of fibers, as highlighted in[100], makes them more susceptible to ingestion or incorporation by organisms. Synthetic fibers, including those from textiles and effluents from the textile industry, as well as those released during domestic washing machine activities[101], contribute significantly to the composition of microplastics. Due to the lightweight and floating nature of microplastics, pelagic fish are more prone to consuming them compared to demersal fish. For instance, the prevalence of fibers in pelagic fish may be attributed to their thin size, allowing them to float on the water's surface, or their form that resembles their natural prey[102]. Interestingly, microplastics exhibit diverse distribution patterns in aquatic environments, dispersing across distinct compartments such as the water surface, water column, and sediment. This dispersion is influenced by variations in shape and density, impacting the availability of microplastics to species at different trophic levels and within different habitats[37,79]. Pelagic organisms, such as phytoplankton[103] and small crustaceans like zooplankton[42], are

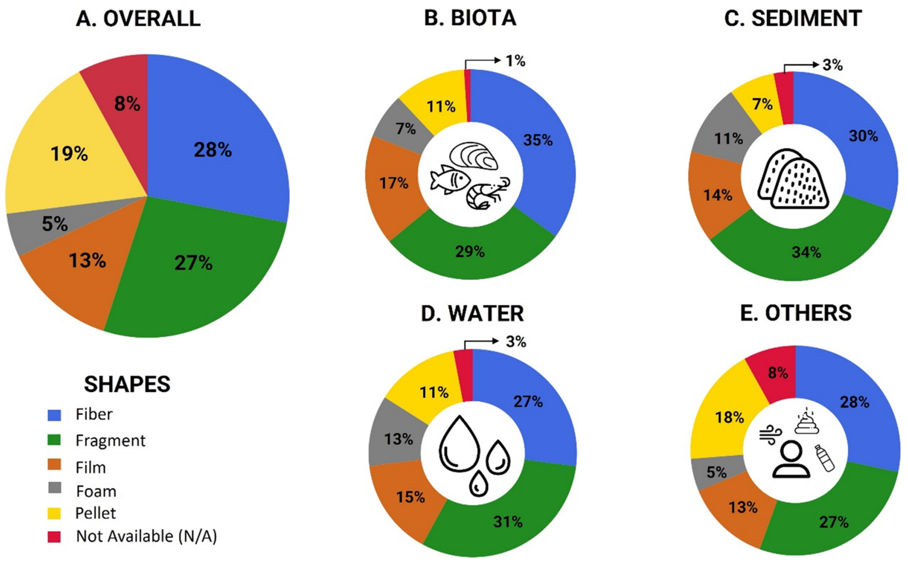

Figure 7. Percentage count of microplastic shapes. (A) Overall; (B) Biota; (C) Sediment; (D) Water; (E) Others. N/A indicates the absence of microplastic polymer data in numerous studies.

more likely to encounter less dense, floating microplastics. In contrast, benthic organisms such as amphipods[104], polychaete worms[105], tubifex worms[106], and echinoderms[107] are more prone to encountering microplastics denser than water. It is widely reported that microplastics can be consumed directly or indirectly by both benthic[17] and pelagic fish[10], where they become part of the prey. Furthermore, these fibers sourced from textiles and other origins can be transported through both air and water before settling in the sediment, leading to widespread distribution and potential ingestion by a variety of organisms including humans through food consumption[79].

The origins of microplastic fragments in the sediment and water ecosystems might be traced back to items such as bags, containers, food wrappers, waste related to tourism, and fishing nets or "ghost nets"[42,108]. Hence, the higher prevalence of microplastic fragments in sediment and water matrices can be ascribed to the gradual breakdown of larger plastic items during their transportation across extensive distances through weathering processes, mechanical abrasion, chemical degradation, and human activities[109]. These broken-down pieces could also sink into the bottom from the surface water and might be the reason for the higher occurrence of fragments in sediment. Additionally, sediment acts as a natural filter, capturing and retaining particles of various sizes of microplastics. Microplastic fragments, being smaller, may be more efficiently trapped and retained in sediment matrices compared to larger plastic items. Additionally, birds and animals[110] that feed on aquatic creatures or inhabit aquatic environments are known to ingest microplastics. The global presence of microplastics in practically all marine and freshwater ecosystems, including in protected and isolated areas around the region, underscores the widespread and potentially harmful nature of these pollutants.

Polymer composition

The overall microplastic polymers observed in environmental matrices of Southeast Asia are illustrated in Figure 8A, and shown in Supplementary Figure 1. In general, PE is the most abundant (22%) microplastic polymer composition in all matrices, followed by PP (17%), PET (10%), PS (10%), PA (9%) and other polymers (12%). Additionally, 13% of publications did not provide polymer identification. Specifically, in biota, the polymer follows the order of PE > PP > PA > PET > PS > PES > PU [Figure 8B], while the order of

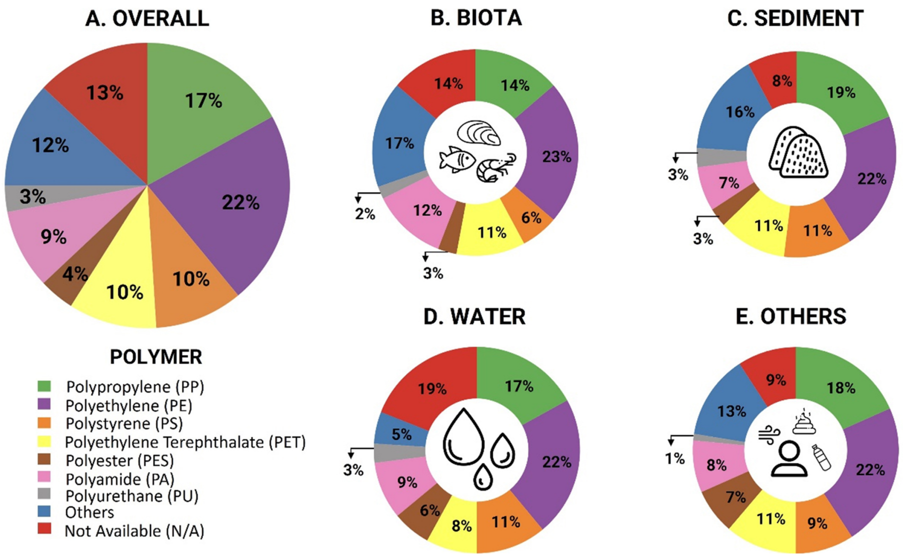

Figure 8. Percentage of seven main polymer compositions. (A) Overall; (B) Biota; (C) Sediment; (D) Water; (E) Others. N/A indicates the absence of microplastic polymer data in numerous studies.

abundance in the sediment matrix is PE > PP > PET > PS > PA > PES >PU [Figure 8C]. The water matrix revealed the microplastic composition of PE > PP > PS > PET > PA > PES > PU [Figure 8D], and the other matrices displayed the abundance in the order of PE > PP > PET > PS > PA > PES > PU [Figure 8E].

PP is a fiber-based material that is commonly used in garments, blankets, and other fiber-based items, as well as food packaging, pipelines, and chemical containers[50]. Fiber PE is widely utilized in the production of films, hollow items, fibers, and everyday necessities such as plastic bags[111]. Since PE and PP stand as the predominant polymer classes in both surface water and sediment, their existence in biota and humans is not surprising[5,112]. In addition, both polymers are known as the most widely produced in the world, satisfying 48.7% of the European plastic demand[89]. Thus, the high demand in the market for PE and PP is the cause of the high detection of these plastics in various environmental matrices in Southeast Asia[2,72,113].

PES, often known as polyester, is found in a wide range of products. The majority of the microplastics found in this investigation were fibers. PS is commonly found in foam products and disposable lunch boxes[114]. It is also utilized in light industrial manufacturing and as a decorative material. PA and PES in the environment mostly originate from the effluents of washing clothes and the usage of fishery tools[115]. PVC is utilized as a film in agricultural cultivation due to its inexpensive cost, and PU is used in adhesives, foams, food-grade coatings, insulators, tyres, sponges, and many more products[116].

Moreover, microplastics can also be distributed in specific water columns according to their polymer density[117]. This enables the penetration of microplastics into aquatic food chains, from the lowest to the highest tropical levels, due to their density-dependent distribution[118-120]. PE, PP, PU, and PS are examples of low-density polymers[121]. These polymers tend to float on the surface water and are likely to be consumed by pelagic species, while benthic species tend to consume dense plastics such as PES, PET, PA, and PVC, as they typically settle on the seabed. Interestingly, high-density polymers such as PET are also found in the surface water rather than in the sediment[4,122]. This can be due to environmental factors such as temperature, wind turbulence, tides, and waves[123]. These denser plastic particles could have also been resuspended from deeper water to the surface[121]. Furthermore, after degradation, aggregation, and biofouling processes, low-density polymers can also reach the seafloor[122]. Biofouling is defined as the accumulation of biological matter on surfaces, which creates biofilms by microorganisms[124]. Subsequently, this may cause an increase in microplastic density, thus resulting in microplastic sinking. The types of biofouling formations on the surface of the microplastic substrates are determined by the local environment in the aquatic habitats and the species of microorganisms.

PHI of microplastics in Southeast Asia

Plastics, a category of polymers comprised of monomers, have been engineered to meet the specific qualities demanded by many applications[125]. The occurrence of incomplete polymerization reactions leads to the existence of hazardous monomers that remain in the polymer, thus impacting its characteristics and also its environment[126]. Furthermore, plasticizers found in plastics, such as phthalates and bisphenols, have been shown to affect hormones[127]. These chemicals are frequently employed to improve the flexibility and durability of plastics such as PVC. While residual monomers in plastics may pose a risk, the presence of plasticizers is another concern because they possess the ability to disrupt hormones. Prospective risk assessment of microplastic particles is critical for determining when and where the ecosystems and human health issues can be anticipated. A study published in 2011 evaluated the environmental and health risks of plastic polymers based on their chemical composition[32]. On a monomer basis, 55 plastic polymers were graded and analyzed. The most hazardous polymers are those that are produced from mutagenic or carcinogenic monomers. Polymers that ranked in this category belong to the families of PU, PVC, epoxy resins, and styrene copolymers due to their high hazard scores[32]. Hence, this study evaluated the environmental toxicity of microplastic polymers in the risk assessment, which includes both environmental exposure and ecotoxicity. This method was used for the hazard score of each polymer, and the value of PHI was calculated based on Equation (1).

The overall hazard categories of Southeast Asia in all four matrices were IV (danger; PHI: 100-1,000) and V (extreme danger; PHI: > 1,000) [Supplementary Table 2]. Singapore, however, was the only country that did not report the type of polymer detected in all four types of matrices; therefore, the value of PHI for Singapore could not be determined [Table 1]. The high PHI value in Malaysia across all environmental matrices, compared to other countries, is due to the presence of polymers with high hazard scores, such as PU, PA, and PS, with hazard scores of 7,384, 47, and 30, respectively [Table 2]. Meanwhile, a low PHI from Brunei may reflect the limited number of studies from this country [Figure 5]. PU is a polymer used to make flexible foams, and has a high hazard score compared to daily plastics used such as PE and PP. As shown in Table 2, PU is composed of carcinogenic propylene oxide monomers that are hazardous to both humans and aquatic organisms. Each year, around millions of tonnes[32] of this polymer are reportedly produced, which may cause it to become more concentrated in the sediment due to its density properties. Meanwhile, the least harmful monomers for the environment are ethylene in PE and propylene in PP, resulting in a low hazard score[32]. Therefore, it is extremely important to identify and chemically characterize the microplastics based on polymer types, not only because each polymer poses different hazard levels, but also because it could be a source of great pollution, since each plastic product uses specific polymers and additives. Thus, this study provides valuable information about the origin of microplastics found in environmental matrices.

In the biota matrix, the majority of the countries were rated as extremely dangerous (red), whereas Vietnam was determined as dangerous with PHI values ranging from 100 to 1,000 [Table 1 and Figure 9A]. This is attributed to the lowest number of hazardous polymers detected in Vietnam in contrast to other countries, which affected the value of PHI evaluated. The sediment matrix showed that most of the countries were extremely dangerous (red), with PHI values of more than 1,000 [Figure 9B]. Sediments have the capacity to serve as a sink for microplastics, which can be permanently stored and have an impact on the

Table 1. The value of PHI in all matrices among Southeast Asia countries

Matrices	Malaysia	Indonesia	Vietnam	Philippines	Thailand	Cambodia	Laos	Myanmar	Brunei	Singapore
No of study	43	63	27	15	34	3	2	3	2	0
Biota	1,016***	47,800***	850**	32,525***	1,321***	0*	0*	0*	0*	0*
Sediment	18,744***	1,508***	25,798***	1,198***	1,130***	148,600***	148,600***	46,650***	1,100***	0*
Water	31,975***	9,835***	1,376***	23,500***	30,861***	0*	0*	0*	0*	0*
Others	29,688***	786**	775**	0*	0*	1,260***	0*	1,140***	867**	0*

*Classified as minor risk category; **Classified as dangerous risk category; ***Classified as extremely dangerous risk category; ****"0" represents "no PHI value" due to no reported polymer. PHI: Polymer hazard index.

Table 2. Detailed information for microplastic polymers detected in this study, including monomer, density, usage, and score

Polymer	Monomer	Number of articles corresponding to the polymer	Main/common application	Score
Polyethylene	Ethylene	180	Toys, bottles, pipes, house ware, *etc.*	11
Polypropylene	Propylene	246	Food packaging, *etc.*	1
Polyamide	Adipic acid	75	Bearings, automotive applications, *etc.*	47
Polystyrene	Styrene	96	Plastic cup, food packaging, spectacles frame, *etc.*	30
Polyethylene Terephthalate	Ethylene glycol	98	Packaging and textile production	4
Polyester	Monoethylene glycol	47	Fabrics, textiles production, *etc.*	3
Polyurethane	Propylene oxide	15	Upholstery, sports mats, packaging bags, *etc.*	7328

environment[76]. Moreover, the majority of the countries in the water matrix have also been indicated as extremely dangerous (red) due to high concentrations of microplastics in each country, whereas others, such as Cambodia, Myanmar, Brunei, and Laos, did not report the polymer identified in this sample matrix [Figure 9C]. The predominant risk level (orange) was reported for other matrices depicted in Figure 9D, where a low number of microplastic studies were reported in each country; this indicates that the majority of the countries are considered to be in danger. However, Malaysia, Cambodia, and Myanmar stand out as areas classified as extremely hazardous (red) based on the PHI. The microplastics that were found could have come from other regions. This is due to the fact that microplastics can travel large distances by wind, water currents, and even migratory animals[128]. As a result, nearby areas may be subjected to similar sources of microplastic contamination, such as rivers, ocean currents, and industrial activity. From the evaluation that has been made, we have concluded that higher hazard scores of the polymers may result in higher values of PHI, even if the microplastic concentration is low. Nevertheless, we cannot overlook the significance of the lowest hazard scores linked to polymers like PP, PE, and PET, given their widespread presence in environmental matrices. When evaluating the risk of microplastic pollution, even materials with lower hazard scores must be considered, as their potential environmental impact becomes significant when they are in high concentrations and/or abundances. This, in turn, contributes to a certain level of environmental risk as reflected in the PHI, while PHI alone cannot be the dominant parameter for ecological assessment and in calculating the hazard index of microplastics. This is because microplastics can also absorb persistent, bioaccumulative, and toxic contaminants from the environment, thus potentially leading to hazards from co-pollutants. These contaminants may include plastic additives, which are chemicals added during the manufacturing of microplastics[129]. The ingestion of microplastics and the accumulation of these contaminants have been a concern for the potential hazards of microplastics in aquatic environments, especially marine environments[1,130]. However, adverse effects of microplastic

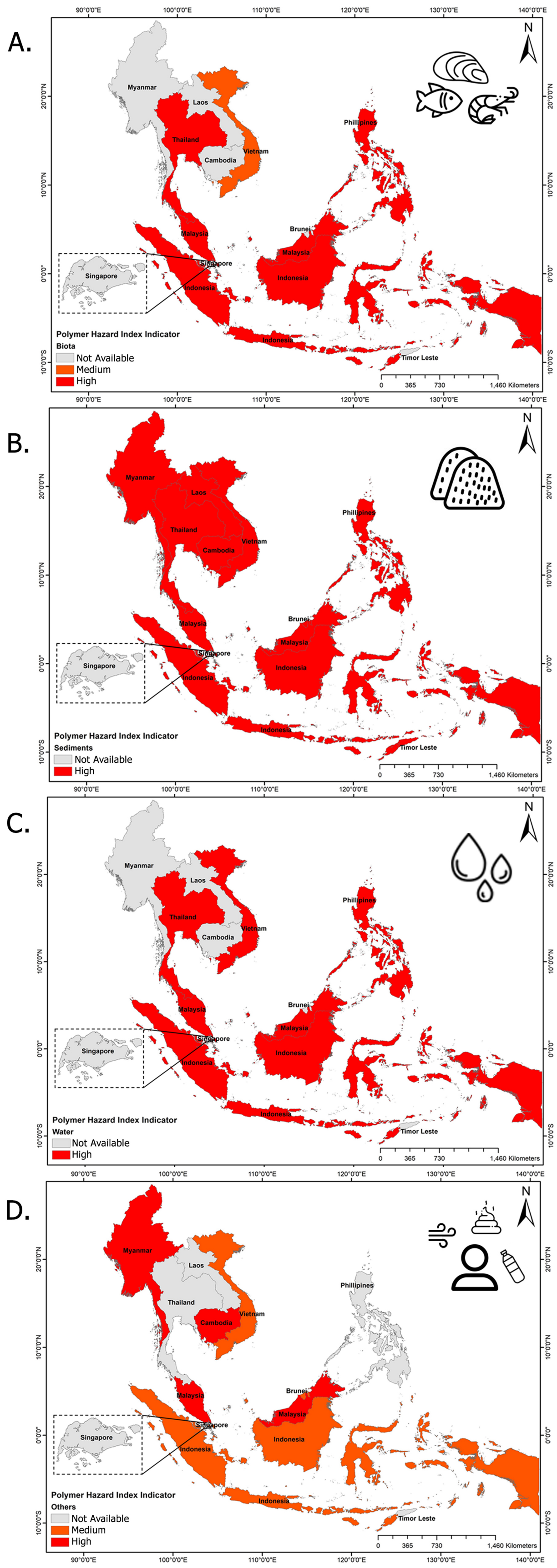

Figure 9. Visualized hazard scores based on Polymer hazard index in environmental matrices. (A) Biota; (B) Sediment; (C) Water; (D) Others.

ingestion have only been observed in laboratory conditions at high exposure concentrations. Further research is needed to fully understand the contribution of plasticizers to the hazard of microplastics, as well as incorporating other related risk assessment calculations such as measured environmental concentration (MEC) and predicted no-effect concentration (PNEC) that are widely used for chemical compounds.

CONCLUSION

The objective of this study was to assess the comprehensive contamination status of microplastics in the Southeast Asia region, considering four matrices - water, sediment, biota, and others. The overall results revealed that microplastic pollution poses a high risk to water, sediment, biota, and other matrices in the Southeast Asia region. The detection of a high concentration of microplastics within an ecosystem suggests a significant environmental impact. Microplastics can enter ecosystems through various avenues such as industrial discharges, improper waste disposal, and degradation of larger plastic items. The fact that the research is conducted mainly in water, followed by sediment and biota or living organisms within the ecosystems, indicates that researchers in Southeast Asian countries are interested in understanding how microplastics are distributed in the ecosystem and how they enter the food web, especially the fate and transport of these emerging contaminants. Additionally, biota can serve as indicators of the overall health of an ecosystem, and the presence of diverse polymer types in these organisms may have implications for the entire ecosystem. The size of microplastics is indeed a crucial factor in understanding their environmental impact. SMP are the predominant size category of microplastics found in Southeast Asia, with biota matrices being the most common habitat for these particles. Additionally, fiber was the predominant microplastic shape found in Southeast Asia. Increased fishing-related activities, shipping activities, and anthropogenic activities in the coastal areas of Southeast Asia may serve as potential contributors. The findings additionally confirmed the presence of PE as the dominant type of microplastic polymer. The PHI toxicity and hazard readings of microplastics in the Southeast Asian region were found to have increased with the presence of high hazard scores of the polymers (PU, PA, and PS). Overall, our results indicated that water, sediment, biota, and others in Southeast Asia are at a high-risk level due to microplastic pollution. However, the different reporting units for microplastic abundance prevent the calculation of pollution load index (PLI) and potential ecological hazard index (PEHI) in environmental matrices within this review. Therefore, it is essential to apply specific methods to assess ecological risks across various research areas in Southeast Asian countries, to enable the identification of the pollution status in the study area, and the precise estimation of microplastics in the environment. Southeast Asia has a major issue with microplastic pollution, underscoring the critical need for effective waste disposal and consumption reduction to mitigate environmental risks and safeguard seafood in the region, as specified by the Coordinating Body on the Seas of East Asia (COBSEA) Regional Action Plan on Marine Litter and ASEAN Regional Action Plan for Combating Marine Debris. More rigorous studies and continuous monitoring are needed from all countries and authorities to establish a "safe standard" or "acceptable limit" for microplastic contaminants, as well as other related regulations for food security and environmental health. Nevertheless, it is envisioned that these data can aid in baseline assessments and address microplastic pollution at specific locations and in various regions of Southeast Asian countries.

GAPS OF EXISTING STUDIES AND FUTURE OUTLOOK

This study highlights the variability in the units used for reporting, thus presenting challenges in establishing a standardized baseline for assessing microplastic pollution in Southeast Asian countries. For instance, the concentrations of microplastics in water may be denoted as items per liter (items/L) or items per cubic meter (items/m^3). Meanwhile, sediment samples may be expressed as items per gram (items/g), items per kilogram (items/kg), or items per square meter (items/m^2), and biota samples may be presented as items per gram tissue (items/g) or items per individual (items/individual), as discussed earlier in this review. This inconsistency poses a difficulty in applying the PLI and PEHI measurements for the evaluation of microplastic risk assessments, as both methods rely on a standardized measure of abundance for accurate comparisons. However, achieving uniformity in reporting units is rather challenging due to the inherent variations in each matrix that have been discussed earlier. Apart from the lack of consistency in reporting units, the divergence in methodologies across research papers poses a significant challenge[131-133]. Some studies attribute their methods to organizations like National Oceanic and Atmospheric Administration (NOAA), Group of Experts on the Scientific Aspects of Marine Environmental Protection (GESAMP), or Intergovernmental Oceanographic Commission of the Western Pacific (IOC-WESTPAC), while others do not specify their sources. This discrepancy complicates the organization of data according to the methods employed, hindering our ability to compare the efficacy of various microplastic sampling methods. Furthermore, there is an inconsistency in the nomenclature of shapes; for instance, the term “pellet” is used interchangeably with “granular”, “sphere”, “beads”, “grains”, “nurdles”, “nibs”, and other variations. Additionally, this variation in naming conventions can lead to confusion, making it challenging to accurately categorize and analyze microplastic shapes. Furthermore, certain publications fail to specify the polymer type of the observed microplastics. Typically, the confirmation for the presence of small particles in various samples (e.g., water, sediment, human cells, air, plants) requires testing through analytical techniques such as Fourier Transform Infrared (FTIR), micro-FTIR, micro-Raman spectroscopy, or pyrolysis-gas chromatography/mass spectrometry (Py-GC/MS) to identify the associated polymers. However, studies with polymer information did not specifically identify the polymers’ assignation based on the shape or color of microplastics found, which could possibly be due to the limitations in costs or resources.

Finally, there is also an absence of information regarding the variations in geological locations for microplastic sampling, which can significantly impact the chosen sampling methods. Different countries exhibit diverse geological features, influencing the design of the sampling methodologies. For instance, when comparing research on microplastics in water from mangrove and sea areas, the methodologies employed may differ. The collection of water samples in mangrove areas often involves the use of the bucket method, while a towing method is commonly employed in sea water or riverine water sampling. Consequently, the observed abundance of microplastics between these two methods may yield disparate outcomes. The lack of consistency in methods makes it difficult to develop a comprehensive picture of the distribution and quantity of microplastics. The complexity of the problem is further increased by Southeast Asia’s varied ecosystems and climate, and influenced by variables including seasonal fluctuations and anthropogenic activity. Large-scale, thorough studies may be difficult to carry out in some of the region’s countries due to a lack of funding and expertise in research infrastructure. For instance, while other Southeast Asian countries are making progress in microplastic research, there is no information in the literature regarding microplastic contamination in East Timor. Similarly, little information has been obtained from Laos, Brunei, Myanmar, and Cambodia.

Additionally, researchers in the Western region have discovered that risk assessments of microplastic polymers are important for assessing their risk to ecosystems and human health; however, in practice, comparing the pollution hazard index of microplastics can be difficult for several reasons, including the diverse nature of microplastics and the variety of factors that must be considered in assessments, as has been highlighted in this review. Apparently, no standardized techniques have been established to determine the ecotoxicity of microplastics in the Southeast Asia region. Different studies may use different methodologies to estimate the risks and hazards, making direct comparisons of results challenging. Moreover, the long-term effects of microplastic exposure are also unknown. While short-term studies can provide information, the long-term consequences of microplastics on ecosystems and organisms are still being studied. To address these issues, continued research should focus on developing standardized procedures for microplastic risk evaluation, understanding the toxicity of various polymer types, and taking into account the larger ecological context in which microplastics are commonly discovered. Future investigations should also prioritize the study of microplastics within terrestrial ecosystems, with a specific emphasis on agricultural land. This focus is essential for advancing our understanding of the biogeochemical dynamics of microplastics in soil-plant systems and for conserving terrestrial and agricultural ecosystems.

The aforementioned studies of microplastics in the Southeast Asian region have a number of difficulties and constraints. While the trend of microplastic research in the region is in line with other research pertaining to microplastics globally, there is also a notable lack of studies focusing on spatial, temporal, and interconnected correlational studies of the matrices within Southeast Asia's environmental ecosystems. As such, little is known about how microplastics are transported within the diverse matrices. Factors such as biological interactions, sedimentation process, and water currents might influence the microplastic distribution, transport, and fate in the region. Therefore, to overcome these limitations, there is a serious need for regional and international harmonization, for instance, in working on standardized procedures, providing more financing/funding, participating in regular monitoring, and sharing capacity in building strong research networks that will expand the knowledge of the scope and effects of microplastic pollution in Southeast Asia. This gap is significant, especially considering the devastating impacts of microplastics on marine ecosystems, health issues, and biodiversity destruction resulting from a substantial increase in plastic pollution on land and in marine environments in the Southeast Asia region. Therefore, collaboration between scientists, policymakers, and environmental organizations is critical for obtaining a thorough understanding of the potential hazards connected with microplastics and developing effective mitigation methods.

DECLARATIONS

Acknowledgements

Authors would like to acknowledge the financial support from the Ministry of Higher Education, Malaysia (FRGS/1/2020/STG04/UMT/02/2; Vote59618) and the continuous technical support from the UNESCO IOC-WESTPAC on microplastic research in Malaysia and Southeast Asia. The authors also would like to thank MRIG members for continuous support during all this time.

Authors' contributions

Conceptualization: Anuar ST, Mohd Ali AA, Ibrahim YS
Data Collection: Mohd Ali AA, Khalid AA, Abd Razak NI, Mohd Maulana NS, Roslan NS, Razmi RSB
Writing - original draft preparation: Mohd Ali AA, Roslan NS, Khalid AA, Abd Razak NI, Mohd Maulana NS, Roslan NS, Anuar ST
Writing - review and editing: Anuar ST, Ibrahim YS, Jaafar M, Shahrudin R, Ismail K, Mohd Ali AA
Visualization: Roslan NS, Wan Ruseli WMA, Mohd Ali AA
Funding acquisition: Anuar ST
All authors have read and approved the final manuscript.

Availability of data and materials

Data will be available in Supplementary Materials and upon request.

Financial support and sponsorship

This work was funded by the Ministry of Higher Education, Malaysia under a Fundamental Research Grant Scheme (FRGS/1/2020/STG04/UMT/02/2; Vote59618).

Conflicts of interest

All authors declared that there are no conflicts of interest.

Ethical approval and consent to participate

Not applicable.

Consent for publication

Not applicable.

Copyright

REFERENCES

1. Cole M, Lindeque P, Halsband C, Galloway TS. Microplastics as contaminants in the marine environment: a review. *Mar Pollut Bull* 2011;62:2588-97. DOI PubMed
2. Anuar ST, Abdullah NS, Yahya NKEM, et al. A multidimensional approach for microplastics monitoring in two major tropical river basins, Malaysia. *Environ Res* 2023;227:115717. DOI
3. Sajorne RE, Cayabo GDB, Gajardo LJA, Mabuhay-omar JA, Creencia LA, Bacosa HP. Disentangling microplastic pollution on beach sand of Puerto Princesa, Palawan Island, Philippines: abundance and characteristics. *Sustainability* 2022;14:15303. DOI
4. Lestari P, Trihadiningrum Y, Firdaus M, Warmadewanthi IDAA. Microplastic pollution in Surabaya River Water and Aquatic Biota, Indonesia. *IOP Conf Ser Mater Sci Eng* 2021;1143:012054. DOI
5. Ibrahim YS, Tuan Anuar S, Azmi AA, et al. Detection of microplastics in human colectomy specimens. *JGH Open* 2021;5:116-21. DOI PubMed PMC
6. Bagheri T, Gholizadeh M, Abarghouei S, et al. Microplastics distribution, abundance and composition in sediment, fishes and benthic organisms of the Gorgan Bay, Caspian sea. *Chemosphere* 2020;257:127201. DOI
7. Duis K, Coors A. Microplastics in the aquatic and terrestrial environment: sources (with a specific focus on personal care products), fate and effects. *Environ Sci Eur* 2016;28:2. DOI PubMed PMC
8. Napper IE, Thompson RC. Release of synthetic microplastic plastic fibres from domestic washing machines: effects of fabric type and washing conditions. *Mar Pollut Bull* 2016;112:39-45. DOI PubMed
9. Ta AT, Babel S. Microplastics pollution with heavy metals in the aquaculture zone of the Chao Phraya River Estuary, Thailand. *Mar Pollut Bull* 2020;161:111747. DOI PubMed
10. Azad SMO, Towatana P, Pradit S, Patricia BG, Hue HT. Ingestion of microplastics by some commercial fishes in the lower Gulf of Thailand: a preliminary approach to ocean conservation. *Int J Agr Technol* 2018;14:1017-32. Available from: https://www.igreenstory.co/wp-content/uploads/2019/10/Ingestion-of-Microplastic-1.pdf. [Last accessed on 18 Apr 2024]
11. Dimassi SN, Hahladakis JN, Yahia MND, Ahmad MI, Sayadi S, Al-ghouti MA. Degradation-fragmentation of marine plastic waste and their environmental implications: a critical review. *Arab J Chem* 2022;15:104262. DOI
12. Andrady AL, Barnes PW, Bornman JF, et al. Oxidation and fragmentation of plastics in a changing environment; from UV-radiation to biological degradation. *Sci Total Environ* 2022;851:158022. DOI PubMed PMC
13. Menzel T, Weigert S, Gagsteiger A, et al. Impact of enzymatic degradation on the material properties of poly(ethylene terephthalate). *Polymers* 2021;13:3885. DOI PubMed PMC
14. Ounjai K, Boontanon SK, Piyaviriyakul P, Tanaka S, Fujii S. Assessment of microplastic contamination in the urban lower Chao Phraya River of Bangkok city, Thailand. *J Water Health* 2022;20:1243-54. DOI PubMed
15. Hamidian AH, Ozumchelouei EJ, Feizi F, Wu C, Zhang Y, Yang M. A review on the characteristics of microplastics in wastewater treatment plants: a source for toxic chemicals. *J Clean Prod* 2021;295:126480. DOI
16. Rochman CM, Brookson C, Bikker J, et al. Rethinking microplastics as a diverse contaminant suite. *Environ Toxicol Chem* 2019;38:703-11. DOI
17. de Sá LC, Oliveira M, Ribeiro F, Rocha TL, Futter MN. Studies of the effects of microplastics on aquatic organisms: what do we know and where should we focus our efforts in the future? *Sci Total Environ* 2018;645:1029-39. DOI
18. Zainuddin AH, Aris AZ, Zaki MRM, Yusoff FM, Wee SY. Occurrence, potential sources and ecological risk estimation of microplastic towards coastal and estuarine zones in Malaysia. *Mar Pollut Bull* 2022;174:113282. DOI PubMed
19. Kisnarti EA, Ningsih NS, Putri MR, Hendriati N, Box C. Microplastic observations in the waters of Labuan Bajo-Gili Trawangan,

Indonesia. *IOP Conf Ser Earth Environ Sci* 2021;925:012043. DOI

20. Maes T, Van der Meulen MD, Devriese LI, et al. Microplastics baseline surveys at the water surface and in sediments of the North-East Atlantic. *Front Mar Sci* 2017;4:135. DOI
21. Khalid N, Aqeel M, Noman A, et al. Linking effects of microplastics to ecological impacts in marine environments. *Chemosphere* 2021;264:128541. DOI
22. Free CM, Jensen OP, Mason SA, Eriksen M, Williamson NJ, Boldgiv B. High-levels of microplastic pollution in a large, remote, mountain lake. *Mar Pollut Bull* 2014;85:156-63. DOI
23. Curren E, Leaw CP, Lim PT, Leong SCY. Evidence of marine microplastics in commercially harvested seafood. *Front Bioeng Biotechnol* 2020;8:562760. DOI PubMed PMC
24. Anderson JC, Park BJ, Palace VP. Microplastics in aquatic environments: implications for Canadian ecosystems. *Environ Pollut* 2016;218:269-80. DOI PubMed
25. Kasamesiri P, Panchan R, Thaimuangphol W. Spatial-temporal distribution and ecological risk assessment of microplastic pollution of inland fishing ground in the Ubolratana Reservoir, Thailand. *Water* 2023;15:330. DOI
26. Tang CN, Kuwahara VS, Leong SCY, Moh PY, Yoshida T. Effect of monsoon on microplastic bioavailability and ingestion by zooplankton in tropical coastal waters of Sabah. *Mar Pollut Bull* 2023;193:115182. DOI PubMed
27. Thushari GGN, Senevirathna JDM, Yakupitiyage A, Chavanich S. Effects of microplastics on sessile invertebrates in the eastern coast of Thailand: an approach to coastal zone conservation. *Mar Pollut Bull* 2017;124:349-55. DOI PubMed
28. Daud A, Mallongi A, Bahar B, Hidayat. Mussel fish (Polymesoda erosa) and microplastics inTallo River, Makassar, Indonesia. *Indian J Forensic Med Toxicol* 2021;15:4539-46. DOI
29. Gallo F, Fossi C, Weber R, et al. Marine litter plastics and microplastics and their toxic chemicals components: the need for urgent preventive measures. *Environ Sci Eur* 2018;30:13. DOI PubMed PMC
30. Blackburn K, Green D. The potential effects of microplastics on human health: what is known and what is unknown. *Ambio* 2022;51:518-30. DOI PubMed PMC
31. Lehel J, Murphy S. Microplastics in the food chain: food safety and environmental aspects. *Rev Environ Contam Toxicol* 2021;259:1-49. DOI PubMed
32. Lithner D, Larsson A, Dave G. Environmental and health hazard ranking and assessment of plastic polymers based on chemical composition. *Sci Total Environ* 2011;409:3309-24. DOI PubMed
33. Xu P, Peng G, Su L, Gao Y, Gao L, Li D. Microplastic risk assessment in surface waters: a case study in the Changjiang Estuary, China. *Mar Pollut Bull* 2018;133:647-54. DOI
34. Prarat P, Hongsawat P. Microplastic pollution in surface seawater and beach sand from the shore of Rayong province, Thailand: distribution, characterization, and ecological risk assessment. *Mar Pollut Bull* 2022;174:113200. DOI PubMed
35. Nguyen MK, Lin C, Quang Hung NT, Hoang HG, Vo DN, Tran HT. Investigation of ecological risk of microplastics in peatland areas: a case study in Vietnam. *Environ Res* 2023;220:115190. DOI
36. Khuyen VTK, Le DV, Fischer AR, Dornack C. Comparison of microplastic pollution in beach sediment and seawater at UNESCO Can Gio Mangrove Biosphere Reserve. *Glob Chall* 2021;5:2100044. DOI PubMed PMC
37. Taha ZD, Md Amin R, Anuar ST, Nasser AAA, Sohaimi ES. Microplastics in seawater and zooplankton: a case study from Terengganu estuary and offshore waters, Malaysia. *Sci Total Environ* 2021;786:147466. DOI PubMed
38. Lahens L, Strady E, Kieu-Le TC, et al. Macroplastic and microplastic contamination assessment of a tropical river (Saigon River, Vietnam) transversed by a developing megacity. *Environ Pollut* 2018;236:661-71. DOI
39. Lebreton LCM, van der Zwet J, Damsteeg JW, Slat B, Andrady A, Reisser J. River plastic emissions to the world’s oceans. *Nat Commun* 2017;8:15611. DOI PubMed PMC
40. Lechthaler S, Waldschläger K, Sandhani CG, et al. Baseline study on microplastics in Indian rivers under different anthropogenic influences. *Water* 2021;13:1648. DOI
41. Meijer LJJ, van Emmerik T, van der Ent R, Schmidt C, Lebreton L. More than 1000 rivers account for 80% of global riverine plastic emissions into the ocean. *Sci Adv* 2021;7:eaaz5803. DOI PubMed PMC
42. Md Amin R, Sohaimi ES, Anuar ST, Bachok Z. Microplastic ingestion by zooplankton in Terengganu coastal waters, southern South China Sea. *Mar Pollut Bull* 2020;150:110616. DOI PubMed
43. Gandhi S, Jones T. Identifying mangrove deforestation hotspots in South Asia, Southeast Asia and Asia-Pacific. *Remote Sensing* 2019;11:728. DOI
44. Song AY, Fabinyi M. China’s 21st century maritime silk road: challenges and opportunities to coastal livelihoods in ASEAN countries. *Marine Policy* 2022;136:104923. DOI
45. Haberstroh CJ, Arias ME, Yin Z, Sok T, Wang MC. Plastic transport in a complex confluence of the Mekong River in Cambodia. *Environ Res Lett* 2021;16:095009. DOI
46. Luo P, Mu Y, Wang S, et al. Exploring sustainable solutions for the water environment in Chinese and Southeast Asian cities. *Ambio* 2022;51:1199-218. DOI PubMed PMC
47. Jambeck JR, Geyer R, Wilcox C, et al. Marine pollution. Plastic waste inputs from land into the ocean. *Science* 2015;347:768-71. DOI
48. Picó Y, Manzoor I, Soursou V, Barceló D. Microplastics in water, from treatment process to drinking water: analytical methods and potential health effects. *Water Emerg Contam Nanoplastics* 2022;1:13. DOI

49. Omeyer LCM, Duncan EM, Abreo NAS, et al. Interactions between marine megafauna and plastic pollution in Southeast Asia. *Sci Total Environ* 2023;874:162502. DOI
50. Wang G, Lu J, Li W, et al. Seasonal variation and risk assessment of microplastics in surface water of the Manas River Basin, China. *Ecotoxicol Environ Saf* 2021;208:111477. DOI
51. Ranjani M, Veerasingam S, Venkatachalapathy R, et al. Seasonal variation, polymer hazard risk and controlling factors of microplastics in beach sediments along the southeast coast of India. *Environ Pollut* 2022;305:119315. DOI
52. Fang C, Zheng R, Chen H, et al. Comparison of microplastic contamination in fish and bivalves from two major cities in Fujian province, China and the implications for human health. *Aquaculture* 2019;512:734322. DOI
53. Nithin A, Sundaramanickam A, Iswarya P, Babu OG. Hazard index of microplastics contamination in various fishes collected off Parangipettai, Southeast coast of India. *Chemosphere* 2022;307:136037. DOI PubMed
54. Lin Q, Zhao S, Pang L, Sun C, Chen L, Li F. Potential risk of microplastics in processed foods: preliminary risk assessment concerning polymer types, abundance, and human exposure of microplastics. *Ecotoxicol Environ Saf* 2022;247:114260. DOI
55. Zhao S, Zhang Z, Chen L, et al. Review on migration, transformation and ecological impacts of microplastics in soil. *Appl Soil Ecology* 2022;176:104486. DOI
56. Rossatto A, Arlindo MZF, de Morais MS, de Souza TD, Ogrodowski CS. Microplastics in aquatic systems: a review of occurrence, monitoring and potential environmental risks. *Environ Adv* 2023;13:100396. DOI
57. Atugoda T, Piyumali H, Liyanage S, Mahatantila K, Vithanage M. Fate and behavior of microplastics in freshwater systems. In: Rocha-santos T, Costa MF, Mouneyrac C, editors. Handbook of microplastics in the environment. Cham: Springer International Publishing; 2022. pp. 781-811. DOI
58. de Smit JC, Anton A, Martin C, Rossbach S, Bouma TJ, Duarte CM. Habitat-forming species trap microplastics into coastal sediment sinks. *Sci Total Environ* 2021;772:145520. DOI PubMed
59. Kaiser D, Kowalski N, Waniek JJ. Effects of biofouling on the sinking behavior of microplastics. *Environ Res Lett* 2017;12:124003. DOI
60. Sharma S, Chatterjee S. Microplastic pollution, a threat to marine ecosystem and human health: a short review. *Environ Sci Pollut Res Int* 2017;24:21530-47. DOI
61. Ageel HK, Harrad S, Abdallah MA. Occurrence, human exposure, and risk of microplastics in the indoor environment. *Environ Sci Process Impacts* 2022;24:17-31. DOI PubMed
62. Ghosh S, Sinha JK, Ghosh S, Vashisth K, Han S, Bhaskar R. Microplastics as an emerging threat to the global environment and human health. *Sustainability* 2023;15:10821. DOI
63. Pironti C, Ricciardi M, Motta O, Miele Y, Proto A, Montano L. Microplastics in the environment: intake through the food web, human exposure and toxicological effects. *Toxics* 2021;9:224. DOI PubMed PMC
64. Munyaneza J, Jia Q, Qaraah FA, et al. A review of atmospheric microplastics pollution: in-depth sighting of sources, analytical methods, physiognomies, transport and risks. *Sci Total Environ* 2022;822:153339. DOI
65. Thinh TQ, Sang TTN, Viet TQ, et al. Preliminary assessment on the microplastic contamination in the atmospheric fallout in the Phuoc Hiep landfill, Cu Chi, Ho Chi Minh city. *VJSTE* 2020;62:83-9. DOI
66. Schwarz AE, Ligthart TN, Boukris E, van Harmelen T. Sources, transport, and accumulation of different types of plastic litter in aquatic environments: a review study. *Mar Pollut Bull* 2019;143:92-100. DOI PubMed
67. Su Y, Zhang Z, Wu D, Zhan L, Shi H, Xie B. Occurrence of microplastics in landfill systems and their fate with landfill age. *Water Res* 2019;164:114968. DOI
68. Zhang Y, Diehl A, Lewandowski A, Gopalakrishnan K, Baker T. Removal efficiency of micro- and nanoplastics (180 nm - 125 μm) during drinking water treatment. *Sci Total Environ* 2020;720:137383. DOI PubMed PMC
69. Kankanige D, Babel S. Contamination by ≥ 6.5 μm-sized microplastics and their removability in a conventional water treatment plant (WTP) in Thailand. *J Water Process Eng* 2021;40:101765. DOI
70. Lehtiniemi M, Hartikainen S, Näkki P, Engström-öst J, Koistinen A, Setälä O. Size matters more than shape: ingestion of primary and secondary microplastics by small predators. *Food Webs* 2018;17:e00097. DOI
71. Ugwu K, Herrera A, Gómez M. Microplastics in marine biota: a review. *Mar Pollut Bull* 2021;169:112540. DOI PubMed
72. Cordova MR, Ulumuddin YI, Purbonegoro T, et al. Abundance and characterization of microplastic pollution in the wildlife reserve, Ramsar site, recreational areas, and national park in northern Jakarta and Kepulauan Seribu, Indonesia. *Chemosphere* 2024;348:140761. DOI
73. Liu S, Chen H, Wang J, et al. The distribution of microplastics in water, sediment, and fish of the Dafeng River, a remote river in China. *Ecotoxicol Environ Saf* 2021;228:113009. DOI
74. Ismanto A, Hadibarata T, Sugianto DN, et al. First evidence of microplastics in the water and sediment of Surakarta city river basin, Indonesia. *Mar Pollut Bull* 2023;196:115677. DOI
75. Akkajit P, Tipmanee D, Cherdsukjai P, Suteerasak T, Thongnonghin S. Occurrence and distribution of microplastics in beach sediments along Phuket coastline. *Mar Pollut Bull* 2021;169:112496. DOI PubMed
76. Li J, Song Y, Cai Y. Focus topics on microplastics in soil: analytical methods, occurrence, transport, and ecological risks. *Environ Pollut* 2020;257:113570. DOI
77. Akhbarizadeh R, Moore F, Keshavarzi B. Investigating a probable relationship between microplastics and potentially toxic elements in fish muscles from northeast of Persian Gulf. *Environ Pollut* 2018;232:154-63. DOI PubMed

78. Yang L, Zhang Y, Kang S, Wang Z, Wu C. Microplastics in freshwater sediment: a review on methods, occurrence, and sources. *Sci Total Environ* 2021;754:141948. DOI
79. Ibrahim YS, Hamzah SR, Khalik WMAWM, Ku Yusof KMK, Anuar ST. Spatiotemporal microplastic occurrence study of Setiu Wetland, South China Sea. *Sci Total Environ* 2021;788:147809. DOI PubMed
80. Issac MN, Kandasubramanian B. Effect of microplastics in water and aquatic systems. *Environ Sci Pollut Res Int* 2021;28:19544-62. DOI PubMed PMC
81. Eriksen M, Lebreton LC, Carson HS, et al. Plastic pollution in the world's oceans: more than 5 trillion plastic pieces weighing over 250,000 tons afloat at sea. *PLoS One* 2014;9:e111913. DOI PubMed PMC
82. Sheng Y, Ye X, Zhou Y, Li R. Microplastics (MPs) act as sources and vector of pollutants-impact hazards and preventive measures. *Bull Environ Contam Toxicol* 2021;107:722-9. DOI
83. Li W, Zu B, Yang Q, Huang Y, Li J. Adsorption of lead and cadmium by microplastics and their desorption behavior as vectors in the gastrointestinal environment. *J Environ Chem Engi* 2022;10:107379. DOI
84. Lee Y, Cho J, Sohn J, Kim C. Health effects of microplastic exposures: current issues and perspectives in South Korea. *Yonsei Med J* 2023;64:301-8. DOI PubMed PMC
85. Chen J, Wang W, Liu H, Xu X, Xia J. A review on the occurrence, distribution, characteristics, and analysis methods of microplastic pollution in ecosystem s. *Env Pollut Bioavail* 2021;33:227-46. DOI
86. Kiran BR, Kopperi H, Venkata Mohan S. Micro/nano-plastics occurrence, identification, risk analysis and mitigation: challenges and perspectives. *Rev Environ Sci Biotechnol* 2022;21:169-203. DOI PubMed PMC
87. Fu L, Li J, Wang G, Luan Y, Dai W. Adsorption behavior of organic pollutants on microplastics. *Ecotoxicol Environ Saf* 2021;217:112207. DOI
88. Wang F, Wang Q, Adams CA, Sun Y, Zhang S. Effects of microplastics on soil properties: current knowledge and future perspectives. *J Hazard Mater* 2022;424:127531. DOI
89. Park TJ, Lee SH, Lee MS, Lee JK, Lee SH, Zoh KD. Occurrence of microplastics in the Han River and riverine fish in South Korea. *Sci Total Environ* 2020;708:134535. DOI
90. Shim WJ, Hong SH, Eo SE. Identification methods in microplastic analysis: a review. *Anal Methods* 2017;9:1384-91. DOI
91. Serrona K, Yu J, Camarin M. Addressing marine litter through sustainable tourism: the case of the Siargao Islands in the Southern Philippines. *SSRN J* 2022. DOI
92. Tanchuling MAN, Osorio ED. The microplastics in Metro Manila Rivers: characteristics, sources, and abatement. In: Stock F, Reifferscheid G, Brennholt N, Kostianaia E, editors. Plastics in the aquatic environment - Part I. Cham: Springer International Publishing; 2022. pp. 405-26. Available from: https://www.researchgate.net/publication/344058681_The_Microplastics_in_Metro_Manila_Rivers_Characteristics_Sources_and_Abatement. [Last accessed on 18 Apr 2024].
93. Praveena SM, Shaifuddin SNM, Akizuki S. Exploration of microplastics from personal care and cosmetic products and its estimated emissions to marine environment: an evidence from Malaysia. *Mar Pollut Bull* 2018;136:135-40. DOI PubMed
94. Sun Y, Ren X, Rene ER, et al. The degradation performance of different microplastics and their effect on microbial community during composting process. *Bioresour Technol* 2021;332:125133. DOI
95. Saengsupavanich C, Ratnayake AS, Yun LS, Ariffin EH. Current challenges in coastal erosion management for southern Asian regions: examples from Thailand, Malaysia, and Sri Lanka. *Anthropocene Coasts* 2023;6:15. DOI
96. Sui L, Wang J, Yang X, Wang Z. Spatial-temporal characteristics of coastline changes in Indonesia from 1990 to 2018. *Sustainability* 2020;12:3242. DOI
97. Moh YC, Manaf LA. Solid waste management transformation and future challenges of source separation and recycling practice in Malaysia. *Resour Conserv Recy* 2017;116:1-14. DOI
98. Tsai FM, Bui T, Tseng M, Wu K. A causal municipal solid waste management model for sustainable cities in Vietnam under uncertainty: a comparison. *Resour Conser Recy* 2020;154:104599. DOI
99. Vaid M, Sarma K, Gupta A. Microplastic pollution in aquatic environments with special emphasis on riverine systems: current understanding and way forward. *J Environ Manage* 2021;293:112860. DOI
100. Vassilenko E, Watkins M, Chastain S, et al. Domestic laundry and microfiber pollution: exploring fiber shedding from consumer apparel textiles. *PLoS One* 2021;16:e0250346. DOI PubMed PMC
101. Šaravanja A, Pušić T, Dekanić T. Microplastics in wastewater by washing polyester fabrics. *Materials* 2022;15:2683. PubMed PMC
102. Hiwari H, Purba NP, Ihsan YN, Yuliadi LPS, Mulyani PG. Condition of microplastic garbage in sea surface water at around Kupang and Rote, East Nusa Tenggara Province. *Pros Sem Indom Biodiv* 2019:5:165-71. Available from: https://smujo.id/psnmbi/article/view/3231. [Last accessed on 18 Apr 2024]
103. Lima ARA, Barletta M, Costa MF. Seasonal distribution and interactions between plankton and microplastics in a tropical estuary. *Estuar Coast Shelf S* 2015;165:213-25. DOI
104. Bronzo L, Lusher AL, Schøyen M, Morigi C. Accumulation and distribution of microplastics in coastal sediments from the inner Oslofjord, Norway. *Mar Pollut Bull* 2021;173:113076. DOI PubMed
105. Hamzah SR, Altrawneh RS, Anuar ST, Khalik WMAWM, Kolandhasamy P, Ibrahim YS. Ingestion of microplastics by the estuarine polychaete, Namalycastis sp. in the Setiu Wetlands, Malaysia. *Mar Pollut Bull* 2021;170:112617. DOI PubMed
106. Zaki MRM, Zaid SHM, Zainuddin AH, Aris AZ. Microplastic pollution in tropical estuary gastropods: abundance, distribution and potential sources of Klang River estuary, Malaysia. *Mar Pollut Bull* 2021;162:111866. DOI PubMed

107. Sawalman R, Werorilangi S, Ukkas M, Mashoreng S, Yasir I, Tahir A. Microplastic abundance in sea urchins (Diadema setosum) from seagrass beds of Barranglompo Island, Makassar, Indonesia. *IOP Conf Ser Earth Environ Sci* 2021;763:012057. DOI
108. Tran MT, Pham TL, Nguyen XT. Reducing plastic waste for the competitiveness of Vietnamese tourist attractions. *E3S Web Conf* 2020;210:01011. DOI
109. Sharma S, Basu S, Shetti NP, Nadagouda MN, Aminabhavi TM. Microplastics in the environment: occurrence, perils, and eradication. *Chem Eng J* 2021;408:127317. DOI PubMed PMC
110. Susanti NKY, Mardiastuti A, Hariyadi S. Microplastics in fishes as seabird preys in Jakarta Bay Area. *IOP Conf Ser Earth Environ Sci* 2022;967:012033. DOI
111. Niu S, Wang X, Rao Z, Zhan N. Microplastics present in sediments of Yushan River: a case study for urban tributary of the Yangtze River. *Soil Sediment Contam* 2021;30:314-30. DOI
112. Wibowo AT, Nugrahapraja H, Wahyuono RA, et al. Microplastic contamination in the human gastrointestinal tract and daily consumables associated with an Indonesian farming community. *Sustainability* 2021;13:12840. DOI
113. Matupang DM, Zulkifli HI, Arnold J, Lazim AM, Ghaffar MA, Musa SM. Tropical sharks feasting on and swimming through microplastics: first evidence from Malaysia. *Mar Pollut Bull* 2023;189:114762. DOI PubMed
114. Blettler MCM, Ulla MA, Rabuffetti AP, Garello N. Plastic pollution in freshwater ecosystems: macro-, meso-, and microplastic debris in a floodplain lake. *Environ Monit Assess* 2017;189:581. DOI
115. Lim KP, Lim PE, Yusoff S, Sun C, Ding J, Loh KH. A meta-analysis of the characterisations of plastic ingested by fish globally. *Toxics* 2022;10:186. DOI PubMed PMC
116. Bhavsar P, Bhave M, Webb HK. Solving the plastic dilemma: the fungal and bacterial biodegradability of polyurethanes. *World J Microbiol Biotechnol* 2023;39:122. DOI PubMed PMC
117. Liu K, Courtene-Jones W, Wang X, Song Z, Wei N, Li D. Elucidating the vertical transport of microplastics in the water column: a review of sampling methodologies and distributions. *Water Res* 2020;186:116403. DOI
118. Au SY, Lee CM, Weinstein JE, van den Hurk P, Klaine SJ. Trophic transfer of microplastics in aquatic ecosystems: identifying critical research needs. *Integr Environ Assess Manag* 2017;13:505-9. DOI PubMed
119. Tang J, Wu Z, Wan L, et al. Differential enrichment and physiological impacts of ingested microplastics in scleractinian corals in situ. *J Hazard Mater* 2021;404:124205. DOI
120. Pradit S, Noppradit P, Sengloyluan K, Nitiratsuwan T, Chuan OM, Towatana P. Low occurrence of microplastic contamination in anchovies, a transboundary species, in Thai waters. *ScienceAsia* 2022;48:459-66. DOI
121. Osorio ED, Tanchuling MAN, Diola MBLD. Microplastics occurrence in surface waters and sediments in five river mouths of Manila Bay. *Front Environ Sci* 2021;9:719274. DOI
122. Saipolbahri N, Anak Bitlus ML, Ismail NA, Fauzi NM, Subki NS. Determination of microplastics in surface water and sediment of Kelantan Bay. *IOP Conf Ser Earth Environ Sci* 2020;549:012059. DOI
123. Frère L, Paul-Pont I, Rinnert E, et al. Influence of environmental and anthropogenic factors on the composition, concentration and spatial distribution of microplastics: a case study of the Bay of Brest (Brittany, France). *Environ Pollut* 2017;225:211-22. DOI
124. Leiser R, Wu GM, Neu TR, Wendt-Potthoff K. Biofouling, metal sorption and aggregation are related to sinking of microplastics in a stratified reservoir. *Water Res* 2020;176:115748. DOI
125. Pillai CKS. Challenges for natural monomers and polymers: novel design strategies and engineering to develop advanced polymers. *Des Monomers Polym* 2010;13:87-121. DOI
126. da Costa JP, Avellan A, Mouneyrac C, Duarte A, Rocha-santos T. Plastic additives and microplastics as emerging contaminants: mechanisms and analytical assessment. *TrAC Trend Anal Chem* 2023;158:116898. DOI
127. Basak S, Das MK, Duttaroy AK. Plastics derived endocrine-disrupting compounds and their effects on early development. *Birth Defects Res* 2020;112:1308-25. DOI PubMed
128. Zhang H. Transport of microplastics in coastal seas. *Estuar Coast Shelf S* 2017;199:74-86. DOI
129. Torres FG, Dioses-Salinas DC, Pizarro-Ortega CI, De-la-Torre GE. Sorption of chemical contaminants on degradable and non-degradable microplastics: recent progress and research trends. *Sci Total Environ* 2021;757:143875. DOI PubMed
130. Huang W, Song B, Liang J, et al. Microplastics and associated contaminants in the aquatic environment: a review on their ecotoxicological effects, trophic transfer, and potential impacts to human health. *J Hazard Mater* 2021;405:124187. DOI
131. Prata JC, da Costa JP, Duarte AC, Rocha-santos T. Methods for sampling and detection of microplastics in water and sediment: a critical review. *TrAC Trend Anal Chem* 2019;110:150-9. DOI
132. Razak NI, Khalid AA, Anuar ST, Ibrahim YS, Mohamad N, Jaafar M. Microplastics in ASEAN freshwater sediments: a review of methodologies, occurrence levels and effects on aquatic organisms. *Malays J Chem* 2023;25:120-38. DOI
133. Bai CL, Liu LY, Hu YB, Zeng EY, Guo Y. Microplastics: a review of analytical methods, occurrence and characteristics in food, and potential toxicities to biota. *Sci Total Environ* 2022;806:150263. DOI PubMed

Gomiero *et al. Water Emerg Contam Nanoplastics* 2024;3:13
DOI: 10.20517/wecn.2023.63

Water Emerging Contaminants & Nanoplastics

Research Article

Open Access

To what extent are wastewater treatment systems a gateway for microplastic particles in the aquatic and terrestrial environments?

Alessio Gomiero[1], Kjell Birger Øysæd[1], Adrián Jaén-Gil[1], Veslemøy Navrestad[1], Geir Skogerbø[2]

[1]Department of Climate and Environment, Norwegian Research Centre (NORCE), Randaberg 4072, Norway.
[2]IVAR IKS, Stavanger 4017, Norway.

Correspondence to: Dr. Alessio Gomiero, Department of Climate and Environment, Norwegian Research Centre (NORCE), Mekjarvik, 12, Randaberg 4072, Norway. E-mail: algo@norceresearch.no

How to cite this article: Gomiero A, Øysæd KB, Jaén-Gil A, Navrestad V, Skogerbø G. To what extent are wastewater treatment systems a gateway for microplastic particles in the aquatic and terrestrial environments? *Water Emerg Contam Nanoplastics* 2024;3:13. https://dx.doi.org/10.20517/wecn.2023.63

Received: 18 Oct 2023 **First Decision:** 14 Dec 2023 **Revised:** 5 Mar 2024 **Accepted:** 25 Mar 2024 **Published:** 7 May 2024

Academic Editors: Antoni Ginebreda, Daoji Li **Copy Editor:** Pei-Yun Wang **Production Editor:** Pei-Yun Wang

Abstract

Sewage treatment plants are designed to handle wastes that include several types of pollutants, including microplastics (MPs), which are synthetic polymer materials fragmented to sizes < 5 mm. Investigating the abundance and removal efficiency rates of MPs in wastewater treatment plants is important because the water body to which plant effluents are discharged may be adversely affected by the released MPs. Therefore, the abundance, characteristics, and removal of MPs at two sewage treatment plants located on the southwest coast of Norway are studied. Twenty-four samples were collected across two sampling sessions by using an ad hoc-designed plastic-free water sampling device, which was improved by applying a cascade of certified stainless-steel sieves. A combined sequence of enzymatic and strong oxidative incubations was performed for sample preparation. The obtained samples were chemically characterized and quantified using thermoanalytical techniques. The overall amounts of polymers in the inlet wastewater and outlet water were 366-616 µg/L and 34-57 µg/L, respectively, indicating an approximate MPs removal efficiency of 78%-85%. Polyethylene (≈ 36%-68%), polypropylene (≈ 7%-48%), polystyrene (≈ 5%-6%), polyvinyl chloride (≈ 15%-26%), polyamide (≈ 2%), polymethacrylate (≈ 3%-4%), polycarbonate (≈ 2%), and polyethylene terephthalate (≈ 9%-32%) were detected in the investigated samples. In biosolids, the overall quantity of MPs was 3.8-5.5 mg/g dry weight across the two investigated sewage treatment plants. Polyethylene (≈ 24%-44%), followed by polyvinyl chloride (PVC) (≈ 11%-

16%), and polyamide (≈ 2%-22%) were the most commonly recurring polymer types. The outcomes of this study indicate that MPs are removed efficiently from wastewaters. However, large amounts of MPs accumulate in biosolids. Therefore, sludge dumping management procedures need to be improved to lower the amount of MPs released into the environment through effluents and biosolids.

Keywords: Microplastics, sewage treatment plants, pyrolysis, sewage sludge

INTRODUCTION

The introduction of plastic materials into our everyday life has indisputably increased our quality of life. Owing to their intrinsic flexibility, plastic materials can be tailored to cater to a wide range of demands, resulting in increased production and usage of plastics in many applications worldwide. However, the massive release of plastic litter and its slow degradation rate are affecting the environment. Microplastics (MPs) are defined as plastics whose sizes are smaller than 5 mm (US NOAA)[1]. They may be either primary or secondary in origin. Primary MPs are manufactured intentionally and used in various applications, including cosmetics and industrial applications such as sandblasting and surface maintenance. Secondary MPs are generated by the photochemical and physical fragmentation of larger macroplastics[2]. While our understanding of the fate and effects of MPs in the marine environment is advancing, knowledge gaps pertaining to plastics in freshwater and terrestrial environments persist.

Sewage treatment plants (STPs) collect sewage from households, industries, and artisanal activities. MPs in sewage may originate from diverse activities, including washing of clothes, floor cleaning, mechanical street washing, plastic beads used in personal care products, and debris from other plastic objects accidentally or deliberately disposed into drains[3]. STPs are complex systems that employ chemical, physical, and biological processes to release an eco-friendly final discharge into terrestrial or aquatic environments. The existing STPs are not engineered to manage plastic microlitter[4]. A significant, but variable, fraction of the MPs arriving at an STP are retained in its final discharge[5]. Therefore, the effluents discharged by STPs have emerged as an important pathway for the entry of plastic microlitter into aquatic environments and, possibly, terrestrial environments through the spreading of sewage sludge on farmland[6]. Nevertheless, substantial data to assess the relevance of STP effluent as a contributor to plastic pollution are lacking, especially in relation to the data available for other sources.

The main objective of this research is to develop a standardized method for collecting, quantifying, and characterizing MPs to accurately estimate the inlet/outlet flux. The results of this work may help clarify the fate and behaviour of MPs in complex STP systems. The focus is on sewage sludge, a valuable byproduct of the sewage treatment process that is utilized in agricultural production.

MATERIALS AND METHODS

Sampling sites

This study was performed at two STPs, namely the North Jæren STP (NJ-STP) and Grødaland STP (GR-STP), located in Rogaland County on the southwest coast of Norway. These plants employ different rinsing systems. The North Jæren STP mainly collects household wastewaters and subjects them to bar screening, grit removal, pre-aeration, primary sedimentation, chemical-physical treatment, and secondary sedimentation. Meanwhile, the Grødaland STP collects industrial discharges and subjects them to bar screening, grit removal, pre-aeration, primary sedimentation, activated sludge treatment, secondary sedimentation, and tertiary filtration. This plant has separate pretreatment systems for (a) food wastes from households and grocery chains; and (b) wastewater sludge, septic sludge, and other organic industrial wastes. Samples were obtained through the filtration of influent and effluent wastewaters. An *ad hoc* designed stainless-steel device was engineered to filter large volumes of wastewater and separate plastic particles into two dimensional classes: > 300 μm (D1) and 300 μm < D2 < 10 μm [Supplementary Figure 1].

The sampling device consisted of two removable plain Dutch weave stainless-steel sieves having a diameter of 30 cm and mesh sizes of 300 and 10 μm, separately. The mesh screens were fixed at the two ends of a 40-cm-long stainless-steel pipe to obtain a filter cascade with the largest mesh size at the top being the first filter unit in touch with the water sample. This design facilitated both the collection of a relatively large volume of wastewater and *in situ* fractionation of MPs. A flow meter was installed at the end of the device to precisely measure the volume of the sampled wastewater. The efficiency of the designed sampling device was validated using replicates of a 100-L tap water sample spiked with 900- and 50-μm-sized polyethylene particles obtained from Goodfellow Ltd. The contributions of each of the size classes of plastics to the spiking mixture were set by mass. To determine the efficiency of the sampling device, 200 mg of the Ø = 900 μm particles and 40 mg of the Ø = 50 μm polyethylene (PE) particles were separately mixed with 100 L of tap water to prepare each replicate. These replicates were subsequently filtered. Thereafter, the filters were removed and dried in an oven at 50 °C for 3 h. The recovered MPs were transferred to an appropriate stainless steel membrane and weighed, and the sampling efficiency of the device was estimated using Equation (1).

$$\text{Efficiency (\%)} = (\text{mass of recovered particles}/\text{mass of added particles}) \times 100 \tag{1}$$

Sampling

The inlet raw water and the outlet wastewater of the two studied STPs were sampled in March and July 2017, and three replicates/site per sampling session were obtained. To reduce any potential variability associated with rain regimes or possible changes in the main flux entering the STPs, the sampling process was repeated for two days. The obtained samples were pooled together. Different volumes of untreated and treated wastewater were sampled [Supplementary Table 1]. As the sampling process, wastewater was pumped from the water stream into the sampling device by using a submersible stainless-steel pump coupled to a rotating bronze head. Influents were collected after the wastewater was passed through a coarse screen (1 cm mesh size) to prevent larger debris from clogging or damaging the pump head. Depending on the status of the wastewater, each sampling event lasted 1-2 h with a maximum flow rate of 5 L/min. After each sampling session, both filters were removed, and their contents were quantitatively transferred to pre-cleaned glass jars by back-flushing the filters and using pre-burned stainless-steel spatulas. To prevent any possible cross-contamination, the sampler was flushed with tap water between sampling events. In total, 24 samples were collected in this study.

Furthermore, a total of 5 L of 5-day digestates were collected from both STPs by pooling together aliquots from the dryer at intervals of five days. The sewage sludges generated by both STPs were further subjected to anaerobic digestion, leading to a decrease in the proportion of organic material by approximately 50%. The anaerobic digesters of both plants received a certain amount (approximately 10% of the dry mass or DM input) of external material, such as sewage sludge, sludge from the aquaculture industry, and food waste, which may have contributed its own MP load. Generally, at the GR-STP, the digestate is dewatered and utilized in agriculture as a soil amendment. Meanwhile, at the NJ-STP, the digestate is dried at 105 °C to approximately 90% DM, additional plant nutrients are added, and the product is marketed as an organic or organic-mineral fertilizer. The anaerobic digestion and dewatering processes were not likely to affect the MP, but at 105 °C, the effects of these processes on MP shape and degradation cannot be ignored. These effects have not been investigated thus far. Solid samples were collected either as dried digestate (NJ-STP) or dewatered digestate (GR-STP). Five litres of digestate samples were collected on five different days from both STPs, and equal aliquots of all samples were pooled and used for analysis. Sample collection was performed using a stainless-steel shovel, and the collected samples were homogenized and stored in glass containers under dark and cold (-20 °C) conditions before further processing. The storage containers were rinsed with Milli-Q and muffled at 500 °C for 3 h beforehand.

Sample preparation

Wastewater

The material trapped by the filter was dried in an oven at 60 °C for 72 h and weighed thereafter. To remove natural organic and inorganic materials before the characterization and quantification analyses of the plastic fragments without damaging their polymer structure, samples were prepared by enzymatic digestion followed by iron-catalysed oxidation incubation in sequence. All the applied enzymes (Sigma Aldrich, Germany) were of technical grade and filtered (0.2 µm) before use. The sample purification process was started by adding 10 mL of sodium dodecyl sulphate (SDS) (5% w/vol) per gram dry weight (DW) of the sample. The samples were then placed in a 300-mL beaker and incubated at 50 °C for 6 h. The SDS-incubated samples were vacuum-filtered on a pre-muffled (500 °C, 3 h) 125 mL glass crucible filter (porosity 4, ROBU, Germany). The digestates were vacuumed off and the remaining material trapped on the sintered glass filtration surface was rinsed by flushing it with 50 mL of GF/A-filtered (1.2 µm) ultrapure water. Approximately 10 mL of a Viscozyme and Cellulclast mixture per gram of sample DW (1:10; v:v) in acetate buffer (0.1 M; pH 4.8) was added to the same crucible, and the resulting sample was placed in an ultrasound bath for 5 min and incubated for 36 h at 50 °C. The digestates were then vacuumed off using the same crucible filter, and the residual material was rinsed again with 50 mL of ultrapure water, digested for 48 h at 30 °C with 10 mL of protease per gram of sample DW (Sigma, Germany) in PBS (1:10 at pH 7.4), vacuumed off, and rinsed with ultrapure water. The digestates were then filtered through the crucible, and the residual material rinsed again with 50 mL of ultrapure water, incubated for 48 h at 30 °C with 50 mL of lipase in PBS (1:5 at pH 7.4), vacuumed off, and rinsed with Milli-Q. The digested material was then filtered through the crucible surface, and the residual material rinsed again with 50 mL of ultrapure water, incubated for 12 h at 40 °C with 50 mL of lignin peroxidase and laccase enzymes in tartarate buffer (1:5 at pH 3.0), vacuumed off, and rinsed with ultrapure water. Finally, the residual organic material was oxidized by performing the iron (II)-catalysed hydrogen peroxide (H_2O_2) reaction (Fenton reaction). H_2O_2 and iron (II) were added to final concentrations of 250 g/L and 2.5 g/L, respectively[7]. The pH of the mixture was adjusted to ~3 with NaOH. The crucible was kept in an ice bath to maintain the temperature between 30 and 40 °C. The oxidized material was vacuumed off, and the residual iron was washed away from the crucible's surface by flushing it with 100 mL of 0.5 M HCl solution and 50 mL of Milli-Q thereafter.

Digestates

The digestate samples stored in glass containers were dried in an oven at 105 °C for 3 days (Thermolab, Norway). The residual water contents of the dehydrated samples were estimated to assess any possible dilution effects of the reagents and enzymes by following the procedure of Gomiero *et al.*[8]. Homogenized digestate sample aliquots of 50 g (n = 5) were subjected to a sequential combination of enzymes followed by strong oxidation treatment before chemical characterization of the processed samples. The samples were initially spiked with 50 µg of d4-PE, was used as an internal standard for all the target plastics because they were extracted using the same method. All the mass concentration values of the sludge analysed in this study were corrected for the recovery percentages of the internal standard, which ranged from 76% to 92%. Sample preparation started with the addition of 10 mL of SDS (5% w/vol) per gram DW of the sample. The samples were placed in a 1-L beaker and treated at 50 °C for 6 h on a Gallenkamp Incubator Shaker (BioNordika, Norway). The SDS-incubated samples were vacuum-filtered using a sintered glass filter funnel with a volume of 1 L (porosity 4, VWR, Norway). The digestates were vacuumed off, and the remaining material trapped on the sintered glass filtration surface was rinsed by flushing it with 100 mL of filtered ultrapure water. Then, 100 mL of a mixture of Viscozyme and Cellulclast per gram of sample DW (1:5, v:v) in acetate buffer (0.1 M; pH 4.8) was added to the same crucible, and the sample was sonicated for 5 min and digested for 48 h at 50 °C. The digestates were then filtered using the same crucible, and the residual material was rinsed again with 100 mL of ultrapure water, incubated for 48 h at 30 °C with 100 mL of protease per gram of sample DW (Sigma, Germany) in PBS (1:5 at pH 7.4), filtered, and rinsed with Milli-Q. The digestates were then filtered, and the residual material was rinsed again with 100 mL of Milli-Q, incubated for 48 h at 30 °C with 100 mL of lipase in PBS (1:5 at pH 7.4), filtered, and rinsed with Milli-Q. The digested material was then filtered, and the remaining material was rinsed again with 100 mL of ultrapure water, incubated for 12 h at 40 °C with 100 mL of lignin peroxidase and laccase in tartarate buffer (1:5 at pH 3.0), vacuumed off, and rinsed with 100 mL of ultrapure water. Finally, the residual organic material was oxidized by performing the Fenton reaction as described above. Approximately 100 mL of 30% peroxide and 2.5 g/L of iron (II) sulphate were added. The oxidized material was filtered, and the residual iron was washed off the crucible surface by flushing it with 100 mL of 0.5 M HCl solution, followed by 50 mL of Milli-Q. Finally, the contents of the crucible were transferred quantitatively to a fiberglass filter (0.7 µm) by following the procedure of Gomiero *et al.* and dried on a glass Petri dish[8]. The 25 mm (Ø) filter surface containing the sample was circularly pressure cut to a final diameter of 10 mm, folded, and transferred into a pre-burned pyrolysis cup. The obtained sample was pyrolyzed after adding 10 µL of 25% TMAH.

Analysis of plastics

Pyrolysis gas chromatograph mass spectrometer (GCMS) measurements were performed using a Shimadzu Optima 2010C GCMS equipped with an Rxi-5ms column (RESTEC, Bellefonte, PA) and coupled to a multi-shot pyrolizer [EGA/PY-3030D, Frontier Lab (Supplier: BioNordika, Norway)], as previously reported[7]. Pyrolysis was performed at 590 °C. Eight polymers, namely polycarbonate (PC), polypropylene (PP), polyvinyl chloride (PVC), polystyrene (PS), polymethyl methacrylate (PMMA), PE, polyethylene terephthalate (PET), and polyamide (PA)6, were selected for chemical characterization and quantification. Standards of polymers with purity > 99% were purchased from Goodfellow Ltd. (Huntingdon, England). These standards were used to set up the calibration and quantification curves. To identify and quantify the target plastics, specific indicator ions were selected, as described and identified previously [Supplementary Table 2][7]. For calibration, between 0.2 and 420 µg of the polymer standards were weighed using an XPE205 DeltaRange Mettler Toledo balance (Germany).

In the water and sludge samples, d4-PE was used as the internal standard. All mass concentration values reported herein were adjusted for recovery of the internal standard added to the samples before extraction. Internal standard recoveries ranged from 81% to 94 %. The limit of detection (LoD) was calculated as described by Hermabessiere *et al.*[9].

Quality control/Quality assessment

Synthetic clothing was avoided by the personnel involved in this study. The use of glass materials was prioritized during sample preparation, and all work surfaces were cleaned with ethanol filtered over a 0.2 mm sieve. Before usage, all lab materials were rinsed with deionized water and ethanol; thereafter, they were covered with aluminium foil. Throughout sample preparation, blanks were used to evaluate sample contamination, as suggested in the literature[10,11]. Any potential airborne contamination was assessed by placing membrane filters on pre-cleaned petri dishes in the workspace for several hours. The membranes were analysed as controls[12]. Procedural blanks consisting of 100 L of filtered (10 µm mesh size) tap water were treated and analysed simultaneously with the STP samples by using the same reagents at the same volumes.

Calculations

The removal efficiency of plastics with sizes > 10 µm was calculated using the following formula:

Removal efficiency (%) = (Influent concentration - effluent)/Concentration Concentration influent × 100.

RESULTS

The effectiveness of the designed sampler was confirmed using 50-µg spikes of the 900- and 50-µm-sized PE particles. The calculated recoveries ranged from 83% to 99%, indicating the suitability of the designed sampling device for the present study [Supplementary Table 3].

Some of the procedural blanks and airborne control samples of plastics were found to be slightly contaminated with plastics. Such contamination consisted predominantly of PE (≈ 11 µg) and PS (≈ 9 µg) [Tables 1 and 2]. The data were not corrected based on the observed levels of contamination in the procedural blanks and airborne contamination controls. MPs were promptly detected in the influents and effluents of both STPs [Table 1]. All the target plastics, namely PE, PP, PS, PVC, PA, PMMA, PC, and PET, were detected in the investigated samples, indicating the omnipresence of plastics in the wastewater system. The total amount of MPs in the NJ-STP influent varied from 616 to 693 µg/L in the spring and summer sampling sessions, respectively. PE (44%), followed by PET (20%), PVC (15%), and PP (7%), were the most common polymer types in the influent waters obtained in the two sampling sessions [Figure 1A].

Significantly lower levels of plastics were observed in the effluent water, and most of the targeted polymers (PP, PS, PVC, PA, PMMA, and PC) were present in quantities lower than their detection limits. The total quantities ranged from 35 µg/L in the samples obtained in the spring sampling session to 54 µg/L in the samples obtained in the summer sampling session. In both cases, PE (68%) and PET (31%) were the most abundant polymers released into aquatic bodies. Similarly, the total amounts of MPs in the GR-STP influent samples obtained in the spring and summer sampling sessions were 366 and 412 µg/L, respectively. PE (40%), followed by PP (25%), PVC (19%), and PET (10%) were the most abundant polymers in the influent water samples obtained in the two sampling sessions [Figure 1B].

Significantly lower levels of plastics were observed in the effluent water, and most of the targeted polymers such as PS, PA, PMMA, PC, and in some cases, PET, were not detected. The total quantity of plastics ranged from 43 µg/L in the sample obtained in the spring sampling session to 57 µg/L in the sample obtained in the summer sampling session. At both STPs, PE (36%-51%), followed by PP (36%-48%) and PVC (26%), were the most abundant polymers released into marine water bodies. In terms of plastic polymer removal from wastewaters, the overall efficiencies of the NJ-STP were 78% and 83%, respectively, in the spring and summer of 2017. Overall, the removal efficiency of PVC was the highest (≈ 94%), followed by those of PP (≈ 90%) and PE-PP-PET (≈ 88%); by contrast, the least efficiently removed polymer was PMMA (≈ 70%). The removal efficiencies of GR-STP were similar at 85% and 83%, respectively, in the spring and summer of 2017. PE and PET were the most efficiently removed polymers from the aqueous phase (87%). The two STPs differ considerably in terms of catchment area composition. The NJ-STP serves a mostly urban area with a population of around 250,000 people, whereas the GR-STP serves a semi-rural population of 5,000 people and an area with a concentration of food industry units. The overall wastewater loads are approximately 42 and 1.7 mln m^3 per year, respectively, resulting in a total annual discharge of 100 kg and 1.4 tons of MPs to the sea (Eastern North Sea) [Figure 2].

Given the lower population density in the GR-STP catchment area, the discharge of MPs per person from this STP is approximately three times that in case of the NJ-STP [Figure 3].

Table 1. Occurrence and distribution of MPs in influent and effluent waters of NJ-STP and GR-STP

	NJ-STP Concentration µg/L								
	PE	**PP**	**PS**	**PVC**	**PA**	**PMMA**	**PC**	**PET**	**Σ**
Influent March-17	271 ± 15	48 ± 4	32 ± 6	96 ± 5	12 ± 3	21 ± 4	11 ± 4	125 ± 7	616 ± 34
Effluent March-17	24 ± 5	< 10	< 8	< 15	< 10	< 15	< 11	11 ± 3	35 ± 9
Influent July-17	311 ± 12	55 ± 3	36 ± 7	110 ± 12	13 ± 2	24 ± 4	< 11	143 ± 12	692 ± 31
Effluent July-17	37 ± 8	< 10	< 8	< 15	< 10	< 15	< 11	17 ± 3	54 ± 12
Procedural blanks (*n* = 10)	< 10	< 10	< 8	< 15	< 10	< 15	< 11	< 10	
Airborne contamination control (*n* = 20)	11	< 10	9	< 15	< 10	< 15	< 11	< 10	
	GR-STP Concentration µg/L								
	PE	**PP**	**PS**	**PVC**	**PA**	**PMMA**	**PC**	**PET**	**Σ**
Influent March-17	147 ± 13	91 ± 5	23 ± 6	70 ± 7	< 10	< 15	< 11	35 ± 4	366 ± 23
Effluent March-17	22 ± 5	21 ± 3	< 8	< 15	< 10	< 15	< 11	< 10	43 ± 8
Influent July-17	165 ± 13	105 ± 10	26 ± 5	75 ± 4	< 10	< 15	< 11	41 ± 8	412 ± 5
Effluent July-17	21 ± 5	21 ± 2	< 8	15 ± 3	< 10	< 15	< 11	< 10 ± 2	57 ± 5
Procedural blanks (*n* = 10)	< 10	< 10	< 8	< 15	< 10	< 15	< 11	< 10	
Airborne contamination control (*n* = 20)	< 10	< 10	< 8	< 15	< 10	< 15	< 11	< 10	

MPs: Microplastics; NJ-STP: North Jæren sewage treatment plant; GR-STP: Grødaland sewage treatment plant; PE: polyethylene; PP: polypropylene; PS: polystyrene; PVC: polyvinyl chloride; PA: polyamide; PMMA: polymethyl methacrylate; PC: polycarbonate; PET: polyethylene terephthalate.

Table 2. Estimated fluxes of MPs in NJ-STP and GR-STP

	NJ-STP	**GR-STP**
MPs generated, mg/m^3 wastewater	655	0.19
MP discharged to sea, mg/m^3 wastewater	45	0.02
MPs generated per p.e. (g/p.e. × year)	62	0.27
MPs discharged to sea per p.e. (g/p.e. × year)	4	0.03

MPs: Microplastics; NJ-STP: North Jæren sewage treatment plant; GR-STP: Grødaland sewage treatment plant.

The differential compositions of the catchment areas allowed for a further comparison between the contributions of households and the food industry to the MP loads. Assuming that the MP contribution per household was the same in the two catchment areas, the NJ-STP figures (mostly household) indicate that the contribution of the food industry was the dominant driver of MPs in the GR-STP influent. The industry contributed an organic load corresponding to approximately 105,000 p.e. (of the total of 110,000 p.e.) to the GR-STP influent. As presented in Table 2, the MP contribution of the food industry as determined from the GR-STP influent sample was negligible compared to that of the household influent sample collected from the NJ-STP. All the analysed digestate samples contained all the targeted polymers. In the digestate solids collected from the NJ-STP, the total amount of polymers ranged from 5.2 mg/g in the sample obtained in the spring sampling session to 5.5 mg/g DW in the sample obtained in the summer sampling session [Table 3]. In case of the NJ-STP, PE was the most commonly recurring polymer in the digestate samples collected in the spring sampling session, accounting for ≈ 40% of the total MPs, followed by PET (≈ 19%), PVC (≈ 16%), and PP (≈ 7%) [Figure 4A].

The relative proportions of polymers in the summer samples obtained from the two plants were approximately the same, with only non-significant variations between the samples. In the digestates

Table 3. Occurrence and distribution of MPs in biosolids of NJ-STP and GR-STP

	NJ-STP Concentration mg/g DW (*n* = 3)								
	PE	**PP**	**PS**	**PVC**	**PA6**	**PMMA**	**PC**	**PET**	**Σ**
Sludge March-17	2.33 ± 0.15	0.41 ± 0.21	0.27 ± 0.09	0.82 ± 0.22	0.19 ± 0.10	0.17 ± 0.09	0.08 ± 0.02	1.0 ± 0.1	5.2 ± 0.5
Sludge July-17	2.33 ± 0.21	0.47 ± 0.25	0.31 ± 0.08	0.94 ± 0.31	0.10 ± 0.10	0.19 ± 0.08	0.05 ± 0.01	1.2 ± 0.2	5.5 ± 0.5
Procedural blanks (*n* = 5)	< 0.1	< 0.1	< 0.05	< 0.2	< 0.1	< 0.12	< 0.05	< 0.1	
Airborne contamination control (*n* = 5)	< 0.1	< 0.1	< 0.05	< 0.2	< 0.1	< 0.12	< 0.05	< 0.1	
	GR-STP Concentration mg/g DW (*n* = 3)								
	PE	**PP**	**PS**	**PVC**	**PA6**	**PMMA**	**PC**	**PET**	**Σ**
Sludge March-17	1.09 ± 0.05	0.67 ± 0.06	0.17 ± 0.05	0.52 ± 0.05	0.97 ± 0.1	0.14 ± 0.05	0.07 ± 0.02	0.9 ± 0.1	3.6 ± 0.2
Sludge July-17	1.23 ± 0.06	0.78 ± 0.09	0.19 ± 0.08	0.55 ± 0.08	0.86 ± 0.1	0.13 ± 0.07	0.05 ± 0.03	0.1 ± 0.1	3.0 ± 0.3
Procedural blanks (*n* = 5)	< 0.1	< 0.1	< 0.05	< 0.2	< 0.1	< 0.12	< 0.05	< 0.1	
Airborne contamination control (*n* = 5)	< 0.1	< 0.1	< 0.05	< 0.2	< 0.1	< 0.12	< 0.05	< 0.1	

MPs: Microplastics; NJ-STP: North Jæren sewage treatment plant; GR-STP: Grødaland sewage treatment plant; DW: dry weight; PE: polyethylene; PP: polypropylene; PS: polystyrene; PVC: polyvinyl chloride; PA: polyamide; PMMA: polymethyl methacrylate; PC: polycarbonate; PET: polyethylene terephthalate.

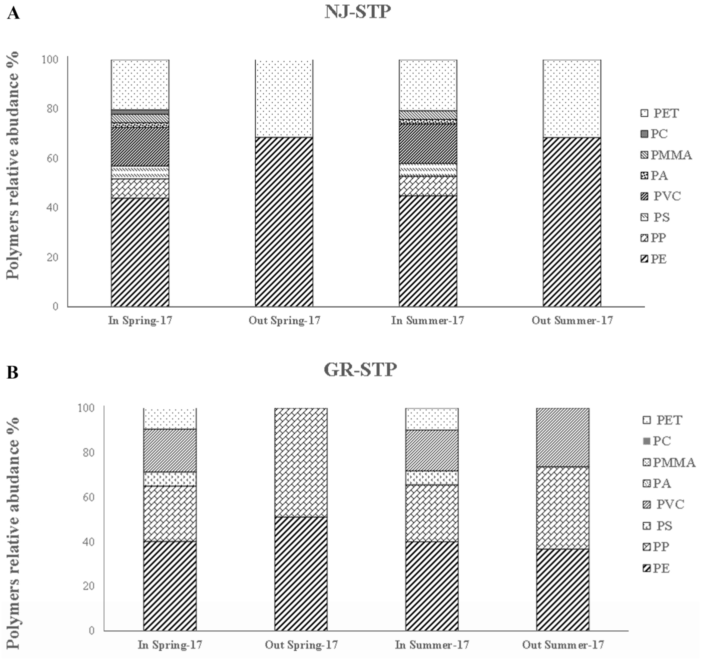

Figure 1. (A) Relative abundance of polymers in the inlet and outlet waters of NJ-STP; (B) Relative abundance of polymers in the inlet and outlet waters of GR-STP. NJ-STP: North Jæren sewage treatment plant; GR-STP: Grødaland sewage treatment plant.

collected from the GR-STP, the total quantity of polymers ranged from 3.5 mg/g in the spring samples to 3.0 mg/g DW in the summer samples. Similar to the results of the samples obtained from the NJ-STP, PE was the predominant plastic detected in the GR-STP digestate samples with a mean concentration of 1.2 mg/g DW and a relative contribution of ≈ 24% to the sum of all plastics. PA (0.86 mg/g), PP (0.78 mg/g), and PVC (0.55 mg/g) were the second (≈ 22%), third (≈ 20%), and fourth (≈ 14%) most recurring polymers in the biosolid samples [Figure 4B].

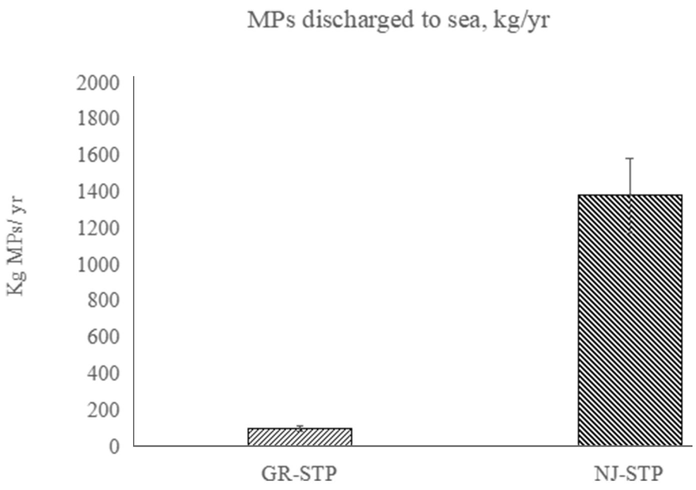

Figure 2. MPs discharged to sea, kg/year from NJ-STP and GR-STP. MPs: Microplastics; NJ-STP: North Jæren sewage treatment plant; GR-STP: Grødaland sewage treatment plant.

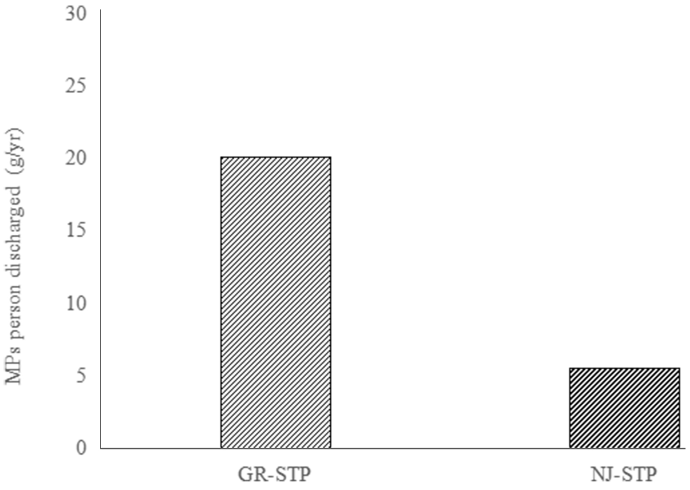

Figure 3. MPs (g/year) per equivalent person discharged to sea, kg/year by NJ-STP and GR-STP. MPs: Microplastics; NJ-STP: North Jæren sewage treatment plant; GR-STP: Grødaland sewage treatment plant.

The variation of plastic concentrations was rather low in terms of either individual plastics or the sum of all plastics. Therefore, the accumulation of plastics throughout the biosolid handling process can be considered comparatively homogeneous. The reproducibility and sensitivity of the proposed method were assessed by splitting one testing sample into five parallels that were analysed separately. Analytical reproducibility stood at RSD ≈ 15% across all detected plastics. Therefore, analytical variability was only a minor source of experimental uncertainty.

DISCUSSION

The results of several studies addressing the characterization and fate of MP litter in wastewater treatment systems, conducted using custom-made sampling devices and state-of-the-art analytical technologies, are available in the literature. However, in most cases, variations in filter selection, sampling frequency, and sample volume hinder comparisons of their results, underscoring the need to promote standardization or

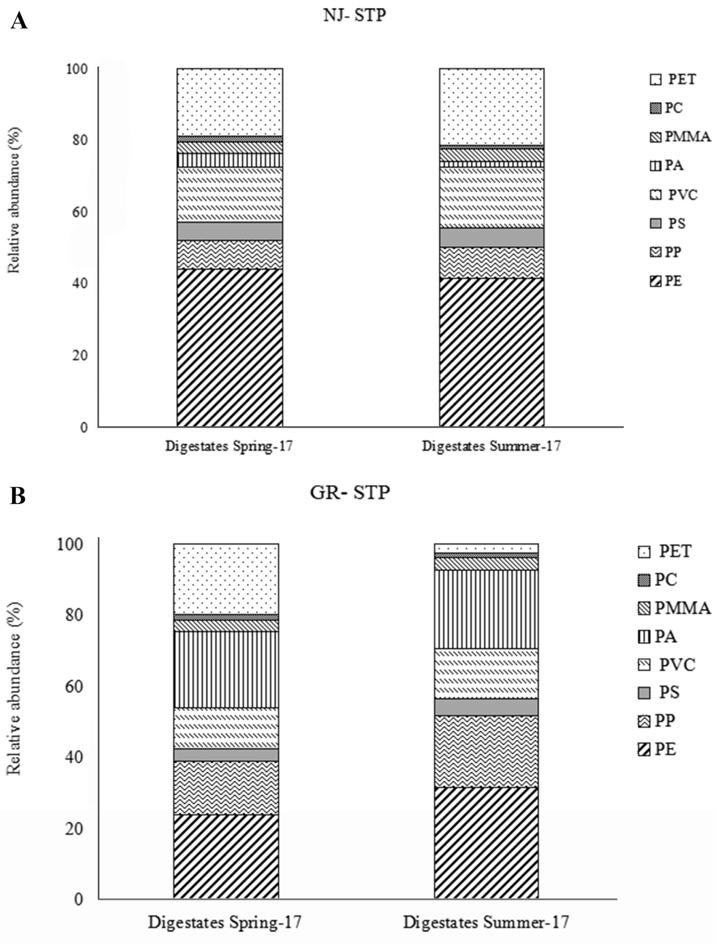

Figure 4. (A) Relative abundance of polymers in digestates of NJ-STP; (B) Relative abundance of polymers in the digestates of GR-STP. NJ-STP: North Jæren sewage treatment plant; GR-STP: Grødaland sewage treatment plant.

harmonization of methodologies. Previous studies have assessed smaller volumes of STP inlet and outlet waters (≈ 50 L) compared to that in the present study. Carr *et al.* managed to process samples of up to 1 m^3 by using tubular filters with filter pore sizes of 45 and 180 μm, which were different from those used herein[13]. The selection of particle size cut-off significantly influences study outcomes, and high MP concentrations have been observed only when finer mesh sizes have been used[14,15]. In terms of analytical approaches, vibrational microscopy-oriented techniques such as micro-Fourier transform infrared analysis (μ-FTIR) and micro-Raman (μ-RAMAN) have been highlighted as robust and reliable methods for chemical characterization of samples, providing valuable information on the numbers, sizes, and shapes of plastic particles, along with their polymeric structures and relative abundances. In addition to vibrational microscopy-oriented analytical techniques, thermoanalytical methods such as pyrolysis coupled with gas chromatography mass spectrometry (pyr-GCMS) and thermal extraction-desorption gas chromatography mass spectrometry (TED-GCMS) have emerged as promising complementary techniques[16,17]. Although thermoanalytical approaches are destructive by nature, they facilitate accurate determination of MP mass, complementing particle-based characterization towards a better understanding of the extent of MP pollution. Because these techniques are designed to report mass-based results, they are particularly useful for wastewater treatment plant managers to study the budget, balance, and partition of plastic materials in complex hydraulic systems.

In the present study, the pyrograms of the analysed water and biosolid samples highlighted the presence of all the targeted polymers such as PVC, PE, PS, PP, PC, PA6, PET, and PMMA. These polymer types have been commonly identified in the influents and effluents of STPs. In a recent review addressing the recognition, occurrence, and removal of plastic particles across 25 sewage treatment plants, Sun *et al.* demonstrated the occurrence of polyester (28%-89%), PE (4%-51%), and PA (3%-30%)[18]. Polyester and PA are extensively used in synthetic clothing, while PEs are used in cosmetics products, including scrubs and creams, as well as in food packaging films[19]. Polymers such as PP, PVC, and PS were observed with relative abundances spanning from 5% to 27%. These multipurpose polymers are heavily used in the food packaging, construction, house maintenance, and automotive production industries, and they are typically found in urban environments[20,21].

The total amounts of MPs and the relative abundances of polymers at the inlets of individual STPs differed significantly, with generally lower levels recorded in case of the GR-STP. This disparity in MP concentrations in the inlet waters of the two STPs likely reflects the compositions of the respective catchment areas, with the NJ-STP serving mainly private households, and the GR-STP serving a large cluster of food industry units. Probably, the former generates larger amounts of MPs from the washing of textiles, use of cosmetics, and various other household activities. Considering the overall wastewater loads, total discharges of 100 kg and 1.4 tons of MPs/year to the Eastern North Sea were estimated for the GR-STP and NJ-STP, respectively. Furthermore, the estimated levels of MPs in the effluent waters (45-50 µg/L) of both STPs could have adverse effects on marine life in the coastal area. Nanoplastic levels and MP levels exceeding 0.14 µg/L are expected to adversely affect 5% (HC5) of key species in the aquatic ecosystem, as reported by the Norwegian Scientific Committee for Food and Environment[22]. Nevertheless, the strong Norwegian Coastal Current rapidly dilutes the effluents and facilitates their long-range dispersion to larger water bodies, resulting in temporary and locally observable expected effects[23,24].

The overall plastic removal rates of the NJ-STP and GR-TP were 78%-83% and 83%-85%, respectively, with no significant differences between the two sampling sessions. Several studies have demonstrated reductions in MPs in STPs, with considerable differences in removal efficiencies. Lv *et al.* reported an overall removal rate of 53% for a full-scale STP located in Eastern China, which employs two parallel alternative wastewater treatment systems[25]. Akarsu *et al.* obtained removal efficiencies ranging from 57% to 96% for three STPs discharging effluents into Mersin Bay, Turkey[26]. Liu *et al.* documented an overall removal efficiency of 64% for a conventional activated-sludge STP in China[27]. Bayo *et al.* (2020) reported an efficient removal rate of 90% for an urban wastewater treatment plant in Cartagena, Spain, that utilizes a system comprising a primary treatment facility and two activated-sludge reactors for sewage processing[28]. Yang *et al.* estimated a removal efficiency of 95% for the Gaobeidian STP in the Chaoyang District of Beijing; this STP is China's largest water recovery plant[29].

The obtained results indicate that the majority of MPs in STPs are retained in the sewage sludge in various treatment steps. Similarly, Talvitie *et al.* calculated that only 20% of the MPs at the wastewater inlet were released through the STP outlet, while the remaining 80% were retained in biosolids[30]. Based on total biosolid production, the authors estimated that approximately 4.6 × 108 MPs were discharged daily from the Finnish STP. Li *et al.* (2018) estimated that 1.56 × 1,014 MPs per year enter the environment though reuse of the biosolids generated by a Chinese STP[31]. Carr *et al.* and Murphy *et al.* found that the biosolids generated by the skimming unit exhibited the highest abundance of MPs (4,000-7,000 MPs per kg WW), which was thousands of times higher than that in the grits and biosolids. These results indicate that the skimming stage of floating solids is an effective step for removing MPs[13,32]. Furthermore, laboratory studies strongly indicate that if sufficient removal of organic particulate materials is achieved, 98%-99% of incoming MPs of all sizes can be removed from the effluent stream[33,34]. The results of these investigations have certainly increased our awareness of the MP problem at STPs. While national guidelines for the removal of MPs from wastewater are yet to be implemented, the expected EU Urban Wastewater Treatment Directive[35] will likely result in upgraded standards for wastewater treatment at both plants, possibly requiring the removal of MPs and other micropollutants. Additionally, the STPs have been informed about the existing efficiency of MP removal, as well as available technologies for monitoring in the future. In this manner, this study has undoubtedly contributed to improving our understanding of the characteristics of plastic particles in STP inlet waters and suggested potential mitigating steps that can be implemented. Moreover, the data obtained in this study have served as the starting point for an extensive survey of the effects of MPs in wastewater sludges and soils published by the Norwegian Water Association[36], thereby expanding the national knowledge base on MPs. Furthermore, these data have facilitated a preliminary correction of exaggerated estimates of MP transfer to soil, reducing the estimated amounts of MPs entering European soils from 60-400,000 tons per year[37] to approximately 2,500 tons per year[38]. Overall conclusions based on investigations on the effects of MPs on plant growth and soil fauna[36] suggest that if sludge-based digestates are applied to soil in the amounts permitted by present legislation[39], the MPs concentrations observed in the present study will not have observable effects on soil fauna and plant growth in the short run, but long-term effects due to accumulation cannot be excluded. As a first step towards mapping the sources and routes of MPs entering and leaving STPs, this investigation provides interesting and useful data. Further efforts should focus on expanding the size range of collectable MPs in wastewater and sludge particles towards finer fractions (< 10 μm). MPs in the near-micron and nanometre range are expected to enter the body organs of living organisms more easily in aquatic systems and, subsequently, those of humans, eliciting diverse toxicological effects[40]. However, further investigations are needed to present a more complete map. The pursuit of such knowledge is advocated because it could aid the formulation of plastic pollution control and prevention measures.

DECLARATIONS

Acknowledgements

The authors are grateful to the staff of the Wastewater Treatment Plant utilities at IVAR IKS for organisational and technical assistance during the sampling campaign.

Authors' contributions

Project administration, conceptualization, methodology, investigation, formal analysis, visualisation, writing - original draft, and writing - review and editing: Gomiero A
Investigation, formal analysis, and visualisation: Øysæd KB
Review and editing: Jaén-Gil A, Navrestad V
Conceptualization, resources, methodology, data curation, writing - original draft, and writing - review and editing: Skogerbø G

Availability of data and materials

The data that support the findings of this study are available on request from the corresponding author Gomiero A.

Financial support and sponsorship

This work was supported by the Norwegian Regional Fund for Rogaland and Hordaland (RFF-Vest) grant #260053.

Conflicts of interest

The author Skogerbø G is employed by IVAR IKS. Other authors declared that there are no conflicts of interest.

Ethical approval and consent to participate

Not applicable.

Consent for publication

Not applicable.

Copyright

REFERENCES

1. Sheavly SB, Register KM. Marine debris & plastics: environmental concerns, sources, impacts and solutions. *J Polym Environ* 2007;15:301-5. DOI
2. Duis K, Coors A. Microplastics in the aquatic and terrestrial environment: sources (with a specific focus on personal care products), fate and effects. *Environ Sci Eur* 2016;28:2. DOI PubMed PMC
3. Tian W, Song P, Zhang H, et al. Microplastic materials in the environment: problem and strategical solutions. *Prog Mater Sci* 2023;132:101035. DOI
4. van Wezel A, Caris I, Kools SA. Release of primary microplastics from consumer products to wastewater in the Netherlands. *Environ Toxicol Chem* 2016;35:1627-31. DOI PubMed
5. Mintenig SM, Int-Veen I, Löder MGJ, Primpke S, Gerdts G. Identification of microplastic in effluents of waste water treatment plants using focal plane array-based micro-Fourier-transform infrared imaging. *Water Res* 2017;108:365-72. DOI PubMed
6. Eerkes-Medrano D, Thompson RC, Aldridge DC. Microplastics in freshwater systems: a review of the emerging threats, identification of knowledge gaps and prioritisation of research needs. *Water Res* 2015;75:63-82. DOI PubMed
7. Simon M, van Alst N, Vollertsen J. Quantification of microplastic mass and removal rates at wastewater treatment plants applying Focal Plane Array (FPA)-based Fourier Transform Infrared (FT-IR) imaging. *Water Res* 2018;142:1-9. DOI PubMed
8. Gomiero A, Øysæd KB, Agustsson T, van Hoytema N, van Thiel T, Grati F. First record of characterization, concentration and distribution of microplastics in coastal sediments of an urban fjord in south west Norway using a thermal degradation method. *Chemosphere* 2019;227:705-14. DOI PubMed
9. Hermabessiere L, Himber C, Boricaud B, et al. Optimization, performance, and application of a pyrolysis-GC/MS method for the identification of microplastics. *Anal Bioanal Chem* 2018;410:6663-76. DOI
10. Magni S, Binelli A, Pittura L, et al. The fate of microplastics in an Italian Wastewater Treatment Plant. *Sci Total Environ* 2019;652:602-10. DOI
11. Liu K, Wang X, Wei N, Song Z, Li D. Accurate quantification and transport estimation of suspended atmospheric microplastics in megacities: implications for human health. *Environ Int* 2019;132:105127. DOI
12. Gomiero A, Strafella P, Øysæd KB, Fabi G. First occurrence and composition assessment of microplastics in native mussels collected from coastal and offshore areas of the northern and central Adriatic Sea. *Environ Sci Pollut Res Int* 2019;26:24407-16. DOI PubMed
13. Carr SA, Liu J, Tesoro AG. Transport and fate of microplastic particles in wastewater treatment plants. *Water Res* 2016;91:174-82. DOI PubMed
14. Leslie HA, Brandsma SH, van Velzen MJ, Vethaak AD. Microplastics en route: field measurements in the Dutch river delta and Amsterdam canals, wastewater treatment plants, North Sea sediments and biota. *Environ Int* 2017;101:133-42. DOI PubMed
15. Fojt J, David J, Přikryl R, Řezáčová V, Kučerík J. A critical review of the overlooked challenge of determining micro-bioplastics in soil. *Sci Total Environ* 2020;745:140975. DOI PubMed
16. Ivleva NP. Chemical analysis of microplastics and nanoplastics: challenges, advanced methods, and perspectives. *Chem Rev* 2021;121:11886-936. DOI PubMed
17. Picó Y, Barceló D. Pyrolysis gas chromatography-mass spectrometry in environmental analysis: focus on organic matter and microplastics. *TrAC Trend Anal Chem* 2020;130:115964. DOI
18. Sun J, Dai X, Wang Q, van Loosdrecht MCM, Ni BJ. Microplastics in wastewater treatment plants: detection, occurrence and removal. *Water Res* 2019;152:21-37. DOI PubMed
19. Ziajahromi S, Neale PA, Rintoul L, Leusch FD. Wastewater treatment plants as a pathway for microplastics: development of a new approach to sample wastewater-based microplastics. *Water Res* 2017;112:93-9. DOI PubMed
20. Andrady AL, Neal MA. Applications and societal benefits of plastics. *Philos Trans R Soc Lond B Biol Sci* 2009;364:1977-84. DOI PubMed PMC
21. Horodytska O, Cabanes A, Fullana A. Plastic waste management: current status and weaknesses. In: Plastics in the aquatic environment - Part I: Current status and challenges. Cham: Springer International Publishing; 2019. pp. 289-306. DOI

22. Microplastics; occurrence, levels and implications for environment and human health related to food. Opinion of the Scientific Steering Committee of the Norwegian Scientific Committee for Food and Environment. 2019. Available from: https://vkm.no/download/18.5b7a016e16dcd89a3977dc60/1571650615867/Microplastics;%20occurrence,%20levels%20and%20implications%20for%20environment%20and%20human%20health%20related%20to%20food.pdf. [Last accessed on 25 Apr 2024].
23. Simonsen M, Lind OC, Saetra Ø, et al. Coastal transport of river-discharged radionuclides: impact of speciation and transformation processes in numerical model simulations. *Sci Total Environ* 2019;669:856-71. DOI
24. Ibrekk HO, Molvær J, Faafeng B. Nutrient loading to norwegian coastal waters and its contribution to the pollution of the North Sea. *Water Sci Technol* 1991;24:239-49. DOI
25. Lv X, Dong Q, Zuo Z, Liu Y, Huang X, Wu W. Microplastics in a municipal wastewater treatment plant: fate, dynamic distribution, removal efficiencies, and control strategies. *J Clean Prod* 2019;225:579-86. DOI
26. Akarsu C, Kumbur H, Gökdağ K, Kıdeyş AE, Sanchez-Vidal A. Microplastics composition and load from three wastewater treatment plants discharging into Mersin Bay, north eastern Mediterranean Sea. *Mar Pollut Bull* 2020;150:110776. DOI PubMed
27. Liu X, Yuan W, Di M, Li Z, Wang J. Transfer and fate of microplastics during the conventional activated sludge process in one wastewater treatment plant of China. *Chem Eng J* 2019;362:176-82. DOI
28. Bayo J, Olmos S, López-Castellanos J. Microplastics in an urban wastewater treatment plant: the influence of physicochemical parameters and environmental factors. *Chemosphere* 2020;238:124593. DOI
29. Yang L, Li K, Cui S, Kang Y, An L, Lei K. Removal of microplastics in municipal sewage from China's largest water reclamation plant. *Water Res* 2019;155:175-81. DOI
30. Talvitie J, Mikola A, Koistinen A, Setälä O. Solutions to microplastic pollution - removal of microplastics from wastewater effluent with advanced wastewater treatment technologies. *Water Res* 2017;123:401-7. DOI PubMed
31. Li X, Chen L, Mei Q, et al. Microplastics in sewage sludge from the wastewater treatment plants in China. *Water Res* 2018;142:75-85. DOI
32. Murphy F, Ewins C, Carbonnier F, Quinn B. Wastewater treatment works (WwTW) as a source of microplastics in the aquatic environment. *Environ Sci Technol* 2016;50:5800-8. DOI PubMed
33. Mitrano DM, Beltzung A, Frehland S, Schmiedgruber M, Cingolani A, Schmidt F. Synthesis of metal-doped nanoplastics and their utility to investigate fate and behaviour in complex environmental systems. *Nat Nanotechnol* 2019;14:362-8. DOI PubMed PMC
34. Schmiedgruber M, Hufenus R, Mitrano DM. Mechanistic understanding of microplastic fiber fate and sampling strategies: synthesis and utility of metal doped polyester fibers. *Water Res* 2019;155:423-30. DOI PubMed
35. European Commission. Urban wastewater. Available from: https://environment.ec.europa.eu/topics/water/urban-wastewater_en. [Last accessed on 25 Apr 2024].
36. A 253 Microplastics in wastewater, wastewater sludge and soil. 2020. (in Norwegian) Available from: https://va-kompetanse.no/butikk/a-253-mikroplast-i-avlopsvann-avlopsslam-og-jord/. [Last accessed on 25 Apr 2024].
37. Nizzetto L, Futter M, Langaas S. Are agricultural soils dumps for microplastics of urban origin? *Environ Sci Technol* 2016;50:10777-9. DOI
38. Ljung E, Olesen KB, Andersson PG, et al. Microplastics in the ecosystem. (in Norwegian). Available from: https://www.svensktvatten.se/contentassets/7be8e202754e4011a400bcff4ed89b1c/mikSVu-rap-8-13.pdf. [Last accessed on 25 Apr 2024].
39. Regulation on organic fertilizers and related products. (in Norwegian) Available from: https://lovdata.no/dokument/SF/forskrift/2003-07-04-951. [Last accessed on 25 Apr 2024].
40. Zhang Y, Kang S, Allen S, Allen D, Gao T, Sillanpää M. Atmospheric microplastics: a review on current status and perspectives. *Earth Sci Rev* 2020;203:103118. DOI

idæa

OPEN ACCESS
Online ISSN: 2831-2597
Volume 3, Issue 3, September 2024

Water Emerging Contaminants & Nanoplastics

oae | WECN
https://oaepublish.com/wecn

Belioka *et al.* *Water Emerg Contam Nanoplastics* 2024;3:14
DOI: 10.20517/wecn.2024.09

Water Emerging Contaminants & Nanoplastics

Review

Open Access

How plastic waste management affects the accumulation of microplastics in waters: a review for transport mechanisms and routes of microplastics in aquatic environments and a timeline for their fate and occurrence (past, present, and future)

Maria-Paraskevi Belioka, Dimitrios S. Achilias

Lab of Polymer and Colours Chemistry and Technology, Department of Chemistry, Aristotle University of Thessaloniki Campus, Thessaloniki 54124, Greece.

Correspondence to: Dr. Maria-Paraskevi Belioka, Prof. Dimitrios S. Achilias, Lab of Polymer and Colours Chemistry and Technology, Department of Chemistry, Aristotle University of Thessaloniki Campus, Thessaloniki 54124, Greece. E-mail: mpelioka@auth.gr; axilias@chem.auth.gr

How to cite this article: Belioka MP, Achilias DS. How plastic waste management affects the accumulation of microplastics in waters: a review for transport mechanisms and routes of microplastics in aquatic environments and a timeline for their fate and occurrence (past, present, and future). *Water Emerg Contam Nanoplastics* 2024;3:14. https://dx.doi.org/10.20517/wecn.2024.09

Received: 14 Mar 2024 **First Decision:** 29 Mar 2024 **Revised:** 27 Apr 2024 **Accepted:** 13 May 2024 **Published:** 23 May 2024

Academic Editor: Roberto Rosal **Copy Editor:** Pei-Yun Wang **Production Editor:** Pei-Yun Wang

Abstract

An increasing global problem is the buildup of improperly handled plastic garbage in the environment. One of the biggest environmental issues facing aquatic ecosystems today is contamination from bulk plastics and plastic detritus. Specifically, microplastics (MPs) and nanoplastics, which are small-scale plastic waste, are now the main causes of pollution in freshwater and marine environments. On the other hand, contamination of aquatic systems is now acknowledged as one of the major environmental hazards facing our world. Currently, concerns have been raised regarding the breakdown of plastic products into micro and nanosized particles, because of the ineffective plastic waste management. To prioritize regions for mitigation policy implementation, it is critical to pinpoint the precise MPs' transport mechanisms and the locations where trash is created. In order to show the historical and contemporary circumstances as well as forecasts and scenarios of global plastic waste management from now until 2060, we used continent-level data on trash management. This study, finally, presents a potential future scenario of estimates on the destiny, transport, and occurrence of plastic waste in aquatic habitats, highlighting the different factors that trigger the transport of MPs into water and the necessity of rational management of plastic waste.

Keywords: Microplastics, nanoplastics, plastic pollution, aquatic environments, plastic waste management, future scenarios

INTRODUCTION

Plastics are currently a great material that is employed in many aspects of daily life, as they are utilized in nearly every industry, including packaging, vehicle, aquaculture, fisheries, biomedical, shipping, agriculture, building and construction, telecommunications, furniture, transportation, textiles, apparel, and personal care items. Because of their low weight, elasticity, resilience, flexibility, low cost, long-term persistence, corrosion resistance, high strength-to-weight ratio, and water-resistant qualities, plastics have supplanted more traditional materials such as glass and metals[1-3].

The number of anthropogenic stressors in aquatic media, including microplastics (MPs), is making a significant contribution to the increasing pollution of the environment[4]. Because plastic goods are used so widely in daily life, an increasing number of plastic particles - primary MPs - are making their way into the water. The global danger that MP pollution poses to human and ecological health is causing the public to grow more concerned about this issue[5,6]. According to the National Oceanic and Atmospheric Administration (NOAA) of the United States, fragments of any kind of plastic that are smaller than 5.0 mm can generally be categorized as MPs[7,8]. It is usual to use the mesh size of the neuston nets (333 μm or 0.33 mm), which was used to collect the samples, even if the bottom limit (size) of the MPs is not stated[4]. The two main processes by which MPs are produced and discharged into a body of water are primary and secondary. MPs come from a variety of sources and have a wide range of features[4,7].

MPs are created when plastics undergo physical, chemical, mechanical, and biological degradation or break down into tiny fractions[9]. Due to their ongoing manufacture, non-biodegradable nature, persistence, and extended environmental life span, these plastics are tiny, ubiquitous particles that have been steadily accumulating in the environment[10]. According to Constant *et al.* (2020), they have been identified as one of the ten emerging pollutants in the United Nations Environmental Programme (UNEP) Year Book 2014 that may pose a hazard to the health of humans and other creatures across all biomes[11].

Scientists worldwide are increasingly concerned about the buildup of MPs in environmental components, with densely inhabited areas showing higher concentrations in lakes, rivers, estuaries, seas, and beaches[12,13]. Due to their tiny size, MPs can potentially affect human health when they enter the human food chain through the consumption of seafood and other terrestrial foods[14-17]. Furthermore, the disposal of plastic trash in municipal waste disposal systems generates toxic leachate, which can damage land and water[18]. Plastic trash will keep rising as a result of inappropriate waste management practices and unprecedented consumption of plastic items[13,19].

Global efforts are focusing on quantifying plastic pollution in seas and freshwater, as it affects marine life and people. The breakdown of macroplastics into MPs complicates identifying pollution sources and implementing mitigation strategies. Studying MP life cycles without estuaries undervalues their contribution to oceans[20]. Over the past 10 years, the relevance of MP debris in freshwater and marine ecosystems has increased[21,22]. The impact of MPs on aquatic organisms is underexplored, with plastic fragmentation primarily induced by weathering, similar to sunlight photodegradation. In marine environments, plastics have a slower rate of degradation due to lower temperatures[21,23,24]. Mechanical elements like turbulence and wave action can fragment plastic debris, while improper disposal can cause secondary MP buildup in marine environments due to non-biodegradable synthetic polymers. Furthermore, the anerobic conditions required for the breakdown of biodegradable polymers are absent from saltwater[4,25,26]. Understanding the mechanisms affecting marine plastic trash dispersion and transit is crucial due to the heterogeneity of plastic particles and their non-linear behavior throughout the water column[27,28]. Variations in density, buoyancy, and residence durations that occur during the MP particle's life cycle in the water are linked to discrepancies in their behavior[28].

The current focus of the study is to gain a better understanding of this behavior, as knowledge of these processes is essential for assessing ecological implications and potential health hazards to humans. Additionally, it helps develop policies and standards for managing coastal areas and put in place appropriate monitoring systems[29]. According to Hardesty *et al.* (2017), numerical models hold great potential for improving our understanding of plastics' behavior in dynamic flow systems. Numerous intricacies linked to flow dynamics can be calculated using numerical models. Furthermore, developments in numerical methods and processing power have made it possible to apply fine grid resolution for the computation of precise and detailed flow patterns, which serve as MP drivers[28,30].

Thus, the goals of this work are to: (a) Review the manner in which fresh water is contaminated by various transport mechanisms; (b) summarize the primary transport mechanisms in the estuaries of some of the heavily polluted rivers or lakes that leak MPs into the seas, (c) to present MPs' routes of transportation via several environmental divisions; (d) to correlate plastic waste management and MPs' occurrence in water; and (e) to analyze the forecasts for plastics and MPs in water by 2060, taking into account the improper handling of plastic trash in the present and the upcoming years.

METHODOLOGY

This mini-review compiles findings from 100 studies about MP transport processes in rivers, lakes, and oceans. The terms "MPs" and "estuary" were combined with the following keywords to extract literature from the databases of Google Scholar, Scopus, and Web of Science: "transport", "fate", "plastic waste", "nanoplastics", "litter", "migration behavior", and "contamination". The retrieved studies were categorized according to the transport mechanisms they covered. Each article located was released between 2010 and 2023. Research addressing the movement of MPs in estuary sediments and water columns was incorporated, whereas studies examining the effects of MPs on estuarine biota were not. Moreover, research conducted in aquatic environments - such as lakes, rivers, and oceans - was also included.

We stopped our search when multiple pages of results in Scopus, Google Scholar, and Web of Science yielded no relevant papers. Since the search was focused on finding publications with literature reviews, case studies, book chapters, conference papers, postgraduate and doctoral theses, and papers written in languages other than English were all excluded. As a result, published articles were filtered using the previously indicated criteria (title, keywords, and abstract), and relevant publications were included in our collection. We reviewed the content of each article, paying particular attention to the abstracts and conclusions. The ideal reference criteria for systematic reviews and meta-analyses set by Moher *et al.* were used in this review paper's research approach [Figure 1][31].

The datasets used in this paper have been taken by OECD Library Global Plastics Outlook as Excel files, and they provide estimates of plastic waste for the different global regions and/or continents. These datasets also provide estimates of plastic waste measured in millions of tons per year, per end-of-life fate after accounting for recycling losses and collected littering, *etc.*[32].

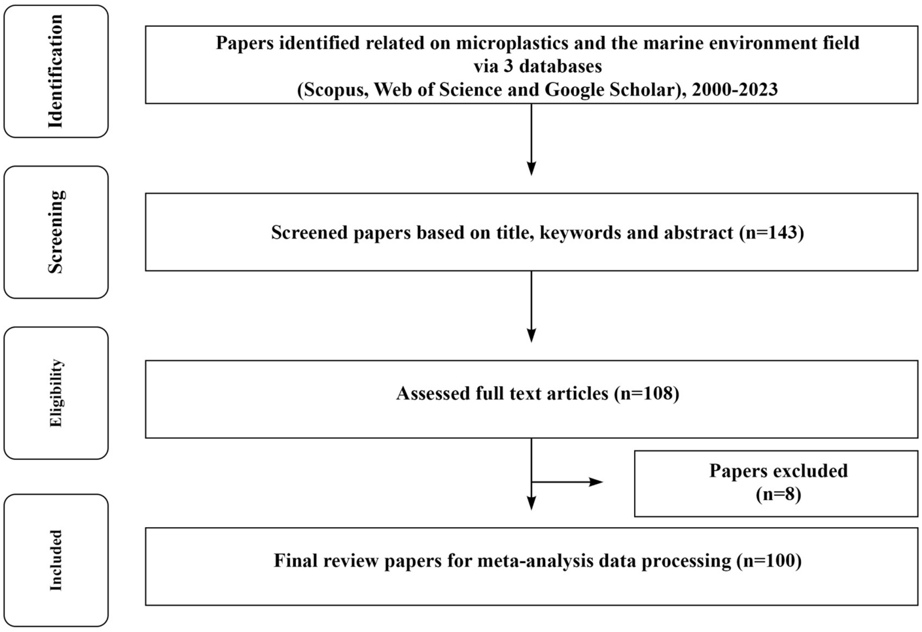

Figure 1. Comprehensive workflow of the research project[31].

TRANSPORT MECHANISMS OF MPS IN FRESHWATER, RIVERS, LAKES AND MARINE ENVIRONMENTS

MPs' occurrence and destiny are influenced by physical properties, environmental interactions, and meteorological and hydrodynamic factors. Factors like size, density, and morphology also influence their dispersion and sinking rates[33]. MPs, due to their size, shape, and durability, are easily transported by wind and water, influenced by human behavior, particle characteristics, weather, and environmental topography[34].

They can enter aquatic habitats through various routes, including runoff, garbage dumping, air deposition, and wastewater treatment plant outfall, as mentioned before. Although treatment plants can retain MPs and filter out some particles, they struggle with synthetic microfibers and nanoplastics[35,36]. Other MP entry mechanisms into terrestrial and aquatic environments relate to agricultural sources, including organic fertilizer products[37].The physical and chemical characteristics of MPs, substrate conditions, and hydrodynamics at the sediment-water interface affect their transit in lakes and rivers, with different origins affecting transport qualities, burial likelihood, and interactions[36,38].

Plastics and MPs can enter the environment through various channels, including terrestrial and marine-based activities, as well as home or commercial drainage systems. For instance, tiny plastic beads commonly found in toothpaste, scrubs, and clothes can easily find their way into the aquatic ecosystem. Similar to this, clothing made of synthetic fibers sheds MPs, which end up as effluents in wastewater treatment facilities or water supplies[39]. Additional pathways for MPs to infiltrate the marine environment include storm drains, wind, and waves. Runoff carries some of them out to sea. Unfavorable weather conditions increase the deposit of macroplastic at shorelines, and the path often passes via landfills and marine recycling ports, which contribute to the breakdown of macroplastic garbage. Sewage sludge, which enters the aquatic ecosystem containing more MPs than garbage, is another possible cause of MP pollution[40,41]. The low concentrations and huge size of MPs allow currents to carry them over greater distances and distribute them widely[42].

Additionally, according to De Witte *et al.* (2014) and Gauquie *et al.* (2015), MPs may be found in a variety of marine animals, including fish, seabirds, bivalves, mammals, and crabs, as well as on beaches and in seabed sediments and surface waters[43,44]. The excrement of zooplankton is another way that MPs might enter the ocean. The MPs were easily consumed by the organisms as they passed through their digestive tracts, were encapsulated in excrement, and were ingested. After being eaten, the excrement dropped to the bottom of the exposure vessel, where it was later consumed by the bigger copepod[45].

Municipal wastewater treatment plants are significant sources of MPs in the environment, primarily removed through sludge settling and solids skimming. The effluent discharges from these plants can influence MP burdens in oceans and surface water habitats[46]. For instance, MP parts from synthetic fibers in garments end up as effluents in wastewater treatment facilities or water, and each day, about 65 million MP particles are released into the receiving water by Glasgow's wastewater treatment works (WWTW), which is situated on the River Clyde[39,45]. Thus, wastewater treatment plant (WWTP) effluent has been highlighted in a number of published studies as a major pathway for the direct transfer of MPs into aquatic and soil habitats[47]. As we said before, in the first stages of the WWT process, large-size MPs and other particles may be held in the grit chamber and mechanical screen. The coagulation/flocculation mechanism causes MP fibers to settle by gravity during the initial treatment phase[13].

The human respiratory system is harmed by MPs of various morphologies that are constantly being carried and settling in soil or sediment after being discharged into the atmosphere. Beaches, seabed sediments, surface waters, and a variety of marine organisms, such as fish, seabirds, bivalves, mammals, and crabs, among others, have been reported to contain MPs[45,48]. MPs can travel by atmospheric fall and marine movement. Its low density and tiny size contribute significantly to the widespread dissemination of MPs in all ecosystems worldwide. According to Obbard *et al.* (2014), polar ice and marine sediments have therefore turned into a worldwide sink for MPs[49].

As to terrestrial system concerns, according to He *et al.* (2018), agricultural operations, precipitation, fractures, and soil organism activities can all introduce MPs into the subsurface soil[50]. These mechanisms have the potential to induce MPs to seep into deep soils containing water and eventually find their way into groundwater[51]. Furthermore, through ingestion, redox, and excretion processes, soil organisms, such as earthworms, insects, nematodes, bacteria, fungi, algae, *etc.*, affect the transport and destiny of MPs[13,52]. MP fragments from wastewater treatment facilities are often retained in sludge due to high efficiency, and large volumes are dumped into Europe for composting and agricultural fertilizer[34]. MPs are not yet taken into account by regulations on hazardous substances found in sludge applied to land, so the mass of MPs unintentionally applied to land each year may surpass 400,000 tons[53]. Sewage treatment effluent contains MPs that can enter the environment through rivers' effluent intake. These particles are primarily applied to land as sludge or discharged directly into the environment. Other methods for disposing of sludge include burning, landfilling, and cement production, making it unlikely for plastic particles to leak[34,51,54]. Other techniques for getting rid of sludge include burning it, dumping it in a landfill, and even using it to make cement that is used in buildings. Under these circumstances, it is improbable that plastic particles would leak into the environment because they are well-contained[51,54,55]. MPs in wastewater treatment plant sewage sludge can be as high as 15,385 items/kg, contaminating agricultural soils. Annual discharges in North America and Europe are estimated to be 63,000-430,000 tons and 440,00-300,000 tons, respectively[53,56].

Organic fertilizers made from composting and fermenting biowaste can introduce MPs into soils, which are often applied to agricultural crops after drying, and are transported through physical, chemical, and biological processes[37]. Plastic film mulching and greenhouse covering have been widely and heavily used in agricultural production because of their efficaciousness in enhancing agricultural quality and production and can be one extra factor for the appearance of MPs in soils[57,58]. The increased concentration of MPs in terrestrial soils may also be caused by other factors such as roadside littering, illicit trash disposal, and tire abrasion[52].

The air-water transfer of materials is influenced by aquatic conditions, including salinity and organic colloids. Bubble bursting, a phenomenon where plastic particles transfer from water to air, is influenced by salinity and gel concentration. In high salinity settings, gel concentration and viscosity significantly affect MP mobility. The addition of proxies for sea surface microlayer components increases the particle transfer rate[59].

The air-water transfer is also reinforced by rivers that are crucial entry points for MPs into the ocean, but the lack of data on their environmental fate makes it difficult to assess danger and design regulatory responses. MP prevalence increases upstream and downstream, correlated with natural and man-made factors. The density and size of MPs influence migration across compartments, with geographic distance being a strong determinant[60,61]. The prevalence of MPs demonstrated significant associations with the increase and geographic location of sampling sites, the distance from the closest city, demographic density, and the rate of urbanization, according to Pearson's correlation analysis provided in a study by Yuan *et al.* 2022[60]. MPs' circulation and final sink are influenced by environmental factors, density, shape, size, hydrodynamics, meteorological conditions, habitat characteristics, and interactions with aquatic biota[62]. The upper soil level is a degradative environment for plastic trash, aided by strong heat, oxygen, and sunlight. Plastics undergo biodegradation and macroplastic breakdown, accelerated by agricultural practices. However, plastic degradation takes decades. MPs enter groundwater systems through leaching and are transported via the biosphere, with soil biota playing a key role in this process[63].

Improper management of rubbish and wind-blown littering might unintentionally introduce plastics from landfills into the terrestrial ecosystem. MPs can travel through the ecosystem thanks to landfills. The polymers might be dispersed far from their sources by wind action[63]. Alternatively, toxic materials derived from plastic garbage may leak into landfills when plastic waste is disposed of there. If left untreated, the leachate from the breakdown and leaching of additives such as plasticizers might release toxins that contaminate the surrounding rivers and groundwater system[64,65].

The amount of plastic litter that is discharged into the environment is difficult to estimate since there are few data and disposal practices for plastic debris vary between countries. Wind-blown trash and plastic discharged onto the land are examples of mismanaged garbage. According to estimates from 2010, the amount of garbage that is mishandled in the European Union (EU) is comparable to that in the US. As demonstrated by the implementation of EU-wide waste management regulations, this is a realistic assumption based on parallels in national income and the development of waste management infrastructure[66]. As mentioned before, the amount of mismanaged plastic garbage (plastic waste - managed waste) in the EU is estimated at 520,000 metric tons. Furthermore, sewage sludge is thought to deposit between 63,000 and 430,000 metric tons of MPs onto land each year[53].

Larger proportions will eventually find their way into the marine environment as a consequence of increased aggregation brought on by rising plastic manufacture and natural erosion. Nonetheless, it is still probable that for a long while to come, more plastic will be deposited and kept in continental ecosystems than will enter the oceans. According to estimates, rivers serve as conduits for the transportation of 70%-80% of marine plastics into the ocean. In addition to being carried by rivers from the land to the ocean, plastic waste may also come back to the ground during high tides or floods. The same elements that influence the movement of sediment also influence the movement of plastic particles within river systems, including environmental parameters and hydrological features[34,53]. Anything may be deposited in areas with low flows and changes in stream depth or flow (such as on bends); on the other hand, high-velocity rainfall and deterioration dislodge previously settled debris to be mobilized instead of introducing particles through runoff[34].

All of the above has been derived from a thorough study of all the published papers included in this review, which include the most prevalent sources and mechanisms of MP transport in aquatic environments. Below in Figure 2, the primary mechanisms of MP transport are illustrated, arranged and quantified based on statistical analysis, ranking from the most dominant and frequent to the least important. More specifically, the main mechanisms that are referred to in the reviewed published papers have been classified in the categories below. This was followed by a quantification of the frequency of occurrence in the examined published papers.

MPS' ROUTES OF TRANSPORTATION VIA SEVERAL ENVIRONMENTAL DIVISIONS

Atmospheric environment

Due to the lack of limits in the air and the fact that the speed, as well as the direction of the air, primarily affect the MPs, the moving of MPs in the atmosphere might result in a large dispersal range for MPs. Variables like temperature, precipitation, wind direction, speed, and pollution concentration gradient influence MPs' movement in the atmosphere, with wind modulation impacting urban transportation and suspension[67,68]. Particle density and sedimentation, wind, and precipitation all affect how long particles remain in the atmosphere and how they fall out or deposit[69]. Low-density MPs are frequently carried by the wind over great distances, which ultimately leads to MP pollution on land and in water[70].

Boucher and Friot (2017) found that wind-borne atmospheric MP transport accounts for 7% of ocean MP contamination. According to air mass trajectories, MPs were carried up to 95 kilometers from their point of origin to a region with a low population density[71]. According to Abbasi *et al.* (2019) and Prata (2018), atmospheric particulates that have settled in the terrestrial environment may also be resuspended in the air or carried to aquatic systems by rainfall or surface runoff and because MPs and dust share the same pattern of degradation, MPs observed in the marine environment can be linked to atmospheric dust fallout[68,72].

Terrestrial environment

Because MPs are resilient, they will build up and come to high concentration levels in the soil, which may have an impact on the biodiversity of soil[73]. Many variables, including abiotic and biotic transport as well as vertical and horizontal mobility, affect how MPs migrate through the soil. The horizontal and vertical motions of MPs in soil are controlled by many elements, such as the surface of the soil, accumulation, and agricultural operations (such as harvesting)[51]. The changes in MP properties and structure (size, shape, hydrophobicity, and chemical composition) also have key roles in MP transport in soil[74]. The retention mechanisms of MPs alter as the size of particles grows, and their attachment effectiveness rises noticeably[75]. Mobility of MP spherules in soil may be improved by raising the UV hydrophilicity and negative surface charge of MP particles[76]. Organic matter and soil water flow rate affect MP transport, with organic matter increasing transport mechanisms and reducing stability. MPs can be transported through natural and man-made processes, and most are fibers, which are easily lifted into the atmosphere. Soil serves as both a source and sink[77,78].

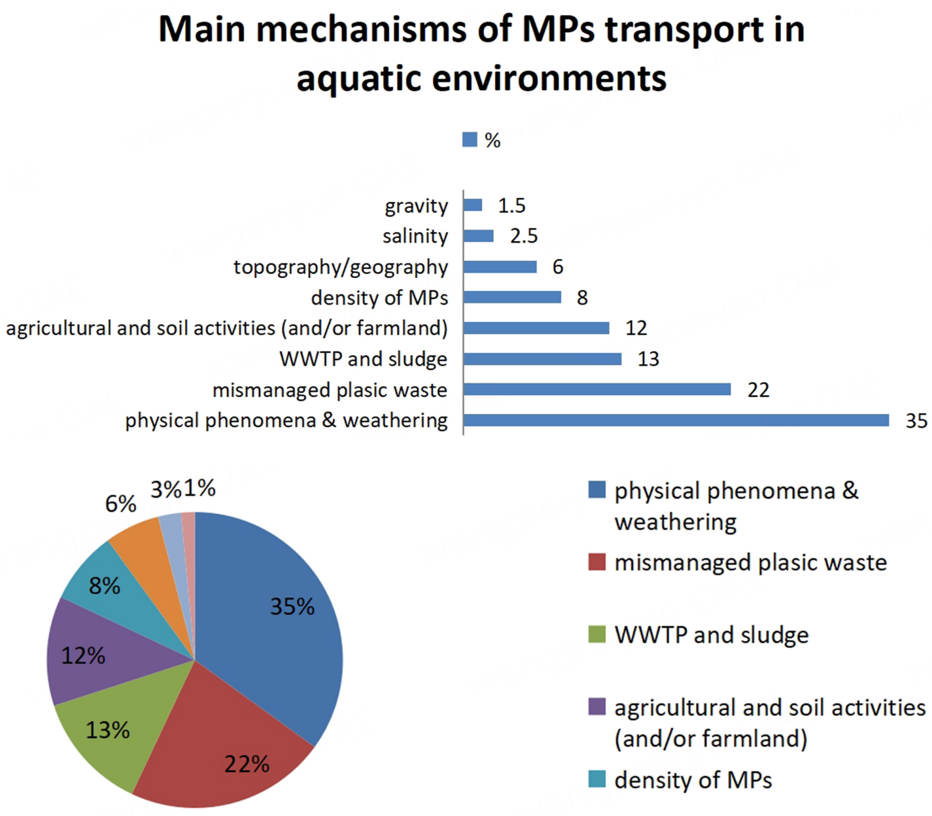

Figure 2. Dominant mechanisms (%) of MP transport in aquatic environments according to the review of the published papers. MP: Microplastic.

Aquatic environment

Strong hydrodynamic forces, such as wind, waves, tides, and thermohaline gradients, constantly affect the aquatic environment, making it an active zone. Thus, climatic pressures and coastal transport mechanisms alter the temporal and geographical distributions of MPs[79]. Plastics are carried by beaching, drifting, and settling pathways from terrestrial, riverine, and marine sources to transient reservoirs on beaches, in tidal wetlands, and in marine sediments. When floodwaters release from upstream locations during wet periods, the largest concentrations of MPs are found around river mouth areas. Although there is little knowledge of the physical mechanisms underlying this process, plastics that are carried to aquatic habitats are maintained nearshore in estuaries, wetland sediments, and beaches[77]. MPs are transported further into grounds and ocean sediments by both terrestrial and aquatic biota, primarily via the processes of bioturbation and biofouling. Various aquatic and soil species can actively participate in the transportation of MPs[50]. As mentioned above, MPs' physical characteristics are influenced by coagulation, photochemical deterioration, mechanical decomposition, and biofouling, affecting particle density, size distribution, geometric form, and surface properties, consequently shaping their ultimate destiny[80,81].

One important factor influencing the buoyancy and movement of MPs in water is particle density. Neutral particles with densities less than seawater float at or close to the sea surface, whereas nonfloating particles with densities greater than seawater often sink to the sea floor[25]. Low-density particles have been discovered in sediments in coastal waters and on the deep ocean floor, suggesting that high-density particles may travel great distances. Because plastics have a high material density and coastal seas are turbulent, it is anticipated that non-buoyant plastic particles will mostly travel by suspended load[82].

Additionally, the size of plastic particles, which plays an instrumental role in the transport of MPs, may be altered by a number of processes, such as flocculation, aggregation, biofouling, and fragmentation. Regardless of their densities, microscopic plastic pieces exhibit the behavior of colloidal particles and typically exist as suspended particles in the water column[80]. As such, the size distribution of plastic particles must be considered a dynamic characteristic that varies with residence duration and transit routes[45]. MPs can become larger and denser by aggregation with both organic and inorganic particles, leading to a quicker deposition of the particles on sediments. Given the large quantities of suspended sediments, particulate organic matter, and detrital particles in the coastal environment, aggregation and subsequent sedimentation could dominate the fate and dispersion of MPs[83].

It has been shown that, like MPs, the Schulze Hardy rule and Derjaguin Landau Verwey Overbeek (DLVO) theory may be used to understand the process behind the behavior of MPs. To put it simply, ionic strength, organic matter, flow velocity, size, and surface charge can all have an impact on MP mobility[83,84]. In relation to their original form (plastic pieces, pellets, fibers, or filaments) and fragmentation processes, marine plastic particles come in a variety of forms[85]. Additionally, the shape and specific surface area of the particles have a significant role in defining the aggregation and biofouling processes that affect the MPs' transit channel. Particles having high surface area to volume ratios (films, fibers, foams) have a greater rate of aggregation/biofouling and may sink sooner than big things[81,83].

All in all, taking into consideration all the aforementioned, we can conclude that MPs can be carried by atmospheric or aquatic currents depending on their weight and density. MPs may move from the pedosphere into the hydrosphere via surface runoff, rainfall, and ocean circulation. Ocean circulation allows MPs to not only move from land to water, but also from water to land[86,87]. In addition, smaller and lighter MPs have the ability to travel great distances, including high altitudes and glacier zones, as they become airborne and are transported by the wind. Denser MPs may collect in the pedosphere (soil) or be buried there, whereas lighter MPs may be carried by wind over the pedosphere[34]. Surface runoff from cities and agricultural regions, together with heavy rains, can introduce MPs into surface waterways (the hydrosphere). Research has indicated that the utilization of plastic mulches to enhance crop development or the addition of household sewage sludge as a soil amendment in agricultural activities may result in the introduction of MPs into the soil[88]. Furthermore, stormwater runoff transports the MPs that are produced by tires wearing down naturally to nearby surface waterways[34]. Furthermore, airborne MPs made of light fibers from trash incineration, landfills, and clothing can travel great distances and deposit themselves in remote locations by atmospheric fallout[88].

PLASTIC WASTE MANAGEMENT AND MPS

Plastic particles are present in the air, drinking water, sediments, seas, snow ice, and agricultural soils, among other things. MPs are being released into the environment at an accelerated rate worldwide, which has an impact on biodiversity, conservation, and water quality. An understanding of the origins, transit, and destiny of plastics in the environment, as well as multidisciplinary research, and regional and global collaboration, are necessary for managing plastics in the environment and guaranteeing effective intervention policies and practices. The accumulation of plastic particles has been found to vary both temporally and geographically, with differences in dispersal and distribution being attributed to anthropogenic causes, time, places, hydrodynamic conditions, and environmental pressure[89]. In addition, the varied distribution of MPs, particularly in adjacent rivers, has been linked to population density, industrial activity, and hydrological conditions[90].

Municipal solid trash contains a sizable portion of post-consumer plastic garbage. Since the 1950s, when commercial manufacture of plastics began, 8,600 million metric tons of plastic have been produced. Of this garbage, 70 percent has been diverted to landfills and the natural environment[19]. For example, plastic leakage in South Africa results in an annual dumping of approximately 40,000 metric tons of plastic waste into the ocean. Concerns about municipal plastic waste (MPW) have arisen in every country, prompting proposals for global legislation and control. Currently, many other nations have banned or imposed taxes on plastics due to popular outcry and political commitment[90].

The greatest solution for a plastics circular economy has been identified as landfill diversion through recycling and energy recovery. On the other hand, the majority of African countries choose to leave their garbage - plastic waste in particular - in landfills or rubbish dumps, with the rare badly managed landfill. While recyclable and reusable items, including plastics, are scavenged and recycled back into the economy, biodegradable materials use these landfills and dumps as composting beds. Africa has a notably distinct approach to managing plastics for socioeconomic and political reasons. Systematic recycling is quite restricted in Africa; the combined capacity for recycling in the most developed systems - South Africa, Ethiopia, Uganda, Rwanda, Morocco, Algeria, Madagascar, Cameroon, and Mozambique - is less than 5%[90,91].

In locations where they have been used, recuperative energy interventions in the plastic waste handling order, such as gasification, pyrolysis, and incineration, have guaranteed a closed-loop system for plastic waste management. However, only developed and middle-income nations that emphasize waste management with circular economy concerns are currently able to implement these costly and more advanced energy recovery technologies. In Africa, there is a dearth of plastic waste-to-energy conversion technologies, which forces people and organizations to engage in open, unregulated burning activities with hazardous environmental effects[90,91].

The growth of plastic garbage in many developing nations has been linked to behavioral psychology, changing consumption habits, and inadequate waste collection and treatment infrastructures[92]. Developing nations frequently have an overwhelming amount of urgent social and infrastructure demands, which prevents them from coordinating appropriate waste management programs with national development initiatives. Thus, as indicated by the widening of streets and rivers, overflow from waste disposal sites, increased composition in municipal solid waste, contamination of shorelines and beaches, and pollution of aquatic systems, the plastic threat is more severe in low- and middle-income nations[93].

Africa and the Middle East stand out as the two continents where the growing buildup of improperly handled plastics has been found. For example, plastic waste in Ghana has been attributed to improper consumption patterns and the rising income of the country’s middle class. The story of plastic leakage is a prevalent environmental aspect, especially in metropolitan areas where careless dumping has led to clogged drains, flooding, cholera and diarrhea outbreaks, an ugly landscape, and a threat to tourism[90,94]. The majority of Africa’s carbon emissions equations do not account for the impact of environmental waste plastics and their carbon footprints, despite the fact that the manufacture of plastic, burning, and poor waste management release greenhouse gases that fuel climate change. The outwardness of plastic mismanagement is mainly attributed to inappropriate social practices and bad political decisions made at the central government level. Africa is thought to have the greatest number of country-level plastic waste management systems worldwide, but the continent is also hindered by a lack of producer-consumer responsibilities, investment and funding channels, and trash management policies[90].

There are huge differences in waste management systems around the globe, and many nations lack any kind of public trash management system. A significant amount of plastic in mixed household garbage nowadays is non-biodegradable and cannot be composted. As a result, over time, plastic will accumulate as a result of traditional garbage disposal techniques including dumping in backyards, rivers, or private or public landfills. Even tiny towns may experience significant environmental pollution due to plastic litter[95]. Furthermore, nations even with well-established waste management systems annually deposit millions of tons of plastic waste into landfills, which is comprised of a sizable amount of controlled and collected post-consumer garbage[96]. Although the implications in terrestrial systems have not yet been well documented, there have been reports of animal consumption and livestock and wildlife entanglement that can prove lethal. According to Lebreton and Andrady (2019), there is a significant potential to reduce the input of plastic and therefore MP (defined as plastic particles < 5 mm) to the environment through better waste management and waste reduction[92]. The annual amounts of mismanaged waste are estimated to triple by 2060 due to continued poor waste management, growing plastic production, and a growing population[96].

As has been noted, municipal trash contains a large number of plastic products, which may wind up in the environment and disintegrate over time, creating secondary MPs. Consequently, municipal garbage represents a huge prospective supply of MPs in the future. Globally, the yearly volumes of garbage have reached hundreds of tonnes and are growing. Consequently, although they mostly exist as macroplastic products now, municipal garbage has the potential to become the greatest source of MPs in the future[92,96].

The majority of plastic debris that finds its way into the marine ecosystem comes from terrestrial sources. Among the involved transportation mechanisms are: (1) rain and wind carry street debris into rivers; (2) inappropriate or forbidden garbage disposal; (3) inadequately maintained landfills; (4) facilities for the production and processing of plastic; (5) spills from drains and treatment of waste; (6) fishing activities; and (7) facilities for disposing of solid waste along the coast[97,98].

Recycling is now the most extensively used method of handling plastics. Global rates have progressively increased to represent 24% of non-fiber plastic garbage generated in 2014. The countries with the highest recycling rates in that year were China (25%) and Europe (30%), with the United States having a rate of 9%, which was average for the globe[19]. Currently, textiles are either burned or disposed of together with other solid trash instead of being recycled. Approximately 53% of plastic trash is recycled, 46% is utilized for energy, and 1% is dumped in landfills. Recycling can extend the lifespan of plastics before they are discarded into the environment, but the recycling process may result in the generation of MPs[97].

The dataset below, from OECD Library Global Plastics Outlook, provides estimates of plastic waste for the different global regions and/or continents. This dataset also provides estimates of plastic waste measured in millions of tons per year, per end-of-life fate after accounting for recycling losses and collected littering, for the period 2000-2019[32]. It is clear that throughout the last two decades, USA, Canada, the European Union, and Asia have been the dominant regions that contribute to the pollution of aquatic environments due to the great increase in plastic waste. In Figure 3, it is clear that industrialized and developed regions produce a higher amount of plastic waste compared to continents such as Oceania, which do not exhibit the same level of industrial development or population as regions like Asia.

The likelihood that poorly managed plastic garbage will find its way into river systems and eventually the ocean varies. Mismanaged plastic waste's likelihood of ending up in the ocean is influenced by a number of

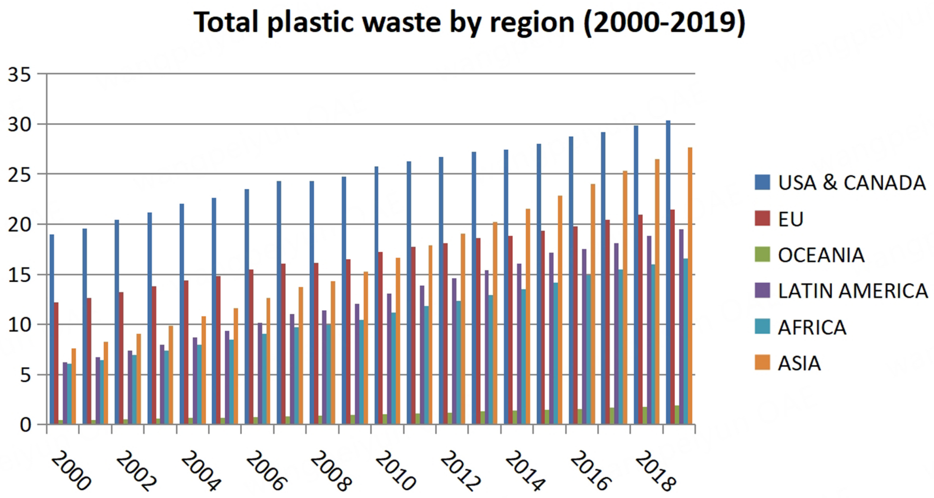

Figure 3. Total plastic waste by region (2000-2019)[32].

factors, including climate, geography, land use, and distances within river basins. The likelihood of improperly managed garbage being released into the ocean is displayed in Figures 4 and 5.

To begin, in areas lacking adequate local waste management techniques, plastic pollution prevails. This indicates that a significant amount of improperly managed plastic debris may initially ends up in rivers and the ocean, underscoring the necessity for improved waste management practices. In addition, cities closest to major polluters typically featured paved areas where plastic waste and water runoff can easily reach river outlets.

While cities in Asia, Africa, or Latin America are often situated alongside relatively small rivers, they contribute significantly to the continent's plastic pollutants. Additionally, possible abundant rainfall in these riverine regions exacerbates the issue, leading to the rapid transportation of plastics into the rivers, which then swiftly flow into the ocean. Furthermore, proximity matters, as cities near the ocean and major river sources tend to cause the highest concentrations of MPs in their waters.

Plastic that ends up in our seas can come from both marine and terrestrial sources. The term "plastics pollution from marine sources" describes the pollution left behind by fishing fleets that employ abandoned boats, fishing nets, lines, and ropes. The proportional contribution of terrestrial and marine sources to ocean pollution is a topic of frequent and heated discussion. Figures 6 and 7 present the origin of MPs in the ocean (regions and application of use correspondingly).

However, it is necessary to underline that surface movements and the direction of the winds in the water have a significant impact on the dispersion and buildup of plastic debris in the ocean. Plastics often travel along the primary surface currents and wind patterns due to their buoyancy, allowing them to float on the ocean's surface. Consequently, they tend to accumulate in gyres within marine cycles, with the highest concentrations found at the centers of ocean basins and lower concentrations at the periphery. Once plastics enter ocean basins from coastal areas, they exhibit a propensity to move toward their central regions.

The most recent estimates indicate that, globally, land-based sources account for around 80% of ocean plastics, with marine sources contributing to the remaining 20%. Roughly half (10 percentage points) of the

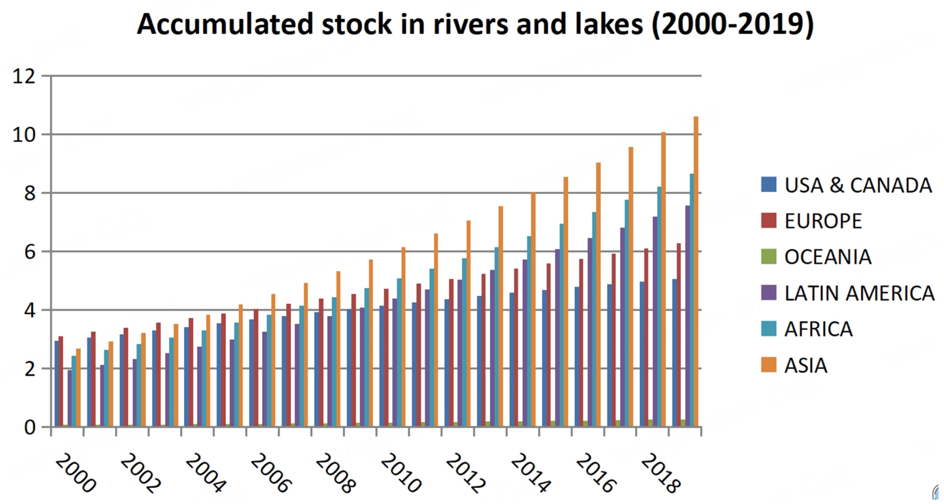

Figure 4. Accumulated stock in rivers and lakes (2000-2019)[32].

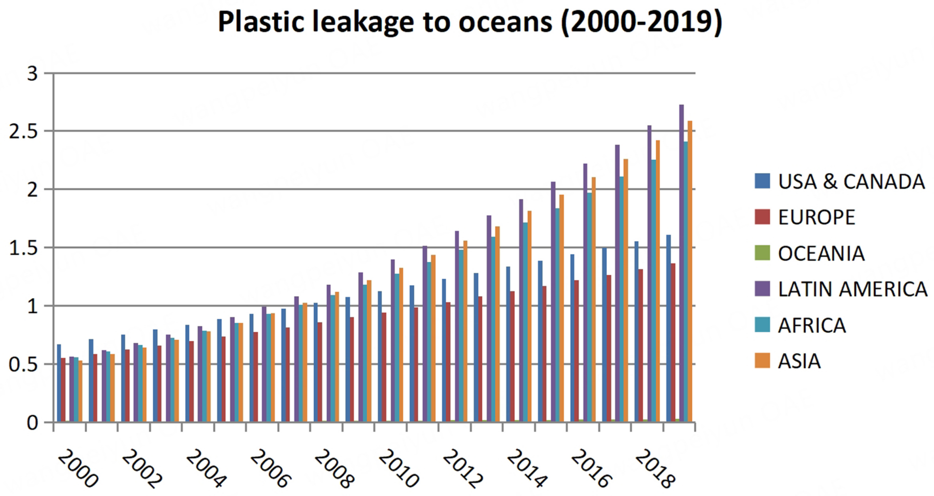

Figure 5. Plastic leakage to oceans (2000-2019)[32].

20% derived from marine sources are thought to come from fishing fleets (such as nets, lines, and damaged ships)[4]. The usage of main plastics by industry is depicted in Figure 5, along with the industry's contribution to plastic trash creation. In addition to the product lifespan, primary plastic use has a significant impact on the development of plastic trash. For example, the active lifespan of packaging is quite short - typically no more than six months. In comparison, plastic use in architecture (building),construction, or transportation has an average lifespan of 35 years. Thus, packaging is the primary source of plastic trash, accounting for about half of the total worldwide.

Figure 8 shows the percentage of plastic garbage generated worldwide in 2000–2019 that is disposed of, recycled (A), burned (B), landfilled (C), littered (D), and mismanaged (E). It is obvious that each region/continent manages the plastic waste in a different way and this has a possible impact or a footprint in the accumulation of MPs in water that is observed. In the past, plastic was typically discarded intact, as recycling or incineration were uncommon practices. However, starting around 1980, the rate of incineration began to increase, and from 1990 onwards, there was a notable rise in recycling rates.

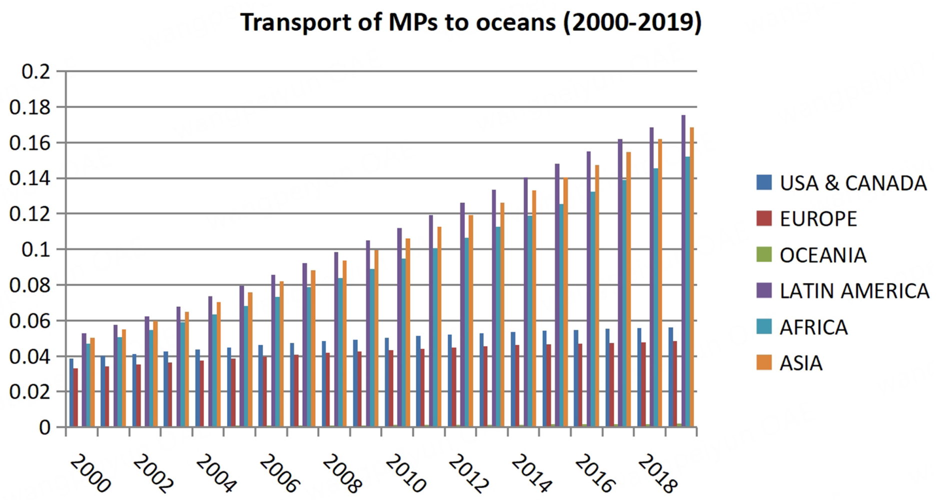

Figure 6. Transport of MPs to oceans (2000-2019)[32]. MPs: Microplastics.

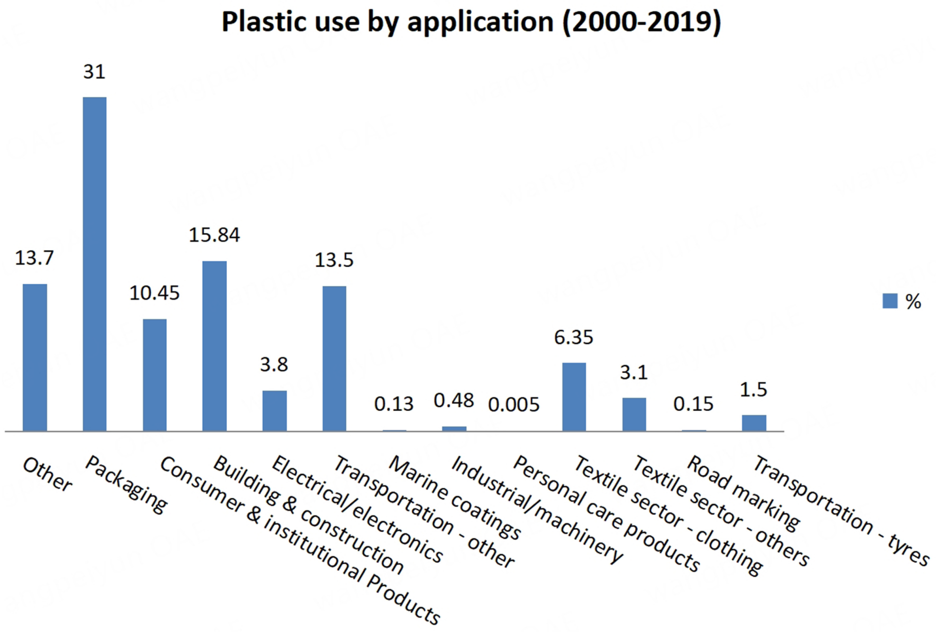

Figure 7. Sources of MPs: Plastic use by application (2000-2019)[32]. MPs: Microplastics.

The greatest solution for a plastics circular economy has been identified as landfill diversion through recycling and energy recovery. Currently, the United States, European Union, and Asia have the highest rates of plastics ending up in landfills. On the other hand, the majority of African countries choose to leave their garbage - plastic waste in particular - in landfills or rubbish dumps, often with inadequate management practices. Africa's approach to plastic waste management is notably distinct due to socioeconomic and political reasons. Formal recycling infrastructure in Africa is relatively limited, with even modern systems in South Africa, Ethiopia, Uganda, Rwanda, Morocco, Algeria, Madagascar, Cameroon, and Mozambique collectively showing less than 5% capacity for recycling. Plastic packaging contributes significantly to Africa's waste stream, especially with the widespread use of bottled and sachet "pure water". In South Africa, for instance, plastic leakage results in an annual oceanic loading of

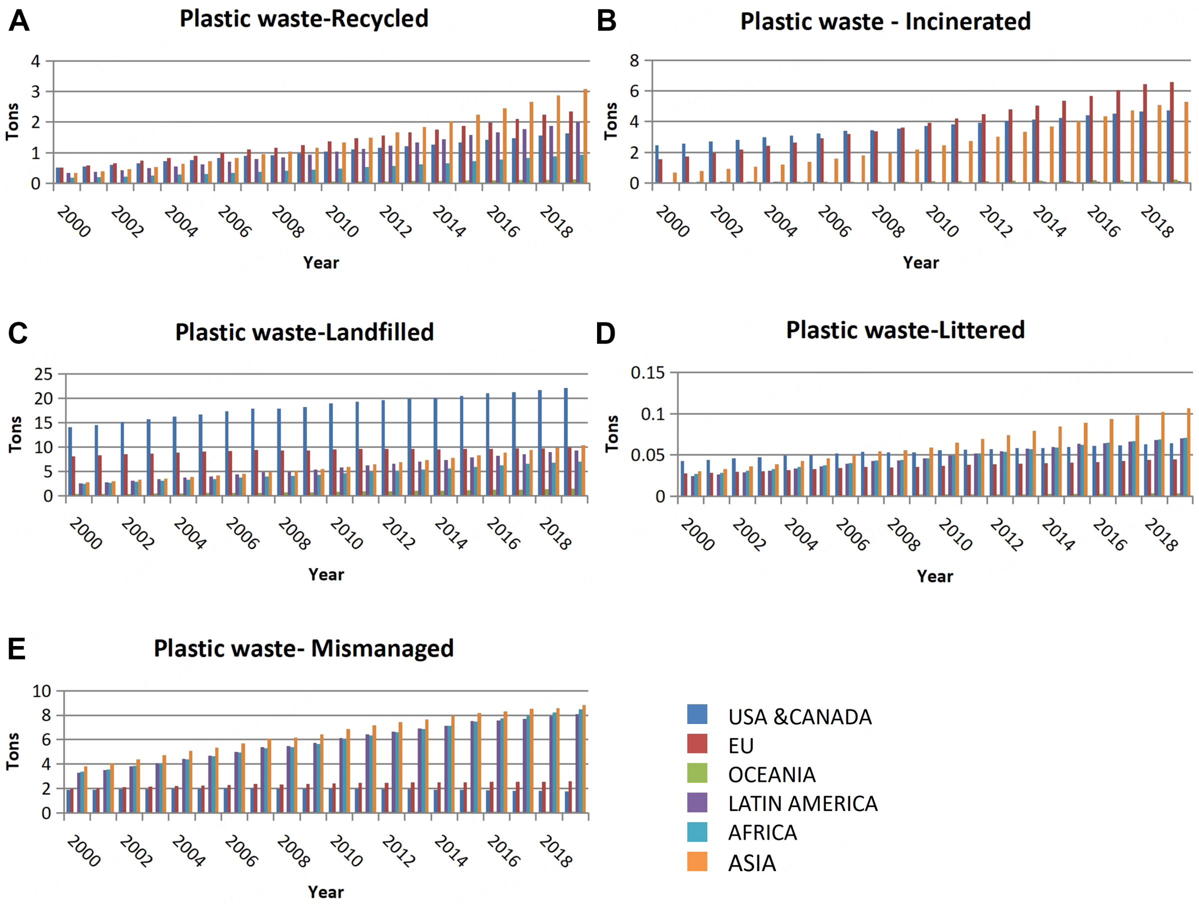

Figure 8. Plastic waste by region (2000-2019). (A) Recycled; (B) Incinerated; (C) Landfilled; (D) Littered; and (E) Mismanaged[32].

approximately 40,000 metric tons of plastic waste[90].

Figures 9 and 10 focus on the analysis of data from the year 2019, specifically examining the presence of macroplastics and MPs in oceans, rivers, and lakes, as well as their origins. Macroplastics in aquatic environments predominantly stem from mismanaged plastic waste, particularly originating from countries with weak economies or/and in stages of development, primarily in Africa, Asia and Latin America. In Figure 10, it is obvious that the main sources of immediate MPs in aquatic environments are MP dust, tyre abrasion, primary pellets, wastewater (WW) sludge, and particles from materials used in road construction.

In the next section, future prospects and estimations concerning the fate of MPs in rivers/lakes and oceans are presented, juxtaposed with the future strategies for plastic waste management. Put simply, by the end of 2060, as depicted in Figure 11, global plastic waste will either undergo recycling or be directed toward landfilling, followed by incineration or, in the worst-case scenario, complete mismanagement. It is imperative to address plastic waste appropriately to mitigate future pollution effects. Whenever feasible, plastics should undergo recycling, and when that is not possible, they should be landfilled hygienically or incinerated with energy recovery. This reduces the amount of improperly managed trash and leaves only difficult-to-treat sources of leakage, such as uncollected litter and MPs. Consequently, international recycling rates will ascend, while rates of improper waste disposal will decline.

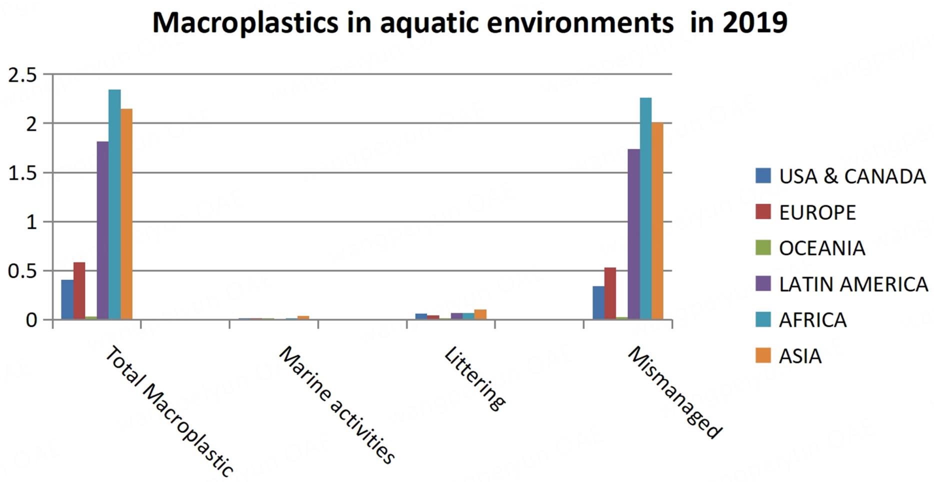

Figure 9. Macroplastics in aquatic environments in 2019[32].

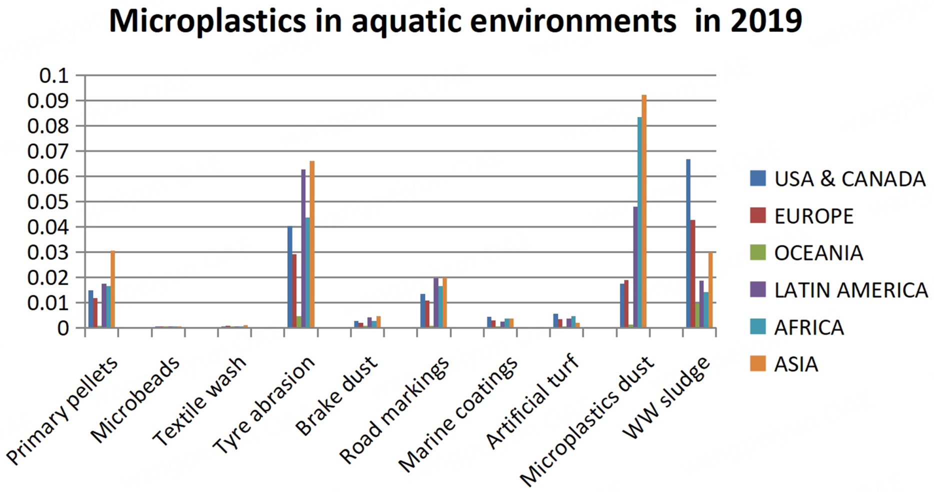

Figure 10. Microplastics in aquatic environments in 2019[32].

The goal of curbing plastic waste reaching rivers and oceans by 2060 hinges on minimizing leakage to aquatic habitats. However, the accumulation of plastic in these water bodies persists until all avenues of leakage are sealed off and the flow completely ceases. Despite efforts, substantial amounts of plastics continue to leak into the environment [Figure 11], with large volumes ending up in aquatic areas. This is due to the approximately 40-year timeframe required to decrease mismanaged garbage to minimal levels. The cumulative volume of plastic will keep rising, mostly in rivers and lakes and less in oceans.

In addition, a future scenario anticipates a decrease in the release of MPs into the environment [Figure 12]. This decline is attributed to the overall economy utilizing less plastic, primarily through recycling and reusing practices. As a consequence of the worldwide effort to control the primary sources of MPs in the water in a sustainable manner, primary pellets, wastewater sludge, and road markings account for the most significant decreases in MP leakage. Future policy measures are poised to prevent a significant rise in primary plastic consumption, with projections indicating an 11% increase in primary plastic production between 2019 and 2060 [Figure 13]. This trend stems from secondary plastics penetrating the market more

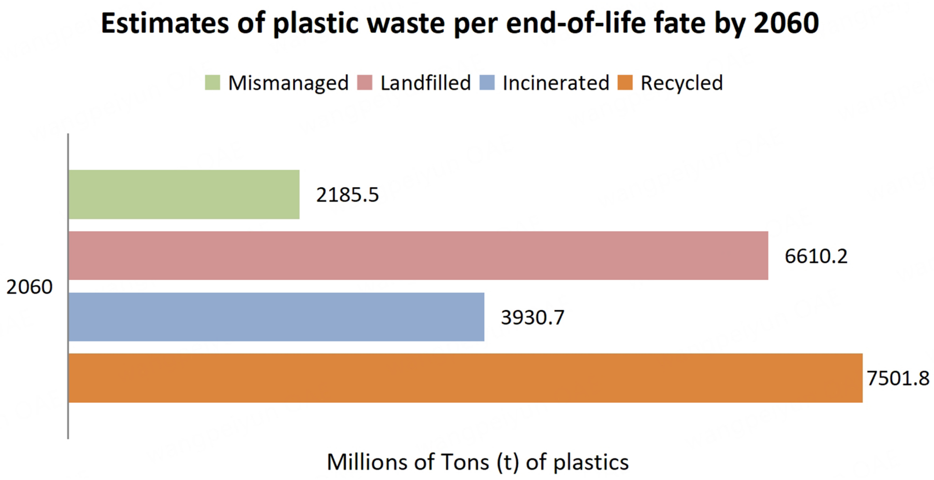

Figure 11. Global estimates of plastic waste per end-of-life fate by 2060[32].

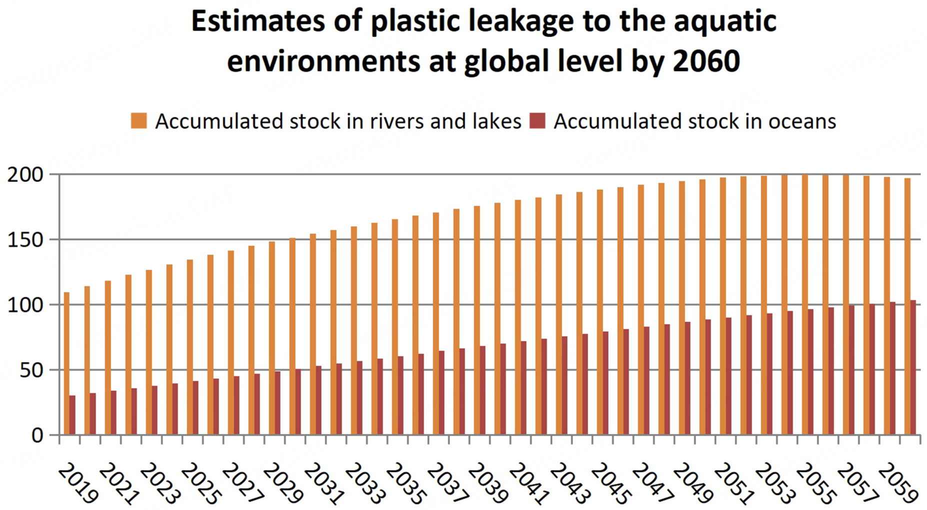

Figure 12. Estimates of plastic leakage [in millions of Tons (t)] to the aquatic environments at the global level by 2060[32].

quickly alongside a diminishing total demand. As targets for recycled content escalate in the coming years, secondary manufacturing is experiencing notably robust growth. This surge is attributable to an overall reduction in plastic manufacturing, leading to decreased demand for plastics and subsequent waste generation, thereby decreasing the amount of recyclable plastic scrap available. Finally, forecasts regarding plastic usage by type up to 2060 [Figure 14], indicate that 89% of MP concentration in aquatic environments will come mainly from the aforementioned primary MPs, shedding light on their prevalent causes and sources.

The amount of plastic debris and particles is growing annually due to the rising global population and greater consumption. These substances pose unknown and untested threats to human health and the environment since they are easily transported over great distances and widely distributed on land, in the sea, and in the air. Despite the possible risks to environmental health, there are very few documented cases of plastic particle pollution of environmental media in Africa. Understanding the origins, transit, and destiny of plastic particles via regional and international collaboration and multidisciplinary research is necessary

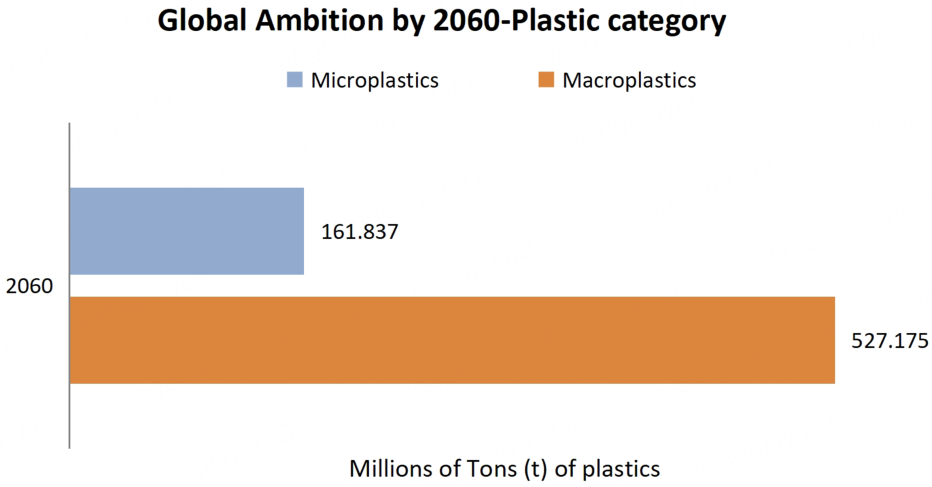

Figure 13. Global Ambition by 2060-Plastic category in aquatic environments[32].

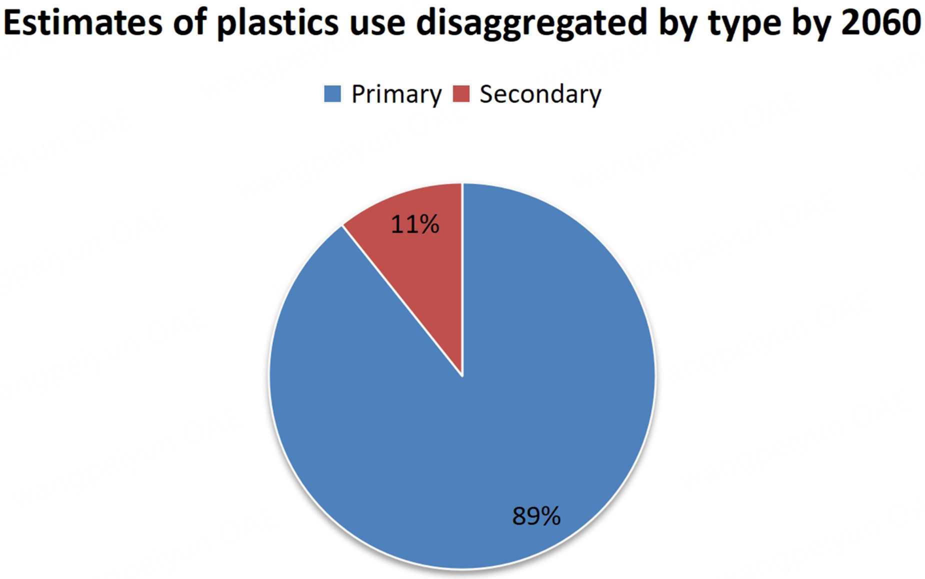

Figure 14. Estimates of plastics use disaggregated by type by 2060[32].

for managing environmental waste plastics and plastic particles and guaranteeing successful intervention policies and practices. We advocate for special control of MPs in consumer items due to the possible harm that plastic particles might cause to ecological functions and health hazards to humans. The data presented in this work contribute to the expanding corpus of knowledge in the global research of micro- and nanoplastic particles, with a focus on developing nations[90].

RESEARCH AND KNOWLEDGE GAPS

The amount of micro- and nanoplastics that are present in the globe is unknown, but due to their detrimental impact on the ecosystem, it is critical to assess the degree of their contamination. It is challenging to assess the degree of damage to human health due to the information gap surrounding this pollution, especially in light of the lack of conclusive data about the impact of micro- and nanoplastics on human health in the human diet. Additionally, it is imperative to furnish precise data to evaluate the exact extent of human exposure to these particles in their everyday diets. This can be achieved through the establishment of standard methodologies for detecting and characterizing micro- and nanoplastics[99,100].

It is difficult to determine the presence of micro- and nanoplastics in marine water and sediment since it depends on the collection technique, sample preparation, and analytical approach. The concentration of particles in nature and the laboratory varied significantly from one another. Furthermore, despite numerous attempts, many environmental influences are unfeasible to replicate in the laboratory; as a result, experimental laboratory conditions and related outcomes are not representative of the field[101].

The fate of micro- and nanoplastics during the metabolism of seafood is not well understood. Opportunities exist in the field of scientific research to close the information gap about the long-term effects of micro- and nanoplastics, particularly with regard to human risk assessment. Numerous investigations have revealed a connection between metabolic, morphological, and behavioral alterations and the presence of micro- and nanoplastics in the food chain. The effects of plastic particle pollution will therefore reach the level of ecosystems. However, the fate of micro- and nanoplastics in marine environments and their consequent environmental effects remain unclear. This lack of clarity poses a challenge in accurately assessing the potential harm to human health posed by micro- and nanoplastics[99].

CONCLUSIONS

This paper was organized into two parts: The first part provides an overview of all published papers focusing on the transport routes of MPs, while the second part analyzes the correlation between improper plastic waste management and high levels of MP accumulation. Identifying precisely where litter is generated is crucial for targeting priority areas for future implementation of mitigation policies regarding MPs in water. Aquatic habitats are threatened by MPs, which have long been recognized as a severe category of pollutants. Therefore, this review covers the mechanics of MPs transport and the handling of plastic trash. The relationship between improperly managed plastic trash and the processes leading to MP accumulation in waterways is not well understood, necessitating further research in this area. After outlining the potential future paths for MPs, we conducted a statistical analysis of several approaches to managing plastic waste to reduce MP pollution. The pervasive presence of MPs in aquatic ecosystems poses a serious threat to both freshwater and marine life. Although research on the presence of MPs in rivers, lakes, and seas has expanded recently, more needs to be learned about the external factors influencing their transit and dispersion in freshwater systems. Given the increasing input of plastic into the environment, the distribution and abundance of MPs in aquatic systems are likely to rise significantly in the coming decades. Unless urgent global action is taken, it is estimated that by 2060, there will be more plastic in the ocean than fish.

DECLARATIONS

Authors' contributions

Validation, formal analysis, investigation, resources, data curation, writing - original draft preparation: Belioka MP
Conceptualization, methodology, writing - review and editing, supervision: Belioka MP, Achilias DS
Both authors have read and agreed to the published version of the manuscript.

Availability of data and materials

The authors used the raw data provided by OECD Library. Global plastics outlook. Available from: https://www.oecd-ilibrary.org/environment/data/global-plastic-outlook_c0821f81-en. [Last accessed on 16 May

2024] and they continued with the further process, using the Microsoft Excel software. Moreover, this is a review paper and all the data and information have been found in the different sources that are mentioned in the "REFERENCES" section.

Financial support and sponsorship
None.

Conflicts of interest
Both authors declared that there are no conflicts of interest.

Ethical approval and consent to participate
Not applicable.

Consent for publication
Not applicable.

REFERENCES

1. Pellini G, Gomiero A, Fortibuoni T, et al. Characterization of microplastic litter in the gastrointestinal tract of *Solea solea* from the Adriatic Sea. *Environ Pollut* 2018;234:943-52. DOI PubMed
2. Zhang K, Hamidian AH, Tubić A, et al. Understanding plastic degradation and microplastic formation in the environment: a review. *Environ Pollut* 2021;274:116554. DOI PubMed
3. Ram B, Kumar M. Correlation appraisal of antibiotic resistance with fecal, metal and microplastic contamination in a tropical Indian river, lakes and sewage. *npj Clean Water* 2020;3:3. DOI
4. Belioka MP, Achilias DS. Microplastic pollution and monitoring in seawater and harbor environments: a meta-analysis and review. *Sustainability* 2023;15:9079. DOI
5. Li W, Luo Y, Pan X. Identification and characterization methods for microplastics basing on spatial imaging in micro-/nanoscales. In: He D, Luo Y, editors. Microplastics in terrestrial environments: emerging contaminants and major challenges. Springer, Cham. 2020. pp. 25-37. DOI
6. Herbort AF, Schuhen K. A concept for the removal of microplastics from the marine environment with innovative host-guest relationships. *Environ Sci Pollut Res Int* 2017;24:11061-5. DOI PubMed
7. Arthur C, Baker JE, Bamford HA. Proceedings of the international research workshop on the occurrence, effects, and fate of microplastic marine debris, September 9-11, 2008, University of Washington Tacoma, Tacoma, WA, USA. 2009. Available from: https://repository.library.noaa.gov/view/noaa/2509. [Last accessed on 16 May 2024].
8. Collignon A, Hecq JH, Galgani F, Collard F, Goffart A. Annual variation in neustonic micro-and meso-plastic particles and zooplankton in the Bay of Calvi (Mediterranean-Corsica). *Mar Pollut Bull* 2014;79:293-8. DOI PubMed
9. Lestari P, Trihadiningrum Y, Wijaya BA, Yunus KA, Firdaus M. Distribution of microplastics in Surabaya river, Indonesia. *Sci Total Environ* 2020;726:138560. DOI PubMed
10. Chamas A, Moon H, Zheng J, et al. Degradation rates of plastics in the environment. *ACS Sustain Chem Eng* 2020;8:3494-511. DOI
11. Constant M, Ludwig W, Kerhervé P, et al. Microplastic fluxes in a large and a small Mediterranean river catchments: the Têt and the Rhône, Northwestern Mediterranean Sea. *Sci Total Environ* 2020;716:136984. DOI PubMed
12. He B, Smith M, Egodawatta P, Ayoko GA, Rintoul L, Goonetilleke A. Dispersal and transport of microplastics in river sediments. *Environ Pollut* 2021;279:116884. DOI PubMed
13. Rose PK, Jain M, Kataria N, Sahoo PK, Garg VK, Yadav A. Microplastics in multimedia environment: a systematic review on its fate, transport, quantification, health risk, and remedial measures. *Groundw Sustain Dev* 2023;20:100889. DOI
14. Bondelind M, Sokolova E, Nguyen A, Karlsson D, Karlsson A, Björklund K. Hydrodynamic modelling of traffic-related microplastics discharged with stormwater into the Göta River in Sweden. *Environ Sci Pollut Res Int* 2020;27:24218-30. DOI PubMed PMC
15. Rist S, Almroth BC, Hartmann NB, Karlsson TM. A critical perspective on early communications concerning human health aspects of microplastics. *Sci Total Environ* 2018;626:720-6. DOI PubMed
16. Sharma S, Chatterjee S. Microplastic pollution, a threat to marine ecosystem and human health: a short review. *Environ Sci Pollut Res Int* 2017;24:21530-47. DOI PubMed
17. Barboza LGA, Gimenez BCG. Microplastics in the marine environment: current trends and future perspectives. *Mar Pollut Bull*

2015;97:5-12. DOI PubMed

18. Rajmohan KVS, Ramya C, Viswanathan MR, Varjani S. Plastic pollutants: effective waste management for pollution control and abatement. *Curr Opin Environ Sci Health* 2019;12:72-84. DOI
19. Geyer R, Jambeck JR, Law KL. Production, use, and fate of all plastics ever made. *Sci Adv* 2017;3:e1700782. DOI PubMed PMC
20. Malli A, Corella-Puertas E, Hajjar C, Boulay AM. Transport mechanisms and fate of microplastics in estuarine compartments: a review. *Mar Pollut Bull* 2022;177:113553. DOI PubMed
21. Zettler ER, Mincer TJ, Amaral-Zettler LA. Life in the "plastisphere": microbial communities on plastic marine debris. *Environ Sci Technol* 2013;47:7137-46. DOI PubMed
22. Cooper DA, Corcoran PL. Effects of mechanical and chemical processes on the degradation of plastic beach debris on the island of Kauai, Hawaii. *Mar Pollut Bull* 2010;60:650-4. DOI PubMed
23. Nelms SE, Coombes C, Foster LC. et al. Marine anthropogenic litter on British beaches: a 10-year nationwide assessment using citizen science data. *Sci Total Environ* 2017;579:1399-409. DOI PubMed
24. Zheng Y, Yanful EK, Bassi AS. A review of plastic waste biodegradation. *Crit Rev Biotechnol* 2005;25:243-50. DOI PubMed
25. Barnes DKA, Galgani F, Thompson RC, Barlaz M. Accumulation and fragmentation of plastic debris in global environments. *Philos Trans R Soc Lond B Biol Sci* 2009;364:1985-98. DOI PubMed PMC
26. Li J, Liu H, Chen JP. Microplastics in freshwater systems: a review on occurrence, environmental effects, and methods for microplastics detection. *Water Res* 2018;137:362-74. DOI PubMed
27. Mahdavimanesh M, Noghrehabadi AR, Behbahaninejad M, Ahmadi G, Dehghanian M. Lagrangian particle tracking: model development. *Life Sci J* 2013;10:34-41. Available from: https://citeseerx.ist.psu.edu/document?repid=rep1&type=pdf&doi=66a90cb17c5aaa3816e504848f152b94c2e5a315. [Last accessed on 16 May 2024].
28. Alosairi Y, Al-Salem SM, Al Ragum A. Three-dimensional numerical modelling of transport, fate and distribution of microplastics in the northwestern Arabian/Persian Gulf. *Mar Pollut Bull* 2020;161:111723. DOI PubMed
29. Rangel-Buitrago N, Vergara-Cortés H, Barría-Herrera J, Contreras-López M, Agredano R. Marine debris occurrence along Las Salinas beach, Viña Del Mar (Chile): magnitudes, impacts and management. *Ocean Coast Manage* 2019;178:104842. DOI
30. Hardesty BD, Harari J, Isobe A, et al. Using numerical model simulations to improve the understanding of micro-plastic distribution and pathways in the marine environment. *Front Mar Sci* 2017;4:30. DOI
31. Moher D, Liberati A, Tetzlaff J, Altman DG; PRISMA Group. Preferred reporting items for systematic reviews and meta-analyses: the PRISMA statement. *Ann Intern Med* 2009;151:264-9. DOI PubMed
32. OECD Library. Global plastics outlook. Available from: https://www.oecd-ilibrary.org/environment/data/global-plastic-outlook_c0821f81-en. [Last accessed on 16 May 2024].
33. Koutnik VS, Leonard J, Alkidim S, et al. Distribution of microplastics in soil and freshwater environments: global analysis and framework for transport modeling. *Environ Pollut* 2021;274:116552. DOI PubMed
34. Horton AA, Walton A, Spurgeon DJ, Lahive E, Svendsen C. Microplastics in freshwater and terrestrial environments: evaluating the current understanding to identify the knowledge gaps and future research priorities. *Sci Total Environ* 2017;586:127-41. DOI PubMed
35. Prata JC, Silva ALP, da Costa JP, et al. Solutions and integrated strategies for the control and mitigation of plastic and microplastic pollution. *Int J Environ Res Public Health* 2019;16:2411. DOI PubMed PMC
36. Krause S, Baranov V, Nel HA, et al. Gathering at the top? Environmental controls of microplastic uptake and biomagnification in freshwater food webs. *Environ Pollut* 2021;268:115750. DOI PubMed
37. Weithmann N, Möller JN, Löder MGJ, Piehl S, Laforsch C, Freitag R. Organic fertilizer as a vehicle for the entry of microplastic into the environment. *Sci Adv* 2018;4:eaap8060. DOI PubMed PMC
38. Alomar C, Estarellas F, Deudero S. Microplastics in the Mediterranean Sea: deposition in coastal shallow sediments, spatial variation and preferential grain size. *Mar Environ Res* 2016;115:1-10. DOI PubMed
39. Murphy F, Ewins C, Carbonnier F, Quinn B. Wastewater treatment works (WwTW) as a source of microplastics in the aquatic environment. *Environ Sci Technol* 2016;50:5800-8. DOI PubMed
40. Cole M, Lindeque P, Halsband C, Galloway TS. Microplastics as contaminants in the marine environment: a review. *Mar Pollut Bull* 2011;62:2588-97. DOI PubMed
41. Leslie HA, Brandsma SH, van Velzen MJM, Vethaak AD. Microplastics en route: field measurements in the Dutch river delta and Amsterdam canals, wastewater treatment plants, North Sea sediments and biota. *Environ Int* 2017;101:133-42. DOI PubMed
42. Eklund B, Hansson T, Bengtsson H, Eriksson Wiklund AK. Pollutant concentrations and toxic effects on the red alga *Ceramium tenuicorne* of sediments from natural harbors and small boat harbors on the west coast of Sweden. *Arch Environ Contam Toxicol* 2016;70:583-94. DOI PubMed
43. De Witte B, Devriese L, Bekaert K, et al. Quality assessment of the blue mussel (*Mytilus edulis*): comparison between commercial and wild types. *Mar Pollut Bull* 2014;85:146-55. DOI PubMed
44. Gauquie J, Devriese L, Robbens J, De Witte B. A qualitative screening and quantitative measurement of organic contaminants on different types of marine plastic debris. *Chemosphere* 2015;138:348-56. DOI PubMed
45. Auta HS, Emenike CU, Fauziah SH. Distribution and importance of microplastics in the marine environment: a review of the sources, fate, effects, and potential solutions. *Environ Int* 2017;102:165-76. DOI PubMed
46. Carr SA, Liu J, Tesoro AG. Transport and fate of microplastic particles in wastewater treatment plants. *Water Res* 2016;91:174-82. DOI PubMed

47. Karbalaei S, Hanachi P, Walker TR, Cole M. Occurrence, sources, human health impacts and mitigation of microplastic pollution. *Environ Sci Pollut Res Int* 2018;25:36046-63. DOI PubMed
48. Hou H, Wang J, Yuan M, et al. Estimating the mitigation potential of the Chinese service sector using embodied carbon emissions accounting. *Environ Impact Assess Rev* 2021;86:106510. DOI
49. Obbard RW, Sadri S, Wong YQ, Khitun AA, Baker I, Thompson RC. Global warming releases microplastic legacy frozen in Arctic Sea ice. *Earths Future* 2014;2:315-20. DOI
50. He D, Luo Y, Lu S, Liu M, Song Y, Lei L. Microplastics in soils: analytical methods, pollution characteristics and ecological risks. *TrAC Trend Anal Chem* 2018;109:163-72. DOI
51. Rillig MC, Ingraffia R, de Souza Machado AA. Microplastic incorporation into soil in agroecosystems. *Front Plant Sci* 2017;8:1805. DOI PubMed PMC
52. Wang W, Ge J, Yu X, Li H. Environmental fate and impacts of microplastics in soil ecosystems: progress and perspective. *Sci Total Environ* 2020;708:134841. DOI PubMed
53. Nizzetto L, Futter M, Langaas S. Are agricultural soils dumps for microplastics of urban origin? *Environ Sci Technol* 2016;50:10777-9. DOI PubMed
54. Browne MA, Galloway T, Thompson R. Microplastic - an emerging contaminant of potential concern? *Integr Environ Assess Manag* 2007;3:559-61. DOI PubMed
55. Dubaish F, Liebezeit G. Suspended microplastics and black carbon particles in the Jade system, southern North Sea. *Water Air Soil Poll* 2013;224:1352. DOI
56. Mahon AM, O'Connell B, Healy MG, et al. Microplastics in sewage sludge: effects of treatment. *Environ Sci Technol* 2017;51:810-8. DOI PubMed
57. Scarascia-Mugnozza G, Sica C, Russo G. Plastic materials in European agriculture: actual use and perspectives. *J Agric Eng* 2011;42:15-28. DOI
58. Kasirajan S, Ngouajio M. Polyethylene and biodegradable mulches for agricultural applications: a review. *Agron Sustain Dev* 2012;32:501-29. DOI
59. Shiu RF, Chen LY, Lee HJ, Gong GC, Lee C. New insights into the role of marine plastic-gels in microplastic transfer from water to the atmosphere via bubble bursting. *Water Res* 2022;222:118856. DOI PubMed
60. Yuan W, Christie-Oleza JA, Xu EG, et al. Environmental fate of microplastics in the world's third-largest river: basin-wide investigation and microplastic community analysis. *Water Res* 2022;210:118002. DOI PubMed
61. Yuan Z, Nag R, Cummins E. Ranking of potential hazards from microplastics polymers in the marine environment. *J Hazard Mater* 2022;429:128399. DOI PubMed
62. Kurniawan TA, Haider A, Ahmad HM, et al. Source, occurrence, distribution, fate, and implications of microplastic pollutants in freshwater on environment: a critical review and way forward. *Chemosphere* 2023;325:138367. DOI PubMed
63. Wong JKH, Lee KK, Tang KHD, Yap PS. Microplastics in the freshwater and terrestrial environments: prevalence, fates, impacts and sustainable solutions. *Sci Total Environ* 2020;719:137512. DOI PubMed
64. Bejgarn S, MacLeod M, Bogdal C, Breitholtz M. Toxicity of leachate from weathering plastics: an exploratory screening study with *Nitocra spinipes*. *Chemosphere* 2015;132:114-9. DOI PubMed
65. Teuten EL, Saquing JM, Knappe DRU, et al. Transport and release of chemicals from plastics to the environment and to wildlife. *Philos Trans R Soc Lond B Biol Sci* 2009;364:2027-45. DOI PubMed PMC
66. Jambeck JR, Geyer R, Wilcox C, et al. Marine pollution. Plastic waste inputs from land into the ocean. *Science* 2015;347:768-71. DOI PubMed
67. Obbard RW. Microplastics in polar regions: the role of long range transport. *Curr Opin Environ Sci Health* 2018;1:24-9. DOI
68. Prata JC. Airborne microplastics: consequences to human health? *Environ Pollut* 2018;234:115-26. DOI PubMed
69. Dris R, Imhof H, Sanchez W, et al. Beyond the ocean: contamination of freshwater ecosystems with (micro-) plastic particles. *Environ Chem* 2015;12:539-50. DOI
70. Horton AA, Dixon SJ. Microplastics: an introduction to environmental transport processes. *WIREs Water* 2018;5:e1268. DOI
71. Boucher J, Friot D. Primary microplastics in the oceans: a global evaluation of sources. 2017. Available from: https://portals.iucn.org/library/sites/library/files/documents/2017-002-En.pdf. [Last accessed on 16 May 2024].
72. Abbasi S, Keshavarzi B, Moore F, et al. Distribution and potential health impacts of microplastics and microrubbers in air and street dusts from Asaluyeh County, Iran. *Environ Pollut* 2019;244:153-64. DOI PubMed
73. Chae Y, An YJ. Effects of micro-and nanoplastics on aquatic ecosystems: current research trends and perspectives. *Mar Pollut Bull* 2017;124:624-32. DOI PubMed
74. Pelley AJ, Tufenkji N. Effect of particle size and natural organic matter on the migration of nano- and microscale latex particles in saturated porous media. *J Colloid Interface Sci* 2008;321:74-83. DOI PubMed
75. Bradford SA, Bettahar M. Concentration dependent transport of colloids in saturated porous media. *J Contam Hydrol* 2006;82:99-117. DOI PubMed
76. Liu M, Lu S, Song Y, et al. Microplastic and mesoplastic pollution in farmland soils in suburbs of Shanghai, China. *Environ Pollut* 2018;242:855-62. DOI PubMed
77. Ali MU, Lin S, Yousaf B, et al. Environmental emission, fate and transformation of microplastics in biotic and abiotic compartments: global status, recent advances and future perspectives. *Sci Total Environ* 2021;791:148422. DOI PubMed

78. Dris R, Gasperi J, Saad M, Mirande C, Tassin B. Synthetic fibers in atmospheric fallout: a source of microplastics in the environment? *Mar Pollut Bull* 2016;104:290-3. DOI PubMed
79. Critchell K, Lambrechts J. Modelling accumulation of marine plastics in the coastal zone; what are the dominant physical processes? *Estuar Coast Shelf Sci* 2016;171:111-22. DOI
80. Filella M. Questions of size and numbers in environmental research on microplastics: methodological and conceptual aspects. *Environ Chem* 2015;12:527-38. DOI
81. Ryan PG. Does size and buoyancy affect the long-distance transport of floating debris? *Environ Res Lett* 2015;10:084019. DOI
82. Shimanaga M, Yanagi K. The Ryukyu Trench may function as a "depocenter" for anthropogenic marine litter. *J Oceanogr* 2016;72:895-903. DOI
83. Zhang H. Transport of microplastics in coastal seas. *Estuar Coast Shelf Sci* 2017;199:74-86. DOI
84. Alimi OS, Budarz JF, Hernandez LM, Tufenkji N. Microplastics and nanoplastics in aquatic environments: aggregation, deposition, and enhanced contaminant transport. *Environ Sci Technol* 2018;52:1704-24. DOI PubMed
85. Hidalgo-Ruz V, Gutow L, Thompson RC, Thiel M. Microplastics in the marine environment: a review of the methods used for identification and quantification. *Environ Sci Technol* 2012;46:3060-75. DOI PubMed
86. Law KL, Morét-Fergusonet S, Maximenko NA, et al. Plastic accumulation in the North Atlantic subtropical gyre. *Science* 2010;329:1185-8. DOI PubMed
87. Zhang Y, Gao T, Kang S, Sillanpää M. Importance of atmospheric transport for microplastics deposited in remote areas. *Environ Pollut* 2019;254:112953. DOI PubMed
88. Haque F, Fan C. Fate and impacts of microplastics in the environment: hydrosphere, pedosphere, and atmosphere. *Environments* 2023;10:70. DOI
89. Hamid F, Bhatti MS, Anuar N, Anuar N, Mohan P, Periathamby A. Worldwide distribution and abundance of microplastic: how dire is the situation? *Waste Manag Res* 2018;36:873-97. DOI PubMed
90. Angnunavuri PN, Attiogbe F, Mensah B. Consideration of emerging environmental contaminants in africa: review of occurrence, formation, fate, and toxicity of plastic particles. *Sci Afr* 2020;9:e00546. DOI
91. Yoshida M. Situation of municipal solid waste management in African Cities - An interpretation of the information provided by the first ACCP meeting. 2018. Available from: http://www.gwopa.org/sites/default/files/2023-06/8_Discussion_Paper_2.pdf. [Last accessed on 16 May 2024].
92. Lebreton L, Andrady A. Future scenarios of global plastic waste generation and disposal. *Palgrave Commun* 2019;5:6. DOI
93. Tackling plastic waste and pollution for human health and marine biodiversity - A call for global action. 2019. Available from: https://www.fauna-flora.org/wp-content/uploads/2023/05/Tearfund-FFI_2020-Tackling-plastic-waste.pdf. [Last accessed on 16 May 2024].
94. Wilson DC, Rodic L, Modak P, et al. Global waste management outlook. 2015. Available from: https://www.uncclearn.org/wp-content/uploads/library/unep23092015.pdf. [Last accessed on 16 May 2024].
95. Free CM. Jensen OP, Mason SA, Eriksen M, Williamson N, Boldgiv B. High-levels of microplastic pollution in a large, remote, mountain lake. *Mar Pollut Bull* 2014;85:156-63. DOI PubMed
96. Haave M, Henriksen T. Sources and fate of microplastics in Urban Systems. In: Rocha-Santos T, Costa MF, Mouneyrac C, editors. Handbook of microplastics in the environment. Springer, Cham. 2022. pp. 849-75. DOI
97. Chaukura N, Kefeni KK, Chikurunhe I, et al. Microplastics in the aquatic environment - the occurrence, sources, ecological impacts, fate, and remediation challenges. *Pollutants* 2021;1:95-118. DOI
98. UNEP. Marine litter: a global challenge. 2009. Available from: https://wedocs.unep.org/bitstream/handle/20.500.11822/7787/-Marine%20Litter_%20A%20Global%20Challenge%20(2009)-2009845.pdf?sequence=3&amp%3BisAllowed=. [Last accessed on 16 May 2024].
99. Al-Thawadi S. Microplastics and nanoplastics in aquatic environments: challenges and threats to aquatic organisms. *Arab J Sci Eng* 2020;45:4419-40. DOI
100. Mattsson K, Jocic S, Doverbratt I, Hansson LA. Chapter 13 - Nanoplastics in the aquatic environment. In: Microplastic contamination in aquatic environments. 2018. pp. 379-99. DOI
101. Vethaak AD, Leslie HA. Plastic debris is a human health issue. *Environ Sci Technol* 2016;50:6825-6. DOI

McAdam *et al. Water Emerg Contam Nanoplastics* 2024;3:15
DOI: 10.20517/wecn.2024.05

Water Emerging Contaminants & Nanoplastics

Research Article

Open Access

Exogenous factors associated with legacy PFAS concentrations in the general U.S. population: NHANES 1999-2018

Jordan McAdam[1], Laura E. Jones[2,3], Xiaobo Xue Romeiko[1], Erin M. Bell[1,3]

[1]Department of Environmental Health Sciences, University at Albany, State University of New York, Rensselaer, NY12144, USA.
[2]Center for Biostatistics, Bassett Research Institute, Cooperstown, NY 13326, USA.
[3]Department of Epidemiology and Biostatistics, School of Public Health, State University of New York, Rensselaer, NY 12144, USA.

Correspondence to: Dr. Erin M. Bell, Departments of Epidemiology and Biostatistics, School of Public Health, State University of New York, 1 University Place, Rensselaer, NY 12144, USA. E-mail:ebell@albany.edu

How to cite this article: McAdam J, Jones LE, Romeiko XX, Bell EM. Exogenous factors associated with legacy PFAS concentrations in the general U.S. population: NHANES 1999-2018. *Water Emerg Contam Nanoplastics* 2024;3:15. https://dx.doi.org/10.20517/wecn.2024.05

Received: 7 Mar 2024 **First Decision:** 26 Apr 2024 **Revised:** 21 May 2024 **Accepted:** 23 May 2024 **Published:** 31 May 2024

Academic Editor: Joana C Prata **Copy Editor:** Pei-Yun Wang **Production Editor:** Pei-Yun Wang

Abstract

To reduce per- and polyfluoroalkyl substances (PFAS) exposure through legislation and other interventions, we must understand factors contributing to individual body burden. Identifying factors associated with serum perfluorinated compounds (PFAS) concentrations also aids in identifying groups at higher risk of adverse health outcomes due to elevated exposure. This exploratory analysis provides initial findings on exposure-related factors associated with legacy PFAS concentrations in the general United States (U.S.) population. We obtained National Health and Nutrition Examination Survey (NHANES) datasets with individual serum PFAS measurements from cycle years 1999-2018 (N = 14,961), excluding the 2001-2002 cycle due to pooled sampling. Over 100 features were evaluated for associations with PFAS concentrations. Data were singly imputed using hot deck and predictive mean matching (PMM) methods, and model performance by imputation method was compared using elastic net regression (ENR) models. Hot-deck imputation explained the most variance in predictive models; thus, a dataset imputed via hot-deck was used for feature selection. ENR models were employed to identify the top variables associated with legacy PFAS concentrations, and selected features were put into linear mixed models to obtain beta estimates and standard errors. Survey year, demographic, income, place of birth and citizenship status, household size, dietary, health, food insecurity, general health and healthcare, housing, social and behavioral, and other characteristics were important factors associated with legacy PFAS concentrations in this nationally representative study population. A better understanding of exogenous factors associated with PFAS concentrations can influence future epidemiological studies, guiding decisions on adjustment for confounding, and advancing our understanding of factors that affect chemical half-lives and toxicokinetics.

Keywords: PFAS, predictors, determinants, demographics, consumer behavior, healthcare, socioeconomics

INTRODUCTION

Per- and polyfluoroalkyl substances (PFAS) are persistent organic pollutants (POPs) and up to 99% of the United States (U.S.) human population has detectable concentrations of PFAS in their blood[1,2]. Though two of the most studied PFAS [i.e., perfluorooctane sulfonate (PFOS) and perfluorooctanoic acid (PFOA)] were phased out of production in many developed countries, concern over health effects associated with exposure to PFOA, PFOS, and other PFAS continues due to their environmental persistence. Many adverse health effects have been associated with PFAS exposure in adults, including dyslipidemia[3-5], changes in liver enzymes[6,7], elevated blood pressure and hypertension[8,9], and kidney and testicular cancer[10]. Because PFAS bioaccumulate in the bodies of adults, transplacental transfer, *in utero*, and breastfeeding, postnatally, can be sources of exposure in offspring[11].

Human exposure to PFAS is complex and varies within and between populations; however, ingestion has been suggested as the main route of exposure to PFAS among the general population. Foods such as fish, meat, offal, eggs, and fruit can be environmentally contaminated[12], but PFAS can also migrate into food from packaging[13-16]. Coated cookware can also leach PFAS into food[17]. Some communities in the U.S. have been highly exposed to PFAS through ingestion of contaminated drinking water[17], though this is not considered a major route of exposure for the general U.S. population. Other routes of PFAS exposure include ingestion of dust, transfer from treated carpets, clothes, and upholstery, inhalation of air, and inhalation of impregnation spray aerosols[18,19]. Though not thought to be a primary route of exposure, there may be dermal exposure from wearing clothing, such as waterproof layers, and from personal care products[18,19]. Serum or plasma concentrations of PFAS are generally used as markers of PFAS body burdens in humans, as they reflect long-term cumulative exposure to the chemicals from all sources of exposure.

To reduce PFAS exposure through legislation and other public health interventions, it is critical to understand factors that may contribute to individual body burden. Identifying factors associated with serum PFAS concentrations can also aid in identifying groups at higher risk of adverse health outcomes due to elevated exposure. Some factors associated with PFAS concentrations, such as parity and breastfeeding history, have been better studied[20-22], but less is known about other factors that may contribute to PFAS body burden in the general adult population. Previous studies evaluating factors associated with PFAS concentrations analyzed a limited number of demographic or dietary factors[23-26]. In addition, many have been conducted in European or Asian populations[24,25,27,28] and are not generalizable to the U.S. population. Given demographic, social and behavioral habits, and regulatory differences, it is important to consider the general U.S. population separately. There has also been a focus on populations living in PFAS-contaminated communities[26,28-30], sensitive populations (i.e., pregnant mothers and neonates)[31-37], and specific demographic or occupational groups[38-40], which are not generalizable to populations with lower, background levels of exposure and non-pregnant adult populations. Due to the paucity of research evaluating a large number of potential factors associated with serum PFAS concentrations in the general U.S. adult population, we aimed to investigate these factors using data from nine cycles of U.S. national health surveys [National Health and Nutrition Examination Survey (NHANES)] as an exploratory analysis.

Unlike previous analyses, we evaluate many potential factors associated with PFAS concentrations using the rich questionnaire data available from NHANES. In this analysis, we focus on exogenous factors (i.e., factors that may be assessed through a questionnaire such as social and behavioral habits, demographic, and household characteristics) that may be associated with PFAS exposure and serum concentrations, and in a separate analysis, we will explore endogenous factors (i.e., factors that may be measured through bloodwork or body measures such as complete blood count panels, environmental chemical concentrations, or body mass index) associated with PFAS concentrations. We evaluate these groups of factors separately due to their potential implications. A better understanding of the exogenous factors associated with PFAS concentrations may influence future epidemiological studies by guiding decisions on adjustment for confounding and furthering toxicological studies by advancing our understanding of factors that affect chemical half-lives, toxicokinetics, and interindividual variation[41,42]. This study is warranted, given that PFAS exposure is multifactorial and complex.

EXPERIMENTAL

Study population

The NHANES is a nationally representative survey conducted by the U.S. National Center for Health Statistics that is designed to assess the health and nutrition status of adults and children in the U.S. through in-home interviews and medical examinations[43]. In this study, we analyzed publicly available data from nine cycles of the NHANES (1999-2000, 2003-2004, 2005-2006, 2007-2008, 2009-2010, 2011-2012, 2013-2014, 2015-2016, 2017-2018). We did not include data collected in the 2001-2002 cycle because PFAS were measured in pooled, rather than individual, serum samples during those years. All study protocols were approved by the National Center for Health Statistics institutional review board and all participants gave written informed consent.

We restricted analyses to participants aged 18 years and older with complete serum PFAS measurements, as there may be differences in social and behavioral factors contributing to PFAS exposure and body burden between adults and children and differences in health outcome etiology for children following PFAS exposure. The final analytic sample was comprised of 14,961 adults. A flow chart showing sample selection and the workflow pipeline is shown in Supplementary Figure 1.

Exposure assessment

Solid phase extraction-high performance liquid chromatography-turbo ion spray ionization-tandem mass spectrometry was used to measure PFAS concentrations in serum samples. Detailed descriptions of the analytic methods have been described previously[44,45]. Our analysis focused on four highly detected PFAS: PFOS, PFOA, perfluorohexane sulfonate (PFHxS), and perfluorononanoic acid (PFNA). Non-detectable concentrations of PFAS were substituted with the respective limit of detection divided by the square root of two[46]. In most cycles, concentrations of PFOS and PFOA were measured in total; however, the 2013-2014, 2015-2016, and 2017-2018 cycles measured linear and branched isomers. To maximize our study population and because many of the regulations and much of the medical guidance surrounding PFAS exposure are based on the summed measures of these congeners[47], we summed these isomers to calculate total PFOS and PFOA concentrations. In the 1999-2000 cycle, PFAS were measured only among individuals with enough surplus sera (approximately 17.8% of participants). For subsequent cycles, PFAS were measured in approximately one-third of the sub-sample of the study cohort at random.

Evaluation of factors associated with serum PFAS concentrations

Each survey cycle contains five components: demographics, dietary, examination, laboratory, and questionnaire data. Each data component has many data files depending on the information collected in that round’s survey and examination assessment. These files are in SAS format and available for download at https://wwwn.cdc.gov/nchs/nhanes/Default.aspx. Datasets used in this analysis from NHANES were downloaded in October and November 2022. The five data components are described below:

- Demographic data: provide individual, family, and household-level information on language, pregnancy status, income, family size, household composition, demographic information, and other selected information such as military service status and country of birth.
- Dietary data: provide detailed dietary intake information from participants, including a 24-hour food and beverage recall, nutrient intake estimates, and supplement use.
- Laboratory and examination data: includes physical measures that can include blood pressure, body measures, oral health examinations, and physical activity monitoring.
- Questionnaire data: provide information on behavior, diet, nutrition, and other factors.

This analysis focused only on potential exogenous factors associated with PFAS concentrations, as described above; therefore, only questionnaire data were utilized in addition to the laboratory measurements of serum PFAS concentrations. We considered data over all cycles combined rather than single cycles at a time to increase the sample size[48].

Given differences across cycles, some variables had a high percent missingness in this larger, combined dataset with all 14,961 participants. Missingness ranged from 0% to 99.38% in the dataset, and 575 variables were identified across all cycles. As PFAS exposure has been associated with numerous health outcomes, variables related to diabetes, blood pressure, kidney conditions, asthma, arthritis, thyroid problems, liver conditions, and cancer, as well as medication use related to these conditions, were excluded from this analysis, given the evidence that PFAS exposure may contribute to these conditions[10,49-55]. Those variables with more than 50% missingness were excluded. This left 100 variables plus 14 demographic covariates for analysis [Figure 1]. The exogenous variables assessed as potential factors associated with serum PFAS concentrations are detailed in Supplementary Table 1. Certain variables from NHANES were re-coded for use in these analyses due to changes in question format across cycles, which are described in Supplementary Table 1. Unless otherwise noted, variables were not re-categorized from what is described in NHANES documentation (https://wwwn.cdc.gov/nchs/nhanes/default.aspx). Reference categories are described where applicable.

Statistical analysis

Data distributions and ranges were calculated and univariate analysis, including heatmaps and intersection analysis to explore missingness between pairs of features, was performed to assess the structure of missingness in the data. First, we describe imputation methods employed to address missingness. Next, we describe methods used to compare imputation methods and select an imputation method for model building. We then describe methods to identify variables best explaining variance in PFAS concentrations and analyses by congener.

Imputation

Because this was a predictive study employing large datasets and we were not performing inference, multiple imputation (MI) - which can be slow and requires pooling of statistical results for inference - was not necessary and was difficult to manage in a machine-learning context[56]. In addition, traditional MI methods have performed poorly on high-dimensional data[57]. We thus chose to explore two efficient donor-based single imputation methods: hot deck and predictive mean matching (PMM).

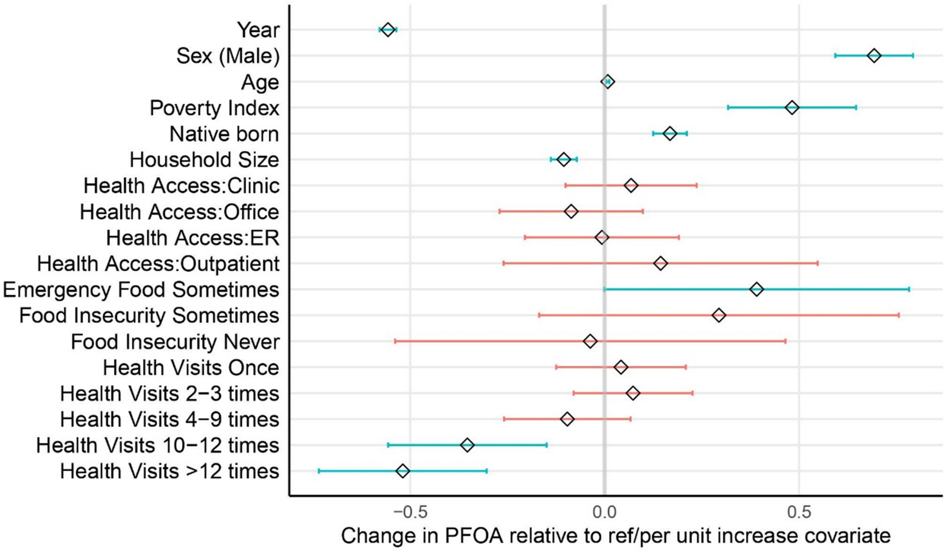

Figure 1. Change in serum PFOA relative to the reference level (for categorical variables) or per unit SD increase for continuous covariates from multivariable mixed-effects regression. See Supplementary Table 2 for details. Blue indicates statistically significant findings, while orange indicates findings that are not statistically significant. PFOA: Perfluorooctanoic acid.

Up to 50% of samples were monotonically missing (i.e., with monotone missingness patterns) for subsets of covariates. Under the assumption that our data were missing at random (MAR), we performed imputation by grouped and sorted simple hot deck and by PMM as described below. Both are donor-based methods that work well with mixed continuous and categorical data and draw replacements from existing observations. Imputations are thus realistic, with no imputed values outside the observed range. Donor-recipient methods such as hot deck are fast and appropriate for large datasets[58].

Hot deck imputation

Simple hot deck is a fast and efficient donor-based method where replacements for missing units (recipients) are randomly selected from complete units (donors) in the same column. Since it is donor-based, hot deck imputation avoids issues with model misspecification that might arise in regression-based methods, and handles large-dimensioned datasets efficiently. While hot deck methods are extensively used, the theory behind the method is less well-developed than other imputation methods[59]. In Hot Deck methods, donor units are randomly selected from a set of complete cases, known as the donor pool. There are multiple ways to specify a donor pool, otherwise known as an imputation class, for each missing unit. For example, columns to be imputed can be sorted and grouped based on other metrics, and sampling occurs from complete units within groupings. We grouped by participant sex, sorted by age, and found appropriate donor values for each missing recipient within the sorted domains by sex and age. Data were imputed using the package "VIM" in R[60].

PMM

PMM is a semi-parametric hot deck method that handles both continuous and categorical data and is robust against model misspecification. As implemented in the "mice" package in R[61], PMM uses an imputation model, for example, regression, to predict missing values, and then matches the predicted value of the missing unit (recipient) with a set of candidate donors from all complete cases that have predicted values closest to that of the missing unit. A donor is randomly chosen from the candidates, and the observed value of the donor is taken to replace the missing value. We assumed donor sets of size five, imputed five iterations, and then combined the datasets into one complete dataset.

Comparison of imputation methods

Elastic net regression (ENR) is a regularized regression method that includes the properties of both ridge regression and least absolute shrinkage and selection operator (LASSO)[62]. By linearly combining ridge and LASSO penalty functions, ENR performs variable selection and continuous shrinkage, and selects groups of correlated variables as a whole.

We compared imputation methods by building ENR models to assess model performance. Data preprocessing involved centering and scaling for continuous variables. All potential factors described in Supplementary Table 1 were entered into the ENR models and model metrics were obtained and compared.

When comparing the models with imputed data from each method, we considered the percent variance explained and R^2 metrics from the ENR model. The goal was to identify the imputation method with the best fitting models that explained the most variance in PFAS concentrations. The dataset from the best fitting imputation method was then used for identification of factors associated with PFAS concentrations.

Imputed datasets from each of the methods described above were randomly split 70/30 for training sets (used to train the models) and testing sets (used to test the models). This method was selected as it is appropriate for datasets with both a large number of rows and columns and is widely used for feature selection.

Identification of factors associated with serum PFAS concentrations

ENR models were used to identify variables that best explain variance in PFAS concentrations. We used the trainControl function in the caret package to specify parameters for model training, where we specified repeated 5-fold cross-validation to identify the optimal model parameters based on the smallest RMSE values. We then trained the ENR model based on the trainControl parameters and made predictions on the test dataset. The varImp (i.e., variable importance) function in the caret library was used to identify the 10 most important variables explaining variance in the five PFAS exposure variables [PFOA; PFOS; PFNA; PFHxS; and the simple sum of PFOA, PFOS, PFNA, and PFHxS (ΣPFAS)]. We computed the simple additive sum, rather than other approaches, to understand the body burden of mixtures of PFAS chemicals, to align with the current health guidance for PFAS exposure and testing that is based on a simple additive sum[47]. The variable importance represents the absolute value of ranked standardized coefficients from the best-fit tuned models. We did not conduct stratified analyses due to the exploratory nature of this analysis and due to differences in variables across the NHANES cycles included in this analysis.

Multivariable modeling

Based on results from feature selection described above, we built multivariable regression models for each of the five PFAS exposure variables, fitted with the 10 most important variables identified. Models were tuned by comparing tested models through analysis of variance (ANOVA) and using the lmeControl function. We extracted beta estimates and standard errors for model interpretation.

All data preprocessing, analysis, and validation were performed using R (version 3.4).

RESULTS AND DISCUSSION

Results

We present the demographic characteristics of participants in Table 1 (missingness was imputed via hot-deck). The smallest share of participants was from the 1999-2000 NHANES cycle (7.43%). The mean (standard deviation) age of participants in this analysis was 47.84 (19.24) years. Most participants were non-Hispanic (NH) White (39.87%-45.85%) and nearly one-third of participants had two persons in their household (29.80%). The PFAS with the highest median serum concentration was PFOS at 10.20 mg/dL. The median serum concentration of ΣPFAS was 16.40 mg/dL [Table 2].

After building the ENR models for each PFAS variable, statistics from the models were compiled to compare the results using the imputation method. Models based on grouped and sorted hot deck imputed data explained the greatest percent variance in PFAS concentrations for each PFAS and had the highest R^2 values for the PFOA, PFOS, PFHxS, and ΣPFAS models (data not shown). Given the overall better model statistics from hot deck imputation, we used this dataset for identification of important variables and for building linear mixed models. Overall, PFOA, PFOS, and ΣPFAS models had the best model fit, with R^2 values ranging from 0.21 to 0.31 (data not shown).

The top 10 variables explaining variance in serum PFAS concentrations, along with beta estimates and standard errors, are presented as forest plots in Figures 1-5 (see Supplementary Table 2 for a description of covariate codings on the Figures) and summarized in Table 3.

Male (relative to female) sex had the largest significant positive effects relative to all serum PFAS [Figures 1-5]. Year (i.e., NHANES cycle) has significant negative associations and had the largest (negative) effect size for PFOA [Figure 1] and PFOS [Figure 2], ΣPFAS [Figure 5] concentrations, suggesting diminishing population exposure or bioaccumulation in the sample populations over time. Age was significantly positively associated with all serum PFAS outcomes except for PFHxS [Figure 3], but effect sizes were small.

Place of birth and/or citizenship were important factors associated with serum PFOA [Figure 1], PFOS [Figure 2], PFHxS [Figure 3], and ΣPFAS concentrations, with being U.S.-born (relative to foreign-born) and possessing U.S. citizenship (relative to not being a U.S. citizen) associated with higher serum concentrations of these PFAS. Household size was an important factor in PFOA [Figure 1], PFOS [Figure 2], and ΣPFAS [Figure 5] models and was negatively associated with these PFAS concentrations. Race/ethnicity were also important factors associated with PFOS [Figure 2], PFNA [Figure 4], and ΣPFAS [Figure 5] concentrations, with the highest concentrations of these PFAS associated with NH Asian ethnicity and the lowest with Mexican-American race/ethnicity (reference group NH White). Three measures of fish and shellfish consumption were identified as important factors associated with serum PFAS concentrations in some models, with fish consumption positively and significantly associated with PFAS concentrations relative to no fish consumption. “Ever” *vs.* “never” freshwater fish consumption (in the last 30 days) was significantly positively associated with PFOS [Figure 2], PFNA [Figure 4], and ΣPFAS concentrations [Figure 5], while “ever” *vs.* “never” shellfish consumption (last 30 days) was significantly associated with PFOS [Figure 2], PFNA [Figure 4], and ΣPFAS [Figure 5] concentrations. “Ever” *vs.* “never” consumption of any fish in the last 30 days was an important factor associated with PFNA concentrations.

Several variables related to healthcare, income, and financial or food security were identified as important factors associated with serum PFAS concentrations. For the PFOA model, where healthcare is accessed (i.e., the ER, hospital outpatient department, a medical clinic, or private medical practice, relative to the reference “another place”), household food insecurity measures, and the number of times a participant received

Table 1. Demographic characteristics of participants, NHANES 1999-2018 (*N* = 14,961)

Variable	Level	*N* (%)
NHANES cycle	1999-2000	1,111 (7.43)
	2003-2004	1,680 (11.23)
	2005-2006	1,657 (11.08)
	2007-2008	1,834 (12.26)
	2009-2010	1,951 (13.04)
	2011-2012	1,648 (11.02)
	2013-2014	1,669 (11.16)
	2015-2016	1,711 (11.44)
	2017-2018	1,700 (11.36)
Sex (mean, SD)	Male	7,247 (48.44)
	Female	7,714 (51.56)
Age (mean, SD)	Years	47.84 ± 19.24
Veteran/military status	Yes	1,707 (11.41)
	No	13,252 (88.58)
Citizenship status	Citizen by birth	12,714 (84.98)
	Not a citizen	2,212 (14.79)
	Refused or don't know	35 (0.23)
Education level	Less than high school	4,228 (28.26)
	High school	3,629 (24.26)
	Greater than high school	7,081 (47.33)
	Refused or don't know	23 (0.15)
Marital status	Married	7,513 (50.22)
	Widowed	1,214 (8.11)
	Divorced	1,465 (9.79)
	Separated	478 (3.19)
	Never married	2,969 (19.84)
	Living with partner	1,316 (8.80)
	Refused	6 (0.04)
Race/ethnicity	Mexican-American	2,944 (19.68)
	Other Hispanic	836 (5.59)
	NH White	6,859 (45.85)
	NH Black	2,991 (19.99)
	Other race	476 (3.18)
	NH Asian	855 (5.71)
Total number of people in family	1	3,144 (21.01)
	2	3,781 (25.27)
	3	2,433 (16.26)
	4	2,102 (14.05)
	5	1,917 (12.81)
	6	775 (5.18)
	≥ 7	809 (5.41)
Annual family income	$0 - $4,999	590 (3.94)
	$5,000 - $9,999	816 (5.45)
	$10,000 - $14,999	933 (6.24)
	$15,000 - $19,999	917 (6.13)
	$20,000 - $24,999	1,106 (7.39)
	$25,000 - $34,999	1,463 (9.78)
	$35,000 - $44,999	1,511 (10.10)
	$45,000 - $54,999	1,055 (7.05)
	$55,000 - $64,999	997 (6.66)
	$65,000 - $74,999	591 (3.95)
	Over $20,000	482 (3.22)
	Under $20,000	128 (0.85)
	$75,000 - $99,999	1,316 (8.80)
	≥ $100,000	2,078 (13.89)
	Refused or don't know	978 (6.54)
Family PIR		2.47 ± 1.62

NHANES: National Health and Nutrition Examination Survey; PIR: poverty income ratio.

healthcare over the past year were important factors [Figure 1]. For the PFOS [Figure 2], PFHxS [Figure 3], PFNA [Figure 4], and ΣPFAS [Figure 5] models, household food security measures were associated with serum concentrations of these PFAS, though the relationships were not clear. For the PFHxS model, telling

Table 2. Legacy serum PFAS distributions (mg/dL), NHANES 1999-2018 (*N* = 14,961)

	Min	**Max**	**P25**	**P50**	**P75**	**IQR**
PFOA	0.07	123.00	1.57	2.70	4.40	2.83
PFOS	0.14	1,403.00	5.00	10.20	19.50	14.50
PFHxS	0.07	82.00	0.80	1.50	2.60	1.80
PFNA	0.058	80.77	0.50	0.83	1.39	0.89
ΣPFAS	0.34	1,418.30	9.00	16.40	28.30	19.30

PFAS: Per- and polyfluoroalkyl substances; NHANES: National Health and Nutrition Examination Survey; Min: minimum; Max: maximum; P25: first quartile; P50: median; p75: third quartile; IQR: interquartile range; PFOA: perfluorooctanoic acid; PFOS: perfluorooctanesulfonic acid; PFHxs: perfluorohexane sulfonate; PFNA: perfluorononanoic acid; ΣPFAS: the simple sum of PFOA, PFOS, PFNA, and PFHxS.

a doctor about trouble sleeping was an important factor and was associated with higher serum PFHxS concentrations [Figure 3].

Factors in the home were important in the PFOS [Figure 2] and PFNA [Figure 4] models. Home missing space ownership status was an important factor in the PFOS model, with renting or having another housing arrangement associated with lower serum PFOS concentrations relative to home ownership [Figure 2]. Having a smoker in the home was associated with lower serum concentrations of PFNA [Figure 4].

Discussion

Exogenous factors associated with PFAS concentrations

In this exploratory analysis, we evaluated over 100 variables collected through questionnaires over nine NHANES cycles between 1999 and 2018 as potential factors associated with PFAS concentrations and presented the top 10 factors for four legacy PFAS and ΣPFAS. We observed that year of survey, demographic, income, place of birth and citizenship status, household size, dietary, health, food insecurity, general health and healthcare, housing, social and behavioral, and other characteristics were important factors associated with legacy PFAS concentrations in this nationally representative study population. The most important factors associated with PFAS concentrations varied by congener, suggesting differing potential sources of exposure to each chemical and differences in toxicokinetics affecting body burden.

Year of collection

In general, exposure to certain legacy PFAS, especially PFOS and PFOA, has been declining over time in the U.S. due to phase outs by manufacturers[63,64], and studies have observed declining concentrations of legacy PFAS over time in humans[65,66]. Our findings support this, as the cycle (year) of NHANES was negatively associated with serum PFOA, PFOS, PFHxS, PFNA, and ΣPFAS concentrations. This may be due to diminishing population-level environmental exposure post-ban.

Demographics and family characteristics

Age

The literature surrounding the relationship between age and legacy PFAS concentrations is mixed, though we observed age to be positively associated with serum PFAS concentrations, albeit with relatively small effect sizes. Legacy PFAS bind to serum albumin[67] and albumin concentrations decrease with age[68]. Additionally, glomerular filtration rate, kidney function, and activity level tend to decrease with age[69-71], so a general increase in legacy PFAS concentrations at older ages could be expected[72]. Contraception use, hysterectomies, and menopause may reduce menstrual blood loss as women age and therefore reduce or eliminate a route of PFAS excretion[73], which could increase PFAS concentrations with age, which supports observations in this study. Though parity has been associated with PFAS concentrations in women of reproductive age[23], in elderly women, it has been shown to have a minor effect on PFAS body burden[74].

Table 3. Hypothesis testing summary of the top 10 variables associated with serum PFAS concentrations, by PFAS congener, NHANES 1999-2018

PFAS	Factor	Reference group (categorical variables only)	S/NS	Direction of association (for categorical variables, compared to reference group) (+/-)
PFOA	Year	-	S	-
	Male sex	Female sex	S	+
	Age	-	S	+
	Poverty index	-	S	+
	Born in U.S.	Born outside of U.S.	S	+
	Household size	-	S	-
	Receive healthcare at clinic	Receive healthcare some other place (i.e., not a clinic, doctor's office, ER, or outpatient center)	NS	+
	Receive healthcare at doctor's office		NS	-
	Receive healthcare at ER		NS	-
	Receive healthcare at outpatient center		NS	+
	Emergency food received sometimes	Emergency food received often	S	+
	Food insecurity experienced sometimes	Food insecurity experienced often	NS	+
	Food insecurity experienced never		NS	-
	Health care visits: once in last year	Health care visits: zero in last year	NS	+
	Health care visits: 2-3 times in last year		NS	+
	Health care visits: 4-9 times in last year		NS	-
	Health care visits: 10-12 times in last year		S	-
	Health care visits: > 12 times in last year		S	-
PFOS	Year	-	S	-
	Male sex	Female sex	S	+
	Age	-	S	+
	Household size	-	S	-
	Shellfish consumption in last 30 days	No shellfish consumption in last 30 days	S	+
	Food insecurity experienced sometimes	Food insecurity experienced often	NS	-
	Food insecurity experienced never		NS	-
	Mexican ethnicity	NH White race	NS	-
	Other Hispanic ethnicity		NS	+
	NH Black race		S	+
	NH Asian race		S	+
	Other race		S	+
	Rent home	Other arrangement	NS	+
	Own home		S	+
PFHxS	Year	-	S	-
	Male sex	Female sex	S	+
	Receive retirement income	Do not receive retirement income	S	+
	Born in U.S.	Born outside of U.S.	S	+
	Ever told doctor trouble sleeping	Never told doctor trouble sleeping	S	+

	Married	Living with partner	NS	+
	Widowed		S	+
	Divorced		NS	+
	Separated		NS	-
	Never married		NS	+
	Receive healthcare at clinic	Receive healthcare some other place (i.e., not a clinic, doctor's office, ER, or outpatient center)	NS	-
	Receive healthcare at doctor's office		NS	+
	Receive healthcare at ER		NS	-
	Receive healthcare at outpatient center		NS	-
	Income level $75,000 - $99,000	Income level < $0 - $4,999	S	-
	Income level < $2,000	Income level < $0 - $4,999	S	+
	Receives retirement income	Does not receive retirement income	S	+
PFNA	Year	-	S	-
	Male sex	Female sex	S	+
	Age	-	S	+
	Smoker in home	No smokers in home	NS	+
	Fish consumption in last 30 days	No fish consumption in last 30 days	S	+
	Shellfish consumption in last 30 days	No shellfish consumption in last 30 days	S	+
	Freshwater fish consumed in last 30 days	No freshwater fish consumption in last 30 days	S	+
	Food insecurity experienced sometimes	Food insecurity experienced often	S	-
	Food insecurity experienced never		NS	-
	Fast duration (in hours) before blood draw		S	-
	Mexican ethnicity	NH White race	S	-
	Other Hispanic ethnicity		NS	-
	NH Black race		S	+
	NH Asian race		S	+
	Other race		NS	+
ΣPFAS	Year	-	S	-
	Male sex	Female sex	S	+
	Age	-	S	+
	Born in U.S.	Born outside of U.S.	S	+
	U.S. citizen	Not a U.S. citizen	S	+
	Household size	-	S	-
	Fish consumption in last 30 days	No fish consumption in last 30 days	S	+
	Shellfish consumption in last 30 days	No shellfish consumption in last 30 days	S	+
	Food insecurity experienced sometimes	Food insecurity experienced often	NS	-
	Food insecurity experienced never		S	-
	Mexican ethnicity	NH White race	NS	-
	Other Hispanic ethnicity		NS	+
	NH Black race		S	+
	NH Asian race		S	+
	Other race		NS	+

PFAS: Per- and polyfluoroalkyl substances; NHANES: National Health and Nutrition Examination Survey; S: significant; NS: non-significant; +: positive; -: negative; PFOA: perfluorooctanoic acid; U.S.: United States; ER: emergency room; PFOS: perfluoroctane sulfonate; NH: non-Hispanic; PFHxS: perfluorohexane sulfonate; PFNA: perfluorononanoic acid; ΣPFAS: the simple sum of PFOA, PFOS, PFNA, and PFHxS.

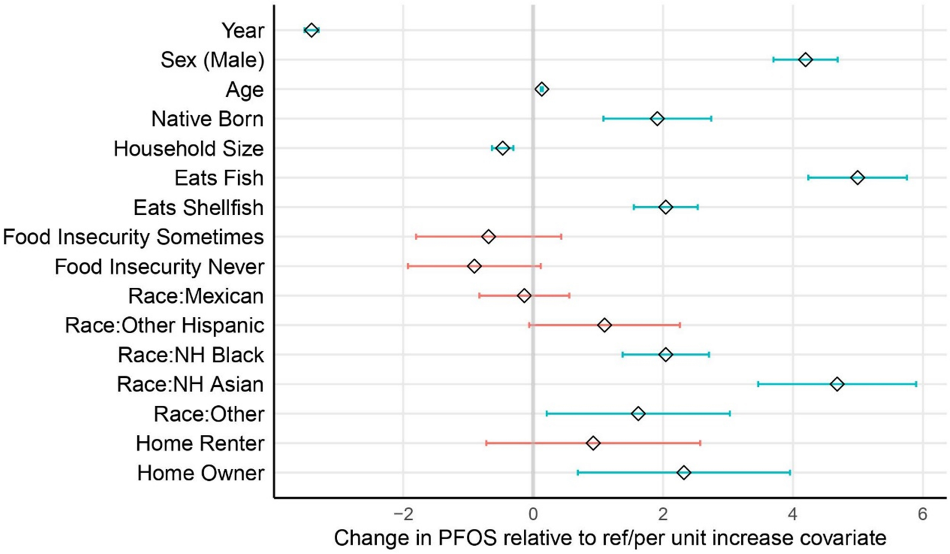

Figure 2. Change in serum PFOS relative to the reference level (for categorical variables) or per unit SD increase for continuous covariates from multivariable mixed-effects regression. See Supplementary Table 2 for details. Blue indicates statistically significant findings, while orange indicates findings that are not statistically significant. PFOS: Perfluorooctane sulfonate.

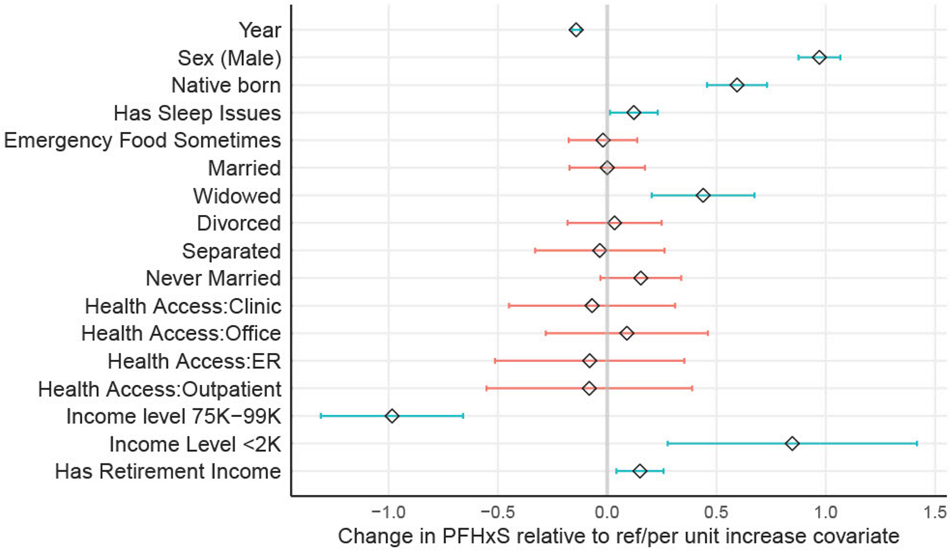

Figure 3. Change in serum PFHxS relative to the reference level (for categorical variables) or per unit SD increase for continuous covariates from multivariable mixed-effects regression. See Supplementary Table 2 for details. Blue indicates statistically significant findings, while orange indicates findings that are not statistically significant. PFHxS: Perfluorohexane sulfonate.

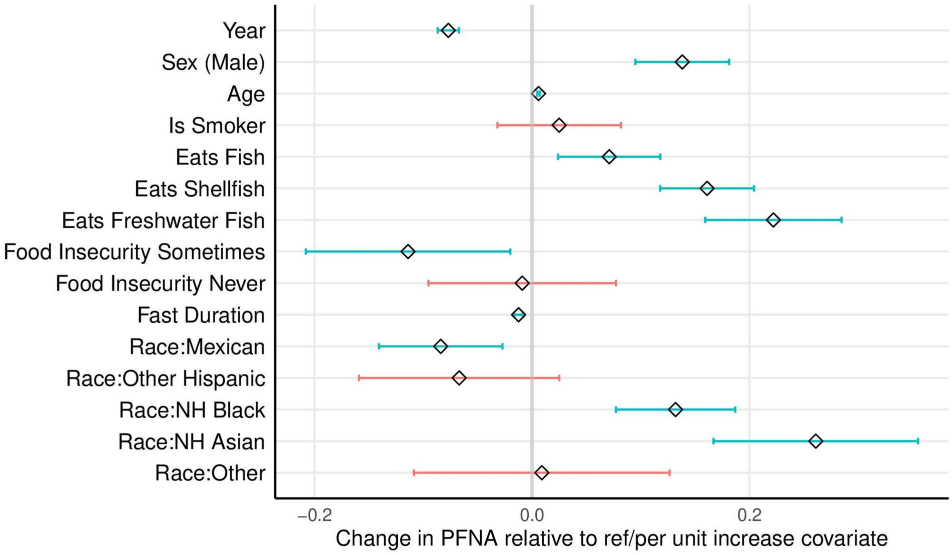

Figure 4. Change in serum PFNA relative to the reference level (for categorical variables) or per unit SD increase for continuous covariates from multivariable mixed-effects regression. See Supplementary Table 2 for details. Blue indicates statistically significant findings, while orange indicates findings that are not statistically significant. PFNA: Perfluorononanoic acid.

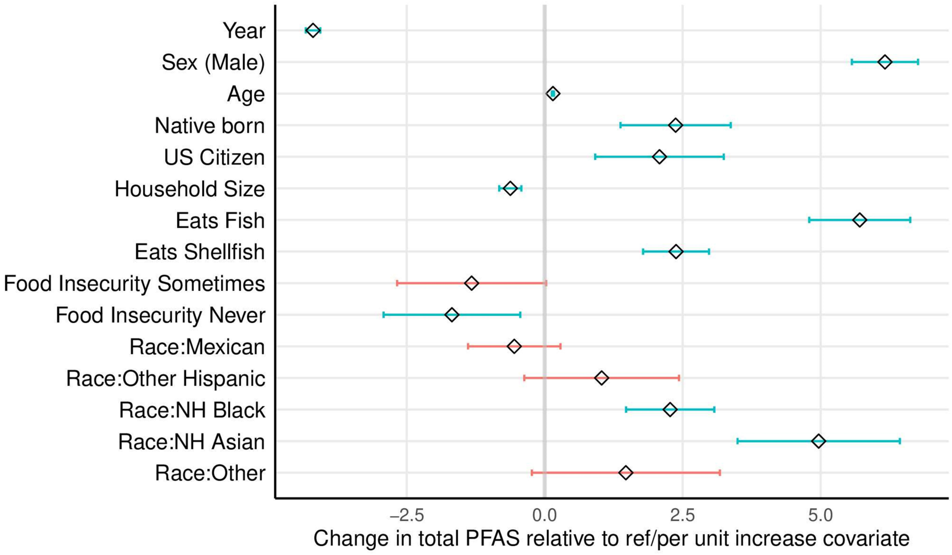

Figure 5. Change in serum ΣPFAS relative to the reference level (for categorical variables) or per unit SD increase for continuous covariates from multivariable mixed-effects regression. See Supplementary Table 2 for details. Blue indicates statistically significant findings, while orange indicates findings that are not statistically significant. ΣPFAS: the simple sum of PFOA, PFOS, PFNA, and PFHxS. PFOA: perfluorooctanoic acid; PFOS: perfluorooctane sulfonate; PFNA: perfluorononanoic acid; PFHxS: perfluorohexane sulfonate.

Citizenship status and place of birth

Though PFOS and PFOA have been phased out in the U.S., they are still in production in parts of the world. In this analysis, we observed U.S. citizenship and being born in the U.S. to be associated with higher concentrations of legacy PFAS concentrations compared to not having U.S. citizenship and being born outside of the U.S. This may be explained in part by cultural habits, imported foods, use of consumer products with PFAS, and social and behavioral differences between immigrants and U.S.-born individuals[75]. Additionally, developed countries may have wider PFAS contamination[76]. A recent review of determinants of PFAS concentrations in pregnant mothers and neonates found nationality, race, and country of origin to be determinants of legacy PFAS concentrations in pregnant mothers[23].

Household size

Household size was negatively associated with legacy PFAS concentrations in this analysis, which may have several explanations. Mothers giving birth to multiple children would be expected to have lower serum PFAS concentrations, as parity is a factor associated with lower legacy PFAS concentrations[23]. Additionally, this could be a proxy measure for socioeconomic status, as larger family size has been a positive predictor of poverty[77] or household members may not be family but roommates. Given our mixed results related to socioeconomic status and serum PFAS concentrations, further study is needed to better understand this finding.

Sex

Overall, male sex predicted higher concentrations of all evaluated PFAS relative to females. This supports a large body of evidence suggesting females have lower serum PFAS concentrations than males, particularly during reproductive years. Females have greater routes of excretion of PFAS, including menstruation, breastfeeding, and childbirth[78-81]. Additionally, a higher renal clearance of PFAS in females has been suggested, and longer half-lives have been observed in males[82,83].

Race/ethnicity

Race/ethnicity were associated with serum concentrations of PFOA, PFOS, and PFNA concentrations. Compared to the NH White race/ethnicity group, the Mexican-American race/ethnicity group generally had lower PFAS concentrations, while other Hispanic, NH Black, “Other” race, and NH Asian race/ethnicity groups had elevated serum concentrations of these congeners. NH Asian race was associated with the highest serum concentrations. Some studies have documented racial disparities in PFAS exposure, with NH Black individuals having higher concentrations of PFOS; however, studies in recent years have shown changes in these trends[45,84-86]. A recent study observed community water systems serving higher proportions of Hispanic/Latino and NH Black residents had significantly increased odds of detecting several PFAS[87], which may reflect disparities in the sites of point sources of PFAS contamination. Our findings in this study suggest a complex relationship between socioeconomic status and serum PFAS concentrations.

Differences in tap water consumption may partially explain our findings. A study assessing NHANES 2011-2016 water consumption trends observed NH White individuals consumed the most tap water, whereas Mexican-American individuals consumed the most bottled water[88], with other studies observing similar results[89-91]. Although bottled water can contain detectable quantities of PFAS[92-94], there are many cases of contaminated public drinking water supplies in the U.S.[95]. The higher concentrations of PFOA, PFOS, and PFNA predicted by NH Asian race compared to other racial and ethnic groups contradict some findings in other studies[21].

Diet

Dietary freshwater fish

Consumption of freshwater fish, such as walleye, trout, pike, perch, or bass, in the last 30 days was significantly associated with higher concentrations of PFOS, PFNA, and ΣPFAS. This is supported by findings from other studies, which have found freshwater fish consumption to be a significant contributor to PFOS concentrations[96-99]. It has been suggested that even infrequent freshwater fish consumption may increase serum PFOS concentrations[97]. Though our findings are based on a binary measure of consumption (i.e., ever *vs.* never in the last 30 days), this suggests that even at a potentially wide range of freshwater fish consumption levels, there is exposure to legacy PFAS. The risks and benefits of freshwater fish consumption may warrant further study.

Dietary shellfish and fish

Shellfish and fish consumption was associated with higher serum concentrations of PFOS, PFNA and ΣPFAS [Figures 2, 4, and 5]. This supports other literature finding evidence of an association between shellfish consumption and serum PFAS concentrations[100-105]. Because our findings are based on a binary measure of consumption, further research in populations consuming shellfish may be helpful in identifying specific species that may result in higher exposure. While NHANES collects information on specific types of shellfish and fish consumed, counts were too small for any specific fish or shellfish to evaluate in this analysis.

Food insecurity

Certain measures of food insecurity (i.e., household food not lasting and household receiving emergency food) were factors associated with all PFAS concentrations, though these relationships were inconsistent. This again suggests a complex relationship between socioeconomic status and serum PFAS concentrations.

Health

Receipt of healthcare

The number of healthcare visits in the last year was associated with PFOA concentrations, though the relationship was not clear. Compared to no visits in the last year, one or two to three visits were associated with higher serum concentrations. Compared to no visits in the last year, 4-9, 10-12, and > 12 visits in the last year were associated with lower concentrations of PFOA. These findings may suggest relationships between overall health, insurance, or socioeconomic status and serum PFAS concentrations. Responding no (*vs.* yes) to “Have you ever told a doctor you had trouble sleeping?” was associated with higher serum concentrations of PFHxS, which may be reflective of healthcare access rather than a relationship between sleeping troubles and serum PFAS concentrations. Additionally, the type of place where healthcare was usually received was associated with PFOA and PFHxS concentrations. Relationships were not clear and may be influenced by healthcare access and socioeconomic status.

Housing and income

Housing characteristics

Renting rather than owning a home was associated with lower concentrations of PFOS. Though associations between housing characteristics and PFAS exposure are not well studied, carpet treatments contain PFAS and have been associated with elevated PFAS concentrations[106,107]. House dust has also been suggested to be an important pathway to human PFAS exposure[108].

Income and consumer spending

Family poverty income ratio (PIR) was positively associated with serum PFOA concentrations, receiving retirement income was positively associated with PFHxS concentrations, and while there was an association between household income and PFHxS concentrations, the relationship did not appear to be linear. The first two measures suggest a positive relationship between income and PFAS concentrations, which may be explained by the increased opportunity to use legacy PFAS containing products such as clothing at higher prices[109].

Comparison to other studies

The R^2 values in this analysis were relatively low, with the highest at 0.31; however, our R^2 results are comparable to or higher than other studies evaluating factors associated with PFAS concentrations[21,26,30,110,111].

Imputation methods

Given the high percent missingness in certain variables and the exploratory nature of this analysis, we tested two donor-based single imputation methods. Imputation involves assumptions that can influence results; therefore, these findings should be interpreted with caution and should be confirmed in future studies. Though the best single imputation methods may vary by dataset and application, research suggests that hot-deck imputation is superior compared to PMM when comparing root mean squared error, unsupervised classification error, supervised classification error, and the time used to run the algorithm[112].

It should be noted that the data in this exploratory analysis had high missingness and a complete-case analysis could not be conducted for comparison due to this and the large number of variables included in models. Further study is needed to understand the best imputation methods for data and modeling of this nature.

Individual congeners vs. additive sums

The recent National Academies of Sciences, Engineering, and Medicine (NASEM) guidance on patient follow-up after PFAS testing was based on ranges of values of the simple additive sum of methylperfluorooctanesulfonamidoacetic acid (MeFOSAA), PFHxS, PFOA, PFDA, perfluoroundecanoic acid (PFUnDA), PFOS, and PFNA in serum or plasma[47]. For patients with < 2 ng/mL serum or plasma PFAS, NASEM recommends providing the usual standard of care. For patients with ≥ 20 ng/mL serum or plasma PFAS, NASEM encourages exposure reduction if point sources can be identified, prioritizing screening for dyslipidemia, conducting thyroid function testing, assessing signs and symptoms of kidney cancer, and assessing signs and symptoms of testicular cancer and ulcerative colitis. Though our analysis could not include MeFOSAA, PFDA, and PFUnDA due to the limited number of NHANES cycles that have evaluated these PFAS, we do show differences in the top factors associated with ΣPFAS (PFOA + PFOS + PFHxS + PFNA) and PFOA, PFOS, PFHxS, and PFNA individually. Therefore, it is important to consider factors associated with simple additive sums of commonly detected PFAS in addition to factors related to single PFAS congeners.

Strengths and limitations

The present study has notable limitations. The first is the cross-sectional nature of the NHANES data. Although legacy PFAS may have half-lives of several years or more[113], which we expect to reduce the risk of exposure misclassification, this does not completely mitigate risk. Additionally, we cannot establish causality and do not draw conclusions as to whether the identified factors cause changes in PFAS concentrations. Second, most of the factors evaluated were collected through self-report. Third, many covariates could not be assessed for their association with PFAS concentrations in this study population due to high missingness. Given the large number of factors that could not be included in this analysis, further research is needed to continue establishing factors associated with PFAS concentrations. Covariates surrounding consumer behavior, diet, housing characteristics, physical activity, and reproductive health, in particular, require further study and may offer further insight into exposure and elimination of PFAS. Fourth, we evaluated the four most measured PFAS, though there are thousands of PFAS. Given the increased use of short-chain and alternative PFAS in recent years, more research is needed to comprehensively understand the factors associated with PFAS concentrations. Fifth, this is an unweighted exploratory study. Although NHANES provides weights for each cycle due to the complex survey design, we did not incorporate them due to the high missingness and methods employed in this exploratory analysis.

Despite these limitations, this work has several notable strengths. First, this was a large study population that was representative of the U.S. general population. Second, this analysis evaluates the largest number of potential factors associated with PFAS concentrations to date. Most studies evaluating factors associated with PFAS concentrations consider a limited number of factors. Third, we used the well-known ENR approach to identify the top factors associated with PFAS concentrations in this study population.

Future directions

It is important to consider the findings here exploratory, and replication in other populations representative of the U.S. general population is needed to confirm these findings. Many of the variables included in this analysis were related to one another or were consequences of others (e.g., poverty index or income and food insecurity). We did not perform stratified analyses due to the exploratory nature of this analysis; therefore, future studies stratified by factors identified here (e.g., socioeconomic status, race, sex, age) are warranted.

Future studies may consider evaluating socioeconomic status in multiple ways (i.e., food insecurity, healthcare access, *etc.*) to further tease out the associations observed here. It may also be beneficial to consider the joint effects of socioeconomic status and PFAS on health effects or socioeconomic status as a moderator in PFAS-health outcome relationships. Given our findings on factors associated with PFAS (i.e., many indicators of socioeconomic status), the potential health effects associated with both PFAS exposure and socioeconomic status, and that PFAS exposure through contaminated drinking water has been associated with socioeconomic and sociodemographic factors[87] and is an important environmental justice issue within the U.S., it is important to explore these relationships further.

This study was motivated by increasing concerns over health effects following PFAS exposure in adults, and our findings raise awareness of potentially vulnerable groups in the general population not occupationally exposed or exposed through highly contaminated drinking water. Future studies should consider prospective analyses where possible to assess potential causality between these factors and serum PFAS concentrations and to further investigate how these factors influence PFAS elimination half-lives. Research should consider adjusting for factors with substantial evidence to suggest they may affect PFAS concentrations, such as age, sex, and year of sample collection, as well as factors specific to the population being studied (i.e., children, adults, pregnant mothers, highly exposed communities, *etc.*). It may be helpful to stratify by factors such as age, sex, year of sample collection, socioeconomic status, and other factors identified here to identify potential effect modifiers in PFAS studies dependent on the research question. Additionally, studies investigating factors associated with PFAS concentrations should consider the inclusion of short-chain and newer PFAS, where little research has been conducted. The R^2 values found in our models suggest other factors may be associated with higher serum PFAS concentrations. Biological factors associated with PFAS concentrations should be explored further, as these factors may affect PFAS toxicokinetics.

CONCLUSIONS

This novel, exploratory study aimed to address the substantial gaps in our understanding of factors associated with serum concentrations of legacy PFAS chemicals in the general U.S. population by employing elastic net regression to evaluate over 100 variables collected via questionnaire in NHANES cycles between 1999-2018. While specific factors varied by the specific PFAS evaluated, we observed the time period of sample collection, sex, age, race, socioeconomic factors, and fish or shellfish consumption to be important factors associated with legacy PFAS concentrations in a large U.S. study population. These preliminary findings may direct research priorities related to PFAS exposure and disparities and highlight gaps in risk assessment. Reducing PFAS exposure through the identification of vulnerable groups may reduce disease burden in the general population and reduce healthcare costs.

DECLARATIONS

Acknowledgments

The authors would like to thank Sana Savadatti, Elizabeth Lewis-Michl, Steven Forand, and Steve Shost for their review of this work and feedback. We thank Megan Kern of Bassett Research Institute for her help with creating our graphic abstract and pipeline flowchart.

Authors' contributions

Conceptualization: McAdam J, Jones LE, Bell EM, Romeiko XX
Methodology, software, visualization, and formal analysis: McAdam J, Jones LE
Writing - original draft: McAdam J, Jones LE, Bell EM
Writing - review and editing: McAdam J, Jones LE, Bell EM, Romeiko XX
Supervision: Bell EM
All authors discussed the results and contributed to the final manuscript.

Availability of data and materials

NHANES datasets are publicly available: https://www.cdc.gov/nchs/nhanes/index.htm.

Financial support and sponsorship

This work was supported by Centers for Disease Control and Prevention Grant # U01TS000303.

Conflicts of interest

All authors declared that there are no conflicts of interest.

Ethical approval and consent to participate

NHANES data were collected under study protocols approved by the National Center for Health Statistics institutional review board and all participants gave written informed consent. More information is available here: https://www.cdc.gov/nchs/nhanes/irba98.htm.

Consent for publication

Not applicable.

Copyright

REFERENCES

1. ATSDR. PFAS exposure assessments. Available from: https://www.atsdr.cdc.gov/pfas/activities/assessments.html. [Last accessed on 29 May 2024].
2. CDC. Fourth national report on human exposure to environmental chemicals, updated tables, March 2021: volume three: analysis of pooled serum samples for select chemicals, NHANES 2005-2016. Available from: https://stacks.cdc.gov/view/cdc/105344. [Last accessed on 29 May 2024].
3. Dunder L, Lind PM, Salihovic S, Stubleski J, Kärrman A, Lind L. Changes in plasma levels of per- and polyfluoroalkyl substances (PFAS) are associated with changes in plasma lipids - a longitudinal study over 10 years. *Environ Res* 2022;211:112903. DOI PubMed
4. Li Y, Barregard L, Xu Y, et al. Associations between perfluoroalkyl substances and serum lipids in a Swedish adult population with contaminated drinking water. *Environ Health* 2020;19:33. DOI PubMed PMC
5. Lin PD, Cardenas A, Hauser R, et al. Per- and polyfluoroalkyl substances and blood lipid levels in pre-diabetic adults-longitudinal analysis of the diabetes prevention program outcomes study. *Environ Int* 2019;129:343-53. DOI PubMed PMC
6. Liu JJ, Cui XX, Tan YW, et al. Per- and perfluoroalkyl substances alternatives, mixtures and liver function in adults: a community-based population study in China. *Environ Int* 2022;163:107179. DOI PubMed

7. Salihovic S, Stubleski J, Kärrman A, et al. Changes in markers of liver function in relation to changes in perfluoroalkyl substances - a longitudinal study. *Environ Int* 2018;117:196-203. DOI PubMed
8. Averina M, Brox J, Huber S, Furberg AS. Exposure to perfluoroalkyl substances (PFAS) and dyslipidemia, hypertension and obesity in adolescents. the fit futures study. *Environ Res* 2021;195:110740. DOI PubMed
9. Pitter G, Zare Jeddi M, Barbieri G, et al. Perfluoroalkyl substances are associated with elevated blood pressure and hypertension in highly exposed young adults. *Environ Health* 2020;19:102. DOI PubMed PMC
10. Bartell SM, Vieira VM. Critical review on PFOA, kidney cancer, and testicular cancer. *J Air Waste Manag Assoc* 2021;71:663-79. DOI PubMed
11. Papadopoulou E, Sabaredzovic A, Namork E, Nygaard UC, Granum B, Haug LS. Exposure of Norwegian toddlers to perfluoroalkyl substances (PFAS): the association with breastfeeding and maternal PFAS concentrations. *Environ Int* 2016;94:687-94. DOI PubMed
12. EFSA Panel on Contaminants in the Food Chain (EFSA CONTAM Panel); Schrenk D, Bignami M, Bodin L, et al. Risk to human health related to the presence of perfluoroalkyl substances in food. *EFSA J* 2020;18:e06223. DOI
13. Schaider LA, Balan SA, Blum A, et al. Fluorinated compounds in U.S. fast food packaging. *Environ Sci Technol Lett* 2017;4:105-11. DOI PubMed PMC
14. Glenn G, Shogren R, Jin X, Orts W, Hart-Cooper W, Olson L. Per- and polyfluoroalkyl substances and their alternatives in paper food packaging. *Compr Rev Food Sci Food Saf* 2021;20:2596-625. DOI PubMed
15. Curtzwiler GW, Silva P, Hall A, Ivey A, Vorst K. Significance of perfluoroalkyl substances (PFAS) in food packaging. *Integr Environ Assess Manag* 2021;17:7-12. DOI PubMed
16. Seltenrich N. PFAS in food packaging: a hot, greasy exposure. *Environ Health Perspect* 2020;128:54002. DOI PubMed PMC
17. ATSDR. Toxicological profile for perfluoroalkyls. 2021. Available from: https://www.atsdr.cdc.gov/toxprofiles/tp200.pdf. [Last accessed on 29 May 2024].
18. Thépaut E, Dirven HAAM, Haug LS, et al. Per- and polyfluoroalkyl substances in serum and associations with food consumption and use of personal care products in the Norwegian biomonitoring study from the EU project EuroMix. *Environ Res* 2021;195:110795. DOI
19. Trudel D, Horowitz L, Wormuth M, Scheringer M, Cousins IT, Hungerbühler K. Estimating consumer exposure to PFOS and PFOA. *Risk Anal* 2008;28:251-69. DOI PubMed
20. Kato K, Wong LY, Chen A, et al. Changes in serum concentrations of maternal poly- and perfluoroalkyl substances over the course of pregnancy and predictors of exposure in a multiethnic cohort of Cincinnati, Ohio pregnant women during 2003-2006. *Environ Sci Technol* 2014;48:9600-8. DOI PubMed PMC
21. Park SK, Peng Q, Ding N, Mukherjee B, Harlow SD. Determinants of per- and polyfluoroalkyl substances (PFAS) in midlife women: evidence of racial/ethnic and geographic differences in PFAS exposure. *Environ Res* 2019;175:186-99. DOI PubMed PMC
22. Sagiv SK, Rifas-Shiman SL, Webster TF, et al. Sociodemographic and perinatal predictors of early pregnancy per- and polyfluoroalkyl substance (PFAS) concentrations. *Environ Sci Technol* 2015;49:11849-58. DOI PubMed PMC
23. McAdam J, Bell EM. Determinants of maternal and neonatal PFAS concentrations: a review. *Environ Health* 2023;22:41. DOI PubMed PMC
24. Nyström J, Benskin JP, Plassmann M, et al. Demographic, life-style and physiological determinants of serum per- and polyfluoroalkyl substance (PFAS) concentrations in a national cross-sectional survey of Swedish adolescents. *Environ Res* 2022;208:112674. DOI PubMed
25. Bartolomé M, Gallego-Picó A, Cutanda F, et al; Bioambient.es. Perfluorinated alkyl substances in Spanish adults: geographical distribution and determinants of exposure. *Sci Total Environ* 2017;603-4:352-60. DOI PubMed
26. Barton KE, Starling AP, Higgins CP, McDonough CA, Calafat AM, Adgate JL. Sociodemographic and behavioral determinants of serum concentrations of per- and polyfluoroalkyl substances in a community highly exposed to aqueous film-forming foam contaminants in drinking water. *Int J Hyg Environ Health* 2020;223:256-66. DOI PubMed PMC
27. Richterová D, Govarts E, Fábelová L, et al. PFAS levels and determinants of variability in exposure in European teenagers - Results from the HBM4EU aligned studies (2014-2021). *Int J Hyg Environ Health* 2023;247:114057. DOI PubMed PMC
28. Pitter G, Da Re F, Canova C, et al. Serum levels of perfluoroalkyl substances (PFAS) in adolescents and young adults exposed to contaminated drinking water in the Veneto Region, Italy: a cross-sectional study based on a health surveillance program. *Environ Health Perspect* 2020;128:27007. DOI PubMed PMC
29. Li Y, Andersson A, Xu Y, et al. Determinants of serum half-lives for linear and branched perfluoroalkyl substances after long-term high exposure - a study in Ronneby, Sweden. *Environ Int* 2022;163:107198. DOI PubMed
30. Cuffney M, Wilkie AA, Kotlarz N, et al. Factors associated with per- and polyfluoroalkyl substances (PFAS) serum concentrations in residents of New Hanover County, North Carolina: the GenX exposure study. *Environ Res* 2023;237:117020. DOI PubMed PMC
31. Fábelová L, Beneito A, Casas M, et al. PFAS levels and exposure determinants in sensitive population groups. *Chemosphere* 2023;313:137530. DOI PubMed PMC
32. Tsai MS, Miyashita C, Araki A, et al. Determinants and temporal trends of perfluoroalkyl substances in pregnant women: the Hokkaido study on environment and children's health. *Int J Environ Res Public Health* 2018;15:989. DOI PubMed PMC
33. Tian Y, Zhou Y, Miao M, et al. Determinants of plasma concentrations of perfluoroalkyl and polyfluoroalkyl substances in pregnant women from a birth cohort in Shanghai, China. *Environ Int* 2018;119:165-73. DOI PubMed

34. Huo X, Liang W, Tang W, et al; Shanghai Birth Cohort Study. Dietary and maternal sociodemographic determinants of perfluoroalkyl and polyfluoroalkyl substance levels in pregnant women. *Chemosphere* 2023;332:138863. DOI PubMed
35. Mahfouz M, Harmouche-Karaki M, Matta J, et al. Maternal serum, cord and human milk levels of per- and polyfluoroalkyl substances (PFAS), association with predictors and effect on newborn anthropometry. *Toxics* 2023;11:455. DOI PubMed PMC
36. Sørensen MM, Fisker AB, Dalgård C, et al. Predictors of serum- per- and polyfluoroalkyl substance (PFAS) concentrations among infants in Guinea-Bissau, West Africa. *Environ Res* 2023;228:115784. DOI PubMed
37. Manzano-Salgado CB, Casas M, Lopez-Espinosa MJ, et al. Variability of perfluoroalkyl substance concentrations in pregnant women by socio-demographic and dietary factors in a Spanish birth cohort. *Environ Int* 2016;92-3:357-65. DOI PubMed
38. Jain RB, Ducatman A. Factors affecting serum PFAS concentrations among US females with surgically and naturally induced menopause: data from NHANES 2003-2018. *Environ Sci Pollut Res Int* 2023;30:84705-24. DOI PubMed
39. Obeng-Gyasi E. Factors associated with elevated per- and polyfluoroalkyl substances serum levels in older adults. *Aging Health Res* 2022;2:100086. DOI PubMed PMC
40. Graber JM, Black TM, Shah NN, et al. Prevalence and predictors of per- and polyfluoroalkyl substances (PFAS) serum levels among members of a suburban US volunteer fire department. *Int J Environ Res Public Health* 2021;18:3730. DOI PubMed PMC
41. Chiu WA, Lynch MT, Lay CR, et al. Bayesian estimation of human population toxicokinetics of PFOA, PFOS, PFHxS, and PFNA from studies of contaminated drinking water. *Environ Health Perspect* 2022;130:127001. DOI PubMed PMC
42. Seshasayee SM, Rifas-Shiman SL, Chavarro JE, et al. Dietary patterns and PFAS plasma concentrations in childhood: project Viva, USA. *Environ Int* 2021;151:106415. DOI PubMed PMC
43. CDC. National health and nutrition examination survey: analytic guidelines, 1999-2010. Available from: https://www.cdc.gov/nchs/data/series/sr_02/sr02_161.pdf. [Last accessed on 29 May 2024].
44. Calafat AM, Wong LY, Kuklenyik Z, Reidy JA, Needham LL. Polyfluoroalkyl chemicals in the U.S. population: data from the National Health and Nutrition Examination Survey (NHANES) 2003-2004 and comparisons with NHANES 1999-2000. *Environ Health Perspect* 2007;115:1596-602. DOI PubMed PMC
45. Kato K, Wong LY, Jia LT, Kuklenyik Z, Calafat AM. Trends in exposure to polyfluoroalkyl chemicals in the U.S. population: 1999-2008. *Environ Sci Technol* 2011;45:8037-45. DOI PubMed
46. Hornung RW, Reed LD. Estimation of average concentration in the presence of nondetectable values. *Appl Occup Environ Hyg* 1990;5:46-51. DOI
47. National Academies of Sciences, Engineering, and Medicine; Health and Medicine Division; Division on Earth and Life Studies; Board on Population Health and Public Health Practice; Board on Environmental Studies and Toxicology; Committee on the Guidance on PFAS Testing and Health Outcomes. Guidance on PFAS exposure, testing, and clinical follow-up. 2022. DOI PubMed
48. Analytic and reporting guidelines: the national health and nutrition examination survey (NHANES). 2005. Available from: https://wwwn.cdc.gov/nchs/data/nhanes/analyticguidelines/05-06-analytic-guidelines.pdf. [Last accessed on 29 May 2024].
49. Zhao Y, Jin H, Qu J, et al. The influences of perfluoroalkyl substances on the rheumatoid arthritis clinic. *BMC Immunol* 2022;23:10. DOI PubMed PMC
50. von Holst H, Nayak P, Dembek Z, et al. Perfluoroalkyl substances exposure and immunity, allergic response, infection, and asthma in children: review of epidemiologic studies. *Heliyon* 2021;7:e08160. DOI PubMed PMC
51. Stanifer JW, Stapleton HM, Souma T, Wittmer A, Zhao X, Boulware LE. Perfluorinated chemicals as emerging environmental threats to kidney health: a scoping review. *Clin J Am Soc Nephrol* 2018;13:1479-92. DOI PubMed PMC
52. Meneguzzi A, Fava C, Castelli M, Minuz P. Exposure to perfluoroalkyl chemicals and cardiovascular disease: experimental and epidemiological evidence. *Front Endocrinol* 2021;12:706352. DOI PubMed PMC
53. Kim MJ, Moon S, Oh BC, et al. Association between perfluoroalkyl substances exposure and thyroid function in adults: a meta-analysis. *PLoS One* 2018;13:e0197244. DOI PubMed PMC
54. Gui SY, Qiao JC, Xu KX, et al. Association between per- and polyfluoroalkyl substances exposure and risk of diabetes: a systematic review and meta-analysis. *J Expo Sci Environ Epidemiol* 2023;33:40-55. DOI PubMed
55. Fenton SE, Ducatman A, Boobis A, et al. Per- and polyfluoroalkyl substance toxicity and human health review: current state of knowledge and strategies for informing future research. *Environ Toxicol Chem* 2021;40:606-30. DOI PubMed PMC
56. Kuhn M, Johnson K. Handling missing data. In: Feature engineering and selection: a practical approach for predictive models. Chapman and Hall; 2019. DOI
57. Emmanuel T, Maupong T, Mpoeleng D, Semong T, Mphago B, Tabona O. A survey on missing data in machine learning. *J Big Data* 2021;8:140. DOI PubMed PMC
58. HotDeckImputation-package: hot deck imputation methods for missing data. Available from: https://www.rdocumentation.org/packages/HotDeckImputation/versions/1.1.0/topics/HotDeckImputation-package. [Last accessed on 29 May 2024].
59. Andridge RR, Little RJ. A review of hot deck imputation for survey non-response. *Int Stat Rev* 2010;78:40-64. DOI PubMed PMC
60. Kowarik A, Templ M. Imputation with the R Package VIM. *J Stat Soft* 2016;74:1-16. DOI
61. van Buuren S, Groothuis-Oudshoorn K. mice: multivariate imputation by chained equations in R. *J Stat Soft* 2011;45:1-67. DOI
62. Zou H, Hastie T. Regularization and variable selection via the elastic net. *J R Stat Soc B* 2005;67:301-20. DOI
63. USEPA. EPA and 3M announce phase out of pfos. 2000. Available from: https://www.epa.gov/archive/epapages/newsroom_archive/newsreleases/33aa946e6cb11f35852568e1005246b4.html. [Last accessed on 29 May 2024].
64. USEPA. PFOA stewardship program baseline year summary report. Available from: https://www.epa.gov/assessing-and-managing-

chemicals-under-tsca/pfoa-stewardship-program-baseline-year-summary-report. [Last accessed on 29 May 2024].
65. Toms LM, Thompson J, Rotander A, et al. Decline in perfluorooctane sulfonate and perfluorooctanoate serum concentrations in an Australian population from 2002 to 2011. *Environ Int* 2014;71:74-80. DOI PubMed PMC
66. Hurley S, Goldberg D, Wang M, et al. Time trends in per- and polyfluoroalkyl substances (PFASs) in California women: declining serum levels, 2011-2015. *Environ Sci Technol* 2018;52:277-87. DOI PubMed
67. Salvalaglio M, Muscionico I, Cavallotti C. Determination of energies and sites of binding of PFOA and PFOS to human serum albumin. *J Phys Chem B* 2010;114:14860-74. DOI PubMed
68. Weaving G, Batstone GF, Jones RG. Age and sex variation in serum albumin concentration: an observational study. *Ann Clin Biochem* 2016;53:106-11. DOI PubMed
69. Denic A, Glassock RJ, Rule AD. Structural and functional changes with the aging kidney. *Adv Chronic Kidney Dis* 2016;23:19-28. DOI PubMed PMC
70. Milanović Z, Pantelić S, Trajković N, Sporiš G, Kostić R, James N. Age-related decrease in physical activity and functional fitness among elderly men and women. *Clin Interv Aging* 2013;8:549-56. DOI PubMed PMC
71. Musso CG, Oreopoulos DG. Aging and physiological changes of the kidneys including changes in glomerular filtration rate. *Nephron Physiol* 2011;119 Suppl 1:p1-5. DOI PubMed
72. Verner MA, Loccisano AE, Morken NH, et al. Associations of perfluoroalkyl substances (PFAS) with lower birth weight: an evaluation of potential confounding by glomerular filtration rate using a physiologically based pharmacokinetic model (PBPK). *Environ Health Perspect* 2015;123:1317-24. DOI PubMed PMC
73. Rickard BP, Rizvi I, Fenton SE. Per- and poly-fluoroalkyl substances (PFAS) and female reproductive outcomes: PFAS elimination, endocrine-mediated effects, and disease. *Toxicology* 2022;465:153031. DOI PubMed PMC
74. Salihovic S, Kärrman A, Lind L, Lind PM, Lindström G, van Bavel B. Perfluoroalkyl substances (PFAS) including structural PFOS isomers in plasma from elderly men and women from Sweden: results from the prospective investigation of the vasculature in Uppsala seniors (PIVUS). *Environ Int* 2015;82:21-7. DOI PubMed
75. Muennig P, Song X, Payne-Sturges DC, Gee GC. Blood and urine levels of long half-life toxicants by nativity among immigrants to the United States. *Sci Total Environ* 2011;412-3:109-13. DOI PubMed
76. Fiedler H, Sadia M. Regional occurrence of perfluoroalkane substances in human milk for the global monitoring plan under the Stockholm Convention on Persistent Organic Pollutants during 2016-2019. *Chemosphere* 2021;277:130287. DOI PubMed
77. Rahman MA. Household characteristics and poverty: a logistic regression analysis. *J Develop Areas* 2013;47:303-17. Available from: http://www.jstor.org/stable/23612271. [Last accessed on 29 May 2024]
78. Cariou R, Veyrand B, Yamada A, et al. Perfluoroalkyl acid (PFAA) levels and profiles in breast milk, maternal and cord serum of French women and their newborns. *Environ Int* 2015;84:71-81. DOI PubMed
79. Lorber M, Eaglesham GE, Hobson P, Toms LM, Mueller JF, Thompson JS. The effect of ongoing blood loss on human serum concentrations of perfluorinated acids. *Chemosphere* 2015;118:170-7. DOI PubMed
80. Manzano-Salgado CB, Casas M, Lopez-Espinosa MJ, et al. Transfer of perfluoroalkyl substances from mother to fetus in a Spanish birth cohort. *Environ Res* 2015;142:471-8. DOI PubMed
81. Mondal D, Weldon RH, Armstrong BG, et al. Breastfeeding: a potential excretion route for mothers and implications for infant exposure to perfluoroalkyl acids. *Environ Health Perspect* 2014;122:187-92. DOI PubMed PMC
82. Fromme H, Tittlemier SA, Völkel W, Wilhelm M, Twardella D. Perfluorinated compounds - exposure assessment for the general population in Western countries. *Int J Hyg Environ Health* 2009;212:239-70. DOI PubMed
83. Li Y, Fletcher T, Mucs D, et al. Half-lives of PFOS, PFHxS and PFOA after end of exposure to contaminated drinking water. *Occup Environ Med* 2018;75:46-51. DOI PubMed PMC
84. CDC. Fourth national report on human exposure to environmental chemicals: updated tables, January 2019, volume one. 2019. DOI
85. Jain RB. Contribution of diet and other factors to the levels of selected polyfluorinated compounds: data from NHANES 2003-2008. *Int J Hyg Environ Health* 2014;217:52-61. DOI PubMed
86. Nelson JW, Scammell MK, Hatch EE, Webster TF. Social disparities in exposures to bisphenol A and polyfluoroalkyl chemicals: a cross-sectional study within NHANES 2003-2006. *Environ Health* 2012;11:10. DOI PubMed PMC
87. Liddie JM, Schaider LA, Sunderland EM. Sociodemographic factors are associated with the abundance of PFAS sources and detection in U.S. community water systems. *Environ Sci Technol* 2023;57:7902-12. DOI PubMed PMC
88. Vieux F, Maillot M, Rehm CD, Barrios P, Drewnowski A. Trends in tap and bottled water consumption among children and adults in the United States: analyses of NHANES 2011-16 data. *Nutr J* 2020;19:10. DOI PubMed PMC
89. Gorelick MH, Gould L, Nimmer M, et al. Perceptions about water and increased use of bottled water in minority children. *Arch Pediatr Adolesc Med* 2011;165:928-32. DOI PubMed
90. Rosinger AY, Herrick KA, Wutich AY, Yoder JS, Ogden CL. Disparities in plain, tap and bottled water consumption among US adults: national health and nutrition examination survey (NHANES) 2007-2014. *Public Health Nutr* 2018;21:1455-64. DOI PubMed PMC
91. Park S, Onufrak S, Patel A, Sharkey JR, Blanck HM. Perceptions of drinking water safety and their associations with plain water intake among US Hispanic adults. *J Water Health* 2019;17:587-96. DOI PubMed PMC
92. Consumer Reports. What's really in your bottled water? 2020. Available from: https://www.consumerreports.org/water-quality/whats-really-in-your-bottled-water-a5361150329/. [Last accessed on 29 May 2024].

93. Chow SJ, Ojeda N, Jacangelo JG, Schwab KJ. Detection of ultrashort-chain and other per- and polyfluoroalkyl substances (PFAS) in U.S. bottled water. *Water Res* 2021;201:117292. DOI PubMed
94. Krachler M, Shotyk W. Trace and ultratrace metals in bottled waters: survey of sources worldwide and comparison with refillable metal bottles. *Sci Total Environ* 2009;407:1089-96. DOI PubMed
95. Stoiber T, Evans S, Temkin AM, Andrews DQ, Naidenko OV. PFAS in drinking water: an emergent water quality threat. 2020. Available from: https://www.ewg.org/sites/default/files/u352/Stoiber_Evans_WaterSolutions_2020.pdf. [Last accessed on 29 May 2024].
96. Augustsson A, Lennqvist T, Osbeck CMG, et al. Consumption of freshwater fish: a variable but significant risk factor for PFOS exposure. *Environ Res* 2021;192:110284. DOI PubMed
97. Barbo N, Stoiber T, Naidenko OV, Andrews DQ. Locally caught freshwater fish across the United States are likely a significant source of exposure to PFOS and other perfluorinated compounds. *Environ Res* 2023;220:115165. DOI PubMed
98. von Stackelberg K, Li M, Sunderland E. Results of a national survey of high-frequency fish consumers in the United States. *Environ Res* 2017;158:126-36. DOI PubMed
99. Wattigney WA, Savadatti SS, Liu M, et al. Biomonitoring of per- and polyfluoroalkyl substances in minority angler communities in central New York State. *Environ Res* 2022;204:112309. DOI PubMed PMC
100. Christensen KY, Raymond M, Blackowicz M, et al. Perfluoroalkyl substances and fish consumption. *Environ Res* 2017;154:145-51. DOI PubMed
101. Haug LS, Thomsen C, Brantsaeter AL, et al. Diet and particularly seafood are major sources of perfluorinated compounds in humans. *Environ Int* 2010;36:772-8. DOI PubMed
102. Lee JH, Lee CK, Suh CH, Kang HS, Hong CP, Choi SN. Serum concentrations of per- and poly-fluoroalkyl substances and factors associated with exposure in the general adult population in South Korea. *Int J Hyg Environ Health* 2017;220:1046-54. DOI PubMed
103. Lindh CH, Rylander L, Toft G, et al. Blood serum concentrations of perfluorinated compounds in men from Greenlandic Inuit and European populations. *Chemosphere* 2012;88:1269-75. DOI PubMed
104. Liu Y, Su J, van Dam RM, et al. Dietary predictors and plasma concentrations of perfluorinated alkyl acids in a Singapore population. *Chemosphere* 2017;171:617-24. DOI PubMed
105. Yamaguchi M, Arisawa K, Uemura H, et al. Consumption of seafood, serum liver enzymes, and blood levels of PFOS and PFOA in the Japanese population. *J Occup Health* 2013;55:184-94. DOI PubMed
106. Beesoon S, Genuis SJ, Benskin JP, Martin JW. Exceptionally high serum concentrations of perfluorohexanesulfonate in a Canadian family are linked to home carpet treatment applications. *Environ Sci Technol* 2012;46:12960-7. DOI PubMed
107. Martin JW, Asher BJ, Beesoon S, Benskin JP, Ross MS. PFOS or PreFOS? Are perfluorooctane sulfonate precursors (PreFOS) important determinants of human and environmental perfluorooctane sulfonate (PFOS) exposure? *J Environ Monit* 2010;12:1979-2004. DOI PubMed
108. Strynar MJ, Lindstrom AB. Perfluorinated compounds in house dust from Ohio and North Carolina, USA. *Environ Sci Technol* 2008;42:3751-6. DOI PubMed
109. Jian JM, Chen D, Han FJ, et al. A short review on human exposure to and tissue distribution of per- and polyfluoroalkyl substances (PFASs). *Sci Total Environ* 2018;636:1058-69. DOI PubMed
110. Cuffney M, Wilkie A, Kotlarz N, et al. Factors associated with per-and polyfluoroalkyl substances (PFAS) serum concentrations in residents of Wilmington, North Carolina: the genx exposure study. *SSRN* 2023. DOI
111. Colles A, Bruckers L, Den Hond E, et al. Perfluorinated substances in the Flemish population (Belgium): levels and determinants of variability in exposure. *Chemosphere* 2020;242:125250. DOI PubMed
112. Raudhatunnisa T, Wilantika N. Performance comparison of hot-deck imputation, K-nearest neighbor imputation, and predictive mean matching in missing value handling, case study: March 2019 SUSENAS Kor dataset. *icdsos* 2022;2021:753-70. DOI
113. Olsen GW, Burris JM, Ehresman DJ, et al. Half-life of serum elimination of perfluorooctanesulfonate,perfluorohexanesulfonate, and perfluorooctanoate in retired fluorochemical production workers. *Environ Health Perspect* 2007;115:1298-305. DOI PubMed PMC

Haave *et al. Water Emerg Contam Nanoplastics* 2024;3:16
DOI: 10.20517/wecn.2024.07

Water Emerging Contaminants & Nanoplastics

Research Article

Open Access

Absence of microplastic bioaccumulation in cod fillets from plastic-polluted western Norwegian waters

Marte Haave[1,2,3], **Emilie Hæggernes**[2], **Alessio Gomiero**[1]

[1]Department of Climate & Environment, NORCE Norwegian Research Centre, Bergen N-5008, Norway.
[2]Department of Chemistry, University of Bergen, Bergen N-5007, Norway.
[3]SALT Lofoten AS, Svolvær 8301, Norway.

Correspondence to: Dr. Marte Haave, Department of Climate & Environment, NORCE Norwegian Research Centre, Nygårdsgt. 112, Bergen N-5008, Norway. E-mail: marte.haave@salt.nu

How to cite this article: Haave M, Hæggernes E, Gomiero A. Absence of microplastic bioaccumulation in cod fillets from plastic-polluted western Norwegian waters. *Water Emerg Contam Nanoplastics* 2024;3:16. https://dx.doi.org/10.20517/wecn.2024.07

Received: 12 Mar 2024 **First Decision:** 29 May 2024 **Revised:** 15 Jun 2024 **Accepted:** 21 Jun 2024 **Published:** 27 Jun 2024

Academic Editor: Joana C Prata **Copy Editor:** Dong-Li Li **Production Editor:** Dong-Li Li

Abstract

Plastics are synthetic, persistent materials that are distributed worldwide. An important concern is whether microplastics (MP) can bioaccumulate in the food chain and pose a threat to human consumers. We studied MP in the fillet of resident coastal cod from a plastic-polluted area in Western Norway, where long-range transported marine litter accumulates and MP are generated on shore. We dissected the fish and processed the samples in an MP-free lab using gentle enzymatic treatment. Micro Fourier transform infrared spectroscopy (μFTIR) was used for identification of particles down to 10 μm. The fish were 40 to 74 cm, corresponding to 2-6 years old. 29 particles were observed in fillets from eight of the 23 individuals. The mean particle count was 1.55 ± 2.75 nMP/100 g, and the mean concentration was 2.81 ± 8.33 μg/kg wet weight. Six polymer groups were identified, where polypropylene (33%) and polyethylene (30%) were the most frequent. The majority (86%) of the particles were fragments ranging from 32-100 μm. Fibers and fragments over 200 μm were observed. The largest particle was a PP particle of 258.2 μm. Controls showed minimal contamination and the procedural blanks were negative. There was no significant correlation between age, body condition, time of capture, and MP concentrations, and no evidence of bioaccumulation of MP in the fillet of older fish after *in situ* exposure. MP in food is of concern for human consumption and emphasizes the importance of understanding MP distribution and fate as well as reducing and controlling plastic release into the environment.

Keywords: Microplastics, bioaccumulation, fish fillet, plastic pollution

INTRODUCTION

Human history has proven that man-made contaminants that are resistant to degradation are distributed far from their source of origin. These substances are often referred to as persistent organic pollutants (POPs). The last decade has documented that microplastics (MP) possess the same traits and have been detected in various environmental samples worldwide, testifying to a global distribution of synthetic polymer particles far from human activities[1-7]. Over the past decade, there has been extensive documentation of MP ingestion by marine organisms[8]. MP have been detected in the muscle and liver of fish and birds, as well as in human blood, placenta, and testes[9-14].

Studies have also provided experimental evidence of micro- and nanoplastic uptake and translocation in animals and humans[12,15-18]. This evidence of omnipresence and uptake into internal organs underscores the need to understand and describe MP kinetics and fate using traditional toxicological terms, such as understanding the routes of exposure and the movement and fate of MP in the food web. We need to understand the fate of MP in organisms and the food web to determine whether they share another common trait of POPs, the ability to bioaccumulate and biomagnify. Bioaccumulation refers to when a substance reaches significantly higher concentrations in an organism compared to its surroundings. Bioaccumulation often leads to biomagnification, which means organisms at higher trophic levels have higher concentrations of the substance due to their inability to excrete or metabolize it. This is of interest to human consumers, since we eat a wide range of foods from different trophic levels and live long lives.

Early experiments on mammals and birds in 1975 showed that MP can be absorbed through the intestines and distributed to different organs and body fluids within minutes of ingestion[16]. This was shown by the absorption of polyvinyl chloride (PVC) particles with an average size of 40 μm (ranging from 10 to 110 μm) in rats, mice, guinea pigs, rabbits, chickens, and dogs. Minutes after exposure, MP were found in the bile, and within the following 24 h, they were excreted via urine, lungs, milk, and placenta, indicating distribution throughout various organs[16]. Later experiments revealed that nanoplastic particles (< 1 μm) reached the brains of fish[15,19-21]. A recent study observed the uptake, distribution, and excretion of palladium-enriched polystyrene nanoparticles in fish and found that they were distributed throughout the body but were also excreted to levels below the detection limit after 48 h of exposure[22]. Similarly, the uptake, distribution, and elimination of ^{14}C-radiolabeled nano polystyrene were demonstrated in clams over a 24-day period, with larger particles (250 nm) still detectable after 48 days, indicating that particle size affects the kinetics[18]. Overall, these studies demonstrate the transfer of micro- and nanoplastics into tissues through barriers such as the intestinal wall and the blood-brain barrier. They also suggest that multiple body fluids and tissues may be affected by the ingestion or inhalation of MP. Furthermore, these findings indicate that micro- and nanoplastic particles may be present in many organs shortly after exposure, although their presence in tissues may be transient. Nonetheless, MP can have permanent deleterious effects, emphasizing the importance of studying chronic exposure to relevant concentrations and compositions of micro- and nanoplastic particles[22,23]. Understanding chronic exposure to relevant levels is thus of importance for understanding the consequences of MP pollution throughout the food web as well as in humans.

Food consumption is one of the most extensively studied routes of MP exposure in humans[24]. Previous studies have demonstrated the presence of MP in edible parts of fish[10,25,26], as well as exposure through seafood that may have become contaminated by plastics during processing, packaging, handling, and cooking[27-31]. The numerous potential sources of MP, differences in sampling methods, dissection techniques, analytical procedures and identification make comparisons between studies, species, and regions challenging[32] and make it hard to differentiate between the effects of trophic level or age and to be able to discern the effects of method uncertainties[33]. When evaluating the evidence for bioaccumulation and the fate of MP in the food web, it is essential to eliminate contamination from sources of MP other than ingestion and trophic transfer, and it is vital to acknowledge limitations and uncertainties related to contamination[34].

This study aimed to elucidate the evidence for bioaccumulation in tissues of naturally exposed wild cod of various sizes and ages, strictly considering the MP that had translocated into tissues from direct or indirect uptake and ingestion of food and water or across respiratory epithelia, using methods sensitive enough to detect a single particle of MP. A high-tech plastic-free laboratory with a strong emphasis on contamination control was used to prevent external contamination. This approach gives the best possibility to investigate and differentiate between MP concentrations in individuals of different ages, and thus investigate the evidence of *in situ* bioaccumulation.

EXPERIMENTAL

The study was conducted using wild-caught cod from a highly plastic-polluted area located in the outer coastal region of southwestern Norway[35] [Figure 1]. The Norwegian Coastal current flows northward along the coastline, carrying marine litter from the North Sea, southern Europe, and even across the Atlantic on the Gulf Stream, as well as locally produced litter. Due to predominantly southwestern winds, floating items are pushed toward the shoreline, where geological formations with numerous islands and inlets act as a physical trap[35,36]. Within this plastic-polluted habitat, the coastal strain of the Atlantic cod (*Gadus morhua*) can be found. The coastal cod was selected for this study because it is a resident, non-migratory species living within a limited area[37,38]. It is a generalist feeder, consuming a wide range of species[39], which makes cod an ideal subject for investigating the uptake and potential bioaccumulation of MP from the environment. A recent study has documented frequent ingestion of plastics in cod from this region[40], and a pilot study identified measurable levels of MP in the muscle and liver of cod from this area[10]. The current study further expanded the sample size to examine the relationship between size (age), body condition, and microplastic concentration in cod. Additionally, updated methods were able to detect small microplastic particles and a plastic-free laboratory was employed to validate the previously observed concentrations of MP in cod from this plastic-polluted region.

Volunteers from the Norwegian Hunters and Anglers' Association captured cod at two locations during two periods between May 7, 2021, and November 2, 2021 [Figure 1 and Table 1]. The two locations were Vindkjeften (4,9771509°E; 60,3322916°N) and Nordre Hola (4,9547007°E; 60,2954264°N).

Only resident cod, which can be distinguished by their size and color, were collected for this study, and the migrant strain of the Atlantic cod was not present in these waters during the sampling period. The resident cod lives its whole life in the same region, and we therefore assume that it is has been exposed to plastics in water and food throughout its lifetime.

According to Norwegian regulations, fish below the minimum size of 40 cm were released back into the water, and thus, the youngest age groups are not represented. The fish collected from the sites were captured using fishing nets or fishing rods. The fish were euthanized by a blow to the head to avoid cutting the skin and potentially contaminating the tissue, wrapped in aluminum foil, and subsequently frozen at -20 °C until further dissection and chemical analysis at NORCE PlastLab.

Contamination control

Given the expected low microplastic concentration in tissues, controlling and recording any external contamination is crucial[41]. All samples were, therefore, processed inside the NORCE PlastLab.

Table 1. Characteristics of cod from two locations in western Norway (Nordre Hola and Vindkjeften), with bodyweight (g), length (cm) and Fulton's condition factor (k-factor), sample weight (g), number of MP by particle shape, MP count (nMP/100 g·ww) and calculated MP mass-concentration (μg/kg·ww)

Fish ID	Capture date	Weight	Length	k-factor	Sample weight	n-fibers/n-fragments	MP count	MP conc.
Location Nordre Hola								
#1	07.05.21	855	43	1.08	71.41	1/1	2.80	2.8
#2*	19.05.21	859	43	1.08	42.13	nd/nd	-	-
#3*	19.05.21	637	40	1.00	69.20	nd/nd	-	-
#4	25.05.21	698	40	1.09	67.96	3/4	10.30	38.9
#5*	30.05.21	863	42	1.17	83.53	nd/nd	-	-
#6	30.05.21	550	42	0.74	72.89	nd/nd	-	-
#7	30.05.21	570	44	0.67	85.02	nd/nd	-	-
#8	07.06.21	400	44	1.02	94.34	nd/nd	-	-
#9	27.10.21	708	42	0.96	78.46	3/nd	3.82	1.3
#10	27.10.21	1,334	44	1.57	91.23	nd/1	1.10	0.8
Location Vindkjeften								
#11	02.11.21	2,299	67	0.76	103.43	nd/4	3.87	11.4
#12	02.11.21	1,285	51	0.97	95.21	nd/nd	-	-
#13	02.11.21	2,059	58	1.06	108.59	nd/nd	-	-
#14	02.11.21	1,855	55	1.11	91.30	nd/nd	-	-
#15	02.11.21	4,639	73	1.19	152.78	nd/nd	-	-
#16	02.11.21	2,229	59	1.09	95.20	nd/nd	-	-
#17	02.11.21	1,459	53	0.98	97.90	nd/4	4.09	1.8
#18	02.11.21	1,823	54	1.16	108.13	nd/1	0.92	0.7
#19	02.11.21	2,023	56	1.15	107.64	nd/nd	-	-
#20	02.11.21	1,959	55	1.18	106.06	nd/nd	-	-
#21	02.11.21	1,356	51	1.02	103.47	nd/nd	-	-
#22	02.11.21	1,796	56	1.02	115.50	nd/5	4.33	7.1
#23	02.11.21	1,770	55	1.06	110.21	nd/nd	-	-
Mean ± SD	-	1,479.45 ± 917.52	50.3 ± 9.42	1.05 ± 0.18	93.50 ± 21.82	Sum: 10/26	1.89 ± 3.10	1.55 ± 2.75

*interference from the presence of protein in the analyses was observed, but samples met the QA/QC requirements of the laboratory. MP: Microplastic; nd: not detected; SD: standard deviation; QA/QC: quality assurance/quality control.

Contamination control, quality assurance/quality control (QA/QC) measures were implemented to minimize and account for any potential sources of microplastic contamination. The laboratory is specially designed to have plastic-free surfaces, including glass, steel, and non-plastic benches and floors. The Plastlab has high-efficiency ultra-low penetration HEPA-14H filtration with an efficiency > 99% for the most penetrating particle size (0.1-0.5 μm). Additional precautions, such as sticky floor mats and an air sluice, were in place to prevent dust from entering. Lab personnel wore clothing made of natural materials like cotton or wool. Glassware, steel filters, and other materials were covered in aluminum foil and burned in a muffle oven at 500 °C before use to remove any traces of MP. Steel filters, glass, and porcelain equipment were used for all procedures, with the only exceptions being silicon tubes, polytetrafluoroethylene (PTFE-Teflon) squeezy bottles, and computers.

Before and after fish dissection or sample preparation, surfaces were rinsed with Milli-Q water that was filtered once more over a Whatman GF/A- filter (1.6 μm) and wiped with tissue paper. Stainless steel filters, tweezers, and other equipment used were rinsed three times and sterilized using a gas burner (FLAMEBOY™, 1,350 °C) between samples. Scalpel blades were changed between samples.

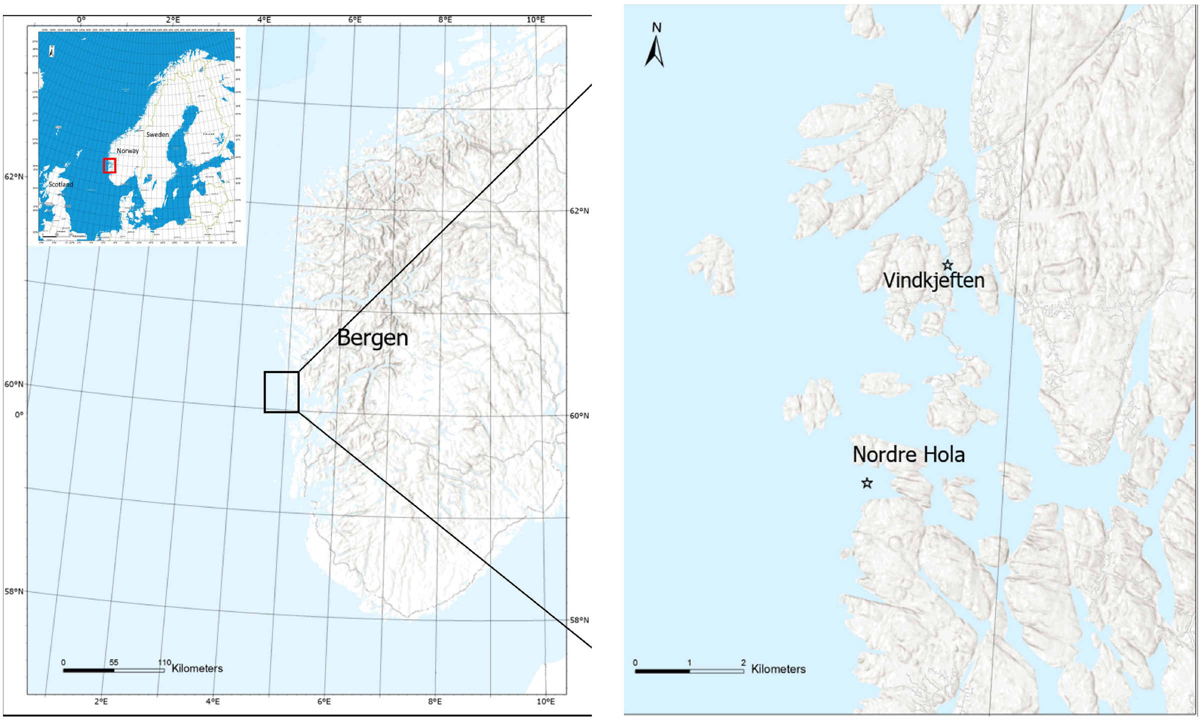

Figure 1. Sampling locations in Western Norway where cod was caught in the spring/summer and autumn of 2021.

To monitor and control for background contamination, open wet traps containing only Milli-Q water were used during the same period as the lab activities. One wet trap was deployed per sample dissection. When microplastic particles were identified in a tissue sample, the corresponding wet trap used during the processing of that sample was also analyzed. In case a plastic particle was detected in the wet trap, particles of the same polymer type were subtracted from the tissue sample results [Supplementary Table 1].

To prevent contamination from the solutions used during the procedure[41], all solutions used were pre-filtered using a glass fiber filter (Whatman GF/A, 1.6 µm) and stored in pre-burnt glass containers until use. Procedural blanks, which used the same solutions and equipment as for sample processing without any sample, were processed simultaneously with the samples.

All 23 fish were measured and weighed during dissection. Body length was measured from the snout to the tip of the tail (caudal length). Based on previously published growth rate curves for resident cod, the age of the cod in this study was estimated to be around two to six years old[37]. As the age of each fish is estimated based on their length, the length is used as a proxy for age. The estimated age of each fish is therefore not given.

Approximately 100 grams from the upper fillet, taken from the region behind the dorsal fin, were used for analysis. The samples were weighed, packed in a double layer of aluminum foil, and frozen at -20 °C until further processing and chemical analysis.

Purification and removal of organic content

To remove the tissue and leave the microplastic particles intact, a gentle enzymatic degradation was performed. The multi-enzymatic extraction protocol for microplastic particles is based on previously published methods[10,42-46]. The method has a recovery rate of 96%-99% and does not damage the plastic polymer[47].

In summary, the purification procedure involved the systematic removal of the muscle tissue, proteins, and fats through a stepwise process outlined in Figure 2. All incubations were done without agitation in a Termaks TS-4115 heating cabinet.

In detail, the cod muscle tissue (up to ~100 grams) was defrosted, cut into cubes, and placed in the sample beaker. First, to permeate cell membranes, 100 mL 5% sodium dodecyl sulphate (SDS) solution was added, and the sample was incubated at 50 °C for a minimum of 3 h [Figure 2].

After incubation in SDS, all the sample was transferred to a vacuum filtration assembly and passed through a 10 μm stainless steel filter. The sample container and filtration system funnel were rinsed with 50% ethanol from a PTFE squeezy bottle. The filter and sample were placed back into the same beaker to prevent loss of material, and 100 mL of 0.1 M glycine buffer at pH 10.0 was added. Ultrasonication was performed on the sample beaker for 10 minutes to release any particles attached to the filter before the filter was rinsed with 1 mL of Milli-Q water. In the second enzyme treatment, 1 mL of protease enzyme (P3111, Sigma Aldrich, Germany) was added, and the beaker was incubated at 50 °C for 48 h before repeating the filtration and ultrasonication steps. The third treatment used 100 mL phosphate buffer saline and 1 mL of lipase enzyme (L0777, Sigma Aldrich, Germany), incubated at pH 5.0 and 50 °C for 24 h.

For the final purification step, a strong oxidative digestion was performed using 50 mL of 30% hydrogen peroxide (H_2O_2) at 50 °C for 12 h to remove fats. The sample was now reduced to a clear liquid [Figure 2]. The sample was filtered to remove the oxidizing agent, sonicated to release any particles from the filter, and rinsed thoroughly with 50% ethanol. The sample was transferred to a tube and the ethanol was evaporated at 50 °C until 1 mL remained. The sample in the tube was transferred to a glass vial for storage, and the tube was washed with 4 × 1 mL of 50% ethanol to transfer all particles, resulting in a total volume of 5 mL in the sample vial. A list of enzymes and buffers can be found in Supplementary Tables 2 and 3.

Prior to identification of the remaining particles, the contents were filtered onto a 0.1 μm Anodisc filter (Whatman, Φ 10 mm) and dried at room temperature in a glass petri dish in the clean PlastLab with a lid until further examination.

Micro Fourier transform infrared spectroscopy identification of microplastics

Identification of polymer types and measurement of particle sizes were automatically performed using micro Fourier transform infrared spectroscopy (μFTIR) with a Thermo Fisher Nicolet iN10 MX Infrared Imaging Microscope. The instrument was equipped with a N_2-cooled 64 × 64 line array mapping detector and a quantum MCT (mercury cadmium telluride) detector. The linear array detector collected 64 scans per sample, and the IR spectra of each microplastic particle were recorded in the mid-IR range of 4,000-850 cm^{-1}, with a spectral resolution of 4 cm^{-1} in transmission mode. The linear array mapping covers the whole Anodisc filter, identifying and measuring the size of every particle on the filter. Currently, the nitrogen-cooled scanning μFTIR- method used in this study is capable of detecting particles down to a theoretical minimum of 6.25 μm according to the technical specifications by Thermo Fisher. As the steel filter mesh used for the pre-treatment is a minimum of 10 μm, we do not regard the method to be quantitative for particles under 10 μm, but smaller particles may stick to the mesh and may be retained nonetheless.

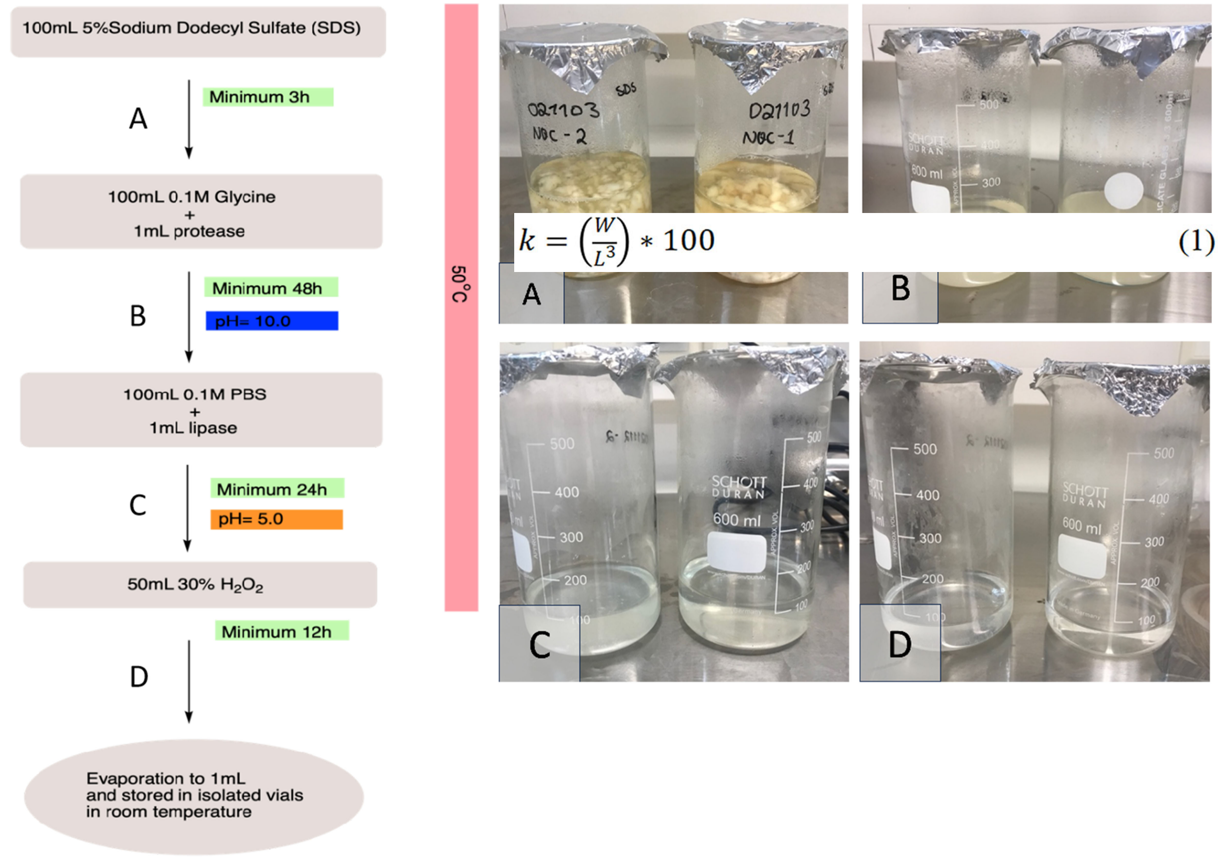

$$k = \left(\frac{W}{L^3}\right) * 100 \quad (1)$$

Figure 2. Detailed flowchart of the stepwise enzymatic treatment that ensured gentle and complete removal of proteins and fats in the cod muscle tissue. The progress of the treatment can be observed in the following stages: (A) the cod muscle tissue after 12 h in 5% SDS; (B) the same sample after 48 h in protease; (C) after 24 h in lipase; (D) and after 12 h in 30% hydrogen peroxide. SDS: Sodium dodecyl sulphate.

Polymer identification was performed automatically by the software by comparing the spectral match of the particles with a reference library (SiMPle, v1.3.1β)[48]. Polymers with a spectral match greater than 70% score were considered automatically positively identified. A spectral match above 65% would be accepted or rejected after manual inspection of the spectrum. The software used for identification and grouping of polymer types also facilitated automatic mass calculations per particle. The mass per particle was estimated by the software by multiplying the particle volume by the density of the polymer type[48]. The particle volume is automatically calculated by the software from the measured major and minor dimensions (length and width) and an estimate of the height (60% of the minor dimension). Particles on the filter that were not of synthetic origin (cellulose from tissue paper and any remaining proteins) were excluded from the results.

For shape classification of plastic particles, fibers were defined as having a length-to-width ratio above three, while fragments had a length-to-width ratio up to three.

Calculations and reporting

Body condition (k-factor)

The condition of the cod was described using Fulton's condition factor (k), as defined by Equation 1, where W represents the weight in grams and L represents the length in centimeters[49]. A healthy body condition factor, indicating that the fish is feeding and well, is typically around one.

$$k = \left(\frac{W}{L^3}\right) * 100 \quad (1)$$

Microplastic mass concentration

The mass concentration of MP was calculated in micrograms per kilogram wet weight (μg/kg·ww) using the estimated mass per particle obtained from the SiMPle software output, and the wet weight of the sample at the time of dissection (Equation 2).

$$MP\ Concentration = \frac{Particle\ mass\ \ (mg)}{Sample\ weight\ (kg\ ww)} \tag{2}$$

Standardized microplastic particle count

The number of detected MP (nMP) was standardized to 100 grams fillet (Equation 3).

$$\frac{nMP}{100g} = \frac{Sample\ weight\ (g)}{100} * n\ detected\ MP \tag{3}$$

Microplastic particle size classes

The MP were categorized into groups based on their size classes determined by their smallest dimension. The size classes included intervals of 10-30, 31-50, 51-100, 101-500, and 500-1,000 μm. In reporting, the focus is on the minor dimension since the smallest dimension is likely the determining factor for retention on the filter during processing.

Statistics

Data management, statistical analyses and calculations were completed using R, (version 2023.12.0+369), Microsoft Excel and IBM SPSS Statistics (version 26.0). To assess the normality of the data, the Shapiro-Wilk test was employed. The results indicated a non-normal distribution for most of the data. Consequently, non-parametric Mann-Whitney *U*-tests were employed to compare means between groups. Spearman's rho correlation test was conducted to examine the correlation between nMP and body length or k-factor. The statistical significance level was set at $\alpha = 0.05$.

RESULTS AND DISCUSSION

Body condition (k-factor) of fish

The k-factor is often used instead of body weight for fish, as it is a parameter that combines both weight and length and indicates if the fish has been feeding and is healthy, which is of relevance to MP exposure and accumulation from the food web. Length and weight, however, are covariates, and are thus statistically dependent; therefore, examination of the correlation between nMP and one of the two variables, weight and length, suffices. Table 1 provides the weight, length, and k-factor for the cod. Based on growth rate curves for resident cod, the age of the cod in this study was estimated to be around two to six years old[37] . Cod from Nordre Hola (mean length: 41.4 ± 2.95 cm), primarily sampled in May, were significantly shorter compared to the cod from Vindkjeften (mean length: 51.37 ± 14.77 cm), sampled in November (Mann-Whitney *U*-test, $U = 0$, $P < 0.001$), which may in part be explained by higher age and growth during summer and early autumn. The fish from both sites were in generally good body condition, with k-factors ranging from 0.67 to 1.57, and a mean k-factor above 1, indicating that most of the fish were healthy and feeding at both sites and times. There was no significant difference in k-factor between sites (Mann-Whitney *U*-test, $U = 53$, $P = 0.475$).

Frequency of occurrence

Out of the 23 samples of cod muscle tissue, MP particles were detected in 8 cod from Nordre Hola (*n* = 4) and Vindkjeften (*n* = 4), resulting in a frequency of occurrence (FO) of 34.78%. As the FO is greatly influenced by the method of analysis, the mass of each sample, and the sensitivity of the detection method, it is subject to large variations among studies. FO up to 100% has been observed[50]. Comparison to previous studies is challenging due to variations in laboratory procedures and reporting, which highlights the importance of using sensitive, harmonized methods and the same format when reporting, for example, FO and size classes across studies. The current low FO in edible tissues of finfish is lower than the FO reported in other studies examining edible tissues and skin of finfish[10,30,50-54], where the FOs were frequently above 40%. Such previously published studies, using a range of different methods, have reported MP from sizes of approximately 100 to 1,000 μm in up to 100% of the samples. The lowest observed FO of 7%[27] used microscopy for manual selection and identified polymers by attenuated total reflectance FTIR (ATR-FTIR), but this method has limitations in detecting particles under 100 μm. In the current study, 93% of the particles were below 100 μm, which theoretically should increase the FO compared to studies that are limited to detection of larger particles. As analytical techniques become more sensitive and accurate, and if size- limits decrease in future studies, it is thus expected that the FO of MP in tissues may increase.

Characteristics of microplastics in cod muscle tissue

There were no significant differences in particle count or particle sizes of microplastic in cod from the two distinct sampling sites and capture periods. As the fish from the two sites were in the same body condition, all the fish were combined to represent the cod population in the local region.

Table 1 presents the microplastic concentration in two ways: particle count standardized to weight (nMP/100 g) and microplastic mass concentration (μg/kg·ww) for all 23 examined cod. The maximum particle concentration was 10.3 nMP/100 g, which equals 0.1 MP/g·ww muscle tissue (cod #4). This is similar to the observed particle concentrations in farmed salmon (*Salmo salar*) from two Norwegian salmon farms of 0.10 ± 0.09 and 0.11 ± 0.12 MP/g ww and in wild salmon with 0.10 ± 0.04 MP/g ww)[50]. The highest observed concentration in this study is lower than the mean concentration observed in the dorsal muscle of European seabass (*Dicentrachus labrax*), Atlantic Horse mackerel (*Trachurus trachurus*), and Atlantic Chub mackerel (*Scomber colias*) from the North East Atlantic, with 0.4 ± 0.7, 0.7 ± 1.3, and 0.6 ± 0.8 MP items/g, respectively[53]. Moreover, fifteen fish showed no detectable MP in the muscle tissue, contributing to a low mean concentration and a large standard deviation of the mean [Table 1]. The mean concentration, when including only the fish with detectable MP, was 4.47 ± 2.99 nMP/100 g, and the mean mass concentration among the same fish was 8.08 ± 13.01 μg/kg.

Polymer types

Six polymer groups were identified: polypropylene (PP), polyethylene (PE), polyester (PES), polystyrene (PS), polyamide (PA), and polyethylene terephthalate (PET). The dominant polymers were PP and PE, which were found in four out of eight positive samples. 38% of the particles in total were PP, and 31% of the particles in total were PE. The distribution of polymers in individual fish can be found in Figure 3, and polymer type, size, and shape per particle are shown in Supplementary Table 1.

MP shape and size

A total of 29 particles were identified as microplastic and passed quality assurance and quality control, of which 21 particles were classified as fragments and eight as fibers. The particle sizes [Figure 4] show that the majority (62%) were smaller than 50 μm. 93% of the particles were smaller than 100 μm in the minor dimension. Fibers and fragments over 200 μm were observed. The largest particle was a PP particle of 258.2 μm.

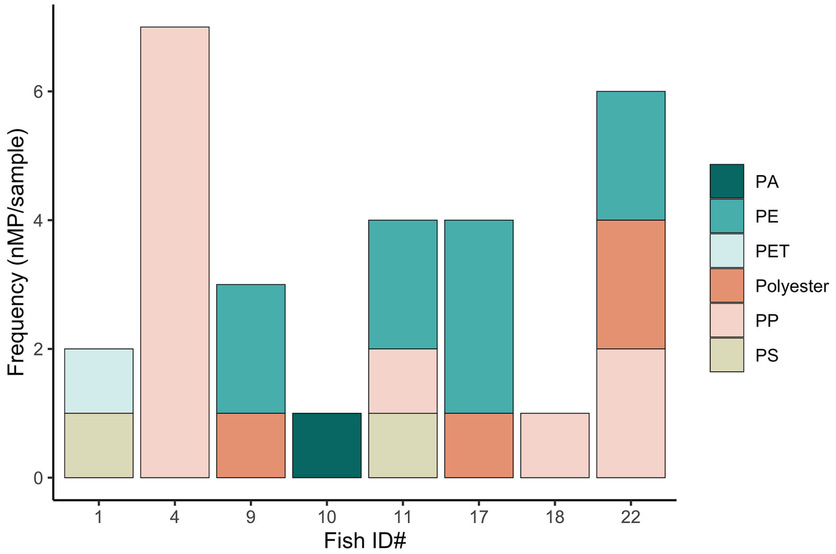

Figure 3. Microplastic concentration (nMP/sample) and polymer distribution in muscle tissue of wild-caught cod from a plastic-polluted area in western Norway 2021. PA: Polyamide; PE: polyethylene; PET: polyethylene terephthalate; PP: polypropylene; PS: polystyrene.

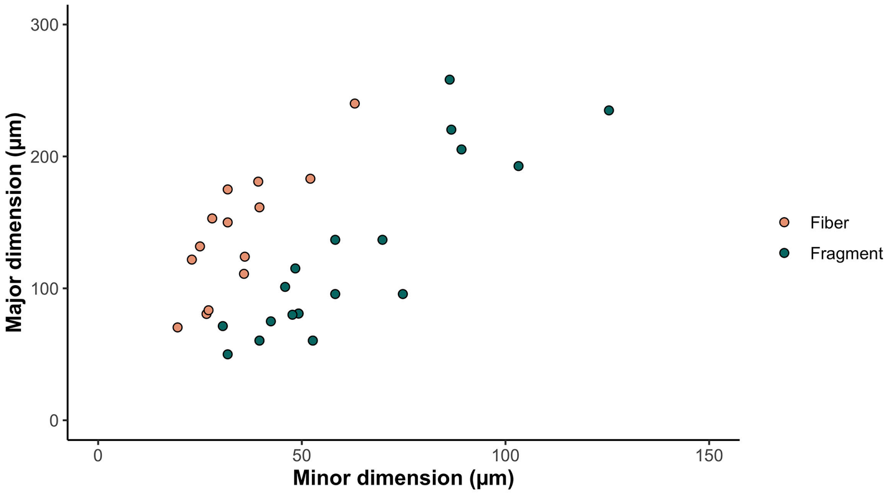

Figure 4. Size distribution of microplastic particles in cod muscle tissue. Major by minor dimension (μm).

Among the eight corresponding wet traps analyzed for quality control, only two contained microplastic particles, which corresponded to the processing of cod #1 and #4. Both wet traps had one PE fiber each, measuring 123 and 310 μm, respectively. Since the color of the PE fibers in the wet traps matched those detected in cod #1, the two PE polymers detected in cod #1 were excluded from the analysis.

Cod #4 exhibited large fragments of polypropylene (PP) up to 235 μm but did not contain any PE which was the polymer type observed in the corresponding wet trap; thus, no subtraction of PE or particles was performed in cod #4. The fishnets used were made of orange PP, but the color did not match the observed particles for cod #4.

No further MP were detected in the wet traps corresponding to fish with observed microplastic particles; thus, the MP are trusted to be from the fish samples, and not contamination from the external lab environment. After subtracting the particles corresponding to wet trap controls, a total of 29 out of 31 particles were included in the results (All particles identified as microplastic are shown in Supplementary Table 1). The procedural blanks did not exhibit any contamination, and therefore, no subtraction of particles was required to account for procedural contamination.

Mass and concentration

MP concentrations in cod muscle tissue (μg/kg·ww) varied greatly, with mean concentrations of 8.08 ± 13.01 μg/kg in the eight cod where MP particles were detected. The highest single concentration of 38.9 μg/kg was found in a 40 cm long fish (cod #4), which had a notable presence of large PP fragments and fibers that significantly impacted the calculated MP mass. However, this concentration, which is considerably higher than the mean for this study, is much lower than the previously reported concentration in the small pilot study of three cod from the same region which observed mean concentrations of 670 ± 470 μg/kg ww in cod muscle tissue[11]. This may be the result of improved analytical methods and the use of a plastic-controlled environment in this study. Cod with both high and low MP concentrations and of different lengths had k-factors above 1, indicating good condition and feeding status irrespective of the MP concentrations observed.

We examined statistically which factors could contribute to the levels and variation of microplastic in the cod muscle tissue. Due to the low number of cod with detected MP particles in the muscle tissue, and the non-normal data distribution, regression analyses could not be performed.

Non-parametric correlation tests were performed on the cod to investigate the correlation between MP occurrence and other likely influencing factors [length (age), body size (weight) and k-factor], combining the cod from the two sites. There were no significant correlations between particle counts (nMP/100 g) and fish body length, weight, or k-factor [Figure 5]. Likewise, there was no correlation between MP mass-concentration (μg/kg·ww) and length (Spearman's rho, r = -0.092, P = 0.68) MP mass-concentration and weight (Spearman's rho, r = -0.014, P = 0.95) or MP mass-concentration and k-factor (Spearman's rho, r = -0.1, P = 0.65). Interestingly, both large and small cod were observed to have zero MP in their muscle tissue [Figure 5]. The results suggest that length (age), body weight, and k-factor are not determining factors for the MP concentration in muscle tissue of cod in plastic-polluted areas. However, the sample size is small, and the low number of cod with positive observations of MP in the fillet hampers statistical analyses. On the other hand, one would expect that if accumulation occurred throughout the lifetime of fish up to six years of age, it would be observable with the sensitive methods used.

Limitations of the study

In this study, we observed a low FO and low concentration of MP in the muscle tissue of wild-caught cod from a highly plastic-polluted area in Western Norway. One potential reason for the low concentrations can be the strict contamination control and good laboratory practice that prevented external contamination from influencing the results[41]. Other influencing factors may theoretically be potential particle losses during the analyses. The use of strong reagents during tissue removal may damage the particle surface, which is why this study instead uses a gentle enzymatic degradation method that has observed a 96%-99% recovery rate. Maintaining the integrity of the polymer particles is important because, if particles close to 10 μm in one dimension experience a small reduction in size, they may be lost through the 10 μm filter mesh.

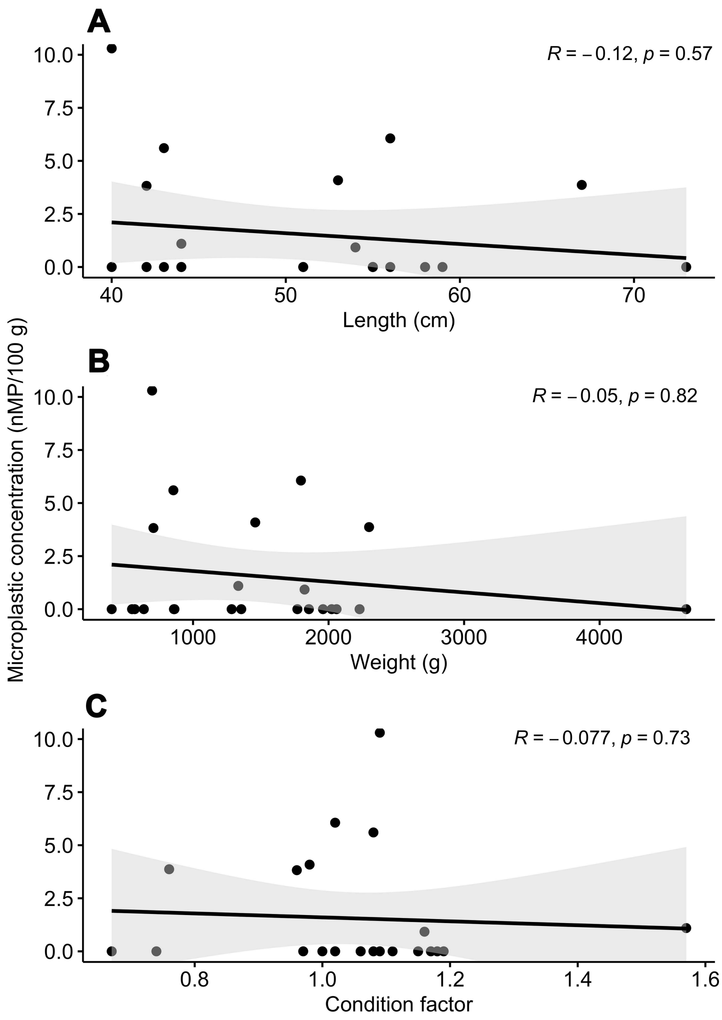

Figure 5. The relationship between nMP/100 g and (A) body length, (B) body weight, and (C) k-factor in resident cod from two locations in Western Norway 2021.

Regarding potential contamination of the samples, which would increase the observed concentrations, strict precautions were taken in the NORCE Plastlab to minimize the introduction of microplastic particles to the samples, in order to strictly quantify the particles that were present due to ingestion in the wild and translocation into fish tissues. The observation of somewhat larger PP fibers and fragments raised some concerns. It is possible that particles larger than 200 µm may have become attached to the fish externally during handling, despite measures taken to minimize contamination. The source of these fibers and fragments remains unidentified, and they do not correspond to the equipment used. This shows how challenging it is to entirely avoid plastic contamination in a plastic-dependent society. Various potential sources of contamination during all procedures, such as fishing gear, clothing, ropes, buckets, and transportation, need to be considered and the use of plastic minimized throughout the procedure. However, removing the larger particles (> 200 µm) from the dataset did not impact the results.

The lack of standardized methods and variation in contamination control measures pose limitations to building knowledge from studies conducted across different regions[32,55]. Previous studies have reported the occurrence of MP in edible parts of finfish[10,25,28,30,51,56,57]. However, due to differences in methods, reported size classes, and variation in contamination control, comparing concentrations and distribution patterns of MP among these studies is challenging.

In terms of replicate analyses, working with a larger number of samples with fewer negative findings is ideal for increased statistical power and understanding method uncertainties. However, microplastic analysis with these sensitive and gentle methods is time-consuming and expensive, making it financially very challenging to expand the sample size to increase data resolution and reduce uncertainties.

The microplastic burden in the water column and sediments of the plastic-polluted region where the cod was caught is assumed to mirror the macroplastic pollution observed on many beaches in the region that are known to receive large volumes of marine debris[35], and it is assumed that the cod had been exposed to macroplastic and MP throughout its lifetime. Cod from this region have been observed to have a higher rate of plastic in their stomach than cod from other areas in Norway[40]. However, direct measurements of the concentrations of MP in these waters and sediments where the fish were caught were not performed, due to funding limitations. A study of MP in sediments from a nearby fjord demonstrated high concentrations of microplastic particles, with the majority being under 100 µm[42], and the polymer composition suggesting both terrestrial and marine sources.

Implications for human consumers

Previous studies have shown that the highest number of microplastic particles are in the lower size classes when using similar methods of analyses[1,42,58]. However, the presence of a high number of small MP in the environment does not necessarily indicate high uptake by organisms or high prevalence in tissues, as studies have demonstrated a low absorption rate of nanoplastics in finfish[22,59].

It has been shown experimentally that fragments over 100 µm can be taken up by organisms[16]. MP have been found to pass through biological tissue either between enterocytes or through phagocytosis by organs such as the gills or gastrointestinal tract[16,60]. The absorption process appears to be influenced by the size of the MP[16,61], but is not fully understood, and a number of studies report larger particles in tissues than what is believed to be able to pass through or between cells. This highlights the need for studies that elucidate the uptake and translocation mechanisms of MP and may provide answers to the most likely size classes to be translocated into, and potentially retained in, tissues.

For human consumers, the presence of MP in our food is of concern, especially if MP are found to accumulate throughout the life of an organism. Our current observations that MP do not increase with age in cod may indicate that the muscle tissue in cod is not the target organ where MP will accumulate, and thus that consumption of old and large fish does not imply a higher exposure to MP. This is in contrast to the known bioaccumulation of several persistent contaminants with the age of the organism, where consumption of older or larger organisms represents a greater risk of exposure, which is therefore advised against.

The Minderoo Monaco Commission has referred to MP as POPs due to their common characteristics[62]. Even without proof of bioaccumulation, persistence and mobility alone are criteria for the POP classification, meaning MP may indeed be classified as POPs. However, the need to thoroughly assess the physico-chemical properties of MP and their bioaccumulation and biomagnification throughout the food web remains. If MP do bioaccumulate, as has been indicated by recent studies of mammalian testis[14], it would warrant increased funding for research into human microplastic exposure and kinetics and support toward the ongoing work to negotiate the international binding treaty on plastic pollution (UNEP-INC), aimed at curbing the production and unregulated release of plastics, as well as monitoring of the generation and distribution of MP in the same way as for the well-known legacy POPs, such as polychlorinated biphenyls (PCBs), dichloro-diphenyl-trichloroethane (DDT) and tetrachlorodibenzodioxins (TCDDs) (dioxins).

Little evidence for bioaccumulation *in situ*

Bioaccumulation of a substance implies that the concentration increases significantly above that of the surrounding environment and can be observed to increase with age due to inefficient excretion or metabolism. This study cannot conclude with evidence of bioaccumulation in the muscle tissue of up to six-year-old cod of increasing length and body mass. Instead, this study adds to a growing number of publications that do not find evidence for microplastic bioaccumulation *in situ*. Similarly, no correlation was found between fish mass and microplastic concentrations in Smallmouth bass (*Micropterus dolomieu*), Lake whitefish (*Coregonus clupeaformis*), and Northern pike (*Esox lucius*), and the study observed no trend of increasing levels in organs over time. A recent study of marine animals at different trophic levels concluded with no evidence of bioaccumulation of MP > 100 μm in the digestive tracts and liver[63].

Similarly, a review of 226 field studies across various fish and seafood species also found no increase in microplastic concentrations per individual with trophic level, challenging the notion of bioaccumulation of plastic[55]. However, the mentioned review cautioned against using the presence of MP in the gastrointestinal tract as an indicator of bioaccumulation, as the transient presence of MP in the gut may simply indicate recent ingestion and could vary over short periods of time due to egestion.

In contrast, another systematic review[33] concluded that bioaccumulation of MP did, in fact, occur within trophic levels, when focusing on the gastrointestinal tract of finfish rather than muscle tissue, which was criticized[55]. The criticized study, however, also concluded with no evidence of biomagnification at higher trophic levels and acknowledged the challenges in identifying such processes over several decades and across the development of different methods for microplastic quantification.

To definitively answer the question of microplastic bioaccumulation, carefully designed *in vivo* experiments or larger datasets from *in situ* observations are needed. For now, the weight of the *in situ* evidence is leaning toward no evidence of bioaccumulation. However, the absence of evidence is not the same as evidence of absence; thus, carefully designed studies and sensitive methods are necessary to settle this question of bioaccumulation of microplastic.

Body distribution of microplastic

The current study focuses on microplastic concentrations in cod muscle tissue. Studies of nanoparticle uptake and depuration in fish do not indicate any specific target organ where nanoplastic particles accumulate[22]. Observations of nanoplastics being taken up, distributed, and eventually eliminated from the liver and other organs may also suggest that the presence of the larger MP in livers is transient and not persistent[17]. In a previous report on MP in salmonids, no significant difference was observed between muscle and liver tissue concentrations, indicating that muscle tissue could serve as equally suitable for monitoring[50]. Similarly, a recent study[63] observed no bioaccumulation in the liver after analyses that included lean fish. Observations confirming the occurrence of MP in the livers of wild fish do not necessarily imply that the liver is a primary target organ for MP accumulation, and studies have shown that MP can be excreted through bile in vertebrates[16], further supporting the likelihood of a transient presence of MP in the liver.

For future studies on cod or fatty fishes, it would be feasible to examine several tissues to determine if there are differences in microplastic distribution after a lifetime of exposure. Furthermore, it is advisable to collect samples from fresh, unfrozen tissue, as freezing and thawing can cause particularly the liver to disintegrate, potentially leading to the loss of microplastic particles. Obtaining sufficiently large liver samples for microplastic analyses may moreover be challenging in small cod.

Although the current evidence suggests that bioaccumulation of MP is not observed using existing analytical methods, it does not imply that exposure to plastic and MP is safe or that plastic pollution is not an environmental concern. The production of plastic involves the use of numerous chemicals, and the uncontrolled release of plastic waste results in the dispersal of unknown quantities of these chemicals into the environment, with increasing and chronic MP exposure to animals and humans. This may be harmful even if the presence in tissues is transient.

Rather than relying on the demonstration of bioaccumulation and biomagnification of MP throughout the food chain, before we take measures against MP pollution, we should consider whether we need more evidence that plastic behaves exactly like the legacy POPs to stop plastic pollution and implement better management practices for plastic materials.

CONCLUSIONS

In conclusion, this study of coastal cod from a plastic-polluted region in Western Norway supports previous observations of the presence of microplastic in the edible tissues of finfish. The study did not find evidence of bioaccumulation in the muscle tissue of two- to six-year-old cod of good body condition. These findings align with previous studies that conclude with no bioaccumulation or biomagnification of MP across different species and trophic levels. The analyses were performed in a state-of-the-art plastic-free laboratory, ensuring minimal external contamination. The study highlights the importance of accurate and sensitive methods and the need for the development of efficient techniques to process larger sample volumes without potentially damaging small microplastic particles. The study found no correlation between fish size, age, body condition, and microplastic concentration; thus, this study provides no support for bioaccumulation with age, but the sample size is small, and the results should be interpreted with care. No bioaccumulation indicates no increased risk for humans of MP ingestion from consuming fillets of large fish. The intake of MP from cod from this region is, based on this study, projected to be low, with a FO of 34.78 % and an average concentration of 2.81 ± 8.33 μg/kg·ww. Future studies could include controlled laboratory experiments to assess the dose-uptake relationship of MP using environmentally relevant exposures. Moreover, humanity already possesses sufficient knowledge about the negative effects of plastic and associated chemicals to justify better management practices and efforts to stop plastic pollution.

DECLARATIONS

Acknowledgments

Kenneth Bruvik and students at TAM/NJFF for providing knowledge of the plastic hot spots suitable for fishing, and for fishing the cod. Thanks to Veslemøy Navrestad (NORCE) for assistance in the lab. Thanks to Rui Pires and Marthe L. Haarr (SALT Lofoten AS) for helping create maps and graphics.

Authors' contributions

Idea, concept, study design, data treatment, graphics, writing, and editing: Haave M
Field work, laboratory work and analysis, data treatment, and proofreading: Hæggernes E
Methodology, data analysis, laboratory supervision, FTIR analyses, QA/QC, and proofreading: Gomiero A

Availability of data and materials

Original FTIR raw data from all cod and the two wet traps with observed MP are available at the Supplementary raw data.

Financial support and sponsorship

The study was funded by NORCE Norwegian Research Centre through internal strategic funding. The University of Bergen supported MSc. Hæggernes E with travel funds for her Master's thesis.

Conflicts of interest

Haave M is currently employed by SALT Lofoten AS, which declares no conflicts of interest regarding the study results. Other authors declared that there are no conflicts of interest.

Ethical approval and consent to participate

Not applicable. The fish used in the experiment were caught as part of teaching for the Norwegian Hunters and Anglers Association in the school project TAM and were subsequently donated for research aimed at MP analyses. The sampled fish were caught from the wild in accordance with Norwegian fishing and hunting regulations. Coastal cod recreational fishing is permitted without requiring ethical approval, provided that minimum size regulations are followed. Rules for recreational fishing and the minimum permissible size can be found at https://lovdata.no/dokument/SF/forskrift/2021-12-23-3910.

Consent for publication:

Not applicable.

Copyright

REFERENCES

1. Bergmann M, Wirzberger V, Krumpen T, et al. High quantities of microplastic in Arctic deep-sea sediments from the HAUSGARTEN observatory. *Environ Sci Technol* 2017;51:11000-10. DOI PubMed
2. Bergmann M, Mützel S, Primpke S, Tekman MB, Trachsel J, Gerdts G. White and wonderful? Microplastics prevail in snow from the Alps to the Arctic. *Sci Adv* 2019;5:eaax1157. DOI PubMed PMC
3. Dris R, Gasperi J, Rocher V, Saad M, Renault N, Tassin B. Microplastic contamination in an urban area: a case study in Greater Paris. *Environ Chem* 2015;12:592-9. DOI
4. Gasperi J, Wright SL, Dris R, et al. Microplastics in air: are we breathing it in? *Curr Opin Environ Sci Health* 2018;1:1-5. DOI
5. Munari C, Infantini V, Scoponi M, Rastelli E, Corinaldesi C, Mistri M. Microplastics in the sediments of Terra Nova Bay (Ross Sea, Antarctica). *Mar Pollut Bull* 2017;122:161-5. DOI PubMed
6. Aves AR, Revell LE, Gaw S, et al. First evidence of microplastics in Antarctic snow. *Cryosphere* 2022;16:2127-45. DOI
7. Cabrera M, Moulatlet GM, Valencia BG, et al. Microplastics in a tropical Andean Glacier: a transportation process across the Amazon basin? *Sci Total Environ* 2022;805:150334. DOI
8. Lusher A, Hollman P, Mendoza-Hill J. Microplastics in fisheries and aquaculture - status of knowledge on their occurrence and implications for aquatic organisms and food safety. FAO Fisheries and Aquaculture Technical Paper. 2017;615. Available from: https://oursharedseas.com/wp-content/uploads/2019/11/FAO_Microplastics_in_fisheries_aquaculture.pdf. [Last accessed on 25 Jun 2024].
9. Ragusa A, Svelato A, Santacroce C, et al. Plasticenta: first evidence of microplastics in human placenta. *Environ Int* 2021;146:106274. DOI
10. Haave M, Gomiero A, Schönheit J, Nilsen H, Olsen AB. Documentation of microplastics in tissues of wild coastal animals. *Front Environ Sci* 2021;9:575058. DOI
11. Zhu L, Zhu J, Zuo R, Xu Q, Qian Y, An L. Identification of microplastics in human placenta using laser direct infrared spectroscopy. *Sci Total Environ* 2023;856:159060. DOI
12. Leslie HA, van Velzen MJM, Brandsma SH, Vethaak AD, Garcia-Vallejo JJ, Lamoree MH. Discovery and quantification of plastic particle pollution in human blood. *Environ Int* 2022;163:107199. DOI PubMed
13. Kutralam-Muniasamy G, Shruti VC, Pérez-Guevara F, Roy PD. Microplastic diagnostics in humans: "the 3Ps" progress, problems, and prospects. *Sci Total Environ* 2023;856:159164. DOI PubMed
14. Hu CJ, Garcia MA, Nihart A, et al. Microplastic presence in dog and human testis and its potential association with sperm count and weights of testis and epididymis. *Toxicol Sci* 2024;200:235-40. DOI

15. Kopatz V, Wen K, Kovács T, et al. Micro- and nanoplastics breach the blood-brain barrier (BBB): biomolecular Corona's role revealed. *Nanomaterials* 2023;13:1404. DOI PubMed PMC
16. Volkheimer G. Hematogenous dissemination of ingested polyvinyl chloride particles. *Ann N Y Acad Sci* 1975;246:164-71. DOI PubMed
17. Clark NJ, Khan FR, Mitrano DM, Boyle D, Thompson RC. Demonstrating the translocation of nanoplastics across the fish intestine using palladium-doped polystyrene in a salmon gut-sac. *Environ Int* 2022;159:106994. DOI
18. Al-Sid-Cheikh M, Rowland SJ, Stevenson K, Rouleau C, Henry TB, Thompson RC. Uptake, whole-body distribution, and depuration of nanoplastics by the scallop pecten maximus at environmentally realistic concentrations. *Environ Sci Technol* 2018;52:14480-6. DOI PubMed
19. Mattsson K, Ekvall MT, Hansson LA, Linse S, Malmendal A, Cedervall T. Altered behavior, physiology, and metabolism in fish exposed to polystyrene nanoparticles. *Environ Sci Technol* 2015;49:553-61. DOI PubMed
20. Mattsson K, Johnson EV, Malmendal A, Linse S, Hansson LA, Cedervall T. Brain damage and behavioural disorders in fish induced by plastic nanoparticles delivered through the food chain. *Sci Rep* 2017;7:11452. DOI PubMed PMC
21. Chae Y, An YJ. Effects of micro- and nanoplastics on aquatic ecosystems: current research trends and perspectives. *Mar Pollut Bull* 2017;124:624-32. DOI PubMed
22. Clark NJ, Khan FR, Crowther C, Mitrano DM, Thompson RC. Uptake, distribution and elimination of palladium-doped polystyrene nanoplastics in rainbow trout (Oncorhynchus mykiss) following dietary exposure. *Sci Total Environ* 2023;854:158765. DOI PubMed
23. WHO. Dietary and inhalation exposure to nano- and microplastic particles and potential implications for human health. 2022. Available from: https://www.who.int/publications/i/item/9789240054608. [Last accessed on 25 Jun 2024].
24. Cox KD, Covernton GA, Davies HL, Dower JF, Juanes F, Dudas SE. Human consumption of microplastics. *Environ Sci Technol* 2019;53:7068-74. DOI PubMed
25. Collard F, Gilbert B, Compère P, et al. Microplastics in livers of European anchovies (*Engraulis encrasicolus*, L.). *Environ Pollut* 2017;229:1000-5. DOI
26. Wootton N, Sarakinis K, Varea R, Reis-Santos P, Gillanders BM. Microplastic in oysters: a review of global trends and comparison to southern Australia. *Chemosphere* 2022;307:136065. DOI PubMed
27. Daniel DB, Ashraf PM, Thomas SN. Microplastics in the edible and inedible tissues of pelagic fishes sold for human consumption in Kerala, India. *Environ Pollut* 2020;266:115365. DOI PubMed
28. Dawson AL, Li JY, Kroon FJ. Plastics for dinner: Store-bought seafood, but not wild-caught from the Great Barrier Reef, as a source of microplastics to human consumers. *Environ Adv* 2022;8:100249. DOI
29. Habib RZ, Kindi RA, Salem FA, et al. Microplastic contamination of chicken meat and fish through plastic cutting boards. *Int J Environ Res Public Health* 2022;19:13442. DOI PubMed PMC
30. Karami A, Golieskardi A, Ho YB, Larat V, Salamatinia B. Microplastics in eviscerated flesh and excised organs of dried fish. *Sci Rep* 2017;7:5473. DOI PubMed PMC
31. Catarino AI, Macchia V, Sanderson WG, Thompson RC, Henry TB. Low levels of microplastics (MP) in wild mussels indicate that MP ingestion by humans is minimal compared to exposure via household fibres fallout during a meal. *Environ Pollut* 2018;237:675-84. DOI PubMed
32. Lusher AL, Hurley R, Arp HPH, et al. Moving forward in microplastic research: a Norwegian perspective. *Environ Int* 2021;157:106794. DOI
33. Miller ME, Hamann M, Kroon FJ. Bioaccumulation and biomagnification of microplastics in marine organisms: a review and meta-analysis of current data. *PLoS One* 2020;15:e0240792. DOI PubMed PMC
34. Shruti V, Kutralam-muniasamy G. Blanks and bias in microplastic research: Implications for future quality assurance. *Trends Environ Anal Chem* 2023;38:e00203. DOI
35. Bastesen E, Haave M, Andersen GL, Velle G, Bødtker G, Krafft CG. Rapid Landscape changes in plastic bays along the Norwegian coastline. *Front Mar Sci* 2021;8:579913. DOI
36. Delandmeter P, van Sebille E. The Parcels v2.0 Lagrangian framework: new field interpolation schemes. *Geosci Model Dev* 2019;12:3571-84. DOI
37. Godø OR, Moksness E. Growth and Maturation of Norwegian coastal cod and Northeast Arctic cod under different conditions. *Fish Res* 1987;5:235-42. DOI
38. Cote D, Moulton S, Frampton PCB, Scruton DA, Mckinley RS. Habitat use and early winter movements by juvenile Atlantic cod in a coastal area of Newfoundland. *J Fish Biol* 2004;64:665-79. DOI
39. Mattson S. Food and feeding habits of fish species over a soft sublittoral bottom in the northeast atlantic: 1. COD (*GADUS MORHUA* L.) (GADIDAE). *Sarsia* 1990;75:247-67. DOI
40. Bråte ILN, Eidsvoll DP, Steindal CC, Thomas KV. Plastic ingestion by Atlantic cod (Gadus morhua) from the Norwegian coast. *Mar Pollut Bull* 2016;112:105-10. DOI PubMed
41. Bai R, Fan R, Xie C, et al. Microplastics are overestimated due to poor quality control of reagents. *J Hazard Mater* 2023;459:132068. DOI
42. Haave M, Lorenz C, Primpke S, Gerdts G. Different stories told by small and large microplastics in sediment - first report of microplastic concentrations in an urban recipient in Norway. *Mar Pollut Bull* 2019;141:501-13. DOI
43. Lorenz C. Detection of microplastics in marine sediments of the German Coast via FT-IR spectroscopy. 2014. DOI

44. Löder MGJ, Imhof HK, Ladehoff M, et al. Enzymatic purification of microplastics in environmental samples. *Environ Sci Technol* 2017;51:14283-92. DOI
45. Gomiero A, Strafella P, Øysæd KB, Fabi G. First occurrence and composition assessment of microplastics in native mussels collected from coastal and offshore areas of the northern and central Adriatic Sea. *Environ Sci Pollut Res Int* 2019;26:24407-16. DOI PubMed
46. Martinelli M, Gomiero A, Guicciardi S, et al. Preliminary results on the occurrence and anatomical distribution of microplastics in wild populations of Nephrops norvegicus from the Adriatic Sea. *Environ Pollut* 2021;278:116872. DOI
47. Gomiero A, Haave M, Kögel T, et al. Tracking of plastic emissions from aquaculture industry (TrackPlast). 2020. Available from: https://hdl.handle.net/11250/2649891. [Last accessed on 25 Jun 2024].
48. Primpke S, Wirth M, Lorenz C, Gerdts G. Reference database design for the automated analysis of microplastic samples based on Fourier transform infrared (FTIR) spectroscopy. *Anal Bioanal Chem* 2018;410:5131-41. DOI PubMed PMC
49. Nash R, Valencia AH, Geffen AJ. The origin of fulton's condition factor - setting the record straight. *Fisheriies* 2006;31:236-8. Available from:https://api.semanticscholar.org/CorpusID:6908259. [Last accessed on 25 Jun 2024]
50. Gomiero A, Haave M, Bjorøy Ø, et al. Quantification of microplastic in fillet and organs of farmed and wild salmonids-a comparison of methods for detection and quantification. 2020. Available from:https://hdl.handle.net/11250/2687619. [Last accessed on 25 Jun 2024].
51. Abbasi S, Soltani N, Keshavarzi B, Moore F, Turner A, Hassanaghaei M. Microplastics in different tissues of fish and prawn from the Musa Estuary, Persian Gulf. *Chemosphere* 2018;205:80-7. DOI PubMed
52. Akhbarizadeh R, Moore F, Keshavarzi B. Investigating a probable relationship between microplastics and potentially toxic elements in fish muscles from northeast of Persian Gulf. *Environ Pollut* 2018;232:154-63. DOI PubMed
53. Barboza LGA, Lopes C, Oliveira P, et al. Microplastics in wild fish from North East Atlantic Ocean and its potential for causing neurotoxic effects, lipid oxidative damage, and human health risks associated with ingestion exposure. *Sci Total Environ* 2020;717:134625. DOI
54. Garcia AG, Suárez DC, Li J, Rotchell JM. A comparison of microplastic contamination in freshwater fish from natural and farmed sources. *Environ Sci Pollut Res Int* 2021;28:14488-97. DOI PubMed
55. Gouin T. Toward an improved understanding of the ingestion and trophic transfer of microplastic particles: critical review and implications for future research. *Environ Toxicol Chem* 2020;39:1119-37. DOI PubMed PMC
56. Karami A, Golieskardi A, Choo CK, Larat V, Karbalaei S, Salamatinia B. Microplastic and mesoplastic contamination in canned sardines and sprats. *Sci Total Environ* 2018;612:1380-6. DOI PubMed
57. Wootton N, Reis-Santos P, Dowsett N, Turnbull A, Gillanders BM. Low abundance of microplastics in commercially caught fish across southern Australia. *Environ Pollut* 2021;290:118030. DOI PubMed
58. Lorenz C, Roscher L, Meyer MS, et al. Spatial distribution of microplastics in sediments and surface waters of the southern North Sea. *Environ Pollut* 2019;252:1719-29. DOI
59. Zeytin S, Wagner G, Mackay-Roberts N, et al. Quantifying microplastic translocation from feed to the fillet in European sea bass *Dicentrarchus labrax*. *Mar Pollut Bull* 2020;156:111210. DOI PubMed
60. Browne MA, Dissanayake A, Galloway TS, Lowe DM, Thompson RC. Ingested microscopic plastic translocates to the circulatory system of the mussel, *Mytilus edulis* (L). *Environ Sci Technol* 2008;42:5026-31. DOI PubMed
61. Deng Y, Zhang Y, Lemos B, Ren H. Tissue accumulation of microplastics in mice and biomarker responses suggest widespread health risks of exposure. *Sci Rep* 2017;7:46687. DOI PubMed PMC
62. Neira M. The Minderoo-Monaco Commission on plastics and human health: editorial to accompany the Minderoo-Monaco Commission on plastics and human health in the journal, *Annals of Global Health*. *Ann Glob Health* 2023;89:22. DOI PubMed PMC
63. Covernton GA, Cox KD, Fleming WL, et al. Large size (>100-µm) microplastics are not biomagnifying in coastal marine food webs of British Columbia, Canada. *Ecol Appl* 2022;32:e2654. DOI PubMed PMC

Magnucka *et al. Water Emerg Contam Nanoplastics* 2024;3:17
DOI: 10.20517/wecn.2024.21

Water Emerging Contaminants & Nanoplastics

Short Communication

Open Access

Occurrence and identification of microplastics retained in corrosion deposits of drinking water transmission pipes

Marta Magnucka, Joanna Świetlik, Agata Lembicz, Piotr Nawrocki, Lilla Fijołek

Faculty of Chemistry, Department of Analytical and Environmental Chemistry, Adam Mickiewicz University, Poznań 61-614, Poland.

Correspondence to: Marta Magnucka, Faculty of Chemistry, Department of Analytical and Environmental Chemistry, Adam Mickiewicz University, Uniwersytetu Poznańskiego 8, Poznań 61-614, Poland. E-mail: marta.magnucka@amu.edu.pl

How to cite this article: Magnucka M, Świetlik J, Lembicz A, Nawrocki P, Fijołek L. Occurrence and identification of microplastics retained in corrosion deposits of drinking water transmission pipes. *Water Emerg Contam Nanoplastics* 2024;3:17. https://dx.doi.org/10.20517/wecn.2024.21

Received: 23 Apr 2024 **First Decision:** 20 Jun 2024 **Revised:** 9 Jul 2024 **Accepted:** 15 Jul 2024 **Published:** 19 Jul 2024

Academic Editors: Yolanda Pico, Marta Otero **Copy Editor:** Pei-Yun Wang **Production Editor:** Pei-Yun Wang

Abstract

The irregular structure and high porosity of corrosion deposits create suitable conditions for the retention, accumulation and adsorption of microplastics (MPs) and nanoplastics (NPs) transported by distributed water. Due to the low mass and continuous degradation of MPs, under certain conditions (e.g., changes in water composition or hydraulic conditions, network failures), these particles can be re-released into the water, causing secondary contamination. This paper presents preliminary results on the degree of MP contamination of sediments lining the inner surface of metal alloy pipes taken from a municipal drinking water distribution network. The isolated particles were assessed in terms of number, shape, residence time in the network, and origin. Plastic fragments classified as MPs and NPs were found in all analyzed corrosion deposits. Fragments smaller than 50 µm predominated, indicating a high level of plastic fragmentation associated with advanced degradation and prolonged residence in the environment. The predominant plastics identified were polyethylene (PE), polyethylene terephthalate (PET), and polyamides. High-carbon particles, most likely NP particles, whose presence in drinking water may pose a high health risk to consumers due to their potential to migrate into body tissues, were very abundant in the sediments but impossible to count with the techniques used. The results indicate the need to intensify research on the content of MPs and NPs not only in drinking water, but also in the sediments covering the interior of distribution pipes, and to identify factors that may cause their secondary release into bulk water.

Keywords: Microplastics, nanoplastics, corrosion deposits, drinking water, drinking water distribution networks

INTRODUCTION

Corrosion deposits covering the internal surfaces of metal-alloy water pipes are formed by co-existing chemical, electrochemical, and biological corrosion[1-9]. The Fe oxides and hydroxides formed in the processes are deposited on the internal surface of the pipes, forming corrosion scales often shaped as undulating "tubercles"[9-12].

The presence of corrosion deposits in water pipes can adversely affect the organoleptic parameters of drinking water[7-9,12,13]. The irregular structure, high porosity, and high undulation of corrosion deposit layer create suitable conditions for the retention, accumulation, and adsorption of various water admixtures, including microplastic (MP) and nanoplastic (NP). Characterized by their small size and irregular shape, MPs[14-17] have a high potential to accumulate on the sediment surface and between tubercles. Due to their small masses and continuous degradation, these particles can be re-released into the bulk water, e.g., when changing the hydraulic conditions in the pipeline, during pipe repairs, or even when changing the quality of the transmitted water. It can, therefore, be assumed that corrosion deposits are one of the potential sources of MPs in drinking water[18].

The occurrence of MP particles in drinking water is highly undesirable. A growing number of literature reports indicate that MP particles can accumulate in the tissues of living organisms[19-23], have the ability to penetrate the blood-brain barrier[24,25], and have the ability to adsorb and carry contaminants that are toxic to living organisms and humans[20,26-28]. For this reason, MP has been included in the list of monitored substances in drinking water in the EU[29].

This article presents the results of a study to determine the extent of MP contamination of sediments deposited on the inner surface of metal alloy pipes used in a metropolitan drinking water distribution network. The isolated particles were assessed in terms of their abundance, shape, residence time in the network, and origin.

EXPERIMENT

Corrosion deposits were taken from fragments of metal alloy pipes from an operational municipal distribution network [Table 1]. Scraped with a steel chisel and dried, the deposits were dissolved using concentrated HCl (Stanlab, Poland). The resulting solutions were vacuum filtered through GF/D glass fiber filters (Whatman, China). The filters with the remaining mineral particles (mainly sand grains) and MP particles were transferred to glass Petri dishes and dried at room temperature.

Microscopic images were taken using a Quanta FEG 250 scanning electron microscope (SEM) (FEI), in low vacuum (70 Pa), at accelerating beam voltages of 10 and 30 kV. Elemental analysis was performed using an Octane silicon-drift detector (SDD) energy dispersive X-ray spectroscopy (EDS) detector (EDAX). Acquisition of EDS spectra was performed at a beam accelerating voltage of 30 kV[18,21,30].

EDS mapping of the carbon regions was used to characterize the MP. To increase particle visibility, images were magnified and contrast was increased. Only particles with clearly visible and edge-limited shapes were counted and sized in precisely scaled 1.5 mm × 2 mm images. The area of the filter area in a single map was 0.025 cm^2, accounting for 1/2,500 of its total area. For each sample, 12-20 images were recorded. The results of the counts were averaged and then converted per cm^2 of filter area and per gram of corrosion deposit [Table 1].

Table 1. Characteristics of tested water pipes, abundance and size distribution of isolated MP particles

Pipes characteristics				Average abundance		Size distribution (μm)				
Material	**Diameter (mm)**	**Exploitation (years)**	**Weight of corrosion deposit (g)**	**MPs/g**	**MPs/cm^2**	**< 50**	**50-100**	**100-150**	**150-200**	**> 200**
Steel 1	32	53	82.48	30,637	10,276	95.57%	1.91%	0.49%	0.12%	0.05%
Steel 2	42	40	69.82	49,760	27,476	98.79%	0.84%	0.13%	0.035%	-
Steel 3	32	30	40.72	41,979	13,661	97.60%	1.61%	0.225%	-	0.009%
Cast iron 1	150	118	16.28	37,665	9,638	98.97%	0.96%	0.07%	-	-
Cast iron 2	115	45	11.34	63,959	11,401	94.39%	4.87%	0.53%	0.21%	-

MP: Microplastic.

A Raman spectrometer equipped with a video microscope (i-Raman® Plus from BWTek) and a 785 nm laser was used for MP identification[29,31-34]. Raman spectra were recorded with BWspec software [BWTek (Metrohm, Poland)][35].

RESULTS AND DISCUSSION

MP particles were found in all sediments, and their numbers ranged from 30-64 × 10^3 particles/g [Table 1]. The highest abundance of MPs was found in the sediment from a cast iron pipe with a diameter of 115 mm, which is probably related to the large volume of water transported through it at a pressure lower than in a pipe with a diameter of 150 mm (high water pressure limits MPs retention). For steel pipes with small diameters (connections to buildings), the number of isolated particles was comparable, and slight variations can be related to the volume of water transported and the average flow rate. No correlation was observed between operating time and the number of retained MPs. Isolated MPs can originate both from water entering the distribution network and from the degradation processes of plastic transmission pipes[30,36]. The particle counts of MPs were high compared to studies by other authors (500-800 MPs/kg of sludge in[18]), which may be related to the longer lifetime of the pipes in this study and/or the underestimation of the number of MPs resulting from the use of Image-Fourier transform infrared spectroscopy (FTIR) for quantitative studies in[18]. The FTIR technique allows reliable estimation of particles > 10 μm in size, whereas the accuracy of the SEM/EDS method is determined in nanometres.

EDS mapping of carbonaceous areas allowed the size distribution of MPs to be determined. Five main size ranges were distinguished: < 50, 50-100, 100-150, 150-200, and > 200 μm [Table 1 and Figure 1]. In all sediments studied, more than 90% were particles < 50 μm. As the size of the particles increases, their content in the sediments decreases. A similar trend was observed in studies for tap water, where particles < 10 μm accounted for the largest percentage among the identified MPs[33,37]. Only two of the analyzed sediments contained particles > 200 μm, probably originating from the degradation of plastic pipes operating in other areas of the network, which is also confirmed by the reported high removal efficiency (up to 90%) of MPs > 10 μm in water treatment processes[13,38,39]. In the case of particles in the 50-200 μm range, an uneven distribution has been observed, most likely linked to the different pipe diameters, thickness, porosity, and build-up time of corrosion deposits. In addition, an important aspect influencing the presence of larger size fractions in the sediments is the remoteness of the intake site from the treatment plant, as plastic water pipes can be a source of secondary contamination of drinking water with MPs.

The origin and estimated residence time of MPs in the distribution network were determined using EDS spectra [Figure 2] and Raman spectra [Figure 3]. Elemental EDS analysis conducted for numerous MP fragments showed that they varied in carbon, chlorine, and oxygen content, indicating their different

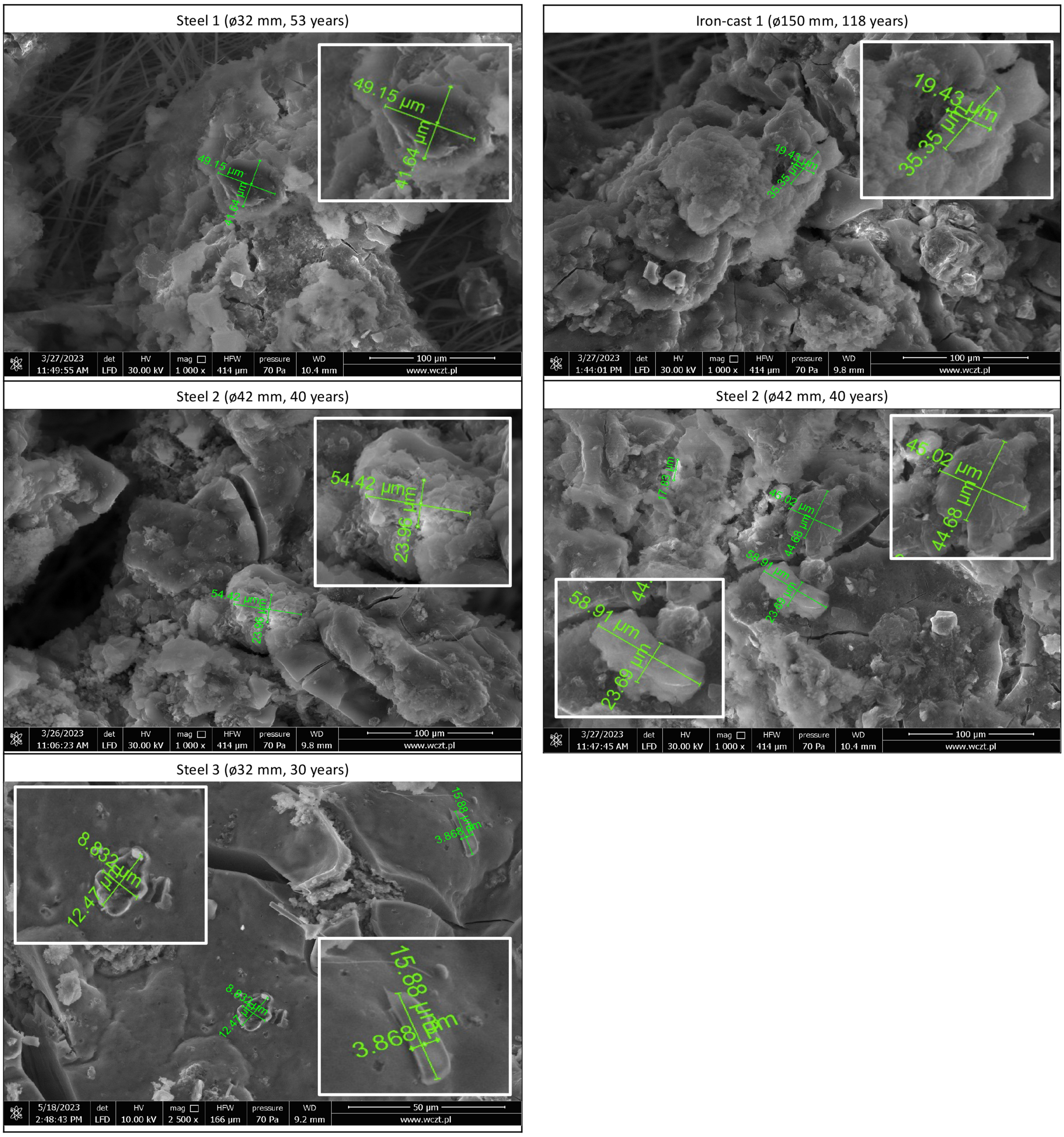

Figure 1. Examples of dimensioned MP particles. MP: Microplastic.

residence times in the water supply network[40] [Figure 2]. The results of the EDS analysis also showed that the MPs accumulated in the sediments originated mainly from plastics consisting of carbon, oxygen, and hydrogen [e.g., polyethylene (PE)/polypropylene (PP), polyethylene terephthalate (PET)], while polymers containing nitrogen in the structure (e.g., polyamides, polyimides, nylon or polyureas) were a less abundant fraction. No fragments of plastics containing high levels of chlorine [e.g., polyvinyl chloride (PVC)] were found. Raman spectroscopy technique was used to identify the isolated particles. The spectra were interpreted on the basis of analysis of the bands constituting "finger prints" of individual polymers[31,32,34] and by comparison with spectra of reference materials. This allowed confirmation of the origin of the isolated particles from PE and PET, and less frequently, from polyamides [Figure 3]. However, with the technique

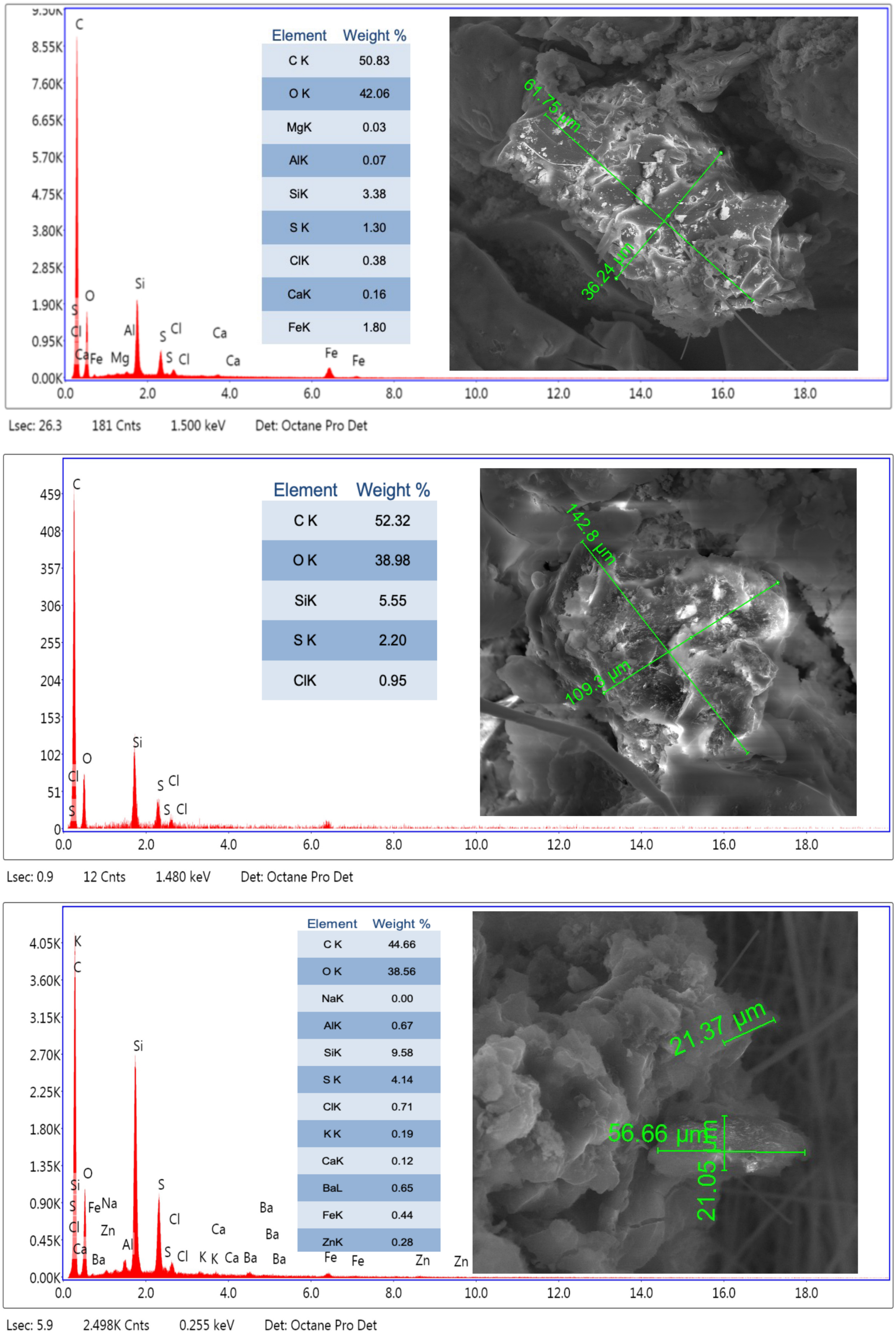

Element	Weight %
C K	50.83
O K	42.06
MgK	0.03
AlK	0.07
SiK	3.38
S K	1.30
ClK	0.38
CaK	0.16
FeK	1.80

Element	Weight %
C K	52.32
O K	38.98
SiK	5.55
S K	2.20
ClK	0.95

Element	Weight %
C K	44.66
O K	38.56
NaK	0.00
AlK	0.67
SiK	9.58
S K	4.14
ClK	0.71
K K	0.19
CaK	0.12
BaL	0.65
FeK	0.44
ZnK	0.28

Figure 2. Elemental composition of selected MP particles. MP: Microplastic.

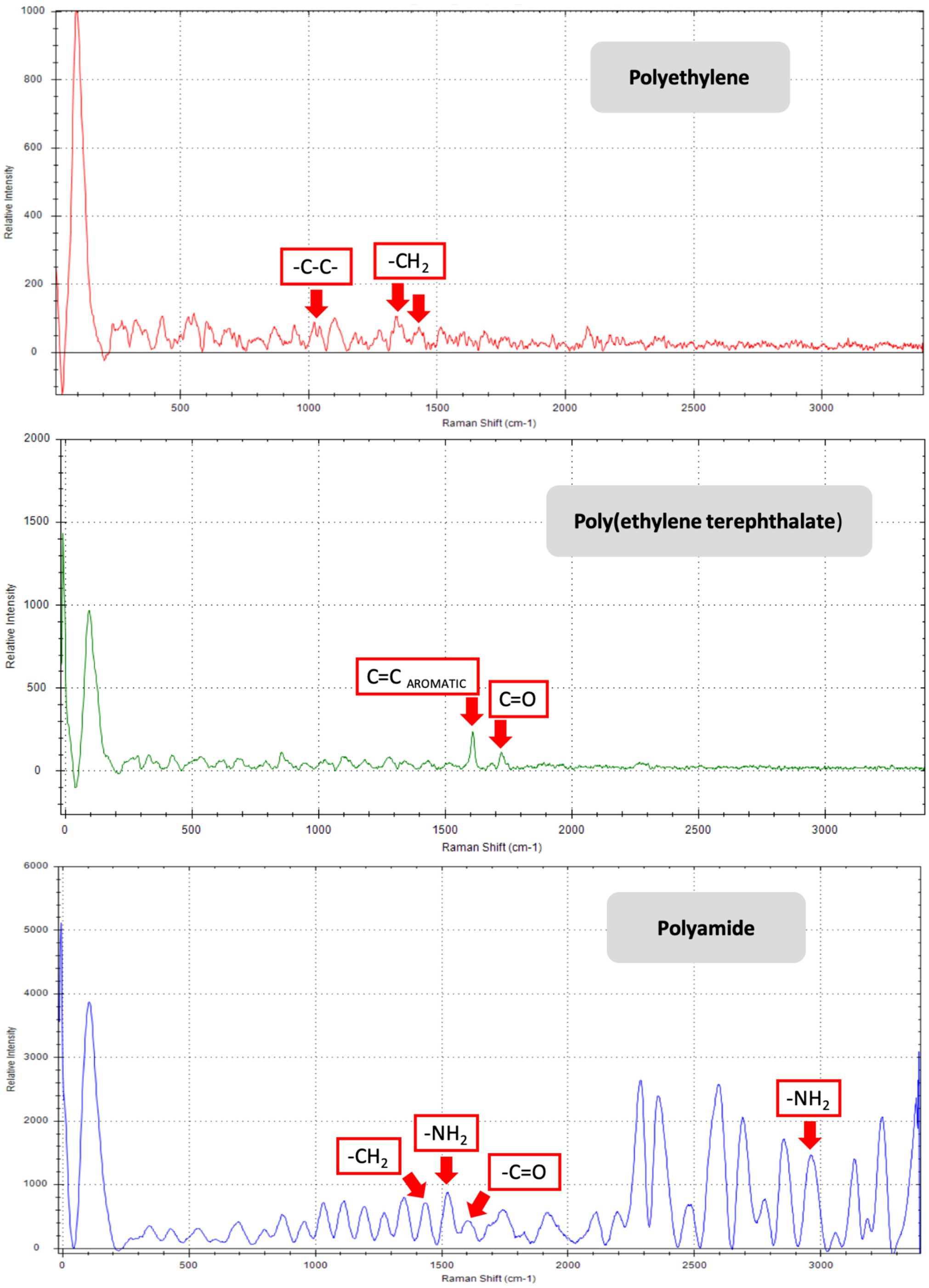

Figure 3. Raman spectra of identified MP particles showing characteristic "finger print" bands. MP: Microplastic.

used, it was not possible to carry out a complete identification of the isolated MP particles, especially those with the smallest dimensions. The results obtained were consistent with those of Johnson *et al.*[41], while in the study of Chu *et al.*[18], the predominant MPs of corrosion deposits were PVC. However, it should be borne in mind that the type of MPs identified is determined by the prevalence of specific plastics in a given area.

CONCLUSION

Plastic fragments classified as MPs and NPs were found in all analyzed corrosion deposits. Among the isolated particles, only a small percentage were MPs > 50 µm, indicating the relatively high efficiency of the applied drinking water treatment technology in removing larger MP fragments from raw water. Among the isolated particles, fragments < 50 µm predominated. The average MP content was 30-64 × 10^3 MPs/g, indicating a high potential for accumulation of the finest MP fractions in corrosion scales. Identification studies showed that the materials forming the MP particles were mainly PE, PET, and polyamides. In addition to particles whose sizes allowed quantitative and qualitative analysis, very abundant particles with high carbon content and very fine sizes were also present in the scales. It was impossible to count and identify them using the techniques used. Most likely, these were NP particles, whose presence in drinking water, due to their potential to migrate into body tissues, could pose a high health risk to consumers. The results indicate the need to intensify research on the content of MPs and NPs in corrosive sludge and the identification of factors that can cause their release into bulk water, and draw attention to the global problem of the ubiquity of the fine fraction of MPs and NPs in the water environment, and the need to monitor the presence and content of these particles not only in drinking water, but also in distribution pipes.

DECLARATIONS

Acknowledgments

This research did not receive any specific grants from funding agencies in the public, commercial, or not-for-profit sectors.

Authors' contributions

Study design and conception, data analysis and interpretation: Magnucka M, Świetlik J
Recording and interpretation of Raman spectra: Nawrocki P
Data collection, technical support: Lembicz A, Fijołek L

Availability of data and materials

Not applicable.

Financial support and sponsorship

None.

Conflicts of interest

All authors declared that there are no conflicts of interest.

Ethical approval and consent to participate

Not applicable.

Consent for publication

Not applicable.

Copyright

REFERENCES

1. Li M, Liu Z, Chen Y, Hai Y. Characteristics of iron corrosion scales and water quality variations in drinking water distribution systems of different pipe materials. *Water Res* 2016;106:593-603. DOI PubMed

2. Kuch A. Investigations of the reduction and re-oxidation kinetics of iron(III) oxide scales formed in waters. *Corros Sci* 1988;28:221-31. DOI
3. American Water Works Association Research Foundation & DVGW- Technologiezentrum Wasser. Internal corrosion of water distribution systems. 2nd edition. 1996. Available from: https://books.google.com/books?hl=zh-CN&lr=&id=F5hKYcQSuSkC&oi=fnd&pg=PA1&dq=Internal+Corrosion+of+Water+Distribution+Systems,+second+ed.%3B+1996%3B&ots=_sIoM3J1H1&sig=5Z6PlCerYpYeZUsZ-ebze3vortU#v=onepage&q=Internal%20Corrosion%20of%20Water%20Distribution%20Systems%2C%20second%20ed.%3B%201996%3B&f=false. [Last accessed on 18 Jul 2024].
4. Camper AK. Involvement of humic substances in regrowth. *Int J Food Microbiol* 2004;92:355-64. DOI PubMed
5. Imran SA, Dietz JD, Mutoti G, Taylor JS, Randall AA. Modified Larsons ratio incorporating temperature, water age, and electroneutrality effects on red water release. *J Environ Eng* 2005;131:1514-20. DOI
6. Imran SA, Dietz JD, Mutoti G, Taylor JS, Randall AA, Cooper C. Red water release in drinking water distribution systems. *J AWWA* 2005;97:93-100. DOI
7. Przywara L, Jaszczurkowska A. Physical and chemical characteristics of corrosion deposits in iron pipes operated in presence of water flow. *Polish J Mat Environ Eng* 2022;4:30-40. DOI
8. Nawrocki J, Raczyk-Stanisławiak U, Swietlik J, Olejnik A, Sroka MJ. Corrosion in a distribution system: steady water and its composition. *Water Res* 2010;44:1863-72. DOI PubMed
9. Swietlik J, Raczyk-Stanisławiak U, Piszora P, Nawrocki J. Corrosion in drinking water pipes: the importance of green rusts. *Water Res* 2012;46:1-10. DOI PubMed
10. Baylis JR. Prevention of corrosion and “red water”. *J AWWA* 1926;15:598-633. DOI
11. Gerke TL, Maynard JB, Schock MR, Lytle DL. Physiochemical characterization of five iron tubercles from a single drinking water distribution system: possible new insights on their formation and growth. *Corros Sci* 2008;50:2030-9. DOI
12. Sarin P, Snoeyink VL, Bebee J, Kriven WM, Clement JA. Physico-chemical characteristics of corrosion scales in old iron pipes. *Water Res* 2001;35:2961-9. DOI PubMed
13. Zimoch I, Dudziak M. Evaluation of toxicity of water and water-pipe deposits in rural water supply systems. 2017. Available from: http://tchie.uni.opole.pl/PECO17_2/Zimoch-Material_PECO17_2.pdf. [Last accessed on 18 Jul 2024].
14. Koelmans AA, Mohamed Nor NH, Hermsen E, Kooi M, Mintenig SM, De France J. Microplastics in freshwaters and drinking water: critical review and assessment of data quality. *Water Res* 2019;155:410-22. DOI PubMed PMC
15. Gruber ES, Stadlbauer V, Pichler V, et al. To waste or not to waste: questioning potential health risks of micro- and nanoplastics with a focus on their ingestion and potential carcinogenicity. *Expo Health* 2023;15:33-51. DOI PubMed PMC
16. Arthur C, Baker JE, Bamford HA. Proceedings of the International Research Workshop on the Occurrence, Effects, and Fate of Microplastic Marine Debris, September 9-11, 2008, University of Washington Tacoma, Tacoma, WA, USA. 2009. Available from: https://repository.library.noaa.gov/view/noaa/2509. [Last accessed on 18 Jul 2024]
17. Wu C, Zhang K, Xiong X. Microplastic pollution in inland waters focusing on Asia. In: Wagner M, Lambert S, editors. Freshwater microplastics. Cham: Springer International Publishing; 2018. pp. 85-99. DOI
18. Chu X, Zheng B, Li Z, et al. Occurrence and distribution of microplastics in water supply systems: in water and pipe scales. *Sci Total Environ* 2022;803:150004. DOI PubMed
19. Cox KD, Covernton GA, Davies HL, Dower JF, Juanes F, Dudas SE. Human consumption of microplastics. *Environ Sci Technol* 2019;53:7068-74. DOI PubMed
20. Mohamed Nor NH, Kooi M, Diepens NJ, Koelmans AA. Lifetime accumulation of microplastic in children and adults. *Environ Sci Technol* 2021;55:5084-96. DOI PubMed PMC
21. Gambino I, Bagordo F, Grassi T, Panico A, De Donno A. Occurrence of microplastics in tap and bottled water: current knowledge. *Int J Environ Res Public Health* 2022;19:5283. DOI PubMed PMC
22. Stock V, Böhmert L, Lisicki E, et al. Uptake and effects of orally ingested polystyrene microplastic particles in vitro and in vivo. *Arch Toxicol* 2019;93:1817-33. DOI PubMed
23. Revel M, Châtel A, Mouneyrac C. Micro(nano)plastics: a threat to human health? *Curr Opin Env Sci Hl* 2018;1:17-23. DOI
24. Wright SL, Kelly FJ. Plastic and human health: a micro issue? *Environ Sci Technol* 2017;51:6634-47. DOI PubMed
25. Koelmans AA, Redondo-hasselerharm PE, Nor NHM, de Ruijter VN, Mintenig SM, Kooi M. Risk assessment of microplastic particles. *Nat Rev Mater* 2022;7:138-52. DOI
26. EFSA Panel on Contaminants in the Food Chain (CONTAM). Presence of microplastics and nanoplastics in food, with particular focus on seafood. *EFSA J* 2016;14:e04501. DOI
27. Mercogliano R, Avio CG, Regoli F, Anastasio A, Colavita G, Santonicola S. Occurrence of microplastics in commercial seafood under the perspective of the human food chain. A review. *J Agric Food Chem* 2020;68:5296-301. DOI PubMed PMC
28. Kadac-Czapska K, Knez E, Grembecka M. Food and human safety: the impact of microplastics. *Crit Rev Food Sci Nutr* 2024;64:3502-21. DOI PubMed
29. EUR-Lex. Directive (EU) 2020/2184 of the European Parliament and of the Council of 16 December 2020 on the quality of water intended for human consumption (recast). 2020. Available from: http://data.europa.eu/eli/dir/2020/2184/oj. [Last accessed on 18 Jul 2024].
30. Świetlik J, Magnucka M. Aging of drinking water transmission pipes during long-term operation as a potential source of nano- and microplastics. *SSRN* 2023. DOI

31. Chakraborty I, Banik S, Biswas R, Yamamoto T, Noothalapati H, Mazumder N. Raman spectroscopy for microplastic detection in water sources: a systematic review. *Int J Environ Sci Technol* 2023;20:10435-48. DOI
32. Fischer J, Wallner GM, Pieber A. Spectroscopical investigation of ski base materials. *Macromol Symp* 2008;265:28-36. DOI
33. Shen M, Zeng Z, Wen X, et al. Presence of microplastics in drinking water from freshwater sources: the investigation in Changsha, China. *Environ Sci Pollut Res Int* 2021;28:42313-24. DOI PubMed
34. Socrates G. Infrared and Raman characteristic group frequencies: tables and charts. 3rd edition. New York; Wiley; 2001. Available from: http://catalysis.eprints.iitm.ac.in/3177/1/George%20Socrates-Infrared%20and%20Raman%20characteristic%20group%20frequencies_%20tables%20and%20charts-Wiley%20%282001%29.pdf. [Last accessed on 18 Jul 2024].
35. B&W TEK. Software. Available from: https://bwtek.com/technology/software/. [Last accessed on 18 Jul 2024].
36. Świetlik J, Magnucka M. Chemical and microbiological safety of drinking water in distribution networks made of plastic pipes. *WIREs Water* 2024;11:e1704. DOI
37. Pivokonsky M, Cermakova L, Novotna K, Peer P, Cajthaml T, Janda V. Occurrence of microplastics in raw and treated drinking water. *Sci Total Environ* 2018;643:1644-51. DOI PubMed
38. Xue J, Samaei SH, Chen J, Doucet A, Ng KTW. What have we known so far about microplastics in drinking water treatment? A timely review. *Front Environ Sci Eng* 2022;16:58. DOI PubMed PMC
39. Dronjak L, Exposito N, Rovira J, et al. Screening of microplastics in water and sludge lines of a drinking water treatment plant in Catalonia, Spain. *Water Res* 2022;225:119185. DOI PubMed
40. Jeong Y, Gong G, Lee HJ, Seong J, Hong SW, Lee C. Transformation of microplastics by oxidative water and wastewater treatment processes: a critical review. *J Hazard Mater* 2023;443:130313. DOI PubMed
41. Johnson AC, Ball H, Cross R, et al. Identification and quantification of microplastics in potable water and their sources within water treatment works in England and Wales. *Environ Sci Technol* 2020;54:12326-34. DOI PubMed

Qian *et al. Water Emerg Contam Nanoplastics* 2024;3:18
DOI: 10.20517/wecn.2024.25

Water Emerging Contaminants & Nanoplastics

Research Article

Open Access

Dyeing sludge-derived biochar for efficient removal of malachite green from dyeing wastewater

Wei Qian[#], Yili Deng[#], Yongzheng Zhang, Yingying Li, Yi Fang, Xiaolong Li, Jialin Liang, Hui Liu

Department of College of Resources and Environment, Zhongkai University of Agriculture and Engineering, Guangzhou 510225, Guangdong, China.
[#]Authors contributed equally.

Correspondence to: Dr. Jialin Liang, Prof. Hui Liu, Department of College of Resources and Environment, Zhongkai University of Agriculture and Engineering, No. 501 Zhongkai Road, Haizhu District, Guangzhou 510225, Guangdong, China. E-mail: jialin.liang@zhku.edu.cn; liuhui@zhku.edu.cn

How to cite this article: Qian W, Deng Y, Zhang Y, Li Y, Fang Y, Li X, Liang J, Liu H. Dyeing sludge-derived biochar for efficient removal of malachite green from dyeing wastewater. *Water Emerg Contam Nanoplastics* 2024;3:18. https://dx.doi.org/10.20517/wecn.2024.25

Received: 10 May 2024 **First Decision:** 17 Jun 2024 **Revised:** 18 Jul 2024 **Accepted:** 23 Jul 2024 **Published:** 25 Jul 2024

Academic Editor: Quan Wang **Copy Editor:** Pei-Yun Wang **Production Editor:** Pei-Yun Wang

Abstract

In light of the rapid advancement of the dyeing industry, the resultant environmental contamination from extensive dye utilization and the subsequent sludge generated by the treatment of dyeing wastewater has escalated, prompting broad apprehension. This study employed the response surface methodology to explore the iodine adsorption capacity of pyrolyzed dyeing sludge peat treated with $ZnCl_2$ [$ZnCl_2$ modified sludge biochar (ZSC)] as the adsorbent material for optimization of the parameters for ZSC preparation. The analysis of the variance of the response surface methods indicated that the pyrolysis temperature emerged as the most pivotal factor. The maximum adsorption capacity of malachite green (MG) by ZSC reached up to 224.0962 mg/g. Moreover, the adsorptive efficacy of ZSC on MG was evaluated under varying environmental conditions, showcasing that the optimal parameters facilitated a remarkable MG removal efficiency of 99.13%. Even after five cycles of reuse, ZSC maintained a substantial decolorization capability of 45% for MG. Characterization of ZSC through scanning electron microscopy (SEM), X-ray diffraction (XRD), Fourier transform infrared spectroscopy (FT-IR), and Brunauer–Emmett–Teller (BET) indicated a high specific surface area of 495.38 m^2/g and the presence of reactive functional groups (–OH and C–O). The adsorption process, upon thermodynamic and kinetic evaluation, aligned more closely with the Langmuir isotherm model and the pseudo-second-order kinetic model. Mechanistic adsorption results revealed that electrostatic attraction, pore-filling, hydrogen bonding, and π-π stacking interactions collectively accounted for the elevated MG removal efficacy by the ZSC. This study represents a promising approach, transforming waste into a treatment solution with the dual purpose of dye removal and resource reclamation from dyeing sludge.

Keywords: Dyeing sludge biochar, adsorption mechanism, malachite green removal, dyeing wastewater

INTRODUCTION

With the swift evolution of the industry, the scourge of textile wastewater contamination is escalating. In China, the annual discharge of textile wastewater amounts to approximately 2.0-2.3 billion tons, representing 11% of the nationwide total wastewater release. Dyeing, the pivotal contributor within the textile industry, generates a large amount of dyeing wastewater daily (300-400 × 10^4 tons), which constitutes 70%-80% of the total effluent in the industry[1,2]. Dyes, extensively employed in textile dyeing, served as the primary source of pollutants in dyeing effluents, engendering wastewater with intense coloration, salinity, heightened organic matter concentration, and intricate compositions[3]. Notably, malachite green (MG) is a dye that also functions as a fungicide, bactericide and parasiticide, characterized by persistence and resistance to natural decomposition. Previous studies have shown that MG possesses a residual period of up to 44 and 342 days in two species of fish, Oreochromis niloticus and Piaractus mesopotamicus, thus posing a significant threat to ecosystems and human well-being[4-6]. Currently, physical and biological treatments[7-11] are predominantly utilized for the remediation of dyeing wastewater; however, substantial sludge would yield and then trigger secondary pollution. Therefore, adsorption treatment has emerged as a widely approved approach due to its efficacy and cost-effectiveness in the removal of dyes from wastewater.

At present, countless endeavors have been dedicated to the development of potent and economical adsorbents for the removal of dyes. Xue *et al.* and He et al. utilized magnetic adsorbents and activated carbon materials for treating dyes, with superior adsorption performance[12,13]. The selection of an adsorbent is paramount in influencing the efficacy of adsorption, with its specific surface area and active sites deemed critical structural and compositional attributes that exert a substantial influence on adsorption phenomena[14]. Presently, carbon-based materials, including biochar and carbon nanotubes, were predominantly acknowledged as adsorbents for extensive application in the decolorization of dye-laden wastewaters, which was attributed to their abundant porous structure, active sites, and elevated specific surface area[15,16]. Notably, biochar, derived from a diverse range of feedstocks, like sludge, lignin-rich biomass, and spent mushroom substrate, has garnered significant interest in the remediation of dyeing-contaminated wastewater because of its exceptional efficacy. For example, Boulanger *et al.* prepared activated carbon for adsorption of activated orange 16 using waste mushroom substrate and virgin birch wood, respectively, and the maximum adsorption was more than 500 mg/g in both cases[17-19]. The advancement and upscaling of biochar application in water purification processes are imperative to foster sustainable practices in wastewater treatment.

In recent years, China has witnessed a dramatic escalation in dyeing sludge output, with the dyeing industry generating ~2.3 million tons of toxic and hazardous dyeing sludge in 2020[20]. Dyeing sludge often comprises polycyclic aromatic hydrocarbons (PAHs), heavy metals, surfactants, dyes, solvents, and detergent compounds. Conventional sludge management strategies like landfilling, incineration, and composting scarcely align with environmental stewardship, particularly concerning dyeing sludge. For example, landfilling of dyeing sludge may pose a risk to the environment as hard-to-degrade pollutants accumulate in the sludge and result in a loss of opportunity to convert the sludge into a resource. Incineration of sludge allows for thermal or electrical energy reduction and energy recovery, but the potential flue gas emissions carry a high environmental risk. Composting of sludge needs to ensure that toxic substances in dye sludge are effectively degraded or controlled during the composting process to avoid contamination of soil and water bodies. Nonetheless, the rich organic content of dyeing sludge offers potential for resource recovery through thermochemical conversion processes[21]. The transformation of sludge into biochar via pyrolysis emerged as a win-win solution that not only reduced sludge volume but also promoted material reclamation. Gong *et al.* utilized life cycle assessments to evaluate the potential of dyeing sludge biochar[20]. Results indicated that the sludge biochar was the most favorable choice for the transformation of dyeing sludge treatment technology due to its low direct pollutant emissions and its ability to replace high-value products. Moreover, pyrolytic carbonization of dyeing sludge promoted the immobilization of heavy metals in the biomass, which reduced the bioavailability and mobility of heavy metals[22]. Although the carbonized dyeing sludge via pyrolysis presented a promising avenue for dyeing sludge treatment, the elevated ash content and diminished organic matter content led to a reduced specific surface area and substandard surface functional group properties, thereby impeding its further utilization[23,24]. To enhance its properties, chemical activation techniques, especially those employing agents like KOH, $ZnCl_2$, H_2SO_4, *etc.*, were increasingly favored[25-30]. Among them, $ZnCl_2$ served as an exemplary activating agent in the preparation of biochar, owing to its ability to transform the material into one with expansive surface areas and finely-tuned pore structure[31]. In this regard, utilizing $ZnCl_2$ could probably enhance the performance of the biochar materials derived from dyeing sludge. Nonetheless, scant research has been dedicated to the fabrication of high-efficacy adsorbent materials targeting dye MG from dyeing sludge waste modified by $ZnCl_2$. The influence of the activation methodology and the pyrolysis process on adsorption efficacy have yet to be comprehensively investigated. Moreover, the underlying adsorption mechanisms warrant a more profound understanding.

Hence, this study employed dyeing sludge as the primary ingredient and $ZnCl_2$ solution as an activator for the synthesis of high-performance adsorbents through pyrolysis. First, the optimization of pyrolysis conditions (pyrolysis temperature, activation ratio, and carbonization duration) on the production of pyrolyzed dyeing sludge treated with $ZnCl_2$ [$ZnCl_2$ modified sludge biochar (ZSC)] was conducted. Second, the adsorption of MG from dyeing wastewater involved a thorough examination of variables such as adsorption equilibrium time, initial pH, initial MG concentration, ZSC dosage, and adsorption temperature, in order to ascertain the favorable conditions for adsorption. Third, the stability of the adsorbent materials was evaluated. Fourth, thermodynamic and kinetic models were used to elucidate the adsorption characteristics of MG in wastewater, shedding light on the underlying mechanism of its adsorption by the ZSC.

MATERIALS AND METHODS

Experimental materials

The dyeing sludge was taken from a dyeing sewage treatment plant in Foshan, Guangdong. I_2, $Na_2S_2O_3$, KIO_3, and $ZnCl_2$ were purchased from Fuchen Chemical Reagent Co. Ltd (Tianjin, China) and MG was obtained from Shandong Yousuo Chemical Technology Co. Ltd (Shandong, China). All chemicals used in the experiments were of analytical grade. The standard solution of MG was prepared with ultrapure water and diluted with distilled water.

Preparation of ZSC

The dyeing sludge was conserved post-drying and crushing. A specific quantity of dried sludge was blended with a $ZnCl_2$ solution (3 mol/L) at a designated mass ratio (ratio of solution to sludge was 1:2, 2:1, and 1:1), and allowed to permeate for 24 h at ambient temperature. Subsequently, the samples were filtered, dried in an oven at 105 °C until attaining a constant mass, and sealed for storage. The sludge samples were placed in a tube-type resistance furnace and heated up to the setting temperature (700-900 °C) at a rate of 10 °C/min and remained for a certain period (1-2 h), and then taken out once the temperature had returned to ambient conditions, thereby obtaining sludge biochar under different preparation conditions. The samples were subjected to an acidification process using a 5% solution of hydrochloric acid to remove soluble ash on the surface of the biochar. Afterwards, the samples were rinsed with water, and subsequently dried to obtain the ZSC, and then sealed for storage.

Adsorption experiment

Simulated wastewater was prepared using MG as the treatment object, and all the experimental operations requiring pH adjustment were carried out using 0.1 M HCl and NaOH[32]. In this experiment, the effects of various influencing factors on the adsorption experiments were considered. The pH of the stock solution was maintained, and the adsorption equilibrium time of ZSC on MG was investigated at a certain concentration and ZSC dosage. The effect of initial pH on adsorption efficiency was investigated at the initial pH range of 2.0-10.0. The effect of initial MG concentration on adsorption experiments was investigated at six different concentrations of MG solution (150-400 mg/L). Seven different ZSC dosages (0.8-5.0 g/L) were used to investigate the effect of ZSC dosage on adsorption. Three temperatures (20, 30, and 40 °C) were used to study the adsorption of MG at different times. Furthermore, the adsorption removal of MG by ZSC was examined after five times of reuse. Comparative tests were conducted using unmodified sludge biochar (SC). Each test was carried out in triplicate.

Characterization

The concentration of MG in the solution was determined using a UV-Vis spectrophotometer at 630 nm (UV-1600-PC, Shanghai, China). The microscopic morphology of ZSC was observed by scanning electron microscopy (SEM, Helios-G4-CX, Thermo Scientific, US). The physical phase of ZSC was analyzed by X-ray diffraction (XRD, D8, Bruker, US). The atomic structure and functional groups of ZSC were analyzed by Fourier transform infrared spectroscopy (FT-IR, Nicolet 6700, Thermo Scientific, US). Nitrogen adsorption/desorption curves were determined by an automated gas sorption analyzer (Autosorb-iQ-MP, Quantachrome, US). The pore structure and other parameters of ZSC were calculated and analyzed using the Brunauer–Emmett–Teller (BET) method.

Analytical methods

A Box-Behnken design (BBD) within the response surface methodology (RSM) was employed to optimize the ZSC adsorption processes, aiming for efficacious iodine adsorption value. The iodine adsorption value was measured using the standard method. The optimal levels were determined from the experiments, and their calculation formulas were as follows [Equations (1-3)]:

$$A = \frac{X}{M} D \tag{1}$$

$$\frac{X}{M} = \frac{5(10c_1 - 1.2c_2V_2) \times 126.93}{m} \tag{2}$$

$$c = \frac{c_2V_2}{10} \tag{3}$$

Where A is the iodine adsorption value of the specimen, mg/g; X/M is the amount of iodine adsorbed per gram of activated carbon, mg/g; D is the correction factor; c_1 is the concentration of the iodine (1/2 I_2) standard solution, mol/L; c_2 is the concentration of the sodium thiosulfate standard solution, mol/L; V_2 is the volume of the sodium thiosulfate standard solution consumed, mL; M is the mass of the specimen, g.

The adsorption removal rate of MG solution was calculated by Equation (4):

$$\text{Adsorption removal (\%)} = \frac{(c_0 - c_t)}{c_0} \times 100\% \tag{4}$$

Where c_0 is the initial concentration of simulated wastewater, mg/L; c_t is the concentration of simulated wastewater after adsorption and decolorization by ZSC, mg/L.

In this paper, Langmuir adsorption isotherm and Freundlich adsorption isotherm were used to fit the adsorption data of MG, respectively. Langmuir and Freundlich's adsorption isotherm expressivity were shown in Equations (5) and (6):

$$\frac{C_e}{q_e} = \frac{1}{q_m} C_e + \frac{1}{K_l q_m} \tag{5}$$

$$\ln q_e = \ln K_f + \ln C_e \frac{1}{n} \tag{6}$$

Where q_e is the amount of adsorbed mass per unit of adsorbent at adsorption equilibrium, mg/g; q_m is the maximum adsorbed mass that can be adsorbed by the monomolecular layer on the surface of the adsorbent during the adsorption process, mg/g; C_e is the concentration of the solute in the equilibrium liquid phase during the adsorption process, mg/L; K_l is the Langmuir adsorption coefficient; K_f is the Freundlich adsorption coefficient; n is the concentration index.

For adsorption kinetic analysis, Lagergren's pseudo-first and pseudo-second adsorption kinetic model and Elovich model were used in this paper. The equations are shown in Equations (7-9):

$$\ln(q_e - q_t) = \ln q_e - k_1 \tag{7}$$

$$\frac{t}{q_t} = \frac{1}{k_2 q_e^2} + \frac{t}{q_e} \tag{8}$$

$$q_t = \frac{1}{\beta} \ln(\alpha\beta) + \frac{1}{\beta} \ln t \tag{9}$$

Where q_e is the amount of adsorbate on the unit adsorbent at adsorption equilibrium, mg/g; q_t is the amount of adsorbate on the unit adsorbent at the moment of t, mg/g; t is the time, min; k_1 is the adsorption rate constant of the pseudo-first kinetic adsorption model; k_2 is the adsorption rate constant of the pseudo-second kinetic adsorption model; α (mg/g/min) is the initial adsorption coefficient; β (g/mg) is the desorption coefficient.

RESULTS AND DISCUSSION

Optimization of pyrolysis conditions

In the RSM study, three factors including pyrolysis temperature (A), carbonization time (B), and activation ratio (C) were used as independent variables, and ZSC iodine adsorption amount was chosen as the response value (Y). The specific experimental factors and levels are shown in Supplementary Table 1. The experimental results are shown in Table 1. The results were regressed using Design Expert 12 software to establish the quadratic regression equation between iodine adsorption amount and the three single factors (pyrolysis temperature, pyrolysis time, and activation ratio). The analysis of variance (ANOVA) of the regression equations is shown in Supplementary Table 2. From the data in Supplementary Table 2, the model F-value was 22.66 and the *P*-value was 0.0002, indicating that the model could well optimize the

Table 1. Experimental design scheme and results

No.	Factor			Iodine adsorption capacity (mg/g)
	Pyrolysis temperature (°C)	Carbonization time (h)	Activation ratio	
1	700	1	1.25	274.16
2	900	1	1.25	289.55
3	700	2	1.25	296.92
4	900	2	1.25	285.2
5	700	1.5	0.5	300.91
6	900	1.5	0.5	303.47
7	700	1.5	2	318.35
8	900	1.5	2	320.66
9	800	1	0.5	300.67
10	800	2	0.5	285.75
11	800	1	2	304.53
12	800	2	2	320.19
13	800	1.5	1.25	324.53
14	800	1.5	1.25	335.21
15	800	1.5	1.25	340.99
16	800	1.5	1.25	339.58
17	800	1.5	1.25	338.79

preparation of biochar from dyeing sludge.

The response surface plots of the interaction effects of the different factors on iodine adsorption were shown in Figure 1. According to the model fitting, it could be obtained that the significance of the three factors was in the order of pyrolysis temperature > activation ratio > carbonization time. The quadratic terms A^2, B^2, and C^2 were all significant for the model ($P < 0.05$), and the interactions of the three factors were non-significant ($P > 0.05$). Figure 1A, C and E showed the interaction of all variables on iodine adsorption. As shown in Figure 1A, when the modification ratio was fixed, both calcination temperature and calcination time would affect iodine adsorption. Increasing calcination temperature could significantly increase iodine adsorption capacity, and the highest point of iodine adsorption appears at a calcination temperature of 800-850 °C for 1.4-1.7 h. As shown in Figure 1C, when the pyrolysis time was fixed, both temperature and modification ratio would affect iodine adsorption. At the same time, at lower temperatures, the iodine adsorption capacity was low, and the improvement of iodine adsorption capacity by modification ratio was not obvious, which meant that the iodine adsorption capacity could be improved at higher temperatures, and the highest point of iodine adsorption appears at 800-850 °C, and the modification ratio was between 1:1 and 2:1. The iodine adsorption of these two figures increased with rising pyrolysis temperatures, and the response surface inclination became more obvious. This suggested that the temperature elevation induced the dissociation of alkyl groups and a subsequent rise in aromaticity within the ZSC[33], thereby facilitating the formation of a porous framework and enhancing the adsorptive capacity. As shown in Figure 1E, when the temperature was fixed, both pyrolysis time and modification ratio would affect iodine adsorption, but the curvature of the surface depicted in Figure 1E was minimal and their impact on the quantity of iodine adsorbed was nearly equivalent. The peak time of iodine adsorption is 1.4-1.7 h, and the modification ratio was 1:1-2:1. As shown in Figure 1B, D and F, we could see that the interaction between the two experimental factors had a significant impact on the response variables. The contour lines in Figure 1B and D were elliptical, indicating that there was an obvious interaction between pyrolysis temperature and pyrolysis time, and between pyrolysis temperature and modification ratio. The contour lines in Figure 1F were close to a circle, indicating that the interaction between pyrolysis time and

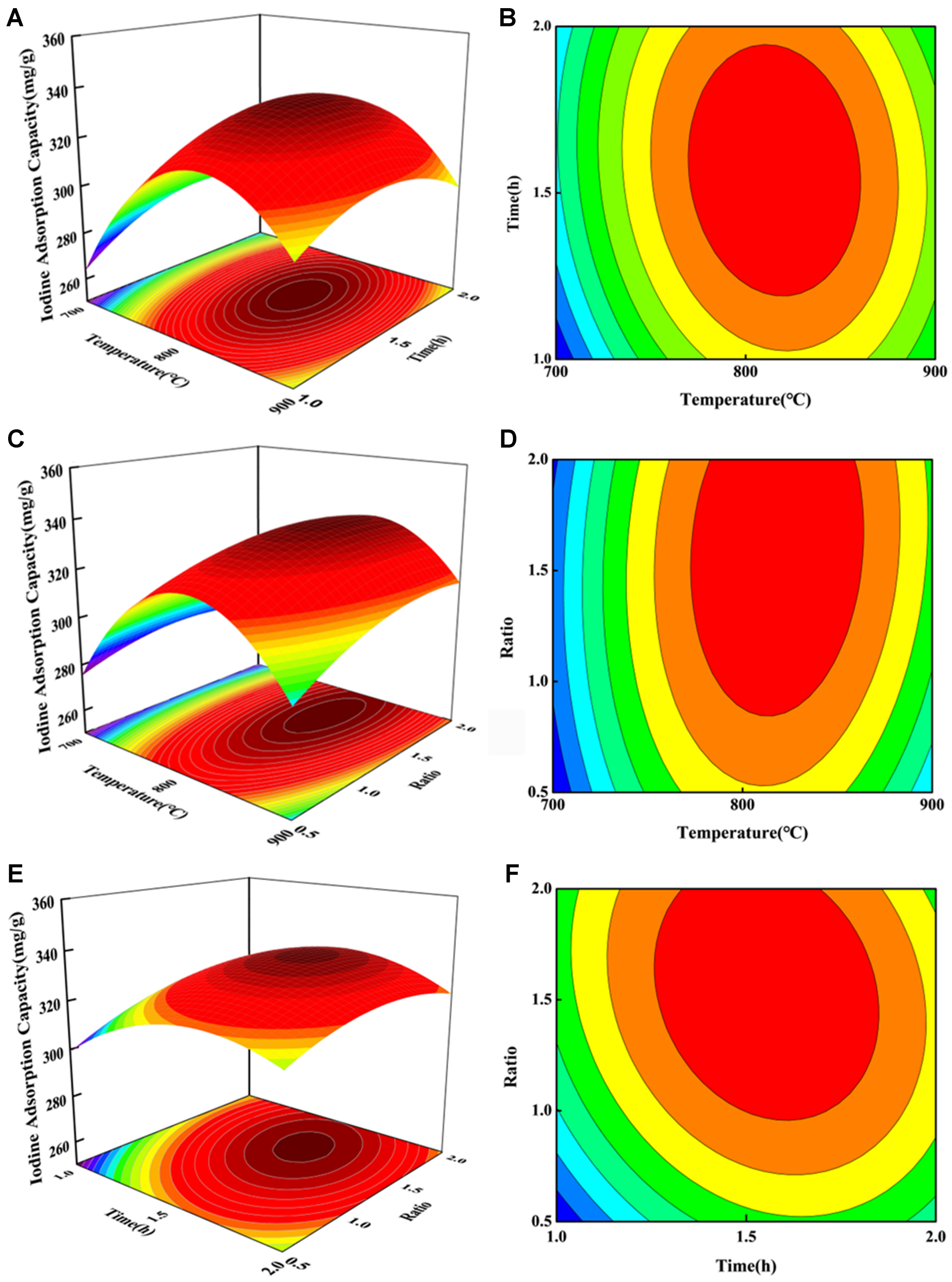

Figure 1. Response surfaces and contours of iodine adsorption by ZSC under three single factors. (A) Three-dimensional response surfaces and (B) contour plots of pyrolysis temperature (700-900 °C) *vs.* pyrolysis time (1.0-2.0 h); (C) Three-dimensional response surfaces and (D) contour plots of pyrolysis temperature (700-900 °C) *vs.* mass ratio of $ZnCl_2$ to sludge (1:2-2:1); (E) Three-dimensional response surfaces and (F) contour plots of pyrolysis time (1.0-2.0 h) *vs.* mass ratio of $ZnCl_2$ to sludge (1:2-2:1). ZSC: $ZnCl_2$ modified sludge biochar.

modification ratio was not significant. Based on the RSM results, the quadratic models for optimization of ZSC preparation were shown in Equation (10). From the model, the optimal preparation process of ZSC from dyeing sludge was selected as an activation temperature of 800 °C, an activation ratio of 1:1, and a carbonization time of 1.5 h. Under such conditions, the predicted iodine adsorption value in the model was 336.63 mg/g. In order to further validate the discrepancy between experimental and model-predicted values, validation experiments were carried out under the above conditions. The corresponding iodine adsorption value was 341.05 ± 1.31 mg/g, confirming the accuracy of this model. In summary, the pyrolysis temperature had the most significant effect on iodine adsorption, followed by the activation ratio and the carbonization time, which was similar to the experimental results obtained by Liang *et al.*[34].

$$Y = -2348.465 + 6.066A + 248.888B + 17.728C - 0.086AB + 0.049AC - 9.613BC - 0.004A^2 - 53.298B^2 - 13.661C^2 \quad (10)$$

Where Y is the iodine adsorption amount, mg/g; A, B, and C are the pyrolysis temperature, carbonization time, and the ratio of immersion activation, respectively.

Characterization of ZSC and SC

The surface morphology of ZSC ($ZnCl_2$ modified sludge biochar) and SC is shown in Figure 2A and B. The SC surface exhibited a sleek texture with minimal pore structure, while the ZSC obtained after $ZnCl_2$ activation showcased a rough and non-uniform surface composition adorned with aggregated fine particles adhering to its surface, alongside a more intricate pore arrangement. This observation was confirmed by the BET surface area [Table 2]. This was probably due to the fact that the $ZnCl_2$ activator promoted water release at higher temperatures (610 °C), leading to the expansion and unsealing of the sludge pores as zinc vapors and various gases were discharged. Accordingly, this process augmented the porosity of the ZSC[35]. Meanwhile, the presence of $ZnCl_2$ could accelerate the fragmentation of the organic matter in the sludge, consequently promoting the pore space in ZSC and enhancing the specific surface area of ZSC[31,36]. Meanwhile, the pore diameter and porosity of ZSC were also enhanced after the acid treatment to remove the metal oxide particles and ash on the surface[37].

The XRD patterns of the sludge biochar before and after modification are shown in Figure 2C. The diffraction patterns of the two sludge biochars exhibited a fundamental similarity involving a range of mineral constituents (such as silicon, calcium, *etc.*). However, the intensity of the diffraction peaks of ZSC surpassed that of SC at certain angles. A large number of diffraction peaks of SC were observed, notably at $2\theta = 20.95°$, 26.72°, and 50.22°, corresponding to the crystal surface reflections of SiO_2 (100), (011), and (112), respectively. Additionally, a peak at 26.65° corresponded to the reflection of graphitic carbon (002) crystals, while a distinct peak at 29.49° indicated the presence of $CaCO_3$, potentially attributed to the large amount of metal content within the sludge. After the modification with $ZnCl_2$, ZSC displayed distinct diffraction peaks, notably with enhanced intensity $2\theta = 20°$ and 26° compared to SC. Moreover, the narrow and sharply defined range of these peaks suggested an improved crystal structure and heightened crystallinity within ZSC. The weak diffraction peak at $2\theta = 45°$ corresponded to the crystalline reflection of graphitic carbon (100), implying that the prepared sample could potentially be a carbon-based material due to the accumulation of irregular aromatic layer structure[25,38].

As shown in Figure 2D, each band in the FT-IR spectra represented the vibration of functional groups in the ZSC and SC. The peaks of the two sludge carbon spectra appeared at basically similar wavelengths but with slightly different intensities. Such differences between ZSC and SC might be attributed to the various contents of surface functional groups. A broad and short peak appeared at a wavelength of 3,400 cm^{-1} (-OH expansion and contraction vibration) in the ZSC and SC samples, indicating that hydroxyl and carboxyl groups existed in both ZSC and SC. The spectral band at 2,923 cm^{-1} correlated with the aliphatic $-CH_3$ stretching vibration; however, this vibration presented as subdued, potentially attributable to the decomposition of aliphatic C–H bonds into gaseous byproducts like CO_2 and CH_4, or their conversion into aromatic configurations under high-temperature conditions, culminating in less pronounced absorption

Table 2. Pore structure characteristics of ZSC and SC

Dyeing sludge-derived biochar	Microporous specific surface area (cm^2/g)	Specific surface area (cm^2/g)	Pore volume (cm^3/g)	Total pore volume (cm^3/g)	Average pore diameter (nm)
ZSC	58.219	495.38	0.054	0.458	3.703
SC	42.227	359.78	0.039	0.333	3.698

ZSC: $ZnCl_2$ modified sludge biochar; SC: unmodified sludge biochar.

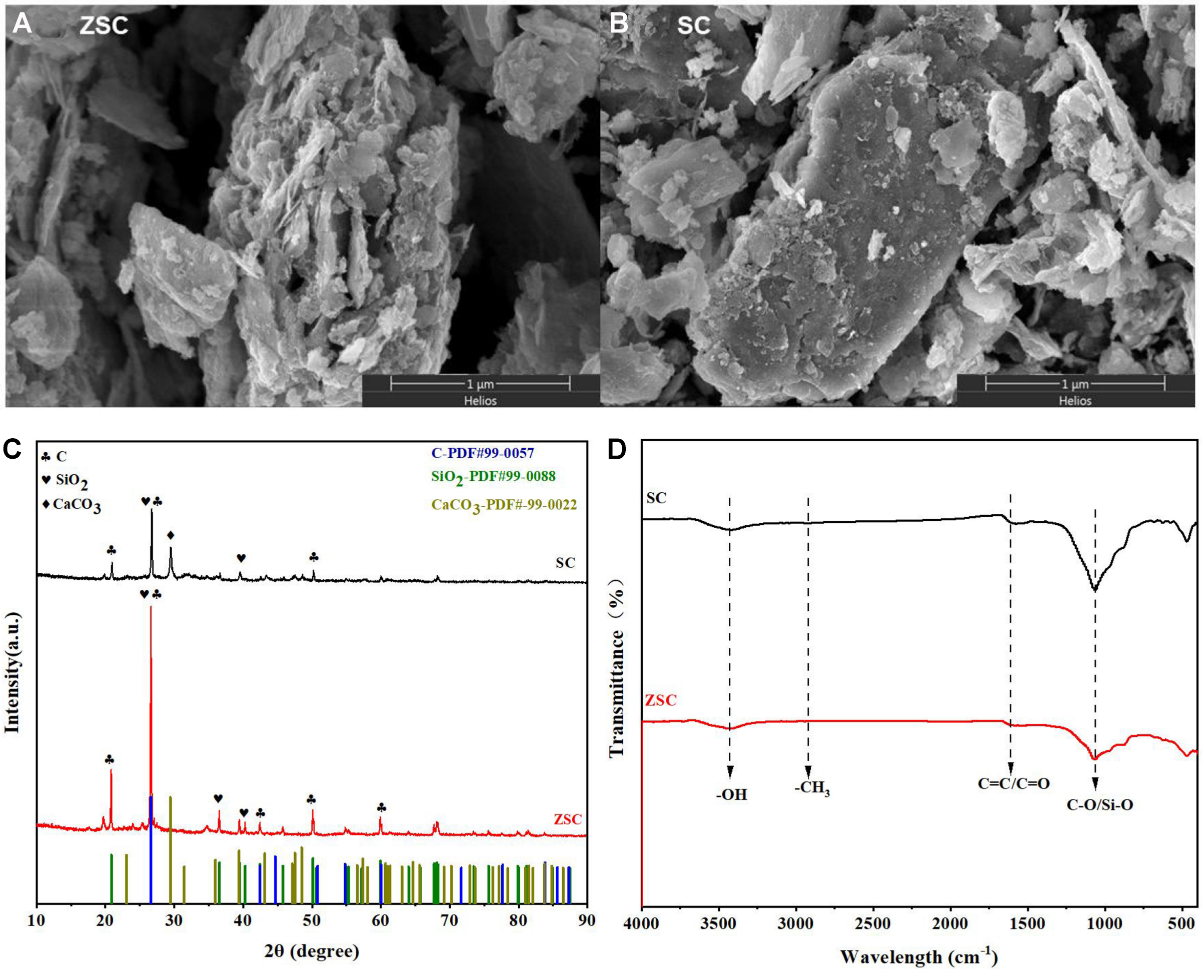

Figure 2. SEM images of (A) ZSC (B) and SC; (C) XRD pattern of ZSC and SC; and (D) FT-IR of ZSC and SC. SEM: Scanning electron microscopy; ZSC: $ZnCl_2$ modified sludge biochar; SC: unmodified sludge biochar; XRD: X-ray diffraction; FT-IR: Fourier transform infrared spectroscopy.

peaks[33]. The corresponding absorption peak at 1,650 cm^{-1} was attributed to the stretching vibration of C=C in the aromatic ring. The weak peaks at 800-1,100 cm^{-1} might be attributed to the stretching vibrations of functional groups such as C–H and C–O–C[39,40]. In addition, two sharp and wide absorption peaks appeared at 1,050 and 800 cm^{-1}, which corresponded to the stretching vibrations of C–O/Si–O and Si–O, respectively[35]. It should be noted that the strengths of functional groups in ZSC, especially in oxygen-containing groups, are weaker than those of SC. During the activation phase, $ZnCl_2$ was capable of engaging not merely with carbon, but also with the oxygen and hydrogen constituents of the biochar[30], attenuating the prominence of these characteristic peaks. This interaction was conjectured to promote the establishment of hydrogen bonds among the nitrogen and oxygen-containing groups on the contaminants.

The pore structure parameters as well as adsorption isotherms and pore size distribution curves of ZSC and SC derived from BET and Barrett-Joyner-Halenda (BJH) methods were shown in Table 2 and Figure 3. As present in Table 2, the specific surface area of ZSC and SC was higher than 350 cm^2/g, while the pore volume was higher than 0.03 cm^3/g. This result indicated high specific surface area and large pore volume in ZSC and SC, which facilitated the efficient and efficacious adsorption of dye, resulting in a markedly superior adsorptive performance[41]. Noticeably, the specific surface area and pore volume of ZSC were > 1.37-fold compared to those of SC, suggesting superior pore structure characteristics in ZSC. This pore structure contributes to better adsorption performance. As could be seen from Figure 3A and C, the adsorption-desorption isothermal curves of ZSC and SC belong to type IV isotherms with H_4 hysteresis loops in the IUPAC classification method, indicating that mesoporous structures existed in both materials. The adsorption and desorption were parallel and nearly horizontal, which might be due to the capillary coalescence phenomenon under low pressure[35,42]. Figure 3B and D showed the pore size distribution of ZSC and SC. The average pore size distribution of ZSC and SC was between 3-120 nm, and both of them were predominantly concentrated in the range of 3-10 nm. This result suggested that the pore structure of both kinds of sludge biochar was predominantly mesoporous, with a small number of macropores present. The results showed that the pore structures of ZSC and SC were suitable for the adsorption of pollutants. Given that ZSC possessed a greater specific surface area, larger pore structure, and an abundance of surface functional groups, it likely exhibited an exceptional adsorptive capacity of MG.

Effect of different factors on MG adsorption

In this study, the effects of five factors on the adsorption process, namely, adsorption equilibrium time, initial MG concentration and initial pH of MG solution, ZSC dosage, and adsorption temperature, were considered, and the results were shown in Figure 4. As depicted in Figure 4A, the rate of decolorization gradually escalated with the extension of the duration of MG adsorption by ZSC, culminating in a heightened adsorption rate until reaching a state of equilibrium, where the pace of adsorption gradually decelerated. The decolorization efficacy surged from 0% to 71% within the initial 120 min, followed by a 2.33% increment in the decolorization efficiency of MG between 120 and 210 min. Accordingly, the adsorption of MG by ZSC showed swiftness within the first 120 min, transitioning gradually to a sluggish adsorption process as time progressed toward equilibrium[43].

The change in solution pH value affects the surface charge of the adsorbent. As such, in this study, the effect of pH in the range of 2-10 on the adsorption process was examined, and the results are shown in Figure 4B. With the increase in pH, the removal rate of MG by ZSC gradually elevated. Notably, the removal rate of MG at pH = 10 was as high as 99.7%, inferring that ZSC was more suitable for MG removal in an alkaline environment. This may be due to the fact that MG was a cationic dye with a positive charge in an aqueous solution and at a pH > 10; this pH level surpassed the zero-charge threshold of ZSC, prompting the deprotonation of the oxygenated functional groups in ZSC[2], thereby facilitating the adsorption of MG. In contrast, in an acidic environment with a lower pH, the anionic groups in ZSC bind with H^+ in the solution and diminish the number of anionic adsorption sites, leading to a lower adsorption rate[44]. Therefore, pH = 10 was selected as the optimal pH for the adsorption process.

Figure 4C reflected the effect of the initial concentration of MG solution on the adsorption process. With the increase in MG concentration, the removal rate of MG gradually decreased. When treating the MG solution with a concentration of 400 mg/L, the removal rate reached about 50%. The reduction of MG removal was due to the saturation of adsorption capacity in ZSC[45]. If treating a high concentration of dye

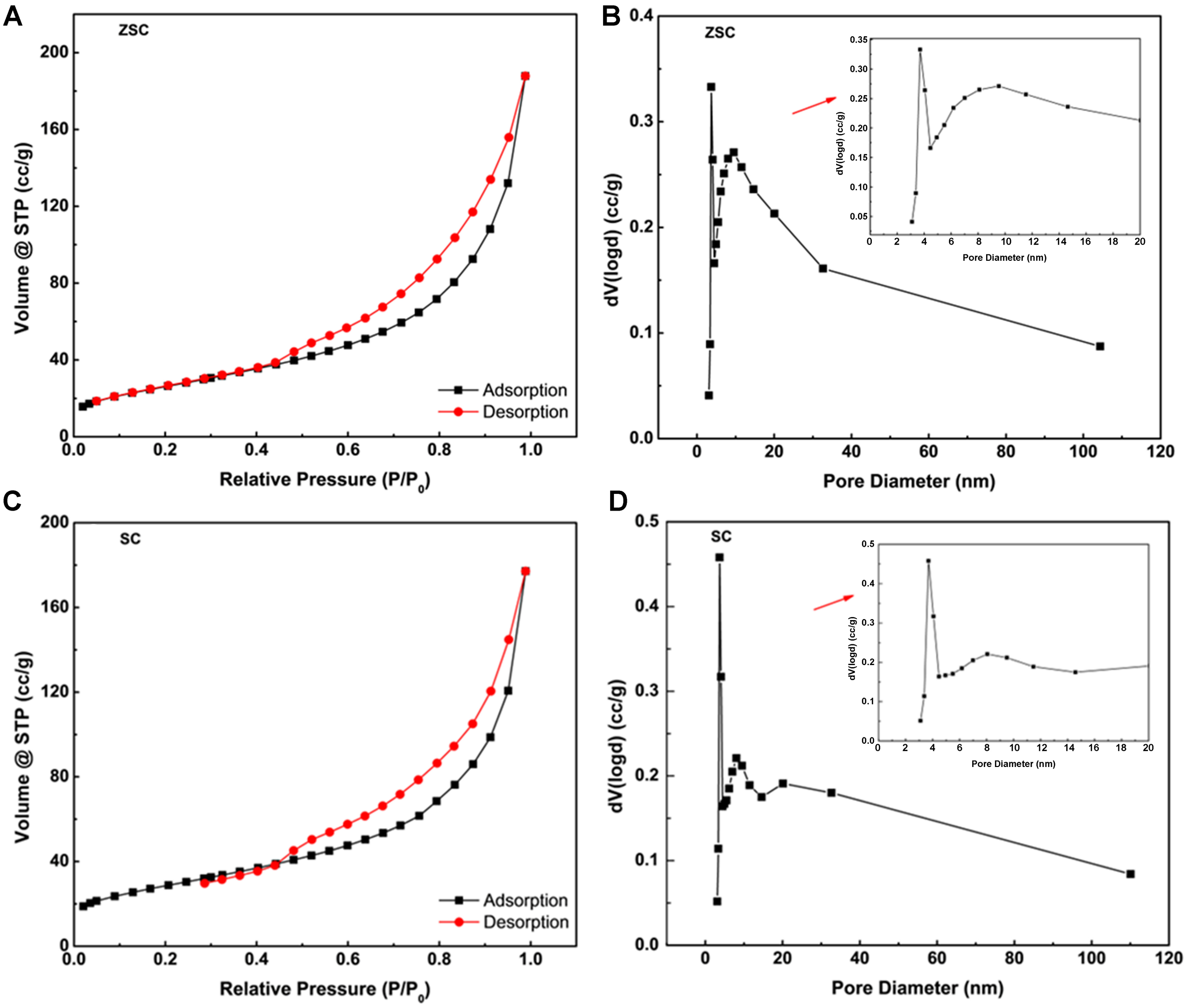

Figure 3. BET N_2-adsorption/desorption isotherm of (A and B) ZSC and (C and D) SC. BET: Brunauer–Emmett–Teller; ZSC: $ZnCl_2$ modified sludge biochar; SC: unmodified sludge biochar.

wastewater, it was necessary to dose more adsorbents in order to achieve a higher removal rate. In practice, the use of small quantities of adsorbents to treat high-concentration wastewater was unsatisfactory. Overall, a concentration of 150 mg/L was chosen as the optimum treatment concentration for the adsorption test.

Figure 4D examined the adsorption performance of MG with different ZSC dosages. The adsorption amount of MG exhibited a remarkable acceleration as the dosage of ZSC surged from 0.8 to 3.2 g/L. Correspondingly, the adsorption amount of MG increased from 79.44 to 261.30 mg/g. Further escalation of the dosage to 5 g/L slowly enhanced the adsorption amount to 298.38 mg/g, suggesting the saturation of adsorption process.

As shown in Figure 4E, temperature has a large influence on the adsorption process. Typically, the adsorption process tends to be inherently exothermic. Surprisingly, as the temperature rises during adsorption equilibrium, rather than a decline in adsorption capacity, there is an upward trend. This may be due to elevated temperatures fostering molecular diffusion, resulting in high adsorption capacity. Nonetheless, under lower temperatures, low adsorption capacity may be due to the influence of mass

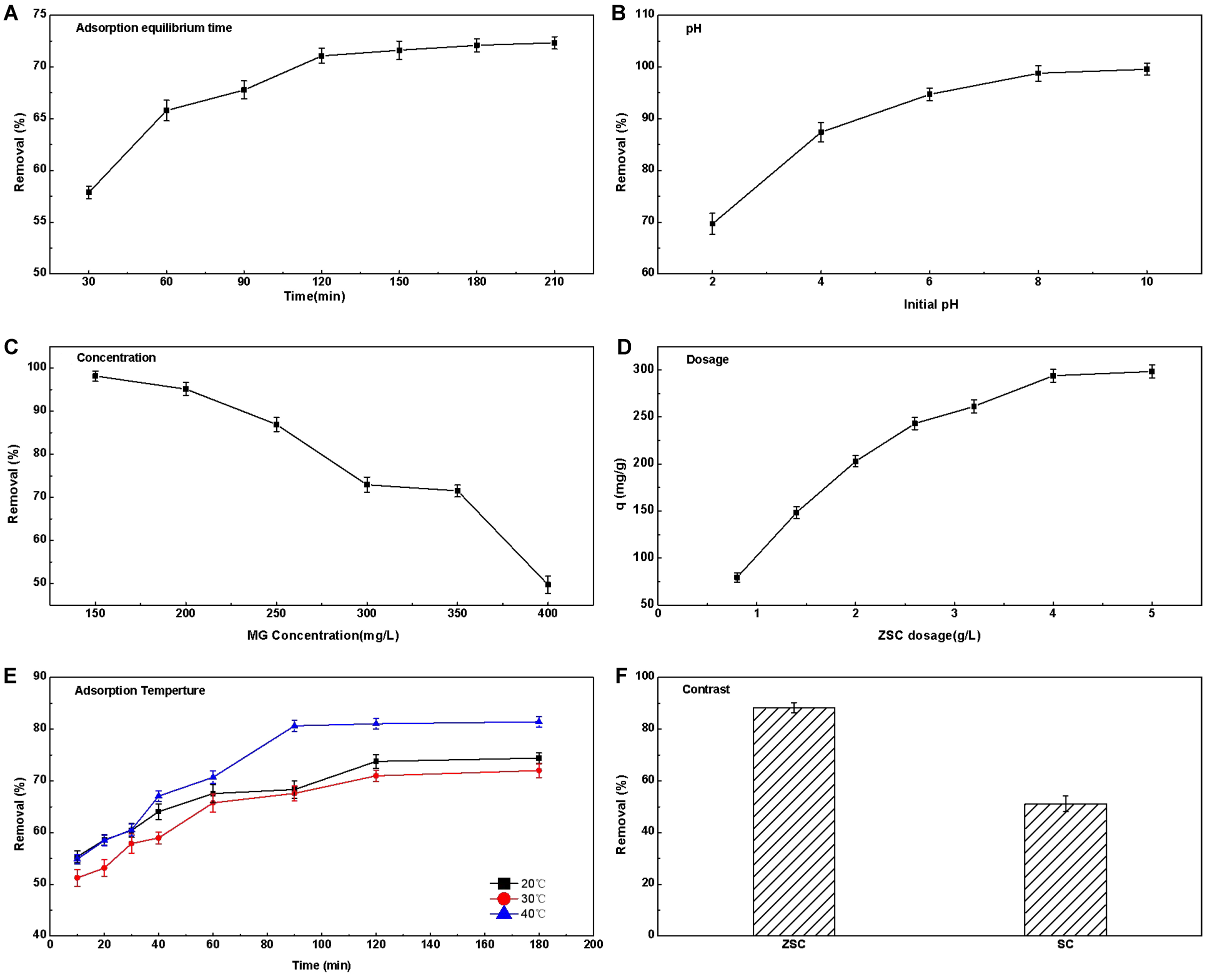

Figure 4. Impacts of different factors of ZSC on the MG adsorption. (A) Adsorption equilibrium time (operation condition: initial pH = stock solution, ZSC dosage = 2 g/L, MG concentration = 300 mg/L, and room temperature); (B) Initial pH of solution (operation condition: reaction time = 120 min, ZSC dosage = 2 g/L, MG concentration = 300 mg/L, and room temperature); (C) MG concentration (operation condition: initial pH = 10.0, reaction time = 120 min, ZSC dosage = 2 g/L, and room temperature); (D) ZSC dosage (operation condition: initial pH = 10.0, reaction time = 120 min, MG concentration = 150 mg/L, and room temperature); (E) Adsorption temperature (operation condition: initial pH = 10.0, reaction time = 120 min, ZSC dosage = 2 g/L, and MG concentration = 150 mg/L); and (F) Comparison results of MG removal rate by ZSC and SC. ZSC: $ZnCl_2$ modified sludge biochar; MG: malachite green; SC: unmodified sludge biochar.

transfer resistance and particle diffusion limiting the rate of adsorption[46,47]. Ebrahimian Pirbazari *et al.* reported an enhancement in adsorption capacity of 57 mg/g when increasing the temperature from 30 to 40 °C, which was attributed to the enhanced diffusion rate of the pollutant molecules in the external boundary layer and internal pores of the adsorbent particles[48]. To expedite the adsorption kinetics, it becomes imperative to elevate the temperature, thereby inducing a phenomenon where the adsorption quantity escalates[2,23]. When the adsorption temperature was 40 °C, the growth of the adsorption rate was obvious in the first 90 min, as indicated by the removal rate of 80.47%. The removal rate began to tend to equilibrium after 120 min. However, at 20 and 30 °C, the growth of the adsorption rate was slow, and the adsorption gradually tended to an equilibrium state after 180 min, as indicated by the MG removal of 75% or less. Therefore, the reaction temperature was selected to be 40 °C.

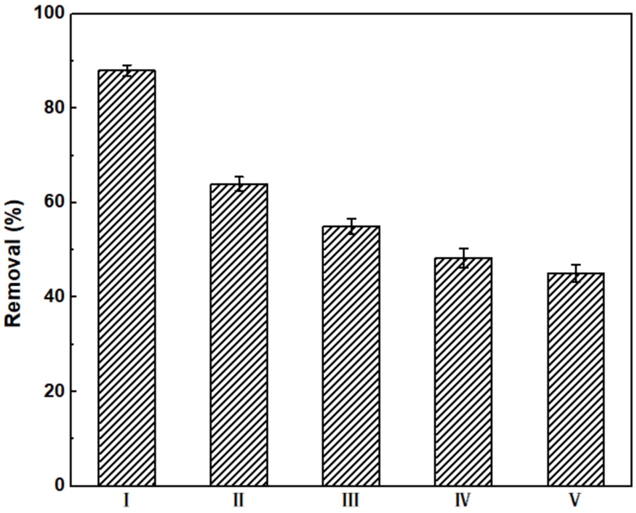

Figure 5. Reusability of ZSC as indicated by the MG removal. ZSC: $ZnCl_2$ modified sludge biochar; MG: malachite green.

In accordance with the above-mentioned results, the optimal conditions for MG removal were chosen as an initial pH of 10, an initial MG concentration of 150 mg/L, a ZSC dosage of 5 g/L, a reaction time of 120 min, and a temperature of 40 °C. Under such conditions, the removal rate of MG was as high as 99.13%.

In order to investigate the adsorption and decolorization effect of ZSC and SC on MG, the removal rate of MG was determined under the same conditions, and the results are shown in Figure 4F. The results showed that the removal rate of MG by ZSC was 37% higher than that of SC under the same conditions, which indicated that the activated sludge biochar had better adsorption performance. Employing dyeing sludge as an adsorbent enhanced the value proposition of sludge utilization, facilitating a more resourceful and sustainable approach to its utilization.

Reusability performance and comparative results of different sludge-derived biochar

In order to evaluate the durability and reusability of the ZSC system, a sequence of five-cycle tests was carried out for MG removal. The results of the adsorption performance of ZSC on MG after reusing were shown in Figure 5. The removal rate of MG by ZSC was close to 90% in the first round, while it was found that the removal rate of MG by ZSC was still around 50% after five cycles. It could be seen that the reusability of sludge-activated carbon was relatively high and could be reused to treat low-concentration dyeing in wastewater.

A comparative analysis of the adsorption efficacy of various sludge-derived biochar materials is presented in Table 3. The adsorption capacities of the modified carbon materials were 2.6-13.1 times higher than those of the unmodified ones, suggesting that chemical modification can promote pore formation and improve the adsorption performance of the materials. In addition, the dyeing sludge-derived biochar activated with $ZnCl_2$ in this study exhibited superior adsorption capabilities and specific surface areas, surpassing the performance of most previously documented adsorbents[49-53]. Unlike other adsorbents necessitating intricate production processes, severe operational conditions, or frequent replacements, this particular biochar can withstand complex conditions and demonstrate practical utility. With an adsorption capacity of 341.0 mg/g and a specific surface area of 495.4 m^2/g, this ZSC biochar exhibited excellent adsorption performance of MG.

Table 3. Comparison of different sludge-derived biochars and their adsorption properties on dyes

Adsorbents	Activating agent	Dye	S_{BET} (m^2/g)	Adsorption capacity (mg/g)	Ref.
Yarn sludge-derived biochar	KI/KOH	MG	1,037.0	498.0	[46]
Sewage sludge-derived biochar	Acetone	MG	17.0	38.6	[47]
Sewage sludge/waterworks sludge-derived biochar	/	Methylene blue	45.5	186.0	[48]
Sewage sludge-derived biochar	/	Remazol brilliant blue R	12.4	87.0	[49]
Sewage sludge/lignin-derived biochar	/	Methylene blue	33.6	38.1	[50]
Dyeing sludge-derived biochar	$ZnCl_2$	MG	495.4	341.0	This study

BET: Brunauer–Emmett–Teller; MG: malachite green.

Adsorption mechanism

Adsorption thermodynamic study

In Supplementary Table 3, it could be seen that the R^2 value of Langmuir isotherm (0.6819) was higher than that of Freundlich isotherm (0.4276), indicating the adsorption behavior of ZSC on MG probably conformed to the Langmuir isotherm. The maximum adsorption of MG by ZSC was 224.0962 mg/g, suggesting that the adsorption of MG occurring at ZSC was monomolecular layer adsorption.

Adsorption kinetic study

Adsorption temperature is a key factor in the removal of pollutants from water by adsorbents[20]. To further evaluate the adsorption kinetic behavior at different temperatures, quasi-primary and quasi-secondary models were used to fit the adsorption curves. Figure 6 and Supplementary Tables 4 and 5 reflected the relevant parameters of adsorption kinetics. In Supplementary Table 4, the maximum adsorption capacity in the pseudo-first model was 35.8234, 43.1939, and 48.9892 mg/g, respectively, at 20, 30, and 40 °C. Correspondingly, in Supplementary Table 5, the largest adsorption capacity at 20, 30, and 40 °C in the pseudo-second model was 114.9425, 112.3596, and 129.8701 mg/g, respectively. Notably, the maximum adsorption capacity in the pseudo-second model was remarkably higher than that of the pseudo-first model. The Elovich model is commonly used to describe the adsorption and desorption processes of chemisorption on non-uniform surfaces, and the results are shown in Figure 6D and Supplementary Table 6. The correlation coefficients indicated that the adsorption process fits well with the Elovich model, and in this experiment, the adsorption rate was much larger than the desorption rate[54]. Furthermore, by comparing the R^2 values of the pseudo-first, pseudo-second kinetic equations and Elovich equations, it was found that the linear correlation coefficient of the pseudo-second kinetic model was closer to 1. Therefore, the process of MG adsorption by ZSC was more suitable to be described by the pseudo-second kinetic model. In addition, this paper further used the intra-particle diffusion model to fit the data on the adsorption capacity of the wastewater treated by the material with time, and the results are shown in Figure 6E and Supplementary Table 7. By segmenting the fitted curves, it was believed that the adsorption process could be roughly divided into two stages: the surface mass transfer stage and the intra-particle diffusion process. By comparing the values of K_d in the different stages, the value of K_{d2} was found to be the smallest in the second stage, which indicated that the rate of the intra-particle diffusion process slowed down until the adsorption rate decreased. Then, the rate of the process slows down until the adsorption is saturated. Meanwhile, the adsorption capacity q_t of the material showed a good linear relationship with $t^{1/2}$, but did not pass through the origin, indicating that the internal diffusion is not the only rapid control step of the adsorption process[55,56]. Based on the above results, it is illustrated that the overall adsorption reaction rate is controlled by the chemical adsorption process rather than by the mass transfer process[20,57].

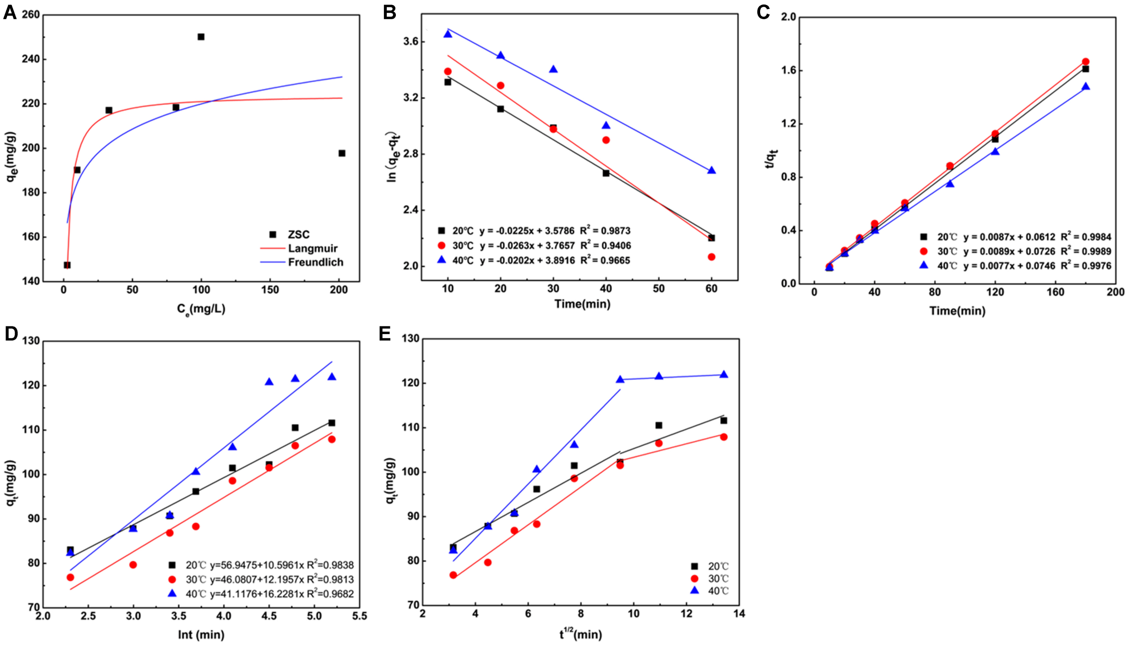

Figure 6. Adsorption isotherms. (A) Langmuir and Freundlich adsorption isotherms, and adsorption kinetic; (B) Pseudo-primary kinetics; and (C) Pseudo-secondary kinetics, (D) Elovich, (E) Intraparticle.

Adsorption summary

According to the literature research, the adsorption mechanism of organic substances by biochar predominantly included pore filling, hydrogen bonding, π-π interactions, electrostatic interactions, and complexation with oxygenated functional groups[58,59]. In this study, the adsorption behavior of ZSC on MG was explored by adsorption isotherms, adsorption kinetics, and experiments with different environmental factors. Results showed that the adsorption of MG by ZSC was notably in accordance with the pseudo-second kinetics and the Langmuir model. As such, the progression of the reaction was primarily ascribed to chemical factors, characterized by monolayer adsorption of individual molecules on a uniform surface, aligning with the results made by Gao *et al.*[21]. ZSC obtained a larger specific surface area and pore structure after pyrolytic carbonization, leading to increased surface active sites, which could be explained by the fact that higher temperature contributes to the decomposition and escape of volatiles, tars, and other products, leading to more microporous structures and larger specific surface area of biochar, and also affects the number of surface active sites of biochar[60]. Upon saturation of the surface active sites, MG slowly diffused into the pores, causing the low removal of MG. This result confirmed that the pore filling was involved in the adsorption process. Additionally, pyrolysis temperature could affect the order of formation of functional groups, and higher pyrolysis temperatures could increase the degree of aromatization of biochar[61]. The FT-IR results showed that ZSC contained functional groups such as –OH, C–O, and C=C, which were able to be attracted to form hydrogen bonding by the nitrogenous groups on the MG that were strongly negatively charged[62]. Moreover, oxygen-containing groups such as C–O were highly aromatized, which were hypothesized to be capable of π-π stacking[63], promoting efficient dye removal. As the pH increased, the acidic groups on the surface of biochar were ionized or dissociated, resulting in an increase in the negative surface charge and the enhancement of the electrostatic interaction of biochar[64], which was consistent with our results [Figure 4B]. The elevation of pH corresponded to a rise in the adsorption capacity of ZSC, suggesting that electrostatic interactions played a more significant role in the adsorption process. Overall, electrostatic interactions, pore filling, hydrogen bonding, and π-π interactions were responsible for the high MG removal in the ZSC adsorption process [Figure 7].

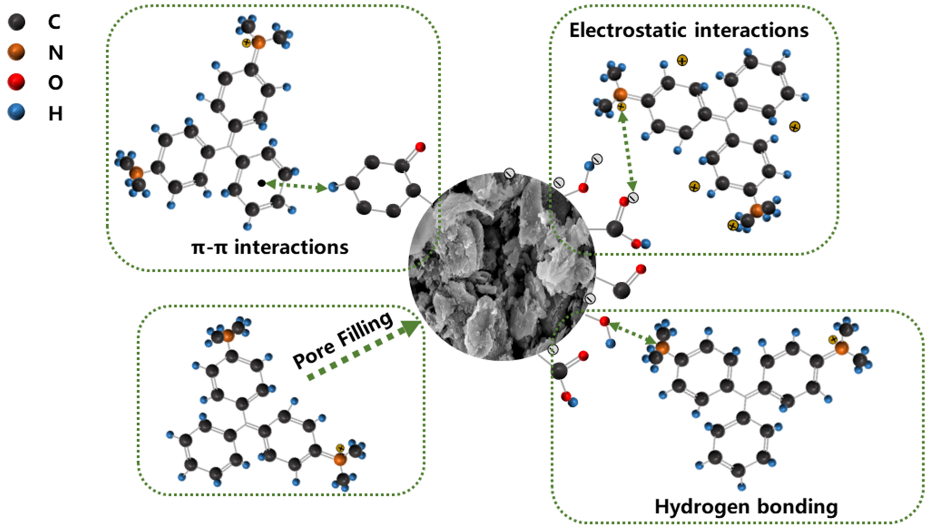

Figure 7. The adsorption mechanism of MG captured by ZSC. MG: malachite green; ZSC: $ZnCl_2$ modified sludge biochar.

CONCLUSION

In this study, a cost-effective dye adsorbent was successfully prepared from dyeing sludge. The combination of pyrolysis temperature, activation ratio, and carbonization time of 800 °C, 1:2 and 1.5 h, respectively, was found to be the optimal preparation conditions by response surface method, and the iodine adsorption value of ZSC was 340.99 mg/g. Meanwhile, the pyrolysis temperature was found to be the main factor affecting the pyrolysis process, followed by the activation ratio through the significance of each factor. The dyeing sludge biochar modified by $ZnCl_2$ activation had a better pore structure with a specific surface area of 495.38 cm^2/g. The adsorption equilibrium time, initial pH, initial MG concentration, ZSC dosage, and adsorption temperature would affect the removal of MG. Under the optimal conditions, the adsorption removal of MG by ZSC was as high as 99.13%. After five reuse cycles, ZSC could still adsorb 45% of MG. The adsorption performance conformed well to the Langmuir-type adsorption isotherm and pseudo-second kinetic model. In the ZSC adsorption process, electrostatic interactions, pore filling, hydrogen bonding, and π-π interactions could reflect the mechanism of high MG removal. In summary, employing sludge-derived activated carbon for the purification of organic wastewater could be a better choice for reducing and recovering sludge, while also proficiently processing dyeing wastewater.

DECLARATIONS

Authors' contributions

Conceptualization, methodology, data analysis: Qian W
Writing - original draft, investigation, data analysis: Deng Y
Investigation: Zhang Y
Data curation: Li Y
Visualization: Fang Y
Data curation, software: Li X
Writing - reviewing and editing, supervision: Liang J
Supervision, funding acquisition: Liu H
All authors listed have made a substantial, direct and intellectual contribution to the work and approved the final manuscript for publication.

Availability of data and materials

Data will be made available upon reasonable request.

Financial support and sponsorship

This work was supported by the Guangdong Basic and Applied Basic Research Foundation (2022A1515110629) and the Basic and Applied Basic Research Project of Guangzhou (2023A04J0957).

Conflicts of interest

All authors declared that there are no conflicts of interest.

Ethical approval and consent to participate

Not applicable.

Consent for publication

Not applicable.

Copyright

REFERENCES

1. Xue G. Technology progress of dyeing wastewater treatment. *Ind Water Treat* 2021;41:10-7. DOI
2. Jia S, Huang MJ, Zhang B, Wei ZY, Cheng H, Li SZ. Research progress of biomass based carbon materials in the treatment of dyeing wastewater. *Chem Ind Forest Prod* 2023;43:145-56. DOI
3. Ou SF, Yang DS, Liao JW, Chen ST. Treating high COD dyeing wastewater via a regenerative sorption-oxidation process using a nano-pored activated carbon. *Int J Mol Sci* 2022;23:4752. DOI
4. Kolya H, Kang CW. Toxicity of metal oxides, dyes, and dissolved organic matter in water: implications for the environment and human health. *Toxics* 2024;12:111. DOI PubMed PMC
5. de Freitas LVP, Silveira JGF, Damaceno MA, et al. Evaluating the persistence of malachite green residues in tilapia and pacu fish. *Environ Toxicol Pharmacol* 2024;106:104382. DOI PubMed
6. Zahuri AA, Abdul Patah MF, Kamarulzaman Y, et al. Decolourisation of real industrial and synthetic textile dye wastewater using activated dolomite. *Water* 2023;15:1172. DOI
7. Dissanayake NSL, Pathirana MA, Wanasekara ND, Mahltig B, Nandasiri GK. Removal of methylene blue and Congo red using a chitosan-graphene oxide-electrosprayed functionalized polymeric nanofiber membrane. *Nanomaterials* 2023;13:1350. DOI PubMed PMC
8. Nguyen DDD, Phan Quang HH, Nguyen XH, Nguyen TP. The treatment of real dyeing wastewater by the electro-Fenton process using drinking water treatment sludge as a catalyst. *RSC Adv* 2021;11:27443-52. DOI PubMed PMC
9. Dong H, Liu H, Yang X, et al. The effect of initial conditions with aerobic biological treatment on aniline dyeing wastewater. *Processes* 2021;9:1329. DOI
10. Lin X, Zhou Q, Xu H, Chen H, Xue G. Advances from conventional to biochar enhanced biotreatment of dyeing wastewater: a critical review. *Sci Total Environ* 2024;907:167975. DOI PubMed
11. Deng D, Lamssali M, Aryal N, Ofori-Boadu A, Jha MK, Samuel RE. Textiles wastewater treatment technology: a review. *Water Environ Res* 2020;92:1805-10. DOI PubMed
12. Xue T, Shao F, Miao H, Li X. Porous polymer magnetic adsorbents for dye wastewater treatment. *Environ Sci Pollut Res Int* 2023;30:97147-59. DOI PubMed
13. He Y, Ni L, Gao Q, et al. Activated carbon with ultrahigh specific surface derived from bamboo shoot shell through K_2FeO_4 oxidative pyrolysis for adsorption of methylene blue. *Molecules* 2023;28:3410. DOI PubMed PMC
14. Castaldo R, Avolio R, Cocca M, Errico ME, Avella M, Gentile G. Amino-functionalized hyper-crosslinked resins for enhanced adsorption of carbon dioxide and polar dyes. *Chem Eng J* 2021;418:129463. DOI
15. Chen S, Tang S, Sun Y, et al. Preparation of a highly porous carbon material based on quinoa husk and its application for removal of dyes by adsorption. *Materials* 2018;11:1407. DOI PubMed PMC
16. Song J, Deng Q, Huang M, Kong Z. Carbon nanotube enhanced membrane distillation for salty and dyeing wastewater treatment by electrospinning technology. *Environ Res* 2022;204:111892. DOI PubMed
17. Boulanger N, Talyzin AV, Xiong S, Hultberg M, Grimm A. High surface area activated carbon prepared from wood-based spent mushroom substrate for supercapacitors and water treatment. *Colloid Surfaces A* 2024;680:132684. DOI
18. Lu J, Zhang Q, An Q, et al. Preparation of activated carbon from sewage sludge using green activator and its performance on dye

wastewater treatment. *Environ Technol* 2023;44:3897-910. DOI

19. Li L, Ai J, Zhang W, et al. Relationship between the physicochemical properties of sludge-based carbons and the adsorption capacity of dissolved organic matter in advanced wastewater treatment: effects of chemical conditioning. *Chemosphere* 2020;243:125333. DOI PubMed
20. Gong Y, Liu F, Liu H, Wang H, Zhao Y, Lin Y. Technology transition strategies for textile-dyeing sludge management in China from the environmental and economic perspectives. *Sustain Prod Consump* 2023;43:363-76. DOI
21. Gao J, Zhou Y, Yang X, et al. Dyeing sludge-derived biochar for efficient removal of antibiotic from water. *Sci Total Environ* 2024;912:169035. DOI PubMed
22. Fan Z, Zhou X, Peng Z, et al. Co-pyrolysis technology for enhancing the functionality of sewage sludge biochar and immobilizing heavy metals. *Chemosphere* 2023;317:137929. DOI PubMed
23. Chen C, Sun J, Li Y, Zhao X, Wu H. Adsorption of methylene blue on activated carbon prepared from printing sludge. *Chin J Environ Eng* 2018;12:1872-8. Available from: http://eekw.rcees.ac.cn/en/article/doi/10.12030/j.cjee.201710068. [Last accessed on 24 Jul 2024]
24. Wong S, Ngadi N, Inuwa IM, Hassan O. Recent advances in applications of activated carbon from biowaste for wastewater treatment: a short review. *J Clean Prod* 2018;175:361-75. DOI
25. Zhang H, Wei Z, Xiong D, et al. Investigation into the structure and properties of biochar co-activated by $ZnCl_2$ and $NaHCO_3$ under low temperature conditions. *Materials* 2024;17:942. DOI PubMed PMC
26. Oke N, Mohan S. Development of nanoporous textile sludge based adsorbent for the dye removal from industrial textile effluent. *J Hazard Mater* 2022;422:126864. DOI PubMed
27. Wei S, Zhu M, Fan X, et al. Influence of pyrolysis temperature and feedstock on carbon fractions of biochar produced from pyrolysis of rice straw, pine wood, pig manure and sewage sludge. *Chemosphere* 2019;218:624-31. DOI PubMed
28. Moško J, Pohořelý M, Skoblia S, et al. Structural and chemical changes of sludge derived pyrolysis char prepared under different process temperatures. *J Anal Appl Pyrol* 2021;156:105085. DOI
29. Zou J, Yu J, Tang L, et al. Analysis of reaction pathways and catalytic sites on metal-free porous biochar for persulfate activation process. *Chemosphere* 2020;261:127747. DOI PubMed
30. Wang RZ, Huang DL, Liu YG, et al. Recent advances in biochar-based catalysts: properties, applications and mechanisms for pollution remediation. *Chem Eng J* 2019;371:380-403. DOI
31. Thue PS, Lima DR, Lima EC, et al. Comparative studies of physicochemical and adsorptive properties of biochar materials from biomass using different zinc salts as activating agents. *J Environ Chem Eng* 2022;10:107632. DOI
32. Ferraro A, Marino E, Trancone G, et al. Assessment of environmental parameters effect on potentially toxic elements mobility in foreshore sediments to support marine-coastal contamination prediction. *Mar Pollut Bull* 2023;194:115338. DOI PubMed
33. Wang X, Li C, Li Z, Yu G, Wang Y. Effect of pyrolysis temperature on characteristics, chemical speciation and risk evaluation of heavy metals in biochar derived from textile dyeing sludge. *Ecotoxicol Environ Saf* 2019;168:45-52. DOI PubMed
34. Liang X, Ning X, Lin C, et al. Optimization of preparation conditions for activated carbons from textile dyeing sludge and sawdust using response surface methodology based on CCD. *Chin J Environ Eng* 2014;8:4937-42. Available from: http://hjhx.rcees.ac.cn/en/article/id/20141161?viewType=HTML. [Last accessed on 24 Jul 2024].
35. Zhao WX, Zhou JY, Chen L, et al. Preparation and adsorption and catalytic performance of municipal sludge biochar. *Chem Res Appl* 2022;34:2531-7. Available from: https://cstj.cqvip.com/Qikan/Article/Detail?id=7108273947&from=Qikan_Search_Index. [Last accessed on 24 Jul 2024].
36. Varela CF, Moreno-aldana L, Agámez-pertuz YY. Adsorption of pharmaceutical pollutants on $ZnCl_2$-activated biochar from corn cob: efficiency, selectivity and mechanism. *J Bioresour Bioprod* 2024;9:58-73. DOI
37. Li Y, Chang F, Huang B, Song Y, Zhao H, Wang K. Activated carbon preparation from pyrolysis char of sewage sludge and its adsorption performance for organic compounds in sewage. *Fuel* 2020;266:117053. DOI
38. Mahapatra U, Chatterjee A, Das C, Manna AK. Chemically activated carbon preparation from natural rubber biosludge for the study of characterization, kinetics and isotherms, thermodynamics, reusability during Cr(VI) and methylene blue adsorption. *Water Sci Technol* 2023;87:635-59. DOI PubMed
39. Jian H, Yang F, Gao Y, et al. Efficient removal of pyrene by biochar supported iron oxide in heterogeneous Fenton-like reaction via radicals and high-valent iron-oxo species. *Sep Purif Technol* 2021;265:118518. DOI
40. Chen J, Bai X, Yuan Y, Zhang Y, Sun J. Printing and dyeing sludge derived biochar for activation of peroxymonosulfate to remove aqueous organic pollutants: activation mechanisms and environmental safety assessment. *Chem Eng J* 2022;446:136942. DOI
41. Zhai S, Li M, Wang D, Ju X, Fu S. Cyano and acylamino group modification for tannery sludge bio-char: enhancement of adsorption universality for dye pollutants. *J Environ Chem Eng* 2021;9:104939. DOI
42. Li K, Lu H, Zhang Q, Li J. Adsorption of Cd(II) and Cu(II) onto clay modified with sludge activated carbon. *KSCE J Civ Eng* 2020;24:1706-16. DOI
43. Wang B, Zhai Y, Wang T, et al. Fabrication of bean dreg-derived carbon with high adsorption for methylene blue: effect of hydrothermal pretreatment and pyrolysis process. *Bioresour Technol* 2019;274:525-32. DOI PubMed
44. Xiao J, Wang L, Ran J, Zhao J, Tao M, Zhang W. Highly selective removal of cationic dyes from water by acid-base regulated anionic functionalized polyacrylonitrile fiber: fast adsorption, low detection limit, reusability. *React Funct Polym* 2020;146:104394. DOI
45. Oladoye PO, Ajiboye TO, Wanyonyi WC, Omotola EO, Oladipo ME. Insights into remediation technology for malachite green wastewater treatment. *Water Sci Eng* 2023;16:261-70. DOI
46. Maiti P, Mangsatabam M, Chatterjee A, Siddiqi H, Mishra A, Meikap B. In-situ synthesis of efficient $ZnCl_2$ doped pyrolyzed biochar

for adsorptive remediation of organic dyes: performance evaluation, mass transfer and mechanism. *Sep Purif Technol* 2024;329:125096. DOI

47. Azim E, Samy M, Hanafy M, Mahanna H. Novel mint-stalks derived biochar for the adsorption of methylene blue dye: effect of operating parameters, adsorption mechanism, kinetics, isotherms, and thermodynamics. *J Environ Manage* 2024;357:120738. DOI PubMed
48. Pirbazari A, Saberikhah E, Badrouh M, Emami MS. Alkali treated Foumanat tea waste as an efficient adsorbent for methylene blue adsorption from aqueous solution. *Water Res Ind* 2014;6:64-80. DOI
49. Tang SH, Zaini MAA. Microporous activated carbon prepared from yarn processing sludge via composite chemical activation for excellent adsorptive removal of malachite green. *Surf Interfaces* 2021;22:100832. DOI
50. Leng L, Yuan X, Huang H, et al. Bio-char derived from sewage sludge by liquefaction: characterization and application for dye adsorption. *Appl Surf Sci* 2015;346:223-31. DOI
51. Zeng H, Qi W, Zhai L, Wang F, Zhang J, Li D. Magnetic biochar synthesized with waterworks sludge and sewage sludge and its potential for methylene blue removal. *J Environ Chem Eng* 2021;9:105951. DOI
52. Raj A, Yadav A, Rawat AP, et al. Kinetic and thermodynamic investigations of sewage sludge biochar in removal of remazol brilliant blue R dye from aqueous solution and evaluation of residual dyes cytotoxicity. *Environ Technol Innov* 2021;23:101556. DOI
53. Dai Q, Liu Q, Zhang X, et al. Synergetic effect of co-pyrolysis of sewage sludge and lignin on biochar production and adsorption of methylene blue. *Fuel* 2022;324:124587. DOI
54. Li Y, Zhao M, Yan H, et al. Silica from rice husk for sludge-based biochar modification: as a novel adsorbent for lead. *J Water Process Eng* 2024;60:105218. DOI
55. Zhao Z, Sun W, Ray MB. Adsorption isotherms and kinetics for the removal of algal organic matter by granular activated carbon. *Sci Total Environ* 2022;806:150885. DOI PubMed
56. Li H, Kong J, Zhang H, et al. Mechanisms and adsorption capacities of ball milled biomass fly ash/biochar composites for the adsorption of methylene blue dye from aqueous solution. *J Water Process Eng* 2023;53:103713. DOI
57. Chen Y, Li M, Li Y, et al. Hydroxyapatite modified sludge-based biochar for the adsorption of Cu^{2+} and Cd^{2+}: adsorption behavior and mechanisms. *Bioresour Technol* 2021;321:124413. DOI PubMed
58. Gayathiri M, Pulingam T, Lee KT, Sudesh K. Activated carbon from biomass waste precursors: factors affecting production and adsorption mechanism. *Chemosphere* 2022;294:133764. DOI PubMed
59. Qu J, Wang Y, Tian X, et al. KOH-activated porous biochar with high specific surface area for adsorptive removal of chromium (VI) and naphthalene from water: affecting factors, mechanisms and reusability exploration. *J Hazard Mater* 2021;401:123292. DOI
60. Zhang W, Du W, Wang F, et al. Comparative study on Pb^{2+} removal from aqueous solutions using biochars derived from cow manure and its vermicompost. *Sci Total Environ* 2020;716:137108. DOI PubMed
61. Liu C, Li H, Ni JQ, et al. Effect of municipal sludge-based biochar produced at different pyrolysis temperatures on humification and oxytetracycline degradation of pig manure composting. *Sci Total Environ* 2024;906:167816. DOI PubMed
62. Zhao W, Zhao Y, Zhang H, Hao C, Zhao P. Efficient removal of cationic and anionic dyes by surfactant modified Fe_3O_4 nanoparticles. *Colloid Surfaces A* 2022;633:127680. DOI
63. Wu JL, He H, Huang JY, Chen YR, Zhang WJ, Wang DS. Preparation of dyeing sludge-based carbon and its adsorption characteristics of dissolved organic matter in dredged residual water. *Saf Environ Eng* 2022;29:174-82. DOI
64. Zeng Y, Lin Y, Ma M, Chen H. Adsorption effect and mechanism of Cd(II) by different phosphorus-enriched biochars. *Environ Sci Pollut Res Int* 2024;31:16642-52. DOI PubMed

Wang *et al. Water Emerg Contam Nanoplastics* 2024;3:19
DOI: 10.20517/wecn.2024.14

Water Emerging Contaminants & Nanoplastics

Review

Open Access

Utilizing microorganisms immobilized on carbon-based materials for environmental remediation: a mini review

Lei Wang[1,2], **Dongle Cheng**[1,2], **Xiaoqing Liu**[3], **Yuanyao Ye**[4]

[1]College of Safety and Environmental Engineering, Shandong University of Science and Technology, Qingdao 266590, Shandong, China.
[2]Institute of Yellow River Delta Earth Surface Processes and Ecological Integrity, Shandong University of Science and Technology, Qingdao 266590, Shandong, China.
[3]Centre for Technology in Water and Wastewater, School of Civil and Environmental Engineering, University of Technology Sydney, Sydney 2007, Australia.
[4]School of Environmental Science and Engineering, Huazhong University of Science and Technology, Wuhan 430074, Hubei, China.

Correspondence to: Prof. Dongle Cheng, College of Safety and Environmental Engineering, Shandong University of Science and Technology, 579 Qianwangang Road, Huangdao District, Qingdao 266590, Shandong, China. E-mail: donglelecheng@gmail.com

How to cite this article: Wang L, Cheng D, Liu X, Ye Y. Utilizing microorganisms immobilized on carbon-based materials for environmental remediation: a mini review. *Water Emerg Contam Nanoplastics* 2024;3:19. https://dx.doi.org/10.20517/wecn.2024.14

Received: 9 Apr 2024 **First Decision:** 20 Jun 2024 **Revised:** 1 Aug 2024 **Accepted:** 6 Aug 2024 **Published:** 19 Aug 2024

Academic Editors: Marta Otero, Joana C Prata **Copy Editor:** Pei-Yun Wang **Production Editor:** Pei-Yun Wang

Abstract

Carbon-based materials have attracted significant interest due to their porous structure and high specific surface area. The stability of carbon provides an optimal environment for microbial growth and activity. This paper presents a comprehensive review of microorganisms immobilized on carbon-based materials. Techniques used to immobilize microorganisms on various carbon-based materials are discussed initially. Subsequently, the review introduces the application of these immobilized microorganisms in the restoration of soil and water environments, including the treatment of organic pollutants, heavy metals, and ammonia nitrogen. Overall, this work enhances our understanding of the microbial pathways facilitated by carbon-based materials.

Keywords: Carbon-based materials, microorganism immobilization, pollutants, remediation

INTRODUCTION

Amid the rapid progression of urbanization and industrialization, toxic pollutants are continuously discharged into the environment, accumulating in the air, water, and soil, and ultimately infiltrating the human body, causing harm to human health. According to the World Health Organization (WHO), nearly a quarter of all human diseases today can be traced back to prolonged exposure to environmental pollution. This indicates the pressing need for effective strategies to mitigate environmental pollution and its impacts on human health[1]. Indeed, environmental pollution remains a major global challenge, and the implementation of appropriate environmental remediation technologies is crucial for preserving human health and safety. Currently, remediation strategies for environmental pollution are primarily classified into physical, chemical, and biological remediation technologies[2]. Among these, biological remediation methods have garnered increasing attention due to their cost-effectiveness and wide applicability. This underscores the potential of microbial remediation as a sustainable and efficient solution for environmental pollution. Nonetheless, although the microbial method for environmental remediation has its advantages, it also has certain limitations. These include the reduction or loss of microbial activity, challenges in separation and recovery post-adsorption, poor genetic stability of microbes leading to easy alterations, and limited adsorption capacity for heavy metals[3]. Consequently, current research is focused on effectively enhancing the treatment efficacy of the microbial method and improving microbial activity. This underscores the necessity for innovative solutions to overcome these limitations and unlock the full potential of microbial remediation for environmental pollution.

Microbial immobilization technology is indeed widely regarded as a potentially effective approach. The process of immobilizing microorganisms offers numerous advantages including high biomass, stability, resistance to loss, rapid reaction speed, strong anti-toxicity, and ease of separation[4]. However, the carrier material employed in this process can exhibit weak mechanical stability and may release toxic elements, leading to a loss of microbial activity. Therefore, the selection of the carrier material is a pivotal aspect of microbial immobilization technology. Despite the challenges that require further investigation, particularly in the selection of carrier materials, the ideal immobilized carrier material should possess attributes such as high biocompatibility, accessibility, stability, a large specific surface area, and low cost. This underscores the necessity for ongoing research in this area to optimize the effectiveness of microbial immobilization technology.

Currently, the primary materials used as carriers include polymers, metal nanoparticles, organometallic frameworks, and carbon materials[5]. Among these, carbon materials have emerged as an ideal platform for microbial carrier materials in recent years. This is attributed to their stable structure, abundant pore structure, and large specific surface area. Additionally, they exhibit excellent biocompatibility, low cost, and are rich in functional groups such as hydroxyl and carboxyl groups. These characteristics render carbon materials particularly suitable for microbial immobilization, enhancing the efficacy of this approach for environmental remediation[6]. However, further research is required to fully exploit the potential of these materials and address any associated challenges. As the use of carbon-based materials for microbial immobilization continues to rise, these materials are assuming an increasingly important role in the treatment of environmental pollutants [Figure 1].

In recent years, some researchers have scrutinized the potential of microbial immobilization techniques in various environmental remediation contexts, introducing a diversity of carrier materials and fixation methods, and deliberating on the factors influencing the microbial immobilization process[7,8]. However, despite the escalating utilization of carbon-based materials in microbial immobilization, a comprehensive review of the application of carbon-based immobilized microorganisms in the treatment of environmental pollutants remains absent.

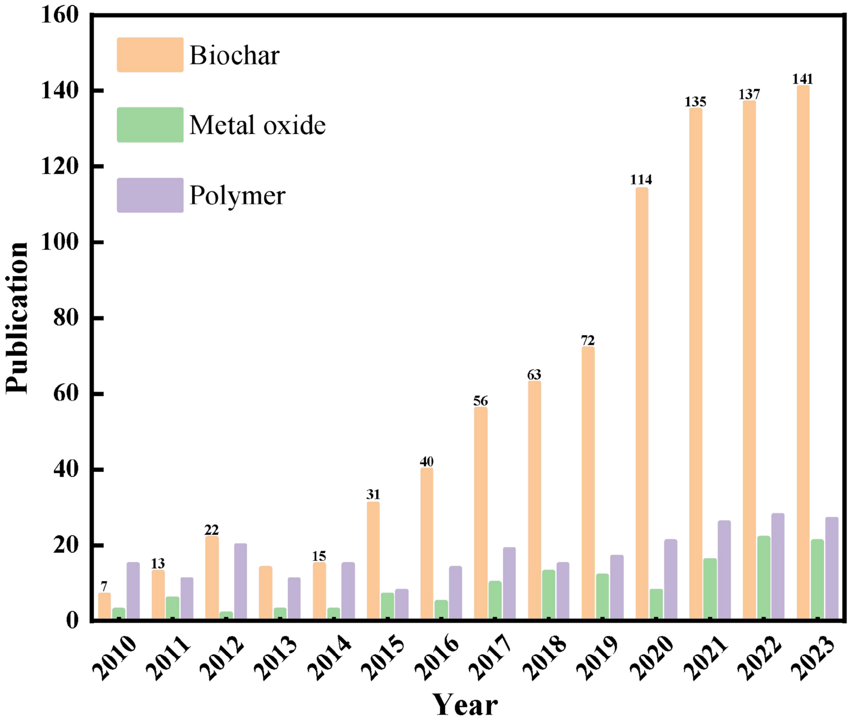

Figure 1. The number of immobilized microorganisms in different materials published per year (Search keywords: immobilized microorganism, biochar, metal oxide, polymer, carbon-based materials. Source: Web of Science, search date: 06-30-2024).

To address this lacuna, we embarked on a meticulous examination of the literature spanning the past two decades, culminating in this exhaustive review. Consequently, we present an overview of the methodologies for immobilizing microorganisms using carbon-based materials such as biochar, activated carbon, carbon nanotubes, and graphene. We further explore their application in the removal of pollutants from aquatic and soil environments. This review aims to serve as a valuable reference for future research on the use of carbon-based materials for microbial immobilization in the remediation of water and soil pollution.

CARBON-BASED MATERIALS

The selection of the carrier material is a crucial factor influencing the immobilization of microorganisms. Different raw materials, along with varying preparation methods and processes, yield different material properties. Key characteristics to consider when selecting a carrier material include its specific surface area, pore size, structure, and mechanical strength, as these significantly impact the microbial load[9].

Recently, carbon-based materials have emerged as some of the most promising nanostructured materials. These materials have garnered significant attention due to their distinctive characteristics, which include high porosity, extensive surface area, functional groups, modifiable surfaces, and a predominantly aromatic structure. Therefore, they are frequently employed as versatile carriers for microbial immobilization. In addition, a thorough understanding of the different characteristics of these carbon-based materials is essential for the effective application of microbial immobilization technology in environmental remediation[10,11]. This highlights the need for continued research and development in this area to identify and optimize the use of suitable carrier materials.

Biochar

Biochar has gained significant attention in recent years as an effective immobilization matrix. Its high carbon content, cation exchange capacity, porosity, stability, and abundance of surface functional groups make it an ideal choice for microbial immobilization[12]. These properties allow biochar to support high enrichment of microorganisms, thereby enhancing the effectiveness of the microbial method for environmental remediation.

This underscores the potential of biochar as a sustainable and efficient solution for environmental pollution. However, further research is needed to fully exploit the potential of biochar and address associated challenges, such as low microbial activity and microbial enrichment and other problems. To address these issues, Han *et al.* investigated the loading of *Bacillus subtilis* 168 onto biochar modified with acid and quaternary ammonium salts to enhance the removal of zearalenone[13]. The study's findings indicated that the modified biochar exhibited an improved pore structure (27.26 nm) compared to pristine biochar (20.41 nm), which contributed to its enhanced bacterial carrying capacity. Moreover, Zhang *et al.* investigated the loading efficiency of biochar derived from various raw materials [honeysuckle residue biochar (HBC), corn stover biochar (CSB)] on *Bacillus subtilis*[14]. The results indicated that the average pore size of HBC and CSB was less than 2 nm, suggesting a predominance of microporous structures on the surface of biochar. Furthermore, the pore volume of HBC exceeded that of CSB, although the average pore size of the two biochars was similar. This suggests that the micropore formation via pyrolysis in HBC surpasses that in CSB, leading to a more developed pore structure in HBC. This enhanced pore structure facilitates microbial growth and reproduction, thereby promoting higher cell density. Zhang *et al.* further emphasize the importance of the physical and chemical properties of biochar in microbial immobilization[15]. The biochar produced from Erding medicine residue (EBC-500) at 500 °C pyrolysis exhibited a more developed pore structure and suitable nutrients, which facilitated the immobilization and proliferation of the degrading strain LZ01. In addition, EBC-500, with a certain degree of alkalinity, can neutralize the acidic intermediates produced during the microbial degradation of chlortetracycline (CTC). This provides a more suitable pH for the growth of LZ01 and enhances the removal efficiency of CTC. Consequently, the removal rate of CTC by EBCM-500 after 2 days reached 82.34%.

To date, the challenge of recovering powdered biochar from aqueous solutions remains a significant limitation to its application. To address this, Zheng *et al.* developed an innovative embedding method by preparing biochar fungal pellets (BFP) that immobilized denitrifying bacteria (*Cupriavidus* sp. H29) for use in bioreactors[16]. The results revealed that the BFP, with its loose and abundant filamentous void structures and a particle size of 5 mm, not only provided ample space and favorable conditions for bacterial adhesion and reproduction but also exhibited excellent solid-liquid separation and reuse performance. Xiang *et al.* present an innovative approach to *Chryseobacterium spH5* strains immobilization using a bead composed of polyvinyl alcohol (PVA), sodium alginate (SA), and biochar for thiamethoxam degradation[17]. The results revealed that the PVA/SA/biochar (0.7%) immobilized microorganisms demonstrated a superior removal effect on thiamethoxam, achieving a removal rate of 90.47%. This was significantly higher compared to the removal rates achieved by PVA/SA immobilized microorganisms (75.06%) and free microorganisms (61.72%). Furthermore, the PVA/SA/biochar (0.7%) immobilized microorganisms exhibited excellent tolerance under extreme environmental conditions. Zeng *et al.* provide valuable insights into the use of ferric tetroxide-modified biochar nanomaterials for the immobilization of *Alcaligenes faecalis* strains[18]. The results demonstrated that the bacteria could sustain growth and maintain robust activity within 48 h under the conditions of 25-40 °C, pH 5-9, initial phenol concentration of 300-500 mg/L, and salinity of 3%.

This demonstrated the potential of modified biochar as an efficacious carrier material for microbial immobilization in environmental remediation. However, further research is required to optimize these modifications and fully harness the potential of biochar.

Activated carbon

Activated carbon, with its large specific surface area and rich pore structure, is highly conducive to cell attachment, making it a popular choice as a solid carrier for the removal of environmental pollutants[19]. As early as 1991, Lin *et al.* explored the co-immobilization system of activated carbon and *Phanerochaete chrysosporium* for the degradation of pentachlorophenol (PCP)[20]. The findings revealed that the normalized PCP mineralization by the co-immobilization system reached 68%. In contrast, only about 17% of the normalized PCP mineralization was observed for the non-immobilized system at 120 h. This is attributed to the solid substrate-activated carbon present in the co-immobilization system, which enhances biodegradation and stability. Furthermore, Annadurai *et al.* demonstrated that the immobilization of microorganisms on activated carbon can notably enhance the degradation efficiency of pollutants, while simultaneously shielding the microorganisms from the impact load of organic pollutants[21]. Hence, the structural characteristics of activated carbon are crucial in microbial loading. Maharaja *et al.* developed a nanoporous activated carbon (NPAC) for the immobilization of microorganisms in bioreactors[22]. The findings indicate that the BET surface area of NPAC is 291 m^2/g and the average pore diameter is 28 Å. The overall removal efficiency of chemical oxygen demand (COD) and biological oxygen demand (BOD) in the reactor are 82% and 85%, respectively, demonstrating the effective carrier properties of NPAC.

To further enhance the efficiency of pollutant removal, Yang *et al.* employed three different methods to modify coconut shell activated carbon: acid, water, and alkali[23]. This modified activated carbon was used to immobilize two microbial communities (ERY-6A and ERY-6B) aimed at degrading erythromycin. The results indicated that both alkali-modified and water-modified activated carbon, in conjunction with the two-bacteria system, exhibited effective erythromycin removal capabilities. The removal efficiency of erythromycin by immobilized cells reached 94.36% within 24 h, which is significantly higher than the 31.90% removal rate by free bacteria. Erythromycin was eliminated by the immobilized cells through mechanisms such as pore adsorption, surface complexation, hydrogen bonding, and biodegradation. Thus, activated carbon also shows potential as a material for microbial immobilization.

Carbon nanotubes

Given that immobilization can augment the activity and stability of microorganisms, carbon nanotubes (CNTs), serving as a carrier for microbial immobilization, have garnered increasing interest in the realm of environmental pollutant removal[24]. CNTs are nanoscale carbon-based materials with a unique surface structure. They offer distinctive properties for the immobilization of microorganisms, owing to their high surface area, superior thermodynamic properties, and low electroosmotic threshold. There exist several types of nanotubes, such as single-walled carbon nanotubes (SCNTs) and multi-walled carbon nanotubes (MCNTs)[25]. While SCNTs consist of only one central carbon tubule, MCNTs are composed of multiple layers of graphite encircling a central carbon tubule. In comparison to SCNTs, MCNTs possess a higher surface area, better dispersibility, and enhanced physicochemical stability, while being more cost-effective and exhibiting lower cytotoxicity[26].

Akyilmaz *et al.* immobilized *Candida tropicalis* onto carbon paste electrodes that contained SCNTs for the detection of dopamine and adrenaline[27]. In a separate study, Boshagh *et al.* examined the hydrogen production process of *Enterobacter aerogenes* PTCC 1221 immobilized by MWCNTs-COOH[28]. The results revealed that MWCNTs-COOH had a higher hydrogen production rate (2.72 L/L·h) than *Enterobacter aerogenes* PTCC 1221. Fourier transform infrared (FTIR) spectroscopy confirmed the successful covalent attachment of the aerogenes to MWCNT-COOH, primarily attributed to the formation of amide bonds between the carboxylic acid groups of the functionalized molecules and the amide groups of the aerogenes.

Therefore, Perchikov *et al.* immobilized cells in a redox-active polymer based on ferrocenecarboxaldehyde-modified bovine serum albumin and CNTs composite for the rapid detection of the phenol index[29]. The findings showed that the detection rate of the redox-active polymer containing CNTs was 502.8 $dm^3/(g \cdot s)$, compared to 193.8 $dm^3/(g \cdot s)$ for the redox-active polymer without carbon nanotubes. Therefore, CNTs-based composites show promise as a potential new material for microbial immobilization.

Graphene

Graphite, graphene and graphene derivative, graphene oxide (GO), is a representative carbon nanomaterial, notable for its large specific surface area and excellent thermal and chemical stability[30]. Despite its inherent antibacterial properties, GO can also foster the growth of microorganisms by adsorbing proteins and supplying ample nutrients, thereby neutralizing its antibacterial capabilities. Consequently, GO can serve as a carrier material for microbial immobilization. Zhao *et al.* constructed microbe- GO composites to adsorb uranium (VI) from aqueous solutions, achieved by immobilizing *Lysinibacillus* sp[31]. The results demonstrated that the maximum adsorption capacity of *Lysinibacillus*-GO for U (VI) was 149.3 mg/g. The primary mechanism of adsorption is attributed to the inner-sphere complexation between U (VI) and oxygen-containing groups.

Liu *et al.* demonstrate the potential of GO/SA aerogel as an adsorption material[32]. By immobilizing heterotrophic nitrifying bacteria FG-06 onto this aerogel, they were able to enhance both the growth of the bacteria and the removal of pollutants. This suggests that GO/SA/FG-06 could be more effective than traditional suspension agents in certain applications. It is another promising step toward more efficient and effective environmental cleanup strategies.

To further enhance environmental applicability, Yong *et al.* developed a method for the immobilization of electroactive microorganisms (*Shewanella oneidensis* MR-1) in microbial fuel cells (MFCs) using graphite/alginate particles[33]. The results indicated that the MFC output of the immobilized cell particles was more stable than that of the suspended cells, and the Coulombic efficiency improved by 0.8-1.7 times compared to the suspended mode. Additionally, MFCs with immobilized cells demonstrated greater resistance to shock from high salt concentrations than MFCs with suspended cells. In another study, Li *et al.* first co-deposited carboxyl graphene (GN-COOH) and gold nanoparticles (AuNPs) onto an electrode, and then immobilized the microbe (*Bacillus subtilis*) onto the modified electrode via covalent bonds[34]. The results showed that this approach shortened the distance between the microbe and the electrode, which is beneficial for electron and mass transfer. Therefore, nanocomposites based on graphene also present a promising new option for microbial immobilization. These studies highlight the potential of carbon-based materials in enhancing the efficiency and stability of microbial processes in environmental applications.

In conclusion, based on current research and technological advancements, biochar offers notable advantages in terms of cost and environmental benefits; however, its performance still requires further enhancement. Activated carbon excels in microbial immobilization due to its high specific surface area and effective adsorption capabilities, but issues related to cost and regeneration need to be addressed. Carbon nanotubes and graphene show significant promise for providing exceptional support and performance, yet challenges related to high costs and environmental impact persist. Future research should concentrate on reducing production costs, enhancing functionalization methods, and evaluating long-term environmental effects to fully harness the potential of these materials in microbial immobilization technologies.

THE FACTORS AFFECTING THE MICROBIAL IMMOBILIZATION

The immobilization of microorganisms on carbon-based materials is influenced by both the intrinsic properties of the carbon-based substrates and a spectrum of environmental factors, such as the initial pollutant concentration, ambient temperature, pH levels, and contact duration. These variables collectively influence the degradation efficiency of pollutants. Consequently, it is imperative to investigate the optimal immobilization conditions to enhance the application of microbial immobilization technology in pollutant removal.

The effect of initial pollutant concentration

Pollutant concentration is a critical parameter in the degradation pathway. Generally, increasing the initial concentration of contaminants enhances their adsorption onto the material until saturation is reached. However, elevated concentrations of pollutants can exert toxic effects on microorganisms, thereby inhibiting their activity. Thus, selecting appropriate carbon-based materials for immobilizing microbial carriers can shield microorganisms from pollutant-induced toxicity, thereby maximizing their pollutant degradation potential.

For instance, Xiang *et al.* observed that increasing the concentration of thiamethoxam from 7 to 42 mg/L resulted in a decrease in the degradation efficiency of free microorganisms from 77.30% to 45.70%[17]. Similarly, the removal efficiency of PVA/SA/biochar-immobilized microorganisms for thiamethoxam decreased from 94.94% to 80.13%. This demonstrates the efficacy of PVA/SA/biochar in protecting microorganisms under high concentrations of contaminants.

pH

pH is another critical parameter; variations in pH not only significantly impact the growth of microorganisms but also alter the surface characteristics of materials and the behavior of pollutants in solution, thereby playing a pivotal role in pollutant removal. Zhang *et al.* observed that biochar-immobilized LZ01 exhibited a higher removal rate of chlortetracycline in neutral and slightly alkaline environments, reaching up to 82.39%[35]. In contrast, the removal rate of chlortetracycline by free LZ01 was 10.31%. Consequently, the influence of pH on the removal rate of immobilized LZ01 is less pronounced compared to free LZ01, primarily because biochar protects microorganisms from adverse pH conditions, thereby enhancing their chlortetracycline removal efficiency. Yu *et al.* proposed considering both the optimal pH for microbial growth and the ideal pH for carrier-microbial binding[36]. This approach can maximize the synergistic benefits of the carrier-microorganism combination in contaminant removal.

Temperature

Temperature is a crucial factor influencing both substance reactions and microbial activity. Generally, the optimal temperature for bioremediation is 25-35 °C, which limits its application under extreme conditions. Consequently, microbial immobilization technology holds promise for enhancing bioremediation in harsh conditions. Manikandan *et al.* observed that the removal rate of Ni^{2+} by wood biochar-immobilized *Pseudomonas stutzeri* increased with rising temperatures[37]. This increase may be attributed to the expansion of pore structures at higher temperatures, creating more surface-active sites for metal ion adsorption. Additionally, temperature influences the solubility of metals and the membrane binding affinity of metal ions to the bacterial cell wall.

The effect of contact time

Contact time is a critical factor influencing the microbial growth curve and cellular activity levels. Zhang *et al.* initially investigated the microbial adsorption capacity of various biochar-based materials, demonstrating that the number of microorganisms on biochar increased with prolonged adsorption time[15]. Although the removal efficiency of pollutants gradually increased with reaction time, it stabilized after approximately two days. This stabilization may be attributed to nutrient depletion and subsequent microbial die-off as the population rapidly grows. Therefore, carbon-based materials offer ample space for microbial growth, effectively shielding strains from toxic substances, increasing bacterial density, and enhancing pollutant degradation by bacteria.

ENVIRONMENTAL APPLICATIONS

The rapid growth of population, industry, urbanization, and intensive agriculture has led to the pollution of soil and water by various pollutants. Microbial immobilization technology has become one of the most successful emerging technologies for soil and water pollution remediation. Among them, Carbon-based materials that immobilize microorganisms have shown great promise in environmental remediation[38]. It has been successfully used to remove a variety of organic and inorganic pollutants from different mediums such as water, soil, and air. These pollutants primarily include toxic metals and organic contaminants[39]. The removal process typically involves biosorption and/or biodegradation mechanisms. This innovative approach leverages the natural abilities of microorganisms and the unique properties of carbon-based materials, offering a potentially effective and sustainable solution for pollution control.

Water pollution remediation

To date, the excessive presence of pollutants in water has detrimental effects on water quality, posing significant health risks[40]. Therefore, it is crucial to explore economical, scalable, efficient, and rapid methods for water treatment. Microbial immobilization methods are emerging as promising technologies for managing water quality. These methods leverage the natural abilities of microorganisms to detect, monitor, and remove target water contaminants. The use of carbon-based materials for microbial immobilization, as discussed earlier, can enhance the efficiency and stability of these processes[41]. These methods are not only cost-effective but also environmentally friendly, making them an attractive option for water treatment. They represent a significant advancement in the field of environmental science and hold great potential for addressing the pressing issue of water pollution. It is an exciting area of research with the potential to make a substantial impact on our environment and health. An *et al.* demonstrated the effectiveness of using *Pseudomonas hibiscicola* L1 strain (Strain L1) immobilized in peanut shell biochar (PBC) for the removal of various pollutants from mixed electroplating wastewater[42]. The pollutants included nickel (II), zinc (II), copper (II), chromium (VI), and ammonia nitrogen. The results showed that PBC not only enhanced the biological activity of Strain L1, but also increased the removal rate of pollutants compared to using PBC alone or free Strain L1. Specifically, the removal rates of the biocarbon-immobilized Strain L1 in mixed electroplating wastewater were as follows: copper (II) (94.92%) > zinc (II) (91.46%) > ammonia nitrogen (79.90%) > nickel (II) (77.02%) > chromium (VI) (34.40%). The removal mechanism proposed by the authors is illustrated in Figure 2A. The removal process primarily involves four mechanisms: (1) nitrate in the solution is utilized by Strain L1 as a nitrogen source for denitrification, forming intermediate nitrite; (2) Cr (VI) is reduced to Cr (III) through electron acceptance by PBC; (3) certain heavy metal ions are removed from the solution via ion exchange; and (4) other heavy metal ions are removed through adsorption processes, which include interactions with functional groups (-OH, -COOH, -CHO), adsorption and accumulation by Strain L1, and electrostatic adsorption by PBC. Huang *et al.* immobilized *Bacillus cereus* RC-1 onto biochar derived from rice straw (SBB-beads), chicken manure (CMB-beads), and sewage sludge (SSB-beads) to facilitate the removal of Cd^{2+} from water[43]. The results demonstrated that SBB-beads achieved the highest Cd^{2+} adsorption capacity at 158.77 mg/g, and the bio-adsorption efficacy of immobilized cells surpassed that of suspended cells. Moreover, the mechanisms underlying Cd^{2+} removal encompass physical adsorption, chemisorption (ion exchange, complexation, precipitation), and intracellular accumulation, which intriguingly may occur independently or synergistically. Additionally, the authors proposed a model delineating the action of different mechanisms

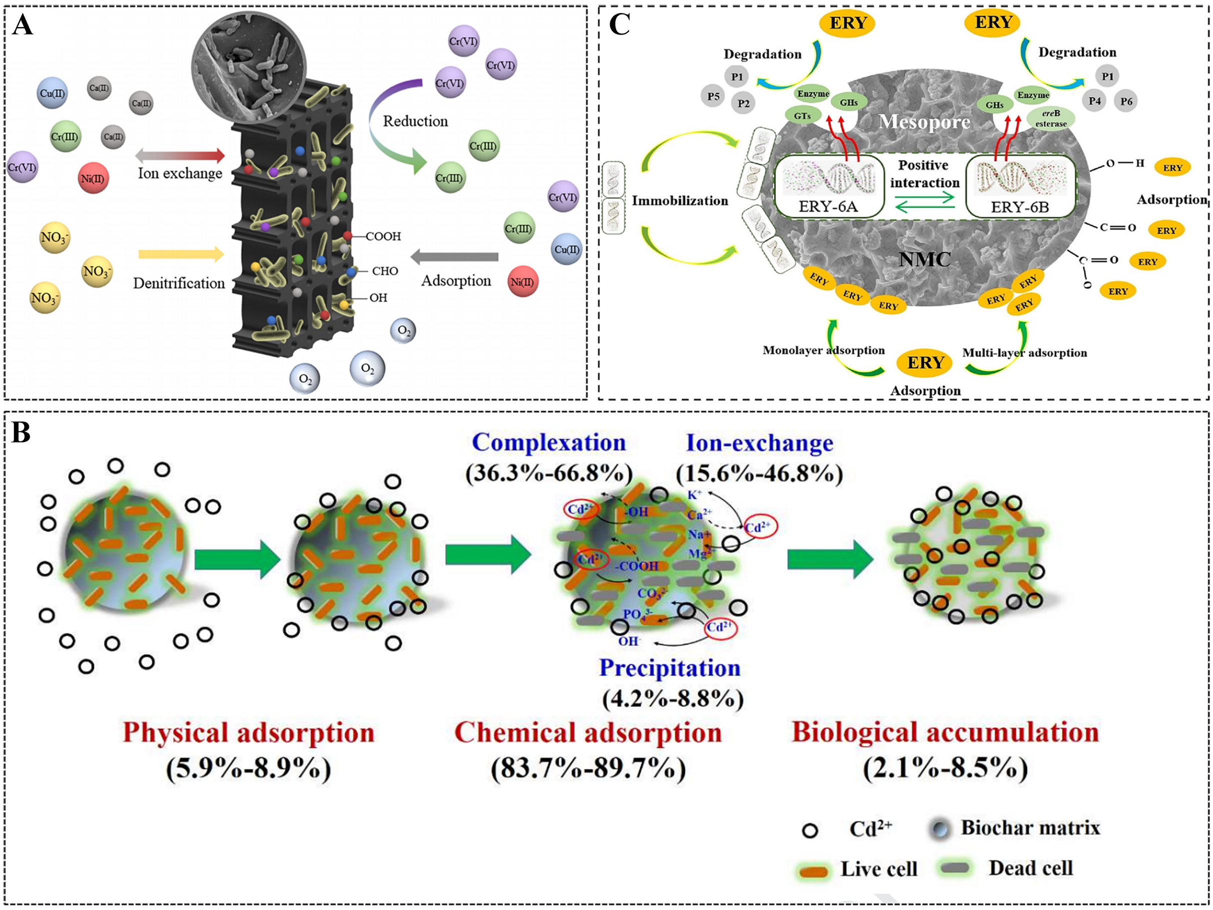

Figure 2. (A) Removal mechanism of co-system; (B) Schematic diagram of the role of immobilized growth cells in the mechanism of Cd^{2+} biosorption; (C) The removal of erythromycin by immobilized cells in mineral salt medium and the potential mechanisms.

[Figure 2B]: initially, metal ions are entrapped and adsorbed onto the material surface by weak physical forces. Subsequently, most metal ions adhere closely to the bio-adsorbents via enhanced chemical adsorption, primarily due to ion exchange and complexation, with a lesser extent due to precipitation. During chemisorption, while some cells perish, others survive, and a fraction of metal ions are transported and sequestered into the cytoplasm.

Nowadays, the rapid industrial and agricultural development in recent years has led to the discharge of large amounts of difficult-to-treat wastewater. Generally, the wastewater contains high concentrations of biodegradable organic pollutants, and even after treatment, it usually fails to meet discharge standards, leading to serious water pollution issues.

In response to this issue, Ouyang *et al.* successfully prepared SA and biochar immobilized GYB1 beads (SC-GYB1) for the biodegradation of 2,3',4,4',5-pentachlorobenzene (PCB 118)[44]. Their results showed that with 2.0% SA, 2.0% wet weight, and 1.5% biochar content, they could degrade 50.50% of PCB 118 within 5 days. Impressively, SC-GYB1 maintained considerable PCB degradation capacity even under 200 mg/L Cd^{2+} stress. In another study, Lu *et al.* prepared Triton X-100 by an adsorption method, adding the non-ionic surfactant Triton X-100 and using biochar as an immobilized carrier to promote biochar immobilized *Pseudomonas aeruginosa* material[45]. This was used for the removal of naphthalene, a refractory organic matter in water. The results showed that low concentrations of Triton X-100 significantly increased the removal rate of naphthalene by 20%-50%, compared with no addition of Triton X-100. This approach not only improved the adsorption capacity of biochar but also promoted the degradation activity of *Pseudomonas aeruginosa*. The authors hypothesize that the two primary removal mechanisms are the adsorption of naphthalene by the biochar itself and the degradation of naphthalene by bacteria immobilized on the biochar.

To enhance pollutant removal efficiency, Yang *et al.* prepared coconut shell activated carbon (NMC) loaded with dual microbial flora (ERY-6A and auriferous bacterium ERY-6B) for erythromycin degradation[23]. The results demonstrated that the immobilized bacteria could remove 95% of 100 mg/L erythromycin within 24 h. As illustrated in Figure 2C, the abundant pore structure on the surface of NMC is a primary factor promoting the removal by dual microbial flora. Additionally, NMC is rich in functional groups (-C=O, -OH, and -COOH), which can easily complex with erythromycin, indicating that surface complexation is another significant factor in its removal. Finally, the surface of NMC contains hydroxyl groups that may form hydrogen bonds with the surface molecules of ERY-6A and ERY-6B. Once the dual bacterial system is immobilized on NMC, a number of degrading enzymes are secreted to degrade erythromycin. Therefore, the main mechanisms of erythromycin removal by immobilized cells include pore adsorption, surface complexation, hydrogen bonding, and enzymatic degradation.

These studies underscore the potential of using carbon-based materials and microbial immobilization for effective wastewater treatment. It is a promising approach toward more sustainable and efficient environmental remediation strategies.

Soil remediation

To date, soil pollution is a significant global issue. Specifically, the leakage and discharge of fossil fuels during extraction, storage, transportation, processing, and use can lead to the accumulation of toxic and harmful substances in the environment[46]. This not only poses a serious threat to human health but also endangers the safety of entire ecosystems. Therefore, soil remediation is an urgent necessity.

Yin *et al.* demonstrate the effectiveness of using rice husk biochar (RHB) and SA as immobilized substrates for complex fungi to create an adsorption system (CFIRHB) and an encapsulation system (CFI-RHB/SA)[47]. The results indicated that CFI-RHB/SA had the highest diesel removal efficiency (64.10%) in highly polluted soil compared to free complex fungi (42.70%). Furthermore, CFI-RHB/SA maintained a stable removal efficiency (> 60%) in soils with higher concentrations of diesel pollution. This is attributed to the key role of fusarium and penicillium in the removal of diesel pollutants. Moreover, the integration of biochar amplifies microbial metabolic capacity, consequently bolstering dehydrogenase (DHA) activity within the soil matrix. Considering that DHA reflects the metabolic reaction of soil microorganisms to diesel oil, increased DHA activity indicates improved efficiency in the oxidative degradation of diesel oil, expediting the transfer of hydrogen atoms from organic substances to specific binding sites.

Li *et al.* investigated a biological carrier constructed from 10%-PVA, 0.5%-SA, and 5%-powdered activated carbon (PAC) for purifying soil contaminated by polycyclic aromatic hydrocarbons (PAHs)[48]. The results indicated that the carrier exhibited no significant cytotoxicity to the immobilized cells, and the live cell population of the immobilized bacteria was 1.86×10^{10} g^{-1}. Furthermore, the biodegradation rates of phenanthrene and pyrene reached 87.0% and 75.4%, respectively, which is twice as high as the rates observed without the use of biological carriers.

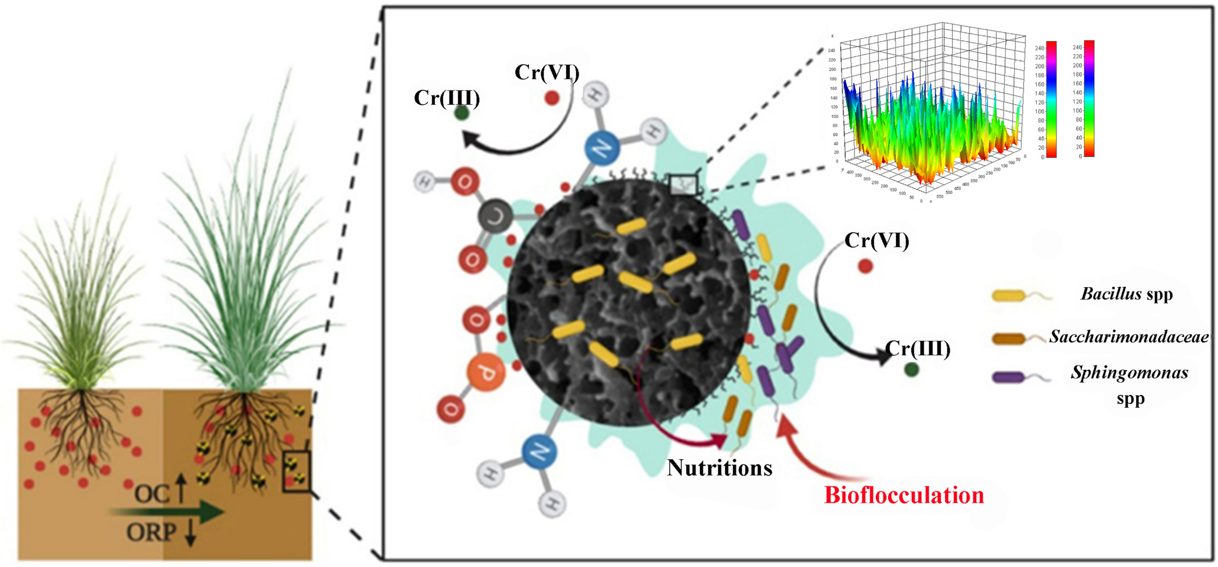

Figure 3. Remediation mechanism of biochar-based Cr-reducing bacteria on Cr-contaminated soil plants.

Chen *et al.* utilized *Enteromorpha prolifera* biochar to immobilize a *Bacillus cereus* WHX-1 reducing strain (WBC), enhancing its Cr (VI) reduction activity, which was subsequently applied to the remediation of Cr-contaminated soil[49]. Experimental results indicated that incorporating WBC elevated the organic carbon content and cation exchange capacity of the soil, decreased the redox potential and bulk density, and markedly enhanced the physicochemical properties of Cr-contaminated soil. Remarkably, 94.22% of Cr (VI) was reduced to Cr (III), representing a 63.38% increase compared to the control group. To elucidate the removal mechanism, scanning electron microscope (SEM) and FTIR analyses revealed that the biochar surface was rough and porous, containing numerous functional groups, such as carboxyl, O-P-O, and amide I, which facilitate the adhesion of biochar to microorganisms. Furthermore, oxygen-containing functional groups act as electron donors, partially reducing Cr (VI). Additionally, biochar supplies nutrients to microorganisms, promoting their growth. Consequently, as depicted in Figure 3, the removal mechanism primarily involves biochar-enriched microbial colonies, thereby forming a stable microbial system in Cr-contaminated soil. This stable microbial aggregation system enhances the reduction of Cr (VI) and decreases the bioavailability of Cr, thereby achieving effective soil remediation.

The remediation of soil co-contaminated by organic pollutants and heavy metals is a significant challenge. Li *et al.* demonstrate the potential of using corncob biochar to immobilize *Citrobacter* strains (IM) for the remediation of soil co-contaminated by petroleum hydrocarbon and heavy metal nickel (Ni)[50]. The results indicated that the degradation rate of petroleum hydrocarbons by solid IM was 45.52%, which was significantly higher than that of free bacteria (30.15%) and biochar alone (25.92%). Importantly, no carcinogenic nickel sulfide was detected after the remediation process in IM. Additionally, the level of soil dehydrogenase activity of IM (0.3956 $\mu g \cdot mL^{-1} \cdot h^{-1} \cdot g^{-1}$) was higher than that of free bacteria (0.2878 $\mu g \cdot mL^{-1} \cdot h^{-1} \cdot g^{-1}$). It is suggested that immobilized microorganism technology is a promising method for the remediation of co-contaminated soil. Table 1 summarizes the application of microbial-carbonaceous immobilized materials for pollutant removal in soil and water environments by detailing the types of pollutants addressed, microbial strains used, carbonaceous materials employed, the effectiveness of pollutant removal, the scale of implementation, and key findings from various studies.

Table 1. Application of microbial-carbon-based materials for removal of pollutant

Carrier material	**Microbes**	**Contaminants**	**Initial concentrate**	**Reaction conditions**	**Removal capacity**	**Medium**	**Scale**	**Ref.**
Rice hull	*Bacillus* H27	Chlorpyrifos	25 mg/L	Time =7 days T = 25 °C Dose = 0.1 g	97.40%	Water	Lab	[51]
Rice husk	*Aeromonas veronii*	Chlorpyrifos	30 mg/L	Time = 24 h T = 30 °C Dose = 1.375 g/L	96.25%	Water	Lab	[52]
			10 mg/kg	Time = 42 days T = 30 °C Dose = 2 g/kg	92.4%	Soil	Lab	
Wheat straw	*Serratia*, *Ralstonia*, and *Enterobacter*	Phenol	1,300 mg/L	Time = 72 h T = 30 °C Dose = 0.6% (w/v)	82.4%	Water	Lab	[53]
PFBCM	*Pseudomonas aeruginosa*	Phenanthrene	80 mg/L	Time = 12 h T = 30 °C pH = 7	50%	Water	Lab	[54]
			41 mg/kg	Time = 6 days T = 30 °C Dose = 2 g	30%	Soil	Lab	
Enteromorpha prolifera	*Bacillus cereus*	Cr (VI)	50 mg/kg	pH = 7.1	94.22%	Soil	Lab	[49]
Rice straw	*Bacillus cereus RC 1*	Cd^{2+}	120 mg/L	pH = 6.0 Time = 20 h	93.02 mg/g	Water	Lab	[55]
Sewage sludge					68.02 mg/g			
Chicken manure					63.95 mg/g			
Maize straw	*Sphingomonas* sp. DZ3	4-bromodiphengl ether	800 mg/L	pH = 7.0 Time = 24 h Dose = 0.1 g T = 40 °C	50.23 mg/g	Water	Lab	[56]
PVA/SA/biochar	*Serratia marcescens*	P-cresol	500 mg/L	pH = 7.0 Time = 3 h T = 30 °C	86.1%	Water	Lab	[57]
Chitosan-biochar	Compound bacteria	Oil	7,881 mg/kg	pH = 7.0 Time = 60 days T = 35 °C Dose = 2.0 g Salinity 1 MS	45.82%	Soil	Lab	[58]
Bamboo charcoal	Degrading bacteria	Nonylphenol	50 mg/L	Time = 24 days	93.95%	Water	Lab	[59]
Activated carbon	*Olivibacter jilunii*	Total nitrogen	249.7 mg/L	Time = 6 days	97.4%	Water	Lab	[60]
		Total phosphorus	19.7 mg/L	Time = 6 days	96.1%	Water	Lab	
		COD	258 mg/L	Time = 6 days	98.0%	Water	Lab	
		Ammonia	221 mg/L		100%			
Granular activated carbon	*Mycobacterium* sp.	TMAH	1.998 mg/L		100%	Water	Lab	[61]
		DOC	4.392 mg/L		78.8%	Water	Lab	
SA/GO	*Bacillus* C5	Crude oil	8,000 mg/kg	Time = 30 days pH = 6.7 Dose = 1.0 kg	64.92%	Soil	Lab	[62]
GO	*Paracoccus aminovorans*	PAHs		Time = 35 days Dose = 0.9 g T = 30 °C	62.86%	Soil	Lab	[63]

PFBCM: Pyrolyzed iron-modified biochar microorganism; PVA: polyvinyl alcohol; SA: sodium alginate; COD: chemical oxygen demand; TMAH: tetra-methyl ammonium hydroxide; DOC: dissolved organic carbon; GO: graphene oxide; PAHs: polycyclic aromatic hydrocarbons.

In summary, these studies underscore the significant potential of immobilized microorganisms supported by carbon-based materials in the removal of various pollutants from soil and wastewater. It is a promising approach toward more sustainable and efficient environmental remediation strategies.

CONCLUSION AND FUTURE PERSPECTIVES

The application of immobilized microorganisms on carbon-based substrates has demonstrated considerable efficacy in the remediation of contaminated soil and water. This strategy harnesses the innate pollutant-degrading capabilities of microorganisms and the adsorption properties of carbon-based materials, yielding a more effective and potentially sustainable solution for environmental remediation. Immobilization techniques can augment the growth stability of microbial cells and extend their tolerance to endure harsh environments. Nevertheless, immobilization techniques encounter several challenges, such as operational complexity, biochar stability, environmental heterogeneity, limitations in mass transfer from the material surface to the immobilized microorganism, and the risk of thick biofilm formation that may hinder efficacy. Additionally, many microorganisms exhibit low tolerance to high concentrations of pollutants, which can result in suboptimal remediation outcomes and prolonged remediation cycles. Furthermore, environmental factors can also influence the effectiveness of immobilized microorganisms. Hence, the selection of novel, effective, and low-cost carbon carriers remains a significant challenge. Biochar and activated carbon are extensively utilized for cell immobilization due to their low toxicity and abundant availability. However, the underlying mechanisms of biochar and activated carbon immobilized bacteria composites in wastewater treatment and soil remediation require further exploration.

Furthermore, microbial immobilization utilizing carbon-based materials represents an advanced technological approach with distinct phases of implementation, each characterized by specific objectives and methodologies. At the laboratory scale, research focuses on the development and optimization of the immobilization technique. This involves conducting experiments with small quantities of carbon-based materials and microorganisms to evaluate key parameters such as microbial activity, substrate interaction, and process efficiency. The outcomes of these studies provide essential data for refining the technology and formulating hypotheses for subsequent stages. Field tests then transition the technology from controlled environments to practical settings, where pilot-scale systems or small-scale trials are employed to simulate environmental conditions. These tests are critical for assessing the stability and performance of the immobilized microorganisms under varied environmental factors, as well as addressing practical challenges related to material durability and microbial viability. The final stage of implementation involves the actual use of the technology in commercial or large-scale applications. This phase requires scaling up the technology, integrating it into existing industrial or environmental systems, and implementing continuous monitoring to ensure operational effectiveness and economic feasibility. The successful transition from laboratory research to field testing and commercial deployment is contingent upon overcoming challenges such as material costs, and integration with existing infrastructure.

DECLARATIONS

Authors' contributions

Conceptualization, investigation, methodology, writing - original draft, supervision, formal analysis: Wang L
Writing - review and editing, methodology, supervision, project administration, funding acquisition, resources: Cheng D
Review and editing, methodology, resources: Liu X
Writing - review and editing, methodology, conceptualization, supervision, resources: Ye Y

Availability of data and materials

Not applicable.

Financial support and sponsorship
This research was supported by The Taishan Scholars Program of Shandong Province (tsqn202211157); Shandong Excellent Youth Science Fund Project (Overseas) (2023HWYQ-077); Project of Shandong Province Higher Educational Young Innovative Talent Introduction and Cultivation Team [Wastewater Treatment and Resource Innovation Team] (ZXQT20211216001); and National Natural Science Foundation of China (No. 52300210).

Conflicts of interest

Cheng D is a Junior Editorial Board member of the journal *Water Emerging Contaminants & Nanoplastics* and the Guest Editor of the Special Issue titled "Elimination of Emerging Contaminants and Micro(nano)plastics in the Anthropogenic Water Cycle", while the other authors have declared that they have no conflicts of interest.

Ethical approval and consent to participate

Not applicable.

Consent for publication

Not applicable.

Copyright

REFERENCES

1. Jiang G. Preface to the special topic on environmental pollution and health risk. *Natl Sci Rev* 2016;3:409. DOI
2. Zamora-Ledezma C, Negrete-Bolagay D, Figueroa F, et al. Heavy metal water pollution: a fresh look about hazards, novel and conventional remediation methods. *Environ Technol Innov* 2021;22:101504. DOI
3. Li Q, Wen D, Qin C, Qian Y, Fu R, Lin S. Physical, chemical, biological, and synergistic technologies for remediation of pesticide-contaminated soil. *Rev Environ Contam T* 2024;262:7. DOI
4. Gannett M, DiTommaso A, Sparks JP, Kao-Kniffin J. Microbial nitrogen immobilization as a tool to manage weeds in agroecosystems. *Agr Ecosyst Environ* 2024;366:108904. DOI
5. Cao Y, Wang L, Wang Y, et al. Functional fungal pellets self-immobilized by mycelium fragments of *Irpex lacteus* WRF-IL for efficient degradation of sulfamethazine as the sole carbon source. *Bioresour Technol* 2023;385:129376. DOI
6. Zhang J, Li F, Liu D, Liu Q, Song H. Engineering extracellular electron transfer pathways of electroactive microorganisms by synthetic biology for energy and chemicals production. *Chem Soc Rev* 2024;53:1375-446. DOI PubMed
7. Wu P, Wang Z, Bhatnagar A, et al. Microorganisms-carbonaceous materials immobilized complexes: synthesis, adaptability and environmental applications. *J Hazard Mater* 2021;416:125915. DOI
8. Jiang Y, Yang F, Dai M, et al. Application of microbial immobilization technology for remediation of Cr(VI) contamination: a review. *Chemosphere* 2022;286:131721. DOI PubMed
9. Zhang J, Yang X, Wang S, et al. Immobilization of zinc and cadmium by biochar-based sulfidated nanoscale zero-valent iron in a co-contaminated soil: performance, mechanism, and microbial response. *Sci Total Environ* 2023;902:165968. DOI PubMed
10. Yuan J, Liu Q, Chen Z, et al. Organic amendments perform better than inorganic amendments in reducing the absorption and accumulation of cadmium in lettuce. *Environ Sci Pollut Res Int* 2023;30:117277-87. DOI PubMed
11. Nor Ashikin NAL, Mohd Fuzi SFZ, Abdul Manaf SA, Abdul Manas NH, Md Shaarani@ Md Nawi S, Md Illias R. Optimization and characterization of immobilized *E. coli* for engineered thermostable xylanase excretion and cell viability. *Arab J Chem* 2022;15:103803. DOI
12. Huang F, Dong F, Chen L, et al. Biochar-mediated remediation of uranium-contaminated soils: evidence, mechanisms, and perspectives. *Biochar* 2024;6:308. DOI
13. Han J, Zhang J, Meng J, et al. Characterization of modified rice straw biochar in immobilizing *Bacillus subtilis* 168 and evaluation on its role as a novel agent for zearalenone-removal delivery. *J Hazard Mater* 2023;453:131424. DOI PubMed
14. Zhang S, Wang J. Removal of chlortetracycline from water by immobilized *Bacillus subtilis* on honeysuckle residue–derived biochar. *Water Air Soil Pollut* 2021;232:236. DOI
15. Zhang S, Wang J. Removal of chlortetracycline from water by *Bacillus cereus* immobilized on Chinese medicine residues biochar. *Environ Technol Innov* 2021;24:101930. DOI
16. Zheng Z, Ali A, Su J, Zhang S, Su L, Qi Z. Biochar fungal pellet based biological immobilization reactor efficiently removed nitrate and cadmium. *Chemosphere* 2022;296:134011. DOI PubMed

17. Xiang X, Yi X, Zheng W, et al. Enhanced biodegradation of thiamethoxam with a novel polyvinyl alcohol (PVA)/sodium alginate (SA)/biochar immobilized *Chryseobacterium* sp H5. *J Hazard Mater* 2023;443:130247. DOI PubMed
18. Zeng Z, Xiao J, Li M, Wu J, Zhang T. Degradation of phenol by immobilized *Alcaligenes faecalis* strain JH1 in Fe_3O_4-modified biochar from pharmaceutical residues. *Water* 2023;15:4084. DOI
19. Zhu P, Zhuo S, Zhang W, Ying X, Huang J, Li X. Performance and application of microbial fuel cells with sodium alginate/agar/activated carbon composite as efficient biocompatible anode. *J Appl Polym Sci* 2023;140:e53999. DOI
20. Lin JE, Wang HY, Hickey RF. Use of coimmobilized biological systems to degrade toxic organic compounds. *Biotechnol Bioeng* 1991;38:273-9. DOI PubMed
21. Annadurai G, Juang RS, Lee DJ. Biodegradation and adsorption of phenol using activated carbon immobilized with *Pseudomonas putida*. *J Environ Sci Heal A* 2002;37:1133-46. DOI PubMed
22. Maharaja P, Mahesh M, Patchaimurugan N, Swarnalatha S, Sekaran G. Treatment of slaughterhouse wastewater by integrated anaerobic/aerobic bioreactors loaded with immobilized nanoporous activated carbon. *J Am Leather Chem As* 2021;116:303-11. https://www.researchgate.net/publication/354311129_Treatment_of_Slaughterhouse_Wastewater_by_Integrated_AnaerobicAerobic_Bioreactors_Loaded_with_Immobilized_Nanoporous_Activated_Carbon. [Last accessed on 18 Aug 2024]
23. Yang J, Xu SY, Zhang T, et al. A dual bacterial alliance removed erythromycin residues by immobilizing on activated carbon. *Bioresour Technol* 2023;384:129288. DOI PubMed
24. Zhai X, Liu X, Dong H, Lin M, Zheng X, Yang Q. Implementation of cytochrome c proteins and carbon nanotubes hybrids in bioelectrodes towards bioelectrochemical systems applications. *Bioprocess Biosyst Eng* 2024;47:159-68. DOI PubMed
25. Kim K, Moon D, Jo M, Ahn H. Carbon nanotube-interlocked Si/CNF self-supporting electrode using continuable spraying architecture system for flexible lithium-ion batteries. *Appl Surf Sci* 2024;656:159663. DOI
26. Alagöz D, Toprak A, Yildirim D, Tükel SS, Fernandez-Lafuente R. Modified silicates and carbon nanotubes for immobilization of lipase from *Rhizomucor miehei*: effect of support and immobilization technique on the catalytic performance of the immobilized biocatalysts. *Enzyme Microb Technol* 2021;144:109739. DOI PubMed
27. Akyilmaz E, Canbay E, Dinçkaya E, Güvenç C, Yaşa İ, Bayram E. Simultaneous determination of epinephrine and dopamine by using *Candida tropicalis* yeast cells immobilized in a carbon paste electrode modified with single wall carbon nanotube. *Electroanalysis* 2017;29:1976-84. DOI
28. Boshagh F, Rostami K, Moazami N. Biohydrogen production by immobilized *Enterobacter aerogenes* on functionalized multi-walled carbon nanotube. *Int J Hydrogen Energ* 2019;44:14395-405. DOI
29. Perchikov RN, Provotorova DV, Kharkova AS, et al. Bioanalytical system for determining the phenol index based on *Pseudomonas putida* BS394(pBS216) bacteria immobilized in a redox-active biocompatible composite polymer "bovine serum albumin-ferrocene-carbon nanotubes". *Polymers* 2022;14:5366. DOI PubMed PMC
30. Manzoor Q, Farrukh MA, Sajid A. Optimization of lead (II) and chromium (VI) adsorption using graphene oxide/ZnO/chitosan nanocomposite by response surface methodology. *Appl Surf Sci* 2024;655:159544. DOI
31. Zhao C, Liu J, Deng Y, et al. Uranium(VI) adsorption from aqueous solutions by microorganism-graphene oxide composites via an immobilization approach. *J Clean Prod* 2019;236:117624. DOI
32. Liu Y, Li Y, Yuan X, Ren R, Lv Y. A self-prepared graphene oxide/sodium alginate aerogel as biological carrier to improve the performance of a heterotrophic nitrifier. *Biochem Eng J* 2021;171:108027. DOI
33. Yong Y, Liao Z, Sun J, Zheng T, Jiang R, Song H. Enhancement of coulombic efficiency and salt tolerance in microbial fuel cells by graphite/alginate granules immobilization of Shewanella oneidensis MR-1. *Process Biochem* 2013;48:1947-51. DOI
34. Li Y, Sun J, Wang J, et al. A microbial electrode based on the co-electrodeposition of carboxyl graphene and Au nanoparticles for BOD rapid detection. *Biochem Eng J* 2017;123:86-94. DOI
35. Zhang S, Wang J, Wang S, Leng S. Effective removal of chlortetracycline and treatment of simulated sewage by *Bacillus cereus* LZ01 immobilized on erding medicine residues biochar. *Biomass Conv Bioref* 2024;14:2281-91. DOI
36. Yu T, Wang L, Ma F, Wang Y, Bai S. A bio-functions integration microcosm: self-immobilized biochar-pellets combined with two strains of bacteria to remove atrazine in water and mechanisms. *J Hazard Mater* 2020;384:121326. DOI PubMed
37. Manikandan SK, Nair V. *Pseudomonas stutzeri* immobilized sawdust biochar for nickel ion removal. *Catalysts* 2022;12:1495. DOI
38. Mittal H, Alfantazi A, Alhassan SM. Recent developments in the adsorption of uranium ions from wastewater/seawater using carbon-based adsorbents. *J Environ Chem Eng* 2024;12:111705. DOI
39. Manoj D, Saravanan R, Raji A, Thangamani A. Carbon-based microelectrodes for environmental remediation: progress, challenges and opportunities. *Carbon Lett* 2023;33:1485-93. DOI
40. González-González RB, Martínez-Zamudio LY, Hernández JAR, González-Meza GM, Parra-Saldívar R, Iqbal HMN. Pharmaceutical pollution fingerprinting and waterbodies remediation using waste-derived carbon dots as sustainable advanced nanomaterials. *Environ Res* 2023;238:117180. DOI PubMed
41. Dhiman P, Goyal D, Rana G, et al. Recent advances on carbon-based nanomaterials supported single-atom photo-catalysts for waste water remediation. *J Nanostruct Chem* 2024;14:21-52. DOI
42. An Q, Jin N, Deng S, et al. Ni(II), Cr(VI), Cu(II) and nitrate removal by the co-system of *Pseudomonas hibiscicola* strain L1 immobilized on peanut shell biochar. *Sci Total Environ* 2022;814:152635. DOI PubMed
43. Huang F, Li K, Wu R, Yan Y, Xiao R. Insight into the Cd^{2+} biosorption by viable *Bacillus cereus* RC-1 immobilized on different biochars: roles of bacterial cell and biochar matrix. *J Clean Prod* 2020;272:122743. DOI
44. Ouyang X, Yin H, Yu X, et al. Enhanced bioremediation of 2,3',4,4',5-pentachlorodiphenyl by consortium GYB1 immobilized on

sodium alginate-biochar. *Sci Total Environ* 2021;788:147774. DOI PubMed

45. Lu L, Li A, Ji X, Yang C, He S. Removal of acenaphthene from water by Triton X-100-facilitated biochar-immobilized *Pseudomonas aeruginosa*. *RSC Adv* 2018;8:23426-32. DOI PubMed PMC
46. Guo S, Yang H, Sun Q, et al. Evaluation of a novel carbon-based micro-nano zero-valent iron composite for immobilization of heavy metals in soil. *J Environ Chem Eng* 2023;11:109740. DOI
47. Yin C, Yan H, Cao Y, Gao H. Enhanced bioremediation performance of diesel-contaminated soil by immobilized composite fungi on rice husk biochar. *Environ Res* 2023;226:115663. DOI PubMed
48. Li P, Wang X, Stagnitti F, et al. Degradation of phenanthrene and pyrene in soil slurry reactors with immobilized bacteria *Zoogloea* sp. *Environ Eng Sci* 2005;22:390-9. DOI
49. Chen Y, Wu H, Sun P, et al. Remediation of chromium-contaminated soil based on *Bacillus cereus* WHX-1 immobilized on biochar: Cr(VI) transformation and functional microbial enrichment. *Front Microbiol* 2021;12:641913. DOI PubMed PMC
50. Li X, Wang Y, Luo T, Ma Y, Wang B, Huang Q. Remediation potential of immobilized bacterial strain with biochar as carrier in petroleum hydrocarbon and Ni co-contaminated soil. *Environ Technol* 2022;43:1068-81. DOI PubMed
51. Liu C, Wen S, Li S, et al. Enhanced remediation of chlorpyrifos-contaminated soil by immobilized strain *Bacillus* H27. *J Environ Sci* 2024;144:172-84. DOI PubMed
52. Manikandan S, Mariyam A, Gowda NK, Singh A, Nair V. Mechanistic understanding of biochar-bacteria system for enhanced chlorpyrifos bioremediation in water and soil medium. *Chem Eng J* 2024;483:149119. DOI
53. Dong J, Xu L, Liu Y, Ren L, Yuan K. Biochar enhances microbial degradation of phenol in water: response surface optimization. *Biochem Eng J* 2024;201:109145. DOI
54. Wang K, Sun Y, Chen D, et al. Enhanced remediation of phenanthrene in water and soil by novel biochar-immobilized bacterial microspheres. *Chem Eng J* 2023;462:141932. DOI
55. Deng M, Li K, Yan YJ, Huang F, Peng D. Enhanced cadmium removal by growing *Bacillus cereus* RC-1 immobilized on different magnetic biochars through simultaneous adsorption and bioaccumulation. *Environ Sci Pollut Res Int* 2022;29:18495-507. DOI PubMed
56. Du J, Sun P, Feng Z, Zhang X, Zhao Y. The biosorption capacity of biochar for 4-bromodiphengl ether: study of its kinetics, mechanism, and use as a carrier for immobilized bacteria. *Environ Sci Pollut Res Int* 2016;23:3770-80. DOI PubMed
57. Jaiswal VK, Sonwani RK, Singh RS. Assessment of enhanced p-cresol biodegradation by encapsulating pre-immobilised *Serratia marcescens* strain HL 1 on tea waste biochar into polyvinyl alcohol/sodium alginate matrix. *Biochem Eng J* 2023;199:109046. DOI
58. Liu Q, Wang Y, Sun S, et al. A novel chitosan-biochar immobilized microorganism strategy to enhance bioremediation of crude oil in soil. *Chemosphere* 2023;313:137367. DOI PubMed
59. Lou L, Huang Q, Lou Y, Lu J, Hu B, Lin Q. Adsorption and degradation in the removal of nonylphenol from water by cells immobilized on biochar. *Chemosphere* 2019;228:676-84. DOI PubMed PMC
60. Huang J, Xiao Y, Chen B. Nutrients removal by *Olivibacter jilunii* immobilized on activated carbon for aquaculture wastewater treatment: *ppk1* gene and bacterial community structure. *Bioresour Technol* 2023;370:128494. DOI PubMed
61. Yang B, Oh H, Lee Y, Jung J, Jahng D. Low-strength electronic wastewater treatment using immobilized cells of TMAH-degrading bacterium followed by activated carbon adsorption. *Desalin Water Treat* 2015;54:3639-45. DOI
62. Liu Q, Chen H, Su Y, et al. Enhanced crude oil degradation by remodeling of crude oil-contaminated soil microbial community structure using sodium alginate/graphene oxide/*Bacillus* C5 immobilized pellets. *Environ Res* 2023;223:115465. DOI PubMed
63. Ren W, Liu H, Mao T, Teng Y, Zhao R, Luo Y. Enhanced remediation of PAHs-contaminated site soil by bioaugmentation with graphene oxide immobilized bacterial pellets. *J Hazard Mater* 2022;433:128793. DOI PubMed

Chandrakanthan *et al. Water Emerg Contam Nanoplastics* 2024;3:20
DOI: 10.20517/wecn.2024.40

Water Emerging Contaminants & Nanoplastics

Research Article

Open Access

Recreational activities as a major source of microplastics in aquatic environments

Kanchana Chandrakanthan[1], **Matthew P. Fraser**[2], **Pierre Herckes**[1]

[1]School of Molecular Sciences, Arizona State University, Tempe, AZ 85287, USA.
[2]School of Sustainable Engineering and the Built Environment, Arizona State University, Tempe, AZ 85287, USA.

Correspondence to: Prof. Pierre Herckes, School of Molecular Sciences, Arizona State University, 551 E University Drive, Tempe, AZ 85287, USA. E-mail: pierre.herckes@asu.edu

How to cite this article: Chandrakanthan K, Fraser MP, Herckes P. Recreational activities as a major source of microplastics in aquatic environments. *Water Emerg Contam Nanoplastics* 2024;3:20. https://dx.doi.org/10.20517/wecn.2024.40

Received: 16 Jun 2024 **First Decision:** 1 Aug 2024 **Revised:** 31 Aug 2024 **Accepted:** 4 Sep 2024 **Published:** 11 Sep 2024

Academic Editors: Zhijie Chen, Joana C Prata **Copy Editor:** Pei-Yun Wang **Production Editor:** Pei-Yun Wang

Abstract

Microplastics (MPs) have been extensively studied in the marine environment in recent years, but their occurrence in recreational waters, and recreational activities as a source of MPs, have been less explored. In this study, we investigate the temporal variation of MPs in the Salt River, a natural surface waterway heavily used for recreation, and in community swimming pools in nearby Tempe, Arizona. Samples were processed using established methodologies and MP shapes and number concentrations were obtained by optical microscopy. The MP concentrations in samples of surface water collected during recreational activity ranged from 27,798 to 222,391 MPs/m^3, with the highest concentrations occurring at 16:00 and lowest at 8:00, consistent with recreational activities. Fibers were the dominant shape (≥ 71%) of MPs overall in the Salt River, accounting for as much as 96% of all MPs at peak activity time (16:00). MP concentrations in water samples from apartment community swimming pools ranged from 59,160 to 254,574 MPs/m^3. In terms of shape, fibers were again dominant (sometimes as high as 87%) in these water samples. Raman spectroscopic characterization of the MPs revealed the presence of polyethylene (PE), polyvinyl chloride (PVC), polyester (PES), polyamide (PA), and polypropylene (PP), showing a larger variety of polymers in the pool samples, while more MP pieces remained chemically unidentifiable. The prevalence of PES and PA fibers indicates that release from synthetic fabrics such as swimwear is a substantial source of MPs in the environment.

Keywords: Microplastics, Salt River, Arizona, swimming pools, polymer composition, weathering

INTRODUCTION

Environmental contamination by plastics has recently developed into an emerging concern, with microplastics (MPs) detection becoming ubiquitous in the environment[1-4]. Environmental MPs - typically defined as plastic particles measuring 5 mm or less in the longest dimension - can originate from the release of primary particles, intentionally engineered and in uniform shapes as microbeads and pre-production pellets[5-7]. More common are secondary MPs, which typically result from the environmental weathering of larger plastics through processes such as photodegradation or mechanical abrasion and tend to have more irregular shapes such as fibers and fragments[8-10].

Environmental research has predominantly focused on MPs in aquatic environments[8,11-20], while fewer studies have been conducted on their presence in atmospheric[21-29] and terrestrial ecosystems[30-35]. Within aqueous environments, most research has concentrated on marine ecosystems, with less than 4% of MP research addressing freshwaters[36]. Freshwater environments, including sources of drinking water, tend to be in closer proximity to the actual sources of MPs. Occurrence data show that the concentrations of MPs in surface waters and the corresponding sediments are higher in areas of high population density[37]. Mismanagement of plastic waste, sewage treatment, agricultural and road runoff, as well as commercial fishing, has been shown to be responsible for MP input into freshwater ecosystems, resulting in rivers being significant to investigate for synthetic MPs[38-40]. MPs, after being released into surface waters, can exhibit remarkable persistence, travel long distances, interact with aquatic organisms, and eventually end up in the oceans[41]. Beaches, often used for recreational activities, have been shown to be significantly contaminated by MPs[42-44]. However, few studies have investigated the occurrence and distribution of MPs in freshwater bodies used for recreational activities, such as lakes, rivers, and swimming pools.

MPs can occur in a variety of shapes, sizes, and colors, but morphologically, fibers appear most common in the gastrointestinal tracts of biota at any trophic level[45-47]. Despite the obvious environmental significance of fibers, shards, films and other fragments tend to be more commonly studied and the environmental sources of fibers remain poorly investigated. Some research reported that the weathering of one gram of polyester (PES) textiles resulted in the release of hundreds of thousands of fibers[48]. Laundry of synthetic fabric and swimwear has also been documented as a substantial source of fibrous MPs[49,50]. To date, there have been few studies that establish the importance of clothing as a source of MP fibers to the environment.

It has been shown that organisms in freshwater, across different habitats and trophic levels, ingest synthetic micro-particles[51]. Freshwater invertebrates such as gammarid amphipods play important roles in the breakdown of particulate organic matter and, therefore, can similarly digest MPs[52]. In addition to their direct toxic effects, these MPs can also act as vectors for other organic contaminants[53-55]. Therefore, investigating freshwater recreational activities as a source of contamination, particularly for synthetic materials such as fiber MPs, is important.

Swimming pools are another class of water system where MPs can be emitted by recreational water use and potentially accumulate. Pools are known to be hotspots for human exposure to pathogens[56] but might also be important in terms of exposure to MPs. Pathogens, including E. coli, Cryptosporidium, and Giardia, are present in such aquatic environments owing to human clustering[57]. MPs might act as a vector for pathogens to be ingested and hence infect humans, especially as smaller microfibers have been documented to evade water treatment processes owing to their size and density[58].

The present work investigates the occurrence of MPs in the Salt River in Arizona, which is used for both recreation and as a drinking water supply. Previous studies have investigated ecological indicators in the river and studied the occurrence of nanomaterials as well as pharmaceuticals and personal care products such as sunscreen[59-62]. A water sampling-based survey was conducted from a single location in the Salt River, in the presence and absence of recreational activities, to assess their impact on MP occurrence. To provide additional context for the occurrence of MPs in recreational waters, community swimming pools in apartment buildings in Tempe, Arizona, were also sampled. MP number concentration and morphology were analyzed using optical microscopy, while the chemistry of the MP was determined by micro-Raman spectroscopy.

EXPERIMENTAL

Sampling of MPs

The Salt River is a surface water system located mostly within the Tonto National Forest (AZ, USA), northeast of Phoenix, Arizona and includes four water reservoirs that form a series of lakes nearly 100 km long[63]. The river is a source of drinking water for the Phoenix metropolitan area and, in the summer months, is a popular destination for recreational activities. There are no commercial activities on the river, such as boating. The Goldfield Recreation area (Mesa, AZ) is a popular river access point (RAP) for recreational activities along the Lower Salt River, and witnesses substantial crowds during the months of June-September [Supplementary Figure 1].

Surface water samples (1 L) were collected at a single location in the Lower Salt River at the Goldfield Recreation area (33.5544° N, 111.6236° W). The samples were collected into clean, pre-fired (450 °C) amber glass bottles from 8 AM to 4 PM on Saturday, July 1st, 2023 (recreational season) and Friday, October 13th, 2023 (absence of recreational activities). The clean sampling bottles were rinsed three times with river water prior to gathering the actual sample, with each time discarding the rinse water downstream.

Triplicate samples were obtained at representative hours of the day (8:00, 12:00, and 16:00) in July to investigate the standard deviation of MP concentrations in water. However, triplicate samples were not obtained for each hourly time stamp due to limitations in logistics, and the relatively low standard deviation between replicates.

Sampling in apartment swimming pools ($n = 7$) in Tempe, Arizona, in July 2023 [Supplementary Figure 2] and October 2023 followed the same protocol. The selected community swimming pools were located in student apartment complexes in Tempe, Arizona, and were accessible for water sampling. Each pool was approximately 20’ × 40’ in size and was used by a substantial number of students during the summer in Arizona. Triplicates were analyzed for three pools with sampling IDs - SP2, SP5, and SP7.

All water samples were refrigerated during transport and stored at 4 °C in the dark until processing in the lab.

Sample processing

All aqueous samples were first passed through a sieve (8”-FH-SS-SS-US-#3-1/2, Hogentogler & Co.Inc., MD, USA) to remove any material larger than 5.6 mm in size. The sample bottles were triple rinsed with ultrapure water (> 18.4 MΩ·cm, Purelab Flex, IL, USA) to extract all MPs sticking to the glass surface of the bottles. The samples were then further processed using a methodology based on recommendations from the National Oceanic and Atmospheric Administration (NOAA) and adapted to water samples[64]. On brief, the first natural organic matter was removed by wet peroxide oxidation using 10 mL of an aqueous 0.05 M Fe (II) solution prepared from $FeSO_4 \cdot 7H_2O$ (Sigma Aldrich, MO, USA), followed by the addition of 10 mL of a 30% hydrogen peroxide (Sigma Aldrich, MO, USA) solution. After letting the resulting mixture rest for

5 min, the solution was heated to 60 °C on a hot plate (Fisher Scientific, NH, USA) to accelerate the digestion of organic matter. This was followed by filtration through pre-fired glass fiber filters (Whatman GF/A, Sigma Aldrich, MO, USA) and drying in an oven (Vulcan 3-1750, CA, USA) at 60 °C.

Since MPs are ubiquitous in all environments, preventive measures must be adopted to minimize contamination of samples and overestimation of MP concentrations[22,65]. In the current study, a blank was obtained during sample handling and processing to evaluate the potential of cross-contamination. An ultrapure water sample (> 18.4 MΩ·cm, Purelab Flex, IL, USA) was transported to the field, was poured into a pre-cleaned and pre-baked (450 °C, overnight) amber glass bottle (similar to the sampling bottle) at the same sampling location, and transported to the lab similar to other water samples. Glassware used during all stages of sample handling, processing, and analyses was washed using a detergent and triple rinsed with ultrapure water (> 18.4 MΩ·cm, Purelab Flex, IL, USA) prior to use. Decontamination measures included subsequent baking of glassware (450 °C overnight). Potential contamination through the deposition of airborne MPs was minimized by covering the clean glassware and equipment used for sample processing and analysis. As MPs are widespread particles that could be found on any surface, lab bench and fume hood surfaces were cleaned with ultrapure water (> 18.4 MΩ·cm, Purelab Flex, IL, USA) and isopropyl alcohol (Fisher Scientific, MA, USA) before sample processing and analyses. The usage of glass materials is generally recommended when processing and analyzing MPs in samples, as plastic materials can release particles and result in contamination and overestimation of MPs[22]. The usage of plastics was minimized during sample handling and analysis, and the recovery rate of MPs from filters was determined to be 93% through matrix spikes with a known number of MPs in the size range 5-5,000 μm (see[25,33] for additional details).

Optical microscopy - shape and number concentrations

Filters were visually analyzed by a digital microscope (Leica DM6B-Z, Germany) (see[33] for details). In brief, the size range was 5-5,000 μm with the higher limit obtained through sieving and based on the typical definition of MPs, while the lower limit of 5 μm was due to the particle size detection limit of the microscope. In terms of shape, an object was considered a fiber when it looked cylindrical and presented an aspect ratio (length/diameter) ≥ 3. The sizes of the MPs were measured along their largest dimension using the software program ImageJ (version 1.5, National Institute of Health, USA, http://imagej.nih.gov/i). MPs were identified under the digital microscope based on criteria reported in literature, including the absence of cellular structures and fibers depicting uniform thickness along their entire length[33,66].

Chemical characterization using micro-Raman spectroscopy

Micro-Raman data were collected using a custom-built Raman spectrometer with a spatial resolution of 1 μm and spectral resolution of 1 cm^{-1}[33]. Raman spectra were collected from 50 to 3,800 cm^{-1}. The excitation source was a Coherent Sapphire solid state continuous wave laser emitting 532 nm. The Raman data were calibrated using cyclohexane with known peak positions.

RESULTS AND DISCUSSION

Temporal variation of MPs in recreational surface waters of the Salt River

MPs were detected in all Salt River surface water samples and an increasing trend in concentrations was observed during the day (July 1st, 2023; Figure 1). The MP concentrations in the surface water samples during recreational activity varied from 27,798 MPs/m^3 in the early morning, prior to recreational activities, to 222,391 MPs/m^3 at 4 PM, at the peak of recreational activities, an increase of a factor of 8 [Figure 1]. The Salt River is accessible in this region for recreational activities from 9:00 daily from June-September. The observed variation in MP concentrations can be ascribed to the micro-particles released from human activities during recreational activities in the Salt River. The relative standard deviation between replicates

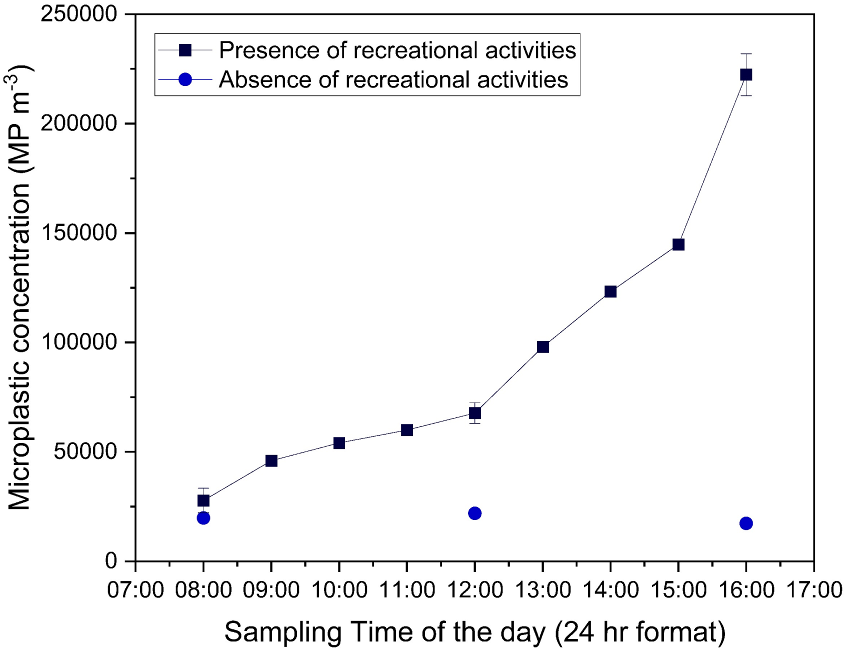

Figure 1. MP occurrence in the Salt River in the presence (July) and absence (October) of recreational activities. MP: Microplastic.

obtained at 8:00, 12:00 and 16:00 during the sampling period in July [Supplementary Table 1] was 10%. MPs were also detected in all samples on October 13th, 2023, in the absence of recreational activities, showing a ubiquitous presence in the Salt River. The MP concentrations observed in October did not vary substantially over the course of the day, ranging from 17,347 to 21,905 MPs/m^3 (the relative standard deviation of concentrations over the day was 11%). The number concentrations in October were similar to that in the surface water sample collected at 8:00 (no recreational activities) in July. MP baseline concentrations during the off-season in the absence of recreational activities are an order of magnitude lower than those observed on July 1st, 2023 [Figure 1]. The Salt River water flow data were retrieved from the closest monitoring station upstream, below Stewart Mountain Dam, from the United States Geological Survey (USGS). The average water flow rates in the river did not show substantial differences (898 ft^3/s on July 1st and 827 ft^3/s on October 13th). Therefore, it is possible to compare the MP concentrations in the Salt River in July and October, negating any dilution effects. Additionally, Mesa (AZ) did not experience rain or dust storms on either of the sampling days (July 1st, 2023 and October 13th, 2023). However, the influence of wind parameters (wind speed and wind direction) on MP concentrations in water on the two sampling days is unknown to us.

Filter blanks used to track contamination showed the presence of 1 to 5 MPs/filter with an average of 2 MPs/filter. MP recovery based on matrix spikes with 5-5,000 µm polydisperse MPs averaged 93%.

Placing the concentrations of MPs in the current study within the context of the existing literature is challenging due to differences in sampling and analytical protocols. Studies on MP occurrence in surface water, especially those used for recreational activities, are sparse. MP concentrations ranging from 0.44 to 9.7 MPs/m^3 have been reported in the waters of Lakes Mead and Mohave, reservoirs along the Colorado River that see some recreational use and are also located in the arid southwestern USA[67]. Even though these basins are sparsely populated, the authors attribute the concentrations observed to the large number of visitors the locations witness[67]. The lower MP size limit in this study was 355 μm, while that of the current study was 5 μm. Even considering only the larger MPs in the Salt River (≥ 355 μm) in the presence of recreational activity at peak time (16:00), the concentrations are 4-5 orders of magnitude higher than those observed in Lakes Mead and Mohave (≥ 355 μm).

This could be attributed to the vast area covered by the two large Colorado River reservoirs (759 km^2) compared to the Salt River, which would result in the dilution of overall MP concentrations in water[67]. Baldwin *et al.* also studied the St. Croix and Mississippi rivers in an earlier study, noting that both were impacted by recreational activities[68]. MP concentrations in these rivers (≥ 333 μm) were similar and of the same order of magnitude as those observed in Lakes Mead and Mohave (Colorado River), and could possibly be ascribed to similar lower size limits of interest. The MP concentrations in the Los Angeles River and Colorado Boulder Creek are 1-3 orders of magnitude lower than those in the Salt River during the absence of recreational activities[69,70]. This observation could be partially ascribed to the smaller lower size cut used in the current study (5 μm), compared to that reported in the aforementioned studies (1,000 μm).

A previous study on the Salt River by Venkatesan *et al.* studied the impact of recreational activities (tubing and swimming) on Ti-containing particles and sunscreen additives. Their findings were consistent with ours in that they saw a significant (80%) increase in the particle concentrations at peak activity time (16:00) over their initial baseline concentration[62]. The change was attributed to the increased recreational activity occurring upstream. Similarly, Chiu *et al.* showed a significant increase in oxybenzone (sunscreen) concentrations in Salt River waters during the day, consistent with an increase in recreational activities[59]. The overall human impact in the study region is documented by ecological studies, such as research that shows a decrease in the herpetofauna diversity along the Salt River, with the increase in urbanization[60]. The Salt River in Arizona is home to fish species including the Castostomus insignis, Gila robusta, Rhinichthys osculus, and the Catostomus clarkii, and the presence of MPs in the riverine ecosystem of interest in our current study can potentially reduce the feeding uptake of such aquatic organisms[71].

Morphological analysis showed that a majority of MPs in the Salt River were fibers [Supplementary Figure 3]. During the day, the fraction of plastics that are fibers increases and they account for 96% of MPs at the peak activity time (4 PM). Even in the absence of recreational river use (October), 72% of the MPs, on average, were fibrous. The overall large percentages of fibrous MPs present in samples collected in July are likely an indication of the secondary synthetic micro-particles originating through the shedding of micro-fibers from fabrics such as swimwear. Compared to regular shaped spherical MPs, fibrous MPs have a larger specific surface area, making them more conducive to ingestion by aquatic organisms and contact with microbes[72]. The recreational activities involve the use of tubes and floating devices; however, the materials commonly used in these devices such as rubber [e.g. poly(isobutylene-co-isoprene) or latex (polyisoprene)] were not observed in the micro-Raman analysis. Therefore, the abundance of fibers is mainly attributed to the shedding of fibers from swimwear. Fibers can also stem from the degradation of larger plastics[73]. Microfibers from synthetic garments were observed in all samples in the current study. This is consistent with studies indicating that a large amount of fibers has been reported to shed from acrylic fabric[74]. Fragments were observed as the only other morphology present and no spherical pellets and beads were observed in surface water samples in the river.

A previous study reporting soil MPs in the same arid region of Phoenix, Arizona, reported samples comprising large fractions of fibers[33], while a study on airborne MPs in nearby Tempe, Arizona, showed that a large fraction were fibers (≥ 82%)[25]. The present study of MPs in the riverine system shows that MPs were largely fibrous with relatively higher fractions than in these other local environmental systems.

Figure 2 shows the evolution of the size distributions of MPs in surface water samples from the Salt River during recreational activity over the course of 8 h. MPs were predominately found in the smallest size fraction (5-50 μm) that we were able to quantify, in water samples collected early in the day (8:00, 9:00, 10:00, and 12:00). Owing to their small size, MPs are ingested by a range of freshwater aquatic organisms that can eventually cause ecotoxicological and physiological changes[75]. Later in the day, MPs were predominately present in larger size classes. A Mann-Whitney Test ($P \leq 0.05$) using OriginPro, Version 2023 (Origin Lab Corporation, Northampton, MA, USA) indicates that the size distribution of MPs at 8:00 is significantly different to that at 16:00 ($P = 0.0064$). As the day progressed, the river saw an increasing number of recreational users, which might have resuspended larger micro-particles previously deposited in sediments. It should be noted that the vertical dynamics of MP distribution within the sediments remain largely understudied and unknown. However, bioturbation can affect the distribution of MPs and litter in river sediments[76].

MPs in apartment community swimming pools

Figure 2 shows the range of MP concentrations observed in surface water samples from community swimming pools ($n = 7$) in Tempe, Arizona. The MP concentrations ranged from 59,160 to 254,574 MPs/m^3 in October 2023 [Figure 3]. While MPs were detected in each pool, the concentrations varied significantly (the average relative standard deviation was 39%). The highest MP concentration was found at site SP5 and the lowest MP concentration was observed at sampling site SP4. Triplicate samples show a low measurement variability, smaller than the observed differences. The variability in MP concentrations between pools likely results from the difference in filter media used. Most swimming pools use sand, cartridge or diatomaceous earth (DE) filters to remove suspended solids as part of the water treatment process implemented to keep water physically attractive, clean, and safe[77]. MP concentrations in swimming pools in the summer (July) were of the same order of magnitude as those observed in October [Figure 3]. This could possibly be due to the rather low drainage frequency of swimming pools (3-7 years)[78]. MPs released from secondary degradation of fabrics could accumulate over time, and may possibly explain the relatively high concentrations observed in our study.

Comparing the results of the current study with existing research is important for contextualizing MP concentrations. However, to date, there are no reported studies investigating the presence of MPs in swimming pools. Overall, the concentrations in the swimming pools are comparable to those in the Salt River during recreational activity in July, and an order of magnitude higher than those in the absence of recreational activities in October. Sources of MPs in swimming pools may also be more limited compared to those in natural environments (Salt River). However, our chemical characterization results for MPs in the Salt River and swimming pools imply the release of synthetic fibers from fabrics. Results from a pilot study investigating MPs in Tempe Town Lake depict concentrations two orders of magnitude lower than those in swimming pools in Tempe [Figure 4]. The Tempe Town Lake is restricted for swimmers and the relatively high water flow in the lake (several hundred to thousand cubic feet per second depending on the season and episodic inflows), as opposed to no flow in swimming pools, could possibly explain the lower concentrations in the lake. The MP concentrations in the swimming pools in Tempe during July are comparable, and of similar magnitude to that in the Salt River during recreational activity [Figure 4]. The concentrations in the swimming pools are of similar magnitude to those in the Tres Rios wetland outflow, a constructed wetland that receives waste-water treatment effluent[79].

Fiber MPs were also the dominant morphology in the swimming pool survey, accounting for as much as 87% (in SP5). Fragments and spherical transparent beads [Supplementary Figure 4] were observed as the only other morphologies observed in these samples. Overall, the highest counts for MPs were observed in the 5-100 μm size fraction in the pool samples.

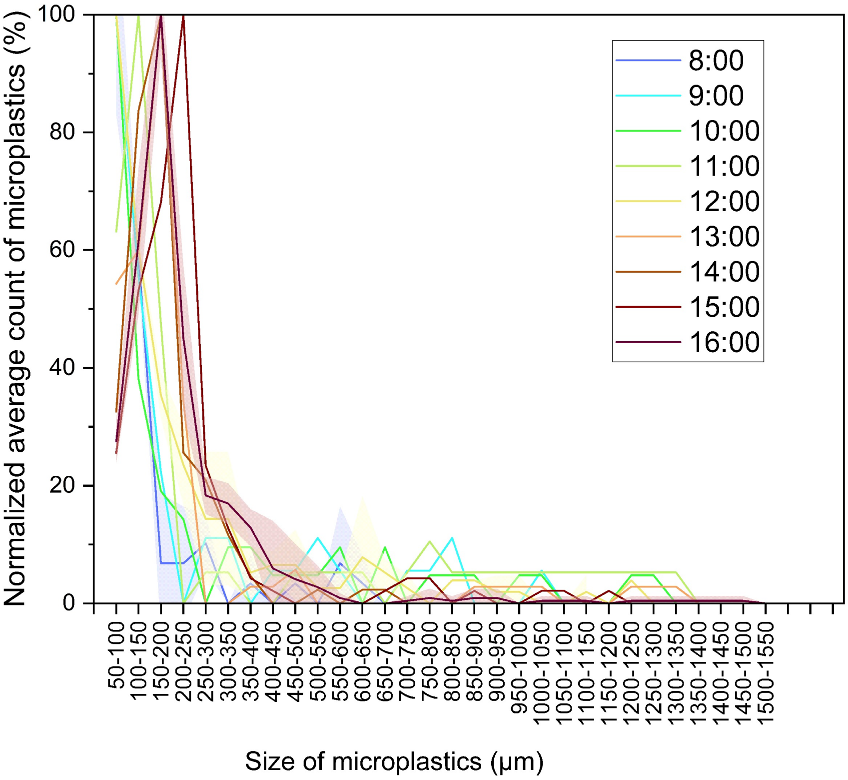

Figure 2. Size distributions of MPs in the Salt River over the course of July 1st, 2023 (Time in 24-hour format). MPs: Microplastics.

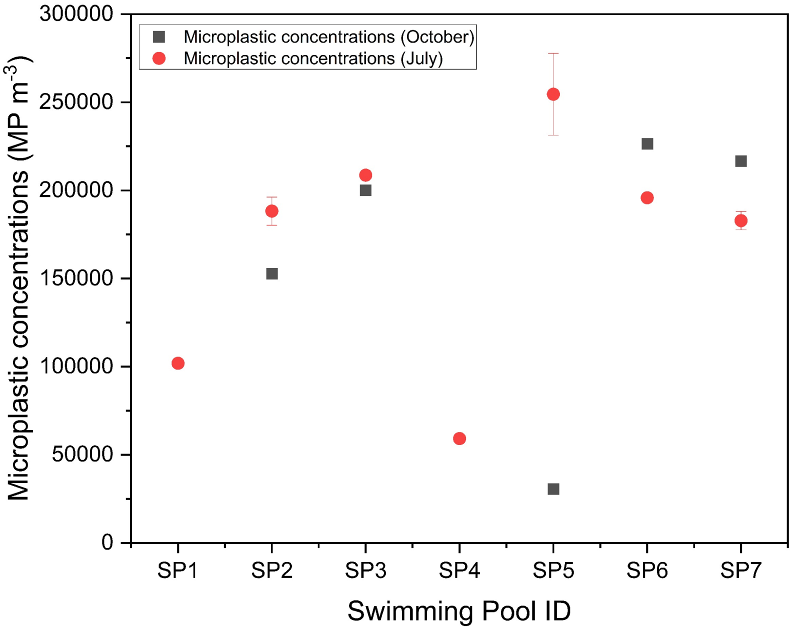

Figure 3. MP concentrations in swimming pools in July and October 2023. Each error bar represents the standard deviation of the mean obtained from three replicate measurements. SP1-SP7 are sampling location IDs of swimming pools. MP: Microplastic.

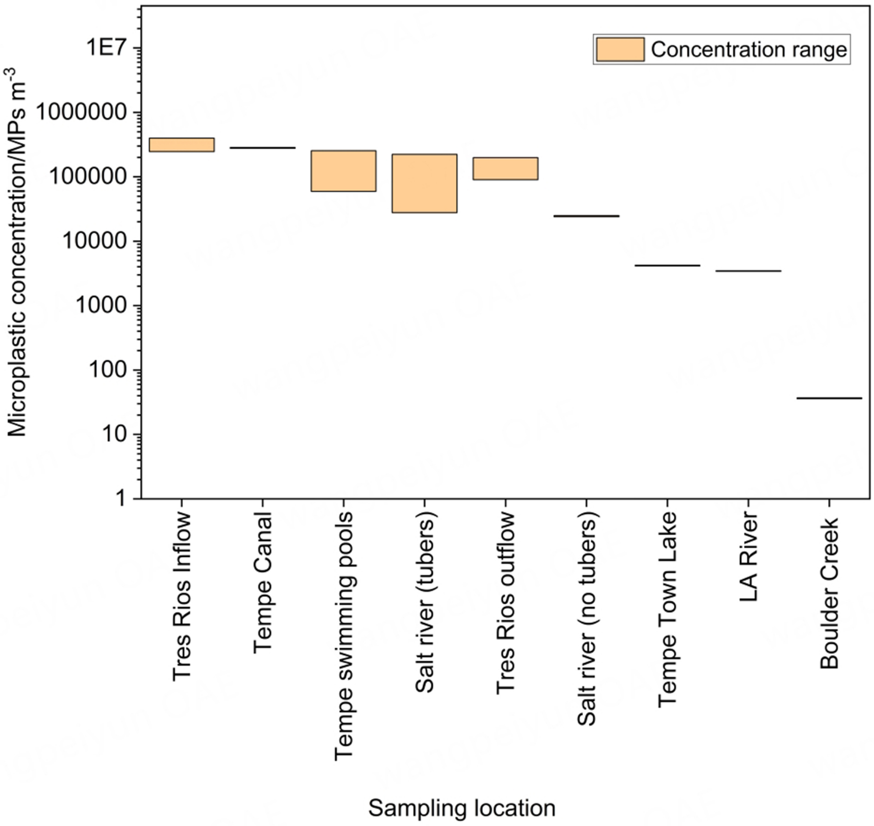

Figure 4. Comparison of MP concentrations in surface waters[67,69,70,79]. MP: Microplastic.

Chemical identification of MPs

Micro-Raman spectroscopy was used to assess the nature of the polymers in the MPs present in the Salt River (July and October) and swimming pools. A large diversity of polymers, including polyethylene (PE), polyvinyl chloride (PVC), polyamide (PA), PES, and polypropylene (PP), were observed and some MPs remained unidentified [Figure 5, Supplementary Figures 5 and 6]. Overall, a majority of the MPs identified were PA and PES. Swimwear is a significant source of microfibers to the environment and consists of interwoven nylon and PES fibers[50]. Raman characterization for MPs in water samples from July revealed that 4% to 40% of the MPs remained chemically unidentified. However, the fraction of unidentified MPs in the aquatic environments (Salt River) was lower than that found in atmospheric and soil environments in Phoenix, Arizona[25,33]. We showed in a previous study that environmental weathering processes can lead to surface modifications that render the MPs unidentifiable by micro-Raman spectroscopy[25]. The relatively lower fractions of unidentified MPs from this study area could possibly be an indication of the recent introduction of synthetic micro-particles from their sources to the aquatic environment (less time for environmental weathering).

PA was present in 67% of the samples from the Salt River during recreational activities and tended to be the most abundant polymer (on average) in all our water samples [Figures 5 and 6]. At peak recreational activity (4 PM), PA accounted for 78% of all MPs. PES was also prominently present in the identified fraction of MPs in samples. These observations, combined with the morphology results, again suggest a high release of MP fibers from synthetic textiles[73]. PES is widely used in fabrics for clothing and is the most produced synthetic fiber on a global scale (~50% of the global fiber market)[9]. PA fibers rank second in the list of the most produced synthetic fibers[80]. The polymer distribution in the swimming pools in Tempe,

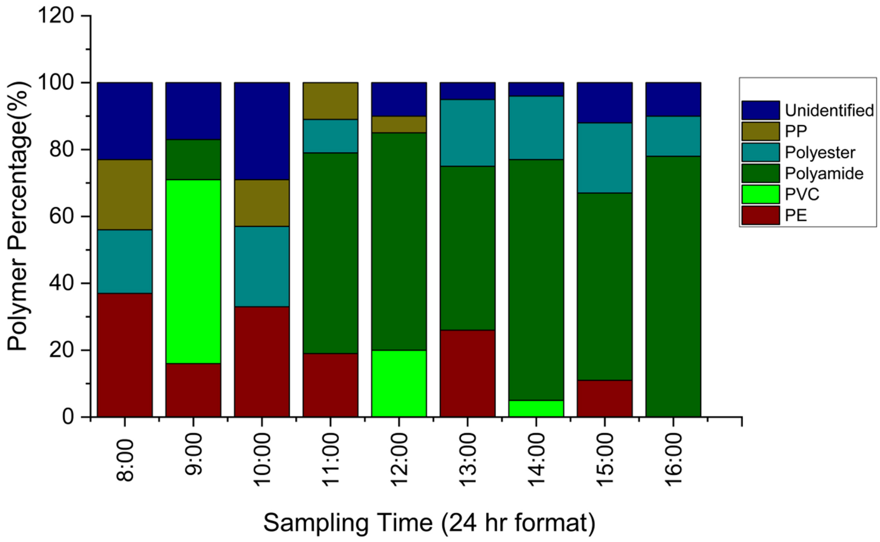

Figure 5. Raman characterization of MPs of heavily used recreational surface water samples in the Salt River. MPs: Microplastics.

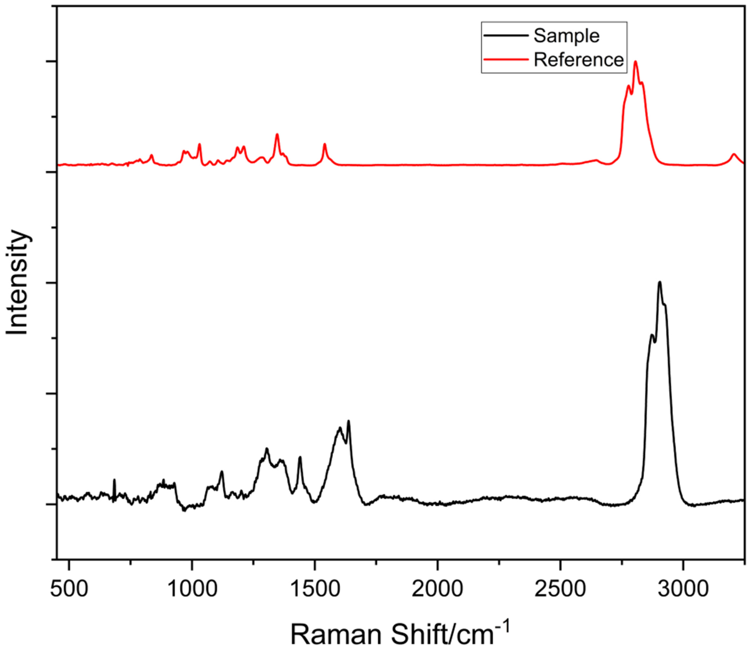

Figure 6. An example spectrum of a MP sample identified as PA compared to that of a reference spectrum. MP: Microplastic; PA: polyamide.

Arizona [Supplementary Figure 6] was similar to the river samples[81]. A recent risk assessment study investigating the impact of different polymeric materials on aquatic organisms states that PA poses the greatest risk, followed by PET[58]. This suggests a non-negligible risk posed by these synthetic materials released to the Salt River in the current study.

CONCLUSION

MPs were ubiquitous in the heavily used recreational waters of the Salt River and local community swimming pools. MP concentrations in surface water samples in the Salt River showed an increase by 8 times at peak recreational activity time compared to baseline concentrations where no recreational activities occurred. MP concentrations depicted substantial variability between apartment swimming pools in Tempe, Arizona, at times as high as 254,574 MPs/m^3. Fibers were the dominant shape of MPs in the tested surface waters, with a majority present in relatively smaller size categories (5-200 µm). Raman characterization for MPs in water samples revealed a diversity of polymers, but 4%-40% of the MPs remained chemically unidentified. The latter is likely the result of weathering processes-induced changes that render the polymers unidentifiable by micro Raman Spectroscopy. However, the fraction of unidentified MPs was smaller in the river during recreational activity compared to those in swimming pools, air and soil samples in the same arid region, indicating the recent introduction of the micro-particles to the riverine system. PA and PES were generally the most abundant polymers, suggesting a secondary origin from synthetic fabrics. Overall, the observations show that recreational activities can be a significant source of MPs in surface waters.

DECLARATIONS

Acknowledgments

We thank Gabrielle Cano, Christine Hubert, Jason Miech, Jesse Molar, and Amelia Stout for their assistance with field sampling for this project. Parts of this paper have appeared in Chandrakanthan K’s doctoral thesis.

Authors’ contributions

Conceptualization, methodology, data, curation, formal analysis, writing - original draft, Writing - review and editing: Chandrakanthan K

Supervision, writing - review and editing: Fraser MP

Writing - review and editing, validation, supervision, project administration: Herckes P

Availability of data and materials

The data that support the findings of this study are available from the corresponding author upon reasonable request.

Financial support and sponsorship

None.

Conflicts of interest

Herckes P is an Editorial Board member of the journal *Water Emerging Contaminants & Nanoplastics*, while the other authors have declared that there are no conflicts of interest.

Ethical approval and consent to participate

Not applicable.

Consent for publication

Not applicable.

Copyright

REFERENCES

1. Geyer R, Jambeck JR, Law KL. Production, use, and fate of all plastics ever made. *Sci Adv* 2017;3:e1700782. DOI PubMed PMC
2. Zhao H, Zhou Y, Han Y, et al. Pollution status of microplastics in the freshwater environment of China: a mini review. *Water Emerg Contam Nanoplastics* 2022;1:5. DOI
3. Bhatia SK, Kumar G, Yang YH. Understanding microplastic pollution: tracing the footprints and eco-friendly solutions. *Sci Total Environ* 2024;914:169926. DOI PubMed
4. Pomata D, La Nasa J, Biale G, et al. Plastic breath: quantification of microplastics and polymer additives in airborne particles. *Sci Total Environ* 2024;932:173031. DOI PubMed
5. Arthur C, Baker JE, Bamford HA. Proceedings of the International Research Workshop on the Occurrence, Effects and Fate of Microplastic Marine Debris, September 9-11, 2008. University of Washington Tacoma, Tacoma, WA, USA. 2009. Available from: https://repository.library.noaa.gov/view/noaa/2509. [Last accessed on 9 Sep 2024].
6. Turner A, Wallerstein C, Arnold R. Identification, origin and characteristics of bio-bead microplastics from beaches in western Europe. *Sci Total Environ* 2019;664:938-47. DOI PubMed
7. Tran TV, Jalil AA, Nguyen TM, Nguyen TTT, Nabgan W, Nguyen DTC. A review on the occurrence, analytical methods, and impact of microplastics in the environment. *Environ Toxicol Pharmacol* 2023;102:104248. DOI PubMed
8. Peller JR, Nelson CR, Babu BG, Iceman C, Kostelnik E. A review of microplastics in freshwater environments: locations, methods, and pollution loads. In: Ahuja S, Loganathan BG, editors. Contaminants in our water: identification and remediation methods. Washington: American Chemical Society; 2020. pp. 65-90. DOI
9. Rebelein A, Int-Veen I, Kammann U, Scharsack JP. Microplastic fibers - underestimated threat to aquatic organisms? *Sci Total Environ* 2021;777:146045. DOI PubMed
10. Ali AAM, Khalid AA, Razak NIA, et al. A review on the presence of microplastics in environmental matrices within Southeast Asia: elucidating risk information through an analysis of microplastic characteristics such as size, shape, and type. *Water Emerg Contam Nanoplastics* 2024;3:12. DOI
11. Andrady AL. Microplastics in the marine environment. *Mar Pollut Bull* 2011;62:1596-605. DOI PubMed
12. Bordós G, Urbányi B, Micsinai A, et al. Identification of microplastics in fish ponds and natural freshwater environments of the Carpathian basin, Europe. *Chemosphere* 2019;216:110-6. DOI PubMed
13. Yuan W, Liu X, Wang W, Di M, Wang J. Microplastic abundance, distribution and composition in water, sediments, and wild fish from Poyang Lake, China. *Ecotoxicol Environ Saf* 2019;170:180-7. DOI PubMed
14. Li C, Busquets R, Campos LC. Assessment of microplastics in freshwater systems: a review. *Sci Total Environ* 2020;707:135578. DOI PubMed
15. Xu S, Ma J, Ji R, Pan K, Miao AJ. Microplastics in aquatic environments: occurrence, accumulation, and biological effects. *Sci Total Environ* 2020;703:134699. DOI PubMed
16. Abbasi S, Turner A. Sources, concentrations, distributions, fluxes and fate of microplastics in a hypersaline lake: Maharloo, south-west Iran. *Sci Total Environ* 2022;823:153721. DOI PubMed
17. Esfandiari A, Abbasi S, Peely AB, et al. Distribution and transport of microplastics in groundwater (Shiraz aquifer, southwest Iran). *Water Res* 2022;220:118622. DOI PubMed
18. Ginebreda A. Emerging contaminants and nanoplastics in the water environment: a matter of rising concern. *Water Emerg Contam Nanoplastics* 2022;1:1. DOI
19. Picó Y, Manzoor I, Soursou V, Barceló D. Microplastics in water, from treatment process to drinking water: analytical methods and potential health effects. *Water Emerg Contam Nanoplastics* 2022;1:13. DOI
20. Leterme SC, Tuuri EM, Drummond WJ, Jones R, Gascooke JR. Microplastics in urban freshwater streams in Adelaide, Australia: a source of plastic pollution in the Gulf St Vincent. *Sci Total Environ* 2023;856:158672. DOI PubMed
21. Eberhard T, Casillas G, Zarus GM, Barr DB. Systematic review of microplastics and nanoplastics in indoor and outdoor air: identifying a framework and data needs for quantifying human inhalation exposures. *J Expo Sci Environ Epidemiol* 2024;34:185-96. DOI PubMed PMC
22. Prata JC, Castro JL, da Costa JP, Duarte AC, Rocha-Santos T, Cerqueira M. The importance of contamination control in airborne fibers and microplastic sampling: experiences from indoor and outdoor air sampling in Aveiro, Portugal. *Mar Pollut Bull* 2020;159:111522. DOI PubMed
23. Giechaskiel B, Grigoratos T, Mathissen M, et al. Contribution of road vehicle tyre wear to microplastics and ambient air pollution. *Sustainability* 2024;16:522. DOI
24. Abbasi S, Turner A. Dry and wet deposition of microplastics in a semi-arid region (Shiraz, Iran). *Sci Total Environ* 2021;786:147358. DOI PubMed
25. Chandrakanthan K, Fraser MP, Herckes P. Airborne microplastics in a suburban location in the desert southwest: occurrence and identification challenges. *Atmos Environ* 2023;298:119617. DOI
26. Liu S, Bai F, Men Z, et al. Spatial distribution, source apportionment and potential ecological risk assessment of suspended atmosphere microplastics in different underlying surfaces in Harbin. *Sci Total Environ* 2023;901:166040. DOI PubMed
27. Zhao X, Zhou Y, Liang C, et al. Airborne microplastics: occurrence, sources, fate, risks and mitigation. *Sci Total Environ* 2023;858:159943. DOI PubMed
28. Abbasi S, Ahmadi F, Khodabakhshloo N, et al. Atmospheric deposition of microplastics in Shiraz, Iran. *Atmos Pollut Res*

2024;15:101977. DOI

29. Din K, Khokhar MF, Butt SI, Qadir A, Younas F. Exploration of microplastic concentration in indoor and outdoor air samples: morphological, polymeric, and elemental analysis. *Sci Total Environ* 2024;908:168398. DOI PubMed
30. Scheurer M, Bigalke M. Microplastics in Swiss Floodplain Soils. *Environ Sci Technol* 2018;52:3591-8. DOI PubMed
31. Zhang GS, Liu YF. The distribution of microplastics in soil aggregate fractions in southwestern China. *Sci Total Environ* 2018;642:12-20. DOI PubMed
32. Abbasi S, Turner A, Hoseini M, Amiri H. Microplastics in the Lut and Kavir Deserts, Iran. *Environ Sci Technol* 2021;55:5993-6000. DOI PubMed
33. Chandrakanthan K, Fraser MP, Herckes P. Microplastics are ubiquitous and increasing in soil of a sprawling urban area, Phoenix (Arizona). *Sci Total Environ* 2024;906:167617. DOI PubMed
34. Palazot M, Soccalingame L, Froger C, et al. First national reference of microplastic contamination of French soils. *Sci Total Environ* 2024;918:170564. DOI PubMed
35. Liu B, Shen Z, Zhou Q, et al. Microplastics in soil aggregates: analytical methods, occurrence patterns, impact analyses and removal approaches. *TrAC Trend Anal Chem* 2024;178:117855. DOI
36. Lambert S, Wagner M. Microplastics are contaminants of emerging concern in freshwater environments: an overview. In: Wagner M, Lambert S, editors. Freshwater microplastics. Cham: Springer International Publishing; 2018. pp. 1-23. DOI
37. Eerkes-Medrano D, Thompson RC, Aldridge DC. Microplastics in freshwater systems: a review of the emerging threats, identification of knowledge gaps and prioritisation of research needs. *Water Res* 2015;75:63-82. DOI PubMed
38. Gatidou G, Arvaniti OS, Stasinakis AS. Review on the occurrence and fate of microplastics in Sewage Treatment Plants. *J Hazard Mater* 2019;367:504-12. DOI PubMed
39. Phuong NN, Duong TT, Le TPQ, et al. Microplastics in Asian freshwater ecosystems: current knowledge and perspectives. *Sci Total Environ* 2022;808:151989. DOI PubMed
40. Gomiero A, Øysæd KB, Jaén-gil A, Navrestad V, Skogerbø G. To what extent are wastewater treatment systems a gateway for microplastic particles in the aquatic and terrestrial environments? *Water Emerg Contam Nanoplastics* 2024;3:13. DOI
41. Koelmans AA, Mohamed Nor NH, Hermsen E, Kooi M, Mintenig SM, De France J. Microplastics in freshwaters and drinking water: critical review and assessment of data quality. *Water Res* 2019;155:410-22. DOI PubMed PMC
42. Claessens M, De Meester S, Van Landuyt L, De Clerck K, Janssen CR. Occurrence and distribution of microplastics in marine sediments along the Belgian coast. *Mar Pollut Bull* 2011;62:2199-204. DOI PubMed
43. Stolte A, Forster S, Gerdts G, Schubert H. Microplastic concentrations in beach sediments along the German Baltic coast. *Mar Pollut Bull* 2015;99:216-29. DOI PubMed
44. Karthik R, Robin RS, Purvaja R, et al. Microplastics along the beaches of southeast coast of India. *Sci Total Environ* 2018;645:1388-99. DOI PubMed
45. Barboza LGA, Dick Vethaak A, Lavorante BRBO, Lundebye AK, Guilhermino L. Marine microplastic debris: an emerging issue for food security, food safety and human health. *Mar Pollut Bull* 2018;133:336-48. DOI PubMed
46. O’Brien S, Okoffo ED, O’Brien JW, et al. Airborne emissions of microplastic fibres from domestic laundry dryers. *Sci Total Environ* 2020;747:141175. DOI PubMed
47. Soltani N, Amini-Birami F, Keshavarzi B, et al. Microplastic occurrence in selected aquatic species of the Persian Gulf: no evidence of trophic transfer or effect of diet. *Sci Total Environ* 2023;892:164685. DOI PubMed
48. Pinlova B, Nowack B. Characterization of fiber fragments released from polyester textiles during UV weathering. *Environ Pollut* 2023;322:121012. DOI PubMed
49. O’Loughlin C. The impact of activewear/swimwear laundering: investigating microplastic-fibre emissions from recycled and non-recycled synthetic textiles. *J Home Econ Inst Aust* 2018;25:2-12. Available from: https://search.informit.org/doi/10.3316/ielapa.107251401188651. [Last accessed on 9 Sep 2024]
50. Rathinamoorthy R, Raja Balasaraswathi S, Madhubashini S, Prakalya A, Rakshana JB, Shathvika S. Investigation on microfiber release from elastane blended fabrics and its environmental significance. *Sci Total Environ* 2023;903:166553. DOI PubMed
51. Imhof HK, Ivleva NP, Schmid J, Niessner R, Laforsch C. Contamination of beach sediments of a subalpine lake with microplastic particles. *Curr Biol* 2013;23:R867-8. DOI PubMed
52. D’Avignon G, Gregory-Eaves I, Ricciardi A. Microplastics in lakes and rivers: an issue of emerging significance to limnology. *Environ Rev* 2022;30:228-44. DOI
53. Costigan E, Collins A, Hatinoglu MD, et al. Adsorption of organic pollutants by microplastics: overview of a dissonant literature. *J Hazard Mater Adv* 2022;6:100091. DOI
54. Whiting QT, O’Connor KF, Potter PM, Al-Abed SR. A high-throughput, automated technique for microplastics detection, quantification, and characterization in surface waters using laser direct infrared spectroscopy. *Anal Bioanal Chem* 2022;414:8353-64. DOI PubMed PMC
55. Hatinoglu MD, Perreault F, Apul OG. Modified linear solvation energy relationships for adsorption of perfluorocarboxylic acids by polystyrene microplastics. *Sci Total Environ* 2023;860:160524. DOI PubMed
56. Schets FM, Schijven JF, de Roda Husman AM. Exposure assessment for swimmers in bathing waters and swimming pools. *Water Res* 2011;45:2392-400. DOI PubMed
57. Ramírez-Castillo FY, Loera-Muro A, Jacques M, et al. Waterborne pathogens: detection methods and challenges. *Pathogens* 2015;4:307-34. DOI PubMed PMC

58. Albarano L, Maggio C, La Marca A, et al. Risk assessment of natural and synthetic fibers in aquatic environment: a critical review. *Sci Total Environ* 2024;934:173398. DOI PubMed
59. Chiu CA, Westerhoff P, Herckes P, Masles M, Elliott G. Monitoring of trace-level pharmaceuticals and personal care products in Salt River Project Waters Final Report. 2009 Available from: https://www.researchgate.net/publication/383877016_Monitoring_of_Trace-Level_Pharmaceuticals_and_Personal_Care_Products_in_Salt_River_Project_Waters_Final_Report_Submitted_to_Salt_River_Project. [Last accessed on 9 Sep 2024].
60. Banville MJ, Bateman HL. Urban and wildland herpetofauna communities and riparian microhabitats along the Salt River, Arizona. *Urban Ecosyst* 2012;15:473-88. DOI
61. Yang Y, Reed R, Schoepf J, Hristovski K, Herckes P, Westerhoff P. Prospecting nanomaterials in aqueous environments by cloud-point extraction coupled with transmission electron microscopy. *Sci Total Environ* 2017;584-5:515-22. DOI PubMed
62. Venkatesan AK, Reed RB, Lee S, et al. Detection and sizing of Ti-containing particles in recreational waters using single particle ICP-MS. *Bull Environ Contam Toxicol* 2018;100:120-6. DOI PubMed
63. Metcalfe AN, Muehlbauer JD, Ford MA, Kennedy TA. Chapter 11 - Colorado River Basin. In: Rivers of North America. Elsevier; 2023. pp. 462-509. DOI
64. Masura J, Baker J, Foster G, Arthur C. Laboratory methods for the analysis of microplastics in the marine environment: recommendations for quantifying synthetic particles in waters and sediments. 2015. Available from: https://repository.oceanbestpractices.org/handle/11329/1076. [Last accessed on 9 Sep 2024].
65. Dawson AL, Santana MFM, Nelis JLD, Motti CA. Taking control of microplastics data: a comparison of control and blank data correction methods. *J Hazard Mater* 2023;443:130218. DOI PubMed
66. Hidalgo-Ruz V, Gutow L, Thompson RC, Thiel M. Microplastics in the marine environment: a review of the methods used for identification and quantification. *Environ Sci Technol* 2012;46:3060-75. DOI PubMed
67. Baldwin AK, Spanjer AR, Rosen MR, Thom T. Microplastics in Lake Mead National Recreation Area, USA: occurrence and biological uptake. *PLoS One* 2020;15:e0228896. DOI PubMed PMC
68. Baldwin AK, King KA, Mason SA, Hoellein TJ, Kim LH, Karns B. Data release for microplastics in water, sediment, fish, and mussels in the St. Croix National Scenic Riverway and Mississippi National River and Recreation Area, Wisconsin and Minnesota, 2015. 2017. Available from: https://www.usgs.gov/data/data-release-microplastics-water-sediment-fish-and-mussels-st-croix-national-scenic-riverway. [Last accessed on 9 Sep 2024].
69. Moore CJ, Lattin GL, Zellers AF. Quantity and type of plastic debris flowing from two urban rivers to coastal waters and beaches of Southern California. *RGCI* 2011;11:65-73. DOI
70. Inland Ocean Coalition. Pilot study finds evidence of microplastics in Colorado's headwater stream. Available from: https://inlandoceancoalition.org/learn/plastic/microplastics-working-group/. [Last accessed on 9 Sep 2024].
71. Mallik A, Xavier KAM, Naidu BC, Nayak BB. Ecotoxicological and physiological risks of microplastics on fish and their possible mitigation measures. *Sci Total Environ* 2021;779:146433. DOI PubMed
72. Hu E, Sun C, Yang F, et al. Microplastics in 48 wastewater treatment plants reveal regional differences in physical characteristics and shape-dependent removal in the transition zone between North and South China. *Sci Total Environ* 2022;834:155320. DOI PubMed
73. Shamskhany A, Li Z, Patel P, Karimpour S. Evidence of microplastic size impact on mobility and transport in the marine environment: a review and synthesis of recent research. *Front Mar Sci* 2021;8:760649. DOI
74. Napper IE, Thompson RC. Release of synthetic microplastic plastic fibres from domestic washing machines: effects of fabric type and washing conditions. *Mar Pollut Bull* 2016;112:39-45. DOI PubMed
75. Thacharodi A, Meenatchi R, Hassan S, et al. Microplastics in the environment: a critical overview on its fate, toxicity, implications, management, and bioremediation strategies. *J Environ Manage* 2024;349:119433. DOI
76. Martin J, Lusher A, Thompson RC, Morley A. The deposition and accumulation of microplastics in marine sediments and bottom water from the Irish Continental Shelf. *Sci Rep* 2017;7:10772. DOI PubMed PMC
77. Wood M, Simmonds L, MacAdam J, Hassard F, Jarvis P, Chalmers RM. Role of filtration in managing the risk from *Cryptosporidium* in commercial swimming pools - a review. *J Water Health* 2019;17:357-70. DOI PubMed
78. United States EPA-832-F-22-015. Jump into pool water efficiency. 2022. Available from: https://www.epa.gov/system/files/documents/2022-09/ws-outdoor-pool-guide.pdf. [Last accessed on 9 Sep 2024].
79. Cisco J. The fate of microplastics in tres rios, a constructed treatment wetland. 2023. Available from: https://keep.lib.asu.edu/system/files/c7/Cisco_asu_0010N_22995.pdf. [Last accessed on 9 Sep 2024].
80. Carr SA. Sources and dispersive modes of micro-fibers in the environment. *Integr Environ Assess Manag* 2017;13:466-9. DOI PubMed
81. Chandrakanthan K. Microplastics in the Desert Southwest: occurrence and characterization in atmospheric, aquatic, and terrestrial environments. 2024. Available from: https://keep.lib.asu.edu/system/files/c7/Chandrakanthan_asu_0010E_23729.pdf. [Last accessed on 9 Sep 2024].

idæa

OPEN ACCESS

Online ISSN: 2831-2597

Volume 3, Issue 4, December 2024

Water Emerging Contaminants & Nanoplastics

oae | WECN

https://oaepublish.com/wecn

Sawma *et al. Water Emerg Contam Nanoplastics* 2024;3:21
DOI: 10.20517/wecn.2024.36

Water Emerging Contaminants & Nanoplastics

Review

Open Access

Environmental management of microplastics and additives: a critical review of treatment technologies and their impact

Marie Joe Sawma, Ramez M. Zayyat, Rand Ghaddar, George M. Ayoub

Department of Civil and Environmental Engineering, American University of Beirut, Beirut 1107 2020, Lebanon.

Correspondence to: Prof. George M. Ayoub, Department of Civil and Environmental Engineering, American University of Beirut, Riad El-Solh Street, Beirut 1107 2020, Lebanon. E-mail: Gayoub@aub.edu.lb

How to cite this article: Sawma MJ, Zayyat RM, Ghaddar R, Ayoub GM. Environmental management of microplastics and additives: a critical review of treatment technologies and their impact. *Water Emerg Contam Nanoplastics* 2024;3:21. https://dx.doi.org/10.20517/wecn.2024.36

Received: 12 Jun 2024 **First Decision:** 12 Aug 2024 **Revised:** 19 Oct 2024 **Accepted:** 23 Oct 2024 **Published:** 30 Oct 2024

Academic Editors: Zhijie Chen, Joana C Prata **Copy Editor:** Pei-Yun Wang **Production Editor:** Pei-Yun Wang

Abstract

Microplastics (MPs) and their associated chemical additives, such as bisphenol A (BPA), nonylphenol (NP), nonylphenol ethoxylate (NEPO), and tetrabromobisphenol (TBBPA), are widely recognized as significant environmental contaminants due to their widespread presence in ecosystems and their potential impact on human health. This review evaluates advanced treatment technologies, such as membrane filtration and oxidation processes, for mitigating these risks and highlights gaps in sustainability and efficiency. Actionable strategies for improving the removal of MPs and MP additives were presented in the assessment of innovative hybrid treatment tailored to different water matrices. The importance of anti-fouling technologies, comprehensive life cycle assessments (LCAs), and standardizing treatment methods to enhance the sustainability and applicability of these technologies were further highlighted. To further improve and optimize treatment processes and ensure sustainability, existing knowledge gaps must be addressed by framing a comprehensive understanding of the long-term ecological effects of MPs and their additives.

Keywords: Microplastics, MP additives, membrane filtration, advanced oxidation, environmental conservation

INTRODUCTION

Plastics began gaining popularity in the 1940s and have since diversified into many types. Recently, annual global plastic production has increased to 359 million tons, with China accounting for 30% of this output[1]. The widespread use of plastics can be attributed to their convenience, affordability, light weight, and durability[1]. They are utilized in numerous sectors, including containers for food and beverages, thermal insulation materials, furniture for homes and offices, electronic gadgets, vehicle interiors, children's toys, textiles, surface coatings, and medical equipment such as prosthetic joints, incubators, intravenous (IV) fluid bags, and drug delivery mechanisms[2]. However, managing plastic waste is a growing concern, as only about 15% of the plastics produced annually are recycled[3]. Thus, the main challenge with plastics is their long-lasting nature, with some lasting hundreds of years before breaking down. This durability contributes to plastic pollution in both land and water environments. Studies show that every year, between 1.15 and 2.41 million metric tons of plastic enter the ocean, leading to large areas of floating debris like the Great Pacific Garbage Patch, which covers about 1.6 million square kilometers[4]. Haque *et al.* (2023) reported that global plastic production increased from 1.3 million tons in 1950 to 359 million tons in 2018, expected to reach 634 million tons by 2025, highlighting the massive global increase in plastic production[5]. Among the various forms of plastic pollution, microplastics (MPs), and MP additives such as bisphenol A (BPA), nonylphenol (NP), and tetrabromobisphenol (TBBPA), have emerged as significant environmental contaminants. These particles are widespread in many ecosystems and pose a serious risk to human health, as well as terrestrial and aquatic environments, due to their persistence and ability to bioaccumulate[6].

Even though the treatment of MPs and MP additives is gaining momentum with new advancements and processes, several significant knowledge gaps persist[7]. The long-term ecological effects of MPs and their additives are not well understood[8]. Additionally, present treatment methods often fall short of complete removal and health effect mitigation of these contaminants, particularly in diverse environmental settings. Furthermore, the lack of standard operating procedures for the analysis and treatment of MPs in different water matrices complicates the evaluation and comparison of treatment performance[9].

In this study, a thorough review of the spread of MPs in the environment and their impacts on health, aquatic systems, and terrestrial systems will be presented. This work also aims to address the current gaps by providing a detailed assessment of advanced treatment technologies, including the innovative integration of membrane filtration with advanced oxidation processes (AOPs). The paper is structured as follows: an overview of the sources and types of MPs, followed by discussions on their environmental and health impacts. The bulk of the review evaluates several treatment techniques, emphasizing advanced oxidation and membrane filtration, with conclusions focusing on sustainability and the need for further research.

SOURCES AND TYPES OF MPS

MPs are small plastic particles, typically less than 5 mm in size, which can exist in various forms such as fibers, films, fragments, beads, and foams[10]. These particles are widespread in the environment due to their resistance to degradation and their persistent nature. MPs are classified into two primary types based on their origin: primary MPs, which are intentionally manufactured for specific purposes, and secondary MPs, which result from the breakdown of larger plastic materials[11].

Primary MPs

Primary MPs, like glitter and microbeads, are intentionally manufactured particles found in personal care products and industrial processes, contributing significantly to environmental contamination due to their small size and persistence[12].

Microbeads are another common form of MPs, and they are small spherical particles often found in personal care products such as exfoliants, cleansers, and toothpaste. These microbeads are added for their abrasive properties, aiding in the removal of dead skin cells or dirt. However, due to their tiny size and inability to be captured by wastewater treatment plants, they easily enter aquatic systems, contributing to widespread pollution[13]. Despite increasing regulatory efforts to ban microbeads in many countries, they remain a persistent problem in regions where regulations are not yet enforced or where existing products containing microbeads are still in use.

Secondary MPs

Secondary MPs are those that result from the breakdown of larger plastics under environmental stressors like UV radiation and mechanical abrasion into smaller particles over time[13-16]. This degradation occurs when macroplastics are exposed to prolonged environmental factors such as sunlight, weather, and moisture[17]. Research by Bajt highlights UV sunlight as the primary factor in this degradation process[18]. UV light breaks chemical bonds in the macroplastics, producing plastic fragments, fibers, or films. This process, known as photodegradation, increases the number of secondary MPs in the environment, contributing to their growing presence in various ecosystems. Mechanical abrasion and chemical interactions further accelerate plastic fragmentation. The continuous production of secondary MPs from plastic waste contributes to their persistent accumulation in marine and terrestrial environments, posing significant ecological challenges[19]. Figure 1 depicts the sources of MPs in the environment.

ENVIRONMENTAL IMPACT OF MPS

MPs have accumulated in significant quantities in both aquatic and terrestrial environments due to inadequate plastic waste management[20]. They often carry various micropollutants that can be harmful to the environment and human health, especially when they enter the food chain. The persistence of MPs in the environment makes understanding their full environmental impact essential for developing effective strategies to mitigate their consequences on both land and water ecosystems, as well as human health.

Impact on aquatic system

MPs in aquatic systems primarily originate from terrestrial environments due to industrial, agricultural, and domestic activities. These insoluble particles enter water bodies through various routes, including wastewater treatment plants, sewer floods, soil erosion, and precipitation[21]. Once in water bodies, MPs attract and accumulate organic and inorganic pollutants from their surroundings, facilitating the spread of contaminants across ecosystems. This contamination not only deteriorates water quality but also disrupts natural habitats and biodiversity. For instance, studies have shown that MPs can inhibit algae's photosynthetic activity, leading to reduced growth rates, which has cascading effects throughout aquatic food webs[22]. Canniff *et al.* deduced that MPs can inhibit the photosynthetic activity of algae. For instance, the paper reports a 30% decline in the growth rate of the algae species Raphidocelis subcapitata due to exposure to MPs[23]. These findings illustrate that even at low concentrations, MPs can have cascading effects on aquatic food webs, ultimately impacting higher trophic levels, including humans.

Impact on terrestrial system

MPs are transported to the soil through natural soil processes like biopores and cracking, as well as through agricultural activities such as harvesting and plowing[24]. Their presence in the soil can significantly damage soil health by harming its microorganisms, as documented by various studies[25-27]. Additionally, improper disposal of plastic products and the accumulation of plastics in landfills pose major environmental challenges. Additionally, MPs block water drainage systems, contributing to flooding and mosquito breeding, which poses public health risks[28,29]. Furthermore, biodegradable MPs contribute to increased production of nitrous oxide (N_2O), a strong greenhouse gas, thereby potentially intensifying global

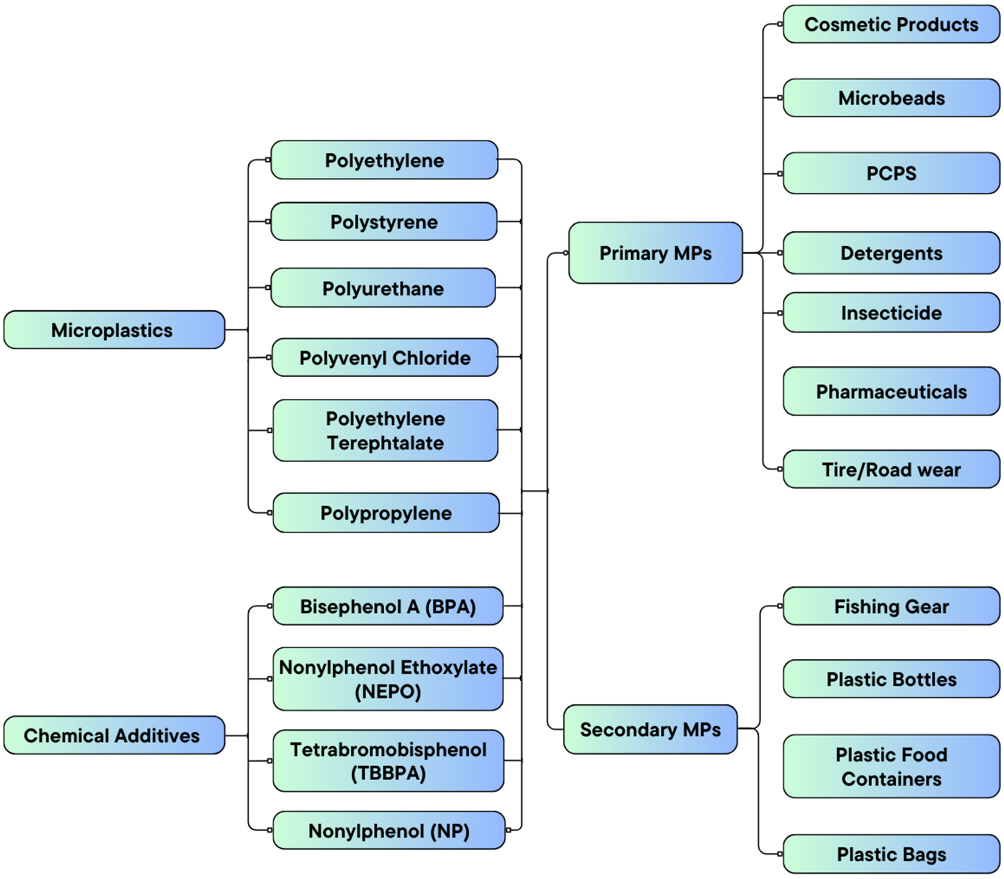

Figure 1. Sources of MPs in the environment. MPs: Microplastics.

warming[30]. The accumulation of MPs in terrestrial environments not only threatens ecosystem health but also contributes to broader environmental issues such as climate change and water management challenges[31].

Impact on human health

MPs can enter the human body through inhalation, ingestion of contaminated food and water, or skin contact[32-34]. Their small size allows them to accumulate in human tissues, leading to oxidative stress, inflammation, and immune system disruptions[30,35]. Prolonged exposure has been linked to chronic conditions such as cardiovascular disease, respiratory issues, and even cancer[36,37]. MPs can also interfere with the human microbiome[28,38,39], potentially leading to metabolic disorders or immune dysfunction[40-43]. The long-term presence of MPs in human tissues underscores their potential for causing cumulative damage, raising serious concerns about public health implications, especially in highly exposed populations. Figure 2 illustrates the environmental impact and sources of MPs.

MP ADDITIVES

MP Additives are chemicals incorporated during the manufacturing process to enhance the physical and chemical properties of the plastics. These additives improve color, transparency, and resistance to temperature, light radiation, moisture, and humidity. Despite their utility in enhancing plastic properties, they pose significant environmental contamination risks, affecting soil, water, air, and human health, similar to what was discussed earlier[44]. Life cycle assessments (LCAs) of these additives have shown that current

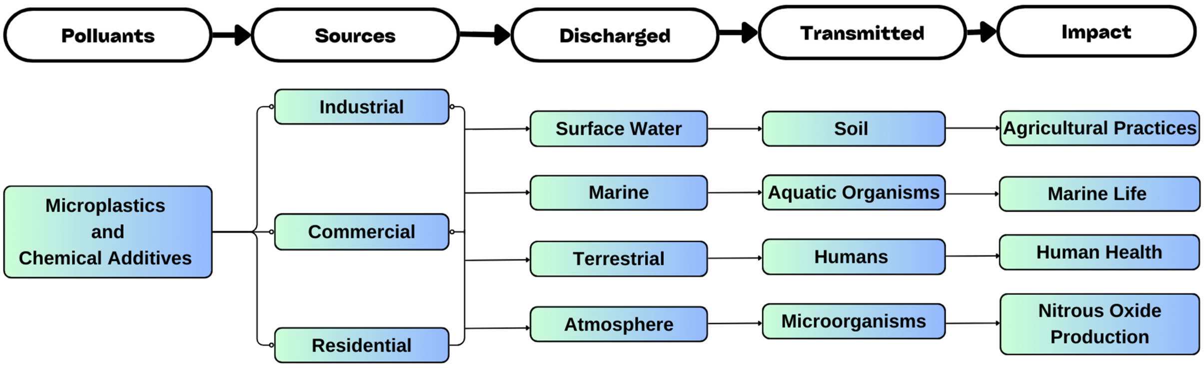

Figure 2. Environmental impact, sources, and pathways of MPs. MPs: Microplastics.

plastic recycling processes are not capable of effectively removing these harmful substances[45]. Common chemical additives used in the production of MPs include BPA, NP, nonylphenol ethoxylate (NEPO), and tetrabromobisphenol A (TTBA). Given their persistence in the environment, these additives continue to accumulate in ecosystems, compounding the challenges associated with plastic pollution and requiring comprehensive strategies for mitigation.

BPA

BPA, also known as 4,4'-(propane-2,2-diyl) diphenol, is a synthetic organic compound widely used in the manufacture of certain plastics and epoxy resins. Its properties enhance the transparency, durability, and heat resistance of these materials, making it a fundamental ingredient in various consumer products. BPA is primarily found in polycarbonate (PC) plastics, which are used to produce items such as water bottles, food storage containers, eyeglass lenses, and dental sealants. It is also used in epoxy resins, which coat food and beverage cans and line water pipes to prevent corrosion. The European Union Water Framework Directive has classified BPA as a priority pollutant due to its environmental impact. It enters the environment through sources such as wastewater treatment plants, runoff, landfill leachate, and industrial discharges. BPA is also classified as one of the endocrine-disrupting compounds (EDCs)[46,47]. Santoro *et al.* argued that BPA possesses estrogen-like and anti-androgenic properties, leading to damage in various tissues and organs, including those of the reproductive, immune, and neuroendocrine systems[48]. Similarly, research conducted by Seachrist *et al.* concluded that early-life exposure to BPA is a risk factor for breast and prostate cancer[49]. The widespread use of BPA in consumer products and its presence in various environmental mediums underscores the need for more stringent regulations and safer alternatives[50].

NP

NP encompasses a group of isomeric compounds, including 4-NP, phenol, p-nonyl-, 4-p-NP, and 4-nonyl-, para nonyl. NP, known as a major environmental contaminant, is present in different environmental mediums, including soil, air, bodies of water, and potable water systems. It is mainly utilized in producing antioxidants, lubricant oil additives, and NEPOs surfactants. As an endocrine disruptor, NP has been extensively studied for its effects on the growth, development, reproduction, and behavior of organisms, including impacts on future generations[51]. NP mimics the natural hormone 17β-estradiol, binding competitively to estrogen receptors and disrupting the endocrine systems of higher organisms[52,53]. Additionally, studies have shown that NP can induce the proliferation of breast tumor cells[54]. The ubiquitous presence, persistence, and resistance to degradation of NP in the environment pose serious concerns[51,55], highlighting the urgent need for rigorous monitoring and effective mitigation strategies to remove NP from water and wastewater systems. Failure to address NP contamination may lead to long-term ecological and human health risks, emphasizing the importance of identifying alternative chemicals and developing more efficient removal technologies[56]. The potential for long-term environmental and public health harm due to NP contamination highlights the need for developing more potent removal techniques and alternative chemical sources.

TBBPA

TBBPA is commonly used as a reagent in the production of epoxy and PC resins, which are commonly found in electronic devices, furniture, and various types of equipment[57,58]. It is extensively present in both abiotic and biotic environments, including air, water, soil, indoor dust, sediments, sewage sludge, and the food chain. Human exposure to TBBPA primarily occurs through dietary intake, ingestion of dust, and dermal contact[59]. Notably, TBBPA has been detected in human breast milk and maternal/cord serum[60], indicating its presence in the blood serum of infants and cord blood[61]. Research has shown that TBBPA can significantly impact growth and development, induce oxidative stress, generate reactive oxygen species (ROS), and affect antioxidant defense systems[62]. Furthermore, TBBPA acts as a thyroid hormone antagonist[63,64], impacting the hypothalamic-pituitary-thyroid axis and related gene expression[62,65]. TBBPA is widely used, and its discovery in human biological fluids raises major concerns about the substance’s long-term health impacts, particularly for vulnerable groups, including expecting mothers and newborns[66].

ADVANCED TREATMENT METHODS FOR MPS AND ADDITIVES

The presence of MPs and additives in both terrestrial and aquatic ecosystems has raised significant concerns regarding their potential impacts on environmental and human health. Addressing these emerging concerns necessitates the implementation of advanced treatment methods that can effectively remove MPs and additives from water. Membrane filtration is a technique used for removing many types of MPs, as it filters out particles larger than its pore size. However, it is not capable of removing dissolved additives associated with MPs. To overcome this limitation, AOPs have been developed to degrade these chemical additives[67].

Membrane filtration

Membrane filtration is a commonly used technology in water treatment because it physically blocks particles larger than the membrane’s pore size, successfully removing MPs from water. Membranes are comprised of a variety of polymers that offer durability and chemical resistance, making them suitable for use in a wide range of municipal, industrial, and residential water treatment systems.

Microfiltration

Microfiltration (MF) consists of a semipermeable membrane with pore sizes typically ranging from 0.1 to 10 micrometers[68]. They are made from various polymers, including polyvinylidene fluoride (PVDF), cellulose acetate (CA), polytetrafluoroethylene (PTFE), olefins, and PC. These polymers are characterized by their excellent film-forming capabilities, mechanical strength, and thermal stability. Additionally, they maintain physical and chemical stability across a broad range of pH levels[69]. The required pressure to force the contaminated water through the membrane is relatively low due to the large pore sizes, allowing for high water flux with minimal resistance[70].

Yahyanezhad *et al.* conducted a study exploring the use of a PVDF membrane with a 0.1 μm pore size for MF[71]. The study utilized an aeration system to prevent membrane fouling and examined three samples with varying concentrations of MPs in wastewater. The MP concentrations in the samples were 220 ± 23, 216 ± 19, and 184 ± 26 MPs/L, with corresponding removal efficiencies of 98%, 100%, and 98.9%, respectively. The results indicated that even at higher concentrations of MPs and their additives, a removal efficiency of 98% can be obtained.

While the study reports a high removal efficiency in removing MPs and their additives, several critical aspects are inadequately addressed, diminishing the robustness of the findings. The paper emphasizes the removal efficiency without sufficiently exploring the long-term sustainability of the MF process, particularly the significant issue of membrane fouling, which can degrade performance over time and increase operational costs. The brief mention of post-treatment needs is insufficient, as the paper does not specify viable methods to address the MPs that still pass through the system, which would have strengthened their conclusions. The experimental design also has limitations, particularly regarding the seasonal variability of samples, yet the study fails to conduct a robust statistical analysis to determine whether these differences are statistically significant. Moreover, the results are based on a specific wastewater treatment plant and the paper does not adequately discuss the limitations of generalizing these findings to other regions with different wastewater compositions or treatment processes.

Expanding on the examination of different membrane materials and their effectiveness, Pizzichetti *et al.* investigated the effectiveness of three different MF PC, CA, and PTFE for removing MPs from tap water[69]. All membranes showed high mass removal efficiencies above 94% for polyamide and polystyrene MPs. Among these, the study found that CA membranes provided an optimal balance between water flux, transmembrane pressure (TMP), and MP removal efficiency, making them suitable for household water filtration. While the authors report high removal efficiencies of above 94% for all tested membranes, they do not adequately address how different membrane materials interact with MPs and their additives, which could affect the generalizability of the findings. The paper also discusses the issue of MPs breaking down into smaller particles during filtration but does not sufficiently explore the implications of this phenomenon, particularly the potential formation of nanoplastics, which could pose even greater environmental risks. Overall, the discussion could be strengthened by addressing these limitations and providing a more critical and comprehensive analysis of the experimental results and their implications. The materials used in MF membranes contribute to the durability and reliability of the system under various operating conditions, maintaining consistent performance over time, thus resulting in reduced maintenance costs and an extended lifespan of the filtration system[72].

Nevertheless, MF encounters several notable challenges in the removal of MPs from water. MF is less effective for removing smaller particles, necessitating supplementary treatment processes for comprehensive removal, leading to increased time and operational costs and increased energy consumption[73]. The efficiency of MF in removing MPs is significantly affected by the density of the particles. High-density MPs, such as polyethylene terephthalate (PET) (1.37 g/cm^3), are more effectively captured by sedimentation and MF processes compared to lower-density MPs like polyethylene (PE) and polypropylene (PP) (0.91-0.97 g/cm^3), which tend to remain buoyant or suspended in the water column. This disparity in density necessitates the implementation of supplementary treatment processes to ensure the comprehensive removal of all MP particles[74]. MF has proven to be a reliable method for removing MPs from water, and its continued application in water treatment systems is crucial for mitigating plastic pollution. However, addressing challenges such as membrane fouling and supplementing MF with other treatment processes will be necessary to achieve long-term sustainability and optimal performance.

Ultrafiltration

Ultrafiltration (UF) is an effective membrane filtration technique that utilizes small pore sizes, typically ranging from 0.001 to 0.1 microns, to selectively retain MPs[75]. The process of filtration begins by applying TMP, which forces water through the membrane and ensures that contaminants, including MPs, are retained on the membrane surface[76]. UF typically operates under a TMP range of 1 to 10 bar (14.5 to 145 psi)[77]. During the UF process, viscosity and total resistance are monitored as they are critical factors affecting water flux. Increased viscosity and resistance decrease the flow rate, thereby reducing flux. While viscosity can be improved by selecting low-resistance membranes and implementing anti-fouling strategies such as regular cleaning, it can also be managed by pre-treating the feed water[78,79].

Tadsuwan and Babel evaluated a pilot-scale UF system within conventional wastewater treatment plants[77]. The goal was to assess the potential of UF as a tertiary treatment stage for removing MPs. The study found that traditional treatment systems removed 86.14% of MPs from the influent. When UF was introduced, the removal efficiency increased significantly to 96.97%. Similarly, a study conducted by Magni *et al.* examined the effectiveness of UF membranes in removing MPs from coastal waters[80]. The study utilized UF membranes with a pore size of 0.04 microns to filter water samples collected from various coastal locations known for high levels of MP pollution. The findings revealed that the UF membranes were highly efficient, achieving a removal efficiency of up to 98% for MPs and additives. It also highlighted that UF could effectively capture a wide range of MP sizes, including those as small as 0.1 microns.

However, the discussion does not sufficiently address the limitations and potential challenges associated with this approach. For instance, while the UF system significantly enhances MP removal, the study does not delve into the operational challenges such as membrane fouling, which could impair long-term efficiency and increase maintenance costs. Additionally, the study's reliance on grab sampling may introduce variability and limit the generalizability of the findings, as this method may not capture the full range of MP sizes in the wastewater. Moreover, the study overlooks the broader environmental implications of the retained MPs in the sludge, which, if not properly managed, could contribute to secondary pollution when the sludge is used in agriculture or disposed of in the environment.

To examine the efficiency of the UF technique under different conditions, UF was evaluated in various applications: wastewater treatment, industrial processes, and drinking water purification. In drinking water purification, UF reaches up to 99% removal efficiency, as the feed water typically has lower concentrations of contaminants, allowing more effective removal of MPs. Pre-treatment processes such as coagulation and sedimentation, which often precede UF in drinking water systems, further reduce the burden on the membranes[81]. In wastewater treatment, UF achieves up to 97% removal efficiency. In industrial processes, UF achieves up to 98% removal efficiency, maintaining product purity and ensuring compliance with regulatory standards. Although UF is a highly effective filtration technology, its performance is heavily influenced by the quality of the feed water, the presence and effectiveness of pre-treatment processes, and the operational conditions in each specific application. A comprehensive evaluation of these factors is essential for optimizing UF performance and ensuring consistent, long-term efficiency across different applications.

UF presents high removal efficiency for MPs and additives, which can be attributed to the ultrafine pore sizes of UF membranes that enable them to effectively capture and eliminate contaminants. Its slightly lower removal efficiency in wastewater treatment compared to drinking water treatment is due to the higher and more varied contaminant loads, including organic matter and oils, which can interfere with the filtration process[82]. Similarly, variations in the efficiency of industrial effluent treatment are attributed to the specific contaminants and MPs[80]. Despite these challenges, UF demonstrates superior performance over MF by effectively handling high densities of contaminants.

In summary, UF demonstrates high removal efficiency for a wide range of MP sizes, making it a valuable tool in water treatment. However, the technique requires further optimization to address issues related to membrane fouling and the handling of MP-laden sludge to ensure long-term sustainability.

Nanofiltration

Nanofiltration (NF) is a membrane filtration process that operates between UF and RO. NF membranes typically have pore sizes ranging from 1 to 10 nanometers and operate at pressures between 4 and 10 bars[83]. As water passes through the NF membrane, MPs and other larger contaminants are retained on the membrane surface, reducing their concentration in the treated water. The shape of MPs can significantly influence their interaction with NF membranes, potentially affecting removal efficiency. A study conducted by Jang *et al.* shows that fibrous MPs can form a dense network on the membrane, leading to more significant fouling and reduced water flux compared to spherical MPs, which tend to form more uniform layers[84]. Furthermore, the density of MPs influences their interaction with the membrane. Higher-density particles are more likely to settle and cause fouling, leading to the formation of a cake layer, which provides additional hydraulic resistance and further reduces the membrane's performance[85].

NF has demonstrated impressive performance in removing MPs from both drinking water and wastewater. Research conducted by Ziajahromi *et al.* indicated that NF membranes could achieve over 90% removal efficiency of MPs from treated wastewater, highlighting their potential to reduce environmental pollution and improve water quality[86]. In this study, wastewater samples were first subjected to pre-treatment processes to remove larger debris and organic matter. The treated wastewater, containing MPs of varying sizes, was then passed through NF membranes under controlled conditions[86,87]. Moreover, Ziajahromi *et al.* conducted an in-depth study focused on the effect of operational pressure on the efficiency of NF membranes in removing MPs from wastewater[86]. The treated wastewater, containing MPs of varying sizes, was then filtered through NF membranes under controlled pressures of 5, 10, and 15 bar. At low pressure (5 bar), larger MPs were effectively removed, but a significant flux decline occurred due to fouling. Medium pressure (10 bar) provided an optimal balance, achieving over 90% removal efficiency for all MP sizes with moderate fouling. High pressure (15 bar) resulted in the highest flux but slightly reduced removal efficiency for smaller MPs and increased fouling due to forceful deposition.

While the study successfully introduced a new method for sampling and processing MPs in wastewater, there are several experimental limitations that warrant critical consideration. The experiment was conducted using a single sampling campaign over a short period, which may not fully capture the temporal variability in MP concentrations within wastewater treatment plants. This limitation raises concerns about the representativeness of the results, as different environmental conditions, such as seasonal changes and varying wastewater compositions, could significantly influence MP levels. Furthermore, the validation of the sampling device was performed using polystyrene MPs in a controlled setting, which does not fully reflect the diversity and complexity of MPs present in actual wastewater samples. This could lead to an overestimation of the method's efficiency in capturing MPs of different compositions and sizes under real-world conditions. Addressing these experimental limitations would strengthen the study's conclusions and provide a more accurate assessment of the effectiveness of the proposed method in diverse wastewater treatment scenarios.

A comprehensive study by Khoo *et al.* examined the fouling behavior of NF membranes compared to UF and MF membranes, specifically focusing on the presence of MPs[88]. Using laboratory-scale filtration units, the researchers maintained consistent operational parameters across all tests and monitored the flux decline and fouling extent over time. Scanning electron microscopy (SEM) and atomic force microscopy (AFM) analyses showed that NF membranes had smoother surfaces, reducing the adhesion of MPs and their additives, which led to lower fouling rates.

The discussion and experiment conducted in the study regarding NF for the removal of micropollutants (MPs) reveal several areas that could benefit from more rigorous analysis and critical reflection.

While the study successfully demonstrates the potential of NF for removing various MPs, the discussion does not adequately address the variability in removal efficiency based on the physicochemical properties of the MPs. The rejection mechanisms, including size exclusion, adsorption, and electrostatic interactions, are complex and can vary significantly depending on the specific characteristics of each pollutant, such as molecular weight, hydrophobicity, and charge. However, the study does not sufficiently explore how these factors influence the performance of the NF membranes. A deeper analysis of these variables and their impact on the efficiency of MP removal would have strengthened the study's conclusions. Compared to other filtration technologies such as MF and UF, NF offers superior performance in removing MPs due to its diffusion mechanism. NF, with its pressure-driven filtration, ensures that even the smallest particles are filtered out, providing a high level of purification. Furthermore, NF is less prone to fouling due to the pressure exerted, which can generate shear forces that are strong enough to effectively mitigate particle adhesion.

While NF has a lower risk of fouling compared to other types of membrane filtration, it can still be affected by organic matter and biofilms commonly found with MPs in wastewater. This fouling can significantly decrease membrane efficiency and lifespan, necessitating frequent cleaning and maintenance, which in turn increases operational costs[87]. Additionally, NF systems have a high initial cost, including the expense of the membranes and the associated infrastructure, which can be prohibitive for smaller or budget-constrained projects[86]. These disadvantages highlight the need for careful consideration and optimization when implementing NF technology for MPs removal in water treatment systems. It could be deduced that despite its high removal efficiency, NF's performance can be significantly impacted by membrane fouling and the variability in MP properties. Further research is needed to optimize NF membranes for broader applications, including handling a wider range of MP shapes and sizes.

Reverse osmosis

Reverse osmosis (RO) is a highly effective water purification method that utilizes a semipermeable membrane to remove MPs from water. The process involves applying pressure to the water, forcing it through the membrane[89]. The applied pressure causes the water molecules to diffuse in the opposite direction - from the contaminated side to the purified side - through the semipermeable membrane. By doing so, contaminants, including MPs, are left behind, and clean water is collected on the other side of the membrane. Notably, the pressure must be high enough to overcome the natural osmotic pressure[89].

Additionally, temperature needs to be controlled during the process since it affects the viscosity of water, thereby impacting the movement of water molecules. At higher temperatures, the viscosity of water decreases, allowing water molecules to move more freely and pass through the RO membrane more easily[90].

Harharah *et al.* assessed the impact of flow rate on the efficiency of RO in removing MPs using artificial wastewater contaminated with MPs of known sizes and concentrations[91]. The researchers varied the flow rates (e.g., 3, 6, 9, and 12 L/min) and monitored the permeate flux and removal efficiency of MPs. The results showed that higher flow rates improved the removal efficiency due to enhanced shear forces, which reduced membrane fouling. At an optimal flow rate of 12 L/min, the RO system achieved up to 99.9% removal efficiency of MPs. Multiple studies investigated the impact of pressure on the efficiency of RO systems for removing MPs. Water samples contaminated with MPs were subjected to RO filtration under varying pressures, ranging from 10 to 20 bar. It was deduced that increasing the pressure improved the removal efficiency from 95% to 99.9%. Researchers used fluorescence microscopy and SEM to observe MP behavior[92-94].

While the study presents promising findings, a more comprehensive analysis of the experimental limitations and practical challenges would be addressed. The reliance on artificial wastewater with predefined MP sizes and concentrations limits the applicability of the findings to real-world situations, where wastewater composition is more complex and variable. Additionally, while the study explores the effect of varying pressures on MP removal, it does not adequately consider the potential consequences, such as increased energy consumption and operational costs, that come with maintaining higher pressures and flow rates. The discussion would be strengthened by a deeper examination of these practical implications, as well as by exploring how these findings could be applied to various wastewater treatment systems.

A case study conducted by researchers at the Guangdong Key Laboratory of Membrane Materials and Separation Technologies was designed to evaluate the impact of MP density and concentration on fouling in RO systems[95]. The researchers used water samples artificially contaminated with MPs of two different sizes: 100 nanometers (nm) and 1 micrometer (μm). These samples were processed through the RO system under controlled conditions. The findings indicated that higher concentrations of MPs led to increased fouling, forming dense particulate layers that significantly reduced membrane performance. Despite these important findings, this study does not explore potential mitigation strategies or how these findings might influence the design and operation of RO systems in practical applications. A more comprehensive analysis that includes diverse MP types, real wastewater conditions, and possible solutions to fouling would provide a more robust understanding of the issue and its implications for RO system performance. RO systems significantly improve water quality by effectively removing a wide range of contaminants, up to 99.9% of MPs, including heavy metals, bacteria, and dissolved solids. This high level of purification results in water that is typically free from unpleasant tastes and odors, providing cleaner and safer drinking water.

ROs have one of the highest removal efficiencies of MPs, but their application is often limited by high running costs and membrane fouling risk. Further research is necessary to adjust operating parameters, like pressure and flow rate, to reduce maintenance costs and strike a balance between efficiency and energy consumption.

Membrane bioreactors

Membrane bioreactors (MBRs) effectively remove MPs from wastewater by integrating biological treatment with membrane filtration. In the biological treatment phase, MPs are reduced through biodegradation and adsorption as microorganisms break them down and produce extracellular polymeric substances (EPS). The EPS form a sticky matrix that facilitates the adsorption of MPs onto microbial floc, a process driven by hydrophobic interactions and van der Waals forces, thereby improving the removal of MPs from aqueous environments in water treatment processes. The filtration process, driven by an exerted pressure or pressure gradient, involves forcing water through the membrane pores, effectively trapping solids, including MPs, on the membrane surface. This combination of biological and physical processes ensures the efficient removal of MPs from wastewater[96-98].

The Gaobeidian Wastewater Treatment Plant in Beijing, China, implemented an MBR system to enhance its wastewater treatment capabilities, focusing on the removal of MPs. The membrane filtration phase employs MF membranes with a pore size of 0.1 μm to retain MPs , and other suspended solids. The implementation of the MBR system resulted in a significant improvement in MP removal efficiency, reducing the concentration of MPs and in the influent from approximately 300 particles per liter to around 1-2 particles per liter in the effluent, achieving an overall removal efficiency of over 99%[96].

The study has several important limitations that need to be addressed. One major issue is the inconsistency in how MPs were detected across different wastewater treatment plants. Additionally, the study relies heavily on visual identification of MPs, which can lead to errors and inaccuracies. Although the authors mention the need for standardized methods, this issue remains unresolved, which limits the study's impact. The discussion also falls short of addressing how these methodological problems could influence the overall conclusions, which might lead to an overestimation of the effectiveness of current wastewater treatment plant (WWTP) processes.

However, Ma *et al.* conducted a comprehensive study tackling the adsorption and absorption mechanisms of MPs in MBR systems and their impact on overall removal efficiency[99]. The study utilized a pilot-scale MBR system combining biological treatment with UF membranes, operating with high mixed liquor suspended solids (MLSS) concentrations ranging from 10,000 to 12,000 mg/L and employing membranes with a pore size of 0.04 micrometers. The study revealed that the adsorption process significantly reduced the concentration of free-floating MPs in the mixed liquor, enhancing their removal efficiency during the membrane filtration phase.

While the discussion effectively summarizes the experimental findings, it lacks a critical analysis of the limitations of the study. The study's reliance on controlled laboratory settings may not accurately reflect the complexity and variability of real-world water treatment environments, which could influence the effectiveness of the coagulation and UF processes. Moreover, the exclusive focus on PE limits the applicability of the findings to a broader range of MP pollutants that vary in size, shape, and chemical composition. This limitation is acknowledged briefly but not critically evaluated in the context of the study's conclusions. Additionally, the discussion does not sufficiently consider the long-term operational challenges associated with membrane fouling, particularly in scenarios involving varying concentrations and types of MPs.

The combination of biological treatment and membrane filtration enhances the overall removal efficiency of MPs. This dual action ensures that a significant portion of MPs will be captured and removed from the treated water before even reaching the membrane filtration stage[100].

Despite the high removal efficiencies of membrane filtration, all technologies face similar challenges, including membrane fouling, high operational pressures, and increased energy consumption[72,101]. Fouling occurs when MPs and organic matter accumulate on the membrane surface, reducing filtration efficiency and requiring frequent cleaning and maintenance. For example, in UF systems, fouling can result in a reduction in permeate flux by up to 50% and can decrease membrane lifespan by 30%-50%, necessitating costly maintenance and downtime[78]. UF systems also require higher operational pressures compared to MF, which increases energy consumption. Despite achieving higher removal efficiencies, UF's need for higher pressures can lead to a 20%-30% increase in energy costs compared to MF systems[72]. The cost of replacing membranes, combined with the energy required to maintain high-pressure systems (especially in NF and RO), increases the overall operational costs. Addressing fouling with anti-fouling technologies and developing self-cleaning membranes could enhance the long-term sustainability of these systems. Studies have shown that the presence of MPs can increase the rate of RO membrane fouling by up to 25% compared to systems without MPs, due to the formation of a dense fouling layer on the membrane surface[102]. For instance, an experiment demonstrated a flux decline of 30% when the concentration of MPs in the feed water was increased from 1 to 10 mg/L[103]. The cake layer formed by MPs on the membrane surface increases the operational pressure required to maintain the desired water flux. This additional pressure can lead to higher energy consumption and operational costs. Golgoli *et al.* reported that the pressure increase could be as much as 20% to 30% in the presence of high concentrations of MPs[104]. Fouling is also a significant threat to the effectiveness of MBR systems where MPs can disrupt microbial activity in the biological treatment phase by providing surfaces for harmful bacteria to grow, leading to imbalances in the microbial community and reducing the degradation of organic pollutants[100]. Additionally, MPs can carry toxic chemicals and heavy metals, further harming microbial communities and compromising the overall treatment efficiency of MBR systems[96].

AOPs

MPs and their chemical additives are effectively broken down by AOPs, which generate reactive radicals that break down complex organic contaminants. AOPs are commonly used in water treatment to remove impurities that are not entirely removed by conventional filtration systems. Fenton reactions, electro-oxidation, and photocatalysis are a few examples of these processes[105,106].

Photocatalysis

Photocatalysis is a chemical process that occurs in the presence of light and a photocatalyst, typically a semiconductor such as titanium dioxide (TiO_2). The process begins with the absorption of photons by the photocatalyst, which creates electron-hole pairs[107]. These pairs generate highly reactive species, such as hydroxyl radicals and superoxide anions, that degrade organic pollutants. Photocatalysis has been particularly effective in removing MP additives like BPA, NP, and TBBPA. For instance, Tang *et al.* reported a 100% removal of NP using hydrophobic TiO_2 nanotubes within 40 min[108].

The study presents promising results in the advanced photocatalytic oxidation of NP using hydrophobic titanium dioxide nanotubes (H-TiO_2NTs), yet several aspects of the experimental design and discussion require further consideration. The hydrophobic modification of TiO_2 nanotubes, while effective in improving NP degradation, suffers from long-term stability issues, as the hydrophobic surface reverts to hydrophilicity under prolonged irradiation, significantly reducing photocatalytic efficiency. This raises concerns about the practicality of using H-TiO_2NTs in continuous or long-term applications, a challenge that the experiment did not fully address. While the study highlights the selective oxidation of NP in the presence of other hydrophilic contaminants, it does not critically evaluate how this selectivity might be affected by the presence of other hydrophobic pollutants, nor does it propose clear future research directions to address these limitations.

Acarer[68] investigates the effectiveness of zinc oxide nanoparticles (ZnO NPs) in promoting the photodegradation of MPs under simulated sunlight. The study extracted MPs from commercial sunscreens and exposed them to ZnO NPs under UV light for 12 h. The results showed a significant increase in the carbonyl index of the MPs, indicating surface oxidation and fragmentation, with a 2.5-fold rise in the carbonyl index reflecting the degree of degradation. Additionally, the study highlighted the enhanced cytotoxicity of the degraded MPs, finding that these transformed particles caused significant increases in lysosomal accumulation and mitochondrial damage. While the study effectively demonstrates the potential of ZnO NPs in accelerating MPs degradation, it does not provide a direct percentage of removal efficiency, focusing instead on the structural changes and biological impacts of the degraded products.

Fenton process

The Fenton process is an advanced oxidation process involving the reaction of H_2O_2 with ferrous iron (Fe^{2+}) to produce hydroxyl radicals, which are potent oxidizing agents. These radicals can degrade a wide range of organic pollutants. The Fenton process is particularly noted for its effectiveness under acidic conditions and its ability to achieve high removal efficiencies.

He *et al.* (2017) discuss the synthesis and application of a bifunctional hollow mesoporous catalyst for the degradation of TBBPA. The $Fe^0CMnFe_2O_4$ catalyst was used in combination with hydrogen peroxide (H_2O_2) and hydroxylamine (NH_2OH) to degrade TBBPA in aqueous solutions. The experiments demonstrated that the catalyst could achieve a removal efficiency of up to 90% within 120 min under optimal conditions, particularly at a neutral pH and with a catalyst dosage of 0.3 g/L. The degradation mechanism involved both reductive debromination and oxidative mineralization processes, facilitated by the generation of hydroxyl radicals (•OH) from H_2O_2 activated by the catalyst. Additionally, the $Fe^0CMnFe_2O_4$ catalyst showed good stability and reusability, retaining nearly 80% of its removal efficiency after 10 cycles of use. These findings suggest that the $Fe^0CMnFe_2O_4$ catalyst is a promising candidate for the effective degradation of persistent organic pollutants like TBBPA, with potential applications in environmental remediation[109]. While the results are promising, the study focuses on optimal conditions without testing the catalyst's robustness in varied environmental scenarios, limiting its real-world applicability. Additionally, the paper lacks an analysis of potential byproducts and long-term catalyst performance in complex wastewater conditions.

To demonstrate the potential of the thermal Fenton reaction for effective environmental remediation of MPs, Hu *et al.* showed that the hydrothermal Fenton system achieved a 95.9% weight loss of ultrahigh-molecular-weight polyethylene (UHMWPE) MPs within 16 h and 75.6% mineralization in 12 h[110]. This efficiency is due to the synergistic effects of hydrothermal hydrolysis and hydroxyl radical production, which break down polymer chains through a two-stage process of chain unfolding and oxidation. The system effectively degrades various plastics and maintains its performance in real-world water samples, including tap, river, and seawater. Toxicity tests with *Escherichia coli* confirmed that the degradation intermediates are non-toxic, highlighting the system's environmental safety.

Electro-oxidation

Electro-oxidation is an electrochemical process where electrical energy is used to generate oxidizing agents directly at the anode surface or indirectly in the bulk solution. This method is effective in treating various organic pollutants, including MP additives.

Ji *et al.* investigated the impact of micelle formation on the electro-oxidation degradation of NEPOs using a Ti_4O_7 anode[111]. Micelle formation was found to significantly inhibit NEPO degradation by creating steric hindrance that prevents hydroxyl radicals from effectively attacking NEPOs. Despite this, the anode achieved 92% degradation within 1 h, with the primary degradation occurring through the cleavage of the Caryl-Oether bond, producing ethoxylated chains and polyethylene glycols (PEGs) as byproducts. Ning *et al.* assessed the effectiveness of a CeO_2-doped PbO_2 anode in degrading polyvinyl chloride microplastics (PVC-MPs) through an electrochemical oxidation process[112]. The experiment explored various operational parameters, such as temperature, current density, pH, initial concentration of PVC-MPs, and electrolyte concentration, to determine their impact on degradation efficiency. The main findings revealed that the CeO_2–PbO_2 anode exhibited superior electrocatalytic activity, achieving a degradation rate of 38.67% after 6 h of electrolysis under optimal conditions. The results showed that higher temperatures, current densities, alkaline pH levels, lower initial concentrations of PVC-MPs, and higher electrolyte concentrations significantly enhanced the degradation process.

The degradation rate achieved is relatively low, especially considering that it was obtained under optimal conditions, with careful adjustments made to key parameters like temperature, current density, pH, and electrolyte concentration. Furthermore, the time required to reach even this limited level of degradation is quite lengthy, which further diminishes the process's practicality for large-scale applications.

Sonocatalysis

Sonocatalysis involves the use of ultrasonic waves to enhance the catalytic degradation of pollutants. The ultrasonic waves generate cavitation bubbles, which, upon collapse, produce localized high temperatures and pressures, leading to the formation of reactive radicals. This method has shown high efficacy in the degradation of organic pollutants.

A hybrid AOP was developed by combining persulfate (PS) activation with nano zero-valent iron (nZVI) supported on reduced graphene oxide (rGO), all enhanced by ultrasound (US). The experiment involved optimizing various parameters, including pH, reaction time, PS concentration, nZVI-rGO dosage, and US power, to maximize the degradation efficiency of NP.

The main findings of the study revealed that the optimized PS/US/nZVI-rGO system achieved a high NP removal efficiency of 98.2%. This result demonstrated a significant synergistic effect compared to other systems lacking one or more of these components. The research also identified the degradation pathway of NP, confirming that sulfate radicals ($SO_4^{\bullet-}$) generated during the process played a predominant role in breaking down the NP molecules. The study concludes that the PS/US/nZVI-rGO system is a highly effective and promising method for treating organic pollutants in water, offering potential for environmental remediation applications[113]. While the study effectively demonstrates the potential of combining PS activation, nano nZVI supported on rGO, and US for the degradation of NP, it does not sufficiently explore the scalability of the process or the economic feasibility of implementing such a system on a larger scale, which are critical factors for practical environmental remediation. The potential environmental impact of the byproducts generated during the degradation process is also not thoroughly examined, particularly regarding the long-term safety of this approach.

Ioannidi *et al.* (2024) investigate the use of palladium-cerium oxide (Pd/CeO_2) as a catalyst for the sonocatalytic degradation of BPA in water. The study focuses on understanding the degradation process, identifying the transformation products formed, and assessing the toxicity of these products. The main findings of the research indicate that the Pd/CeO_2 catalyst significantly enhances the degradation of BPA when combined with US, achieving a degradation efficiency of 95% within 60 min. The process was influenced by various operational parameters, including US power and catalyst loading. The study also identified nine transformation products formed during the degradation process, some of which exhibited reduced toxicity compared to the parent compound BPA, although a few remained toxic[114].

This work highlights the potential of using sonocatalysis with Pd/CeO_2 nanoparticles for the effective degradation of BPA, while also underscoring the importance of understanding the environmental impact of the resulting byproducts. However, while the focus on BPA is important, the study's limited scope does not account for how this system might perform with other pollutants. Furthermore, while the optimization of operational parameters is discussed, the study does not fully examine the interactions between these parameters, which could provide valuable insights for improving process efficiency. Addressing these limitations would strengthen the study's relevance and applicability for broader environmental remediation efforts. Anastopoulos *et al.* investigated the use of palladium-cerium oxide (Pd/CeO_2) for the sonocatalytic degradation of BPA in water, achieving 95% degradation within 60 min[115]. The study identified nine transformation products, some with reduced toxicity. While the research demonstrates the effectiveness of Pd/CeO_2 in degrading BPA, it lacks examination of other pollutants and the interactions between operational parameters, limiting broader environmental applicability.

Catalytic oxidation

Catalytic oxidation processes involve the use of catalysts to accelerate the oxidation of pollutants, often using agents such as oxygen, ozone, or hydrogen peroxide. These processes are highly effective in degrading various organic compounds.

A study conducted by Zanaty *et al.* (2024) explores the use of a novel nanocomposite for the catalytic oxidation and removal of MPs. The research focuses on the effectiveness of this material in breaking down pollutants, demonstrating high removal efficiencies with 97% degraded through catalytic oxidation. Additionally, the study highlights the nanocomposite's recyclability, retaining 78% efficiency after six cycles, positioning it as a promising candidate for sustainable water treatment[116].

While the study presents promising results, the study does not provide a detailed analysis of the potential environmental impact of the degradation byproducts, which could be significant in real-world applications. Furthermore, the recyclability of the material does not examine the potential loss of catalytic activity over extended cycles, which could affect its practicality for large-scale use. Addressing these limitations would provide a more robust understanding of the nanocomposite's applicability and effectiveness in real-world water treatment.

The use of catalysts in AOPs for the degradation of MPs in water, when enhanced with metals like Ag or Pt, is highly effective in generating reactive radicals such as hydroxyl radicals (•OH), which play a crucial role in breaking down MPs into smaller, less harmful fragments. The research highlights that photocatalytic systems such as TiO_2 and ZnO can achieve near-complete degradation of certain MPs under optimal conditions, with reported efficiencies approaching 100%. The study also explores the potential of hybrid catalyst systems, which combine different catalytic materials to further enhance the degradation efficiency, making these processes promising for real-world water treatment applications[117]. However, while the catalytic approaches show great promise, the discussion also points to the need for further research to address challenges such as the potential formation of secondary pollutants and the economic feasibility of large-scale applications. Figure 3 summarizes the treatment methods employed for MPs and their additives.

Approach to combined treatment methods

In the effort to improve the efficiency of water treatment processes in removing MPs, it has become evident that no single treatment method can address all the challenges effectively. Therefore, implementing a combined treatment approach becomes crucial to enhance the removal of MPs and their additives, reduce operational costs, minimize environmental impact, and improve overall water quality. To provide a clear overview, Table 1 summarizes the advantages, disadvantages, and removal efficiencies of various membrane technologies employed in removing MPs, while Table 2 summarizes the methods of AOPs. Integrating UF with AOPs, specifically TiO_2 Photocatalysis, offers an efficient solution. UF is well-regarded for its capability to remove a broad spectrum of MPs due to its diffusion mechanism. However, UF membranes suffer from fouling, where organic matter and other impurities accumulate on the membrane surface, thereby reducing their efficiency and lifespan. TiO_2 photocatalysis can mitigate this issue by using titanium dioxide as a catalyst and it is also able to degrade the additives of MPs efficiently. This process prevents the accumulation of organic matter on UF membranes, enhancing the removal efficiency of both MPs and organic contaminants, while reducing the need for frequent membrane cleaning and maintenance. This

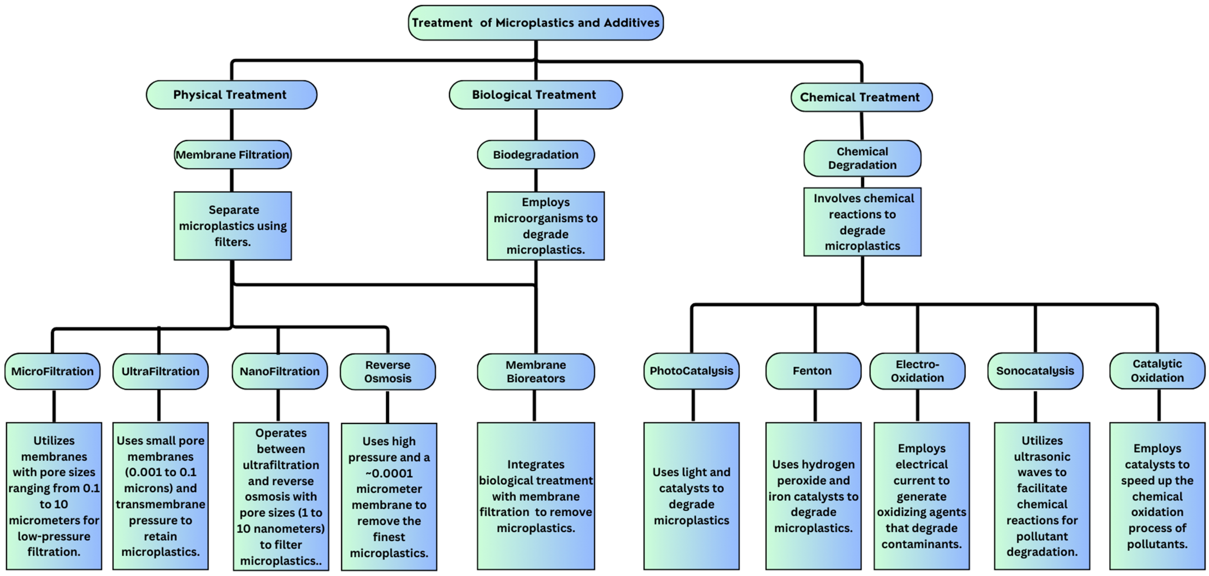

Figure 3. Treatment methods for MPs and additives. MPs: Microplastics.

combination results in a more comprehensive and efficient water treatment system.

Similarly, combining NF with MBR presents a synergistic approach to water treatment. NF is effective in removing smaller MPs and various other contaminants due to its diffusive characteristics. However, NF membranes are prone to fouling by organic matter and biofilms, which can decrease their effectiveness and increase operational costs. MBR systems, which integrate biological treatment with membrane filtration, can alleviate this issue. By integrating NF with MBR, the biological treatment reduces the organic load before it reaches the NF membrane, thus minimizing fouling and extending the membrane's lifespan. This approach benefits from the high removal efficiency of NF while benefiting from the comprehensive treatment capabilities of MBR. Figure 4 depicts the hybrid MBR UF/MF system with percent removal of select MPs and MP additives.

RO and catalytic oxidation effectively eliminate organic pollutants and MP while resolving RO's problems with fouling and high operating pressure. Catalytic oxidation enhances performance while consuming less energy and requiring less maintenance by decomposing chemical additives. This integration improves the therapy's efficiency and cost-effectiveness. Table 3 summarizes the cost-benefit analysis by contrasting the initial, continuing, and maintenance costs of each strategy while emphasizing its overall efficacy and environmental impact[68,72,100,103,104,118].

It can be deduced from Table 3 that although all three hybrid systems are effective, their costs vary from low to high; therefore, the optimum choice will depend on the type of water. Surface water, which is regularly contaminated by pollutants from runoff and organic debris, is the ideal application for the UF/AOP hybrid system. For wastewater treatment, the MBR/NF system is recommended since it combines biological degradation with fine filtration for comprehensive treatment. Because the RO/Catalytic Oxidation system efficiently removes salts and contaminants to produce high-purity water, it is ideal for brackish and seawater.

Table 1. Advantages and disadvantages of various membrane technologies employed in removing MPs

Method	Removal efficiency	Advantages	Disadvantages
MF	94% to 100%	- High removal efficiency for larger MPs - Low energy consumption due to low-pressure operation - Durable and stable membranes	- Less effective for smaller particles - Frequent cleaning and potential membrane replacement due to fouling - Efficiency affected by the density of MPs
UF	96% to 99%	- High removal efficiency for a broad range of MPs - Longer membrane lifespan and resistance to fouling	- Higher energy requirements due to increased operational pressures - Significant fouling issues, particularly with organic matter - Increased operational costs due to energy and maintenance
NF	90%	- Very high removal efficiency for smaller MPs - Lower fouling rates compared to MF and UF	- Susceptibility to fouling by organic matter and biofilms - High initial cost and infrastructure expenses - Limited removal efficiency for very small particles
RO	95% to 99.9%	- Extremely high removal efficiency for all MPs - Comprehensive removal of various contaminants	- Significant membrane fouling issues - High operational pressures and energy consumption - High initial and operational costs
MBR	99%	- Very high removal efficiency for MPs - Combines biological and physical treatment for comprehensive contaminant removal	- Significant membrane fouling - Potential disruption to biological processes - High operational complexity and costs

MPs: Microplastics; MF: microfiltration; UF: ultrafiltration; NF: nanofiltration; RO: reverse osmosis; MBR: membrane bioreactor.

Table 2. Removal efficiencies of MPs and their additives using AOPs

Treatment method	Pollutants	Removal efficiency	Limitations
Photocatalysis	NP	100% for NP	Hydrophobic modification of TiO_2 suffers from long-term stability issues
Fenton process	TBBPA	Up to 90%	Potential byproducts and their environmental impacts not thoroughly analyzed
	UHMWPE	95.9%	Long-term performance and environmental impact of degradation intermediates not fully assessed
Electro-oxidation	NEPOs	Over 92%	Micelle formation inhibits degradation. Controlled lab conditions may not reflect real-world wastewater complexities. Lack of alternative mitigation strategies
	MPs	38.67%	Low efficiency and lengthy treatment time under optimal conditions
Sonocatalysis	NP	98.2%	Scalability and economic feasibility not explored. Environmental impact of byproducts not thoroughly examined
	BPA	95%	Interactions between operational parameters not fully explored. Broader applicability and environmental impact need further study
Catalytic oxidation	MPs	97%	Recyclability and loss of catalytic activity over cycles not thoroughly assessed

AOPs: Advanced oxidation processes; NP: nonylphenol; TBBPA: tetrabromobisphenol; UHMWPE: ultrahigh-molecular-weight polyethylene; NEPOs: nonylphenol ethoxylates; MPs: microplastics; BPA: bisphenol A.

Table 3. Cost-benefit analysis for each combined treatment method

Method	Initial cost	Operational cost	Maintenance cost	Efficiency	Environmental impact
Hybrid UF + AOP (TiO_2 photocatalysis)	High	Moderate	Moderate	Extremely high for all particles and contaminants	Positive (less waste, moderate energy)
Hybrid NF + MBR	High	High	Moderate to high	Very high for smaller particles	Mixed (high resource use, extended lifespan)
Hybrid RO + catalytic oxidation	Very high	High	Moderate	Extremely high for all particles and contaminants	Mixed (high energy, reduced fouling)

UF: Ultrafiltration; AOP: advanced oxidation process; NF: nanofiltration; MBR: membrane bioreactor; RO: reverse osmosis.

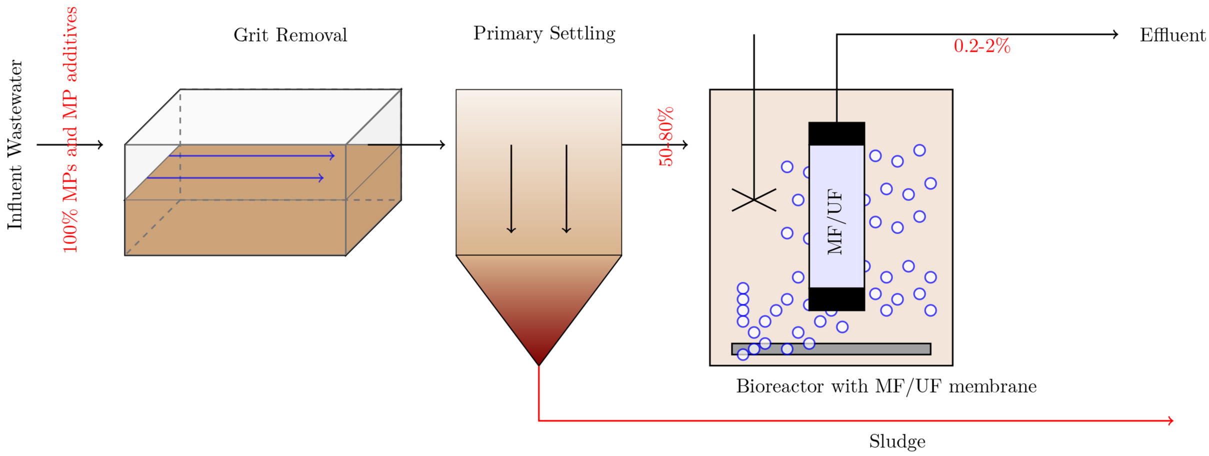

Figure 4. Schematic of hybrid MBR-UF/MF treatment system. MBR: Membrane bioreactor; UF: ultrafiltration; MF: microfiltration.

REMOVAL MECHANISMS

Understanding the mechanisms of removal of MPs and MP additives from water and wastewater is essential to ensuring the effectiveness of treatment methods and optimizing their performance. These systems can be broadly divided into two groups: physical processes that trap and retain pollutants, and chemical processes that convert pollutants into less recalcitrant forms.

Physical removal mechanisms are mainly highlighted using membrane treatment processes, where size exclusion, adsorption, and in the case of RO and NF, ionic diffusion through the membrane. On the other hand, the premise behind chemical removal in processes such as coagulation\flocculation involves the addition of a chemical that forms bonds with the MP surface and later combines multiple particles due to electrostatic interaction[Figure 5][119]. Guo *et al.* concluded that electrostatic interaction was the dominant force between surface functionalized 2-acrylamido-2-methylpropane sulfonic acid polymer nanoparticle and aluminum oxide particle in the flocculation process of MPs[120]. Furthermore, Khan *et al.* deduced that coagulation of MPs is highly dependent on optimizing various factors such as coagulant type, dosage, pH, and the physical characteristics of MPs[121].

On the other hand, photocatalysis, Fenton reactions, and electro-oxidation involve the generation of reactive species, mainly hydroxyl radicals, that break down MPs into less harmful byproducts. Photocatalysis using TiO_2 can effectively degrade NP and other additives, converting them into harmless byproducts. Figure 6 illustrates the breakdown of PVC using Fenton oxidation, where the hydroxyl radicals produced electrochemically enable the breakdown of polymer chains into smaller, less harmful molecules, ultimately converting them into CO_2 and H_2O. To improve MPs' environmental management, increase treatment efficacy, and decrease the long-term impacts of MP-related pollution, further research into these mechanisms is required.

FUTURE NEEDS AND GAPS

Future research needs to address several critical gaps in our understanding of MPs and their environmental impact. Comprehensive studies are necessary to identify and quantify the primary sources of MPs and understand their transport mechanisms from these sources to aquatic and terrestrial environments. This requires robust models that simulate their movement through various environmental matrices, including soil, water, and air. Additionally, the long-term ecotoxicological impact of MPs on different levels in aquatic

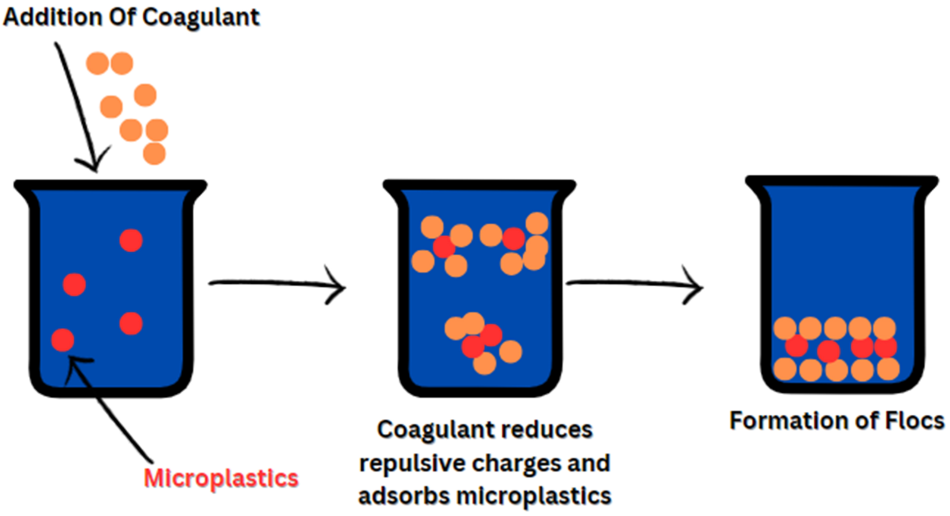

Figure 5. Schematic of coagulation/flocculation of MPs. MPs: Microplastics.

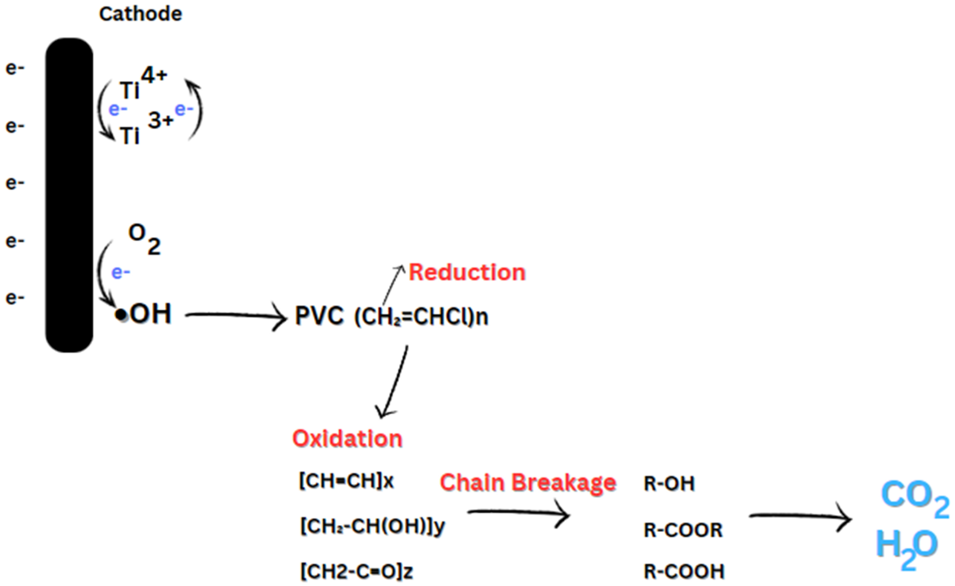

Figure 6. Breakdown of PVC using Fenton oxidation. PVC: Polyvinyl chloride.

and terrestrial ecosystems needs further exploration, especially regarding chronic exposure effects on organisms and potential bioaccumulation and biomagnification in food webs. While MF and UF are effective in removing MPs, fouling remains a significant challenge, highlighting the need to develop anti-fouling coatings and self-cleaning membranes to enhance system longevity and efficiency. Integrating UF with AOPs has shown promise in degrading MPs into harmless byproducts, and future research should optimize these systems for large-scale, cost-effective, and environmentally sustainable applications. The development of mixed matrix membranes (MMMs) that incorporate adsorbents for enhanced MP capture represents a significant advancement, necessitating further research into novel materials that offer higher selectivity, durability, and resistance to fouling. Conducting pilot-scale studies in diverse environmental settings will provide valuable data on the practical feasibility, efficiency, scalability, and environmental sustainability of these hybrid systems, ensuring reliable implementation for comprehensive water treatment.

LCA OF MPS AND THEIR ADDITIVES

A substantial gap persists in the understanding of the full life cycle of MPs and their additives, from production to environmental degradation and remediation, necessitating LCA studies. At every stage of the MP life cycle, LCA provides a framework for evaluating the environmental costs of extracting and manufacturing raw materials, using them, disposing of them, and causing environmental degradation. MPs are a particularly serious environmental issue because they remain in ecosystems and emit toxic substances that may have negative effects on biodiversity and human health. Addressing this issue requires assessing the carbon footprint of MPs and their additives, including their production, usage, and disposal, which is crucial for quantifying associated greenhouse gas emissions and developing strategies to minimize their environmental impact. A novel method for incorporating patent literature into projected LCAs has been presented by Spreafico *et al.*[122]. Through the identification of innovative eco-design solutions and state-of-the-art technology in MP collection and treatment, this method provides a more forward-looking assessment of the environmental effects. By incorporating patent analysis into LCA, future advancements in MP remediation, such as membrane filtering and AOPs, can be evaluated for their potential to significantly reduce the environmental effect of MP-related technologies. This strategy helps close the gap between current practices and the possible environmental advantages of technological advancement.

Applying proper LCA to MPs is still difficult because of data shortages and difficulties in assessing long-term environmental repercussions, as many studies rely on imprecise data addressing MP release, degradation, and ecological effects. Jiao *et al.* claim that the lack of consistent reporting makes it difficult to conduct comprehensive assessments of the life cycle impacts of MPs[123]. The persistence of MPs in ecosystems and their capacity to generate toxic metabolites complicate evaluations. Future LCA research must use multi-scale data and advanced modeling to more precisely predict MP behavior across ecosystems. Policy frameworks that cover the whole lifespan of MPs from production to disposal will help foster innovation in treatment technologies and reduce the environmental impact of MPs by expanding knowledge and creating sustainable solutions.

CONCLUSION

In this study, we have comprehensively examined the issue of MPs and their additives, including their sources, impacts, and treatment methods, highlighting key strategies for improving removal efficiency. MPs and their additives pose significant ecological risks. Advanced treatment technologies, while promising, require optimization and further research, especially concerning fouling and byproduct management. AOPs and membrane filtration are two examples of treatment technologies that offer promising ways to mitigate the environmental risks that MPs generate. By addressing problems like membrane fouling and optimizing treatment processes, these technologies support sustainable water management techniques. However, further research into novel materials is required to improve their performance and resistance to fouling. The development of innovative materials and hybrid treatment approaches further enhances the practical applicability of these methods in diverse environmental settings. The paper highlights the need for LCA studies, which include carbon footprint analysis to develop mitigation plans, to assess the environmental impacts of MPs and their additives over the duration of their lifecycle. Standardization of sampling and reporting practices is necessary to ensure data consistency. Highlights of the paper include pointing out significant research gaps and offering a thorough analysis of MPs' causes, effects, and treatment modalities. In conclusion, managing MPs necessitates advanced treatment technology, comprehensive environmental evaluations, and strong regulatory frameworks. Effective treatment options are essential to safeguarding both human and environmental health.

DECLARATIONS

Authors' contributions

Worked on writing-original draft: Sawma MJ, Ghaddar R
Writing-review and editing: Zayyat RM
Validation, supervision, and conceptualization: Ayoub GM

Availability of data and materials

Not applicable.

Financial support and sponsorship

None.

Conflicts of interest

All authors declared that there are no conflicts of interest.

Ethical approval and consent to participate

Not applicable.

Consent for publication

Not applicable.

Copyright

REFERENCES

1. Dissanayake PD, Kim S, Sarkar B, et al. Effects of microplastics on the terrestrial environment: a critical review. *Environ Res* 2022;209:112734. DOI PubMed
2. Hale RC, Seeley ME, La Guardia MJ, Mai L, Zeng EY. A global perspective on microplastics. *JGR Oceans* 2020;125:e2018JC014719. DOI
3. Shen L, Worrell E. Chapter 31 - Plastic recycling. In: Handbook of recycling. Elsevier; 2024. pp. 497-510. DOI
4. Alhazmi H, Almansour FH, Aldhafeeri Z. Plastic waste management: a review of existing life cycle assessment studies. Sustainability 2021;13:5340. DOI
5. Haque F, Fan C. Fate of microplastics under the influence of climate change. *iScience* 2023;26:107649. DOI PubMed PMC
6. McMullen K, Vargas FH, Calle P, Alavarado-Cadena O, Pakhomov EA, Alava JJ. Modelling microplastic bioaccumulation and biomagnification potential in the Galápagos penguin ecosystem using Ecopath and Ecosim (EwE) with Ecotracer. *PLoS One* 2024;19:e0296788. DOI PubMed PMC
7. Matavos-Aramyan S. Addressing the microplastic crisis: a multifaceted approach to removal and regulation. *Environm Adv* 2024;17:100579. DOI
8. Li XF, Mitch WA. Drinking water disinfection byproducts (DBPs) and human health effects: multidisciplinary challenges and opportunities. *Environ Sci Technol* 2018;52:1681-9. DOI PubMed
9. Sutkar PR, Gadewar RD, Dhulap VP. Recent trends in degradation of microplastics in the environment: a state-of-the-art review. *J Hazard Mater Adv* 2023;11:100343. DOI
10. Pothiraj C, Amutha Gokul T, Ramesh Kumar K, et al. Vulnerability of microplastics on marine environment: a review. *Ecol Indic* 2023;155:111058. DOI
11. Ziani K, Ioniţă-Mîndrican CB, Mititelu M, et al. Microplastics: a real global threat for environment and food safety: a state of the art review. *Nutrients* 2023;15:617. DOI PubMed PMC
12. An L, Liu Q, Deng Y, Wu W, Gao Y, Ling W. Sources of microplastic in the environment. In: He D, Luo Y, editors. Microplastics in terrestrial environments. Cham: Springer International Publishing; 2020. pp. 143-59. DOI
13. Singh A, Mishra BK. Microbeads in personal care products: an overlooked environmental concern. *J Clean Prod* 2023;427:139082. DOI
14. Anbumani S, Kakkar P. Ecotoxicological effects of microplastics on biota: a review. *Environ Sci Pollut Res Int* 2018;25:14373-96. DOI PubMed
15. Nabi I, Bacha A, Zhang L. A review on microplastics separation techniques from environmental media. *J Clean Prod* 2022;337:130458. DOI

16. Rillig MC. Microplastic in terrestrial ecosystems and the soil? *Environ Sci Technol* 2012;46:6453-4. DOI PubMed
17. Yang Y, Jalalah M, Alsareii SA, et al. Plastic wastes (PWs) and microplastics (MPs) formation: management, migration, and environmental impact. *J Environ Chem Eng* 2024;12:112926. DOI
18. Bajt O. From plastics to microplastics and organisms. *FEBS Open Bio* 2021;11:954-66. DOI PubMed PMC
19. Dube E, Okuthe GE. Plastics and micro/nano-plastics (MNPs) in the environment: occurrence, impact, and toxicity. *Int J Environ Res Public Health* 2023;20:6667. DOI PubMed PMC
20. Wu P, Huang J, Zheng Y, et al. Environmental occurrences, fate, and impacts of microplastics. *Ecotoxicol Environ Saf* 2019;184:109612. DOI
21. Rossatto A, Arlindo MZF, de Morais MS, de Souza TD, Ogrodowski CS. Microplastics in aquatic systems: a review of occurrence, monitoring and potential environmental risks. *Environ Adv* 2023;13:100396. DOI
22. Wright SL, Thompson RC, Galloway TS. The physical impacts of microplastics on marine organisms: a review. *Environ Pollut* 2013;178:483-92. DOI PubMed
23. Canniff PM, Hoang TC. Microplastic ingestion by daphnia magna and its enhancement on algal growth. *Sci Total Environ* 2018;633:500-7. DOI PubMed
24. Rillig MC, Ziersch L, Hempel S. Microplastic transport in soil by earthworms. *Sci Rep* 2017;7:1362. DOI PubMed PMC
25. Huang Y, Liu Q, Jia W, Yan C, Wang J. Agricultural plastic mulching as a source of microplastics in the terrestrial environment. *Environ Pollut* 2020;260:114096. DOI
26. Kumar M, Xiong X, He M, et al. Microplastics as pollutants in agricultural soils. *Environ Pollut* 2020;265:114980. DOI
27. de Souza Machado AA, Kloas W, Zarfl C, Hempel S, Rillig MC. Microplastics as an emerging threat to terrestrial ecosystems. *Glob Chang Biol* 2018;24:1405-16. DOI PubMed PMC
28. Dad FP, Khan WU, Kirkham MB, Bolan N, Tanveer M. Microplastics: a review of their impacts on different life forms and their removal methods. *Environ Sci Pollut Res Int* 2023;30:86632-55. DOI PubMed
29. Oliveira M, Almeida M, Miguel I. A micro(nano)plastic boomerang tale: a never ending story? *TrAC Trend Anal Chem* 2019;112:196-200. DOI
30. Chen G, Feng Q, Wang J. Mini-review of microplastics in the atmosphere and their risks to humans. *Sci Total Environ* 2020;703:135504. DOI
31. Conti G, Rapisarda P, Ferrante M. Relationship between climate change and environmental microplastics: a one health vision for the platysphere health. *One Health Adv* 2024;2:17. DOI
32. Chen C, Pan J, Xiao S, et al. Microplastics alter nitrous oxide production and pathways through affecting microbiome in estuarine sediments. *Water Res* 2022;221:118733. DOI
33. Prata JC, da Costa JP, Lopes I, Duarte AC, Rocha-Santos T. Environmental exposure to microplastics: an overview on possible human health effects. *Sci Total Environ* 2020;702:134455. DOI PubMed
34. Yu Y, Chen H, Hua X, et al. Polystyrene microplastics (PS-MPs) toxicity induced oxidative stress and intestinal injury in nematode Caenorhabditis elegans. *Sci Total Environ* 2020;726:138679. DOI
35. Persiani E, Cecchettini A, Ceccherini E, Gisone I, Morales MA, Vozzi F. Microplastics: a matter of the heart (and vascular system). *Biomedicines* 2023;11:264. DOI PubMed PMC
36. Segovia-Mendoza M, Nava-Castro KE, Palacios-Arreola MI, Garay-Canales C, Morales-Montor J. How microplastic components influence the immune system and impact on children health: focus on cancer. *Birth Defects Res* 2020;112:1341-61. DOI PubMed
37. Sharma MD, Elanjickal AI, Mankar JS, Krupadam RJ. Assessment of cancer risk of microplastics enriched with polycyclic aromatic hydrocarbons. *J Hazard Mater* 2020;398:122994. DOI PubMed
38. Çobanoğlu H, Belivermiş M, Sıkdokur E, Kılıç Ö, Çayır A. Genotoxic and cytotoxic effects of polyethylene microplastics on human peripheral blood lymphocytes. *Chemosphere* 2021;272:129805. DOI PubMed
39. Kratina P, Watts TJ, Green DS, Kordas RL, O'Gorman EJ. Interactive effects of warming and microplastics on metabolism but not feeding rates of a key freshwater detritivore. *Environ Pollut* 2019;255:113259. DOI
40. Kannan K, Vimalkumar K. A review of human exposure to microplastics and insights into microplastics as obesogens. *Front Endocrinol* 2021;12:724989. DOI PubMed PMC
41. Sheng Y, Ye X, Zhou Y, Li R. Microplastics (MPs) act as sources and vector of pollutants-impact hazards and preventive measures. *Bull Environ Contam Toxicol* 2021;107:722-9. DOI PubMed
42. Shruti VC, Pérez-Guevara F, Elizalde-Martínez I, Kutralam-Muniasamy G. First study of its kind on the microplastic contamination of soft drinks, cold tea and energy drinks - future research and environmental considerations. *Sci Total Environ* 2020;726:138580. DOI PubMed
43. Watts AJR, Lewis C, Goodhead RM, et al. Uptake and retention of microplastics by the shore crab *Carcinus maenas*. *Environ Sci Technol* 2014;48:8823-30. DOI PubMed
44. Costa JPD, Avellan A, Mouneyrac C, Duarte A, Rocha-Santos T. Plastic additives and microplastics as emerging contaminants: mechanisms and analytical assessment. *TrAC Trend Ana Chem* 2023;158:116898. DOI
45. Hahladakis JN, Velis CA, Weber R, Iacovidou E, Purnell P. An overview of chemical additives present in plastics: migration, release, fate and environmental impact during their use, disposal and recycling. *J Hazard Mater* 2018;344:179-99. DOI PubMed
46. Kitamura S, Suzuki T, Sanoh S, et al. Comparative study of the endocrine-disrupting activity of bisphenol A and 19 related compounds. *Toxicol Sci* 2005;84:249-59. DOI

47. Zielińska M, Bułkowska K, Cydzik-Kwiatkowska A, Bernat K, Wojnowska-Baryła I. Removal of bisphenol A (BPA) from biologically treated wastewater by microfiltration and nanofiltration. *Int J Environ Sci Technol* 2016;13:2239-48. DOI
48. Santoro A, Chianese R, Troisi J, et al. Neuro-toxic and reproductive effects of BPA. *Curr Neuropharmacol* 2019;17:1109-32. DOI PubMed PMC
49. Seachrist DD, Bonk KW, Ho SM, Prins GS, Soto AM, Keri RA. A review of the carcinogenic potential of bisphenol A. *Reprod Toxicol* 2016;59:167-82. DOI PubMed PMC
50. Adamovsky O, Groh KJ, Białk-Bielińska A, et al. Exploring BPA alternatives - environmental levels and toxicity review. *Environ Int* 2024;189:108728. DOI PubMed
51. Yang W, Gao X, Wu Y, et al. The combined toxicity influence of microplastics and nonylphenol on microalgae *Chlorella pyrenoidosa*. *Ecotoxicol Environ Saf* 2020;195:110484. DOI PubMed
52. Brix R, Hvidt S, Carlsen L. Solubility of nonylphenol and nonylphenol ethoxylates. On the possible role of micelles. *Chemosphere* 2001;44:759-63. DOI PubMed
53. Soares A, Guieysse B, Jefferson B, Cartmell E, Lester JN. Nonylphenol in the environment: a critical review on occurrence, fate, toxicity and treatment in wastewaters. *Environ Int* 2008;34:1033-49. DOI PubMed
54. Noorimotlagh Z, Mirzaee SA, Martinez SS, Rachoń D, Hoseinzadeh M, Jaafarzadeh N. Environmental exposure to nonylphenol and cancer progression Risk-A systematic review. *Environ Res* 2020;184:109263. DOI PubMed
55. Ömeroğlu S, Murdoch FK, Sanin FD. Investigation of nonylphenol and nonylphenol ethoxylates in sewage sludge samples from a metropolitan wastewater treatment plant in Turkey. *Talanta* 2015;131:650-5. DOI PubMed
56. Wang F, Xiang L, Sze-Yin Leung K, et al. Emerging contaminants: a one health perspective. *Innovation* 2024;5:100612. DOI
57. Covaci A, Voorspoels S, Abdallah MA, Geens T, Harrad S, Law RJ. Analytical and environmental aspects of the flame retardant tetrabromobisphenol-A and its derivatives. *J Chromatogr A* 2009;1216:346-63. DOI PubMed
58. Yu Y, Yu Z, Chen H, et al. Tetrabromobisphenol A: disposition, kinetics and toxicity in animals and humans. *Environ Pollut* 2019;253:909-17. DOI PubMed
59. Barghi M, Shin ES, Kim JC, Choi SD, Chang YS. Human exposure to HBCD and TBBPA via indoor dust in Korea: estimation of external exposure and body burden. *Sci Total Environ* 2017;593-4:779-86. DOI PubMed
60. Cariou R, Antignac JP, Zalko D, et al. Exposure assessment of French women and their newborns to tetrabromobisphenol-A: occurrence measurements in maternal adipose tissue, serum, breast milk and cord serum. *Chemosphere* 2008;73:1036-41. DOI
61. Kim UJ, Oh JE. Tetrabromobisphenol A and hexabromocyclododecane flame retardants in infant-mother paired serum samples, and their relationships with thyroid hormones and environmental factors. *Environ Pollut* 2014;184:193-200. DOI PubMed
62. Parsons A, Lange A, Hutchinson TH, et al. Molecular mechanisms and tissue targets of brominated flame retardants, BDE-47 and TBBPA, in embryo-larval life stages of zebrafish (danio rerio). *Aquat Toxicol* 2019;209:99-112. DOI
63. Kitamura S, Kato T, Iida M, et al. Anti-thyroid hormonal activity of tetrabromobisphenol A, a flame retardant, and related compounds: affinity to the mammalian thyroid hormone receptor, and effect on tadpole metamorphosis. *Life Sci* 2005;76:1589-601. DOI PubMed
64. Zhang YF, Xu W, Lou QQ, et al. Tetrabromobisphenol A disrupts vertebrate development via thyroid hormone signaling pathway in a developmental stage-dependent manner. *Environ Sci Technol* 2014;48:8227-34. DOI PubMed
65. Zhu B, Zhao G, Yang L, Zhou B. Tetrabromobisphenol A caused neurodevelopmental toxicity via disrupting thyroid hormones in zebrafish larvae. *Chemosphere* 2018;197:353-61. DOI PubMed
66. Miao B, Yakubu S, Zhu Q, Issaka E, Zhang Y, Adams M. A review on tetrabromobisphenol A: human biomonitoring, toxicity, detection and treatment in the environment. *Molecules* 2023;28:2505. DOI PubMed PMC
67. Sturm MT, Myers E, Schober D, et al. Comparison of AOP, GAC, and novel organosilane-based process for the removal of microplastics at a municipal wastewater treatment plant. *Water* 2023;15:1164. DOI
68. Acarer S. A review of microplastic removal from water and wastewater by membrane technologies. *Water Sci Technol* 2023;88:199-219. DOI PubMed
69. Pizzichetti ARP, Pablos C, Álvarez-Fernández C, Reynolds K, Stanley S, Marugán J. Evaluation of membranes performance for microplastic removal in a simple and low-cost filtration system. *Case Stud Chem Environ Eng* 2021;3:100075. DOI
70. Malucelli LC, Ozeri I, Matos M, Magalhães WLE, Filho MASC, Eisen MS. High-flux, porous and homogeneous PVDF/cellulose microfiltration membranes. *Cellulose* 2022;29:1943-53. DOI
71. Yahyanezhad N, Bardi MJ, Aminirad H. An evaluation of microplastics fate in the wastewater treatment plants: frequency and removal of microplastics by microfiltration membrane. *Water Pract Technol* 2021;16:782-92. DOI
72. Gul A, Hruza J, Yalcinkaya F. Fouling and chemical cleaning of microfiltration membranes: a mini-review. *Polymers* 2021;13:846. DOI PubMed PMC
73. Singh S, Kalyanasundaram M, Diwan V. Removal of microplastics from wastewater: available techniques and way forward. *Water Sci Technol* 2021;84:3689-704. DOI PubMed
74. Long Z, Pan Z, Wang W, et al. Microplastic abundance, characteristics, and removal in wastewater treatment plants in a coastal city of China. *Water Res* 2019;155:255-65. DOI PubMed
75. Zhang Y, Diehl A, Lewandowski A, Gopalakrishnan K, Baker T. Removal efficiency of micro- and nanoplastics (180 nm-125 µm) during drinking water treatment. *Sci Total Environ* 2020;720:137383. DOI PubMed PMC
76. Zhang Y, Jiang H, Wang H, Wang C. Removal strategies for aquatic microplastics. In: Khan A, Wang C, Asiri AM, editors.

Microplastic sources, fate and solution. Singapore: Springer Nature Singapore; 2023. pp.71-88. DOI

77. Tadsuwan K, Babel S. Microplastic abundance and removal via an ultrafiltration system coupled to a conventional municipal wastewater treatment plant in Thailand. *J Environ Chem Eng* 2022;10:107142. DOI
78. Zhang J, Li G, Yuan X, et al. Reduction of ultrafiltration membrane fouling by the pretreatment removal of emerging pollutants: a review. *Membranes* 2023;13:77. DOI PubMed PMC
79. Xiao T, Zhu Z, Li L, Shi J, Li Z, Zuo X. Membrane fouling and cleaning strategies in microfiltration/ultrafiltration and dynamic membrane. *Sep Purif Technol* 2023;318:123977. DOI
80. Magni S, Gagné F, André C, et al. Evaluation of uptake and chronic toxicity of virgin polystyrene microbeads in freshwater zebra mussel *Dreissena polymorpha* (Mollusca: Bivalvia). *Sci Total Environ* 2018;631-2:778-88. DOI
81. Le LT, Bui XB, Tran CS, Chiemchaisri C, Pandey A. Chapter 9 - Membrane and filtration processes for microplastic removal. In: Current developments in biotechnology and bioengineering. Elsevier; 2023. pp.203-20. DOI
82. Michielssen MR, Michielssen ER, Ni J, Duhaime MB. Fate of microplastics and other small anthropogenic litter (SAL) in wastewater treatment plants depends on unit processes employed. *Environ Sci Water Res Technol* 2016;2:1064-73. DOI
83. Oatley-Radcliffe DL, Walters M, Ainscough TJ, Williams PM, Mohammad AW, Hilal N. Nanofiltration membranes and processes: a review of research trends over the past decade. *J Water Process Eng* 2017;19:164-71. DOI
84. Jang H, Kang S, Kim J. Identification of membrane fouling with greywater filtration by porous membranes: combined effect of membrane pore size and applied pressure. *Membranes* 2024;14:46. DOI PubMed PMC
85. Fang Y, Duranceau SJ. Study of the effect of nanoparticles and surface morphology on reverse osmosis and nanofiltration membrane productivity. *Membranes* 2013;3:196-225. DOI PubMed PMC
86. Ziajahromi S, Neale PA, Rintoul L, Leusch FD. Wastewater treatment plants as a pathway for microplastics: development of a new approach to sample wastewater-based microplastics. *Water Res* 2017;112:93-9. DOI PubMed
87. Pivokonsky M, Cermakova L, Novotna K, Peer P, Cajthaml T, Janda V. Occurrence of microplastics in raw and treated drinking water. *Sci Total Environ* 2018;643:1644-51. DOI PubMed
88. Khoo YS, Goh PS, Lau WJ, et al. Removal of emerging organic micropollutants via modified-reverse osmosis/nanofiltration membranes: a review. *Chemosphere* 2022;305:135151. DOI PubMed
89. Sturm MT, Schuhen K, Horn H. Method for rapid biofilm cultivation on microplastics and investigation of its effect on the agglomeration and removal of microplastics using organosilanes. *Sci Total Environ* 2022;806:151388. DOI PubMed
90. Wang L, He J, Heiranian M, et al. Water transport in reverse osmosis membranes is governed by pore flow, not a solution-diffusion mechanism. *Sci Adv* 2023;9:eadf8488. DOI PubMed PMC
91. Harharah RH, Abdalla GMT, Elkhaleefa A, Shigidi I, Harharah HN. A study of copper (II) ions removal by reverse osmosis under various operating conditions. *Separations* 2022;9:155. DOI
92. Popov K, Oshchepkov M, Pervov A, et al. A case study of calcium carbonate crystallization during reverse osmosis water desalination in presence of novel fluorescent-tagged antiscalants. *Membranes* 2022;12:194. DOI PubMed PMC
93. Yu YH, Jenne D. Numerical modeling and dynamic analysis of a wave-powered reverse-osmosis system. *J Mar Sci Eng* 2018;6:132. DOI
94. Sheriff I, Awang NA, Halim HB, et al. Extraction and analytical methods of microplastics in wastewater treatment plants: isolation patterns, quantification, and size characterization techniques. *Desalin Water Treat* 2024;318:100399. DOI
95. Wang Z, Liu K, Gao Y, et al. Removal and fouling influence of microplastics in fertilizer driven forward osmosis for wastewater reclamation. *Membranes* 2021;11:845. DOI PubMed PMC
96. Sun J, Dai X, Wang Q, van Loosdrecht MCM, Ni BJ. Microplastics in wastewater treatment plants: detection, occurrence and removal. *Water Res* 2019;152:21-37. DOI PubMed
97. Kraatz S, Libra JA, Drastig K, Hunstock U, Zare M, Jacobs H. Water use indicators at farm scale - an agro-hydrological software solution. *Sci Total Environ* 2019;678:133-45. DOI PubMed
98. Wang Z, Lin T, Chen W. Occurrence and removal of microplastics in an advanced drinking water treatment plant (ADWTP). *Sci Total Environ* 2020;700:134520. DOI PubMed
99. Ma B, Xue W, Hu C, Liu H, Qu J, Li L. Characteristics of microplastic removal via coagulation and ultrafiltration during drinking water treatment. *Chem Eng J* 2019;359:159-67. DOI
100. Zhang J, Xue Y, Eshtiaghi N, Dai X, Tao W, Li Z. Evaluation of thermal hydrolysis efficiency of mechanically dewatered sewage sludge via rheological measurement. *Water Res* 2017;116:34-43. DOI PubMed
101. Tang N, Zhang S, Si Y, Yu J, Ding B. An ultrathin bacterial cellulose membrane with a Voronoi-net structure for low pressure and high flux microfiltration. *Nanoscale* 2019;11:17851-9. DOI PubMed
102. Ozden S, Monti S, Tozzini V, et al. Egg protein derived ultralightweight hybrid monolithic aerogel for water purification. *Mater Today* 2022;59:46-55. DOI
103. Okamoto Y, Lienhard JH. How RO membrane permeability and other performance factors affect process cost and energy use: a review. *Desalination* 2019;470:114064. DOI
104. Golgoli M, Khiadani M, Shafieian A, et al. Microplastics fouling and interaction with polymeric membranes: a review. *Chemosphere* 2021;283:131185. DOI PubMed
105. Wang J, Wang S. Reactive species in advanced oxidation processes: formation, identification and reaction mechanism. *Chem Eng J* 2020;401:126158. DOI

106. Hübner U, Spahr S, Lutze H, et al. Advanced oxidation processes for water and wastewater treatment - guidance for systematic future research. *Heliyon* 2024;10:e30402. DOI PubMed PMC
107. Ameta R, Solanki MS, Benjamin S, Ameta SC. Chapter 6 - Photocatalysis. In: Advanced oxidation processes for waste water treatment. Academic Press; 2018. pp.135-75. DOI
108. Tang C, Huang X, Wang H, Shi H, Zhao G. Mechanism investigation on the enhanced photocatalytic oxidation of nonylphenol on hydrophobic TiO_2 nanotubes. *J Hazard Mater* 2020;382:121017. DOI PubMed
109. He F, Ji Y, Wang Y, Zhang Y. Preparation of bifunctional hollow mesoporous $Fe^0@C@MnFe_2O_4$ as Fenton-like catalyst for degradation of tetrabromobisphenol A. *J Taiwan Inst Chem Eng* 2017;80:553-62. DOI
110. Hu K, Zhou P, Yang Y, et al. Degradation of microplastics by a thermal fenton reaction. *ACS EST Eng* 2022;2:110-20. DOI
111. Ji Y, Niu J, Fang Y, Tan Nou A, Warsinger DM. Micelles inhibit electro-oxidation degradation of nonylphenol ethoxylates. *Chem Eng J* 2022;430:133167. DOI
112. Ning Z, Duan X, Li Y, Zhao X, Chang L. Degradation of polyvinyl chloride microplastics via electrochemical oxidation with a CeO_2 –PbO_2 anode. *J Clean Prod* 2023;432:139668. DOI
113. Rahmani AR, Salari M, Shabanloo A, Shabanloo N, Bajalan S, Vaziri Y. Sono-catalytic activation of persulfate by nZVI-reduced graphene oxide for degradation of nonylphenol in aqueous solution: process optimization, synergistic effect and degradation pathway. *J Environ Chem Eng* 2020;8:104202. DOI
114. Ioannidi AA, Bampos G, Antonopoulou M, et al. Sonocatalytic degradation of bisphenol A from aquatic matrices over Pd/CeO_2 nanoparticles: kinetics study, transformation products, and toxicity. *Sci Total Environ* 2024;919:170820. DOI
115. Anastopoulos I, Kyzas GZ. Are the thermodynamic parameters correctly estimated in liquid-phase adsorption phenomena? *J Mol Liq* 2016;218:174-85. DOI
116. Zanaty M, Zaki A, El-Dek S, Abdelhamid HN. Zeolitic imidazolate framework@hydrogen titanate nanotubes for efficient adsorption and catalytic oxidation of organic dyes and microplastics. *J Environ Chem Eng* 2024;12:112547. DOI
117. Zoppas F, Sacco N, Soffietti J, Devard A, Akhter F, Marchesini FA. Catalytic approaches for the removal of microplastics from water: recent advances and future opportunities. *Chem Eng J Adv* 2023;16:100529. DOI
118. Truppi A, Petronella F, Placido T, et al. Visible-light-active TiO_2-based hybrid nanocatalysts for environmental applications. *Catalysts* 2017;7:100. DOI
119. Zhang Y, Wang X, Li Y, et al. Improving nanoplastic removal by coagulation: Impact mechanism of particle size and water chemical conditions. *J Hazard Mater* 2022;425:127962. DOI
120. Guo Y, Kong F, Fatehi P. Generation and use of lignin-g-AMPS in extended DLVO theory for evaluating the flocculation of colloidal particles. *ACS Omega* 2020;5:21032-41. DOI PubMed PMC
121. Khan MT, Ahmad M, Hossain MF, et al. Microplastic removal by coagulation: a review of optimizing the reaction conditions and mechanisms. *Water Emerg Contam Nanoplastics* 2023;2:22. DOI
122. Spreafico C, Landi D, Russo D. A new method of patent analysis to support prospective life cycle assessment of eco-design solutions. *Sustain Prod Consump* 2023;38:241-51. DOI
123. Jiao H, Ali SS, Alsharbaty MHM, et al. A critical review on plastic waste life cycle assessment and management: challenges, research gaps, and future perspectives. *Ecotoxicol Environ Saf* 2024;271:115942. DOI PubMed

Mouatchô *et al. Water Emerg Contam Nanoplastics* 2024;3:22
DOI: 10.20517/wecn.2024.39

Water Emerging
Contaminants &
Nanoplastics

Research Article

Open Access

Use of a fluorescent molecular rotor probe for nanoplastics assessment in epiphytic biofilms growing on submerged vegetation of Lake Saint Pierre (St. Lawrence River)

Linsey Yvette Mouatchô[1], Eva Roubeau Dumont[2], Dominic E. Ponton[3], François Gagné[2], Marc Amyot[3], Isabelle Lavoie[1]

[1]National Institute of Scientific Research, Quebec City G1K 9A9, Quebec, Canada.
[2]Aquatic Contaminants Research Division, Environment and Climate Change Canada, Montreal H2Y 2E7, Quebec, Canada.
[3]GRIL, Department of Biological Sciences, University of Montreal, Montreal H2V 0B3, Quebec, Canada.

Correspondence to: Linsey Yvette Mouatchô, National Institute of Scientific Research, 490 de la Couronne Street, Quebec City G1K 9A9, Quebec, Canada. E-mail: mouatcho.linsey@gmail.com

How to cite this article: Mouatchô LY, Roubeau Dumont E, Ponton DE, Gagné F, Amyot M, Lavoie I. Use of a fluorescent molecular rotor probe for nanoplastics assessment in epiphytic biofilms growing on submerged vegetation of Lake Saint Pierre (St. Lawrence River). *Water Emerg Contam Nanoplastics* 2024;3:22. https://dx.doi.org/10.20517/wecn.2024.39

Received: 14 Jun 2024 **First Decision:** 3 Sep 2024 **Revised:** 18 Oct 2024 **Accepted:** 4 Nov 2024 **Published:** 27 Nov 2024

Academic Editors: Jie Wang, Zhijie Chen **Copy Editor:** Pei-Yun Wang **Production Editor:** Pei-Yun Wang

Abstract

Studies on plastic pollution conducted in freshwaters mainly focused on monitoring plastic debris in the water column or in the sediments. Few studies have investigated the occurrence of plastic debris in benthic biofilms (periphyton). Yet, algal biofilms may potentially act as a sink for plastic debris, trapping it within their mucilaginous or filamentous matrix. Biofilms may also represent a source of plastic debris by sloughing when they become senescent. In addition, plastic debris accumulated within biofilms may enter the food web via primary consumers. Considering these observations, this study aims to quantify nanoplastics (NPs) accumulated in biofilms growing on aquatic vegetation from Lake Saint Pierre (LSP), a fluvial lake of the St. Lawrence River, and its archipelago. Biofilms were removed from submerged plants and the presence of NPs was assessed by spectrophotometry using the fluorescent molecular rotor probe 9(dicyanovinyl)-julolidine (DCVJ). The results of this study confirm the biofilms' ability to act as a sink for NPs. Despite the fact that the determination of the absolute nanoparticle number and size distribution remains a challenge, we estimated a median concentration of 1.05 × 10^9 NP/mg of biofilm dry weight (DW) when using 100 nm polystyrene beads for calibration. Concentrations were significantly different between water masses, with higher concentrations in samples collected in the two lateral water masses compared to the central water mass. Our study provides, for the first time, a quantitative assessment of NPs from epiphytic biofilms in a large river under the influence of anthropogenic sources.

Keywords: Plastic pollution, nanoplastics, freshwater, epiphytic biofilm, fluorescent probe

INTRODUCTION

Since the year 1950, when global plastic production was around 0.5 million tons[1], its annual production has grown steadily, reaching 400 million tons per year in 2022[2]. North America produced 17% of these plastics in 2022[2]. With increasing production, extensive usage of plastic products, as well as poor waste management combined with insufficient regulation, plastic pollution raised global concerns as debris [i.e., mesoplastics 5 to 25 mm, microplastics (MPs) 1 µm to 5 mm, and nanoplastics (NPs) ≤ 1 µm[3]] has been detected in all ecosystems worldwide[4]. For instance, hundreds of research articles assessed the presence and fate of plastic debris in the aquatic environment over the past decade, with a particular focus on MPs in marine ecosystems and in the water column[5]. In the water compartment, plastic debris of 0.45 to 505 µm in size has been detected in concentrations ranging between 3×10^{-8} to 2 particles per mL[6]. Several studies focusing on marine ecosystems highlighted the adverse effects of plastic debris on the biota. Plastic pollution can cause physical damage, such as the entanglement of animal appendages or the obstruction of their digestive tract[7]. Biological and chemical effects such as oxidative stress or DNA damage have also been reported[6], and have been related to the presence of additives compounds such as plasticizers used during plastic production or to the presence of sorbed contaminants[8].

Compared to the marine environment, there are fewer studies that investigated the occurrence of plastic debris in freshwater ecosystems and their ecotoxicity[6]. However, streams and rivers are the major pathways for plastic debris into marine ecosystems[9], and studies suggest that these freshwaters may be at least as contaminated as marine waters[10]. For example, the sediment compartment of the St. Lawrence River is among the 25% most polluted in the world, with concentrations ranging from 65 to 7,562 plastic particles per kg dry weight (DW)[11]. Concentrations ranging from 48 to 187 particles per L were recorded in the water column of the Amsterdam canal (the Netherlands), which was higher than concentrations recorded in the North Sea coast (the Netherlands), where the mean concentration recorded was 27 particles per L[12].

Studies conducted in freshwaters mainly focused on monitoring plastic debris concentrations in the water column or in the sediments, while their occurrence and abundance in periphytic biofilms (or periphyton) have been largely overlooked. Periphyton is a key compartment at the base of aquatic and terrestrial food webs; it is a consortium of viruses, archaea, bacteria, algae, protozoa, fungi, and meiofauna, embedded in a matrix of extracellular polymeric substances. Periphyton colonizes all types of substrates exposed to light[13]. This biological matrix may function as a sink for plastic debris as particles get trapped and incorporated and may also represent a source of plastic particles for higher trophic levels[14]. Trapped plastic debris may have several ecotoxicological consequences on the microorganisms composing the periphyton, as reviewed in Guasch *et al.* (2022)[15]. For example, a study by Merbt *et al.* (2022) conducted on periphyton exposed to virgin and aged polyethylene (PE) beads (1-4 µm, 0.96 g/mL) for 28 days revealed their incorporation in the periphyton and showed a significant shift in microbial community composition[16]. A study by Miao *et al.* (2019) observed that periphyton exposed for 3 h to polystyrene beads (0.1 µm, 0.1 mg/mL) led to a significant decrease in chlorophyll concentration and impaired activity of functional enzymes, such as β-glucosidase and leucine aminopeptidase[17]. Plastic debris also acts as vectors for contaminants and may consequently influence their bioavailability[18] for the microorganisms of the periphyton and for consumers.

Biofilms influence the degradation of plastic particles by promoting their fragmentation by microorganisms that secrete enzymes capable of breaking covalent bonds[14]. Plastic debris accumulated within the periphyton may enter the food web via primary consumers feeding on this basal resource[19]. Considering that periphytic biofilms might act as a sink of plastic particles, dietary exposure of consumers might be more important than direct exposition through the water column[15]. Despite the key role periphytic biofilms play in freshwaters, little is known about their ability to trap and accumulate plastic particles[14]. To our knowledge, the article by Wang *et al.* (2023) is the only field study that provides evidence supporting the hypothesis that periphyton can incorporate plastic debris[20]. They recorded MPs, mainly fibers, in concentrations ranging from 419 to 1,314 items/m^2 in the CaoE River, China[20]. The authors focused on particle sizes in the mm range (≤ 0.5, 0.5-1, 1-2, 2-5 mm) as plastic debris was handpicked under an optical stereomicroscope prior to identification through Raman microscope spectroscopy.

To this date, less research has focused on NPs as compared to MPs; nanosize particles require complex analytical methods to be accurately quantified[21] and only a few studies measured particles smaller than 10 µm in the environment[6]. However, the ecotoxicity of plastic debris is likely to increase with decreasing size. Indeed, surface area in contact with contaminants increases with decreasing particle size[22], thus making NPs a particularly concerning hazard to biota. In addition, tissue translocation of NPs has been observed in laboratory experiments where nanometer-sized particles can passively cross tissue membranes[23,24]. To our knowledge, no studies have investigated the presence of NPs accumulated in periphyton. The following keywords were used in a Web of Science search TI = [*plastics AND (biofilms OR periphyt* OR "microbial communit*") AND (fresh$water* OR river* OR stream*)] and returned 16 results with only 4 of them addressing periphytic biofilms as a sink for plastic debris. Among those four publications, two were related to experimental exposure of periphyton to MPs[16,25], and one study was related to the quantification of MPs larger than 500 µm in periphyton collected in the field[20]. The fourth article by Holzer *et al.* (2022) was the only study specific to NPs, in which the authors investigated the bioaccumulation and toxicity of NPs in stream periphyton, as well as their transfer and resulting effects on the aquatic snail *Physa acuta*[26]. In their experiment, they exposed periphyton grown on glass slides in microcosms containing palladium-doped polyacrylonitrile coated with a polystyrene shell (160 nm, 0.5 mg/L) for 24 h and performed a feeding trial with the contaminated periphyton for 14 days. Their study revealed a strong accumulation of NPs in periphyton, where 90% of the NPs added to the microcosms were no longer in the overlying media.

Based on the scarcity of studies conducted to address plastic pollution in freshwaters, especially within the biofilm compartment, additional knowledge is needed to assess the extent to which this primary resource may act as a sink for NPs and as a source of contamination to consumers. The main objective of this study was to estimate NPs accumulated in periphyton growing on aquatic vegetation (i.e., epiphyton) from Lake Saint Pierre (LSP), a fluvial lake of the St. Lawrence River, and its archipelago (Quebec, Canada). LSP is an exceptionally rich ecosystem, both biologically and economically[27]. This widening of the St. Lawrence River is recognized as an ecosystem of international importance under the Ramsar Convention and is identified as a World Biosphere Reserve by UNESCO[28]. Plant beds of submerged/rooted aquatic vegetation are one of the key components of LSP, as they play an essential role in regulating various physical parameters such as current velocity and sedimentation of suspended particulate matter[29]. These dense plant communities provide essential habitats for the survival of many species of invertebrates and fish[29], and the epiphyton growing on this vegetation is a key component of the food web as several consumers rely on this resource[30]. Aquatic plants also form the basis of waterfowl diets[31], which may be exposed to NPs accumulated within the epiphyton.

Seventy percent of the water flowing through LSP comes from Lake Ontario[27]. This water is of relatively good quality and mainly flows through the navigation channel[32]. The shallower areas of the lake are thus isolated by this central water mass and show degraded water quality due to certain highly impacted tributaries entering the lake[33]. Because the main sources of water coming into LSP mix very little[34], they form three distinct water masses with different physico-chemical characteristics. The different origins of the three water masses and their water quality led to the hypothesis that NP concentrations accumulating in the epiphyton will differ depending on sampling locations within the LSP system (north, south, and central water masses). A second hypothesis was formulated around the upstream-downstream longitudinal gradient, where NP concentrations were projected to be higher in the epiphyton collected at the upstream stations compared to downstream stations. This hypothesis was based on the assumption that dense aquatic vegetation will favor NPs accumulation in the epiphyton and thus act as a filter for plastic particles.

The secondary objective of this study was to explore the feasibility of assessing polystyrene-like NPs (PSNPs) in the epiphyton by spectrophotometry using the fluorescent molecular rotor probe 9(dicyanovinyl)-julolidine (DCVJ). In this study, NPs detection was based on the probe's sensitivity to changes in hydrophobicity[35,36]. Briefly, a hydrophobic interaction between the probe and polystyrene nanoplastic beads (PSN) occurs at the PSN's surface, which produces a fluorescent signal[36]. After calibration with PSN, this signal is correlated to the presence of PSN and/or PSNP polymers, and its intensity is proportional to their concentration. The method allows for relative quantification of NPs in biofilm samples with PSN as the reference polymer. This method was previously used to assess PSN in diverse biological samples such as mussels[35-37] or radish sprout[35] and was tested here for the first time in the complex and heterogenous periphyton matrix.

MATERIALS AND METHODS

Study area

Lake Saint Pierre [Figure 1], stretching from Sorel to Trois-Rivières, is a widening of the St. Lawrence River and is characterized by a lentic hydrology (except for the central water mass)[38]. The system is 32 km long and 13 km wide, covers an area of 500 km^2 and has an average depth of 3 m with a maximum depth of 11.3 m at the center due to a man-made navigation channel[27]. The channel forms a physical barrier between the northern water body, mainly fed by the Ottawa, Yamachiche, Maskinongé and du Loup rivers, and the southern water body of the lake with waters from Richelieu, Saint-François, Yamaska, and Nicolet rivers[27]. Those tributaries drain highly anthropized lands, such as agricultural areas, which account for 37.7% of the lake's watershed[32]. As for the central water body, it is mainly fed by Lake Ontario[27]. The water quality from the central water body differs from the lateral water masses that exhibit a lower quality[27] due to tributaries such as the Yamaska River which is among the most agriculturally and industrially polluted rivers in the Province of Quebec[39]. In addition, the northern water mass receives wastewater effluents from Montreal, the world's 3rd largest treatment plant of its kind[40]. The water masses of the lake also differ by the spatial distribution of the submerged vegetation[32], with greater abundances in the littoral zones and around the archipelago[34]. The floodplains of the lateral masses are exposed to heavy anthropization, such as dense road networks, sewer overflows, row crops, and several municipalities and industries[32,33].

Biofilm sampling and water physicochemistry

In August 2023, 14 stations were visited across LSP and its archipelago. To minimize secondary contamination of samples with plastic debris, field staff were dressed in cotton clothing and used sampling tools made of metal or glass. No gloves were used during sampling to avoid potential contamination with plastic-like material. Biofilm samples were collected on submerged plants such as *Vallisneria americana*, *Potamogeton pusillus*, and *Potamogeton perfoliatus*. Submerged vegetation was harvested using a metal rake and transferred to a steel bucket containing 750 mL of lake water. Plants were then manually vigorously

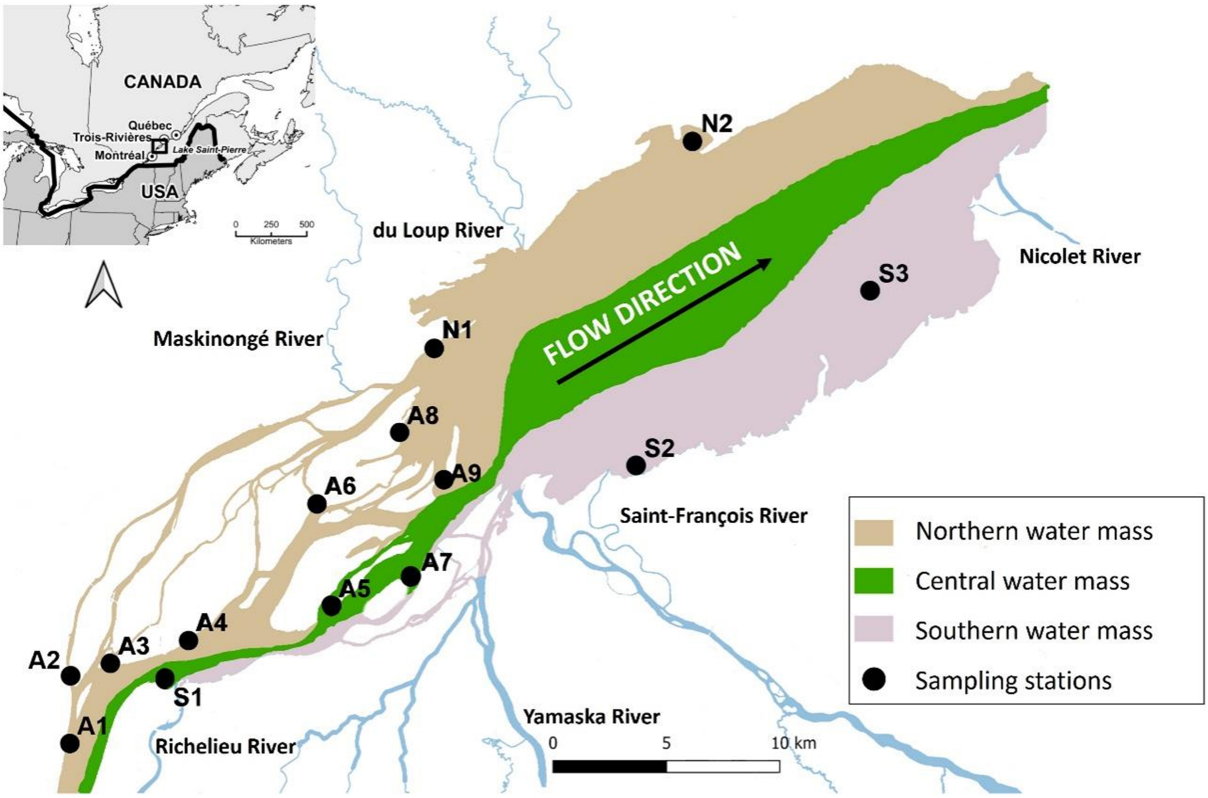

Figure 1. Distribution of water masses within Lake Saint-Pierre (Quebec, Canada) and the stations visited in 2023. Out of the 14 stations sampled, nine were located in the lake's archipelago area (stations A1 to A9), three on the south shore (stations S1, S2, and S3), and two on the north shore (stations N1 and N2). Nine stations (A1 to A4, A6, A8, A9, N1, and N2) were located in the northern water body, three (A5, A7, and S1) in the central water body and two (S2 and S3) in the southern water body.

shaken to detach the epiphython. The content was then transferred into 1-liter glass jars after filtration on a 0.5 mm pore size metal sieve to remove plant debris and large invertebrates. Samples were preserved in coolers in the field and stored at 4 °C in the dark until arrival at the laboratory. In order to obtain representative samples, each of the 14 stations was sampled along a transect of three sampling points that were 10-20 meters apart. Conductivity, temperature, and pH were measured on site using the ORION Thermo Scientific multi-probe field instrument [Supplementary Table 1]. Once in the laboratory, biofilm samples were oven-dried at 50 °C to preserve the physicochemistry of potential plastic polymers[41], and stored at room temperature in obscurity until further analyses.

Sample digestion and detection of PSNPs by spectrophotometry

A subsample (referred to as samples hereafter) from each of the 42 biofilm samples (14 stations × 3 points per transect) was rehydrated in ultrapure water (5 mL per gram of dry mass) and manually stirred with a stainless steel spatula. To ensure complete rehydration, samples were placed on an orbital shaker at 300 rpm for one week (room temperature in obscurity). Afterwards, potassium hydroxide (KOH 20%) was added to each sample (v/v for a 10% final KOH concentration) to digest organic content[42] without degrading PSN, and the samples were left for agitation for one additional week after thorough vortexing. After one week under agitation, the digestates were left to stand for 3 h to allow for microparticles to settle. The supernatants were then collected for analysis. Potassium dihydrogen phosphate (KH_2PO_4, pH 6.5, 100 mM) was added (0.5 v/v) to neutralize KOH and avoid interference with the quantification method[42]. Levels of NPs were then estimated by spectrophotometry using the fluorescent molecular rotor probe DCVJ.

The commercial DCVJ probe (Sigma Aldrich, CAS 58293-56-4) was dissolved in methanol at a concentration of 1 mM to serve as a stock solution. The stock solution was diluted at 0.4 µM in ultrapure water for a daily solution used for fluorescence analysis. A volume of 30 µL collected from the sample's supernatant was mixed with 160 µL of DCVJ probe and 10 µL of ultrapure water in 96-well microplates. The fluorescence intensity of the microplates was analyzed using a microplate reader (Agilent, BioTek, Synergy Neo 2) with the excitation wavelength at 450 nm and the emission wavelength at 620 nm. PSNPs detected in biofilm samples were assumed to have a maximum size of 100 nm as standard solutions of PSN beads of 50 and 100 nm (Polyscience, Polybead® Microspheres) were used for method calibration [Supplementary Figure 1]. Biofilm NP concentrations were calculated using the 100 nm low concentration calibration curve as they fit best the fluorescence intensity range, except for station S2 which had a higher fluorescence than the range provided by the 100nm low concentration curve, and as such levels were calculated with the 100 nm high concentration calibration curve (i.e., above 5,000). The influence of plastic material autofluorescence[43] on the detection of PSNPs with the fluorescent DCVJ probe was also investigated and no autofluorescence was detected at 620 nm [Supplementary Table 2].

Quality assurance and quality control of the DCVJ probe assay

Several procedural controls were implemented in the protocol and were analyzed with the samples to assess (1) the potential contamination during the sample treatment process (i.e., negative controls); and (2) the efficiency of PSN recovery during the digestion process (digestion controls). Negative controls consisted of ultra-pure water samples that were digested using the same protocol as for biofilm samples, and the digestion controls were suspensions of PSN of a known theoretical concentration suspended in deionized water (8.41×10^{13} 50 nm PSN/mL; 1.15×10^{13} 100 nm PSN/mL) and digested also using the same protocol as for biofilm samples. Deionized water samples (water blanks) were analyzed to ensure the specificity of the DCVJ probe with PSN and to assess the background noise. Biological controls were performed during the method development and involved spiked biofilm samples (pooled biofilm samples, and the addition of a known theoretical concentration of 8.35×10^{12} PSN/mL) to assess fluorescence signal in the presence of the biofilm matrix and potential interactions. As for the limit of detection (LOD), its theoretical value (blank standard deviation × 2) was estimated at 65 ng/mL and the blank standard consisted of the DCVJ probe diluted in water (Gagné, 2019). Standard curves using suspensions of PSN (50 and 100 nm) were generated to validate the linearity of the signal using the DCVJ probe (R^2 ranged between 0.92 and 0.99 depending on particle size; Supplementary Figure 1).

Data representation and analysis

Mapping of the sampling stations at the scale of LSP was carried out using QGIS-Server, QGIS software (version 3.26.1). Estimated levels of PSNPs in the biofilms growing on submerged vegetation at each station were graphically presented to allow for inter-station comparison, and a Pearson correlation was conducted to explore a potential upstream-downstream longitudinal gradient. Sampling stations were subsequently classified according to their respective water masses (i.e., northern, central, or southern water mass). Differences in terms of PSNP concentrations between the three water masses were assessed by a Kruskal-Wallis test followed by a Dunn post-hoc test using the FSA package. Significant differences were set at $P < 0.05$ and statistical analyses were conducted using the softwares R (version 4.3.0) and R studio (version 2024.04.0+735).

RESULTS

Quality assurance and quality control

Water blanks and negative controls used for the quality assurance and quality control (QAQC) assay did not emit any fluorescent signal (values not shown), contrary to samples containing PSN (i.e., digestion and biological controls). No autofluorescence from PSN controls was measured at 450:620 nm in the absence of

Table 1. Average concentrations of polystyrene nanoplastic beads (PSN/mL) of 50 and 100 nm detected in the sample used for quality assurance and quality control

PSN size	Sample type	Emission 620 nm (AU)	Initial theoretical concentration	Final measured concentration
50 nm	Water blanks	NA	-	NA
	Negative controls	NA	-	NA
	Digestion controls	5,615	8.41×10^{13}	3.29×10^{10}
	Biological controls	2,827	8.02×10^{13}	4.26×10^{10}
100 nm	Water blanks	NA	-	NA
	Negative controls	NA	-	NA
	Digestion controls	6,683	1.15×10^{13}	1.24×10^{12}
	Biological controls	1,792	8.35×10^{12}	4.16×10^{11}

Fluorescence intensities are expressed as AU and were determined at 450 nm excitation wavelength. Water blanks: deionized water; negative controls: digested deionized water; digestion controls: PSN suspensions of a known theoretical concentration; biological controls: spiked biofilm samples. PSN: Polystyrene nanoplastic beads; AU: arbitrary units; NA: not applicable.

DCVJ, indicating that the observed fluorescent signal in the presence of both PSN and DCVJ was specific to their interaction. Hence, biological controls emitted a fluorescent signal that was not related to the autofluorescence of plastic materials[44], as confirmed by the autofluorescence assay [Supplementary Table 2]. Samples containing PSN showed a loss, especially with PSN of 50 nm [Table 1]. For 50 nm PSN beads, there was a difference of a factor of 2,000 for digestion controls and of a factor of 1,000 for biological controls between the theoretical and the measured PSN concentrations. As for PSN of 100 nm, there was a ninefold and a twentyfold difference (digestion and biological controls, respectively) in PSN concentration between the initial theoretical concentration and the final measured concentration.

Detection of PSNPs in biofilms

Samples' fluorescence at 620 nm was mostly below 5,000 AU and ranged from 320 to 4,800 AU [Supplementary Table 3]. The three samples from the most contaminated station emitted a fluorescence signal above 5,000 at 620 nm (i.e., 5,316, 5,355, and 6,253). All samples' fluorescence signal fell along the linear part of the 100 nm PSN calibration curve [Supplementary Figure 1], implying that samples contained PSNPs. Estimated levels of PSNPs ranged from 1.05×10^7 to 5.61×10^9 PSNP/mg biofilm DW with a median concentration of 1.05×10^9 PSNP/mg biofilm DW. The average (± standard-deviation, SD) concentration was $1.34 \times 10^9 \pm 1.10 \times 10^9$ PSNP/mg biofilm DW. As a general trend, PSNP concentrations observed in the three samples collected along the transect at each station were relatively similar, except for A5, where PSNPs were in much lower concentrations in one sample. There was a twenty-eight-fold difference in PSNP concentration between the most contaminated station, S2, and the least contaminated station, A5 [Figure 2]. Overall, PSNP concentrations at the different sampling stations seemed to be mainly related to the three water masses rather than to an upstream-downstream longitudinal gradient. Indeed, no significant correlation was observed between the distance (km) from the most upstream station (A1) and PSNP concentrations ($r = 0.26$; $P > 0.05$).

Sampling stations were grouped according to their water mass (central, northern, and southern). The central water mass was the least contaminated with PSNPs, where a median concentration of 5.24×10^8 PSNP/mg biofilm DW and an average concentration of $5.01 \times 10^8 \pm 3.06 \times 10^8$ PSNP/mg biofilm DW were estimated. The southern water mass was the most contaminated, with a median concentration of 3.02×10^9 PSNP/mg biofilm DW and a mean concentration of $3.18 \times 10^9 \pm 1.78 \times 10^9$ PSNP/mg biofilm DW. As for the northern water mass, it was three times less contaminated than the southern water mass, and twice as contaminated as the central water mass. The median concentration in the northern water mass was 1.03×10^9 PSNP/mg biofilm DW and the average concentration was $1.16 \times 10^9 \pm 5.02 \times 10^8$ PSNP/mg biofilm DW.

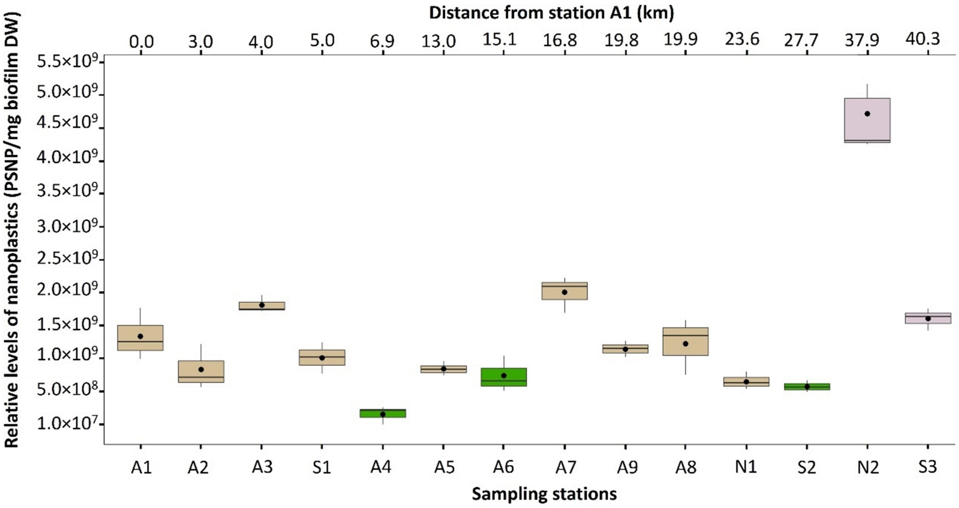

Figure 2. Estimated concentrations of nanoplastic (PSNP/mg DW) in the biofilm samples collected across the 14 stations (× 3 sampling points) visited at Lake St-Pierre. Codes on the X-axis represent station location where A = archipelago, N = north shore, S = south shore. Colors represent water masses, where brown for the northern water body, green for the central water body, and lilac for the southern water body. The solid black line represents the median concentration, and the black dot represents the mean concentration. Stations are presented from upstream to downstream, with station A1 being the most upstream station. Distances in km from station A1 are also indicated. PSNP: Polystyrene-like nanoplastics; DW: dry weight.

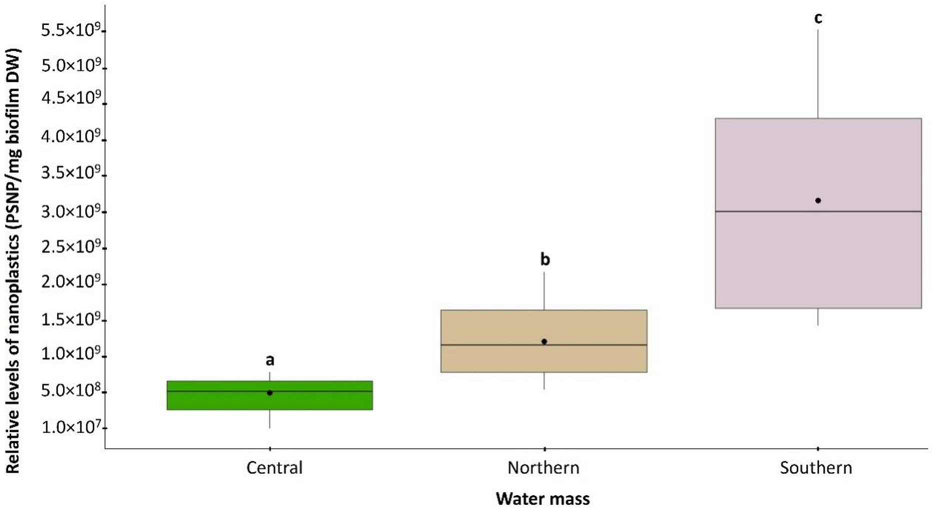

Figure 3. Estimated concentrations of nanoplastic (PSNP/mg DW) in the biofilm samples collected across the 14 stations grouped according to their respective water mass (central, northern and southern). The central water body includes three stations (A5, A7 and S1), the northern water body includes nine stations (A1 to A4, A6, A8, A9, N1 and N2), and the southern water body includes two stations (S2 and S3). The solid black line represents the median concentration, and the black dots represent the mean concentration. The letters a, b, and c indicate significant differences in estimated concentrations of nanoplastics between water masses. PSNP: Polystyrene-like nanoplastics; DW: dry weight.

A Kruskall-Wallis test performed to assess the difference in PSNP concentrations between the three water masses showed that there was a significant effect of water mass ($P < 0.001$) [Figure 3]. The Dunn post-hoc test revealed significant differences between central and northern water masses ($P = 0.002$), southern and central water masses ($P < 0.001$), and northern and southern water masses ($P = 0.015$). The epiphyton from the submerged vegetation collected in the southern water mass appeared to have accumulated six times more PSNP/mg biofilm DW than the epiphyton from the central water mass.

DISCUSSION

Methodological development of the DCVJ probe

Water blanks and digestion controls used in the QAQC assay did not exhibit a fluorescence signal at 620 nm contrarily to PSN suspensions, meaning that water, reagents, and sample processing did not contribute to the observed signal at 620 nm in biofilm samples, i.e., if plastic contamination occurred, it was below LOD. Digestion controls and biological controls showed a loss of PSN, especially for the smallest PSN size (50 nm), which might imply a size-dependent efficiency of the analytical method. However, given the NPs' tendency to aggregate, even more so as concentration increases[45] and particle size decreases[46], the particle loss was considered minor, given the overall PSN concentration and the fact that the primary goal was to compare contamination levels between sampling stations. Preliminary tests with biological controls helped confirm a potential interaction between KOH, biofilm organic matter, and spiked PSN, which slightly decreased the fluorescent signal at 620 nm for both particle sizes. The extent of this interaction remains to be quantified, as it is directly linked to (1) biofilm composition, (2) NP concentration, and (3) NPs size. Furthermore, the size and concentration of NP particles are well known to strongly influence their propension to aggregate in suspension, especially in the absence of surface surfactants[47,48].

Overall, the QAQC assay, in addition to the autofluorescence assay [Supplementary Table 2], demonstrated the method's ability to detect NPs resembling PSN in the complex epiphyton matrix, and enabled a comparison of NP contamination between stations and between water masses of LSP. However, there might be a marked underestimation of PSNPs detected in biofilm samples, given the loss of PSN used in the QAQC assay. Therefore, the DCVJ probe currently provides information on whether or not epiphythic biofilms can accumulate NPs from LSP and enables comparison between stations but cannot be used for absolute quantification. Further research and method development are needed to improve the quantitative assessment of PSN in periphyton samples, such as studying the interaction between organic matter and the DCVJ probe, and to link periphyton biochemical properties to potential interactions (such as lipid content). The use of the DCVJ probe could be coupled with other analytical methods, such as nanoparticle tracking analysis (NTA) or pyrolysis-GC/MS. These methods also require handling and sample processing, with the potential introduction of other methodological biases.

Developing protocols and methods to properly analyze and quantify NPs is an ongoing process with multiple challenges due to the complex nature of NPs contamination[49,50]. There are currently very few methodologies enabling rapid quantitative analysis of plastic particles, and most of them solely focus on MPs in environmental water samples[51-53], which are less complex than organic matrices such as periphytic biofilms. The DCVJ probe has been successfully applied to quantify PSN in diverse aquatic and terrestrial organisms[35,37,54], demonstrating promise for high-throughput analysis of environmental samples and organisms. The approach allows for effective means of comparison between treatments or sampling stations, although it still needs further development and adjustments to improve quantification depending on the nature and biochemical complexity of the samples being analyzed.

Presence of PSNPs in biofilms

Lower concentrations of PSNPs in the central water mass of LSP compared to the lateral water masses might be linked to the water residence time and, therefore, to the water flow regime. In this zone, the water flow regime is higher, with a residence time of 20 h, while it can reach up to 72 h and even several weeks during the summer low-water period in the lateral water masses[55]. High water flow regime, such as in the central water mass, may promote the dispersal and movements of particles[56] and thus prevent NP accumulation in biofilms. The lower PSNP concentrations observed in the central water mass might also be linked to the origin of the water coming from Lake Ontario, where this lentic environment favors particle sedimentation. Another factor that can drive NP contamination is point sources[57], and direct effluent sources potentially containing plastic pollution may not be as present in this central zone of the lake compared to the lateral water masses. For example, station A5 (lowest estimated PSNP concentration) is surrounded by a protected area[27], which can help limit inputs of plastic debris.

High concentrations of PSNPs observed in the epiphyton collected in lateral water masses might be attributed to the proximity to sources of pollution along the lake shore[58]. This observation is consistent with the results by Crew *et al.* (2020), who assessed MPs in the sediments of the St. Lawrence River and found a fourfold difference between MP concentrations in sampling points located around the LSP archipelago (n = 3) and the one station located on the north shore of LSP[11]. In lateral water masses, sources of pollution seem mainly linked to agricultural land use and urban areas. In the southern water mass, elevated NP concentrations were mainly driven by station S2, where the average concentration reached $4.73 \times 10^9 \pm 7.56 \times 10^8$ particles/mg DW. This station is located downstream of the Yamaska and Saint-François rivers, which flow through agricultural watersheds[59,60]. In addition, the Yamaska River is among the most polluted rivers in the province of Quebec, partly due to the presence of industrial activities. Indeed, the Yamaska River runs through the municipality of Granby, which is home to 271 industries, including 28 plastic/rubber industries[61]. In the northern water mass, elevated PSNP concentrations were mainly driven by stations A8 and N1 with average concentrations of $2.02 \times 10^9 \pm 2.76 \times 10^8$ particles/mg biofilm DW and $1.24 \times 10^9 \pm 4.31 \times 10^8$ particles/mg biofilm DW, respectively. Both stations were located in agricultural areas, with station N1 located downstream (1.4 km) of a small agricultural stream that also drains large proportions of agricultural lands[62]. Agriculture is one major source of plastic debris into the environment[9]; therefore, it is not surprising to observe elevated PSNP concentrations in the epiphyton collected on the submerged aquatic vegetation growing along the south and the north shores.

Finally, differences in PSNP concentrations between the northern and southern water masses might reflect the general pollution level of their affluents. For instance, the water quality (i.e., nitrogen, phosphorus, suspended particle matter, and bacteriological loads) is poorer in the tributaries of the south shore compared to those of the north shore[63]. For example, at the St. Lawrence River scale, the annual total suspended particle load between 2013 and 2017 was 1.3 times higher in the tributaries of the south shore than in the tributaries of the north shore[63]. Higher concentrations of all other parameters (i.e., nitrogen, phosphorus and bacteriological loads) were also observed in water samples collected from the south shore than in samples collected from the north shore. For instance, Maskinongé River, which is in close proximity to station A8 in the northern water body, exhibited a better water quality than Yamaska and St-François rivers, which were the main tributaries discharging upstream of the most contaminated station (S2) in the southern water body.

Comparing PSNP concentrations in the biofilm growing on submerged vegetation from LSP with NP concentrations found in other systems around the world is difficult as, to our knowledge, there are no other studies focusing on NPs in this biological compartment. The same goes for other benthic compartments, such as the sediments, as empirical data are lacking due to technical limitations to retrieving NPs particles[64] or analytical limitations to detecting nanoscale particles[57]. However, laboratory experiments highlighted a continuum between MPs and NPs, where MPs subsequently degrade into NPs[3]. For example, Wagner and Lambert (2016) investigated the degradation of different plastic types under aqueous conditions and observed that PS of 1 × 1 cm squares size generated the highest number of particles (6.4×10^8 particles/mL) in the 30-2,000 nm size range[65]. Based on this, the elevated PSNP concentrations observed in the epiphyton of LSP seem plausible, considering the elevated concentrations of MPs found in the sediments of the St. Lawrence River[11].

CONCLUSION

The present study is the first to investigate NPs (resembling polystyrene) contamination in the biofilm growing on the submerged vegetation. The DCVJ fluorescent probe was used to detect and quantify these NPs. This analytical method provided insights into a rapid and cost-effective approach enabling the quantification of PSNPs and laid the foundations for the development of field monitoring protocols in a context where standardized and accessible protocols are lacking. However, the method needs further improvement, particularly in its ability to detect and quantify a broader range of plastic polymers. Moreover, the DCVJ probe can currently only be employed as a diagnostic tool for plastic pollution as the quantified particles need to be correlated with a calibration standard, in this case, PSN. Therefore, it is essential to compare the DCVJ method with other techniques, such as pyrolysis-GC/MS, to obtain absolute quantification and to provide valuable complementary information from a qualitative perspective. Finally, insights into samples' biochemical composition (e.g., lipids, amino acids) could help to better understand the potential *in situ* interactions between biofilms and NPs contamination.

Overall, the analysis of biofilm samples collected from submerged vegetation revealed an important accumulation of PSNPs, supporting the hypothesis that periphyton can act as a sink for plastic particles. Estimated levels of PSNPs were linked to the three water masses of LSP with higher concentrations in stations located in lateral waters compared to the central water mass, suggesting an important influence of land-based sources from the tributaries. Further research is needed to better assess the link between specific anthropogenic activities at the watershed scale and NPs pollution.

DECLARATIONS

Authors' contributions

Field sampling: Mouatchô LY, Ponton DE, Amyot M, Lavoie I
Sample preparation: Mouatchô LY
Laboratory analyses: Roubeau Dumont E
Data analysis: Mouatchô LY
Study design: Lavoie I, Ponton DE, Amyot M, Mouatchô LY
Funding acquisition: Lavoie I, Gagné F, Amyot M
Manuscript writing: Mouatchô LY, Roubeau Dumont E, Lavoie I
Manuscript review and editing: Mouatchô LY, Roubeau Dumont E, Ponton DE, Gagné F, Amyot M, Lavoie I
All authors have read and approved the final manuscript.

Availability of data and materials

The data are available in Supplementary Materials and can also be available from the corresponding author upon reasonable request.

Financial support and sponsorship

This research was supported by a grant from Fonds de recherche du Québec - Nature et technologies (FRQNT) to Lavoie I and fundings from Groupe de Recherche Interuniversitaire en Limnologie (GRIL) provided to Mouatchô LY.

Conflicts of interest

Gagné F is an Editorial Board member of the journal *Water Emerging Contaminants & Nanoplastic*, while the other authors have declared that they have no conflicts of interest.

Ethical approval and consent to participate

Not applicable.

Consent for publication

Not applicable.

Copyright

REFERENCES

1. Thompson RC, Moore CJ, vom Saal FS, Swan SH. Plastics, the environment and human health: current consensus and future trends. *Philos Trans R Soc Lond B Biol Sci* 2009;364:2153-66. DOI PubMed PMC
2. Plastics Europe. Plastics - the fast facts 2023. Available from: https://plasticseurope.org/knowledge-hub/plastics-the-fast-facts-2023/. [Last accessed on 9 Nov 2024].
3. Ter Halle A, Jeanneau L, Martignac M, et al. Nanoplastic in the North Atlantic subtropical gyre. *Environ Sci Technol* 2017;51:13689-97. DOI PubMed
4. Kalčíková G, Skalar T, Marolt G, Jemec Kokalj A. An environmental concentration of aged microplastics with adsorbed silver significantly affects aquatic organisms. *Water Res* 2020;175:115644. DOI PubMed
5. Granek EF, Brander SM, Holland EB. Microplastics in aquatic organisms: improving understanding and identifying research directions for the next decade. *Limnol Oceanogr Lett* 2020;5:1-4. DOI
6. Bucci K, Tulio M, Rochman CM. What is known and unknown about the effects of plastic pollution: a meta-analysis and systematic review. *Ecol Appl* 2020;30:e02044. DOI PubMed
7. Laist DW. Impacts of marine debris: entanglement of marine life in marine debris including a comprehensive list of species with entanglement and ingestion records. In: Coe JM, Rogers DB, editors. Marine debris. New York: Springer; 1997. pp. 99-139. DOI
8. Revel M, Roman C, Châtel A. Is cell culture a suitable tool for the evaluation of micro- and nanoplastics ecotoxicity? *Ecotoxicology* 2021;30:421-30. DOI PubMed
9. Campanale C, Dierkes G, Massarelli C, Bagnuolo G, Uricchio VF. A relevant screening of organic contaminants present on freshwater and pre-production microplastics. *Toxics* 2020;8:100. DOI PubMed PMC
10. Peng J, Wang J, Cai L. Current understanding of microplastics in the environment: occurrence, fate, risks, and what we should do. *Integr Environ Assess Manag* 2017;13:476-82. DOI PubMed
11. Crew A, Gregory-Eaves I, Ricciardi A. Distribution, abundance, and diversity of microplastics in the upper St. Lawrence River. *Environ Pollut* 2020;260:113994. DOI PubMed
12. Karlsson TM, Vethaak AD, Almroth BC, et al. Screening for microplastics in sediment, water, marine invertebrates and fish: method development and microplastic accumulation. *Mar Pollut Bull* 2017;122:403-8. DOI PubMed
13. Battin TJ, Besemer K, Bengtsson MM, Romani AM, Packmann AI. The ecology and biogeochemistry of stream biofilms. *Nat Rev Microbiol* 2016;14:251-63. DOI PubMed
14. Kalčíková G, Bundschuh M. Aquatic biofilms-sink or source of microplastics? A critical reflection on current knowledge. *Environ Toxicol Chem* 2022;41:838-43. DOI PubMed
15. Guasch H, Bernal S, Bruno D, et al. Interactions between microplastics and benthic biofilms in fluvial ecosystems: knowledge gaps and future trends. *Freshw Sci* 2022;41:442-58. DOI
16. Merbt SN, Kroll A, Tamminen M, et al. Influence of microplastics on microbial structure, function, and mechanical properties of stream periphyton. *Front Environ Sci* 2022;10:928247. DOI
17. Miao L, Hou J, You G, et al. Acute effects of nanoplastics and microplastics on periphytic biofilms depending on particle size, concentration and surface modification. *Environ Pollut* 2019;255:113300. DOI PubMed
18. Wagner M, Lambert S. Freshwater microplastics: emerging environmental contaminants? Springer International Publishing: Cham; 2018. DOI
19. Krause S, Baranov V, Nel HA, et al. Gathering at the top? Environmental controls of microplastic uptake and biomagnification in freshwater food webs. *Environ Pollut* 2021;268:115750. DOI
20. Wang B, Lan X, Zhang H, Hu Y. Benthic biofilms in riverine systems: a sink for microplastics and the underlying influences. *Environ Pollut* 2023;337:122607. DOI
21. Chatterjee S, Krolis E, Molenaar R, Claessens MM, Blum C. Nile red staining for nanoplastic quantification: overcoming the challenge of false positive counts due to fluorescent aggregates. *Environ Chall* 2023;13:100744. DOI
22. Gallitelli L, Cera A, Cesarini G, Pietrelli L, Scalici M. Preliminary indoor evidences of microplastic effects on freshwater benthic macroinvertebrates. *Sci Rep* 2021;11:720. DOI PubMed PMC
23. Osman DM, Yuan W, Shabaka S, et al. The threat of micro/nanoplastic to aquatic plants: current knowledge, gaps, and future perspectives. *Aquat Toxicol* 2023;265:106771. DOI PubMed
24. Triebskorn R, Braunbeck T, Grummt T, et al. Relevance of nano- and microplastics for freshwater ecosystems: a critical review. *TrAC*

Trend Anal Chem 2019;110:375-92. DOI

25. Castaño-Ortiz JM, Romero F, Cojoc L, et al. Accumulation of polyethylene microplastics in river biofilms and effect on the uptake, biotransformation and toxicity of the antimicrobial triclosan. *Environ Pollut* 2024;344:123369. DOI
26. Holzer M, Mitrano DM, Carles L, Wagner B, Tlili A. Important ecological processes are affected by the accumulation and trophic transfer of nanoplastics in a freshwater periphyton-grazer food chain. *Environ Sci Nano* 2022;9:2990-3003. DOI
27. MELCCFP. Lake Saint-Pierre, a jewel to be restored. 2013. (in French). Available from: https://belsp.uqtr.ca/id/eprint/421. [Last accessed on 9 Nov 2024].
28. RSIS Lake Saint-Pierre. Ramsar sites information service. (in French). Available from: https://rsis.ramsar.org/fr/ris/949. [Last accessed on 9 Nov 2024].
29. Doucet C, Girard C, Clément-Robert G, Slevan-Tremblay I, Royer Boutin P, Boissonneault Y. Regional integrated management plan for Lake Saint-Pierre. 2018. (in French). Available from: https://belsp.uqtr.ca/id/eprint/1428/1/TCRLSP%201_2018_%20Plan_gestion_int%c3%a9gr%c3%a9e_A.pdf. [Last accessed on 9 Nov 2024].
30. Lalonde S, Cusson B, Longpré D. Current state of knowledge regarding the vegetation on the south shore of Lake Saint-Pierre. 2003. (in French). Available from: https://belsp.uqtr.ca/id/eprint/331/1/Lalonde%20et%20al_2003_vegetation%20rive%20sud%20lac%20St-Pierre_A.pdf. [Last accessed on 9 Nov 2024].
31. Richard G, Côté D, Mingelbier M, Jobin B, Morin J, Brodeur P. Land cover of the Lake Saint-Pierre (St. Lawrence River) floodplain between the years 1950, 1964 and 1997: interpretation of aerial photographs, digitation and preparation of a georeferenced database. (in French). Available from: https://belsp.uqtr.ca/id/eprint/497/. [Last accessed on 9 Nov 2024].
32. TCRLSP. Fact sheet regarding improvements to water quality in Lake Saint-Pierre. 2018. (in French). Available from: https://belsp.uqtr.ca/id/eprint/1432/1/TCRLSP%204_2018_qualit%C3%A9_eau_Fiche%20synth%C3%A8se_A.pdf. [Last accessed on 9 Nov 2024].
33. TCRLSP. Introductory document to the regional integrated management plan for Lake Saint-Pierre, 2018. (in French). Available from: https://belsp.uqtr.ca/id/eprint/1428. [Last accessed on 9 Nov 2024].
34. Restoration of Habitats in Lake Saint-Pierre: a prerequisite for recovery of the Yellow Perch. *natcan* 2014;138:50-61. DOI
35. Moraz A, Breider F. Detection and quantification of nonlabeled polystyrene nanoparticles using a fluorescent molecular rotor. *Anal Chem* 2021;93:14976-84. DOI PubMed
36. Gagné F. Detection of polystyrene nanoplastics in biological tissues with a fluorescent molecular rotor probe. *J Xenobiot* 2019;9:8147. DOI PubMed PMC
37. Gagné F, Roubeau-Dumont E, André C, Auclair J. Micro and nanoplastic contamination and its effects on freshwater mussels caged in an urban area. *J Xenobiot* 2023;13:761-74. DOI PubMed PMC
38. Description des caractéristiques du lac Saint-Pierre. Source: Ministère de l'Environnement et de la Faune, Lac Saint-Pierre. Fiche d'information sur les zones humides Ramsar, 1998, pp. 1-3. Available from: https://oraprdnt.uqtr.uquebec.ca/portail/gscw031?owa_no_site=665&owa_no_fiche=109. [Last accessed on 9 Nov 2024].
39. Genovese A, Hudon C, Martel AL, Cattaneo A. Molluscan assemblages under multiple stressors in a large fluvial lake. *Fund Appl Limnol* 2016;188:289-307. DOI
40. Villemure I. I Impact of trophic exposure to a major municipal effluent on the physiological responses of two mobile predator fish species. Theses, University of Quebec in Trois-Rivières: Trois-Rivières, 2015. Available from: https://depot-e.uqtr.ca/id/eprint/7801/1/031118297.pdf. [Last accessed on 9 Nov 2024] DOI
41. Li J, Liu H, Paul Chen J. Microplastics in freshwater systems: a review on occurrence, environmental effects, and methods for microplastics detection. *Water Res* 2018;137:362-74. DOI PubMed
42. Thiele CJ, Hudson MD, Russell AE. Evaluation of existing methods to extract microplastics from bivalve tissue: adapted KOH digestion protocol improves filtration at single-digit pore size. *Mar Pollut Bull* 2019;142:384-93. DOI PubMed
43. Morgana S, Casentini B, Tirelli V, Grasso F, Amalfitano S. Fluorescence-based detection: a review of current and emerging techniques to unveil micro/nanoplastics in environmental samples. *TrAC Trend Anal Chem* 2024;172:117559. DOI
44. Monteleone A, Brandau L, Schary W, Wenzel F. Using autofluorescence for microplastic detection - Heat treatment increases the autofluorescence of microplastics1. *Clin Hemorheol Microcirc* 2020;76:473-93. DOI PubMed
45. Lee CH, Fang JK. Effects of temperature and particle concentration on aggregation of nanoplastics in freshwater and seawater. *Sci Total Environ* 2022;817:152562. DOI PubMed
46. Peiponen KE, Roussey M. Prediction of nanoplastics aggregation in wastewaters. *Water Emerg Contam Nanoplastics* 2023;2:12. DOI
47. Pradel A, Catrouillet C, Gigault J. The environmental fate of nanoplastics: what we know and what we need to know about aggregation. *NanoImpact* 2023;29:100453. DOI PubMed
48. Katsumiti A, Losada-Carrillo MP, Barros M, Cajaraville MP. Polystyrene nanoplastics and microplastics can act as Trojan horse carriers of benzo(a)pyrene to mussel hemocytes in vitro. *Sci Rep* 2021;11:22396. DOI PubMed PMC
49. Jakubowicz I, Enebro J, Yarahmadi N. Challenges in the search for nanoplastics in the environment - a critical review from the polymer science perspective. *Polym Test* 2021;93:106953. DOI
50. Choi S, Lee S, Kim MK, Yu ES, Ryu YS. Challenges and recent analytical advances in micro/nanoplastic detection. *Anal Chem* 2024;96:8846-54. DOI PubMed
51. Huber MJ, Ivleva NP, Booth AM, et al. Physicochemical characterization and quantification of nanoplastics: applicability, limitations and complementarity of batch and fractionation methods. *Anal Bioanal Chem* 2023;415:3007-31. DOI PubMed PMC

52. Okoffo ED, Thomas KV. Quantitative analysis of nanoplastics in environmental and potable waters by pyrolysis-gas chromatography-mass spectrometry. *J Hazard Mater* 2024;464:133013. DOI PubMed
53. Wang X, Li Y, Kroll A, Mitrano DM. Differentiating microplastics from natural particles in aqueous suspensions using flow cytometry with machine learning. *Environ Sci Technol* 2024;58:10240-51. DOI PubMed
54. Chakraborty N, Silswal A, Koner AL. Julolidine-based fluorescent molecular rotor: a versatile tool for sensing and diagnosis. *Sens Diagn* 2024;3:585-98. DOI
55. Comité ZIP of Lake Saint-Pierre Summary sheet on improving water quality in Lake Saint-Pierre. 2018. (in French). Available from: https://belsp.uqtr.ca/id/eprint/1432/1/TCRLSP%204_2018_qualit%C3%A9_eau_Fiche%20synth%C3%A8se_A.pdf. [Last accessed on 9 Nov 2024].
56. He B, Smith M, Egodawatta P, Ayoko GA, Rintoul L, Goonetilleke A. Dispersal and transport of microplastics in river sediments. *Environ Pollut* 2021;279:116884. DOI PubMed
57. Hale RC, Seeley ME, La Guardia MJ, Mai L, Zeng EY. A global perspective on microplastics. *JGR Oceans* 2020;125:e2018JC014719. DOI
58. Eerkes-Medrano D, Thompson RC, Aldridge DC. Microplastics in freshwater systems: a review of the emerging threats, identification of knowledge gaps and prioritisation of research needs. *Water Res* 2015;75:63-82. DOI PubMed
59. COGESAF. Water master plan for the Saint-François River watershed. 2014. (in French). Available from: https://cogesaf.qc.ca/PDE/COGESAF_PDE_2014-2023.pdf. [Last accessed on 9 Nov 2024].
60. MRC. Haute Yamaska Revised water master plan (2017-2021) - For healthy lakes and streams in Haute-Yamaska. 2017. (in French). Available from: https://haute-yamaska.ca/wp-content/uploads/2018/08/PDE-version-finale_3-mai-2018-web.pdf. [Last accessed on 9 Nov 2024].
61. Granby. Industrial business directory. (in French). Available from: https://granby-industriel.com/entreprises/. [Last accessed on 9 Nov 2024].
62. MRC. Maskinongé Revised land use and development plan. Plan 9.9C - Maskinongé: Lake Saint-Pierre shoreline zoning. 2022. (in French). Available from: https://mrcmaskinonge.ca/wp-content/uploads/schema-amenagement-plan-9-9c.pdf?v=1620672520. [Last accessed on 9 Nov 2024].
63. MELCCFP. Loadings of six physicochemical and bacteriological parameters at the mouth of the main tributaries of the St. Lawrence River - 2013-2017. 2024. (in French). Available from: https://www.environnement.gouv.qc.ca/Eau/flrivlac/physicochimie-bacteriologie/rapport-charges-six-parametres-physicochimiques-bacteriologique.pdf. [Last accessed on 9 Nov 2024].
64. Uddin S, Fowler SW, Habibi N, Behbehani M. Micro-nano plastic in the aquatic environment: methodological problems and challenges. *Animals* 2022;12:297. DOI PubMed PMC
65. Lambert S, Wagner M. Formation of microscopic particles during the degradation of different polymers. *Chemosphere* 2016;161:510-7. DOI PubMed

Brirmi *et al. Water Emerg Contam Nanoplastics* 2024;3:23
DOI: 10.20517/wecn.2024.60

Water Emerging Contaminants & Nanoplastics

Review

Open Access

Progress and challenges in heterocyclic polymers for the removal of heavy metals from wastewater: a review

Nour El Houda Brirmi[1], Taha Chabbah[2], Saber Chatti[1], Kamel Alimi[3,4], Hatem Ben Romdhame[5], Regis Mercier[2], Catherine Marestin[2], Nicole Jaffrezic-Renault[6]

[1]Laboratory of Natural Substances (LSN), National Institute of Research and Physicochemical Analysis (INRAP), Biotechnopole of Sidi Thabet, Ariana 2020, Tunisia.
[2]Institute of Polymer Materials IMP-INSA, UMR 5223, University of Lyon, Villeurbanne 69100, France.
[3]Analytical Platform (PA), National Institute of Research and Physicochemical Analysis (INRAP), Biotechnopole of Sidi Thabet, Ariana 2020, Tunisia.
[4]LR18ES19, University of Monastir, Monastir 5019, Tunisia.
[5]LR99ES14, University Tunis El Manar, El Manar 2092, Tunisia.
[6]Institute of Analytical Sciences, UMR 5280, CNRS-UCBL, University of Lyon, Villeurbanne 69100, France.

Correspondence to: Prof. Nicole Jaffrezic-Renault, Institute of Analytical Chemistry, UMR 5280, CNRS-UCBL, University of Lyon, 5 La Doua street, Villeurbanne 69100, France. E-mail: nicole.jaffrezic@univ-lyon1.fr

How to cite this article: Brirmi NEH, Chabbah T, Chatti S, Alimi K, Romdhame HB, Mercier R, Marestin C, Jaffrezic-Renault N. Progress and challenges in heterocyclic polymers for the removal of heavy metals from wastewater: a review. *Water Emerg Contam Nanoplastics* 2024;3:23. https://dx.doi.org/10.20517/wecn.2024.60

Received: 24 Aug 2024 **First Decision:** 18 Oct 2024 **Revised:** 10 Nov 2024 **Accepted:** 12 Nov 2024 **Published:** 27 Nov 2024

Academic Editors: Xianhua Liu, Zhijie Chen **Copy Editor:** Ting-Ting Hu **Production Editor:** Ting-Ting Hu

Abstract

Water contamination by heavy metals has emerged as a global environmental problem. Their toxicity, non-degradability, and persistent nature make them a serious threat to human health, flora, and fauna. Therefore, several techniques have been developed for the removal of these pollutants from wastewater. Recently, linear aromatic polymers have received increasing attention for wastewater treatment due to the presence of various heterocyclic moieties containing electron-donating atoms such as nitrogen, oxygen, or sulfur on their backbone, which can be easily coordinated with metals, resulting in excellent affinity for heavy metals. This review article is specifically devoted to providing an overview of the various linear-architecture heterocyclic polymers that have been synthesized to be used as adsorbent phases for the removal of heavy metals from wastewater over the past fifteen years. The importance of incorporating heterocyclic units as efficient chelating sites for ion binding is highlighted. The adsorption mechanisms of different aromatic polymers are presented; their adsorption isotherms can primarily be modeled with the Langmuir model and their kinetics follow a pseudo-second-order kinetic model. The ways to improve the adsorption capacities of the linear aromatic polymers by increasing their specific surface area are discussed in the perspective paragraph, along with strategies to improve their reusability by choosing the proper acidic washing step.

Keywords: Adsorption, heterocyclic linear polymers, polyimides, polyamides, heavy metals, wastewater

INTRODUCTION

In recent years, water pollution caused by heavy metal contamination has become a global concern[1]. Due to the rapid growth of industrialization and anthropogenic activities including metal plating, mining operations, tannery, batteries, chemical, automobile radiator manufacturing, and other industries, a dramatic increase in heavy metal pollution has occurred in the aquatic environment[2,3]. Extensive use of heavy metals in the above industries results in industrial wastewater rich in heavy metals that mix with lakes, rivers, oceans, and other drinking water sources, leading to water pollution[4,5]. There are various kinds of heavy metals, but the most predominant in industrial effluents are copper (Cu) (1.45 ± 1.22 mg/L), chromium (Cr) (65.81 ± 40.01 mg/L), lead (Pb) (21.28 ± 6.85 mg/L), iron (Fe) (90.52 ± 32.08), zinc (Zn) (62.90 ± 8.63 mg/L), cadmium (Cd) (25.65 ± 6.60 mg/L), mercury (Hg) (6.78 ± 3.36 mg/L), and nickel (Ni) (0.74 ± 0.80 mg/L)[6,7]. These heavy metal compounds are extremely toxic, persistent, non-biodegradable, and highly soluble in aqueous media[8,9]. They, therefore, rapidly penetrate into food chains and accumulate in living organisms, causing severe threats to humans and aquatic ecosystems[10,11]. Although the consumption of limited amounts of certain heavy metals is extremely essential for human beings due to their unique role in the human metabolic system, excessive intake can lead to harmful health effects[12]. For example, nickel (Ni) can be useful at non-hazardous levels; it functions as an enzyme activator and is involved in many important metabolic processes. However, the excessive ingestion of Ni may cause lung and kidney damage, gastrointestinal disorders, dermatitis, and breathlessness[13,14]. Zn is a versatile element that plays critical roles in various cellular processes, making it indispensable for all living organisms[15,16]. At excess levels, Zn can cause serious health problems such as neuronal and respiratory disorders, vomiting, nausea, anemia, and prostate cancer[17]. Although Cu is an essential metal for humans, it is also potentially toxic above supra-optimal levels[18]. Cobalt (Co) serves as a metal component of vitamin B12 (cyanocobalamin), but can be hazardous to the human body following excessive exposure[19]. Heavy metal levels in drinking water are strictly controlled by powerful organizations such as the World Health Organization (WHO) and the US Environmental Protection Agency (USEPA)[20] [Table 1].

Therefore, efforts have been devoted to researching effective technologies for removing toxic metals from wastewater[5]. Numerous water decontamination techniques have been applied, including chemical precipitation[21], ion exchange[22], membrane filtration[23], and electrochemical processes[24,25]. However, these techniques are difficult to remove heavy metals in low concentrations[26]. Up to now, adsorption has been considered the best process for removing damaging metals from water resources, thanks to its higher efficiency, simplicity, ease of accessibility, cost-effectiveness, and environmentally-friendly nature[27,28]. The additional advantage of adsorption is that adsorbents can be easily regenerated using an appropriate desorption process[29-31]. Many adsorbents are employed to trap heavy metals in wastewater. The conventional adsorbents are activated carbons, activated clays, zeolites, and silica gels[32-37]. In recent decades, many efforts have been made to remove heavy metals, using several types of organic linear polymers bearing heterocyclic moieties in their main or lateral chains. Heterocyclic polymer based-adsorbents are one of the best alternatives for heavy metal adsorption due to the presence of heteroatom groups on their chains that can be chelating sites for metals, thus making the resulting polymers effective

Table 1. Acceptable heavy metal levels according to WHO and USEPA

Heavy metals	WHO	USEPA
Cd	3 µg/L	5 µg/L
Hg	6 µg/L	2 µg/L
Cr total	50 µg/L	100 µg/L
Cu	2,000 µg/L	1,300 µg/L
Pb	10 µg/L	15 µg/L
Ni	70 µg/L	100 µg/L
Fe	1,000-3,000 µg/L	300 µg/L
Zn	3,000 µg/L	5,000 µg/L

WHO: World Health Organization; USEPA: US Environmental Protection Agency.

adsorbent phases to remove different metals from wastewater. Moreover, the incorporation of heteroaromatic rings on the polymer chains is the most common approach for increasing the chemical and thermal stability of the resulting polymers and their hydrophilicity, which is a necessary property to extract inorganic pollutants from water media[38,39]. The recent developments in synthesized heterocyclic polymers-based adsorbents for the extraction of various toxic metals from wastewater are reviewed here. This review was based on the querying of the scientific database (Web of Science, Scopus, and Google Scholar) through the main keywords: Adsorption, heterocyclic linear polymers, polyimides (PIs), polyamides, heavy metals, wastewater, and through a selection of the published papers in the last 15 years. To our knowledge, no other review specifically oriented to the use of heterocyclic polymers for the removal of heavy metals from wastewater has been published until now. The published reviews, such as the one by Malik *et al*., have cited all types of adsorbents used for heavy metal removal, but only a few examples of polymers have been mentioned[5].

HEAVY METALS AND THEIR IMPACT ON HUMAN HEALTH

Heavy metals are part of the natural environment, and their traces are essential for human health. However, their excessive use on an industrial scale generates considerable pollution in water systems, due to their discharge through industrial wastewater, posing a severe threat to the ecological environment and public health. Many heavy metals, including Hg, Cd, Pb, Zn, Cr, As, Cu, Fe, Mn, Ag, Co, and Ni, have been identified as the most abundant in water and soil[40]. These metals are highly soluble in water and easily accumulate in plants and the human body through the food cycle[41]. Long-term exposure to heavy metals leads to serious diseases and an increased risk of some cancers[42,43]. Exposure to high levels of Hg affects the central nervous system and can damage the functionality of the brain, kidneys, and liver[44-46]. Cd is known as a carcinogenic metal and can cause kidney dysfunction, cardiovascular diseases, lung cancer, hypertension, and testicular atrophy[47,48]. Pb is another heavy metal with negative effects on human health, such as Alzheimer's disease, kidney damage, mental retardation, reproductive system dysfunction, and cancers[49,50]. Chronic exposure to Zn has been reported to cause fertility disorders, cancer, and cholesterol imbalance[51,52]. Arsenic exposure has been linked with heart disease, bronchitis, dermatitis, mental disorders, and lung and skin cancers[53,54]. Cr exists as a trivalent ion [Cr(III)] and as a hexavalent ion [Cr(IV)], which is the form most harmful to humans, plants, and animals. It can cause lung tumors, digestive tract cancer, mutagenicity and embryotoxicity, hemorrhage, and skin irritation[55,56]. Cu toxicity has been associated with kidney disorders, vomiting, diarrhea, gastroenteritis, liver damage, and even death[57,58]. Excessive silver consumption causes serious toxicological issues, such as changes in blood cells, and liver and kidney damage[59].

ADSORBENTS

Several adsorbents have been used for the adsorption method that can be sorted into three main families: industrial adsorbents, bioadsorbents, and polymeric adsorbents. Industrial adsorbents generally present specific surface areas greater than 100 m^2/g, up to 1,000 m^2/g. The most popular industrial adsorbents are activated carbons, zeolites, silica gels, and activated clays. Approximately 150.000 t/year of activated zeolites, 400.000 t/year of activated carbons, 400.000 t/year of activated clays, and 25.000 t/year of silica gels have been produced[60]. The most popular industrial adsorbents are activated carbons, zeolites, silica gels, and activated clays, all of which demonstrate excellent adsorption capacities for metal removal. Zeolites consist of micropores and aluminosilicate compounds that form a network of SiO_4 and AlO_4^- tetrahedra, linked by common oxygen atoms[61]. These materials present a large specific surface area, high cation exchange capacity, non-emission of toxic compounds, and excellent heat resistance, which make them suitable for the removal of undesired heavy metals[62]. Due to the low ion exchange capacities of natural zeolites, chemical or physical methods are frequently used to enhance their adsorption performance[63]. Álvarez *et al.* compared the adsorption efficiency of activated zeolite with that of natural zeolite for removing Cr (VI)[64]. They reported that adsorption capacity depended on the type of activation and decreased in the following order: activated zeolite with NaOH (82%) > natural zeolite (34%) > activated zeolite with HCl (13%). Mehdi *et al.* also prepared an activated zeolite as an adsorbent material for Ni^{2+} removal from an aqueous solution[65]. The study revealed that the adsorption process was temperature-dependent. The maximum adsorption capacity expected from Langmuir isotherm was found to be 28.79 mg/g at 20 °C. In addition, the values of Freundlich constant n relating to the adsorption intensity were increased from 2.52 to 3.11, with increasing temperature of solution from 20 to 60 °C, indicating better adsorption at a higher temperature.

Adsorption onto activated clay can also constitute an efficient technique for decontaminating water polluted by toxic metals. Khalfa *et al.* studied the removal of several metals Cu^{2+}, Pb^{2+}, Zn^{2+}, and Cd^{2+} using natural and activated clay to assess the effectiveness of these abundant materials in treating wastewater[66]. The authors reported that the heavy metal adsorption properties of natural and activated clay were $Pb^{2+} > Cu^{2+} > Cd^{2+} > Zn^{2+}$. They also noted that activated clay has eliminated greater amounts of metals than pure clay. In fact, after sulfuric acid treatment of clay, the adsorption capacity of Pb^{2+}, Cu^{2+}, Cd^{2+}, and Zn^{2+} was found to increase from 29.11, 22.30, 21.93, and 20.86 mg/g to 50.94, 33.66, 26.74, and 26.44 mg/g, respectively. Dim *et al.* treated the natural clay using hydrochloric acid for Cr (VI) and Fe (III) adsorption from a wastewater medium[67]. The study revealed that the highest removal recorded on activated clay for Cr (VI) and Fe (III) was 18.15 and 39.80 mg/g, respectively. Based on the value of n, activated clay showed a greater affinity to Cr (VI) ($n = 1.76$) than Fe (III) ($n = 0.356$).

Activated carbon is the most commonly used and widely produced adsorbent for wastewater treatment. It has recently received significant interest for the removal of heavy metals due to the large surface area, suitable surface functional groups, and appropriate pore diameter[68]. Numerous researchers have examined the adsorption capacity of activated carbon as a function of changes in preparation factors [Table 2]. It has been shown that the nature of raw material, the preparation conditions (temperature, heating rate, and duration), and the type of activation method (physical or chemical) have a significant influence on the physicochemical properties of activated carbon and therefore on adsorption performance[69-74].

However, the use of activated carbon is limited by its high production cost, poor selectivity, difficult functionalization, and low regeneration. Its regeneration requires high energy (500-900 °C) with a 10%-15% loss of the carbonaceous material and a limited adsorption capacity. The recovery of the adsorbed heavy metals decreases the process cost; nevertheless, eluents should not damage the adsorbent and should be cost-effective and eco-friendly. Diluted HCl solutions were used to recover the heavy metals[75]. Therefore,

Table 2. Adsorption behavior of activated carbon prepared under different conditions

Used raw material	Temperature of preparation (°C)	Time of preparation (min)	Surface area (m^2/g)	Heavy metal	Adsorption capacity (mg/g)	1/n[a]	Ref.
Rape straw	300	120	699.9	Pb (II)	253.2	0.181	[69]
Sugar beet bagasse	450	120	748	Cr (VI)	52.8	0.592	[70]
Rice straw	400	240	4.39	Cd (II)	37.14	-	[71]
Gingko leaf	800	90	310	Cu (II)	59.90	0.3785	[72]
Rice husk	600	10	768.98	Hg^0	0.016	-	[73]
Pine bark	600	24	-	Cd (II)	85.8	0.3364	[74]

[a] 1/n: The correction factor related to the intensity of adsorption (Freundlich isotherm).

the adsorption onto economic sorbents such as bio-based materials has been the subject of numerous studies, due to their availability, inexpensiveness, biodegradability, biocompatibility, and renewability. These parameters have a great impact on environmental practices. There are several agricultural by-products, such as banana peel[76], green tea waste[77], rice husk[78], and treated olive pulp[79], that have been employed as bio-adsorbents to remove heavy metals in water.

Polysaccharides are the most abundant carbohydrate and possess excellent properties for use as bio-based adsorbents for metals[80-82]. These natural polymers, such as cellulose, carrageenan, alginate, starch, cyclodextrin, chitin, and its derivative chitosan, have obtained vast attention as practical and low-cost adsorbents as opposed to activated carbons. Many attractive properties of polysaccharides, such as their specific structure, high reactivity, chemical stability, and excellent selectivity for metals, have made them such smart alternative adsorbents. Moreover, the chemistry of their surface can be modified by grafting functional groups onto chains to acquire new adsorption properties. Yu *et al.* proposed the grafting of amino-terminated hyperbranched polyamide (HP) onto the surface of cellulose-bearing aldehyde groups for efficient removal of metals[83]. This material shows excellent adsorption performance for Cu^{2+} with an adsorption capacity of 138 mg/g. Guleria *et al.* developed a poly-(acrylamide-co-acrylic acid) functionalized cellulose adsorbent to improve its heavy metal adsorption performance[84]. Triazole groups have also been grafted onto cellulose chains by Yin[85] to eliminate Gd(III) and by Mahalakshmi[86] to adsorb efficiently Pb^{2+}, Co^{2+}, Ni^{2+}, and Cd^{2+}. This study revealed that incorporating heteroatoms as chelating units in the cellulose backbone plays a major role in the adsorption process with the coordination reaction between nitrogen atoms in triazole and metals.

Polymeric adsorbents including ion exchange resins, molecularly imprinted polymers (MIPs), and porous organic polymers (POPs) have been utilized extensively in the remediation of metals from water[87-89], but the usage of linear organic polymers as adsorbents is less reported. Over the last few years, heterocyclic polymer-based adsorbents, such as polypyrroles, polyamides, PIs [Table 3], have received increasing attention from researchers because of their potential applications in the uptake of various heavy metals and the fact that the incorporation of different functional groups in polymer matrices enables them to be used as adsorbents capable of efficiently absorbing numerous organic and inorganic pollutants. In addition, these polymers can easily be regenerated under mild conditions.

HETEROCYCLIC LINEAR POLYMER-BASED ADSORBENTS

A review of recent adsorbents used in metal removal from contaminated wastewater is presented here, with a focus on linear functional polymeric adsorbents. These polymers can be produced from different polymerizations of heterocyclic monomers. Furthermore, the impact of different factors such as the pH of

Table 3. Heavy metal ions adsorption using various linear aromatic polymers

Polymer adsorbent	**Repetitive unit**	**Metal ion**	**Adsorption capacity (mg/g) or %**	**Affinity Parameter (1/n)**	**Ref.**
Quinoxaline-based PTIs	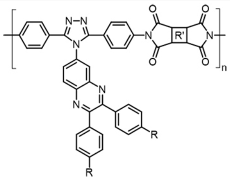	$Cr_2O_7^{2-}$, Pb^{2+}, Hg^{2+}, Cd^{2+}, Zn^{2+}, Co^{2+}, Mn^{2+}, Cr^{3+}	28%, 33%, 40%, 44%, 50%, 60%, 85%, 89% (pH = 8)	-	[90]
Phenoxy quinoline-based PTAIs	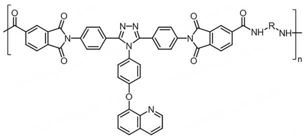	F^-, $Cr_2O_7^{2-}$, Cr^{3+}, Cd^{2+}, Pb^{2+}, Hg^{2+}	9.50, 8.56, 6.60, 6.66, 7.97, 8.76 mmol/g (pH = 3). 5.96, 4.99, 7.99, 7.90, 8.94, 9.2 mmol/g (pH = 10)	-	[91]
Phenoxy quinoline-based PTIs	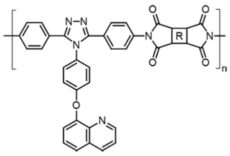	F^-, $Cr_2O_7^{2-}$, Cr^{3+}, Cd^{2+}, Pb^{2+}, Hg^{2+}	8.91, 7.55, 5.0, 4.2, 5.5, 5.71 mmol/g (pH = 3) 5.0, 4.0, 6.1, 7.0, 8.38, 8.8 mmol/g (pH = 10)	-	[92]
Polyimides containing imidazole and xanthene pendants	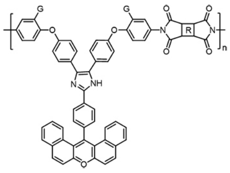	Hg^{2+}, Cr^{3+}, Cd^{2+}, Co^{2+}, Pb^{2+}	37.9, 32.65, 28.6, 21.15, 19.80 mmol/g	-	[93]
Polyimides containing pyridine and xanthene pendants	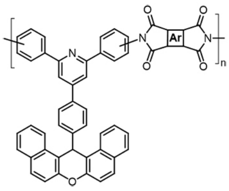	Cr (VI)	91%	-	[94-96]
Porphyrin-based PIs	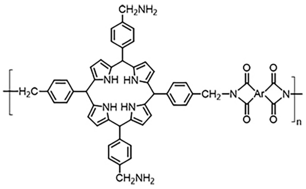	Cd^{2+}, Hg^{2+}	28.59, 27.73 mmol/g	-	[97,98]
Biosourced polyimides	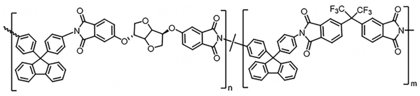	Pb^{2+}, Ni^{2+}, Cd^{2+}, Hg^{2+}	0.726, 0.818, 0.488, 0.084	0.096, 0.064, 0.102, 0.181	[99]
PXIs	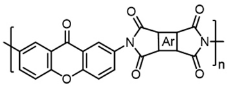	Cd^{2+}, Pb^{2+}, Cu^{2+}, Ni^{2+}, Co^{2+}, Cr (VI)	57.3%, 47%, 45.2%, 42%, 41.1%, 39%	-	[100]
Polyimides bearing1,3,4-oxadiazole and pyridine units	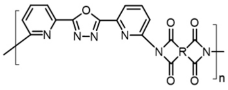	Co^{2+}, Ni^{2+}	110.4, 100.5 mmol/g	-	[101]
Sulfonated copolyimides	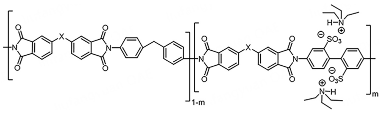	Pb^{2+}	99%	-	[102]
Chlorobenzylidine-based polyamides	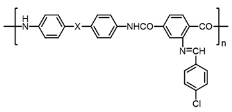	Pb^{2+}, Cr^{3+}	274.6, 255.2 mmol/g	-	[103]

PAMAs	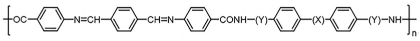	Cu^{2+}, Cd^{2+}, Pb^{2+}	470.7, 462.3, 452.1 mmol/g	0.345, 0.393, 0.413	[104]
Pyridine-containing polyamides	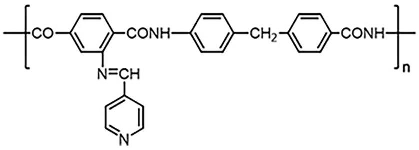	Cu^{2+}, Pb^{2+}	389.9, 403.1 mmol/g	-	[105]
1,2,4-triazole-based polyamides	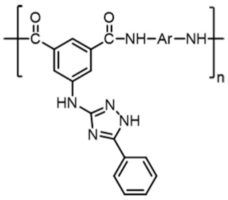	Hg^{2+}	99%	-	[106]
Imidazole-based polyimides	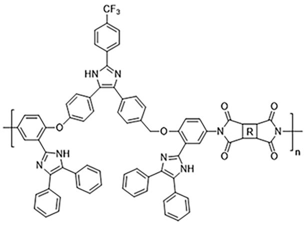	Cr^{3+}, Co^{2+}, Cd^{2+}, Hg^{2+}, Pb^{2+}	38.45, 26.20, 20.5, 18.40, 13.30 mmol/g	-	[107]
Imidazole-based polyamides	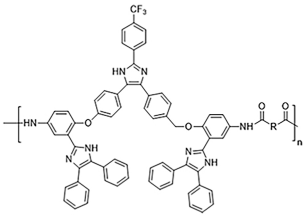		43.90, 30.80, 25.10, 21.60, 19.60 mmol/g		
Sulfonated polyamides	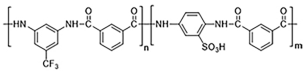	Pb^{2+}, Hg^{2+}	11.87, 5.17 mmol/g	-	[108]
PAS	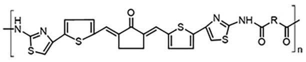	Hg^{2+}	47.95 mmol/g	0.14	[109]
	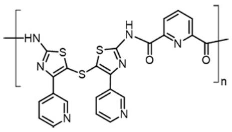	Pb^{2+}	714 mmol/g	0.059	[110-113]
Poly(amide-hydrazide-imide)s	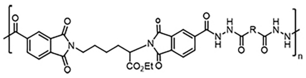	Pb^{2+}, Cd^{2+}, Cu^{2+}, Zn^{2+}, Hg^{2+}	0.99, 075, 0.47, 0.31, 0.037 mmol/g	-	[114]
	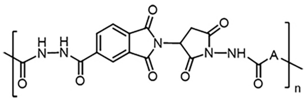	Pb^{2+}, Cd^{2+}, Cu^{2+}, Zn^{2+}, Hg^{2+}	1.70, 0.71, 0.54, 0.29, 0.43 mmol/g		[115]
Poly(2-aminothiazole)	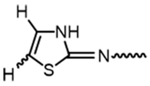	Ag^{+}	336.98	0.233	[116]
1,2,3-triazole based-poly(ionic liquid)	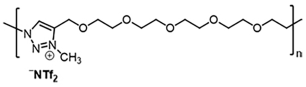	Cr (VI)	13.545	0.289	[117]
1,2,3- triazole containing polystyrene	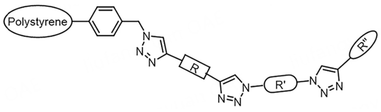	Mg^{2+}, Zn^{2+}	3, 30%	-	[118]

Polyazomethines	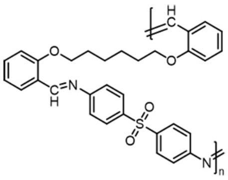	Co^{2+}, Cu^{2+}, Au^{3+}	21.28, 31.25, 35.71	-	[119]
	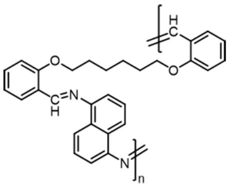	Ni^{2+}, Cu^{2+}, Co^{2+}	25.64, 15.38, 31.25		[120]
Poly(etherphosphine)s	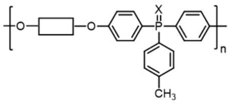	Pb^{2+}, Cd^{2+}, Hg^{2+}, Ni^{2+}	-	-	[121]
Diethylphosphonate-containing poly(arylene ether nitrile)s	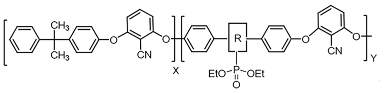	Pb^{2+}, Cd^{2+}, Hg^{2+}, Ni^{2+}	-	-	[122]

PTIs: Poly(triazole-imide)s; PTAIs: poly(triazole-amide-imide)s; PTIs: poly(triazole-imide)s; PIs: polyimides; PXIs: poly(xanthone-imide)s; PAMAs: poly(azomethine amide)s; PAS: polyamide-sulfide.

the solution, the adsorbent dosage, the initial concentration of heavy metals, and the contact time on the adsorption capacity of polymers-based adsorbents are studied.

PIs

PIs are one of the most important aromatic polymer classes, offering excellent thermal stabilities, sufficient chemical resistance, and high mechanical and electrical properties. However, they present very poor hydrophilicity, and therefore, many efforts have been undertaken to incorporate heterocyclic functional groups into their backbone or side groups to generate new PIs with enhanced thermal properties and improved chelating properties.

Among various heterocycle structures, 1,2,4-triazole has been the subject of numerous studies, mainly due to its stability under diverse conditions and the well-established role of triazole units as binding sites for metals. Therefore, insertion of the triazole ring into the main chains produces materials with high hydrophilicity, enabling them to interact with metals. Bazzar *et al.* synthesized a series of PIs bearing 1,2,4-triazole moiety in the principal chain and quinoxaline as a pendant group, according to a two-step procedure that involves the condensation of diamines with dianhydrides followed by the imidization process[90]. The obtained poly(triazole-imide)s were used as adsorbents of Cr^{3+}, Co^{2+}, Zn^{2+}, Pb^{2+}, Cd^{2+}, Hg^{2+}, Cr^{VI}, and Mn^{2+} individually or in mixtures, at a range of pH values (1-14). The removal percentage of metals was increased in the order of $Cr^{3+} > Mn^{2+} > Co^{2+} > Zn^{2+} > Cd^{2+} > Hg^{2+} > Pb^{2+}$, which is contrary to the order of their ion radii. The maximum adsorption of 98% was given to the smallest metal ion (Cr^{3+}), while 35% removal was observed for the largest metal ion (Pb^{2+}) [Figure 1A].

A series of solutions at different pH values ranging from 1.0 to 14.0 was prepared to study the effect of initial solution pH on metal ion removal. As shown in Figure 1B, the percentage of Cr^{3+} removal was low in the pH zone between 1 and 5, and increased with increasing pH, reaching a maximum of 98% at a basic pH of 10. While the adsorption efficiency of $Cr_2O_7^{2-}$ anion was 80% at pH 1.0 and decreased as pH increased [Figure 1C]. This finding can be explained by the fact that in the acidic pH range, nitrogen atoms of the

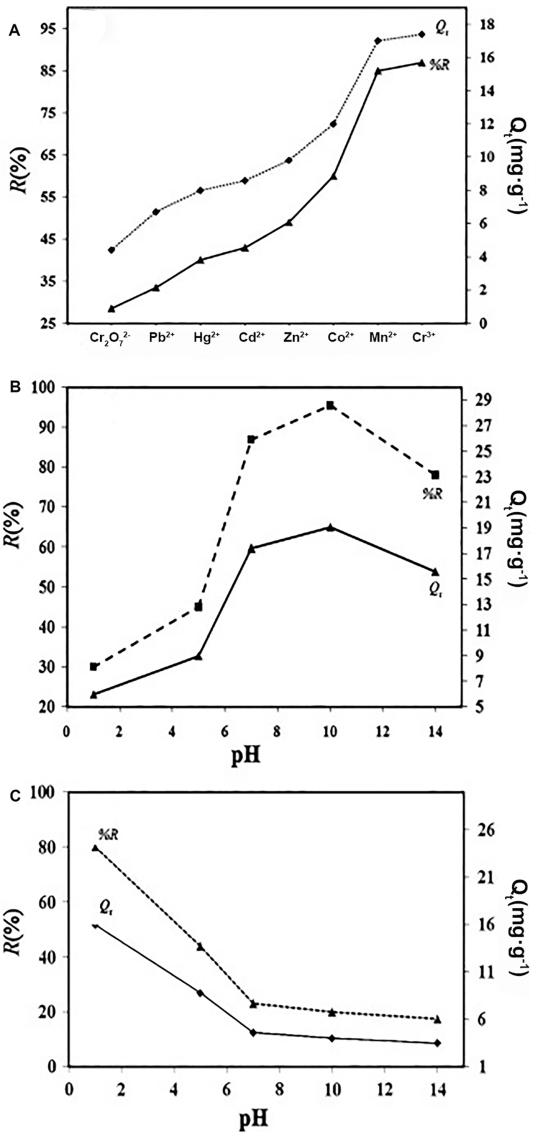

Figure 1. (A) The quantity of adsorbed metals (Qt) and adsorption efficiency (%R) at pH = 8 by poly(triazole-imide); (B) effect of pH variation on the adsorption amount of Cr^{3+} cation; (C) effect of pH variation on the amount of adsorption of $Cr_2O_7^{2-}$ anion. From[90] with permission.

triazole and quinoxaline cycles are protonated, resulting in a repulsive interaction between the positive ions and the positively charged polymer surface that reduces the adsorption of the Cr^{3+} cation. On the other hand, the negative-charged $Cr_2O_7^{2-}$ is electrostatically attracted to positive bonding groups on the PI surface. The solution pH is an important parameter as it can affect the adsorbent's functional group ionization and can determine the attractive or repulsive interaction between the adsorbent and the metals to enhance or reduce adsorption efficiency. Ghaemy *et al.* also reported the influence of pH on metal adsorption ability using triazole-based poly(amide-imide) bearing a pendant phenoxy quinoline unit[91]. The polycondensation reaction was performed between a diimide-diacid and three commercial diamines in the presence of thiamine pyrophosphate as an activator in NMP (N-méthyl-2-pyrrolidone)/Pyridine mixture containing LiCl and $CaCl_2$. At acidic media pH = 3, the highest extraction percentages of 95% and 85% were found for F^- and $Cr_2O_7^{2-}$ anions, respectively, and the adsorption of Cr^{3+} and Cd^{2+} cations showed the lowest value of 66% at this pH. The adsorption study revealed that polymer removal performance depended mainly on the structure and hydrophilic character of the diamine moiety in the polymer backbone. The highest adsorption percentage was observed with the polymer containing two hydrophilic triazole rings in the repeating unit, increasing its hydrophilic character and adsorption capacity. The same authors[92] reported the design of another family of phenoxy quinoline-based poly(triazole-imide)s for the efficient removal of metals. The triazole and phenoxy quinoline groups were identified as effective chelating and host units for heavy metals. According to this research, structural modification of PI by incorporating heterocyclic rings can be an interesting approach to improving their adsorption capacity.

Flexible ether linkages, imidazole rings, and xanthene as a pendant group have been successfully added to PIs by Amininasab *et al.*[93]. The use of Imidazole heterocyclic rings and their derivatives is advantageous due to their high electron affinity and good thermal stability. The prepared PIs showed an enhanced adsorption capacity for adsorbing heavy metals due to the increased presence of –NH and –O groups along the adsorbent's backbone. The adsorption capacities for Hg^{2+}, Cr^{3+}, Cd^{2+}, Co^{2+}, and Pb^{2+} were 37.90, 32.65, 28.60, 21.15, and 19.80 mg/g, respectively. For efficiently removing Cr (VI) from wastewater, PIs were functionalized with pyridine and xanthene groups[94].

The pyridine heterocyclic ring has been reported to improve the processability, solubility, and adsorption performance of PIs due to its aromaticity and polarizability resulting from nitrogen heteroatoms[95], which are recognized as the main adsorption sites and effective binding sites for heavy metals to form metal complexes which are known as the main adsorption site and as an effective binding site of heavy metals to form a metal complex[96]. The adsorption behavior of these polymers at different Cr (VI) concentrations (1, 5, and 10 mg/L) showed that the adsorption capacity (91%) was higher when the concentration of hexavalent Cr in aqueous solution was 5%. Rafiee *et al.*, in turn, described the development of new PIs having porphyrin units utilizing four tetracarboxylic dianhydrides and tetramine through a two-step imidization technique for the adsorption of Cd^{2+} and Hg^{2+}[97]. Porphyrins are regarded as an attractive class of heterocyclic materials with a high capacity to bind with a diverse array of metals and create stable complexes. The nitrogen atoms in the tetrapyrrolic core, due to their electron-donating properties, can serve as ligand sites to adsorb various metals, allowing their efficient extraction[98]. Adsorption tests were performed by dissolving 5 mg of a single PI in 25 mL of individual aqueous metal ion solutions at pH 7 and stirring for 3 days. The results showed that the utilized PI had an excellent adsorption capacity toward $Cd^{2+} > Hg^{2+}$.

Bio-sourced coPIs were used as adsorbent films which is similar to the order

f Pb^{2+}, Ni^{2+}, Cd^{2+}, and Hg^{2+} from aqueous solution[99]. These polymers were synthesized by combining, from 100% to 0%, three monomers (isosorbide-based dianhydride, petroleum-based dianhydride, and cardo diamine). It was noted that adsorption efficiency increased as the proportion of isosorbide moieties in the PI backbones increased. Thus, the homopolyimide, obtained from 100% of biobased dianhydride and diamine, exhibited the highest adsorption efficiency toward metals. This rise is mainly due to the incorporation of isosorbide into the polymer structure, which can generate attractive hydrophilicity and wettability, increasing their tendency to remove contaminants from water. Comparing the adsorption capacity of metals on this polymer, the order was as follows: $Pb^{2+} \approx Ni^{2+} > Cd^{2+} > Hg^{2+}$. Based on the 1/n values, the adsorption of Ni^{2+} (0.064) and Pb^{2+} (0.096) is deemed to be more advantageous, while the adsorption of Hg^{2+} (0.181) is less favorable. In addition, the proposed adsorption mechanism was mainly based on oxygen-heavy metal interactions [Figure 2].

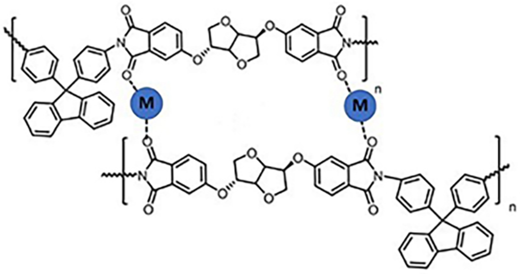

Figure 2. The metal-polyimide complex formed via oxygen-heavy metal interaction. From[99] with permission.

Lakouvaj *et al*. also investigated the extraction of metals including Cr (VI), Co (II), Ni (II), Cu (II), Pb (II), and Cd (II) from aqueous solutions using a new class of poly(xanthone-imide)s (PXIs)[100]. The authors revealed that the adsorption efficiency (%) increased in the order of $Cd^{2+} > Pb^{2+} > Cu^{2+} > Ni^{2+} > Co^{2+} >$ Cr(VI), which is similar to the order of their ionic radii. They stated that the carbonyl functional groups in PI chains act as coordination sites for chelation with metals [Figure 3].

Mansoori *et al*., in a similar research, reported the synthesis of PIs containing 1,3,4-oxadiazole and pyridine moieties for removing Co^{2+} and Ni^{2+}[101]. It has been demonstrated that variations in solution pH impact the coordination capabilities of PIs toward metals. Consequently, the highest metal uptake capacities for Co (II) and Ni (II) were 110.4 and 100.5 mg/g, respectively, at pH 7.0. This finding was reported by Manzoor *et al*. It was shown that variations in solution pH affect the coordination capacities of PIs toward metals[102]. Thus, the highest metal uptake capabilities of Co^{2+} and Ni^{2+} were 110.4 and 100.5 mg/g, respectively, at pH 7.0. Manzoor *et al*. prepared two aromatic sulfonated copolyimides (SPIs), FBM and OBM, using two distinct dianhydrides FDA [4,4'-(hexafluoroisopropylidene)-diphthalic anhydride] and ODPA (4,4'-oxydiphthalic anhydride), along with stoichiometric amounts of sulfonated [BDSA (Benzidine-2,2'-disulfonic acid)·TEA (triethylamine)] and non-sulfonated [MDA (4,4′-methylenedianiline)] diamines as comonomers, aiming for effective Pb adsorption from aqueous solutions[102]. They reported that incorporating anionic sulfonate groups into the PI backbone improved hydrophilicity, resulting in enhanced Pb^{2+} adsorption.

The authors employed quantum chemical simulations using Molecular Operating Environment software (MOE) to identify the structural factors affecting the sorption efficiency of Pb^{2+} onto SPI adsorbents. It was observed that OBM has a hydrophilic surface area larger than that of FBM, as shown in Figure 4. The enhanced hydrophilicity of the OBM copolyimide contributes to its increased adsorption capacity, which is consistent with experimental results, with data showing higher adsorption of Pb ions on the OBM surface (99%) compared to FBM (30%).

Polyamides

Heterocyclic polyamides represent one of the most important classes of high-performance materials, which are ideal candidates for use as heavy metal ion adsorbent from aqueous solutions. Significant attention has been drawn to the synthesis of polyamides containing –CONH–, –CSNH–, –N=CH–, and heterocyclic groups that can serve as metal-complexing ligands. The presence of these chelating functionalities in an aromatic polyamide backbone is expected to enhance metal ion adsorption capacity and stability for reuse.

Ravikumar *et al.* synthesized aromatic polyamides and polythioamides incorporating pendant chlorobenzylidine rings via direct polycondensation of a dicarboxylic acid with diamines and thioamines, respectively, for the removal of toxic metals from water[103].

Figure 3. Chelation of metals with PXIs[100]. PXIs: Poly(xanthone-imide)s.

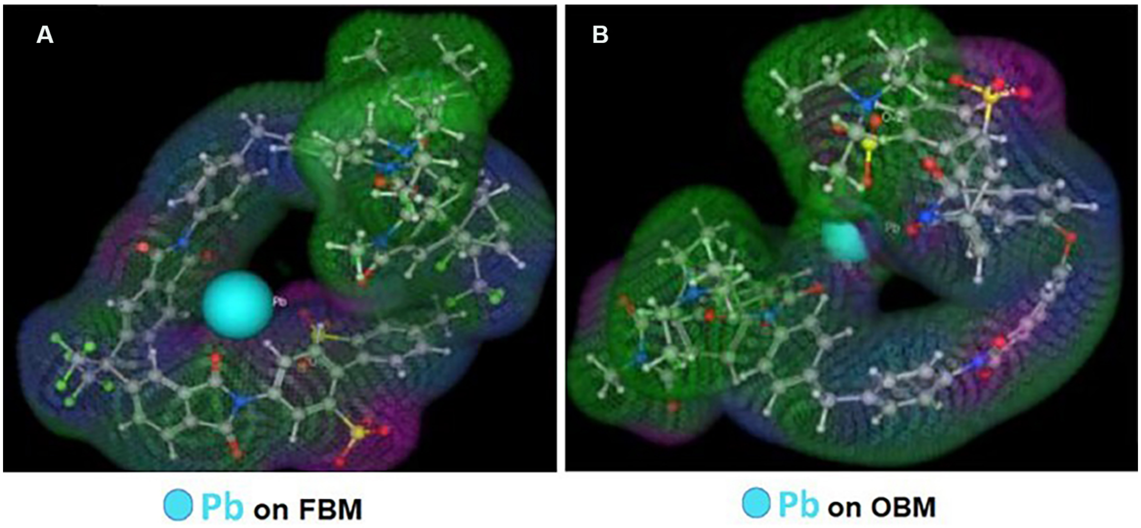

Figure 4. Hydrophobic regions (depicted as green dots) and hydrophilic regions (represented by blue and purple areas) of two sulfonated aromatic copolyimides, the sulfonated FBM (A) and non-sulfonated OBM (B) complex with Pb. From[102] with permission.

They reported that the amide, carbonyl, and azomethine groups in the polymer backbone enhanced the adsorption capacity of Pb^{2+} and Cr^{3+} from water. The highest adsorption capacity for Pb^{2+}, 274.6 mg/g, was achieved at pH 10, while the maximum adsorption for Cr^{3+}, 255.2 mg/g, occurred at pH 6.

Murugesan *et al.*, on the other hand, examined the elimination of Pb^{+2}, Cu^{+2}, and Cd^{+2}, using aromatic poly(azomethine amide)s[104]. Their results showed that the removal of metals varied with pH, peaking at pH 6. They also reported an increase in adsorption efficiency as the contact time increased and equilibrium was observed in 60 min. The polyamide exhibited maximum adsorption capacities of 470.7 mg/g for Cu^{2+}, 462.3 mg/g for Cd^{2+}, and 452.1 mg/g for Pb^{2+}. In an additional study[105], they investigated the adsorption efficiency of newly developed polyamides incorporating pyridyl and azomethine pendant groups for the removal of Cu (II) Pb (II) metals. The highest adsorption capacities of Cu (II) and Pb (II) ions, determined by Langmuir models, were determined to be 389.9 and 403.1 mg/g, respectively. Gómez-Valdemoro *et al.* fabricated aromatic polyamides bearing pendant 1,2,4-triazole groups to extract Hg cations from aqueous media[106]. The study demonstrated that the polar triazole unit significantly enhanced the hydrophilicity of polyamides, rendering these polymers effective solid phases for the high extraction (99%) of Hg^{2+} from aquatic environments. Soleimani *et al.* have also highlighted the importance of incorporating a heterocyclic imidazole ring into polyamide backbones as a hydrophilic chelating agent for heavy metals[107]. They reported high percentage removal of 87.80%, 61.60%, 50.20%, 43.09%, and 39.30% for Cr^{3+}, Co^{2+}, Cd^{2+}, Hg^{2+}, and Pb^{2+}, respectively. Santiago *et al.* prepared a series of sulfonated aromatic polyamides and evaluated their uptake performance to eliminate Pb and Hg ions[108]. It was found that the polyamides exhibited higher adsorption capacities for Pb^{2+} compared to Hg^{2+}.

Albukhari *et al.* synthesized a series of four heteroaromatic sulfur-containing polyamides by polycondensation of diamine with diacid chlorides for the selective removal of heavy metals from wastewater[109]. The obtained polymers demonstrated a remarkably high selectivity for Hg (II) ions, with the maximum adsorption capacity reaching 47.95 mg/g by the Langmuir model. The effect of pH (ranging from

1 to 9) on the adsorption of Hg^{+2} was also studied. It has been reported that the highest percentage of Hg^{+2} extraction, 98.75%, was achieved at pH 1. This increase was explained by the electrostatic attraction forces that can occur between protonated sites formed at pH 1, such as secondary amine groups and carbonyl groups in the polymer backbones, with the negatively charged species including $HgCl_4^{-2}$, neutral $HgCl_2$, and another chloroanionic complex $HgCl_3^{-1}$. In another study, Rezania *et al*. prepared a polyamide-sulfide (PAS) incorporating pyridine and thiazole heterocycles for Pb removal from water[110]. They observed that the synthesized polymer is an excellent adsorbent of Pb(II) ions, demonstrating a significant adsorption capacity of around 714 mg/g.

Replacing polyamides with copolyamides such as poly(amide-imide)s (PAIs) may be beneficial for increasing the polarity of the polymer chain to extract heavy metals with more affinity. Due to the presence of both amide and imide units in their polymer repeating units, PAIs exhibit properties that are different from those of polyamides and PIs. As a result, this class of polymers provides a good combination of excellent thermal stability, processability, and high uptake of heavy metals[111-113].

The adsorption of PAIs was enhanced by incorporating hydrazide functional groups in their backbone. This improvement is attributed to the polar characteristics of the hydrazide group (–CO–NH–NH–CO–), which readily engages with metals to create complexes[114]. These heterocyclic polymers were prepared by polycondensation of a diacid monomer containing imidic rings with various dihydrazides for the extraction of heavy metal cations such as Pb, Cd, Cu, and Zn. Among heavy metals, Pb demonstrated the highest adsorption capacity at 0.99 mmol/g, while Cd ions were adsorbed with a capacity of 0.75 mmol/g. A comparative study was carried out using another family of poly(amide-hydrazide-imide) obtained from the reaction of an acid chloride-anhydride monomer with dihydrazides, which resulted in more efficient adsorption of Pb^{2+} (1.70 mmol/g)[115].

Other heterocyclic polymers

Powerful adsorption of silver ions was obtained utilizing a poly(2-aminothiazole)P-2AT prepared via the polymerization of 2-aminothiazole with benzoyl peroxide (BPO) as an initiator in 1,4-dioxane at 80 °C for 24 h[116]. The adsorption tests were performed at different pH levels (3-6), contact times (15-90 min), and initial Ag^+ concentrations (100-1,200 mg/L) to study the effect of these parameters on adsorption capacity. It revealed that adsorption efficiency increased with the increasing initial concentrations and the contact time. The maximum adsorption capacity of Ag^+ on P-2AT was found to be 336.98 mg/g for 1,200 mg/L Ag (I) solution at pH 5 after 90 min of contact. An attractive heavy metal adsorbent based on a poly(ionic liquid) bearing 1,2,3-triazole moiety was developed by Puguan and Kim for Cr (VI) extraction[117]. It was prepared by Cu-catalyzed cycloaddition CuAAC of α-azide-ω-alkyne monomer in the presence of CuIP $(OEt)_3$ followed by quaternization and anion exchange. The Langmuir isotherm model described the adsorption of Cr (VI) on the poly(ionic liquid) as monolayer adsorption with an adsorption capacity of 13.545 mg/g at room temperature and pH 2. The adsorption was the result of van der Waals and electrostatic forces between the amines in the triazole ring and the dissociated Cr (VI) in water. The 1,2,3-triazole unit has also been grafted into polystyrene chains [Figure 5] to be tested as sorbents for the removal of Mg and Zn present in wastewater[118]. These polymers showed a low selectivity for Mg, with an extraction percentage of below 3%, while for Zn, the removal percentage was around 30%.

Qureshi *et al*. synthesized polyazomethine through a polycondensation reaction of dialdehyde and diamine for the adsorption of Co^{2+}, Cu^{2+}, and Au^{3+} from wastewater[119]. The sorption process followed the Langmuir monolayer adsorption model, and the adsorption capacities for Co^{2+}, Cu^{2+}, and Au^{3+} were 21.28, 31.25, and 35.71 mg/g, respectively. The results indicated a chemisorption/ion-exchange nature of adsorption. The

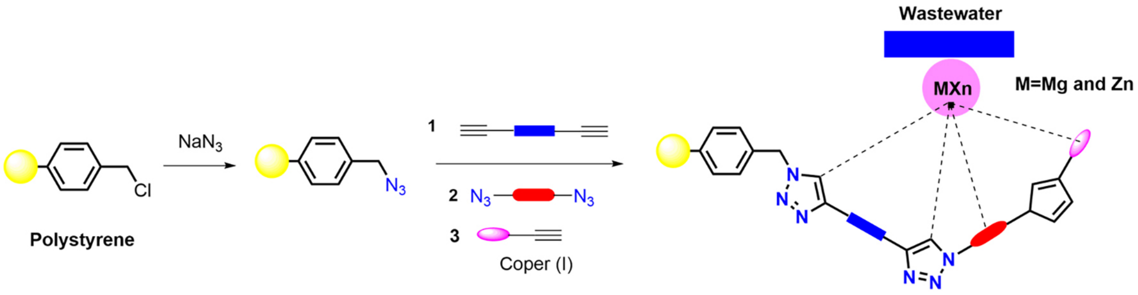

Figure 5. Synthetic Scheme of 1,2,3-Triazoles-Based Polystyrene and its application in the Extraction of Zn and Mg from Wastewater. From[118] with permission.

authors varied several parameters, including initial ion concentration (10-50 mg/L), pH levels (2-8), the quantity of polymer adsorbent (10-50 mg), and the contact time (10-180 min), to obtain maximum adsorption capacity from the optimum adsorbent. The ideal conditions obtained for the highest adsorption capacity of Co^{2+}, Cu^{2+}, and Au^{3+} are at a pH value of 8 for Co^{2+} and Cu^{2+} and 2 for Au^{3+}. The corresponding adsorption capacities were 4.32, 51.8, and 41.32 mg/g, respectively.

Likewise, a polyazomethine derived from another diamine[120] was also prepared and used for the efficient extraction of Ni^{2+}, Cu^{2+}, and Co^{2+}. This material removed up to 77% of Ni^{2+}, 98% of Cu^{2+}, and 72% of Co^{2+} from wastewater. Chabbah *et al.* developed phosphorous polymers for the detection of Pb^{2+}, Cd^{2+}, Hg^{2+}, and Ni^{2+} heavy metals[121,122]. Their results showed that the synthesized polymers display a performing ability for the decontamination of water.

ADSORPTION MECHANISMS

The Langmuir adsorption model assumes that a polymer has a fixed number of binding sites. All the binding sites show the same affinity for the adsorbent. Therefore, each site adsorbs only one molecule and forms a single monolayer.

The linear form of the Langmuir model can be written as:

$$1/q_e = 1/bq_m\,(1/C_e) + 1/q_m \qquad \text{(Eq. 1)}$$

Where q_e (mg/g) is the amount of heavy metals adsorbed onto the polymer at equilibrium, Ce (mg/L) is the equilibrium concentration, q_m (mg/g) denotes the maximum adsorption capacity, and b (L/mg) is the Langmuir constant related to free energy. The Langmuir constants q_m and b were calculated from the slope and the intercept of the Langmuir plot of $1/q_e$ *vs.* $1/C_e$.

The linear form of the Freundlich model is given as:

$$\ln q_e = 1/n \ln C_e + \ln k_F \qquad \text{(Eq. 2)}$$

Where q_e (mg/g) represents the amount of heavy metals adsorbed per unit mass of adsorbent, C_e (mg/L) is the equilibrium concentration of heavy metals, and n and k_F are Freundlich constants. These constants can be determined from the linear plot of $\ln q_e$ *vs.* $\ln C_e$.

The Redlich-Peterson isotherm combines Langmuir and Freundlich models. At higher concentrations, it approximates the Freundlich model, while at lower concentrations, it aligns with the Langmuir equation. The equation is given as:

$q_e = (K_R C_e)/(1 + a_R C_e^b)$ (Eq. 3)

where K_R is the Redlich-Peterson isotherm constant (L/g), α_R is the Redlich-Peterson isotherm constant (L/mg), and β is the exponent that lies between 0 and 1. The constant β can characterize the isotherm as: if $\beta = 1$, the Langmuir will be the preferable isotherm, while if $\beta = 0$, the Freundlich isotherm will be the preferable isotherm.

The Temkin isotherm model contains a factor that explicitly takes into account the adsorbing species - adsorbate interactions. This model assumes the following conditions: (1) the heat of adsorption of all the molecules in the layer decreases linearly with the coverage due to adsorbent-adsorbate interactions; and (2) the adsorption is characterized by a uniform distribution of binding energies, up to some maximum binding energy. The derivation of the Temkin isotherm assumes that the fall in the heat of sorption is linear rather than logarithmic, as implied by the Freundlich equation. The Temkin isotherm has commonly been applied in the following form:

$q_e = B\ln(AC_e)$ (Eq. 4)

where $B = RT/b$ and A is Temkin constant.

The kinetics of heavy metal adsorption onto the different fabricated polymers were analyzed at various time intervals using the pseudo-first-order and pseudo-second-order kinetic models. The pseudo-first-order kinetic model is expressed as:

$\ln(q_e - q_t) = -k_1 t + \ln q_e$ (Eq. 5)

where q_t and q_e (mg/g) are the amount of heavy metals adsorbed at time t (min) and equilibrium time, respectively. The parameter k_1 (min^{-1}) denotes the rate constant of the pseudo-first-order kinetic model. The rate constant of the pseudo-first-order kinetic model and q_e values are derived from the slope and the intercept of the linear plots of $\ln(q_e - q_t)$ *vs.* time (min), respectively. The pseudo-first-order kinetic model assumes that one heavy metal ion is sorbed onto one sorption site on the surface of a polymer.

The pseudo-second-order kinetic model can be written as:

$1/q_t = t/q_e + 1/k_2 q_e^2$ (Eq. 6)

where k_2 (g/mg/min) is the rate constant of the pseudo-second-order kinetic model. This model assumes that one heavy metal ion is sorbed onto two sorption sites on the surface of an adsorbent. The rate constant of the pseudo-second-order kinetic model and q_e are estimated from the intercept and the slope of the linear plots of t/q_t *vs.* time (min), respectively.

The adsorption isotherms were best fitted with Langmuir model for the adsorption of heavy metals on biosourced PI[99], polyamide sulfide[109], 1,2,3-triazole based-poly(ionic liquid)[117], and polyazomethines[119].

Redlich-Peterson model allowed the best fitting of the adsorption isotherms of heavy metals on poly(azomethine amide)s[104]. This point suggests that the polymer surface presents a homogeneous surface with specific adsorption sites.

The pseudo-second-order kinetic model allowed the best fitting of the adsorption of heavy metals on poly(azomethine amide)s[104], 1,2,3-triazole based-poly(ionic liquid)[117], and polyazomethines[119], suggesting that the rate-limiting step of heavy metal adsorption is mainly chemisorption process.

PERSPECTIVES AND CHALLENGES

The main factors characterizing the adsorbent qualities are its affinity, represented by the factor 1/n (with a lower value indicating higher affinity), and its adsorption capacity. Some quantitative data for conventional adsorbents can be found in the literature [Table 4].

For zeolites[65], 1/n is equal to 0.39 and the adsorption capacity is 28.79 mg/g for Ni (II) ions at 20 °C. For activated clays[71], 1/n is equal to 0.56 for Cr (VI) and 2.80 for Fe (III), and adsorption capacities are 18.15 mg/g and 39.80 mg/g, respectively. For activated carbon, depending on the raw materials [Table 2], 1/n varies from 0.181 for Pb (II) to 0.592 for Cr (VI) and adsorption capacities vary from 37.14 mg/g for Cd (II) to 253.2 mg/g for Pb (II). The characteristics of heterocyclic linear polymers are compared to those of the conventional adsorbents to select the best of them. Biosourced PIs[99] present a value of 1/n equal to 0.064 for Ni (II) and PASs[110] has a value of 0.059 for Pb (II). Such low values were not obtained with conventional adsorbents. Moreover, certain heterocyclic linear polymers demonstrated selectivity for specific heavy metal ions; for example, poly(etherphosphine)[121] and diethylphosphonate-containing poly(arylene ether nitrile)[122] were selective for Pb(II). This selectivity is particularly relevant for the recovery of pure heavy metals in diluted acidic media or complexing media. Concerning the adsorption capacities of heterocyclic linear polymers for Pb (II), they could vary from less than 1 mg/g[121] to 403.1 mg/g[105] and 452.1 mg/g[104] with respectively a pyridine-containing polyamide and a poly(azomethine amide)s. To enhance the adsorption capacities of linear polymeric phases, inorganic compounds such as silica gel, graphene, graphene oxide (GO), clay, and monoliths can be coated with them. The resulting materials significantly present a larger specific surface area and then a higher adsorption capacity; an example shows that the capacity of adsorption of PI for Cu^{2+} ion increased by a factor of 77 after PI/silica coprecipitation[123]. Another way to increase the specific surface area is the electrospinning of the heterocyclic linear polymers. Amino-rich functionalized PIs-polyethyleneimine (PEI) fibers with a diameter of 13 μm and a surface roughness of Rq = 17.10 nm were successfully synthesized. These fibers present numerous amine groups at the surface and were able to adsorb Cr (VI) ions with a capacity of adsorption of 50 mg/g[124]. Electrospun Fe_3O_4/MWCNTs/polyamide 6 nanofibers with a diameter of 101 nm enabled the adsorption of Pb (II) ion through the OH groups at their surface; an adsorption capacity of 49.3 mg/g was obtained[125]. Electrospun PA6/CaO nanofibers presented an adsorption capacity of 39 mg/g for Pb (II) ions and 33 mg/g for Cr (VI) ions[126].

Adsorbent regeneration is important for repeated use in different applications, as well as for reducing the quantity of adsorbent material, which in turn lowers the cost of the adsorbent. Studies have shown that adsorbents based on aromatic linear polymers can be reused for numerous cycles without significant loss of adsorption capacity.

Pyridine-based polyamide designed for removing Pb(II) and Cu(II) ions was successfully regenerated with various acids, including H_2SO_4, HCl, and CH_3COOH, and used for seven adsorption-desorption cycles [Figure 6][105]. Among these, aq. H_2SO_4 and aq. HCl proved more effective than aq. CH_3COOH for the

Table 4. Comparison of the characteristics of heterocyclic polymers to other popular heavy metal absorbents

Adsorbent	Heavy metal	Adsorption capacity mg/g	Affinity (1/n)	Ref.
Zeolite	Ni	28.79	0.39	[65]
Activated clay	Cr	18.15	0.56	[71]
	Fe	39.80	2.80	[71]
Activated carbon	Pb	253.2	0.181	[69]
	Cd	85.8	0.3364	[74]
Biosourced polyimides	Ni		0.064	[99]
Polyamide-sulfides	Pb		0.059	[110]
Poly(etherphosphine)	Pb	1		[121]
Poly(azomethine amide)	Pb	403.1		[105]
	Pb	452.1		[104]
Functionalized amino-rich PI-PEI fibers	Cr	50		[124]
Electrospun Fe_3O_4/MWCNTs/polyamide 6 nanofibers	Pb	49.3		[125]
Electrospun PA6/CaO nanofibers	Pb	39		[126]
	Cr	33		

PI: Polyimide; PEI: polyethyleneimine.

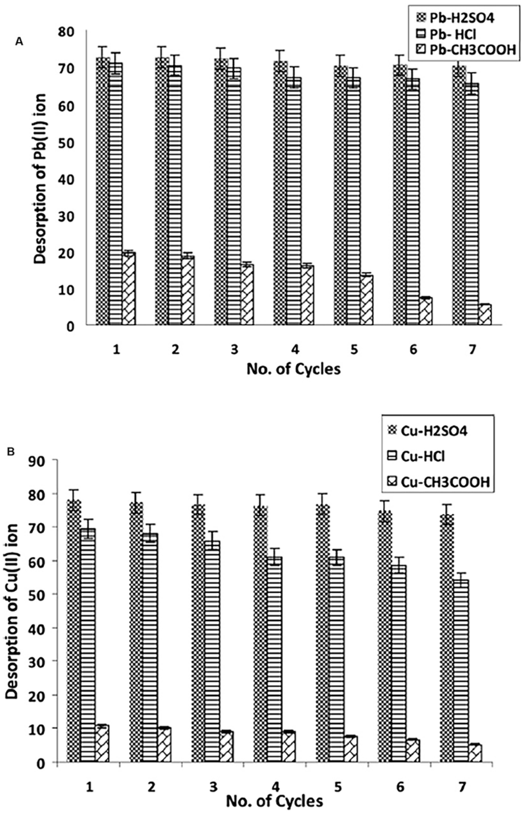

Figure 6. Adsorption-desorption of Pb^{2+} (A) and Cu^{2+} (B) onto adsorbent polyamide. From[105] with permission.

desorption of Cu (II) and Pb (II) ions. Additionally, the adsorbent demonstrated sustained efficiency in removing Cu (II) and Pb (II) ions, without considerable loss of efficiency even after seven adsorption-desorption cycles.

Similarly, polyamide and polythioamide bearing chlorobenzylidine moieties retain their original removal capacity for removing Cr^{2+}, Pb^{2+}, Cd^{3+}, and Cu^{2+} after four consecutive adsorption-desorption cycles[103]. Adsorbent regeneration was carried out using an aqueous solution of HCl (2N). The reusability results, presented in Table 5, revealed that the capacities of both polyamide P3 and polythioamide P5 remained practically unchanged for all metals, even after four cycles of adsorption-desorption.

Bıyıkoğlu *et al.* also examined the reusability of poly(2-aminothiazole) P-2AT after four adsorption-desorption cycles[116]. To remove the previously adsorbed Ag^+ ion, the P-2AT was treated with 0.1 M HNO_3 solution. As shown in Figure 7, the Ag^+ adsorption capacity was almost the same on the second use and decreased on the fourth cycle to 23.84 mg/g. This suggests that P-2AT can be used repeatedly to remove Ag (I) ions.

Table 5. Metal ion adsorption capacity of polyamide P3 and polythioamide P5 after four cycles of adsorption-desorption[103]

Cycle no.	Adsorption capacity (mg/g) of polyamide P3			
	Pb(II)	Cu(II)	Cr(II)	Cd(III)
1	108.7	102.5	91.8	60.1
2	106.4	102.4	71.1	58.2
3	104.9	100.9	65.7	53.8
4	99.7	98.1	64.7	49.6
	Adsorption capacity (mg/g) of polythioamide P5			
1	109.4	108.5	82.6	60.1
2	107.5	100.9	71.8	56.5
3	105.9	99.5	71.1	44.6
4	103.8	96.7	65.7	37.8

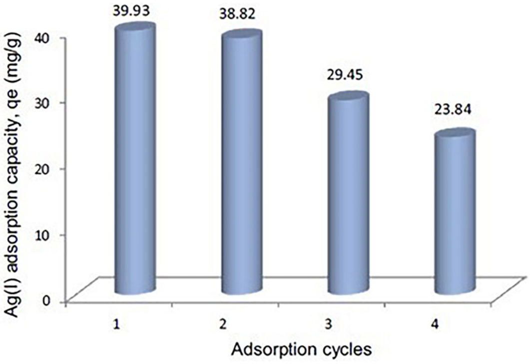

Figure 7. Adsorption capacity of Ag (I) onto poly(2-aminothiazole) after four adsorption cycles. From[116] with permission.

After selecting the best formula and configuration for the heterocyclic polymers, the further challenge is achieving large-scale production at a reduced cost.

CONCLUSION

This study aims to present an overview of heterocyclic polymer-based adsorbents for the extraction of heavy metals to reduce water pollution. The various parameters affecting the adsorption capacity of heavy metals are studied. The removal of heavy metals from wastewater through adsorption is a cost-effective alternative to conventional costly methods, making it an optimal choice for wastewater treatment. Heterocyclic linear polymers are effective adsorbents of toxic metals due to their chemical and physical stability, their specific affinity, their adsorption capacity that can be improved, and their easy regeneration. The heterocyclic functional groups contained in the polymer backbone are responsible for the increased adsorption efficiency and recyclability of heavy metal ions in aqueous media. These groups act as attractive chelating sites and tend to eliminate ions through electrostatic interactions. The regeneration of the adsorbent polymers showed that the adsorption-desorption process is reversible, indicating that aromatic linear polymers have a strong potential for reuse, as the active sites are physically bonded to the polymer backbone. The successful use of heterocyclic polymer-based materials also opens up new possibilities for eliminating hazardous organic pollution from wastewater.

DECLARATIONS

Authors' contributions

Writing - original draft preparation: Brirmi NEH, Chabbah T, Chatti S, Marestin C
Conceptualization: Alimi K, Ben Romdhame H, Mercier R
Writing - review and editing: Jaffrezic-Renault N

Availability of data and materials

Not applicable.

Financial support and sponsorship

The authors would like to acknowledge the financial support of the POLYAM project, funded by the High Ministry of Education and Research in Tunisia. The CNRS is acknowledged for its support of the IRP NARES. The research was funded by the European Union Horizon 2020 (TUNTWIN) research and innovation program under grant agreement (No. 952306). The authors acknowledge the financial support from the EU H2020 WIDESPREAD Program entitled Bionanosens grant agreement (No. 951887).

Conflicts of interest

Jaffrezic-Renault N is an Editorial Board member of the journal *Water Emerging Contaminants & Nanoplastics*, while the other authors declared that there are no conflicts of interest.

Ethical approval and consent to participate

Not applicable.

Consent for publication

Not applicable.

Copyright

REFERENCES

1. Beidokhti MZ, Naeeni ST, Abdi Ghahroudi MS. Biosorption of nickel (II) from aqueous solutions onto pistachio hull waste as a low-cost biosorbent. *Civ Eng J* 2019;5:447-57. DOI
2. Liu J, Liu YJ, Liu Y, Liu Z, Zhang AN. Quantitative contributions of the major sources of heavy metals in soils to ecosystem and human health risks: a case study of Yulin, China. *Ecotoxicol Environ Saf* 2018;164:261-9. DOI PubMed
3. Shen F, Mao L, Sun R, Du J, Tan Z, Ding M. Contamination evaluation and source identification of heavy metals in the sediments from the Lishui River watershed, Southern China. *Int J Environ Res Public Health* 2019;16:336. DOI PubMed PMC
4. Sharma R, Saini KC, Rajput S, et al. Environmental friendly technologies for remediation of toxic heavy metals: pragmatic approaches for environmental management. In: Aravind J, Kamaraj M, Karthikeyan S, editors. Strategies and tools for pollutant mitigation. Cham: Springer International Publishing; 2022. pp. 199-223. DOI
5. Malik L A, Bashir A, Qureashi A, Pandith A H. Detection and removal of heavy metal ions: a review. *Environ Chem Lett* 2019;17:1495-521. DOI
6. Ishaq S, Jabeen G, Arshad M, et al. Heavy metal toxicity arising from the industrial effluents repercussions on oxidative stress, liver enzymes and antioxidant activity in brain homogenates of Oreochromis niloticus. *Sci Rep* 2023;13:19936. DOI PubMed PMC
7. Gutwiński P, Cema G, Ziembińska-buczyńska A, Wyszyńska K, Surmacz-górska J. Long-term effect of heavy metals Cr(III), Zn(II), Cd(II), Cu(II), Ni(II), Pb(II) on the anammox process performance. *J Water Process Eng* 2021;39:101668. DOI
8. Özdemir S, Serkan Yalçın M, Kılınç E. Preconcentrations of Ni(II) and Pb(II) from water and food samples by solid-phase extraction using *Pleurotus* ostreatus immobilized iron oxide nanoparticles. *Food Chem* 2021;336:127675. DOI PubMed
9. Ali S, Hussain S, Khan R, et al. Renal toxicity of heavy metals (cadmium and mercury) and their amelioration with ascorbic acid in rabbits. *Environ Sci Pollut Res Int* 2019;26:3909-20. DOI PubMed
10. Byber K, Lison D, Verougstraete V, Dressel H, Hotz P. Cadmium or cadmium compounds and chronic kidney disease in workers and the general population: a systematic review. *Crit Rev Toxicol* 2016;46:191-240. DOI PubMed
11. Liu S, Shi J, Wang J, Dai Y, Li H, Li J, Zhang P. Interactions between microplastics and heavy metals in aquatic environments: a review. *Front Microbiol* 2021;12:652520. DOI PubMed PMC
12. Duan C, Ma T, Wang J, Zhou Y. Removal of heavy metals from aqueous solution using carbon-based adsorbents: a review. *J Water Process Eng* 2020;37:101339. DOI
13. Genchi G, Carocci A, Lauria G, Sinicropi MS, Catalano A. Nickel: human health and environmental toxicology. *Int J Environ Res Public Health* 2020;17:679. DOI PubMed PMC
14. Mokhtari N, Dinari M, Rahmanian O. Novel porous organic triazine-based polyimide with high nitrogen levels for highly efficient removal of Ni(II) from aqueous solution. *Polym Int* 2019;68:1178-85. DOI
15. Patil R, Sontakke T, Biradar A, Nalage D. Zinc: an essential trace element for human health and beyond. *Food Health* 2023;5:13. DOI
16. Kambe T, Taylor KM, Fu D. Zinc transporters and their functional integration in mammalian cells. *J Biol Chem* 2021;296:100320. DOI PubMed PMC
17. Taiwo AM, Oyeleye OF, Majekodunmi BJ, et al. Evaluating the health risk of metals (Zn, Cr, Cd, Ni, Pb) in staple foods from Lagos and Ogun States, Southwestern Nigeria. *Environ Monit Assess* 2019;191:167. DOI PubMed
18. Shabbir Z, Sardar A, Shabbir A, et al. Copper uptake, essentiality, toxicity, detoxification and risk assessment in soil-plant environment. *Chemosphere* 2020;259:127436. DOI PubMed
19. Leyssens L, Vinck B, Van Der Straeten C, Wuyts F, Maes L. Cobalt toxicity in humans-a review of the potential sources and systemic health effects. *Toxicology* 2017;387:43-56. DOI PubMed
20. Fei Y, Hu YH. Design, synthesis, and performance of adsorbents for heavy metal removal from wastewater: a review. *J Mater Chem A* 2022;10:1047-85. DOI
21. Esalah J, Husein MM. Removal of heavy metals from aqueous solutions by precipitation-filtration using novel organo-phosphorus ligands. *Separation Sci Technol* 2008;43:3461-75. DOI
22. Dabrowski A, Hubicki Z, Podkościelny P, Robens E. Selective removal of the heavy metal ions from waters and industrial wastewaters by ion-exchange method. *Chemosphere* 2004;56:91-106. DOI PubMed
23. Oatley-radcliffe DL, Walters M, Ainscough TJ, Williams PM, Mohammad AW, Hilal N. Nanofiltration membranes and processes: a review of research trends over the past decade. *J Water Process Eng* 2017;19:164-71. DOI

24. Tran T, Leu H, Chiu K, Lin C. Electrochemical treatment of heavy metal-containing wastewater with the removal of COD and heavy metal ions: electrochemical treatment of heavy metal containing wastewater. *J Chin Chem Soc* 2017;64:493-502. DOI
25. Aarfane A, Bensemlali M, Elmelouky A, et al. Electrocoagulation efficiency probed using electrochemical impedance spectroscopy. *Chin J Chem Eng* 2024;75:266-73. DOI
26. Elgarahy A, Elwakeel K, Mohammad S, Elshoubaky G. A critical review of biosorption of dyes, heavy metals and metalloids from wastewater as an efficient and green process. *Clean Eng Technol* 2021;4:100209. DOI
27. Masoumi A, Ghaemy M. Adsorption of heavy metal ions and azo dyes by crosslinked nanochelating resins based on poly(methylmethacrylate-co-maleic anhydride). *Express Polym Lett* 2014;8:187-96. DOI
28. Chai WS, Cheun JY, Kumar PS, et al. A review on conventional and novel materials towards heavy metal adsorption in wastewater treatment application. *J Clean Prod* 2021;296:126589. DOI
29. Samiey B, Cheng CH, Wu J. Organic-inorganic hybrid polymers as adsorbents for removal of heavy metal ions from solutions: a review. *Materials* 2014;7:673-726. DOI PubMed PMC
30. Geng Z, Lin Y, Yu X, et al. Highly efficient dye adsorption and removal: a functional hybrid of reduced graphene oxide-Fe_3O_4 nanoparticles as an easily regenerative adsorbent. *J Mater Chem* 2012;22:3527. DOI
31. Crini G. Recent developments in polysaccharide-based materials used as adsorbents in wastewater treatment. *Prog Polym Sci* 2005;30:38-70. DOI
32. Chakraborty R, Asthana A, Singh AK, Jain B, Susan ABH. Adsorption of heavy metal ions by various low-cost adsorbents: a review. *Int J Environ Anal Chem* 2022;102:342-79. DOI
33. Oladoye PO. Natural, low-cost adsorbents for toxic Pb(II) ion sequestration from (waste)water: a state-of-the-art review. *Chemosphere* 2022;287:132130. DOI PubMed
34. Abdollahi N, Moussavi G, Giannakis S. A review of heavy metals' removal from aqueous matrices by metal-organic frameworks (MOFs): state-of-the art and recent advances. *J Environ Chem Eng* 2022;10:107394. DOI
35. Sikiru S, Abiodun OA, Sanusi YK, et al. A comprehensive review on nanotechnology application in wastewater treatment a case study of metal-based using green synthesis. *J. Environ Chem Eng* 2022;10:108065. DOI
36. Boraah N, Chakma S, Kaushal P. Attributes of wood biochar as an efficient adsorbent for remediating heavy metals and emerging contaminants from water: a critical review and bibliometric analysis. *J Environ Chem Eng* 2022;10:107825. DOI
37. Abdel-magied AF, Abdelhamid HN, Ashour RM, et al. Magnetic metal-organic frameworks for efficient removal of cadmium(II), and lead(II) from aqueous solution. *J Environ Chem Eng* 2022;10:107467. DOI
38. Gomri M, Abderrazak H, Chabbah T, et al. Adsorption characteristics of aromatic pollutants and their halogenated derivatives on bio-based poly (ether-pyridine)s. *J Environ Chem Eng* 2020;8:104333. DOI
39. Brirmi NEH, Chabbah T, Chatti S, et al. Effect of the pendent groups on biobased polymers, obtained from click chemistry suitable, for the adsorption of organic pollutants from water. *Polym Adv Technol* 2022;33:3551-71. DOI
40. Gupta S, Sireesha S, Sreedhar I, Patel C M, Anitha K L. Latest trends in heavy metal removal from wastewater by biochar based sorbents. *J Water Process Eng* 2020;38:101561. DOI
41. Järup L. Hazards of heavy metal contamination. *Br Med Bull* 2003;68:167-82. DOI PubMed
42. Ali H, Khan E. Bioaccumulation of non-essential hazardous heavy metals and metalloids in freshwater fish. Risk to human health. *Environ Chem Lett* 2018;16:903-17. DOI
43. Paithankar JG, Saini S, Dwivedi S, Sharma A, Chowdhuri DK. Heavy metal associated health hazards: an interplay of oxidative stress and signal transduction. *Chemosphere* 2021;262:128350. DOI PubMed
44. Rae IB, Gibb SW, Lu S. Biosorption of Hg from aqueous solutions by crab carapace. *J Hazard Mater* 2009;164:1601-4. DOI PubMed
45. Hu XF, Lowe M, Chan HM. Mercury exposure, cardiovascular disease, and mortality: a systematic review and dose-response meta-analysis. *Environ Res* 2021;193:110538. DOI PubMed
46. Chen R, Xu Y, Xu C, et al. Associations between mercury exposure and the risk of nonalcoholic fatty liver disease (NAFLD) in US adolescents. *Environ Sci Pollut Res Int* 2019;26:31384-91. DOI PubMed
47. Hensawang S, Chanpiwat P. Health impact assessment of arsenic and cadmium intake via rice consumption in Bangkok, Thailand. *Environ Monit Assess* 2017;189:599. DOI PubMed
48. Genchi G, Sinicropi MS, Lauria G, Carocci A, Catalano A. The effects of cadmium toxicity. *Int J Environ Res Public Health* 2020;17:3782. DOI PubMed PMC
49. Musfirah M, Rangkuti AF. The lead exposure risk due to wells water consumption in code riverside community, Yogyakarta city. *Kemas* 2019;14:318-25. DOI
50. Thongsringklee M, Robson MG, Siriwong W. Health effects of low level exposure to lead among communication radio repair workers at Samutsakhon province, Thailand. *Hum Ecol Risk Assess* 2021;27:344-51. DOI
51. Rizwan M, Ali S, Hussain A, et al. Effect of zinc-lysine on growth, yield and cadmium uptake in wheat (Triticum aestivum L.) and health risk assessment. *Chemosphere* 2017;187:35-42. DOI PubMed
52. Yahya EB, Alqadhi AM. Recent trends in cancer therapy: a review on the current state of gene delivery. *Life Sci* 2021;269:119087. DOI PubMed
53. Ren C, Zhou Y, Liu W, Wang Q. Paradoxical effects of arsenic in the lungs. *Environ Health Prev Med* 2021;26:80. DOI PubMed PMC

54. Rahaman MS, Rahman MM, Mise N, et al. Environmental arsenic exposure and its contribution to human diseases, toxicity mechanism and management. *Environ Pollut* 2021;289:117940. DOI PubMed

55. Rahman Z, Singh V P. The relative impact of toxic heavy metals (THMs) (arsenic (As), cadmium (Cd), chromium (Cr)(VI), mercury (Hg), and lead (Pb)) on the total environment: an overview. *Environ Monit Assess* 2019;191:1-21. DOI PubMed

56. Yoshinaga M, Ninomiya H, Al Hossain MMA, et al. A comprehensive study including monitoring, assessment of health effects and development of a remediation method for chromium pollution. *Chemosphere* 2018;201:667-75. DOI PubMed

57. Peixoto S, Henriques I, Loureiro S. Long-term effects of $Cu(OH)_2$ nanopesticide exposure on soil microbial communities. *Environ Pollut* 2021;269:116113. DOI PubMed

58. Neff E, Dharmarajan G. The direct and indirect effects of copper on vector-borne disease dynamics. *Environ Pollut* 2021;269:116213. DOI PubMed

59. Salih HHM, El Badawy AM, Tolaymat TM, Patterson CL. Removal of stabilized silver nanoparticles from surface water by conventional treatment processes. *Adv Nanopart* 2019;8:21-35. DOI PubMed PMC

60. Krou NJ. Etude expérimentale et modélisation d’un procédé séquentiel AD-OX d’élimination de polluants organiques. Génie des procédés 2010. (in French). Available from: https://theses.hal.science/tel-04272164. [Last accessed on 20 Nov 2024].

61. Taamneh Y, Sharadqah S. The removal of heavy metals from aqueous solution using natural Jordanian zeolite. *Appl Water Sci* 2017;7:2021-8. DOI

62. Ugwu EI, Othmani A, Nnaji CC. A review on zeolites as cost-effective adsorbents for removal of heavy metals from aqueous environment. *Int J Environ Sci Technol* 2022;19:8061-84. DOI

63. Taffarel SR, Rubio J. On the removal of Mn^{2+} ions by adsorption onto natural and activated Chilean zeolites. *Min Eng* 2009;22:336-43. DOI

64. Álvarez AM, Guerrón DB, Montero Calderón C. Natural zeolite as a chromium VI removal agent in tannery effluents. *Heliyon* 2021;7:e07974. DOI PubMed PMC

65. Mehdi B, Belkacemi H, Brahmi-ingrachen D, Braham LA, Muhr L. Study of nickel adsorption on NaCl-modified natural zeolite using response surface methodology and kinetics modeling. *Groundwater Sustain Dev* 2022;17:100757. DOI

66. Khalfa L, Sdiri A, Bagane M, Cervera ML. Multi-element modeling of heavy metals competitive removal from aqueous solution by raw and activated clay from the Aleg formation (Southern Tunisia). *Int J Environ Sci Technol* 2020;17:2123-40. DOI

67. Dim PE, Termtanun M. Treated clay mineral as adsorbent for the removal of heavy metals from aqueous solution. *Appl Sci Eng Prog* 2021;14:511-24. DOI

68. Angin D, Sarikulce S. The effect of activation temperature on properties of activated carbon prepared from wine industry pressing waste. *Desal Water Treat* 2017;73:373-9. DOI

69. Zhang Z, Wang T, Zhang H, Liu Y, Xing B. Adsorption of Pb(II) and Cd(II) by magnetic activated carbon and its mechanism. *Sci Total Environ* 2021;757:143910. DOI PubMed

70. Ghorbani F, Kamari S, Zamani S, Akbari S, Salehi M. Optimization and modeling of aqueous Cr(VI) adsorption onto activated carbon prepared from sugar beet bagasse agricultural waste by application of response surface methodology. *Surf Interfaces* 2020;18:100444. DOI

71. Deng Y, Huang S, Laird DA, Wang X, Meng Z. Adsorption behaviour and mechanisms of cadmium and nickel on rice straw biochars in single- and binary-metal systems. *Chemosphere* 2019;218:308-18. DOI PubMed

72. Lee ME, Park JH, Chung JW. Comparison of the lead and copper adsorption capacities of plant source materials and their biochars. *J Environ Manage* 2019;236:118-24. DOI PubMed

73. Zhao W, Geng X, Lu J, et al. Mercury removal performance of brominated biomass activated carbon injection in simulated and coal-fired flue gas. *Fuel* 2021;285:119131. DOI

74. Park JH, Wang JJ, Kim SH, et al. Cadmium adsorption characteristics of biochars derived using various pine tree residues and pyrolysis temperatures. *J Colloid Interface Sci* 2019;553:298-307. DOI PubMed

75. Lata S, Singh PK, Samadder SR. Regeneration of adsorbents and recovery of heavy metals: a review. *Int J Environ Sci Technol* 2015;12:1461-78. DOI

76. Afolabi F, Musonge P, Bakare B. Evaluation of lead (II) removal from wastewater using banana peels: optimization study. *Pol J Environ Stud* 2021;30:1487-96. DOI

77. Çelebi H, Gök G, Gök O. Adsorption capability of brewed tea waste in waters containing toxic lead(II), cadmium (II), nickel (II), and zinc(II) heavy metal ions. *Sci Rep* 2020;10:17570. DOI PubMed PMC

78. Khalil U, Shakoor MB, Ali S, et al. Selective removal of hexavalent chromium from wastewater by rice husk: kinetic, isotherm and spectroscopic investigation. *Water* 2021;13:263. DOI

79. Amar MB, Walha K, Salvadó V. Evaluation of olive stones for Cd(II), Cu(II), Pb(II) and Cr(VI) biosorption from aqueous solution: equilibrium and kinetics. *Int J Environ Res* 2020;14:193-204. DOI

80. Varghese AG, Paul SA, Latha MS. Remediation of heavy metals and dyes from wastewater using cellulose-based adsorbents. *Environ Chem Lett* 2019;17:867-77. DOI

81. Begum S, Yuhana NY, Md Saleh N, Kamarudin NHN, Sulong AB. Review of chitosan composite as a heavy metal adsorbent: material preparation and properties. *Carbohydr Polym* 2021;259:117613. DOI PubMed

82. Tarabukin DV, Torlopov MA, Shchemelinina TN, et al. Biosorbents based on esterified starch carrying immobilized oil-degrading microorganisms. *J Biotechnol* 2017;260:31-7. DOI PubMed

83. Yu D, Wang Y, Wu M, Zhang L, Wang L, Ni H. Surface functionalization of cellulose with hyperbranched polyamide for efficient adsorption of organic dyes and heavy metals. *J Clean Prod* 2019;232:774-83. DOI
84. Guleria A, Kumari G, Lima EC. Cellulose-g-poly-(acrylamide-co-acrylic acid) polymeric bioadsorbent for the removal of toxic inorganic pollutants from wastewaters. *Carbohydr Polym* 2020;228:115396. DOI PubMed
85. Yin W, Liu L, Tang S, Zhang H, Pan X, Chi R. Facile synthesis of triazole and carboxyl-functionalized cellulose-based adsorbent via click chemistry strategy for efficient Gd(III) removal. *Cellulose* 2019;26:7107-23. DOI
86. Mahalakshmi R, Saravanan R, Selvakumar P, Karthikeyan MS, Ravikumar L. Polymeric substitution of triazole moieties in cellulosic schiff base for heavy metal complexation studies. *J Polym Environ* 2022;30:360-72. DOI
87. Dinari M, Mokhtari N, Hatami M. Covalent triazine based polymer with high nitrogen levels for removal of copper (II) ions from aqueous solutions. *J Polym Res* 2021;28:2463. DOI
88. Chu S, Feng X, Liu C, Wu H, Liu X. Advances in chelating resins for adsorption of heavy metal ions. *Ind Eng Chem Res* 2022;61:11309-28. DOI
89. Wu H, Lin G, Liu C, Chu S, Mo C, Liu X. Progress and challenges in molecularly imprinted polymers for adsorption of heavy metal ions from wastewater. *Trends Environ Anal Chem* 2022;36:e00178. DOI
90. Bazzar M, Ghaemy M, Alizadeh R. Synthesis and characterization of new fluorescent polyimides bearing 1,2,4-triazole and 1,2-diaryl quinoxaline: study properties and application to the extraction/elimination of metallic ions from aqueous media. *React Funct Polym* 2013;73:492-8. DOI
91. Ghaemy M, Qasemi S, Ghassemi K, Bazzar M. Nanostructured composites of poly(triazole-amide-imide)s and reactive titanium oxide by epoxide functionalization: thermal, mechanical, photophysical and metal ions adsorption properties. *J Polym Res* 2013;20:278. DOI
92. Ghaemy M, Ghassemi K, Qasemi S, Bazzar M. Synthesis, characterization and properties of new poly(triazole-imide)s and their composites with silane-modified nanoclay. *Polym Bull* 2015;72:2435-53. DOI
93. Amininasab SM, Esmaili S, Taghavi M, Shami Z. Fabrication and characterization of novel high-performance fluorinated polyimides with xanthene pendent architecture: study of thermal, photophysical, antibacterial and heavy metal ion adsorption behavior. *React Funct Polym* 2016;192:48-57. DOI
94. Amininasab SM, Esmaili S, Shami Z. High-performance polyimides based on pyridine and xanthene pendant groups; synthesis, characterization, photoactivity, thermal, antibacterial, and Cr(VI) ion adsorption properties. *High Perform Polym* 2020;32:371-82. DOI
95. Huang X, Li H, Liu C, Wei C. Design and synthesis of high heat-resistant, soluble, and hydrophobic fluorinated polyimides containing pyridine and trifluoromethylthiophenyl units. *High Perform Polym* 2019;31:107-115. DOI
96. Ghorbani M, Eisazadeh H. Removal of COD, color, anions and heavy metals from cotton textile wastewater by using polyaniline and polypyrrole nanocomposites coated on rice husk ash. *Compos Part B Eng* 2013;45:1-7. DOI
97. Rafiee Z, Golriz L, Karimipour G, Kowkabi S. Preparation and properties of polyimides having porphyrin moieties for heavy metals removal. *Polym Bull* 2021;78:481-92. DOI
98. Natale C, Monti D, Paolesse R. Chemical sensitivity of porphyrin assemblies. *Mater Today* 2010;13:46-52. DOI
99. Jlalia I, Zouaoui F, Chabbah T, et al. Adsorption characteristics of WFD heavy metal ions on new biosourced polyimide films determined by electrochemical impedance spectroscopy. *J Inorg Organomet Polym* 2021;31:2471-82. DOI
100. Lakouraj MM, Rahpaima G, Azimi R. Organosoluble xanthone-based polyimides: synthesis, characterization, antioxidant activity and heavy-metal sorption. *Mater Tehnol* 2016;50:471-8. DOI
101. Mansoori Y, Ghanbari M. Novel polyimides obtained from a new aromatic diamine (BAPO) containing pyridine and 1,3,4-oxadiazole moieties for removal of Co(II) and Ni(II) ions. *Polymers for Advanced Techs* 2015;26:658-64. DOI
102. Manzoor A, Kalsoom S, Khan YK, Siddiqi HM, Shah MH. Synthesis of sulfonated copolyimides by thermal imidization for efficient lead ion adsorption from aqueous media. *ACS Appl Polym Mater* 2022;4:5660-9. DOI
103. Ravikumar L, Kalaivani SS, Murugesan A, et al. Synthesis, characterization, and heavy metal ion adsorption studies of polyamides, polythioamides having pendent chlorobenzylidine rings. *J of Applied Polymer Sci* 2011;122:1634-42. DOI
104. Murugesan A, Ravikumar L, Sathyaselvabala V, et al. Removal of Pb(II), Cu(II) and Cd(II) ions from aqueous solution using polyazomethineamides: Equilibrium and kinetic approach. *Desalination* 2011;271:199-208. DOI
105. Kirupha SD, Murugesan A, Vidhyadevi T, Baskaralingam P, Sivanesan S, Ravikumar L. Novel polymeric adsorbents bearing amide, pyridyl, azomethine and thiourea binding sites for the removal of Cu(II) and Pb(II) ions from aqueous solution. *Separation Sci Technol* 2012;48:254-62. DOI
106. Gómez-valdemoro A, San-josé N, García FC, De La Peña JL, Serna F, García JM. Novel aromatic polyamides with main chain and pendant 1,2,4-triazole moieties and their application to the extraction/elimination of mercury cations from aqueous media. *Polym Chem* 2010;1:1291. DOI
107. Soleimani B, Taghavi M, Ghaemy M. Synthesis, characterization and heavy metal ion adsorption behavior of imidazole-based novel polyamides and polyimides. *J Mex Chem Soc* 2017:61. DOI
108. Santiago AA, Ibarra-palos A, Cruz-morales JA, et al. Synthesis, characterization, and heavy metal adsorption properties of sulfonated aromatic polyamides. *High Perform Polym* 2018;30:591-601. DOI
109. Albukhari SM, Hussein MA, Abdel Rahman MA, Marwani HM. Highly selective heteroaromatic sulfur containing polyamides for Hg^{+2} environmental remediation. *Des Monomers Polym* 2020;23:25-39. DOI PubMed PMC

110. Rezania H, Vatanpour V, Salehi E, Gavari N, Shockravi A, Ehsani M. Wholly heterocycles-based polyamide-sulfide containing pyridine and thiazole rings: a super-adsorbent polymer for lead removal. *J Polym Environ* 2019;27:1790-800. DOI
111. Hsiao S, Guo W, Kung Y, Lee Y. Redox-active and electrochromic aromatic poly(amide-imide)s with 2,4-dimethoxytriphenylamine chromophores. *J Polym Res* 2011;18:1353-64. DOI
112. Faghihi K, Hajibeygi M, Shabanian M. New photosensitive and optically active organo-soluble poly(amide-imide)s from N,N′-(bicyclo[2,2,2]oct-7-ene-tetracarboxylic)-bis-L-amino acids and 1,5-bis(4-aminophenyl)penta-1,4-dien-3-one: synthesis and characterization. *J Polym Res* 2010;17:379-90. DOI
113. Thiruvasagam P, Vijayan M. Synthesis of new diacid monomers and poly(amide-imide)s: study of structure-property relationship and applications. *J Polym Res* 2012;19:9845. DOI
114. Alborzi A, Zahmatkesh S, Yazdanpanah A. l-Lysine-derived optically active poly(hydrazide-imide)s: synthesis, characterization and their application in removal of heavy metal ions. *Polym Bull* 2013;70:3359-72. DOI
115. Vakili MR, Zahmatkesh S, Panahiyan MJ, Jafarizadeh T. Poly(amide-hydrazide-imide)s containing L-aspartic acid: synthesis, characterization, and their applications in removal of heavy metal ions. *Des Monomers Polym* 2015;18:315-22. DOI
116. Bıyıkoğlu M, Çiftçi H. Adsorption of Ag(I) ions from wastewaters using poly(2-aminothiazole): kinetic and isotherm studies. *Polym Bull* 2020;77:6161-74. DOI
117. Puguan JMC, Kim H. Synthesis of free-standing poly(ionic liquid) bearing 1,2,3-triazole group for the adsorptive elimination of Cr^{6+} from aqueous solution. *J Environ Chem Eng* 2020;8:104084. DOI
118. Ouerghui A, Dardouri M, Elamari H, Ammari F, Girard C. Chemical modification of polystyrene merrifield: extraction of zinc and magnesium located in wastewater. *AJPST* 2019;5:73. DOI
119. Qureshi F, Memon SQ, Khuhawar MY, Jahangir TM. Removal of Co^{2+}, Cu^{2+} and Au^{3+} ions from contaminated wastewater by using new fluorescent and antibacterial polymer as sorbent. *Polym Bull* 2021;78:1505-33. DOI
120. Qureshi F, Memon SQ, Khuhawar MY, Jahangir TM, Channar A. Synthesis and application of fluorescent and thermally stable polyazomethine as adsorbent in the remediation of Ni (II), Cu (II) and Co (II) from wastewater systems. *J Polym Res* 2021;28:2582. DOI
121. Chabbah T, Abderrazak H, Souissi R, et al. A sensitive impedimetric sensor based on biosourced polyphosphine films for the detection of lead ions. *Chemosensors* 2020;8:34. DOI
122. Chabbah T, Chatti S, Jaffrezic-renault N, Weidner S, Marestin C, Mercier R. Impedimetric sensors based on diethylphosphonate-containing poly(arylene ether nitrile)s films for the detection of lead ions. *Polym Adv Technol* 2023;34:2471-81. DOI
123. Huang J, Zheng Y, Luo L, et al. Facile preparation of highly hydrophilic, recyclable high-performance polyimide adsorbents for the removal of heavy metal ions. *J Hazard Mater* 2016;306:210-9. DOI PubMed
124. Jia W, Du J, Jiang M, et al. Preparation and Cr (VI) adsorption of functionalized polyimide fibers. *J of Applied Polymer Sci* 2022;139:e52799. DOI
125. Bassyouni D, Mohamed M, El-ashtoukhy E, El-latif MA, Zaatout A, Hamad H. Fabrication and characterization of electrospun Fe_3O_4 /o-MWCNTs/polyamide 6 hybrid nanofibrous membrane composite as an efficient and recoverable adsorbent for removal of Pb (II). *Microchem J* 2019;149:103998. DOI
126. Hafiz Ahmed A, Mohamed W, El Hamouly S, Maziad N, Abd Elmonam M. Preparation, characterization and water treatment application of electro-spun polyamide 6 nanocomposite. *Egypt J Chem* 2022;0:0-0. DOI

Mirza *et al. Water Emerg Contam Nanoplastics* 2024;3:24
DOI: 10.20517/wecn.2024.70

Water Emerging Contaminants & Nanoplastics

Research Article

Open Access

Prediction of arsenic (III) adsorption from aqueous solution using non-neural network algorithms

Nazmul Hassan Mirza, **Takeshi Fujino**

Department of Environmental Science and Technology, Saitama University, Saitama 338-8570, Japan.

Correspondence to: Prof. Takeshi Fujino, Department of Environmental Science and Technology, Graduate School of Science and Engineering, Saitama University, 255 Shimo-Okubo, Sakura-Ku, Saitama 338-8570, Japan. E-mail: fujino@mail.saitama-u.ac.jp

How to cite this article: Mirza NH, Fujino T. Prediction of arsenic (III) adsorption from aqueous solution using non-neural network algorithms. *Water Emerg Contam Nanoplastics* 2024;3:24. https://dx.doi.org/10.20517/wecn.2024.70

Received: 24 Oct 2024 **First Decision:** 12 Nov 2024 **Revised:** 18 Nov 2024 **Accepted:** 22 Nov 2024 **Published:** 10 Dec 2024

Academic Editors: Zhijie Chen, Roberto Rosal **Copy Editor:** Pei-Yun Wang **Production Editor:** Pei-Yun Wang

Abstract

Heavy metals such as arsenic can be effectively removed through adsorption. Through material property evaluation and adsorption parameter optimization, machine learning (ML) modeling provides an alternative to lengthy laboratory experimentation. In this work, adsorption data from an earlier study employing a waste-material composite were used. To create prediction models, four non-neural network algorithms - support vector machines (SVM), Gaussian process regression (GPR), linear regression, and ensemble approaches - were used and contrasted with neural network algorithms. Nine predictors were utilized, ranging from adsorbent composition alterations to experimental circumstances. Using principal component analysis (PCA) and feature selection, together with the F-test and minimum redundancy maximum relevance (MRMR) algorithms for feature reduction, optimization was accomplished. With an R-squared of 0.939, mean absolute error (MAE) of 5.778, and root mean squared error (RMSE) of 7.119 for training and an R-squared of 0.942, MAE of 5.450, and RMSE of 6.870 for testing, the optimized GPR method offered the best predictive performance. The best R-squared values found for other algorithms were: SVM (0.922), linear regression (0.925), and ensemble (0.927). The most important variables influencing adsorption efficiency were initial arsenic concentration, time, and the iron salt content. Local interpretable model-agnostic explanations (LIME), partial dependence plot (PDP), and Shapley additive explanations (SHAP) plots were used to explain these results. This work shows that, based on model-derived parameters, non-neural network algorithms may efficiently simulate and optimize arsenic adsorption tests, providing a trustworthy substitute for neural network techniques and markedly increasing adsorption efficiency.

Keywords: Adsorption, arsenic removal, machine learning, non-neural network regression, water quality

INTRODUCTION

The ecosystem and human health can suffer greatly when toxic heavy metals, even in trace amounts, are released into groundwater[1]. Most often, various industrial and agricultural activities, urbanization, and other factors release this type of hazardous element into the land, water, and atmosphere[2]. Arsenic (As) is one of the most well-known heavy metals for its toxicity. The current estimate of the affected population worldwide is approximately 150 million, which is certain to rise as more afflicted places are identified[3]. All natural waterways contain arsenic, which can originate from biological processes as well as natural processes occurring in the Earth's crust[4]. There are two primary types of inorganic arsenic: arsenite [As(III)] and arsenate [As(V)][5]. Arsenate is the main species present in naturally occurring surface water basins, while arsenite is the predominant form in groundwater[6]. While As(III) and As(V) are not equally dangerous, As(III) is approximately 60 times more poisonous[7]. Since As(III) frequently exists in neutral, undissociated forms, removal of it is quite challenging[8]. Arsenic poses a global health danger to humans. Long-term exposure to arsenic, mostly from tainted food and water, can cause serious illnesses such as lung, kidney, liver, and skin cancers[9]. The World Health Organization (WHO) has set a maximum allowable concentration of arsenic in drinking water at 10 μg/L[10].

Hence, it is still imperative to completely eradicate this toxic heavy metal. In addition to biological approaches, coagulation, precipitation, reverse osmosis, filtering, and adsorption are some of the ways that have been developed to remove arsenic[11,12]. Adsorption is arguably the most successful strategy among these[13]. With modified adsorbents such as chars, activated carbons, activated aluminium, thiol-functionalized chitin nanofibers, goethite-based adsorbent, zero-valent iron, synthetic siderite, titanium dioxide, and many more, adsorption is a commonly used physical separation method for the removal of hazardous heavy metals from groundwater[14]. For the removal of both organic and inorganic contaminants, adsorption is the method of choice in the water and wastewater sectors due to its ease of handling, low sludge production, affordability, and regeneration potential[15]. Adsorbents derived from solid waste are frequently employed in water and wastewater treatment procedures[16-18]. Moringa waste, a type of agricultural solid waste, can serve as a biosorbent to adsorb heavy metals[19]. Various parts of the Moringa oleifera plant, including seeds, leaves, and bark, have also been shown to possess the ability to remove heavy metals[20,21]. Metal salts, such as iron and aluminum, are frequently used to remove arsenic[22]. On the other hand, porous composite materials formed of metal salts combined with solid waste are employed to extract heavy metals. It is crucial to evaluate the many control elements affecting adsorption and overall efficiency in order to optimize composite adsorbents. Historically, mathematical models have been employed to optimize efficiency and evaluate the influence of parameters[23,24].

Currently, the water and wastewater treatment industry is increasingly employing machine learning (ML) to forecast treatment procedures, thanks to improvements in computational efficiency resulting from enhanced hardware and software[25-28]. Developing high-performance solid adsorbents typically involves intuition-based, factor-by-factor techniques, with response surface procedures serving as the primary means of experimental design[29]. The aqueous phase adsorption of heavy metals involves many factors, including the interaction between adsorbents and adsorbates and ambient variables[30,31]. A growing number of ML algorithms, including artificial neural networks (ANN), tree-based techniques, and support vector regression, are being used to simulate and examine the processes of heavy metal adsorption by solid adsorbents[32-34]. However, some research has been undertaken without considering appropriateness or context[35,36] and several papers omitted the findings of the present experiment and instead only incorporated a limited portion of data from previous publications[37,38]. Adsorption isotherms and batch studies are two common methods used to analyze the adsorption behavior of heavy metals and organic pollutants in the aqueous phase. However, both methods can be laborious and ineffective[39]. ML can be used to automatically map complex systems and produce the mapping relationship between input and output variables[40]. The foundation of ML is sufficient and high-quality data, which effect model performance[41]. The ANN was first created to replicate the workings of the human brain using a rigorous data analysis technique. Consequently, numerous environmental studies pertaining to water pollution have been using an expanding number of different ANN methodologies. The ANN technique was effectively applied by Mandal *et al.* to model an As(III) removal process[42]. According to Sakizadeh, ANN have various shortcomings, especially in the environmental sciences, despite their effective application in many modeling studies[43]. One of the main constraints is the lack of sufficient data records. Training on a limited dataset may result in overfitting, a situation in which the model exhibits good generalization ability when it performs well on training data but badly on unseen data. In addition to ANN, the applications of other advanced machine learning algorithms (MLAs) such as support vector machine (SVM)[44,45] random forest (RF)[46], gradient boosted regression tree[47], Bayesian network[48], adaptive network-based fuzzy inference system[49], and Ensemble models[50] have been proven to be accurate and useful for different learning problems in multiple domains. A recent study investigated the adsorption of arsenic (III) using a porous filter media block (PFMB). The study employed classical isotherm and kinetic models alongside ANN modeling to analyze the adsorption process[51]. A PFMB made of biochar and moringa bark as bio-adsorbents and enhanced with sodium bicarbonate, ferric chloride, aluminum sulfate, and commercial gypsum was examined for its capacity to adsorb arsenic. Seven different PFMB samples, each prepared with different amounts of aluminum-iron salts and moringa-based bio-adsorbents (biomass and biochar), were used in batch studies. The experimental parameters encompassed different agitation rates, pH levels, duration, initial concentration, and quantity of adsorbent. This study will employ identical data sets to assess non-neural network approaches in forecasting arsenic adsorption and juxtapose them with the neural network model.

This study aims to predict the adsorption capacity of the PFMB using a total of four non-neural network machine-learning algorithms. The best non-neural network algorithms will be evaluated and compared with neural network results from the previous study. ANN were used in the previous study; although they are successful, they are computationally demanding and perform best with huge datasets. In order to overcome those constraints, this paper investigates non-neural network approaches for assessing adsorption trials. It draws attention to the effectiveness, relevance, and insights offered by non-neural models by contrasting neural with non-neural methods. The study provides a unique comparative examination of different approaches, with a focus on algorithm selection, model performance optimization, and finding critical experimental conditions. The efficacy of four non-neural network strategies - SVM, ensemble approaches, Gaussian process regression (GPR), and linear regression - in predicting adsorption capacity and identifying contributors in the PFMB will be evaluated. To provide a thorough explanation of the model results, the study will make use of Shapley additive explanations (SHAP), partial dependence plot (PDP) analysis, and local interpretable model-agnostic explanations (LIME).

METHODS

Data collection and preprocessing

A total of 507 data sets were gathered from batch experiments conducted in a previous study to facilitate ML analysis[51]. The dataset included nine predictive parameters, with arsenic uptake capacity serving as the response parameter [Table 1]. Modeling was performed using MATLAB R2023b, implementing four non-neural network algorithms: linear regression, SVM, ensemble methods, and GPR.

The first step in non-neural network modeling after data gathering is data preprocessing, which cleans and formats the data. Data preprocessing is an essential phase in the ML process that involves cleaning, transforming, and preparing raw data for training ML models[52]. This phase has a major impact on the final

Table 1. Data collection for the non-neural network analysis

Parameters	Ranges	Nos	Role
Initial concentration of arsenic [As(III)] in ppm (initial conc.)	0.25-4.0	507	Predictor
Amount of adsorbent used (g per 50 mL solution) (adsorbent)	0.25-1.0	507	Predictor
pH of the solution (pH)	2.5-11.3	507	Predictor
Shaking speed in revolutions per minute (rpm) (shaking)	100-200	507	Predictor
Contact time in minutes (time)	30-300	507	Predictor
$FeCl_3·6H_2O$ used in PFMB preparation (g per 50 g of media) (Fe/Iron salt)	0.25-0.75	507	Predictor
$[Al_2(SO_4)_3]$ used in PFMB preparation (g per 50 g of media) (Al salt)	0.25-0.75	507	Predictor
Moringa bark biomass included in PFMB (g per 50 g of media) (M. Biomass)	0.25-0.75	507	Predictor
Moringa bark biochar included in PFMB (g per 50 g of media) (M. Biochar)	0.25-0.75	507	Predictor
Adsorption capacity for As(III) in micrograms per gram (μg/g) (arsenic uptake)		507	Response

PFMB: Porous filter media block.

models' efficacy and performance. Among the crucial phases in data preprocessing are data cleaning, data transformation, feature engineering, data normalization, scaling, normalizing, and encoding categorical information into numerical representations, which are common transformations[53,54]. Each predictor's significance was examined independently using the F-test technique, and the features were ranked based on the analysis of the p-values obtained from the F-test findings. In ML and data analysis, the minimum redundancy maximum relevance (MRMR) test is a feature selection technique that helps find a subset of characteristics with high relevance to the target variable while preserving low redundancy among the features chosen. The best feasible set of characteristics that can maximally and mutually diverge from one another and accurately represent the response variable was chosen using the MRMR algorithm. Principal component analysis (PCA) is a dimensionality reduction approach used in feature importance analysis that can be used to characterize the association between descriptors and output variables[55]. Information gain is used to demonstrate the significance of the descriptors[56]. Most of the information present in a big set of variables can be retained when converting it into a smaller set of variables using PCA[57]. A new variable that corresponds to a linear combination of the original variables is the resultant main component[58]. In regression learners, dimensionality reduction can produce regression models that lessen the risk of overfitting. Next, the data are divided into testing and training sets. The model is trained using algorithms such as ensemble techniques, GPR, SVM, and linear regression on the training data. Reliability is ensured using validation techniques such as cross-validation, and the model's performance is assessed on the testing set. Lastly, the model's predictions are interpreted and important characteristics influencing arsenic adsorption are identified using respective techniques [Figure 1].

Non-neural network algorithms

Adsorption behavior can be modeled by researchers using ML techniques, considering a range of parameters including arsenic concentrations, adsorbent properties, and environmental factors. Non-neural network ML algorithms have shown great promise in the field of arsenic adsorption modeling utilizing PFMBs[59]. Cost-effective and practical descriptors for assessing adsorbent properties and predicting adsorption efficiency encompass macro-level factors such as operational parameters (adsorbent dosage, adsorbate concentration, contact time, and stirring speed)[60] and synthesis conditions (composition and proportion of raw materials, synthesis duration, and pH)[61]. In model training, output variables that are easily accessible and have cost-effective experimental attributes, such as adsorption capacity, removal rate, and efficiency, are commonly used[62,63]. The main goal of regression analysis is to identify a linear, planar, or hyperplanar model that minimizes the gap between the observed and predicted values[64,65]. ML can be classified into four main types based on the nature of the datasets and their corresponding labels:

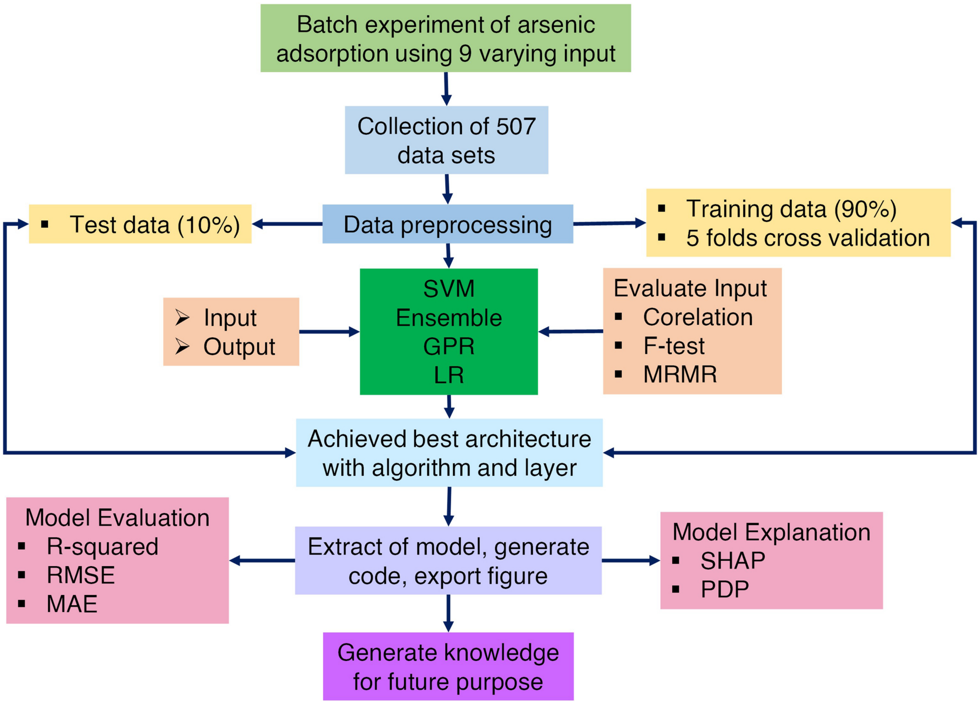

Figure 1. Schematic flow chart of ML toolbox. ML: Machine learning; SVM: support vector machines; GPR: Gaussian process regression; MRMR: minimum redundancy maximum relevance; RMSE: root mean squared error; MAE: mean absolute error; SHAP: Shapley additive explanations; PDP: partial dependence plot.

supervised, unsupervised, semi-supervised, and reinforcement learning[66]. The objective of this study is to utilize supervised ML to target the adsorption capacity. The techniques used for estimating adsorption capacity and identifying major contributing factors include ensemble methods, GPR, SVM, and linear regression. These techniques provide robust frameworks for these purposes [Table 2].

Linear regression is a simple and widely used statistical method for modeling the relationship between a dependent variable (target) and one or more independent variables (features) by fitting a linear equation to the observed data. A linear relationship between the independent variable X and the dependent variable y is assumed by the linear regression model. The model can be expressed as follows:

$$y = \beta0 + \beta1\cdot x1 + \beta2\cdot x2 + \ldots + \beta n\cdot xn + \epsilon$$

When the error term is represented by ϵ, the coefficients for the independent variables are xi, the intercept term is $\beta0$, and the coefficients for the independent variables are βi. According to linear regression, there must be a linear relationship between the variables, a normally distributed distribution of the errors, and a constant variance (homoscedasticity) of the errors. Among various available techniques, linear, interactions linear (IL), robust linear, and stepwise linear (SL) regression were evaluated in this study. The two best-performing models, interaction linear regression and stepwise linear regression, were chosen for further evaluation with varying input features, both with and without the application of PCA.

SVM regression concentrates on identifying a hyperplane that captures a given fraction of the data inside a margin around the predicted values[57], in contrast to classic regression models that seek to directly reduce the mean squared error. Finding the hyperplane that best fits the data while permitting some variation or error is the goal of SVM regression[67]. SVM maps the input space derived from the independent variables in

Table 2. Algorithms evaluated for each model

GPR	SVM	Linear regression	Ensembles of trees
Rational quadratic GPR	Linear SVM	Linear	Boosted trees
Squared exponential GPR	Quadratic SVM	Interactions linear	Bagged trees
Matern 5/2 GPR	Cubic SVM	Robust linear	Optimizable trees
Exponential GPR	Fine/medium/coarse SVM	Stepwise linear	
Optimizable GPR	Optimizable SVM		

GPR: Gaussian process regression; SVM: support vector machines.

a kernel function and focuses mostly on the border between classes[68]. The epsilon (ε), kernel function, and penalty parameter are all connected to the prediction accuracy of SVR. The parameter ε, which is utilized for training data fitting, governs the function of the ε-insensitive zone width. From available different presets, linear, quadratic, cubic, fine/medium/coarse and optimizable SVM were evaluated and the best one was selected as SVM. SVM, which operates based on statistical learning theory, is regarded as an exacting ML methodology[69]. SVM has been considered for regression analysis because of its great flexibility and a small number of tuning factors[70].

Ensemble methods, a supervised ML modeling technique for simulating the heavy metal adsorption process, are tree-based techniques[62]. It incorporates a variety of techniques, including decision trees, gradient boosting (GB), and RF, and can adapt to both classification and regression scenarios[71]. One of the ensemble learning methods, the boosting technique, is used to train the GB method[72]. By minimizing the prediction error for a regression problem, boosting is usually used to combine several weak prediction models into a final strong model with improved predictive performance. Bootstrap sampling is used in the RF algorithm to randomly choose the input variables and split the training data so that the trees develop independently of one another[73]. Cross-validation and other similar approaches are frequently used in hyperparameter tuning[74]. Among various Ensembles of trees, boosted trees, bagged trees, and optimizable trees were evaluated in this study before selecting the best one to train and model.

GPR is a non-parametric Bayesian regression technique that uses a distribution over functions to model the connection between input data and output values. When providing uncertainty estimates for forecasts, it is an effective way to capture intricate and non-linear interactions. A covariance (kernel) function and a mean function constitute a Gaussian Process. A key factor in GPR is the kernel function selection. It is crucial to select the right hyperparameters, such as those found in the kernel function. To increase the likelihood of the observed data, these hyperparameters are frequently optimized for GPR. Among various available techniques, rational quadratic, squared exponential, Matern 5/2, exponential, and optimizable GPR were tried and evaluated in this study.

Parameters optimization and model selection

Each of the four regression approaches, namely GPR, SVM, linear regression, and ensemble methods, offers a variety of pre-existing algorithms to choose from. The algorithms underwent rigorous testing and were evaluated based on their predictive accuracy. The algorithm with the highest effectiveness for each method was chosen, and feature selection techniques were subsequently utilized to improve the performance of the model. The feature selection approach entailed systematically lowering the least significant features to discover the ideal subset for each regression model, by assessing different combinations. Later on, PCA was utilized both with and without feature selection to assess its influence on model correctness. The integration of feature selection and PCA resulted in improved model accuracy. Ultimately, an optimization strategy was employed to further refine the model, utilizing the most effective combinations of PCA and feature selection

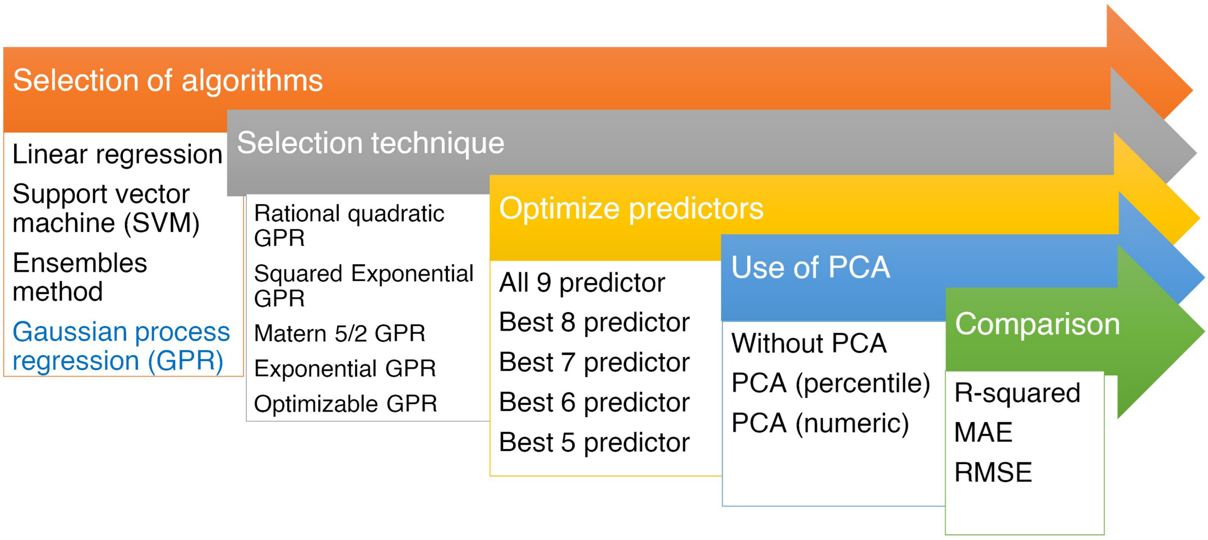

Figure 2. Evaluation and optimization of model (GPR). GPR: Gaussian process regression; PCA: principal component analysis; MAE: mean absolute error; RMSE: root mean squared error.

[Figure 2]. In order to achieve optimization, three techniques were taken into consideration: Bayesian optimization, grid search, and random search. Eventually, Bayesian optimization was chosen to fine-tune the models.

Evaluation of model and validation

In order to overcome the constraints and possible shortcomings of ML models utilized in arsenic adsorption research from aqueous solutions, evaluation and validation are essential. Inadequate or non-representative datasets, sensitivity to hyperparameters, or problems such as underfitting or overfitting can all pose problems for these models. To maximize the model's performance and adaptability for adsorption investigations under various experimental settings, rigorous validation guarantees the accuracy of predictions. In order to ensure the data's excellent quality, preprocessing procedures were employed. Both the trial-and-error methodology and hyperparameter tuning approaches, specifically Bayesian optimization in this case, were employed to fine-tune the hyperparameters. Regression models are assessed using several approaches, such as the coefficient of determination (R^2), mean absolute error (MAE), and root mean squared error (RMSE)[75]. Training ML models requires avoiding both overfitting and underfitting[76]. By adding a regularization loss function and expanding the training dataset, overfitting can be prevented[77]. On the other hand, lowering regularization parameters and raising the model's complexity - for example, by utilizing larger polynomial terms or more features - can lessen underfitting[78]. Three types of validation schemes are available: cross-validation, holdout validation, and resubstitution. Resubstitution is incapable of preventing overfitting, whereas holdout validation is more effective for large datasets. Cross-validation is an effective approach for evaluating a model's ability to generalize and handle variations[79]. Ten percent of the data in this study were allocated for testing, while the remaining 90% were used to train the model randomly using five-fold cross-validation[80]. After the training process, a random selection of 10% of the data was set aside to test the model and confirm its validation. ML models are often interpreted using the PDP, SHAP, and LIME. By visualizing the correlation between certain input properties and the anticipated result, PDP offers valuable insights into how modifications to particular variables impact the model's predictions. SHAP provides consistent and thorough explanations for the entire dataset by quantifying the contribution of each feature to the model's prediction using cooperative game theory. Rather than discussing the complete model, LIME concentrates on elucidating specific predictions. It achieves this by constructing a localized, simplified model approximation around the specific prediction being examined. When used in tandem, these techniques improve comprehension of intricate ML models and make them more accessible and useful. R^2, RMSE and MAE equations are as follows: (1), (2), and (3). In these Equations, y represents the response value (sorption capacity), $\overline{y}$ represents the average response value, $\hat{y}$ is the model predicted value, and N is the observation number.

$$R^2 = 1 - \frac{\sum(y_i - \hat{y})^2}{\sum(y_i - \bar{y})^2} \tag{1}$$

$$\text{RMSE} = \sqrt{\frac{1}{N}\sum_{i=1}^{N}(y_i - \hat{y})^2} \tag{2}$$

$$\text{MAE} = \frac{1}{N}\sum_{i=1}^{N} |y_i - \hat{y}| \tag{3}$$

RESULTS AND DISCUSSION

Data collection and preprocessing

The initial data analysis involved calculating the mean, minimum, maximum, and standard deviation. Additionally, preprocessing processes were performed when required. No missing values were present. The histogram plot of all predictors is shown in Figure 3. In order to be suitable for regression analysis, data must undergo preprocessing techniques such as standardization, normalization, and modification. From the histogram plot, data transformation was done to make it normally distributed as much as possible. Figure 4 shows the correlation coefficient values of arsenic adsorption capacity with nine variables among them. There was no presence of collinearity among the nine variables examined in the study. The significance levels of the different factors were consistent, and the Pearson correlation coefficients revealed a similar level of linkage among these variables.

These plots did not include fixed parameters beyond those used in the plot. The strongest correlation between the adsorption capacity and the starting concentration amount was observed. Since there are more ions available for adsorption, a higher initial concentration of arsenic leads to higher adsorption. Furthermore, it might decrease at low adsorbent concentrations, which would leave fewer sites available for adsorption[81,82]. The correlation plot revealed that the amount of iron salt utilized in the production of PFMB, together with the duration of the batch experiment, were identified as the two most significant elements impacting the outcome. The plot of adsorbent quantity utilization demonstrates an initial increase with higher amounts, followed by a subsequent drop with further increases in quantity. Once a location becomes accessible for adsorption, it can significantly enhance the effectiveness of removal.

Oversaturation can lead to ineffective adsorption since more adsorption sites might go unused, which would reduce overall efficiency[83,84]. The observed decline in correlation was partly caused by variations in the relationship between the parameters, which were shown by the correlation plot. For example, 125 rpm was the shaking speed that resulted in the best adsorption efficiency, but both lower and higher speeds decreased adsorption[51]. As shaking speed increased, desorption increased and adsorption decreased at lower speeds. Additionally, as iron salts were more successful in adsorbing heavy metals, the adsorption capacity was negatively correlated with adsorbent quantities and the substitution of iron salts for aluminum salts[85]. Interestingly, despite the fact that biomass and charcoal were supposed to improve porosity, their presence had no discernible effect on adsorption. Research has shown that biosorbents made from Moringa

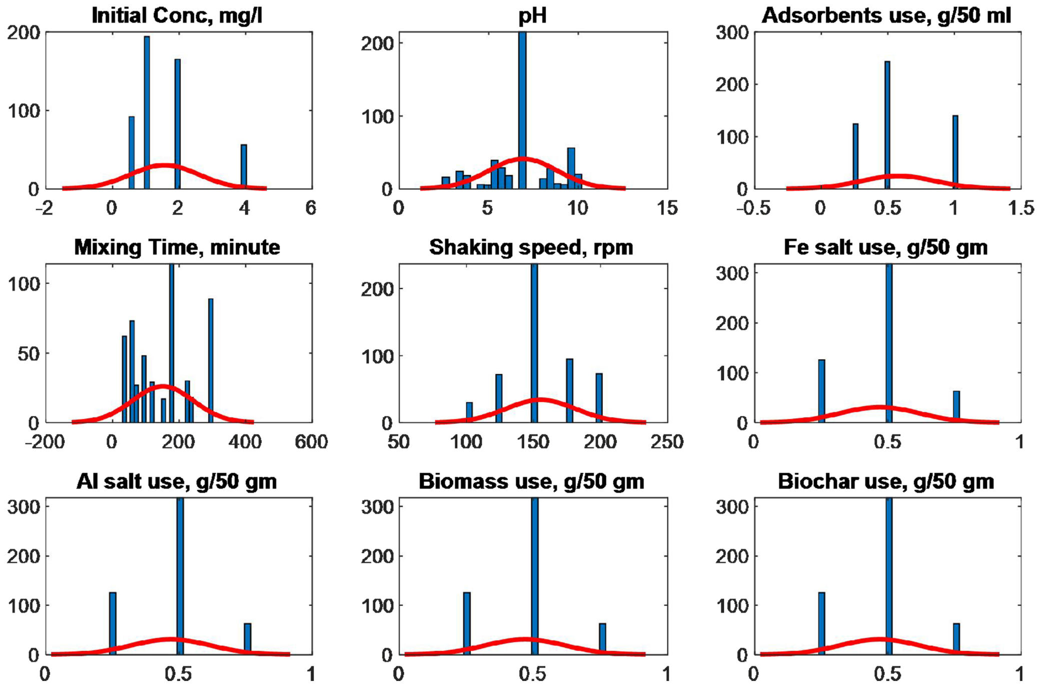

Figure 3. Histogram plot of 09 predictors (507 nos).

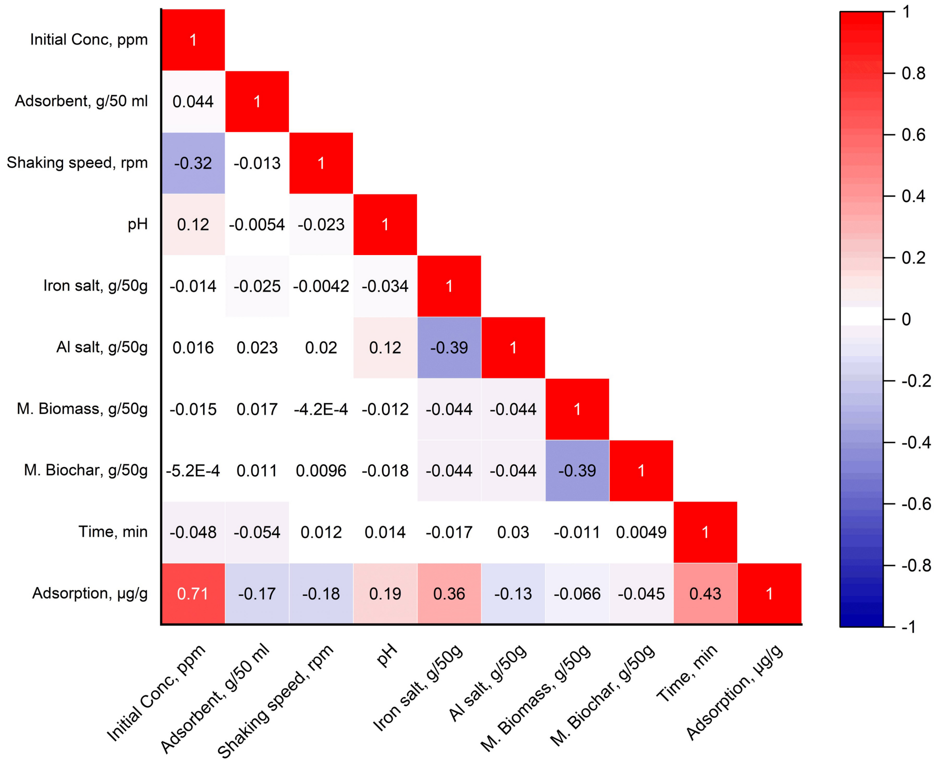

	Initial Conc, ppm	Adsorbent, g/50 ml	Shaking speed, rpm	pH	Iron salt, g/50g	Al salt, g/50g	M. Biomass, g/50g	M. Biochar, g/50g	Time, min	Adsorption, µg/g
Initial Conc, ppm	1									
Adsorbent, g/50 ml	0.044	1								
Shaking speed, rpm	-0.32	-0.013	1							
pH	0.12	-0.0054	-0.023	1						
Iron salt, g/50g	-0.014	-0.025	-0.0042	-0.034	1					
Al salt, g/50g	0.016	0.023	0.02	0.12	-0.39	1				
M. Biomass, g/50g	-0.015	0.017	-4.2E-4	-0.012	-0.044	-0.044	1			
M. Biochar, g/50g	-5.2E-4	0.011	0.0096	-0.018	-0.044	-0.044	-0.39	1		
Time, min	-0.048	-0.054	0.012	0.014	-0.017	0.03	-0.011	0.0049	1	
Adsorption, µg/g	0.71	-0.17	-0.18	0.19	0.36	-0.13	-0.066	-0.045	0.43	1

Figure 4. Correlation coefficient plot for predictors and response.

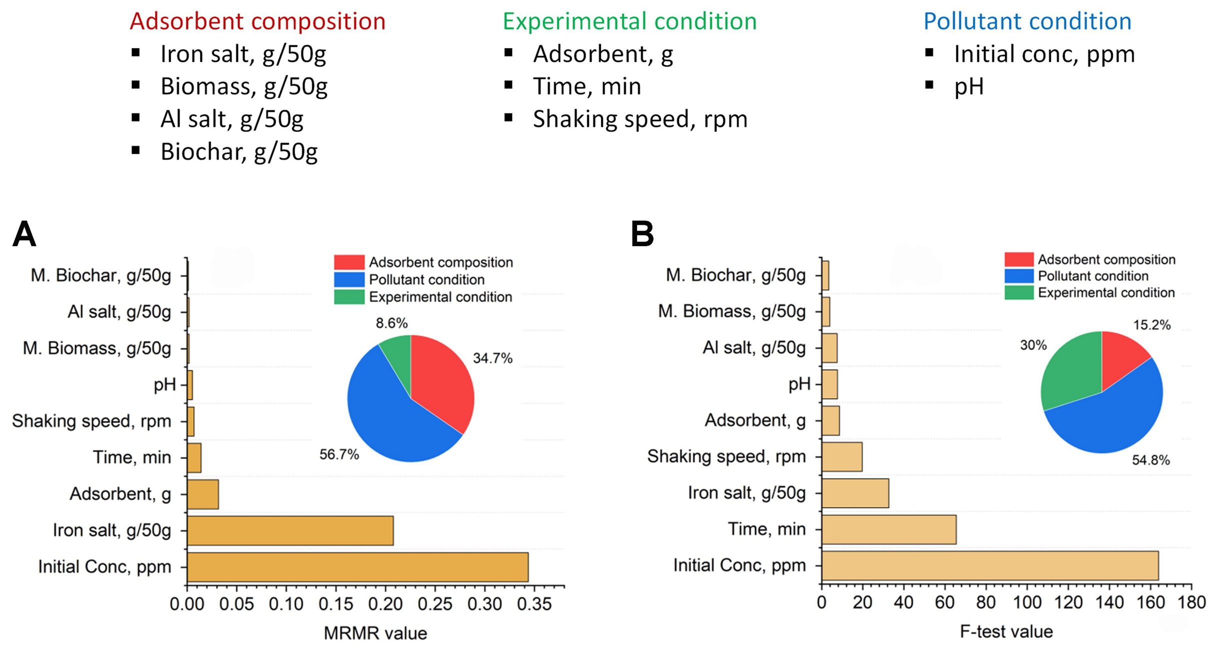

Figure 5. The analysis of feature importance using (A) MRMR and (B) F-test algorithms. MRMR: Minimum redundancy maximum relevance.

oleifera are effective in adsorption; nevertheless, compared to iron salts, metal salts may degrade composite performance[86]. Furthermore, interactions between the adsorbent and particular types of arsenic are significantly influenced by the point of zero charge (PZC). Higher pH values, usually between 5 and 10, improve adsorption, according to the link between pH and adsorption effectiveness[87]. Excellent As(III) adsorption capabilities were demonstrated by mesoporous iron oxide in the pH range of 5-9, with peak adsorption occurring at pH 8.0[88].

The analysis of feature importance using the MRMR and F-test algorithms is displayed in Figure 5. After that, the nine predictors were divided into three groups: composition of the adsorbent, condition of the pollutant, and experimental condition. The findings from both algorithms were quite similar, showing that the state of the pollutant had a greater influence on adsorption than any other factor, accounting for over 50% of the total. The adsorbent composition had the least significant impact on adsorption.

ML models

SL and IL were the two methods used in the linear regression model. Using the F-test and MRMR to assess each feature's relevance, the nine features were reduced to the top five. In addition, PCA was used. Based on the evaluation, it was determined that the IL model with six essential features produced the best results for training and validation when neither PCA nor the robust form were used. The three unused features were biochar, biomass, and Al salt. With a training duration of 7.7448 s, this model was able to predict 8,800 observations per second. Evaluation parameters for the most efficient model were as follows: RMSE 7.867, MSE 61.89, R-squared 0.92503, and MAE 6.4483 for training validation; and RMSE 8.6876, MSE 75.475, R-squared 0.9194, and MAE 7.4623 for testing [Figure 6].

The quadratic SVM was found to be the most effective model for our adsorption analysis during the training and testing phases of the SVM algorithm. The appropriate algorithms were chosen, and then feature selection, PCA, and optimization were carried out. The quadratic SVM, which employed an

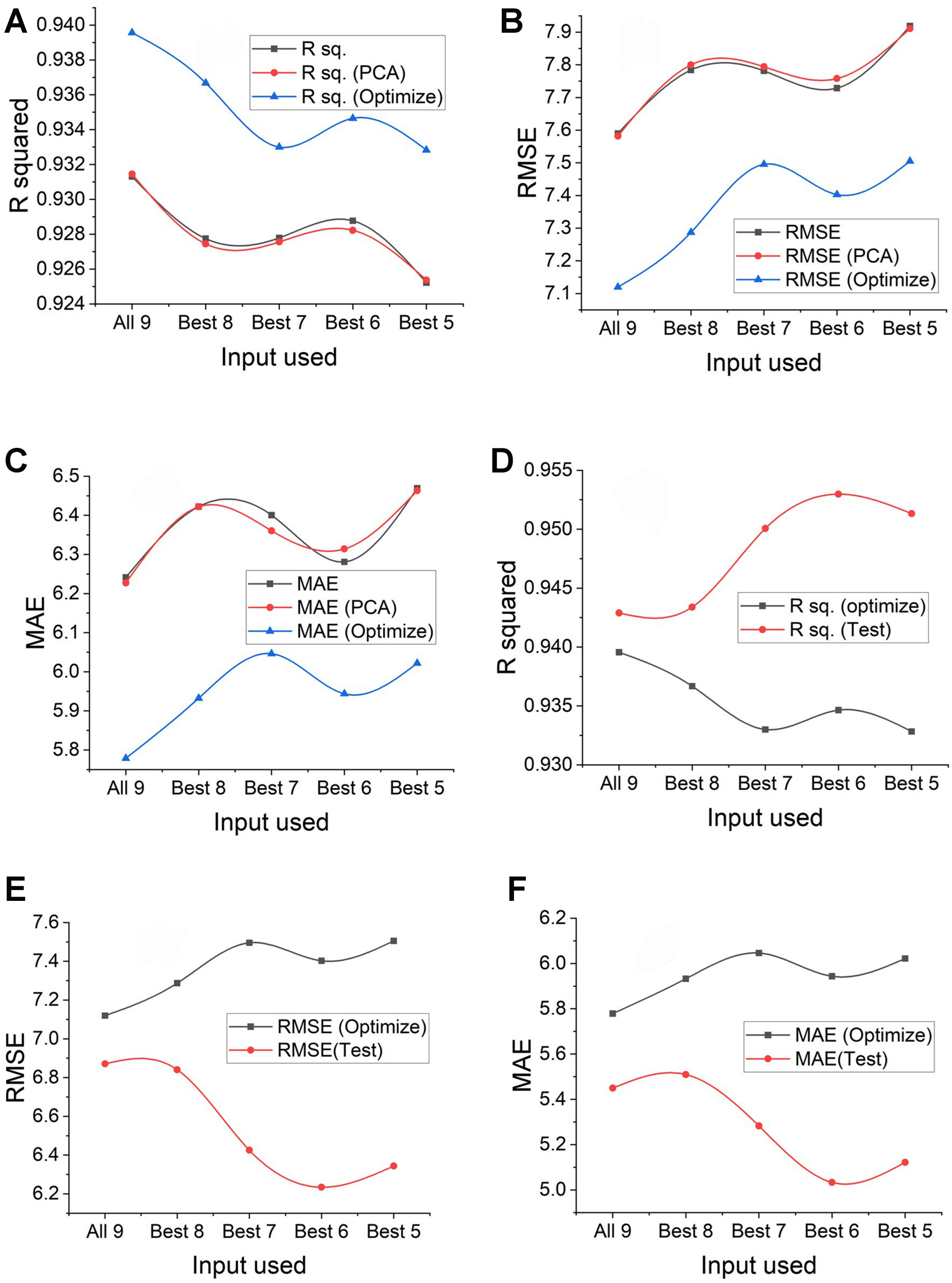

Figure 6. GPR, GPR with PCA, and GPR optimize algorithms were used with variating input features to (A) R squared; (B) RMSE; and (C) MAE. Model of GPR optimize algorithm was tested with (D) R squared; (E) RMSE; and (F) MAE. GPR: Gaussian process regression; PCA: principal component analysis; RMSE: root mean squared error; MAE: mean absolute error.

automatic epsilon, automatic box constant, automatic kernel size, and quadratic kernel function, was the best SVM model. PCA was used, without optimization, keeping nine numerical components with all nine features that were chosen. The model's prediction speed was about 4,200 observations per second, and its training time was 4.7034 s. We next compared these outcomes with those of other models. For training and validation, the most efficient SVM model showed RMSE of 8.0644, MSE of 65.034, R-squared of 0.92188, and MAE of 6.5322; for testing, the results showed RMSE of 8.2772, MSE of 68.513, R-squared of 0.91671, and MAE of 6.7366 [Figure 6].

We used the bagged tree, boosted tree, and optimizable tree algorithms in the ensemble regression analysis. After applying feature selection, PCA was employed with every feature that had been chosen. The ensemble methods were then optimized, and the outcomes were contrasted to assess the performance of the regression. With an R-squared value of 0.92739, it was verified that the optimization ensembles including all 9 characteristics produced the best outcomes without the use of PCA. The strong predictive performance of this model is indicated by the close alignment of test results and training time validation findings. Table 3 lists all of the parameters that were used in the best ensemble model. An optimizable ensemble, the most efficient model, showed the following assessment metrics: RMSE was 7.7964, MSE was 60.784, R-squared was 0.92739, and MAE was 6.0745 for training and validation; RMSE was 6.85, MSE was 46.923, R-squared was 0.94389, and MAE was 5.414 for testing [Figure 6].

The GPR algorithm was used for regression analysis and modeling. Three presets were used: Matern 5/2 GPR, rational quadratic GPR, and squared exponential GPR. The Matern 5/2 preset yielded the best results out of all of them and was kept for additional examination. After that, feature selection was used to examine the top 8, 7, 6, and 5 features with and without PCA. To preserve numerical values and the 95% variance, PCA was used. Thereafter, an optimizable GPR model was used and contrasted with alternative GPR models. The optimizable GPR with all 9 characteristics and no PCA produced the best results [Figure 6]. Table 4 provides a thorough breakdown of the parameters used in the optimized GPR model. The optimized GPR model demonstrated the subsequent assessment measures, making it the most efficient model: In testing, RMSE was 6.8707, MSE was 47.207, R-squared was 0.94289, and MAE was 5.45; in training and validation, RMSE was 7.1194, MSE was 50.686, R-squared was 0.93956, and MAE was 5.7789.

Comparison of ML models

Upon evaluating the efficacy of distinct ML methods in forecasting arsenic (III) adsorption capacity through the utilization of PFMBs, significant insights become apparent. The optimal GPR model performed better than the others, with the highest R^2 values (0.94289 for the test and 0.93956 for validation) and the lowest RMSE (7.1194 for validation and 6.8707 for the test), demonstrating higher accuracy and dependability [Table 5]. For this approach, the test and training outcomes are likewise close, indicating the model's accuracy. Figure 7 displays the true reaction and forecast, demonstrating how the perfect prediction and true values line up. According to the optimization iteration, after about 30 iterations, the lowest MSE difference between the observed and model values was reached. With an R^2 of 0.94389 and a test RMSE of 6.85, the improved ensemble model performed admirably, closely trailing the GPR in terms of predictive power. Comparing the parameters of a neural network model with a non-neural network model (GPR) using similar data sets showed that the neural network performed better than the GPR model during the validation stage. However, in the testing phase, the non-neural network model exhibited superior efficiency. The allocation of data varied among the training, validation, and testing stages for each model. Within the neural network, 70% of the dataset was allocated for training purposes, while 15% was designated for validation and the other 15% was set aside for testing. Conversely, in the case of non-neural network models, 90% of the data were utilized for training the model, which involved validation using five-fold cross-validation. The remaining 10% was set aside specifically for testing purposes. This comparison demonstrates that non-neural network techniques can be equally effective as neural network algorithms when used in these experimental data sets. In comparison to GPR and the ensemble model, the SVM with PCA showed lower R^2 values (0.92188 for validation and 0.91671 for test) and somewhat higher error metrics (validation RMSE of 8.0644 and test RMSE of 8.2772), despite being effective. Using fewer features led to less accurate predictions, as evidenced by the interaction linear model with the best six features

Table 3. The parameters were used for the best Ensemble algorithms

ML model	Prediction speed	Training time	Preset	Method	Minimum leaf size	Nos of learners	Learning rate	Nos of predictors used	iterations	Training time limit
Ensemble	~600 obs/s	225.76 s	Optimize	Boosted trees	1	14	0.38311	9	30	False

ML: Machine learning.

Table 4. The parameters were used for the best GPR algorithms

ML model	Prediction speed	Training time	Signal standard deviation	Optimize numeric parameters	Basic function	Kernel function	Kernel scale	Sigma	iterations	Training time limit
GPR optimize	~1,300 obs/s	1,305.9 s	20.4671	Yes	Constant	Nonisotropic rational quadratic	0.12835	0.0020662	30	False

GPR: Gaussian process regression; ML: machine learning.

Table 5. Four ML algorithms with best model input conditions and results

Algorithms used	Feature used	RMSE (validation)	R squared (validation)	MAE (validation)	MAE (test)	RMSE (test)	R squared (test)
SVM (PCA)	All 9	8.0644	0.92188	6.5322	6.736	8.2772	0.91671
GPR (optimize)	All 9	7.1194	0.93956	5.7789	5.45	6.8707	0.94289
Ensemble (optimize)	All 9	7.7964	0.92739	6.0745	5.414	6.85	0.94389
Interaction linear	Best 6	7.867	0.92503	6.4483	7.4623	8.6876	0.9194
Neural network[51]	All 9	6.75	0.955			7.76	0.928

ML: Machine learning; RMSE: root mean squared error; MAE: mean absolute error; SVM: support vector machines; PCA: principal component analysis; GPR: Gaussian process regression.

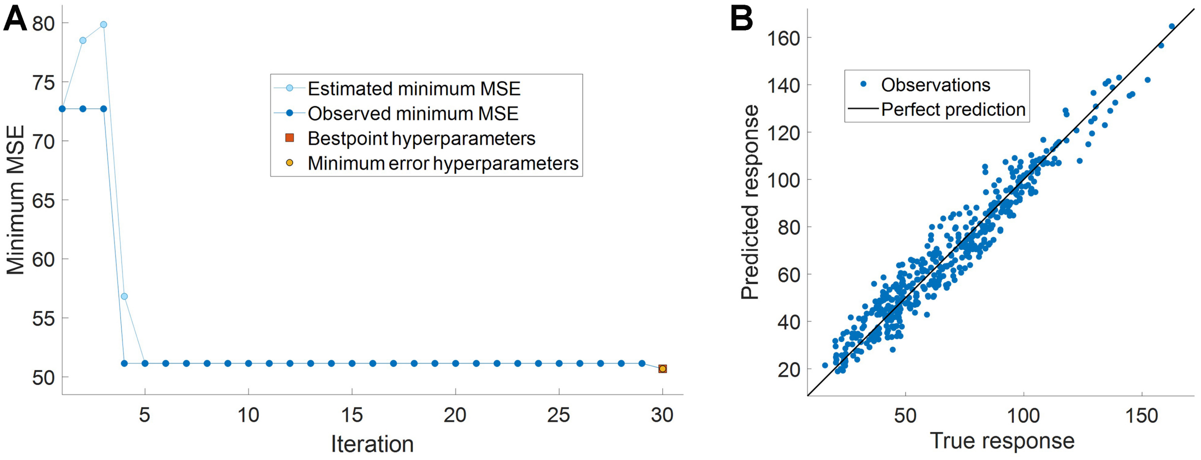

Figure 7. (A) Model plots of optimizable GPR minimum MSE plot, and (B) prediction *vs.* true response plot of optimized GPR. GPR: Gaussian process regression; MSE: mean squared error.

having the greatest error metrics (validation RMSE of 7.867 and test RMSE of 8.6876). The investigation, taken as a whole, emphasizes the value of ensemble approaches and feature optimization in reaching high

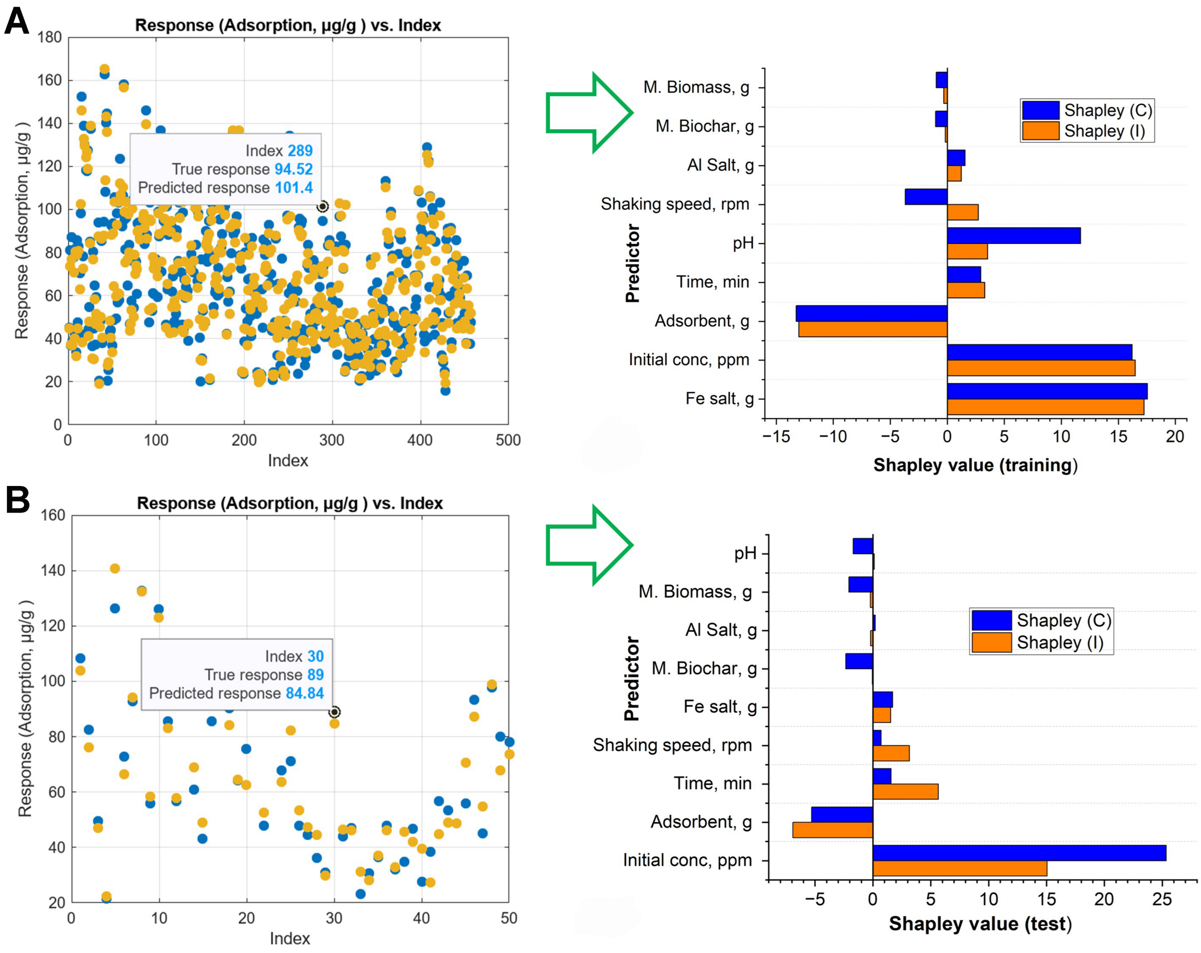

Figure 8. Shapley plot for training [(A) for index:289], and for test [(B) for index: 30] with response plot of the model optimized GPR. GPR: Gaussian process regression.

predicted accuracy for adsorption capacity.

Model explanations

In this investigation, the contributions of individual variables to the adsorption capacity predictions were interpreted using SHAP. The SHAP values suggest that the initial concentration of arsenic and the time of contact have the most significant beneficial impact on adsorption efficiency. This highlights the critical roles that these factors play in the process. Furthermore, the interactions between features were emphasized using SHAP value distributions. For example, the combined impacts of temperature and pH had a greater influence on adsorption capacity than each variable alone. These observations are consistent with theoretical interpretations of adsorption dynamics, confirming the resilience of the model and improving our understanding of the underlying mechanisms. SHAP analysis was carried out utilizing both conditional and interventional approaches for a particular training data point (index 289), where the true value was 94.52 and the predicted value was 101.4, and a test data point (index 30), with a true value of 89 and a predicted value of 84.84 [Figure 8]. The use of iron salt and the starting concentration of arsenic were shown to have the greatest effects in both situations, whereas the amount of adsorbent had the opposite impact. The dependability of the model's explanations is supported by the consistency of these outcomes across approaches. These results were visually verified by the SHAP plots, which displayed the various contributions to the model's predictions and how well they matched the actual values[89,90]. PCA was used to

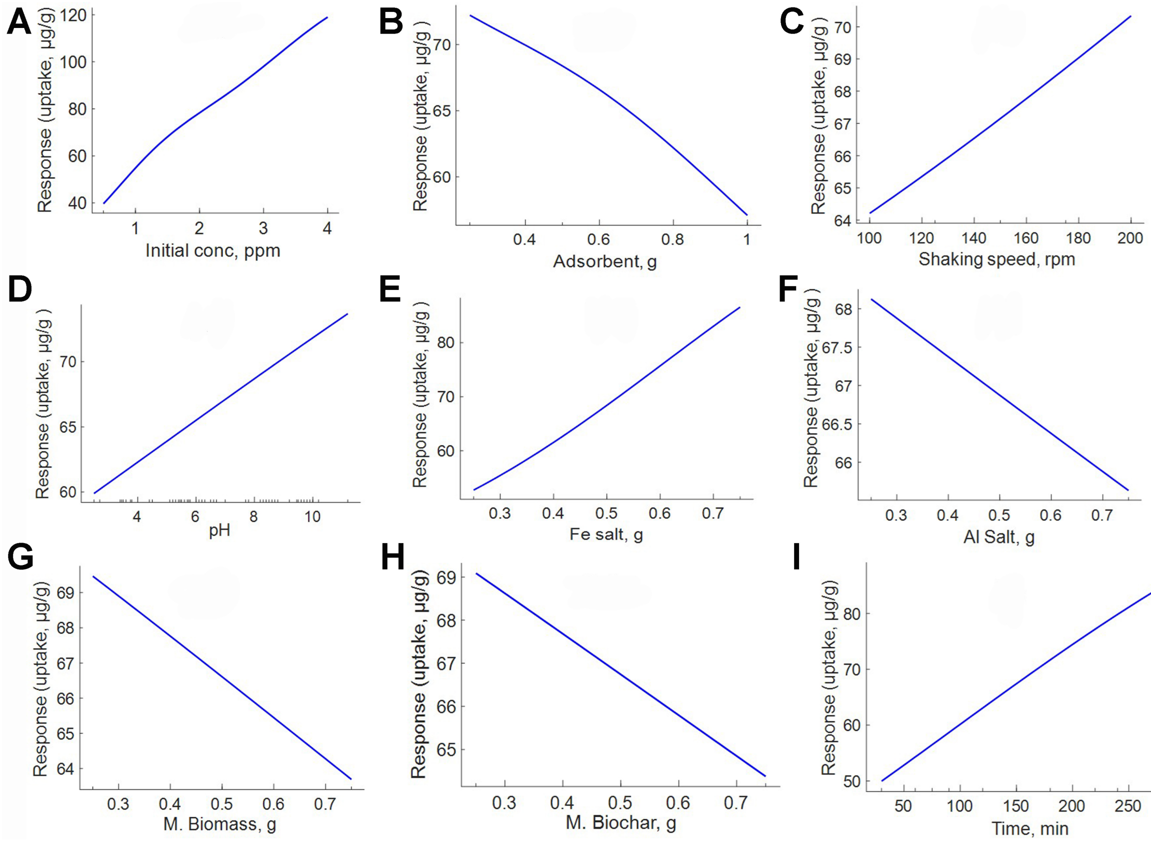

Figure 9. PDP of the optimized GPR model. PDP: Partial dependence plot; GPR: Gaussian process regression.

reduce components to improve accuracy and simplify the model. PCA was applied in both available ways: by specifying explained variance and the number of components. For this study, all regression analyses showed better results when specifying the number of components than the explained variance. The figure shows the number of components required to explain 95% of the variance in the data.

The optimized GPR model was used to illustrate the association between nine important factors and the anticipated adsorption capacity of arsenic (III) onto PFMBs using PDPs [Figure 9]. The PDPs have detected some noteworthy tendencies, which are as follows: A direct correlation was observed between the sorption efficiency and the starting arsenic concentration, as the adsorption capacity increased rapidly from 40 to 120 µg/g with an increase in the initial arsenic concentration ranging from 0.5 to 4 ppm. However, the sorption efficiency decreased from 75 to 55 µg/g when the quantity of adsorbent was raised from 0.25 to 1 g per 50 mL. The adsorption capacity exhibited a slight increase from 60 to 70 µg/g and 60 to 75 µg/g, respectively, with varying shaking speeds (100 to 200 rpm) and pH levels (3 to 12). The pH range specified denotes the optimal range for achieving maximum efficiency. The addition of iron salt (used as 0.25 to 0.75 g per 50 g) enhanced the adsorption capacity from 50 to 90 µg/g. However, the addition of aluminum salt somewhat decreased it from 68 to 65 µg/g. The addition of 0.25 to 0.75 g of biochar and biomass reduced the adsorption capacity from 70 to 60 µg/g. Capacity rose from 50 to 90 µg/g when the adsorption duration was extended from 30 to 300 min. These results draw attention to the intricate interactions between variables and offer suggestions for improving adsorbent formulations and testing setups[91,92].

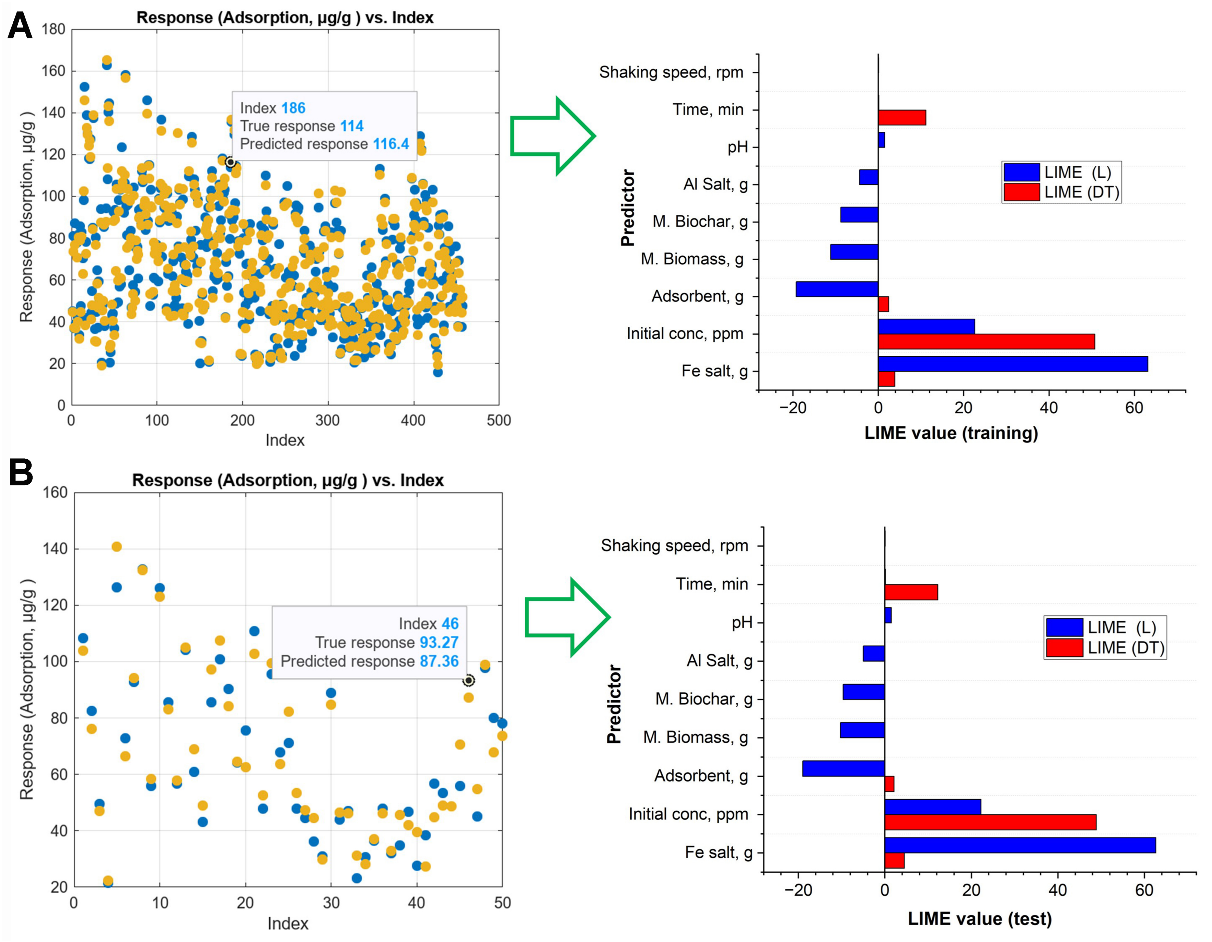

Figure 10. LIME plots for training [(A) index:186], and for test [(B) index: 46] with response plot of the model optimized GPR using linear and decision tree model. LIME: Local interpretable model-agnostic explanations; GPR: Gaussian process regression.

Here, optimized GPR predictions on adsorption capacity were analyzed using artificial predictor data with 5,000 samples, and LIME was used to provide an explanation. At index 46, where the experimental adsorption capacity was 93.27 and the model anticipated 87.36, we looked at the test data while maintaining a focus on local data locality with 1,500 neighbors and a kernel width of 0.75. Indicating that the linear model offered a closer approach to the model's prediction, the LIME explanation values were 86.56 for the linear model and 63.89 for the tree-based model. As can be seen in Figure 10, the LIME explanations for the training data at index 186, with an experimental value of 114 and a model prediction of 116.4, were 112.04 for the linear model (with a kernel width of 0.95) and 113.38 for the tree-based model. This implies that although the tree-based model can also give plausible explanations depending on the situation, the linear model constantly provides closer approximations.

CONCLUSIONS

Arsenic removal is sometimes difficult and expensive; however, using inexpensive adsorbents is a viable way to produce safe water. An efficient method for estimating adsorbent capacity without requiring a lot of trial-and-error laboratory testing is ML modeling. In this work, we employed non-neural network algorithms as a feasible substitute for conventional neural network techniques in modeling arsenic adsorption studies. The data used in this work came from earlier batch tests on the adsorption of arsenic using a PFMB made of biomass, aluminum salt, gypsum-based iron salt, and moringa bark biochar. Predictive models were created using four non-neural network algorithms: ensemble techniques, linear regression, GPR, and SVM. Nine predictors were considered, including variations in the adsorbent composition, such as the proportions of iron salt, aluminum salt, moringa biochar, and moringa biomass, as well as experimental circumstances such as pH, shaking speed, initial concentration, adsorbent amount, and time. Every algorithm underwent optimization via feature selection and PCA application. F-test and MRMR algorithms were utilized for feature reduction. Using R-squared, MAE, and RMSE values for comparative study, it was shown that the optimized GPR algorithm performed the best in terms of prediction. The most important variables in adsorption efficiency were the initial arsenic concentration, time, and iron salt content in the adsorbent. This was further clarified using SHAP, LIME, and PDP plots, which also demonstrated the effectiveness of the most efficient model. This paper shows that adsorption tests can be efficiently modeled by non-neural network techniques, and the performance of adsorbents may be optimized by using parameters that are generated from the model. By adding more controllable parameters or predictors, such as more specific physicochemical characteristics and experimental settings, the model's effectiveness can be further increased. For the effective removal of heavy metals or other contaminants, this methodology provides a useful way to optimize composite adsorbents in removal technologies. In order to optimize the efficacy of the adsorbent composition and potentially expand its use in a variety of environmental cleanup initiatives, future research should investigate the integration of these extra components.

DECLARATIONS

Authors' contributions

Conceived and designed collaboratively: Mirza NH, Fujino T
Experimental data collection: Mirza NH
Computational model development and simulations: Mirza NH
Data analysis, interpretation of results, and manuscript writing: Mirza NH, Fujino T
Both authors approved the final version of the manuscript before submission.

Availability of data and materials

The datasets used in the study are available from the corresponding author upon reasonable request.

Financial support and sponsorship

None.

Conflicts of interest

All authors declared that there are no conflicts of interest.

Ethical approval and consent to participate

Not applicable.

Consent for publication

Not applicable.

Copyright

REFERENCES

1. Ren X, Chen C, Nagatsu M, Wang X. Carbon nanotubes as adsorbents in environmental pollution management: a review. *Chem Eng J* 2011;170:395-410. DOI

2. Chung JY, Yu SD, Hong YS. Environmental source of arsenic exposure. *J Prev Med Public Health* 2014;47:253-7. DOI PubMed PMC
3. Ravenscroft P, Brammer H, Richards K. Arsenic pollution: a global synthesis. Oxford, UK: Wiley-Blackwell, 2009. DOI
4. Smedley P, Kinniburgh D. A review of the source, behaviour and distribution of arsenic in natural waters. *Appl Geochem* 2002;17:517-68. DOI
5. Chutia P, Kato S, Kojima T, Satokawa S. Arsenic adsorption from aqueous solution on synthetic zeolites. *J Hazard Mater* 2009;162:440-7. DOI PubMed
6. Song W, Zhang M, Liang J, Han G. Removal of As(V) from wastewater by chemically modified biomass. *J Mol Liq* 2015;206:262-7. DOI
7. Sigdel A, Park J, Kwak H, Park P. Arsenic removal from aqueous solutions by adsorption onto hydrous iron oxide-impregnated alginate beads. *J Ind Eng Chem* 2016;35:277-86. DOI
8. Sun J, Zhang X, Zhang A, Liao C. Preparation of Fe-Co based MOF-74 and its effective adsorption of arsenic from aqueous solution. *J Environ Sci* 2019;80:197-207. DOI
9. Wang C, Luan J, Wu C. Metal-organic frameworks for aquatic arsenic removal. *Water Res* 2019;158:370-82. DOI PubMed
10. Holm TR. Effects of CO_3^{2-}/bicarbonate, Si, and PO_4^{3-} on Arsenic sorption to HFO. *J AWWA* 2002;94:174-81. DOI
11. Bissen M, Frimmel FH. Arsenic - a review. Part II: oxidation of Arsenic and its removal in water treatment. *Acta hydrochim hydrobiol* 2003;31:97-107. DOI
12. Choong TS, Chuah T, Robiah Y, Gregory Koay F, Azni I. Arsenic toxicity, health hazards and removal techniques from water: an overview. *Desalination* 2007;217:139-66. DOI
13. Norberto J, Zoroufchi Benis K, Mcphedran KN, Soltan J. Microwave activated and iron engineered biochar for arsenic adsorption: life cycle assessment and cost analysis. *J Environ Chem Eng* 2023;11:109904. DOI
14. Masue Y, Loeppert RH, Kramer TA. Arsenate and arsenite adsorption and desorption behavior on coprecipitated aluminum:iron hydroxides. *Environ Sci Technol* 2007;41:837-42. DOI PubMed
15. Mohan D, Pittman CU Jr. Arsenic removal from water/wastewater using adsorbents - a critical review. *J Hazard Mater* 2007;142:1-53. DOI PubMed
16. Lee B, Kim Y, Lee H, Yi J. Synthesis of functionalized porous silicas via templating method as heavy metal ion adsorbents: the introduction of surface hydrophilicity onto the surface of adsorbents. *Micropor Mesopor Mat* 2001;50:77-90. DOI
17. Ahmaruzzaman M. Industrial wastes as low-cost potential adsorbents for the treatment of wastewater laden with heavy metals. *Adv Colloid Interface Sci* 2011;166:36-59. DOI PubMed
18. Zhang L, Zeng Y, Cheng Z. Removal of heavy metal ions using chitosan and modified chitosan: a review. *J Mol Liq* 2016;214:175-91. DOI
19. Tizhe B, Osemeahon S, Nkafamiya I, Shagal M. Biosorption of metal ions from aqueous solution by immobilized moringa oleifera bark. *IRJPAC* 2015;5:238-44. DOI
20. Barua S, Rahman IMM, Nazimuddin M, Hasegawa H. Evaluation of Moringa oleifera carbon for the As(III) removal from contaminated groundwater. *Int J Innov Appl Stud* 2014;8:1390-9. Available from: https://www.cabidigitallibrary.org/doi/full/10.5555/20153089415. [Last accessed on 7 Dec 2024]
21. Mirza NH, Fujino T. Gypsum-based porous media filter with solid waste: a novel composite for removing arsenic (III) from aqueous solution. *Int J Eng* 2025;38:735-43. DOI
22. Ouyang D, Zhuo Y, Hu L, Zeng Q, Hu Y, He Z. Research on the adsorption behavior of heavy metal ions by porous material prepared with silicate tailings. *Minerals* 2019;9:291. DOI
23. Mazloom G, Farhadi F, Khorasheh F. Kinetic modeling of pyrolysis of scrap tires. *J Anal Appl Pyrol* 2009;84:157-64. DOI
24. Khraibet SA, Mazloom G, Banisharif F. Comparative study of different two-phase models for the propane oxidative dehydrogenation in a bubbling fluidized bed containing the $VO_x/\gamma\text{-}Al_2O_3$ catalyst. *Ind Eng Chem Res* 2021;60:9729-38. DOI
25. Jaffari ZH, Abbas A, Kim CM, et al. Transformer-based deep learning models for adsorption capacity prediction of heavy metal ions toward biochar-based adsorbents. *J Hazard Mater* 2024;462:132773. DOI
26. Yaseen ZM. An insight into machine learning models era in simulating soil, water bodies and adsorption heavy metals: Review, challenges and solutions. *Chemosphere* 2021;277:130126. DOI PubMed
27. Xiong T, Cui J, Hou Z, et al. Prediction of arsenic adsorption onto metal organic frameworks and adsorption mechanisms interpretation by machine learning. *J Environ Manage* 2023;347:119065. DOI
28. Liu R, Zuo L, Zhang P, Zhao J, Tao D. A deep learning neural network approach for predicting the factors influencing heavy-metal adsorption by clay minerals. *Clay Miner* 2022;57:70-6. DOI
29. Shaheen SM, Niazi NK, Hassan NE, et al. Wood-based biochar for the removal of potentially toxic elements in water and wastewater: a critical review. *Int Mater Rev* 2019;64:216-47. DOI
30. Mongioví C, Crini G, Gabrion X, et al. Revealing the adsorption mechanism of copper on hemp-based materials through EDX, nano-CT, XPS, FTIR, Raman, and XANES characterization techniques. *Chem Eng J Adv* 2022;10:100282. DOI
31. Mallik AK, Moktadir MA, Rahman MA, Shahruzzaman M, Rahman MM. Progress in surface-modified silicas for Cr(VI) adsorption: a review. *J Hazard Mater* 2022;423:127041. DOI PubMed
32. Ismail UM, Onaizi SA, Vohra MS. Aqueous Pb(II) removal using ZIF-60: adsorption studies, response surface methodology and machine learning predictions. *Nanomaterials* 2023;13:1402. DOI PubMed PMC

33. Abdi J, Mazloom G. Machine learning approaches for predicting arsenic adsorption from water using porous metal-organic frameworks. *Sci Rep* 2022;12:16458. DOI PubMed PMC
34. Aftab RA, Zaidi S, Danish M, Ansari KB, Danish M. Novel machine learning (ML) models for predicting the performance of multi-metal binding green adsorbent for the removal of Cd (II), Cu (II), Pb (II) and Zn (II) ions. *Environ Adv* 2022;9:100256. DOI
35. Zhu X, Wan Z, Tsang DC, et al. Machine learning for the selection of carbon-based materials for tetracycline and sulfamethoxazole adsorption. *Chem Eng J* 2021;406:126782. DOI
36. Yin G, Jameel Ibrahim Alazzawi F, Mironov S, et al. Machine learning method for simulation of adsorption separation: comparisons of model's performance in predicting equilibrium concentrations. *Arab J Chem* 2022;15:103612. DOI
37. Dashti A, Raji M, Riasat Harami H, Zhou JL, Asghari M. Biochar performance evaluation for heavy metals removal from industrial wastewater based on machine learning: application for environmental protection. *Sep Purif Technol* 2023;312:123399. DOI
38. Almalawi A, Khan AI, Alqurashi F, Abushark YB, Alam MM, Qaiyum S. Modeling of remora optimization with deep learning enabled heavy metal sorption efficiency prediction onto biochar. *Chemosphere* 2022;303:135065. DOI PubMed
39. Elbana TA, Magdi Selim H, Akrami N, Newman A, Shaheen SM, Rinklebe J. Freundlich sorption parameters for cadmium, copper, nickel, lead, and zinc for different soils: influence of kinetics. *Geoderma* 2018;324:80-8. DOI
40. Ducamp M, Coudert F. Prediction of thermal properties of zeolites through machine learning. *J Phys Chem C* 2022;126:1651-60. DOI
41. Ma S, Liu Z. Machine learning for atomic simulation and activity prediction in heterogeneous catalysis: current status and future. *ACS Catal* 2020;10:13213-26. DOI
42. Mandal S, Mahapatra S, Sahu M, Patel R. Artificial neural network modelling of As(III) removal from water by novel hybrid material. *Process Saf Environ* 2015;93:249-64. DOI
43. Sakizadeh M. Artificial intelligence for the prediction of water quality index in groundwater systems. *Model Earth Syst Environ* 2016;2:63. DOI
44. Guo Y, Bartlett PL, Shawe-Taylor J, Williamson RC. Covering numbers for support vector machines. *IEEE Trans Inform Theory* 2002;48:239-50. DOI
45. Durbha SS, King RL, Younan NH. Support vector machines regression for retrieval of leaf area index from multiangle imaging spectroradiometer. *Remote Sens Environ* 2007;107:348-61. DOI
46. Čeh M, Kilibarda M, Lisec A, Bajat B. Estimating the performance of random forest versus multiple regression for predicting prices of the apartments. *IJGI* 2018;7:168. DOI
47. Wei L, Yuan Z, Zhong Y, Yang L, Hu X, Zhang Y. An improved gradient boosting regression tree estimation model for soil heavy metal (arsenic) pollution monitoring using hyperspectral remote sensing. *Appl Sci* 2019;9:1943. DOI
48. Cha Y, Kim YM, Choi JW, Sthiannopkao S, Cho KH. Bayesian modeling approach for characterizing groundwater arsenic contamination in the Mekong River basin. *Chemosphere* 2016;143:50-6. DOI
49. Jang JSR. ANFIS: adaptive-network-based fuzzy inference system. *IEEE Trans Syst Man Cybern* 1993;23:665-85. DOI
50. Abdullahi J, Rufai I, Rimtip NN, Orhon D, Aslanova F, Elkiran G. A novel approach for precipitation modeling using artificial intelligence-based ensemble models. *Desalin Water Treat* 2024;317:100188. DOI
51. Mirza NH, Fujino T. Aqueous arsenic (III) removal using a novel solid waste based porous filter media block: traditional and machine learning (ML) approaches. *Desalin Water Treat* 2024;319:100536. DOI
52. Zhu JJ, Yang M, Ren ZJ. Machine learning in environmental research: common pitfalls and best practices. *Environ Sci Technol* 2023;57:17671-89. DOI PubMed
53. Zhao S, Li J, Chen C, Yan B, Tao J, Chen G. Interpretable machine learning for predicting and evaluating hydrogen production via supercritical water gasification of biomass. *J Clean Prod* 2021;316:128244. DOI
54. Li J, Li L, Tong YW, Wang X. Understanding and optimizing the gasification of biomass waste with machine learning. *Green Chem Eng* 2023;4:123-33. DOI
55. Alemneh ST, Emire SA, Hitzmann B, Zettel V. Comparative study of chemical composition, pasting, thermal and functional properties of Teff (Eragrostis tef) flours grown in Ethiopia and South Africa. *Int J Food Prop* 2022;25:144-58. DOI
56. Smith A, Keane A, Dumesic JA, Huber GW, Zavala VM. A machine learning framework for the analysis and prediction of catalytic activity from experimental data. *Appl Catal B Environ* 2020;263:118257. DOI
57. Li J, Zhang L, Li C, et al. Data-driven based in-depth interpretation and inverse design of anaerobic digestion for CH_4-rich biogas production. *ACS EST Eng* 2022;2:642-52. DOI
58. Jamei M, Karbasi M, Alawi OA, et al. Earth skin temperature long-term prediction using novel extended Kalman filter integrated with artificial intelligence models and information gain feature selection. *Sustain Comput Infor* 2022;35:100721. DOI
59. Breiman L. Random forests. *Mach Learn* 2001;45:5-32. DOI
60. Zhu X, Wang X, Ok YS. The application of machine learning methods for prediction of metal sorption onto biochars. *J Hazard Mater* 2019;378:120727. DOI
61. Pathy A, Meher S, P B. Predicting algal biochar yield using eXtreme Gradient Boosting (XGB) algorithm of machine learning methods. *Algal Res* 2020;50:102006. DOI
62. Kooh MRR, Thotagamuge R, Chou Chau Y, Mahadi AH, Lim CM. Machine learning approaches to predict adsorption capacity of Azolla pinnata in the removal of methylene blue. *J Taiwan Inst Chem Eng* 2022;132:104134. DOI
63. Ghaedi M, Daneshfar A, Ahmadi A, Momeni M. Artificial neural network-genetic algorithm based optimization for the adsorption of phenol red (PR) onto gold and titanium dioxide nanoparticles loaded on activated carbon. *J Ind Eng Chem* 2015;21:587-98. DOI

64. Zhang S, Yuan Y, Liu C, et al. Modeling and optimization of porous aerogel adsorbent for removal of cadmium from crab viscera homogenate using response surface method and artificial neural network. *LWT* 2021;150:111990. DOI
65. Jiang H, Yang Z, Li Z. Non-parallel hyperplanes ordinal regression machine. *Knowl Based Syst* 2021;216:106593. DOI
66. Emmert-Streib F, Dehmer M. Taxonomy of machine learning paradigms: a data-centric perspective. *WIREs Data Min Knowl* 2022;12:e1470. DOI
67. Ye H, Ma X, Yang T, Hou Y. Comparative study on the performance prediction of fuel cell using support vector machine with different kernel functions. In: Proceedings of China SAE Congress 2018: Selected Papers; Singapore. 2020. pp. 337-51. DOI
68. Lee SH, Li J, Wang X, Yang K. Online-learning-aided optimization and interpretation of sugar production from oil palm mesocarp fibers with analytics for industrial applications. *Resour Conserv Recy* 2022;180:106206. DOI
69. Zhang L, Chao B, Zhang X. Modeling and optimization of microbial lipid fermentation from cellulosic ethanol wastewater by Rhodotorula glutinis based on the support vector machine. *Bioresour Technol* 2020;301:122781. DOI
70. Da T, Ren H, He W, Gong S, Chen T. Prediction of uranium adsorption capacity on biochar by machine learning methods. *J Environ Chem Eng* 2022;10:108449. DOI
71. Li J, Zhang W, Liu T, et al. Machine learning aided bio-oil production with high energy recovery and low nitrogen content from hydrothermal liquefaction of biomass with experiment verification. *Chem Eng J* 2021;425:130649. DOI
72. Li J, Suvarna M, Pan L, Zhao Y, Wang X. A hybrid data-driven and mechanistic modelling approach for hydrothermal gasification. *Appl Energy* 2021;304:117674. DOI
73. Cai J, Xu K, Zhu Y, Hu F, Li L. Prediction and analysis of net ecosystem carbon exchange based on gradient boosting regression and random forest. *Appl Energy* 2020;262:114566. DOI
74. Dehghanian N, Ghaedi M, Ansari A, et al. A random forest approach for predicting the removal of Congo red from aqueous solutions by adsorption onto tin sulfide nanoparticles loaded on activated carbon. *Desalin Water Treat* 2016;57:9272-85. DOI
75. He Z, Wang Q, Rao P, et al. WS_2 significantly enhances the degradation of sulfachloropyridazine by Fe(III)/persulfate. *Sci Total Environ* 2022;850:157987. DOI PubMed
76. Haq MA, Rahim Khan MA. DNNBoT: deep neural network-based botnet detection and classification. *Comput Mater Con* 2022;71:1729-50. DOI
77. Koeshidayatullah A. Optimizing image-based deep learning for energy geoscience via an effortless end-to-end approach. *J Pet Sci Eng* 2022;215:110681. DOI
78. Fan Y, Yang W. A backpropagation learning algorithm with graph regularization for feedforward neural networks. *Inform Sci* 2022;607:263-77. DOI
79. Yaqoob U, Younis MI. Chemical gas sensors: recent developments, challenges, and the potential of machine learning - a review. *Sensors* 2021;21:2877. DOI
80. Yuan X, Li J, Lim JY, et al. Machine learning for heavy metal removal from water: recent advances and challenges. *ACS EST Water* 2024;4:820-36. DOI
81. Alam MA, Shaikh WA, Alam MO, et al. Adsorption of As (III) and As (V) from aqueous solution by modified Cassia fistula (golden shower) biochar. *Appl Water Sci* 2018;8:839. DOI
82. Nguyen TH, Pham TH, Nguyen Thi HT, et al. Synthesis of iron-modified biochar derived from rice straw and its application to arsenic removal. *J Chem* 2019;2019:1-8. DOI
83. Yang S, Wu Y, Aierken A, et al. Mono/competitive adsorption of Arsenic(III) and Nickel(II) using modified green tea waste. *J Taiwan Inst Chem Eng* 2016;60:213-21. DOI
84. Imran M, Iqbal MM, Iqbal J, et al. Synthesis, characterization and application of novel MnO and CuO impregnated biochar composites to sequester arsenic (As) from water: modeling, thermodynamics and reusability. *J Hazard Mater* 2021;401:123338. DOI
85. Giles DE, Mohapatra M, Issa TB, Anand S, Singh P. Iron and aluminium based adsorption strategies for removing arsenic from water. *J Environ Manage* 2011;92:3011-22. DOI
86. Sumathi T, Alagumuthu G. Adsorption studies for arsenic removal using activated *Moringa oleifera*. *Int J Chem Eng* 2014;2014:1-6. DOI
87. Bae J, Kim S, Kim KS, Hwang H, Choi H. Adsorptive removal of arsenic by mesoporous iron oxide in aquatic systems. *Water* 2020;12:3147. DOI
88. Mudzielwana R, Gitari WM, Ndungu P. Removal of As(III) from synthetic groundwater using Fe-Mn bimetal modified kaolin clay: adsorption kinetics, isotherm and thermodynamics studies. *Environ Process* 2019;6:1005-18. DOI
89. Islam SR, Eberle W, Bundy S, Ghafoor SK. Infusing domain knowledge in AI-based “black box” models for better explainability with application in bankruptcy prediction. arXiv. [Preprint.] May 30, 2019 [accessed 2024 Dec 7]. Available from: https://doi.org/10.48550/arXiv.1905.11474.
90. Li J, Pan L, Suvarna M, Tong YW, Wang X. Fuel properties of hydrochar and pyrochar: prediction and exploration with machine learning. *Appl Energy* 2020;269:115166. DOI
91. Goldstein A, Kapelner A, Bleich J, Pitkin E. Peeking inside the black box: visualizing statistical learning with plots of individual conditional expectation. *J Comput Graphical Stat* 2015;24:44-65. DOI
92. Yuan X, Suvarna M, Low S, et al. Applied machine learning for prediction of CO_2 adsorption on biomass waste-derived porous carbons. *Environ Sci Technol* 2021;55:11925-36. DOI PubMed

Tang. *Water Emerg Contam Nanoplastics* 2024;3:25
DOI: 10.20517/wecn.2024.53

Water Emerging Contaminants & Nanoplastics

Review

Open Access

Valorization of organic waste as biosorbents for wastewater treatment

Kuok Ho Daniel Tang

Department of Environmental Science, The University of Arizona, Tucson, AZ 85721, USA.

Correspondence to: Prof. Kuok Ho Daniel Tang, Department of Environmental Science, The University of Arizona, 1177E. 4th Street, Tucson, AZ 85721, USA. E-mail: daniel.tangkh@yahoo.com

How to cite this article: Tang KHD. Valorization of organic waste as biosorbents for wastewater treatment. *Water Emerg Contam Nanoplastics* 2024;3:25. https://dx.doi.org/10.20517/wecn.2024.53

Received: 3 Aug 2024 **First Decision:** 14 Oct 2024 **Revised:** 16 Nov 2024 **Accepted:** 26 Nov 2024 **Published:** 21 Dec 2024

Academic Editor: Marco Race **Copy Editor:** Pei-Yun Wang **Production Editor:** Pei-Yun Wang

Abstract

With increasing population and waste generation, organic waste disposal has presented an unprecedented challenge. Valorization of the waste for wastewater treatment emerges as a feasible way to recycle or upcycle the waste. Agricultural and non-agricultural waste has been successfully converted into biosorbents to remove various pollutants. Through reviewing 126 papers, this review aims to provide a comprehensive overview of the effectiveness and mechanisms of biosorbents from organic waste in adsorbing different organic and inorganic waste. Most recent studies have focused on using biosorbents to remove dyes, pharmaceuticals, and heavy metals. The biosorbents were synthesized primarily through drying and pulverization, or pyrolysis. Some biosorbents have been chemically treated with acids, alkalis, or salts to increase their surface functional groups. Furthermore, different biomass materials have also been combined to synthesize biocomposite sorbents. The extraction of lignocellulose and chitin from biomass as biosorbents is also common. Biosorption occurs via chemisorption and physisorption, with the former more prevalent among organic pollutants and the latter among inorganic pollutants. The Langmuir isotherm model, which indicates monolayer sorption, and the pseudo-second-order kinetic model, which implies chemisorption as rate-limiting, best describe most of the biosorption data. Biosorption is governed mainly by pH, temperature, initial pollutant concentrations, dosage and size of biosorbents, and contact time. This review highlights the need to standardize optimization procedures and develop cost-effective and scalable biosorption systems. It highlights the potential of biosorbents, especially biochar, as potential substitutes for activated carbon in the column adsorption process of tertiary wastewater treatment.

Keywords: Biosorption, dyes, heavy metals, pyrolysis, Langmuir isotherm, valorization

INTRODUCTION

Organic waste is a term used to describe biodegradable materials that originate from plant or animal sources. This category includes a wide variety of items such as uneaten food, coffee grounds, fruit and vegetable peels, eggshells, yard waste, fallen leaves, branches, weeds, cut flowers, pet food, livestock manure, untreated wood, and paper or packaging stained with food [Figure 1][1]. Annually, the world produces 2.01 billion tonnes of municipal solid waste, with a conservative estimate suggesting that at least 33% of this is not managed in an environmentally friendly way. Despite making up only 16% of the global population, high-income countries are responsible for about 34%, or 683 million tonnes, of the world's waste[2]. By 2050, global waste is projected to increase to 3.40 billion tonnes, which is more than twice the expected population growth during the same period. The amount of waste produced in low-income countries is predicted to rise more than threefold by 2050. Middle- and low-income countries contribute 53% and 57% of food and green waste, respectively, with the proportion of organic waste increasing as the level of economic development decreases[2].

Each year, an estimated 11.2 billion tonnes of solid waste is collected globally. The decomposition of the organic portion of solid waste contributes to about 5 percent of global greenhouse gas emissions[3]. It produces a substantial amount of methane, a powerful greenhouse gas that plays a significant role in climate change. Organic waste can also contain substances such as antibiotics, chemicals, and pathogens that can infiltrate the soil and groundwater as the waste decomposes[4]. The appropriate handling of organic waste is vital for the sustainability of our environment. Valorization of organic waste into products with commercial values has been probed as the global shift toward the circular economy gains momentum[5,6]. Organic waste can be valorized through conversion into raw materials for energy sources or incorporation into finished goods. The latter is usually achieved by recycling and upcycling, which involve salvaging and reprocessing the waste into new, useful items[4]. Composting and aerobic digestion could convert organic waste into organic fertilizers and soil additives that add nutrients to the soil, as well as biogas, serving as a renewable energy source[7]. Organic waste contains a variety of essential phytochemicals, antioxidants, enzymes, and other bioactive compounds that can be extracted. Crop residues and by-products from food can provide the materials for manufacturing biofuels, bioplastics, and other biomaterials[8].

Organic waste can also be valorized as biosorbents. Biosorbents are materials of biological origin that can be used for sorption, particularly in removing contaminants from wastewater. Biosorption is generally a passive process that does not require energy[9]. The capacity of a biosorbent to eliminate contaminants relies on its kinetic equilibrium and surface characteristics. Since organic waste is made of cellular structures, contaminants are adsorbed to these structures when organic waste is employed as biosorbents[10]. Biosorbents play a crucial role in environmental cleanup efforts and are seen as a cost-effective solution for extracting toxic heavy metals from industrial wastewater, contributing to environmental remediation. They are capable of effectively eliminating toxic heavy metal ions, such as mercury, arsenic, lead, cadmium, and chromium, from polluted water[9]. Biosorbents can also remove other pollutants, such as dyes, pesticides, phenolic compounds, and fossil fuels. In wastewater treatment, these sorbents can be packed in an adsorption column where effluent with contaminants is fed into the column from the top[11]. The biosorbents adsorb the contaminants, and the clean effluent exits the column at the bottom. This process can be reversed to flush out the contaminants adsorbed. The biosorbents can then be reused or discarded and replaced[11].

Despite the rising interest in valorizing organic waste as biosorbents, the existing review is fragmented. Karim *et al.* reviewed the potential use of fibrous food waste for the biosorption of heavy metals. However, fibrous food waste is only a type of organic waste[12]. Though heavy metals have been the primary focus of

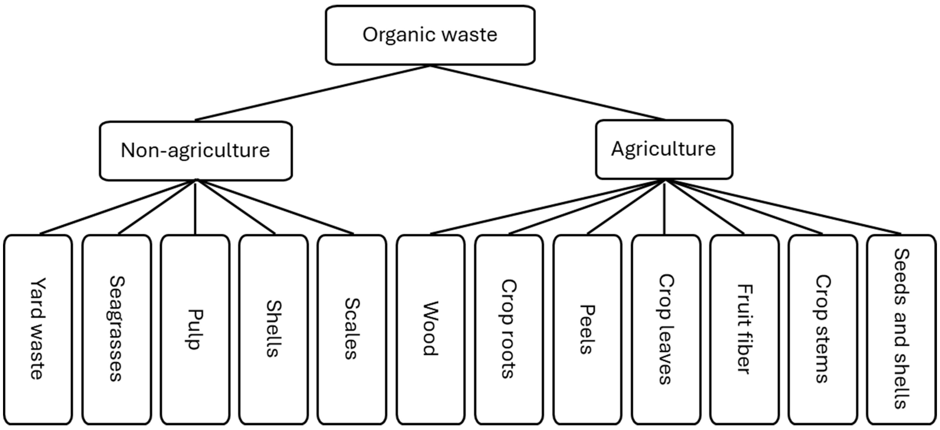

Figure 1. Examples of agricultural and non-agricultural organic waste. Agricultural organic waste originates from agricultural activities such as crop and fruit farming, while non-agricultural organic waste comes from food waste, yard waste, and various organic materials from natural habitats.

studies related to biosorbents, other types of pollutants in wastewater deserve attention. Okoro *et al.* were interested in reviewing the use of nanomaterial-based biosorbents to eliminate certain organic pollutants in wastewater. These nano-biosorbents comprise algae, bacteria, chitosan/chitin, and fungi[13]. Except for chitosan, which can be extracted from seafood waste, particularly the shells of crustaceans, other biosorbents are not considered organic waste. Additionally, seafood waste is one of the many different types of organic waste generated. The use of agricultural waste to produce biosorbents has garnered much review attention[14-16]. Agricultural waste, typically including waste from farms, poultry houses, and slaughterhouses, is a major constituent of organic waste but not its entirety. Organic waste also encompasses non-agricultural waste, such as food waste, yard waste, wood waste, and paper waste. Moreover, there is more interest in reviewing the ability of agricultural waste-derived biosorbents to remove heavy metals than other pollutants[15-17]. Park *et al.* gave an overview of the history, raw materials, and mechanisms of biosorption, as well as the synthesis of biosorbents. The overview did not examine the different types of organic waste that can be used for biosorbent synthesis and their specific adsorption performances and mechanisms in aqueous environments. Additionally, the overview was published over 10 years ago[18].

This review, therefore, aims to provide more comprehensive coverage of a wider array of organic waste for the biosorption of different pollutants from wastewater. Specifically, it aims to examine the efficiency and mechanisms of biosorbents derived from different types of organic waste in removing various pollutants from wastewater. It contributes to a better understanding of the feasibility of various biosorbents in treating wastewater while highlighting the latest innovations in their applications for wastewater treatment and future research directions.

METHODS

This review employed a narrative approach to comprehensively present the biosorbents derived from a wide array of organic waste for wastewater treatment. The literature search was conducted using databases primarily consisting of Web of Science, Scopus, and ScienceDirect. The keywords used in the search include adsorbent, biosorbent, organic, waste, water, wastewater, treatment, and household. To refine the search, the keywords were combined into key phrases such as organic adsorbent for water treatment, biosorbent for wastewater treatment, adsorbent from household waste, and adsorbent from organic waste. A total of 249 articles were retrieved from the databases and were screened using these criteria: (1) the articles must have been published in the past 10 years, with those in the past 5 years prioritized; (2) they must be related to adsorbents from organic waste; (3) they must include the use of the biosorbents to treat various wastewater contaminants, ideally with the efficiency and mechanism specified. The screening resulted in 126 articles to be included in this review.

AGRICULTURE-DERIVED ORGANIC WASTE

Agricultural waste crops that have undergone physical and chemical treatments can be utilized to eliminate contaminants from wastewater. The adsorption capacity of the biosorbents is influenced by their chemical composition and physical properties, such as density, porosity, particle size, specific surface area, and the size and distribution of pores[19]. These factors determine the ability of the biosorbents to adsorb a wide variety of ions and molecules[9]. Through appropriate functionalization, the selectivity of the biosorbents can be "engineered". This enables customization of their affinity toward the intended pollutants and allows for their use in multiple applications[20]. For instance, acid modification of walnut shells was found to improve their biosorption of metals through the enhancement of sulfur-containing functional groups on their surfaces that facilitate complexation with metals[21] [Figure 2]. Agricultural waste may consist of crop waste, such as corn straw, rice and wheat, and sugar cane, as well as fruit waste, such as peels, pits, and shells. These types of waste are usually rich in cellulose, hemicellulose, and lignin, making them good candidates for activated carbon production [Figure 1][16].

Biosorbents can be physically synthesized from dried pulverized organic waste or chemically by converting organic waste to activated carbon [Figure 3]. The feasibility and adsorption efficiency of activated carbon production depends on the carbon content of the waste and the carbonization process[11]. The carbonization procedure frequently involves a combination of thermochemical and/or chemical methods to produce cost-effective materials with high adsorption capabilities [Figure 3]. The production of activated carbon primarily involves pyrolysis, a thermochemical method conducted at elevated temperatures or combined methods that include the use of chemical substances and a somewhat reduced operating temperature [Figure 3][23]. At times, pyrolysis becomes the sole technique for carbonizing raw materials, especially when the biomass contains harmful compounds. However, if a combined carbonization approach is employed, intricate chemical reactions can take place effectively. Typically, the most desirable properties are achieved by activating with bases, acids, and mineral acid salts[24].

The thermochemical method is essentially a thermal treatment, which involves heating at temperatures ranging from 827 to 1,027 °C using air, steam, or supercritical CO_2. Meanwhile, the combined method requires both thermochemical and chemical procedures[25]. While pyrolysis results in less environmental pollution and has a lesser environmental impact, biosorbents with superior adsorption characteristics are typically produced through chemical activation[25]. Comparatively, the physical method of producing biosorbent is simpler, often involving drying, crushing, and pulverizing of biomass or subjecting the biomass to ultrasound treatment [Figure 3]. This method can be combined with chemical treatments, as with pyrolysis, to enhance the biosorbent's functional groups [Figure 3][16].

Adsorption of organic pollutants

Wastewater contains a myriad of organic pollutants, including pesticides, pharmaceutical and personal care products, polycyclic aromatic hydrocarbons (PAHs), dyes, and microplastics. Dyes are significant contaminants for wastewater from textile, paper-making, leather, and cosmetic industries, though their presence in municipal wastewater is not generally significant. Furthermore, they have received substantial attention in studies on applying biosorbents for organic pollutant removal[10,14,26]. They are, thus, included in the list of organic pollutants in this review. Some of the organic pollutants are persistent organic pollutants[27]. These are artificial organic chemical compounds that are either intentionally or

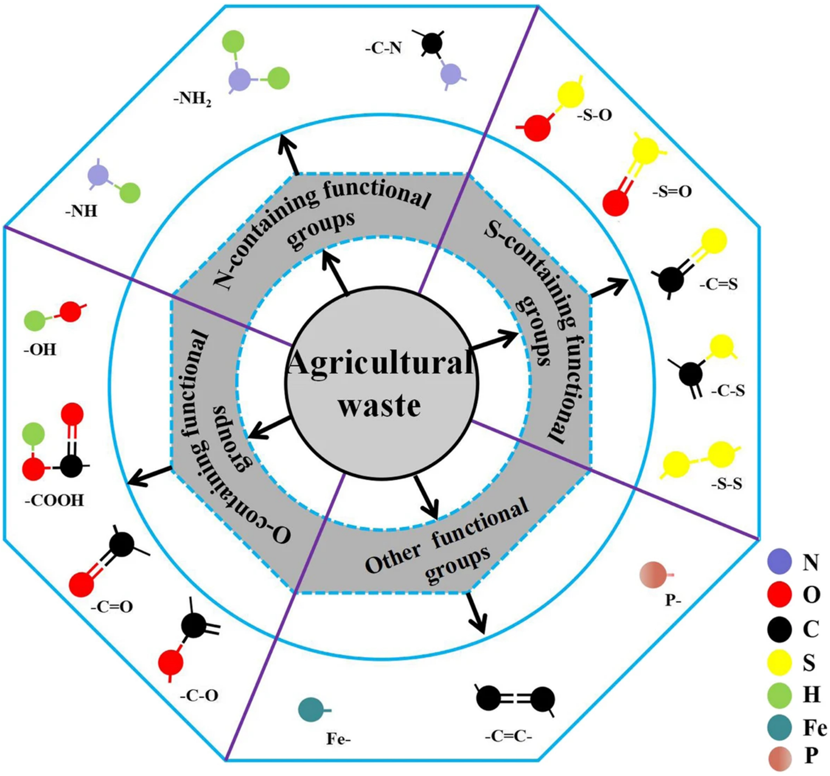

Figure 2. Various functional groups on the surface of biosorbents[22].

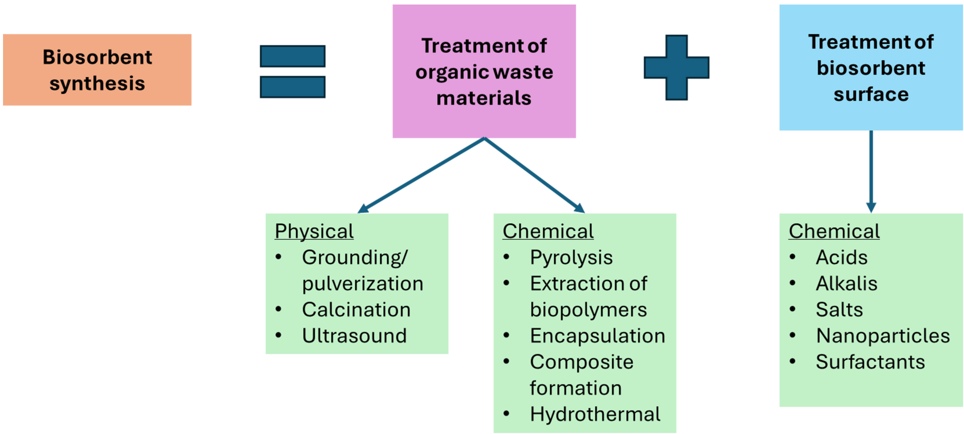

Figure 3. Synthesis of biosorbents. Organic waste can be physically or chemically treated to obtain the biosorbent materials, which are subsequently subjected to surface treatments or modifications to increase the adsorption capacity.

unintentionally produced. They pose a significant environmental threat due to their toxicity, persistence, ability to be transported over long distances, bioaccumulation, and potential harmful effects on living organisms[26]. The United States Environmental Protection Agency (USEPA) has defined the organic priority pollutants, which comprise multiple substances such as halogenated hydrocarbons, organochlorine pesticides, monocyclic aromatics, phthalate acid esters, PAHs, polychlorinated biphenyls, *etc.*[28]. Organic micropollutants are another group of organic pollutants characterized by their small sizes and low environmental concentrations. They could be persistent or non-persistent. Microplastics, polychlorinated biphenyls, and certain pharmaceutical products are examples of persistent organic micropollutants[29]. These pollutants can be removed from wastewater via adsorption, with activated carbon being the most common sorbent.

Biosorbents from husks and shells

Biosorbents can serve as a sustainable alternative to activated carbon. As aforementioned, there is a wide variety of agriculture-derived waste types, such as husks, shells, peels, and stone fruits. Husks and shells are plentiful agricultural by-products that possess significant stability, extensive specific surface area, and good mechanical strength. They are primarily made up of lignin and polysaccharides[11]. Numerous studies have demonstrated the effectiveness of sorbents derived from these materials under experimental conditions for the biosorption of metal ions and organic compounds comprising bisphenol A, carbamazepine, diclofenac, naproxen, quinoline, and tetracycline[14]. They have also been used to reduce chemical oxygen demand (COD) and remove dyes. The capacity of crude and modified coconut shells, as well as waste coconut fiber, to remove various pollutants from wastewater samples has been studied. These pollutants include Congo Red (98.9%), Rhodamine-B (99.2%), phenol (64%), and diamond green (85%)[30-33]. Studies found that these biosorbents performed well in treating complex samples such as landfill leachate and industrial effluents, where multiple pollutants can be eliminated concurrently[34,35] [Table 1]. When landfill leachate samples were subjected to 5- to 25-time dilution, the efficiency of removing COD and dye using rice husk increased significantly[34] [Table 1].

However, a study also showed that the efficiency of removing certain pharmaceuticals like carbamazepine and diclofenac from both ultrapure water and wastewater effluents was lower in real samples compared to simulated ones. This lower efficiency could be due to the presence of solid substances and soluble organic compounds in wastewater, which give rise to a matrix effect, evident when the presence of numerous components in a sample affects the accuracy of measuring the analyte concentration[50,51]. Another study demonstrated the effective removal of crystal violet (97%) using *Camellia oleifera* shells modified with citric acid. The removal was due mainly to surface adsorption, intraparticle diffusion, and chemical interactions between the dye and the surface functional groups of the biosorbent[36]. Furthermore, it has been highlighted that rice husk can be used in constructed wetlands augmented with microorganisms to remove textile dyes from industrial wastewater. The efficiency of removing Black-5 azo dye using the biosorbent varied with the pH of the pollutant solution, achieving elimination efficiencies of 84%, 52%, and 55% at pH 4, 7, and 10, respectively[37]. This indicates the potential of using biosorbents together with other strategies to improve pollutant removal efficiency.

Biosorbents from fruit and vegetable peels

Additionally, fruit and vegetable peels are popular alternatives for biosorbents. Examples of common waste peels used for this purpose include avocados, bananas, lemons, oranges, pomegranates, and potatoes. These waste peels are commonly used for biosorption probably because they are widely consumed globally[14]. Due to their availability, they provide a cost-effective option for biosorbent production. Research has shown that raw banana peels and orange peels have a wide range of practical uses in treating wastewater. For instance, raw banana peels have been found to be effective in removing various organic contaminants such as PAHs, phenol, benzoic acid, salicylic acid, and Rhodamine-B dye from both simulated and real wastewater samples, with efficiencies more than 90%, except for phenol (60%) and benzoic acid (88.7%)[38,40,52,53].

Similarly, orange peel has displayed its potential in removing methylene blue and reducing total dissolved solids (TDS) and COD in real wastewater samples at efficiencies of 90%, 92.3%, and 88.8%, respectively[41] [Table 1]. In all these applications, the main interaction explaining the effectiveness of these materials has

Table 1. Adsorption performance of biosorbents from agricultural waste for organic pollutants

Biosorbent	Contaminant	Initial pollutant concentration	pH	Temperature	Reaction time	Sorption capacity	Removal (%)	Ref.
Sulfuric acid-activated coconut husk	Rhodamine-B	200-1,000 mg/L	7	30-50 °C	120 min	16,666.7 mg/g	99.2%	[31]
Coconut shell	Phenol	50-250 mg/L	NA	25 °C	2 h	18.1 mg/g	64%	[32]
Coconut shell	Brilliant green dye	10-100 mg/L	2-12 (optimal 8)	NA	100 min	NA	85%	[33]
H_3PO_4-activated rice husk	COD, color, NH_4^+	880 mg/L COD; 18 mg/L NH_4^+	NA	30 °C	24 h	NA	80% COD; 90% color; 100% NH_4^+	[34]
Citric acid-modified *Camellia oleifera* shell	Crystal violet	50-300 mg/L	7	20-40 °C	5 h	141.8 mg/g (40 °C)	97%	[36]
Rice husk mixed with soil at a 1:1 ratio	Black-5 azo dye	100 mg/L	4	25 °C	48 h	NA	84%	[37]
Banana peel	Naphthalene, fluorene, phenanthrene	20 mg/L	7	25 °C	1.33 h	333.3 mg/g naphthalene; 285.7 mg/g fluorene; 217.4 mg/g phenanthrene	95% naphthalene; 98% fluorene; 98% phenanthrene	[38]
Pomegranate peel	C.I. reactive yellow	125 mg/L	2	25 °C	1-100 min	209.7 mg/g (at 53.9 min)	75%	[39]
NaOH-treated avocado peel	Alcian blue; brilliant blue; neutral red; methylene blue	5-200 mg/L	2-12	30 °C	0-25 h	31 mg/g Alcian blue; 3.2 mg/g brilliant blue; 6.9 mg/g neutral red; 62.1 mg/g methylene blue	99.6% Alcian blue; 99.5% brilliant blue; 99.8% neutral red; 99.7% methylene blue	[40]
HNO_3-activated orange peel	Methylene blue	5-60 mg/L	NA	25 °C	5-120 min	NA	No mixing: 84.2% (5 min); 88.7 (120 min) With mixing: 90.2% (5 min); 94.2% (120 min)	[41]
Raw orange peel (A); orange peel modified with instant controlled pressure drop (B); orange peel modified with NaOH and instant controlled pressure drop (C); orange peel modified with NaOH, citric acid, and instant controlled pressure drop (D)	RR-272; phenol	RR-272 (50-800 mg/L); phenol (0-2,000 mg/L)	pH 5 (RR-272); pH 7 (phenol)	25 °C	NA	RR-272: 2.1 mg/g (A); 15.2 mg/g (B); 12.2 mg/g (C); 39.8 mg/g (D) Phenol: 4.6 mg/g (A); 17.8 mg/g (B); 34.3 mg/g (C); 14.9 mg/g (D)	640% (RR-272, raw orange peel); 1,812% (phenol, raw orange peel) (The percentage refers to adsorption capacity in comparison to orange peel)	[42]
Raw cactus peel	BR46	200 mg/L	6	25 °C	180 min	82.6 mg/g	NA	[43]
Barley straw with H_3PO_4 and microwave treatments	Norfloxacin	10-100 mg/L	7.03	25-55 °C	1-168 h	349 mg/g (25 °C); 359 mg/g (35 °C); 387 mg/g (45 °C); 441 mg/g (55 °C)	95.5% (25 °C); 93.3% (35 °C); 95.4% (45 °C)	[44]
Corncob and sugarcane bagasse biochar	Chlortetracycline	200 mg/L	3-7	25 °C	48 h	36.1 mg/g (pH 7, corncob); 25.7 mg/g (pH 7, sugarcane bagasse)	59.6% (pH 5, corncob); 84,5% (pH 4, sugarcane bagasse)	[45]
Citric acid functionalized magnetic graphene oxide coated corn straw (CA-mGO; CA-mGO_5CS; CA-$mGO_{10}CS$)	Methylene blue	1,000 mg/L	8	25 °C	3 h	276.5 mg/g (CA-mGO); 300.3 mg/g (GA-mGO_{10} CS); 315.5 mg/g (GA-mGO_5CS)	77% (CA-mGO); 82.4% (CA-$mGO_{10}CS$); 84% (CA-mGO_5CS)	[46]

Rice straw and *Phanerochaete chrysosporium*	Methylene blue	400 mg/L	5	37 °C	24 h (straw); 12 days (straw + *P. chrysosporium*	140.4 mg/g	88% (28.4% biodegraded and 59.6% adsorbed)	[47]
Mango stones treated with iron oxide magnetic nanoparticles	Chloroquine; sertraline	20 mg/L	5-6	43 °C	24 h	49.4 mg/g (chloroquine); 64.8 mg/g (sertraline)	86% (contaminant mixture)	[48]
Algerian date stone	Methylene blue	10-100 mg/L	7	25-55 °C	10-120 min	6.7 mg/g (25°C)	98.8% (60 min)	[49]

NA: COD: chemical oxygen demand; RR-272: reactive red 272.

been identified as chemisorption, where the contaminant molecules form strong chemical bonds with the surface of the biosorbents. A study showed that using NaOH and citric acid to modify orange peel in moderate conditions, along with thermal activation, greatly increased the efficiency of phenol biosorption by over 18 times and enhanced the removal of reactive-red dye (RR-272) by more than 6 times, indicating that chemical modification could potentially enhance the efficiency of biosorption[42] [Table 1]. Specifically, NaOH modifies and improves the structural properties of biosorbents, increasing their surface area and porosity, while citric acid can introduce more functional groups onto the surface of biosorbents. Akkari *et al.* utilized dried ground raw cactus fruit peel as an inexpensive and eco-friendly sorbent to eliminate basic red 46 (BR46) from water-based solutions. They found that the maximum adsorption capacity was 82.58 mg/g. The biosorption isotherm was better represented by the Freundlich model, while the kinetic biosorption data were well described by the pseudo-second-order model. The Freundlich model describes the adsorption process on heterogeneous surfaces, which is not limited to a monolayer. The pseudo-second-order kinetics suggest chemisorption as a likely mechanism. Moreover, their reuse study demonstrated that the biosorbent could be regenerated after three successive cycles using HCl as a chemical reagent. As with other studies, the biosorption process was spontaneous and exothermic[43] [Table 1].

Biosorbents from straws and corn cobs

Rice, wheat, and barley straws, as well as corn cobs, are frequently utilized as biosorbents. They are obtained from the fibrous remains of the plant body and are rich in lignin, cellulose, and hemicellulose. These agricultural residues have sparked considerable interest due to being valuable by-products of the plant cultivation process. They are notable not only for their abundant supply but also for their cost-effectiveness and widespread availability[54]. Barley straw was treated with phosphoric acid and exposed to microwave radiation to create a modified adsorbent. 0.5 mg of the modified barley straw was then tested for its effectiveness in removing 100 mg/L of norfloxacin at a neutral pH. The results showed a sorption capacity of 349 mg/g at 25 °C, 359 mg/g at 35 °C, 387 mg/g at 45 °C, and 441 mg/g at 55 °C[44] [Table 1]. Two types of agricultural waste, corn cob and sugar cane, were utilized to remove the organic pollutant chlortetracycline. The reported removal efficiency for both biosorbents was over 90% at an optimal reaction time of 20 h[45] [Table 1]. Corn straw modified with citric acid and graphene oxide proved effective in adsorbing at least 80% of methylene blue at pH 8[46] [Table 1].

Using biosorption in conjunction with biodegradation provides another efficient option for eliminating methylene blue from wastewater. For example, when a mixture of 1.0 g of rice straw and a 5 mL suspension of the white rot fungus (*Phanerochaete chrysosporium*) spore was used, 88% of methylene blue with an initial concentration of 400 mg/L was removed at pH 5.0. This removal process involved 28.4% of the total removed dye being broken down by *P. chrysosporium*, while the remainder was subjected to biosorption by fungal cells and biodegraded rice straw[47] [Table 1]. Similarly, a study conducted with a combination of rice straw and *Bacillus subtilis* showed at least 90% of methylene blue with a starting concentration of 400 mg/L was removed by 0.5 g of rice straw mixed with 0.2 mL of spore suspensions. The pH of the process was maintained at 7. The presence of both *P. chrysosporium* and *B. subtilis* led to an increase in the specific surface area of the straw and the generation of more functional groups, resulting in a considerable enhancement in removing methylene blue. Additionally, microbial biodegradation played a crucial role in the overall dye-removal process[55].

Biosorbents from stone fruits

Biosorbents can also be produced from stone fruits, particularly the seeds of fruits such as avocados, apricots, and peaches, due to their properties. Like other biosorbents derived from crops, fruit stones have high cellulose, hemicelluloses, and lignin content. The surface hydroxyl groups on these biosorbents can facilitate the introduction of various functional groups to enhance biosorption [Figure 2][10]. A study utilized oven-dried ground mango stones treated with iron oxide magnetic nanoparticles (MS-Fe_3O_4) to eliminate chloroquine and sertraline from polluted water[48] [Table 1]. Both contaminants required an optimal adsorbent dosage of 0.01 g. The pH level significantly affected their adsorption on MS-Fe_3O_4, with the most effective outcomes observed within a pH range of 5-6. Analysis of kinetic data suggested that the pseudo-second-order model provided the best fit, with equilibrium attained at 16 and 4 h for chloroquine and sertraline, respectively. Isotherm studies indicated maximum adsorptive capacities of 49.42 mg/g for chloroquine and 64.79 mg/g for sertraline at 318 K, highlighting the favorable impact of elevated temperatures. The Sips model was observed to explain the adsorption more precisely. It combines elements from the Langmuir and Freundlich isotherms and is particularly useful for fitting adsorption data in cases where the adsorption surface is not uniform. It is, therefore, appropriate for systems with both homogenous and heterogenous adsorption sites at low and high adsorbate concentrations, respectively[48]. In another study, Algerian date pits were examined for their utility as a biosorbent to eliminate methylene blue from water solutions. The Freundlich model was determined to provide the most accurate representation of the adsorption isotherm. Upon conducting a kinetic study, it was observed that the pseudo-second-order model effectively described the adsorption process[49] [Table 1]. However, most of the studies on the use of stone fruits as biosorbents center on the biosorption of metal ions. This is further illustrated in the subsequent section.

Biochar and organically derived activated carbon

In addition to drying and pulverization, biosorbents can also be synthesized through carbonization to produce biochar or activated carbon. Carbonization can be performed on a wide variety of organic waste, and like non-carbonized biosorbents, they can be chemically treated to enhance sorption and recyclability[56]. An investigation was conducted to evaluate the effectiveness of using activated carbon derived from coconut shells to remove pentachlorophenol added to aqueous solutions passing through a column. The biosorbent exhibited a notable sorption capacity of 36.82 mg/g, particularly noteworthy for its efficacy under neutral pH and relatively gentle and economically feasible conditions, involving a 6-hour duration of contact and a temperature of 37 °C[57]. Naghdi *et al.* highlighted the effectiveness of activated carbon derived from pine wood in removing carbamazepine, which is commonly found in surface waters, even at very low concentrations ranging from 0.5 to 20 μg/L. This significant adsorption capacity was observed across a broad pH range of 3.0 to 8.0. The study also revealed that nanobiochar exhibited an adsorption capacity of 0.074 μg/g after 3 h of contact time. Furthermore, the results indicated that increasing the pH from 3 to 8 led to an improvement in the adsorption efficiency[58]. In a spiked sample containing an initial methylene blue and Rhodamine B concentration of 1,000 mg/L at neutral pH, the cationic dyes were effectively captured using 20 mg of porous carbon derived from banana peels. This carbon material exhibited impressive sorption capacities of 744.39 mg/g for methylene blue and 520.29 mg/g for Rhodamine B, showcasing its potential for efficient dye sequestration[59]. In a study, carbonized yam peels were used to create a magnetic adsorbent to remove 2,4-dichlorophenoxyacetic acid (2,4-D). The activated carbon was modified using magnetite nanoparticles. The results showed higher adsorption at high 2,4-D concentration, low pH, and room temperature. The process was found to be exothermic and spontaneous. The magnetized activated carbon can be easily separated from water, and it retained 60% of its adsorption capacity after five cycles[56].

Implications

A wide variety of agricultural waste has been demonstrated to be potential adsorbents for various organic pollutants, particularly dyes and pharmaceuticals, and in some cases, COD in general. This waste often contains functional groups such as hydroxyl, carboxyl, and amino groups, which can facilitate the adsorption of a wide range of contaminants [Figure 2]. Using this waste aligns with circular economy principles, as it reduces waste, promotes resource recovery, and minimizes reliance on non-renewable resources[60]. The perishable nature of agricultural waste does introduce some challenges but generally does not significantly limit its potential as an adsorbent. In fact, with proper processing and treatment, perishable agricultural waste can be effectively transformed into stable, high-performance adsorbents[60]. Perishable agricultural waste can be converted into biochar or activated carbon through pyrolysis or carbonization. It can also be dried and pulverized. These processes transform short-lived organic materials into valuable, long-lasting adsorbents.

However, these biosorbents have varied biosorption efficiencies under different conditions and when applied to different pollutants. In practical use, owing to the different physicochemical characteristics of wastewater, optimization experiments are crucial to increase the performance of these biosorbents [Figure 4]. Biosorption has shown the flexibility of integrating with other methods, such as biodegradation, for better performance. Biosorbents can be synthesized physically, thermochemically, or via both methods, with different potential chemical treatments to enhance their surface functional groups for better performance. In most instances, biosorption of organic pollutants is characterized by the Langmuir or Freundlich isotherms and the pseudo-second-order kinetics, with chemisorption being more predominant.

Adsorption of inorganic pollutants

There are comparatively more studies conducted on the adsorption of inorganic pollutants, particularly metal ions, using biosorbents from agricultural waste. The remarkable performance of these biosorbents has been confirmed through their ability to eliminate over 90% of metals, including Cu^{2+}, Cd^{2+}, Pb^{2+}, and Zn^{2+} [Table 2][61,62]. Among the tested metals, Pb^{2+} appears to be the most examined[71,63]. The primary mechanism driving biosorption is physisorption.

Biosorbents from husks and shells

A study compared the effectiveness of using 0.5 g/L of dried and ground almond, hazelnut, peanut, pistachio, and almond shells to extract Cd, Pb, and Hg from polluted water. Hazelnut shells demonstrated the highest potential for this purpose when tested with single and multiple contaminants in mineral water [Table 2][63]. Variations in the effectiveness of the different shells were attributed to the varying proportions of their cellulose, hemicellulose, and lignin. The presence of a complex heavy metal mixture in the water caused a decrease in Cd removal, likely due to reduced electrostatic interaction and complexation with anions such as Cl^-. When all three contaminants were present in the water, they competed with each other,

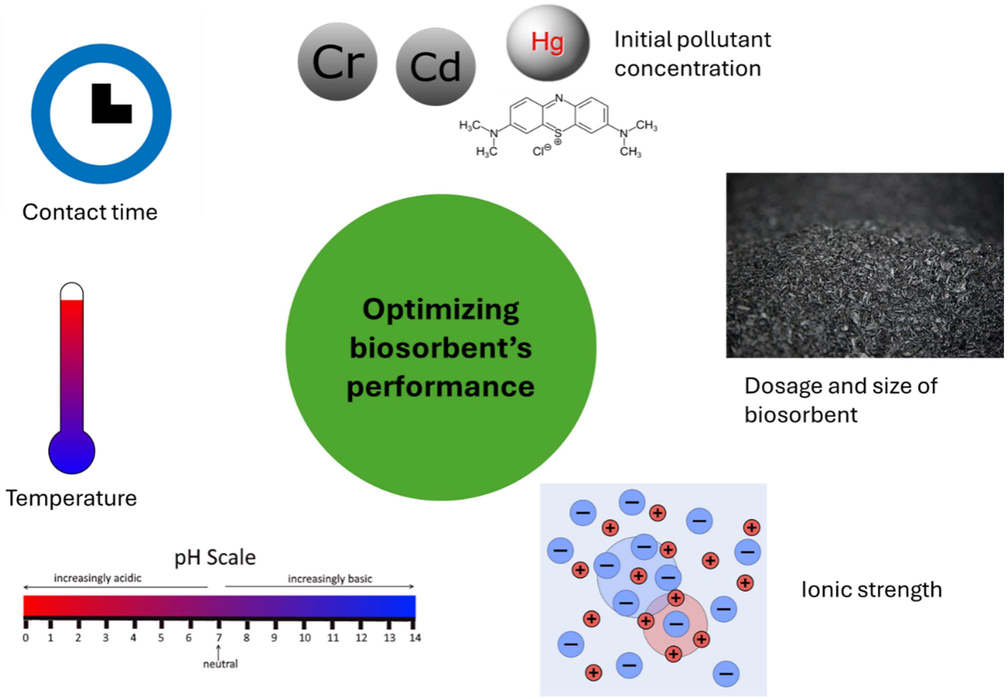

Figure 4. Optimization of a biosorbent's performance typically takes into account the temperature, pH, and ionic strength of the reaction medium, the initial pollutant concentration, the dosage and size of the biosorbent, and the contact time between the sorbate and biosorbent.

with lead demonstrating a greater affinity for the sorbent than mercury[63].

Walnut shell powder was subjected to chemical modification using sodium hydroxide and citric acid to create modified biosorbents with numerous pores serving as binding centers[64]. Analysis of Cr^{6+} adsorption at pH 2 using isotherm and kinetic models revealed that the adsorption behavior of Cr^{6+} was effectively explained by the Langmuir model, indicating the formation of a monolayer of the adsorbate on the surface of the biosorbents. The citric acid-modified biosorbent exhibited the highest maximum adsorption capacity for Cr^{6+} at 75.26 mg/g, followed by the sodium hydroxide-modified biosorbent at 69.56 mg/g, and walnut shell powder at 64.82 mg/g [Table 2][64]. Sodium hydroxide-treated dried and pulverized rice hulls were employed for the concentration, extraction, and reclamation of metal ions in both batch and column operations. The treatment notably enhanced the effectiveness of removing various metal ions[72]. The process was rapid for several ions (Ba, Co, Cd, Cu, Ni, Sr, and Zn), showing promise for efficiently removing low-level metal ions at high throughput. The primary removal mechanism is presumed to be the electrostatic attraction between the rice hulls and the metal ions. A pH level of 5 was found to be optimal for the biosorption of most metal ions[72]. This forms a significant difference from the adsorption of organic pollutants using husks and shells, which often relies on interactions such as van der Waals forces, hydrogen bonding, and hydrophobic interactions. However, polar organic pollutants also exhibit electrostatic interactions with biosorbents. Like organic pollutants, chemical modifications tend to improve the adsorption efficiency of biosorbents for metal ions.

Biosorbents from fruit and vegetable peels

The removal of Cd^{2+}, Cr^{3+}, and Pb^{2+} ions from real industrial wastewater at pH 6 using banana peel resulted in high biosorption efficiencies. Specifically, the removal efficiencies were 97.77% for Cd^{2+}, 98.9% for Cr^{3+},

Table 2. Adsorption performance of biosorbents from agricultural waste for inorganic pollutants

Biosorbent	**Contaminant**	**Initial pollutant concentration**	**pH**	**Temperature**	**Reaction time**	**Sorption capacity**	**Removal (%)**	**Ref.**
Rice husks	Cu^{2+}	100-500 mg/L	2-7	25 °C	240 min	12.8 mg/g	100% (4 g biosorbent, 100 mg/L Cu^{2+})	[61]
Risk husks treated with CS_2 to enhance sulfur-bearing groups	Cd^{2+}	250 mg/L	7	15 °C	120 min	138.9 mg/g	90%	[62]
Peanut, hazelnut, pistachio, walnut and almond shells	Cd, Pb, and Hg in single-element solutions	2 μmol/L	6.5-7	22 °C	48 h	Hazelnut shell (408-449 μg/g Cd; 693-767 μg/g Pb; 656-731 μg/g Hg)	Peanut shell (97% Cd, 92% Pb, 65% Hg); hazelnut shell (98% Cd, 97% Pb, 90% Hg); pistachio shell (88% Cd, 91% Pb, 77% Hg); walnut shell (93% Cd, 72% Pb, 77% Hg); almond shell (81% Cd, 89% Pb, 79% Hg)	[63]
Walnut shell powder modified with alkali and citric acid	Cr^{6+}	20-120 mg/L	2	25 °C	40 min	64.82 mg/g (unmodified); 69.56 mg/g (alkali-modified); 75.25 mg/g (citric acid-modified)	73.4% (unmodified); 69% (alkali-modified); 63.8% (citric-acid-modified)	[64]
Banana peel	Cd^{2+}, Cr^{3+}, Pb^{2+}	Cd^{2+} (0.0003 mg/L); Cr^{3+} (0.05 mg/L); Pb^{2+} (0.1 mg/L)	6	25 °C	60 min	Cd^{2+} (2.23 mg/g); Cr^{3+} (1.1 mg/g); Pb^{2+} (3.1 mg/g)	Cd^{2+} (97.8%); Cr^{3+} (98.9%); Pb^{2+} (96.9%)	[65]
Banana peel	Th, U	U (55.8 mg/L); Th (18.8 mg/L)	4.1	25 °C	25 h	U (8.99 mg/g); Th (0.0362 mg/g)	U (70%); Th (100%)	[66]
Orange peel and *Aspergillus niger*	Cd^{2+}, Pb^{2+}	50-250 mg/L	5-6	30 °C	300 min	Simulated sample: Cd^{2+} (370.4 mg/g, pH = 5); Pb^{2+} (286 mg/g, pH = 6)	Simulated sample: Cd^{2+} (96%, 300 min); Pb^{2+} (90%. 300 min) Competitive sorption: Cd^{2+}or Pb^{2+} (65%, 60 min)	[67]
Unmodified and citric acid-treated *Byrsonima crassifolia* endocarp	Cd^{2+}, Ni^{2+}	25-100 mg/L	5	30 °C	24 h	Unmodified in single solution: Cd^{2+} (1.71 mg/g); Ni^{2+} (0.95 mg/g) Modified in single solution: Cd^{2+} (3.10 mg/g); Ni^{2+} (2.45 mg/g)	All biosorbents in binary solutions: Cd^{2+} (7.5-75%); Ni^{2+} (8.5%-97.4%)	[68]
Peach stone modified by citric acid	Cd^{2+}, Cu^{2+}, Pb^{2+}	6-120 mg/L	2-7	30 °C	180 min	Cd^{2+} (37.5 mg/g), Cu^{2+} (32.2 mg/g), Pb^{2+} (118.8 mg/g)	Cd^{2+} (89.6%), Cu^{2+} (97.2%), Pb^{2+} (93.4%)	[69]
Avocado seeds	As^{3+}	5-30 mg/L	6	25-40 °C	120 min	93.75 mg/g	65% at 20 mg/L As^{3+}	[70]

and 96.9% for Pb^{2+} [Table 2][65]. It is worth noting that raw banana peels were found to have the same purification efficiency when used as a separation medium for thorium and uranium in laboratory and mine wastewater samples from South Africa [Table 2][66]. Orange peel has shown great potential for various applications, including the removal of metal ions such as Cu^{2+}, Fe^{2+}, and Mn^{2+}[73]. In a study, a hybrid sorbent consisting of orange peel and the fungus *Aspergillus niger* demonstrated a 65% elimination efficiency in the simultaneous removal of Cd^{2+} and Pb^{2+} ions from real water samples with a pH of 5.5. This remarkable performance was achieved using just 0.5 mg of the hybrid sorbent [Table 2][67]. A study utilized banana, orange, and potato peels to create biosorbent beads for removing heavy metals from a solution. The beads showed higher uptake of As and Pb at neutral pH but decreased uptake of Cd, Cu, Hg,

and Ni at higher pH. At equilibrium, the beads could remove up to 92%, 87%, 84%, and 90% of Cd, Cu, Hg, and Ni, respectively. The adsorption was primarily physisorption, following the pseudo-first-order model. Banana peel and orange peel beads were more efficient than potato peel beads due to their higher surface heterogeneity[74]. Another study used melon peel as a biosorbent to effectively remove Cu, Cd, and Pb from water. The NaOH-modified melon peel biosorbent showed increased functional groups and surface area, which are important for heavy metal adsorption. The Langmuir isotherm model fitted the heavy metal biosorption better. Maximum capacities for adsorbing a single metal (Cu, Cd, and Pb) were 77.76, 76.16, and 191.93 mg/g, respectively[75].

Biosorbents from straws

As for crop-derived sorbents, three types of rice straw-based biosorbents - raw rice straw, alkali-treated rice straw, and rice straw biochar - were analyzed for their ability to adsorb Cd^{2+} and Zn^{2+}. Raw rice straw showed the highest adsorption, with 20.9% for Cd^{2+} and 8.4% for Zn^{2+}[76]. The optimum pH for Cd^{2+} adsorption was 5 for all three adsorbents, while the optimum pH for Zn^{2+} was 4. The adsorption capacity best fitted the Freundlich isotherm for all adsorbents, indicating a heterogeneous property and a favorable adsorption process[76]. In a recent study, an environmentally friendly straw-based adsorbent was developed via acrylamide and citric acid surface modification to remove $Cr_2O_7^{2-}$ and Cu^{2+} from water. The adsorption capacities of the modified biosorbent for $Cr_2O_7^{2-}$ and Cu^{2+} in a mixed system saw significant increases (196% and 151%, respectively), attributed to a collaborative effect through electrostatic attraction. Both the functional groups and adsorbed pollutants served as adsorption sites[77].

Since crop-based biosorbents are rich in lignin, hemicellulose, and cellulose, studies have also been conducted to extract these materials for biosorption. Yu *et al.* investigated the performance and stability of carboxyl group-modified straws and their cellulose, lignin, and hemicellulose extracts for removing Pb^{2+}[78]. It was revealed that modification significantly improved both the adsorption capacity and stability of the materials, with modified hemicellulose showing the highest adsorption capacity, followed by both modified lignin and straw and, finally, modified cellulose. The optimal pH range for Pb^{2+} adsorption was found to be between 4.0 and 5.0, with modified cotton and rape straw being more stable than modified maize straw within this range[78]. Mohammadabadi and Javanbakht used ultrasonic and gelation-solidification methods to extract lignin to synthesize a biocomposite as a biosorbent for lead[79]. The biocomposite beads were effective in lead removal from water under various conditions. Its maximum adsorption capacity was reported to be 344.83 mg/g at an initial lead concentration of 210 mg/L, a temperature of 328 K, and a pH level of 5. The study also investigated the adsorption kinetics and isotherms and found that they followed the pseudo-second-order kinetic model, as well as the Langmuir and Temkin isotherms[79]. This aligns with frequently reported Langmuir isotherm in other biosorption studies, though other isotherm models were also reported at times.

Biosorbents from stone fruits

As with organic pollutants, attempts have been made to synthesize biosorbents for inorganic pollutants from seeds and fruit stones. Monroy-Figueroa studied the effectiveness of using natural and chemically modified *Byrsonima crassifolia* endocarp for removing Cd^{2+} and Ni^{2+} ions[68] [Table 2]. Treating the biomass with citric acid improved its ability to adsorb these ions under competitive conditions. The citric acid modification increased the functional groups on the biosorbent's surface through reactions with lignocellulosic materials. The process involves an ion-exchange mechanism, potentially involving surface carboxylic, hydroxyl, phenolic groups, and Ca^{2+} replacement. This is supported by the findings that the main elements found in the biomass were C, O, and Ca^{2+}[68]. The peach stone modified with citric acid has been found to effectively remove Cu^{2+} at a sorption capacity of 118.8 mg/g, Pb^{2+} at 93.4 mg/g, and Cd^{2+} at

89.6 mg/g from solutions. This was observed under conditions of an initial metal ion concentration of 200 mg/L, pH 5, and an adsorbent mass of 0.1 g [Table 2][69]. Additionally, when avocado pits were modified with citric, sulfuric, or tartaric acid, they exhibited enhanced sorption capacities between 3.3 and 21.8 mg/g for Cd^{2+}, Cu^{2+}, Ni^{2+}, Pb^{2+}, Zn^{2+}, as compared to untreated avocado seeds, with sorption capacities between 2.5 and 5.6 mg/g[70].

While acids, whether mineral or organic, are commonly used to functionalize the surfaces of biosorbents, basic functionalization has also been reported. For instance, Šoštarić *et al.* utilized apricot stone waste, which was treated with a 1.0 mol/L NaOH solution, to remove Cu^{2+}, Pb^{2+}, and Zn^{2+} (with an initial concentration of 400 mg/L) from a solution at a pH of 5.0[80]. The process involved using 0.5 g of biosorbent, resulting in the elimination of 81% of Cu^{2+}, 87% of Pb^{2+}, and 97% of Zn^{2+}[80]. A recent study used jackfruit seed powder to efficiently remove As^{5+}, Cd^{2+}, and Cr^{6+} from water. The study optimized various conditions and found that the powder worked best at an adsorbent weight of 0.5 g, initial metal concentrations of 40 μg/L (As^{5+}), 30 mg/L (Cd^{2+}), and 30 mg/L (Cr^{6+}), temperatures between 25 and 30 °C, and a pH range of 7-7.5[81]. The results aligned well with Langmuir (As^{5+}, Cd^{2+}, Cr^{6+}), Freundlich (As^{5+}, Cr^{6+}), and Dubinin-Radushkevich (Cd^{2+}, Cr^{6+}) isotherm models, indicating that heavy metal biosorption may not be limited to a specific isotherm model[81]. Nonetheless, the Langmuir isotherm has been more consistently mentioned than other isotherms. A study used dried and powdered *Phyllanthus emblica* fruit stones to remove Pb^{2+} and Cd^{2+} from water through adsorption. The biosorbent removed 80% of both heavy metal ions within 60 min at pH 6. The process was determined to be endothermic, spontaneous, and feasible[82].

Biochar and organically derived activated carbon

Like organic pollutants, biosorbents are commonly subjected to chemical modifications, particularly treatments with acids and alkalis, to increase their sorption capacities. The lignocellulosic components of agricultural waste have been extracted for the biosorption of inorganic pollutants. Thermochemical treatment has also been employed to synthesize biosorbents in the form of biochar for inorganic pollutant removal. A type of magnetic biochar derived from banana peels exhibited high biosorption potential for Cu^{2+} (75.9 mg/g), Hg^{2+} (83.4 mg/g), and Zn^{2+} (72.8 mg/g) in individual systems at pH 6 within 3 h[83]. However, in multi-component systems, Hg^{2+} significantly inhibited the biosorption of Cu^{2+} and Zn^{2+}. Additionally, the biochar showed higher biosorption affinity toward Hg^{2+} compared to Cu^{2+} and Zn^{2+}[83]. Dieme *et al.* evaluated the effectiveness of activated charcoal composed of a combination of cashew shells, millet stalks, and rice pomace[84]. This charcoal was enhanced by a coating of Fe^{3+} ions to increase its chemical reactivity. The study focused on its ability to remove oxyanion As (V), and the results showed that the charcoal had an adsorption capacity ranging from 0.236 to 0.301 mg/g[84]. Erabee *et al.* studied the performance of activated biochar from coconut shells, modified with $KMnO_4$, in adsorbing ammonia nitrogen (NH_3–N) and S^{2-} ions from leachate[85]. They found that the positively charged surface of the sorbent influenced the efficient binding of NH_3–N and S^{2-}, leading to biosorption capacities of 0.1979 and 0.0065 mg/g, respectively[85].

Wang *et al.* (2019) explored the pyrolysis of pinewood biomass and natural hematite mixtures at different temperatures (300, 450, and 600 °C) under a nitrogen (N_2) environment to create nanocomposites, designated as P1, P2, and P3, respectively[86]. The findings indicated that P1 could adsorb up to 0.0194 mg/g of Cd^{2+} and 0.0228 mg/g of Cu^{2+}, P2 could adsorb up to 0.0155 mg/g Cd^{2+} and 0.0109 mg/g Cu^{2+}, and P3, 0.0146 mg/g Cd^{2+}, and 0.0125 mg/g Cu^{2+}. It was observed that increasing the pH from 3 to 5 enhanced the sorption of both Cd^{2+} and Cu^{2+}, while higher ionic strength resulted in decreased Cd^{2+} sorption. Notably, Cd^{2+} sorption was reduced by over four times in the presence of Cu^{2+} in a binary system[86]. While the study indicates the effect of pyrolysis temperature on the adsorption capacity of a biosorbent, it also shows that individual pollutants in a multi-component system could mutually affect the respective adsorption efficiencies. Furthermore, fifteen types of *Caragana korshinskii* biochar were synthesized by pyrolysis at varying temperatures and times in an oxygen-free environment[87]. The results indicated that the pyrolysis at 650 °C for 3 h yielded biochar with the best performance. The maximum adsorption capacities were 220.94 mg/g for Pb^{2+} and 42.43 mg/g for Cd^{2+}. The amounts of biochar producing the optimal adsorption were 3 g/L for Pb^{2+} and 2.2 g/L for Cd^{2+}[87]. At pH ranges of 3-6 and 6-7.5, adsorption was optimum for Pb^{2+} and Cd^{2+}, respectively. The adsorption fitted the Langmuir and Freundlich isotherm models, as well as the pseudo-second-order kinetic model. The adsorption mechanisms were characterized by cationic-π interactions, electrostatic adsorption, intraparticle diffusion, ion exchange, physisorption, and precipitation, among others[87].

Implications

Similar to organic pollutants, the optimal conditions for biosorption of inorganic pollutants considerably vary, depending on the types of biosorbents and pollutants, thus prompting optimization studies specific to wastewater types [Figure 4]. Most of the studies on inorganic biosorption have been conducted on heavy metals due mainly to their toxic effects and environmental concerns. The biosorbents can be tailored via chemical treatments, pyrolysis at different temperatures, combining to form composites, and extraction of specific materials such as lignocellulosic components from biomass. While the Langmuir and Freundlich isotherms generally describe the adsorption behavior, the former is more commonly mentioned. Physisorption, particularly electrostatic interactions, is the predominant sorption mechanism. However, that does not rule out chemisorption, especially surface complexation, which is also common between inorganic pollutants and biosorbents. The presence of other metal ions has been reported to affect the adsorption of certain metal ions in binary or multi-component systems, confirming that a biosorbent may not be equally effective in removing different inorganic species from wastewater. This is also the largest limitation of biosorbent.

The studies reviewed highlight the potential matrix effect in real wastewater due to the complex mixture of substances therein that can influence the action and efficiency of biosorbents. This could be due to competitive adsorption, where different contaminants in wastewater can compete for the same binding sites on biosorbents, and the presence of organic matter, which can coat the biosorbent surface, blocking active sites or changing the surface charge[88]. In addition, high concentrations of dissolved ions can impact biosorbent performance, resulting in “screening effects”, which diminish the electrostatic interactions between biosorbents and charged contaminants, especially sorption involving ion exchange. Additionally, when multiple contaminants are present, biosorbents may exhibit varied affinities toward different substances[63]. For instance, Oladipo *et al.* reported that Cu^{2+} and Zn^{2+} biosorption was substantially hampered in the presence of Hg^{2+} in a multi-component aqueous system, while Wang *et al.* observed a reduction of Cd^{2+} biosorption in a binary system[83,86]. Additionally, Aranda-García *et al.* found that the biosorption efficiency of Ni^{2+} by a biosorbent from oak acorn shell decreased as the ionic strength in the solution rose from 2 to 2,000 mM. Higher ionic strength likely introduces competing ions, particularly divalent ions like Ca^{2+} and Mg^{2+}, which have a greater negative effect on Ni^{2+} uptake than monovalent ions such as Na^{+} and K^{+}[89].

The presence of matrix effects in wastewater highlights a major drawback of the current designs of biosorption studies, which often employ single-contaminant systems. These systems may not represent the multi-component nature of real wastewater. Pertile *et al.* pointed out that a NaOH-activated biosorbent from cones at a concentration of 0.1 mol/L adsorbed 96% Ni and 19% Zn from the wastewater of a neutralization station containing other heavy metals over a 20-min treatment. Despite these significant reductions, the treated water did not conform to the required emission limits for safe discharge into the sewer system[90]. This limits the practical applications of biosorbents and underscores the importance of their modifications and optimization for enhanced performance.

NON-AGRICULTURE-DERIVED ORGANIC WASTE

Though agricultural activities generate a myriad of organic waste, this waste can also come from non-agricultural sources. For instance, household waste containing food scraps and yard waste is a significant source of organic waste. Industrial and municipal solid waste, such as pulp, paper, and textile materials, is also rich in organic matter [Figure 1]. These types of waste have the potential to be converted into biosorbents. Nonetheless, studies on the production of biosorbents from non-agricultural organic waste are fewer than those on biosorbents from agricultural waste. The methods for converting these types of waste into biosorbents are the same as those for agricultural waste, often involving physical, chemical, and thermochemical methods, with or without chemical treatments.

Adsorption of organic pollutants

Huge amounts of fish scales are discarded as solid waste from seafood processing plants and fish markets. This biowaste can be used as a biosorbent in the treatment of wastewater. Devasena *et al.* investigated the use of waste fish scales as a biosorbent to treat pollutants in seafood processing plant wastewater[91]. The treatment showed over 70% removal of nitrite, phosphate, and biological oxygen demand (BOD), and over 95% removal of ammonia and COD. The best adsorption for BOD, COD, and ammonia was attained when a biosorbent dosage of 1 g/100 mL was used, with a contact time of 90 min. The adsorption was characterized by the Langmuir and Freundlich isotherm models[91]. A study examined the process of removing methylene blue from a water solution using fish scales modified with Fe_3O_4 nanoparticles[92]. The biosorbent's structure contained collagen fibers, apatite crystals, and nano-magnetite particles. Methylene blue adsorbed onto the biosorbent through physisorption, which was best characterized with the Sips isotherm equation. Its maximum adsorption capacities estimated with the Langmuir and Sips models were 68.72 and 60.87 mg/g, respectively. Its adsorption kinetics fitted the pseudo-second-order model[92]. Neves *et al.* examined the impact of NaCl and surfactant on the removal of reactive blue 5G dye using unmodified fish scales[93]. Using phenomenological modeling, the researchers found that despite the nonporous nature of the fish scales, they displayed a notable adsorption capacity of approximately 291 mg/g. This high adsorption capacity is attributed to the strong affinity between the adsorbent and the adsorbate, as well as the adsorption of dye aggregates onto the biosorbent. The addition of NaCl and a surfactant raised the sorption capacity to 291 and 299 mg/g, respectively[93]. These findings highlight fish scales as a viable biosorbent.

Food waste containing pollutants is a major concern for disposal. Traditional methods for handling food waste are not effective when the waste contains harmful chemicals such as As^{3+}. Vakili *et al.* recommend using an alkali pre-treatment process to decontaminate the waste and reutilize it as an adsorbent for wastewater treatment[94]. The research findings indicate that treating the contaminated food waste with 0.8 M NaOH at 60 °C for 4 h successfully removes As^{3+} with an impressive removal efficiency of 99.8%. The alkali-treated waste displayed a strong adsorption capacity for methylene blue, achieving an adsorption capacity as high as 534.6 mg/g when the pH was 9 and the adsorbent dosage was 40 g/L[94]. The adsorption aligned with the intraparticle diffusion and Temkin models. Additionally, the adsorbent can be reused for not less than 4 cycles without losing its efficiency in removing methylene blue substantially, thus highlighting its practical potential[94]. Attempts were made to utilize brewery residue for organic pollutant removal. A study investigated the use of brewery residue (*Saccharomyces pastorianus*) to remove methylene blue from water[95]. The findings showed that immobilizing *Saccharomyces pastorianus* in sodium alginate resulted in effective dye removal. Microencapsulation of the residue, a pH of 9, a biosorbent dose of 5.28 g/L, and a contact time of approximately 100 min resulted in the most effective sorption[95]. The Langmuir model best represented the biosorption isotherm. The maximum biosorption capacity estimated with the model was 188.7 mg/g at room temperature. The biosorption mechanism was chemical or physical in nature and was found to be influenced by biosorbent particle size[95].

Attempts to use the shells of marine organisms to adsorb organic pollutants show varying results. The potential of using the shells of *Corbicula fluminea* as a natural sorbent for treating toxic olive oil mill waste was studied[96]. The results showed that the shells were not effective in adsorbing chemicals from mill waste, particularly aromatic structures, after a 14-day treatment. An increase in pH and COD levels of the mill waste and spectroscopy data implied that the shell dissolved partially[96]. In a different study, snail shell dust from *Bellamya bengalensis* was utilized to treat industrial wastewater[97]. The study examined variations in multiple water quality parameters, including BOD, COD, dissolved oxygen, pH, and the levels of inorganic ions, after the treatment. The results indicated that with a 15 g/L application rate over 4 days, all parameters except dissolved oxygen displayed a significant decrease in concentration, in contrast to the findings of the previous study using the shells of *Corbicula fluminea*[97]. A study used shrimp shell chitin to remove COD and polyphenols from olive mill wastewater[98]. The optimized conditions for maximum removal were found to occur at a pH of 12, an adsorbent concentration of 10 g/L, a contact time of 24 h, and a stirring speed of 420 rpm. The maximum adsorption capacity for polyphenols reached 69.47%, while the maximum COD removal achieved 43%, contrary to another study on olive mill wastewater decontamination using *Corbicula* shells[96,98]. Kinetic studies showed that the pseudo-second-order model provided a better fit for the adsorption behavior than the intraparticle diffusion and pseudo-first-order models[98]. This implies that the types of shells used could have opposing or different effects on the same kind of wastewater. Chitin could be the main material in shells that confers its adsorbent characteristics[11]. Generally, when shells are pulverized to a smaller particle size, the surface area increases, and more chitin is exposed. The findings from an adsorption study revealed that finer waste oyster shell powder (average 8.15 μm) adsorbed Congo red and methylene blue to a substantially greater extent, with an increase of 48.3% and 62.5%, respectively, compared to the ordinary shell powder (average 27.75 μm). Notably, the adsorbent can remove more Congo red than methylene blue, because of the presence of cationic chitin[99].

There has been increasing interest in using *Eichhornia crassipes*, an aquatic weed, to remove synthetic dyes due to its wide availability. Saufi *et al.* explored the potential of the dried leaves and roots of *E. crassipes* in removing Rhodamine B[100]. Their findings indicated that the leaves had a greater capacity for adsorbing Rhodamine B compared to the roots. Additionally, they observed that increasing the initial dye concentrations and the duration of contact between the biosorbent and dye solution led to enhanced removal of the dye by both the roots and leaves. The adsorption data were effectively represented by the pseudo-second-order kinetic model and the Langmuir isotherm model[100]. In a study by Kulkarni *et al.*, the biosorption capacity of dried roots of *E. crassipes* for crystal violet dye was examined[101]. It was reported that higher temperatures intensify the bond between the dye molecules and the bonding sites within the roots of *E. crassipes* (when sprayed). The adsorption behavior was tested with the Langmuir and Freundlich isotherm models. The authors concluded that the Freundlich model fitted the biosorption equilibrium data better. Additionally, they found that the pseudo-second-order model offered the best representation of the biosorption kinetic data[101]. Patil *et al.* studied the use of live roots of *E. crassipes* to remove crystal violet from water[102]. They found that the Freundlich isotherm model best described the biosorption process, indicating multilayer biosorption on an energetically heterogeneous surface. They also observed that the pseudo-second-order model was most suitable for describing the adsorption kinetics[102].

The pseudo-second-order model seems to primarily govern the kinetics of organic pollutant biosorption using various non-agricultural biosorbents. While the Langmuir isotherm predominantly describes the adsorption behavior, other isotherms, such as Freundlich and Sips, are also frequently mentioned. Other than the variability caused by different biosorbents and pollutants, this review highlights the possibility of magnetizing the biosorbents to facilitate their separation, and immobilizing the microbial consortia in certain waste such as brewery waste for biosorption. In addition, some biosorbents may not be suitable for certain types of wastewater and may worsen contamination. This prompts the careful selection of biosorbents according to the purpose for optimal performance.

Adsorption of inorganic pollutants

A study revealed that mussel shells can effectively remove ammonium from water. Optimal adsorption was observed to occur over 90 min using 700 mg/25 mL of ground mussel shells, with an initial ammonium concentration of 40 mg/L and a pH level of 8[103]. The maximum adsorption capacity was 2.33 mg/g, with an efficiency of 46.6%. The adsorption process was well described by the Freundlich isotherm model and both pseudo-first-order and pseudo-second-order kinetics[103]. Esmaeili *et al.* (2020) successfully employed the calcined shell of the *Solamen vaillanti* snail for the extraction of Cu^{2+}, Co^{2+}, and Pb^{2+} from a solution[104]. The optimal conditions for the removal process were observed at a pH of 5 for Co^{2+} and Pb^{2+} and a pH of 4 for Cu^{2+}. Optimal adsorption occurred at a temperature of 25 °C, with an initial metal ion concentration of 10 mg/L and an adsorbent dose of 2 g/L, over a contact time of 60 min. Moreover, the Langmuir model indicated the highest adsorption capacities for Pb^{2+}, Co^{2+}, and Cu^{2+} to be 26.04, 29.41, and 33.55 mg/g, respectively[104]. Similar to the extraction of lignocellulosic materials from crop residues as biosorbents, specific shell components can also be extracted for the synthesis biosorbents. Ali *et al.* conducted a study where they used chitosan nanoparticles derived from shrimp shells for the adsorption of Fe^{2+} and Mn^{2+} from wastewater[105]. Through batch experiments, it was found that the maximum adsorption capacity for Fe^{2+} was 99.8% at 116.2 mg/g, and for Mn^{2+} was 95.3% at 74.1 mg/g. The pH levels of 4 and 5 were optimal for Fe^{2+} and Mn^{2+} adsorption, respectively, where the initial ion concentration was 40 mL/g. Optimal adsorption occurred over a contact time of 100 min with an adsorbent dose of 10 g/L[105]. As with other studies[103,104], the adsorption was best described by the pseudo-second-order and the Langmuir models.

Foroutan *et al.* explored the process of extracting Pb^{2+} from an aqueous solution using Vanami shrimp peel[106]. They achieved an impressive removal efficiency of 98% by optimizing various factors, including maintaining a pH of 6, a temperature of 30 °C, a contact time of 130 min, employing an adsorbent dose of 5 g/L, and starting with a Pb^{2+} concentration of 60 mg/L. Utilizing the Langmuir model, they were able to determine the maximum adsorption capacity, measuring at 24.331 mg/g[106]. In a study using the Taguchi method, oyster shell powder was used to remove Cd^{2+} from water[107]. Optimal removal was recorded when the biosorbent was calcined at 900 °C, and the reaction pH was 10. Biosorbent calcination at 900 °C or higher temperatures led to a larger surface area. The study also found pH to contribute most significantly to the adsorption performance of the biosorbent, followed by temperature, pollutant concentration, biosorbent dosage, and contact time[107]. This study also highlights the potential of thermochemical methods, in this case calcination, in synthesizing or improving the performance of biosorbents.

Other than organic pollutants, fish scales also show potential for removing inorganic pollutants. A study focused on using waste fish scales as a biosorbent to remove Cr^{3+} metal ions through batch experiments[108]. The highest removal of Cr^{3+}, at 99.8%, occurred using 0.8 g of the biosorbent, a solution pH of 5, and a contact time of 90 min, with an initial Cr^{3+} concentration of 150 mg/L. The Langmuir isotherm model best described the experimental data, with a maximum adsorption capacity of 18.3 mg/g. Additionally, the adsorption kinetics were observed to follow the pseudo-first and second models well[108]. Conversion of fish scales to biochar through a thermochemical approach has been conducted. Devasena *et al.* focused on using waste fish scales to create biosorbents for treating pollutants in fish processing wastewater[91]. The findings showed that fish scale biochar effectively reduced BOD by 87% and COD by 84% within 150 min. The ideal pH range was identified as 6-8, and the experimental results aligned well with the Langmuir isotherm and pseudo-second-order kinetic models[91]. Fish scale biochar was also used in another study aiming to assess its effectiveness in removing toxic Cd^{2+} from contaminated water. Key design parameters and biosorption performance were investigated through batch and fixed-bed experiments. Batch experiments revealed that the maximum adsorption capacity of the biosorbent was 99.14 mg/g, and it was monolayer (Langmuir) in nature. The removal efficiency was 95.4% under a batch mode and 99% under a dynamic flow mode. The biosorbent retained a biosorption capacity of more than 78 mg/g and a recovery rate of 99% after 10 sorption/desorption cycles. Cd^{2+} was found to be immobilized by the –NH, –OH, and carboxyl groups[109].

In a study, food waste was combined with iron to yield Fe-loaded food waste biochar, which was then examined for its capacity to adsorb phosphate from water[110]. The study involved adjusting the temperature, pyrolysis time, and iron concentrations. The findings demonstrated that the biochar effectively captured phosphate, with the adsorption process explained by pseudo-second-order and Elovich kinetic models. The Freundlich and Redlich–Peterson isotherm models provided a more precise representation of the phosphate adsorption onto the biochar compared to the Langmuir isotherm model[110]. In another study, a similar iron-infused food waste biochar was employed to adsorb Se^{6+} from water[111]. The study revealed that the duration of pyrolysis did not significantly affect the Se^{6+} adsorption capacity of the biosorbent, but the temperature and Fe concentration were influential factors. Pyrolysis over 3.5 h, at 495.0 °C, with 0.44 M Fe added, resulted in optimal adsorption[111]. Se^{6+} adsorption best fitted the pseudo-second-order and pseudo-first-order kinetic models. Additionally, the Freundlich model was a better fit for the equilibrium adsorption data compared to the Langmuir model. The biosorbent can adsorb Se^{6+} at a capacity as high as 11.7 mg/g[111].

Though not as prevalent as other organic waste, dead or loose seaweeds floating in water or accumulating on beaches can constitute a portion of the waste. The potential of seaweeds as biosorbents has been explored. In a study, the ability of *Sargassum tenerrimum* to remove Cr^{6+} was examined through batch experiments[112]. Biosorption was observed to be maximum at 25 °C and pH 2, with a biosorbent particle size of 0.6 mm. The Langmuir isotherm model satisfactorily described the adsorption behavior and gave a maximum adsorption capacity of 37.7 mg/g dry biomass. Employing the biosorbent for batch treatment of real tannery wastewater under optimal conditions revealed a Cr^{6+} removal efficiency of around 88%[112]. Al-Homaidan *et al.* (2018) investigated the use of three types of green algae, namely *Enteromorpha intestinalis*, *Microspora amoena*, and *Cladophora glomerata* as biosorbents to remove Cr^{6+} from the water via batch experiments[113]. They found that *C. glomerata* had the highest removal efficiency of up to 66.6% at pH 2.0 and 45 °C over 60 min when a dosage of 1.0 g dried algal cells/100 mL and a starting Cr^{6+} level of 20 mg/L were used. They also determined that the Freundlich model provided a better fit for the equilibrium data[113]. Additionally, a biosorbent derived from *Jania adhaerens* was employed to adsorb Cu^{2+} from water[114]. The kinetics data were suitably described using the pseudo-second-order model. The Langmuir model best represented the adsorption isotherm and demonstrated the highest adsorption of 67 mg/g. The biosorption was facilitated by amine, carboxyl, and sulfonate functional groups [Figure 2]. A main mechanism underlying the biosorption was identified to be ion exchange[114].

Again, here, the Langmuir and the pseudo-second-order models satisfactorily describe the isotherm and kinetics of most of the studies reviewed. A study on various factors influencing biosorption found the influence of pH to be the strongest[107]. The presence of salts and surfactants in the aqueous solutions can also affect or increase biosorption efficiency, implying that modifying wastewater could be an option to improve biosorption.

DISCUSSIONS

Adsorption has gained significant attention compared to other wastewater treatment methods because of its effectiveness in removing various contaminants, cost-effectiveness, and simplicity. In particular, biosorbents have been highlighted for their potential, as they are often derived from agricultural by-products, making them more affordable and sustainable than activated carbon, another commonly used adsorbent[115]. They are biodegradable and some can be regenerated for reuse, simplifying disposal and management. However, biosorbents may suffer variable performance, influenced by the type of biosorbent used, the nature of the pollutants, and environmental conditions. Furthermore, they may have lower adsorption capacities than activated carbon[15,116]. A study comparing the adsorption capabilities of commercial adsorbents and biosorbents for fluoxetine in water found that among commercial options, granulated activated carbon (233.5 mg/g) topped the list, followed by zeolite 13× (32.11 mg/g) and zeolite 4A (21.86 mg/g). For low-cost biosorbents, the order was spent coffee grounds (14.31 mg/g), then pine bark (6.53 mg/g), and cork waste (4.74 mg/g)[117]. This indicates the superior adsorption capacities of commercial adsorbents. However, a cost analysis showed that commercial adsorbents had a higher cost per gram of fluoxetine removed, with zeolite 4A costing 6.85 €/g, zeolite 13× costing 3.13 €/g, and granulated activated carbon costing 1.07 €/g. In comparison, low-cost biosorbents offered lower costs: pine bark was 0.92 €/g, cork waste was 0.41 €/g, and spent coffee grounds were the least expensive at 0.16 €/g[117]. Biosorbents were generally more cost-effective for the same amount of contaminant removed.

The variability of biosorbents is also demonstrated in this review, where the adsorption capacities of different biosorbents vary with different pollutants, as shown in Table 3. Avocado peel stands out as an effective biosorbent for dyes, while H_3PO_4-activated rice husk could remove all ammonium from water. Rice husk also eliminated Cu^{2+} in an experiment. Hazelnut shells and banana peels perform excellently as adsorbents of multiple heavy metals. Chitosan nanoparticles, Vannamei shrimp peels, fish scales, and fish scale biochar are also good adsorbents of metal ions [Table 3]. Chitosan is derived from the exoskeletons of crustaceans, confirming the potential of shrimp peels as a biosorbent. Additionally, the abundance of these waste types makes them good candidates for biosorbent production. For instance, approximately 8.4 million tonnes of avocados were produced worldwide in 2021, and with the peel accounting for about 10%-15% of an avocado's total weight, it is estimated that 840,000 to 1.26 million tonnes of avocado peel waste is produced annually. The annual generation of risk husk is estimated at 100 million tonnes, while that of banana peel is approximated at 36 to 48 million tonnes[118]. Valorizing these waste materials as low-cost biosorbents could substantially reduce the volume of organic waste bound for landfills. Turning these waste materials into biosorbents substantially extends their lives, and this process typically requires only drying to reduce the moisture content without the need for extensive and energy-consuming preservation procedures, such as freezing.

In some instances, the carbonization of the biosorbent materials increases their performance. A study comparing the effectiveness of *Euryale ferox* Salisbury seed coat and its activated carbon in removing Pb^{2+} ions revealed that the activated carbon achieved an impressive removal efficiency of 99.9% for Pb^{2+}, while the seed coat itself only managed to remove 89.5% of the ions at neutral pH[119]. Another study reported that biochar was notably more efficient than woodchip in reducing COD, total organic carbon, and fecal indicator bacteria. The reasons for this could be its higher porosity, larger surface area, and greater chemical stability after carbonization[120]. Additionally, biochar can be customized through additional treatment to target specific pollutants. Different feedstocks can be mixed to produce biochar, further alleviating the concern for raw material supply for biosorbent production[121]. Mixing feedstocks may enhance functional group diversity, which can improve the adsorption of a wider range of contaminants from wastewater.

Table 3. Best-performing biosorbent with more than 90% removal efficiency based on pollutant type

Pollutant	Biosorbent	Removal (%)
Rhodamine-B	Sulfuric acid-activated coconut husk	99.2%
NH_4^+	H_3PO_4-activated rice husk	100%
Crystal violet	Citric acid-modified *Camellia oleifera* shell	97%
Naphthalene Fluorene Phenanthrene	Banana peels	95% 98% 98%
Alcian blue Brilliant blue Neutral red Methylene blue	Avocado peels	99.6% 99.5% 99.8% 99.7%
Norfloxacin	Barley straw with H_3PO_4 and microwave treatments	95.5%
Cu^{2+}	Rice husks	100%
Cd Pb Hg	Hazelnut shells	98% 97% 90%
Cr^{2+} Cr^{3+} Pb^{2+} Th	Banana peels	97.8% 98.9% 96.9% 100%
As^{3+}	Food waste treated with NaOH	99.8%
Fe^{2+} Mn^{2+}	Chitosan nanoparticles	99.8% 95.3%
Pb^{2+}	Vanami shrimp peels	98%
Cr^{3+}	Fish scales	99.8%
Cd^{2+}	Fish scale biochar	99%

Carbonization to produce biochar incurs additional costs. An analysis of life cycle environmental and economic performance performed by Alhashimi and Aktas revealed that biochar presents a more favorable energy demand and a reduced global warming potential compared to activated carbon. Specifically, biochar has an energy requirement of 6.1 MJ/kg, while activated carbon's demand is significantly higher at 97 MJ/kg[122]. Regarding greenhouse gas emissions, biochar generates an average of -0.9 kg CO_2eq/kg, in stark contrast to activated carbon's emissions of 6.6 kg CO_2eq/kg. When assessing heavy metal adsorption as the primary function, biochar typically exhibits lower environmental impacts, displaying a significant difference of about one order of magnitude between the two materials. This conclusion holds even after accounting for the environmental effects associated with transporting biochar over long distances[122]. Additionally, the cost associated with using biochar to adsorb chromium and zinc is lower than that for activated carbon. For lead and copper, however, the adsorption costs were found to be similar for both materials[122].

In actual wastewater treatment, biosorbents, including biochar, can be applied in column biosorption in tertiary treatment, where wastewater is passed through a column packed with biosorbents. As the water flows through, pollutants are adsorbed onto the materials. This system is suitable for continuously treating large volumes of wastewater in industrial or municipal settings[123]. Biosorbents can be used in stabilization ponds or filtration systems to improve the removal of suspended solids and pollutants[124]. In some cases, more biochar is needed than activated carbon to treat the same amount of wastewater, primarily due to differences in their adsorption capacities and characteristics, thus resulting in more waste biosorbent generated. This waste could be reduced by enhancing the reusability of the biosorbents or channeling it for anaerobic digestion to recover energy while reducing waste volume[15]. Its uses for composting and soil amendment are controversial due to the presence of contaminants and the reentry of these contaminants into the environment. For the same reason, the use of activated sludge has been controversial. It is a regulated waste in countries such as China, Germany, and the Netherlands[125]. Thompson *et al.* also stated that biochar from biosolids performed worse environmentally than powdered activated carbon and wood biochar because of the energy requirement for drying biosolids and the additional adsorbent needed[126]. Furthermore, due to its inorganic content, it has not been included in this review. It is noteworthy that the matrix effect of wastewater could limit the effectiveness of biosorbent, as discussed in Section "Implications".

CONCLUSION

A large inventory of organic waste has shown the potential of being converted into biosorbents. In fact, most studies show that organic waste, particularly agricultural waste, can be used for biosorption, and the efficiency can be improved with optimization of pH, temperature, biosorbent dosage, and contact time according to the physicochemical properties of the wastewater treated. Modifications, such as pulverization, chemical treatments, pyrolysis, calcination, immobilization, and composite production, can also be made to the biosorbents, whether individually or in combination. Despite their versatility and flexibility, certain barriers to their wide application must be addressed. Their major limitations are (1) biosorbents may experience decreased efficiency after several regeneration cycles, and their regeneration could be complex and costly; (2) biosorbents may lack specificity in their actions and may be suitable when it comes to removing a specific contaminant from the wastewater; (3) used biosorbents contribute to secondary waste that needs to be treated or disposed of carefully; (4) the performance of biosorbents vary considerably for different types of pollutants under different operational conditions; and (5) utilization of biosorbents may require specialized technology and equipment.

To overcome these barriers, it is recommended that (1) the efficiency and cost-effectiveness of regeneration techniques, often including chemical, thermal, or biological approaches, can be enhanced to improve the recyclability of biosorbents; (2) more studies can be dedicated to functionalization and modification of biosorbents to increase their performance in removing certain pollutants; (3) the biosorption process can be optimized to reduce chemical and energy requirements, hence operational costs; (4) the optimization procedures are standardized by addressing the major factors influencing biosorption, and this can be facilitated with artificial intelligence; (5) user-friendly and scalable biosorption systems can be developed, for instance, by designing biosorption modules that can be added to the existing wastewater treatment facilities. This includes the development of column technologies to pack the biosorbents. This review highlights the potential use of biosorbents, especially biochar, as a substitute for high-cost, energy-intensive activated carbon in the column adsorption process of tertiary wastewater treatment or filtration systems of small-scale water treatment. It also sheds light on the possibility of combining different feedstocks for biochar production to ensure an adequate supply of raw materials. It contributes to the circular economy by turning waste into resources. In relation to the recommendations, future studies could focus on improving the regeneration potential of biosorbents, the synthesis of biosorbents with better performance, and their applications in pilot- or full-scale wastewater treatment, as well as the use of artificial intelligence for optimization of the treatment process.

DECLARATIONS

Authors' contributions

Conceptualization, visualization, project administration, writing - original draft, writing - review and editing: Tang KHD

Availability of data and materials

Not applicable.

Financial support and sponsorship

None.

Conflicts of interest

Tang KHD is the Guest Editor of the Special Issue titled "New Advances in Green Adsorbents for Wastewater Treatment" of the *Water Emerging Contaminants* & *Nanoplastics* journal.

Ethical approval and consent to participate

Not applicable.

Consent for publication

Not applicable.

Copyright

REFERENCES

1. Fang Y, Wang P, Zhang L, et al. A novel Zr-P-modified nanomagnetic herbal biochar immobilized Cd and Pb in water and soil and enhanced the relative abundance of metal-resistant bacteria: biogeochemical and spectroscopic investigations to identify the governing factors and potential mechanisms. *Chem Eng J* 2024;485:149978. DOI
2. The World Bank. Trends in solid waste management. Available from: https://datatopics.worldbank.org/what-a-waste/trends_in_solid_waste_management.html. [Last accessed on 16 Dec 2024].
3. UN Environment Programme. Solid waste management. Available from: https://www.unep.org/explore-topics/resource-efficiency/what-we-do/cities/solid-waste-management. [Last accessed on 16 Dec 2024].
4. Lizundia E, Luzi F, Puglia D. Organic waste valorisation towards circular and sustainable biocomposites. *Green Chem* 2022;24:5429-59. DOI
5. Tang KHD. Valorization of plastic waste through incorporation into construction materials. *Civ Sustain Urban Eng* 2022;2:96-109. DOI
6. Tang KHD. Attitudes towards plastic pollution: a review and mitigations beyond circular economy. *Waste* 2023;1:569-87. DOI
7. Wang Y, Wang J, Yi G, et al. Sulfur-aided aerobic biostabilization of swine manure and sawdust mixture: humification and carbon loss. *Bioresour Technol* 2023;387:129602. DOI
8. Srivastava A, Mishra A. Food waste valorization for handling environmental problems: a review. *Environ Sustain* 2022;5:401-21. DOI
9. Mo J, Yang Q, Zhang N, Zhang W, Zheng Y, Zhang Z. A review on agro-industrial waste (AIW) derived adsorbents for water and wastewater treatment. *J Environ Manage* 2018;227:395-405. DOI
10. Torres E. Biosorption: a review of the latest advances. *Processes* 2020;8:1584. DOI
11. Nematollahzadeh A, Vaseghi Z. Biosorbents in industrial wastewater treatment. In: Karchiyappan T, Karri RR, Dehghani MH, editors. Industrial wastewater treatment. Springer International Publishing: Cham; 2022. pp. 101-32. DOI
12. Karim A, Raji Z, Karam A, Khalloufi S. Valorization of fibrous plant-based food waste as biosorbents for remediation of heavy metals from wastewater - a review. *Molecules* 2023;28:4205. DOI PubMed PMC
13. Okoro HK, Pandey S, Ogunkunle CO, et al. Nanomaterial-based biosorbents: adsorbent for efficient removal of selected organic pollutants from industrial wastewater. *Emerg Contam* 2022;8:46-58. DOI
14. Karić N, Maia AS, Teodorović A, et al. Bio-waste valorisation: agricultural wastes as biosorbents for removal of (in)organic pollutants in wastewater treatment. *Chem Eng J Advs* 2022;9:100239. DOI
15. Anastopoulos I, Pashalidis I, Hosseini-Bandegharaei A, et al. Agricultural biomass/waste as adsorbents for toxic metal decontamination of aqueous solutions. *J Mol Liq* 2019;295:111684. DOI
16. Tokay B, Akpınar I. A comparative study of heavy metals removal using agricultural waste biosorbents. *Bioresour Technol Rep* 2021;15:100719. DOI
17. Shakoor MB, Niazi NK, Bibi I, et al. Remediation of arsenic-contaminated water using agricultural wastes as biosorbents. *Crit Rev Env Sci Technol* 2016;46:467-99. DOI
18. Park D, Yun Y, Park JM. The past, present, and future trends of biosorption. *Biotechnol Bioproc E* 2010;15:86-102. DOI
19. Dai Y, Sun Q, Wang W, et al. Utilizations of agricultural waste as adsorbent for the removal of contaminants: a review. *Chemosphere*

2018;211:235-53. DOI

20. Popovic AL, Rusmirovic JD, Velickovic Z, et al. Kinetics and column adsorption study of diclofenac and heavy-metal ions removal by amino-functionalized lignin microspheres. *J Ind Eng Chem* 2021;93:302-14. DOI
21. Godinho D, Nogueira M, Bernardo M, et al. Recovery of Cr(III) by using chars from the co-gasification of agriculture and forestry wastes. *Environ Sci Pollut Res Int* 2019;26:22723-35. DOI
22. Liu G, Dai Z, Liu X, Dahlgren RA, Xu J. Modification of agricultural wastes to improve sorption capacities for pollutant removal from water - a review. *Carbon Res* 2022;1:25. DOI
23. De Gisi S, Lofrano G, Grassi M, Notarnicola M. Characteristics and adsorption capacities of low-cost sorbents for wastewater treatment: a review. *Sustain Mater Technol* 2016;9:10-40. DOI
24. Kosheleva RI, Mitropoulos AC, Kyzas GZ. Synthesis of activated carbon from food waste. *Environ Chem Lett* 2019;17:429-38. DOI
25. Pathak PD, Mandavgane SA, Kulkarni BD. Fruit peel waste as a novel low-cost bio adsorbent. 2015;31:361-81. DOI
26. Tang KHD. Advances and feasibility of biocatalytic technologies for dye removal. *Res in Ecol* 2024;6:1-15. DOI
27. Tang KHD, Darwish NM, Alkahtani AM, Abdelgawwad MR, Karácsony P. Biological removal of dyes from wastewater: a review of its efficiency and advances. *Trop Aqua Soil Pollut* 2022;2:59-75. DOI
28. Sawicka B, Messaoudi M, Vambol V, et al. Organic micropollutants in wastewaters: advances in sustainable management and treatment methods. In: Bhadouria R, Tripathi S, Singh P, Singh R, Singh HP, editors. Organic micropollutants in aquatic and terrestrial environments. Springer, Cham; 2024. pp. 225-47. DOI
29. Kumar A, Deepika, Tyagi D, Tarkeshwar, Kapinder. Organic micropollutants and their effects on the environment and human health. In: Bhadouria R, Tripathi S, Singh P, Singh R, Singh HP, editors. Organic micropollutants in aquatic and terrestrial environments. Springer Nature Switzerland: Cham; 2024. pp. 87-105. DOI
30. Rani KC, Naik A, Chaurasiya RS, Raghavarao KSMS. Removal of toxic Congo red dye from water employing low-cost coconut residual fiber. *Water Sci Technol* 2017;75:2225-36. DOI PubMed
31. Bello OS, Adegoke KA, Fagbenro SO, Lameed OS. Functionalized coconut husks for rhodamine-B dye sequestration. *Appl Water Sci* 2019;9:1051. DOI
32. Karri RR, Sahu J, Jayakumar N. Optimal isotherm parameters for phenol adsorption from aqueous solutions onto coconut shell based activated carbon: error analysis of linear and non-linear methods. *J Taiwan Instf Chem Eng* 2017;80:472-87. DOI
33. Saritha B, Chockalingam MP. Adsorption study on removal of basic dye by modified coconut shell adsorbent. *Int J Civ Eng Technol* 2017;8:1370-4. Available from: https://iaeme.com/MasterAdmin/Journal_uploads/IJCIET/VOLUME_11_ISSUE_8/IJCIET_08_08_149.pdf. [Last accessed on 16 Dec 2024]
34. Luo Y, Li R, Sun X, Liu X, Li D. The roles of phosphorus species formed in activated biochar from rice husk in the treatment of landfill leachate. *Bioresour Technol* 2019;288:121533. DOI
35. Kumar A, Singha S, Dasgupta D, Datta S, Mandal T. Simultaneous recovery of silica and treatment of rice mill wastewater using rice husk ash: an economic approach. *Ecol Eng* 2015;84:29-37. DOI
36. Guo H, Yan L, Song D, Li K. Citric acid modified Camellia oleifera shell for removal of crystal violet and Pb(II): parameters study and kinetic and thermodynamic profile. *Desalin Water Treat* 2016;57:15373-83. DOI
37. Saba B, Jabeen M, Khalid A, Aziz I, Christy AD. Effectiveness of rice agricultural waste, microbes and wetland plants in the removal of reactive black-5 azo dye in microcosm constructed wetlands. *Int J Phytoremediation* 2015;17:1060-7. DOI
38. Gupta H, Gupta B. Adsorption of polycyclic aromatic hydrocarbons on banana peel activated carbon. *Desalin Water Treat* 2016;57:9498-509. DOI
39. Ali MEM, Abdelsalam H, Ammar NS, Ibrahim HS. Response surface methodology for optimization of the adsorption capability of ball-milled pomegranate peel for different pollutants. *J Mol Liq* 2018;250:433-45. DOI
40. Mallampati R, Xuanjun L, Adin A, Valiyaveettil S. Fruit peels as efficient renewable adsorbents for removal of dissolved heavy metals and dyes from water. *ACS Sustain Chem Eng* 2015;3:1117-24. DOI
41. Jusufi K, Korça B, Berisha A, et al. Potential application of orange peels as bio-sorbents in the removal of organic molecules from wastewater. In: Proceedings of the Fourth International Conference on Radiation and Applications in Various Fields of Research, Serbia. 2016; pp. 176-8. Available from: https://www.rad-proceedings.org/papers/RadProc.2016.41.pdf. [Last accessed on 16 Dec 2024].
42. Romero-Cano LA, Gonzalez-Gutierrez LV, Baldenegro-Perez LA, Medina-Montes MI. Preparation of orange peels by instant controlled pressure drop and chemical modification for its use as biosorbent of organic pollutants. *Rev Mex Ing Quím* 2016;15:481-91. Available from: https://www.redalyc.org/pdf/620/62046829015.pdf. [Last accessed on 16 Dec 2024]
43. Akkari I, Graba Z, Bezzi N, et al. Biosorption of basic red 46 using raw cactus fruit peels: equilibrium, kinetic and thermodynamic studies. *Biomass Conv Bioref* 2024;14:1825-36. DOI
44. Yan B, Niu CH, Wang J. Kinetics, electron-donor-acceptor interactions, and site energy distribution analyses of norfloxacin adsorption on pretreated barley straw. *Chem Eng J* 2017;330:1211-21. DOI
45. Zhang L, Tong L, Zhu P, et al. Adsorption of chlortetracycline onto biochar derived from corn cob and sugarcane bagasse. *Water Sci Technol* 2018;78:1336-47. DOI
46. Ge H, Wang C, Liu S, Huang Z. Synthesis of citric acid functionalized magnetic graphene oxide coated corn straw for methylene blue adsorption. *Bioresour Technol* 2016;221:419-29. DOI
47. Cheng M, Zeng G, Huang D, et al. Combined biological removal of methylene blue from aqueous solutions using rice straw and

Phanerochaete chrysosporium. *Appl Microbiol Biotechnol* 2015;99:5247-56. DOI

48. Ribeiro AC, Januário EFD, Vidovix TB, Vieira AMS, Duarte EDCNFA, Bergamasco R. Synthesis of a novel functionalized biosorbent from mango stone and its application in the pharmaceutical's removal from water and a synthetic mixture. *Chemosphere* 2024;346:140520. DOI
49. Khelifi O, Mehrez I. Equilibrium, kinetics and thermodynamics studies of methylene blue adsorption from aqueous solutions by biosorbent derived from Algerian date stones. *J Water Sci Environ Technol* 2016. Available from: https://revues.imist.ma/index.php/JOWSET/article/view/6830. [Last accessed on 16 Dec 2024]
50. Bo L, Gao N, Liu J, Gao B. The competitive adsorption of pharmaceuticals on granular activated carbon in secondary effluent. *Desalin Water Treat* 2016;57:17023-9. DOI
51. Chang EE, Wan JC, Kim H, Liang CH, Dai YD, Chiang PC. Adsorption of selected pharmaceutical compounds onto activated carbon in dilute aqueous solutions exemplified by acetaminophen, diclofenac, and sulfamethoxazole. *ScientificWorldJournal* 2015;2015:186501. DOI PubMed PMC
52. Ali A, Saeed K. Phenol removal from aqueous medium using chemically modified banana peels as low-cost adsorbent. *Desalin Water Treat* 2016;57:11242-54. DOI
53. Pawar S, Theodore T, Hiremath PG. Synthesis of hydroxyapatite from avocado fruit peel and its application for hexavalent chromium removal from aqueous solutions-adsorption isotherms and kinetics study. *Adsorption* 2019;12:1964-72. DOI
54. Wu C, Huang L, Xue SG, et al. Arsenic sorption by red mud-modified biochar produced from rice straw. *Environ Sci Pollut Res Int* 2017;24:18168-78. DOI
55. Guo J. Enhancing biological removal of methylene blue from aqueous solutions using *Bacillus subtilis* inoculated rice straw. *J Environ Eng* 2019;145:1478. DOI
56. Herrera-García U, Castillo J, Patiño-Ruiz D, Solano R, Herrera A. Activated carbon from yam peels modified with Fe_3O_4 for removal of 2,4-dichlorophenoxyacetic acid in aqueous solution. *Water* 2019;11:2342. DOI
57. Mohamed G, El-Shafey O, Fathy NA. Preparation of carbonaceous hydrochar adsorbents from cellulose and lignin derived from rice straw. *Egypt J Chem* 2017;60:793-804. DOI
58. Naghdi M, Taheran M, Pulicharla R, et al. Pine-wood derived nanobiochar for removal of carbamazepine from aqueous media: adsorption behavior and influential parameters. *Arab J Chem* 2019;12:5292-301. DOI
59. Yu P, Liu Z, Wu D, Chen M, Lv W, Zhao Y. Accumulation of polystyrene microplastics in juvenile Eriocheir sinensis and oxidative stress effects in the liver. *Aquat Toxicol* 2018;200:28-36. DOI
60. Debnath B, Saha I, Mukherjee T, Mitra S, Das A, Das A. Chapter 12 - Sorbents from waste materials: a circular economic approach. In: Sorbents materials for controlling environmental pollution. Elsevier: 2021. pp. 285-322. DOI
61. Konga A, Arunsanjay KS, Hariharaprabhu T, Sudhagar P, Solaman TR. Studies o n removal of Cu^{2+} from effluent water by using rice husk. *Asian J Microbiol Biotechnol Environ Exp Sci* 2015;17:115-21. Available from: https://www.researchgate.net/publication/281874723_Studies_on_removal_of_Cu2_from_effluent_water_by_using_rice_husk. [Last accessed on 16 Dec 2024]
62. Qu J, Meng X, You H, Ye X, Du Z. Utilization of rice husks functionalized with xanthates as cost-effective biosorbents for optimal Cd(II) removal from aqueous solution via response surface methodology. *Bioresour Technol* 2017;241:1036-42. DOI
63. Dias M, Pinto J, Henriques B, et al. Nutshells as efficient biosorbents to remove cadmium, lead, and mercury from contaminated solutions. *Int J Environ Res Public Health* 2021;18:1580. DOI PubMed PMC
64. Garg R, Garg R, Sillanpää M, et al. Rapid adsorptive removal of chromium from wastewater using walnut-derived biosorbents. *Sci Rep* 2023;13:6859. DOI PubMed PMC
65. Ajmi RN, Sultan M, Hanno SH. Bioabsorbent of chromium, cadmium and lead from industrial waste water by waste plant. *J Pharm Sci Res* 2018;10:672-4. Available from: https://www.jpsr.pharmainfo.in/Documents/Volumes/vol10Issue03/jpsr10031853.pdf. [Last accessed on 16 Dec 2024]
66. Oyewo OA, Onyango MS, Wolkersdorfer C. Application of banana peels nanosorbent for the removal of radioactive minerals from real mine water. *J Environ Radioact* 2016;164:369-76. DOI
67. Singh J, Ali A, Jaswal VS, Prakash V. Desalination of Cd^{2+} and Pb^{2+} from paint industrial wastewater by Aspergillus niger decomposed Citrus limetta peel powder. *Int J Environ Sci Technol* 2015;12:2523-32. DOI
68. Monroy-Figueroa J, Mendoza-Castillo DI, Bonilla-Petriciolet A, Pérez-Cruz MA. Chemical modification of Byrsonima crassifolia with citric acid for the competitive sorption of heavy metals from water. *Int J Environ Sci Technol* 2015;12:2867-80. DOI
69. Yan J, Lan G, Qiu H, et al. Adsorption of heavy metals and methylene blue from aqueous solution with citric acid modified peach stone. *Sep Sci Technol* 2018;53:1678-88. DOI
70. Díaz-Muñoz LL, Bonilla-Petriciolet AB, Reynel-Ávila HE, Mendoza-Castillo DI. Sorption of heavy metal ions from aqueous solution using acid-treated avocado kernel seeds and its FTIR spectroscopy characterization. *J Mol Liqs* 2016;215:555-64. DOI
71. Lu XG, Guo YT. Removal of Pb (II) from aqueous solution by sulfur-functionalized walnut shell. *Environ Sci Pollut Res Int* 2019;26:12776-87. DOI PubMed
72. Dan Y, Xu L, Qiang Z, Dong H, Shi H. Preparation of green biosorbent using rice hull to preconcentrate, remove and recover heavy metal and other metal elements from water. *Chemosphere* 2021;262:127940. DOI
73. Surovka D, Pertile E, Sarcakova E, Svidrova L, Bendova M. Adsorptive removal of sulphates from aqueous matrix using a fixed bed column packed with orange peel. In: Proceedings of the 15th International Multidisciplinary Scientific GeoConference (SCEM); Albena, Bulgaria. 2015; pp. 33-40.

74. Nathan RJ, Martin CE, Barr D, Rosengren RJ. Simultaneous removal of heavy metals from drinking water by banana, orange and potato peel beads: a study of biosorption kinetics. *Appl Water Sci* 2021;11:1457. DOI
75. Ahmadi H, Hafiz SS, Sharifi H, Rene NN, Habibi SS, Hussain S. Low cost biosorbent (Melon Peel) for effective removal of Cu (II), Cd (II), and Pb (II) ions from aqueous solution. *Case Stud Chem Environ Eng* 2022;6:100242. DOI
76. Bhadoria P, Shrivastava M, Khandelwal A, et al. Preparation of modified rice straw-based bio-adsorbents for the improved removal of heavy metals from wastewater. *Sustain Chem Pharm* 2022;29:100742. DOI
77. Liu Q, Li Y, Chen H, et al. Superior adsorption capacity of functionalised straw adsorbent for dyes and heavy-metal ions. *J Hazard Mater* 2020;382:121040. DOI
78. Yu H, Wang J, Yu J, Wang Y, Chi R. Adsorption performance and stability of the modified straws and their extracts of cellulose, lignin, and hemicellulose for Pb^{2+}: pH effect. *Arab J Chem* 2020;13:9019-33. DOI
79. Mohammadabadi SI, Javanbakht V. Lignin extraction from barley straw using ultrasound-assisted treatment method for a lignin-based biocomposite preparation with remarkable adsorption capacity for heavy metal. *Int J Biol Macromol* 2020;164:1133-48. DOI PubMed
80. Šoštarić TD, Petrović MS, Pastor FT, et al. Study of heavy metals biosorption on native and alkali-treated apricot shells and its application in wastewater treatment. *J Mol Liq* 2018;259:340-9. DOI
81. Maity S, Bajirao Patil P, SenSharma S, Sarkar A. Bioremediation of heavy metals from the aqueous environment using Artocarpus heterophyllus (jackfruit) seed as a novel biosorbent. *Chemosphere* 2022;307:136115. DOI PubMed
82. Kushwaha S, Suhas, Chaudhary M, et al. Utilization of *Phyllanthus emblica fruit stone* as a potential biomaterial for sustainable remediation of lead and cadmium ions from aqueous solutions. *Molecules* 2022;27:3355. DOI PubMed PMC
83. Oladipo AA, Ahaka EO, Gazi M. High adsorptive potential of calcined magnetic biochar derived from banana peels for Cu^{2+}, Hg^{2+}, and Zn^{2+} ions removal in single and ternary systems. *Environ Sci Pollut Res Int* 2019;26:31887-99. DOI
84. Dieme MM, Villot A, Gerente C, Andres Y, Diop SN, Diawara CK. Sustainable conversion of agriculture wastes into activated carbons: energy balance and arsenic removal from water. *Environ Technol* 2017;38:353-60. DOI PubMed
85. Erabee IK, Ahsan A, Jose B, et al. Adsorptive treatment of landfill leachate using activated carbon modified with three different methods. *KSCE J Civ Eng* 2018;22:1083-95. DOI
86. Wang S, Zhao M, Zhou M, et al. Biomass facilitated phase transformation of natural hematite at high temperatures and sorption of Cd^{2+} and Cu^{2}. *Environ Int* 2019;124:473-81. DOI
87. Wang T, Zheng J, Liu H, Peng Q, Zhou H, Zhang X. Adsorption characteristics and mechanisms of Pb^{2+} and Cd^{2+} by a new agricultural waste-Caragana korshinskii biomass derived biochar. *Environ Sci Pollut Res Int* 2021;28:13800-18. DOI
88. Escudero LB, Quintas PY, Wuilloud RG, Dotto GL. Recent advances on elemental biosorption. *Environ Chem Lett* 2019;17:409-27. DOI
89. Aranda-García E, Chávez-Camarillo GM, Cristiani-Urbina E. Effect of ionic strength and coexisting ions on the biosorption of divalent nickel by the acorn shell of the oak *Quercus crassipes* Humb. & Bonpl. *Processes* 2020;8:1229. DOI
90. Pertile E, Vaclavik V, Dvorsky T, Heviankova S. The removal of residual concentration of hazardous metals in wastewater from a neutralization station using biosorbent - a case study company Gutra, Czech Republic. *Int J Environ Res Public Health* 2020;17:7225. DOI PubMed PMC
91. Devasena SS, Padmavathy P, Rani V, Ganesan P, Pereira JJ. Studies on the efficiency of fish scale adsorbents for treatment of fish processing effluent. *Env Prog Sustain Energy* 2023;42:e14195. DOI
92. Gholami N, Dadvand Koohi A, Ebrahimian Pirbazari A. Fabrication, characterization, regeneration and application of nanomagnetic Fe_3O_4@fish scale as a bio-adsorbent for removal of methylene blue. *J Water Environ Nanotechnol* 2018;3:219-34. DOI
93. Neves D, Sobral P, Ferreira JL, Pereira T. Ingestion of microplastics by commercial fish off the Portuguese coast. *Mar Pollut Bull* 2015;101:119-26. DOI PubMed
94. Vakili M, Gholami F, Zwain HM, et al. Treatment of As(III)-contaminated food waste using alkali treatment and its potential application for methylene blue removal from aqueous solutions. *J Water Proc Eng* 2023;55:104100. DOI
95. Blaga AC, Tanasă AM, Cimpoesu R, Tataru-Farmus RE, Suteu D. Biosorbents based on biopolymers from natural sources and food waste to retain the methylene blue dye from the aqueous medium. *Polymers* 2022;14:2728. DOI PubMed PMC
96. Domingues A, da Costa JP, Rocha-Santos TAP, Gonçalves FJM, Pereira R, Pereira JL. Biosorption potential of the shell of Corbicula fluminea towards olive oil mill waste. *Int J Environ Sci Technol* 2022;19:5689-96. DOI
97. Sharma A, Devi I. A sustainable biosorption technique for treatment of industrial wastewater using snail shell dust (Bellamya bengalensis). *Environ Monit Assess* 2023;195:389. DOI PubMed
98. Elayadi F, Achak M, Beniich N, Belaqziz M, El Adlouni C. Factorial design for optimizing and modeling the removal of organic pollutants from olive mill wastewater using a novel low-cost bioadsorbent. *Water Air Soil Pollut* 2020;231:4695. DOI
99. Su H, Guo X, Zhang X, et al. Ultrafine biosorbent from waste oyster shell: a comparative study of Congo red and Methylene blue adsorption. *Bioresource Technol Rep* 2022;19:101124. DOI
100. Saufi H, Alouani ME, Aride J, Taibi M. Rhodamine B biosorption from aqueous solution using Eichhornia crassipes powders: Isotherm, kinetic and thermodynamic studies. *Chem Data Collect* 2020;25:100330. DOI
101. Kulkarni MR, Revanth T, Acharya A, Bhat P. Removal of crystal violet dye from aqueous solution using water hyacinth: equilibrium, kinetics and thermodynamics study. *Resour Efficient Technol* 2017;3:71-7. DOI
102. Patil SR, Sutar SS, Jadhav JP. Sorption of crystal violet from aqueous solution using live roots of Eichhornia crassipes: kinetic,

isotherm, phyto and cyto-genotoxicity studies. *Environ Technol Innov* 2020;18:100648. DOI

103. Nguyen VQ, Van HT, Sy HL, Nguyen TML, Nguyen DK. Application of Mussell-derived biosorbent to remove NH_4^+ from aqueous solution: equilibrium and kinetics. *SN Appl Sci* 2021;3:4462. DOI
104. Esmaeili H, Tamjidi S, Abed M. Removal of Cu (II), Co (II) and Pb (II) from synthetic and real wastewater using calcified Solamen Vaillanti snail shell. *Desalin Water Treat* 2020;174:324-35. DOI
105. Ali MEA, Aboelfadl MMS, Selim AM, Khalil HF, Elkady GM. Chitosan nanoparticles extracted from shrimp shells, application for removal of Fe(II) and Mn(II) from aqueous phases. *Sep Sci Technol* 2018;53:2870-81. DOI
106. Foroutan R, Esmaeili H, Fard MK. Equilibrium and kinetic studies of Pb (II) biosorption from aqueous solution using shrimp peel. *Int Res J Appl Basic Sci* 2015;9:1954-65. Available from: https://www.researchgate.net/publication/289673152_Equilibrium_and_kinetic_studies_of_Pb_II_biosorption_from_aqueous_solution_using_shrimp_peel. [Last accessed on 16 Dec 2024]
107. Yen HY. Taguchi optimization for Cd(II) removal from aqueous solutions using oyster shell powders. *Desalin Water Treat* 2016;57:20430-8. DOI
108. Teshale F, Karthikeyan R, Sahu O. Synthesized bioadsorbent from fish scale for chromium (III) removal. *Micron* 2020;130:102817. DOI PubMed
109. Akar T, Karadağ Atılgan M, Celik S, Sayin F, Tunali Akar S. Highly effective fish scale–based biochar as a recyclable and green material for toxic cadmium ion bioremoval from liquid phase. *Biomass Conv Bioref* 2024;14:4869-82. DOI
110. Kang J, Seo E, Lee C, Park S. Fe-loaded biochar obtained from food waste for enhanced phosphate adsorption and its adsorption mechanism study via spectroscopic and experimental approach. *J Environ Chem Eng* 2021;9:105751. DOI
111. Hong SH, Lyonga FN, Kang JK, et al. Synthesis of Fe-impregnated biochar from food waste for Selenium(VI) removal from aqueous solution through adsorption: Process optimization and assessment. *Chemosphere* 2020;252:126475. DOI
112. Bazzazzadeh R, Soudi M, Valinassab T, Moradlou O. Kinetics and equilibrium studies on biosorption of hexavalent chromium from leather tanning wastewater by Sargassum tenerrimum from Chabahar-Bay Iran. *Algal Res* 2020;48:101896. DOI
113. Al-Homaidan AA, Al-Qahtani HS, Al-Ghanayem AA, Ameen F, Ibraheem IBM. Potential use of green algae as a biosorbent for hexavalent chromium removal from aqueous solutions. *Saudi J Biol Sci* 2018;25:1733-8. DOI PubMed PMC
114. Pouya MR, Behnam S. Adsorption behavior of copper ions on alga *Jania adhaerens* through SEM and FTIR analyses. *Sep Sci Technoly* 2017;52:2062-8. DOI
115. Salman M, Demir M, Tang KHD, et al. Removal of cresol red by adsorption using wastepaper. *Ind Domest Waste Manag* 2022;2:1-8. DOI
116. Lee KK, Tang KHD. Agaricales (Gilled Mushrooms) as biosorbents of synthetic dye. *Mal J Med Health Sci* 2020;16:10-7. Available from: https://medic.upm.edu.my/upload/dokumen/2020112512045902_2020_0295.pdf. [Last accessed on 16 Dec 2024]
117. Silva B, Martins M, Rosca M, et al. Waste-based biosorbents as cost-effective alternatives to commercial adsorbents for the retention of fluoxetine from water. *Sep Purif Technol* 2020;235:116139. DOI
118. Food and Agriculture Organization of the United Nations. Statistics Division (ESS). Available from: https://www.fao.org/about/who-we-are/departments/statistics-division. [Last accessed on 16 Dec 2024].
119. Devi B, Goswami M, Rabha S, Kalita S, Sarma HP, Devi A. Efficacious sorption capacities for Pb(II) from contaminated water: a comparative study using biowaste and its activated carbon as potential adsorbents. *ACS Omega* 2023;8:15141-51. DOI PubMed PMC
120. Kaetzl K, Lübken M, Gehring T, Wichern M. Efficient low-cost anaerobic treatment of wastewater using biochar and woodchip filters. *Water* 2018;10:818. DOI
121. Taherymoosavi S, Joseph S, Munroe P. Characterization of organic compounds in a mixed feedstock biochar generated from Australian agricultural residues. *J Anal Appl Pyrolysis* 2016;120:441-9. DOI
122. Alhashimi HA, Aktas CB. Life cycle environmental and economic performance of biochar compared with activated carbon: a meta-analysis. *Resour Conserv Recy* 2017;118:13-26. DOI
123. Verma L, Singh J. Removal of As(III) and As(V) from aqueous solution using engineered biochar: batch and fixed-bed column study. *Int J Environ Sci Technol* 2023;20:1961-80. DOI
124. Chen J, Jiang X, Tang X, Sun Y, Zhou L. Use of biochar/persulfate for accelerating the stabilization process and improving nitrogen stability of animal waste digestate. *Sci Total Environ* 2021;757:144158. DOI
125. Wiśniowska E, Grobelak A, Kokot P, Kacprzak M. 10 - Sludge legislation-comparison between different countries. In: Industrial and municipal sludge, prasad. Butterworth-Heinemann: 2019. pp. 201-24. DOI
126. Thompson KA, Shimabuku KK, Kearns JP, Knappe DRU, Summers RS, Cook SM. Environmental comparison of biochar and activated carbon for tertiary wastewater treatment. *Environ Sci Technol* 2016;50:11253-62. DOI PubMed

Kelly *et al. Water Emerg Contam Nanoplastics* 2024;3:26
DOI: 10.20517/wecn.2024.66

Water Emerging Contaminants & Nanoplastics

Research Article

Open Access

Microplastics in Southern Ocean sea ice: a pan-Antarctic perspective

Anna Kelly[1], **Thomas Rodemann**[2], **Klaus M. Meiners**[3,4,5], **Heidi J. Auman**[1], **Sebastien Moreau**[6], **Francois Fripiat**[7], **Bruno Dellile**[8], **Delphine Lannuzel**[1,4,5]

[1]Institute for Marine and Antarctic Studies, University of Tasmania, Hobart 7001, Tasmania, Australia.
[2]Central Science Laboratory, University of Tasmania, Hobart 7001, Tasmania, Australia.
[3]Australian Antarctic Division, Department of Climate Change, Energy, the Environment and Water, Kingston 7050, Tasmania, Australia.
[4]Australian Antarctic Program Partnership, University of Tasmania, Hobart 7001, Tasmania, Australia.
[5]Australian Centre for Excellence in Antarctic Science, Institute for Marine and Antarctic Studies, University of Tasmania, Hobart 7004, Tasmania, Australia.
[6]Norwegian Polar Institute, Fram Centre, Tromsø 9007, Norway.
[7]Laboratoire de Glaciologie, Université Libre des Bruxelles, Brussels 1050, Belgium.
[8]Chemical Oceanography Unit, Freshwater and Oceanic Sciences Unit of Research, University of Liège, Liège 4000, Belgium.

Correspondence to: Anna Kelly, Institute for Marine and Antarctic Studies, University of Tasmania, Private Bag 129, Hobart 7001, Tasmania, Australia. E-mail: anna.kelly@utas.edu.au

How to cite this article: Kelly A, Rodemann T, Meiners KM, Auman HJ, Moreau S, Fripiat F, Dellile B, Lannuzel D. Microplastics in Southern Ocean sea ice: a pan-Antarctic perspective. *Water Emerg Contam Nanoplastics* 2024;3:26. https://dx.doi.org/10.20517/wecn.2024.66

Received: 16 Oct 2024 **First Decision:** 18 Nov 2024 **Revised:** 13 Dec 2024 **Accepted:** 17 Dec 2024 **Published:** 30 Dec 2024

Academic Editors: Jie Wang, Giuseppe Suaria **Copy Editor:** Pei-Yun Wang **Production Editor:** Pei-Yun Wang

Abstract

Microplastic (MP; plastic particles < 5 mm) pollution is pervasive in the marine environment, including remote polar environments. This study provides the first pan-Antarctic survey of MP pollution in Southern Ocean sea ice by analyzing sea ice cores from several diverse Antarctic regions. Abundance, chemical composition, and particle size data were obtained from 19 archived ice core samples. The cores were melted, filtered, and chemically analyzed using Fourier-transform infrared spectroscopy and 4,090 MP particles were identified. Nineteen polymer types were found across all samples, with an average concentration of 44.8 (± 50.9) particles·L^{-1}. Abundance and composition varied with ice type and geographical location. Pack ice exhibited significantly higher particle concentrations than landfast ice, suggesting open ocean sources of pollution. Winter sea ice cores had significantly more MPs than spring and summer-drilled cores, suggesting ice formation processes play a role in particle incorporation. Smaller particles dominated across samples. Polyethylene (PE) and polypropylene (PP) were the most common polymers, mirroring those most identified across marine habitats. Higher average MP concentrations in developing sea ice during autumn and winter, contrasting lower levels observed in spring and summer, suggest turbulent conditions and faster growth rates are likely responsible for the increased incorporation of particles. Southern Ocean MP contamination likely stems from both local and distant sources. However, the circulation of deep waters and long-range transport likely contribute to the accumulation of MPs in regional gyres, coastlines, and their eventual incorporation into sea ice. Additionally, seasonal sea ice variations likely influence regional polymer compositions, reflecting the MP composition of the underlying waters.

Keywords: Microplastic, marine debris, sea ice, plastic pollution, Antarctica, Southern Ocean

INTRODUCTION

Despite the ubiquity of microplastics (MPs; plastic particles < 5 mm) in the global oceans and their noted presence within remote polar regions, the majority of polar reports have come from the Arctic Ocean, where significant levels of MPs have been recorded in surface waters[1], snow[2], and sea ice[3,4]. In the Southern Ocean, the subtropical front (STF) and the Antarctic circumpolar current (ACC) have long been considered active barriers[5], specifically to buoyant MPs at the sea surface[6,7], thus potentially limiting MP contamination being transported to the Southern Ocean from lower latitudes. However, since their discovery in the Southern Ocean, there have been an increasing number of contrasting MP reports in the region[8-10], suggesting higher exchange across the ACC than previously thought[11]. Plastic contamination has been noted in Antarctic surface waters[12,13], sea ice[14,15], snow[16], and deep-sea sediments[17]. The geography and oceanographic processes in the Arctic and Antarctic vary widely, and thus, we focus solely on the Antarctic in this work when speculating on incorporation and transport mechanisms. To date, there has been a significant lack of comprehensive research surrounding MPs in Antarctic sea ice, with only three previous studies (totaling four ice cores) having been published to date. One of the three studies is our initial work, which first indicated the presence of MPs in Southern Ocean sea ice[14]. However, our methodology was significantly different, making cross-study comparisons difficult. Cunningham *et al.* (2022) did not identify MPs down to their polymeric composition, only noting their presence and confirming the particles were synthetic in nature[18]. Similarly, Materic *et al.* (2022) analyzed one ice core for nanoplastics[15], and thus, our studies are incompatible for comparison. As such, this research truly provides a foundation for subsequent sea ice MP studies and future comparisons.

The remoteness of the ice-covered Southern Ocean and its total encompassment within the ACC provide unique insights regarding marine debris in isolated regions and its transport to areas largely devoid of human activity. Global contaminants have been known to reach the Southern Ocean via long-range atmospheric transport (LRAT) and oceanic currents[19,20]. The ACC is an eastward-flowing current, dividing the Southern Ocean from the surrounding Indian, Atlantic, and Pacific oceans[21]. If MPs from lower latitudes are transported past the ACC - or locally sourced from research, tourist, and fishing activities - they can be pulled toward the continent by southern-flowing tracts of regional gyres such as in the Ross or Wedell Sea[13,22,23] and drawn further into coastal waters as a result of localized eddies, storm-forced surface waves, wave-driven advection such as Stoke's drift, and frontal meandering[11,24]. MPs directed nearest the continent can then interact with the westward-flowing Antarctic coastal current, leading to further dispersal and their exposure to local processes like tidal interactions, eddies, and seawater convection[25]. Therefore, it should be noted that while it is easier for plastics to enter the Antarctic than previously thought, it is unlikely that MP debris is being moved out of the Southern Ocean at a rate of equal exchange once it has found its way there, but rather is being captured by marine mediums and cycled through Antarctic food webs.

The Antarctic sea ice growth cycle is one of the largest seasonally driven events on Earth, exhibited by the vast changes to sea ice extent from ~3 million km^2 in late austral summer to ~19 million km^2 at its height in early spring[26]. Antarctic sea ice has been suggested to serve as a temporal sink for MP debris[14], and the large seasonal variability in sea ice coverage may facilitate a large and recurring particle flux for MP debris into the global ocean. Sea ice has been suggested to serve as a temporal sink for MPs in polar regions. In autumn and winter, MP particles may be harvested from surface waters during frazil ice formation, where they adhere to and are scavenged by ice crystals as the crystals rise in the water column to become incorporated in newly formed sea ice[27]. As ice continues to form, MPs can become incorporated into growing sea ice via basal accretion until their release in spring when sea ice melts[6]. Additionally, in a well-established ice column, the ice-water interface allows for the sieving of particulate matter in and out of the ice[28,29]. Lastly, MP accumulation may occur by means of LRAT of snow or aerosols[16]. Small, lightweight particles (often fibrous) are easily carried by southward-moving air masses where they can be deposited onto the ice and incorporated into its upper layers, e.g., by snow metamorphic processes, including snow-ice formation[2,30].

To our knowledge, no study has assessed the abundance of MP pollution in sea ice from a pan-Antarctic perspective. This study sought to assess the distribution, abundance, polymer composition, and size spectra of MPs to determine if MP contamination varied significantly across sampling sites, geographical regions, and ice types. We conducted the first comprehensive analysis of MP particles in Antarctic sea ice from near-shore fast ice and open-ocean pack ice. Antarctic landfast ice is sea ice attached to the coastline or grounded icebergs, remaining stationary, while pack ice consists of free-floating sea ice that drifts with wind and ocean currents. Sampling both allows us to compare the sources, transport mechanisms, and temporal deposition of MPs, as landfast ice is stationary and may capture local inputs over time, while pack ice is dynamic and integrates materials from diverse regions, offering insights into the distribution and fate of MPs in polar environments. We conducted MP analysis on 19 sea ice cores from 10 individual research expeditions across distinct Southern Ocean regions: The Antarctic Peninsula, the Bellinghausen Sea, the Weddell Sea, Queen Maud Land, Prydz Bay, Wilkes Land, Mawson Sea, the Ross Sea, and McMurdo Sound, and sampled during austral summers spanning 2004-2022 [Figure 1]. From this analysis, we report the average MP concentration in Antarctic sea ice and analyze the spatial variability of MPs around the Southern Ocean to attain a broader understanding of MP contamination in the Southern Ocean.

MATERIALS AND METHODS

Core collection

The 19 archived sea ice cores used for this study were collected between 2004 and 2022 [Figure 1]. Cores were drilled in austral autumn/winter (March-Aug), spring (Sept-Nov), and late summer season (Dec-Feb) under trace-metal-clean conditions. Of these, 10 cores were first-year pack ice and 9 were first-year landfast ice [Table 1]. Cores drilled during the DML campaign were collected using a Kovacs Mark II corer with an internal diameter of 9 cm, while the rest of the cores were drilled with an electropolished stainless steel corer, suited for trace metal analysis[31], with an internal diameter of 8 or 14 cm. Ice cores were stored in PE plastic bags for transport and freezer storage and decontaminated for MP analysis, as outlined below.

Laboratory processing

All chemicals and reagents used in this study were pre-filtered over 1.2 µm Whatman GF/C (glass microfiber, 47 mm) filters to mitigate MP contamination from packaging. A Dupont™ Tyvek full-coverage suit (Bioclean-D non-sterile coverall with hood, manufactured by Cleanroom Garments) was worn during all ice-core cutting and handling in the field, ensuring consistency with the attire used in trace-metal-clean sea ice coring. For laboratory work, 100% cotton clothing was worn as a precaution to minimize contamination from polymer-blend and synthetic textile fibers. Additionally, cotton fibers were excluded

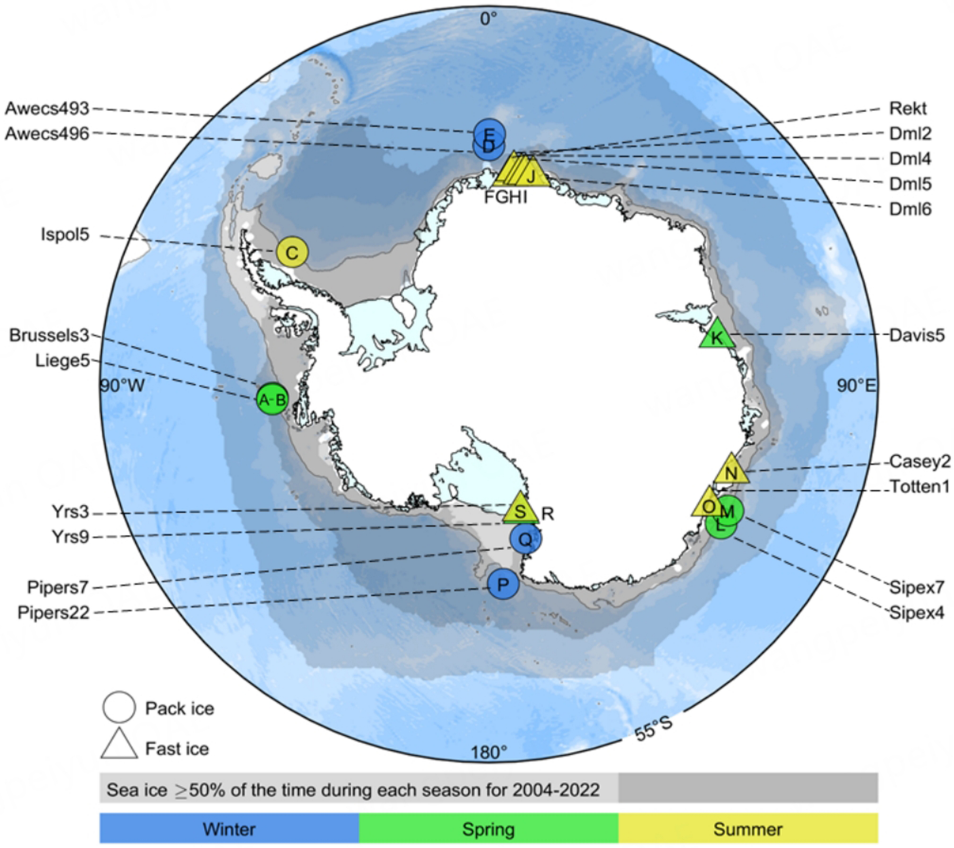

Figure 1. Map of sampling sites for Antarctic ice cores collected from 2004-2022 coupled with mean sea ice concentrations across associated summers. Winter and spring sea ice extent are combined (light gray), while summer sea ice extent is shown in dark gray.

from all analyses to further reduce potential contamination. All glassware was pre-rinsed with ethanol and washed in a glassware-only dishwasher, followed by acid rinses with 1% HCl solution. All glassware was covered in aluminum foil to prevent contamination. Nitrile gloves were not worn during the study, except when handling hazardous chemicals, due to evidence suggesting they can contaminate samples and cause false positives[32]. During each sample transfer step, glassware was thoroughly rinsed with MilliQ™ water to ensure particles had not adhered to the walls of any containers.

As the ice cores were archived samples, processing occurred across three different institutions: the Norwegian Polar Institute (NPI; Tromsø, Norway), the Institute for Marine and Antarctic Studies (IMAS; Hobart, Tasmania), and the Université Libre des Bruxelles (ULB; Brussels, Belgium). Therefore, ice core handling varied slightly based on laboratory infrastructure. The following is a brief overview of the ice-core processing method used to isolate and identify MPs.

All ice cores were cut with individual consideration for the ice crystal structure and ice algal biomass (chlorophyll *a* and particulate organic carbon) within the ice. The cutting of the 19 cores resulted in a total of 60 ice-core horizons for processing and analysis. To ensure there was no contamination due to ice-core storage in LDPE bags for transport and storage, the outside of the core (approx. 1-2 mm) was scraped off with a ceramic knife (Kyocera) pre-cleaned with MilliQ™ water. Core horizons were melted in glass containers at room temperature. Oxidative digestions using 2% sodium dodecyl sulfate (SDS; BDH Laboratory Supplies, England) solution and 35% hydrogen peroxide (H_2O_2; Chem-Supply) were performed

Table 1. Ice core data for the 19 archived sea ice cores used for analysis

Core ID	Original campaign	Sample location	Sampling date	Latitude (°N)	Longitude (°E)	Core length (m)	Ice type
Brussels3	SIMBA	Bellingshausen Sea	11 Oct 2007	-70.06	-93.68	0.59	Pack
Liege5	SIMBA	Bellingshausen Sea	21 Oct 2007	-70.04	-94.08	0.98	Pack
Ispol5	ISPOL	Weddell Sea	19 Dec 2004	-68.06	-55.30	0.95	Pack
Awecs493	AWECS	Weddell Sea	21 June 2017	-66.44	0.12	0.58	Pack
Awecs496	AWECS	Weddell Sea	24 June 2017	-67.46	-0.02	0.59	Pack
Rekt	REKT	Queen Maud Land	12 Jan 2021	-70.18	5.61	1.73	Fast
Dml2	DML	Queen Maud Land	12 Jan 2022	-69.66	6.47	1.385	Fast*
Dml4	DML	Queen Maud Land	13 Jan 2022	-69.84	8.49	1.65	Fast*
Dml5	DML	Queen Maud Land	13 Jan 2022	-69.84	9.62	1.26	Fast*
Dml6	DML	Queen Maud Land	14 Jan 2022	-69.86	11.62	1.85	Fast*
Davis5	DAVIS	Prydz Bay, Davis Station	29 Nov 2015	- 68.57	77.96	1.68	Pack
Sipex4	SIPEX II	Mawson Sea	7 Oct 2012	-65.08	121.67	0.75	Pack
Sipex7	SIPEX II	Mawson Sea	19 Oct 2012	-65.15	118.55	0.80	Pack
Casey2	AAV2	O'Brien Bay, Wilkes Land	23 Dec 2016	-66.30	110.50	1.30	Fast
Totten1	AAV2	Moscow University Ice Shelf, Wilkes Land	31 Dec 2016	-66.80	119.50	1.05	Fast
Pipers7	PIPERS	Terra Nova Bay Polynya, Ross Sea	1 May 2017	-74.97	166.95	0.29	Pack
Pipers22	PIPERS	Central Ross Sea	28 May 2017	-71.07	176.02	0.45	Pack
Yrs3	YROSIAE	Cape Evans, McMurdo Sound	8 Dec 2011	-77.63	166.38	1.48	Fast
Yrs9	YROSIAE	Cape Evans, McMurdo Sound	7 Nov 2012	-77.38	166.23	1.7	Fast

Ice type* indicates cores that were drilled as part of free-floating pack ice, but ice texture analysis and high platelet content indicate they may have originated as landfast sea ice.

over the course of 48 h at 50 °C to reduce biological material in each sample. Next, the treated meltwater was filtered through silica sand (50-70 µm particle size, Sigma-Aldrich) and the filtrate was discarded to waste. Density separations were then performed on the sand mixture (and potentially entrapped MPs) by being placed in a supersaturated NaCl solution (NaCl > 99%, Sigma-Aldrich), stirred for approximately 15 min, and left to settle for about 3 h. NaCl was chosen based on its sufficiency in MP isolation following Quinn *et al.* (2017), even for denser polymers such as polyvinyl chloride (PVC) and polyethylene terephthalate (PET)[33]. The supernatant was filtered onto Whatman anodisc aluminum oxide filters (0.2 µm porosity, 25 mm diameter). Each filter was then placed in an oven to dry for 24 h at 50 °C, following an established oxidative digestive protocol shown to have minimal impact on polymers[34].

Cores processed at NPI (Rekt, Dml2, Dml4, Dml5, Dml6) and ULB (Brussels3, Liege5, Ispol5, Awecs493, Awecs496, Pipers7, Pipers22, Yrs3, Yrs9) were cut in cold rooms; therefore, additional cold gear was necessary. Thin PE gloves were worn over wool gloves. This additional precaution was not found to increase MPs found in blanks at either institution (see next section). Additionally, ULB cores were cut using a powered band saw, and the outside ice layer of each core horizon was removed with the band saw blade.

Blanks and recovery tests

As cores were cut under slightly different circumstances, laboratory blanks were run at all three institutions in triplicate to ensure reliable MP data from our environmental samples. At each institution, blank ice cores were created with ultrapure MilliQ™ water and cylindrically frozen. They were then processed identically to our real samples, allowing us to identify potential laboratory contamination and avoid polymer overestimation. Noted total MPs in blanks by institution are as follows: one polyurethane (PUR) and one polystyrene (PS) particle at NPI (mean 0.22 ± 0.38 particles·L^{-1}), one polyamide (PA) and five PP particles at

IMAS (mean 0.67 ± 0.67 particles·L^{-1}), one PUR, one PS, and two PP particles at ULB (mean 0.44 ± 0.38 particles·L^{-1}). These particle numbers were subtracted from their relevant samples for final calculations and statistical tests.

Three additional blanks, referred to as "spiked blanks", were prepared for recovery rate testing. These blanks were made by spiking 1 L of MilliQ^{TM} water with 50 blue PE beads (20-27 μm diameter; 1.08 g·mL^{-1}) (Cospheric LLC). The recovery samples were processed in the same manner as the previous blanks and environmental samples. The PE beads were identified and counted using a light microscope, and the average recovery rate was determined to be 96 (±3)%. One of the filters was used for micro-Fourier-transform spectroscopy (μFTIR) analysis to verify that the Purency Microplastic Finder (PMF; Purency; version 4.17) accurately detected the beads and corresponded with visual observations.

μFTIR/chemical imaging and data analysis

Data were collected via μFTIR spectroscopy. A Hyperion 3000 microscope attached to a Vertex 70 spectrometer (both Bruker Optics) was used for chemical imaging of all sample filters. Sample analysis was conducted with OPUS 8.7 software (Bruker), using 128 scans for the background and 16 scans for each frame, with an IR microscope objective of ×3.5 magnification. The 64 × 64 FPA detector was selected (no binning), resulting in 64 × 64 spectra per frame (784 × 784 μm^2) with a pixel resolution of ~12.25 × 12.25 μm^2. Each filter was analyzed by combining 16 × 16 FPA frames to create a hyperspectral image containing over 5 million spectra per filter (12.544 × 12.544 mm^2).

The collated OPUS data were exported as an ENVI file and particle analysis was conducted with PMF, an automated analysis software for μFTIR imaging. Machine learning is used in conjunction with an integrated spectral library to directly compare OPUS spectral data and the spectra of known polymers. A baseline confidence rate (hit level) of 90% was set for PA to ensure the software could differentiate true PA particles from similar-looking biological spectra, while 60% was set for all remaining polymer types. For each particle categorized as an MP, software-provided particle area was used to calculate the equivalent spherical diameter (ESD) of each MP. Polymer-dependent false-color images were then generated by PMF to map polymer types, sizes, and locations on each sample filter.

To determine whether variables had normal distributions prior to correlation analyses, the Shapiro-Wilk test was conducted. The non-parametric Mann-Whitney-U test was performed to determine if there was a significant difference in median MP abundances by sampling season and ice type, as well as investigating differences in median particle size between pack and fast ice, and across the ice core's sampling seasons. All tests were performed using the statistical analysis software R (version 4.4.1).

RESULTS AND DISCUSSION

MP abundance in entire sea ice cores

MP contamination was identified in every sampled sea ice core [Figure 2]. In total, 4,090 MP particles were found in this study, averaging a concentration of 44.8 (± 50.8, median = 23.3) particles·L^{-1}. There was a significant difference in median particle abundance between autumn/winter vs. spring cores ($P = 0.038$) and autumn/winter *vs.* summer cores ($P = 0.019$), though there was no statistical difference found between spring and summer concentrations ($P = 0.529$).

Cores collected during austral spring (Brussels3, Liege5, Davis5, Sipex4, Sipex7, Yrs9) and summer (Ispol5, Rekt, Dml2, Dml4, Dml5, Dml6, Casey2, Totten1, Yrs3) reported median MP quantities of 10.1 and 16.4 particles·L^{-1}, respectively [Figure 2]. These are much lower quantities than those recorded in our winter

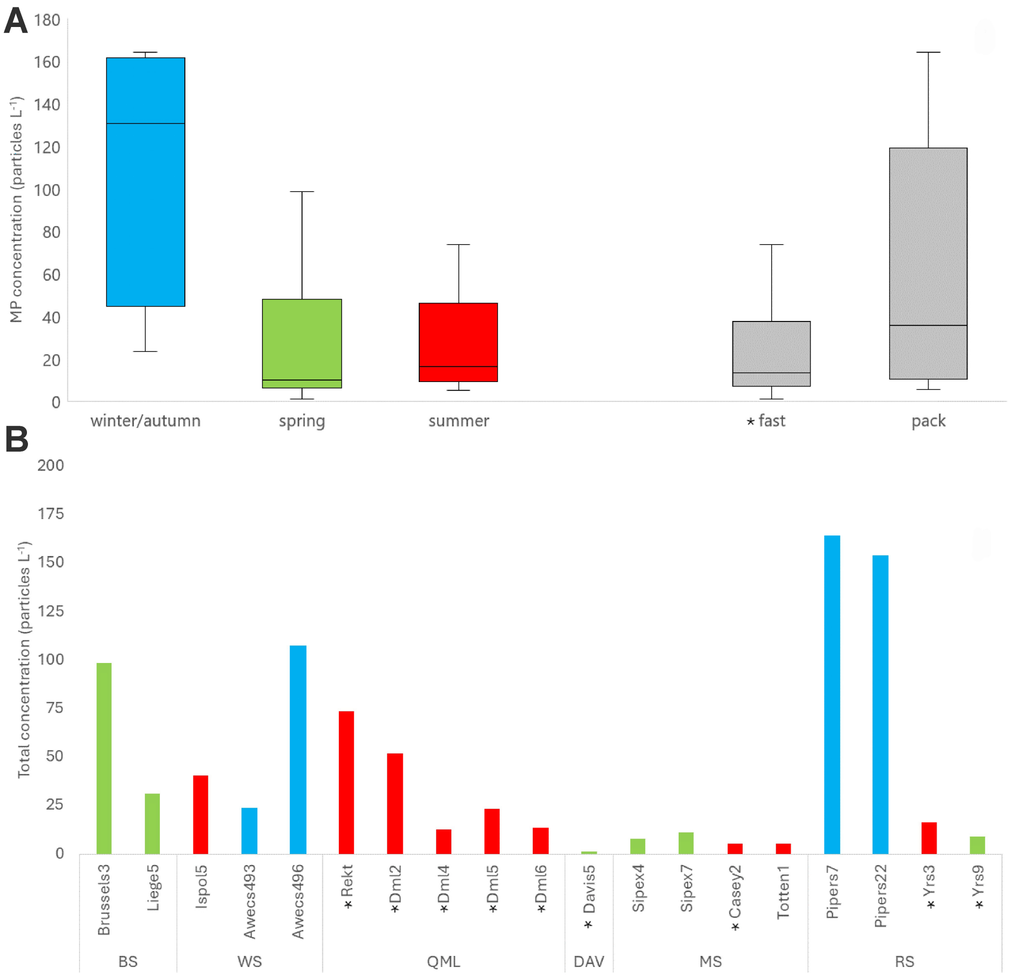

Figure 2. (A) MP concentrations (particles·L^{-1}) grouped by season (winter samples colored in blue, spring in green, and summer in red) and ice type (*denotes landfast ice cores); and (B) presented as the total concentration of MPs per ice core delineated by region: BS, WS, QML, DAV, MS, and RS. MP: Microplastic; BS: Bellinghausen Sea; WS: Weddell Sea; QML: Queen Maud Land; DAV: Davis Station; MS: Mawson Sea; RS: Ross Sea.

cores (Awecs493, Awecs496, Pipers7, Pipers22) at 130.6 particles·L^{-1}. Landfast cores showed a lower median concentration of MPs at 13.4 particles·L^{-1}, compared to pack ice, which had a median of 35.8 particles·L^{-1}, though this was not found to be statistically significant ($P = 0.133$).

Across all 19 cores, we calculate an average integrated MP concentration of 2.2 × 10^{5} (± 2.6 × 10^{5}) particles·m^{-2} in Antarctic sea ice. Our results do not suggest differences in MP counts between years, with no clear temporal trend or variation based on sampling location. Instead, the time of year appears to be the major driver of MP dynamics in sea ice. Integrated concentrations by seasonality are as follows: 3.3 × 10^{5} (± 2.8 × 10^{5}) particles·m^{-2} in autumn and winter ice, 9.7 × 10^{4} (± 4.3 × 10^{4}) particles·m^{-2} in spring, and 2.3 × 10^{5} (± 3.2 × 10^{5}) particles·m^{-2} in summer. The median integrated concentration of MPs in pack ice is 1.2 × 10^{5} particles·m^{-2}, compared with 1.8 × 10^{5} particles·m^{-2} in fast ice, though this difference was not statistically significant ($P = 0.242$).

Polymeric composition

A total of 19 polymer types were identified across all samples (see Table 2 for polymer abbreviations and contributions). Polymer types in pack versus fast ice were largely the same. Polyoxymethylene (POM) (19 particles), silicone (2 particles), and polyphenylsulfone (PPSU) (1 particle) were only noted in fast ice samples, while polyetheretherketone (PEEK) (1 particle) was only found in pack ice; the presence of all other polymers was noted in both ice types. PP and PE consistently dominated across the majority of ice core horizons, with only one exception in which PET was the dominant polymer (Pipers22).

Polymer abundance across pack and fast ice was similar but exhibited a few notable differences. The top ten polymers identified for both ice types were the same (PE, PP, PET, PUR, PAN, PVC, PS, PBT, PA, ABS). Pack ice had slightly higher relative concentrations of all polymers, but most notably PET and PUR, which comprised ≈21% of MPs, compared to ≈11% in fast ice. Compositionally, over 18% of MPs found in fast ice were PAN (350/1,927 particles) compared to 4% in pack ice (88/2,163 particles).

Overall, polymer composition across individually sampled sea ice cores was highly variable. However, when regionally grouped, the relative contribution of each polymer was fairly similar between regions [Figure 3].

Particle size

Over 80% of identified particles were ≤ 1,000 μm^2 and the average particle area for all polymers was 1,033.73 (± 4,501.83) μm^2. ESD of particles ranged from 13.0 to 506.6 µm, with a mean ESD of 27.4 (± 23.7) µm. A significant difference in median particle size was found between pack and landfast ice cores ($P = 0.0015$). The mean particle area of landfast cores was 769.4.0 (± 1,640.7) μm^2, and a mean ESD of 25.6 (± 18.0) µm. Pack ice exhibited a larger mean particle area of 1,258.5 (± 5,747.6) μm^2, and a mean ESD of 28.9 (± 27.7) µm. The median particle area by season is as follows: 365.1 μm^2 in winter cores, 315.1 μm^2 in spring cores, and 265.2 μm^2 in summer cores. As such, significant differences were found between the median particle area for autumn/winter *vs.* summer cores ($P = 2.6 \times 10^{-5}$) and for spring *vs.* summer cores ($P = 0.002$); however, no significant difference in median particle area was found between winter and spring cores ($P = 0.366$).

We found that, in general, particles increased in abundance with decreasing size [Figure 4], and this remained true for both pack and fast ice. The smallest noted particle size was 121 μm^2 in area (several different polymers) and constituted over 51% of all identified particles (2,099/4,090). The largest particle found in our samples was a piece of PS with an area of 201,561 μm^2. In fact, PS had the largest mean area across samples [Table 2].

Spatial and seasonal variability

The spatial and seasonal presence of MPs in sea ice is variable, as seen in Figure 2. Our analysis indicates that coastal sea ice exhibits lower MP abundances than open ocean sea ice. Ice textures are indicative of sea ice growth history, and could help elucidate the mechanisms of MP incorporation, enrichment, and release, as well as the varying levels of MP contamination across drill sites. Pack ice generally has higher frazil ice contributions compared to landfast ice which is mostly made of columnar ice[35]. The more turbulent conditions associated with open ocean regions due to strong winds and wave action lend themselves to frazil ice formation[36], in which randomly shaped ice crystals rise from up to 100 m depth[37] through the water column in autumn and winter, congealing into slush or pancake ice at the ocean surface. We suspect that MPs may get scavenged by frazil ice crystals as they rise to the sea surface, similar to processes suggested for algae and Fe incorporation[38-41]. Alternatively, frazil ice crystals may use MPs as condensation nuclei and subsequently rise to the ocean surface[42], leading to MP incorporation into newly formed ice. It has also been suggested that the number of times an ice crystal encounters a particle will determine how

Table 2. Total polymeric composition and particle size data for all 19 sea ice cores

Abbr.	Polymer	Particle count	Mean area (stdev) (μm^2)	Total area percentage	Mean ESD (stdev) (μm)
PP	Polypropylene	1,338	1,049 (± 3,649)	33.4%	28 (± 24)
PE	Polyethylene	969	758 (± 1,424)	18.2%	26 (± 18)
PAN	Polyacrylonitrile	438	1,750 (± 5,134)	17.5%	35 (± 31)
PET	Polyethylene terephthalate	376	862 (± 1,485)	9.4%	27 (± 19)
PUR	Polyurethane	298	899 (± 1,948)	7.7%	28 (± 19)
PVC	Polyvinyl chloride	228	702 (± 1,882)	6.4%	23 (± 20)
PS	Polystyrene	200	1,972 (± 14,480)	3.8%	29 (± 41)
PBT	Polybutylene terephthalate	55	368 (± 358)	0.5%	20 (± 9)
ABS	Acrylonitrile butadiene Styrene	53	1,551 (± 3,246)	0.5%	35 (± 27)
PA	Polyamide	47	326 (± 1,087)	0.4%	16 (± 13)
PMMA	Polymethyl mathacrylate	19	662 (± 1,032)	0.3%	23 (± 18)
EVOH	Ethylene-vinyl alcohol copolymer	19	192 (± 157)	0.09%	15 (± 5)
POM	Polyoxymethylene	19	140 (± 30)	0.06%	13 (± 1)
EVAc	Ethylene vinyl acetate	12	885 (± 1,886)	0.3%	26 (± 22)
PPSU	Polyphenylsulfone	8	133 (± 0)	0.02%	13 (± 0)
PC	Polycarbonate	5	816 (± 658)	0.1%	30 (± 12)
CA	Cellulose acetate	3	221 (± 77)	0.02%	17 (± 3)
silicone	Silicone	2	199 (± 94)	< 0.001%	16 (± 4)
PEEK	Polyetheretherketone	1	265	< 0.001%	19

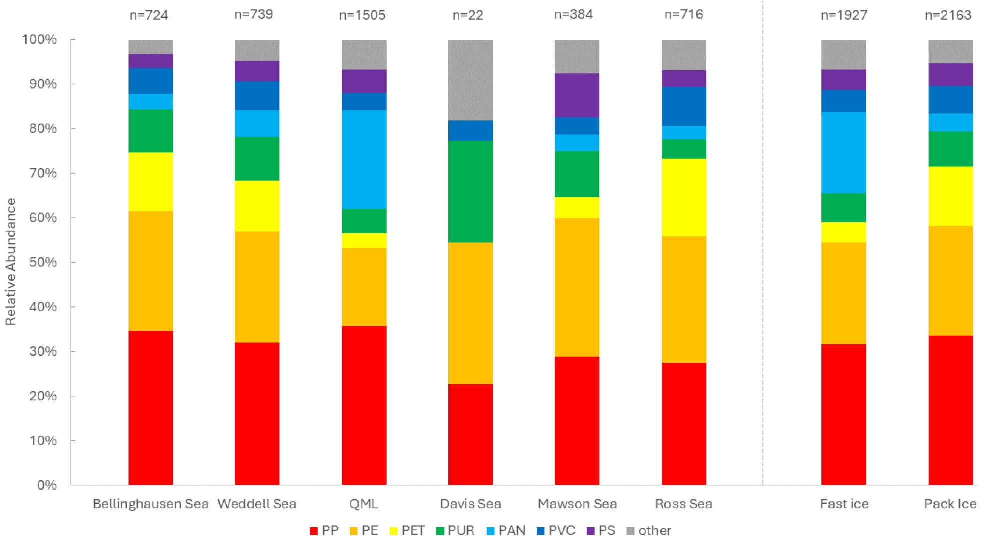

Figure 3. Polymer composition by geographic region and by ice type, where n equals the total particle abundance.

much material gets entrained in sea ice[43], and that convection of sea ice brines and under-ice water, as well as wave action, contribute to particle entrapment[44]. In contrast, landfast ice often forms in calmer conditions and exhibits higher inclusions of columnar ice growing at the bottom of an existing ice cover[45]. The bioaccumulation of MPs by algal growth and associated exopolymeric substances (EPS) in the skeletal layer could explain the incorporation of MPs into columnar ice, as suggested in the case of iron, macronutrients, and ice algae[39,46-49]. Additionally, some of the landfast cores (Yrs and Dml) consisted of

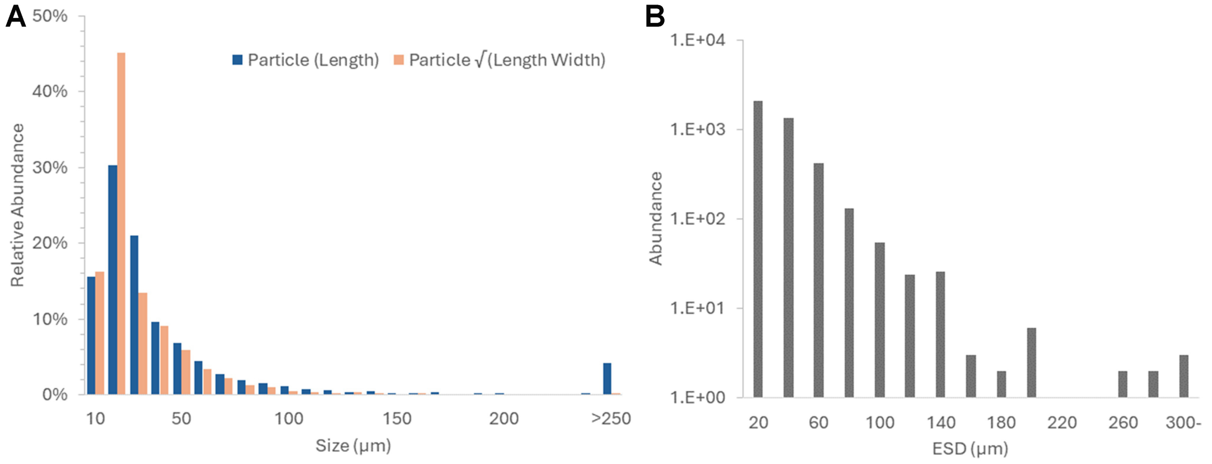

Figure 4. (A) Relative MP particle size distribution from all analyzed stations (n_p = 4,090). Dark blue bars represent particles by length. Light orange bars represent the geometric mean of particle size based on length and width. Particle lengths and widths were measured using PMF; (B) Polymer size abundance across all sea ice samples shown as ESD on a logarithmic scale. MP: Microplastic; PMF: Purency Microplastic Finder; ESD: equivalent spherical diameter.

platelet ice, which facilitates further incorporation mechanisms for MPs. Basal melting can occur when glacial ice comes into contact with relatively warmer waters, leading to underlying supercooled seawater, which may create favorable conditions for platelet ice formation, buoyant rise, and accumulation under the adjacent landfast sea ice[50] along with potential entrapment of any MPs present.

We noted that cores collected in spring and summer had significantly lower MP quantities than in winter. Because samples were not obtained from one site across different seasons, it is difficult to make assumptions about the seasonal MP flux during the sea ice growth/melt cycle. However, ice sampled in late winter/early spring is likely to have the highest levels of MP contamination, as suggested for other sea ice variables such as macronutrients and trace metals[51-53]. This was true for our study as the autumn and winter cores (Awecs493, Awecs496, Pipers7, Pipers22) exhibited the highest mean MP concentrations of all samples [Figure 2]. Sea ice growth rate is fastest in winter and the ice itself is often more frazil-dominant, which, as discussed above, could result in autumn/winter ice cores having higher incorporation rates of MPs than cores collected later in the year. Additionally, turbulent sea ice growth conditions in winter could help explain why the average MP size was significantly larger in winter cores compared to summer cores. Based on mean particle size results from Chen *et al.* (2023), larger particles are more easily entrapped in ice, and the fast and tumultuous growth conditions for sea ice in winter might assist with particle incorporation into a growing ice column[54]. Furthermore, our theory on MP flux in the seasonal ice cover is supported through a deeper look at cores sampled later in the sea ice season. As sea ice melts in spring, ice porosity increases, and brine channels can expand and connect with underlying seawater, where particulate matter such as algae (and suspected MPs) may get released from the ice[55]. Casey2 and Totten1 from late summer in the eastern Antarctic are a prime example of this. Both cores were collected off Wilkes Land in late December, by which point the ice exhibited highly permeable textures with typical characteristics of decaying ice, such as large brine channels and melt holes[56]. These two cores were among those with the lowest mean concentrations of MPs. Time series are needed to test these hypotheses. Alternatively, mesocosm experiments could be conducted to simulate both sea ice growth and melt phases (e.g., Geilfus *et al.*, 2019)[27].

Transport mechanisms

MPs in the Southern Ocean may originate from both local and distant sources. While the ACC is thought to keep the Southern Ocean from accumulating MPs from northern latitudes[19], it has been suggested that both its surface and sub-surface waters are penetrable to MPs[13,57]. Passive MP transport is heavily influenced by ocean currents and mixing such as meridional overturning circulation (MOC) and Southern Ocean upwelling. Baroclinic wind instability transports mass to the poles and yields southward eddy advection[58]. Therefore, MPs in surface waters in mid to low latitudes in the upper cell of the MOC are being drawn down into the Southern Ocean and across the axis of the ACC. We noted higher abundances of MPs in pack ice than fast ice may support the theory that contamination is likely coming from northern latitudes, rather than as a direct result of local and intercoastal activities from research bases or fishing ventures. The presence of MPs in Southern Ocean air samples further indicates that MPs can be transported by diffuse sources[18,59]. The dominance of smaller MPs across our samples was consistent with other Antarctic MP studies that found MP abundance decreased with increasing size[12,60]. Concurrently, the majority of MPs are less than 10 μm in length, indicating that atmospheric and oceanic long-range transport may assist in MP accumulation across our sea ice sampling sites[59,61]. In addition, snow deposition may also play a role in depositing MPs into sea ice as MP fragments and fibers are likely to be incorporated into snow mixtures due to their low particle density and pre-enrichment in materials entrained by winds, as it has been observed on the continent at DML stations and reported elsewhere in the literature[16,62]. However, small MP sizes could simply indicate that particles - whether they originate from local sources or not - are being mechanically degraded over time via marine consumption[63] or in highly dynamic atmospheric and oceanic conditions[61,64] and re-enriched into sea ice and surface waters during subsequent seasons. The abundance of MPs in the autumn/winter cores of the Weddell and Ross Seas could indicate that these large oceanic gyres allow for the accumulation of MP contamination during sea ice formation, rather than their re-dispersal in more open ocean regions. Both these regions are characterized as major areas where northern-sourced deep waters cross the ACC before upwelling southward and toward the surface[23]. The upwelling of deep waters in the Weddell and Ross gyres is a good source candidate of MPs for the surface waters (hence the pack sea ice) in the Southern Ocean since the highest concentration of MPs is found between 200 and 600 m depth in offshore waters of the World's ocean (e.g., Choy *et al.*, 2019)[65]. For example, Isobe *et al.* (2017) observed higher MP concentrations in surface waters south of the Polar Front than in waters north of it[12]. This hypothesis is further supported by the significantly higher MP concentration found in offshore waters of the Weddell Gyre (where deep-water upwelling prevails) compared to waters on the Weddell Sea continental shelf by Leistenschneider *et al.* (2024)[66]. On the contrary, waters on the Antarctic Shelf may be protected from this MP contamination by the Southern Ocean slope front, just north of the continental slope, which partially protects the continental shelf from the intrusion of deeper waters. Further research on pathways of particle transport in the Southern Ocean and sea ice is needed to garner a deeper understanding of contamination levels, and to accurately predict MP sinks as plastic production continues to increase.

In conjunction with seasonal ice characteristics, sampling locations may also help explain the disparity between volumetric MP concentrations in the autumn/winter cores versus the summer/spring cores. We suspect accumulation trends may result from a combination of faster sea ice growth during autumn/winter (and thus more efficient MP entrapment), proximity to external sources of pollution transported by means of wind, subsurface waters (particularly for neutrally buoyant MPs), and local hydrographic features. An MP accumulation model[6] showed that the Antarctic was initially reasonably well protected from MPs sourced externally to the Southern Ocean, but at the end of the 50-year time span, MP contamination had heavily penetrated the Southern Ocean and was present around the entire Antarctic coastline, with MP abundance remaining most dense in Pacific Ocean sectors during winter. This corresponds with our findings, as Pipers7 and Pipers22 sampled during winter near the Ross Sea[67] accounted for the highest particle abundances across all our cores (163.1 and 153.8 particles·L^{-1}, respectively). The remaining cores collected during the sea ice growth phase in the Weddell Sea (Awecs493 and Awecs496)[68] also exhibited higher MP concentrations than any spring/summer cores. As the model progressed, the region with the highest winter accumulation was the Bellinghausen Sea. Brussels3 and Liege5 were drilled during austral spring in this region and maintained significantly higher MP abundances than any other spring/summer cores (average of 98.4 and 31.1 particles·L^{-1}, respectively). Researchers noted that sea ice permeability was significantly reduced for Brussels3 in particular, which could explain the high concentration of particles within this core[69], despite cycles of warming beginning in early spring, thus retaining MPs that were enriched during winter. In contrast, cores drilled in East Antarctica during the sea ice melt phase (Davis5, Sipex4, Sipex7, Casey2, Totten1) exhibited the lowest mean concentrations of MPs among all samples. This could be because the largest hydrological features in the eastern Antarctic remain the ACC and the Antarctic Coastal Current, and the region lacks a large gyre system that can potentially entrap MPs. Simultaneously, we speculate that this could be a result of low vessel traffic, and greater distance from tourist and research hotspots. Cunningham *et al.* (2022) demonstrated that air masses and wind are transport mechanisms for MP entering the Southern Ocean and noted that MPs in their study were likely to have originated from South America[18], which would likely be the case for some of our Weddell Sea ice cores. Perhaps because the eastern Antarctic is further removed from the southern land masses of Africa and South America, airborne MP pollution is not as significant of a factor. This, coupled with the lower rates of tourism and marine activities, could explain the lower MP counts in these cores.

Potential sources for MPs in sea ice

We suspect MP particles are scavenged from surrounding environmental media and incorporated into the sea ice matrix during its growth phase. Based on comparisons with MP studies in surface and subsurface waters, sea ice is a temporary sink for MPs. The mean concentrations of particles·L^{-1} across our cores were consistently four to six orders of magnitude higher than concentrations in seawater [Table 3]. Note that at the time of the current study, there are no comparable reports of MP concentrations in the Bellinghausen or Mawson Seas. In general, the lack of standardized methods for MP extraction from seawater and chemical identification remains a hindrance to consistent cross-study comparisons. Additionally, most studies in the Antarctic are focused on regions with long-standing research stations or those experiencing higher levels of anthropogenic pressures. As such, there have been mixed reports of MP presence in Antarctic surface waters, with some studies finding high levels of MPs in offshore surface waters[19] while others reporting little to no presence of MPs at all[7,73]. Thus, MP incorporation during initial sea ice growth may coincide with the higher abundances of MPs we noted in our autumn/ winter cores compared to those sampled during spring and summer. It may also account for why studies reporting contamination continually note MPs in Antarctic sub-surface waters[60] and sediments[17,74] but vary widely in their findings for upper-surface waters in both coastal and offshore regions.

Air masses may also contribute MPs in sea ice. To date, little remains known about the presence of airborne MPs in Antarctica, though it remains highly probable that at least some portion of MPs found in Southern Ocean Sea ice arise from atmospheric contributions. Backwards, air mass trajectories from the first study of MPs in Antarctic snow indicated that MPs entering the Southern Ocean likely arrive via long-range transport, most notably from South America, upwards of 6,000 km away from their sampling sites in the Ross Sea region, though local sources from Scott Base and McMurdo Station contributed as well[16]. Similarly, air mass trajectories conducted for a cruise from East Asia to Antarctica indicate that MPs likely originated from the continents of South Asia and Oceania[61], with non-fibrous MP concentrations decreasing with increasing latitude. Finally, the ocean-atmosphere exchange of MPs may also contribute locally to our sea ice concentrations[75]. Particles - particularly in coastal surface waters - can be re-entrained in the atmosphere via sea mist[75]. With these combined conclusions, it may be that long-range transport

Table 3. Study summaries of MP concentrations in Antarctic seawater and air masses compared to findings in sea ice in the corresponding regions for our study sites

Ref.	Location	Sample medium	Mean MP concentration (particles$\cdot$L^{-1})	Regional sea ice concentration (particles$\cdot$L^{-1})
Leistenschneider *et al.*, 2024[66] Leistenschneider *et al.*, 2021[70]	Weddell Sea	Surface waters Subsurface waters	1.0×10^{-5} 4.35×10^{-2}	57.1
Pakhomova *et al.*, 2022[71]	Weddell Sea	Subsurface waters	4.3×10^{-4}	57.1
Cincinelli *et al.*, 2017[72]	Ross Sea	Subsurface waters	1.7×10^{-4}	85.8
Zhang *et al.*, 2022[60]	Ross Sea Davis Sea	Subsurface waters Subsurface waters	1.85×10^{-3} 1.91×10^{-3}	85.8 1.1
Aves *et al.*, 2022[16]	Ross Sea	Air	29	85.8

MP: Microplastic.

facilitates MP contamination across the STF, where a portion of airborne MPs become incorporated into surface waters for inclusion into growing ice. An additional portion of MP particles that remain or become airborne could integrate into sea ice via snow deposition. Cunningham *et al.* (2022) found MP types consistent in air masses and seawater, and thus, they similarly speculate that atmospheric and oceanic processes influence Antarctic MP presence in tandem[18].

It is difficult to pinpoint specific sources of MP contamination. However, the MP fragments found in our samples are typically abundant in the marine environment and have several uses in and out of a marine context. PP, PE, PUR, PVC, PET, and PS are the most abundant marine MPs, comprising approximately 80% of total plastic production[76], and all six polymers were found in high abundance in our study, totaling 78.9% of all MPs identified [Table 2]. The most abundant polymer types were PP and PE and were present in all 19 ice cores. This coincides with PP and PE being the most abundant marine MPs globally and around the Southern Ocean[7,66,72], and aligns with global production rates[77,78]. PP and PE are commonly associated with maritime and fishing activities and land-based beach litter, and this, combined with their low density, makes them readily abundant in surface waters[79]. Additionally, PP was the most abundant polymer found in atmospheric deposition samples inland of the Ross Sea region (coastal Victoria Land), and was linked to potential human activities at nearby research stations[80]. PET accounted for 49% of polymers found in a study of Antarctic snow, with the authors suggesting that both local and distant sources could be contributing to this phenomenon[16]. PET and PA are commonly used in textiles and have high correlations with wastewater[81,82]; thus, while all polymers could penetrate the Southern Ocean via long-range transport, there is potential that these polymers originate from local Antarctic stations or - what is more likely - vessels. Interestingly, PAN and PVC were also found in relatively high quantities across our samples, ranked in the top three for marine polymers of concern[83]. Despite their densities being higher than that of seawater, they have been found in other Southern Ocean samples[7,84]. For cores collected over shallower water depths, we suspect that plastic-laden marine sediments may be resuspended during storms or other turbulent conditions, allowing for the incorporation of these denser MPs into sea ice. Compositionally, PAN was the third most prevalent polymer in fast ice, accounting for over 22% of all MPs, compared to just 6% for pack ice. Ultimately, the high variability in abundance and polymeric composition across our samples makes it difficult to draw conclusions regarding the immediate sources of this debris.

CONCLUSION

Here, we have provided the first pan-Antarctic study of MPs in Southern Ocean sea ice. MP concentrations across our ice cores were high, particularly when compared to concurrent regional seawater studies, indicating sea ice is a reservoir for plastic pollution in the Southern Ocean. High MP concentrations in growing sea ice during autumn and winter, compared to lower average MP abundances in spring and summer, indicate that turbulent and faster growth processes are a likely driver for particle incorporation. The increase in ice porosity and the widening of brine channels as sea ice melts could allow for a return of MPs to surrounding surface waters, suggesting that while sea ice is a sink for MPs, it is a highly seasonal one. It is suspected that Southern Ocean MP contamination is originating from both local and distant sources, but that circulation of northerly deep waters and long-range transport have a heavy impact on MP accumulation across Southern Ocean regional gyres, coastlines, and their eventual inclusion into sea ice. Finally, due to strong seasonal components in the Southern Ocean sea ice cycle, regional polymer compositions are likely largely dependent on the MP composition of underlying waters.

MPs in the Southern Ocean have the potential to accumulate over time. While we know MPs are incorporated into the ice during sea ice growth in autumn and winter, the fate of MPs remains unknown once they are released from the ice again. The low density and small sizes of MPs give them the ability to remain in surface waters to be further broken down by consumption[63] or re-incorporated into sea ice during the following growth season. Even particles that have sunken out of the surface waters to settle in sediments can be resuspended in the water column during storms[39,85] in shallower coastal areas, and thus again have the potential to become entrapped in a growing ice column. Currently, there is a lack of data to conduct analyses on Southern Ocean MP accumulation trends. This could be remedied by conducting time-series sampling, where sea ice is analyzed from subsequent years to determine if there is accumulation over time, as well as further analysis of Southern Ocean sediments to determine if they are an ultimate sink for MPs. The Southern Ocean is known for its variable and highly dynamic conditions, which may make it difficult to pinpoint individual transport and enrichment mechanisms for MPs in sea ice. However, this work provides a step toward particle flux modeling of MPs in sea ice and their effects on the rest of the biogeochemical cycle, both locally and more broadly, around the Southern Ocean.

DECLARATIONS

Authors' contributions

Methodology, validation, writing - original draft, investigation, formal analysis: Kelly A
Conceptualization, data curation: Kelly A, Rodemann T
Funding acquisition: Lannuzel D
Supervision: Lannuzel D, Rodemann T, Meiners KM, Auman HJ, Moreau S, Fripiat F
Writing - review and editing: Lannuzel D, Rodemann T, Meiners KM, Auman HJ, Moreau S, Fripiat F, Dellile B
Resource acquisition: Lannuzel D, Meiners KM, Dellile B, Fripiat F, Moreau S

Availability of data and materials

All data relevant to this study are available via the Australian Antarctic Data Center (doi: 10.26179/qzf5-tr20).

Financial support and sponsorship

Meiners KM was supported by the Australian government through Australian Antarctic Science project #4546, and Lannuzel D by an ARC Future Fellowship (FT190100688). Moreau S is supported by the Norwegian Research Council project I-CRYME (Impact of CRYosphere Melting on Southern Ocean Ecosystems and biogeochemical cycles, 11993). This work contributes to the Antarctic Science

Collaboration Initiative program (project ID ASC1000002) and the Australian Research Council (ARC)'s Australian Centre for Excellence in Antarctic Science (project number SR200100008).

Conflicts of interest
All authors declared that there are no conflicts of interest.

Ethical approval and consent to participate
Not applicable.

Consent for publication
Not applicable.

Copyright

REFERENCES
1. Kanhai DK, Gardfeldt K, Krumpen T, Thompson RC, O'Connor I. Microplastics in sea ice and seawater beneath ice floes from the Arctic Ocean. *Sci Rep* 2020;10:5004. DOI PubMed PMC
2. Bergmann M, Mützel S, Primpke S, Tekman MB, Trachsel J, Gerdts G. White and wonderful? Microplastics prevail in snow from the Alps to the Arctic. *Sci Adv* 2019;5:eaax1157. DOI PubMed PMC
3. Obbard RW, Sadri S, Wong YQ, Khitun AA, Baker I, Thompson RC. Global warming releases microplastic legacy frozen in Arctic Sea ice. *Earth's Future* 2014;2:315-20. DOI
4. Peeken I, Primpke S, Beyer B, et al. Arctic sea ice is an important temporal sink and means of transport for microplastic. *Nat Commun* 2018;9:1505. DOI PubMed PMC
5. Fraser CI, Kay GM, Plessis MD, Ryan PG. Breaking down the barrier: dispersal across the Antarctic Polar Front. *Ecography* 2017;40:235-7. DOI
6. Mountford AS, Morales Maqueda MA. Modeling the accumulation and transport of microplastics by sea ice. *JGR Oceans* 2021;126:e2020JC016826. DOI
7. Suaria G, Perold V, Lee JR, Lebouard F, Aliani S, Ryan PG. Floating macro- and microplastics around the Southern Ocean: results from the Antarctic circumnavigation expedition. *Environ Int* 2020;136:105494. DOI PubMed
8. De-la-Torre GE, Santillán L, Dioses-Salinas DC, et al. Assessing the current state of plastic pollution research in Antarctica: knowledge gaps and recommendations. *Chemosphere* 2024;355:141870. DOI
9. da Silva JRMC, Bergami E, Gomes V, Corsi I. Occurrence and distribution of legacy and emerging pollutants including plastic debris in Antarctica: sources, distribution and impact on marine biodiversity. *Mar Pollut Bull* 2023;186:114353. DOI PubMed
10. Tirelli V, Suaria G, Lusher AL. Microplastics in polar samples. In: Rocha-Santos T, Costa MF, Mouneyrac C, editors. Handbook of microplastics in the environment. Cham: Springer International Publishing; 2022. pp. 281-322. DOI
11. Fraser CI, Morrison AK, Hogg AM, et al. Antarctica's ecological isolation will be broken by storm-driven dispersal and warming. *Nature Clim Change* 2018;8:704-8. DOI
12. Isobe A, Uchiyama-Matsumoto K, Uchida K, Tokai T. Microplastics in the Southern Ocean. *Mar Pollut Bull* 2017;114:623-6. DOI PubMed
13. Waller CL, Griffiths HJ, Waluda CM, et al. Microplastics in the Antarctic marine system: an emerging area of research. *Sci Total Environ* 2017;598:220-7. DOI
14. Kelly A, Lannuzel D, Rodemann T, Meiners KM, Auman HJ. Microplastic contamination in east Antarctic sea ice. *Mar Pollut Bull* 2020;154:111130. DOI PubMed
15. Materić D, Kjær HA, Vallelonga P, Tison JL, Röckmann T, Holzinger R. Nanoplastics measurements in Northern and Southern polar ice. *Environ Res* 2022;208:112741. DOI PubMed
16. Aves AR, Revell LE, Gaw S, et al. First evidence of microplastics in Antarctic snow. *The Cryosphere* 2022;16:2127-45. DOI
17. Cunningham EM, Ehlers SM, Dick JTA, et al. High abundances of microplastic pollution in deep-sea sediments: evidence from Antarctica and the Southern Ocean. *Environ Sci Technol* 2020;54:13661-71. DOI
18. Cunningham EM, Rico Seijo N, Altieri KE, et al. The transport and fate of microplastic fibres in the Antarctic: the role of multiple global processes. *Front Mar Sci* 2022;9:1056081. DOI
19. Lacerda ALDF, Rodrigues LDS, van Sebille E, et al. Plastics in sea surface waters around the Antarctic Peninsula. *Sci Rep* 2019;9:3977. DOI PubMed PMC
20. Zhang Y, Gao T, Kang S, Sillanpää M. Importance of atmospheric transport for microplastics deposited in remote areas. *Environ Pollut* 2019;254:112953. DOI

21. Nowlin WD, Klinck JM. The physics of the Antarctic circumpolar current. *Rev Geophys* 1986;24:469-91. DOI
22. Ryan S, Schröder M, Huhn O, Timmermann R. On the warm inflow at the eastern boundary of the Weddell Gyre. *Deep Sea Res Pt I* 2016;107:70-81. DOI
23. Tamsitt V, Drake HF, Morrison AK, et al. Spiraling pathways of global deep waters to the surface of the Southern Ocean. *Nat Commun* 2017;8:172. DOI PubMed PMC
24. Pennel R, Kamenkovich I. On the factors controlling the eddy-induced transport in the Antarctic circumpolar current. *J Phys Oceanogr* 2014;44:2127-38. DOI
25. Rintoul SR, Naveira Garabato AC. Dynamics of the Southern Ocean circulation. Ocean circulation and climate - a 21st century perspective. Elsevier; 2013. pp. 471-92. DOI
26. National Snow and Ice Data Center. NOAA/NSIDC climate data record of passive microwave sea ice concentration, version 4. Available from: https://nsidc.org/data/g02202/versions/4. [Last accessed on 23 Dec 2024].
27. Geilfus NX, Munson KM, Sousa J, et al. Distribution and impacts of microplastic incorporation within sea ice. *Mar Pollut Bull* 2019;145:463-73. DOI
28. Spindler M. Notes on the biology of sea ice in the Arctic and Antarctic. *Polar Biol* 1994;14:BF00238447. DOI
29. Leventer A. Particulate flux from sea ice in polar waters. In: Thomas DN, Dieckmann GS, editors. Sea ice. Wiley; 2003. pp. 303-32. DOI
30. Jeffries MO, Krouse HR, Hurst-Cushing B, Maksym T. Snow-ice accretion and snow-cover depletion on Antarctic first-year sea-ice floes. *Ann Glaciol* 2001;33:51-60. DOI
31. Lannuzel D, de Jong J, Schoemann V, Trevena A, Tison J, Chou L. Development of a sampling and flow injection analysis technique for iron determination in the sea ice environment. *Anal Chim Acta* 2006;556:476-83. DOI
32. Witzig CS, Földi C, Wörle K, et al. When good intentions go bad-false positive microplastic detection caused by disposable gloves. *Environ Sci Technol* 2020;54:12164-72. DOI
33. Quinn B, Murphy F, Ewins C. Validation of density separation for the rapid recovery of microplastics from sediment. *Anal Methods* 2017;9:1491-8. DOI
34. López-Rosales A, Andrade JM, Grueiro-Noche G, Fernández-González V, López-Mahía P, Muniategui-Lorenzo S. Development of a fast and efficient method to analyze microplastics in planktonic samples. *Mar Pollut Bull* 2021;168:112379. DOI PubMed
35. Thomas DN, Dieckmann GS. Sea ice - an introduction to its physics, chemistry, biology and geology. London: Wiley Blackwell; 2003. Available from: https://www.wiley.com/en-us/Sea+Ice%3A+An+Introduction+to+its+Physics%2C+Chemistry%2C+Biology+and+Geology-p-9780632058082. [Last accessed on 23 Dec 2024].
36. Barrette PD. Understanding frazil ice: the contribution of laboratory studies. *Cold Reg Sci Technol* 2021;189:103334. DOI
37. Ito M, Ohshima KI, Fukamachi Y, Mizuta G, Kusumoto Y, Nishioka J. Observations of frazil ice formation and upward sediment transport in the Sea of Okhotsk: a possible mechanism of iron supply to sea ice: frazil ice and upward sediment transport. *J Geophys Res Oceans* 2017;122:788-802. DOI
38. Dieckmann GS, Lange MA, Ackley SF, Jennings JC. The nutrient status in sea ice of the Weddell Sea during winter: effects of sea ice texture and algae. *Polar Biol* 1991;11:449-56. DOI
39. Lannuzel D, Schoemann V, de Jong J, et al. Distribution of dissolved iron in Antarctic sea ice: spatial, seasonal, and inter□annual variability. *J Geophys Res* 2010;115:2009JG001031. DOI
40. Garrison DL, Ackley SF, Buck KR. A physical mechanism for establishing algal populations in frazil ice. *Nature* 1983;306:363-5. DOI
41. Spindler M, Dieckmann GS. Distribution and abundance of the planktic foraminifer Neogloboquadrina pachyderma in sea ice of the Weddell Sea (Antarctica). *Polar Biol* 1986;5:185-91. DOI
42. Weeks WF, Ackley SF. The growth, structure, and properties of sea ice. In: Untersteiner N, editor. The geophysics of sea ice. Boston: Springer US; 1986. pp. 9-164. DOI
43. Garrison D, Close A, Reimnitz E. Algae concentrated by frazil ice: evidence from laboratory experiments and field measurements. *Antartic Sci* 1989;1:313-6. DOI
44. Weissenberger J, Grossmann S. Experimental formation of sea ice: importance of water circulation and wave action for incorporation of phytoplankton and bacteria. *Polar Biol* 1998;20:178-88. DOI
45. Fraser AD, Wongpan P, Langhorne PJ, et al. Antarctic landfast sea ice: a review of its physics, biogeochemistry and ecology. *Rev Geophys* 2023;61:e2022RG000770. DOI
46. Roukaerts A, Deman F, Van der Linden F, et al. The biogeochemical role of a microbial biofilm in sea ice. *Elem Sci Anth* 2021;9:00134. DOI
47. van der Merwe P, Lannuzel D, Nichols CM, et al. Biogeochemical observations during the winter–spring transition in East Antarctic sea ice: evidence of iron and exopolysaccharide controls. *Mar Chem* 2009;115:163-75. DOI
48. de Jong J, Schoemann V, Maricq N, et al. Iron in land-fast sea ice of McMurdo Sound derived from sediment resuspension and wind-blown dust attributes to primary productivity in the Ross Sea, Antarctica. *Mar Chem* 2013;157:24-40. DOI
49. Meiners K, Gradinger R, Fehling J, Civitarese G, Spindler M. Vertical distribution of exopolymer particles in sea ice of the Fram Strait (Arctic) during autumn. *Mar Ecol Prog Ser* 2023;248:1-13. Available from: http://www.int-res.com/articles/meps2003/248/m248p001.pdf. [Last accessed on 24 Dec 2024]
50. Hoppmann M, Richter ME, Smith IJ, et al. Platelet ice, the Southern Ocean's hidden ice: a review. *Ann Glaciol* 2020;61:341-68. DOI

51. Fripiat F, Meiners KM, Vancoppenolle M, et al. Macro-nutrient concentrations in Antarctic pack ice: overall patterns and overlooked processes. *Elementa Sci Anthrop* 2017;5:13. DOI
52. Lannuzel D, Chever F, van der Merwe PC, et al. Iron biogeochemistry in Antarctic pack ice during SIPEX-2. *Deep Sea Res Pt II* 2016;131:111-22. DOI
53. Meiners KM, Michel C. Dynamics of nutrients, dissolved organic matter and exopolymers in sea ice. In: Thomas DN, editor. Sea ice. Wiley; 2017. pp. 415-32. DOI
54. Chen Z, Elektorowicz M, An C, Tian X. Entrainment and enrichment of microplastics in ice formation processes: implications for the transport of microplastics in cold regions. *Environ Sci Technol* 2023;57:3176-86. DOI PubMed
55. Tison J, Worby A, Delille B, et al. Temporal evolution of decaying summer first-year sea ice in the Western Weddell Sea, Antarctica. *Deep Sea Res Pt II* 2008;55:975-87. DOI
56. Corkill M, Moreau S, Janssens J, et al. Physical and biogeochemical properties of rotten East Antarctic summer sea ice. *JGR Oceans* 2023;128:e2022JC018875. DOI
57. Reisser J, Slat B, Noble K, et al. The vertical distribution of buoyant plastics at sea: an observational study in the North Atlantic Gyre. *Biogeosciences* 2015;12:1249-56. DOI
58. Marshall J, Speer K. Closure of the meridional overturning circulation through Southern Ocean upwelling. *Nature Geosci* 2012;5:171-80. DOI
59. Obbard RW. Microplastics in polar regions: the role of long range transport. *Curr Opin Environ Sci Health* 2018;1:24-9. DOI
60. Zhang S, Zhang W, Ju M, et al. Distribution characteristics of microplastics in surface and subsurface Antarctic seawater. *Sci Total Environ* 2022;838:156051. DOI
61. Chen Q, Shi G, Revell LE, et al. Long-range atmospheric transport of microplastics across the southern hemisphere. *Nat Commun* 2023;14:7898. DOI PubMed PMC
62. Bullard JE, Ockelford A, O'brien P, Mckenna Neuman C. Preferential transport of microplastics by wind. *Atmos Environ* 2021;245:118038. DOI
63. Dawson AL, Kawaguchi S, King CK, et al. Turning microplastics into nanoplastics through digestive fragmentation by Antarctic krill. *Nat Commun* 2018;9:1001. DOI PubMed PMC
64. Andrady AL. Microplastics in the marine environment. *Mar Pollut Bull* 2011;62:1596-605. DOI PubMed
65. Choy CA, Robison BH, Gagne TO, et al. The vertical distribution and biological transport of marine microplastics across the epipelagic and mesopelagic water column. *Sci Rep* 2019;9:7843. DOI PubMed PMC
66. Leistenschneider C, Wu F, Primpke S, Gerdts G, Burkhardt-Holm P. Unveiling high concentrations of small microplastics (11-500 μm) in surface water samples from the southern Weddell Sea off Antarctica. *Sci Total Environ* 2024;927:172124. DOI PubMed
67. Tison J, Maksym T, Fraser AD, et al. Physical and biological properties of early winter Antarctic sea ice in the Ross Sea. *Ann Glaciol* 2020;61:241-59. DOI
68. Tison J, Schwegmann S, Dieckmann G, et al. Biogeochemical impact of snow cover and cyclonic intrusions on the winter Weddell Sea ice pack. *JGR Oceans* 2017;122:9548-71. DOI
69. Lewis M, Tison J, Weissling B, et al. Sea ice and snow cover characteristics during the winter–spring transition in the Bellingshausen Sea: an overview of SIMBA 2007. *Deep Sea Res Pt II* 2011;58:1019-38. DOI
70. Leistenschneider C, Burkhardt-Holm P, Mani T, Primpke S, Taubner H, Gerdts G. Microplastics in the Weddell Sea (Antarctica): a forensic approach for discrimination between environmental and vessel-induced microplastics. *Environ Sci Technol* 2021;55:15900-11. DOI PubMed
71. Pakhomova S, Berezina A, Lusher AL, et al. Microplastic variability in subsurface water from the Arctic to Antarctica. *Environ Pollut* 2022;298:118808. DOI
72. Cincinelli A, Scopetani C, Chelazzi D, et al. Microplastic in the surface waters of the Ross Sea (Antarctica): occurrence, distribution and characterization by FTIR. *Chemosphere* 2017;175:391-400. DOI
73. Kuklinski P, Wicikowski L, Koper M, et al. Offshore surface waters of Antarctica are free of microplastics, as revealed by a circum-Antarctic study. *Mar Pollut Bull* 2019;149:110573. DOI
74. Munari C, Infantini V, Scoponi M, Rastelli E, Corinaldesi C, Mistri M. Microplastics in the sediments of Terra Nova Bay (Ross Sea, Antarctica). *Mar Pollut Bull* 2017;122:161-5. DOI PubMed
75. Allen S, Allen D, Moss K, Le Roux G, Phoenix VR, Sonke JE. Examination of the ocean as a source for atmospheric microplastics. *PLoS One* 2020;15:e0232746. DOI PubMed PMC
76. Almroth B, Eggert H. Marine plastic pollution: sources, impacts, and policy issues. *Rev Env Econ Policy* 2019;13:317-26. DOI
77. Geyer R, Jambeck JR, Law KL. Production, use, and fate of all plastics ever made. *Sci Adv* 2017;3:e1700782. DOI PubMed PMC
78. Bråte IL, Halsband C, Allan I, Thomas K. Report made for the Norwegian Environment Agency: microplastics in marine environments; occurrence, distribution and effects. Available from: http://www.miljodirektoratet.no/Documents/publikasjoner/M319/M319.pdf. [Last accessed on 24 Dec 2024].
79. Erni-Cassola G, Zadjelovic V, Gibson MI, Christie-Oleza JA. Distribution of plastic polymer types in the marine environment; a meta-analysis. *J Hazard Mater* 2019;369:691-8. DOI PubMed
80. Illuminati S, Notarstefano V, Tinari C, et al. Microplastics in bulk atmospheric deposition along the coastal region of Victoria Land, Antarctica. *Sci Total Environ* 2024;949:175221. DOI
81. Henry B, Laitala K, Klepp IG. Microplastic pollution from textiles: a literature review. 2018. Available from: https://hdl.handle.net/20.

500.12199/5360. [Last accessed on 24 Dec 2024].

82. Šaravanja A, Pušić T, Dekanić T. Microplastics in wastewater by washing polyester fabrics. *Materials* 2022;15:2683. DOI PubMed PMC
83. Yuan Z, Nag R, Cummins E. Ranking of potential hazards from microplastics polymers in the marine environment. *J Hazard Mater* 2022;429:128399. DOI PubMed
84. Barboza LGA, Frias JP, Booth AM, et al. Microplastics pollution in the marine environment. World seas: an environmental evaluation. Elsevier; 2019. pp. 329-51. DOI
85. Dethleff D, Kempema EW. Langmuir circulation driving sediment entrainment into newly formed ice: tank experiment results with application to nature (Lake Hattie, United States; Kara Sea, Siberia). *J Geophys Res* 2007;112:2005JC003259. DOI

AUTHOR INSTRUCTIONS

1. Submission Overview

Before you decide to publish with us, please read the following items carefully and make sure that you are well aware of Editorial Policies and the following requirements.

1.1 Topic Suitability

The topic of the manuscript must fit the scope of the journal. Please refer to Aims and Scope for more information.

1.2 Open Access and Copyright

The journal adopts Gold Open Access publishing model and distributes content under the Creative Commons Attribution 4.0 International License. Copyright is retained by authors. Please make sure that you are well aware of these policies.

1.3 Publication Fees

Water Emerging Contaminants & Nanoplastics is an open access journal. When a paper is accepted for publication, authors are required to pay Article Processing Charges (APCs) to cover its editorial and production costs. The APC for each submission is $1500. There are no additional charges based on color, length, figures, or other elements. For more details, please refer to OAE Publication Fees.

1.4 Language Editing

All submissions are required to be presented clearly and cohesively in good English. Authors whose first language is not English are advised to have their manuscripts checked or edited by a native English speaker before submission to ensure the high quality of expression. A well-organized manuscript in good English would make the peer review even the whole editorial handling more smooth and efficient.

If needed, authors are recommended to consider the language editing services provided by OAE to ensure that the manuscript is written in correct scientific English before submission. An extra charge is required to enjoy this service. Please visit https://www.oaepublish.com/services or contact English-Editing@oaepublish.com for more details.

1.5 Work Funded by the National Institutes of Health

If an accepted manuscript was funded by National Institutes of Health (NIH), the author may inform Editors of the NIH funding number. The Editors are able to deposit the paper to the NIH Manuscript Submission System on behalf of the author.

1.6 Financial Disclosure and Conflict of Interest

Please provide financial disclosure and any conflict of interest on the title page of manuscript.

2. Submission Preparation

2.1 Cover Letter

A cover letter is required to be submitted accompanying each manuscript. It should be concise and explain why the study is significant, why it fits the scope of the journal, and why it would be attractive to readers, *etc.*
Here is a guideline of a cover letter for authors' consideration:
In the first paragraph: include the title and type of the manuscript, a brief on the background of the study, the question the author sought out to answer and why;
In the second paragraph: concisely explain what was done, the main findings and why they are significant;
In the third paragraph: indicate why the manuscript fits the Aims and Scope of the journal, and why it would be attractive to readers;
In the fourth paragraph: confirm that the manuscript has not been published elsewhere and not under consideration of any other journal. All authors have approved the manuscript and agreed on its submission to the journal. Journal's specific requirements have been met if any.
If the manuscript is contributed to a Special Issue, please also mention it in the cover letter.
If the manuscript was presented partly or entirely in a conference, the author should clearly state the background information of the event, including the conference name, time and place in the cover letter.

2.2 Types of Manuscripts

There is no restriction on the number of figures, tables and references, provided that the manuscript is concise and comprehensive. The journal publishes Research Articles, Reviews and Systematic Reviews, Short Communications, Commentaries, *etc*. For more details about paper type, please refer to the following table.

Manuscript Type	**Definition**	**Word Limit**	**Abstract**	**Keywords**	**Main Text Structure**
Research Article	A Research Article describes detailed results from novel research. All findings are extensively discussed.	8000 max	Unstructured abstract. No more than 250 words.	3-8 keywords	The main content should include four sections: Introduction, Experimental, Results and discussion, and Conclusions.
Review	A review article should provide readers with an in-depth understanding of a field by summarizing existing literature, and highlight key gaps and challenges to address future research.	10000 max	Unstructured abstract. No more than 250 words.	3-8 keywords	The main text may consist of several sections with unfixed section titles. We suggest that the author include an "Introduction" section at the beginning, several sections with unfixed titles in the middle part, and a "Conclusion" section in the end.
Systematic Review	A Systematic Review collects and critically analyzes multiple research studies, using methods selected before one or more research questions are formulated, and then finding and analyzing related studies and answering those questions in a structured methodology.	3000 max	Structured abstract including Aim, Methods, Results and Conclusion. No more than 250 words.	3-8 keywords	The main content should include four sections: Introduction, Methods, Results and Discussion.
Short Communication	Short Communications are short papers that present original and significant material for rapid dissemination. Short articles include, but are not limited to: discovery or development of new materials, cutting-edge experiments and theory, novelty in simulation and modeling, elucidation of mechanisms.	1500 max	Unstructured abstract. No more than 250 words.	3-8 keywords	/
Commentary	A Commentary is to provide comments on a newly published article or an alternative viewpoint on a certain topic.	2500 max	Unstructured abstract. No more than 250 words.	3-8 keywords	/
Editorial	An Editorial is a short article describing academic news or opinions of Editorial Board members.	1000 max	None required.	None required.	/
Letter to Editor	A Letter to Editor is usually an open post-publication review of a paper from its readers, often critical of some aspect of a published paper. Controversial papers often attract numerous Letters to Editor.	800 max	Unstructured abstract (optional). No more than 250 words.	3-8 keywords (optional)	/
Opinion	An Opinion usually presents personal thoughts, beliefs, or feelings on a topic.	1200 max	Unstructured abstract. No more than 250 words.	3-8 keywords	/
Perspective	A Perspective provides personal points of view on the state-of-the-art of a specific area of knowledge and its future prospects. Links to areas of intense current research focus can also be made. The emphasis should be on a personal assessment rather than a comprehensive, critical review. However, comments should be put into the context of existing literature. Perspectives are usually invited by the Editors.	2000 max	Unstructured abstract. No more than 250 words.	3-8 keywords	/
Technical Guide	A Technical Note is a short article giving a brief description of a specific development, technique or procedure, or it may describe a modification of an existing technique, procedure or device applied in research.	1200 max	Unstructured abstract (optional). No more than 250 words.	3-8 keywords	/

2.3 Manuscript Structure

Trials, observational studies, systematic reviews, meta-analyses and qualitative research should be described and reported according to standard guidelines, as presented by the Equator Initiative, such as CONSORT, STROBE or PRISMA guidelines.

2.3.1 Front Matter

2.3.1.1 Title

The title of the manuscript should be concise, specific and relevant, with no more than 16 words if possible. When gene or protein names are included, the abbreviated name rather than full name should be used.

2.3.1.2 Authors and Affiliations

Authors' full names should be listed. The initials of middle names can be provided. Institutional addresses and email addresses for all authors should be listed. At least one author should be designated as corresponding author. In addition, corresponding authors are suggested to provide their Open Researcher and Contributor ID upon submission. Please note that any change to authorship is not allowed after manuscript acceptance.

2.3.1.3 Abstract

The abstract should be a single paragraph with word limitation and specific structure requirements (for more details please refer to Types of Manuscripts). It usually describes the main objective(s) of the study, explains how the study was done, including any model organisms used, without methodological detail, and summarizes the most important results and their significance. The abstract must be an objective representation of the study: it is not allowed to contain results which are not presented and substantiated in the manuscript, or exaggerate the main conclusions. Citations should not be included in the abstract.

2.3.1.4 Graphical Abstract

The graphical abstract is essential as this can catch first view of your publication by readers. We recommend you to submit an eye-catching figure. It should summarize the content of the article in a concise graphical form. It is recommended to use it because this can make online articles get more attention. The graphic abstract should be submitted as a separate document in the online submission system. Please provide an image with a minimum of 730 × 1,228 pixels (h × w) or proportionally more. The image should be readable at a size of 7 × 12 cm using a regular screen resolution of 96 dpi. Preferred file types: TIFF, PSD, AI, JPG, JPEG, EPS, PNG, ZIP and PDF files.

2.3.1.5 Keywords

Three to eight keywords should be provided, which are specific to the article, yet reasonably common within the subject discipline.

2.3.2 Main Text

Manuscripts of different types are structured with different sections of content. Please refer to types of manuscripts to make sure which sections should be included in the manuscripts.

2.3.2.1 Introduction

The introduction should contain background that puts the manuscript into context, allow readers to understand why the study is important, include a brief review of key literature, and conclude with a brief statement of the overall aim of the work and a comment about whether that aim was achieved. Relevant controversies or disagreements in the field should be introduced as well.

2.3.2.2 Methods

Methods should contain sufficient details to allow others to fully replicate the study. New methods and protocols should be described in detail while well-established methods can be briefly described or appropriately cited. Experimental participants selected, the drugs and chemicals used, the statistical methods taken, and the computer software used should be identified precisely. Statistical terms, abbreviations, and all symbols used should be defined clearly. Protocol documents for clinical trials, observational studies, and other non-laboratory investigations may be uploaded as supplementary materials.

2.3.2.3 Results

This section contains the findings of the study. Results of statistical analysis should also be included either as text or as tables or figures if appropriate. Authors should emphasize and summarize only the most important observations. Data on all primary and secondary outcomes identified in the section Methods should also be provided. Extra or supplementary materials and technical details can be placed in supplementary documents.

2.3.2.4 Discussion

This section should discuss the implications of the findings in context of existing research and highlight limitations of the study. Future research directions may also be mentioned. A paragraph describing the limitations of the study presented should be explicitly included in the Discussion.

2.3.2.5 Conclusion

It should state clearly the main conclusions and include the explanation of their relevance or importance to the field.

2.3.3 Back Matter

2.3.3.1 Acknowledgments

Anyone who contributed towards the article including those who provided professional writing services or materials, should be acknowledged. Authors should obtain permission to acknowledge from all those mentioned in the Acknowledgments section. This section is not added if the author does not have anyone to acknowledge.

2.3.3.2 Authors' Contributions

Each author is expected to have made substantial contributions to the conception or design of the work, or the acquisition, analysis, or interpretation of data, or the creation of new software used in the work, or have drafted the work or substantively revised it.

Please use Surname and Initial of Forename to refer to an author's contribution. For example: made substantial contributions to conception and design of the study and performed data analysis and interpretation: Salas H, Castaneda WV; performed data acquisition, as well as provided administrative, technical, and material support: Castillo N, Young V.

If an article is single-authored, please include "The author contributed solely to the article." in this section.

2.3.3.3 Availability of Data and Materials

In order to maintain the integrity, transparency and reproducibility of research records, authors should include this section in their manuscripts, detailing where the data supporting their findings can be found. Data can be deposited into data repositories or published as supplementary information in the journal. Authors who cannot share their data should state that the data will not be shared and explain it. If a manuscript does not involve such issue, please state "Not applicable." in this section.

2.3.3.4 Financial Support and Sponsorship

All sources of funding for the study reported should be declared. The role of the funding body in the experiment design, collection, analysis and interpretation of data, and writing of the manuscript should be declared. Any relevant grant numbers and the link of funder's website should be provided if any. If the study is not involved with this issue, state "None." in this section.

2.3.3.5 Conflicts of Interest

Authors must declare any potential conflicts of interest that may be perceived as inappropriately influencing the representation or interpretation of reported research results. If there are no conflicts of interest, please state "All authors declared that there are no conflicts of interest." in this section. Some authors may be bound by confidentiality agreements. In such cases, in place of itemized disclosures, we will require authors to state "All authors declare that they are bound by confidentiality agreements that prevent them from disclosing their conflicts of interest in this work.". If authors are unsure whether conflicts of interest exist, please refer to the "Conflicts of Interest" of OAE Editorial Policies for a full explanation.

2.3.3.6 Ethical Approval and Consent to Participate

Research involving human subjects, human material or human data must be performed in accordance with the Declaration of Helsinki and approved by an appropriate ethics committee. An informed consent to participate in the study should also be obtained from participants, or their parents or legal guardians for children under 16. A statement detailing the name of the ethics committee (including the reference number where appropriate) and the informed consent obtained must appear in the manuscripts reporting such research.

Studies involving animals and cell lines must include a statement on ethical approval. More information is available at Editorial Policies.

If the manuscript does not involve such issue, please state "Not applicable." in this section.

2.3.3.7 Consent for Publication

Manuscripts containing individual details, images or videos, must obtain consent for publication from that person, or in the case of children, their parents or legal guardians. If the person has died, consent for publication must be obtained from the next of kin of the participant. Manuscripts must include a statement that a written informed consent for publication was obtained. Authors do not have to submit such content accompanying the manuscript. However, these documents must be available if requested. If the manuscript does not involve this issue, state "Not applicable." in this section.

2.3.3.8 Copyright

Authors retain copyright of their works through a Creative Commons Attribution 4.0 International License that clearly states how readers can copy, distribute, and use their attributed research, free of charge. A declaration "© The Author(s)

2025." will be added to each article. Authors are required to sign License to Publish before formal publication.

2.3.3.9 References

References should be numbered in order of appearance at the end of manuscripts. In the text, reference numbers should be placed in square brackets and the corresponding references are cited thereafter. Only the first five authors' names are required to be listed in the references, other authors' names should be omitted and replaced with "et al.". Information from manuscripts accepted but not published should be cited in the text as "Unpublished material" with written permission from the source. The names of journals should be italicized.

References should be described as follows, depending on the types of works:

Types	**Examples**
Journal articles by individual authors	Weaver, D. L.; Ashikaga, T.; Krag, D. N. Effect of occult metastases on survival in node-negative breast cancer. *N. Engl. J. Med.* **2011**, *364*, 412-421. DOI: 10.1056/NEJMoa1008108
Organization as author	Diabetes Prevention Program Research Group. Hypertension, insulin, and proinsulin in participants with impaired glucose tolerance. *Hypertension* **2002**, *40,* 679-686. DOI: 10.1161/01.HYP.0000035706.28494.09
Both personal authors and organization as author	Vallancien, G.; Emberton, M.; Harving, N.; van Moorselaar, R. J.; Alf-One Study Group. Sexual dysfunction in 1,274 European men suffering from lower urinary tract symptoms. *J. Urol.* **2003**, *169*, 2257-2261. DOI: 10.1097/01.ju.0000067940.76090.73
Journal articles not in English	Zhang X.; Xiong H.; Ji T. Y.; Zhang Y. H.; Wang Y. Case report of anti-N-methyl-D-aspartate receptor encephalitis in child. *J. Appl. Clin. Pediatr.* **2012**, *27*, 1903-1907. (in Chinese)
Journal articles ahead of print	Odibo, A. O. Falling stillbirth and neonatal mortality rates in twin gestation: not a reason for complacency. *BJOG.* **2018**, Epub ahead of print [DOI: 10.1111/1471-0528.15541]
eBook	Hammond, C. *The Basics of Crystallography and Diffraction*, 4th ed.; Oxford University Press, 2015. DOI: 10.1093/acprof:oso/9780198738671.001.0001
Book in print	Frankel, F. *Picturing Science and Engineering*; MIT Press, 2018.
ebook chapter	Hammond, C. Crystal Symmetry. In *The Basics of Crystallography and Diffraction*, 4th ed.; International Union of Crystallography Texts on Crystallography, Vol. 21; Oxford University Press, 2015; pp 99−134. DOI: 10.1093/acprof:oso/9780198738671.003.0004
ebook with editors	*Mom the Chemistry Professor: Personal Accounts and Advice from Chemistry Professors Who Are Mothers*, 2nd ed.; Woznack, K., Charlebois, A., Cole, R. S., Marzabadi, C. H., Webster, G., Eds.; Springer, 2018. DOI: 10.1007/978-3-319-78972-9
ebook series	Cable, M. L. Life in Extreme Environments: Lanthanide-Based Detection of Bacterial Spores and Other Sensor Design Pursuits. Ph.D. Dissertation, California Institute of Technology, Pasadena, CA, 2010. http://resolver.caltech.edu/CaltechTHESIS:05102010-145436548 (accessed 2019-09-10).
Thesis or dissertation	Tian D, Araki H, Stahl E, Bergelson J, Kreitman M. Signature of balancing selection in Arabidopsis. *Proc Natl Acad Sci U S A*. Forthcoming 2002.
Thesis or dissertation in print	Enander, R. T. Lead particulate and methylene chloride risks in automotive refinishing. Ph.D. Thesis, Tufts University, Medford, MA, 2001.
Website	*World Health Organization Home Page*. https://www.who.int/ (accessed 2019-02-21).
Newspaper	Beauge, J. School district sued over burns girl suffered during chemistry class demonstration. *PennLive* (*Harrisburg, PA*), November 17, 2018, updated November 17, 2018. https://www.pennlive.com/news/2018/11/school_district_sued_over_burn.html (accessed 2019-02-22).
Conference abstract	Okita, J.; Iwamoto, T.; Kira, M. Novel synthetic route for hydrosilyllithiums. In *Book of Abstracts, 2000 International Chemical Congress of Pacific Basin Societies (PACIFICHEM 2000)*, Honolulu, HI; Paper INOR 216.
Conference proceedings	Nilsson, A.; Petersson, F.; Persson, H. W.; Jönsson, H.; Laurell, T. Manipulation of suspended particles in a laminar flow. In *Micro Total Analysis Systems 2002, Proceedings of the µTAS 2002 Symposium*, Nara, Japan, November 3−7, 2002; Baba, Y., Shoji, S., van den Berg, A., Eds.; Kluwer Academic Publishers: Dordrecht, The Netherlands, 2002; Vol. 2, pp 751−753. DOI: 10.1007/978-94-010-0504-3_50
Database	*SpectraBase*. Bio-Rad Laboratories. https://spectrabase.com/ (accessed 2020-01-05).
Patent	Stern, M. K.; Cheng, B. K. M. Process for preparing N-(p-nitroaryl)amides via reaction of nitrobenzene with nitriles. US 5380946, 1995.
Preprint	Yamamoto T. S.; Inui R.; Tada Y.; Yokoyama S. Prospects of detection of subsolar mass primordial black hole and white dwarf binary mergers. *arXiv* 2004, arXiv:2401.00044. Available online: https://arxiv.org/abs/2401.00044 (accessed 29 December 2023).

2.3.3.10 Supplementary Materials

Additional data and information can be uploaded as Supplementary Materials to accompany the manuscripts. The supplementary materials will also be available to the referees as part of the peer-review process. Any file format is acceptable, such as data sheet (word, excel, csv, cdx, fasta, pdf or zip files), presentation (powerpoint, pdf or zip files), image (cdx, eps, jpeg, pdf, png or tiff), table (word, excel, csv or pdf), audio (mp3, wav or wma) or video (avi, divx, flv, mov, mp4, mpeg, mpg or wmv). All information should be clearly presented. Supplementary materials should be cited in the main text in numeric order (e.g., Supplementary Figure 1, Supplementary Figure 2, Supplementary Table 1, Supplementary Table 2, etc.). The style of supplementary figures or tables complies with the same requirements on figures or tables in main text. Videos and audios should be prepared in English, and limited to a size of 500 MB.

2.4 Manuscript Format

2.4.1 File Format

Manuscript files can be in DOC,DOCX and Latex formats and should not be locked or protected.

2.4.2 Length

The word limit is specified in the item "Types of Manuscripts". There are no restrictions on number of figures or amount of supporting documents. Authors are encouraged to present and discuss their findings concisely.

2.4.3 Language

Manuscripts must be written in English.

2.4.4 Multimedia Files

- The journal supports manuscripts with multimedia files. The requirements are listed as follows:
- Video or audio files are only acceptable in English. The presentation and introduction should be easy to understand. The frames should be clear, and the speech speed should be moderate.
- A brief overview of the video or audio files should be given in the manuscript text.
- The video or audio files should be limited to a size of up to 500 MB.
- Please use professional software to produce high-quality video files, to facilitate acceptance and publication along with the submitted article. Upload the videos in mp4, wmv, or rm format (preferably mp4) and audio files in mp3 or wav format.

2.4.5 Figures

- Figures should be cited in numeric order (e.g., Figure 1, Figure 2) and placed after the paragraph where it is first cited;
- Figures can be submitted in format of tiff, psd, AI or jpeg, with resolution of 300-600 dpi;
- Figure caption is placed under the Figure;
- Diagrams with describing words (including, flow chart, coordinate diagram, bar chart, line chart, and scatter diagram, *etc.*) should be editable in word, excel or powerpoint format. Non-English information should be avoided;
- Labels, numbers, letters, arrows, and symbols in figure should be clear, of uniform size, and contrast with the background;
- Symbols, arrows, numbers, or letters used to identify parts of the illustrations must be identified and explained in the legend;
- Internal scale (magnification) should be explained and the staining method in photomicrographs should be identified;
- All non-standard abbreviations should be explained in the legend;
- Permission for use of copyrighted materials from other sources, including re-published, adapted, modified, or partial figures and images from the internet, must be obtained. It is authors' responsibility to acquire the licenses, to follow any citation instruction requested by third-party rights holders, and cover any supplementary charges.

2.4.6 Tables

- Tables should be cited in numeric order and placed after the paragraph where it is first cited;
- The table caption should be placed above the table and labeled sequentially (e.g., Table 1, Table 2);
- Tables should be provided in editable form like DOC or DOCX format (picture is not allowed);
- Abbreviations and symbols used in table should be explained in footnote;
- Explanatory matter should also be placed in footnotes;
- Permission for use of copyrighted materials from other sources, including re-published, adapted, modified, or partial tables from the internet, must be obtained. It is authors' responsibility to acquire the licenses, to follow any citation instruction requested by third-party rights holders, and cover any supplementary charges.

2.4.7 Abbreviations

Abbreviations should be defined upon first appearance in the abstract, main text, and in figure or table captions and used consistently thereafter. Non-standard abbreviations are not allowed unless they appear at least three times in the text. Commonly-used abbreviations, such as DNA, RNA, ATP, *etc.*, can be used directly without definition. Abbreviations in titles and keywords should be avoided, except for the ones which are widely used.

2.4.8 Italics

General italic words like *vs.*, *et al.*, *etc.*, *in vivo*, *in vitro*; t test, F test, U test; related coefficient as r, sample number as n, and probability as P; names of genes; names of bacteria and biology species in Latin.

2.4.9 Units

SI Units should be used. Imperial, US customary and other units should be converted to SI units whenever possible. There is a space between the number and the unit (i.e., 23 mL). Hour, minute, second should be written as h, min, s.

2.4.10 Numbers

Numbers appearing at the beginning of sentences should be expressed in English. When there are two or more numbers in a paragraph, they should be expressed as Arabic numerals; when there is only one number in a paragraph, number < 10 should be expressed in English and number > 10 should be expressed as Arabic numerals. 12345678 should be written as 12,345,678.

2.4.11 Equations

Equations should be editable and not appear in a picture format. Authors are advised to use either the Microsoft Equation Editor or the MathType for display and inline equations.

2.5 Submission Link

Submit an article via https://www.oaecenter.com/login?JournalId=wecn.

3. Research and Publication Ethics

3.1 Research Involving Human Subjects

All studies involving human subjects must be in accordance with the Helsinki Declaration and seek approval to conduct the study from an independent local, regional, or national review body (e.g., ethics committee, institutional review board, *etc*.). Such approval, including the names of the ethics committee, institutional review board, *etc*., must be listed in a declaration statement of Ethical Approval and Consent to Participate in the manuscript. If the study is judged exempt from ethics approval, related information (e.g., name of the ethics committee granting the exemption and the reason for the exemption) must be listed. Further documentation on ethics should also be prepared, as Editors may request more detailed information. Manuscripts with suspected ethical problems will be investigated according to COPE Guidelines.

3.1.1 Consent to Participate

For all studies involving human subjects, informed consent to participate in the studies must be obtained from participants, or their parents or legal guardians for children under 16. Statements regarding consent to participate should be included in a declaration statement of Ethical Approval and Consent to Participate in the manuscript. If informed consent is not required, the name of the ethics committee granting the exemption and the reason for the exemption must be listed. If any ethical violation is found at any stage of publication, the issue will be investigated seriously based on COPE Guidelines.

3.1.2 Consent for Publication

All articles published by OAE are freely available on the Internet. All manuscripts that include individual participants' data in any form (i.e., details, images, videos, *etc*.) will not be published without Consent for Publication obtained from that person(s), or for children, their parents or legal guardians. If the person has died, Consent for Publication must be obtained from the next of kin. Authors must add a declaration statement of Consent for Publication in the manuscript, specifying written informed consent for publication has been obtained.

3.2 Research Involving Animals

Experimental research on animals should be approved by an appropriate ethics committee and must comply with institutional, national, or international guidelines. OAE encourages authors to comply with the AALAS Guidelines, the ARRIVE Guidelines, and/or the ICLAS Guidelines, and obtain prior approval from the relevant ethics committee. Manuscripts must include a statement indicating that the study has been approved by the relevant ethical committee and the whole research process complies with ethical guidelines. If a study is granted an exemption from requiring ethics approval, the name of the ethics committee granting the exemption and the reason(s) for the exemption should be detailed. Editors will take account of animal welfare issues and reserve the right to reject a manuscript, especially if the research involves protocols that are inconsistent with commonly accepted norms of animal research.

3.3 Research Involving Cell Lines

Authors must describe what cell lines are used and their origin so that the research can be reproduced. For established cell lines, the provenance should be stated and references must also be given to either a published paper or to a commercial source. For de novo cell lines derived from human tissue, appropriate approval from an institutional review board or equivalent ethical committee, and consent from the donor or next of kin, should be obtained. Such statements should be listed on the Declaration section of Ethical Approval and Consent to Participate in the manuscript.

Further information is available from the International Cell Line Authentication Committee (ICLAC). OAE recommends that authors check the NCBI database for misidentification and contamination of human cell lines.

3.4 Research Involving Plants

Experimental research on plants (either cultivated or wild), including collection of plant material, must comply with institutional, national, or international guidelines. Field studies should be conducted in accordance with local legislation, and the manuscript should include a statement specifying the appropriate permissions and/or licenses. OAE recommends that authors comply with the IUCN Policy Statement on Research Involving Species at Risk of Extinction and the Convention on the Trade in Endangered Species of Wild Fauna and Flora.

For each submitted manuscript, supporting genetic information and origin must be provided for plants that were utilized. For research manuscripts involving rare and non-model plants (other than, e.g., Arabidopsis thaliana, Nicotiana benthamiana, Oriza sativa, or many other typical model plants), voucher specimens must be deposited in a public herbarium or other public collections providing access to deposited materials.

3.5 Publication Ethics Statement

OAE is a member of the Committee on Publication Ethics (COPE). We fully adhere to its Code of Conduct and to its Best Practice Guidelines.

The Editors of this journal enforce a rigorous peer-review process together with strict ethical policies and standards to guarantee to add high-quality scientific works to the field of scholarly publication. Unfortunately, cases of plagiarism, data falsification, image manipulation, inappropriate authorship credit, and the like, do arise. The Editors of *Water Emerging Contaminants & Nanoplastics* take such publishing ethics issues very seriously and are trained to proceed in such cases with zero tolerance policy.

Authors wishing to publish their papers in *Water Emerging Contaminants & Nanoplastics* must abide to the following:

- The author(s) must disclose any possibility of a conflict of interest in the paper prior to submission.
- The authors should declare that there is no academic misconduct in their manuscript in the cover letter.
- Authors should accurately present their research findings and include an objective discussion of the significance of their findings.
- Data and methods used in the research need to be presented in sufficient detail in the manuscript so that other researchers can replicate the work.
- Authors should provide raw data if referees and the Editors of the journal request.
- Simultaneous submission of manuscripts to more than one journal is not tolerated.
- Republishing content that is not novel is not tolerated (for example, an English translation of a paper that is already published in another language will not be accepted).
- The manuscript should not contain any information that has already been published. If you include already published figures or images, please get the necessary permission from the copyright holder to publish under the CC-BY license.
- Plagiarism, data fabrication and image manipulation are not tolerated.
- Plagiarism is not acceptable in OAE journals.

Plagiarism involves the inclusion of large sections of unaltered or minimally altered text from an existing source without appropriate and unambiguous attribution, and/or an attempt to misattribute original authorship regarding ideas or results, and copying text, images, or data from another source, even from your own publications, without giving credit to the source.

As to reusing the text that is copied from another source, it must be between quotation marks and the source must be cited. If a study's design or the manuscript's structure or language has been inspired by previous studies, these studies must be cited explicitly.

If plagiarism is detected during the peer-review process, the manuscript may be rejected. If plagiarism is detected after publication, we may publish a Correction or retract the paper.

Falsification is manipulating research materials, equipment, or processes, or changing or omitting data or results so that the findings are not accurately represented in the research record.

Image files must not be manipulated or adjusted in any way that could lead to misinterpretation of the information provided by the original image.

Irregular manipulation includes: introduction, enhancement, moving, or removing features from the original image; grouping of images that should be presented separately, or modifying the contrast, brightness, or color balance to obscure, eliminate, or enhance some information.

If irregular image manipulation is identified and confirmed during the peer-review process, we may reject the manuscript. If irregular image manipulation is identified and confirmed after publication, we may publish a Correction or retract the paper.

OAE reserves the right to contact the authors' institution(s) to investigate possible publication misconduct if the Editors find conclusive evidence of misconduct before or after publication. OAE has a partnership with iThenticate , which is the most trusted similarity checker. It is used to analyze received manuscripts to avoid plagiarism to the greatest extent possible. When plagiarism becomes evident after publication, we will retract the original publication or require modifications, depending on the degree of plagiarism, context within the published article, and its impact on the overall integrity of the published study. Journal Editors will act under the relevant COPE guidelines.

4. Authorship

Authorship credit of OAE journals should be solely based on substantial contributions to a published study, as specified in the following four criteria:
1. Substantial contributions to the conception or design of the work, or the acquisition, analysis, or interpretation of data for the work;
2. Drafting the work or revising it critically for important intellectual content;
3. Final approval of the version to be published;
4. Agreement to be accountable for all aspects of the work in ensuring that questions related to the accuracy or integrity of any part of the work are appropriately investigated and resolved.

All those who meet these criteria should be identified as authors. Authors must specify their contributions in the section Authors' Contributions of their manuscripts. Contributors who do not meet all the four criteria (like only involved in acquisition of funding, general supervision of a research group, general administrative support, writing assistance, technical editing, language editing, proofreading, *etc.*) should be acknowledged in the section of Acknowledgement in the manuscript rather than being listed as authors.

If a large multiple-author group has conducted the work, the group ideally should decide who will be authors before the work starts and confirm authors before submission. All authors of the group named as authors must meet all the four criteria for authorship.
AI and AI-assisted technologies should not be listed as an author or co-author.

5. Reviewers Exclusions

You are welcome to exclude a limited number of researchers as potential Editors or reviewers of your manuscript. To ensure a fair and rigorous peer review process, we ask that you keep your exclusions to a maximum of three people. If you wish to exclude additional referees, please explain or justify your concerns—this information will be helpful for Editors when deciding whether to honor your request.

6. Editors and Journal Staff as Authors

Editorial independence is extremely important and OAE does not interfere with editorial decisions.

Editorial staff or Editors shall not be involved in the processing their own academic work. Submissions authored by editorial staff/Editors will be assigned to at least three independent outside reviewers. Decisions will be made by other Editorial Board members who do not have conflict of interests with the author. Journal staffs are not involved in the processing of their own work submitted to any OAE journals.

7. Policy of the Use of AI and AI-assisted Technologies

7.1 AI Authorship

Generative AI and AI-assisted technologies (e.g., large language models) are increasingly employed in content creation. However, their use in manuscript preparation is strictly limited:

- Prohibited applications: These tools must not be used to perform core research tasks, including generating scientific insights, analyzing/interpreting data, or drawing scientific conclusions.
- Permitted applications: They may only be used to enhance manuscript readability and language quality.

All AI technologies must be used under human oversight, as they may produce inaccurate or biased content. AI tools cannot be listed as authors/co-authors or cited as such. Authors retain full responsibility for all content, including AI-generated material.

Exceptions for methodological use:
If AI tools are integral to the research design/methodology, authors must:
1. Document usage transparently in the *Materials and Methods* section, specifying:
- Tool/model name
- Version/extension number
- Manufacturer

2. Include a declaration titled "*Declaration of Generative AI Use*" before the reference section, stating:
"*During the preparation of this work, the author(s) used [TOOL NAME] due to [reason]. The author(s) reviewed and edited all AI-generated content and accept full responsibility for the published material.*"
Note: No declaration is required for basic grammar/spelling checkers or reference managers.

7.2 Generative AI in Visual Content

OAE prohibits the use of generative AI/AI-assisted tools to create or modify images, including:
- Graphical abstracts
- Cover images
- Figures within manuscripts

Permitted adjustments limited to:
- Brightness/contrast correction
- Color balance optimization

provided these edits do not obscure, delete, or misrepresent original image data.

7.3 AI Use in Peer Review

Confidentiality requirements:
- Reviewers must not upload manuscripts/materials to AI platforms, as this:

1. Violates OAE's confidentiality policies
2. Risks intellectual property infringement
3. May compromise personal data in identifiable content

Review integrity standards:
- Peer review must remain human-driven – AI tools cannot replace critical scholarly judgment.
- Reviewers must not use AI for manuscript evaluation due to risks of:

1. Inaccurate/incomplete assessments
2. Algorithmic bias

Declaration requirement: Reviewers retain full accountability for their reports, if any aspect of the manuscript's evaluation was supported in any way by an AI tool, reviewers must explicitly disclose it in their report.

OAE will periodically reassess this policy to align with technological advancements and academic standards.

8. Conflict of Interests

OAE journals require authors to declare any possible financial and/or non-financial conflicts of interest at the end of their manuscript and in the cover letter, as well as confirm this point when submitting their manuscript in the submission system. If no conflicts of interest exist, authors need to state "The authors declare no conflicts of interest". We also recognize that some authors may be bound by confidentiality agreements, in which cases authors need to sate "The authors declare that they are bound by confidentiality agreements that prevent them from disclosing their competing interests in this work".

9. Editorial Process

9.1 Initial check

9.1.1 Initial manuscript check

New submissions are initially checked by the Managing Editor from the perspectives of originality, suitability, structure and formatting, conflicts of interest, background of authors, etc. Poorly-prepared manuscripts may be rejected at this stage. If your manuscript does not meet one or more of these requirements, we will return it for further revisions.

9.1.2 Publishing ethics

All manuscripts submitted to *Water Emerging Contaminants & Nanoplastics* are screened using iThenticate powered by CrossCheck to identify any plagiarized content. Your study must also meet all ethical requirements as outlined in our Editorial Policies. If the manuscript does not pass any of these checks, we may return it to you for further revisions or decline to consider your study for publication.

9.2 Editorial assessment

Once your manuscript has passed the initial check, our editorial team will assign it to an Academic Editor, i.e., the Editor-in-Chief in the case of regular submissions, the Guest Editor in the case of Special Issue submissions, or an Editorial Board member in case of a conflict of interest, who will be notified of the submission and invited to check and recommend reviewers. The Academic Editors may reject manuscripts that they deem highly unlikely to pass peer review without further consultation.

9.3 Process

Water Emerging Contaminants & Nanoplastics operates a single-blind review process. The technical quality of the research described in the manuscript is assessed by a minimum of three independent expert reviewers. The Academic Editor is responsible for the final decision regarding acceptance or rejection of the manuscript. For controversial manuscripts, the Editor-in-Chief is responsible for making the final decision.

9.4 Decisions

Your research will be judged on technical soundness only, not on its perceived impact as judged by Editors or referees. There are three possible decisions: Accept (your study satisfies all publication criteria), Invitation to Revise (more work is required to satisfy all criteria), and Reject (your study fails to satisfy key criteria and it is highly unlikely that further work can address its shortcomings).

10. Contact Us

Managing Editor
Serein Hu
Email: watercontaminants@oaemesas.com

Locations
Los Angeles Office
245 E Main Street Ste 107, Alhambra CA 91801, USA
Tel: +1 323 9987086

Xi’an Office
Suite 1504, Plaza A, Xi’an National Digital Publishing Base, No. 996 Tiangu 7th Road, Gaoxin District, Xi’an 710077, Shaanxi, China
Tel: +86 (0)29 8954 0089

Water Emerging Contaminants & Nanoplastics
(*WECN*)
Los Angeles Office
245 E Main Street ste 107, Alhambra,
CA 91801, USA
Tel: +1 323 9987086
E-mail: watercontaminants@oaemesas.com
Website: https://www.oaepublish.com/wecn